

Environmental Assessment of the Alaskan Continental Shelf

Volume 3

Principal Investigators' Reports
October - December 1976



- VOLUME 1. RECEPTORS (BIOTA):
MARINE MAMMALS; MARINE BIRDS; MICROBIOLOGY
- VOLUME 2. RECEPTORS (BIOTA):
FISH; PLANKTON; BENTHOS; LITTORAL
- VOLUME 3. EFFECTS; CONTAMINANT BASELINES; TRANSPORT
- VOLUME 4. HAZARDS; DATA MANAGEMENT

Environmental Assessment of the Alaskan Continental Shelf

October-December 1976 quarterly reports from Principal Investigators participating in a multi-year program of environmental assessment related to petroleum development of the Alaskan Continental Shelf. The program is directed by the National Oceanic and Atmospheric Administration under funding from and for use by the Bureau of Land Management.

ENVIRONMENTAL RESEARCH LABORATORIES

Boulder, Colorado

February 1977

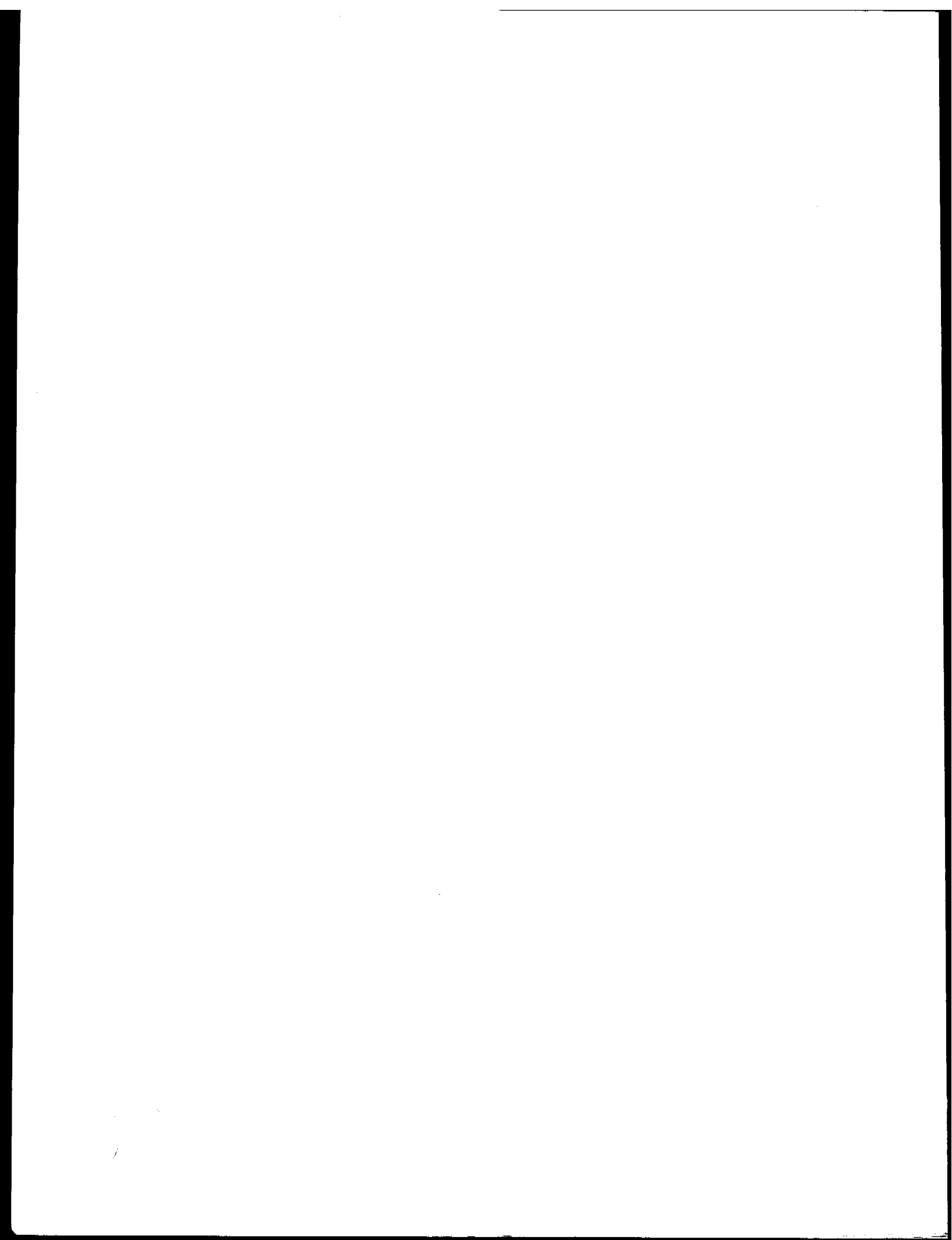
NOTICE

The Environmental Research Laboratories do not approve, recommend, or endorse any proprietary product or proprietary material mentioned in this publication. No reference shall be made to the Environmental Research Laboratories or to this publication furnished by the Environmental Research Laboratories in any advertising or sales promotion which would indicate or imply that the Environmental Research Laboratories approve, recommend, or endorse any proprietary product or proprietary material mentioned herein, or which has as its purpose an intent to cause directly or indirectly the advertised product to be used or purchased because of this Environmental Research Laboratories publication.

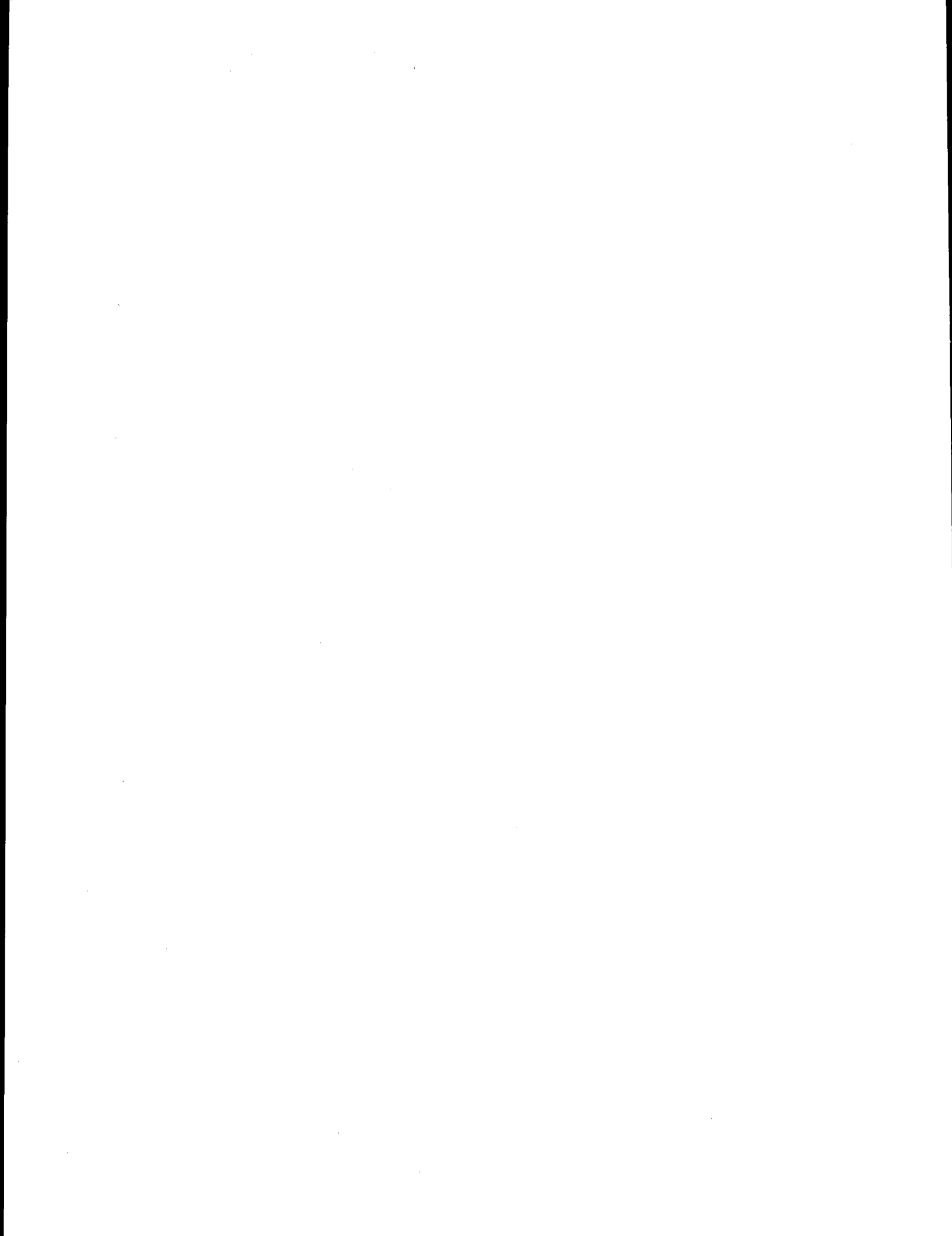
VOLUME 3

CONTENTS

EFFECTS	1
CONTAMINANT BASELINES	181
TRANSPORT	307



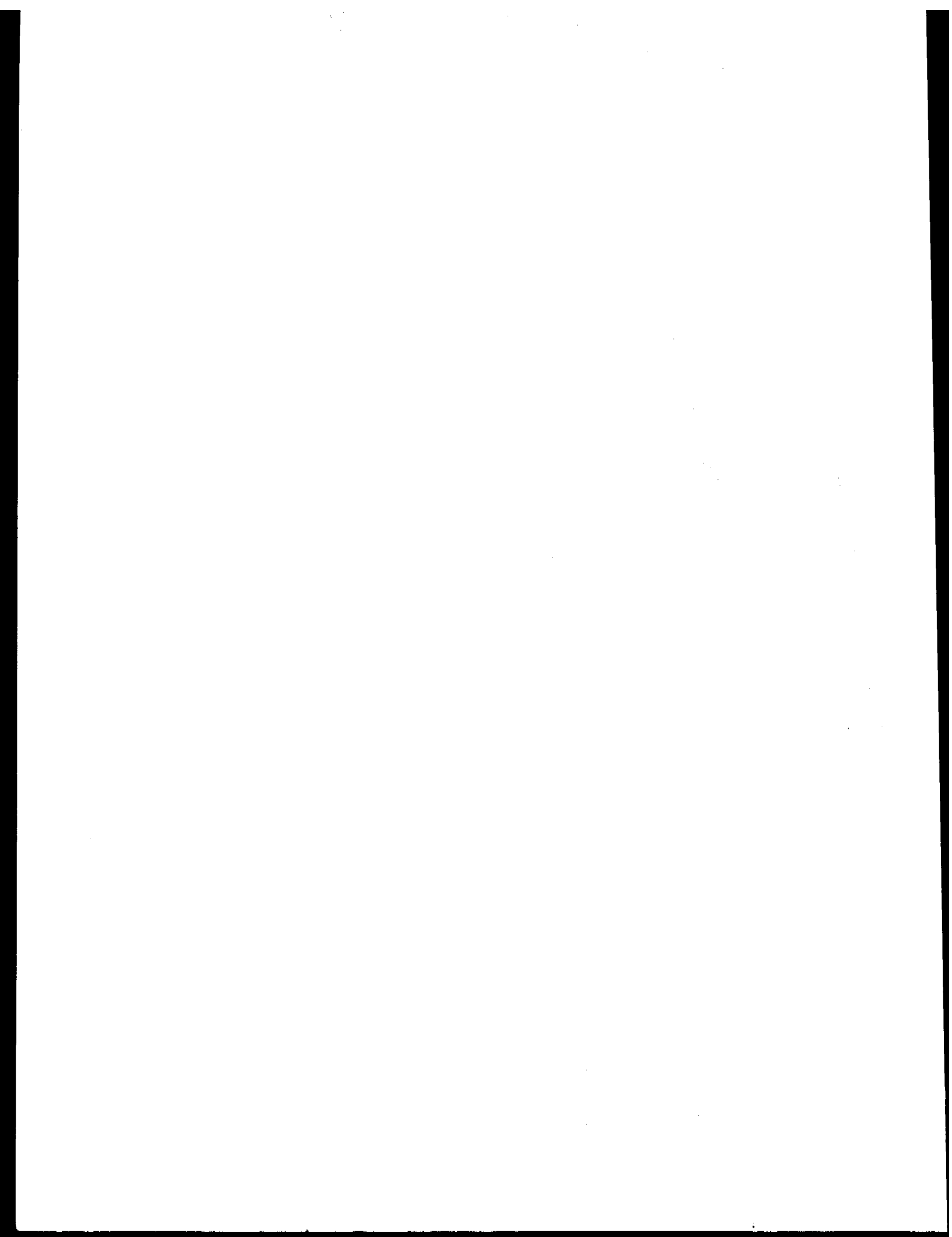
EFFECTS



EFFECTS

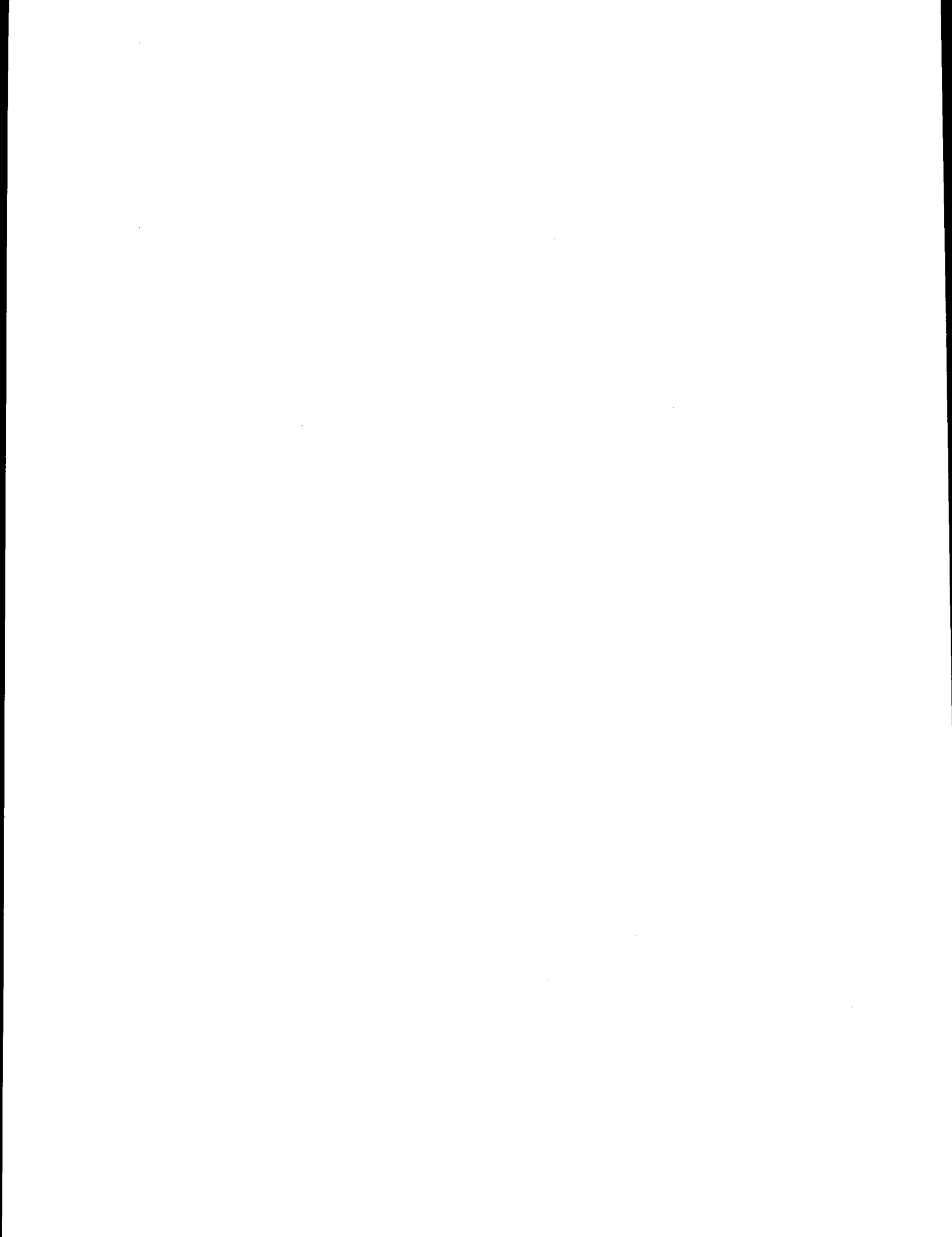
*Indicates Final Report

<u>Research Unit</u>	<u>Proposer</u>	<u>Title</u>	<u>Page</u>
62	Arthur L. DeVries Phy. Research Lab. Scripps Inst. of Ocean	Study of Effects of Acute and Chronic Exposure to Hydrocarbons in Shallow Water Bering Sea Fishes	1
*71	Gerald L. Kooyman et al. NMFS/NWFC	Physiological Impact of Oil on Pinnipeds	3
72	S. D. Rice J. F. Karinen NMFS/Auke Bay Fisheries Lab.	Acute and Chronic Toxicity, Uptake, and Depuration, and Sublethal Meta- bolic Response of Alaskan Marine Organisms to Petroleum Hydrocarbons	27
73/ 74	D. C. Malins et al. NMFS/NWFC	Sublethal Effects as Reflected by Morphological, Chemical, Physiological, Behavioral, and Pathological Indices	46
75	D. C. Malins Maurice E. Stansby NMFS/NWFC	Assessment of Available Literature on Effects of Oil Pollution on Biota in Arctic and Subarctic Waters	87
77	T. Laevastu F. Favorite NMFS/NWFC & AFC	Ecosystem Dynamics, Eastern Bering Sea	89
96	Samuel M. Patten, Jr. Johns Hopkins U.	Effects of Petroleum Exposure on Hatching Success of Glaucous-winged Gulls (<i>Larus glaucescens</i>) on Egg Island, Copper River Delta	149
123	Ronald L. Smith IMS/U. of Alaska	Acute Toxicity - Pacific Herring Roe in the Gulf of Alaska	153
*183	Richard S. Caldwell et al Oregon State U. Marine Sciences Center	Effects of a Seawater-Soluble Fraction of Alaskan Crude Oil and Its Major Aro- matic Components on Larval Stages of the Dungeness Crab, <i>Cancer Magister</i> Dana	157
305	C. Peter McRoy IMS/U. of Alaska	Sublethal Effects on Seagrass Photosyn- thesis	169
389	Jeanette W. Struhsaker NMFS/SWFC	Transport, Retention, and Effects of the Water-soluble Fraction of Crude Oil in Experimental Food Chains	174



RU# 62

NO REPORT WAS RECEIVED



PHYSIOLOGICAL IMPACT OF OIL ON PINNIPEDS

by

Gerald L. Kooyman*

Roger L. Gentry**

and

W. Bruce McAlister**

Submitted as the Final Report

for Research Unit #71

OUTER CONTINENTAL SHELF ENERGY ASSESSMENT PROGRAM

Sponsored by

U.S. Department of the Interior

Bureau of Land Management

December 1976

* Scripps Institution of Oceanography, PRL, La Jolla, CA 92037

** Northwest & Alaska Fisheries Center, National Marine Fisheries Service,
NOAA, 7600 Sand Point Way N.E., Seattle, WA 98115

I. Summary of objectives, conclusions and implications with respect to OCS oil and gas development.

A. The objective of this study was to measure the effects of oil contamination on the northern fur seal through studies on the thermal conductance of pelts, dive performance, and alterations in the metabolic rate before and after contact with oil. A second objective was to compare thermal conductance in pelts of fur-bearing marine mammals with that of nonfur-bearing species to determine whether surface fouling might be a major route of impact for all species.

B. Conclusions. The study has shown that small amounts of crude oil have large effects on thermal conductance of fur-bearing pelts, and no effect on nonfur-bearing pelts. In living animals light oiling of approximately 30% of the pelt surface area resulted in a 1.5-fold increase in metabolic rate while immersed in water of various temperatures. Furthermore, this effect lasted at least 2 weeks. Although normal diving was measured, we did not obtain post-oiling data to show the effect of oil contact on dive performance.

C. Implications. Any contact with oil at any time of year would have a profound influence on the health of individual northern fur seals through increases in pelt conductance with concomitant increases in metabolic rate. That death would inevitably follow such contact cannot be verified from the present effort. However, considering that (a) oiled animals have greatly increased maintenance costs, and (b) they are extremely reluctant to enter sea water (where their food is found), it is clear that the health of oiled animals would be in serious jeopardy. Light crude oils, coated heavily enough to have a severe metabolic impact, may not be visually detectable on the pelt. Therefore, oiled animals on the rookery may not be obvious which would make ineffective any rehabilitation program following an oil spill.

II. Introduction

A. General nature and scope of study.

We anticipated that oil would have an impact on pinnipeds through (1) alterations of the insulative properties of the fur with resultant increased maintenance costs, (2) impaired diving and feeding abilities, and (3) direct metabolic effects of ingested oil. We anticipated that different routes of impact might be of different magnitude, depending on whether the animal used fur, fur and blubber, or blubber alone for thermoregulation, and depending further on whether the type of thermoregulation used differed at different life stages of the individual. Since it was not practical to investigate all these lines simultaneously, this research project was limited to detailed investigations of the impact of oil contamination on maintenance costs and diving ability in one fur bearing species (the northern fur seal), and to a broad survey of the impact of oil on insulative properties of pelts in many pinniped species.

B. Specific Objectives

1. Measure thermal conductance of pelts of many species to quantify the insulative properties of fur and of hair.
2. Measure thermal conductance of pelts after oiling and after cleaning with detergents.
3. Measure heat loss during immersion of oiled vs. nonoiled northern fur seals (subadult males only), using standard O_2 analysis.
4. Measure heat loss during immersion of oiled animals after washing with detergents.
5. Measure effects of oil on feeding and diving behavior of lactating female fur seals through the number and depth of dives made during feeding excursions, and through the duration of feeding excursions.

C. Relevance to problems of petroleum development

The northern fur seal is the most numerous pinniped within the Alaskan area where petroleum development might occur; their major breeding grounds are the Pribilof Islands, very close to the St. George Basin lease site. As fur bearers they are among the marine mammals most likely to be affected by oil. Furthermore, since the northern fur seal is harvested by the U.S. Government as part of its obligation to the Interim Convention on Conservation of North Pacific Fur Seals, any oil-related accident which resulted in substantial loss of the herd would also carry economic and international implications. By measuring the physiological responses of individual animals to surface contamination, the present research effort provides basic information from which the impact on the herd of a major oil spill in the fur seal's range can be predicted.

III. Current state of knowledge

The effects of oil spills on marine mammals have been reviewed recently by Smith and Geraci (1975), and by Davis and Anderson (1976). From both these sources it appears that hair bearing marine mammals (either adult or immature) are not usually killed by simple surface contact with oil. However, fur-bearing marine mammals (either young or adult) are much more susceptible, and may be killed by such contact. Ingestion of oil-contaminated food may cause measurable tissue changes (Smith and Geraci, 1975), but unless ingestion is chronic these changes appear to be reversible. To date the effects of chronic contact with petroleum are not known.

Metabolic rates of immersed seals have been measured in the past (Irving and Hart, 1957; Miller et al., 1976; Iverson and Krog, 1973), and are useful only in comparisons with the control animals used in the present study. No metabolic measurements of oiled marine mammals have been made, although such studies have been done with the muskrat (McEwan et al, 1974).

The characteristics of heat flux in aquatic animals have been the subject of several studies. The thermal conductance (C) of seal blubber was studied by Scholander et al., (1950), Hart and Irving (1959), and Bryden (1964). Flensed blubber was found to conduct about the same as asbestos, and the blubber of the living animal with its flow of blood was about 50% higher (Hart and Irving, 1959). Changes in (C) of dry and immersed pelts of beaver and polar bear also have been determined by Scholander et al., (1950). The influence of flow-rate, guard hairs and undercoat on (C) has been assessed by Frisch et al., (1974).

IV. Study area

Laboratory studies were done at the Physiological Research Laboratory, Scripps Institution of Oceanography, La Jolla, California. All field studies were done on St. George Island, Pribilof Group, Alaska. Seals whose feeding excursions were measured were probably feeding off the Continental Shelf near St. George Island.

V. Sources, methods and rationale of data collection

A. Thermal conductance studies

Fresh, blubber-free pelts from several species of pinnipeds were collected and kept frozen until the time for the heat flux measurements. The pelts studies are listed in Table 1. The pelts were mounted on wooden frames with enough stretching so that there was little slack in the skin.

The heat flux measurements were made with a Beckman-Whiteley heat flow transducer, Model T200-3. The transducer consists of a silver-constantan thermopile sandwiched between thin bakelite plates. Heat flow through the thermopile generates an electromotive force due to the difference in temperature between the thermocouple junctions of the thermopile. The output was measured with a Leeds and Northrup Model 8686 potentiometer.

Mounted on the bottom side of the transducer was a brass chamber with the edges and bottom surface insulated with 5 cm of styrofoam. Water at 37°C (< 0.1°C variation) was circulated from a Thermomix 1420 circulator. Over the top surface of the transducer was placed a 30 by 30 cm water bath with a thin (0.1 mm thick) sheet of plastic as the bottom of the container. The mounted pelts were bonded to the plastic sheet by means of a thin film of grease (Crisco). The pelt was then held tightly in place with four mounting brackets which pressed against the wooden frame. A Lauda/Brinkmann circulator K-2/RD pumped water into and out of the bath through two manifolds which distributed the water evenly across the pelt. Flow-rate through the bath was 25 cm · min⁻¹. The water depth was about 3 cm. The water temperature selected was usually about 12°C, and the variation in temperature through the course of a run was 0.1°C. Plate (skin temperature) and water temperatures were read with a Leeds and Northrup 8686 potentiometer whose reference temperature source was a distilled water and ice slush. Conductance

Table 1. Thermal conductance of immersed pinniped pelts. P = pup; SA = subadult; A = adult. Bracketed samples are from the same animal.

Family	Genus and species ^{1/}	Age	Pelt thickness (Cm)	Fur thickness (Cm)	Conductance (W · M ⁻² · °C ⁻¹)
Mustelidae	<u>Enhydra lutris</u>	P	2.2	1.9	7
	" "	A	1.1	0.7	26
	" " ^{2/}	A	2.1	1.7	23
	" "	A	1.3	0.9	22
	" "	A	2.6	2.3	22
Phocidae	<u>Erignathus barbatus</u>	A	1.2	-	27
	<u>Phoca groenlandica</u>	A	0.4	-	52
	<u>Lobodon carcinophagus</u>	A	0.8	-	37
	<u>Hydrurga leptonyx</u>	SA	0.6	-	34
	<u>Leptonychotes weddelli</u>	P ^{3/}	1.5	0.4	28
	" "	P ^{3/}	1.5	0.4	28
Otariidae	<u>Zalophus californianus</u>	A	0.4	-	58
	<u>Callorhinus ursinus</u>	SA	1.0	0.5	26
	" "	SA	0.8	0.4	26
	" "	P	1.2	0.3	40
Odobenidae	<u>Odobenus rosmarus</u>	SA	2.5	-	15

^{1/} In accordance with the Marine Mammal Commission nomenclature list.

^{2/} Same fur sample as previous measurements but combed and fluffed.

^{3/} Pup long-haired fur (lanugo).

was computed as the heat flow per unit area divided by the difference in plate and water temperatures, and it was expressed in $W \cdot M^{-2} \cdot ^\circ C^{-1}$. In order to achieve thermal stability a run lasted from 8 to 12 hours.

After the initial run the pelts were "squeezed" dry and 10 to 20 ml (.02 ml x cm^{-2}) of Prudhoe Bay Crude oil was painted into the fur, except for the sea otter pup pelt which was thoroughly drenched. The paint strokes ran with the grain on the fur. The pelt was left sitting for about 5 min. and then rinsed with fresh water for 15 sec. It was then placed in the water bath.

Pelts were cleaned in a series of washings and rinsings, in which a brisk rubbing was done to scrub out the oil. The pelt was then blotted dry with paper towels. Afterwards the fur was blown dry at room temperature and placed in the water bath.

B. Diving effort

A depth-time recording instrument was designed for studying the diving behavior of the fur seal. The instrument consists of two basic systems; (1) the film transport system; and (2) the pressure transducer package. Photographic film is loaded on a spool, and passes over guide surfaces to an uptake spool. A dc timing motor with accompanying gear train are attached to and drive the uptake spool. Various tensioning devices are built into the film transport system. The pressure transducer is of the helical Bourdon-tube type. The time-depth recorder is coupled to the outside environment only through this pressure transducer. As the outside pressure changes the pressure transducer moves a pointer through an arc which is proportional to the change in pressure. An LED (Light-Emitting-Diode) is fixed to the end of the pointer. Its light is masked with the exception of a 0.004 mm hole immediately above the photographic film. Orienting the plane of the arc perpendicular to the direction of the film transport and parallel to the film plane, the movements of the LED are recorded on the unexposed film which passes beneath it in a chart-like configuration. Placing transparent overlays on the exposed and developed film, the time and depth bases can be read.

The instrument is housed in an aluminum cylinder measuring 19.8 by 5.3 cm, weighing 709 grams (with film and batteries) in air, with time resolution of 30 seconds and depth resolution to 3 meters. Recording time, using Kodak bomb burst film #2476 is 7 days. The instrument is attached to the animal by means of a nylon harness. In 1975 this instrument differed in that pressure-sensitive paper was used in place of photographic film, and a stylus replaced the LED.

In the 1975 field season, three lactating fur seals were equipped with dummy depth-time recorders, and five were fitted with functional recorders. In the 1976 field season, nine depth-time recorders were sent out, six on females and three on subadult males. Two of the females had been oiled prior to release. Oiling was accomplished by brushing approximately 100-180 ml of Prudhoe Bay crude oil onto the pelt with a paint brush. Only the pelage posterior to the neck and dorsal to the

mid-sagittal plane, that is about 30% of the total surface area of the body (including the flippers), was coated. This coated pelt could not be visually distinguished from a noncoated pelt.

As a control for the effects of the harness and instrument on duration of the feeding cycle, eight females were marked by clipping and bleaching numbers in their pelt, and their departures from and returns to the rookery were observed from late May through mid-October. Data were collected directly on computer code sheets regarding the hour of day, location, and behavior of each female several times per day.

C. Metabolic rates during immersion

Fur seals were held for several months at Scripps, and for several weeks on St. George Island. Those at Scripps were two females and one male that were 3 years old, and one female that was 2 years old. The five males used on St. George Island were all 2 to 3 years old. During the metabolic studies their weights did not vary more than 10%.

The St. George fur seals were weighed dry on a platform beam balance just prior to the metabolic run. The Scripps fur seals were weighed wet on a spring scale. Soon after weighing all animals were placed in the metabolic test chamber specially designed for these studies. The chamber, which was 151 cm long, 84 cm wide, 84 cm deep, and which held about 1400 liters of fresh water, was constructed of styrofoam sheets (about 95 cm thick) which were coated with wood and fiber glass for strength. The lid of the chamber was fastened tightly over a neoprene gasket and the box was filled with fresh water to 2 cm above the lip of a 60 cm diameter lucite dome projecting above the chamber top. Opposed ports in the lower portion of the dome functioned as intake and exhaust for air drawn through this air space. The rate of air flow was measured with a Wright respirometer. Humidity was determined with a dial hygrometer, and barometric pressure was measured with an aneroid barometer.

Air temperature and water temperature of the box were measured with thermocouple probes, one of which was placed at the mouth of the air intake and the other on the upper portion of the chamber wall about 2 cm below the lid. Water was slowly, constantly and uniformly stirred in the box by means of a series of outlet and inlet manifolds. Water temperature usually varied less than 0.5°C. Readout of the thermocouple probes was with a Bailey Batt 4 coupled to a digital voltmeter which made possible the reading of temperatures to 0.1°C.

Deep body temperatures were obtained by feeding the animals an encapsulated radio transmitter, the pulse rate of which varied with temperature. The signal was received on a standard AM radio and the pulses were counted with a hand counter and converted to temperature readings.

A sample of the exhaust from the dome was drawn through a glass "U" tube filled with drierite, two "U" tubes containing CO₂ absorber, and a final "U" tube of drierite before entering the sensing cell of an AEI O₂ analyzer. In those experiments with oiled or washed animals a "U" tube of 4-12 mesh activated charcoal preceded the first drierite "U" tube. This material absorbed all oil fumes, and it was changed after every 30-minute run.

The AEI O₂ analyzer signal was continuously recorded on a 25 cm chart recorder adjusted to record from 19-21% full scale. At 30-minute intervals the inlet air sample was checked, and the instrument's reference cell adjusted if it had drifted. Once a session the analyzer was calibrated by flushing the sensing cell with outside air and then reducing its pressure a known amount and recording the drop on the chart paper.

All runs started at 1900 and ended by 0700 hours. During the runs all lights in the laboratory were turned out. An open window next to the chamber provided light and fresh air.

The plotted curves of O₂ concentration changes were smoothed by eye and the difference in O₂ concentration from the intake and exhaust were determined every minute. The averages for 30-minute intervals were collated. Appropriate factors for correction of gas volumes to STPD were incorporated into a computer program, and oxygen consumption rates were calculated on a Data General Corporation, Nova 2, computer.

Fur seals were oiled by first putting them lightly to sleep with gas anesthesia (Halothane). This was accomplished by placing the seal's head in a plastic mask and flowing gas through the mask at a known concentration. Gas flow rate and concentration were maintained with a Bird Mk 5 respirator and fluotéc vaporizer. Prudhoe Bay crude oil was then brushed over the back of the animal from the base of the skull to the tail. About 100 ml of oil was brushed onto the fur. The rest of the animal was left oil-free. This process took no more than 15 minutes. After oiling the animals were permitted to swim in a clean pool of sea water for several hours before the night's metabolic test.

One day following the metabolic test the animals were cleaned. The cleaning took 30-45 minutes so that the animals were anesthetized, intubated, and maintained under light anesthesia. Animal RF was cleaned with ShellSol 70, an oil solvent, and animal YN was cleaned with Basic H detergent. Animal R.B. was not cleaned.

The surface area (SA) of one 2-year-old male, taken in the commercial harvest, was determined by removing the pelt and one fore and one hind flipper. These parts were laid out on a stiff sheet of drawing plastic and the slightly stretched flippers were outlined. A planimeter was used to determine the area of these drawings.

VI. Results

A. Thermal conductance studies

The fur of the three long-haired animals that we studied, the Weddell seal pup, fur seal, and sea otter, had quite different appearances from each other. The Weddell seal was a woolly, rather disheveled looking fur that wetted rapidly when immersed. The sea otter pelt had a woolly, loose appearance superficially, but had a very dense underfur or wool. Kenyon (1969) cites an examination of the fur by Scheffer in which hair densities of 101,000 fibers $\cdot \text{cm}^{-2}$ were estimated. The fur did not lie as flat as that of the fur seal, but it did seem more water repellent.

The fur seal pelt was a dense, smooth, orderly looking fur that was a water-resistant barrier. Water penetrated slowly into the underfur. The wetting seemed to be hastened if the guard hairs were parted. We found that if the fur were pressed hard and the pressure advanced with the grain of the fur, water was forced out and the underfur appeared dry. After watching fur seals groom we suspect that process may achieve similar results.

The texture and density of the fur seal pelt is discussed in Scheffer's monograph (1962). The hair density of the mature pelt is 57,000 hairs $\cdot \text{cm}^{-2}$, and that of the pup fur was 9,000 hairs or fibers $\cdot \text{cm}^{-2}$. He notes that 75 to 80% of the pup fur was underhair which is coarser than underfur or wool of older animals. Scheffer also noted that when it rains the pups soak to the skin. Considering these differences in physical characteristics the greater (C) of the pup pelt compared to that of the subadults is expected (Table 1).

Of all the sea mammal pelts tested the best insulator, or the one in which (C) was the least was that of the sea otter pup, Enhydra lutris (Table 1). Its conductance value was $7 \text{ W} \cdot \text{M}^{-2} \cdot ^\circ\text{C}^{-1}$. The next lowest (C) was the skin of the walrus, Odobenus rosmarus. Several species had about the same (C) values of between $20\text{-}30 \text{ W} \cdot \text{M}^{-2} \cdot ^\circ\text{C}^{-1}$. These were the adult sea otters, subadult fur seals, Callorhinus ursinus, Weddell seal pups, Leptonychotes weddelli, and the bearded seal, Erignathus barbatus. The highest (C) was recorded from the California sea lion, Zalophus californianus, pelt of $58 \text{ W} \cdot \text{M}^{-2} \cdot ^\circ\text{C}^{-1}$.

The most profound effects of oiling were on the Enhydra pup and the subadult Callorhinus in which (C) increased 2.1, and 1.7 to 2.0 times, respectively (Table 2).

The (C) of the naturally oiled Enhydra, an animal that apparently swam through an oil slick and whose partially oiled carcass was later found, was nearly the same as the pelt we oiled with Prudhoe Bay Crude. However, the density of the two oils was different. The Prudhoe Bay Crude was much lighter, was not tarry and did not clump the fur. Oil caused no change in (C) of Erignathus or Zalophus.

Table 2. Thermal conductance of oiled and immersed pelts.
 Symbols are the same as Table 1.

Subject	Age	Pelt thickness (Cm)	Conductance ($W \cdot M^{-2} \cdot ^\circ C^{-1}$)	Multiple of control
<u>E. lutris</u>	P	1.1	15	2.1
" " <u>1/</u>	A	-	26	-
" " <u>2/</u>	A	-	29	1.3
" " <u>2/</u>	A	-	26	1.1
<u>E. barbatus</u>	A	1.2	27	1.0
<u>L. weddelli</u>	P	0.9	42	1.5
<u>Z. californianus</u>	A	0.4	56	1.0
<u>C. ursinus</u>	SA	1.0	53	2.0
" "	SA	0.8	45	1.7
" "	P	0.7	54	1.4

1/ Naturally oiled with heavy crude.

2/ Compared to combed and fluffed fur.

The most improvement due to cleaning was in Callorhinus, but the(C) was still 1.5 x greater than the control (Table 3). However, the pup Callorhinus pelt had a lower(C) after cleaning than the control. This was probably because the loft due to fluffing of the fur after cleaning and drying was better in the cleaned than in the control pelt. The(C) of the adult Enhydra pelt was about the same as the control. The pup sea otter pelt deteriorated and no measurements were possible. There was no change in Zalophus.

B. Diving effort

In 1975, all the dummy recorders, and four of the five functional dive recorders were recovered. Almost 3,000 dives were recorded in 608 hours of continuous recording from these instruments. These data have been published and appear as Appendix I.

In 1976, three of the nine recorders were recovered, and only one of the recorders contained a usable record. Neither of the two oiled animals returned to the rookery, and records of their diving performance, on which a determination of the effects of oil fouling was to be based, were not recovered. Visual inspection of the one record recovered did not show any significant deviations from the other controls, and therefore the data obtained from this recorder were not analyzed for this report.

Eighty-eight different feeding excursions were quantified for eight females which were visually marked but not instrumented. Figure 1 shows that when the duration of feeding cycle (in days spent at sea) is plotted against time (with day of parturition as day zero) a straight line function results with a slope of $b = 0.39$. This slope is significantly different from zero, indicating that length of the feeding cycle increases throughout the season.

C. Metabolic measurements

Six different normal (control) fur seals were tested once each at water temperatures of 6.5°C (Table 4). Three of these seals were subsequently oiled and were measured again at the same water temperature; two of the three oiled seals were tested a third time after they had been washed with solvents. Mean oxygen consumption for oiled and control animals was significantly different (paired t test means \leq controls, $P < .025$).

One animal, RB, was not cleaned after oiling. The average rate of oxygen consumption ($\dot{V}O_2$) for the metabolic test conducted the day of the oiling was 36.3 ml O_2 /min · kg in 6.5°C water. Eleven days later a second test was conducted, and $\dot{V}O_2$ was measured as 39.7 ml O_2 /min · kg. Fifteen days later a third test was conducted in 10°C water and the $\dot{V}O_2$ measured 33.2 ml O_2 min · kg. It should be noted that this animal experienced an extremely heavy loss of hair and underfur between the second and third tests.

Animals spent more time resting during the pre-oiling trial than in either the oiled or washed trials. Animal RB was an exception (Table 5).

Table 3. Thermal conductance of cleaned and immersed pelts. Cleaning agent was Basic-H detergent*. Symbols the same as Table 1.

Subject	Age	Pelt Thickness (Cm)	Conductance ($W \cdot M^{-2} \cdot ^\circ C^{-1}$)	Multiple of Control
<u>E. lutris</u>	A	1.9	21	0.9**
" "	A	2.6	20	0.9**
<u>Z. californianus</u>	A	0.4	56	1.0
<u>C. ursinus</u>	SA	1.0	38	1.5
" "	SA	0.9	40	1.5
" "	P	1.4	34	0.9

* Shakelee products.

** Compared to combed and fluffed fur.

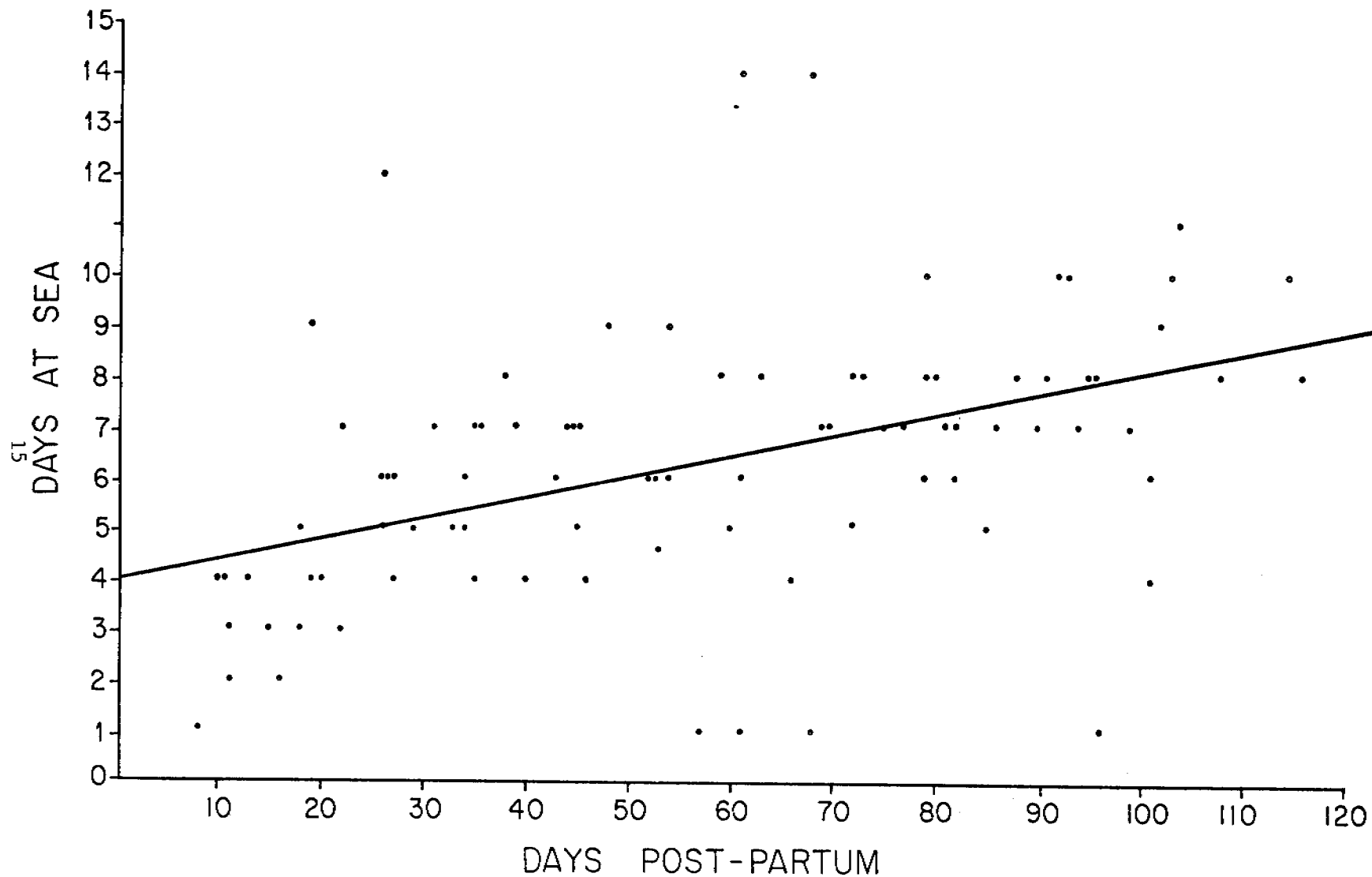


Figure 1. Duration of feeding cycles of eight marked Callorhinus females at St. George Island, 1976. Each data point represents one completed cycle. N=88 observations.

Table 4. Average $\dot{V}O_2$ for night run of control, oiled and washed fur seals at 6-10°C water temperature

Subject	Control			Oiled			Washed		
	$\dot{V}O_2$ ml O ₂ /kg·min	R	s.d.	$\dot{V}O_2$ ml O ₂ /kg·min	R	s.d.	$\dot{V}O_2$ ml O ₂ /kg·min	R	s.d.
<u>Scripps 6-10°C</u>									
Theophalus	20.5	(32.0-14.3)	5.49						
<u>St. George 6°C</u>									
R.F.	25.0	(28.9-18.0)	3.2	43.4	(50.9-35.2)	4.7	50.0	(65-38)	8.7
Y.N.	20.4	(24.3-15.7)	2.5	31.1	(55.8-24.5)	9.9	38.1	(57-26)	11.8
T.C.	31.2	(44.6-24.0)	6.4						
R.B.	23.8	(31.0-18.0)	4.5	36.3	(51.2-25.2)	10.0	37.8	(53.4-28.7)	8.1
L.F.	26.9	(32.5-19.1)	3.9						

Table 5. Percent time spent resting and grooming, $\dot{V}O_2$ of resting and grooming in control oiled and washed fur seals at 6°C

Subject	Control				Oiled				Washed			
	% rest	$\dot{V}O_2$	% groom	$\dot{V}O_2$	% rest	$\dot{V}O_2$	% groom	$\dot{V}O_2$	% rest	$\dot{V}O_2$	% groom	$\dot{V}O_2$
R.F.	57	22	43	32	36	31	64	49	38	40	62	64
Y.N.	92	18	8	32	70	26	30	49	52	27	48	49
T.C.	41	27	59	41								
R.B.	52	21	48	29	59	27	41	50	64	31	36	53
L.F.	72	25	28	43								

Subject	% rest	$\dot{V}O_2$		% grooming	$\dot{V}O_2$	
		ml	O ₂ /kg.min		ml	O ₂ /kg.min
Theophalus*	77		16	23		27

*Scripps animal.

$\dot{V}O_2$ during the specific activities of resting or grooming was extracted from the continuously recorded data of the metabolic run, and is presented in Table 5 also. Grooming $\dot{V}O_2$ is at least half again higher than resting $\dot{V}O_2$, even though the type of rest measured during these runs was usually quite fitful and consequently higher than if the animals had slept soundly.

A number of runs were made at water temperatures higher than 6°C. The results are plotted in Figure 2. There is a tendency for the $\dot{V}O_2$ of the control group to decline as the water temperature rises. The curve seems to be leveling off at about 20° to 25°C. The $\dot{V}O_2$ of the animals held at Scripps tend to be lower than for the animals tested at St. George Island. The $\dot{V}O_2$ of oiled RB and washed YN were higher than for other animals at all temperatures.

The surface area of the one 20.4 kg 2-year-old fur seal male was 0.53 m². Of this total area, 27% was attributable to the rear flippers, and 19% to the foreflippers.

VII. Discussion

A. Thermal conductance

The various pelts studied might be grouped into three major categories: (1) the sparsely furred, wettable pelts of walrus, sea lions, and seals, which depend wholly upon a thick blubber layer for insulation rather than upon fur. (2) The fur seal pelt which is a dense fur that may gradually wet unless groomed. This fur is probably the sole insulation even though some subcutaneous fat is present. (3) The sea otter which has no subcutaneous fat and the pelage is the barrier to heat loss. With this grouping in mind, Figure 3 summarizes the effects of oiling and cleaning of adult sea otter and sea lion and subadult fur seal pelts.

Thermal conductance is very high in the sea lion pelt. Oiling and washing do not alter the insulative properties much. These results are consistent with the nature of their pelage. Such an effect would be similar in all those species in which blubber was the primary insulator.

The increase in (C) in the sea otter and especially the fur seal after oiling (Fig. 3, Table 2) stems from a serious degradation of the fur. If the animals are unable to reverse this effect by some means, such as grooming, they probably could not endure cold water immersion long. Washing the fur, particularly that of the fur seal does not decrease (C) to the extent that maintenance costs are reduced more than halfway back to control levels.

The pelt of the nearly hairless walrus was a poor conductor because the skin was so thick, nearly 5 cm. In the live animal any blood flowing through the skin would increase its (C). No doubt the most important thermal barrier would be the thick subcutaneous blubber layer.

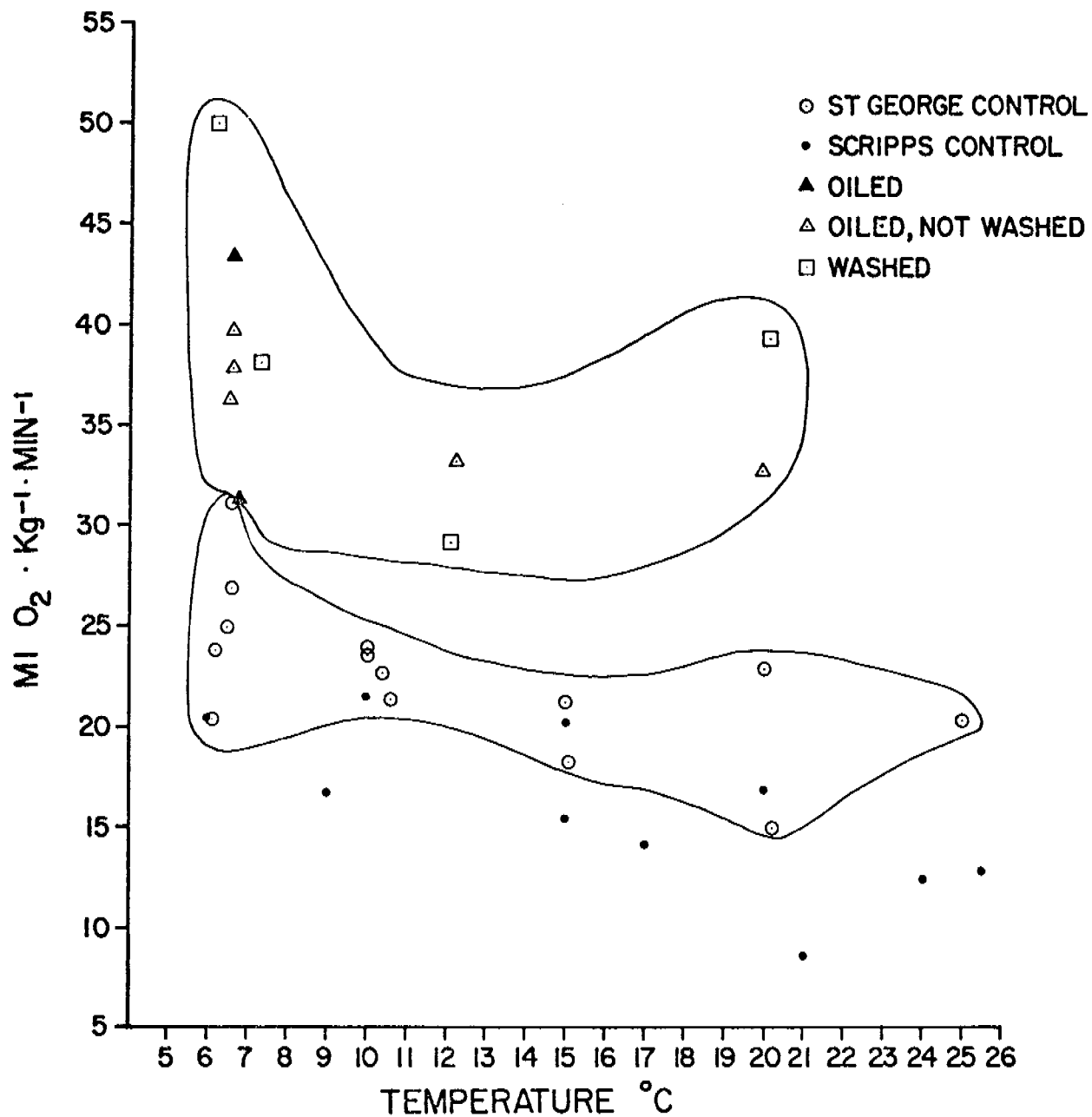


Figure 2. Overall $\dot{V}O_2$ averages for fur seals tested at different water temperatures.

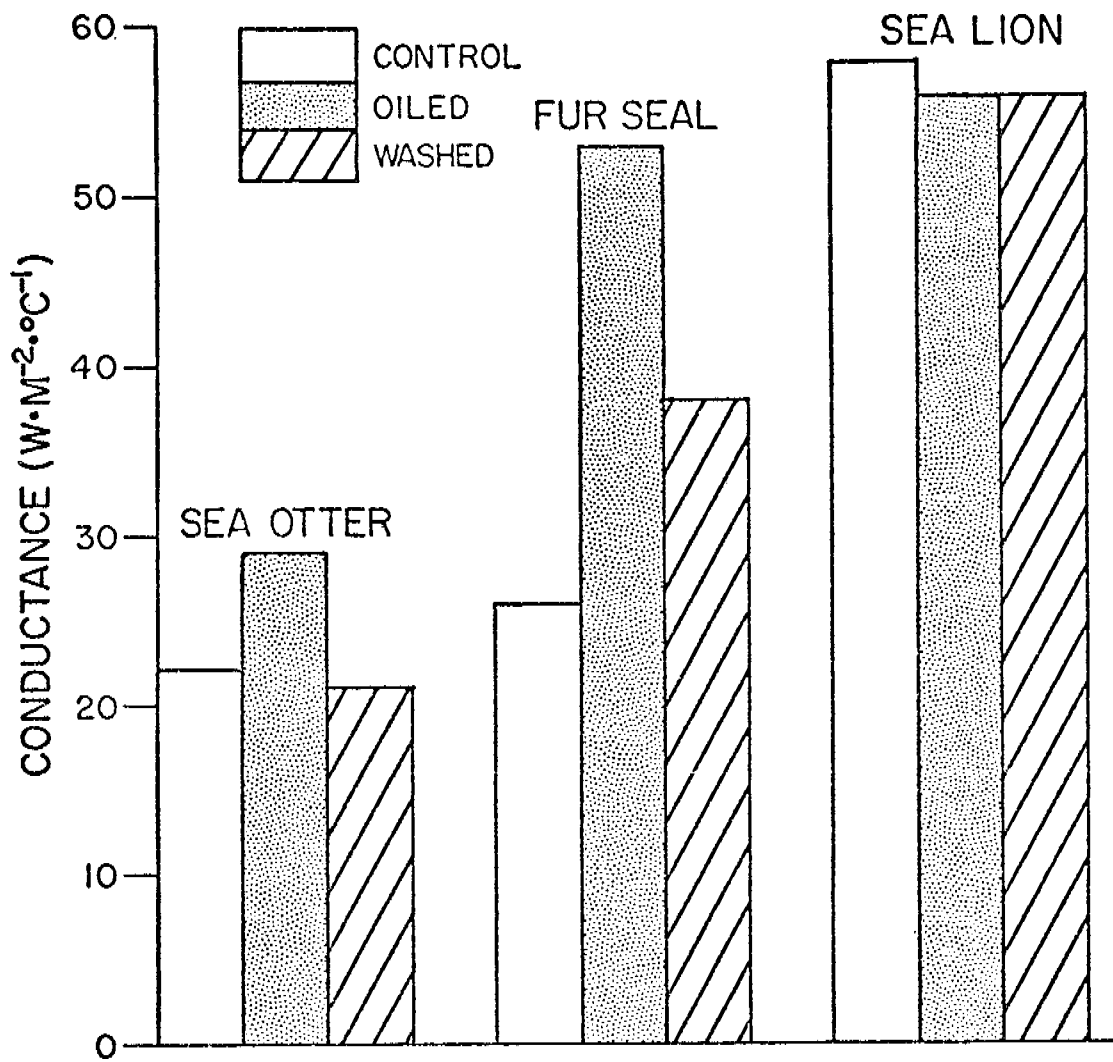


Figure 3. Thermal conductance of sea otter, fur seal, and sea lion pelts during normal immersion, after oiling, and after cleaning.

The (C) through the skin and pelage of the earless seals (phocids) and the sea lion were high compared with the sea otter and fur seals. This is not surprising considering that these species possess a thick, sub-cutaneous blubber layer which serves as the main barrier to heat loss. It was found previously that (C) through skin, fur, and 4 to 5 cm of blubber was about $3.5 \text{ W} \cdot \text{M}^{-2} \cdot ^\circ\text{C}^{-1}$ in the ringed seal, *P. hispida* (Scholander et al., 1950). This is a tenth of the (C) we measured in the skin and fur only of seals. However, as we mentioned earlier, Hart and Irving (1959) determined that blubber in the live animal is not so effective an insulator. (C) is about 50% higher than the value previously determined by Scholander et al. (1950).

For a short time after birth all species of polar seal pups possess a long-haired pelt called lanugo. This coat functions as the main barrier to heat loss until a thick blubber layer develops as the pup nurses. Until the blubber layer develops the pups usually do not enter the water. If they were to do so the pelt quite likely would wet through and there would be a large heat loss such as that which we measured of $28 \text{ W} \cdot \text{M}^{-2} \cdot ^\circ\text{C}^{-1}$ for Weddell seals. Considering that the thermal gradient, that is the difference between the body temperature and the sea water temperature, would be about 37°C , this loss represents a total output of over $1,000 \text{ W} \cdot \text{M}^{-2}$. Estimating that a 27-kg pup has a surface area of about 0.93 M^2 (Meek's surface area equation $\text{SA} = 10\text{W}^{0.67}$; Drent and Stonehouse, 1971) the total heat loss would be 930 W. This is about 12 times the predicted heat production based on body weight (Hart and Irving, 1959). The newborn pups probably cannot sustain such a high metabolic rate and thus they could not tolerate immersion long.

Thermal conductivity results seem unrealistically high for control pelts of the sea otter and fur seal. Based on calculations similar to those for the Weddell seal the (C) of the pelt is more than 5 times greater than it should be. Apparently some important property of the pelt is lost after removal from the animal. The important missing element may be grooming. Without this activity water may leak into the fur, and is not removed. Thus, any agent that increases the watability of the fur will increase (C) of the pelt.

B. Diving effort

This study has produced baseline data on diving effort in lactating females carrying a recording device. It has also produced data on the length of feeding cycles of uninstrumented females which indicate that wearing the harness and instrument somewhat increased the length of the feeding cycle. We cannot determine from this study whether the pattern in diving depth was altered by presence of the harness. Since no diving records were retrieved from oiled animals, we can make no comparisons between experimental and control groups.

C. Metabolic measurements

The lowest $\dot{V}O_2$ which was achieved by animal YN, may be due to behavior. This seal held itself up in the dome of the test chamber for much of the time and it was scored as "resting." In this position 40-60% of the body was out of water. After oiling animal RB also assumed this same position when resting. The animals are behaviorally thermoregulating by lifting themselves out of cold water into an air environment of 10-15°C. This may explain why animal RB's percent of time resting actually went up after oiling (Table 5). However, the differences between $\dot{V}O_2$ before and after oiling and washing are distinct even though two of the animals made some advantageous behavioral changes while in the metabolic chamber. This increase is substantial even though the oiling was light (60-100 ml of oil) and though only 30 to 40% of the pelage was coated. Two weeks after oiling animal RB, the one animal not cleaned, still showed a heat production as high as the first day after oiling.

There were some other noteworthy behavioral changes. For a few days after oiling of animal RB and after oiling and washing of animal YN, they swam with their backs arched and out of the water. This resulted in a peculiar swimming pattern. Animal RF rarely volunteered to enter the water after oiling and cleaning. It was necessary, therefore, to feed him in the dry pen where he appeared ravenous at every meal.

Neither cleaning agent (Basic H detergent, or ShelSol 70 solvent) reduced the heat loss that was induced by the oil. Indeed, the solvent seemed to have worsened the situation.

The animals held at Scripps had consistently lower $\dot{V}O_2$ values than the St. George seals, even though they had spent the previous 8-10 months at water temperatures of 10-20°C rather than the normal 3-6°C. Much of this difference must be attributable to the previous months of training and close association with humans of the Scripps animals.

The minimum resting $\dot{V}O_2$'s measured during a 30-minute period at 6°C were 2.5 times greater for the Scripps animals and 2.9 to 4.7 times greater for the St. George seals than predicted for terrestrial mammals of similar size (Kleiber, 1961). The $\dot{V}O_2$'s seemed to drop as the water temperature was raised (Fig. 2). The lowest $\dot{V}O_2$ recorded was for animal Louise at a water temperature of 20°C. The overall $\dot{V}O_2$ average for the total metabolic run in which this measure occurred was only 30% higher than predicted by the standard metabolic equation.

Resting metabolic rates during immersion which were 2 to 3 times greater than predicted for other mammals have been noted by others (Irving and Hart, 1957; Miller et al., 1976; Morrison et al., 1974). Similarly elevated metabolic rates have also been noted in immersed penguins (Kooyman et al., 1976).

If some assumptions are made the total (C) of the animals can be estimated in order to compare these results with the results of flensed pelts. The assumptions are: (1) the respiratory quotient (R.Q.) of the fur seal is about 0.8; (2) at an R.Q. of 0.8 one L. of O₂ consumed produces 4.6 kcal of heat; (3) heat lost through evaporation and respiration is insignificant because the air above the immersed seal is cool and saturated; (4) the surface area of the measured fur seal does not match Meek's equation $SA = 10W^{0.67}$, and we are justified in changing the constant 10 to 6.8 so that we may calculate the SA of other fur seals.

The mean C of three controls at 6°C using the lowest $\dot{V}O_2$ for a 30-minute period was $8 W \cdot M^{-2} \cdot ^\circ C$ and $11 W \cdot M^{-2} \cdot ^\circ C$ for three oiled animals. If we consider that half the total SA is due to the flippers, and we assume that there is no loss of heat through the flippers, then (C) doubles in each instance to 16 and $22 W \cdot M^{-2} \cdot ^\circ C$. In this case (C) is surprisingly high. The (C) of terrestrial mammals in air is about $1 W \cdot M^{-2} \cdot ^\circ C$ and in the immersed Adelle penguin it is about $6 W \cdot M^{-2} \cdot ^\circ C$ (Kooyman et al., 1976).

We are handicapped by not knowing (C) of the flippers. Furthermore, if there is some heat loss in the flippers of controls which is reduced or stopped during the cold stress induced by oiling, the (C) through the pelts of oiled animals would be even greater than the results indicate.

With all the pitfalls in such estimates we cautiously note that (C) estimates of control animals of $16 W/m^2 \cdot ^\circ C$ is 60% of the pelt (C) measurements (Table 1). In oiled animals the (C) of the oiled section of the pelt could be as high as $34 W/m^2 \cdot ^\circ C$ if we assume only one-third of the pelt is oiled, that the overall average (C) is $22 W/m^2 \cdot ^\circ C$, and that (C) of nonoiled portions is $16 W/m^2 \cdot ^\circ C$. This is 70% of the values directly measured from hides with a heat flow transducer (Table 2).

Despite these apparently high losses of heat we never noted a decline in the body temperature during the five oiled or washed runs in which body temperature was measured.

VIII. Conclusions

A. Thermal conductance

The method of determining heat flow through pelts that was described in this study is an uncomplicated way of obtaining relative information about conductance. A shortcoming of this technique is that it tells nothing about what effects the behavior, especially grooming, of the animal may have on conductance. Therefore, the relative effects of oiling and cleansing may be substantially different in the living animals.

A mild oiling of the pelt with a light crude oil does not increase heat loss during immersion significantly in seals and sea lions. The(C)of the pelts of the otter and fur seal were unrealistically high even in the controls. This is suspected to be due to loss of water repellency for some unknown reason. These results emphasize the importance of pelt integrity and the calamitous effects of its loss. Oiling increases the(C) of the pelt presumably by reducing water repellency. The consequences would be gravely serious for these species if they were not able to overcome quickly the oiling effects. Removing the oil from the fur with a detergent does not improve the quality much.

B. Diving effort

Since the oiled seals failed to return to land with the depth-time recorders, we can draw no conclusions about the effects of oil contamination on diving effort, depth, or duration.

C. Metabolic tests

Heat production of fur seals while immersed is exceptionally high in controls. The added burden of oiling, which raises heat production at least another 50% and probably much more if the oiling were extensive, makes it questionable that oiled seals could sustain themselves long if they remained in cold water. In due course they would probably experience exhaustion, hypothermia, and death. The reluctance of oiled animals to enter the water to eat while in the holding pens supports this conclusion. Furthermore, after at least 2 weeks the oiling effects on the thermal properties of the coat still persist.

IX. Needs for further study

Fruitful areas of continued study on determining or helping to reduce the impact of oil on fur seals are the following:

1. Develop a technique to remotely identify whether a fur seal has been oiled, both when it is in and out of the water.
2. Assess the long term effects of oiling on fur seals. Determine how long an elevated heat production will persist in an immersed animal. Determine what would be the final outcome of young males after oiling, i.e., how long would they remain ashore before going to sea, how long would their at-sea period last, and what weight losses would they experience at this time?
3. Search for cleaning agents that would restore the pelt to its original condition after contact with oil.
4. Obtain more detailed quantitative information on the degree and areas of heat loss over the body. Particularly, how much heat is lost through the flippers under varying conditions of immersion?

X Summary of 4th quarter operations

See Quarterly report for period 7/1/76 to 9/30/76.

LITERATURE CITED

- BRYDEN, M. M.
1964. Insulative capacity of the subcutaneous fat of the southern elephant seal. *Nature*, 203: 1299-1300.
- DAVIS, J. E., AND S. S. ANDERSON.
1976. Effects of oil pollution on breeding gray seals. *Mar. Pollut. Bull.* 7(6): 115-118.
- DRENT, R. H., AND B. STONEHOUSE.
1971. Thermoregulatory responses of the Peruvian penguin Spheniscus humboldti. *Comp. Biochem. Physiol.* 40A: 689-710.
- FRISCH, J., N. A. ØRITSLAND, AND J. KROG.
1974. Insulation of furs in water. *Comp. Biochem. Physiol.* 47A: 403-410.
- HART, J. S., AND L. IRVING.
1959. The energetics of harbor seals in air and in water with special consideration of seasonal changes. *Can. J. Zool.* 37: 447-457.
- IRVING, L., AND J. S. HART.
1957. The metabolism and insulation of seals as bare-skinned mammals in cold water. *Can. J. Zool.* 35: 497-511.
- IVERSON, J. A., AND J. KROG.
1973. Heat production and body surface area in seals and sea otters. *Norwegian J. Zool.* 21: 51-54.
- KENYON, K. W.
1969. The sea otter in the eastern Pacific Ocean. *North Amer. Fauna*, #68, 352 p.
- KLEIBER, M.
1961. *The fire of life; an introduction to animal energetics.* Wiley & Sons, New York. 454 p.
- KOONYMAN, G. L., R. L. GENTRY, W. P. BERGMAN, AND H. T. HAMMEL.
1976. Heat loss in penguins during immersion and compression. *Comp. Biochem. Physiol.* 54A: 75-80.
- McEWAN, E. H., N. AITCHISON, AND P. E. WHITEHEAD.
1974. Energy metabolism of oiled muskrats. *Can. J. Zool.* 52: 1057-1062.
- MILLER, K., M. ROSEMANN, AND P. MORRISON.
1976. Oxygen uptake and temperature regulation of young harbor seals (Phoca vitulina richardi) in water. *Comp. Biochem. Physiol.* 54A: 105-107.

- MORRISON, P., M. ROSEMAN, AND J. A. ESTES.
1974. Metabolism and thermoregulation in the sea otter. *Physiol. Zool.* 47: 218-229.
- SCHEFFER, V. B.
1962. Pelage and surface topography of the northern fur seal. *North Amer. Fauna*, #64, 206 p.
- SCHOLANDER, P. F., V. WATERS, R. HOCK, AND L. IRVING.
1950. Body insulation of some arctic and tropical mammals and birds. *Biol. Bull. Mar. Biol. Lab. Woods Hole*, 99(2): 225-236.
- SMITH, T. G., AND J. R. GERACI.
1975. The effect of contact and ingestion of crude oil on ringed seals of the Beaufort Sea. *Beaufort Sea Tech. Rept.* #5.
- KOOSMAN, G. L., R. L. GENTRY and D. L. URQUHART.
30 July 1976. Northern Fur Seal Diving Behavior: A New Approach to Its Study. *Science* 193: 411-412.

QUARTERLY REPORT

Contract #
Research Units #72, 331, 334
Report Period October 1, 1976 - December 30, 1976
Number of Pages 10

ACUTE AND CHRONIC TOXICITY, UPTAKE, AND DEPURATION,
AND SUBLETHAL METABOLIC RESPONSE OF ALASKAN MARINE ORGANISMS
TO PETROLEUM HYDROCARBONS

Stanley D. Rice

John F. Karinen

Northwest and Alaska Fisheries Center Auke Bay Fisheries Laboratory
National Marine Fisheries Service, NOAA
P. O. Box 155, Auke Bay, Alaska 99821

December 15, 1976

I. Task Objectives

A. Objectives, experimental designs, manpower allocations.

1. Determine the acute toxicity of the water-soluble fraction (WSF) of crude oil (1.3 man years):
 - a. Continue experiments with species not tested previously. Static tests will be phased out and flow-through tests phased in.
 - b. Continue experiments with larvae of species not tested previously. Tests will be static. Emphasis will be on intertidal species, such as mussels, barnacles, snails, and sea urchins.
2. Determine which components of oil account for toxicity (3.25 man years):
 - a. Assess the toxicity role of phenols and heterocycles by determining quantities in oil and WSF's, and determining the acute toxicity to three species of the major compounds found in the WSF. Toxicity tests will be static.
 - b. Determine toxicity of a natural WSF and a synthetic WSF to three species with flow-through tests to determine whether the synthetic WSF accounts for all the toxicity. Compounds that are difficult to analyze for, or that may be in trace quantities, can probably be eliminated as major components responsible for toxicity. Future tests will be with altered synthetic WSF's.
 - c. Determine time-dependent toxicity recovery curves with mono- and di-nuclear aromatics to three species with flow-through tests. Tests will be with individual compounds and with combined mixtures. This will be a beginning effort to assess the relative toxicity importance of mono- and di-nuclear aromatics.
3. Determine the long-term effects of WSF's on growth and gonad histology of three species under flow-through conditions. Tests will be 30 to 90 days long. Tissue burden levels of hydrocarbons will be determined (see 6 b). (1.5 man years).
4. Determine the effects of short-term exposures to WSF's on the survival of tagged marine organisms that are returned to the environment. Two species (limpets and mussels) will be tagged, exposed, and returned to their "home" spots. Their survival will be monitored for up to 3 months. Tests with pure aromatic fractions will also be used. Preliminary tests have confirmed this study's feasibility. Survival in the environment will be compared to survival of laboratory-held organisms. (1.3 man years).
5. Determine the effects of WSF's of oil and pure aromatics on the metabolic rate of untested invertebrate species and on larvae of shrimp and crabs. A Gilson respirometer will be used with larvae, and a flow-through set up for larger invertebrates. Oxygen uptake will be monitored by a blood-gas analyzer,

and heart rate may be measured in some species. Experiments will be coordinated with uptake-depuration experiments (tissue burden experiments) for the assessment of the animal's capacity to oil uptake. (2 man years).

6. Determine the tissue burden of several species exposed to oil, and their ability to rid themselves of hydrocarbons. Analysis will be by NOAA National Analytical Laboratory. (1 man years).

a. Larvae will be tested with WSF's spiked with labelled isotopes. The form of the isotope (parent hydrocarbon versus metabolite) will be checked by the method of Roubal et al. (1976), no determination of metabolite identity will be attempted. Eggs will also be tested.

b. The tissue burden of animals exposed in the long-term flow-through tests (see 3). Mono- and dinuclear aromatic hydrocarbon concentrations will be determined by two GC runs per sample, and verified by two GC-MS determinations per series of 12.

c. Additional uptake-depuration experiments will be conducted on three additional species using flow-through exposures. Choice of species will depend on results of experiments in progress.

7. Determine the pathway and rate of elimination of labelled mono- and di-nuclear aromatics in fish and crabs; identify the labelled compounds as "parent" or "metabolite". Gills and excretory organs will be treated separately. Isotopes will be introduced via a WSF. Isotope form (parent hydrocarbon introduced vs. metabolite) will be determined using the method of Roubal et al. (1976). (0.4 man years).

8. Determine the burrowing behavior of three species (Dungeness crabs, Macoma clams, and polychaete worms) when exposed to varying levels of contaminated sediments. Doses will be determined on a volume-added basis and by GC. (0.4 man years).

9. Determine the fate and distribution of trace metal-organic hydrocarbon (e.g. naphthols) complexes in the WSF of crude oils, to evaluate the potential significance of oil-contaminated particles ingested by detrital and filter feeding organisms. (0.5 man years):

a. The loss of metals from the WSF and appearance of metals in organic precipitates will be monitored under various light, temperature, and salinity regimes. Metals will be analyzed by atomic absorption. Fate of naphthols in the solution will be determined by GC.

b. The proportion of selected labelled aromatic and heterocyclic compounds partitioning into soluble, colloidal, and settleable fractions will be determined in the presence and absence of microorganisms.

II. Laboratory Activities

A. General Methods

Standard bioassay techniques, modified for the special requirements of working with hydrocarbons, are used in the majority of our experiments. Animals exposed to oil are monitored for death, sublethal physiological effects, behavioral changes, and metabolism of hydrocarbons.

All bioassays are done at the Auke Bay Laboratory. The majority of organisms are collected in the vicinity of Auke Bay, Alaska.

Cook Inlet crude oil is obtained from Shell Oil Company in 55-gallon drums. No. 2 fuel oil was taken from the laboratory heating system fuel tanks. Benzene, toluene, and naphthalene were reagent grade.

1. Mixing

WSF's are prepared by gently mixing a 1-percent oil-to-water suspension. Depending on the volume needed, the oil-water mixture is prepared in either an 18-liter bottle, a 100-liter glass aquarium, a 55-gallon polyethylene-lined metal barrel, or an 800-liter fiberglass tank. In each case, electric motors with mixing paddles are adjusted to the proper mixing energy to allow the oil vortex to descend one-third of the depth of the container. The mixing continues for 20 hours followed by a 3-hour settling period. The WSF is then siphoned off from beneath the oil slick and diluted for use in exposure.

2. Exposure

Most exposures are static, aerated, and at a tissue-to-volume ratio of 1 gram per liter or less. Oil concentrations are measured analytically at the beginning of the exposures. Organism responses (mortality or some other parameter) are analyzed by computerized probit statistics. Repetitive dosing is used for several studies. The oil concentration is periodically monitored

and brought up to the initial concentration by addition of 100 percent water-soluble fraction. The concentration deviation is minimized by frequent redosing.

5. Analytical Techniques

Our oil-water solutions (WSF's) are routinely analyzed by infrared (IR) and ultraviolet (UV) spectrophotometry, as well as by gas-liquid chromatography (GC).

The IR method is from Gruenfeld (1973), and involves determining the absorbance of light at 3412 nanometer wave length by the oil-derived hydrocarbons. Aliphatic compounds, which are not very toxic, absorb most strongly at this wave length. The method does not measure toxic aromatic or polar compounds. We use this method as a general indication of relative differences between successive WSF preparations, and as a means of comparing our work with that of other investigations. Despite its limitations, this method of determining oil in water is far superior to measuring only the volume of oil added to water, since the amount of oil that enters the water column is dependent on the mixing energy and duration.

A second method that we routinely employ is a modified version of the UV method of Neff and Anderson (1975). This method involves determining the absorbance of oil-derived hydrocarbons at 221 nanometers. Naphthalene and methyl-substituted naphthalenes absorb most strongly at this wave length, although high concentrations of mononuclear aromatics (such as benzene, toluene, xylene, etc.) can also cause appreciable absorption. The naphthalenes have been implicated in several toxicity studies. We use this method principally as a means of predicting the toxicity of successive WSF preparations. Since

the different methyl-substituted naphthalenes have slightly different molar absorptivities at 221 nanometers, we report results by this method as naphthalene equivalents. This is the amount of pure naphthalene that would account for most of the absorbance observed in a given sample measured at 221 nanometers.

The third method we employ routinely involves gas-liquid chromatography (GLC). We use a column suggested by Supelco, Inc., which is especially suited for separating aromatic hydrocarbons. In this method we extract the WSF with two aliquots of methylene chloride, and then analyze from 1 to 10 microliters of the combined extracts immediately by GLC for mononuclear aromatics. Then we concentrate the extract to 500 microliters, and analyze from 1 to 10 microliters again by GLC for the higher aromatics.

We have established the identity of most of the aromatic peaks by comparing retention times with known standards, by spiking WSF's with known aromatics, and by mass spectroscopic (MS) identification of selected samples. The results from these different methods have always been in agreement. The MS study (conducted at the Northwest Fisheries Center in Seattle) also established that both normal and some branched paraffins elute from our column, and in some cases they elute simultaneously with some of the aromatic compounds. On the basis of this information we are now able to correct for this interference.

4. Bioassay Statistics

When possible, all of our bioassay results are analyzed by a computerized probit analysis by Finney (1971). This statistical technique calculates a maximum likelihood estimation of the oil concentration that would cause 50 percent of the exposed animals to respond after exposure to the WSF for some given time.*

*We call this concentration of oil in the W F the median tolerance limit, or T_{lm}.

behavioral responses.

In addition, the probit analysis estimates a slope function with 95 percent fiducial limits, as well as the 95 percent fiducial limits about the T_{Lm}. This slope function is the rate at which the proportion of animals responding changes with changing oil concentrations in the WSF. From it, one can estimate the most likely proportion of animals that would respond at WSF oil concentrations other than the T_{Lm}. It is related to the tolerance distribution of the species being tested.

In some cases our bioassay results are not amenable to probit analysis. Probit analysis requires at least two dose levels of WSF at which the proportion of animals responding is observed to be between zero and one. Occasionally our dose levels will be so distributed that none of the animals respond in some set of lower doses, and all of them respond in the next highest dose and all higher doses. Or, there will be only one dose at which the proportion of animals responding is observed to lie between zero and one. In the former case we estimate the T_{Lm} as the antilog of the sum of the log of the highest dose where no animals respond, plus the log of the lowest dose where all of the animals respond, divided by two. In the latter case we estimate the T_{Lm} by plotting the dose versus the percent of the animals responding, and noting the dose level that corresponds to 50 percent response. This is the method of Doudoroff et al. (1951).

B. Methods and Scheduling of Individual Studies

1. Flow-through exposure methodology is being developed. Larval assays with flow-through apparatus are scheduled for the spring 1977.

2(a) Prudhoe Bay and Cook Inlet crude oils and No. 2 fuel oil samples have been sent to the National Analytical Center for phenolic and heterocyclic

compound analyses using gas chromatograph-mass spectrometry. The WSF's of Prudhoe Bay and Cook Inlet crude oils and fuel oil are also being analysed by the same procedure to determine the persistence of these phenolic compounds during a 96-hour period.

A standard 96-hour static assay was completed with phenol and the shrimp, Pandalus goniurus. An attempt was made to test naphthol with the same species.

2(b) A study of synthetic WSF's is scheduled for spring 1977.

2(c) A study to determine toxicity of oil components under flow-through conditions has started. The toxicity of each of 15 to 20 different aromatics (selected by their relative concentrations in oil WSF's) will be determined using a flow-through bioassay dosing apparatus and brine shrimp as the test animal. For each different batch of shrimp, a reference bioassay will be conducted using benzene to correct for sensitivity changes between batches. These data will allow us to predict the toxicity of any mixture of the aromatics tested. We will compare the predicted toxicity with the experimentally determined toxicity of several mixtures of aromatics, and with oil WSF's. This will allow us to determine if the joint toxicity of the aromatics is additive, since that is the assumption used to formulate the prediction of toxicity.

5. Long term growth studies are scheduled for summer of 1977.

4. A study to determine effects of petroleum hydrocarbons on rates of byssal thread attachments by the mussel Mytilus edulus, has begun. This study will provide information on the feasibility of using byssal thread rate as a parameter in later field studies where (1) mussels are exposed in the lab and then their condition monitored in the field, as well as (2) using byssal thread attachment rates to monitor chronic pollution in the field.

Mussels are collected, acclimated in the lab then glued individually to glass plates and suspended in test solutions with WSF's. The mussels are examined daily for number of byssal threads attached to the glass during and after the exposure period.

5. Studies of metabolic effect of oil are scheduled for winter of 1977. King crab juveniles will be wired for heart rate measurements and exposed to four aromatic components singularly under flow-through conditions. Heart rate and aromatic uptake, accumulation and excretion will be monitored simultaneously to determine if aromatic compound accumulation and metabolism correlates with a metabolic effect.
6. Tissue burden studies are scheduled for winter and summer 1977.
7. Uptake studies are scheduled for spring and summer 1977.
8. Effects of oil on burrowing behavior of three species is scheduled for spring and summer 1977.
9. The fate of trace metal aromatic hydrocarbon complexes in seawater is scheduled for winter 1977.

III. Results

(Refer to Task Objectives, p. 1)

1. Bioassays completed this quarter include:

<u>Species</u>	<u>Common Name</u>	<u>Toxicant</u>
<u>Pandalus goniurus</u>	humpy shrimp	phenol
<u>Salvelinus malma</u>	Dolly Varden char	Prudhoe Bay crude and No. 2 fuel oil
<u>Theragra chalcogrammus</u>	pollock	Cook Inlet crude and No. 2 fuel oil

2(a) Results from the phenolic compound analyses of WSF's and crude oils is being interpreted. Some phenols and substituted phenolic compounds were found in both crude oil and WSF's of crude oils. Final results are due in January 1977.

2(b) Considerable progress has been made on continuous dosing apparatus. Apparatus for continuous dosing of benzene, toluene, xylenes, naphthalene, methylnaphthalene, and dimethylnaphthalene has been developed and is being tested. A continuous flow crude oil WSF prototype device has been developed and should be operational by spring 1977.

2(c) The study on oil component toxicity started in November with final results due by April 1977.

3. No progress.

4. The rate of byssal thread attachment in mussels decreases when exposed to oil and shows a dose related response. Tests with toluene, naphthalene, and WSF's of Cook Inlet crude and No. 2 fuel oil have been completed. Mussels which are unable to lay down byssal threads would likely to be detached from the substrate. This laboratory study and field studies will be completed by fall 1977.

5. Much of the effort during the first quarter of the fiscal year was on preparation of manuscripts and planning new 1977 research. Five papers were presented at the NOAA/EPA Symposium in Seattle on November 10-12, 1976, on "Fate and Effects of Petroleum Hydrocarbons in Marine Ecosystems and Organisms". Manuscripts of three of the papers presented at the symposium were accepted for publication. Abstracts of the five papers presented at the Seattle symposium are attached to this report. Also attached is the abstract of a manuscript by Broderson et al, on sensitivity of larvae to hydrocarbons; it will be presented at the Oil Spill Conference sponsored by API, EPA, and USCG in New Orleans in March 1977.

IV. Interpretation of Results

Interpretation of results is included in manuscripts prepared for publication, six abstracts of which are attached to this report.

V. Problems Encountered

1. The sample oxidizer and supplies did not arrive and become operational until November 1976. This caused delays in processing of uptake samples with isotopes from last quarter's temperature-uptake study.
2. Considerable effort has been required to develop satisfactory continuous-flow oil exposure devices that are capable of delivering stable concentrations of toxicant at a high enough concentration. Available systems did not meet the above criteria. Most of the problems have been solved and we are ready to begin flow-through toxicity experiments on schedule.

Note: This manuscript has not received review external to the Auke Bay Fisheries Laboratory and should not be released or distributed without permission of the authors.

EFFECTS OF TEMPERATURE, VOLATILITY, AND BIODEGRADATION ON
THE PERSISTENCE OF AROMATIC HYDROCARBONS IN SEAWATER

D. Loren Cheatham, Rob S. McMahon, Susan J. Way,
Jeffrey W. Short, and Stanley D. Rice

Northwest Fisheries Center Auke Bay Fisheries Laboratory
National Marine Fisheries Service, NOAA
P.O. Box 155, Auke Bay, AK 99821

NOAA-EPA Symposium on Fate and Effects of Petroleum Hydrocarbons,
Seattle, Washington, November 1976.

ABSTRACT

A Cook Inlet crude oil water-soluble fraction was monitored at 5°, 8°, and 12°C by gas chromatography to determine the effect of temperature and the temperature-dependent factors of volatilization and biodegradation on the loss of individual mononuclear and dinuclear aromatic hydrocarbons from seawater. The importance of temperature-dependent factors was assessed at each temperature by using aeration and mercuric chloride as experimental conditions. Lower temperature inhibited the loss of all mononuclear and dinuclear aromatic hydrocarbons; this was expected because the vapor pressures of these hydrocarbons decrease with decreasing temperature. Volatility was a significant factor in the loss of mononuclear aromatics due to their relatively high vapor pressures. Biodegradation had little effect on mononuclear aromatics, but had a significant effect on dinuclear aromatics, particularly naphthalene. This effect was diminished with decreasing temperature, presumably because of decreased activity of micro-organisms which can utilize aromatic hydrocarbons as substrates at colder temperatures. Oil and seawater mixtures could be expected to be more toxic at lower temperatures because mononuclear and dinuclear aromatic hydrocarbons would persist longer.

EFFECTS OF TEMPERATURE ON THE ACUTE TOXICITY OF TOLUENE,
NAPHTHALENE, AND THE WATER-SOLUBLE FRACTION OF
COOK INLET CRUDE OIL TO PINK SALMON AND SHRIMP

Sid Korn, D. Adam Moles, and Stanley D. Rice

Northwest Fisheries Center Auke Bay Fisheries Laboratory
National Marine Fisheries Service, NOAA
P.O. Box 155, Auke Bay, AK 99821

ABSTRACT

We conducted toxicity tests at different temperatures to determine the effects of temperature on survival of shrimp and fish exposed to oil and oil component solutions. Exposure concentrations declined with time, and at different rates for each temperature, simulating a point source spill in the environment.

Shrimp (Pandalus goniurus and Eualus spp.) and pink salmon (Oncorhynchus gorbuscha) were tested (96-h bioassays) with toluene, naphthalene, and the water-soluble fraction (WSF) of Cook Inlet crude oil at 4°, 8°, and 12°C. Median tolerance limits (96-h TLm) were computed by probit statistics. Oil concentrations were measured by ultraviolet spectrophotometry.

The effect of different temperatures on the toxicity of toluene, naphthalene, and the WSF of Cook Inlet crude oil solutions depended on species and toxicant. Survival of shrimp exposed to toluene and naphthalene was significantly less at higher temperatures. In contrast, survival of pink salmon exposed to toluene was significantly less at lower temperatures. Other tests did not yield significant temperature effects (Non-overlapping 95% fiducial limits).

Temperature can affect toxicity in three ways: (1) it affects the persistence of the toxicant in water, (2) it affects the organism by changing the rate of hydrocarbon uptake, metabolism (if any), and excretion, and, (3) extreme temperatures can act as synergistic stresses with oil toxicity. It is likely that hydrocarbons will be toxic for longer time periods at lower temperatures because they persist longer at lower temperatures. However, since animals have different tolerances to oil and temperature, we cannot say whether the sensitivity of any particular animal will be increased or decreased at lower temperatures.

EFFECTS OF CRUDE OIL EXPOSURE ON KING CRAB
(PARALITHODES CAMTSCHATICA) GILL MORPHOLOGY

Mary Ann Smith

Geophysical Institute, University of Alaska, Fairbanks, AK 99701

Malin B. Bonnett

Northwest Fisheries Center Auke Bay Fisheries Laboratory
National Marine Fisheries Service, NOAA, P.O. Box 155, Auke Bay, AK 99821

ABSTRACT

Juvenile king crabs (Paralithodes camtschatica) were exposed in seawater periodically replenished with a sublethal dose of the water-soluble fraction of Cook Inlet crude oil for 3 days. Tissues were sampled at 3 h, corresponding to decrease in heart rate, and after the end of exposure period at 6 days. These tissues were fixed, processed, and examined with light and transmission electron microscopy.

The gills from 3-h-exposed crabs show essentially the same features as control gills. The morphology of gills taken from crabs after the end of the exposure period (6 days) showed the following changes: (1) the plasma membrane was separated from cytoplasm and cell size was reduced, (2) cytoplasm and nucleus showed more electron dense granules, (3) there were many large vacuoles within cells, (4) mitochondria were fewer and their shape was altered, (5) smooth endoplasmic reticulum appeared swollen, and (6) the interdigitation of lateral cell surfaces was interrupted. Blood cells present in these samples were also altered; the perinuclear space was enlarged and vacuoles were present in the cytoplasm.

Some of these changes in the gills indicate morphological damage following altered metabolic response to sublethal crude oil exposure,

SENSITIVITY OF LARVAL AND ADULT ALASKAN SHRIMP AND CRABS
TO ACUTE EXPOSURES OF THE WATER-SOLUBLE FRACTION
OF COOK INLET CRUDE OIL

C. C. Brodersen, S. D. Rice, J. W. Short, T. A. Mecklenburg, and J. F. Karinen

Northwest and Alaska Fisheries Center Auke Bay Fisheries Laboratory
National Marine Fisheries Service, NOAA
P.O. Box 155, Auke Bay, AK 99821
907-789-7231

ABSTRACT

We measured the sensitivity of adult and larval Alaskan shrimp and crabs to the water-soluble fraction (WSF) of Cook Inlet crude oil. All tests were 96-hr static bioassays at temperatures these animals normally encounter. Oil concentrations in seawater were measured by infrared spectrophotometry. Larval crustaceans were found to die more slowly than adults, making it necessary to measure sensitivity in terms of concentrations causing moribundity (death imminent) instead of in terms of concentrations causing death during exposure. The cessation of all motion and reaction was found to indicate moribundity in adults and the cessation of swimming was found to indicate moribundity in larvae exposed for 96 hr.

Ninety-six-hr LC_{50} 's for moribundity for stage I larvae ranged from 0.95 to 1.8 ppm depending on species, while 96-hr LC_{50} 's for adults ranged from 1.9 to 4.2 ppm oil. Sensitivities for stage I-VI larvae of coonstripe shrimp ranged between 0.24 ppm and 1.9 ppm.

Larvae were more sensitive to oil than adults. The sensitivity of larvae depended on species and developmental stage. Larvae are probably more vulnerable than adults to oil exposure because of greater sensitivity to oil and greater susceptibility to predation. Cold water species may be particularly vulnerable because of increased time spent as developing larvae.

KEY WORDS: Larvae, Crustaceans, Acute toxicity, Alaska, Crude oil.

MOLTING AND SURVIVAL OF KING CRAB (*PARALITHODES CAMTSCHATICA*)
AND COONSTRIPE SHRIMP (*PANDALUS HYP SINOTUS*) LARVAE
EXPOSED TO COOK INLET CRUDE OIL WATER-SOLUBLE FRACTION

T. Anthony Mecklenburg, Stanley D. Rice, and John F. Karinen

Northwest and Alaska Fisheries Center Auke Bay Fisheries Laboratory
National Marine Fisheries Service, NOAA
P. O. Box 155, Auke Bay, AK 99821

ABSTRACT

Larvae of coonstripe shrimp and king crab were exposed to solutions of the water-soluble fraction (WSF) of Cook Inlet crude oil in a series of bioassays on intermolt stages I and II and the molt period from stage I to stage II. Molting larvae were more sensitive than intermolt larvae to the WSF, and molting coonstripe shrimp larvae were more sensitive than molting king crab larvae. When molting larvae were exposed to high concentrations of the WSF (1.15-1.87 ppm total hydrocarbons) for as little as 6 hr, molting success was reduced by 10-30% and some deaths occurred. When larvae were exposed to these high concentrations for 24 hr or longer, molting declined 90-100% and the larvae usually died. The lowest concentrations tested (0.15-0.55 ppm total hydrocarbons) did not inhibit molting at any length of exposure, but many larvae died after molting. Median lethal concentrations (LC50's) based on 144 hr of observation for molting coonstripe shrimp and 120 hr for molting king crab were much lower than the 96-hr LC50's, showing that the standard 96-hr LC50 is not always sufficient for determining acute oil toxicity. Although our LC50's for intermolt larvae are higher than levels of petroleum hydrocarbons reported for chronic and spill situations, some of our LC50's for molting larvae exposed 24 hr and longer are similar to or below these environmental levels. Comparisons of sensitivity to oil between different crustacean species or life stages should be based on animals tested in the same stage of the molt cycle, such as intermolt.

Key Words: Molting, crustaceans, larvae, *Paralithodes camtschatica*, *Pandalus hypsinotus*, crude oil, Alaska.

RESPONSE OF THE CLAM, *MACOMA BALTHICA* (LINNAEUS), EXPOSED TO PRUDHOE BAY CRUDE OIL AS UNMIXED OIL, WATER-SOLUBLE FRACTION, AND OIL-CONTAMINATED SEDIMENT IN THE LABORATORY

Tamra L. Taylor and John F. Karinen

Northwest and Alaska Fisheries Center Auke Bay Fisheries Laboratory
National Marine Fisheries Service, NOAA
P. O. Box 155, Auke Bay, AK 99821

ABSTRACT

The small clam, *Macoma balthica* (Linnaeus 1758), will likely be subjected to oil slicks layered on the mud and to water-soluble fractions of crude oil or oil-contaminated sediment. Groups of adult clams in or on their natural sediment were exposed in flow-through aquaria at 7°-12°C to various concentrations of Prudhoe Bay crude oil layered on the mud surface, the water-soluble fraction (WSF) of the crude oil, and oil-treated sediment (OTS).

Gentle settling of crude oil over clam beds had negligible effects on clams observed for 2 months. Water-soluble and oil-treated sediment fractions of Prudhoe Bay crude oil inhibited burrowing and caused clams to move to the sediment surface. Responses were directly proportional to concentrations of the WSF or amount of OTS. The 1-hr and 72-hr effective median concentrations of the WSF for the responses of burrowing by unburied clams and surfacing by buried clams were 0.234 and 0.367 ppm naphthalene equivalents respectively. The interpolated amount of OTS needed for a 50% surfacing response within 24 hr was 0.67 g OTS cm⁻².

Although short-term exposures of clams to the WSF of crude oil and OTS caused few deaths, behavioral responses of clams to oil may be of great importance to their survival in the natural environment. In these laboratory tests, many of the clams recovered, but in nature clams that come to the sediment surface may be eaten by predators or die from exposure.

Key Words: *Macoma balthica*, crude oil, Alaska.

OCSEAP QUARTERLY REPORT - RU 73/74

Contract #: R7120819

Reporting Period: October 1 - December 31, 1976

Number of Pages: 39

SUBLETHAL EFFECTS AS REFLECTED BY MORPHOLOGICAL, CHEMICAL,
PHYSIOLOGICAL, BEHAVIORAL, AND PATHOLOGICAL INDICES

Donald C. Malins, Edward H. Gruger, Jr.

Harold O. Hodgins, Douglas D. Weber

Environmental Conservation Division
National Marine Fisheries Service, NOAA
Northwest and Alaska Fisheries Center
2725 Montlake Boulevard East
Seattle, Washington 98112

December 1976

I. TASK OBJECTIVES

The general objective of these studies is to identify and evaluate in selected marine organisms the effects of chronic exposure to petroleum hydrocarbons and trace metals.

Under the general task objective, behavioral, morphological, chemical, physiological, and pathological parameters are being investigated. The specific objectives for studies described in this quarter are as follows:

1. Behavioral

Effects of petroleum on salmon homing:

To determine if petroleum hydrocarbons present in water modify the behavior of homing adult salmon by (a) causing them to avoid their home stream or (b) disrupting their homing capability.

2. Morphological

Effects of petroleum on fish eye lenses:

To further elucidate effects of long-term exposure of petroleum in the diet on structure of eye lenses of rainbow trout.

3. Chemical

a. Biotransformation of petroleum hydrocarbons:

To define and evaluate accumulation, bioconversion, and excretion of petroleum hydrocarbons in salmon, flatfish, and invertebrates (e.g., shrimp).

b. Trace metal concentrations in flatfish skin and mucus:

To define and evaluate uptake, accumulation, and discharge of trace metals from epidermal mucus and skin of starry flounder.

c. Biotransformation of trace metal compounds:

To define and evaluate accumulation and excretion of trace metals in salmon and flatfish; to delineate important cellular and subcellular interactions in organisms.

4. Pathological

Pathological effects of exposure to oil-contaminated sediment:

To determine the frequency and nature of pathological changes occurring in flatfish as a result of exposure to oil-contaminated sediment.

II. FIELD OR LABORATORY ACTIVITIES

A. Ship or Field Trip Schedule N/A

B. Scientific Party

Names, affiliation, and roles of investigators conducting these studies are listed in the FY 77 OCSEAP Research Unit #73/74 proposal. Particularly see pages 19-20, 23, and 26.

C. Methods

1. Behavioral

Effect of petroleum on salmon homing:

Three studies were initiated in October 1976 to evaluate the effect of petroleum hydrocarbons on the homing of adult coho (Oncorhynchus kisutch) and chinook (O. tshawytscha) salmon. Two of the studies are designed to determine if exposure (24 to 28 hours) to petroleum components has an effect on a salmon's homing capability. These experiments are currently in progress and will be reported in the next quarter.

The third experiment, which is complete and the results of which are presented below, was designed to determine if salmon will avoid their home stream when petroleum hydrocarbons are present in the water.

Oil introduced into the home stream water consisted of the major water-soluble components of Prudhoe Bay crude oil (hereafter termed synthetic oil). Components of the mixture were determined from gas chromatographic and mass spectral data taken from five representative samples of the water-soluble fraction (WSF) of Prudhoe Bay crude oil. (For details of the analytical approach, see OCSEAP Quarterly Report RU 74, September 1976, and for the method of generating the WSF analyzed, see OCSEAP Annual Report RU 74, April 1976.) All hydrocarbons used in the synthetic mixture were of spectrophotometric grade or distilled in glass. The percent, by volume, of each hydrocarbon in the synthetic oil mixture is given in Table 1.

The avoidance study was conducted at the Northwest and Alaska Fisheries Center (NWAFC), Seattle, using chinook salmon returning to a freshwater holding area (Fig. 1). The holding area consists of a 25-meter raceway with trap, and a 10-meter entrance ladder. At a distance of 12 meters from the ladder, 11 liters of water per minute were diverted from the raceway into a sealed 38-liter glass mixing chamber. The glass chamber contained 17 baffles and an electrically powered propellor for initial mixing. Synthetic oil was metered into the inflow of the glass chamber with a peristaltic pump, and this initial oil-water mixture reintroduced at the head of the fish ladder through a diffuser 30 cm beneath the water surface. Further mixing took place through water turbulence in the ladder.

Water samples for hydrocarbon analysis were collected from the center of the water column in the fish ladder at the termination of each test. On the day of water sample collection, two 100-ml aliquots of water were

TABLE 1

Synthetic oil mixture. Hydrocarbon order on basis of increasing GC retention times.

Hydrocarbon	Percent by volume
Cyclohexane	2.19
Benzene	5.85
Toluene	64.10
Methylcyclohexene	5.55
Ethylbenzene	0.99
Xylene-m	7.92
Xylene-o	4.84
Xylene-p	4.96
Ethyltoluene-o	0.96
Ethyltoluene-m	0.99
1,2,3-trimethylbenzene	0.48
1,3,5-trimethylbenzene	0.50
1,2,4-trimethylbenzene	0.49
C ₃ -benzene	*
C ₄ -benzene	**
Naphthalene	0.16
Methylnaphthalene	***

* Isopropanol benzene is less than 0.40% of the WSF and is not included.

** Four C₄ benzenes noted in the WSF constitute 2.05% of the total WSF and are not included.

*** 1-Methylnaphthalene and 2-methylnaphthalene are not included since they constitute less than 0.5% of the total WSF and were not consistently identified by GC as being present in the WSF.

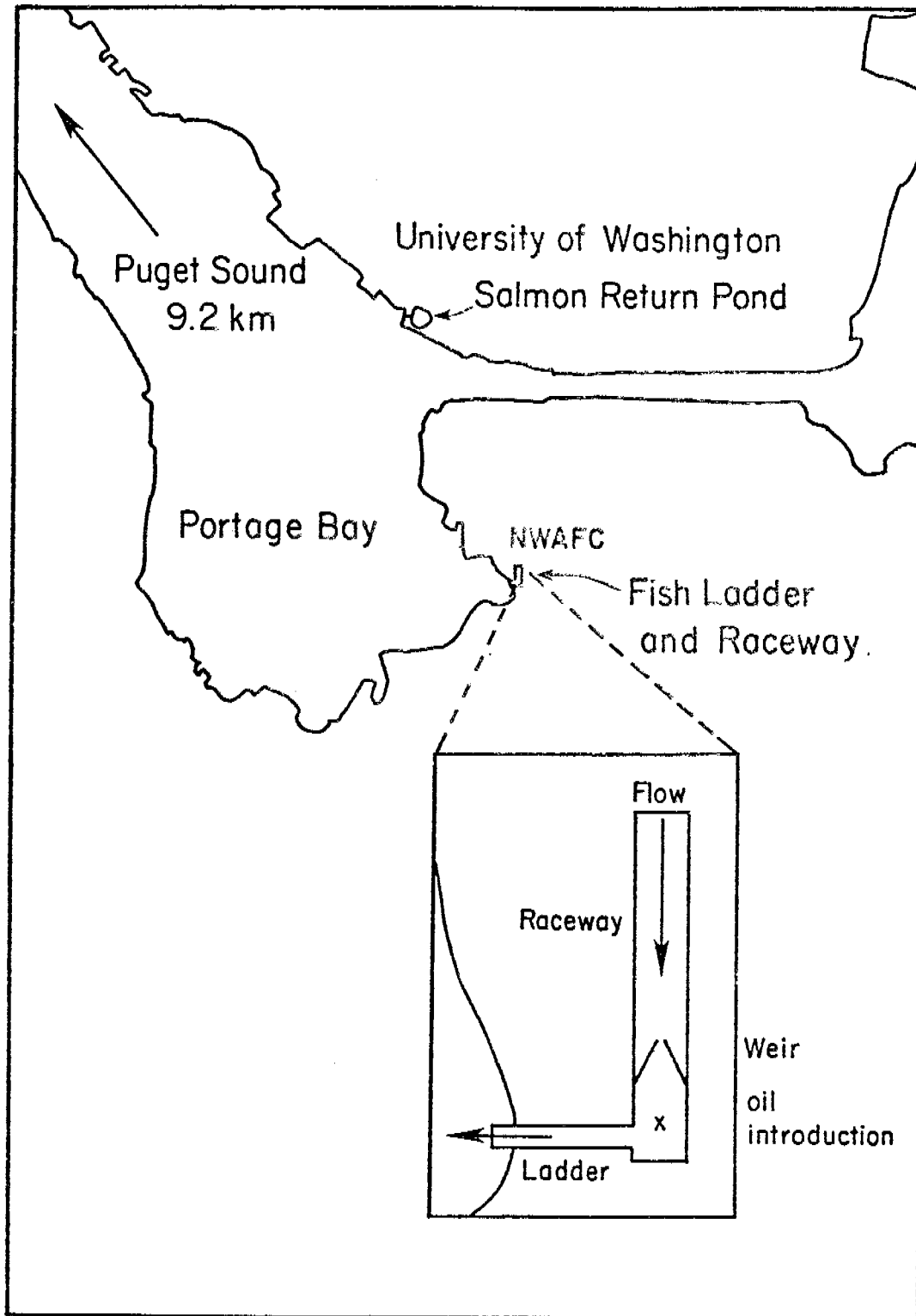


Figure 1. Map of area to which adult chinook salmon were returning in the homing study with expanded diagram of details of the fish ladder and weir.

extracted three times with a total of 15 ml of CS₂; the CS₂ was evaporated to 0.5 ml, internal standard was added, and 3 µl were injected into a gas chromatograph. Characteristics of the gas chromatograph are:

Column: 1 meter glass, 6 mm O.D., 2 mm I.D.

Packing: 0.2% Carbowax 1500 on 60/80 mesh Carbopack C (Sufelco, Bellefonte, Pennsylvania)

Gas flow: carrier flow at 44.4 ml/min (of N₂)

Temperature conditions: initial 40°C

final 215°C

rate 15°C/min

injection temperature 200°C

detector temperature 300°C

Chinook salmon returning to the NWAFC predominately enter the fish ladder and raceway during hours of twilight and darkness. The number of salmon entering the raceway trap were recorded daily. On test days, the synthetic oil was introduced continuously starting at 1600 hours and terminated at 0800 hours the following day. Flow rates for the synthetic oil were taken at the start and end of each test: total water flow in the raceway and ladder were considered to be constant at 5900 l/min.

2. Morphological

Effects of petroleum on fish eye lenses;

Lenses were obtained from 3-year-old rainbow trout (Salmo gairdneri) that were either fed food treated with 1 g Prudhoe Bay crude oil/kg Oregon moist pellet fish food (OMP) or OMP without added petroleum. Feeding was initiated in July 1975 and continued for more than a year. Details of the oil incorporation in food are given in OCSEAP Quarterly

Report RU 73, September 1976 (page 1 under the Physiological Section). Details of preparation of samples for scanning electron microscopy are presented in the first OCSEAP RU 73 Quarterly Report of 1975.

Hydration experiments were conducted with lenses freshly excised from rainbow trout that had no history of exposure to petroleum. The lenses were placed in hypotonic media consisting of a dilution series of Dulbecco's Saline (Cell Biology, 1976, Altman and Katz, eds., Fed. Am. Soc. Exp. Biol. Med., p. 61), ranging from full strength saline (280 mosm.) to distilled water. The solution and lenses were maintained at 2°C except when the measurements were taken.

3. Chemical

a. Biotransformation of petroleum hydrocarbons:

Shrimp

Challenge experiments were conducted employing a high specific activity tritiated naphthalene which facilitates the identification of very small amounts of individual metabolites of aromatic hydrocarbons and allows for the autoradiography of tissue sections from exposed larval and post-larval invertebrates. Studies with post-larval shrimp, Pandalus hypsinotus, were carried out using continuous-flowing seawater containing 6 ppb of tritiated naphthalene for 144 hours followed by 48 hours depuration. Other details of the laboratory procedures were included in the previous OCSEAP progress report for RU 74. Work in this area is continuing and details will be provided in a later report.

One-year old spot shrimp, Pandalus platyceros, were exposed to the WSF of Prudhoe Bay crude oil at a concentration of 0.11 ppm for seven days. The WSF was obtained from the solubilizer designed by Roubal et al.

(Roubal, Wm.T., D. Bovee, T.K. Collier, and S.I. Stranahan, Flow-through system for chronic exposure of aquatic organisms to seawater-soluble hydrocarbons from crude oil: Construction and applications, 1977 Oil Spill Conference, New Orleans, March 1977). The animals were washed, extracted, and analyzed for accumulated hydrocarbons by gas-liquid chromatography (GLC)/mass spectrometry (MS).

Biotransformation of petroleum hydrocarbons:

Marine Fish

Coho salmon and starry flounder (Platichthys stellatus) were exposed to the WSF of Prudhoe Bay crude oil obtained from the flow-through system described by Roubal et al. (above). For salmon and flounder the total concentration of hydrocarbons in the flow-through seawater was 0.8 ppm. The coho salmon were exposed to the WSF for six weeks and starry flounder for two weeks. After this time salmon and flounder were placed in clean seawater to evaluate their capability to deplete tissues.

b. Trace metal concentrations in flatfish skin and mucus:

Starry flounder averaging 25 g were exposed to 3 or 150 ppb of water-borne radioactively-labeled lead (Pb^{210}) and cadmium (Cd^{109}) at 4° and 10°C for a period of up to 30 days (details of exposure regimes are given in previous OCSEAPRU 73 reports). Following exposure, fish were placed in metal-free waters for two weeks.

At each data point, samples of mucus and skin (ventral and dorsal) were collected from three fish. Levels of metals in the samples were determined by liquid scintillation spectrometry. Because very little (<1 g) of mucus was obtained from the flatfish, it was not possible to carry out rheometric measurements. Total protein in the mucus was

determined by Lowry's method (Lowry, O.H., N.J. Rosebrough, A.L. Farr, and R.J. Randall, 1951, Protein determination in biological tissues, J. Biol. Chem. 193, 265).

c. Biotransformation of trace metal compounds:

Marine Fish

Coho salmon and starry flounder were exposed to 5 or 150 ppb of lead for 15 days. The exposure conditions and relevant chemical analyses are given in previous OCSEAP RU 74 progress reports. Additional data was obtained with coho salmon and starry flounder on the subcellular distribution of lead following exposure at 10°C. Details of the laboratory and workup procedures in obtaining the subcellular fractions of liver and kidney were given in OCSEAP RU 74 Quarterly Report, September 1976.

4. Pathological

Pathological effects on flatfish of exposure to oil-contaminated sediments

Preparation of oil-contaminated sediment:

Sediment was collected from a beach near Sequim, Washington. A homogeneous mixture of the sediment will be analyzed for baseline levels of hydrocarbons and for particle sizes.

The remainder of the procedure for mixing the sediment with oil is similar to the protocol used by Dr. Jack Anderson of Battelle Northwest Sequim, Washington (Anderson, J.W. and L.J. Moore, Bioavailability of sediment-sorbed naphthalenes to the sipunculid worm, Phascolosoma agassizii, In: Fate and Effects of Petroleum Hydrocarbons in Marine Ecosystems and Organisms, Pergamon Press, In Press). The sediment is being frozen and thawed three times to kill as many sediment-associated organisms as possible without destroying its absorptive properties. Upon arrival of

a new shipment of Prudhoe Bay crude oil (expected January 1977), the sediment will be mixed with 0.2% (v/v) oil using a modified cement mixer. About 30 liters of oil-soaked sediment can be prepared at a time. Sediment prepared in this manner will be placed in the test aquarium and equilibrated with running seawater for 24 hours before addition of fish.

Chemical and pathological analyses:

Analyses for petroleum hydrocarbons, particularly the 2 to 5 ring aromatic compounds, will be performed on the sediment, water, and fish, by the NOAA National Analytical Facility, NWAFC. The projected schedule for sediment analyses employing duplicate samples is the following: Day 1 (when test fish are added), day 2, day 7, day 14, day 21, day 28, after 6 weeks, after 2 months, and if the sediment is not renewed at this point, at two-week intervals thereafter until the end of the experiment.

Analyses for petroleum hydrocarbons in incoming seawater and in water from the test aquarium will be performed at two-week intervals. In addition, at weekly intervals, analyses for dissolved oxygen and ammonia will be done on the water near the sediment.

Four types of analyses will be performed on experimental fish: (1) gross examination of visible lesions or tumors; (2) histopathological examination of critical tissues, such as liver, kidney, skin, and gills; (3) determination of petroleum hydrocarbons in tissues from liver, gall bladder, or muscle; and (4) hematological tests on blood, such as hematocrit and differential blood cell counts. Gross examination of fish will be performed weekly. All of the latter three analyses will be performed on each of two fish sacrificed at two- to three-week intervals.

Experimental facilities and fish care:

Exposure experiments will be performed at the NWAFC's Mukilteo Facility. Fish will be held in 2 x 2 x 7 ft fiberglass tanks supplied with flowing seawater; the tanks will have 2 inches (about 60 liters) of either untreated or oil-soaked sediment layered on a false bottom made of fine mesh fiberglass screening and fiberglass supports. Seawater will flow over and under the sediment. Depending upon the size of English sole (Parophrys vetulus) or starry flounder available at the time of collection, between 30 and 50 fish will be used per aquarium.

C. N/A

D. N/A

III. RESULTS

1. Effects of petroleum on salmon homing.

Presence of petroleum hydrocarbons at levels of 600 ppb and less did not prevent adult chinook salmon from entering their home stream. As shown in Figure 2, a synthetic oil mixture was introduced into the fish ladder on four occasions in November 1976. There was an increase in fish returns following the November 2-3 exposure. The exact amount introduced into the water in this test was not accurately evaluated due to malfunction of the delivery system, but was estimated at 600 ppb.

The introduction of hydrocarbons after November 2-3 coincided with a natural daily decrease in returning fish. That this decrease was not due to the presence of hydrocarbons is supported by the occurrence of a similar decline in chinook salmon returns to the University of Washington. The University of Washington fishway is 0.6 kilometers from the NWAFC and has the same basic salmon stock and water drainage system.

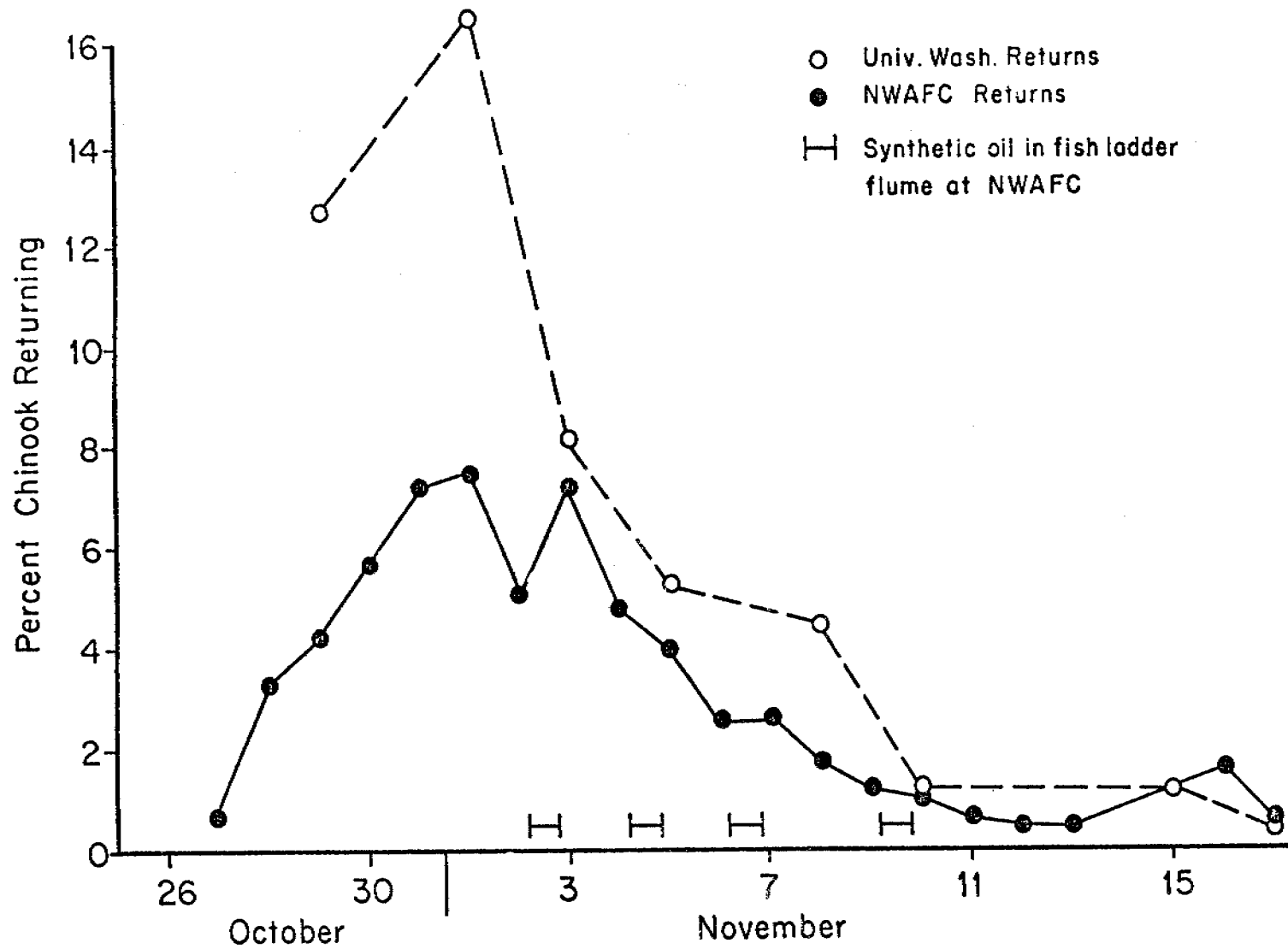


Figure 2. Percent chinook salmon returning to the University of Washington and the Northwest and Alaska Fisheries Center (NWAFC) by date (percentages do not sum to 100% since salmon were returning before and after time period depicted). Horizontal lines (—) represent 16-hour periods during which synthetic oil was introduced into the NWAFC fish ladder.

Table 2 lists the amount of synthetic oil in the water as measured by: (1) flow rates taken at the beginning and end of each test, (2) concentration determined by gas chromatographic analysis of two water samples taken at the termination of each test. The variation in levels of synthetic oil as measured by gas chromatography may be indicative of incomplete mixing.

2. Morphological

Effects of petroleum on fish eye lenses.

In the last OCSEAP report for RU 73, a marked increase in volume of lenses of mature rainbow trout fed petroleum was described.

Work on the lenses has continued this quarter and the change in size appears to be largely the result of hydration. The enlarged lenses from oil-fed fish were soft, and with mild pressure were easily compressed and remained deformed; whereas, the lenses from control trout (non-oil-fed) returned to their normal geometry after equivalent pressure.

The lens is composed of ribbon-like filaments which interdigitate, forming a spherical mass. The filaments have simple projections on their broad surfaces which fit into pits on the adjacent fiber. In addition, there are complex interlocking protuberances along the edge of each fiber (Fig. 3). After treatment with petroleum, the fiber structure appears changed: the broad surface is wrinkled and the interdigitating protuberances are not smooth and regular as in untreated fish (Fig. 4). The fibers look shriveled, as if the fixative were hyperosmotic, suggesting that the increase in size is largely due to hydration rather than to an increase in mass resulting from cell proliferation or cell secretory activity.

TABLE 2

Amount of synthetic oil in home stream water and percent of fish returning

Test date	ppb synthetic oil determined by:		% change in returns
	Flow rate	GC analysis	
November 2-3	600*	**	+43
November 4-5	200,130+	35,31++	-23
November 6-7	200,130	129,121	+ 7
November 9-10	400,285	336,124	-17

* Estimated.

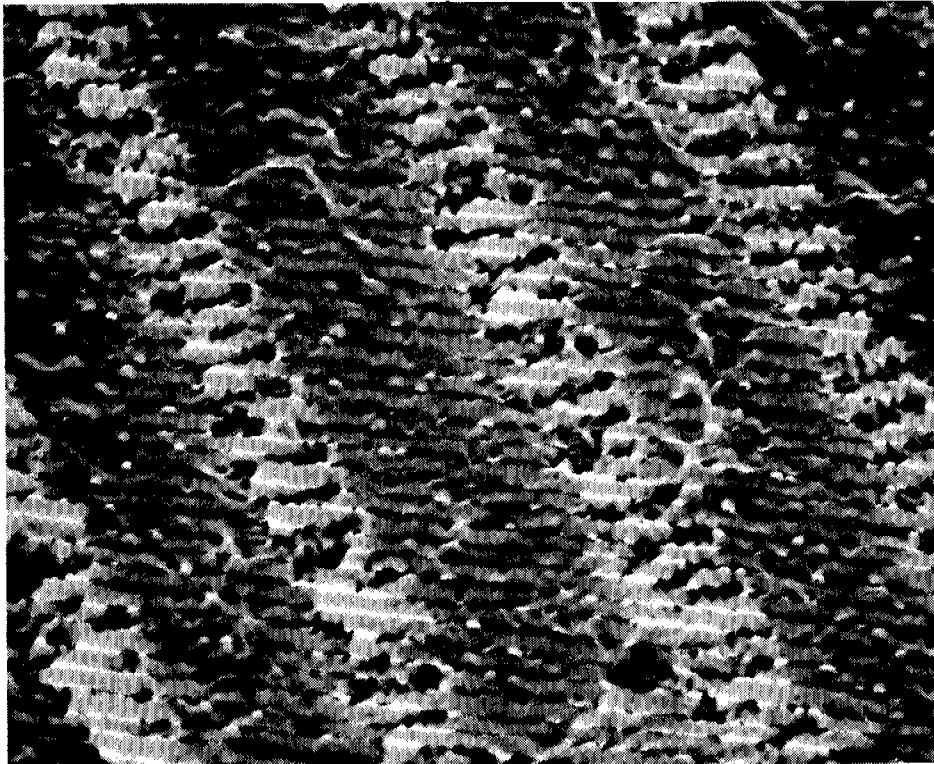
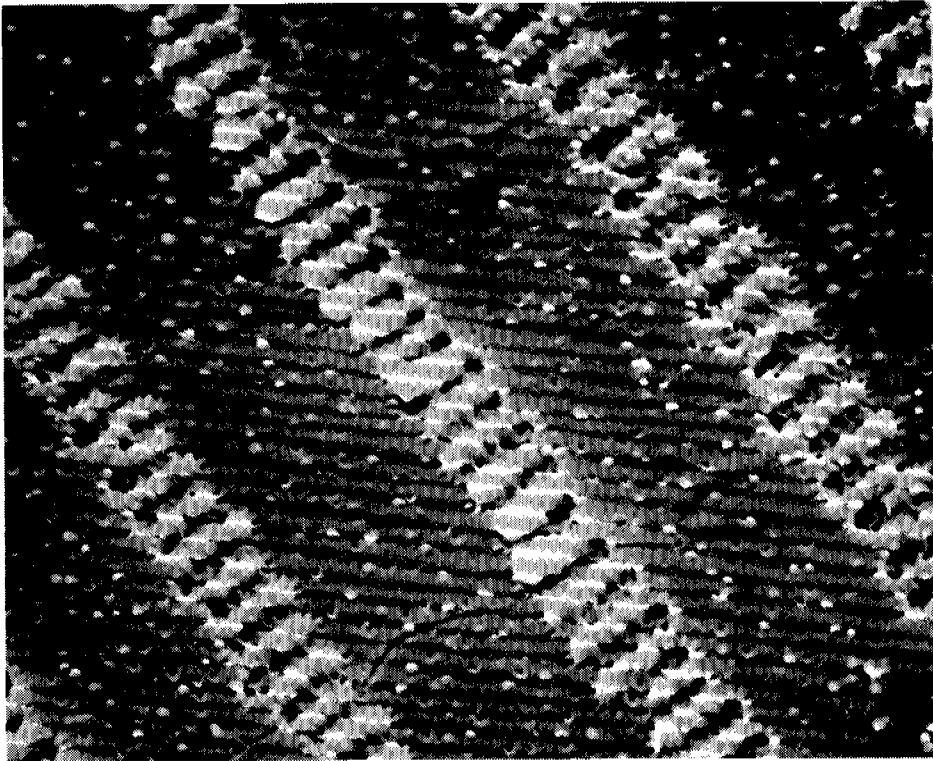
** Not determined.

+ The two values represent concentrations of oil in home stream water at the beginning and end of each test.

++ The two values represent duplicate home stream water samples taken at the end of each test.

Figure 3. (upper micrograph). Scanning electron micrograph of lens fibers from an untreated rainbow trout (X 2600).

Figure 4. (lower micrograph). Lens fibers from a rainbow trout exposed to crude oil in the diet for one year. Note the undulated surface of the fiber compared to the control (X 2600).



To test the hydration hypothesis, lenses were removed from normal rainbow trout, measured, and placed in hypotonic media. Within about 5 hours in distilled water there was a 64% increase in lens volume (Fig. 5), demonstrating that hydration could account for much of observed increases in trout eye lens volume after oil exposure.

3. Chemical

a. Biotransformation of petroleum hydrocarbons:

Shrimp

The data on accumulation of water-soluble hydrocarbons in one-year old spot shrimp suggests that significant levels of low molecular weight aromatic hydrocarbons are readily accumulated in thoracic segments (Table 3). In contrast, abdominal segments were found to contain no more than trace levels of identified aromatic hydrocarbons. The data given in Table 3 represent hydrocarbon accumulations in experimental animals with respect to data obtained from a control group.

Other studies on the cellular distribution of radioactivity associated with accumulated isotopically-labeled naphthalene and metabolites are being carried out by autoradiography. Metabolite formation is being investigated via radiometric techniques.

Biotransformation of petroleum hydrocarbons:

Marine Fish

Data are provided on the accumulation of hydrocarbons in coho salmon exposed to a WSF of Prudhoe bay crude oil equaling 0.8 ppm of total hydrocarbons in seawater. After one week of exposure no hydrocarbons were detected in muscle tissue (Table 4). Exposures from two to six weeks, however, resulted in the accumulation of significant amounts of

Volume change of lenses in distilled water

% diff $.70 - 1.15 = 64.3\%$

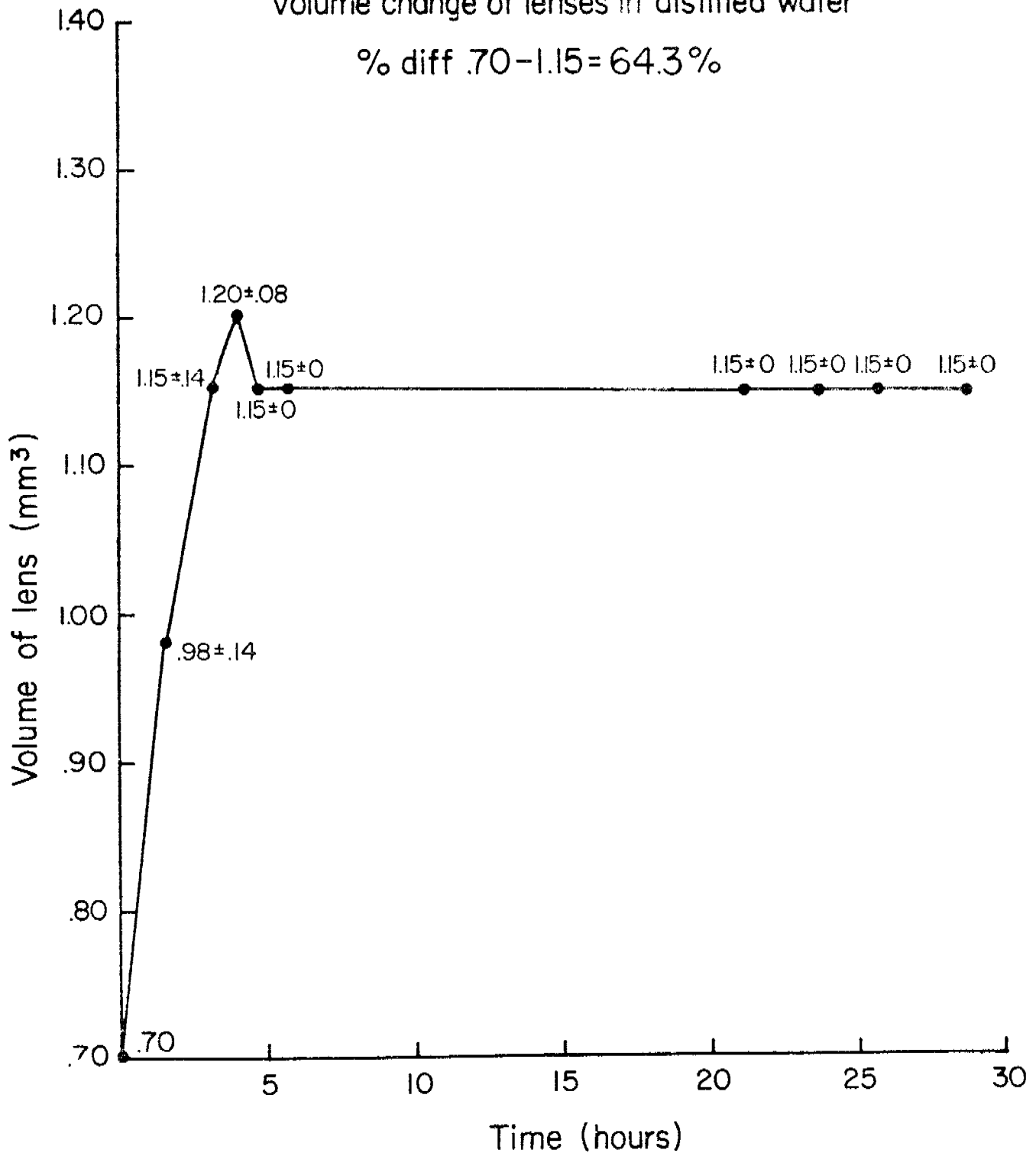


Figure 5. Mean volume changes \pm standard deviations of enucleated lenses from rainbow trout. One lens from each of three trout was placed in distilled water for 30 hours, the diameters were measured and converted to volumes.

TABLE 3

*Hydrocarbons in thoracic and abdominal segments of one-year old spot shrimp exposed to a water-soluble fraction of Prudhoe Bay crude oil using flow-through system.**

Compound	Thoracic Segments (ng/g wet wt)	Abdominal Segments (ng/g wet wt)
C ₂ -Substituted benzenes	25	Trace**
C ₃ -Substituted benzenes	17	Trace
C ₄ - & C ₅ -Substituted benzenes	2	Trace
Naphthalene	1	Trace
1- & 2-Methylnaphthalenes	19	Trace
C ₂ -Substituted naphthalenes	18	Trace
C ₃ -Substituted naphthalenes	15	Trace

* 0.11 ppm total hydrocarbons in flow-through water.

** Trace - below measurable limit.

TABLE 4

Hydrocarbons in muscle tissue of coho salmon (*Oncorhynchus kisutch*) exposed to the water-soluble fraction of Prudhoe Bay crude oil using a flow-through system*

Compound	Weeks Exposure				
	1	2 ng/g dry tissue	3 ng/g dry tissue	5 ng/g dry tissue	6** ng/g dry tissue
C ₂ -Substituted benzenes	--***	310	660	490	270
C ₃ -Substituted benzenes	--	300	880	1,500	390
C ₄ - & C ₅ -Substituted benzenes	--	1,500	1,700	5,500	2,000
Naphthalene	--	70	140	240	120
2-Methylnaphthalene	--	100	310	560	200
1-Methylnaphthalene	--	90	220	400	160
C ₂ -Substituted naphthalenes	--	310	360	850	440
C ₃ -Substituted naphthalenes	--	230	150	680	390

* 0.8 ppm (total hydrocarbons) in flow-through water. Samples are composites from two fish; no evidence was found from interfering compounds in control animals. Limits of detection for individual hydrocarbons will be given later.

** After a six-week exposure period, the fish were placed in oil-free seawater. After one week, hydrocarbons representative of the WSF were below detectable limits.

*** Compounds not detected.

substituted and unsubstituted benzenes and naphthalenes. The C₄ and C₅-substituted benzenes were prominent constituents of muscle reaching 5,500 ng/g dry weight of tissue after five weeks of exposure. Interestingly, when fish exposed for six weeks were transferred to clean water detectable levels of hydrocarbons were not found on week thereafter. Thus, as suggested in previous reports, coho salmon have a significant capability of depurating muscle tissue of accumulated low molecular weight hydrocarbons. The data given in Table 4 replace the provisional and essentially qualitative data included in the previous progress report (Table 4).

Table 5 lists data on hydrocarbon accumulation in muscle, liver, and gills, of starry flounder exposed to a WSF of Prudhoe Bay crude oil equaling 0.8 ppm of the total hydrocarbons in seawater. After one week of exposure, high levels of hydrocarbons of the WSF were observed in tissues in contrast to the findings obtained with salmon.

b. Trace metal concentrations in flatfish skin and mucus:

Data on concentrations of lead and cadmium in flatfish mucus and skin are given in Figures 6 to 9 and Table 6.

Mucus

The findings were that the flatfish mucus sequestered large amounts of lead and cadmium giving rise to a bioconcentration factor (conc. of metal in mucus/conc. of metal in water) of about 12 to 14 (Figs. 6 to 8) within the first few days of exposure to either lead nitrate or cadmium nitrate. For example, starry flounder exposed to 150 ppb lead nitrate at 10°C for four days accumulated 1,800 ppb of lead in the mucus. The initial high concentrations of metal declined steeply during the rest of the exposure period reaching about 300 ppb at the end of 14 days (Fig. 7).

TABLE 5

Hydrocarbons in selected tissues of starry flounder (*Platichthys stellatus*) exposed to the water-soluble fraction of Prudhoe Bay crude oil using a flow-through system*

Compound	Tissue											
	Muscle				Liver				Gills			
	Exposure		Depuration		Exposure		Depuration		Exposure		Depuration	
	1**	2**	1**	2**	1	2	1	2	1	2	1	2
ng/g dry tissue												
C ₂ -Substituted benzenes	5,500	1,700	270	NF***	1,600	2,600	230	180	1,800	1,100	1,100	60
C ₃ -Substituted benzenes	15,000	5,500	180	300	5,900	9,600	380	190	5,000	3,100	3,400	NF
C ₄ - & C ₅ -Substituted benzenes	93,000	33,000	9,800	26,000	36,000	110,000	29,000	ND***	30,000	21,000	23,000	ND
Naphthalene	2,100	950	290	800	1,500	3,300	870	ND	440	750	470	310
2-Methyl-naphthalene	8,300	2,700	330	590	3,000	6,200	870	NF	2,300	1,200	490	NF
1-Methyl-naphthalene	6,100	2,100	340	820	2,400	5,000	990	NF	1,800	940	480	NF
C ₂ -Substituted naphthalenes	24,000	8,800	2,700	7,000	9,700	28,000	8,900	250	7,900	3,200	3,900	220
C ₃ -Substituted naphthalenes	17,000	6,400	2,100	7,600	5,300	22,000	9,800	NF	7,600	3,500	4,300	NF

* 0.8 ppm (total hydrocarbons) in flow-through seawater. Samples were composites of five fish (muscle) and ten fish (liver and gills); corrections in data were made with reference to values from control animals. Limits of detection for individual hydrocarbons will be given later.

** Weeks.

*** NF = not found; ND = not detected.

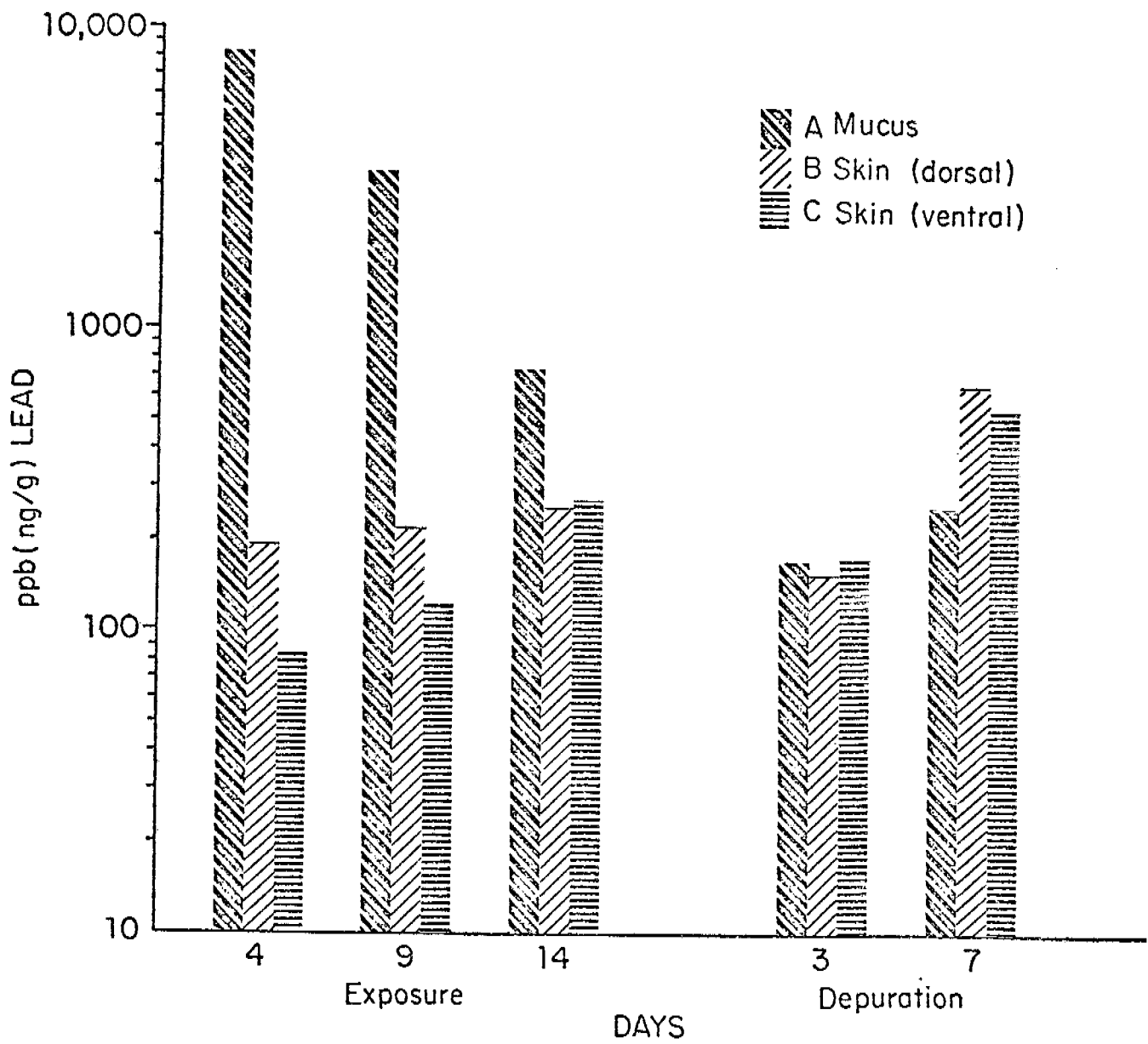


Figure 6. Starry flounder exposed to 150 ppb of $Pb(NO_3)_2$ at 4°C.

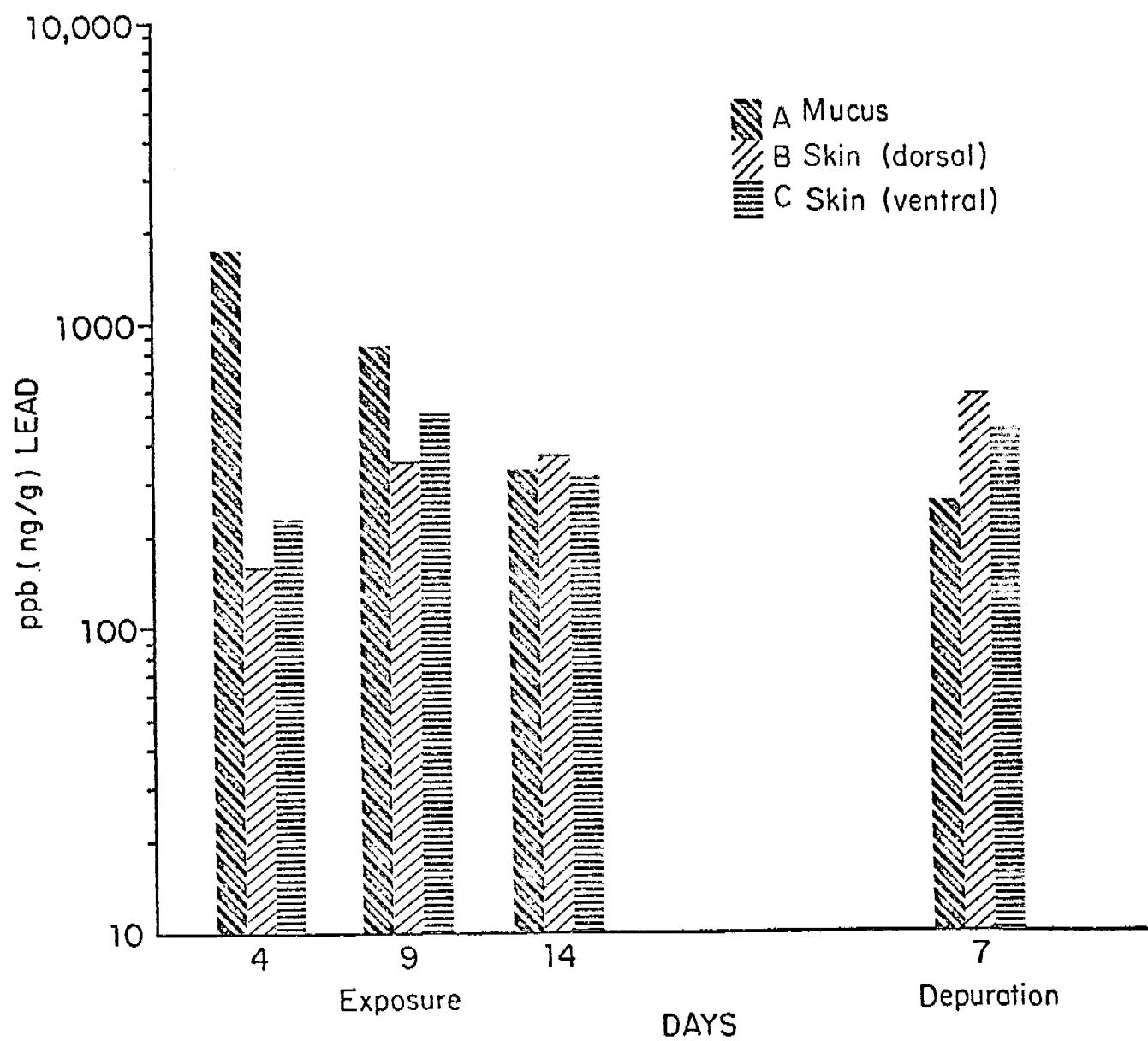


Figure 7. Starry flounder exposed to 150 ppb of $Pb(NO_3)_2$ at $10^\circ C$.

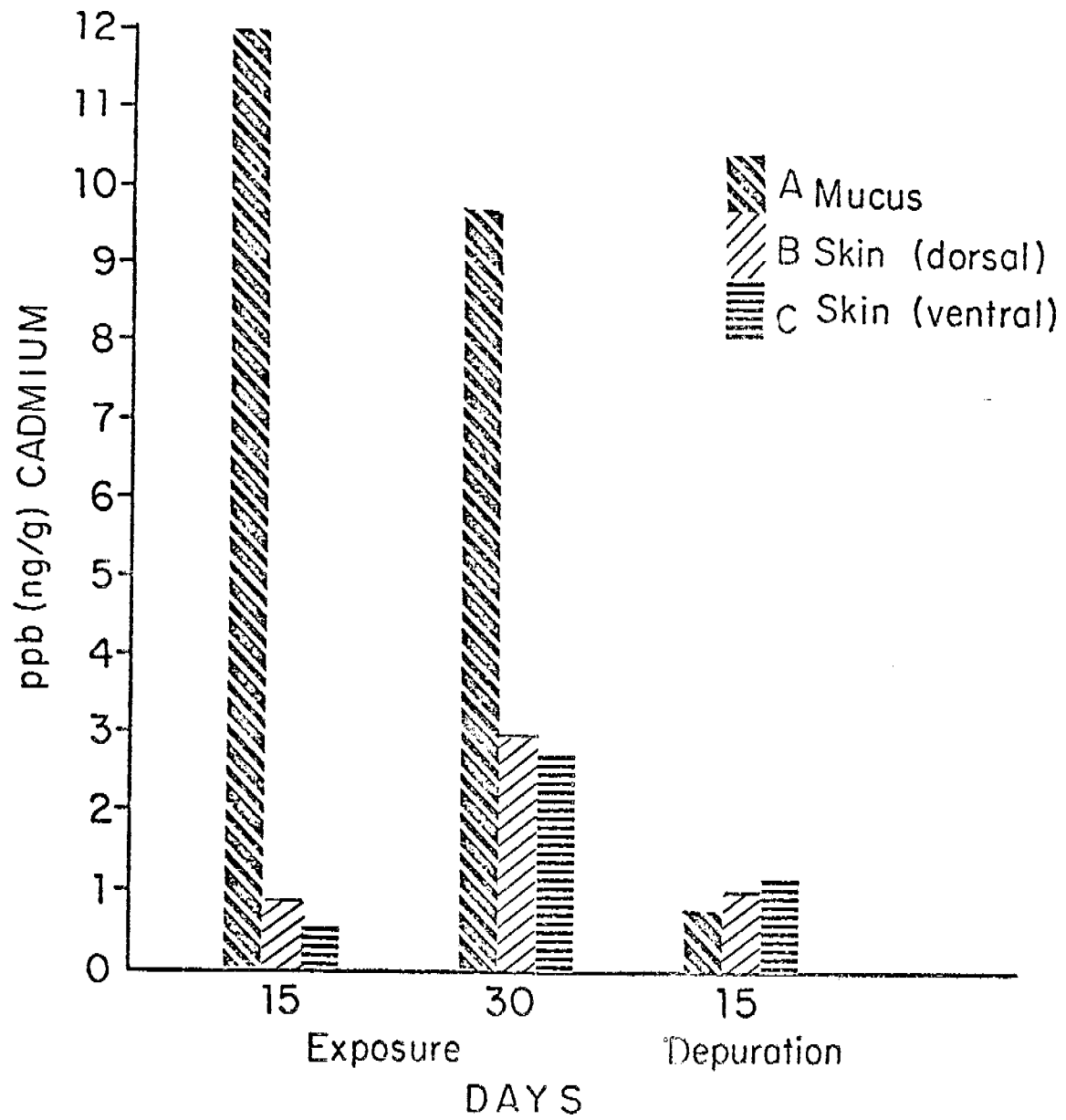


Figure 8. Starry flounder exposed to 150 ppb of $\text{Cd}(\text{NO}_3)_2$ at 10°C .

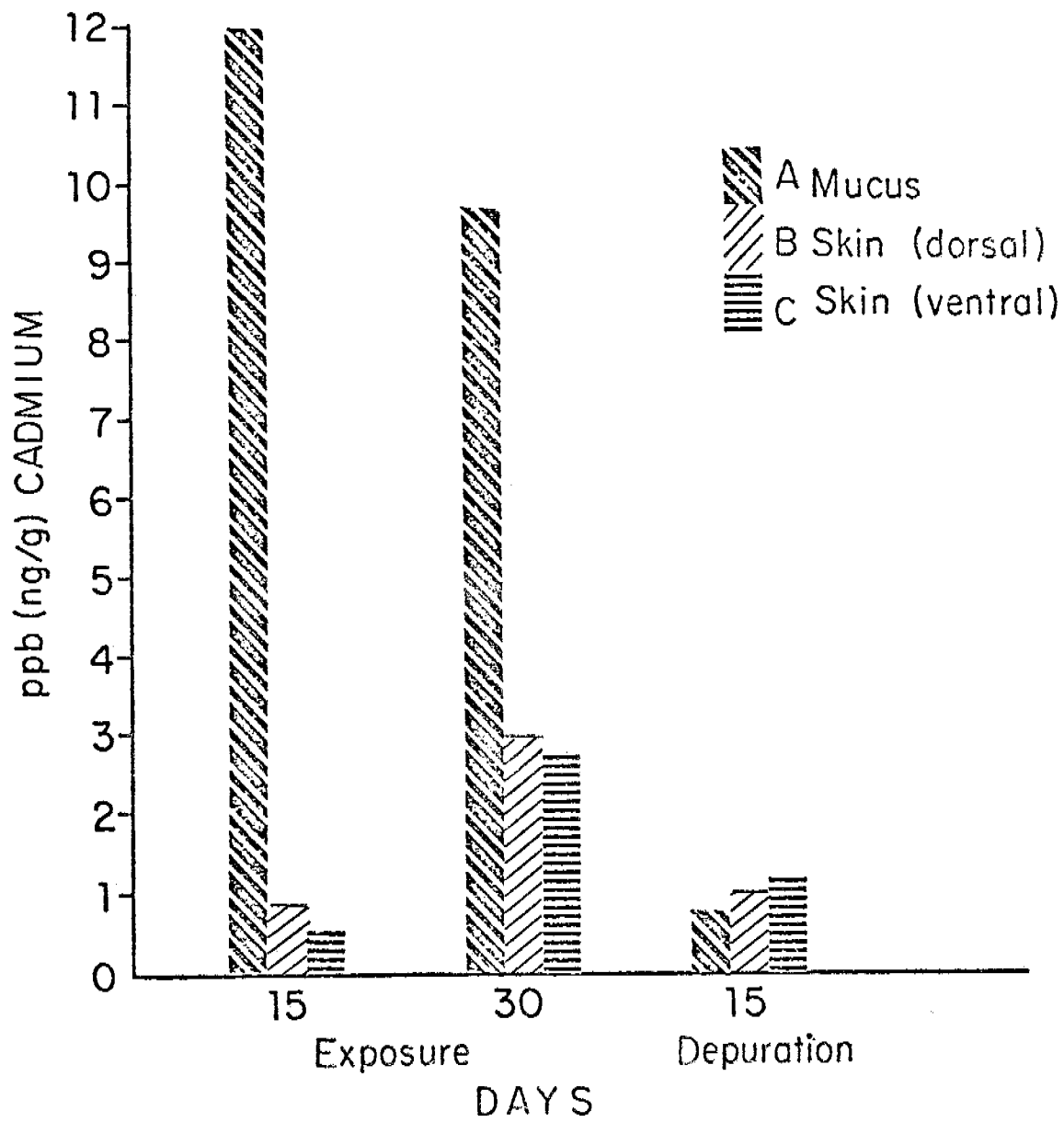


Figure 9. Starry flounder exposed to 3 ppb of $\text{Cd}(\text{NO}_3)_2$ at 10°C .

TABLE 6

Bioconcentration factors* for lead and cadmium in starry flounder (*Platichthys stellatus*)** exposed to water-borne $Pb(NO_3)_2$ and $Cd(NO_3)_2$

Metal	Level of exposure ppb (ng/g)	Epidermal mucus		Skin (dorsal)		Skin (ventral)	
		4°C	10°C	4°C	10°C	4°C	10°C
Pb	3	***	2.3	***	2.5	***	2.1
	150	4.7	2.2	1.8	2.4	1.9	2.1
Cd	150	1.3	1.3	0.3	0.4	0.18	1.2

* Bioconcentration factor - Concentration of metal in tissue/conc. of metal in water.

** Fish were exposed to metals for a period of two weeks and tested immediately.

*** Not determined.

This residual amount of metal persisted in the mucus even when the test fish were returned to metal-free environment for a period of seven days. For the lead-exposed fish, temperature had a definite inverse effect on the concentrations of the metal in the mucus (Table 6). That is, the fish exposed at 4°C accumulated much higher amounts of lead than those exposed at 10°C. However, no such temperature effect was observed for the cadmium-exposed fish. Both lead and cadmium were accumulated to a similar extent in the mucus of the fish challenged at 10°C; however, cadmium discharged at a faster rate than lead when the fish were placed in metal-free water for depuration.

The pattern of accumulation and discharge of metals exhibited by the flatfish mucus is quite different from that observed for coho salmon mucus (OCSEAP Quarterly Report RU 73, September 1976). On freeze-drying the mucus samples, it was found that samples from both species contained about 98% water. However, flatfish mucus contained 250 ± 20 mg percent total protein and coho salmon mucus contained 140 ± 30 mg percent total protein. Mucus from the two species is currently being analyzed for amino acids to discern any differences that may be correlated with the differential capacity of these mucuses to bind or sequester metals.

Skin

Concentrations of metals increased continuously in the flatfish skin during the entire exposure period (Figs. 6 to 9). Scales were not separated from the skin before analyses. Lead was accumulated to a much greater extent than cadmium in the skin of test fish (Table 6). Concentrations of lead in the skin increased during depuration of lead-exposed starry flounder indicating that the skin/scales was a storage site for lead. A similar situation was not observed for cadmium.

c. Biotransformation of trace metal compounds:

Marine Fish

The data in Tables 7, 8, 9, and 10 give results on the accumulation and subcellular distribution of lead in coho salmon and starry flounder exposed to ppb levels of this metal in surrounding seawater. The accumulation of lead in coho salmon and starry flounder is characterized by significant bioconcentration factors in both gills and kidney (Tables 7 and 8). The posterior kidney is a prominent site for lead accumulation in both species of fish. Moreover, after 8 and 37 day depuration periods substantial levels of lead still persist in both organs. The data also indicate that starry flounder show a notable tendency to accumulate lead in the brain in comparison to coho salmon. For example, after 15 days of exposure to 150 ppb of lead at 10°C, brain of salmon was found to contain 6 ppb of this metal; however, under similar conditions starry flounder brain was found to contain over 500 ppb of lead. In both species, the blood, notably the erythrocytes, contained substantial amounts of accumulated lead.

In the cell fractionation studies with liver and kidney of coho salmon and starry flounder it is notable that a significant portion of accumulated lead appeared in the enzyme-rich microsomal and cytosol fractions.

4. Pathological

Pathological effects on flatfish of exposure to oil-contaminated sediment

a. Sediment preparation:

Approximately 1,200 lbs of sediment have been collected from a selected beach north of Sequim, Washington, on the Strait of Juan de Fuca. This sediment is presently being frozen and thawed and analyzed

TABLE 7

Accumulation of lead in coho salmon (*Oncorhynchus kisutch*) and starry flounder (*Platichthys stellatus*) in exposures at 5 ppb in seawater

Species Temperature Exposure period	Coho salmon 10°C		Starry flounder 10°C	
	28-Day U* ppb	28-Day U ppb	18-Day D** ppb	54-Day D ppb
Gills	12			
Liver	5	13	18	21
Kidney	19	7	11	22
anterior				
Kidney	53	6	12	19
posterior				
Blood	2	21	14	14
Erythrocytes	9			
Plasma	<1			
Brain	<1	4	9	10

* U = uptake

** D = depuration

TABLE 8

Accumulation of lead in coho salmon (*Oncorhynchus kisutch*) and starry flounder (*Platichthys stellatus*) in a 15-day exposure at 150 ppb in seawater.

Species Temperature Exposure period	Coho salmon					Starry flounder			
	4°C		10°C			4°C		10°C	
	15-Day U* ppb	7-Day D** ppb	15-Day U ppb	8-Day D ppb	37-Day D ppb	15-Day U ppb	7-Day D ppb	15-Day U ppb	8-Day D ppb
Gills	1,062	1,102	1,533	1,433	760	404	417	1,546	709
Liver	269	297	409	447	225	578	500	744	1,138
Kidney anterior	272	304	468	673	677	557	557	1,871	568
Kidney posterior	1,094	1,760	1,798	1,985	2,218	701	852	1,288	716
Blood	282	206	179	132	26	314	344	525	544
77 Erythrocytes	539	444	784	461	189				
Brain	4	8	6	14	7	202	363	529	491

* U = uptake

** D = depuration.

TABLE 9

Subcellular distribution of lead in coho salmon (*Oncorhynchus kisutch*) after exposure to 150 ppb of lead at 10°C in seawater

Exposure Organ	15-Day U*			8-Day D**		
	Liver percent	Kidney anterior percent	Kidney posterior percent	Liver percent	Kidney anterior percent	Kidney posterior percent
Cell fraction						
cellular debris	18	34	40	7	25	33
mitochondrial	26	22	21	13	28	15
microsomal	20	13	14	40	33	28
cytosol	30	11	10	40	14	10
Percent of total metal recovered	94	80	85	100	100	86

* U = uptake

** D = depuration

TABLE 10

Subcellular distribution of lead in starry flounder (*Platichthys stellatus*) after exposure to 5 ppb of lead at 10°C in seawater

Exposure period Organ	30-Day U*			18-Day D**			54-Day D		
	Liver percent	Kidney anterior percent	Kidney posterior percent	Liver percent	Kidney anterior percent	Kidney posterior percent	Liver percent	Kidney anterior percent	Kidney posterior percent
Cell fraction									
cellular debris	20	51	41	23	40	38	33	78	68
mitochondrial	6	8	7	4	8	10	11	9	9
microsomal	21	4	7	12	11	11	15	13	14
cytosol	46	33	35	55	41	46	43	6	17
Percent of total metal recovered	93	96	93	94	100	105	102	106	108

* U = uptake

** D = depuration

for hydrocarbons and particle sizes. Upon arrival of a new lot of Prudhoe Bay crude oil, the sediment and oil will be mixed.

b. Experimental facilities and fish care:

Existing aquaria are presently being modified by replacing the sheet fiberglass false bottoms with supports containing fine mesh screens. Arrangements have been made to obtain experimental fish from unpolluted areas of Puget Sound, Washington.

IV. PRELIMINARY INTERPRETATION OF RESULTS

1. Behavioral

Effects of petroleum on salmon homing:

Electrophysiological studies indicate that salmon detect aromatic hydrocarbons in the water at levels well below 1 ppm (See OCSEAP Quarterly Report RU 73, June 1976). Exact thresholds of hydrocarbon detection have not been determined. However, extrapolation of data based on amplitude of olfactory neural response and concentrations tested suggest that salmon should certainly be capable of detecting aromatics at levels less than 100 ppb. The results of the present experiment indicate that adult chinook salmon, though almost surely capable of detecting the presence of the tested hydrocarbons at the concentrations used (up to 600 ppb calculated by flow rate or 336 ppb by gas chromatography), do not avoid home stream water when the hydrocarbons are present.

2. Morphological

Effects of petroleum on fish eye lenses:

Such drastic changes as were observed in the size of the lens could produce severe myopia. It should be re-emphasized, however, that the amount of oil applied to food (1 g/kg) in these studies was very large.

Factors contributing to the etiology of lens enlargement are still being studied, as well as possible adverse effects on the fish of such changes. Lens enlargement could be a reflection of eye-specific effects of oil exposure or could reflect alterations in fluid balance that result, for example, from kidney tubule damage. Particular emphasis is being placed on studies to determine if much lower levels of oil than previously fed can induce similar lens abnormalities.

3. Chemical

a. Biotransformation of petroleum hydrocarbons:

Shrimp

The findings with shrimp imply that the mature animals readily sequester hydrocarbon components of a WSF in a period of one week. The thoracic segments appear to be a predominant site for accumulating the low molecular weight benzenes and naphthalenes. The fact that only trace amounts of hydrocarbons were detected in abdominal segments suggests that the spot shrimp tend to selectively deposit the more water-soluble hydrocarbons in certain body tissues. At present no information is available on the ability of these organisms to deplete thoracic segment tissues.

Biotransformation of petroleum hydrocarbons:

Marine Fish

The data presented in Tables 4 and 5 on the accumulation of hydrocarbons from the WSF of Prudhoe Bay crude oil by both coho salmon and starry flounder indicate that dramatic species differences exist in the tendency to deposit the low molecular weight hydrocarbon structures in key tissues. The C₄ and C₅-substituted benzenes are prominent in the muscle, liver, and gills, of exposed starry flounder and the muscle of

exposed coho salmon. Yet substantially greater concentrations of these aromatic structures appear to occur in the muscle of exposed starry flounder compared to that of muscle of coho salmon; the differences often exceeding an order of magnitude. Moreover, as mentioned in the previous report, hydrocarbons were not detected in either the liver or gills of coho salmon exposed to WSF of Prudhoe Bay crude oil. Nevertheless, with starry flounder, substantial accumulation of substituted and unsubstituted naphthalenes and benzenes were found in liver and gills as shown in Table 5. Present data indicate that starry flounder accumulate very large proportions of water-soluble hydrocarbons in comparison to salmonids. It seems reasonable to speculate from our data that levels of Prudhoe Bay WSF in the fraction of a ppm range may result in readily detectable accumulations of hydrocarbons in starry flounder after exposures of a week or greater durations. Experiments are in progress to verify these conclusions. It will be interesting to determine whether the tendency demonstrated by starry flounder to accumulate high proportions of aromatic hydrocarbons from surrounding water is reflected in animals exposed to oil-impregnated sediments.

b. Biotransformation of trace metal compounds:

Marine Fish

The results obtained for coho salmon and starry flounder exposed to ppb levels of lead indicate that a one- to three-week exposure can result in bioconcentration factors of about 10 in organs such as gills and posterior kidney. Because lead is a neurotoxin it is of interest to note that starry flounder tends to accumulate a relatively high level of this metal in the brain. Also of interest is the fact that both species tend to deposit a high proportion of lead, accumulated in kidney and

liver, in enzyme-rich fractions of the cell, such as the microsomes and cytosol.

c. Trace metal concentrations in flatfish skin and mucus:

Compared to coho salmon mucus (OCSEAP Quarterly Report RU 73, June-September 1976) flatfish mucus accumulated much higher concentrations of metals. In the case of coho mucus, maximum levels of metals (bioconcentration factors of 2 to 3) were reached within a few hours of exposure and these levels remained virtually constant for the rest of the exposure period. On the other hand, flatfish mucus accumulated substantial amounts of either lead or cadmium (bioconcentration factors of 12 to 14) initially and then the levels began to decline steeply for the rest of the exposure period. Furthermore, flatfish mucus was much more elastic or viscous and was very difficult to dissolve in water. Coho mucus was quite fluid and was easily dissolved in water. Rosen and Cornford (Rosen, M.W. and N.E. Cornford, 1971, Fluid and friction of fish slimes, Nature 234, 49-51) have proposed that rheological or viscoelastic properties of mucus are related to the swimming habits of fish. That is, faster swimming fish apparently possess mucus that is more effective in reducing friction when dissolved in water and also the mucus is more easily soluble in water. Differences observed in physical properties of coho mucus and flatfish mucus may be related to this phenomenon.

Different patterns of uptake and accumulation of metals in the flatfish and coho mucus prompts us to speculate that flatfish mucus may contain more binding sites for metals than coho mucus. Further, in contrast to coho mucus, when the metals lead and cadmium are sequestered by the flatfish mucus, they do not appear to exist primarily in a labile

equilibrium with the metals in the water. The initial high concentrations of metals which accumulated in the flatfish mucus and which were followed by a steep decline, suggests that the presence of lead or cadmium in the mucus, after an induction period of several hours, triggers a more rapid turnover of mucus in the flatfish. However, at present we do not have any substantiating evidence to support such an hypothesis.

It should be noted that significant concentrations of metals, especially lead, persist in the mucus of fish returned to clean water for several days. Whether the presence of high concentrations of metals induces any structural alterations in the mucus remains to be seen.

It may be that as with coho salmon, lead in the flatfish is associated primarily with the scales, rather than the skin. Concentration of lead in the skin/scales increased during the depuration period, indicating a role of the skin and/or scales in the storage of lead. The presence of high concentrations of lead persistent in the skin, scales, and mucus, may be deleterious to the well-being of the fish in several ways, although at present little is known about this.

4. Pathological

Pathological effects on flatfish of exposure to oil-contaminated sediment

No experiments have been completed.

V. PROBLEMS ENCOUNTERED/RECOMMENDED CHANGES

1. Behavioral: None

2. Morphological: None

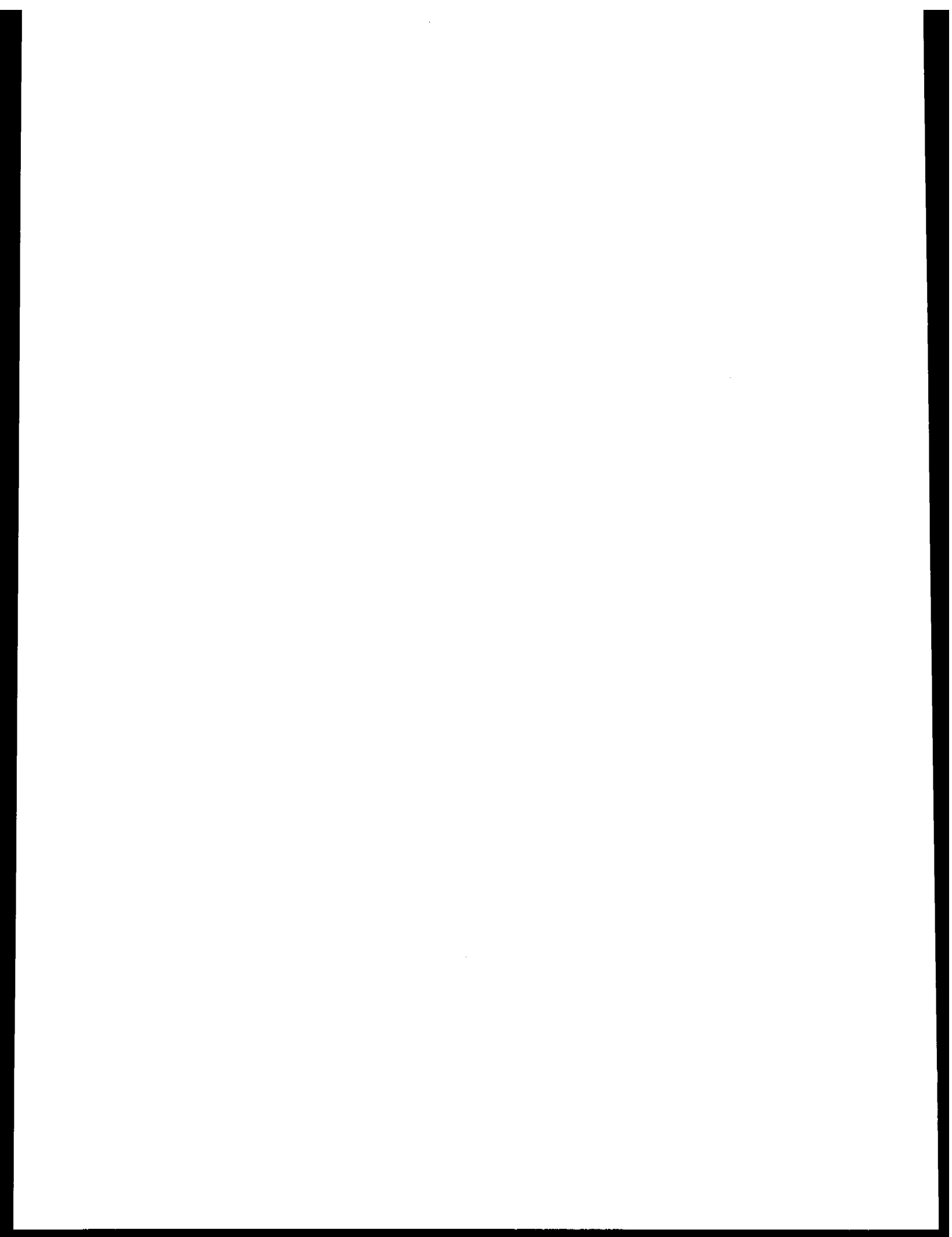
3. Chemical: A correction is required for some data given in Table III of the progress report for RU 74 for April-June 1976. Values given for picograms HC/mg dry weight should be multiplied by 1.46.

4. Pathological: We are presently unable to begin exposing flatfish to oil-contaminated sediments because of the lack of sufficient quantities of fresh Prudhoe Bay crude oil.

VI. ESTIMATE OF FUNDS EXPENDED

Salaries including Environmental Conservation Division:

October	7,280.78
November	8,863.33
December	<u>9,426.93</u>
Total	25,571.04
<u>Travel:</u>	613.99
<u>Rents (phone):</u>	464.71 (Dec. estimates)
<u>Printing:</u>	49.00
<u>Services:</u>	2,120.51
<u>Supplies:</u>	7,877.44
<u>Equipment:</u>	<u>7,601.60</u>
Total	44,298.29



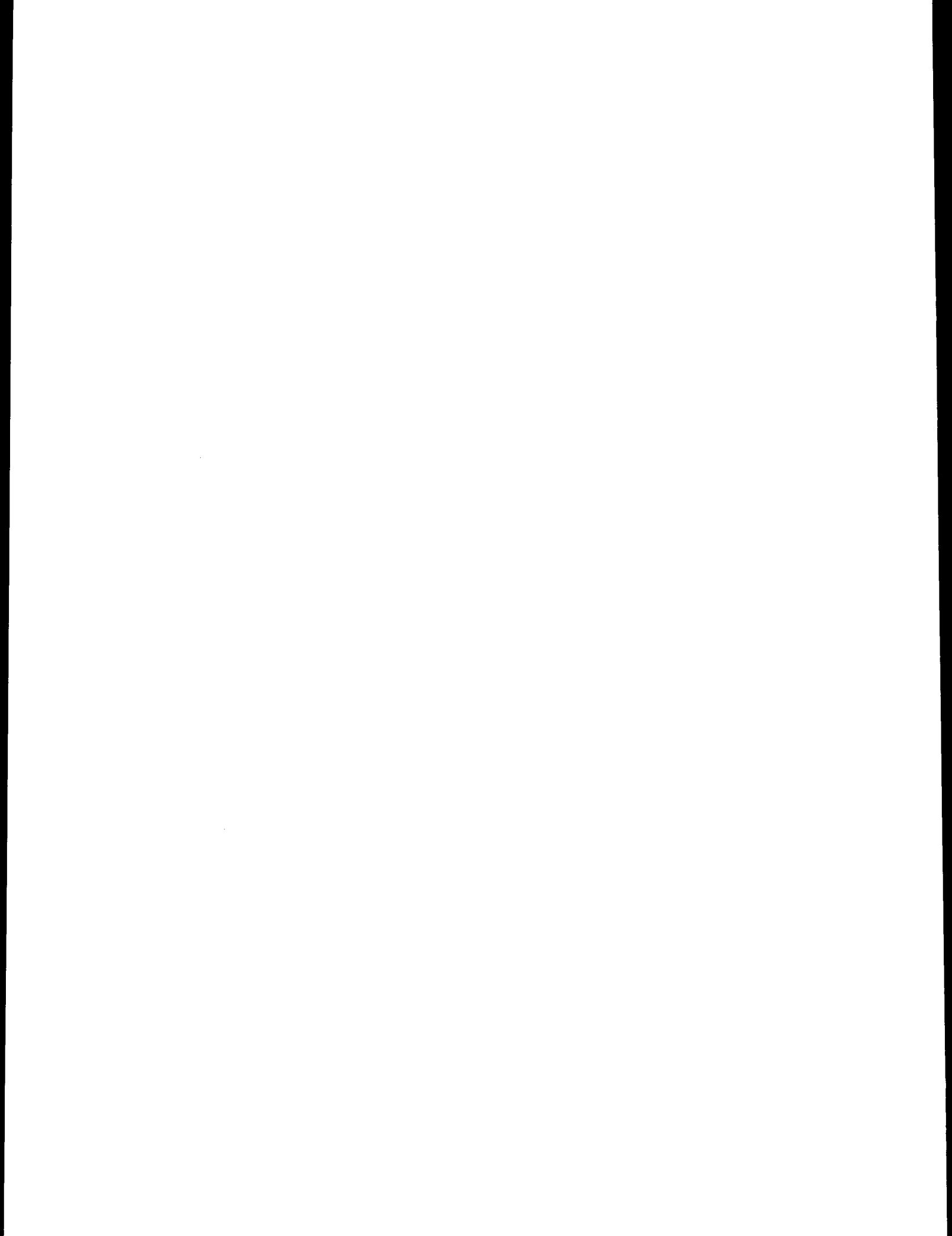
RU# 75

NO REPORT RECEIVED

A final report is expected next quarter

Supplemental reference:

Malins, D. C., Editor. Effects of Petroleum on Arctic
and Subarctic Marine Environments and Organisms,
Academic Press, NY (In Press, 1977)



QUARTERLY REPORT

Contract No.	:None
Research Unit No.	:RU-77
Reporting Period	:Oct 1 - Dec 31, 1976
Number of Pages	:1 (+ two attachments)

ECOSYSTEM DYNAMICS, EASTERN BERING SEA

Co-Principal Investigators

Taivo Laevastu and Felix Favorite
National Marine Fisheries Service
Northwest and Alaska Fisheries Center

I. Task Objective:

Formulation of a multicomponent, dynamic, numerical ecosystem model for the eastern Bering Sea.

II. Field or Laboratory Activities:

A. N/A

B. T. Laevastu, K. Larson

C. Restructuring of sub-model formats, and the acquisition of data on whales.

D. N/A

E. N/A

III. Results:

This contract was not renewed promptly in October, thus new results are not available at this time. However, two reports based on initial use of the 8-component model (see RU-77 Annual Report for 1976) are attached: Evaluation of standing stocks of marine resources in the eastern Bering Sea (Laevastu and Favorite), NWAFC Processed Report, 1976, 35 p; and Consumption of copepods and euphausiids in the eastern Bering Sea as revealed by a numerical ecosystem model (Laevastu, Dunn and Favorite), NWAFC Processed Report, 196, 18 p.

IV. Preliminary Interpretation of Results:

None

V. Problems Encountered/Recommended Changes:

None

VI. Estimate of Funds Expended:

\$6,700.00

Northwest and Alaska Fisheries Center

Processed Report

EVALUATION OF STANDING STOCKS OF
MARINE RESOURCES IN THE EASTERN BERING SEA

(using a static-trophic numerical
Bulk Biomass Model BBM)

by

T. Laevastu and F. Favorite

Resource Ecology Task

Resource Ecology and Fisheries Management Division

U.S. Department of Commerce
National Oceanic and Atmospheric Administration
National Marine Fisheries Service
Northwest and Alaska Fisheries Center
2725 Montlake Blvd. East
Seattle, Washington 98112

October 1976

Contents

Abstract.

1. Dynamics of the standing stocks in relation to ecosystem internal consumption.
 - 1.1 Purpose of the model study.
 - 1.2 Basic relations between standing stock, growth, and consumption, and a method for determination of plausible standing stock.
2. Bulk Biomass Model (BBM).
3. Plausible standing stocks in the eastern Bering Sea and their trophic interactions.
4. Fishery in relation to ecosystem trophodynamics.
5. Starvation and/or efficient food conversion in marine ecosystem and their consequences.
6. References.

List of Figures

- Figure 1. Schematic presentation of quasi-equilibrium state of a standing stock.
- Figure 2. Schematic food flow diagram for BBM model.
- Figure 3. Iteration scheme.
- Figure 4. Marine mammals and birds in eastern Bering Sea (monthly mean biomass, kg/km^2).
- Figure 5. Consumption of pelagic marine ecological groups by mammals and birds.
- Figure 6. Consumption of demersal marine ecological groups by mammals and birds.
- Figure 7. Simulated simplified monthly standing stocks of phyto- and zooplankton in eastern Bering Sea.

III

List of Tables

- Table 1. Mammals (excluding whales) in eastern Bering Sea and their food composition (input to BBM model).
- Table 2. Composition of food of major ecological groups in eastern Bering Sea (input to BBM model).
- Table 3. Growth, mortality, and food coefficients for major ecological groups in eastern Bering Sea (input to BBM model).
- Table 4. Monthly growth rates in percent.
- Table 5. Annual consumption in eastern Bering Sea, kg/km^2 (as computed with BBM model).
- Table 6. Annual mean consumptions, standing stocks, and mean annual turnover rates (kg/km^2) in eastern Bering Sea (as computed with BBM model).
- Table 7. Ecosystem internal consumption and fishery in eastern Bering Sea, assuming $800,000 \text{ km}^2$ area (as computed with BBM model).

Evaluation of Standing Stocks of Marine Resources
in the Eastern Bering Sea

by

T. Laevastu and F. Favorite

Northwest and Alaska Fisheries Center
Seattle, Washington

ABSTRACT

Standing stock size of any marine ecological group is dependent, besides recruitment, on ecosystem internal consumption and growth, and on mortality rates. Growth-rate data are generally available, as are fishing and natural mortality rate estimates. The ecosystem internal consumption can be determined by food requirements (for growth and for maintenance) and composition of food of all components of the marine ecosystem. A static-trophic numerical Bulk Biomass Model that computes the ecosystem internal consumption is programmed and uses an iterative technique to derive plausible standing stocks of various ecological groups, using growth and mortality data. Model computations indicate that the availability of food is the main factor limiting the size of standing stocks of most ecological groups above herbivores; the need for further research on food coefficients, composition of food, and feeding habits is emphasized.

Model results indicate that: (1) only a small fraction of the annual phytoplankton production is used directly by herbivorous zooplankton and pelagic fish (<10%), and the bulk of this production

must go to a regeneration cycle or sink to the bottom where it is consumed as detritus by benthos; (2) the estimated consumption of zooplankton is considerably higher than the standing stock and production (as ascertained from available data) would permit, indicating that the present quantitative zooplankton data are deficient and/or starvation is rather common in the sea; and (3) there must be considerable standing stocks of squids and small pelagic fish (Pacific herring, Clupea harengus pallasii; capelin, Mallotus villosus; smelt, family Osmeridae; etc.) in the Bering Sea ($>3.5 \text{ ton/km}^2$ and ca 8 ton/km^2 , respectively) to satisfy the food requirements for other ecological groups grazing upon them.

Plausible standing stocks of various ecological groups in the eastern Bering Sea are presented. In general, it can be postulated that the food coefficients of the fish (both for growth and maintenance) are lower (i.e., fish is more efficient in food utilization) than assumed heretofore and that a considerable part of the biomass of fish is in recruitment juveniles, which have high growth coefficients.

1. DYNAMICS OF THE STANDING STOCKS IN RELATION TO ECOSYSTEM

INTERNAL CONSUMPTION

1.1 Purpose of the model study

A marine ecosystem is characterized by a complex web of interspecies interactions (i.e., one preying upon the other), and by interactions between the species and the environment. There is an intense competition for living space and food, and the removal of part of one component of this ecosystem by the fishery will cause an increase and/or decrease in other components, by altering the delicate balance (or imbalance). Thus, in order to evaluate changes in abundances and distributions of different marine living resources, realistic quantitative numerical models, which depict processes in the ecosystem, must be used; the conventional, single-species fisheries models are no longer adequate. A complex, dynamic, numerical, marine ecosystem (DYNUMES) model development is in progress at the Northwest and Alaska Fisheries Center (NWAFC), and prior to applying some features of this model to the eastern Bering Sea area, it was deemed necessary to program a static-trophic Bulk Biomass Model (BBM). The latter permits determination of the plausible sizes of standing stocks of various ecological groups in the eastern Bering Sea, and provides quantitative insight into the ecosystem internal consumption as compared to the loss due to the fishery. This model has provided a considerable amount of preliminary information on trophic conditions in the Bering Sea ecosystem. Some results are reported below.

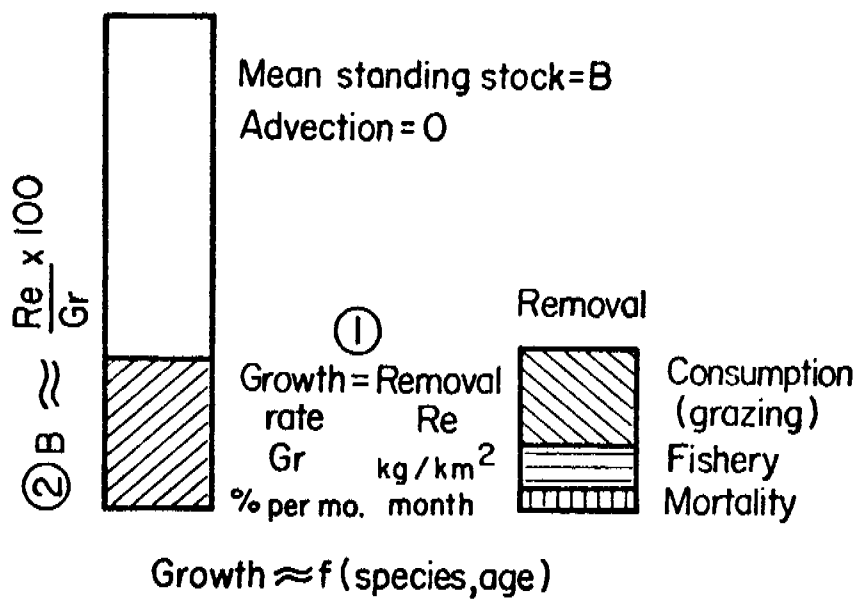


Fig. 1--Schematic presentation of quasi-equilibrium state of a standing stock.

1.2 Basic relations between standing stock, growth, and consumption; a method for determination of plausible standing stock

Assuming that the magnitude of a given standing stock does not fluctuate materially from year to year (i.e., quasi-steady-state), its growth should equal consumption (grazing) plus losses due to the fishery and mortality (by old age and diseases) (see Fig. 1 for schematic presentation). It is assumed that there is no advection into or out of the area. This assumption would not cause any noticeable error on three accounts: First, the model deals with an overall mean (square kilometers as basic areal unit) for the eastern Bering Sea. Secondly, the eastern Bering Sea is a semi-closed sea, with relatively little in and out flow as well as little in and out migration. Thirdly, if noticeable migration in and out of the area occurs (e.g., birds, mammals) then the quantities present in each time step are prescribed and not determined iteratively within the model.

Some information on growth rates of various age groups of marine animals is available, as are estimates of the exploitable biomass for certain species, but the size of the total standing stock (biomass) is unknown. Thus, in order to estimate the latter, it is necessary to determine the sum of the consumption and natural and fishing mortalities and to equate this with growth and to compute the biomass:

$$B \approx \frac{Re \times 100}{Gr}$$

where B is biomass (e.g., mean value in kg/km^2)

Re is the sum of ecosystem internal consumption, mortality from old age and diseases, and removal by the fishery (also computed as biomass in kg/km^2)

Gr is biomass (bulk) growth rate, given in percentage in unit time (and/or time step used in the model, i.e., % per month).

Ecosystem internal consumption can be computed only if a relatively complete ecosystem is considered. However, certain simplifications can be made by lumping ecologically similar species into ecological groups, such as semi-demersal fish, called hereafter "roundfish" (e.g., Arctic cod, Boreogadus saida; saffron cod, Eleginus gracilis; Pacific cod, Gadus macrocephalus; walleye pollock, Theragra chalcogramma, etc.), small pelagic fish (e.g., capelin, Mallotus villosus; Pacific herring, Clupea harengus pallasii; etc.), and zooplankton (e.g., copepods and euphausiids, etc.). Mean composition of food and food coefficients (total, or separated by growth and maintenance requirements) must be estimated and prescribed for these ecological groups. A reasonable first guess estimate of a standing stock of one of the major ecological groups must also be available; this first guess can be altered in iterative computations. The (natural) mortality from "old age" and from diseases is, in most ecological groups, relatively small; possible errors affect the following iterative estimates of standing stock relatively little. Thus, the real natural mortality rate in our model refers to real mortality from "old age" and diseases and is not the same

as the conventionally used natural mortality in fisheries population dynamics, which includes also grazing. In our model the grazing (which is in most cases much greater than real natural mortality) is computed separately and not used as input parameter.

The "food flow diagram" for computation of grazing is shown on Figure 2 and the iterative procedure for computation of standing stock is schematically shown on Figure 3.

After the first iteration some quantitative information on consumption of most ecological groups is obtained and initial estimations of their standing stocks can be made by assuming maximum possible growth rates for the given ecological group. In order to adjust bulk growth rate, information on age composition of given ecological groups is useful, as the growth rate is fast in juvenile stages and decreases rapidly with age (i.e., it seems that a greater proportion of food is used for growth in young fish, whereas old fish use the food more for maintenance). Thus, the iterative method allows some indirect estimates to be made of the relative proportion of the prefishery population; such estimates have not been customarily made in the past. Using maximum growth rates and minimum consumption (i.e., estimate of low food coefficient) a minimum estimate of standing stock can be obtained.

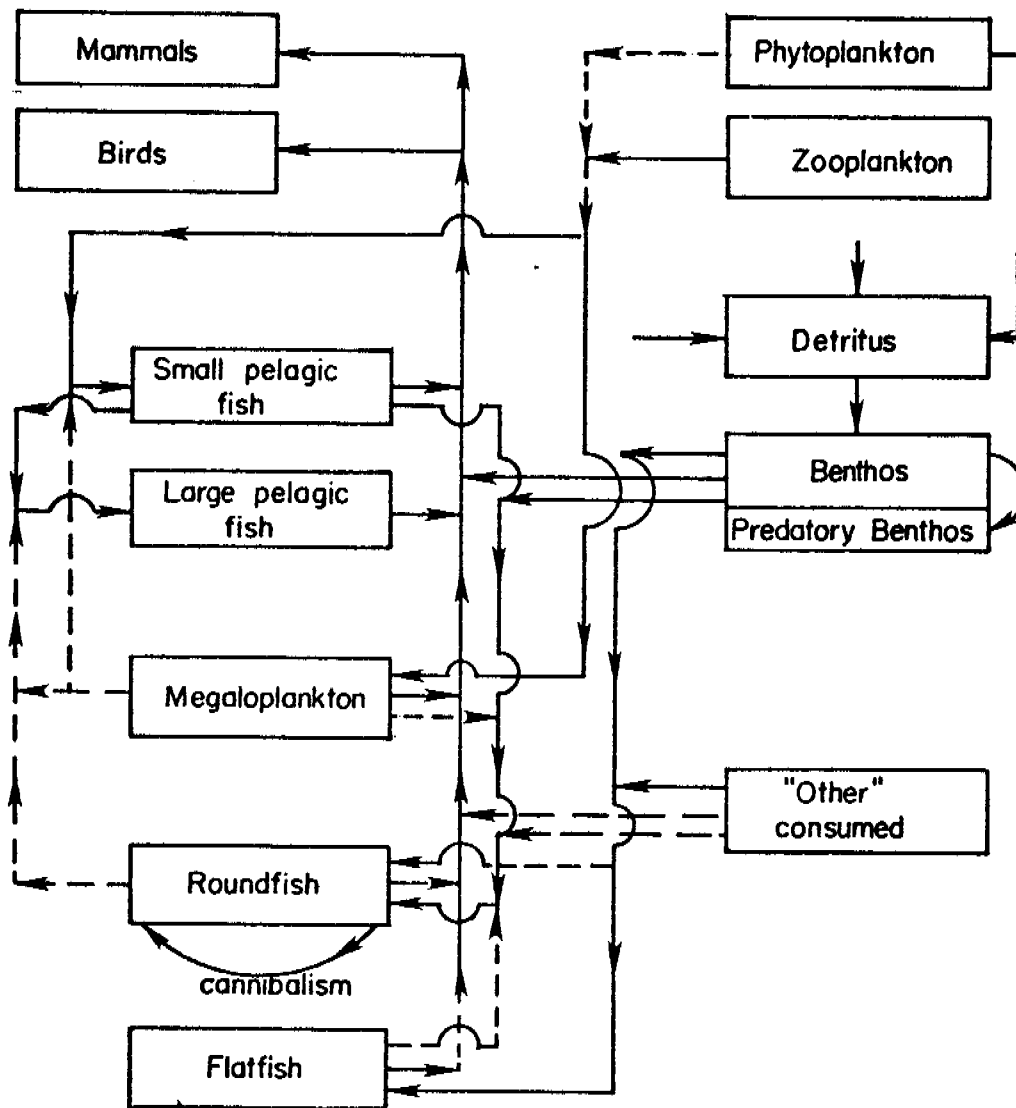


Fig. 2--Schematic food flow diagram for BBM model
 _____ major contribution; --- minor contribution

Figure 3.--Iteration scheme
(descriptive)

Notes: Food composition, food coefficients, fishery yield, and natural mortality prescribed.
Growth coefficients, below possible maximum, prescribed, changed in iterative tuning.
Mammal and bird populations prescribed.

<u>Computation</u>	<u>Assumptions, adjustments</u>	<u>Remarks</u>
A. Full year, each ecological group, in monthly time steps		
1. Consumption by mammals, birds	Popul. biomasses prescribed	Store consumptions of different groups, (for use in following comp.)
2. Consumption and biomass of roundfish	Initial biomass $6t/km^2$ Cannibalism 20% of cons.	Store consumptions (applies to all steps below)
3. Annual loss/gain of roundfish	Readjust biomass (1/15 of gain/loss)	Iterate until loss gain <10% pop. biom.
4. Consumption and biomass of large pelagic fish	Initial biomass=3x estimated mean salmon run	(Main cons. by mammals already computed)
5. Comp. as 3 above		
6. Consumption and biomass of small pelagic fish	Initial biomass=consumption to this step	(Assuming one turn-over a year)
7. Comp. as 3 above		
Continue with all ecological groups in similar manner		
B. Whole ecosystem by month through 3 years		
1. Consumption and biomass of all groups	Compute loss/gain Readjust growth coeff. and/or biomass	Use consumption of previous month
2. Repeat computation until quasi-equilibrium established for 3 years in whole ecosystem		Gain-decrease biomass Loss-adjust growth coeff. to max., there-after increase biomass (applies to individual groups)

2. BULK BIOMASS MODEL (BBM)

The food flow diagram of the Bulk Biomass Model (BBM) is shown in Figure 2. The following basic formulas--although modified as required for computation of different ecological groups, as indicated later--are used in the model.

Monthly biomass balance formula:

$$Q_{i,t} = Q_{i,t-1} (2 - e^{-g_{i,t}}) e^{-n} - C_{i,t} \quad (1)$$

$$\text{where: } g_{i,t} = g_{i,o} + g_{i,a} \cos(\alpha t - \mathcal{H}_{i,a}) \quad (2)$$

Food requirement and food proportioning formulas:

$$F_{i,t} = Q_{i,t-1} (2 - e^{-g_{i,t}}) K_{i,g} + Q_{i,t} K_{i,m} \quad (3)$$

$$C_{i,j,t} = F_{i,t} \rho_{i,j} \quad (4)$$

$$C_{i,k,t} = F_{i,t} \rho_{i,k} \text{ -- etc.}$$

$$C_{i,t} = C_{j,i,t} + C_{k,i,t} + \dots C_{n,i,t} \quad (5)$$

The symbols in the above equations are:

$Q_{i,t}$ - biomass (e.g., kg/km²) of ecological group i in month t
 $g_{i,t}$ - monthly bulk growth coefficient (approximately growth in % per month) (g_o is mean growth coefficient and g_a is the annual range of its change; \mathcal{H} is phase lag and α phase speed = 30° per month).

$F_{i,t}$ - food requirement for growth and maintenance (computed as kg/km²)

K_g - food coefficient for growth (e.g., 1:2 - 2 kg of food biomass gives 1 kg of growth)

K_m - food coefficient for maintenance (in terms of body (biomass) weight per time step)

$C_{i,t}$ - total amount of ecological group consumed by other groups in unit time (month)

$\rho_{i,j}$ - proportion of ecological group in the food of group i

The estimated number of mammal species (excluding whales) in the eastern Bering Sea is available (McAlister and Perez, 1976), together with the estimates of their mean weight and average composition of food (Table 1). An annual curve was fitted through the summer and winter biomass, computed as kg/km^2 (using 800,000 km^2 for the portion of the central and southern eastern Bering Sea area under consideration). The food requirement for mammals is reported as 6% to 8% of body weight daily (Sergeant, 1969); and the lower value (6%) was used in our model. Estimates on the total number of marine birds, their mean weight and average food composition, was taken from Straty and Haight (1976) and an annual curve was also fitted to the estimates. Although the marine birds' food requirement is usually estimated at 20% of body weight daily (Wiens and Scott, 1975), a lower value of 12% was used in our model, as a conservative (low) estimate was desired.

The first-guess input fields of fish groups (roundfish, flatfish, etc.) were based on a summarization of data available in voluminous literature. As walleye pollock (a roundfish) is the most abundant species in the eastern Bering Sea (see Low, 1976),

Table 1

Mammals (excluding whales) in Eastern Bering Sea
and their food composition (input to BBM Model)

Species	Average Number of Animals		Mean Weight (kg)	Percent Composition of Food					
	Summer	Winter		Roundfish	Herring	Salmon	Squids	Benthos	Others
Fur seal	550,000	96,000	65	80	5	2	11	--	2
Seal lion	100,000	50,000	400	80	10	10	--	--	--
105 Harbor seal	190,000	315,000	140	30	12	2	30	21	5
Ringed & ribbon seals	175,000	350,000	70	35	34	1	10	15	5
Bearded seal	75,000	200,000	240	8	8	1	8	70	5

it became the "basic species" for the start of iterations (i.e., its estimated standing stock of 5 million tons was prescribed as a first-guess field), and the formulas 1 to 5 (above) were used for iterative computations of the standing stocks of fish ecological groups (see Figure 3 and Tables 2 and 3 for input data).

The zooplankton consumption was computed on the basis of ecological groups that use these organisms as food (separated into copepods and euphausiids, when available data on composition of food permitted). The annual zooplankton and phytoplankton standing crop curves were simulated only in general terms; no attempt was made for their exact reproduction, except that the highest plausible standing stock values ascertained from the literature were used. A high value was also selected for benthos ($200\text{g}/\text{m}^2$), and it was assumed that only 25% of the benthos biomass consists of predatory benthos; model computations indicated that even with this relatively low proportion of predatory benthos, a large part of benthos food requirements must be satisfied by detritus.

Squids, decapods, amphipods, etc., were combined into an ecological group, called megaloplankton. Very little quantitative data are available on species belonging to this group, except some of these species that occur at times and areas as important food items in stomach analyses (e.g., squids).

Finally it was necessary to create an additional ecological group, called "others": stomach analyses often indicate unidentified food items that cannot be assigned to any of the other groups.

Table 2

Composition of Food of Major
Ecological Groups in Eastern Bering Sea
(Input to BBM Model)

Ecological group	Food	
	Item	Percentage
Megaloplankton (squids, etc.)	Copepods	30
	Phytoplankton	60
Small pelagic fish (herring, etc.)	Copepods	60
	Euphausiids	30
	Others	10
Large pelagic fish (salmon, etc.)	Euphausiids	10
	Squids	15 ^{1/}
	Herring	40 ^{1/}
	Roundfish	15 ^{2/}
	Others	20
Benthos	(Detritus, other benthos)	
Roundfish (pollock, etc.)	Herring	20
	Benthos	20
	Euphausiids	15
	Copepods	10
	Others	10
	Roundfish (cannibalism)	25
Flatfish (yellowfin sole, etc.)	Benthos	85
	Flatfish	15
	(cannibalism)	

1/ Herring includes smelt and capelin

2/ Mostly juvenile pollock

Table 3

Growth, Mortality, and Food Coefficients
for Major Ecological Groups in Eastern Bering Sea
(Input to BBM Model)

	Growth coefficient ^{1/}	Mortality coefficient	Food coefficients ^{2/}	
			Growth	Maintenance
Megaloplankton (squids, etc.)	15.6	4.5	1:6	--
Small pelagic fish (herring, etc.)	14.6	1.5 ^{3/}	1:3	+ 1.0
Large pelagic fish (salmon, etc.)	6.0	3.6	1:3	+ 1.3
Benthos (predatory benthos)	13.2	6.0	--	(0.67)
Roundfish	9.2	2.2	--	1.3
Flatfish	8.4	2.2	--	1.0

^{1/} % per month, most coefficients, except small pelagic fish, includes fishing mortality, which is computed separately.

^{2/} % body weight daily

^{3/} excludes fishery

Table 4

Monthly Growth Rates in Percent

Age interval (years)	Yellowfin sole ^{1/}	Alaska plaice ^{2/}	Pacific herring ^{3/4/}	Cod ^{5/}	Walleye pollock ^{6/}
1 to 2	14.30	15.17	6.35 to 7.08	14.35	10.83
2 - 3	7.46	7.26	2.57 to 3.09	6.31	5.69
3 - 4	4.39	4.46	1.74 to 1.88	3.97	3.03
4 - 5	3.74	3.27	1.29 to 1.53	2.70	2.14
5 - 6	2.06	2.60	0.82 to 0.95	1.87	1.69
6 - 7	1.66	1.95	0.82 to 0.99	1.35	1.22
7 - 8	1.62	1.99	0.56 to 0.60	0.99	1.20
8 - 9	1.61	1.43	--	--	1.11
9 - 10	0.85	1.12	--	--	0.92

^{1/} Slow growth in first year (3.9 g).

^{2/} Growth in first year, 8 g.

^{3/} Fast growth in first year (ca 30 g). Upper and lower limits given.

^{4/} Lower growth rate in herring applies to fish which had grown fast in first year and continues to grow fast.

^{5/} Very fast growth in first year (190 g).

^{6/} Growth in first year ca 50 g.

The addition of an artificial ecological group also contributes to lower estimates of specific standing stocks by decreasing the real consumption, which has been assigned to this artificial group, "others". This consumption can be later apportioned, either speculatively or on the basis of new food consumption data to real ecological groups.

3. PLAUSIBLE STANDING STOCKS IN THE EASTERN BERING SEA AND THEIR TROPHIC INTERACTIONS

The prescribed standing stocks of mammals and birds (Table 1) are converted to kg/km^2 , using a total area of $800,000 \text{ km}^2$ (Fig. 4). These bulk biomasses, together with food coefficients and composition of food, as described in previous sections, provide the bases for computations of consumptions by these organisms. As the estimates of standing stocks are relatively conservative, the consumptions of various marine ecological groups are also considered conservative (Figs. 5 and 6). Annual consumptions of various ecological groups by consumer groups are summarized in Table 5.

Model results indicate that the annual consumption of small pelagic fish (e.g., Pacific herring) by birds is six times as high as the annual catch of herring (see Table 7, column 4). It is most probable that a significant part of the small pelagic fish consumed is not herring but capelin and/or other pelagic species; however, this must be verified by additional bird stomach analyses. Such analyses would also permit estimating the consumption of juvenile

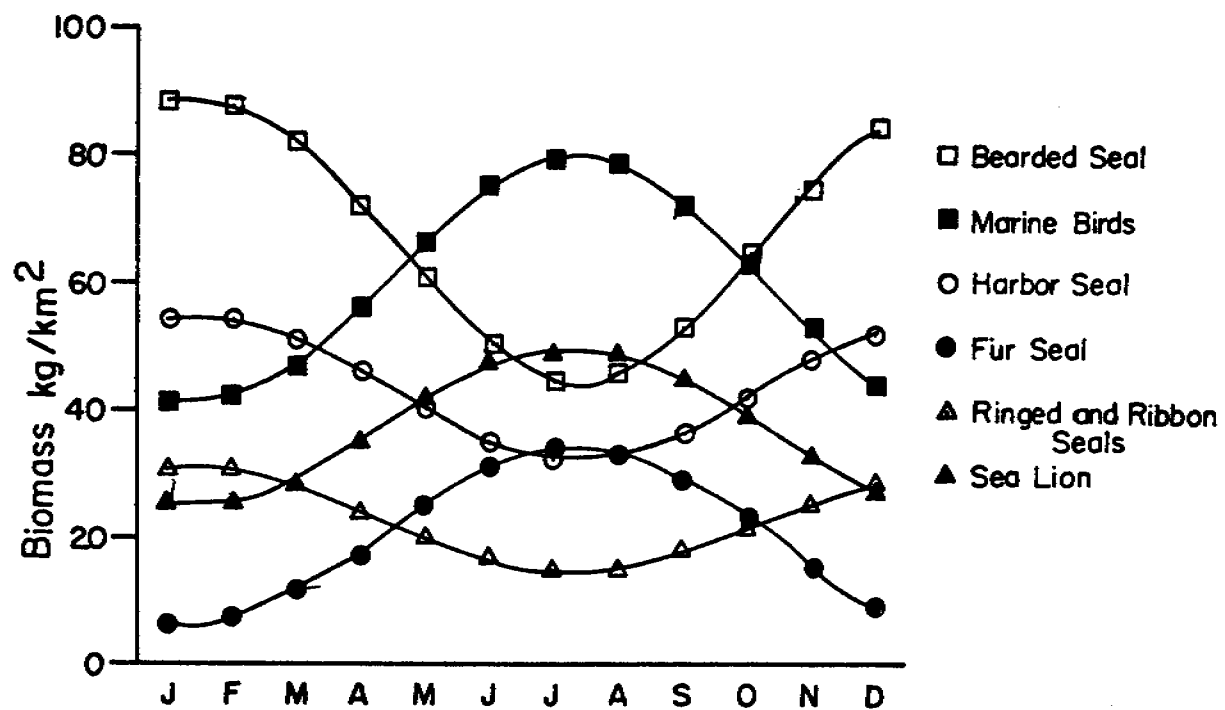


Fig. 4.--Marine mammals and birds in the eastern Bering Sea (monthly mean biomass, kg/km²).

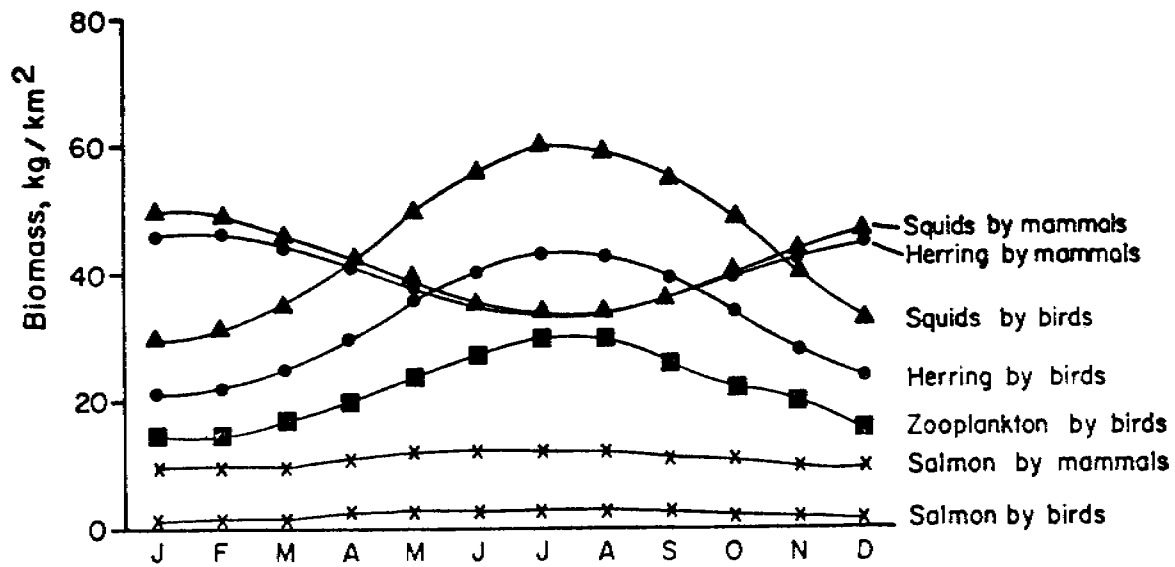


Fig. 5--Consumption of pelagic marine ecological groups by mammals and birds.

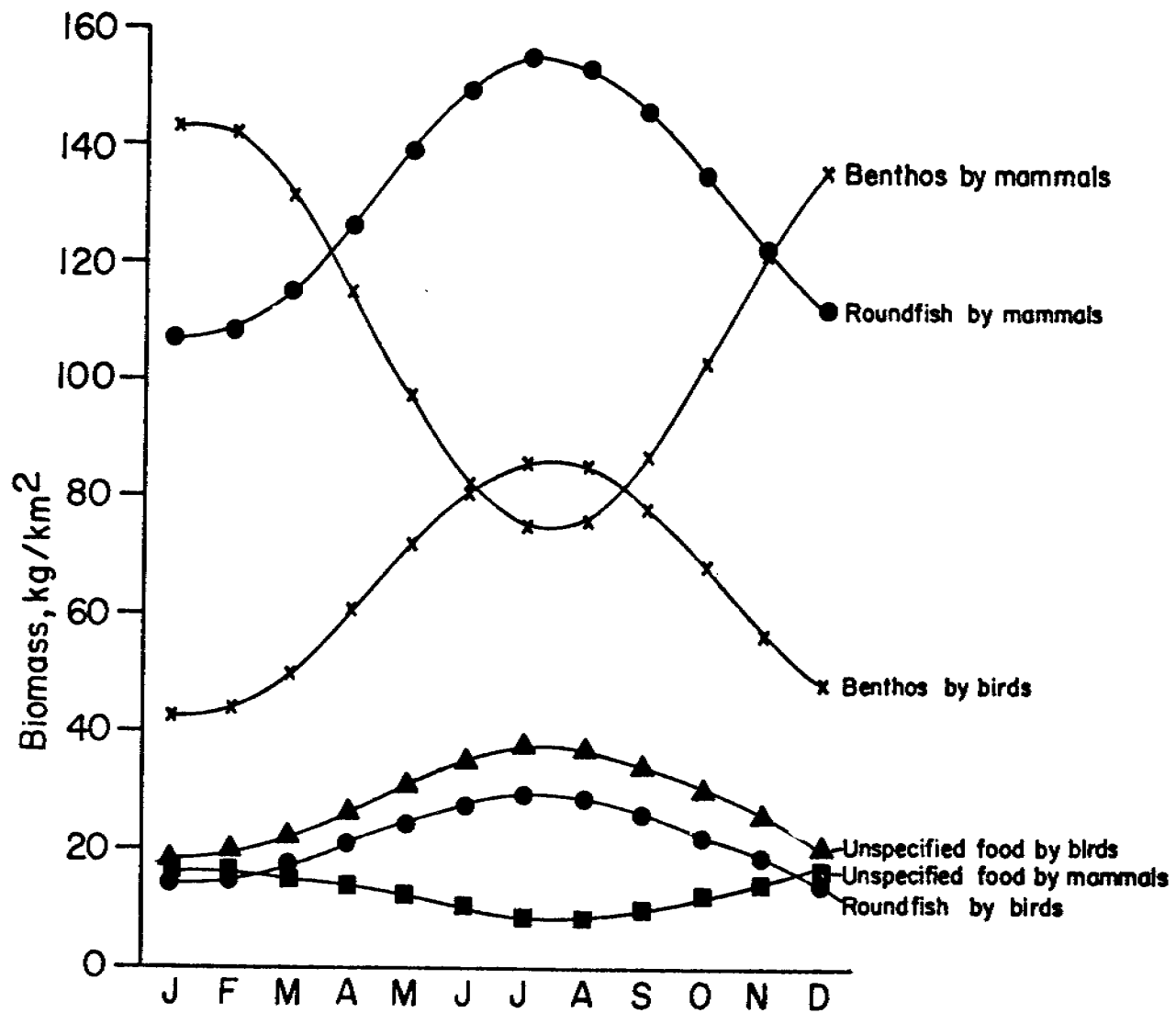


Fig. 6--Consumption of demersal marine ecological groups by mammals and birds.

Table 5

Annual Consumption in Eastern Bering Sea
kg/km² (as computed with BBM Model)

Consumer	Phytoplankton	Zooplankton	Squids	Herring	Salmon	Benthos	Roundfish	Flatfish	Others
Birds	--	(150)	540	390	(25)	780	260	--	340
Mammals	--	--	500	480	130	1,310	1,570	--	150
Zooplankton	(676) ^{1/} 33,800	--	--	--	--	--	--	--	--
Squids (megaloplankton)	--	15,000	--	--	--	--	--	--	--
Herring (small pelagic fish)	3,050	68,670	2,290	--	--	--	--	--	7,620
⁷¹¹ Salmon (large pelagic fish)	--	--	800	2,130	--	--	800	--	800
Benthos	--	--	--	--	--	(122,590) ^{2/}	--	--	--
Roundfish (pollock, etc.)	--	11,810	--	9,460	--	9,460	1,990	--	4,720
Flatfish	--	--	670	500	--	14,430	670	--	670
Totals	36,850	85,630	4,800	12,960	155	25,980 (148,570) ^{3/}	5,290	(1,200) ^{4/}	14,300

^{1/} mg/m³^{2/} Consumption by predatory benthos^{3/} Includes consumption by predatory benthos^{4/} Cannibalism, etc. computed as part of "others"

Pacific salmon, genus Oncorhynchus, by birds. Preliminary estimates indicate that birds may consume nearly half as much salmon (25 kg/km^2), as smolts and small juveniles, as the total commercial catch of salmon (ca 50 kg/km^2).

The quantitative BBM model indicates also that mammals might consume more than twice as much adult salmon (130 kg/km^2) and more than seven times as much Pacific herring (480 kg/km^2) as the total commercial catches of these species. The consumption of roundfish by birds is relatively insignificant (ca 12% of commercial catch), whereas the consumption of roundfish by mammals is about 75% of the total commercial catch.

Whereas some rough estimates of the monthly biomass of mammals and birds can be prescribed from available estimates of the numbers of these animals, the biomass of the fish must be derived through more indirect ways. An iterative procedure, which is based essentially on a trophodynamic approach, permits balancing of the internal and external consumption. Thus, it is necessary to introduce an average composition of food of various fish ecological groups into the model. Many qualitative notes on the composition of food of various species are available in the literature, which indicate that for any given species it varies within relatively wide limits (depending on species), both in space and time. Quantitative data on the composition of food are sparse; thus, additional research in this area is badly needed. Preliminary estimates of the mean composition of food of the ecological groups as used in the calculations reported in this paper are given in Table 2.

Food coefficients (or transfer or conversion efficiencies) are as important parameters in a trophodynamic bulk biomass model as the estimates of the composition of food. Unfortunately, the data on food requirements (and conversion) for growth and for maintenance are also scarce and variable. The food coefficient estimates for fish, available in the literature, vary from 1:3 to 1:15 (also dependent on species), the most common being between 1:5 - 1:10 (i.e., 10 g of food would give a 1 g increase in predator biomass). Rarely is a distinction made between the food coefficient for growth and the food coefficient for maintenance. Although some experimental data are available, specially for salmon, the general estimate for maintenance (food) energy requirement is ca 2% of body weight of food daily (1% per day being lowest value found in the literature). Obviously, the food (energy) requirements for growth and maintenance vary, not only from species to species, but also with age. This aspect of the food requirements, as well as of the growth relationships, is discussed briefly later. The average food coefficients used in the BBM model run reported here (Table 3) are also conservative.

The growth coefficients (Table 3) are "tunable" variables in the model within reasonable limits, as is the biomass which is being iteratively determined: if a given biomass decreases with time, it can be brought to equilibrium by either increasing the growth or increasing the initial biomass estimates. Data on growth are available in the literature for most species--however,

the growth rate varies with age of the species (Table 4), being high in the first 2 years and decreasing rapidly thereafter. This decrease of growth rate (biomass or weight change per unit time) can be interpreted two ways: first, the conversion of food to growth is more efficient in young populations than in old populations, the old population converting most of their food intake for maintenance energy; and second, the older, larger species might not be able to capture enough food in proportion to their weight due to a scarcity of food and its dispersed state. The growth coefficients, tuned to the values given in Table 3 are relatively high because of attempts to iterate minimum standing stocks; thus, these high growth coefficients also signify relatively young populations. Considering the measured growth coefficients (Table 4) and these used in the model (Table 3) it seems possible that more than half of the biomass of exploited populations is in pre-fishery juveniles.

The mortality coefficients (old age and diseases only, fishing mortality is computed separately) are estimated by considering the fishery and the age of the species (i.e., the fish populations which grow older, but are heavily fished, have low mortality rates). In most cases, the natural mortality of old age and of diseases is small in most exploited fish populations (<1.5% per month) as compared to ecosystem internal consumption (i.e., being eaten by others). The ecosystem internal consumption, computed with the BBM model, is based on biomass size, food coefficients (food requirements), and composition of food.

The annual consumption of different ecological groups by other groups in the eastern Bering Sea, summarized in Tables 5 and 6, is presented as kg per km². The only directly underutilized ecological group seems to be phytoplankton. Latest revised estimates in the literature support this result (e.g., most Russian reports show that between 5.5% and 15% of phytoplankton is utilized by zooplankton). However, two considerations must be added to this observation: first, phytoplankton must be considered as the main source of food (detritus) for benthos in this relatively shallow sea--preliminary computations show that the availability of detritus food is limiting the growth of the benthonic biomass; and second, the available estimates of the standing stocks of zooplankton (generally <400 mg/m³ or ca 20 g/m²) are apparently too low. Relatively crude simulated monthly standing stocks of phytoplankton and zooplankton are estimated (Fig. 7); these are used only for comparison with consumption in the model and do not enter into the direct computational loop for iteration of standing stocks of other ecological groups.

The main consumers of zooplankton are small pelagic fish (Pacific herring, smelt, capelin), squids, and juvenile roundfish (walleye pollock, cod). If we consider the annual consumption in relation to the highest value of mean standing stock as reported in the literature (Table 6), we find that the annual consumption alone would require an annual turnover rate of 4.3, which is an impossibility according to present knowledge on zooplankton production in the Bering Sea. Two explanations are offered: first, the present

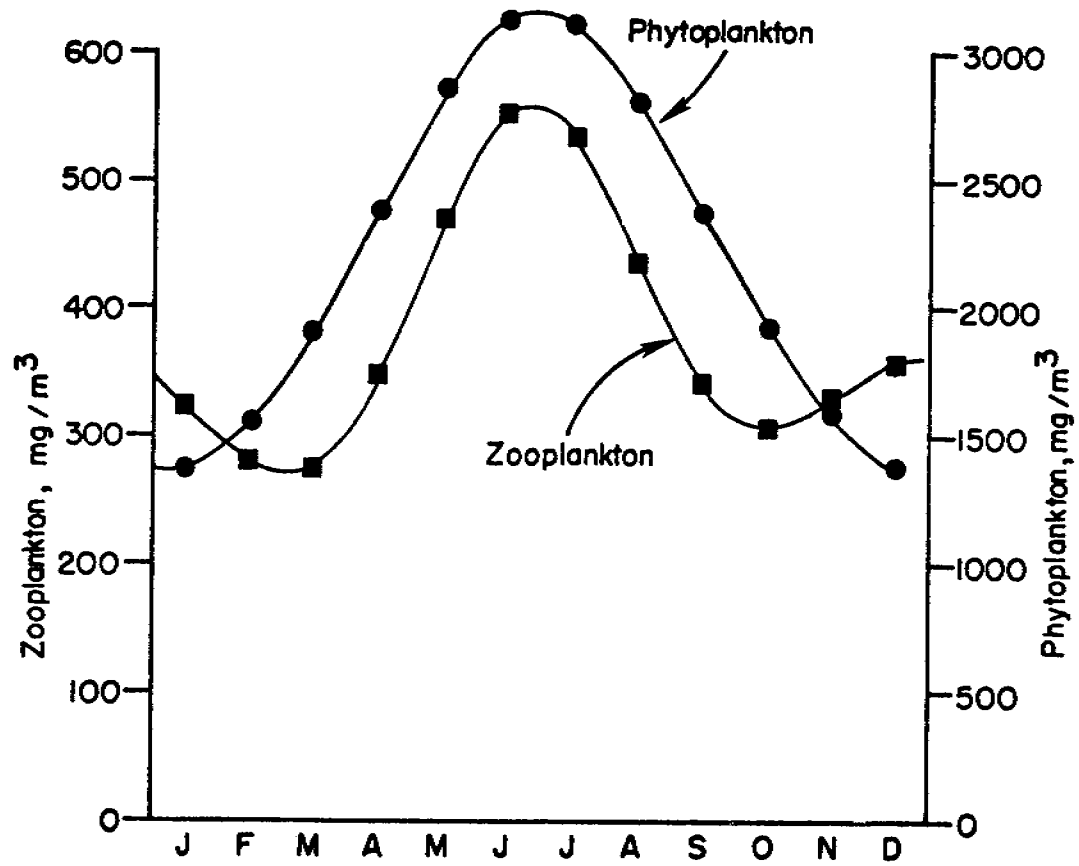


Fig. 7--Simulated simplified monthly standing stocks of phyto and zooplankton in the eastern Bering Sea.

Table 6

Annual Mean Consumptions, Standing Stocks, and Mean Annual Turnover Rates
(kg/km²) in Eastern Bering Sea (as Computed with BBM Model)

Ecological group	Monthly mean standing stock	Annual consumption ^{1/}	Mean natural annual turnover rate ^{2/}
Phytoplankton	(2,000) ^{3/} 100,000	36,850	(0.4)
Zooplankton (copepods, euphausids)	(400) ^{3/} 20,000	85,630	4.3
Megaloplankton (squids, etc.)	3,800	4,800	1.3
Small pelagic fish (herring, etc.)	8,200	12,960	1.6
Large pelagic fish (salmon, etc.)	760	155	(0.2)
Benthos	200,000	25,980	--
(predatory benthos)	(50,000) ^{4/}	(148,570) ^{5/}	(0.8)
Roundfish	9,800	5,290	0.5
Flatfish	4,700	(1,200) ^{6/}	(0.3)
Others	?	14,300	?

^{1/} All exclude fishery

^{2/} Standing crop/consumption (excluding fishery)

^{3/} mg/m³

^{4/} Predatory benthos

^{5/} Total consumption, including consumption by predatory benthos

^{6/} Cannibalism and consumption by roundfish, mammals ("incidental")

zooplankton sampling methods are deficient and do not permit catching the more mobile euphausiids; and second, starvation caused by insufficient availability of zooplankton prevails in the sea.

Squids are reported as food items in variable quantities in stomach analyses of birds, mammals, and various fish species. Besides some qualitative taxonomic studies of squids in the Bering Sea, nearly nothing is known about their abundance. Our present model estimates their abundance to be 3.8 tons/km^2 (or 3 million tons in the eastern Bering Sea). If their abundance is less, their relative quantitative occurrence in the diet of other ecological groups in the eastern Bering Sea must be smaller than estimated in our inputs and the difference must be replaced by other food items. What other organisms would serve as replacements is difficult to suggest because computations show all other food items to be in short supply.

The small pelagic fish, exemplified in the model by Pacific herring but including also such species as smelt and capelin, is assumed to feed mainly (90%) on zooplankton (copepods and euphausiids). The rest of the food (10%) is assumed to consist of phytoplankton, juvenile and small squids, and other unspecified food (meroplankton, mysids, decapods, amphipods, etc.). On the other hand, these small pelagic fish serve as important food items for most of the other fish, especially roundfish and mammals. The model estimate of the standing stock of the small pelagic fish in the eastern Bering Sea is 8.2 tons/km^2 , or 6.6 million tons. Unfortunately, little research has been carried out on this resource, as only herring has been subject to a fishery, whereas smelt and capelin are of no commercial importance.

The abundance of salmon has been estimated from the mean size of returning adult sockeye runs. These salmon enter the food web as food for some mammals (e.g., seals) and as consumers of small pelagic fish. As seaward migrating smolts, they mainly consume zooplankton. Due to the relatively rapid shoreward movement across the eastern Bering Sea, adult sockeye salmon, O. nerka, do not substantially influence the annual food budget in the eastern Bering Sea. However, the short term effects (monthly) may be substantial.

Most flexible in food habits are the roundfish (semi-demersal fish--walleye pollock, cod, etc.), which obtain their food from pelagic fish and benthos. The flexibility of food habits might be one of the reasons why pollock is the most abundant species in the Bering Sea. In addition to the general flexibility in food habits, pollock are also cannibalistic, the cannibalism increasing with age of the fish so that 65% of the food of fish longer than 50 cm is reported to consist of younger pollock. Cannibalism in pollock can cause long-period fluctuations in abundance; interactions in the fishery and the removal of the larger (more cannibalistic) pollock by fishery could result in an increase in standing stock. These phenomena will be reported and explained in a forthcoming report. In the present model, pollock is assumed to be only moderately cannibalistic. The mean standing stock of roundfish in the eastern Bering Sea is found by our iterative model to be 9.8 tons/km² or 7.8 million tons. This includes exploitable as well as prefishery populations. The main consumers of roundfish are mammals, roundfish (cannibalism) and the fishery. It could be postulated that the degree of cannibalism is a function of the availability or lack of food. 122

Although the flatfish can be divided into two groups by the composition of food and feeding habits--the large-mouth flatfish feeding mainly on benthos, and the small-mouth flatfish having food habits similar to roundfish--only one group was considered in our model, and it was made largely dependent on benthic food. The preliminary computations with the present model gives 4.7 tons/km^2 , or 3.8 million tons, in the eastern Bering Sea (total population, including prefishery juveniles). The computations of flatfish standing stock with the present model is, however, less certain than the computation of other ecological groups, largely because it has the smallest trophic interactions with the rest of the ecosystem as presently programmed.

The standing stock of benthos was assumed to be 200 g/m^2 , and 25% of it was assumed to be predatory benthos (possibly an underestimate). All the food of "fish food benthos" and half the food of the predatory benthos was assumed to be detritus. The consumption of the benthos was computed as dictated by the composition of food of the other ecological groups.

4. FISHERY IN RELATION TO ECOSYSTEM TROPHODYNAMICS

The computed monthly mean standing stocks of ecological groups of fish in the eastern Bering Sea, their annual consumption within the ecosystem, and mean annual catch (in recent years) are summarized (Table 7). The ecosystem internal consumption is compared to the fishery by computing the percentage of the latter from the former in the same table. A monthly mean fishing mortality coefficient

Table 7

Ecosystem Internal Consumption and Fishery in Eastern Bering Sea,
 assuming 800,000 km² area (as computed with BBM Model)

Ecological group	Standing stock	Ecosystem internal consumption	Fishery	Fishery (in % of internal consumption)	Monthly mean fishing mortality coefficient (%)
Pelagic fish (e.g. herring)	8,200	12,960	63	0.5	0.06
Roundfish	9,800	5,290	2,075	39	1.76
Flatfish	4,700	(1,200)	215	(18)	(0.38)
Salmon	760	155	50	33	0.55
Others (crabs, etc.)	?	(14,300)	(250)	(1.8)	—

(% of mean standing stock removed by fishery per month) is also given. The greatest component in relation to ecosystem internal consumption and the largest in general is that of roundfish (walleye pollock). This might be caused partly by the beneficial effects of the fishery on the standing stock of this species, as mentioned earlier.

The next largest fishery in relation to consumption is that of salmon, but the ecosystem internal consumption is relatively small in relation to the total biomass of the system.

The smallest fishery, but one subject to the largest ecosystem internal consumption, occurs in small pelagic fish (e.g., Pacific herring), which are also often called forage fish. It could be postulated that this fishery has a relatively small effect on fluctuations of the standing stock of herring; however, the pollock fishery by affecting the size and abundance of the main consumer of herring, should have a marked effect on herring abundance. As herring is under considerable pressure as forage, an additional, relatively small removal of herring can markedly affect the size and growth of its standing stock. This will be described in another report (demonstrated with a more complex ecosystem model DYNUMES).

5. STARVATION AND/OR EFFICIENT FOOD CONVERSION IN MARINE ECOSYSTEM AND THEIR CONSEQUENCES

Computations afforded by the BBM model show that the greatest part of most of the ecological groups are consumed as food by other ecological groups. Furthermore, the high growth coefficients together with high standing stocks (which are higher than any other estimates heretofore) indicate that the greater part of the biomass of the standing stocks must be juveniles.

All iterative computations in the model are made with very conservative (low) food coefficients, implying very efficient food conversion and/or starvation. Most of the quantitative results of the model depend on the above mentioned inputs. These inputs are, however, rather crude estimates, due to lack of proper data. It can be assumed that if availability of food is a limiting factor of production in the sea, as the model indicates, there must be a considerable spatial and temporal variability in the composition of food of any species. Further research in this matter is highly desirable as well as research in food requirements and conversion related to growth and maintenance.

Recent laboratory investigations have shown that one important consequence of partial starvation is the nonmaturation of gonads (Fluchter and Trommsdorf, 1974). This suggests that all adult fish might not spawn every year and that the size of the spawning stock would vary from year to year, depending on availability of food. Furthermore, the timing of the spawning period and its length might

well be influenced by food availability and temperature anomalies-- the influence of the latter being known from a number of other investigations.

The BBM model also indicates that the trophically controlled marine ecosystem is unstable and that minor changes in one component can influence other components rather profoundly by competition for food and availability of food. Thus, minor perturbations propagate rapidly through the whole ecosystem. Many further research needs are suggested by the model, such as the possible dependence of year-class strength on grazing on eggs and larvae being one of the principal causes of year class fluctuations.

Finally, the BBM model underlines the fact that enhanced evaluation and management of marine resources requires consideration of the dynamics of the marine ecosystem as a whole, rather than by individual studies of single species. A relatively complete Dynamical Numerical Marine Ecosystem (DYNUMES) model, presently in an advanced stage of development at the Northwest and Alaska Fisheries Center will (when completed) provide the basis for new and more effective research and management schemes.

6. REFERENCES

Fluchter, T., and H. Trommsdorf.

1974. Nutritive stimulation of spawning in common sole (Solea solea L.). Ber. Dtsch. wiss. Komm. Meeresforsch. 23:352-359.

Low, L. L.

1976. Status of major demersal fishery resources of the north-eastern Pacific: Bering Sea and Aleutian Islands. Natl. Mar. Fish. Serv., NOAA, Northwest and Alaska Fisheries Center, Seattle, Wash. Unpubl. Manuscr.

McAlister, W.B. and M.S. Perez.

1976. Preliminary estimates of pinniped-finfish relationships in the Bering Sea. Natl. Mar. Fish. Serv., NOAA, Northwest and Alaska Fisheries Center, Seattle, Wash. Unpubl. Manuscr.

Sergeant, D.E.

1969. Feeding rates of cetacea. Norway, Fiskeridir. Skr., Ser. Havunders. 15:246-258.

Straty, R. R. and R.E. Haight.

1976. Interaction of marine birds and commercial fish in the eastern Bering Sea. Natl. Mar. Fish. Serv., NOAA, Northwest and Alaska Fisheries Center, Auke Bay, Alaska. Unpubl. Manuscr.

Wien, J.A. and J.M. Scott.

1975. Model estimation of energy flow in Oregon coastal seabird populations. Condor 77:439-452.

CONSUMPTION OF COPEPODS AND EUPHAUSIDS
IN THE EASTERN BERING SEA AS REVEALED
BY A NUMERICAL ECOSYSTEM MODEL

by

Taivo Laevastu, Jean Dunn, and Felix Favorite*

September 1976

*Northwest and Alaska Fisheries Center, National Marine Fisheries Service,
NOAA, 2725 Montlake Boulevard East, Seattle, WA 98112

CONTENTS

	Page
Abstract.....	1
Introduction.....	2
Numerical Ecosystem Model.....	4
Zooplankton composition.....	4
Zooplankton consumption.....	6
Starvation or Inadequate Plankton Sampling?.....	13
Future Research.....	14
Summary.....	16
Literature Cited.....	18

CONSUMPTION OF COPEPODS AND EUPHAUSIDS
IN THE EASTERN BERING SEA AS REVEALED
BY A NUMERICAL ECOSYSTEM MODEL

By Taivo Laevastu, Jean Dunn, and Felix Favorite

ABSTRACT

The Division of Resource Ecology and Fisheries Management is formulating a Dynamic Numerical Marine Ecosystem (DYNUMES) Model for use in evaluating interactions of environmental and biological components. Initially, the model will be used in reference to the economically important eastern Bering Sea area, and a preliminary submodel which permits evaluation of the interactions of only 8 representative biological components in the area has been tuned to assess rough biomass balances. As a first step we have modelled general zooplankton consumption and compared this with zooplankton abundance. Results indicate that the monthly consumption is roughly equivalent to the monthly standing stock, an impossible situation. The usefulness of existing plankton data, which are obviously more qualitative than quantitative, in biological or ecosystem models is challenged, and cooperative integrated plankton and fisheries field studies are recommended to resolve the apparent dilemma.

INTRODUCTION

It was nearly a century and a half ago that the plankton net revolutionized marine biology studies and, although the cataloging of these microscopic forms has been reasonably complete for a number of years, there have been numerous controversies concerning the quantification of plankton data. The variety of sampling devices, net mesh sizes, and towing procedures are ample evidence of the difficulties in acquiring accurate samples. The variability in samples obtained by paired nets and replicate tows (in many instances as much as an order of magnitude or more) bear strong testimony as to the small-scale patchiness of organism distributions--not to mention the inherent large scale patchiness due to areas of convergence and divergence of various temporal and spatial dimensions. Fisheries groups have largely been willing to let biological oceanographers wrestle with this problem and have concentrated their efforts on ichthyoplankton assessments. However, the realization that only limited knowledge of fish species would stem from single species studies and that multi-species studies are required, has raised the issue that perhaps only through total ecosystem studies will adequate information on any one species be forthcoming.

During our attempts to formulate a conceptual ecosystem model of the eastern Bering Sea in order to evaluate the difficulties and complexities of such an undertaking, we were confronted with conflicting and confusing zooplankton data even though numerous studies have been made. In spite of the gross assumptions made with respect to the various coefficients used, there is a serious deficiency in the amount of zooplankton reported in the literature and an obvious requirement for forage by fish stocks calculated to be present. This, of course, poses a challenge to those

ecosystem models that begin with primary and secondary production estimates. We believe that it is important to point out these discrepancies because extensive and costly plankton surveys are being made in the eastern Bering Sea as a result of requirements for environmental impact statements prior to awarding offshore oil leases, and routine, standard sampling of the plankton biomass especially to an arbitrary depth level (e.g., 80, 100, 150 m, etc.) may result in a totally unrealistic assessment of these populations.

The eastern Bering Sea is unique in that it has not only one of the widest continental shelves (>500 km) of the world's oceans, but this area is relatively isolated by the land masses of the Alaskan Peninsula and eastern Siberia from the usual alongshore flows that sweep along the lengths of most continents--although Bering Strait provides a narrow, shallow passage into the Arctic Ocean. In addition, the shelf area is largely covered with ice each winter, resulting in homogeneous water temperatures less than -1°C ; but, in summer, surface temperatures in excess of 15°C occur, particularly in inshore areas. The varying conditions result in onshelf and offshelf movements of various biological components. It is an oceanic area that can reasonably be considered and treated as a fundamental ecosystem.

NUMERICAL ECOSYSTEM MODEL

The relatively complex conceptual numerical ecosystem model (DYNUMES), under development at the Northwest and Alaska Fisheries Center, has been described elsewhere (Laevastu, Favorite, and McAlister, 1976), and only those brief notes which are necessary to explain the findings presented in this paper are given below. The present 8-component model, a submodel of the DYNUMES model, permits deriving plausible standing stocks of pollock and herring using available data from the literature and an iterative method; other biological components such as mammals and birds are prescribed as monthly fields. The populations are distributed as available knowledge on migrations and occurrence dictates. Growth, fishing mortalities, and consumption by other species are computed in monthly time steps. Available data from literature on stomach content and food coefficients are used for computation of consumption rates, but in the present formulation, these factors do not have temporal and spatial variability. The food coefficient is computed as 1:2 for growth and 1% of body weight for maintenance, so an average food coefficient of ca 1:5 was used. The consumption of various "food items" (i.e., species or groups of species) is used, among others, to compute changes in population size of the consumed species and is stored on discs for various outputs, including summation over the entire computational area. Here we focus attention on the consumption of copepods and euphausiids as computed by the model and discuss the consequences of the findings to fisheries problems.

Zooplankton Composition

There are considerable data on zooplankton in the Bering Sea reported by various U.S., Japanese and Soviet scientists. Although the mean standing

stock reported varies between 100 and 300 mg/m³, 700 to 800 mg/m³ have been reported in the upper 20 meters of the water column during late summer in some areas, and maximum values of 2.5 g/m³ have occurred. The species composition as well as the frequency of occurrence of major species is well agreed upon, however, reproduction cycles are not well known. Although there are about four dominant species of copepods (Eucalanus bungii, Calanus plumchrus, C. cristatus, and Metridia pacifica) present in summer, eurythermic plankters (Oithona similis, Sagitta elegans, Calanus glacialis, Parathemisto libellula) are predominant in winter. Acartia longiremis and Pseudocalanus spp. are dominant forms in inshore waters. Generally, copepods produce only one generation annually (Metridia pacifica may produce up to four) and these occur at different times: C. cristatus in early winter; C. glacialis in late spring, followed by Eucalanus bungii; and Metridia pacifica from late spring to late fall. About 70 to 80% of the plankton biomass is considered to consist of copepods. The four dominant forms of euphausiids are Thysanoessa raschii, T. inermis, T. longipes, and T. spinifera, the first being primarily an inshore form, and it may require 2 years for these forms to reach maturity.

The data on zooplankton production are even less reliable than on standing stock, due to various indirect methods used for its estimation. The most frequently reported values of production are around 110 to 140 g/m² per year, variably referred to as copepod production and total zooplankton production. This value is in disagreement with some earlier estimates of zooplankton production in the Atlantic (3 to 8% of standing stock daily).

The zooplankton standing stock in the present submodel is created on the basis of available quantitative knowledge. It is made a function of time (month), latitude, and specific location (e.g., such as the continental shelf, etc.). Due to difficulty in obtaining reasonable values of zooplankton standing stock in time and space, it is more advantageous in the construction of an ecosystem model to compute the plausible consumption of zooplankton and to use only the relative zooplankton abundance for estimate of density dependent feeding. An example of areal distribution of zooplankton standing stock (in mg/m^3) as generated in our submodel for month of July, is shown in Figure 1. The monthly consumption of copepods and euphausiids was computed in other subroutines, in connection with food requirements (in the DYNUMES model, the zooplankton standing stock size at any given location and time will be used for computation of food availability; in this paper, we use it merely for comparison to consumption).

Zooplankton Consumption

The major consumers of zooplankton in our submodel are herring (and ecologically related species) and juvenile (pre-fishery) pollock. The total monthly amounts consumed are relatively constant through the year, fluctuating only little with the fluctuating biomass of consumers (Table 1), because the present submodel does not account for food density dependent feeding, nor variation of food coefficient with temperature. The monthly values of total zooplankton consumption in the Bering Sea imply that (a) there is little variation of total amounts consumed from month to month (the food composition and rate of consumption is constant year around in the present model, the zooplankton consumption by migratory birds is

ZOOPLANKTON, MG/M³, No. 7

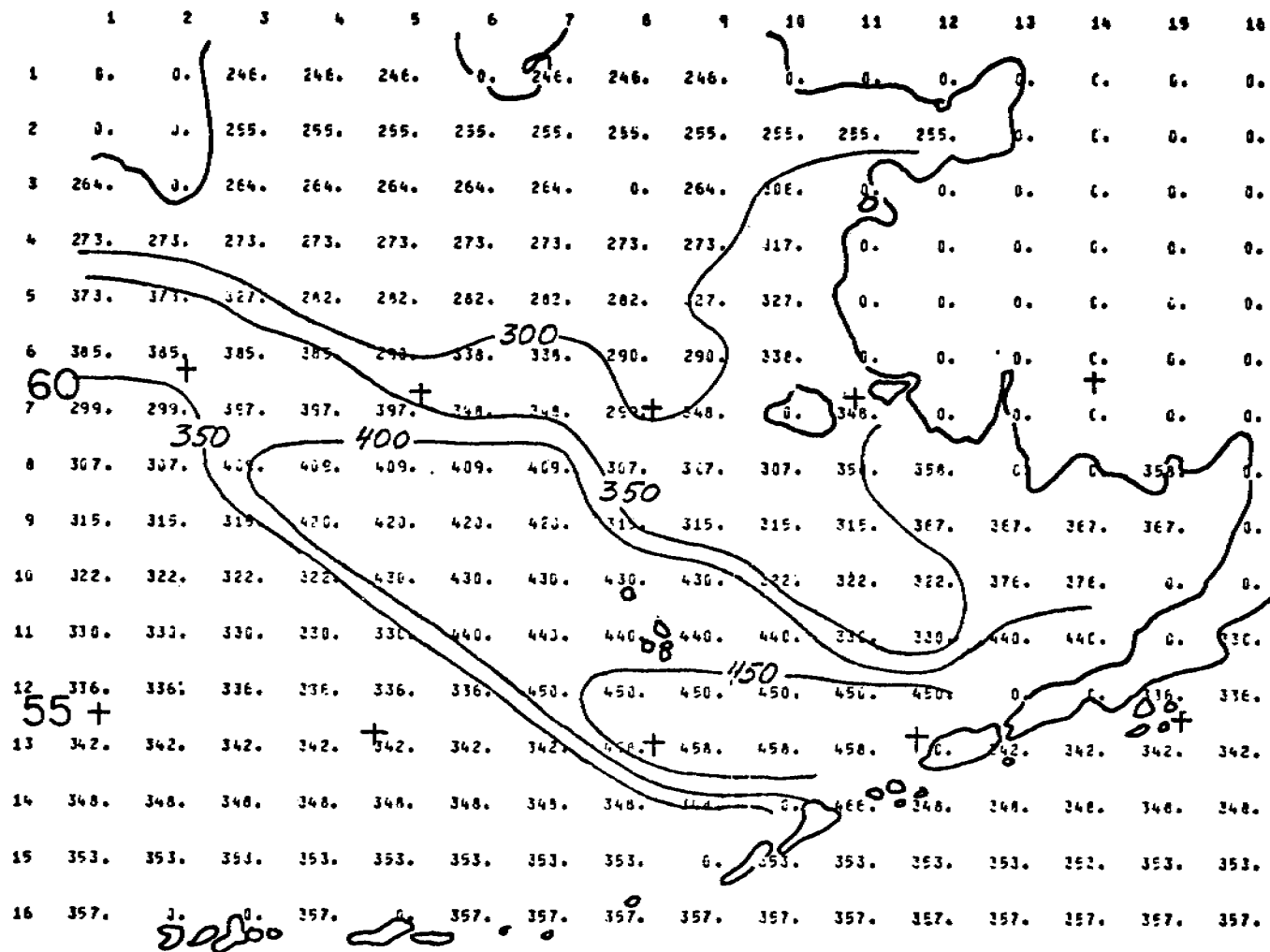


Figure 1.--Simulated standing stock of zooplankton (mg/m³) in the eastern Bering Sea in July.

Table 1.--Examples of midseason monthly values of total consumption of copepods, euphausiids, herring and pollock, in the Bering Sea, as computed with 8-component ecosystem submodel (in thousand tons).

Month	Copepods	Consumption of Euphausiids	Herring	Pollock
February	2145	1704	114	176
May	2183	1706	122	192
August	2094	1564	103	216
November	2010	1509	99	178

relatively minor, and consumption by whales is not considered); and (b) the copepod consumption is approximately 60% whereas the euphausiid consumption is 40%. An interesting observation from Table 1 is that the consumption of zooplankton and consumption of next lower link in food chain (e.g., herring) is about 1:10 to 1:20 (these numbers will change with additional tuning of model), supporting indirectly the general "one order magnitude less" relation between various food chain links in the ocean; this relation is a result of model computations rather than model input.

Examples of monthly consumption of zooplankton (the numbers represent mg/m^3 , assuming a 50 m homogenous depth distribution) are shown in Figures 2 to 4. In April (Fig. 2), there were two areas of high consumption of zooplankton: (1) over the deep water off the shelf, where the bulk of pollock biomass is located, and (2) over the outer edge of continental shelf where the herring population has moved. By June (Fig. 3) the area of high consumption is over the central part of the continental shelf. In October (Fig. 4), the area of high zooplankton moves back toward the continental slope and, during winter, the area of zooplankton consumption is over deep water off the continental slope. Examination of these figures indicates that there are large areas where the zooplankton consumption is light and much of the production is consequently going primarily into a nutrient regeneration cycle and/or sinks to the bottom where it will be used by detritus feeding benthos. Furthermore, the seasonal shifts of areas of high consumption apparently allow subsequent recovery of standing stock and production in areas heavily grazed in periods before and, surely, some replenishment also occurs through transport of zooplankton by currents into these previously heavily grazed areas.

TOTAL ZOOPL. CONS. M³

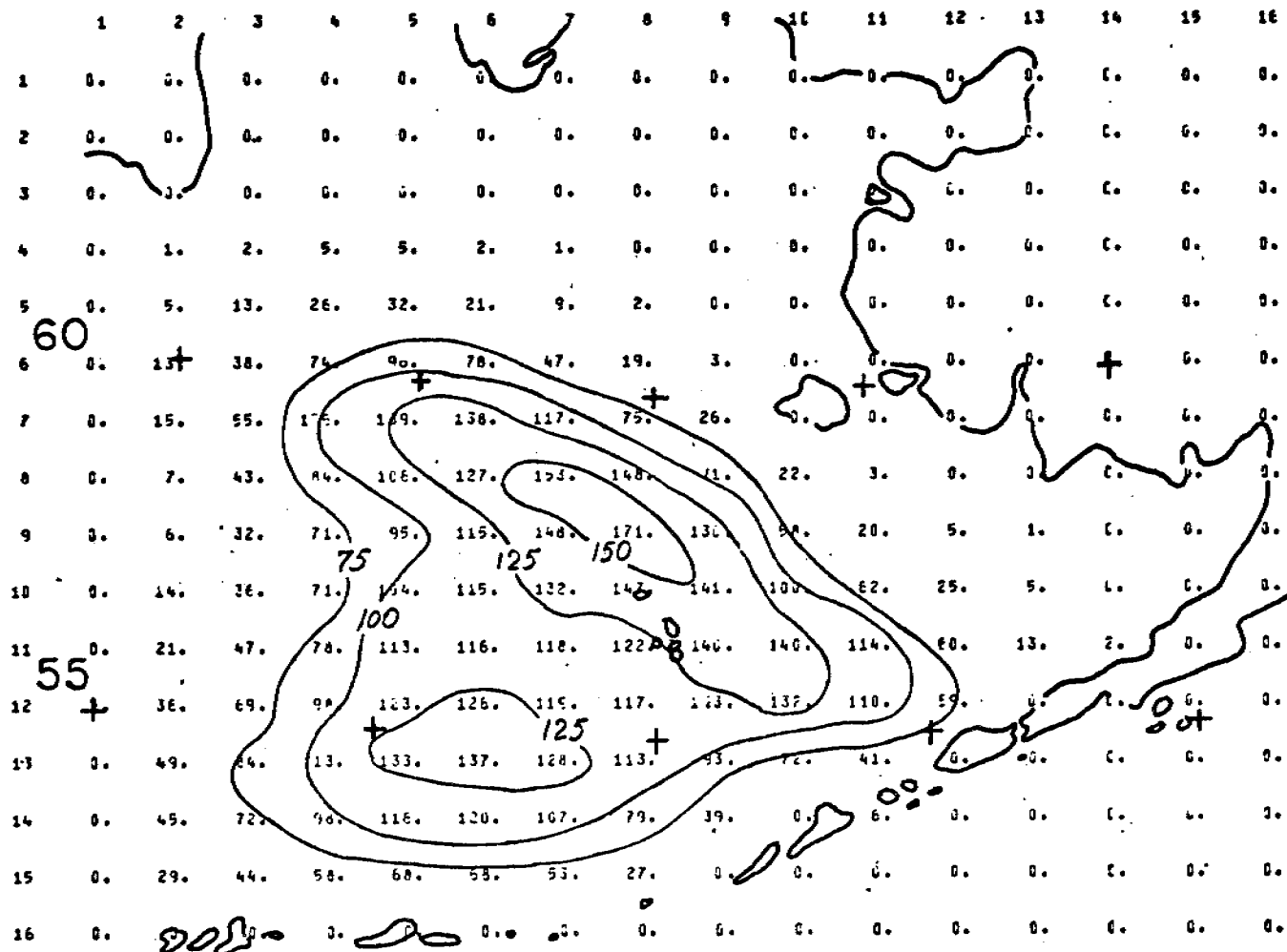


Figure 2.--Computed consumption of zooplankton (mg/m³) in the eastern Bering Sea in April.

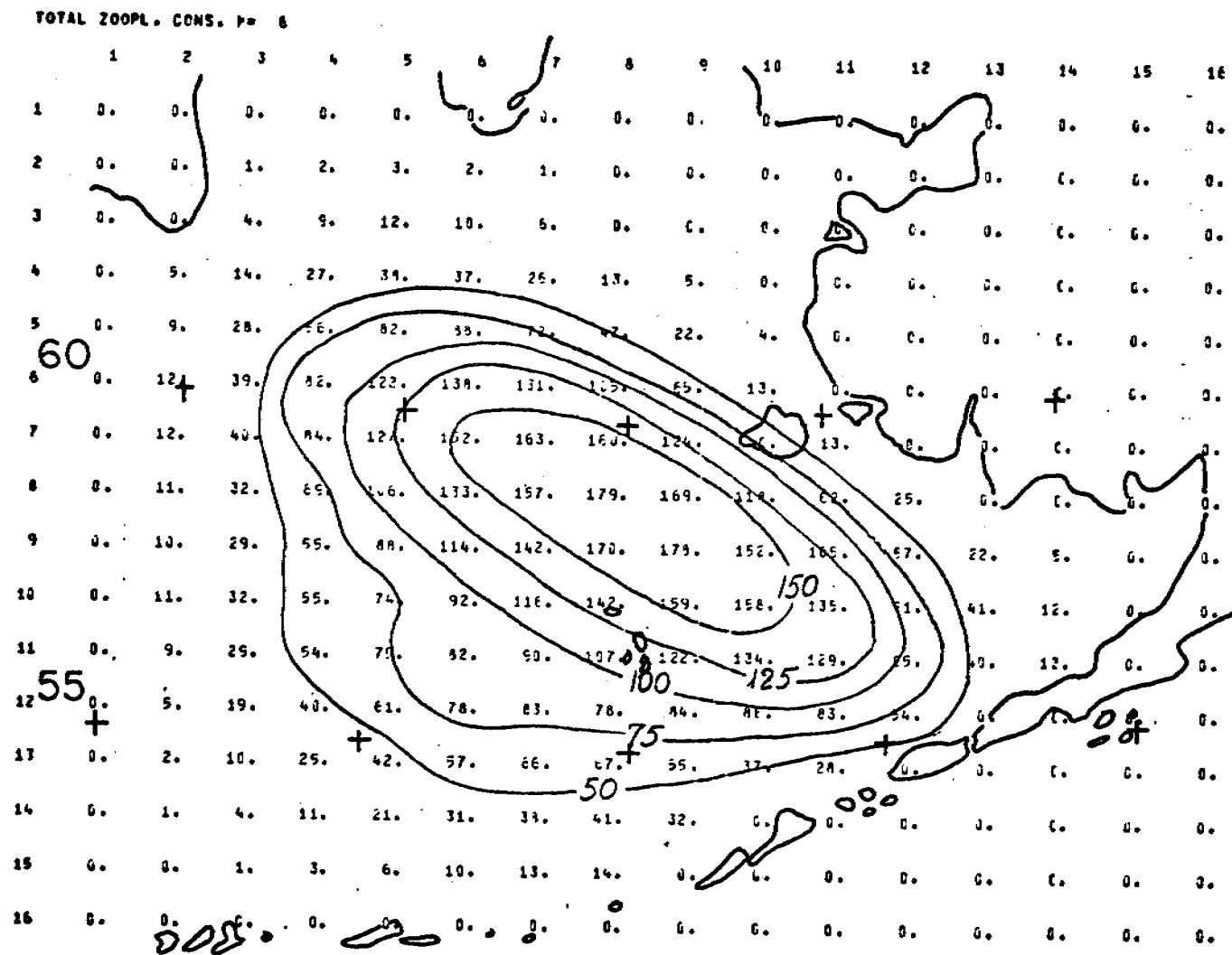


Figure 3.--Computed consumption of zooplankton (mg/m^3) in the eastern Bering Sea in June.

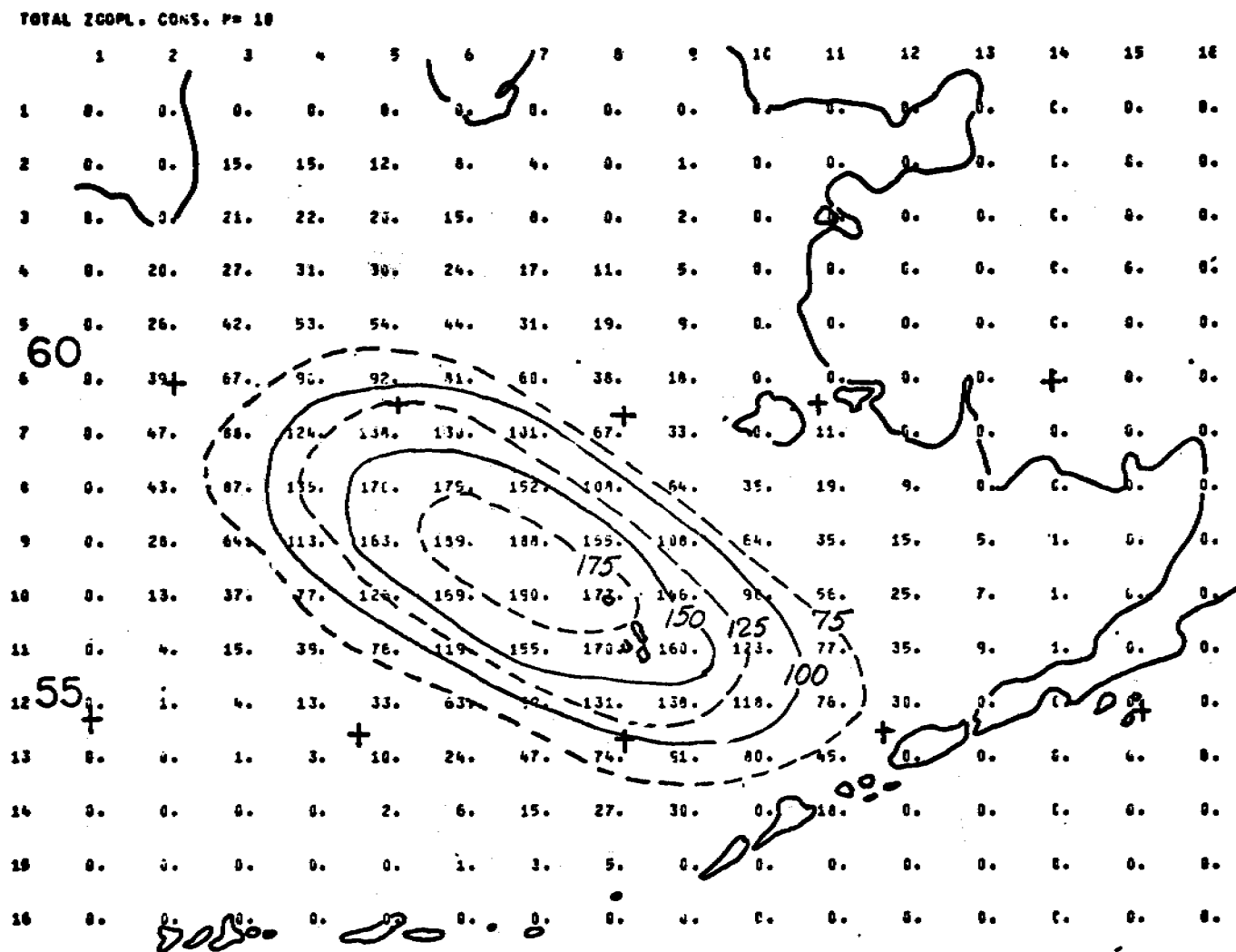


Figure 4.--Computed consumption of zooplankton (mg/m^3) in the eastern Bering Sea in October.

STARVATION OR INADEQUATE PLANKTON SAMPLING?

In comparing, quantitatively, the reported standing stock of zooplankton (Fig. 1) with the computed consumption (Figs. 2 to 4), one finds that in relatively large areas the monthly zooplankton consumption nearly equals or is only slightly lower than the standing stock. In reality, this is not possible. Thus, the cause of the discrepancy (too low standing stock or too high consumption) must be sought either in the model results or in the zooplankton data.

Excessive consumption values can be obtained by the model only if (a) the actual food coefficient is much lower than about 1:5; (b) the proportion of plankton in the diet of grazers is lower than that prescribed; (c) the standing stock of grazers (fish and birds) is lower than assumed in the model; (d) there is widespread starvation, which implies that availability of food is the limiting factor for abundance and growth for most species in the marine ecosystem; or (e) our quantitative knowledge of zooplankton standing stocks is inadequate. Condition (a), above, seems very unlikely, considering the pertinent data available in the literature. Condition (b) also seems unlikely, as the lowest possible values were selected for this particular model run. Likewise, condition (c) seems unlikely, as relatively low estimates of the consumers of plankton were used and not all fish species which consume plankton were included in the present model (also whale consumption is excluded); pollock and herring standing stocks were iteratively determined in other subroutines as the smallest biomass which is sustainable with the lowest possible ecosystem internal consumption and maximum fishery, even assuming highest possible growth rate and considering

natural mortality (i.e., the mortality from "old age"), nearly nil. This leads us to accept conditions (d) or (e) as a proper conclusion. That there may be widespread starvation in other biological components is supported by the results from other subroutines in the model. It also suggests that our quantitative knowledge of zooplankton standing stocks is inadequate, (which is probably true with respect to larger, more mobile organisms, such as euphausids, which are relatively scarce in quantitative zooplankton reports, but which occur in stomach content analyses).

The requirement for high zooplankton abundance also raises an important question about the grazing on ichthyoplankton (fish eggs and larvae) and its consequences. If the zooplankton is grazed down to a low level, the ichthyoplankton would be grazed to the same degree, or possibly to a higher degree, if selective feeding occurs. If areas of high consumption coincide with areas of high concentrations of pelagic fish eggs and larvae, the spawning success, and consequent year class strength, may be determined largely by pelagic, post-spawning grazing, rather than by number of spawners.

FUTURE RESEARCH

As the large and more mobile zooplankters, such as euphausids, constitute a large proportion of the forage for fish and, as selective feeding is expected on such larger organisms and, as our quantitative knowledge on these organisms is scarce indeed, it seems to be desirable to emphasize quantitative studies on this group of organisms with fine-meshed midwater trawls and especially, near the bottom, with similar fine-meshed beam (or slide) trawls.

At the same time we need "synoptic" studies of the fish and other grazers, especially their stomach content, to establish the "selectivity coefficient" of various species in relation to the species spectrum present. Such "synoptic" plankton-fish studies might enlighten other open questions, such as 1) is there a lower threshold value of plankton concentrations which causes plankton feeding fish to disperse and leave the low standing stock area for search of more adequate food, 2) or does starvation and its consequences, such as slower or no growth, higher mortality and non-maturation of gonads, prevail for longer periods in given areas and conditions.

It would be worthwhile to investigate where and when areas of high zooplankton consumption might coincide with areas of known abundance of pelagic egg and larvae of given species. The possible effect of excessive consumption of ichthyoplankton during periods of low standing stock of zooplankton raises interesting questions concerning fish behavior that would be difficult to answer in an oceanic regime but might be addressed in an isolated regime such as the eastern Bering Sea. Certainly the marked external and internal environmental factors provide an easily recognized time-frame. Although fish spawning occurs as a cyclic event, dictated by instinct and environmental and other factors, it is possible that predation on eggs and larvae is a result of learned behavior rather than by instinct or chance encounter. If so, one might ask that if in an area where the shallow depths could permit spatial orientation do the predators use time-space guideposts in the search for ichthyoplankton (much like the fisherman who returns to a particular fishing location) or do they seek, in addition, the environmental conditions that trigger the

various spawning events? If unable to associate the latter, then large year classes could result from the spawners adjusting to anomalous geographical displacements of optimum spawning conditions, where the eggs and larvae would not be subjected to normal predation. Further studies on zooplankton abundance, distribution (including depth distribution under the ice) and related fish behavior, particularly data on feeding behavior under the ice are also definitely needed.

The exciting aspect of the model is that fish population dynamics is considered in the context of variability in its environment, thereby providing insights into those factors which affect their distribution, abundance and productivity, and ultimately lead to quantification of these relationships and prediction models. However, the ability to compute accurate assessments of these interactions will require extensive and orderly acquisition of vast amounts of new information related to the entire ecosystem.

SUMMARY

A numerical, gridded ecosystem model with 8 components was used to compute the consumption of copepods and euphausiids in the eastern Bering Sea. The principal zooplankton consumers in this model were pollock, herring, and marine birds.

Zooplankton consumption was, in some areas and months, nearly equal to zooplankton standing stock as ascertained from available literature, even though the model does not include all zooplankton consumers, and relatively low coefficients of consumption were used. After evaluating other possible causes for this discrepancy, it was concluded that either our existing knowledge on standing stock, production, and turnover rates

of zooplankton is deficient, or starvation in the sea is rather common. Either there is a lack of quantitative data on the larger, more mobile zooplankton organisms such as euphausiids (which occur in relatively large proportions in stomachs of pollock, herring, and ecologically related species, but whose numbers are not caught sufficiently in routine plankton survey work), or the data on the number of generations and production rates of zooplankton need considerable revision.

The model indicates that areas of high consumption of copepods and euphausiids change monthly, primarily due to the migrations of grazers, and that, on the other hand, there are large areas where zooplankton consumption is very low and production goes into a regeneration cycle or is consumed by benthos. The transport of copepods and euphausiids by currents seems to be an important factor both for providing food for grazers and providing brood stock to areas of high consumption. If the areas of high utilization of zooplankton coincide with the areas of abundance of ichthyoplankton, survival of fish larvae and, subsequently, year class strength of a given species in these areas may be determined almost entirely by grazing.

As the process of feeding on plankton, including selective feeding, is a prey density-dependent process, it is important in fisheries research to know how food availability affects the behavior of fish, such as migrations, dispersals, etc. Thus, it is necessary to couple zooplankton research intimately with other fisheries research operations. Other information on planktivorous fish (e.g., abundance by sonar surveys and experimental fishing, stomach analyses, etc.) must be collected concurrently with plankton sampling. Knowledge of abundance, survival and behavior of zooplankton and fish during periods of ice cover is also required.

LITERATURE CITED

Laevastu, T., F. Favorite, and W. B. McAlister

1976. A dynamic numerical marine ecosystem model for evaluation of marine resources in eastern Bering Sea. Final report RU-77, Ecosystem dynamics birds and marine mammals, Part III. Natl. Oceanic Atmos. Admin., Natl. Mar. Fish. Serv., Northwest Fish. Center, Seattle, Wash. 69 p. + 36 p. appendix (Processed.)

QUARTERLY REPORT

Research Unit : 86-77
Reporting Period: summer 76
Number of Pages: 5

Effects of Petroleum Exposure on Hatching Success of Alaskan
Glaucous-winged Gulls (Larus glaucescens) on Egg Island,
Copper River Delta

Samuel A. Patten, Jr.
M. Sc. Ph.D. cand.

Associate Investigator
Department of Pathobiology
The Johns Hopkins University

1 January 1977

QUARTERLY REPORT

I. Task Objectives:

Effects of Petroleum Exposure on Hatching Success of Alaskan Glaucous-winged Gulls (Larus glaucescens) on Egg Island, Copper River Delta.

A partial analysis of potential effects of OCS development and tanker traffic on the ecosystem of the Copper River Delta.

An ongoing investigation of the effect of North Slope Crude Oil on ecological community structure and productivity.

II. Field Activities:

We are examining the effects of North Slope Crude Oil exposure on breeding success of the Glaucous-winged Gull, a common inshore and marine scavenger nesting in colonies. We are examining the largest gull colony in the NEMOA, Egg Island, which is located 10 km SE of Point Whitsned and 20 km south of Cordova ($60^{\circ} 23' N$, $145^{\circ} 46' W$). The counterclockwise onshore currents of the Gulf and strong tidal interchange make barrier islands such as Egg Island susceptible to contamination from tanker traffic and oil lease sites of Middleton Island and those between Cape Suckling and Icy Bay.

Oiling of eggs has been carried out during the 1976 breeding season. Onset of incubation was late May and incubation continued far beyond the normal period until mid-July in oiled clutches.

The investigators (Patten & Patten) were on site from 20 May 1976 to 24 Aug 1976. Our affiliation is the Department of Pathobiology, School of Hygiene and Public Health, The Johns Hopkins University. Our role is to fulfill contract obligations as Associate Investigator and Research Technician.

Methods:

Colonial nesting and synchronization of the breeding cycle leave marine bird populations including gulls open to catastrophic events such as major oil spills (e.g. recent Liberian tanker accidents) which could eliminate the productivity of the breeding season. In addition, bird species may be susceptible to chronic low-level oil pollution since recent evidence indicates high toxicity to eggs with very low levels (microliters) of oil exposure (Dieter F&WS, pers. comm.)

North Slope Crude Oil provided to us in May, 1976 by NEFS Auke Bay Laboratory under sponsorship of Dr. Jay Quast, NOAA, has been used to test toxic effects on eggs. Commercially available mineral oil (non-toxic) has been used to test neutral blocking agent effects on respiration (gas exchange) on developing embryos.

We are comparing our experimental results with four years previous information on the breeding success of the Herring Gull, two years of which are from Egg Island.

Oil was delivered to completed clutches of three (3) eggs in the second week of incubation in 50 marked nests (of 75) on the ocean slope of Egg Island covered dunes SW of Egg Island Light (60° 216' N, 145° 451' W). 25 clutches received 1cc/egg surface application of #3 Crude, and 25 clutches received 1cc/egg mineral oil. Both treatments were delivered by drops from calibrated syringes. Delivery date was 11 June 1976. 25 clutches received no treatment.

#3 Crude was more viscous than mineral oil and covered about 25% egg surface. Mineral oil at this dose covered about 50% egg surface. Air temperature was 60°F at the time of application, winds were variable from NW to SW, with bright sunshine. Clutches in the experimental area were inspected the next day. Most evidence of oil exposure had disappeared except for slight petroleum odor.

Clutches were then inspected at weekly intervals in order to keep disturbance to a minimum.

We continued our R0,96-76 investigation of the adjacent colony of 186 nests for reproductive success using methods identical to 1975 but with an attempt to lower disturbance in the study area. On other parts of Egg Island we banded 2500 gull chicks and color-dyed adult gulls to determine local and migratory movements (15 adult birds).

III. Results:

1. The egg oiling experiments had decided effects; with North Slope Crude we report nearly complete mortality (approaching 100%) of all samples. We also report high mortality of the non-toxic mineral oil egg samples.
2. Adult gulls continued to brood oiled eggs well beyond the normal incubation period into mid-July (approximately +25 days).
3. Non-oiled clutches in the experimental area hatched normally, but with a usual predation rate, which accounted for disappearance of both oiled and un-oiled eggs. Final fledging success in the adjacent control colony was 1.14 chicks fledged per nest.
4. Adult gulls incubating oiled clutches well past the normal period did not re-nest and gradually abandoned unmatched clutches.

IV. Preliminary interpretation of results:

Analysis continues at present. We offer the following interpretation: At this high dose there are apparently both physical (smothering) and chemical (toxic) effects on developing gull embryos. This treatment has an explosive physiological effect in both cases. This is not satisfactory, because it simply provides us with a yes/no answer; yes there is an effect. Hence our plans for revised methodology in the 1977 field season.

- V. Problems encountered/recommended changes:
We must have more refined methods and much lower doses to approach LD_{50} . We must differentiate the effect of the toxic vs. non-toxic (sootering) oil exposures. Doseage was far too high.

A key feature in additional research will be capture of incubating adult gulls and subsequent oiling of breast feathers, feet, or food to test transfer of oil to eggs and chicks. We appreciate input from NMFS into planning of experiments to consider all likely pathways of oil exposure, including possible transport by wind or debris from an oiled beach.

Oiling of adults and chicks will be carried out during the 1977 breeding season. Effects on chicks may include: external thermoregulatory disturbance; internal metabolic disturbance due to ingestion or inhalation; or disruption of visual patterns by which adults recognize young.

Oil will be administered to chicks to simulate beach or intertidal oiling; or to head feathers to evaluate disruption of recognition patterns.

- VI. Financial Statement, Milestone Chart and Data Submission Schedule follow.

Our main activity this past quarter has been completion of our RU#96-FY76 Final Report.

Quarterly Report

Contract #03-5-022-56
Research Unit #123
Task Order #18
Reporting Period 10/1 - 12/31/76
Number of Pages 3

ACUTE TOXICITY - PACIFIC HERRING ROE IN
THE GULF OF ALASKA

Dr. Ronald L. Smith
Institute of Marine Science
University of Alaska
Fairbanks, Alaska 99701

I. Task Objectives

Objectives for this quarter included hiring and overseeing a technician for the hydrocarbon analyses. We have also tried to make arrangements for scanning electron microscopy of control and experimental herring larvae.

II. Field and Laboratory Activities

A. Ship or field work:

None.

B. Scientific party involved in project:

R. L. Smith	Principal Investigator
J. Pearson	Associate Investigator
J. A. Cameron	Research Assistant
C. Akert	Research Technician

C. Methods:

Scanning EM work was performed on herring larvae using standard EM procedures employed at Oregon State University. Gas chromatographic analyses of tissues and water samples collected during this project were performed using the techniques of Dr. David Shaw, IMS, University of Alaska. GC-MS techniques were employed in an effort to identify the fractions appearing on the chromatographs.

D. Sample localities:

None.

E. Data analyzed:

Some 60 scanning electron microscope photographs were taken of a variety of control and exposed larvae. Copies of some of these photos will be included in the final report on this project. Those photographs illustrate several malformations which could not be observed under the dissecting microscope. These include the following:

- erosion of pectoral fin
- malformed mouth, incapable of closing completely
- missing branchiostegal membrane
- missing maxillary bone.

Chromatographic analyses show that the exposed larvae and unhatched eggs did accumulate hydrocarbons. We will report on the identity of these hydrocarbons in the final project report, soon upcoming.

IV. Problems Encountered

One very critical problem encountered during this quarter deals with the procedures used in sample preparation for gas chromatography. Either through imprecise instructions or sloth on the part of the technician (or both) no internal marker was added to the tissue and water sample extracts. Since these extracts were not evaporated to a uniform volume, we have no way of expressing hydrocarbon levels quantitatively. In the final report we will only be able to make qualitative statements about what is there and some observations about relative levels in the different exposure groups compared to the controls. This will be the major drawback of the entire study.

OCS COORDINATION OFFICE

University of Alaska

ENVIRONMENTAL DATA SUBMISSION SCHEDULE

DATE: December 31, 1976

CONTRACT NUMBER: 03-5-022-56

T/O NUMBER: 18

R.U. NUMBER: 123

PRINCIPAL INVESTIGATOR: Dr. R. L. Smith

No environmental data are to be taken by this task order as indicated in the Data Management Plan. A schedule of submission is therefore not applicable¹.

The final report is being prepared.

NOTE: ¹ Data Management Plan has been approved and made contractual.

EFFECTS OF A SEAWATER-SOLUBLE FRACTION OF
ALASKAN CRUDE OIL AND ITS MAJOR AROMATIC
COMPONENTS ON LARVAL STAGES OF THE
DUNGENESS CRAB, *CANCER MAGISTER* DANA

R. S. CALDWELL, E. M. CALDARONE and M. H. MALLON
Department of Fisheries and Wildlife
Marine Science Center
Oregon State University
Newport, Oregon 97365

Abstract

Larval stages of the Dungeness crab, *Cancer magister* Dana, were exposed continuously to dilutions of Alaskan crude oil water-soluble fraction (WSF) or seawater solutions of naphthalene or benzene for periods lasting up to 60 days. Effects on survival, duration of larval development and size were employed as indicators of toxic effects. By these criteria the toxic threshold for exposure to the WSF was estimated as 4.0% of the full strength WSF (0.0049 mg/l as naphthalene or 0.22 mg/l as total dissolved aromatics). The lowest concentration at which toxic effects were observed with naphthalene was 0.13 mg/l and with benzene was 1.1 mg/l.

The concentrations of aromatic hydrocarbons in the WSF were inversely related to the degree of alkylation in each of the benzene and naphthalene families, but the acute toxicity of the 12 compounds was directly related to the degree of alkyl-substitution. In addition, naphthalene and its derivatives were more toxic than benzene and its derivatives. Because of these relationships, the individual aromatic compounds, contributed approximately equally to the acute toxicity of the WSF. The collective toxicity of these compounds tested individually accounted for only 8.45% of the WSF acute toxicity. Since benzene contributed a greater fraction of the WSF toxicity in the chronic experiments (approximately 30%) it is suggested that the toxicity of this compound may involve a different mechanism in long term exposures than in acute tests.

Key words: Crustacea, zoeae, *Cancer magister*, petroleum, aromatic hydrocarbons, crude oil, benzene, naphthalene, toxicity

Introduction

Studies of the biological effects of oil pollution in marine waters have intensified in recent years as a result of the publicity created by large oil spills and the trend toward development of offshore oil fields. Recent reviews have summarized much of this work (Nelson-Smith, 1970; 1973). Although the developmental stages of organisms are often more sensitive to toxicants than adults, relatively little work with oil or components of oil has yet been done on these forms. Struhsaker et al. (1974) have studied the effects of benzene on developmental stages of two marine fish. Wells and Sprague (1976) have found that emulsions of Venezuelan crude oil were toxic to lobster larvae at concentrations as low as 0.14 mg/l. Katz (1973) reported that cultured larvae of the crab, *Neopanope texana* showed reduced survival when exposed throughout the zoeal stages to a seawater-soluble fraction of Venezuelan crude oil. In this paper we report on the results of a study that was carried out to test the toxic effects of a seawater-soluble fraction of Alaskan crude oil and its major aromatic components on larval stages of the Dungeness crab, *Cancer magister* Dana.

Materials and Methods

Long term exposure of Dungeness crab larvae to dilutions of a 1% (1 part crude oil to 100 parts seawater) Cook Inlet crude oil water-soluble fraction (WSF) and to benzene and naphthalene dissolved in seawater were conducted in flowing water laboratory culture systems (Buchanan et al., 1975). In the first of two test series, larvae were the

This research was supported by NOAA Task Order No. 3, Contract No. 03-5-022-68, Technical Paper No. 4377, Oregon Agricultural Experiment Station. The authors are grateful to Dr. J. Karinan, NMFS, Auke Bay, Alaska for collection and shipment of several Alaskan female crabs.

progeny of a female crab obtained off the coast of Oregon and in the second series the larvae were the progeny of a female obtained from Auke Bay, Alaska. Toxicant exposures were begun within a few hours of hatching of the first stage zoeae by the females. Larvae were cultured at 13°C (10.5-14.2°C) in filtered sterile seawater (29-34‰) saturated with air. The photoperiod was 11 hr of darkness and 13 hr of light. In each test the initial numbers of larvae were approximately 300 in the control treatment and 100 in each of the toxicant exposure treatments. During the culture period the larvae were transferred to clean culture containers three times per week and fed newly hatched nauplii of San Francisco brine shrimp, *Artemia salina*. Crab larvae reaching the fifth zoeal stage in the first test were fed one week old brine shrimp larvae. Mortality and molt data were recorded daily and the lengths of the cephalothorax of the surviving larvae were taken at the termination of each experiment to evaluate effects on growth. The criterion of death was development of an opaque appearance to the larvae.

Stock solutions of WSF, benzene and naphthalene used in the long term tests were prepared daily using a procedure similar to that of Anderson et al. (1974). The materials to be tested, 180 ml of crude oil, 3.0 ml of benzene and 360 mg of naphthalene, were added to the surface of 18 l. of seawater in each of three 19 l. pyrex bottles, and the contents were stirred nonturbulently with magnetic stirrers for 20 hours at 13°C. After allowing the contents to remain undisturbed for an additional 3 hr, these stock solutions were transferred without contamination by surface materials to the Mariotte bottles of the diluter system through glass delivery tubing. Test solutions (Table 1) were obtained by a continuous flow serial dilution of the toxicant solutions.

The acute toxicity of the WSF and twelve of its major aromatic hydrocarbon components to newly hatched first instar zoeae was determined in 96-hr static bioassays at 13°C in 30‰ seawater. Larvae were obtained from an Alaskan female crab and were not fed during the experiment. Stock solutions of individual aromatic hydrocarbons were prepared daily by nonturbulent mixing at 13°C of each hydrocarbon with 900 ml of sterile 30‰ seawater. Stock solutions of the WSF were prepared as in the long term tests. The concentrations of the stock solutions, siphoned from the bottom of the vessels, were determined, and the solutions were diluted to provide logarithmic series of toxicant concentrations. At least 50 larvae were used per test concentration. Deaths were recorded at 24-hr intervals, and the criterion of death was the same as in the chronic bioassays. The acute toxicity of each compound is expressed as 48-hr and 96-hr LC50s, determined according to the graphical interpolation method of the American Public Health Association (1971).

Routine monitoring of seawater toxicant concentrations in both chronic and acute experiments was performed by UV absorption methods employing a Bausch and Lomb Spectronic 505 spectrophotometer. Extraction of toxicants from seawater was made into UV-quality n-hexane with efficiencies greater than 95% and absorbances at the measuring wavelengths greater than 0.3. The concentrations of the hexane solutions of pure aromatic hydrocarbons were determined by comparison of their absorbances at appropriate wavelength maxima with those of standard solutions. The wavelength maximum employed for benzene was 255 nm; that for naphthalene was 221 nm. The concentration of the WSF was routinely monitored by measurement of the 221 nm peak in hexane extracts of seawater and expressed as naphthalene.

Detailed analyses of the aromatic hydrocarbon composition of the WSFs were performed by gas-liquid chromatography using a Hewlett-Packard 5700 series gas chromatograph equipped with a flame ionization detector and temperature programming. Hexane extracts of the WSF employing 1:10 and 1:100 ratios of hexane to seawater were chromatographed without additional treatment. Extraction efficiencies in all determinations were greater than 95%. Extracts were chromatographed on 2 sets of columns: 6'x1/8" stainless steel packed with 10% SE-30 on 100/120 mesh Chromosorb W HP or 10% TCEP [1,2,3-tris(2-cyanoethoxy)propane] on 80/100 mesh Chromosorb P AW. Nitrogen was used as the carrier gas at 20 ml/min with each column. The injection port and detector temperatures were 250°C and 300°C, respectively. Separations on 10% TCEP were performed isothermally at 80°C, whereas temperature programming was employed with the 10% SE-30 columns. The programming rate was 8°C/min with an initial temperature of 80°C held for 8 min, and a final temperature of 260°C. Qualitative and quantitative analyses were accomplished by reference to pure standards of each hydrocarbon.

Cook Inlet crude oil was purchased from Shell Oil Company. Reagent grade naphthalene was obtained from J.T. Baker Chemical Company, chromatography m- and o-xylene and reagent grade toluene from Matheson, Coleman and Bell and UV-grade n-hexane and benzene from Burdick and Jackson Laboratories, Inc. Other aromatic hydrocarbons were purchased from Chem Service, Inc., West Chester, Pa. Column packing materials were purchased from Hewlett-Packard, Inc. and Supelco, Inc.

Statistical differences in mean duration of larval development to each stage and in larval sizes were determined with Student's t-test.

TABLE 1. Toxicant concentrations employed in the chronic toxicity bioassays

Toxicant	Test I		Test II	
	Concentration (mg/l.) *	N	Concentration (mg/l.)	N
<u>Crude Oil WSF*</u>				
low	0.0022 ± 0.0010**	5	0.0013 ± 0.0003	10
high	0.0083 ± 0.0019	11	0.0049 ± 0.0005	10
<u>Benzene</u>				
low	0.18***		0.17 ± 0.04	11
medium	1.1 ± 0.1	4	1.2 ± 0.2	11
high	7.0 ± 1.6	8	6.5 ± 0.4	11
<u>Naphthalene</u>				
low	0.019 ± 0.001	3	0.021 ± 0.004	10
High	0.17 ± 0.03	13	0.13 ± 0.02	10

*As naphthalene

**Mean ± S.D.

***Estimated by dilution

Discussion

In our studies, the 96-hr LC50 for Cook Inlet crude oil WSF was found to be 31% of the stock WSF. Larval cultures were not affected by continuous exposures to WSFs representing 1.8 and 1.1% of the stock fractions (0.0022 and 0.0013 mg/l. as naphthalene, respectively). The threshold of toxic effects during chronic exposures appeared to occur near 4.0% of the full strength WSF (0.0049 mg/l. as naphthalene) since survival was slightly reduced (Fig. 2) and a retardation of developmental rate was noted (Table 2) in the second experiment at this concentration, but the size of surviving larvae was not affected (Table 3). No effects were seen, however, in the first test at 6.8% of the WSF (0.0083 mg/l. as naphthalene). The differences in response of larvae in the two tests could represent differences in the sensitivity of Oregon and Alaskan populations of the crab to the WSF. Such variability of response may, however, be expected even within a single population as has been seen with the larvae of *Callinectes sapidus* for the pesticide mirex.

Since the sum of concentrations of the measured aromatics in our WSF is 5.52 mg/l. (Table 4), a lethal threshold concentration of 4.0% of the stock WSF would be equivalent to 0.22 mg/l. as aromatics. Anderson et al. (1974), in studies with WSFs of two crude oils, found that the concentration of aromatics was approximately 50% of the total dissolved hydrocarbons. By assuming a similar relationship, we would expect the total dissolved hydrocarbons in our WSF at the threshold concentration to be approximately 0.44 mg/l. This result appears to be in fair agreement with the results of Katz (1973) and Wells and Sprague (1976) who studied the toxicity of Venezuelan crude oil to larval crabs and lobsters, respectively.

Katz (1973) found that the larvae of *N. texana* exposed to full strength 1% WSF from the day of hatching, experienced about 60% mortality between days 2 and 5 of culture, but thereafter experienced only a low rate of dying until the termination of the experiment on day 14. Larvae exposed to the WSF beginning with the second zoeal stage on day 4 until the end of the experiment, however, did not die at a significantly greater rate than the control larvae. Although Katz did not employ dilutions of his WSF, his results with delayed exposures suggest that the full strength fraction was close to the lethal threshold. The concentration of the WSF was reported to be 4.0 ppm, about 10 times our estimate of the threshold concentration of total dissolved hydrocarbons in our WSF.

Our results are not as easily compared with those of Wells and Sprague (1976) since they employed dispersions of oil in water rather than WSFs. They found, however, that the 30-day LC50 for lobster larvae and the threshold of retardation of larval development were both about 0.14 mg/l. for larvae starting the test as first instars; a concentration remarkably similar to our estimate (0.44 mg/l. as total dissolved hydrocarbons) of the toxic threshold concentration of Alaskan crude oil WSF to Dungeness crab larvae.

Little information is available in the published literature on the toxicity of individual chemical species found in crude oil WSFs that might allow a reconstruction of the toxicity of the whole fraction. Our acute toxicity studies established that the toxicity of aromatic hydrocarbons to zoeae increased with the degree of alkylation within each of the benzene and naphthalene families of compounds. Additionally, the naphthalene derivatives were substantially more toxic than the benzene derivatives. McAuliffe (1966) has shown that the alkylation of benzene results in decreasing water solubility; at 20°C the solubilities of benzene, toluene, o-xylene, ethylbenzene and 1,2,4-trimethylbenzene are 1780, 515, 175, 152 and 57 ppm, respectively. These data suggest that the relative toxicity of the various aromatic compounds is largely a function of their ability to partition into the lipophilic components of the larvae, presumably the cell membranes. A similar conclusion was reached by Currier (1951) who found that the herbicidal effectiveness of benzene and several of its methylated derivatives to plants was inversely correlated with the water to paraffin oil partition coefficients.

The concentrations of the individual aromatics in the WSF is a function both of the water solubility of the compound and its concentration in the parent oil. Probably due largely to the water solubility characteristics of the compounds, the concentrations of the specific aromatics in our WSF tended to decrease with increasing alkyl-substitution of the aromatic rings. As a result the most toxic compounds were found in the lowest concentrations and consequently the fractional toxicities of the compounds were all similar based on acute toxicity experiments (Table 6). Since the aromatics are generally considered to be the most toxic components in crude oils (Boylan and Tripp, 1971; Moore and Dwyer, 1974; Struhsaker et al., 1974), it is curious that we have been able to account for only 8.45% of the toxicity of the whole WSF by these compounds. These results suggest either that the alkanes and cycloalkanes are more toxic relative to the aromatics than previously supposed, that other very highly toxic compounds which are present only in low concentration occur in the WSF, or that the toxicity of the aromatics, and possibly other compounds, is more than additive in the whole fraction. At present we do not have sufficient information to evaluate these several alternatives.

Although benzene accounted for only 0.95% of the acute toxicity of the WSF, this compound contributed a higher fraction of the toxicity of the WSF in long-term tests. At the toxic threshold concentration of 4.0% of the stock WSF in chronic tests the concentration of benzene would be 0.13 mg/l. We found in chronic exposures that 1.1 mg/l. benzene markedly affected larval survival, but 0.18 mg/l. did not (Fig. 1).

TABLE 2. Effect of the crude oil WSF, benzene and naphthalene on the duration of larval development to the end of the first, second, third and fourth zoeal stages

Toxicant (mg/l.)	First stage			Second stage			Third stage			Fourth stage		
	N	Duration (days)	t	N	Duration (days)	t	N	Duration (days)	t	N	Duration (days)	t
TEST I												
SW control	107	12.4 ± 1.1*		68	22.1 ± 2.2		38	33.8 ± 2.2		27	49.1 ± 3.6	
Crude oil WSF												
0.0022	45	12.4 ± 1.8	-0.12	31	21.5 ± 1.3	1.19	23	34.6 ± 2.8	-1.31	16	49.6 ± 3.1	-0.45
0.0083	35	12.1 ± 0.7	1.45	23	22.0 ± 1.2	0.21	15	33.9 ± 1.4	-0.18	8	47.0 ± 1.2	1.65
Benzene												
0.16	37	12.4 ± 1.0	-0.09	25	21.9 ± 1.5	0.37	20	34.8 ± 2.2	-1.68	9	49.7 ± 1.7	-0.42
1.1	12	12.5 ± 0.9	-0.32	6	24.5 ± 1.8	-2.61**	0	---	---	0	---	---
7.0	0	---	---	0	---	---	0	---	---	0	---	---
Naphthalene												
0.019	33	12.9 ± 1.2	-2.37**	24	22.7 ± 2.1	-1.24	16	34.8 ± 2.4	-1.51	10	50.3 ± 3.6	-0.86
0.17	32	12.6 ± 1.4	-0.68	22	22.0 ± 1.2	-0.02	15	34.3 ± 2.6	-0.78	4	48.2 ± 2.6	0.48
TEST II												
SW control	186	12.2 ± 0.8		120	21.6 ± 1.8		117	32.3 ± 2.3				
Crude oil WSF												
0.0013	67	12.4 ± 0.9	-1.58	51	21.7 ± 1.8	-0.27	48	32.6 ± 2.4	-0.80			
0.0049	44	13.6 ± 1.3	-8.83***	30	23.1 ± 2.6	-3.60***	24	35.2 ± 3.4	-4.88***			
Benzene												
0.17	54	12.1 ± 1.0	1.05	39	21.3 ± 1.7	1.04	39	31.7 ± 2.1	1.45			
1.2	31	12.0 ± 0.8	0.26	11	21.8 ± 1.3	-0.30	9	32.6 ± 1.7	-0.29			
6.5	0	---	---	0	---	---	0	---	---			
Naphthalene												
0.021	63	12.2 ± 0.9	0.16	54	21.5 ± 1.5	0.60	52	31.4 ± 1.6	2.38			
0.13	64	13.0 ± 0.9	-6.60***	43	23.1 ± 1.8	-4.65***	42	33.8 ± 2.8	-3.15***			

*Mean ± one standard deviation.

**Value of Student's t significant at the 0.05 level.

***Value of Student's t significant at the 0.01 level.

TABLE 3. Effect of the crude oil WSF, benzene and naphthalene on the size of surviving fifth stage zoeae at the termination of the first chronic exposure test and on the size of surviving fourth stage zoeae at the termination of the second chronic exposure test

Toxicant (mg/l.)	N	Mean size (mm)	S.D.	t	d.f.
TEST I					
SW control	5	2.54	0.12		
<u>Crude oil WSF</u>					
0.0022	8	2.41	0.05	1.85	11
0.0083	6	2.74	0.14	-2.59*	9
<u>Benzene</u>					
0.18	6	2.50	0.12	0.48	9
1.1	0	----	----	----	----
7.0	0	----	----	----	----
<u>Naphthalene</u>					
0.019	3	2.52	0.22	0.15	6
0.17	2	2.50	0.10	0.32	5
TEST II					
SW control	105	1.86	0.08		
<u>Crude oil WSF</u>					
0.0013	45	1.84	0.10	0.80	148
0.0049	17	1.85	0.08	0.31	120
<u>Benzene</u>					
0.17	31	1.87	0.09	0.38	134
1.2	8	1.79	0.08	1.60	111
6.5	0	----	----	----	----
<u>Naphthalene</u>					
0.021	24	1.88	0.10	-0.80	127
0.13	38	1.84	0.09	1.09	141

*Significant at the 0.05 level

TABLE 4. Concentration of the principal aromatic hydrocarbons in three full strength 1% Cook Inlet crude oil WSFs

Compound	Water-soluble fraction			Mean \pm S.D. (mg/l.)
	A (mg/l.)	B (mg/l.)	C (mg/l.)	
Benzene	3.00	2.82	3.63	3.15 \pm 0.43
Toluene	1.37	1.47	1.73	1.52 \pm 0.18
m-, p-xylenes	0.25	0.32	0.34	0.30 \pm 0.05
o-xylene	0.16	0.20	0.21	0.19 \pm 0.03
Ethylbenzene	0.11	0.13	0.14	0.13 \pm 0.02
Naphthalene	0.05	0.06	0.08	0.06 \pm 0.02
1,2,4-trimethylbenzene	0.05	0.06	0.06	0.06 \pm 0.01
2-methylnaphthalene	0.03	0.03	0.04	0.03 \pm 0.01
1-methylnaphthalene	0.02	0.03	0.03	0.03 \pm 0.01
Dimethylnaphthalenes	0.02	0.02	0.03	0.02 \pm 0.01
1,3,5-trimethylbenzene	0.01	0.01	0.02	0.01 \pm 0.01
1,2,4,5-tetramethylbenzene	0.01	0.01	0.01	0.01 \pm 0.00
Total measured aromatics	5.08	5.16	6.32	5.52 \pm 0.69
WSF concentration as naphthalene (by UV absorption method)	0.116	0.112	0.137	0.122 \pm 0.013

TABLE 5. Acute toxicity of the crude oil WSF and the principal aromatic hydrocarbon components of the WSF to the first instar zoeae

Toxicant	LC50 (mg/l.)	
	48-hr	96-hr
Crude oil WSF (as naphthalene)	0.082	0.038
Benzene	>347.	108.
Toluene (methylbenzene)	170.	28.
Ethylbenzene	40.	13.
m-xylene (1,3-dimethylbenzene)	33.	12.
o-xylene (1,2-dimethylbenzene)	38.	6.0
1,2,4-trimethylbenzene	17.	5.1
Mesitylene (1,3,5-trimethylbenzene)	13.	4.3
Durene (1,2,4,5-tetramethylbenzene)	>3.1	2.1
Naphthalene	-----	>2.0
1-methylnaphthalene	8.2	1.9
2-methylnaphthalene	5.0	1.3
Dimethylnaphthalene (mixture of isomers)	3.1	0.60

TABLE 6. Fractional toxicity of specific aromatic hydrocarbons in Cook Inlet WSF

Compound	Percent of the 96-hr toxic concentration of each compound	
	In full strength WSF (0.122 mg/l. as naphthalene)	In the 96-hr toxic concentration of the WSF (0.038 mg/l. as naphthalene)
Benzene	2.92	0.91
Toluene	5.43	1.69
Ethylbenzene	1.00	0.31
m-xylene	2.50	0.78
o-xylene	3.17	0.99
1,2,4-trimethylbenzene	1.18	0.37
1,3,5-trimethylbenzene	0.23	0.07
1,2,4,5-tetramethylbenzene	0.48	0.15
naphthalene	<3.00	<0.93
1-methylnaphthalene	1.58	0.49
2-methylnaphthalene	2.31	0.72
Dimethylnaphthalene	3.33	1.04
Total	27.13	8.45

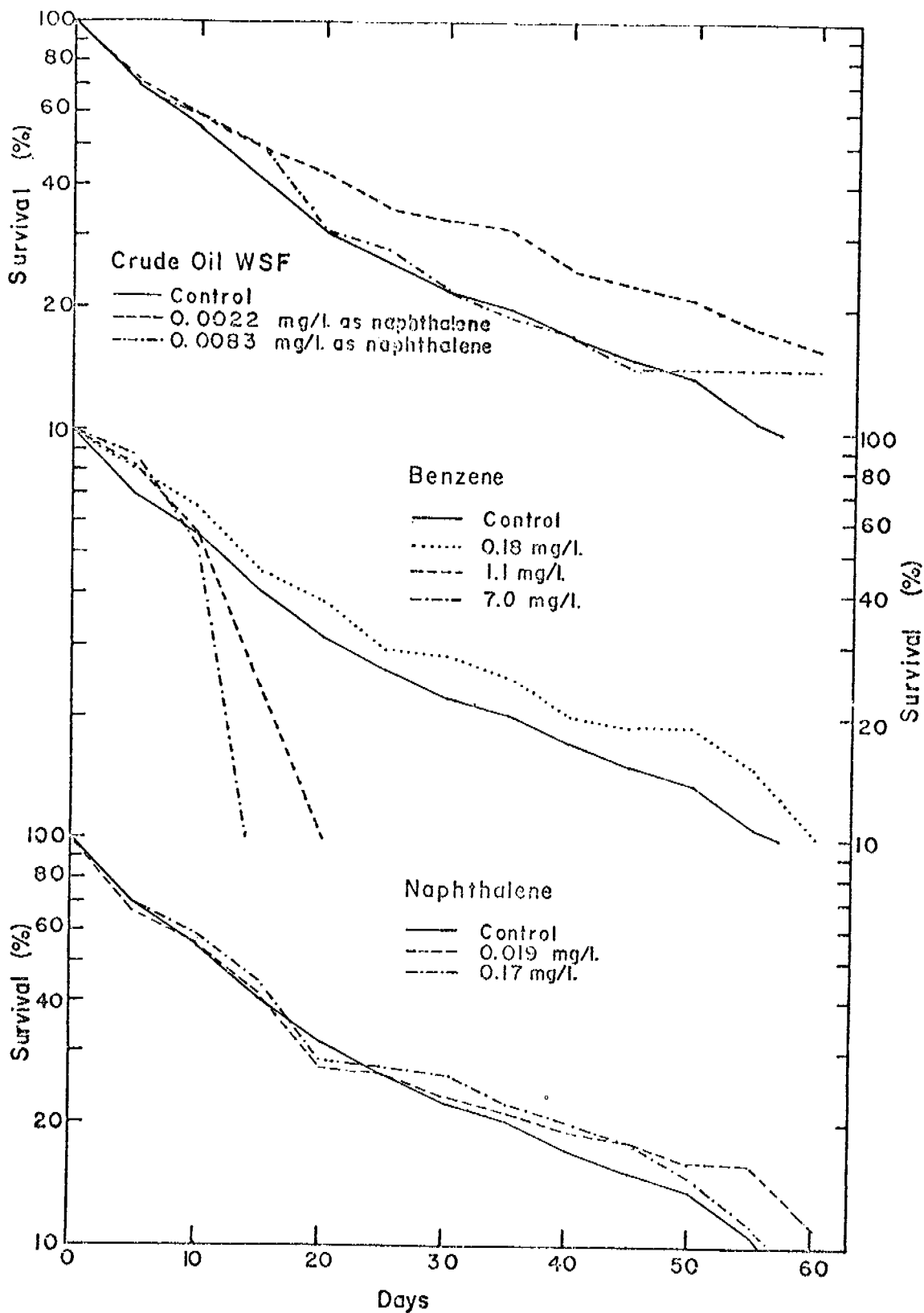


Fig. 1. Survival of *C. magister* zoeae exposed continuously to different concentrations of crude oil WSF, benzene and naphthalene. Results are from the first long-term experiment which employed the progeny of an Oregon female crab.

Results

Dungeness crab zoeae reared in dilutions of the WSF and in naphthalene seawater solutions in the initial long term tests did not exhibit a higher rate of dying than control zoeae even at the highest concentrations tested, 0.0083 mg/l. as naphthalene for the WSF and 0.17 mg/l. naphthalene (Fig. 1). Similarly, the highest naphthalene concentration tested in the second experiment, 0.13 mg/l., had no effect on survival, but larvae exposed to the highest concentration of the WSF, 0.0049 mg/l. as naphthalene, exhibited a slightly poorer survival than control animals (Fig. 2). At the end of the test on day 40, only 20% of the original number of larvae in this treatment survived compared with 36% of the control zoeae.

Exposures of larvae to benzene at concentrations of 1.1 and 7.0 mg/l. in the first test and 1.2 and 6.5 mg/l. in the second test had substantial effects on survival (Figs. 1 and 2). In each of these treatments an accelerated rate of dying first became apparent after day 10 and was coincident with the timing of the first molt in control larvae. At the higher concentrations larvae appeared unable to molt and died as first stage zoeae. Even before day 10, the condition of these larvae appeared to be poor. At the lower two concentrations, 1.1 and 1.2 mg/l., the rates of dying were slower than at 7.0 and 6.5 mg/l. benzene, but even at these lower concentrations the majority of deaths occurred before day 20. Larvae exposed to 0.18 and 0.17 mg/l. benzene in the two tests survived as well as the controls.

In contrast to its adverse effect on survival, benzene, even at lethal concentrations (1.1 and 1.2 mg/l.), had little apparent effect on the duration of larval stages (Table 2). The only exception was a slight delay ($P=0.05$) in the mean time to the second molt of larvae exposed to 1.1 mg/l. benzene. In addition, benzene did not affect the size of larvae surviving the tests (Table 3).

Neither the WSF nor naphthalene appeared to influence the duration of larval development in the first test which employed Oregon larvae, but exposure of Alaskan larvae to the highest concentrations of each of these toxicants in the second series of tests resulted in significant delays to each of the first, second and third molts (Table 2). By the time of the third molt, the mean delay of larvae exposed to the highest concentration of the WSF was 2.85 days and that of zoeae exposed to 0.13 mg/l. naphthalene was 1.44 days. No significant delays were observed at the lower concentrations of these two toxicants.

Naphthalene did not affect the size of larvae surviving the exposures compared with controls in either test even at the highest concentrations (Table 3). In the tests with the WSF, the only significant difference between treatments and controls was with the highest concentration of the WSF in the first test with Oregon larvae. In this group the small number of surviving larvae were larger than the controls by 0.20 mm, averaging 2.74 mm across the carapace (Table 3).

Since the aromatic hydrocarbons are often considered to be the most toxic components of crude oil (Boylan and Tripp, 1971; Moore and Dwyer, 1974; Struhsaker et al., 1974) we decided that an analysis of these compounds in our WSF together with a determination of their relative acute toxicities to first stage crab larvae might be valuable in identifying the most important contributors to the toxicity of oil WSFs. Table 4 lists the concentrations of 12 of the principal aromatics in our WSF. Benzene, at 3.15 mg/l, was the most abundant aromatic hydrocarbon. There were lesser amounts of the alkylated benzenes; their concentrations bearing an inverse relationship with the degree of alkylation. The concentrations of naphthalene and its alkylated derivatives in the WSF were also inversely related to the degree of side chain substitution, but, in contrast to benzene, the concentration of naphthalene was only 0.06 mg/l.

Table 5 lists the acute toxicities of the same 12 aromatic hydrocarbons to first stage zoeae along with the acute toxicity of the WSF. The 96-hr LC50 for the WSF was 0.038 mg/l. as naphthalene, a concentration 31% of the full strength WSF (Table 4). Of the individual aromatic components, benzene was the least toxic with a 96-hr LC50 of 108 mg/l., while dimethylnaphthalene (a mixture of isomers) was the most toxic with a 96-hr LC50 of 0.60 mg/l. Within both the benzene and naphthalene series, the acute toxicities of these compounds exhibited a clear pattern of increasing toxicity with increasing side chain substitution. Furthermore, naphthalene and its alkylated derivatives were more toxic than benzene and its derivatives. Although only one ethyl-substituted aromatic was tested, the results suggest that ethyl-substitution results in greater toxicity than methyl-substitution; the 96-hr LC50 for toluene (methylbenzene) was 28 mg/l. compared with a 96-hr LC50 of 13 mg/l. for ethylbenzene.

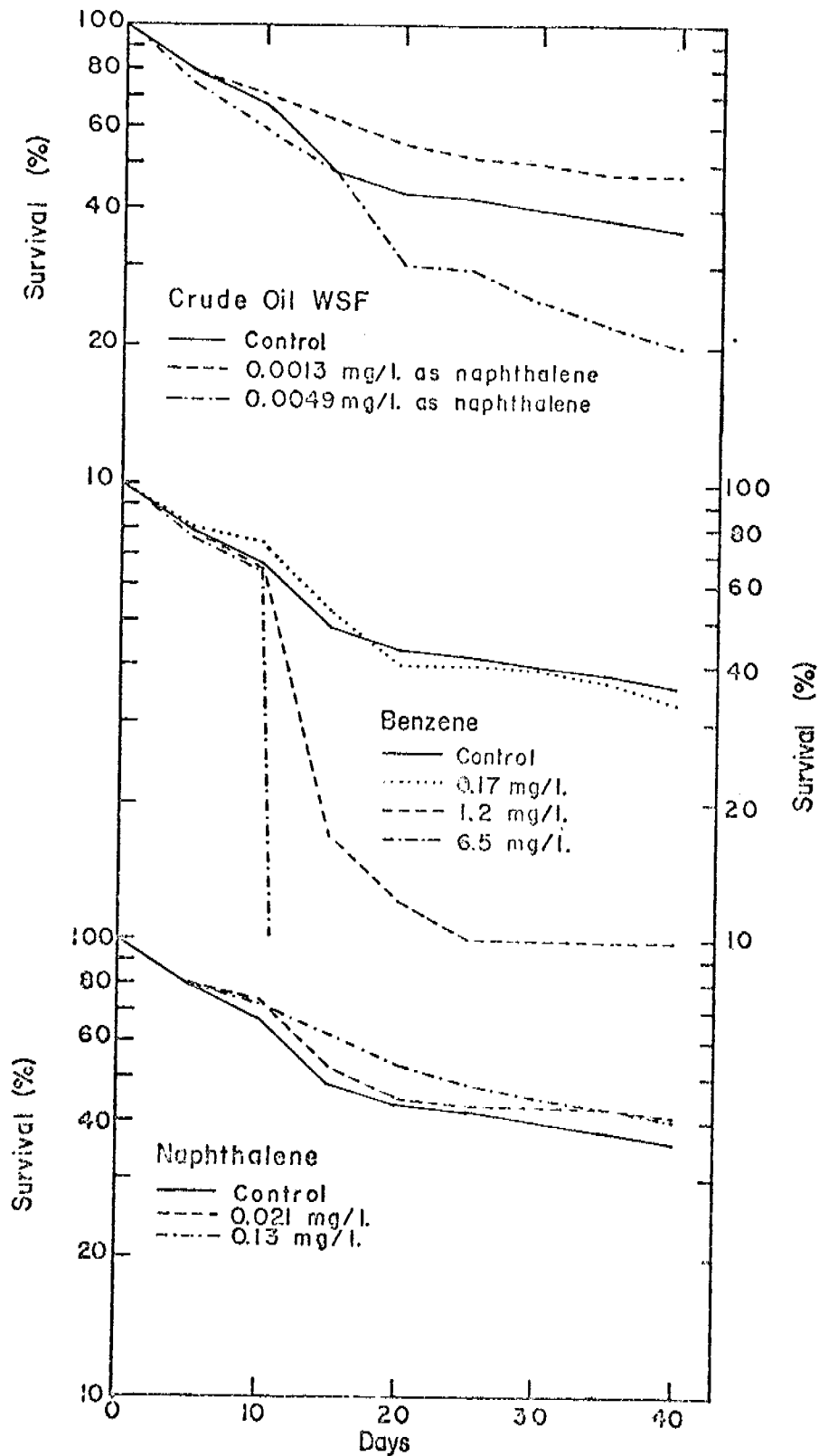


Fig. 2. Survival of *C. magister* zoeae exposed continuously to different concentrations of crude oil WSF, benzene and naphthalene. Results are from the second long-term experiment which employed the progeny of an Alaskan female crab.

The threshold of benzene toxicity therefore lies between these two concentrations, say 0.44 mg/l., the logarithmic average of 1.1 and 0.18 mg/l, and benzene would account for 30% of the toxicity of the WSF in the chronic toxicity experiments. Employing the same reasoning for naphthalene where 0.13 mg/l. may be taken as the threshold concentration for this compound (Table 2), this diaromatic compound would account for only 1.8% of the threshold toxicity of the WSF. While the latter percentage is in fair agreement with the fractional toxicity of naphthalene as determined in the acute toxicity experiments (Table 6), that for benzene is not, suggesting that the mechanism of benzene toxicity may be different in acute and chronic exposures. Such a suggestion is consistent with our observation that the death of benzene exposed larvae in the long term tests was conspicuously associated with the time of molting in control larvae.

References

- Anderson, J. W., J. M. Neff, B. A. Cox, H. E. Tatem and G. M. Hightower, Characteristics of dispersions and water-soluble extracts of crude and refined oils and their toxicity to estuarine crustaceans and fish, Marine Biology 27, 75 (1974).
- American Public Health Association, American Water Works Association and Water Pollution Control Federation, Standard Methods for the Examination of Water and Wastewater, 13th ed, Amer. Public Health Assoc., Washington, D.C., 1971.
- Bookhout, C. G. and J. D. Costlow, Jr., Effects of mirex on the larval development of blue crab, Water, Air, Soil Pollut. 4, 113 (1975).
- Boylan, D. B. and B. W. Tripp, Determination of hydrocarbons in seawater extracts of crude oil and crude oil fractions, Nature 230, 44 (1971).
- Buchanan, D. V., M. J. Myers and R. S. Caldwell, An improved flowing water apparatus for the culture of brachyuran crab larvae, J. Fish. Res. Bd. Canada 32, 1880 (1975).
- Currier, H. B., Herbicidal properties of benzene and certain methyl derivatives, Hilgardia 20, 383 (1951).
- Katz, L. M., The effects of water soluble fractions of crude oil on larvae of the decapod crustacean Neopanope texana (Say), Environ. Pollut. 5, 199 (1973).
- McAuliffe, C., Solubility in water of paraffin, cycloparaffin, olefin, acetylene, cycloolefin, and aromatic hydrocarbons, J. Phys. Chem. 70, 1267 (1966).
- Moore, S. F. and R. L. Dwyer, Effects of oil on marine organisms: a critical assessment of published data, Water Res. 8, 819 (1974).
- Nelson-Smith, A., The problem of oil pollution in the sea, Adv. Marine Biology 8, 215 (1970).
- Nelson-Smith, A., Oil Pollution and Marine Ecology, Plenum Press, New York, 1973.
- Struhsaker, J. W., M. B. Eldridge and T. Echeverria, Effects of benzene (a water-soluble component of crude oil) on eggs and larvae of Pacific herring and northern anchovy, pg. 253, In: Pollution and Physiology of Marine Organisms (Vernberg, F. J. and W. B. Vernberg, eds.) Academic Press, New York, 1974.
- Wells, P. G. and J. B. Sprague, Effects of crude oil on American lobster (Homarus americanus) larvae in the laboratory, J. Fish. Res. Bd. Canada 33, 1604 (1976).

QUARTERLY REPORT

Contract #03-5-022-56
Research Unit #305
Reporting Period - 1 July 1976
to 1 Oct. 1976

SUBLETHAL EFFECTS ON SEAGRASS PHOTOSYNTHESIS

C. Peter McRoy
Institute of Marine Science
University of Alaska
Fairbanks, Alaska 99701
SS #333-32-8153

6 October 1976

Task Objectives

Task objectives were modified because of the replacement of Dr. Pearson by Dr. McRoy as principal investigator. The modifications shifted an emphasis on the chemistry to the ecology of seagrass beds. The specific tasks performed were b and c of the proposal for research. These specific tasks were:

b. An evaluation of uptake rates by eelgrass of the selected contaminants on the basis of: (1) photoperiod; (2) light intensity; (3) salinity; (4) temperature.

c. An evaluation of the effect of the contaminants on the kinetics of photosynthetic carbon uptake in the limiting kinetic situations.

Field/Laboratory Work

During July and August, 1976 field and laboratory experiments were performed in Izembek Lagoon, Cold Bay, Alaska. Laboratory experiments were controlled exposure of uprooted seagrass to hydrocarbons and subsequent measurement of their productivity as estimated by ^{14}C uptake. In situ exposure to hydrocarbons was done on the grassbeds and results were followed for two weeks.

In addition observations on situations in nature where eelgrass is exposed to hydrocarbons were made during a cruise of the R/V ACONA in southeast Alaska.

Methods

Injection of hydrocarbon into the sediment of a grassbed.

Ten plots were staked in a 20m x 5m area of an intertidal bed of Zostera marina. Care was exerted to minimize trampling of the area. In each sample plot a 10x10 cm quadrat was marked and the leaves of Z. marina were clipped to a reference line that allowed a photosynthetic area to remain (approximately 5 cm of leaf). On the following day 50 ml of a kerosene: seawater emulsion (1:1 by volume) was injected into five of the quadrats using a syringe with a spinal tap needle. The maximum depth of injection was 8.5 cm and 15 points were injected in each quadrat. The remaining five plots were designated as control areas. Clipping and injection were done during lowtide.

A separate plot was marked and injected with 20 ml toluene. Plots were observed for the effect of the injections and regrowth of the leaves was allowed for 2 weeks. The resultant regrow on leaves were clipped to the reference line. A subsample of 15 leaves from each quadrat was measured. The total regrowth was dried at 90°C for 24 hr, weighed and converted to $\text{g(dry)} \cdot \text{m}^{-2} \cdot \text{day}^{-1}$.

A sediment core was taken on the day of injection in the general sample area. Interstitial water was extracted from sections 0-5 cm and 5-10 cm from the surface and collected in vacutainers for analysis of ambient hydrocarbon concentrations.

Samples of kerosene and toluene used for injection were saved in poly-bottles.

In the laboratory in Fairbanks, leaves were combusted using a dry combustion technique. The radioactive carbon dioxide released was trapped by a scintillation fluid and counted in a liquid scintillation counter. Counts were corrected for combustion efficiency, counter efficiency, quench, and background. Corrected counts were converted to productivities after the formula

$$P = \frac{(DPM_{\text{leaf}}) (CA) (1.05) (V)}{(DPM_{\text{ampoule}}) (T) (W)} = \text{mg C fixed/g-dry-hr}$$

where DPM = disintegrations per minute

CA = carbonate carbon available per liter

V = volume incubation bottle

T - incubation time (hr)

W = weight of leaf in gm

1.05 = correction factor for differential uptake of C isotopes.

Incubation of plants exposed to hydrocarbon: ^{14}C uptake.

Intact intertidal plants were removed from the lagoon, cleaned of epiphytes and sediment, and placed in beakers. Each beaker was filled with an emulsion of a hydrocarbon and lagoon water; one beaker was a control containing only seawater. Emulsions were made by vigorously shaking lagoon water and the hydrocarbon mixed by volume. Concentrations used were 1:10 toluene:seawater, 1:100 kerosene:seawater, 1:10 kerosene:seawater, 1:1 kerosene:seawater. Exposure to the hydrocarbon proceeded for 5.5 hr at air temperature (8°C).

After exposure, one half of the plants from each beaker were rinsed with seawater and incubated in triplicate stoppered glass bottles filled with filtered seawater spiked with ^{14}C (experiment A). Each bottle contained up to 4 turions connected by a piece of rhizome. Incubation proceeded in full sunlight at air temperature. The temperature, salinity and pH of the water in the bottles was recorded and alkalinity was calculated subsequently. After a 4 hr. incubation the plants were removed and rinsed with fresh water. Roots and rhizomes were separated from the leaves and discarded. Leaves were dried at 90°C for 24 hr, foiled wrapped, and stored in a dessicator.

The other half of the plants were rinsed in seawater and replaced in rinsed beakers containing new seawater. The plants were kept in seawater for 6 hr, changing water once. Incubation procedure was then followed.

Results and Interpretation

Injection of hydrocarbon into the sediment of a grassbed.

The mean productivity of the untreated plants was higher (0.96 ± 0.61 g(dry) \cdot $m^{-2} \cdot day^{-1}$) than the mean productivity of the treated plants (0.75 ± 0.27). The mean growth of the plants exposed to hydrocarbon was only 79% of the untreated plants, although the range in productivity of the treated plants falls into the range of the untreated plants. While the biomass grown in two weeks differed, the length of leaf regrown was the same for both exposed and unexposed plants.

The plants exposed to toluene showed no visible ill effects.

^{14}C incubation after exposure to hydrocarbon.

After the emulsion separated, plants tended to remain in the lower layer of seawater, except where the emulsion was 1:1 kerosene:seawater.

Plants treated with toluene were dark brown at the end of 5.5 hr and their productivity was reduced 7.4 times when compared to control plants.

In every case but one (experiment A, .01 part kerosene) the mean productivity of kerosene-treated plants was lower than the untreated plants. Plants exposed to 1:1 kerosene:seawater exhibited the lowest mean productivity, reduced 1.6-1.9 times the control. Although the means for plants exposed to .01 and .1 parts kerosene were lower than the mean of the controls, the difference does not appear significant.

Plants exposed to hydrocarbons in their natural habitats showed much less drastic results than those exposed in bottles, and indicated laboratory manipulations should not be the sole basis of the extrapolation of impact on natural systems. Considerations such as tidal flushing and time of contamination relative to lowtide play unquantified controlling influence on the magnitude of the effect of contamination. While a major spill at lowtide in Izembek Lagoon may probably have a drastic effect, seagrass exposed to low level continuous contamination is able to survive and grow well. This was demonstrated in the small boat harbor of Sitka, Alaska where an oil slick of boat fuels was seen on the water over a flourishing eelgrass bed, and on lowtide the plants were directly exposed to the slick.

Problems

A serious problem is duplication of contamination conditions. Laboratory experimentation does not allow for the favorable modifications dynamic physical conditions of the seagrass habitat may make on exposure or for adaptation of the plants to conditions of exposure. If one considers only bottle experiments the results are contradictory to the observation of eelgrass growing in low-level continuous exposure situations such as in boat harbors.

Variation intrinsic in the experimental methods is large and therefore differences in the response of treated to untreated plants was not clearly shown.

The injection of hydrocarbon into the grassbed sediments was hard to limit to the sediment and therefore not the leaves of the seagrass. The hydrocarbon immediately rose out of the injection point and spread as a slick over the water, resting in the plant's leaves. How much hydrocarbon actually remained in the sediment is unknown.

November 21, 1976

Quarterly Progress Report

TASK TITLE: Transport, retention, and effects of the water-soluble fraction of crude oil in experimental food chains

I. TASK OBJECTIVES:

The water-soluble fraction of crude oil contains components that are highly toxic to marine organisms. The fate and effects of chronic concentrations of this fraction in marine food chains are poorly understood and will be investigated in this task. Determinations will be made of the rates of uptake of the water-soluble fraction of crude oil from water, food, and water and food by phytoplankton, clams, and starry flounder as well as the physiological and behavioral effects of the fraction. Also to be determined are the tolerance levels of each species of test organisms exposed continuously to the water-soluble fraction under flow-through (open-cycle) conditions.

(For further detailed information, see attached work statement-Attachment A)

II. PLANNING AND WORK SCHEDULING:

A. Literature review

1. During this quarter, a thorough review of existing oil (and related subjects) literature was made. The review included information on field measurements of oil in marine ecosystems, lethal and chronic effects of petroleum products on marine and freshwater organisms, techniques for analyzing oil in water and animal and plant tissue, and experimental techniques for exposing organisms to water-soluble oil fractions. A manuscript was prepared by Dr. Whipple during this quarter which reviews some of this literature (Physiological effects of the water-soluble aromatics in crude oil on fishes and the potential significance of chronic oil exposure to fisheries populations-Attachment B, publications list).

B. Reviews of our proposed experiments and analyses

1. The design of experiments in the oil task received technical review from a number of sources during the quarter. These sources included:

- a. Tiburon Laboratory Research Council via a task review
 - b. Dr. Stanley D. Rice, Auke Bay Fisheries Laboratory (NMFS).
 - c. Dr. John Stegeman, Wood Hole Oceanographic Institute.
 - d. Dr. Steven Klein, University of California, Berkeley.
 - e. Dr. Donald Malins, Northwest Fisheries Center (NMFS)
 - f. Mr. George Snyder, Northwest Fisheries Center (NMFS).
 - g. Dr. Jack Anderson, Battelle Northwest Laboratories, Sequim, Washington.
 - h. Mr. Herb Sanborn, Northwest Fisheries Center (NMFS)
 - i. Dr. Joyce Hawkes, Northwest Fisheries Center (NMFS)
2. The oil analytical methods for our experiments were reviewed by a number of outside investigators including:
- a. Dr. William McLeod, National Analytical Laboratory, Northwest Fisheries Center (NMFS).
 - b. Dr. Donald Brown, National Analytical Laboratory, Northwest Fisheries Center (NMFS).
 - c. Dr. John S. Warner, Battelle Memorial Laboratories, Columbus, Ohio.
 - d. Dr. Jack Anderson, Battelle Northwest Laboratories, Sequim, Washington.
 - e. Dr. Stanley D. Rice, Auke Bay Fisheries Laboratory (NMFS).
 - f. Mr. Sid Korn, Auke Bay Fisheries Laboratory (NMFS).
 - g. Dr. Fred Weiss, Shell Development Co., Houston.

- h. Dr. Douglas Wolfe, ERL, Boulder.
 - i. Dr. Ted Roubal, Northwest Fisheries Center (NMFS).
- C. The following trips were made and discussions held with individuals at each organization, institution or meeting:
- 1. Jeannette Whipple
 - a. Alaska - August
 - 1) OCS hearings - Dept. Interior - Anchorage & Homer.
 - 2) Alaska Fish & Game - Anchorage.
 - 3) AEIDC - OCS Data Center - Anchorage.
 - 4) EPA - Anchorage.
 - 5) OCS/NOAA Project Office - Juneau
 - 6) NMFS, EAD Office - Juneau
 - 7) NMFS, Auke Bay Laboratory
 - b. Seattle, Washington - November
 - Meeting: Fate and Effects of Petroleum Hydrocarbons in Marine Ecosystems and Organisms.
 - 2. Thomas Yocom
 - a. Washington, D.C. - August
 - Meeting: Sources, Effects, and Sinks of Hydrocarbons in the Aquatic Environment.
 - b. Seattle, Washington - November
 - Meeting: Fate and Effects of Petroleum Hydrocarbons in Marine Ecosystems and Organisms.
 - 3. Pete Benville
 - a. Fairbanks, Alaska - August
 - Meeting: 27th Alaska Science Conference, University of Alaska.

b. NMFS Auke Bay Laboratory

c. Seattle, Washington - November

Meeting: Fate and Effects of Petroleum Hydrocarbons in Marine Ecosystems and Organisms.

D. Work Scheduling and description of work accomplished during the quarter:

1. A revised work schedule was prepared in October as part of an NMFS Current Year Task Plan (NOAA Form 32-14A - see Attachment C).
2. An apparatus was designed during the quarter to produce a continuous flow of the water-soluble fraction of crude oil for dosing animals in our experiments. We believe that this solubilizer is a major breakthrough for studies of the acute and chronic effects of the water-soluble fractions of crude oil or petroleum products. The first draft of a manuscript describing the apparatus (as well as the reasons why we developed it) was prepared this quarter and a portion of it is attached (Attachment D).
3. The seawater supply system to the Tiburon Laboratory was completely overhauled during the quarter to minimize the possibility of breakdowns. Plans were made to install a standby generator in the event of electrical power failure (to help insure success of long-term chronic tests).
4. Analytical gear (UV-spectrophotometer, spectrofluorometer, gas chromatograph columns) and bioassay equipment (test tanks, racks, temperature control equipment) were ordered and received during the quarter.
5. Preliminary experiments were run to determine the toxicity of the water-soluble fraction (WSF) of Cook Inlet crude oil (as obtained from our solubilizer) to starry flounder in a flow-through test situation. The WSF was introduced into a 20-gallon test tank which was full of oil-free seawater. The concentration of WSF gradually increased in the tank over a 3 1/2 hour period. At about this point the flounder lost equilibrium. The test-tank concentration of six

monocyclic aromatics (benzene through the xylenes) was 5.1 ppm and the ultraviolet optical density was 0.09.

6. Informal bids were solicited for water and tissue sample analyses that cannot be conducted at the Tiburon Laboratory; we contacted Dr. John S. Warner, Battelle Memorial Laboratory, Columbus, Ohio (Attachment E) and Dr. William McLeod, Manager, National Analytical Laboratory, NMFS, Seattle.

III. Justification of revision of work scheduling.

(The FY 77 current year Task Plan - Attachment C - reflects a number of work schedule slides when compared to the work statement upon which the OCSEAP funding was approved).

A. Delay in release of funds

The original proposal stated that work would begin on April 1, 1976. Release of funds and approval to hire personnel did not occur until June, 1976.

B. Delay in hiring of personnel

Mr. Yocom was hired in late June 1976 on a temporary (rather than the requested term) appointment. A NOAA-wide freeze on hiring restricted us from bringing any of the three technical assistants on board. To date, we have approval to hire a half-time GS-3 Biological Aide. Recently we received approval to hire two full-time technicians on term appointments. As such, the oil task has operated with only a full-time fishery biologist (Yocom), a half-time chemist (Benville), a quarter-time fishery biologist (Whipple), intermittent technical assistance from personnel borrowed from other tasks, and some volunteer personnel.

C. Delay in acquisition of Cook Inlet crude oil

To date, we have been unable to acquire an adequate supply of Cook Inlet crude oil to begin experimentation. In July, 1976, Dr. Douglas Wolfe was contacted, and he informed us that he was ordering a shipment of oil to supply a number of laboratories, including ours. He said, however, that shipment would not be expected before November, 1976.

Dr. Stanley D. Rice at the Auke Bay Fisheries Laboratory agreed to order some oil for us through Shell Oil Co., with whom he had done contract work. We were promised 110 gallons of crude oil by November 1, 1976.

In August, we contacted Mr. Edward Mertens of Chevron Oil Co. (and API), and he told us that Union 76 Oil Co. in Oleum, California (across the Bay from the Tiburon Laboratory) had a supply of Cook Inlet crude oil. Through him, we contacted personnel at Union 76 (Forrest Bottomley, Al Granquist). Two weeks after being told, initially, that they would supply us with oil, they refused to sell us any. We subsequently contacted (through Ed Mortens again) the Atlantic Richfield Co. We again were told, initially, that they would supply us with oil (contacted June Siva and John Nakagana), but the day before our truck was due to arrive to pick up the oil, they refused to sell us any.

After these failures to acquire oil, we again contacted Dr. Douglas Wolfe, who suggested that we wait for his shipment. In the interim, we have been running preliminary tests with small quantities of oil graciously supplied by the Auke Bay Fisheries Laboratory.

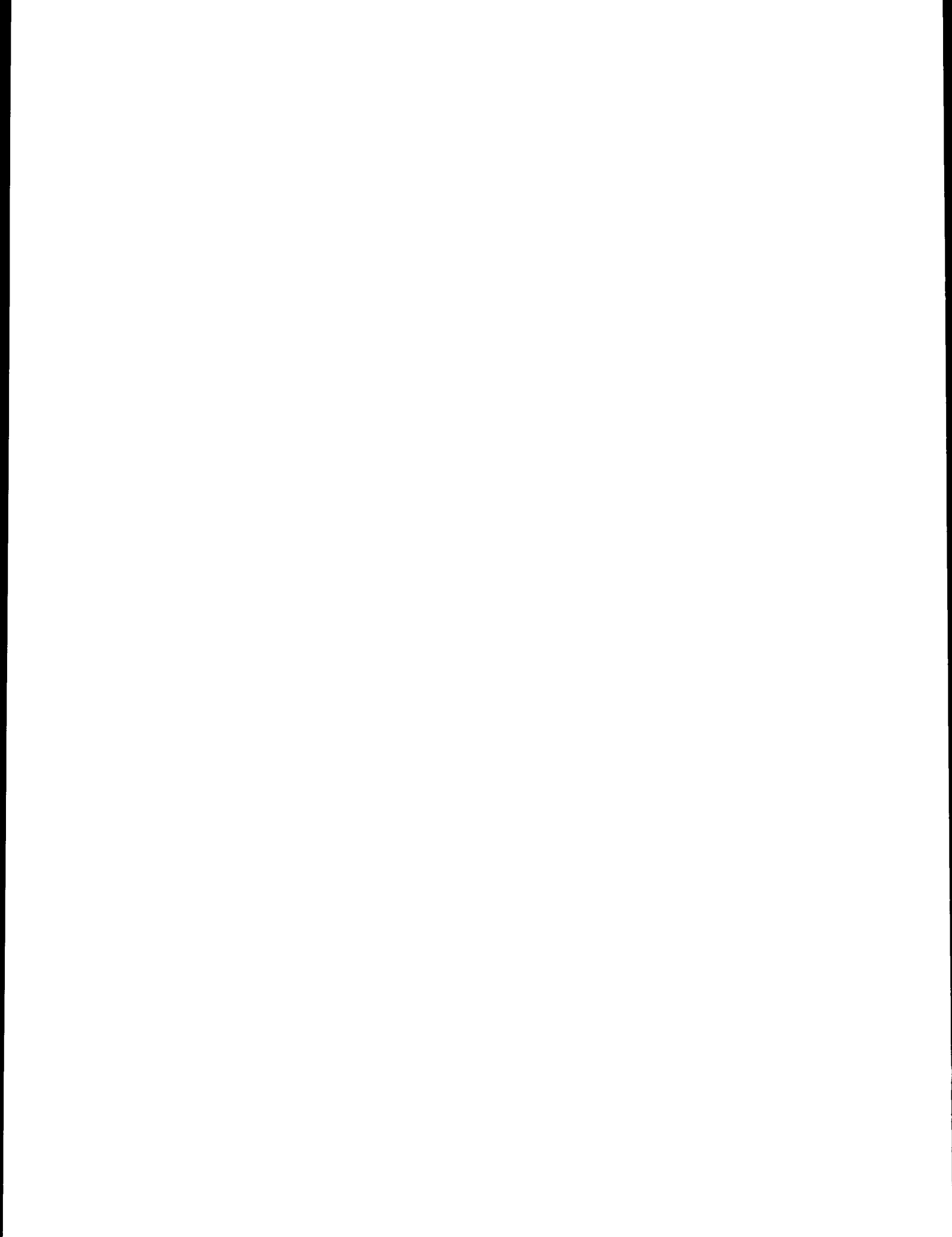
We are hopeful that the oil arrives soon and that further delays in personnel hiring will be minimal so that we can avoid any additional slides in schedule.

IV. Experiments to be undertaken next quarter.

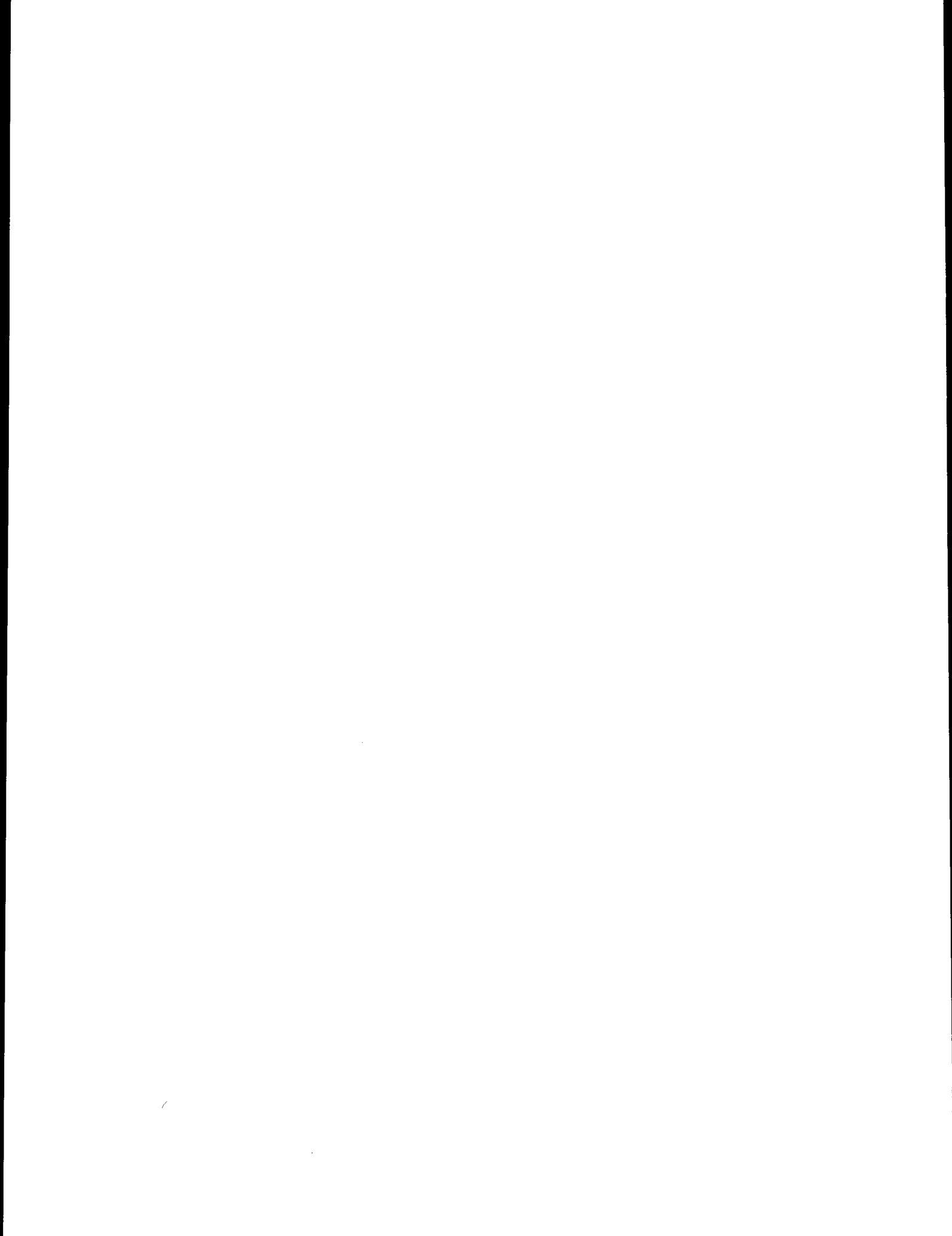
Attached (Attachment F) is a detailed outline of the acute and chronic toxicity tests that we will conduct to determine the tolerance of our experimental animals to the water soluble fraction of Cook Inlet crude oil and to determine the fate of that fraction in a simple food chain.

V. Physiology Investigations

Attached (Attachment G) is a list of staff in the Physiology Investigations.

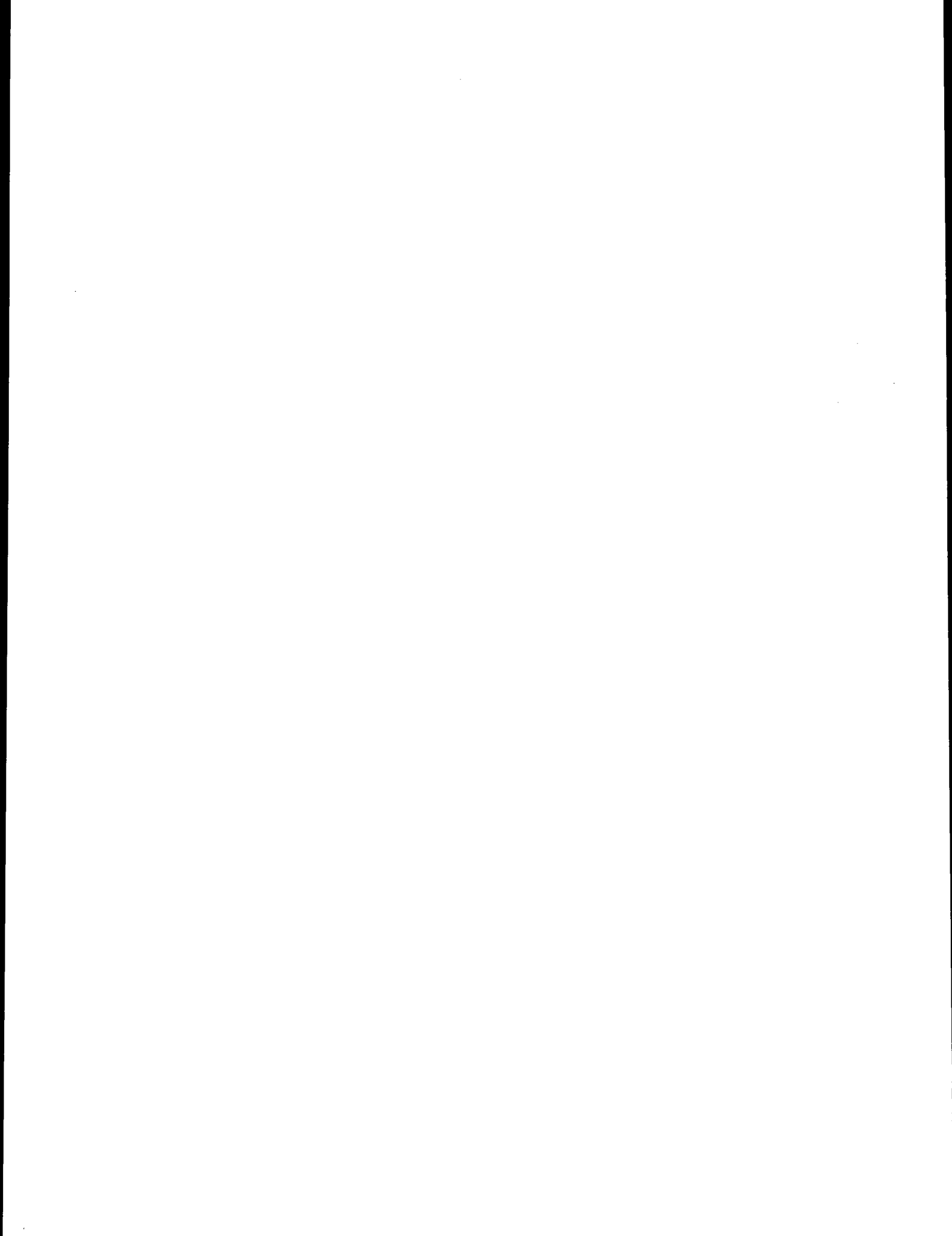


CONTAMINANT BASELINES



CONTAMINANT BASELINES

<u>Research Unit</u>	<u>Proposer</u>	<u>Title</u>	<u>Page</u>
43	Stephen N. Chesler et al. Bioorganic Stds. Sec. NBS	Trace Hydrocarbon Analysis in Previously Studied Matrices and Methods Development for: (A) Trace Hydrocarbon Analysis in Sea Ice and at the Sea Ice-Water Interface, (B) Analysis of Individual High Molecular Weight Aromatic Hydrocarbons	185
47	Philip LaFleur Analytical Chem Div NBS	Environmental Assessment of Alaskan Waters - Trace Element Methodology - Inorganic Elements	189
152	Richard A. Feely Joel D. Cline PMEL/NOAA	Distribution, Composition, Transport, and Hydrocarbon Absorption Characteristics of Suspended Matter in the Gulf of Alaska, Lower Cook Inlet, and Shelikof Strait	191
153	Joel Cline PMEL/NOAA	Distribution of Light Hydrocarbons, C ₁ - C ₄ , in Norton Sound and Chukchi Sea	215
162	David C. Burrell IMS/U. of Alaska	Natural Distribution and Environmental Background of Trace Heavy Metals in Alaskan Shelf and Estuarine Areas	262
275	D. G. Shaw IMS/U. of Alaska	Hydrocarbons: Natural Distribution and Dynamics on the Alaskan Continental Shelf	299
278	Robert J. Barsdate IMS/U. of Alaska	Microbial Release of Soluble Trace Metals from Oil Impacted Sediments	303
413	Hans Nelson USGS	Trace Metal Content of Bottom Sediment in Northern Bering Sea	305



Quarterly Report

Contract #01-6-022-11469
Research Unit #43/44/45

Reporting Period
October 1, 1976 - December 31, 1976

Stephen N. Chesler
Harry S. Hertz
Willie E. May
Stephen A. Wise

Trace Organic Analysis Group
Bioorganic Standards Section
Analytical Chemistry Division
National Bureau of Standards
Washington, D.C. 20234

December 31, 1976

I. TASK OBJECTIVES

The task reported herein relates to serving as a quality assurance laboratory for hydrocarbon analyses of marine waters, sediments and tissues. This objective will be met by: 1) Conducting a second series of interlaboratory comparisons on sediment homogenized at NBS; 2) Conducting an interlaboratory comparison study on tissue samples of Mytilus homogenized by NBS; 3) Acting as a sample-split coordinating-laboratory (10% of all samples collected by NOAA P.I.'s will be sent for NBS analysis and/or redistribution); 4) Acting as a consultant laboratory to other NOAA P.I.'s involved in hydrocarbon analysis.

II. FIELD AND LABORATORY ACTIVITIES

A. Field Activities

There was one field trip during the period covered by this report. The trip occurred on November 18-19, 1976.

B. SCIENTIFIC PARTY

Harry S. Hertz, National Bureau of Standards - principal investigator;

Stephen N. Chesler, National Bureau of Standards - principal investigator;

Kihlo Park, NOAA - staff scientist OCSEAP.

C. METHODS

Sampling and laboratory methods are the same as described in previous reports.

D. SAMPLE LOCALITIES

Twenty-five kg of Mytilus was collected from the steel pilings off Elwood Pier. This pier is located approximately 2 miles downstream from active oil seeps at Coal Oil Point, Santa Barbara, CA.

F. REVISED MILESTONE CHART

<u>Milestones</u>	<u>Date</u>
1) Collect intertidal sediment samples at Katalla River and Hinchinbrook Island for intercalibration exercises. (Mussels also collected.) Sufficient material collected to allow periodic analyses over the course of two years.	5/76

<u>Milestones</u>	<u>Date</u>
2) Return of first intercalibration exercise results (sediment) to NBS and completion of detailed lab analysis of sediment by NBS.	1/77*
3) NBS report to NOAA on results of FY-76 quality assurance program.	3/77*
4) Coal Oil Point mussel collection for intercalibration.	12/76
5) Send out samples for second sediment intercalibration exercise. These samples will be obtained by blending the Katalla and Hinchinbrook samples.	6/77*
6) Completion of mussel homogeneity studies.	4/77
7) Dissemination of mussel samples to participating laboratories (contingent upon satisfactory results in homogeneity study).	4/77
8) Return of second sediment intercalibration exercise results to NBS and completion of detailed lab analysis by NBS.	9/77*
9) Return of mussel intercalibration exercise results to NBS and completion of detailed lab analysis by NBS.	7/77
10) Split of P.I. field samples for quality assurance purposes.	when received
11) NBS report to NOAA on results of FY-77 quality assurance program.	10/77

*Revised milestones. These revisions are due to the lack of response from the laboratories participating in the initial sediment round robin.

III. RESULTS

A. Sediment Round Robin

The round robin sediment material has been analyzed at NBS. We are not releasing our results at the present time due to the extremely slow response from the participants. Of the four NOAA contractors, we have received results from only one laboratory - W. MacLeod, NOAA, Seattle.

B. Sample Split Analyses

We have not received any sample splits from NOAA contractors and thus have not performed this task during this period.

IV. PROBLEMS ENCOUNTERED/RECOMMENDED CHANGES

The problems we encounter continue to be the same as mentioned in earlier reports. We still have not received any sample splits from the other hydrocarbon investigators and have to date received only one round robin response from a NOAA laboratory.

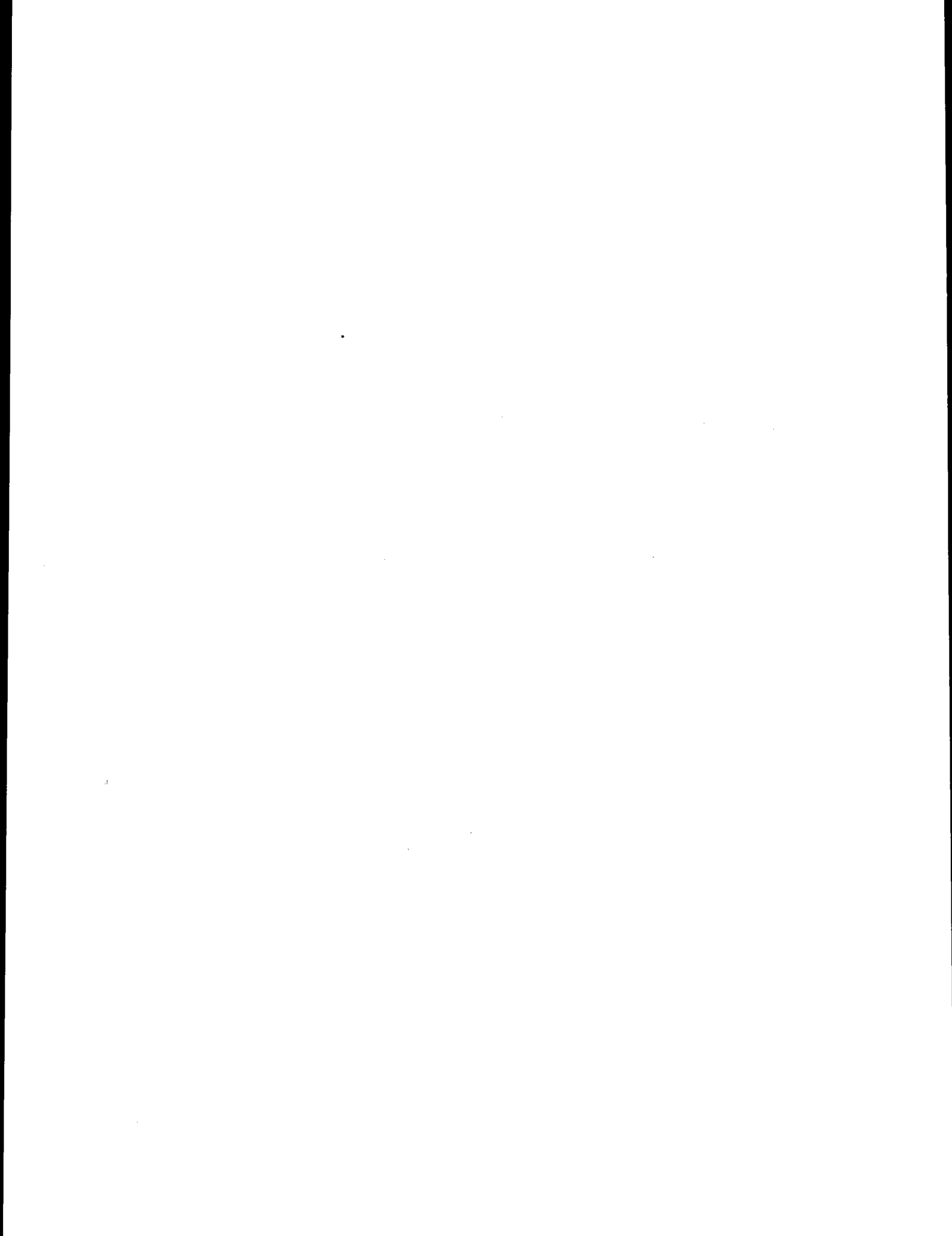
V. ESTIMATED FUNDS EXPENDED

Approximately \$78K have been spent through December 1, 1976.

RU# 47

NO REPORT WAS RECEIVED

A final report is expected next quarter



QUARTERLY REPORT

Research Unit: #152
Reporting Period: 10/1/76-12/31/76

The Distribution, Composition, Transport, and Hydrocarbon
Adsorption Characteristics of Suspended Matter in the
Gulf of Alaska, Lower Cook Inlet, and Shelikof Strait

Principal Investigators: Richard A. Feely, Oceanographer
Joel D. Cline, Oceanographer

Pacific Marine Environmental Laboratory
3711 - 15th Avenue N.E.
Seattle, Washington 98105

I. Task Objectives

The major objectives of the suspended matter program include:

- (1) determination of the seasonal variability of the distribution and composition of suspended matter in Lower Cook Inlet and Shelikof Strait;
- (2) an investigation of the processes controlling resuspension and redistribution of bottom sediments; and
- (3) an investigation of the adsorptive characteristics of Cook Inlet suspended matter for crude oil.

II. Field or Laboratory Activities

A. Field Activities

No field activities occurred during the reporting period.

B. Laboratory Activities

1. Methods

The major (Mg, Al, Si, K, Ca, Ti, and Fe) and trace (Cr, Mn, Ni, Cu, Zn, and Pb) element chemistry of the particulate matter is being determined by x-ray secondary emission (fluorescence) spectrometry utilizing a Kevex[®] Model 0810A-5100 x-ray energy spectrometer and the thin film technique (Baker and Piper, 1976; and Massoth *et al.*, in preparation). The inherent broad band of radiation from an Ag x-ray tube is used to obtain a series of characteristic emission lines from a single element secondary target which then more efficiently excites the thin film sample. Se and Zr secondary targets are used to analyze the samples for both major and trace elements. Standards are prepared by passing suspensions of finely ground USGS standard rocks (W-1, G-2, GSP-1, AGV-1, BCR-1, PCC-1) and NBS trace element standards through a 37 μ m mesh polyethylene screen followed by collection of the size fractionated suspensates on Nuclepore[®] filters identical to those used for sample acquisition. The coefficient of variation for

ten replicate analyses of a largely inorganic sample of approximately mean mass was less than 3 percent for the major constituents and as high as 5 percent for the trace elements. However, when sampling precision is considered, the coefficients of variation increase, averaging 12 and 24 percent for major and trace elements, respectively.

Analysis of total particulate carbon and nitrogen is carried out with a Hewlett Packard model 185B C-H-N analyzer. In this procedure, particulate carbon and nitrogen compounds are combusted to CO_2 and N_2 (micro Dumas method), chromatographed on Poropak[®] Q, and detected sequentially with a thermal conductivity detector. NBS acetanilide is used for standardization. Analyses of replicate surface samples yield coefficients of variation ranging from 2 to 10 percent for carbon and 7 to 14 percent for nitrogen.

2. Data Collected

To date we have completed all five cruises in the Gulf of Alaska and southeastern Bering Shelf scheduled for FY76. The first cruise (RP-4-Di-75B-III) was conducted in the southeastern Bering Shelf during the fall of 1975 (12 September-5 October). The second cruise was conducted in the northeastern Gulf of Alaska during late fall of the same year (21 October-10 November). The third cruise, also in the northeastern Gulf, was conducted in early spring of 1976 (13-30 April). The fourth cruise was conducted in the southeastern Bering Shelf in early summer of 1976 (24 June-9 July). The last cruise was conducted in the northeastern Gulf of Alaska during the summer of 1976 (19-31 July).

In addition to the five cruises, two field expeditions, designed to collect suspended matter samples from the major rivers discharging

into the southeastern Bering Shelf and the northeastern Gulf of Alaska, have been completed. At this point, approximately 1500 samples have been collected and weighed for suspended load determinations. In addition, approximately 600 samples have been collected for elemental analysis of the particulate material.

3. Sample Locations

The sample locations for cruises one through three have been given in previous reports. Figure 1 shows the locations of the suspended matter stations in the southeastern Bering Shelf for cruise four (RP-4-MW-76B-VIII). A number of the EBBS stations were omitted during this cruise because of insufficient time. Figure 2 gives the station positions for cruise five (RP-4-Di-76B-I). Figures 3 and 4 respectively show the locations of the suspended matter stations for the river sampling expeditions in the southeastern Bering Shelf and northeastern Gulf of Alaska.

III. Results

A. Particulate Matter Distributions

The data on the distribution of suspended matter in the southeastern Bering Shelf and the northeastern Gulf of Alaska for the fall cruises (RP-4-Di-75B-III and RP-4-Di75C-I) are complete and have been described in the First Annual Report. We have also completed the analyses of the samples from the spring cruise in the northeastern Gulf (RP-4-Di-76A-IV) and these data were discussed in the 6th Quarter Report. The data from the summer cruises (RP-4-MW-76B-VIII in the southeastern Bering Shelf and RP-4-Di-76B-I in the northeastern Gulf of Alaska) and the two river sampling expeditions are complete and will be described below.

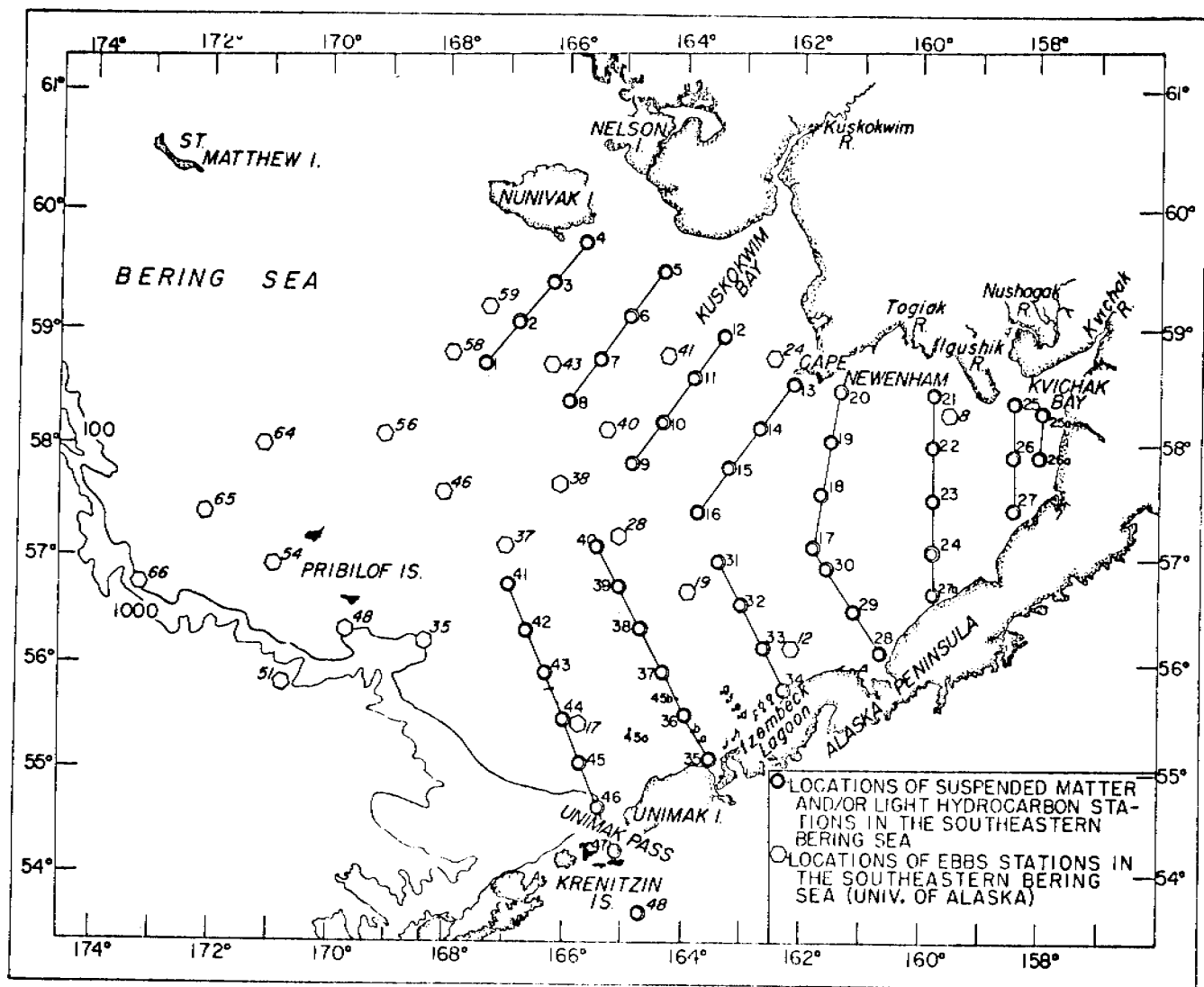


Figure 1. Locations of suspended matter stations in the southeastern Bering Shelf (Cruise RP-4-MW-76B-VIII, 24 June - 9 July, 1976)

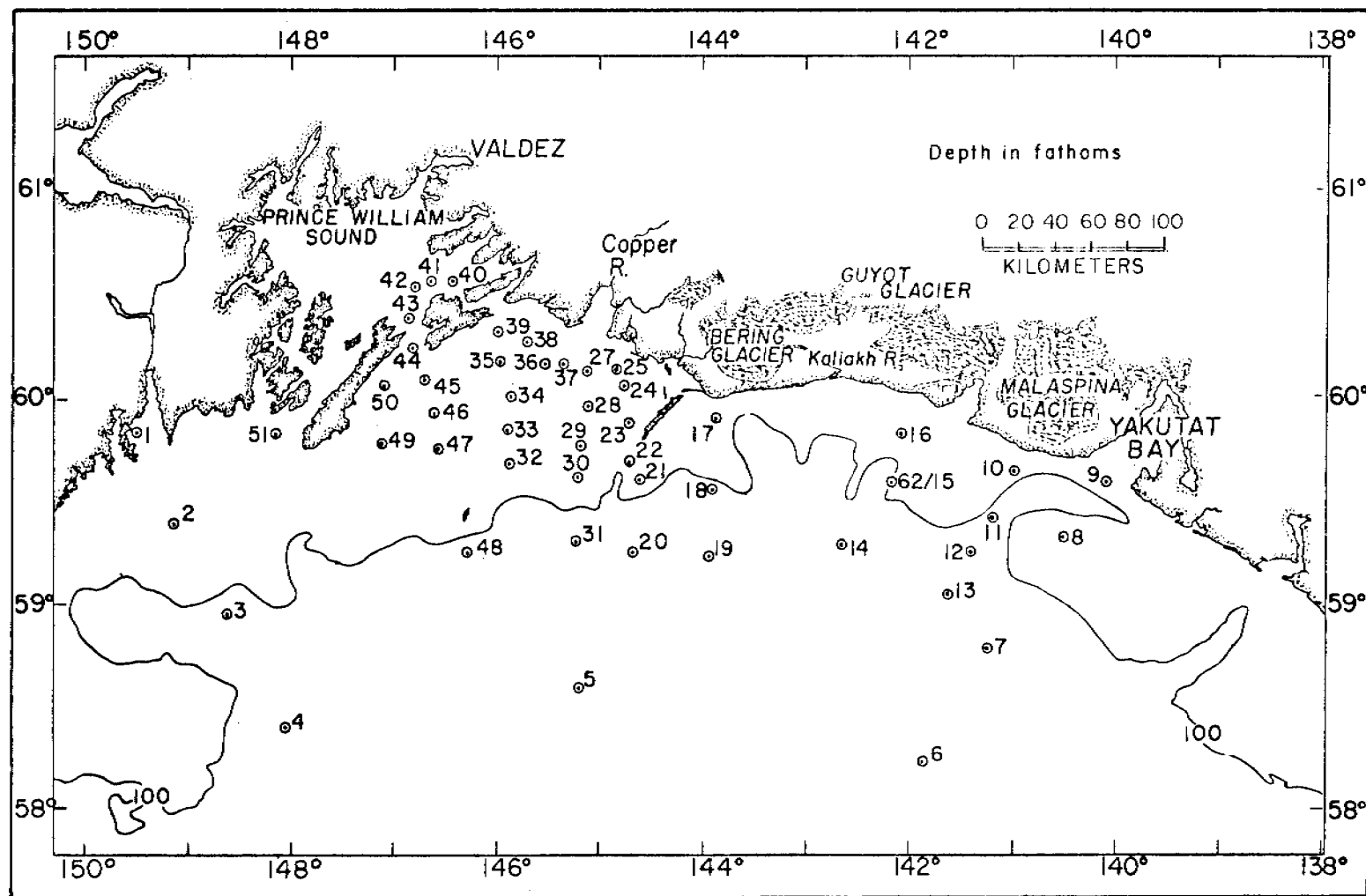


Figure 2. Locations of suspended matter stations in the northeastern Gulf of Alaska (Cruise RP-4-Di-76B-1, 19 - 31 July, 1976)

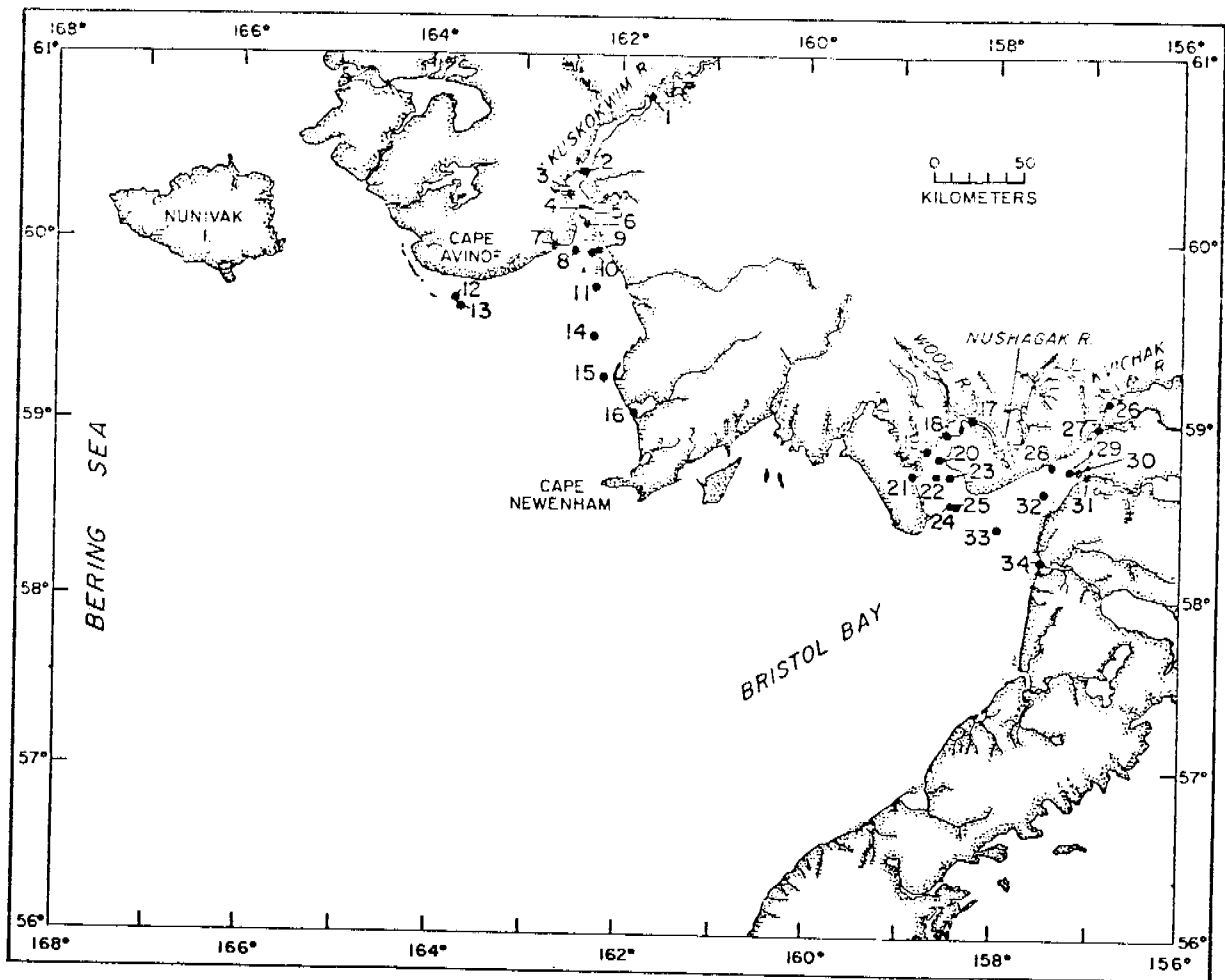


Figure 3. Locations of suspended matter stations in the major rivers draining into the southeastern Bering Shelf (12 - 21 Sept., 1976)

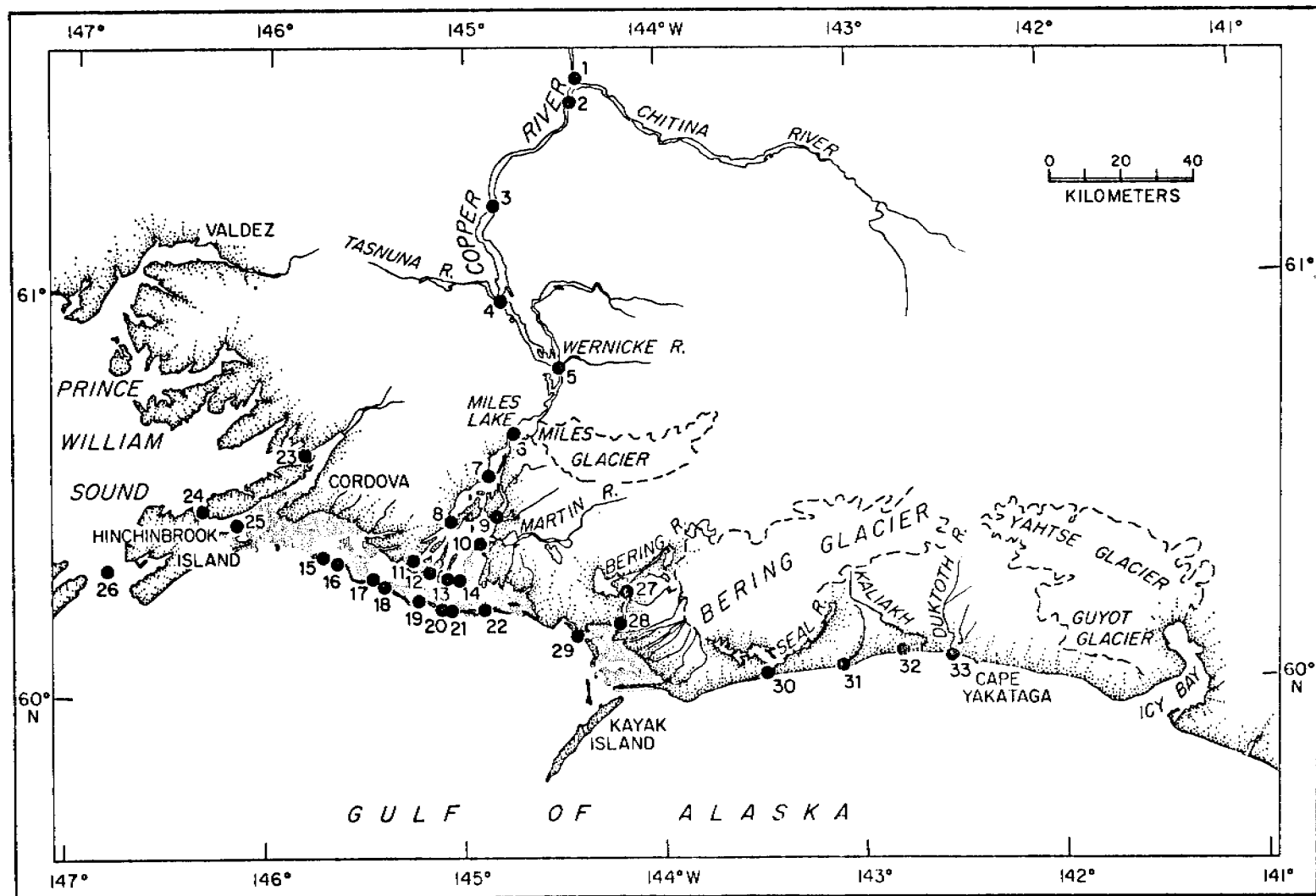


Figure 4. Locations of suspended matter stations in the major rivers draining into the northeastern Gulf of Alaska (22 - 27 June, 1976)

1. Southeastern Bering Shelf

Figures 5 and 6 show the distribution of suspended matter at the surface and 5 m above the bottom during the summer cruise in the southeastern Bering Shelf (RP-4-MW-76B-VIII, 24 June-9 July 1976). The surface particulate matter distributions are dominated by the discharge of suspended material from the northern rivers. Large plumes of suspended matter extend to the southwest from Kuskokwim Bay and the region east of Cape Newenham. Similar plumes were observed during the fall cruise (First Annual Report) and at that time the plumes consisted of inorganic suspended material originating from the Kuskokwim, Kvichak, and Nushagak Rivers. It is expected that these plumes consist of suspended matter from similar sources. However, we are presently conducting chemical analyses of the samples from this region for the purpose of documenting the sources and these data will be presented in a future report.

Along the Alaska Peninsula surface suspended matter concentrations decrease rapidly away from the coast. This is due to rapid mixing of the highly turbid shelfwater with the relatively clear Pacific Ocean water which originates from the passes of the Alaskan Peninsula and is deflected to the northeast along the coast of the Alaskan Peninsula. Near Unimak Island and in the region west of the northern end of the Alaska Peninsula, two surface plumes are evident which were not observed during the fall cruise. These plumes might be attributed to the large seasonal variations in primary productivity which are characteristic of this region. Sharma et al. (1974) observed turbid plumes in the region northwest of Unimak Pass which he attributed to similar processes.

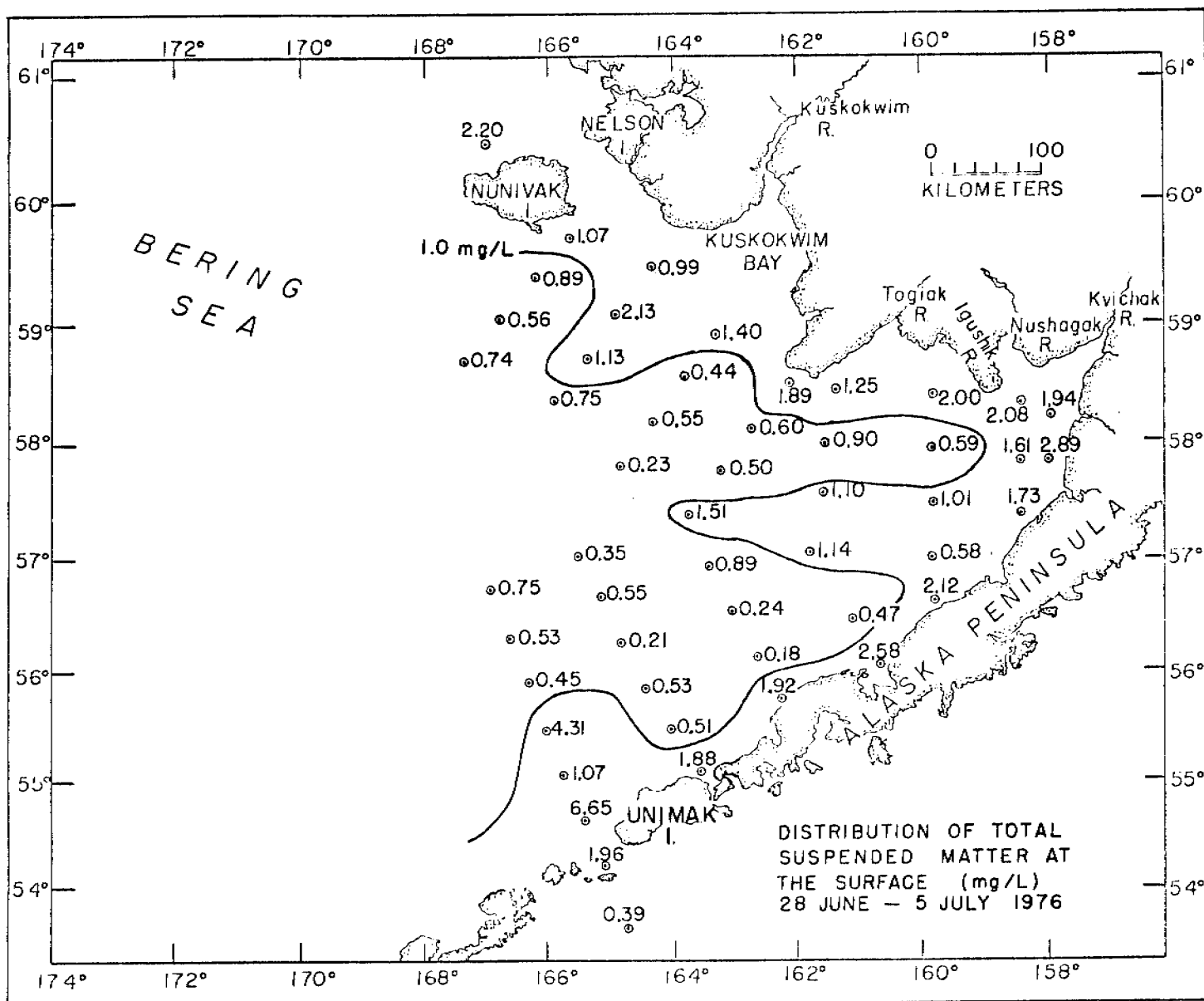


Figure 5. Distribution of total suspended matter at the surface in the southeastern Bering Shelf (Cruise RP-4-MW-76B-VIII, 24 June - 9 July, 1976)

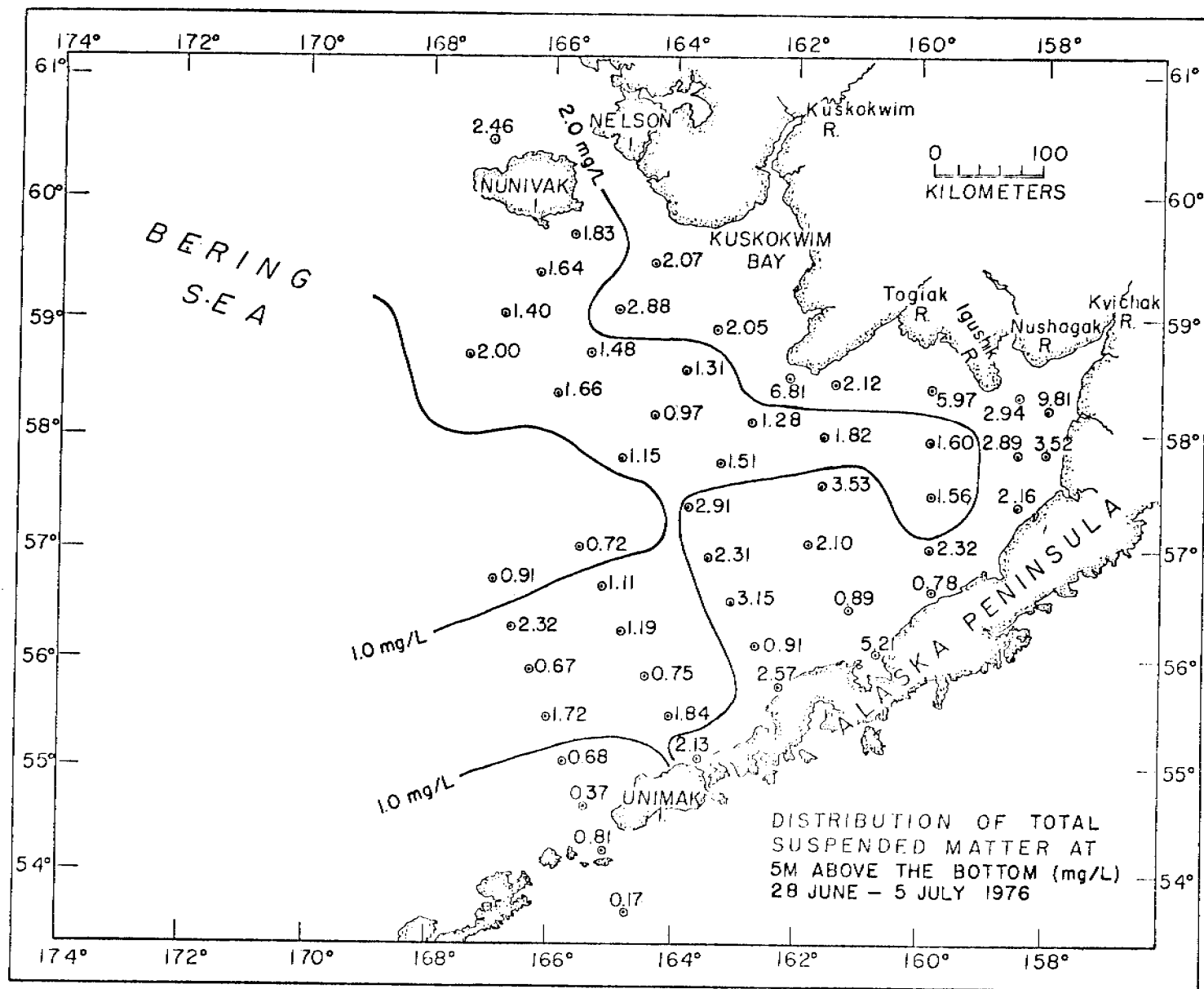


Figure 6. Distribution of total suspended matter at 5 m above the bottom in the southeastern Bering Shelf (Cruise RP-4-MW-76B-VIII, 24 June - 9 July, 1976)

Near the bottom, suspended matter concentrations are high (> 1.0 mg/L) throughout most of the study region, indicating possible resuspension of bottom sediments. Figure 7 shows a vertical cross-section of broken lines of stations from Kuskokwim Bay to Unimak Island. The figure shows increasing suspended matter gradients near the bottom which are attributed to resuspension and redistribution of bottom sediments. Since Bristol Bay is a relatively shallow embayment, it is entirely possible that waves and tides play a major role in the resuspension processes. Sharma et al. (1972) have presented evidence from grain size distributions of Bristol Bay sediments to show that wave energy on the bottom plays a predominant role in the redistribution of sediments.

2. Northeastern Gulf of Alaska

Since there are no gauging stations near the mouths of the major rivers discharging into the northeast Gulf of Alaska, there is very little information about the quantities of sedimentary materials that are discharged into the Gulf of Alaska from these important sources. From careful analysis of discharge data for the Copper River near Chitina, Reimnitz (1966) estimated that approximately 1.07×10^{14} g yr⁻¹ of fine grain material are delivered annually to the Gulf by way of the Copper River system.

In order to obtain an order of magnitude verification of the estimates made by Reimnitz, river samples were collected near the mouths of the major rivers discharging into the northeast Gulf (see Figure 4). River samples were obtained with a precleaned 4-liter polyethylene bottle lowered from a Bell 206B helicopter hovering within 2 m of the water surface, June 22-27, 1976. Figure 8 shows

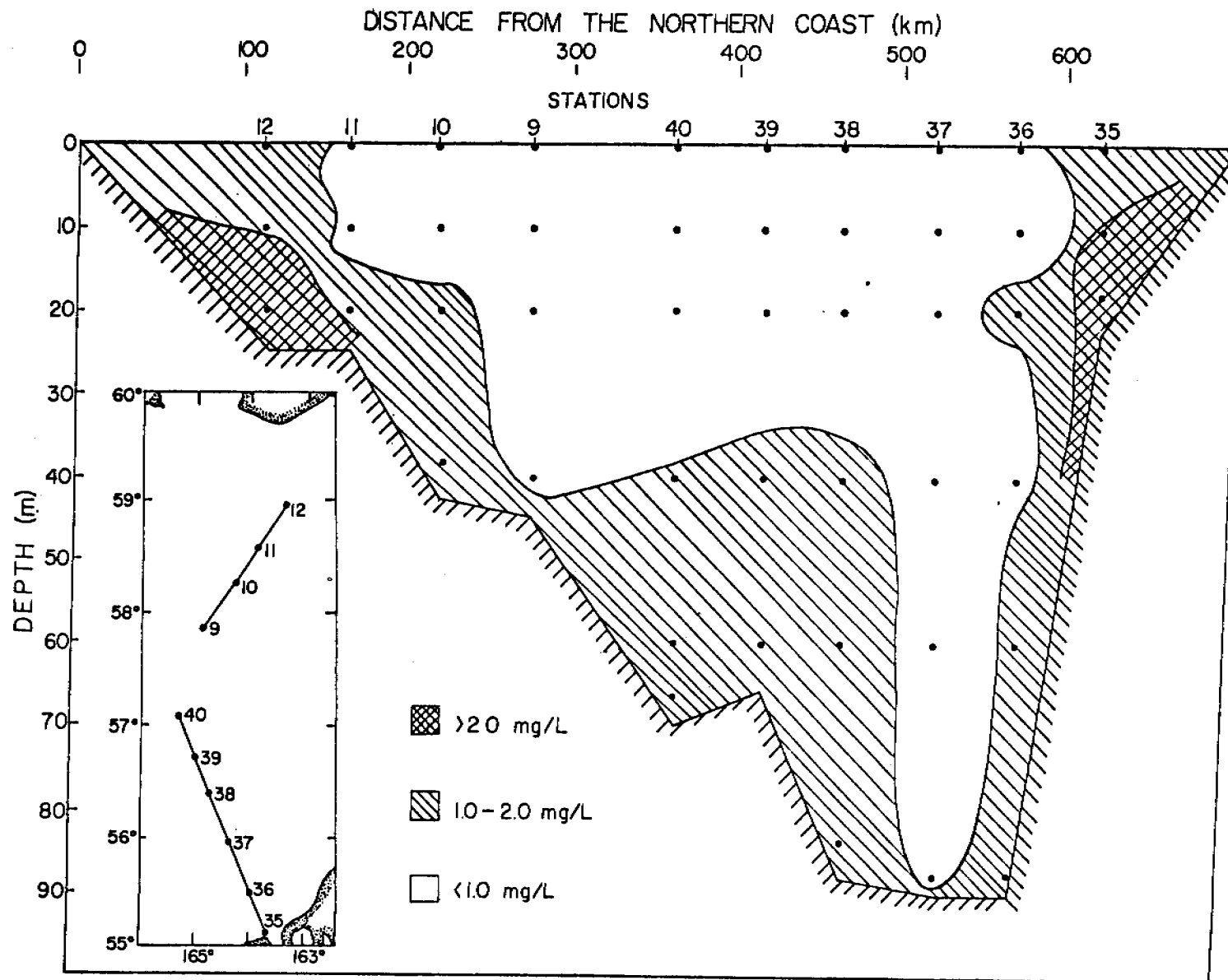


Figure 7. Vertical cross section of the distribution of total suspended matter for stations 9 thru 12 and 36 thru 40 in the southeastern Bering Shelf (Cruise RP-4-MW-76B-VIII, 24 June - 9 July, 1976)

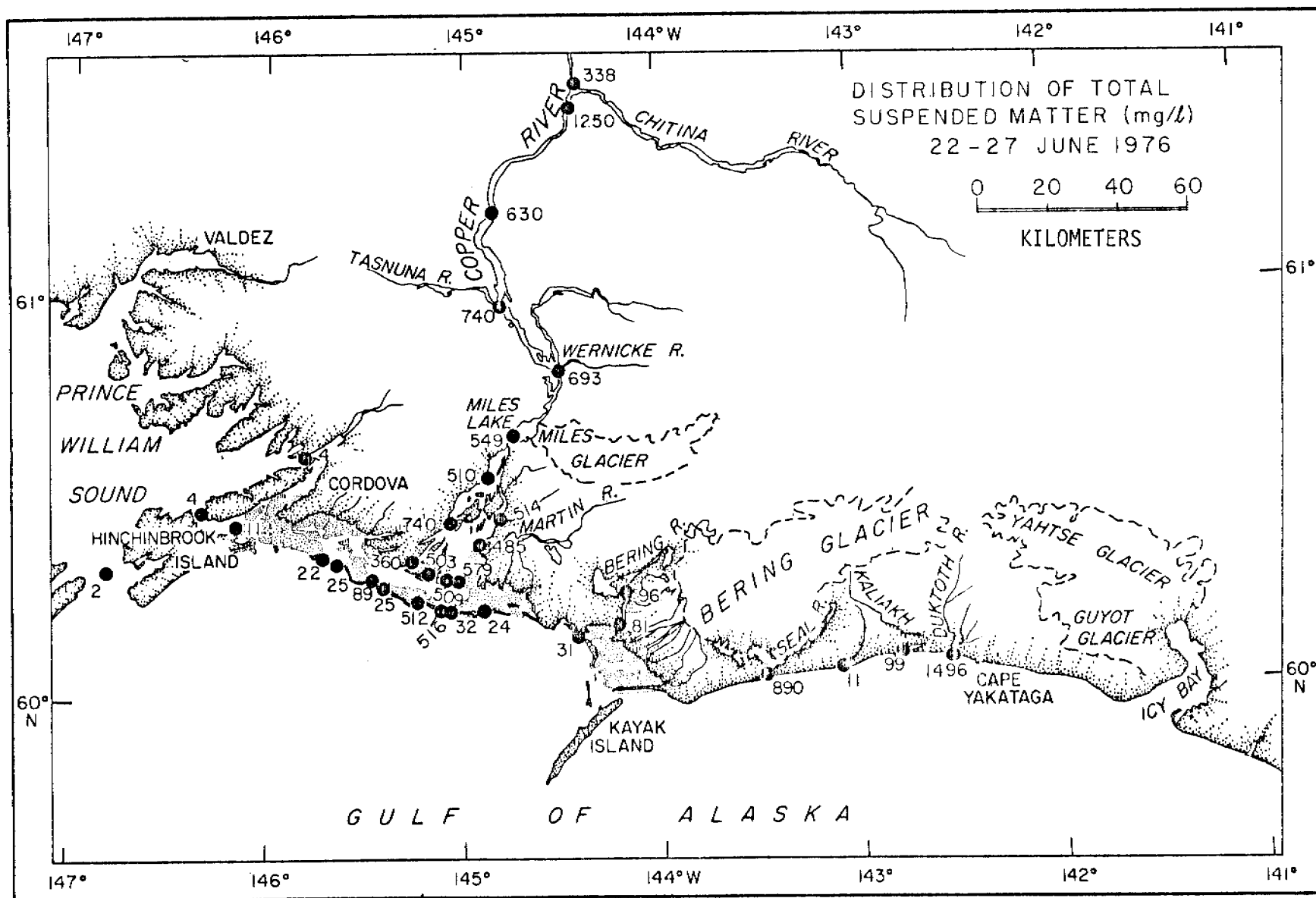


Figure 8. Distribution of total suspended matter at the surface in the major rivers draining into the northeastern Gulf of Alaska (22 -27 June, 1976)

the results of those measurements. Near the mouth of the Copper River suspended matter concentrations average $0.525 \pm .09$ g/l. Using this value and the approximation of the annual water discharge at the mouth of the Copper River (estimated by Reimnitz to be approximately 8.0×10^{13} l yr⁻¹), the estimated annual mean discharge of approximately 0.42×10^{14} g yr⁻¹ is calculated. This estimate is approximately 2.5 times lower than the estimate of Reimnitz. However, considering the large variations that may result from annual and seasonal fluctuations in discharge rates and sediment concentrations, the small difference between these estimates may not be significant. More accurate determinations of annual sediment fluxes are not possible without permanent gauging stations.

East of Kayak Island the coastal rivers which drain the Bering, Guyot and Malaspina Glaciers have widely varying suspended matter concentrations. Surface concentrations at the river mouths range from 11 mg/l for the Tsivat River to 1496 mg/l for the Ducktooth River. These variations are probably related to the water and suspended matter discharge patterns of the nearby glaciers. At this time no estimates of water discharge from these rivers are available, and consequently, no estimates of sediment fluxes can be made.

While the available information on the sediment fluxes from the major rivers discharging into the Gulf of Alaska is sketchy, it does suggest that significant seasonal variations occur which would affect seasonal patterns of suspended matter distributions in the Gulf. Figures 9 and 10 show the distribution of suspended matter at the surface and 5 m above the bottom during the summer cruise in the northeastern Gulf of Alaska (RP-4-Di-76B-I, 19-31 July 1976). The

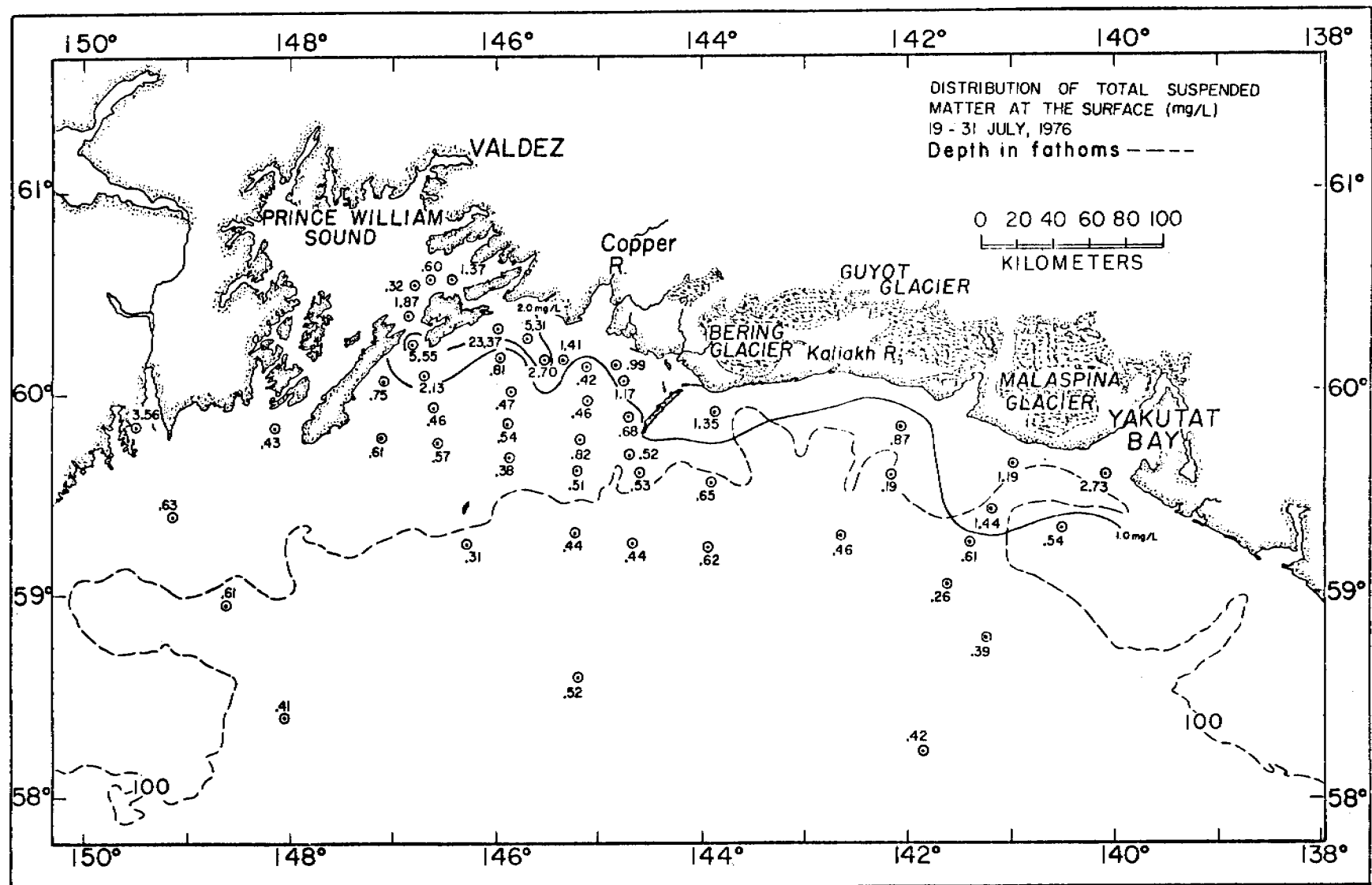


Figure 9. Distribution of total suspended matter at the surface in the northeastern Gulf of Alaska (Cruise RP-4-Di-76B-I, 19 - 31 July, 1976)

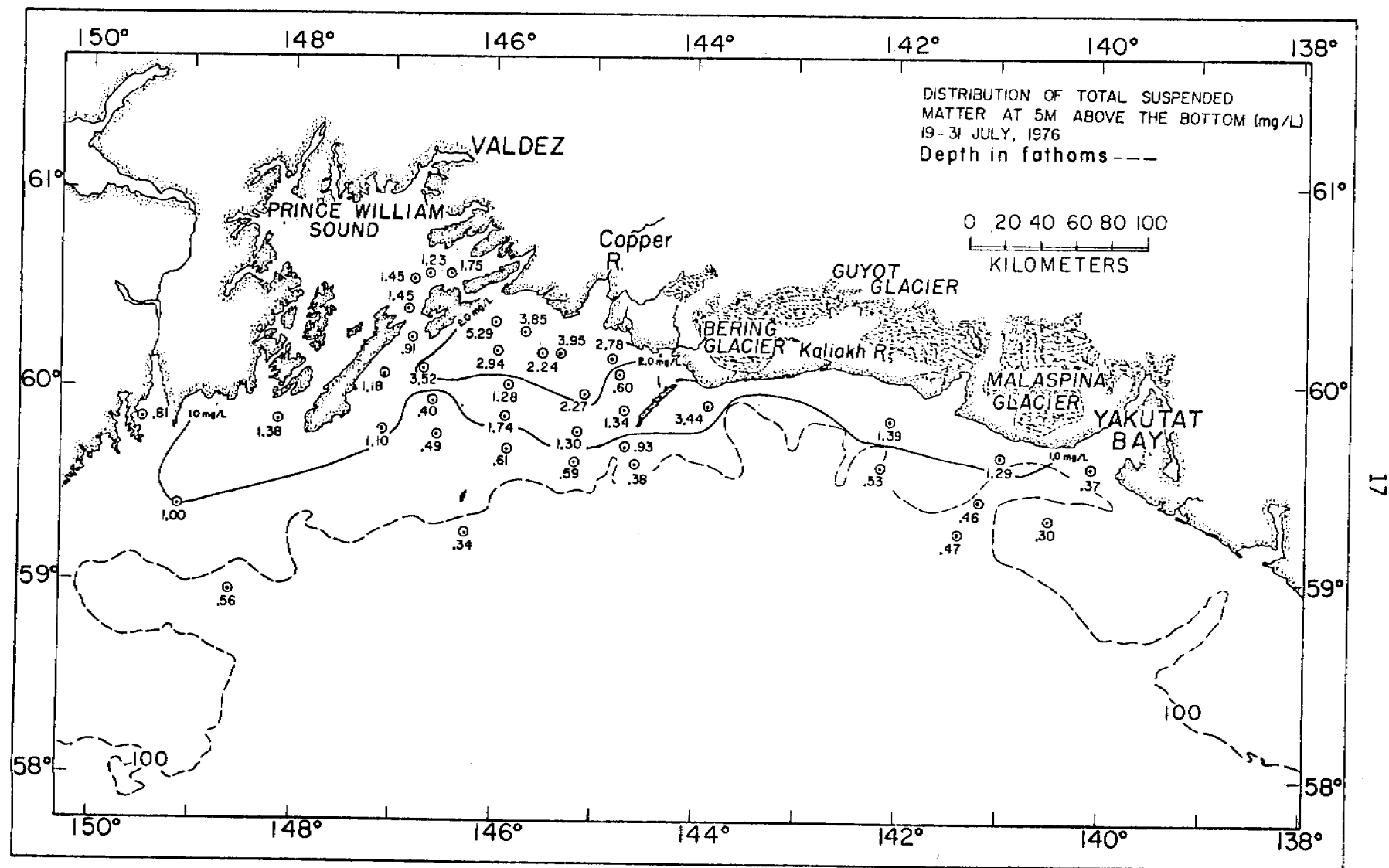


Figure 10. Distribution of total suspended matter at 5 m above the bottom in the northeastern Gulf of Alaska (Cruise RP-4-Di-76B-I, 19 - 31 July, 1976)

surface suspended matter distribution pattern for the summer cruise is different from the previous two cruises. For example, in the region just south of Malaspina Glacier a plume of turbid water extends outward from the coastline. This plume was not observed during either of the previous two cruises and may be the result of increased sediment flux from the coastal rivers during the summer. However, from careful analysis of ERTS imagery for this region Burbank (1974) observed that occasionally wind-generated counterclockwise eddies were formed which transported significant quantities of terrestrial material seaward. It is probable that both factors, high sediment flux and the formation of wind-generated eddies, contribute to the offshore transport of suspended matter in this region. Although such ephemeral processes are difficult to document without extensive supportive physical oceanographic data, there is a strong possibility that these eddies play a major role in the offshore transport of suspended matter.

During the fall and spring cruises significant quantities of terrestrial suspended matter were transported to the southwest from Kayak Island by what was presumed to be a large clockwise eddy. The summer cruise showed no evidence that a similar transport mechanism was in effect. Turbid plumes of terrestrially derived suspended matter remain relatively close to the coastline on either side of Kayak Island. Apparently, the large clockwise eddy which is characteristic of this region was not present at the time of the summer cruise.

In the vicinity of the Copper River a plume of highly turbid water extends offshore as far as 40 km. Suspended matter

concentrations within the plume are high, averaging 6.7 mg/L, which reflects the increased sediment discharge during the summer months. As with the previous two cruises, the sedimentary material from the Copper River is carried to the west along the coast until it reaches Hinchinbrook Island, where a portion of the material passes into Prince William Sound and the remaining material is carried to the southwest along the southeastern coast of Montague Island.

B. Elemental Chemistry of the Particulate Material

At this point, we have completed the analyses of the samples from the fall cruises in the Gulf of Alaska and southeastern Bering Shelf. The results of the analyses were described in previous reports and, therefore, will not be described here. Work is progressing on the samples from the spring and summer cruises. However, no data are available at this time.

C. Sampling and Analytical Precision

In order to compare the reproducibility of the analytical techniques for determining the chemical composition of the suspended matter with the variability of the samples, a number of replicate experiments were conducted during the fall cruise in the Gulf. A surface sample from station 9 was collected in a 10-liter Niskin bottle and simultaneously filtered through ten 0.4 μm pore size Nuclepore[®] filters. All ten filters were analyzed for major and trace inorganic elements and the results are shown in Table I. In addition, a single rock standard was prepared in exactly the same manner as the samples and analyzed once a day during 53 sequential days of analysis and the results are shown in Table II. Table I shows the variability of the samples and Table II shows the precision of the x-ray fluorescence technique. As shown in Table II, the analytical precision ranges from 1.2 to 3.1 percent for the major elements and 2.2 to 8.9

TABLE I

Replicate study of ten individually filtered water samples from a single Niskin[®] bottle taken from the surface at station 9 in the northeastern Gulf of Alaska (RP-4-Di-75C-I, 21 Oct.-10 Nov., 1975)

Replicate#	Mg(wt.%)	Al(wt.%)	Si(wt.%)	K(wt.%)	Ca(wt.%)	Ti(wt.%)	Cr(ppm)	Mn(ppm)	Fe(wt.%)	Ni(ppm)	Cu(ppm)	Zn(ppm)	Pb(ppm)
1	6.94	9.04	23.95	1.37	4.48	0.42	84.2	956	5.70	42.1	52.2	159.8	71.5
2	7.82	11.77	31.02	1.74	5.50	0.55	150.6	1227	7.45	61.0	74.9	212.5	84.4
3	7.72	11.17	30.11	1.65	5.91	0.53	117.8	1212	7.21	147.7	64.6	191.9	77.7
4	6.88	10.71	29.67	1.68	5.94	0.54	117.3	1188	7.30	49.6	60.5	175.7	74.5
5	7.41	11.20	31.02	1.71	5.86	0.56	119.5	1241	7.51	53.5	63.0	201.8	72.6
6	6.54	10.04	27.44	1.53	5.08	0.49	101.9	1098	6.61	49.6	71.3	198.0	103.2
7	7.69	11.47	30.15	1.64	5.78	0.53	114.3	1189	7.16	52.8	77.1	232.1	99.1
8	7.52	11.42	32.87	1.80	6.28	0.59	131.1	1348	8.14	57.2	79.1	225.9	97.0
9	5.92	9.01	25.86	1.42	5.17	0.48	96.0	1053	6.37	40.7	54.6	203.9	73.0
10	6.22	11.83	32.25	1.94	3.05	0.54	138.2	1220	6.55	46.2	50.6	179.7	84.8
Mean	7.40	10.76	29.44	1.65	5.30	0.52	117.0	1173	6.99	60.1	64.8	198.1	83.8
STD. DEV.	1.22	1.06	2.84	0.17	0.94	0.05	19.8	110	0.69	31.4	10.5	22.4	12.0
Coeff. of variation (%)	16.4	9.8	9.6	10.3	17.9	9.3	16.9	9.4	9.9	52.3	16.1	11.3	14.3

TABLE II

Ten replicate analyses of a single USGS W-1 standard. The rock standard was prepared by passing a suspension of the rock material through a 37 μm polyethylene mesh followed by collection of the suspensate on a Nuclepore[®] filter (0.4 μm nominal pore size, 2.5 cm^2 active collection area). Replicates were randomly chosen from 53 sequential days of analysis.

Replicate #	Seq. #	Mg (wt. %)	Al (wt. %)	Si (wt. %)	K (wt. %)	Ca (wt. %)	Ti (wt. %)	Cr (ppm)	Mn (ppm)	Fe (wt. %)	Ni (ppm)	Cu (ppm)	Zn (ppm)
1	2	3.99	7.57	24.72	0.53	7.82	0.62	105	1,266	7.70	86	104	90
2	16	4.23	8.27	25.42	0.57	7.95	0.65	106	1,308	7.83	86	125	94
3	17	4.19	8.30	25.75	0.57	8.08	0.66	115	1,315	7.93	90	123	88
4	23	4.18	8.08	25.70	0.57	7.99	0.67	116	1,338	7.89	87	130	93
5	26	4.00	8.18	25.24	0.57	7.95	0.65	112	1,299	7.85	91	126	93
6	31	4.17	8.27	25.42	0.56	7.93	0.65	108	1,287	7.80	87	130	93
7	34	4.20	8.34	25.87	0.57	8.05	0.66	111	1,314	7.87	86	136	93
8	38	4.05	7.80	24.67	0.55	7.80	0.64	107	1,264	7.67	85	132	91
9	39	3.96	8.27	25.34	0.56	7.85	0.65	107	1,303	7.72	90	136	89
10	49	4.03	7.95	25.13	0.56	7.84	0.64	106	1,291	7.72	89	149	93
Mean		4.10	8.10	25.33	0.56	7.93	0.65	109	1,299	7.80	88	129	92
Std. Dev.		0.10	0.25	0.41	0.02	0.10	0.01	4	23	0.09	2	12	2
Coef. of Variation (%)		2.5	3.1	1.6	2.3	1.2	2.1	3.6	1.7	1.2	2.4	8.9	2.2

percent for the trace elements. In contrast, the sampling precision ranges from 9.6 to 17.9 percent for the major elements and 9.4 to 52.3 percent for trace elements. These results clearly illustrate that with respect to the quantities of material analyzed the sample-to-sample variability is significantly greater than the analytical variability for all the elements that were studied.

IV. Preliminary Interpretation of the Results

The distribution patterns of particulate material in the southeastern Bering Shelf and northeastern Gulf of Alaska indicate significant seasonal variations which are the result of a number of processes acting concurrently. These include: the rate of supply of sedimentary material from the coastal rivers; the rate of primary production; and local variations in surface currents. During the summer months when both the supply of sedimentary material from the coastal rivers and primary productivity are at a maximum, local variations in suspended matter distributions are common. Plumes of river-derived suspended matter are most intense at this time and significant offshore transport is effected by wind-generated surface eddies.

Near the bottom, suspended matter concentrations generally increase with depth. A bottom nepheloid layer covers most of the shelf. The quantity of suspended matter in the nepheloid layer and its height above the bottom is highly variable in space and time and appears to be most intense in the fall and winter months when tidal and storm-induced bottom currents are of sufficient velocity to resuspend bottom sediments.

A comparison of the analytical precision for a single standard with a replicate study of ten individually filtered subsamples from a Niskin bottle clearly demonstrates that for all the elements studied the sample-

to-sample variability is greater than the analytical precision of the x-ray fluorescence techniques applied.

V. Problems Encountered

We have no significant problems to report at this time.

VI. Estimate of Funds Expended

Since we have only recently received the FY77 funds for this project, no estimates of expenditures are available at this time.

References

Reimnitz, E., 1966. Late Quaternary history and sedimentation of the Copper River Delta and vicinity, Alaska (unpublished Ph.D. dissertation). Univ. California, La Jolla, 225 p.

Sharma, G. D., 1972. Graded sedimentation on the Bering Shelf. 24th IGC. Section 8.

→ Sharma, G. D., Wright, F. F., Burns, J. J., and Burbank, D. C., 1974. Sea surface circulation, sediment transport, and marine mammal distribution, Alaska Continental Shelf, report prepared for the National Aeronautics and Space Administration.

Quarterly Report

Research Unit: 153-77
Reporting Period: 1 Oct. - 31 Dec. 1976
Number of Pages: 46

DISTRIBUTION OF LIGHT HYDROCARBONS, C₁-C₄,
IN NORTON SOUND AND CHUKCHI SEA

Dr. Joel Cline

Pacific Marine Environmental Laboratory
3711 - 15th Avenue N.E.
Seattle, Washington 98105

December 31, 1976

I. OBJECTIVES

The low molecular weight hydrocarbon program was initiated in the OCS of Alaska in response to the environmental guidelines set forth in the Environmental Study Plan for the Gulf of Alaska, Southeastern Bering Sea and the Beaufort Seas (January, 1975). Briefly, the purpose was to establish the spatial and temporal variations (seasonal and diurnal) in the low molecular weight hydrocarbon fraction prior to exploration, development, and production of fossil fuel reserves in the proposed lease areas. These components have proven to be valuable indicators of petroleum input arising from drilling, production, and transportation of crude oil and refined products.

In support of the basic objectives, attention was given to natural hydrocarbon sources, namely gas and oil seeps, production of hydrocarbons from near-surface bottom sediments, and biogenic hydrocarbon sources within the water column. Of particular importance is the ephemeral nature of the low molecular weight hydrocarbon fraction arising from local sources and their importance as reliable indicators of petroleum accumulations.

In this contract period, LMWH studies will focus on site specific regions of Lower Cook Inlet, Tarr Bank and Kayak Island (NEGOA), southeastern Kodiak Shelf, and Norton Sound. Emphasis will be placed on the identification of petroleum or natural gas hydrocarbons arising from natural source regions. These studies will be directed toward the assessment of low molecular weight hydrocarbons (aliphatics and aromatics) as useful indicators of petroleum hydrocarbons. Our present capability will be supplemented by the analysis of the low molecular weight aromatics (e.g., benzene, toluene, ethylbenzene, etc.) as we feel that these components may be strongly indicative of petroleum sources. Because of very low natural background levels, these components will prove to be valuable plume tracers.

II. FIELD ACTIVITIES

A. Field Schedule

During the reporting period 1 October thru 31 December 1976, no field activities were conducted. However, results from the Norton Sound/Chukchi Sea cruise conducted in September 1976 (RP-4-DI-76B-4) will be presented at this time. Because of the timing of this cruise, these results could not be included in the previous 6th Quarter Report. Other pertinent data relative to participating scientists, station and trackline data may be obtained from the aforementioned report.

B. Laboratory Schedule

In preparation for FY77 studies, two equipment and laboratory objectives must be met. The first of these is the final design and construction of the interstitial water gas sampler. The final design has been agreed upon by us and the Department of Oceanography (UW), and construction will commence in late January 1977. Scheduled completion should be in advance of the April 1977 cruise to the northeast Gulf of Alaska. Field testing of the instrument will be conducted in early March 1977.

The new LMWH program envisioned will augment the analysis of waters for the low molecular weight aromatics. Equipment is currently on hand and studies are currently underway evaluating several adsorption resins for the retention of the aromatics. This program will be implemented by April 1977.

C. Scientific Party

See semi-annual report: 1 July - 30 Sept. 1976.

D. Methods

See semi-annual report: 1 July - 30 Sept. 1976.

E. Sampling Grid

For clarity, the station grids occupied in Norton Sound and the Chukchi Sea are included in this report (Figures 1 and 2). They are also shown in the semi-annual report.

F. Data Collected and Analyzed

See semi-annual report: 1 July - 30 Sept. 1976.

III. RESULTS

A. Chukchi Sea and Kotzebue Sound

The spatial and vertical distribution of the low molecular weight hydrocarbons (LMWH) was determined during the month of September 1976 as a continuation of our sampling program in the OCS of Alaska.

The sampling grid employed is shown in Figure 1.

1. Methane

The areal distributions of methane in n1/1 (STP) are shown for the surface layers (Figure 3) and 5 meters from the bottom (Figure 4). Surface concentrations of methane (excluding Kotzebue Sound proper) are rather uniform, ranging from a low of 100* n1/1 at the northern extremity of the survey grid to a high of 215 n1/1 near the coast northwest of Kotzebue. The average concentration was 130 ± 25 n1/1. Presumably this represents near equilibrium conditions with the atmosphere. In contrast, surface concentrations within inner Kotzebue Sound are significantly higher (338 ± 110 n1/1), primarily due to a vertical flux from methane-rich water below.

*In accord with our nominal sampling and analytical errors, all methane values have been rounded to the nearest 5 n1/1. This procedure also facilitates contouring.

The distribution of methane in the near bottom waters is highly variable, reflecting both localized and advective sources. An example of the former is shown in Kotzebue Sound where the concentration of methane exceeds 3000 n1/l. At the time of these observations, the water column in Kotzebue Sound was highly stratified with warm low salinity water at the surface ($S = 25 \text{ ‰}$, $T = 9^{\circ}\text{C}$) and cold, relatively high salinity water at the bottom ($S = 28 \text{ ‰}$, $T < 1^{\circ}\text{C}$). Methane released from the anoxic bottom sediments was trapped below the resulting pycnocline. It will be shown in subsequent sections that these elevated concentrations of methane were not supported by similarly high levels of other LMWH (e.g., ethane, ethylene, etc.).

The plume of methane-rich water emerging from the western Chukchi Sea appears to be an artifact of circulation. In Figures 5 and 6 are shown the surface and near bottom distribution of temperature. Both of these thermal surfaces reveal the intrusion of relatively cold water ($< 4^{\circ}\text{C}$) into the survey region from the west. More will be said about this water mass later in the report.

The average near bottom concentration of methane (excluding Kotzebue Sound) is $360 \pm 130 \text{ n1/l}$. These levels of methane are rather typical for shelf waters over the OCS of Alaska based on our previous measurements. The lowest concentrations of methane near the bottom were observed near the coast (Figure 4), where a low bottom source is anticipated.

2. Ethane and Ethylene

The surface distribution of ethane and ethylene is shown in Figures 7 and 8. Both components reveal little spatial variability, suggesting the absence of well-defined localized sources or sinks. The average ethane

concentration in the surface layers is $0.6^* \pm 0.2$ n1/1 and compares favorably with our observations in Bristol Bay and NEG OA.

Surface concentrations of ethylene are systematically higher than those of ethane, presumably reflecting low level primary productivity. The average is 1.2 ± 0.4 n1/1, or a factor of two above the average concentration of ethane.

Near bottom concentrations of ethane and ethylene are shown in Figures 9 and 10. Both of these components correlate strongly with the near bottom temperature (Figure 6) and salinity distributions, suggesting that circulation is the dominant factor.

The average near bottom concentration of ethane and ethylene is 1.1 ± 0.6 n1/1 and 2.6 ± 1 n1/1. On the average, the concentration of ethylene exceeds that of ethane by a factor of 2.6. This is in excellent agreement with our findings in both the Gulf of Alaska and southeastern Bering Sea, where the factor ranges from 2 to 3. These results are biased in that the plume of C₂-rich water at 68°N is characterized by unusually high concentrations of ethane relative to ethylene. This observation will be treated more fully in the discussion section.

3. Propane and Propylene

The surface distribution of propane and propylene is depicted in Figures 11 and 12. As was the case with the surface distributions of the C₂ aliphatics, no localized sources or sinks were observed. The average surface concentrations of ethane and ethylene are 0.2 ± 0.1 n1/1 and 0.4 ± 0.2 n1/1. Concentrations of propylene less than .05 n1/1 are reflected as zero (Figure 12).

*All values for ethane, ethylene, propane, and propylene have been rounded to the nearest 0.1 to reflect actual analytical and sampling variability.

Concentrations of propane and propylene near the bottom are revealed in Figures 13 and 14. Propane, not unlike that of ethane and ethylene, is correlated with near bottom circulation (Figure 13). Average concentrations of propane and propylene are 0.6 ± 0.3 n1/1 and 0.6 ± 0.2 n1/1, respectively. These average values are rather typical for near bottom Alaskan shelf waters with the exception of the plume of propane-rich water emerging from the western Chukchi Sea. In the core of the plume the concentration of propane exceeds propylene by a factor of 3 (Figures 13 and 14). This is an unusual circumstance and reflects the rather unique hydrocarbon composition of this water mass.

4. Iso- and n-butanes

The concentrations of iso- and n-butanes were uniformly below 0.1 n1/1. Because of inherent low-level contamination of water samples, the uncertainty in the concentrations of butane below the 0.1 n1/1 level is very large. In most cases, the concentration of C₄ aliphatics, after correction for the carrier blank, was below the detection limit of .03 n1/1.

5. Discussion - Chukchi Sea and Kotzebue Sound

In the general sense, the observed distributions of LMWH's in the Chukchi Sea appears to be typical in comparison to other OCS regions of Alaska that we have investigated. The levels of concentrations and the compositional ranges are those expected from biogenic sources within the sediments and water column. Sedimentary sources of LMWH's are presumably supplemented by small amounts arising from low temperature thermal cracking of indigenous organic matter.

The single anomalous feature observed in the Chukchi Sea is the plume of methane-rich water intruding from the western Chukchi Sea near 68°N latitude

(see Figure 4). This water mass, as indicated by the temperature and salinity distribution, is also characterized by anomalously high concentrations of ethane, ethylene, and propane. In all OCS regions we have investigated to date (excluding Norton Sound, see below), the concentration of ethylene near the bottom exceeds that of ethane by a factor of 2 to 3. This appears to be the result of a similar compositional flux from the underlying sediments. If the depth of water is shallow and little stratification is evident, surface productivity may increase the ethylene/ethane ratio to a value greater than 3.

Inspection of Figures 9 and 10 reveals that the ethylene/ethane ratio approaches 1 near the western boundary of the grid. Although no definitive statement can be made about the origin of these hydrocarbons, the anomalous ethylene/ethane ratio suggests a petroleum or natural gas source. If this speculation is true, the source exists to the west along the northern coast of Siberia. That the ethylene/ethane ratio is rapidly approaching normal values near Pt. Hope, also suggests that considerable dilution and modification of the original LMWH composition in this water mass has occurred enroute.

Another possible explanation is the unique production of ethane and propane not accompanied with the normal production of the C_2 and C_3 olefins. We have not observed this phenomenon elsewhere in the shelf waters of Alaska. Moreover, if this were the result of a unique biological process, it must be occurring in a water mass which is sinking.

B. Norton Sound

The horizontal and vertical distribution of the LMWH was determined in September 1976 at the stations shown in Figure 2. Because of unusual accumulations of ethane and propane discovered in the near bottom waters just south of Nome, station spacing in this area was reduced to 5 naut. mi. rather than the usual 30 naut. mi. spacing used in our general survey studies. This grid

pattern is shown in Figure 15.

In this report, only the salient features of the LMWH distributions will be presented with in-depth analysis to follow in the final report. Considerable attention will be given to the unusual distributions of hydrocarbons observed south of Nome.

1. Methane

Surface concentrations of methane in n1/1 are shown in Figure 16. The dominant feature is the large plume of methane-rich water emanating from Safety Sound due east of Cape Nome. The highest surface concentration of methane in this region was 600 n1/1, representing approximately 6-fold supersaturation with respect to partial pressure of methane in the atmosphere. The occurrence of methane-rich surface waters near lagoons is not uncommon as we have observed similar distributions in Bristol Bay.

There also appears to be a surface source of methane in the eastern extremity of Norton Sound. However, it is likely that this surface feature has resulted from a vertical flux of methane from below, where extremely high concentrations of methane were found.

The near bottom distribution of methane is depicted in Figure 17. A strong bottom source of methane exists east of Stuart Island, where concentrations exceed 2000 n1/1. The elevated concentrations of methane detected near the bottom are probably due to thermal stratification (see Figures 18 and 19), or a strong production of methane from the bottom, or both. Without detailed knowledge of the strength of benthic methane sources, or at least the distribution of organic carbon in the surficial sediments, we can not evaluate the relative merits of each process.

Although the distribution of methane reveals strong localized sources, the average concentration in the surface and near bottom waters is 230 ± 150 n1/1

and 410 ± 190 nl/l. The near bottom average was calculated neglecting the singularly high value of 2240 nl/l observed east of Stuart Island.

2. Ethane and Ethylene

The surface distributions of ethane and ethylene are shown in Figures 20 and 21. Ethane is sporadically variable in the surface layers with no well-defined sources. A single high value (1.4 nl/l) was observed near St. Lawrence Island with all other values less than 1 nl/l. The average concentration of ethane in the surface layers is 0.5 ± 0.3 nl/l, a value near that observed for the surface waters of the Chukchi Sea.

In contrast, the concentration of ethylene in the surface waters is significantly higher and its distribution reveals localized sources (Figure 21). The strongest source of ethylene appears northwest of Nome and presumably reflects local primary productivity. Concentrations of ethylene in the core of the plume exceed 2 nl/l. Average concentration of ethylene is 1.3 ± 0.5 nl/l. The mean ethylene/ethane ratio in the surface layers is 2.6.

The near bottom concentration of ethane is shown in Figure 22. The dominant feature of the region is the plume of ethane-rich water extending northwest along the coast. In order to more precisely document the nature and extent of the plume, a small-scale sampling grid was implemented, the detail or fine structure of which are shown in Figure 23. As is apparent in Figure 23, the plume extends north then west along the coast in accord with the general near bottom circulation patterns. During this study, we were able to trace the plume for about 100 km. Recent conversations with Drs. Mark Holmes and Hans Nelson of the USGS indicate that geological conditions are ideal for gas and/or petroleum seeps in the region. In fact, a west trending fault, passing nearly through the locus of the plume, has been identified by Dr. Nelson. Also, the geological strata are tilted upward allowing an avenue of escape for gas or

natural hydrocarbons. Comparison of Figures 22 and 23 indicate that the concentration of ethane in the core of the plume is approximately 20-fold above background. Unexpectedly, near bottom methane concentrations in the region are not indicative of the seep (see Figure 17). Additional comments on the nature of the gas seep will be discussed below.

The mean concentration of ethane to the east and south of the seep area is 0.5 ± 0.3 n1/1. To the west of the seep area, it is not possible to distinguish clearly the ambient levels of ethane from those brought about by the influence of the seep itself.

The concentration of ethylene within 5 m of the bottom is reflected in Figure 24. Concentrations of ethylene increase toward the west and generally correlate with the distributions of salinity and temperature (Figures 5 and 6). On this basis we would judge the ethylene to be transient, characteristic of the water mass rather than being produced locally. The range in concentrations of ethylene is from 4 n1/1 near St. Lawrence Island to less than 1 n1/1 north of Stuart Island at the eastern extremity of Norton Sound.

3. Propane and Propylene

The surface concentrations of propane and propylene are shown in Figures 25 and 26. As is evident from the diagrams, both propane and propylene are uniformly distributed over the region with no apparent localized sources. Average concentrations of propane and propylene are 0.2 ± 0.1 n1/1 and 0.5 ± 0.2 n1/1, respectively.

The concentration of propane within 5 m of the bottom is shown in Figure 27. As was evident from the near bottom distribution of ethane, the concentration of propane also is anomalously high in the presumed seep area south of Nome. Maximum concentration observed was 1.4 n1/1, a value approximately 5-fold above the ambient levels observed toward the east (0.3 n1/1).

A detailed plot of the near bottom propane distribution is shown in Figure 28. In this view the maximum observed concentration was 2.5 n1/1 along a line running due south from Nome. The "puff" nature of the dispersion plume may represent multiple sources or the episodic nature of the seep itself. Because the sampling was not synoptic in time, we can not be sure of the reason for the plume characteristics. The general drift of the plume is in accord with the circulation of the region. The plume is a recognizable entity "down-stream" for approximately 60 km.

The distribution of propylene near the bottom is reflected in Figure 29. It shows no strong sources and is sporadically variable over the entire region. Average concentration is 0.4 ± 0.1 n1/1 with the lowest concentrations found at the eastern extremity of the sound.

4. Iso- and n-butanes

The concentrations of iso- and n-butanes over most of the region were at or below the detection limit (0.03 n1/1), except in the region of the seep. In this location, both butanes reached maximum concentrations of 0.5 n1/1 at the point where maxima also were observed in the concentrations of ethane and propane. The distribution of the plume is identical to that observed for the aforementioned hydrocarbons. The ratio of iso-butane to n-butane is approximately 1 as suggested by the average concentration in the plume. Both were 0.2 ± 0.2 n1/1.

There was also evidence of C₅ hydrocarbons in the seep area. Several of the chromatograms were allowed to "run" beyond the normal elution time of the C₄'s to ascertain the presence of higher molecular weight hydrocarbons (i.e., pentanes, hexanes, and possibly low molecular weight aromatics). At two stations where evidence indicated the presence of unusually high concentrations of ethane and propane, a complex, partially resolved mixture was evident on

the chromatogram at the retention times of the C₅'s. These results were not quantified as neither the extraction procedure nor the chromatographic analysis is quantitative for the heavier hydrocarbons.

5. Discussion - Norton Sound

The most conspicuous feature observed in Norton Sound is the presumed gas seep south of Nome, although at this point it is not known whether heavier fractions of petroleum might be present as well. Hopefully in-depth studies proposed for next summer, including hydrocarbon analyses of sediments, waters, and biota, will elucidate the nature and extent of the seep.

Several unique features of the seep should be mentioned. The first of these is the relatively small concentration of methane observed in the region of the seep. Since most natural gases analyzed show a preponderance of methane, it is surprising that little or no increases above ambient levels were detected. If a bubble of methane gas were to come to equilibrium with the bottom waters in Norton Sound (2 atm. hydrostatic pressure, approx. 20 m), the concentration of methane in the water column at the point of introduction would be approximately 5.0×10^7 n1/1, or a factor of nearly 10^5 above the present observed concentration.

If the mode of entry is via bubbles, the concentration of methane in the water column will depend on bubble size and frequency, transfer rates, as well as the partial pressure of methane in the bubble. It is conceivable that the bulk of the gas escaping may be nitrogen or carbon dioxide, but until further studies can be performed, no definite conclusions can be drawn at this time.

Another indicator of hydrocarbons of nonbiogenic origin is the ratio of methane to ethane plus propane. This plot is shown in Figure 30. A minimum in this ratio is observed south of Nome (i.e., 50) with values increasing rapidly to 500 toward the east and 300 toward the west. This parameter has

been used successfully in the Gulf of Mexico by Dr. Brooks of TAMU to delineate nonbiogenic sources of LMWH.

Other characteristics of the seep are shown in the ratio of ethane to propane and ethane to ethylene. The first of these is shown in Figure 31 where the seep gas appears to have a fixed ethane-propane composition. The dark circles represent all near bottom samples taken in the region of the seep where the ethane/ethylene ratio is greater than 1. The least squares equation of the line passing through the solid circles is

$$C_3 = 0.34 C_2 - 0.04.$$

In order to accurately assess the original composition of the gas seep, solubilities of the individual components and the degree of mixing that has occurred between seep gases and normal sediment gases must be considered. Methane notwithstanding, the solubilities of the $C_2 - C_4$ hydrocarbon fraction in seawater are not well known. However, based on fresh water measurements, the solubilities of ethane and propane are nearly equal. To the extent that mixing has occurred in the sediments, it would appear that the ratio of ethane to propane is about 3.

The open circles, representing only a portion of the actual data taken, indicate the ambient relationship that exists between ethane and propane (ethane/ethylene < 1) in Norton Sound. The equation of this line (open circles) is

$$C_3 = 0.37 C_2 + .08,$$

and is not statistically different than the relationship observed in the region of the seep. Unfortunately, the range of concentration was minimal while the scatter in the data was large.

The ethane-ethene (ethylene) relationship is depicted in Figure 32. Only the nonseep data points have been included. The normal ethane/ethene ratio is

0.34 compared to 0.5 observed in the northeast Gulf of Alaska. In the region of the seep the ratio is 6.5 and clearly shows the predominance of ethane over ethylene. This is the only region investigated to date in the OCS of Alaska where the concentration of ethane exceeded that of ethylene. Based on over 2000 samples analyzed, it appears that the ethane/ethene ratio is a useful indicator of nonbiogenic LMWH, at least in the OCS waters of Alaska.

IV. PROBLEMS ENCOUNTERED/RECOMMENDED CHANGES

There are no serious problems to date; the program is running smoothly.

V. ESTIMATE OF FUNDS EXPENDED

	<u>Allocated</u>	<u>Expended to Date</u>	<u>Balance</u>
Salaries and overhead	41.2K	8.1K	33.1K
Major equipment	8.4K	0	8.4K
Expendable supplies	4.5K	1.0K	3.5K
Travel and per diem	4.1K	0	4.1K
Shipping	1.0K	0	1.0K
Publications	1.0K	0	1.0K
Contract costs	0.6K	0	0.6K
FY76 carryover	<u>4.0K</u>	<u>0</u>	<u>4.0K</u>
	64.8K	9.1K	55.7K

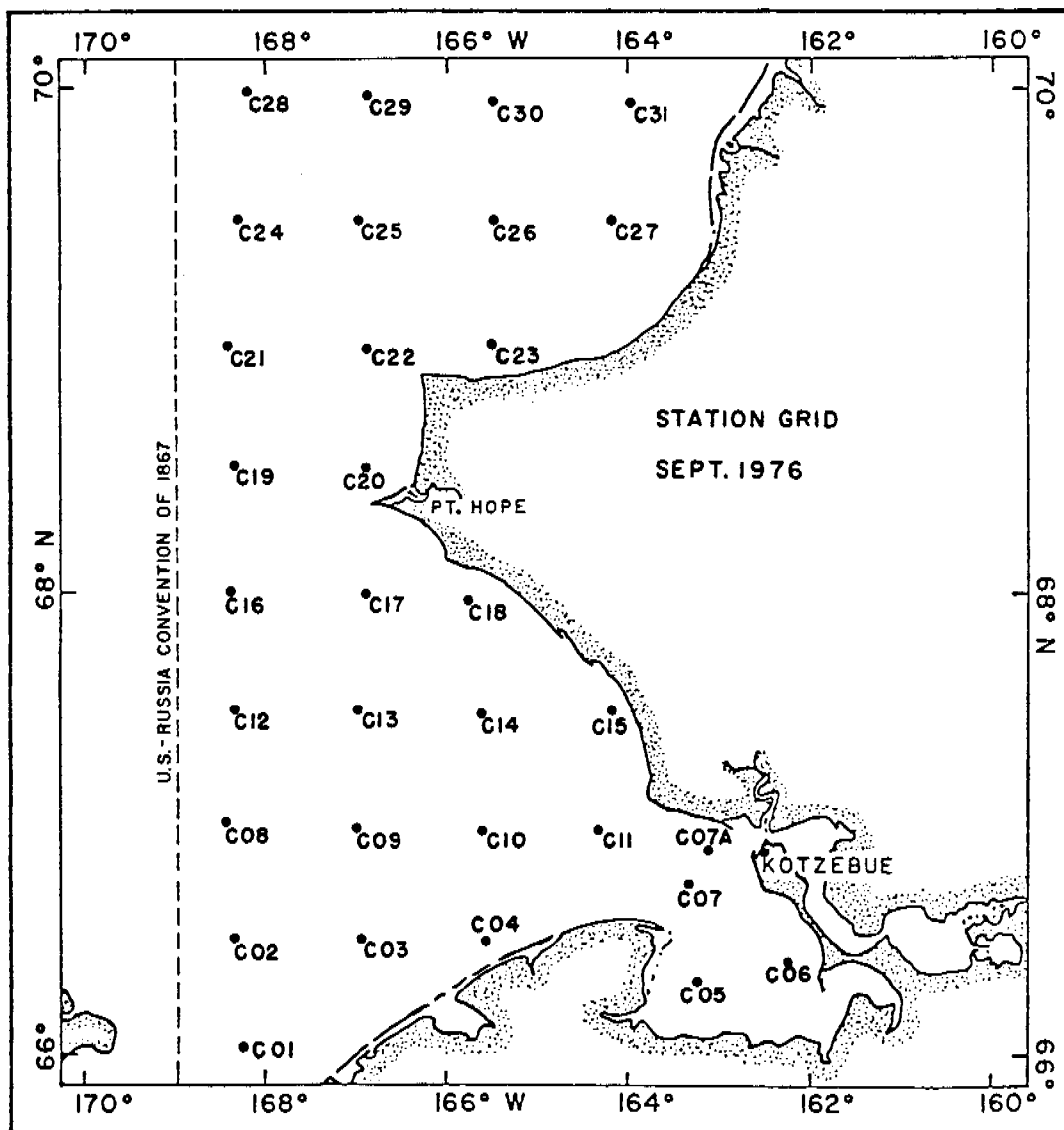


Figure 1. Station locations in southeastern Chukchi Sea and Kotzebue Sound.

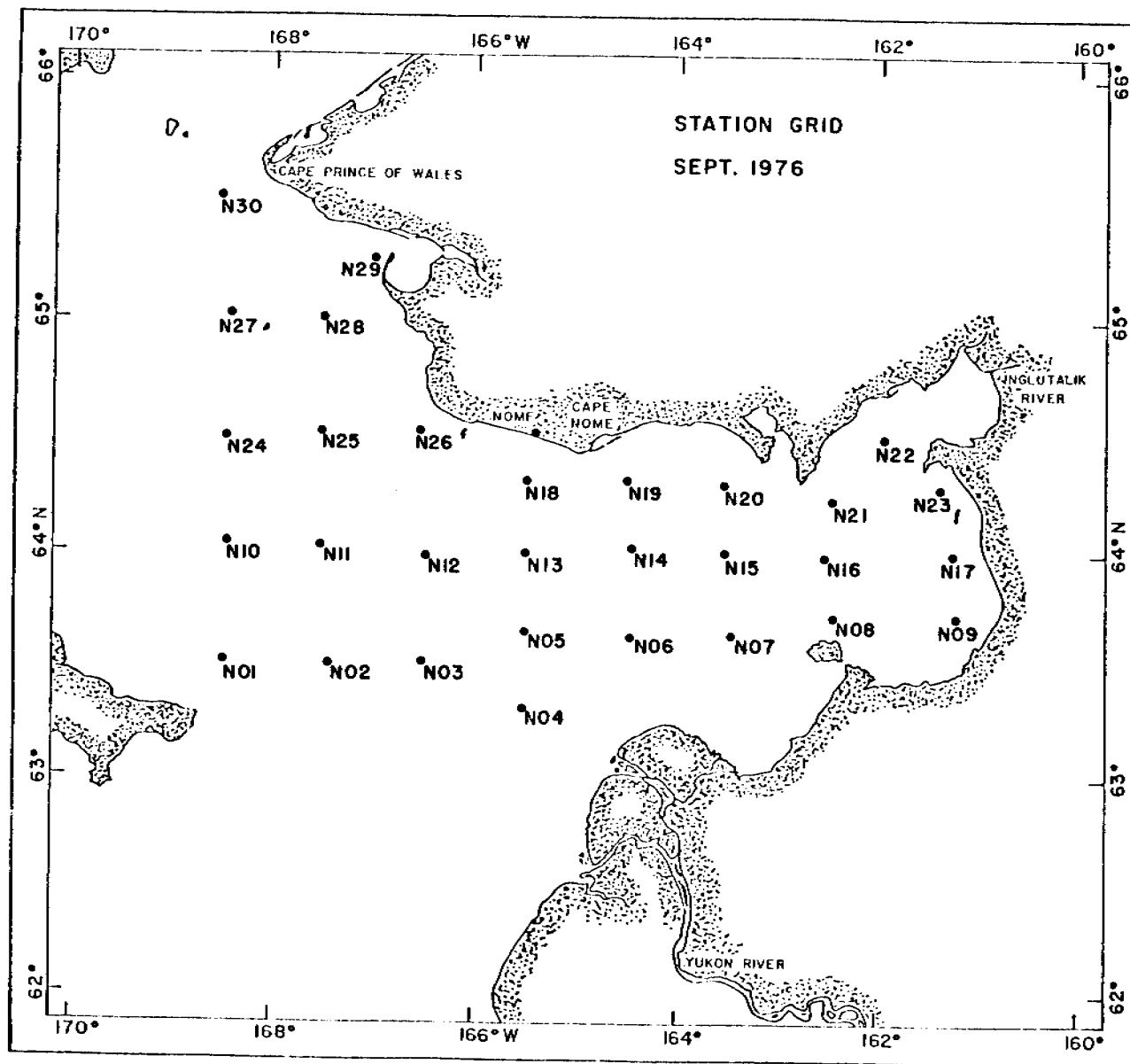


Figure 2. Station locations in Norton Sound and northern Bering Sea.

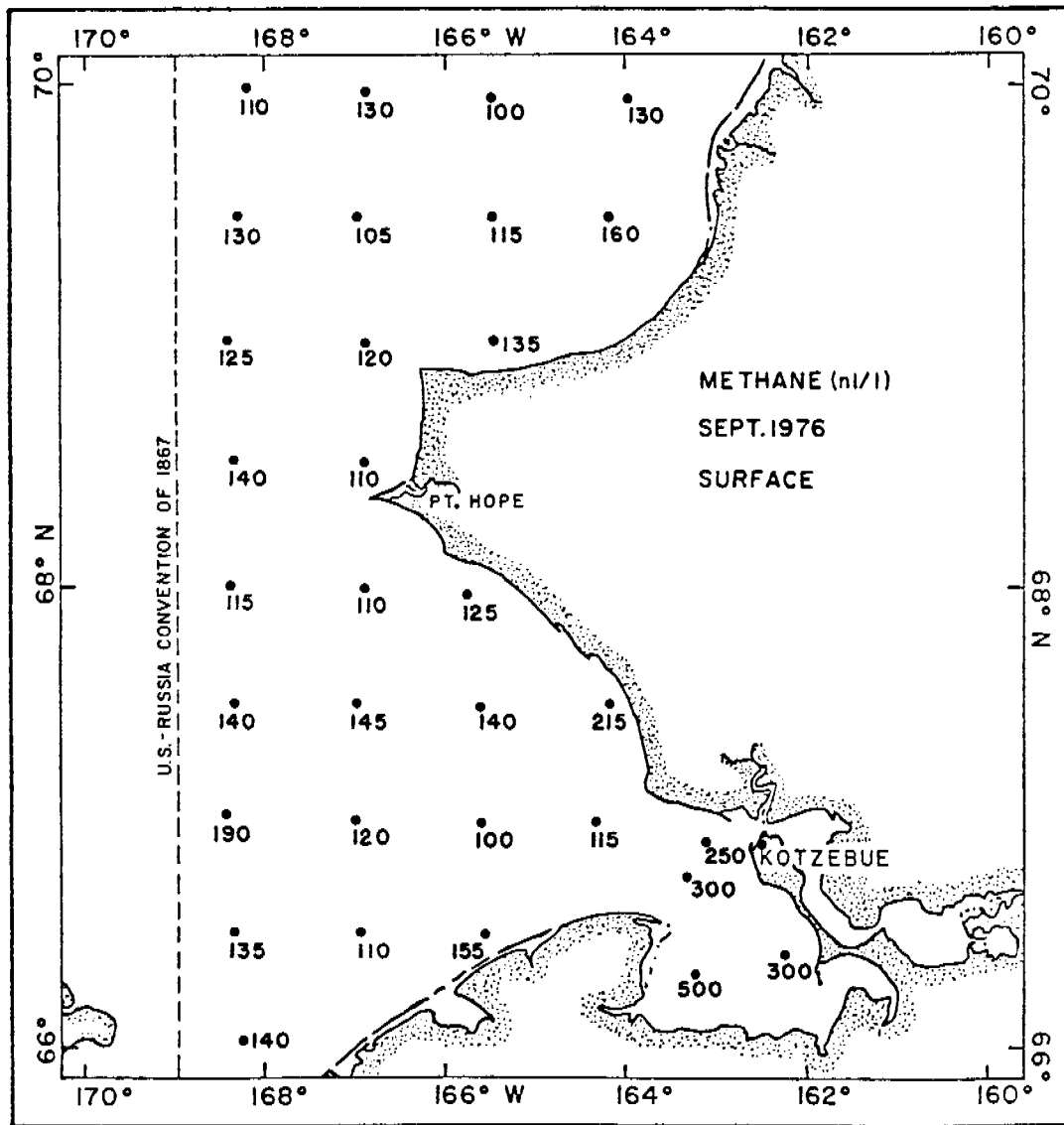


Figure 3. Surface distribution of methane in Sept. 1976. Concentrations are expressed in nl/l (STP).

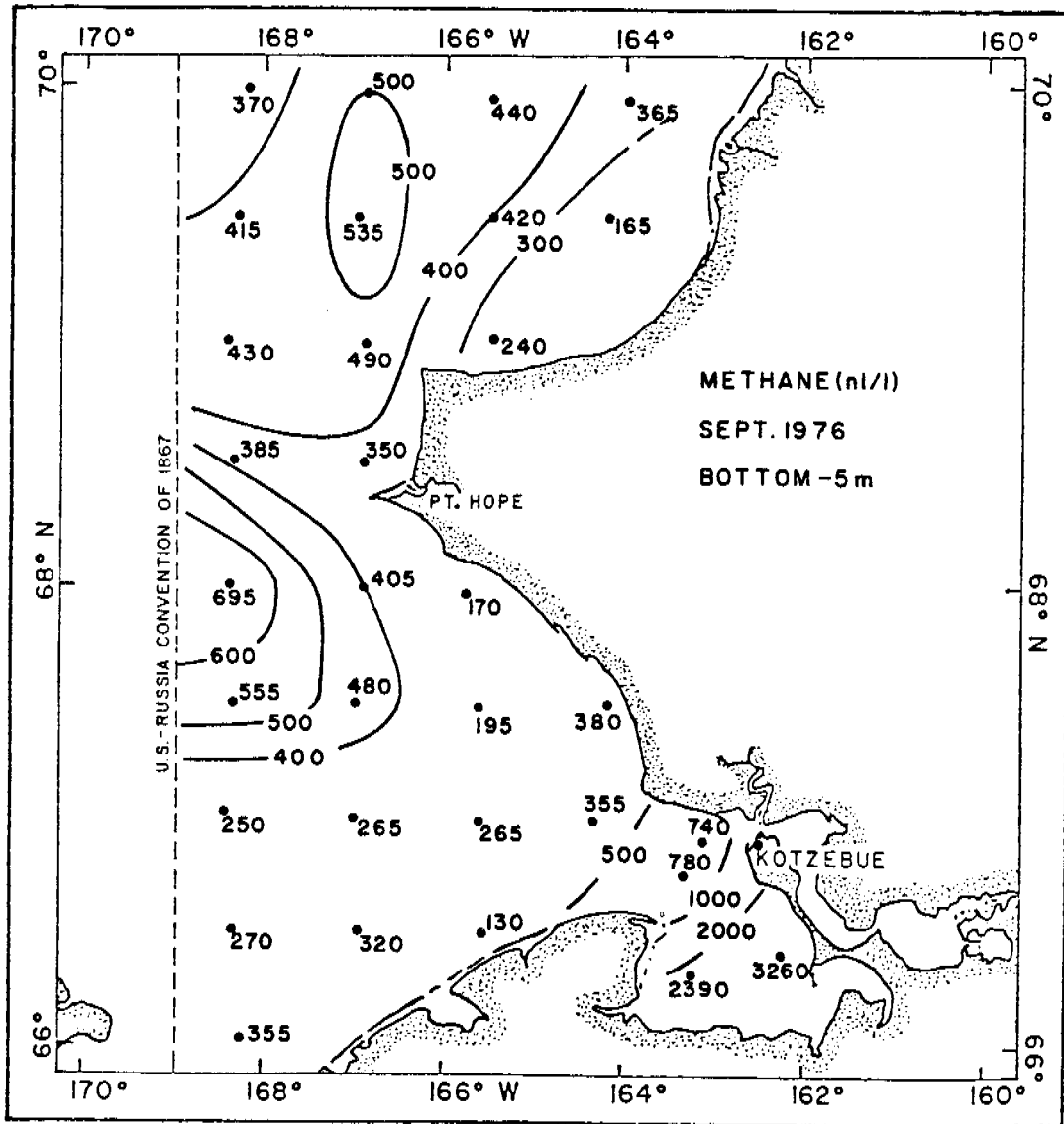


Figure 4. Areal distribution of methane 5 m from the bottom in Sept. 1976. Concentrations are expressed in n1/l (STP).

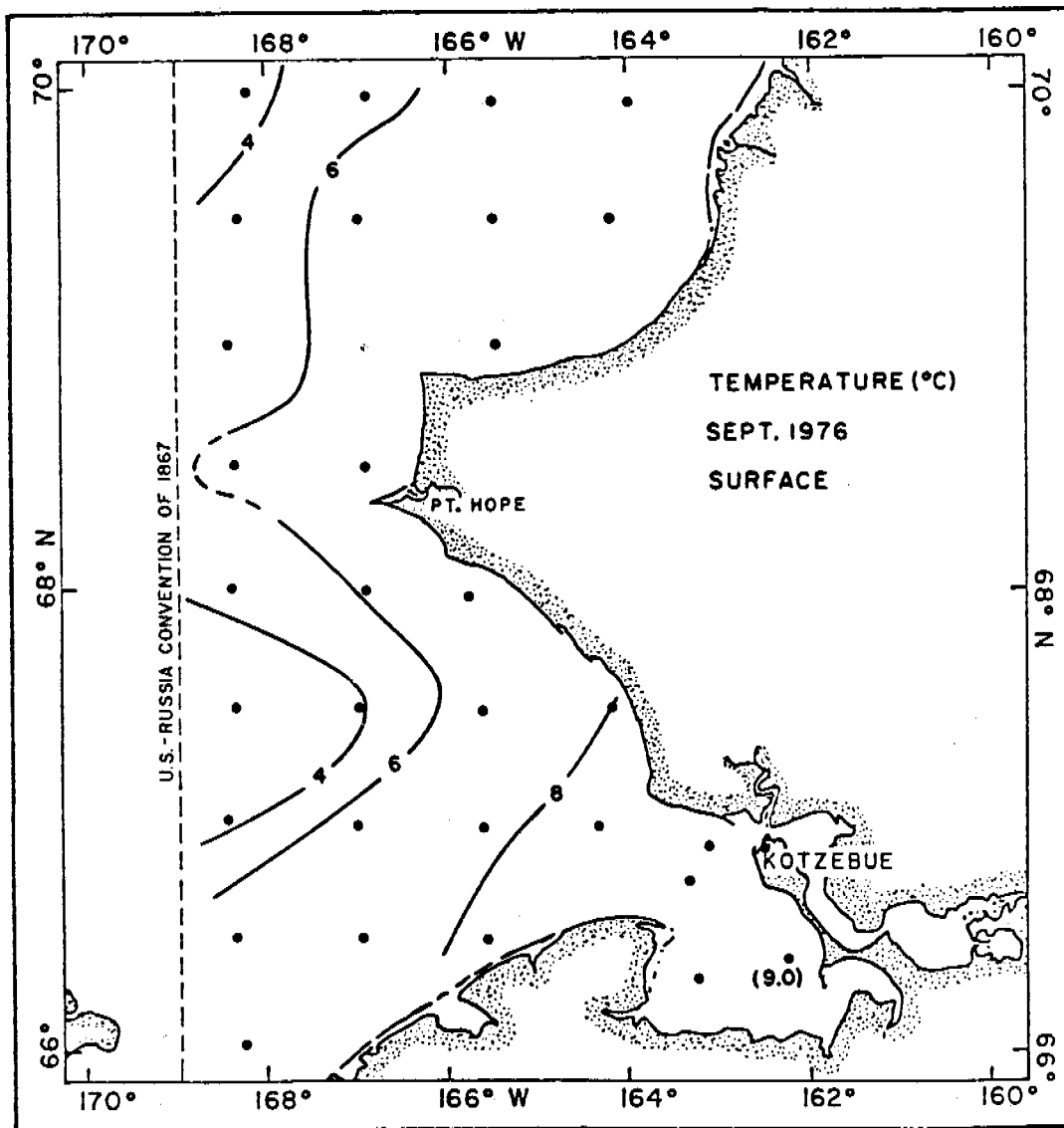


Figure 5. Surface distribution of temperature in Sept. 1976.

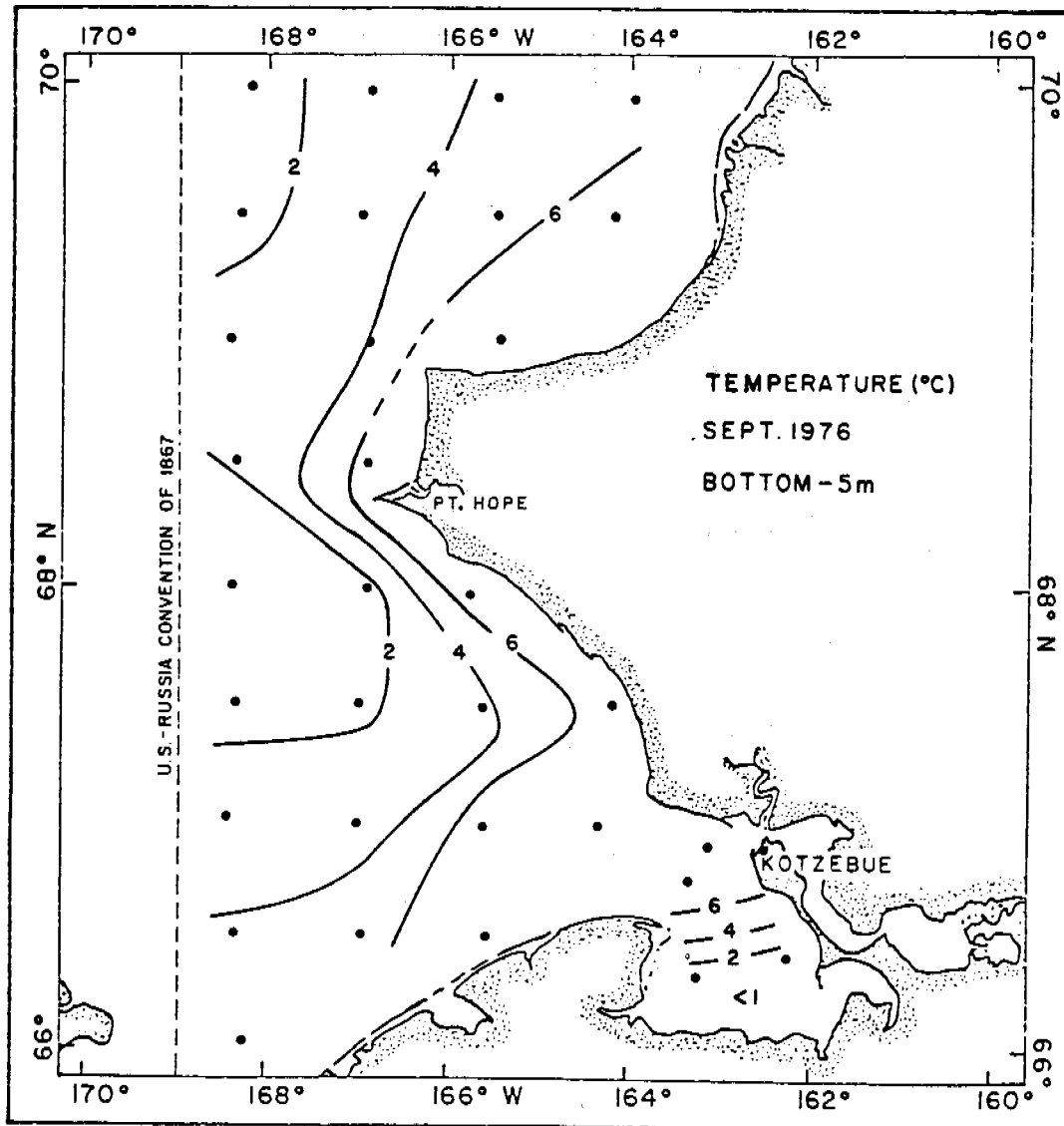


Figure 6. Areal distribution of temperature 5 m from the bottom in Sept. 1976.

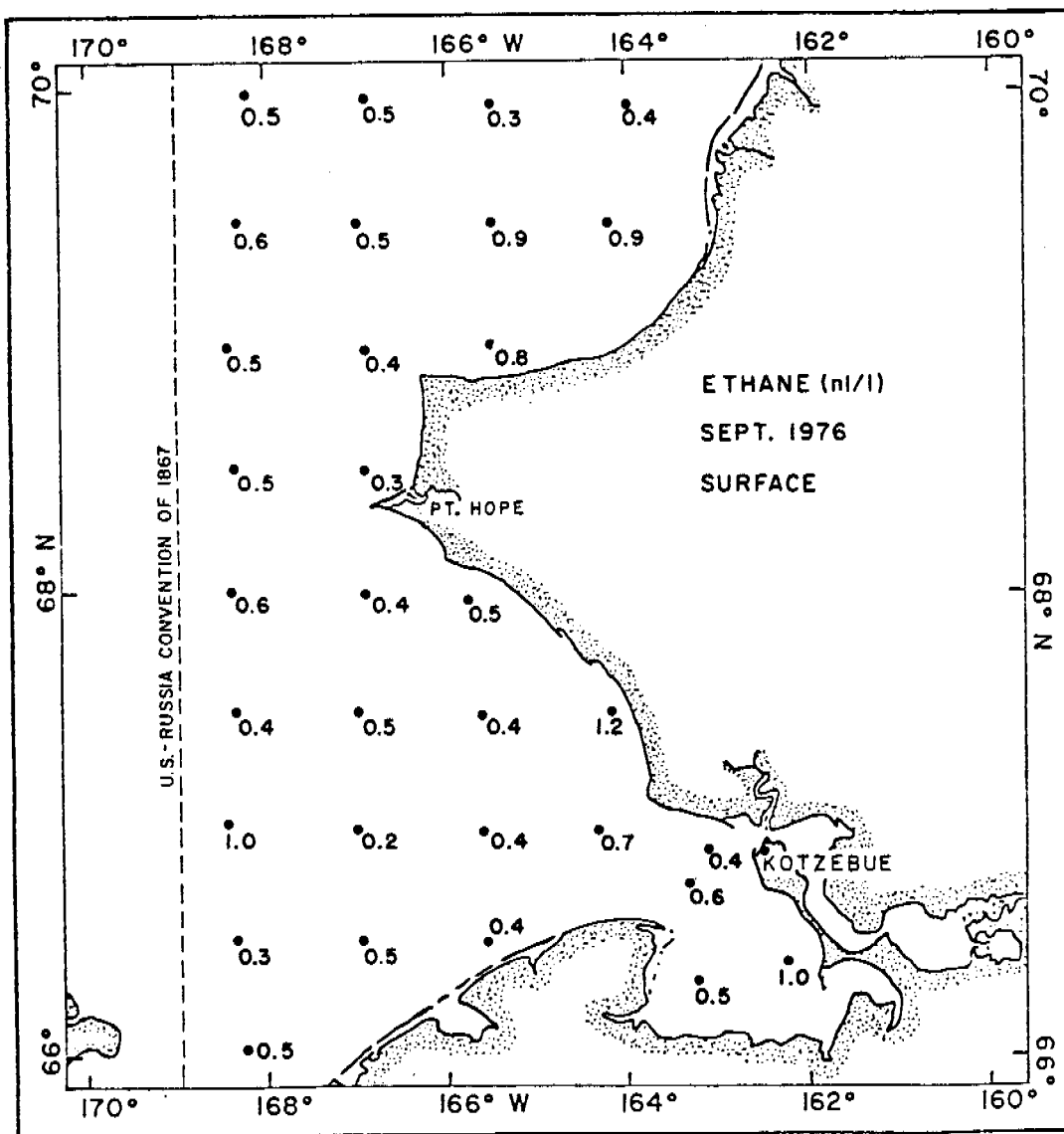


Figure 7. Surface distribution of ethane in Sept. 1976. Concentrations are expressed in n1/l (STP).

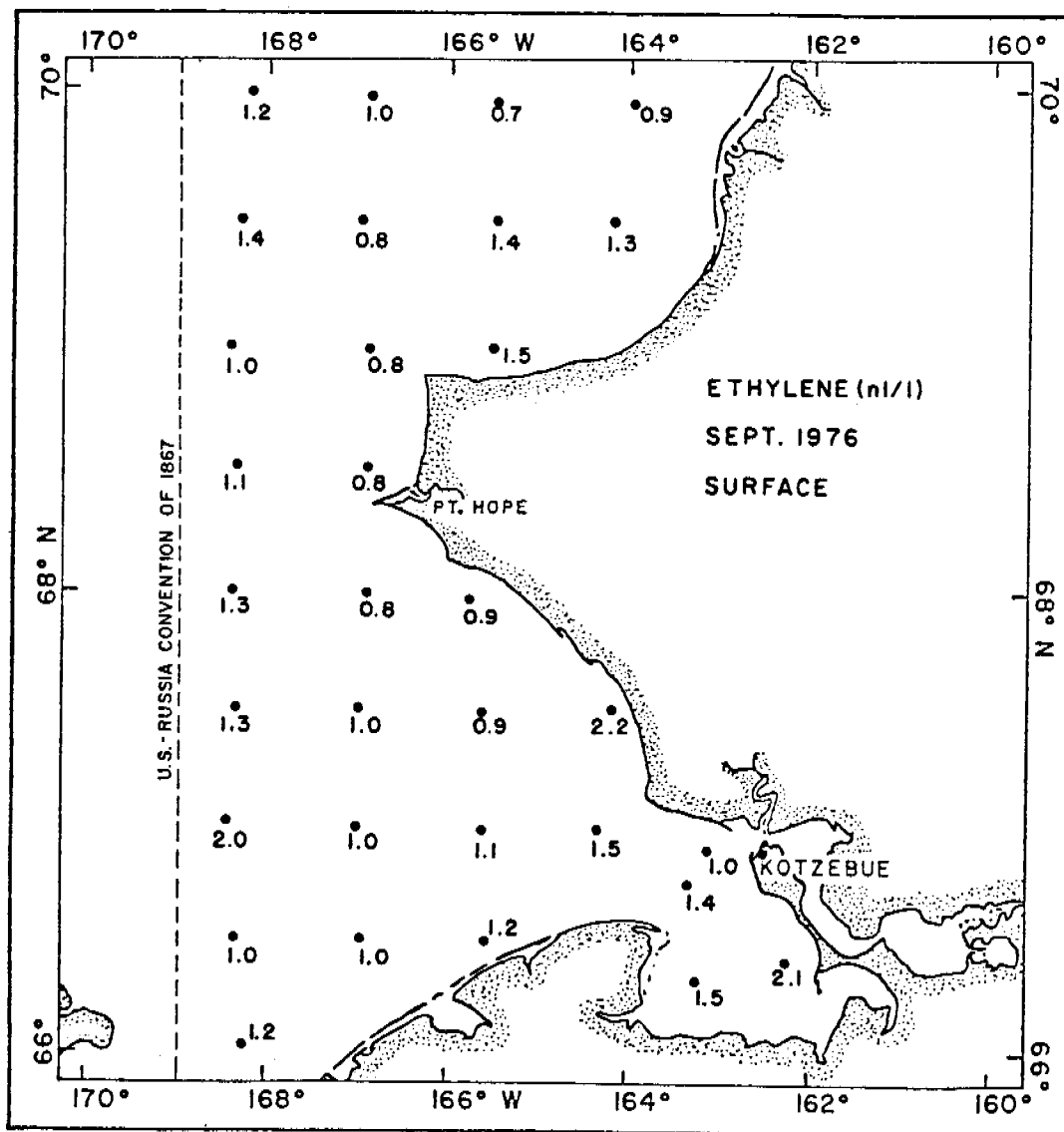


Figure 8. Surface distribution of ethylene (ethene) in Sept. 1976. Concentrations are expressed in n1/1 (STP).

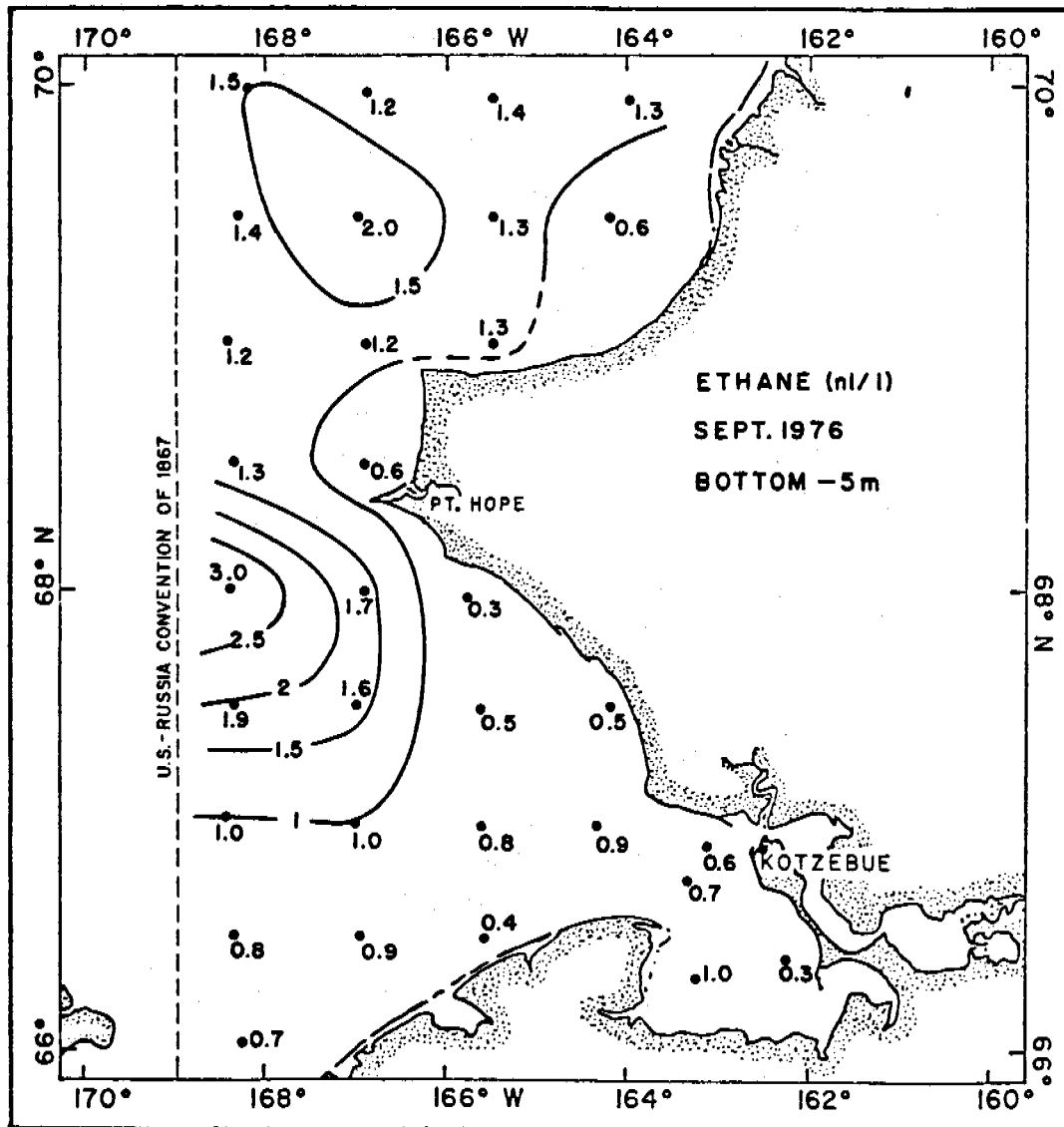


Figure 9. Areal distribution of ethane 5 m from the bottom in Sept. 1976. Concentrations are expressed in nl/l (STP).

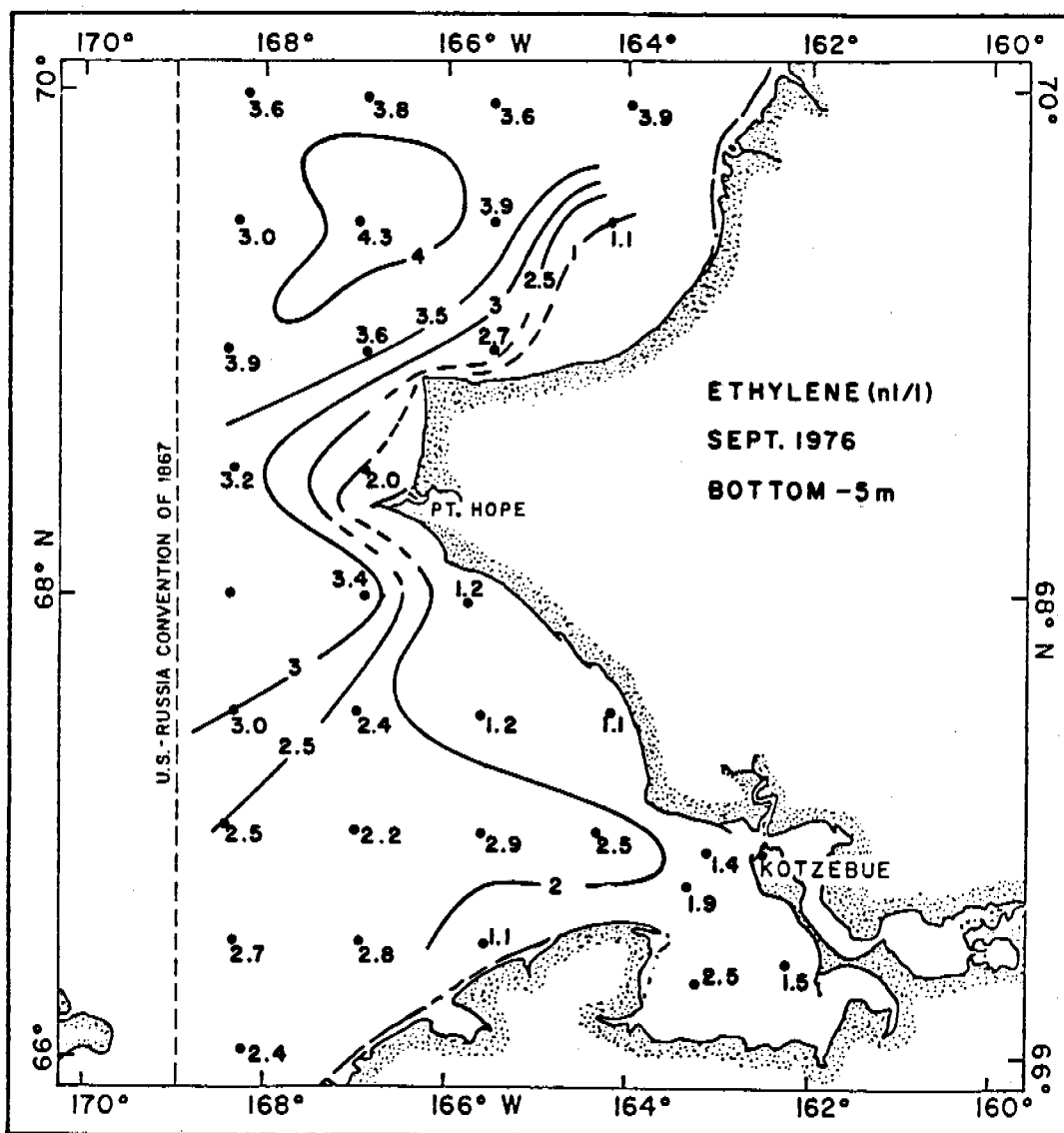


Figure 10. Areal distribution of ethylene (ethene) 5 m from the bottom in Sept. 1976. Concentrations are expressed in nl/l (STP).

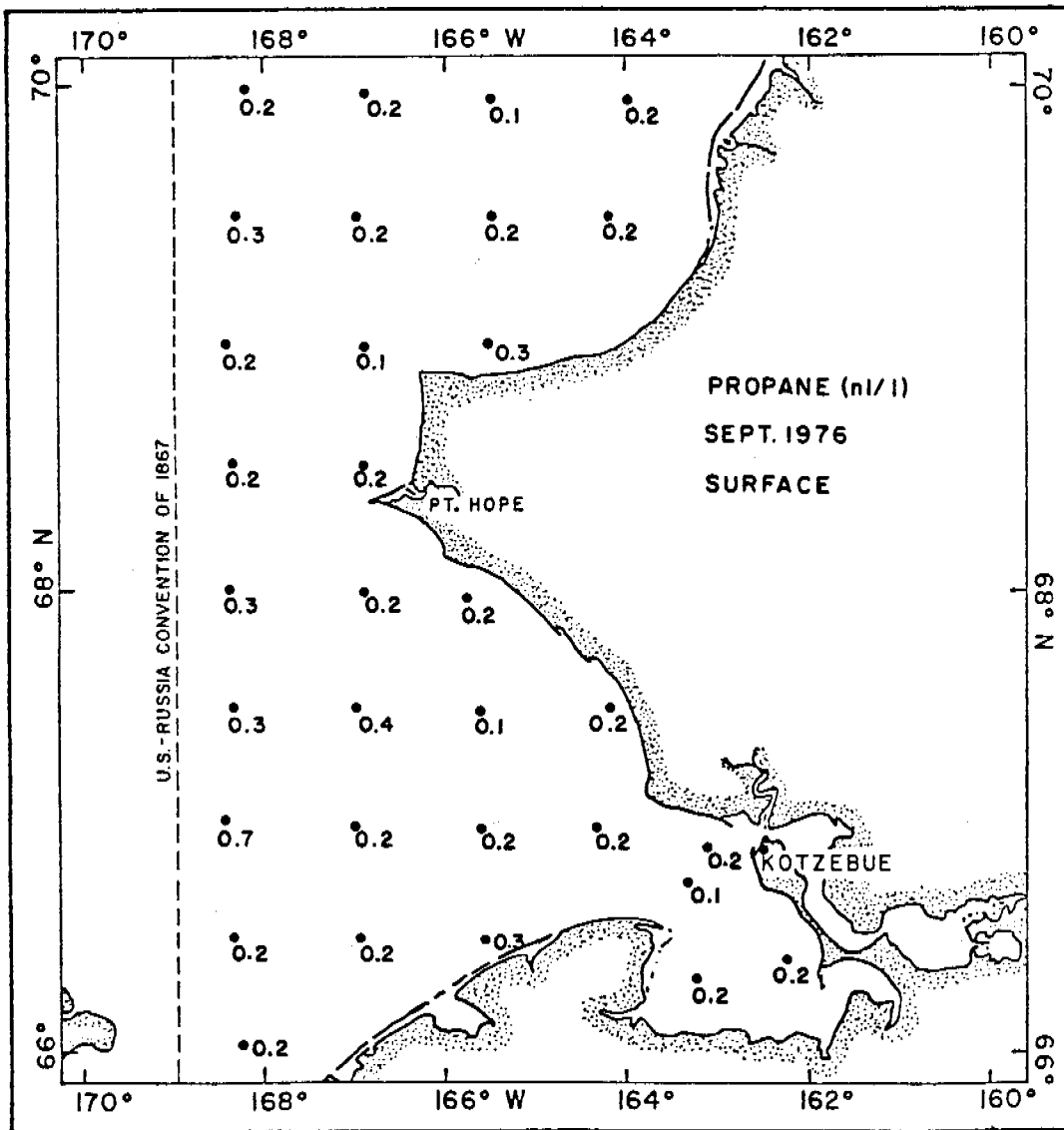


Figure 11. Surface distribution of propane in Sept. 1976. Concentrations are expressed in nl/l (STP).

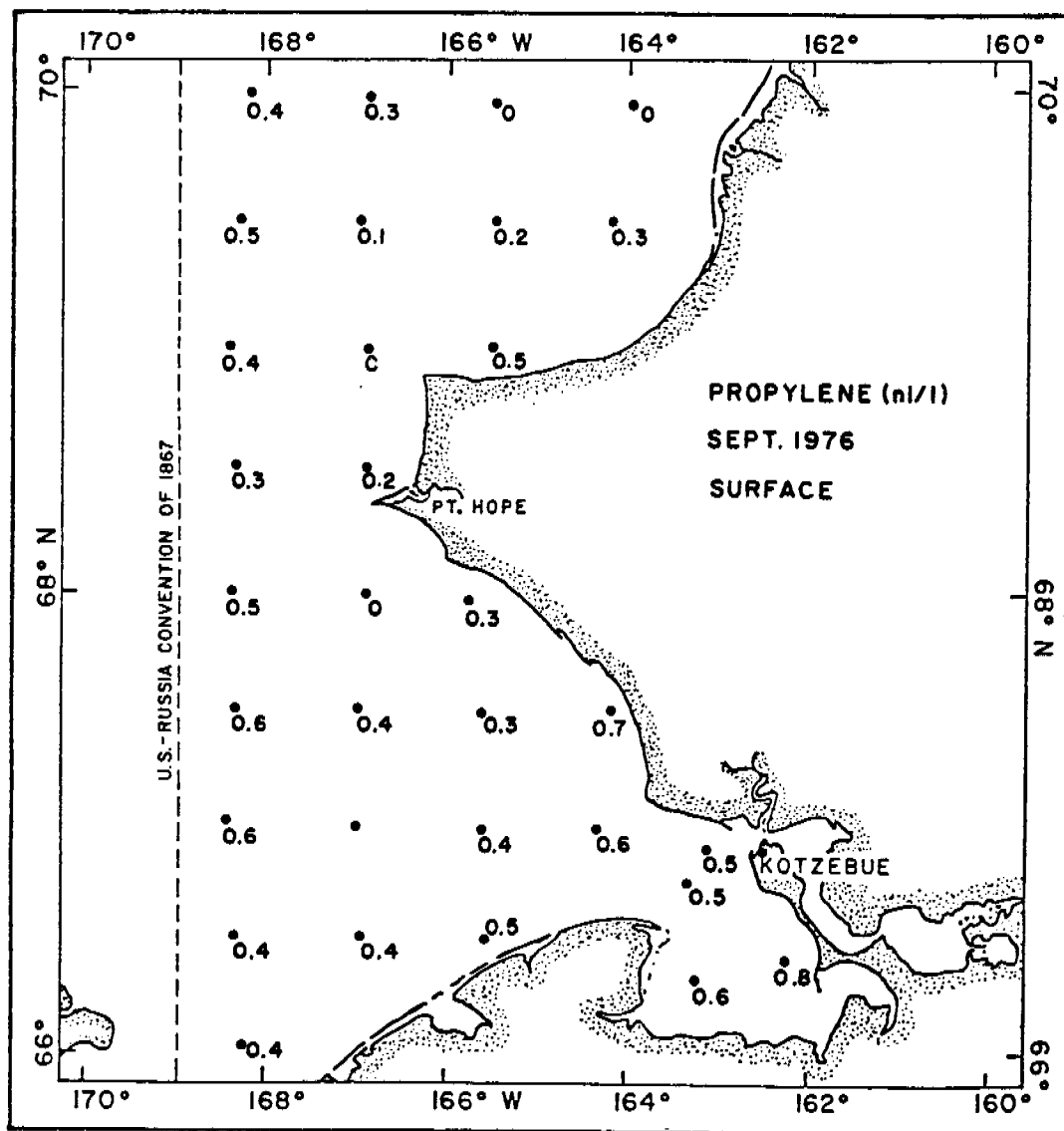


Figure 12. Surface distribution of propylene (propene) in Sept. 1976. Concentrations are expressed in nl/l (STP).

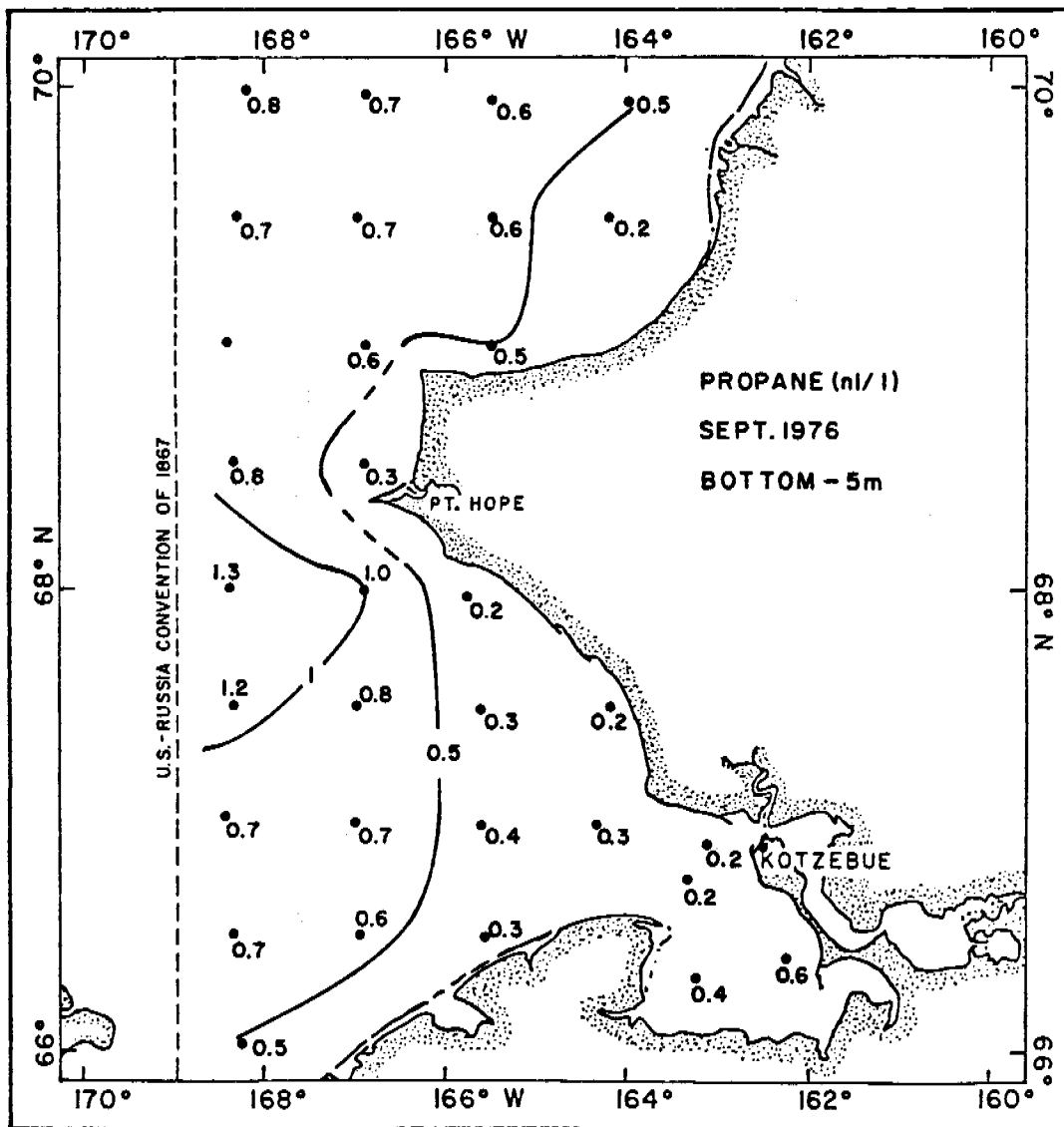


Figure 13. Areal distribution of propane 5 m from the bottom in Sept. 1976. Concentrations are expressed in n1/1 (STP).

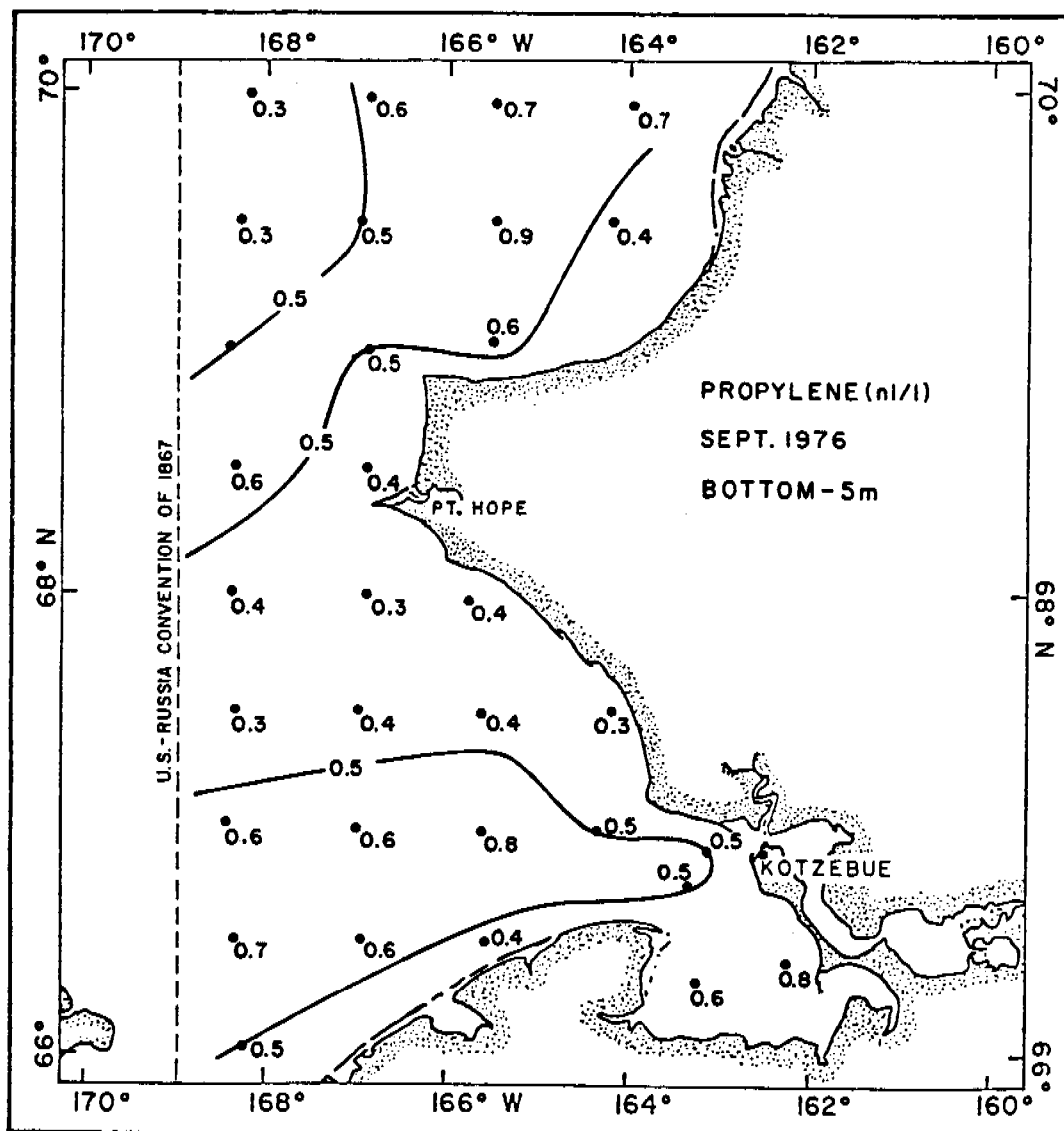


Figure 14. Areal distribution of propylene (propene) 5 m from the bottom in Sept. 1976. Concentrations are expressed in nl/l (STP).

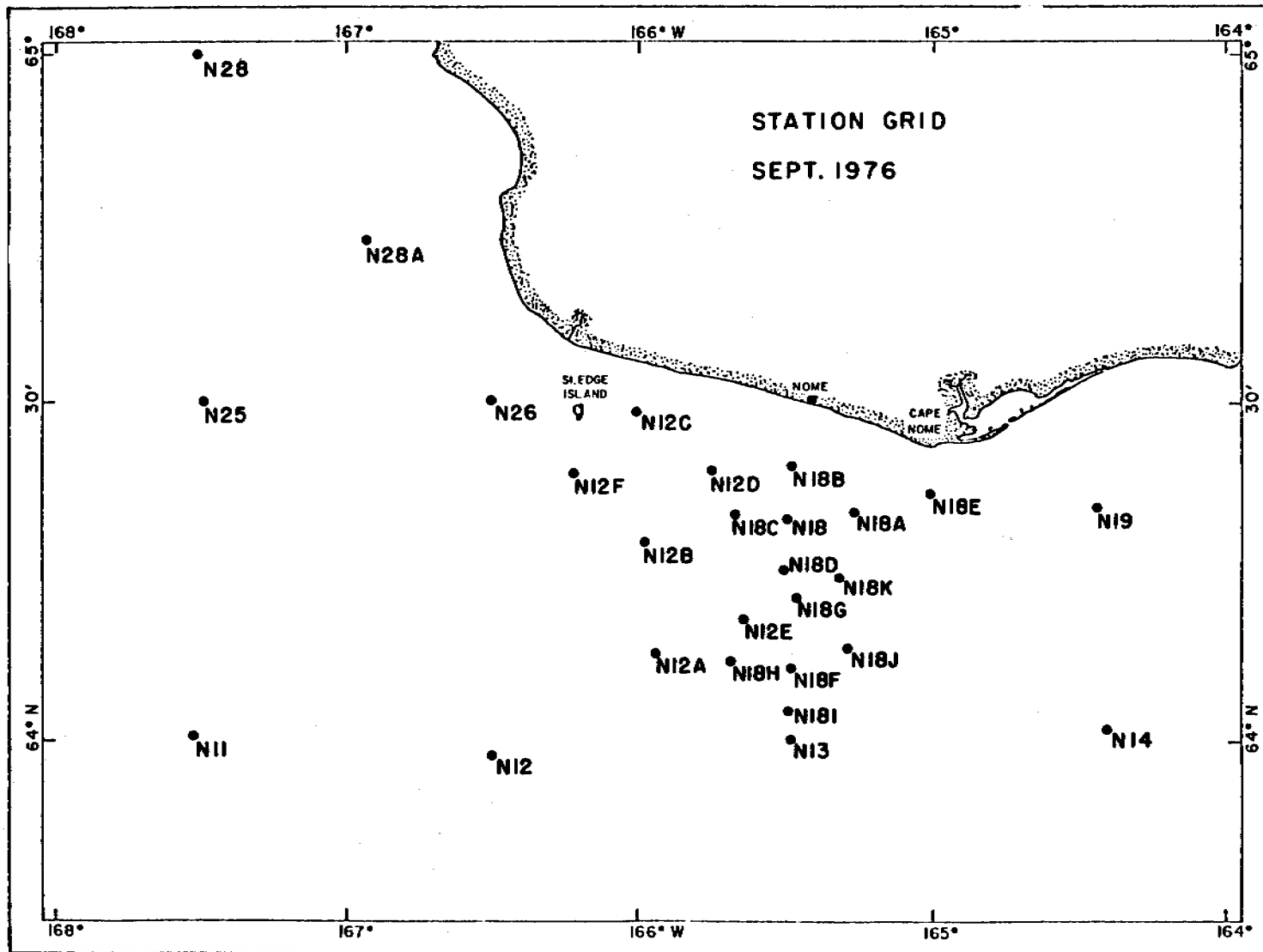


Figure 15. Station locations in the vicinity of the gas seep.

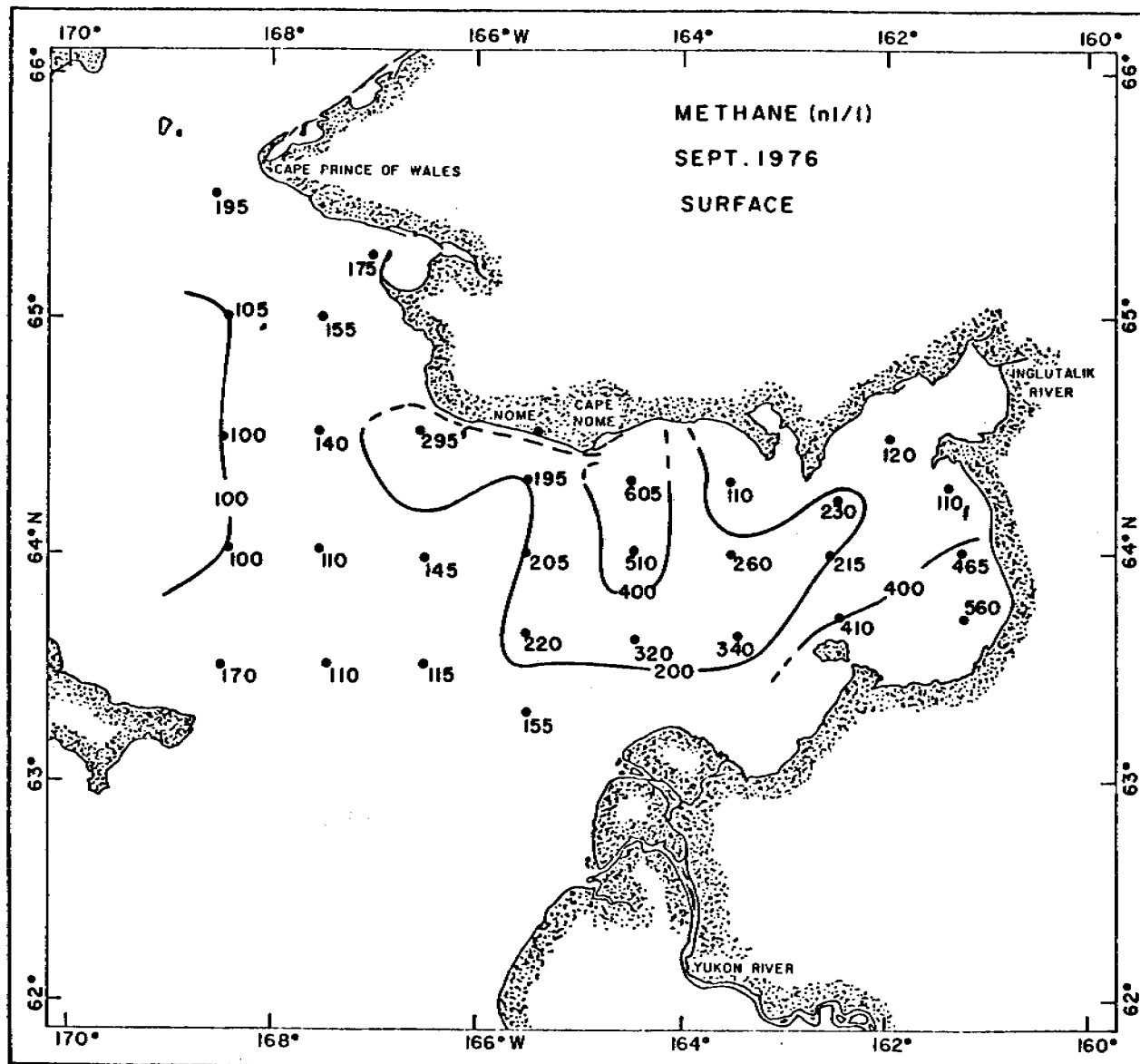


Figure 16. Surface distribution of methane in Sept. 1976. Concentrations are expressed in n1/1 (STP).

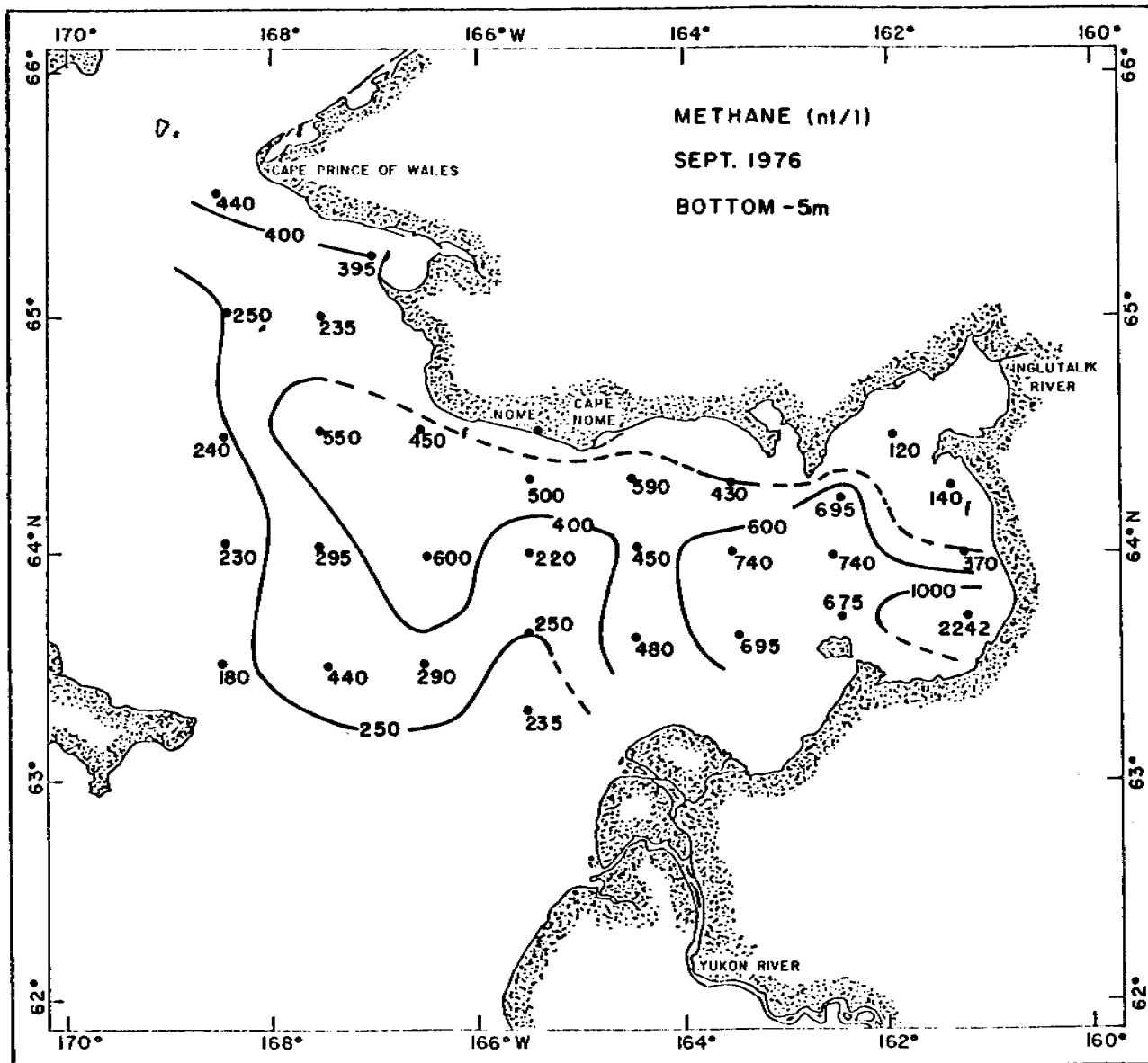


Figure 17. Areal distribution of methane 5 m from the bottom in Sept. 1976. Concentrations are expressed in n1/1 (STP).

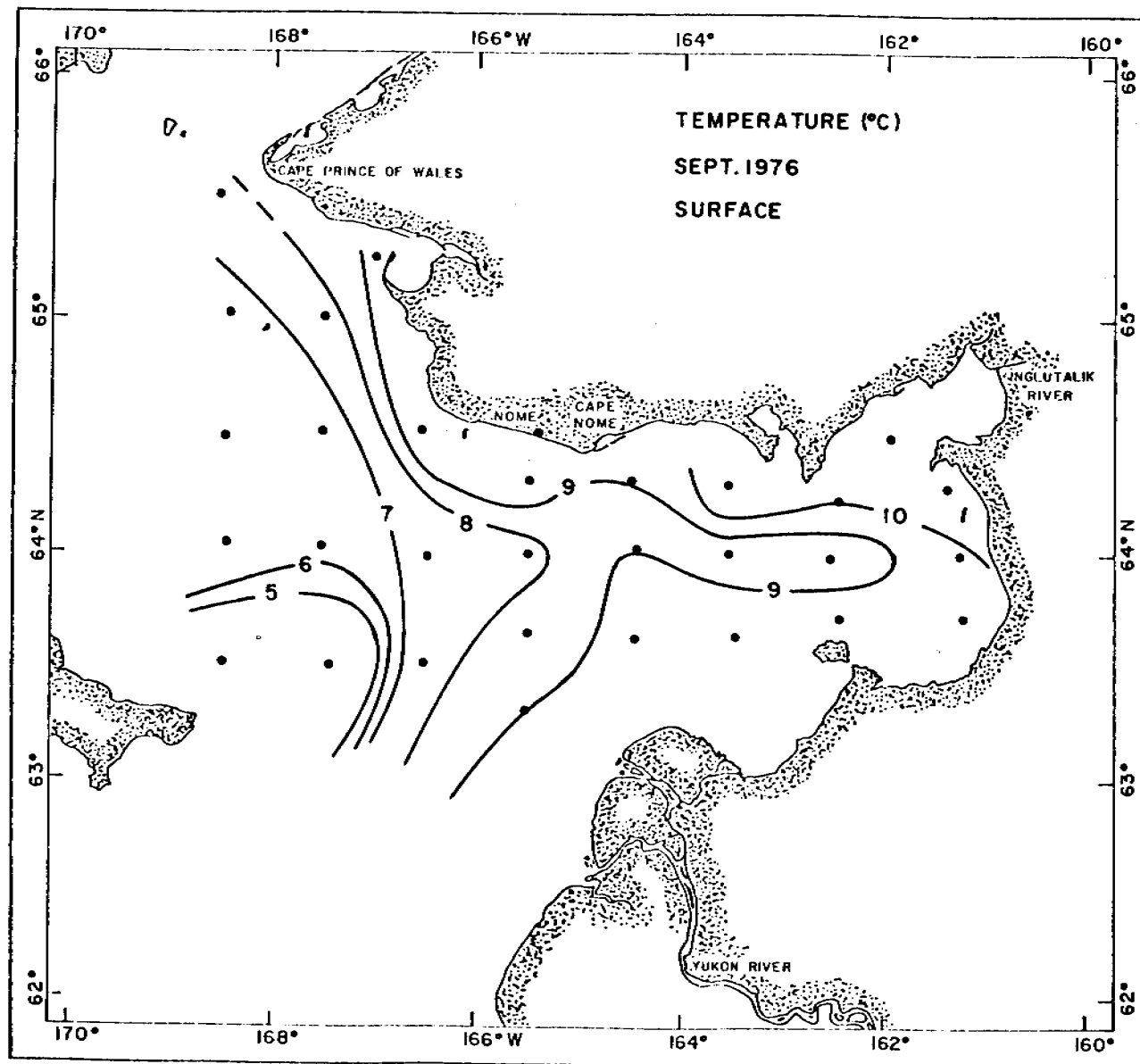


Figure 18. Surface distribution of temperature in Sept. 1976.

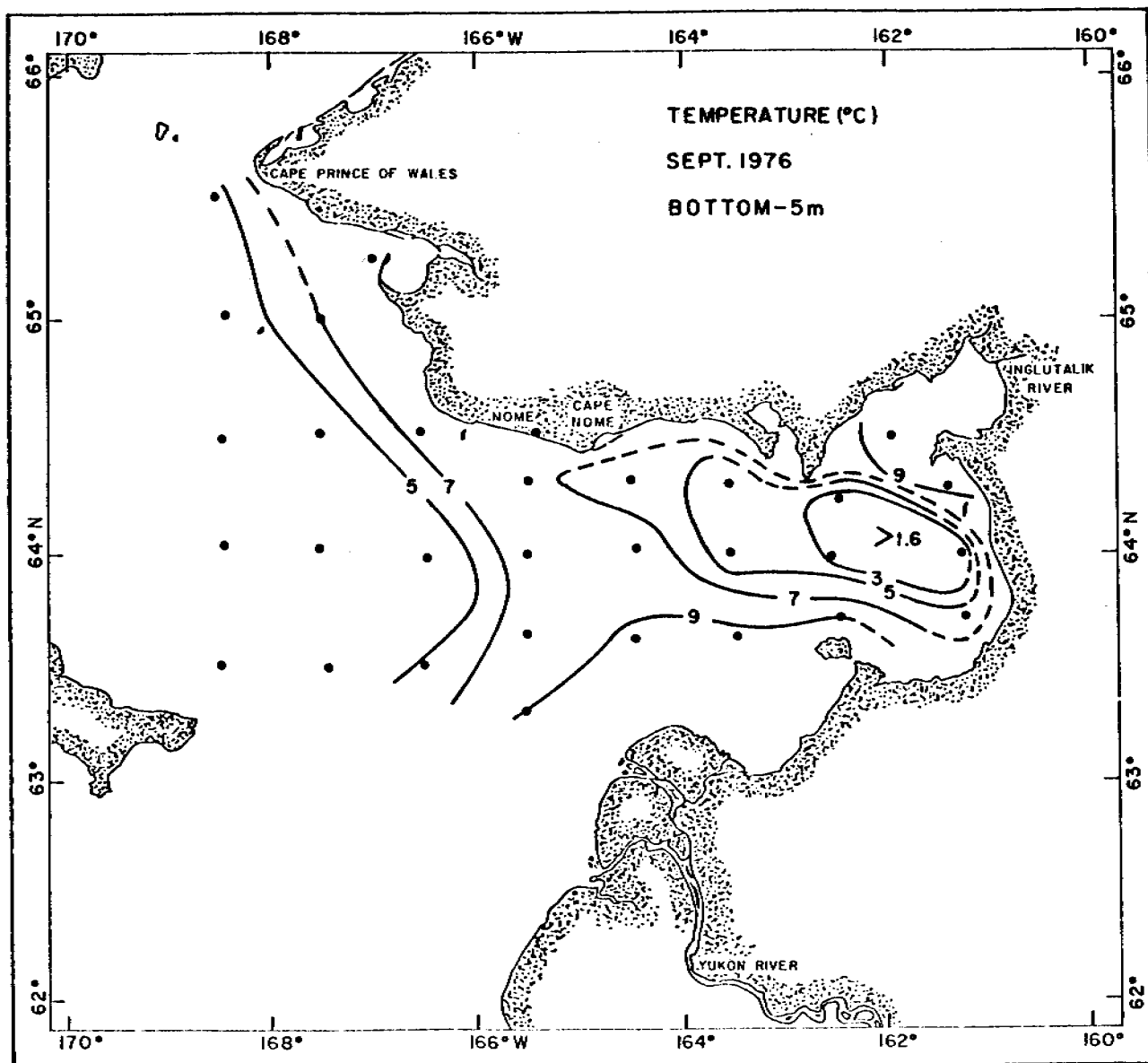


Figure 19. Areal distribution of temperature 5 m from the bottom in Sept. 1976.

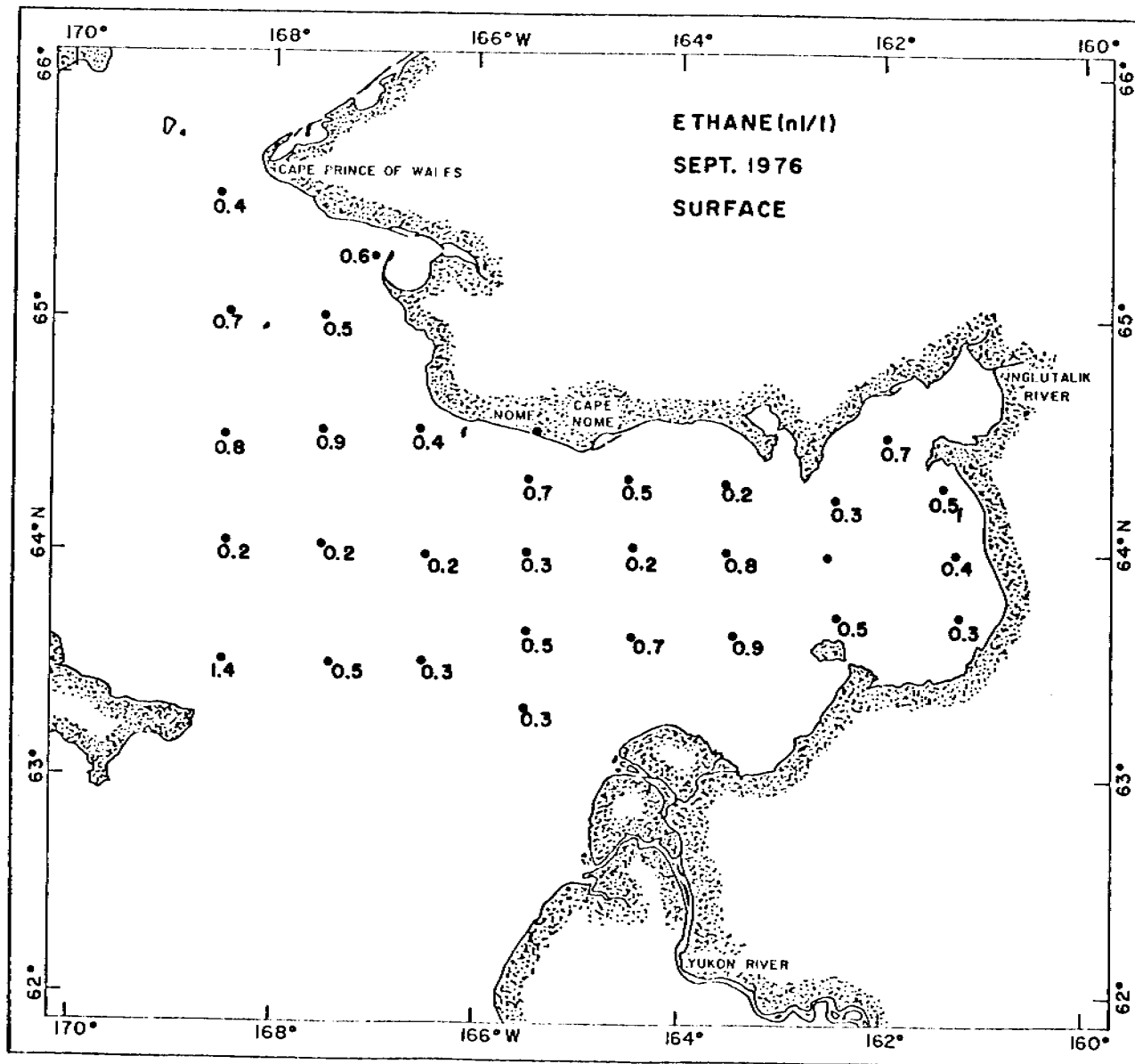


Figure 20. Surface distribution of ethane in Sept. 1976. Concentrations are expressed in n1/l (STP).

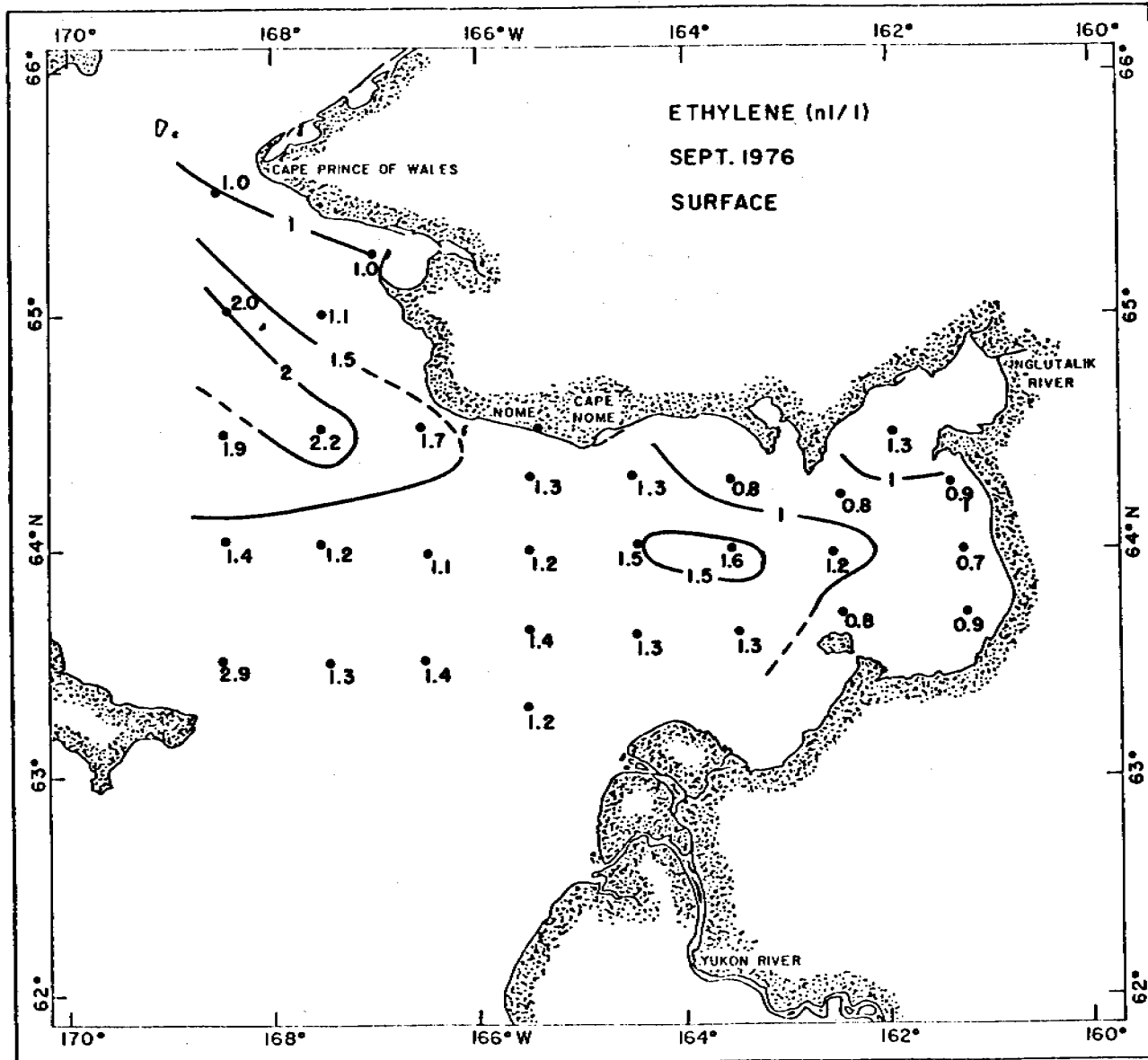


Figure 21. Surface distribution of ethylene (ethene) in Sept. 1976. Concentrations are expressed in n1/1 (STP).

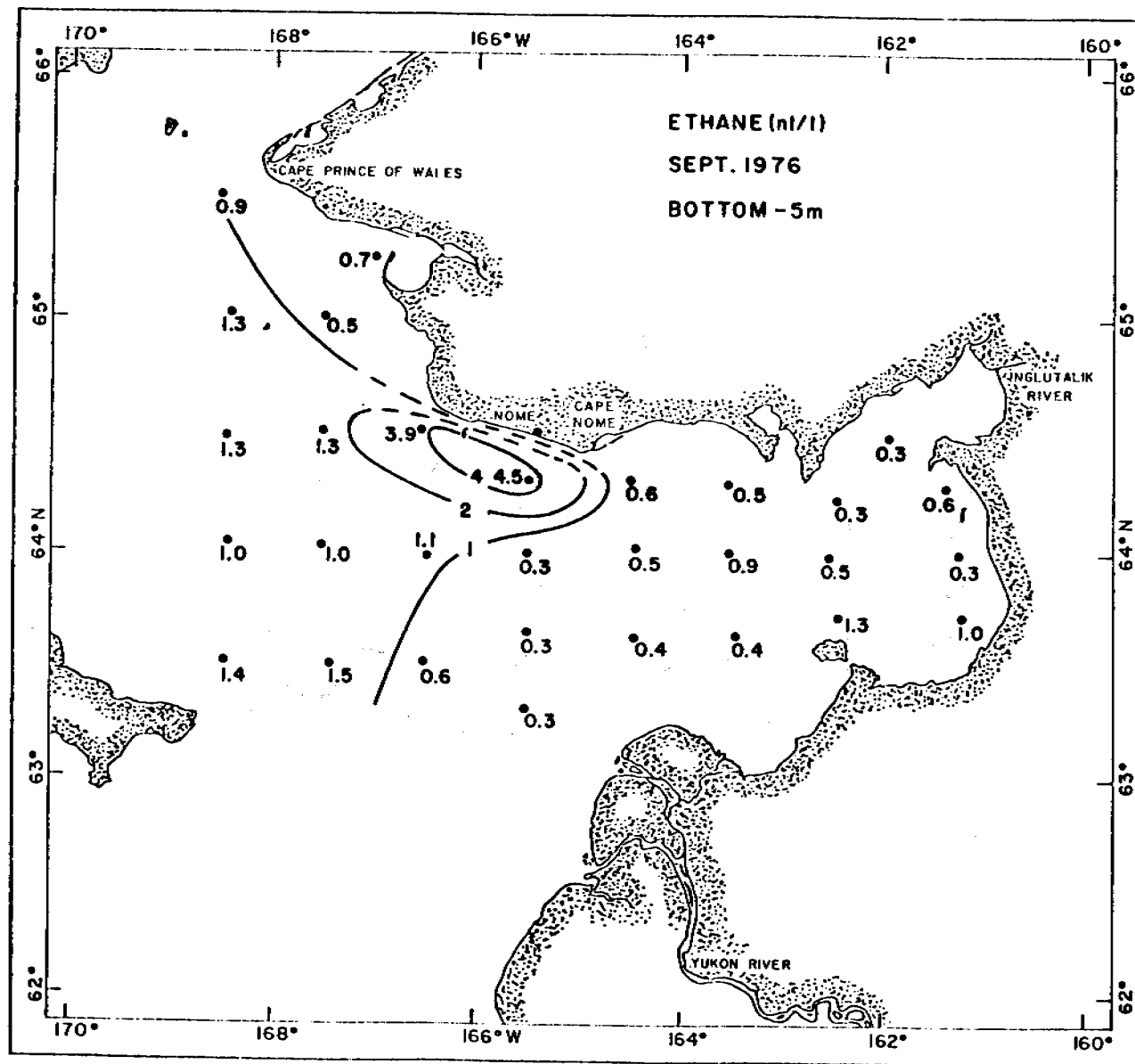


Figure 22. Areal distribution of ethane 5 m from the bottom in Sept. 1976. Concentrations are expressed in n1/1 (STP).

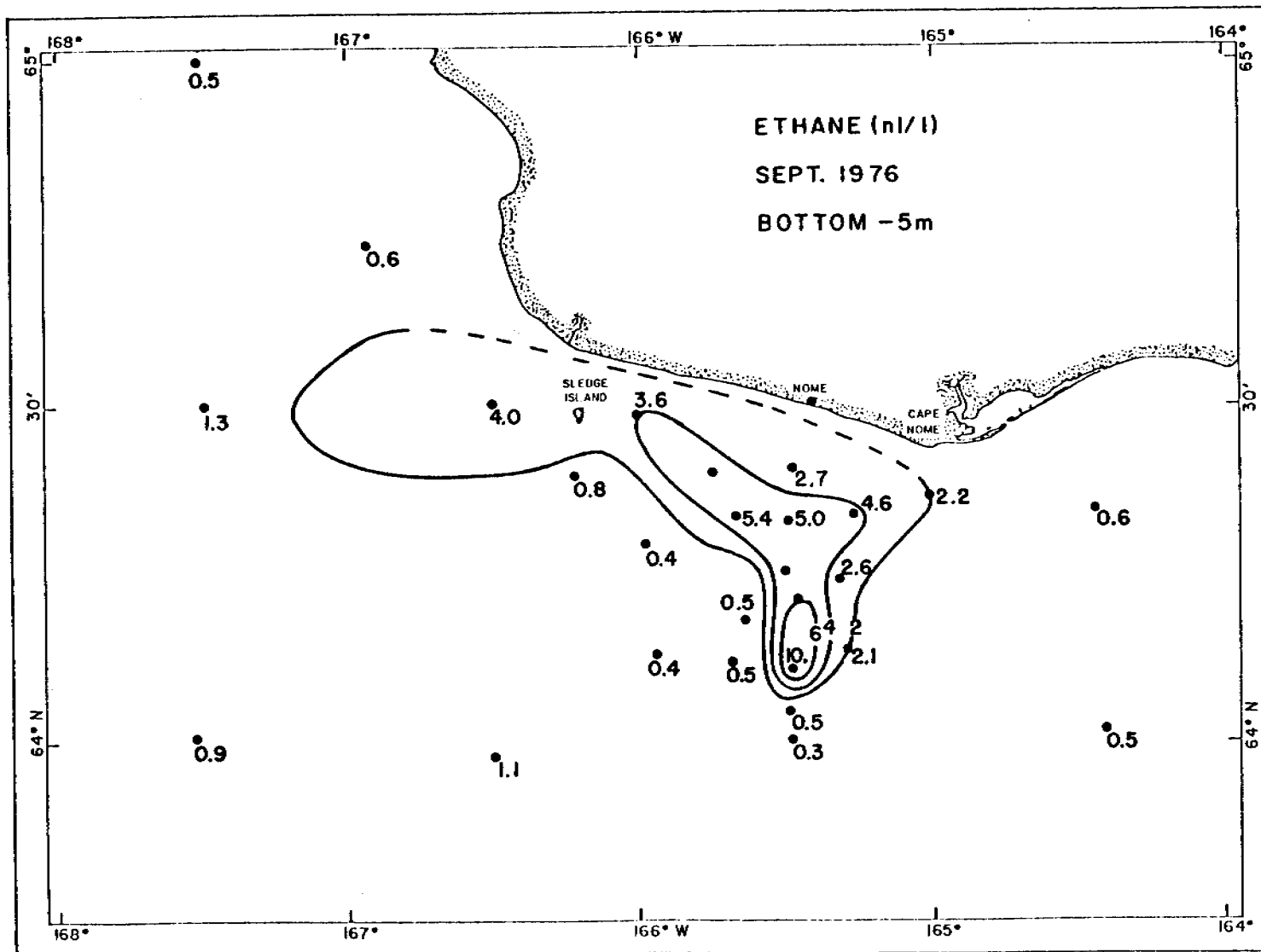


Figure 23. Dispersion plume of ethane within 5 m of the bottom in Sept. 1976. Concentrations are expressed in n/l (STP).

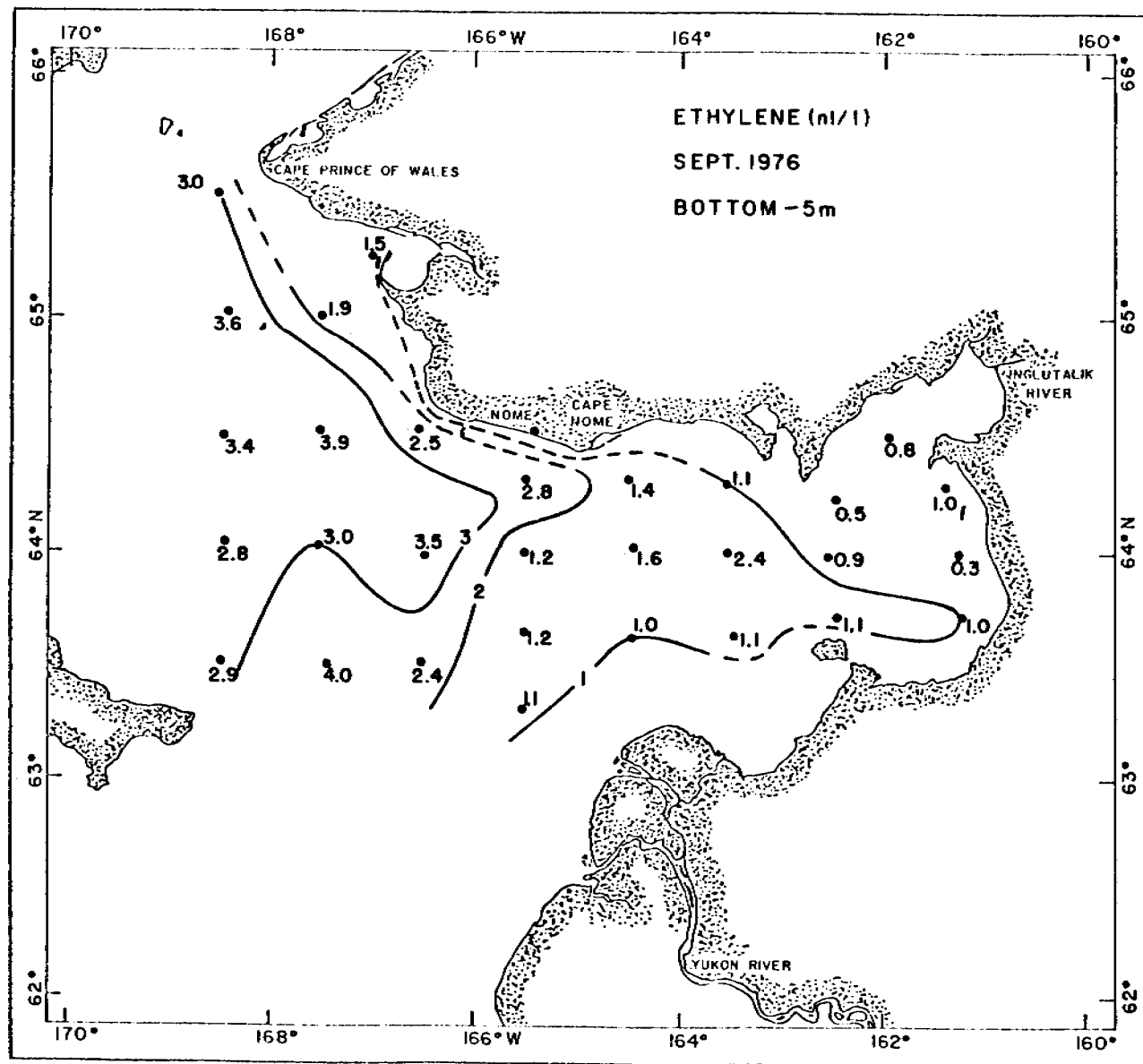


Figure 24. Areal distribution of ethylene (ethene) 5 m from the bottom in Sept. 1976. Concentrations are expressed in n1/1 (STP).

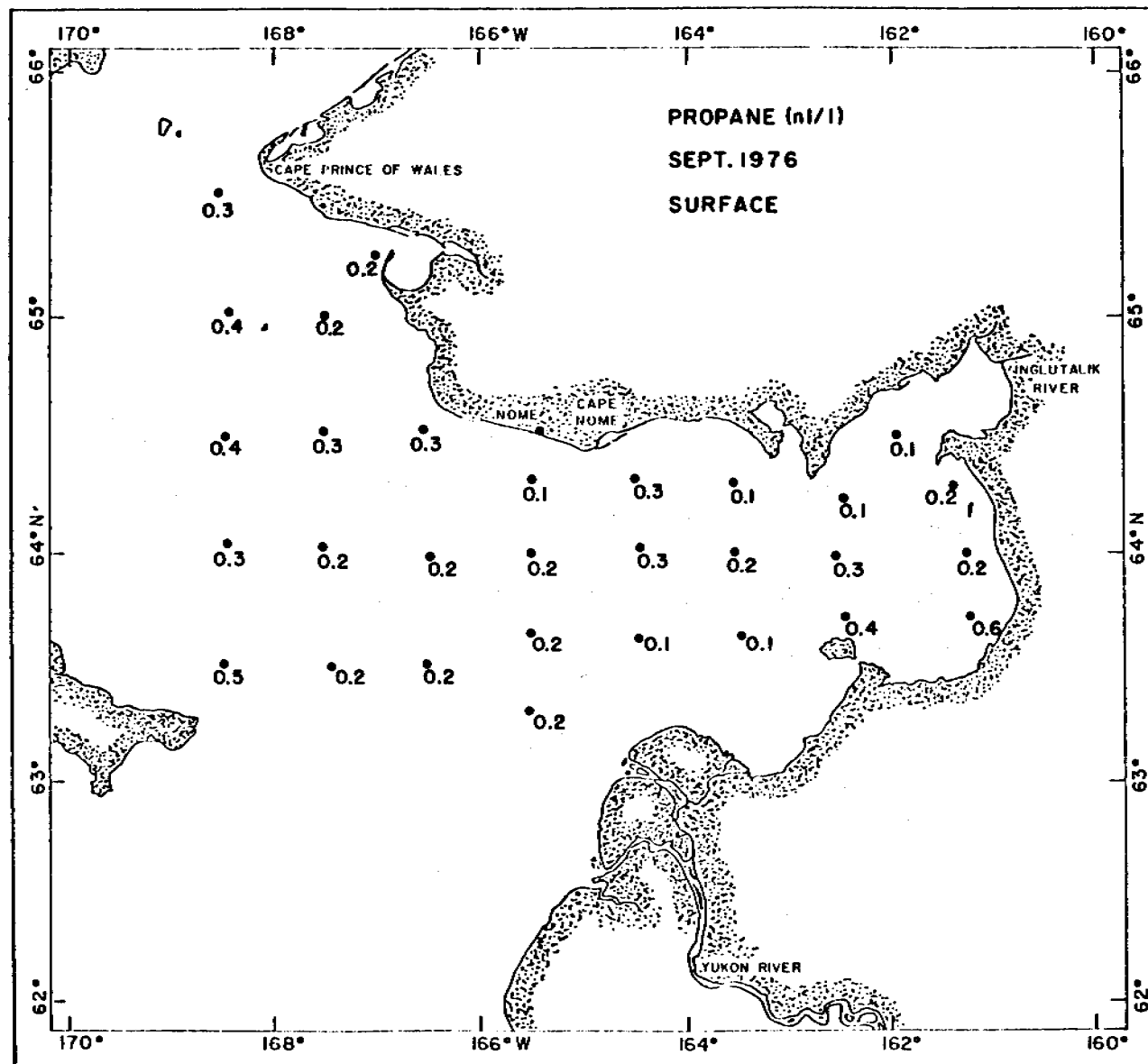


Figure 25. Surface distribution of propane in Sept. 1976. Concentrations are expressed in n/1 (STP).

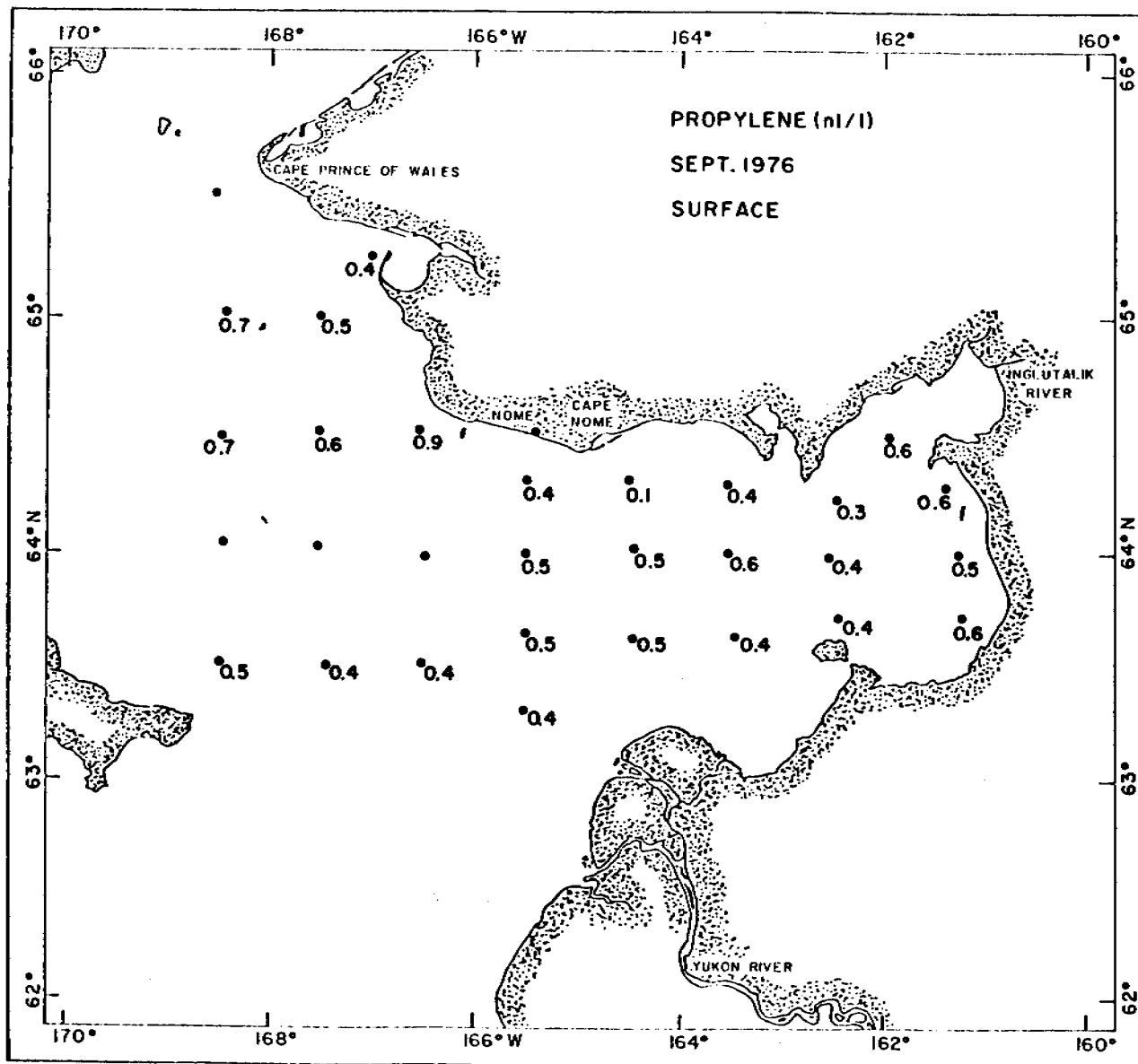


Figure 26. Surface distribution of propylene (propene) in Sept. 1976. Concentrations are expressed in nI/l (STP).

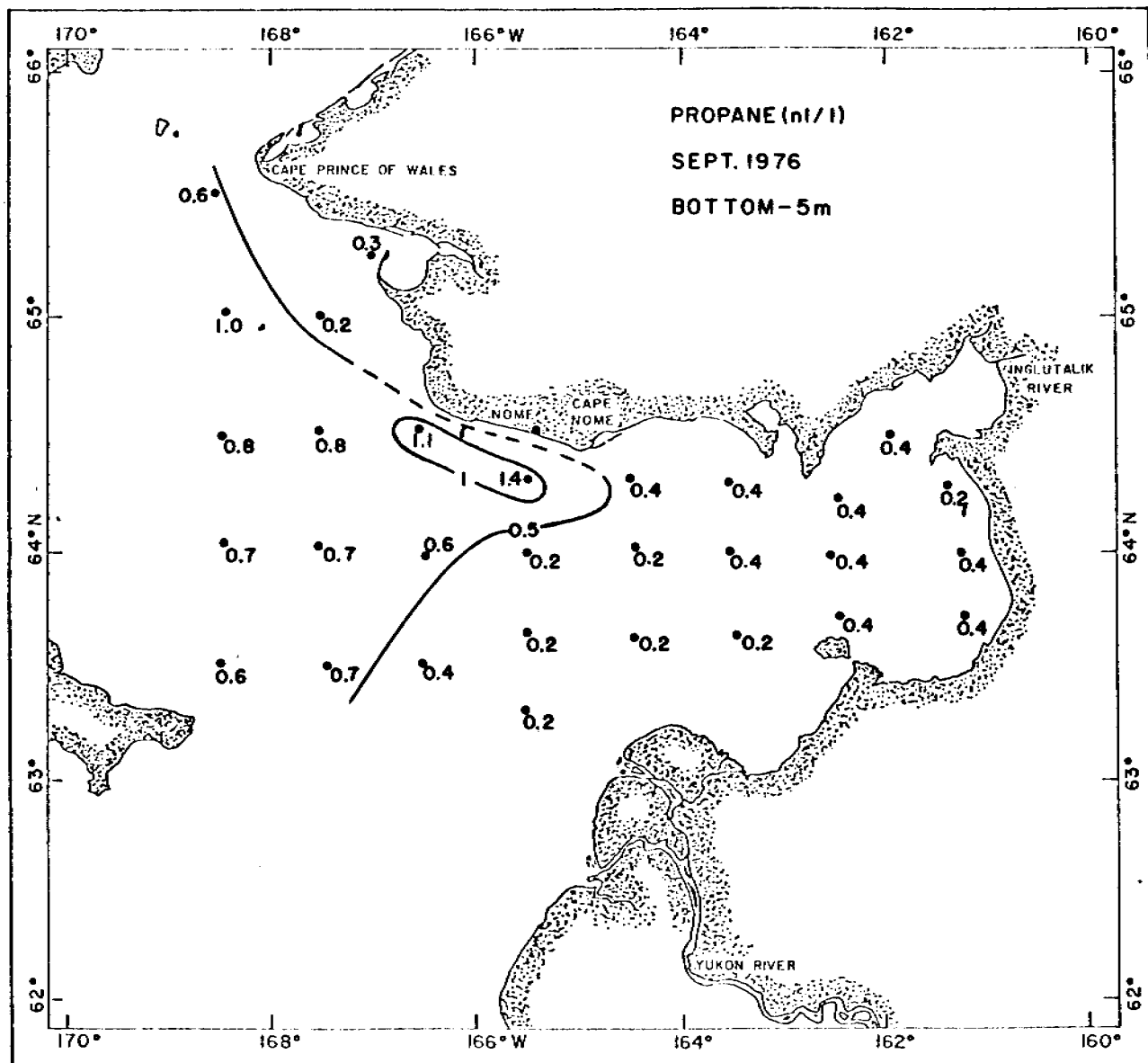


Figure 27. Areal distribution of propane 5 m from the bottom in Sept. 1976. Concentrations are expressed in nl/l (STP).

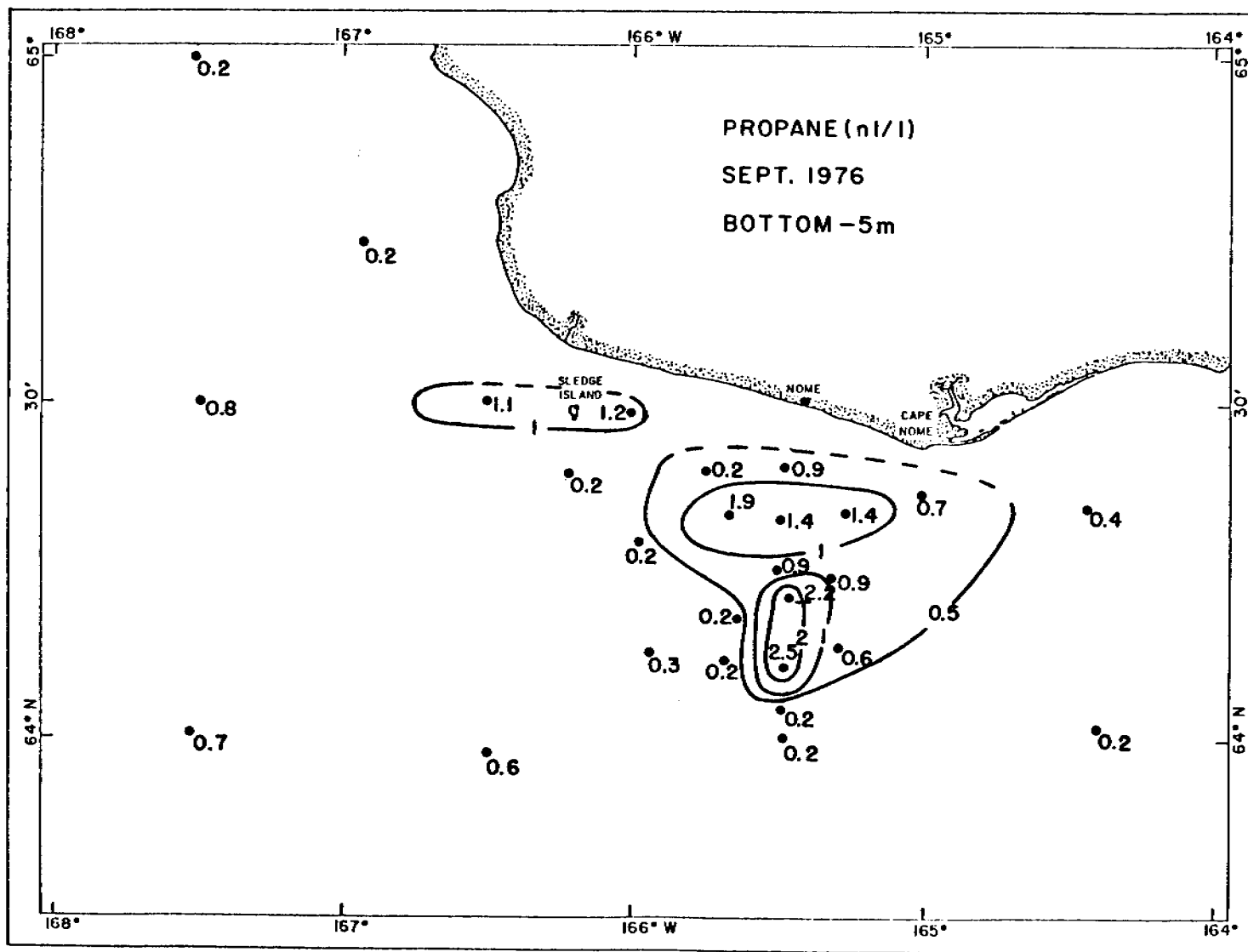


Figure 28. Dispersion plume of propane within 5 m of the bottom in Sept. 1976. Concentrations are expressed in nl/l (STP).

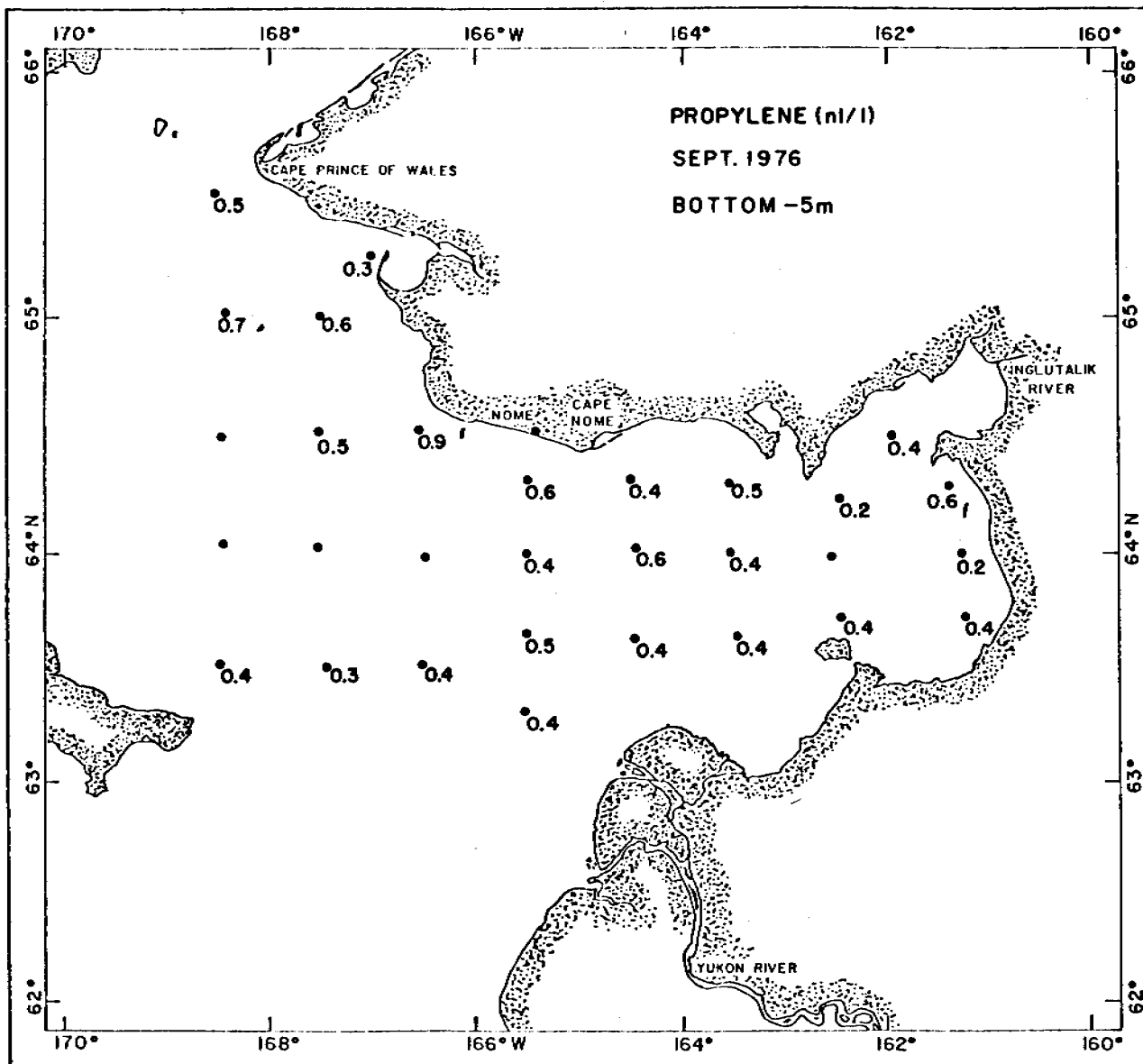


Figure 29. Areal distribution of propylene (propene) 5 m from the bottom in Sept. 1976. Concentrations are expressed in n1/1 (STP).

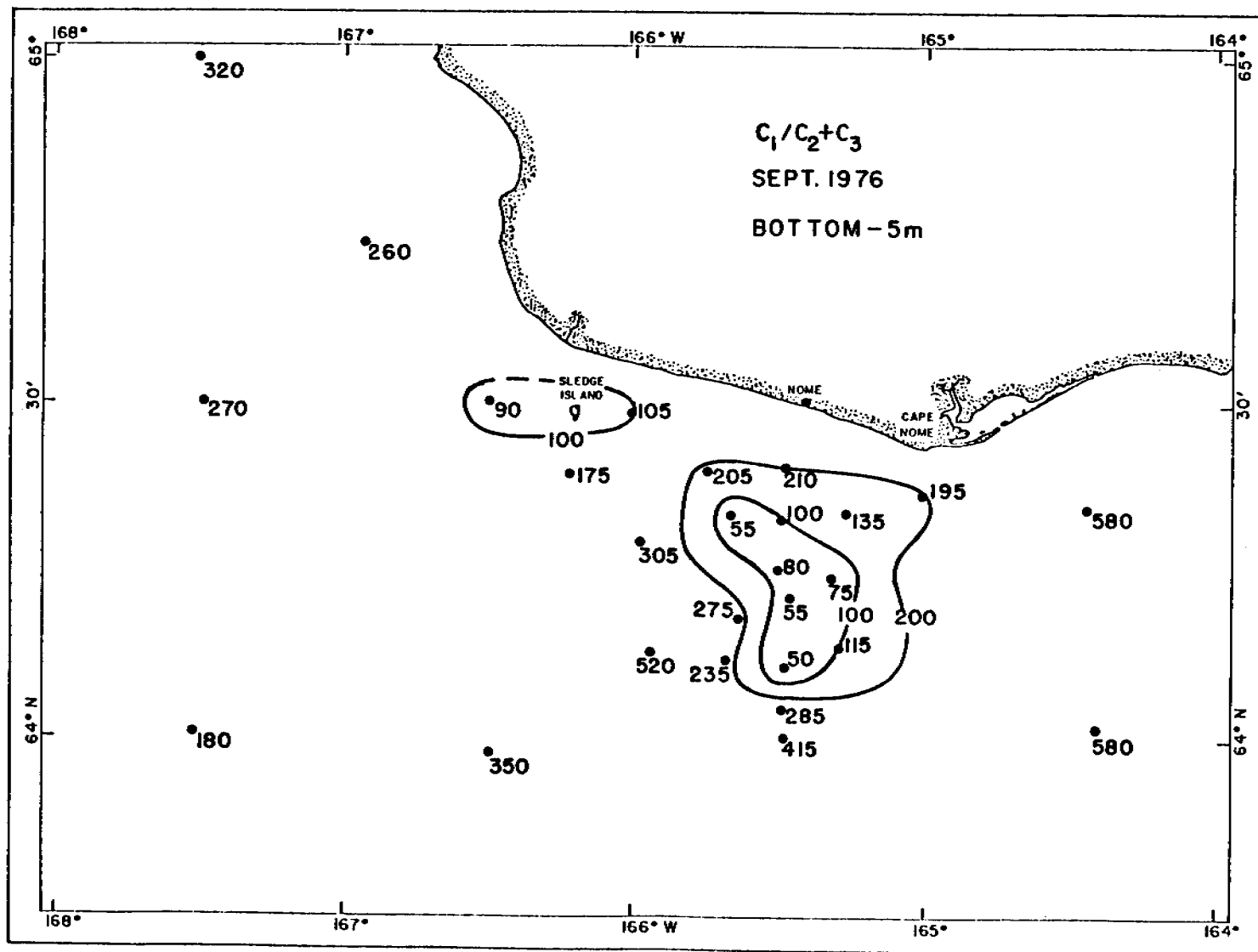


Figure 30. The distribution of the alkane ratio, $C_1/C_2 + C_3$, near the bottom in the vicinity of the gas seep.

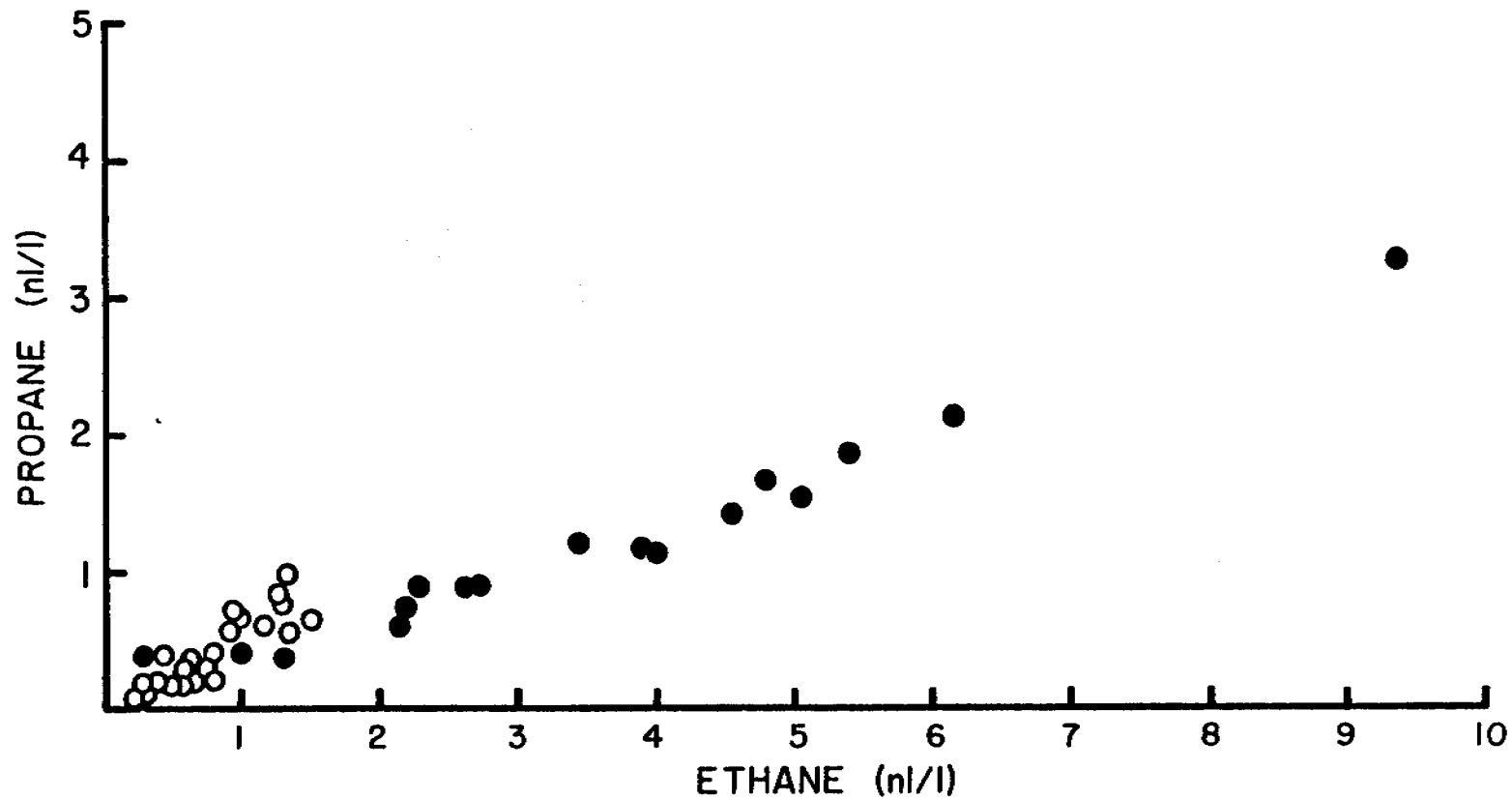


Figure 31. The relationship between the concentration of ethane and propane in the near bottom waters. The solid circles represent observations in the vicinity of the seep (ethane/ethylene > 1), open circles represent all other samples. For clarity, only a portion of the nonseep data is shown.

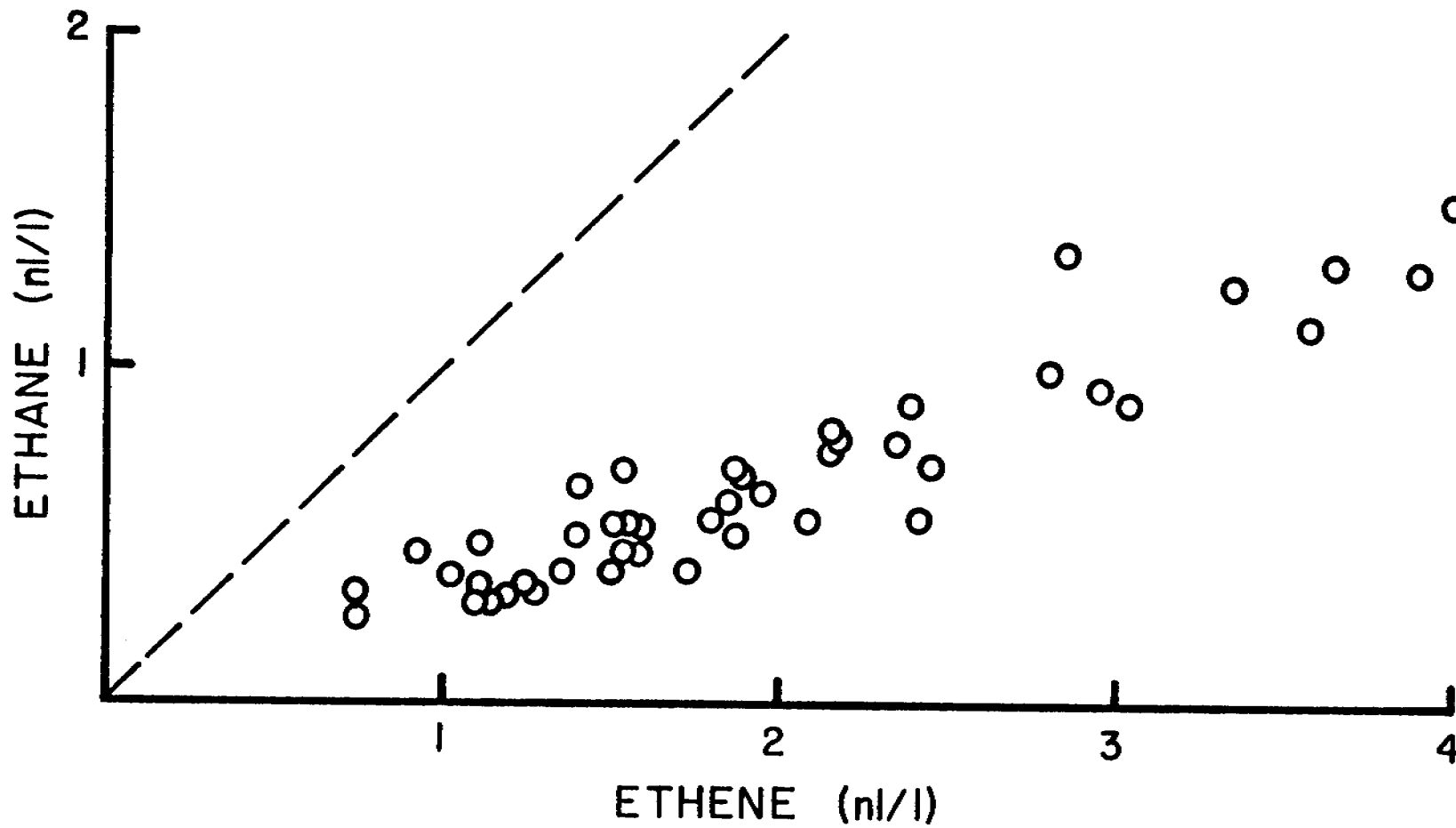


Figure 32. The relationship between the concentration of ethane and ethylene (ethene) in the near bottom waters. The dashed line represents an ethane/ethylene ratio of 1. All observations in the seep area would plot well above the 45° line.

Quarterly Report

Contract #03-5-022-56
Research Unit #162/163/288/293/310
Task Order #12
Reporting Period 10/1 - 12/31/76
Number of Pages 35

NATURAL DISTRIBUTION AND ENVIRONMENTAL BACKGROUND OF
TRACE HEAVY METALS IN ALASKAN SHELF AND ESTUARINE AREAS

Dr. David C. Burrell
Professor of Marine Science
Institute of Marine Science
University of Alaska
Fairbanks, Alaska 99701

January 1, 1977

I. TASK OBJECTIVES

The primary objective of this program is to characterize the trace metal contents of seawater, sediment, and selected indigenous biota in the three originally specified study areas (Gulf of Alaska, S. Bering Sea, Beaufort Sea) plus those regions added through later contract modifications (Lower Cook Inlet, Norton Sound). This program also incorporates sediment grain-size analysis, clay mineralogy analysis and "previous work" literature searches as described in the original Work Statement.

II. FIELD AND LABORATORY ACTIVITIES

A. Field Work

1. NEGOA Specific Study Site - Icy Bay

R/V *Acona* cruise September 11-16, 1976

Personnel: D. C. Burrell

A reconnaissance survey of Icy Bay, the agreed choice for the specific study site in the N.E. Gulf of Alaska. Approximately 10 miles of bathymetric track were run and two hydrographic stations occupied. Data from this cruise is currently being processed.

2. N. Bering Sea (Norton Sound) and Chukchi Sea

OSS *Discoverer* Leg IV, September 8-24, 1976

Personnel: T. Manson

Sixty water column samples were taken at 39 stations. In addition, 31 uncontaminated Haps core samples for heavy metal analysis, and 62 van Veen grab samples for sediment size analysis were collected. Sample localities are given in Figure 1 (Norton Sound) and Figure 2 (Chukchi Sea).

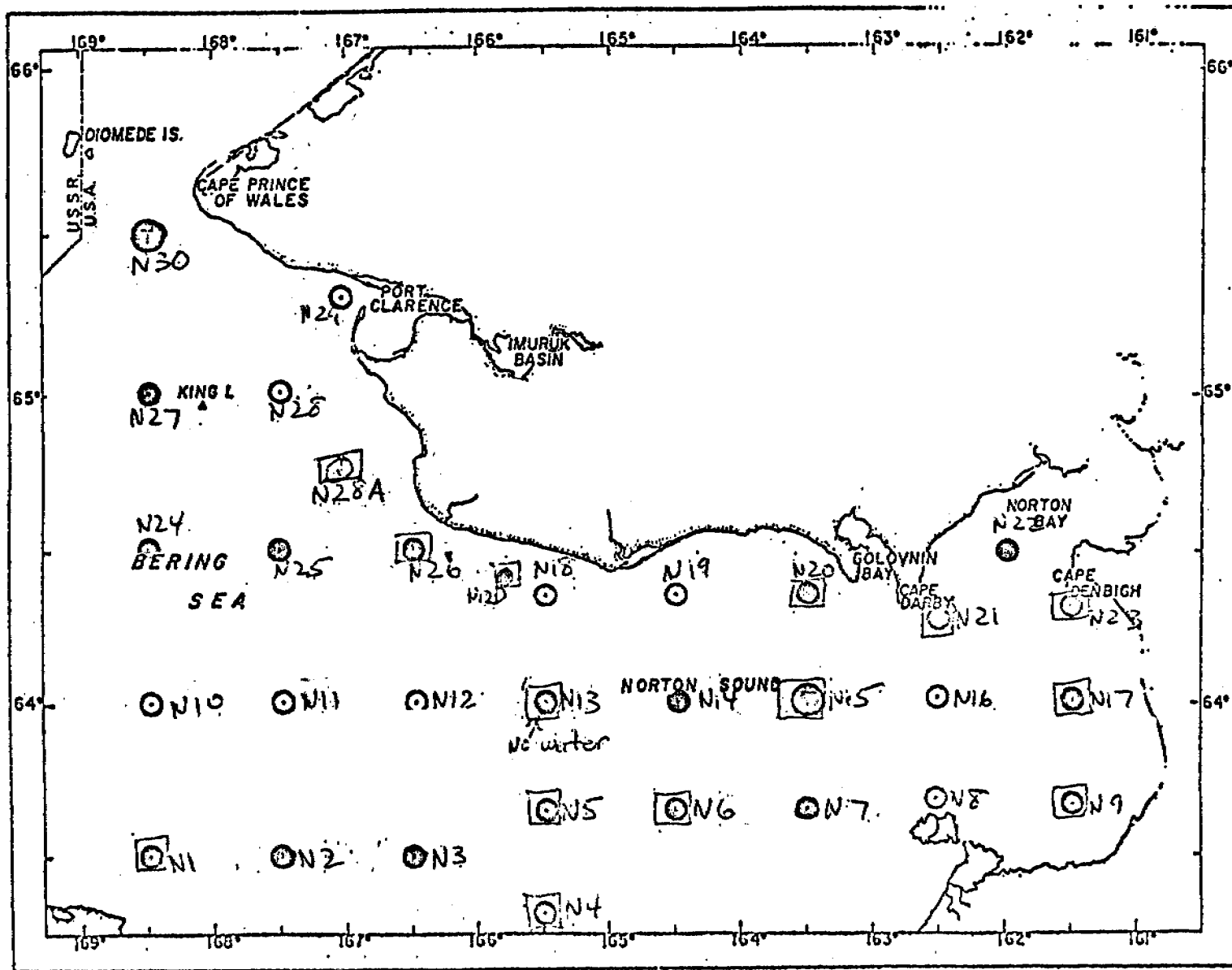


Figure 1. N. Bering Sea (Norton Sound) *Discoverer* Leg IV September 8-24, 1976. Station locations: Solid circle = water column samples, open squares = Haps cores.

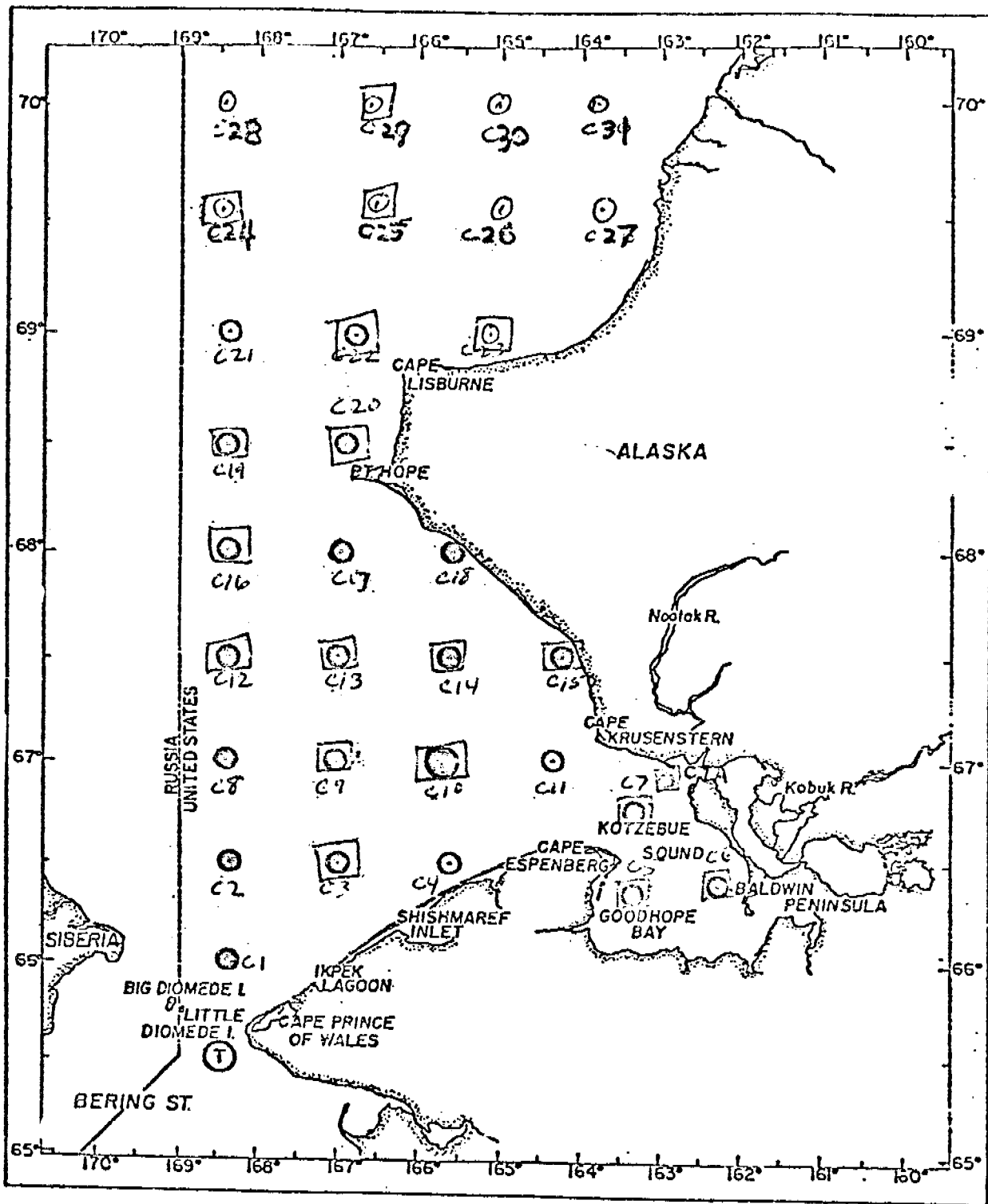


Figure 2. Chukchi Sea *Discoverer* Leg IV September 8-24, 1976. Station locations: Solid circles - water column samples, open squares - Haps cores.

B. Scientific Parties

As noted above.

C. Field Collection Methods

Sample collection and storage were as described in the Annual Report. Water samples were collected in ship's drop-top Niskin bottles and filtered through an in-line 0.45 μm filter. Core samples were taken using the standard Haps corer. Each of these samples was sectioned vertically into two segments.

D. Sample Localities

Sample localities for the N. Bering Sea (Norton Sound) and Chukchi Sea are shown in Figures 1 and 2.

E. Laboratory Analysis Programs

1. Vanadium in seawater by neutron activation analysis (Dr. D. E. Robertson):

To accomplish this analysis the V must be separated and concentrated from the seawater matrix prior to the neutron activation. We employed a new technique, recently developed under another program, to perform these measurements. Vanadium-48 ($t_{1/2} = 16$ days) tracer was produced by proton bombardment of a titanium foil in the University of Washington cyclotron, and carrier-free ^{48}V was radiochemically separated and used as a tracer in the methods development.

To 100 ml aliquots of seawater in precleaned polystyrene beakers was added 5 mg of high purity iron solution and 250 μl of phenol red indicator (0.1 gm per 250 ml of 0.001M NaOH). High purity 1.5M NH_4OH was then added dropwise while stirring until the first permanent color change from yellow to red occurred at a pH of about 7.8 ± 0.3 . The

Fe(OH)₃ precipitates were allowed to settle for about 20 minutes and the precipitates were then centrifuged and washed 3 times with 0.5M ammonium acetate containing 1 g/l of Magnifloc.

The precipitates were then transferred to 2/5 dram pre-cleaned polyethylene snap-top vials and were dried slowly under a heat lamp. The vials were then sealed in polyethylene bags and encapsulated in 2 dram polyethylene vials for neutron activation. Vanadium standards (14.2 µg) were prepared by pipetting 10 µl of standard solution onto discs of high purity IPC filter media, drying the discs and encapsulating them in the same manner as the Fe(OH)₃ precipitates. The samples and standards were neutron irradiated at the Washington State University Triga reactor, one at a time, standards interspersed between samples, for 2.0 minutes each. Following the irradiation the samples were allowed to decay for 2.0 minutes and were then counted directly on a Ge(Li) diode detector for 10 minutes to measure the 1434 keV γ-ray of ⁵²V (3.8 minutes).

The chemical recovery of vanadium for this procedure was 95.6 ± 1.4%, and the precision and accuracy were estimated to be less than 10%. The average procedural blank amounted to 0.11 ± 0.03 µg/l.

2. Intercalibration of methods used for water column analyses (Dr. D. C. Burrell):

Extra samples were taken on the *Discoverer* Leg IV, November 23 - December 2, 1975 cruise to enable comparisons to be made for some metals using various analytical techniques. The results of this work are still not yet available. However, filament atomic absorption analysis was compared with d.c. anodic stripping voltammetry for Cu,

Pb and Cd with unsatisfactory results as outlined below. A second set of samples was subsequently collected, from the surface, from within Resurrection Bay out into the Gulf. The analysis of those has just been completed.

3. Cu, Cd, Ni and Zn in biota by flameless atomic absorption (Dr. D. C. Burrell):

During this quarter we have analysed intertidal samples from the Gulf and S. Bering Sea lease areas collected for us by Dr. Zimmerman's group. The standard localities for those samples were listed in the previous quarterly report. In addition, *Neptunea* samples from the S. Bering Sea have been completed.

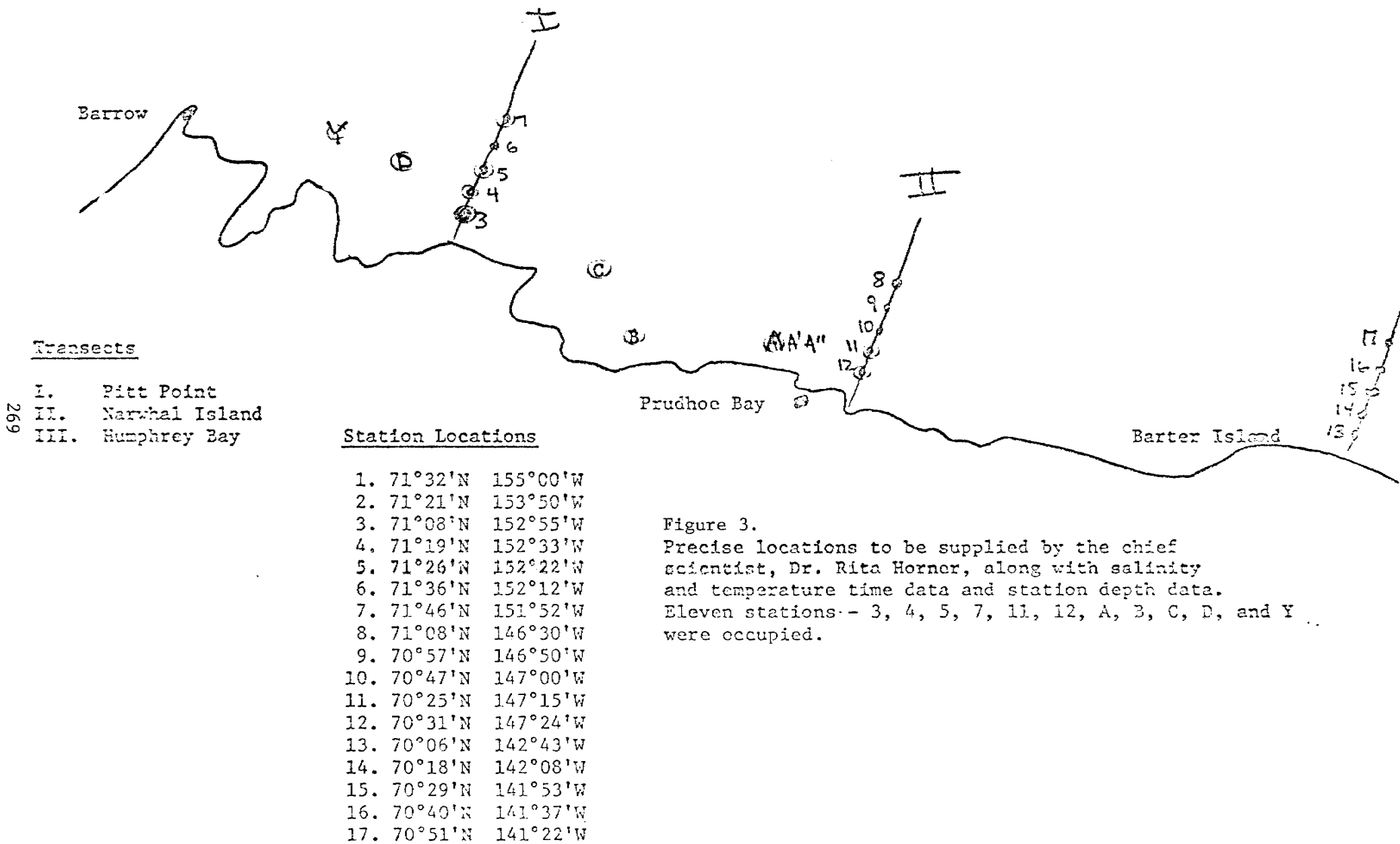
4. Se in biota by GC (Dr. T. A. Gosink):

The selenium contents of biota and parts of organisms from the S. Bering Sea have been determined.

5. Cr, Se and Al in sediment extracts by GC (Dr. T. A. Gosink):

Cr and Se analyses of sediment extracts (see Annual Report) collected in the N.W. Gulf of Alaska, S. Bering Sea and the Beaufort Sea have been completed. Sample locations for the latter area are given in Figure 3. The program has also included analysis of archived samples from the Beaufort Sea as discussed in the Annual Report. Extractable Al contents of N.W. Gulf of Alaska and S. Bering Sea samples have also been determined.

6. Total contents of heavy metals in sediment by neutron activation analysis (Dr. D. E. Robertson):



6. (Continued)

Presented here are the results of neutron activation analyses of Alaskan OCS sediments for As, Ba, Co, Cr, Fe, Sb and Sc. These measurements were made by irradiating 100 to 200 mg subsamples of sediments in the WSU Triga reactor for approximately 6 hours, storing the samples for predetermined time periods to allow short-lived interfering activation products to decay, and then counting the samples on Ge(Li) diode detectors.

It is not possible to measure Ag by this direct counting method because of an interference from high levels of ^{46}Sc produced in the activated samples. We are, therefore, developing a rapid radiochemical separation of $^{110\text{m}}\text{Ag}$ (252d) from the neutron irradiated sediment samples by lithium metaborate fusion, followed by solvent extraction of the $^{110\text{m}}\text{Ag}$ with dithizone in strong acid solution. The separated silver will then be counted in a NaI(Tl), high efficiency well crystal.

7. Heavy metals in archived Beaufort Sea sediment samples (Dr. A. S. Naidu):

The concentrations of some heavy metals in the total and non-lithogenous component of gravel-free sediment from the Beaufort Sea have been determined. These samples were collected before the commencement of the OCS program. Sample localities were given in the Annual Report.

8. Clay mineral analysis program (Dr. A. S. Naidu):

The weighed peak area percentages of clay minerals in S. Bering Sea sediment samples have been determined. Analyses have been performed on <2 and $<1 \mu\text{m}$ fractions with various chemical treatments.

III. RESULTS

1. Vanadium in seawater by neutron activation analysis (Dr. D. E. Robertson):

Data for the eastern and western Gulf of Alaska and for the Bering Sea are given in Tables I-III, respectively.

2. Intercalibration of methods used for water column analysis (Dr. D. C. Burrell):

See Section IV.

3. Cu, Cd, Ni and Zn in biota by flameless atomic absorption (Dr. D. C. Burrell):

Heavy metal contents of intertidal *Mytilus* and *Fucus* samples from all three primary lease areas are given in Tables IV and V. Data for *Neptunea* samples collected in the S. Bering Sea or the April 1-16, 1976 *Miller Freeman* cruise are given in Table VI. Table VII lists our most recent accuracy values.

4. Se in biota by GC (Dr. T. A. Gosink):

The selenium contents (mg/kg dry weight) of whole and portions of organisms collected in the S. Bering Sea on the 19 August - September 1975 *Miller Freeman* cruise are given in Table VIII.

5. Cr, Se and Al in sediment extracts by GC (Dr. T. A. Gosink):

Values for Se, Cr and Al contents of extracts from surface sediment samples from the N.W. Gulf of Alaska and S. Bering Sea are given in Tables IX and X, respectively. Se and Cr data for extracts from sediments collected on the August 1976 *Glacier* cruise in the Beaufort Sea

TABLE I

N.E. Gulf of Alaska

Discoverer Leg III 23 November - 2 December, 1975

D. E. Robertson, Analyst

Soluble vanadium contents of filtered (0.4 μ m) water • (μ g/kg).

Station	Depth	V
02	178	1.6
05	162	1.7
08	10	1.3
	274	1.6
15	10	1.4
	1500	1.6
26	10	1.6
	136	1.6
29	71	1.5
30	42	1.3
33	10	1.1
	205	1.6
44	10	1.2
	165	1.4
48	10	1.3
	447	1.6
52	74	1.3
53	10	1.3
	204	1.4
55	10	1.3
	110	1.2
58	82	1.4

TABLE II

N. W. Gulf of Alaska
Discoverer Leg IV 8-16 October, 1975
 D. E. Robertson, Analyst

Soluble vanadium contents of filtered (0.4 μm) water \cdot ($\mu\text{g}/\text{kg}$).

Station	Depth	V
101	1	1.2
	80	1.4
104	1	1.6
	96	1.4
108*	10	1.5
	226	1.6
119	204	1.5
121	1	1.3
	220	1.7
124	1	1.6
	105	1.7
133	1	1.3
	68	1.3
135	1	1.4
	141	1.3
137	1	1.3
	95	1.6
145	1	1.4
	63	1.5
148	1	1.3
	100	1.3
157	1	1.4
	59	1.2
160	1	1.5
	132	1.6

**Discoverer* Leg III 23 November - 2 December, 1975

TABLE III

S. Bering Sea
Discoverer Leg II 2-19 June, 1975
D. E. Robertson, Analyst

Soluble vanadium contents of filtered (0.4 μm) water \cdot ($\mu\text{g}/\text{kg}$).

Station	Depth	V
17	110	1.0
24	40	1.3
34	175	1.3
37	0	1.3
41	0	1.3
43	0	1.5
56	0	1.4
59	30	1.3
64	0	1.5
	80	1.5, 1.4

TABLE IV

Heavy metal contents of *Mytilus* ($\mu\text{g/g}$ dry weight).
Intertidal collection summer 1976.

	Cd	Cu	Ni	Zn
A. N.E. GULF				
Port Dick	11.0	8.4	2.2	80.3
Day Harbor	10.4	5.5	1.2	68.2
Katalla	6.0	10.8	4.3	90.0
Boswell Bay	2.9	6.4	1.2	39.6
La Touche Point	5.5	8.6	3.5	52.1
B. N.W. GULF AND KODIAK ISLAND				
Sundstrom Island	10.3	8.0	3.4	106.5
Cape Nukshak	9.0	9.0	3.2	81.9
C. S. BERING SEA				
Makushin	6.0	6.0	1.4	80.7
Otter Island	24.6	6.0	1.8	156.4

TABLE V

Heavy metal contents of *Fucus* ($\mu\text{g/g}$ dry weight).
Intertidal collection, summer 1976.

	Cd	Cu	Ni	Zn
A. N.E. GULF OF ALASKA				
Kayak Island	3.8	6.0	15.0	16.7
Anchor Cove (Day Harbor)	2.8	6.8	14.5	12.5
B. N.W. GULF OF ALASKA				
Cape Nukshak	4.3	7.0	9.3	14.9
C. S. BERING SEA				
Otter Island	3.1	5.0	5.1	8.1

TABLE VI

S. Bering Sea

Miller Freeman collection April 1-16, 1976Heavy metal contents of *Neptunea* ($\mu\text{g/g}$ dry weight).A. Tissue

Sample No.	Cd	Cu	Ni	Zn
15	13.0	215.9	<0.63	72.8
19	5.0	127.0	<0.63	85.9
22	32.0	241.3	0.92	133.1
31	<1.3	111.2	0.70	56.8
50	2.5	155.8	0.63	84.8

B. Digestive gland and reproductive organ

Sample No.	Cd	Cu	Ni	Zn
15	292.9	1495	0.93	1263
19	155.0	460	8.50	1325
22	200.0	875	4.63	275
31	65.0	140	1.88	350
50	280.0	6200	2.13	7000

TABLE VII

Accuracy data for biota analysis.

A. <u>NBS Standard #1571 Orchard Leaves</u>		
Element	This Study	NBS Certified
Cu	10.6, 11.4, 11.4, 12.5	12 ± 1
Ni	0.8, 0.9, 1.2, 2.5	1.3 ± 0.2
Zn	23.0, 23.5	25 ± 3

B. <u>NBS Standard #1577 Bovine Liver</u>		
Element	This Study	NBS Certified
Zn	148.5, 150.0	130 ± 10

TABLE VIII

S. Bering Sea

Miller Freeman Cruise 19 August - 3 September, 1975

Samples collected by M. Hoberg, T. A. Gosink, Analyst

Selenium contents of biota (mg/kg dry weight).

Station	Specimen Identification	Se (ppm)
1. 59°41'N 171°15'W	<i>Spirontocaris</i> sp.	0.21
2. 59°60'N 171°17'W	<i>Spirontocaris</i> sp.	0.71
3. 59°20'N 171°50'W	Wattled eelpout (eyes)	0.48
4. 59°20'N 171°50'W	Wattled eelpout (skin)	1.08
5. 58°30'N 170°14'W	Kelp	0.45
6. 58°00'N 170°16'W	Kelp	0.44
7. 60°00'N 168°40'W	King salmon (liver)	11.1
8. 60°00'N 168°40'W	Pollock (eyes)	0.08, 0.37
9. 60°00'N 168°40'W	Pollock (skin)	0.58
10. 59°20'N 171°48'W	<i>Chionoecetes opilio</i> (meat)	ND
11. 60°00'N 169°17'W	Agarum cribosum	0.38
12. 57°41'N 169°35'W	Capelin (whole)	1.29

ND = not detected

TABLE IX

N. W. Gulf of Alaska
Discoverer Leg IV 8-16 October, 1975
T. A. Gosink, Analyst

Selenium, chromium and aluminium contents of
surface sediment extracts ($\mu\text{g/g}$).

Station	Se	Cr	Al
101	-	ND	227
105	ND	ND	518
119	ND	ND	599
121	ND	ND	369
124 (1 cm)	0.17	0.6	117
(25 cm)	0.20	1.3	189
133	0.02	1.8	103
137	ND	ND	18
160	0.02	2.1	55

ND = not detected above blank level

TABLE X

S. Bering Sea

Discoverer Leg III 25 September - 3 October, 1975

T. A. Gosink, Analyst

Selenium, chromium and aluminium contents of
surface sediment extracts ($\mu\text{g/g}$).

Station	Se	Cr	Al
8	0.02	0.4	92
17	ND	ND	342
19	ND	ND	178
24	0.01	ND	103
35	0.09	0.4	102
40	ND	ND	ND
43	ND	1.7	55
46	ND	0.5	84
51	ND	0.9	122
54	0.02, 0.03	0.3	211
56	ND	ND	60
65	ND	1.9	138

ND = not detected

5. (Continued)

are presented in Table XI, and the Cr contents of Beaufort Sea archived samples in Table XII.

6. Total contents of heavy metals in sediments by neutron activation analysis (Dr. D. E. Robertson):

Total concentrations of As, Ba, Co, Cr, Sb and Sc (in $\mu\text{g/g}$) and Fe (%) for the eastern and western Gulf of Alaska are given in Tables XIII and XIV. Total Ba and As contents for S. Bering Sea samples are given in Table XV.

7. Heavy metals in archived Beaufort Sea sediment samples (Dr. A. S. Naidu):

Data for total and non-lithogenous fractions are given in Table XVI.

8. Clay mineral analysis program (Dr. A. S. Naidu):

Data for S. Bering Sea samples are given in Table XVII.

IV. PRELIMINARY INTERPRETATION

1. Vanadium in seawater by neutron activation analysis (Dr. D. E. Robertson):

Fifty-eight seawater samples collected at the surface and near the bottom at 36 stations in the Bering Sea and Gulf of Alaska have been analyzed. The vanadium concentrations in these samples averaged $1.5 \pm 0.2 \mu\text{g/l}$, and ranged from 1.0 to $1.7 \mu\text{g/l}$. The observed range in concentration in these samples is much less than that reported in the literature (0.2 to $4 \mu\text{g/l}$). The vanadium concentrations in particulate matter filtered from these samples was included in the June 30, 1976 progress report. Particulate vanadium concentrations ranged from

TABLE XI

Beaufort Sea

Glacier Leg II 23 August - 3 September, 1976

T. A. Gosink, Analyst

Selenium and chromium contents of surface
sediment extracts ($\mu\text{g/g}$).

Station	Cr	Se
3	ND	0.29
4	-	0.41
5	-	0.27
6	Tr	0.20
7	ND	0.47
8	ND	0.04
9	0.03	0.15
10	ND	0.43
12	-	0.24

ND = not detected above blank level

TABLE XII

Beaufort Sea
Archived samples*
T. A. Gosink, Analyst

Chromium contents of sediment extracts (mg/kg).

Station No.	Cr
71 AJ T-5 (31)	1.34
GLA 71-19 (4)	2.68
BSS-83 (30)	2.09
GLA 71-3 (44)	2.30
71 AJ T-20 (33)	1.50
PDB74-43 (3)	0.92

*Archived samples provided by A. S. Naidu, see 1975-1976 Annual Report for localities. Hydroxyl amino - acetic acid extracts.

TABLE XIII

N. E. Gulf of Alaska
Discoverer Leg III 23 November - 2 December, 1975
 D. E. Robertson, Analyst

Total heavy metal contents of bottom sediments
 ($\mu\text{g/g}$ except Fe %).

Station	Interval	As	Ba	Co	Cr	Fe(%)	Sb	Sc
2	0-2	5.3	700 \pm 190	16	115	4.20	0.61 \pm 0.19	14
	6-8	7.8	930 \pm 140	22	166	5.91	0.90 \pm 0.16	20
	10-12	7.7	710 \pm 130	19	134	5.02	0.71 \pm 0.13	17
	14-16	8.0	890 \pm 140	22	156	5.64	0.74 \pm 0.16	19
	18-20	6.3	770 \pm 110	19	112	4.96	0.81 \pm 0.13	17
5	8-10	2.2	500 \pm 100	20	130	5.14	0.59 \pm 0.10	18
	14-16	9.5	720 \pm 140	23	119	5.14	0.90 \pm 0.15	18
26	0-2	1.8	540 \pm 120	20	124	4.95	0.43 \pm 0.11	18
	4-6	<2.0	460 \pm 130	16	88	4.14	0.49 \pm 0.12	16
	8-10	3.5	490 \pm 120	20	126	4.98	0.57 \pm 0.10	19
	12-14	3.1	340 \pm 140	17	98	4.27	0.58 \pm 0.14	16
30	Top 2 cm	7.2	460 \pm 110	12	112	3.10	0.16 \pm 0.09	14
51	0-2	8.7	540 \pm 100	27	162	6.84	0.44 \pm 0.28	24
	4-6	7.9	530 \pm 130	20	138	4.94	0.37 \pm 0.10	17
59A	v.v.	1.6 \pm 0.6	570 \pm 160	17	156	4.52	0.66 \pm 25	19
58	0-2	2.7 \pm 0.7	430 \pm 160	18	145	4.80	0.35 \pm 0.08	20
	4-6	2.3 \pm 0.6	250 \pm 160	17	131	4.37	0.40 \pm 0.07	15
	8-10	2.3 \pm 0.7	480 \pm 170	18	153	5.19	0.45 \pm 0.09	21
57	0-2	2.1 \pm 0.6	350 \pm 180	18	134	4.37	0.46 \pm 0.16	16
	4-6	1.9 \pm 0.7	490 \pm 170	15	79	3.79	0.43 \pm 0.09	12
56	0-2	2.2 \pm 0.5	620 \pm 140	19	116	4.23	0.24 \pm 0.07	20
	4-6	1.9 \pm 0.8	770 \pm 180	12	88	2.99	0.30 \pm 0.05	9
	8-10	3.2 \pm 0.6	740 \pm 160	22	171	5.73	0.56 \pm 0.09	24
	12-14	2.7 \pm 0.7	530 \pm 170	18	142	4.68	0.47 \pm 0.08	17
33	0-2	2.6 \pm 0.6	450 \pm 160	16	114	5.23	0.81 \pm 0.07	16
	4-6	1.5 \pm 0.7	450 \pm 140	11	79	3.33	0.63 \pm 0.06	12
	8-10	1.4 \pm 0.6	350 \pm 100	12	32	2.27	0.40 \pm 0.05	10
48	0-2	2.5 \pm 0.4	550 \pm 130					
	4-6	2.3 \pm 0.7	500 \pm 120	16	104	4.41	0.51 \pm 0.09	17
	8-10	2.1 \pm 0.4	440 \pm 140					

TABLE XIII (Continued)

Station	Interval	As	Ba	Co	Cr	Fe(%)	Sb	Sc
44	0-2	2.7 ± 0.7	450 ± 120	15	112	4.36	0.42 ± 0.08	18
	4-6	0.8 ± 0.4	400 ± 130	16	55	2.97	0.33 ± 0.05	16
49	0-2	4.4 ± 0.9	350 ± 150	18	129	4.86	0.41 ± 0.10	23
	4-6	3.4 ± 0.4	540 ± 120	18	144	5.25	0.36 ± 0.08	22
	8-10	3.4 ± 0.7	530 ± 140	19	66	3.46	0.35 ± 0.06	21
	12-14	2.2 ± 0.3	670 ± 110	20	78	3.67	0.29 ± 0.04	25
	16-18	2.6 ± 0.4	380 ± 60	17	58	3.04	0.39 ± 0.06	18
50	0-2	3.0 ± 0.2	500 ± 70	19	74	3.44	0.26 ± 0.05	21
	8-10	2.4 ± 0.4	370 ± 130	12	98	2.84	<0.16	9
	12-14	3.2 ± 0.4	410 ± 140	20	136	5.08	0.35 ± 0.08	20
	18-20	2.3 ± 0.4	510 ± 110	16	110	3.76	0.28 ± 0.06	10
52	0-2	4.3 ± 0.5	770 ± 140	19	137	4.90	0.59 ± 0.09	14
	4-6	2.9 ± 0.4	720 ± 120	21	142	5.44	0.57 ± 0.25	17
	8-10	2.5 ± 0.5	580 ± 140	20	94	4.26	0.58 ± 0.05	14
	12-14	2.9 ± 0.4	520 ± 120	17	122	4.12	0.51 ± 0.08	12
	14-16	3.5 ± 0.5	690 ± 80	22	136	5.41	0.56 ± 0.09	18

TABLE XIV

N. W. Gulf of Alaska
Discoverer Leg IV 8-16 October, 1975
 D. E. Robertson, Analyst

Total heavy metal contents of bottom sediments
 ($\mu\text{g/g}$ except Fe %).

Station	Interval	As	Ba	Co	Cr	Fe(%)	Sb	Sc
105	0-2	4.7	460 \pm 80	5	192	1.32	0.26 \pm 0.06	-
	4-6	1.8	560 \pm 120	16	82	3.72	0.70 \pm 0.08	-
120	4-6	2.9	670 \pm 60	16	97	3.85	0.49 \pm 0.10	14
	8-10	2.6	1100 \pm 60	17	102	4.18	0.97 \pm 0.12	15
	12-14	5.2	790 \pm 80	16	100	3.96	0.96 \pm 0.11	14
	16-18	2.6	610 \pm 60	15	89	3.63	0.81 \pm 0.09	13
121	0-2	5.4	760 \pm 80	15	117	4.10	0.82 \pm 0.12	15
	4-6	3.8	710 \pm 80	15	106	3.93	0.73 \pm 0.12	14
	8-10	5.6	670 \pm 70	13	96	3.39	0.82 \pm 0.09	13
122	0-2	2.9	260 \pm 30	3	15	0.83	0.17 \pm 0.06	3
124	0-2	2.8	630 \pm 60	8	67	2.75	0.52 \pm 0.10	10
	4-6	3.3	570 \pm 70	9	61	2.73	0.43 \pm 0.09	10
	8-10	3.7	460 \pm 60	9	59	2.96	0.33 \pm 0.09	9
133	Grab	3.8	400 \pm 80	16	31	4.10	0.35 \pm 0.10	14
134	0-2	6.6	670 \pm 90	16	77	4.17	0.51 \pm 0.12	16
	4-6	5.7	620 \pm 100	15	75	4.08	0.64 \pm 0.14	16
	8-10	7.3	820 \pm 120	21	75	4.61	0.69 \pm 0.14	18
	12-14	8.8	830 \pm 110	18	75	4.73	0.73 \pm 0.14	18
	16-18	5.1	490 \pm 110	14	66	3.87	0.48 \pm 0.10	15
135	0-2	4.3	710 \pm 130	16	74	4.90	0.56 \pm 0.15	18
	4-6	4.5	680 \pm 110	15	54	4.49	0.50 \pm 0.12	16
	8-10	5.1	250 \pm 110	16	77	4.73	0.56 \pm 0.13	17

TABLE XV

S. Bering Sea
Discoverer 2-19 June, 1975
 D. E. Robertson, Analyst

Total heavy metal contents of bottom sediments ($\mu\text{g/g}$).

Station	Interval	Ba	As
8	0-2	370 \pm 230	4.1 \pm 0.4
	4-6	230 \pm 210	5.1 \pm 0.3
	8-10	310 \pm 220	4.1 \pm 0.4
	12-14	<210	3.9 \pm 0.4
19	0-2	440 \pm 140	3.7 \pm 0.4
30	0-4	200 \pm 190	3.4 \pm 0.6
	4-8	<260	2.1 \pm 0.5
	8-12	<370	1.5 \pm 0.5
37	0-2	430 \pm 190	4.1 \pm 0.6
	4-6	500 \pm 150	3.1 \pm 0.5
	8-11	750 \pm 150	5.8 \pm 0.4
41	0-2	480 \pm 140	3.0 \pm 0.4
43	0-2	<420	3.2 \pm 0.5
	4-6	390 \pm 200	3.5 \pm 0.3
56	0-2	<260	0.7 \pm 0.6
	4-6	460 \pm 280	4.3 \pm 0.6
	8-10	570 \pm 440	2.8 \pm 0.6
	12-18	<500	4.0 \pm 0.7
59	0-2	1070 \pm 340	4.0 \pm 0.4
	4-6	<350	3.8 \pm 0.4
64	0-2	1030 \pm 340	2.7 \pm 0.8
	4-6	500 \pm 270	3.6 \pm 0.6
	8-10	<280	2.9 \pm 0.6
	12-14	810 \pm 300	3.6 \pm 0.6
	16-20	400 \pm 260	4.6 \pm 0.5
	20-24	600 \pm 240	6.5 \pm 0.4
12	0-3	650 \pm 170	4.3 \pm 0.5
28	0-3	490 \pm 170	2.9 \pm 0.5
29	0-4	530 \pm 220	7.2 \pm 0.5

TABLE XVI

Beaufort Sea*

A. S. Naidu, Analyst

Total heavy metal contents of sediments (gravel free, dry weight).

Sample No.	Fe %			Mn %			Cu $\mu\text{g/g}$			Zn $\mu\text{g/g}$			Ni $\mu\text{g/g}$			V $\mu\text{g/g}$		
	Total	NL	%NL	Total	NL	%NL	Total	NL	%NL	Total	NL	%NL	Total	NL	NL%	Total	NL	NL%
BSS-62	4.18	0.25	6	270	88	33	43	5	12	130	25	19	50	3	6	275	9.9	4
BSS-83	3.44	0.43	13	270	88	33	43	7	16	75	33	44	41	3	7	170	16.7	10
BSS-88	3.08	0.48	16	300	220	73	61	8	13	90	40	44	47	6	13	185	10.6	6
GLA71-1	2.18	0.53	24	280	150	54	28	19	68	87	24	28	45	5	11	-	-	-
GLA71-3	2.40	0.48	20	260	200	77	24	3	13	75	-	-	39	2	5	120	10.9	-
GLA71-12	2.80	0.51	18	340	260	77	39	7	18	95	40	42	53	6	11	-	-	-
GLA71-23	2.80	0.73	26	440	275	63	38	6	16	101	32	32	57	4	7	160	9.5	6
GLA71-25	2.55	0.55	22	500	400	80	35	7	20	98	25	26	55	3	5	150	11.1	7
GLA71-27	1.55	0.29	19	1460	550	38	18	7	39	72	21	29	33	2	6	-	-	-
GLA71-44	2.22	0.51	23	590	490	83	25	6	24	77	23	30	45	2	4	120	14.4	12
GLA71-63	2.75	0.91	33	490	360	74	35	12	34	92	40	44	51	6	12	160	-	-
GLA71-71	2.12	0.73	34	370	260	70	60	6	10	85	32	38	49	4	8	120	10.9	9
GLA71-72	2.80	0.78	28	1000	700	70	44	19	43	79	36	58	51	8	16	-	-	-
GLA71-78	3.55	0.80	23	630	420	67	47	12	26	95	44	46	66	6	9	225	16.2	7
GLA71-80a	3.25	0.60	19	590	400	68	38	14	37	100	27	27	62	4	6	190	11.3	6
GLA71-80b	3.25	0.55	17	590	400	68	38	11	29	100	27	27	62	4	6	190	12.1	6
GLA71-80c	3.25	0.58	18	590	400	68	38	11	29	100	31	31	62	4	6	190	11.9	6
PDB74-34a	1.33	0.28	21	230	143	62	16	12	75	95	15	16	33	2	6	60	3.2	6
PDB74-34b	1.33	0.23	17	230	138	60	16	11	69	95	17	18	33	2	6	-	-	-
PDB74-39a	1.03	0.15	15	270	90	33	13	1	8	123	13	11	37	2	5	25	2.8	11
PDB74-39b	1.03	0.13	13	270	80	30	13	1	8	123	15	12	37	3	8	-	-	-
PDB74-41	1.48	0.21	14	350	150	43	28	1	4	104	21	20	44	3	7	25	3.2	13
PDB74-43	1.26	0.05	4	290	120	41	12	1	8	123	8	7	25	Tr	Tr	25	2.2	9
70BS-22	1.65	0.38	23	270	138	51	24	4	17	84	25	30	37	2	5	75	9.8	13
71AJT-5	1.48	0.20	14	240	123	51	13	2	15	60	15	25	24	0	0	25	3.8	15
71AJT-20	1.70	0.43	25	320	180	56	26	5	19	100	31	31	43	3	7	75	10.2	14
71AER-15	1.85	0.29	16	310	200	65	24	1	4	91	19	21	43	3	7	75	2.5	3
72AJT-5	1.48	0.33	22	240	120	50	13	2	15	60	27	45	24	2	8	25	6.4	26
72AJT-6	1.43	0.16	11	270	150	56	10	1	10	60	19	32	22	2	9	25	4.9	20
72AJT-8	-	-	-	-	-	-	32	4	13	115	29	25	51	4	8	75	10.2	14
72AER-129a	2.40	1.03	43	310	250	81	30	8	27	108	40	37	45	3	7	100	13.9	14
72AER-129b	2.40	1.23	51	310	245	79	30	6	20	108	46	43	45	4	9	-	-	-
72AER-134	1.20	0.28	23	250	128	51	39	4	10	115	21	18	52	2	4	100	7.2	7
72AER-137	0.98	0.18	18	150	55	37	10	1	10	38	15	40	19	0	0	25	3.2	13
72AER-166	2.58	0.38	15	240	150	63	22	3	14	58	27	47	40	3	8	50	6.6	13
73AER-168	2.68	0.33	12	270	155	57	28	2	7	108	21	19	43	2	5	50	4.6	9

* Archived samples, see 1975-1976 Annual Report for locations.

NL = non-lithogenous fraction.

TABLE XVII

S. Bering Sea

Discoverer 2-19 June 1975

A. S. Naidu, Analyst

Clay mineralogy (weighted peak area percents).

Station No.	Sample Saturation	Expandable		Illite		Kaolinite		Chlorite	
		< 2 m μ	< 1 m μ	< 2 m μ	< 1 m μ	< 2 m μ	< 1 m μ	< 2 m μ	< 1 m μ
2	Glycol	-	2	-	61	-	15	-	22
	K ⁺ & Glycol	-	-	-	-	-	-	-	-
	Mg ⁺⁺ & Glycol	-	-	-	-	-	-	-	-
8	Glycol	45	50	10	17	17	10	28	23
	K ⁺ & Glycol	0	-	52	-	0	-	48	-
	Mg ⁺⁺ & Glycol	44	-	13	-	0	-	43	-
10	Glycol	43	46	19	25	12	Tr	26	29
	K ⁺ & Glycol	0	-	62	-	0	-	38	-
	Mg ⁺⁺ & Glycol	33	-	30	-	5	-	32	-
13	Glycol	26	36	31	26	11	10	32	28
	K ⁺ & Glycol	0	-	43	-	0	-	57	-
	Mg ⁺⁺ & Glycol	25	-	33	-	0	-	42	-
14	Glycol	26	35	31	32	6	8	37	25
	K ⁺ & Glycol	-	-	-	-	-	-	-	-
	Mg ⁺⁺ & Glycol	17	-	30	-	7	-	46	-
19	Glycol	26	40	34	20	10	7	30	33
	K ⁺ & Glycol	-	-	60	-	0	-	40	-
	Mg ⁺⁺ & Glycol	21	-	47	-	0	-	32	-
21	Glycol	25	35	33	29	8	9	34	27
	K ⁺ & Glycol	18	-	41	-	7	-	34	-
	Mg ⁺⁺ & Glycol	28	-	29	-	9	-	34	-

TABLE XVII (Continued)

Station No.	Sample Saturation	Expandable		Illite		Kaolinite		Chlorite	
		< 2 m μ	< 1 m μ	< 2 m μ	< 1 m μ	< 2 m μ	< 1 m μ	< 2 m μ	< 1 m μ
26	Glycol	24	32	38	26	10	12	28	30
	K ⁺ & Glycol	7	-	45	-	0	-	48	-
	Mg ⁺⁺ & Glycol	23	-	31	-	0	-	46	-
31	Glycol	25	30	35	35	11	0	29	35
	K ⁺ & Glycol	3	-	39	-	0	-	58	-
	Mg ⁺⁺ & Glycol	22	-	41	-	4	-	34	-
34	Glycol	28	33	33	33	12	Tr	27	34
	K ⁺ & Glycol	12	-	40	-	12	-	36	-
	Mg ⁺⁺ & Glycol	13	-	43	-	6	-	38	-
41	Glycol	19	28	37	31	12	9	32	32
	K ⁺ & Glycol	0	-	47	-	8	-	45	-
	Mg ⁺⁺ & Glycol	24	-	38	-	7	-	31	-
43	Glycol	33	36	30	33	8	8	29	23
	K ⁺ & Glycol	11	-	46	-	13	-	30	-
	Mg ⁺⁺ & Glycol	29	-	34	-	9	-	28	-
48	Glycol	30	36	35	36	0	4	35	24
	K ⁺ & Glycol	0	-	50	-	0	-	50	-
	Mg ⁺⁺ & Glycol	23	-	31	-	0	-	46	-
57	Glycol	15	29	41	38	10	8	34	25
	K ⁺ & Glycol	-	0	48	-	0	-	52	-
	Mg ⁺⁺ & Glycol	24	-	40	-	4	-	32	-
60	Glycol	13	21	52	43	7	14	28	22
	K ⁺ & Glycol	0	-	53	-	15	-	32	-
	Mg ⁺⁺ & Glycol	20	-	43	-	10	-	27	-
62	Glycol	25	25	33	42	10	8	32	25
	K ⁺ & Glycol	0	-	58	-	8	-	34	-
	Mg ⁺⁺ & Glycol	27	-	39	-	5	-	29	-

TABLE XVII (Continued)

Station No.	Sample Saturation	Expandable		Illite		Kaolinite		Chlorite	
		< 2 m μ	< 1 m μ	< 2 m μ	< 1 m μ	< 2 m μ	< 1 m μ	< 2 m μ	< 1 m μ
64	Glycol	22	22	45	39	Tr	10	33	29
	K ⁺ & Glycol	9	-	51	-	8	-	32	-
	Mg ⁺⁺ & Glycol	26	-	38	-	9	-	27	-
65	Glycol	14	27	52	40	6	5	28	28
	K ⁺ & Glycol	-	-	-	-	-	-	-	-
	Mg ⁺⁺ & Glycol	-	-	-	-	-	-	-	-
69	Glycol	23	25	36	42	12	5	29	28
	K ⁺ & Glycol	43	-	31	-	4	-	22	-
	Mg ⁺⁺ & Glycol	38	-	37	-	4	-	21	-

<0.007 to 0.77 $\mu\text{g}/\ell$, but averaged about 0.05 $\mu\text{g}/\ell$, or approximately 3% of the total vanadium.

It appears that this neutron activation procedure possesses that required sensitivity, accuracy and precision to show that dissolved vanadium is rather homogeneously distributed in the oceans at an average concentration of about 1.5 $\mu\text{g}/\ell$ -- an important conclusion for establishing reliable baseline data for this trace element in the oceans. The present interest stems mainly from the fact that vanadium is present in relatively high concentration in crude oil (1 to 6000 ppm), and the effects of vanadium on marine ecosystems from potential oil spills during shipping and off-shore drilling are largely unknown. Certain marine ascidians and tunicates have an organo-vanadium compound as a respiratory pigment, and the effects on these inter-tidal and benthic animals from accumulated organo-vanadium compounds present in crude oils could be detrimental.

2. Intercalibration of methods used for water column analysis (Dr. D. C. Burrell):

Values for the eastern Gulf of Alaska intercalibration stations for Cd, Cu and Pb by filament atomic absorption were higher than by d.c. anodic stripping voltammetry by up to an order of magnitude. Unfortunately, at the present time we do not have data by neutron activation analysis. We suspected the large errors have to be associated with the particular batch of small volume collection tubes used. Subsequent work on large volume samples directly collected from the surface (i.e., not *via* a wire-hung sampler) has given considerably closer agreement. However, it would appear that the precision of the atomic

absorption procedure is around \pm 50-100%. In view of the fact that much of the data on soluble trace metal contents extant in the literature is in error by one or more orders of magnitude, these findings do not necessarily reject atomic absorption as a possible procedure for survey purposes. A comprehensive report on this sub-project is presently being prepared.

3. Cu, Cd, Ni and Zn in biota by flameless atomic absorption (Dr. D. C. Burrell):

Mytilus and *Fucus* are proving to be excellent indicator species. There are no obvious anomalies through the E. and W. Gulf and Bering Sea study areas. *Mytilus* should prove to be sensitive to Zn and Cd and *Fucus* to Ni. For some reason the latest periodic accuracy test is less satisfactory for zinc than previously, although earlier start-up problems with this metal have generally been eliminated. In view of our more recent data, the earliest values for zinc in *Mytilus* (tabulated in Annual Report) should now be discarded.

The heavy metal contents of the *Neptunea* samples are most interesting. The initial batch of data for samples from the N.E. Gulf of Alaska (Table XXIX in 1975-1976 Annual Report) showed elevated Cu and remarkably high Cd contents. For the latest batch taken from the S. Bering Sea we have separated gut and reproductive organs and analysed this portion and remaining tissue sample separately. From Table VI it may be seen that the former fraction is elevated in Cu, Cd and Zn by several orders of magnitude. Unfortunately, very little appears to be known about the biology of this animal.

4. Se in biota by GC (Dr. T. A. Gosink):

Biota samples show normal values with specific organs (liver, skin and some eyes) showing very high concentrations.

5. Cr, Se and Al in sediment extracts by GC (Dr. T. A. Gosink):

Selenium analyses of sediments show the anticipated pattern of being present in very low concentrations. Cr shows no unusual characteristics.

6. Total contents of heavy metals in sediments by neutron activation analysis (Dr. D. E. Robertson):

Within the limits of analytical error, no large, systematic variations in concentrations of these trace metals with core depth were observed. However, some geographical variability of trace metals in surface (0-2 cm) sediment distributions was observed.

Unusually high Ba concentrations were observed at Stations 59 and MB in the S. Bering Sea. Curiously, these areas of high Ba are in close proximity to Stations 56 and 43 where some of the lowest Ba concentrations were found. The distribution of Ba illustrates that rather large geographical variations in concentrations can exist over relatively small distances.

The surface areal distribution of chromium in the sediments shows minimum concentrations at eastern Gulf of Alaska Stations 133, 134 and 135. Station 122 contains very low Cr concentrations as well as most other trace metals. The sediment at Station 122 is highly calcareous (26.9% Ca compared to 2.3% Ca for other adjacent stations), and reflects a greatly different trace metal composition.

V. PROBLEMS ENCOUNTERED

The Hanford "N" Reactor, which had been shut down because of a strike has just now been restarted. The "N" Reactor was the only reactor in the western U.S. which possesses the necessary highly thermalized neutron flux to perform direct instrumental neutron activation analyses of seawaters. We were, therefore, unable to perform many of the trace metal analyses of Alaskan coastal seawater samples during this period. We have commenced analyses of these samples now that the reactor has restarted.

OCS COORDINATION OFFICE

University of Alaska

ENVIRONMENTAL DATA SUBMISSION SCHEDULE

DATE: December 31, 1976

CONTRACT NUMBER: 03-5-022-56

T/O NUMBER: 12

R.U. NUMBER:
162/163/288/293/312

PRINCIPAL INVESTIGATOR: Dr. D. C. Burrell

Submission dates are estimated only and will be updated, if necessary, each quarter. Data batches refer to data as identified in the data management plan.

<u>Cruise/Field Operation</u>	<u>Collection Dates</u>		<u>Estimated Submission Dates</u> ¹			
	<u>From</u>	<u>To</u>	<u>Batch 1</u>	<u>2</u>	<u>3</u>	<u>4</u>
Discoverer Leg II #808	6/2/75	6/19/75	*	*	None	*
Silas Bent Leg I #811	8/31/75	9/14/75	None	None	None	None
Discoverer Leg IV #812	10/8/75	10/16/75	*	*	None	*
Miller Freeman	8/16/75	10/20/75	None	None	Unknown	None
Discoverer Leg III #810	9/12/75	10/3/75	None	None	None	*
North Pacific	4/25/75	8/7/75	None	None	Unknown	None
Intertidal Biota		1975	None	None	Unknown	None
Discoverer #816	11/12/75	12/2/75	*	*	None	*
Contract 03-5-022-34	Last	Year	*	None	None	None
USCGC Glacier	-	-	Data batches as yet not determined			
Discoverer	9/10/76	9/24/76	Funding for analysis not provided.			

Note: ¹ Data Management Plan has been approved by M. Pelto, we await approval by the Contract Officer.

<u>Cruise/Field Operation</u>	<u>Collection Dates</u>		<u>Estimated Submission Dates</u> ¹			
	<u>From</u>	<u>To</u>	<u>Batch 5</u>	<u>6</u>	<u>7</u>	<u>8</u>
Discoverer Leg II 808	6/2/75	6/19/75	*	None	None	None
Silas Bent Leg I 811	8/31/75	9/14/75	None	None	None	None
Discoverer Leg IV 812	10/8/75	10/16/75	*	*	None	None
Miller Freeman	8/16/75	10/20/75	None	Lost	*	*
Discoverer Leg III 810	9/12/75	10/3/75	None	*	None	None
North Pacific	4/25/75	8/7/75	None	Lost	Lost	Lost
Intertidal Biota		1975	None	None	*	*
Discoverer 816	11/23/75	12/2/75	*	None	None	None
Contract 03-5-022-34	Last	year	*	None	*	*
Glacier	8/23	9/3/76		*		

<u>Cruise/Field Operation</u>	<u>Collection Dates</u>		<u>Estimated Submission Dates</u> ¹	
	<u>From</u>	<u>To</u>	<u>Batch 9</u>	<u>10</u>
Discoverer Leg II 808	6/2/75	6/19/75	*	*
Silas Bent Leg I 811	8/31/75	9/14/75	*	*
Discoverer Leg IV 812	10/8/75	10/16/75	9/30/76	*
Miller Freeman	8/16/75	10/20/75	none	none
Discoverer Leg III 810	9/12/75	10/3/75	none	none
North Pacific	4/25/75	8/7/75	none	none
Intertidal Biota		1975	none	none
Discoverer 816	11/23/75	12/2/75	*	*
Contract 03-5-022-34	Last	year	*	none
Moana Wave	3/76	4/15/76	*	none
Beaufort Sea Sediments			*	*

* These data have been submitted in tabular form in the Annual and Quarterly Reports for T/O 12 including the Final report of contract 03-5-022-34.

Quarterly Report

Contract #03-5-022-56
Research Unit #275/276/294
Task Order #5
Reporting Period 10/1 - 12/31/76
Number of Pages 2

HYDROCARBONS: NATURAL DISTRIBUTION AND DYNAMICS ON
THE ALASKAN CONTINENTAL SHELF

Dr. David G. Shaw
Institute of Marine Science
University of Alaska
Fairbanks, Alaska 99701

January 1, 1977

I. Task Objectives

The primary objectives of this program are to produce data on the kinds and amounts of hydrocarbons in waters, biota and sediment of Alaskan OCS areas, and to develop a quantitative understanding of factors that control these distributions.

II. Field and Laboratory Activities

A. Field

1. Surface water samples and seston were collected on a cruise of the USNOSS Discoverer in Norton Sound and the Chukchi Sea during September, 1976.
2. Surface water samples and seston were collected on a cruise of the R/V Moana Wave in the Western Gulf of Alaska and adjacent waters during October, 1976.
3. As this report is being transmitted, intertidal collections of sediment and plant materials are being made in Lower Cook Inlet.

B. Laboratory

1. Analyses of biota, water and seston are all proceeding satisfactorily.
2. Operational plans for site specific studies in Lower Cook Inlet, the Bering Sea, and the Beaufort Sea are being developed. The Lower Cook Inlet plan is sufficiently developed that one sampling is now being made (see II. A. 3 above).
3. Investigations of (1) the interaction of hydrocarbons with suspended sediments and (2) the role of zooplankton in the transfer of dispersed hydrocarbons from the pelagic to the benthic environment are continuing.

III. Results

Baseline data continues to show no major surprises. Petroleum was found in two (of 14) water samples collected in the Beaufort Sea but ship contamination is suspected. Preliminary results of our hydrocarbon sediment interaction study indicate that only a small fraction of hydrocarbons are sorbed to suspended sediments from the Gulf of Alaska under laboratory conditions.

IV. Problems Encountered

1. FY '77 funding has not been received in final form. This has stifled all but routine aspects of this work.
2. The intercalibration program is still not operating as proposed.

OCS COORDINATION OFFICE

University of Alaska

ENVIRONMENTAL DATA SUBMISSION SCHEDULE

DATE: December 31, 1976

CONTRACT NUMBER: 03-5-022-56 T/O NUMBER: 5 R.U. NUMBER: 275/276/294

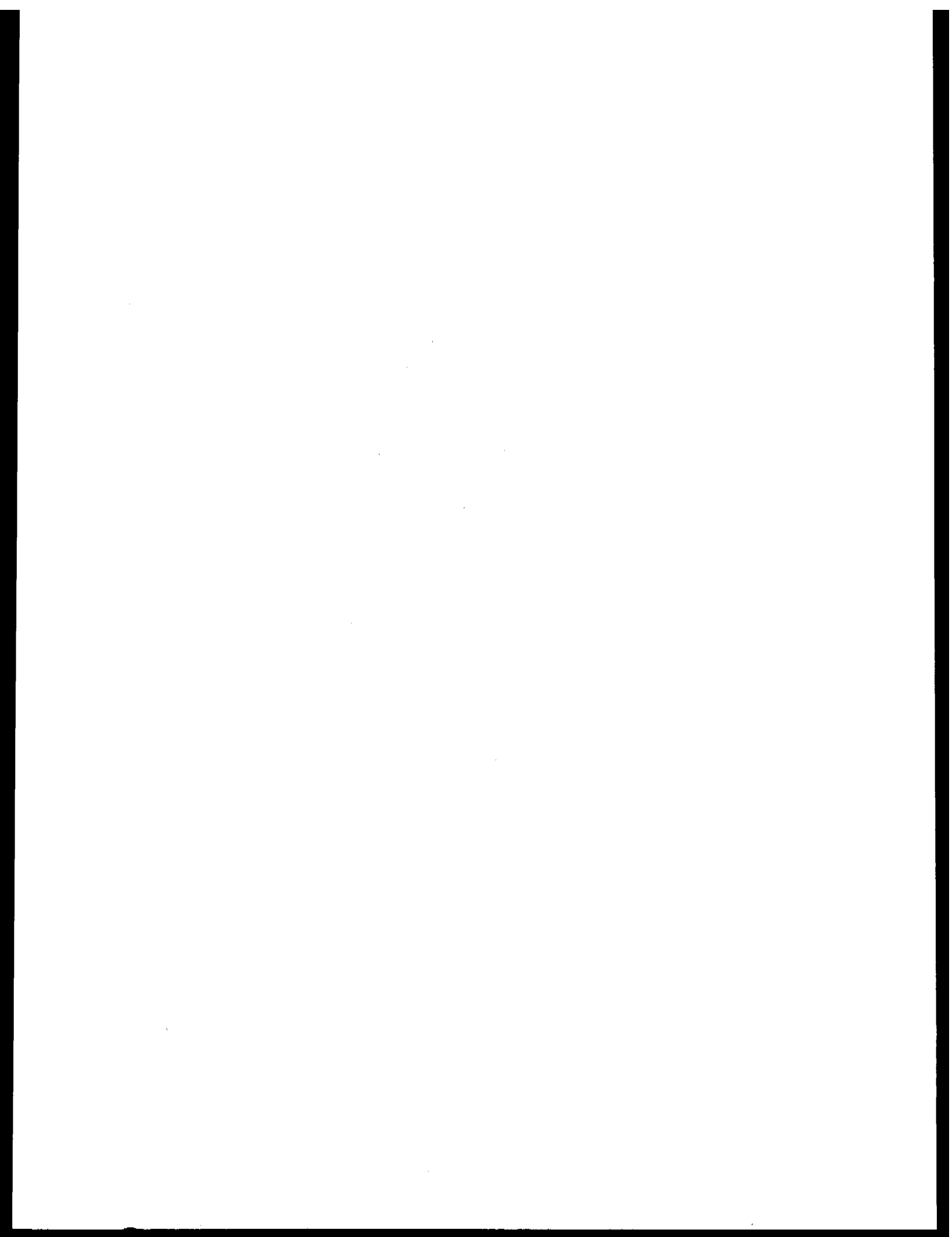
PRINCIPAL INVESTIGATOR: Dr. D. G. Shaw

Submission dates are estimated only and will be updated, if necessary, each quarter. Data batches refer to data as identified in the data management plan.

<u>Cruise/Field Operation</u>	<u>Collection Dates</u>		<u>Estimated Submission Dates</u> ¹		
	<u>From</u>	<u>To</u>	<u>Batch 1</u>	<u>2</u>	<u>3</u>
Silas Bent Leg I #811	8/31/75	9/14/75	None	submitted	submitted
Discoverer Leg III #810	9/12/75	10/3/75	None	None	submitted
Discoverer Leg IV #812	10/3/75	10/16/75	9/30/76	None	submitted
Surveyor #814	10/28/75	11/17/75	None	submitted	None
North Pacific	4/25/75	8/7/75	submitted	None	None
Contract 03-5-022-34	Last	Year	submitted	submitted	submitted
Moana Wave MW 001	2/21/76	3/5/76	None	9/30/76	9/30/76
Miller Freeman	5/17/76	6/4/76	9/30/76	None	None
Glacier	-	-	None	(a)	None
Discoverer	9/10/76	9/24/76	None	(a)	(a)
Moana Wave	10/7/76	10/16/76	None	(a)	(a)

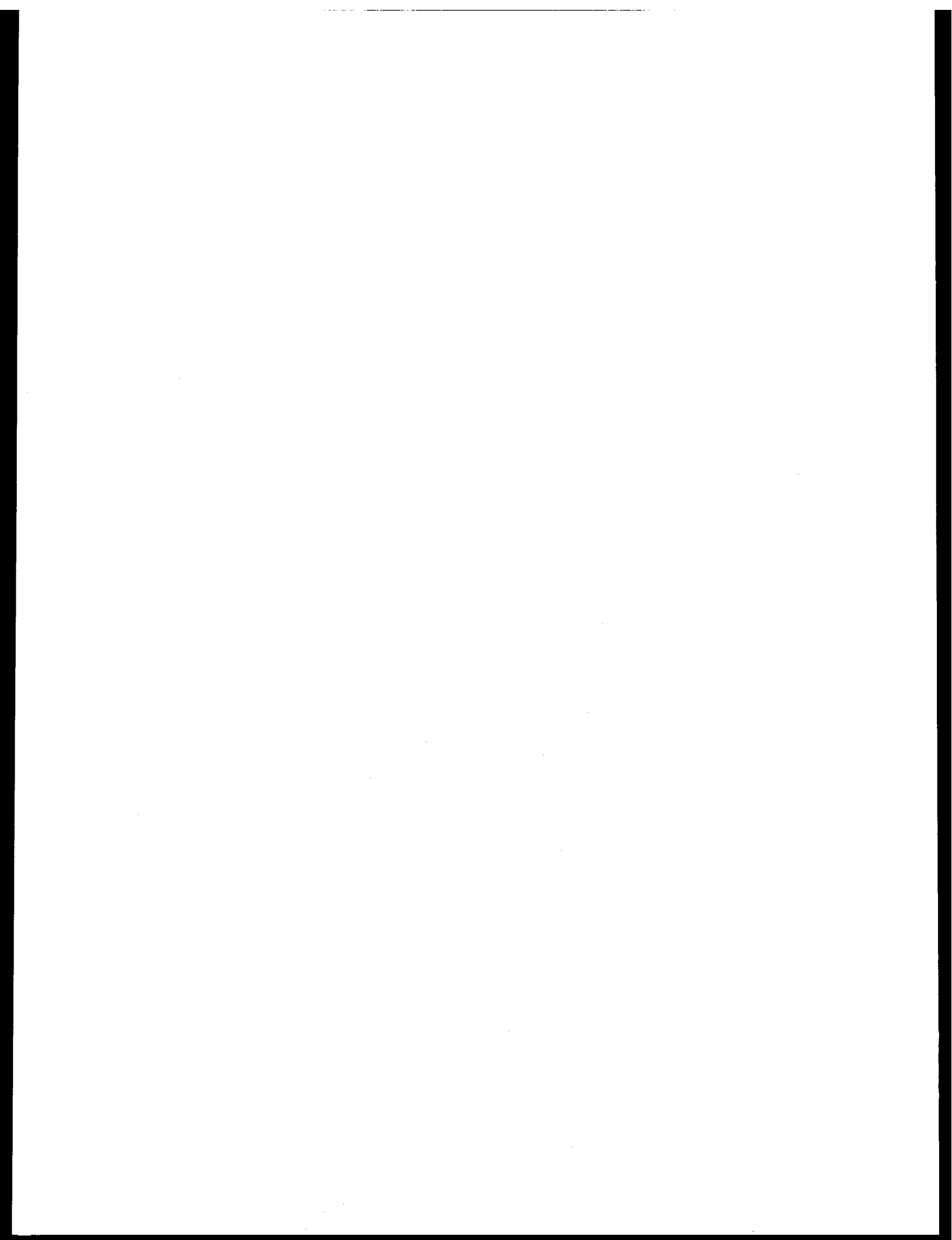
Note: ¹ Data Management plan has been approved and made contractual.

(a) Data will be processed and submitted in FY '77, contingent upon receiving funding for Fy '77.



RU# 278

NO REPORT WAS RECEIVED



QUARTERLY REPORT

Contract RK6-6074
Research Unit 413
Reporting Periods:

1 October 1976
1 January 1977

413 - Trace Metal Content of Bottom Sediment in Northern Bering Sea

Hans Nelson
Pacific-Arctic Branch of Marine Geology
345 Middlefield Road
Menlo Park, CA 94025

January, 1977

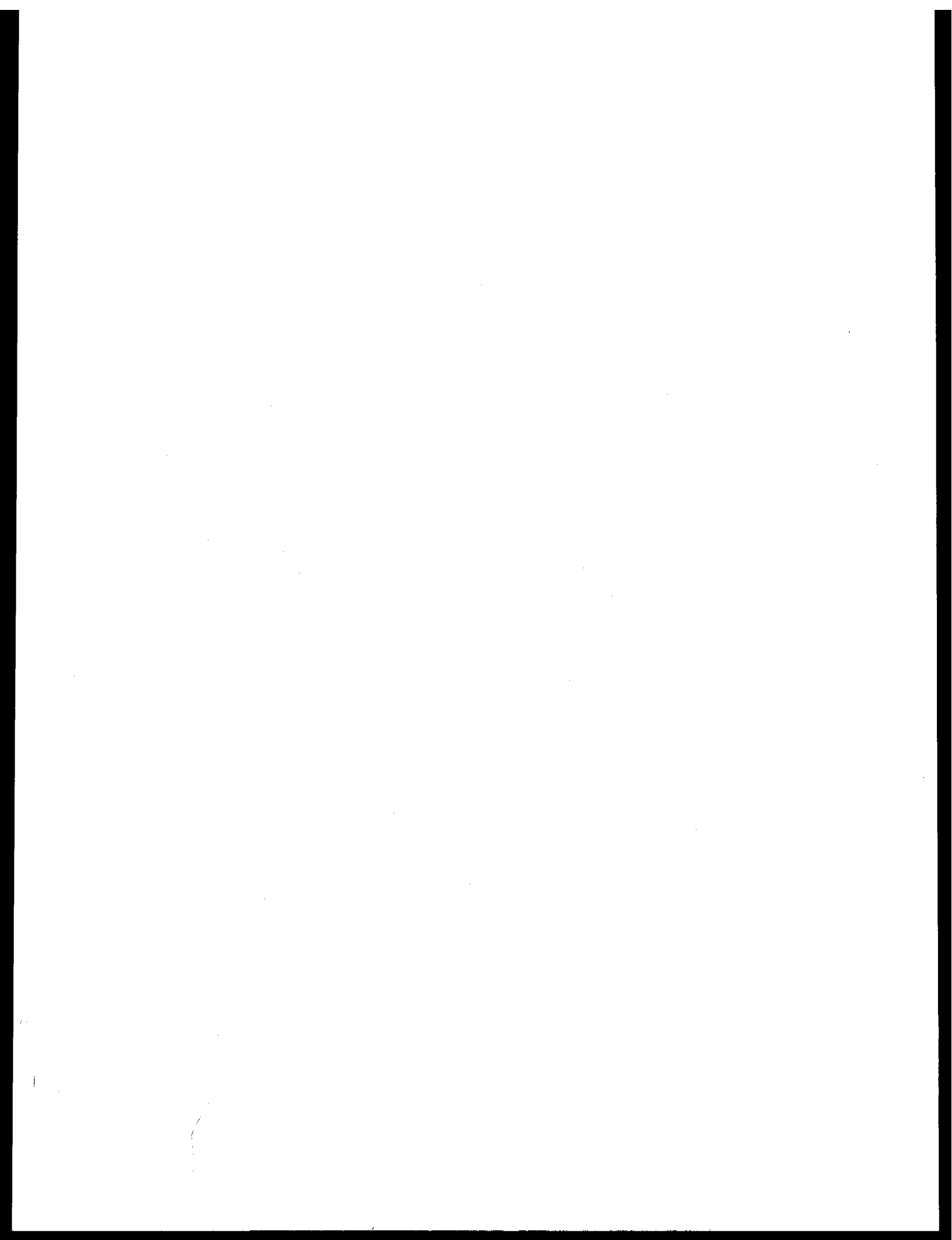
Oct. 1 - RU 413

Bulk sediments from samples collected in previous studies were submitted for semi-quantitative emission spectrographic analysis. These samples included mainly surface samples with a smaller number of subsurface box core samples. Thirty replicate analyses and five standard rock samples were also included in the total of 300 analyses. After sample preparation 30 duplicate splits were sent to Mr. David Robertson for neutron activation analysis at Batelle Northwest. An additional suite of 30 surface samples were collected by the "chemically clean" Soutar Van Veen during the October cruise and these were frozen for future trace metals analysis.

Jan. 1 - RU 413

The USGS Analytical Laboratories in Menlo Park, CA completed the emission spectrographic analyses for the 300 bulk sediment samples. Sample control at the USGS in Denver is in process of computer punching and entering data into RASS files. In Menlo Park, Brad Larsen is retrieving old data files with bulk sediment analyses and programming computer operations to form one complete bulk data set of all old and new data for northern Bering Sea. He is also performing computer operations to create one complete data set of all pan concentrate trace metal analyses. In addition, analysis of clay mineralogy has been completed for northern Bering Sea samples by Dr. James Hein and analysis of C content is underway at Menlo Park and at UCLA by Mark Sandstrom. Analysis of sediment texture for Oct. 1976 cruise samples has been nearly completed at our Menlo Park laboratories. These data will be combined with previous textural analyses completed by the University of Washington and USGS on northern Bering sea bulk sediments collected for the heavy metals program from 1967 - 1972.

TRANSPORT



TRANSPORT

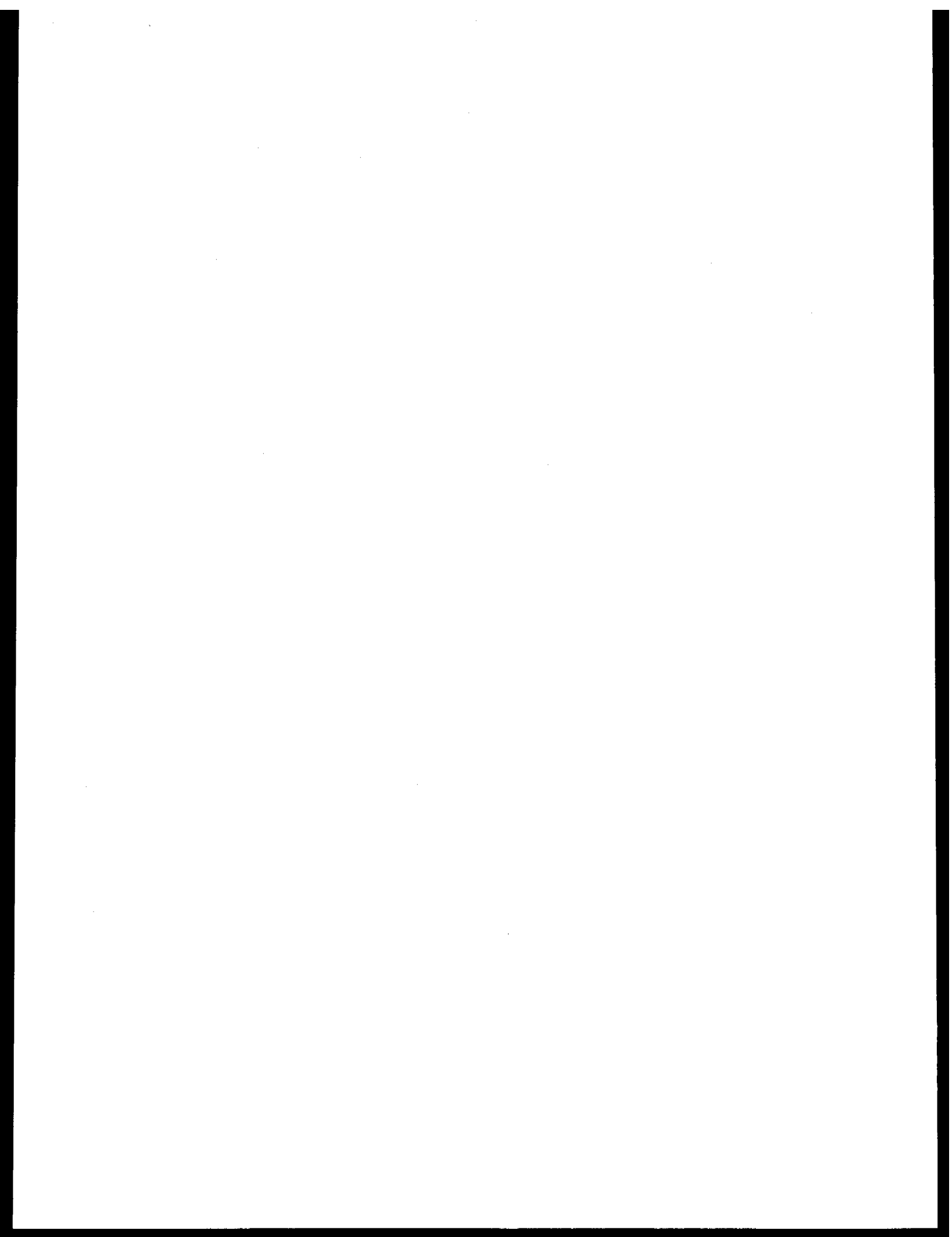
<u>Research Unit</u>	<u>Proposer</u>	<u>Title</u>	<u>Page</u>
48	Donald E. Barrick WPL/NOAA	(July-Sept. 1976 and Oct.-Dec. 1976) Development and Operation of HF Ocean Current Mapping Radar Units - Physical Oceanography	313
81	G. L. Hufford U.S. Coast Guard	Beaufort Shelf Surface Currents	327
91	K. Aagaard Dept. of Ocean. U. of Wash.	Current Measurements in Possible Dis- persal Regions of the Beaufort Sea	339
111	Robert Carlson Inst. of Water Res- sources U. of Alaska	Effects of Seasonability and Variabil- ity of Streamflow in Nearshore Coastal Areas	351
123	Ronald L. Smith IMS/U. of Alaska	Acute Toxicity - Pacific Herring Roe in the Gulf of Alaska	353
138	Stanley P. Hayes James D. Schumacher PMEL/NOAA	Gulf of Alaska Study of Mesoscale Oceanographic Processes (GAS-MOP)	357
140	Jerry Galt PMEL/NOAA	(July-Sept. 1976 and Oct.-Dec.1976) Numerical Studies of Alaskan OCS	361
141	J. D. Schumacher et al. Dept. of Ocean. U. of Wash.	Bristol Bay Oceanographic Processes (B-BOP)	375
141E	L. K. Coachman et al. Dept. of Ocean. U. of Wash.	Norton Sound/Chukchi Sea Oceanographic Processes (N-COP)	383
151	Knut Aagaard Dept. of Ocean. U. of Wash.	STD Measurements in Possible Dispersal Regions of the Beaufort Sea	394
208	William R. Dupre U. of Houston	Yukon Delta Coastal Processes Study	399
217	Donald V. Hansen AOML/NOAA	Outer Continental Shelf Energy Program	407

TRANSPORT

<u>Research Unit</u>	<u>Proposer</u>	<u>Title</u>	<u>Page</u>
244	Roger G. Barry INSTAAR	Study of Climatic Effects on Fast Ice Extent and Its Seasonal Decay Along the Beaufort and Chukchi Coasts	409
250	Lewis H. Shapiro William H. Harrison Geophys. Inst. U. of Alaska	Mechanics of Origin of Pressure Ridges, Shear Ridges and Hummock Fields in Landfast Ice	473
257/ 258	W. J. Stringer Geophys. Inst. U. of Alaska	Morphology of Beaufort, Chukchi and Bering Seas Near Shore Ice Conditions by Means of Satellite and Aerial Remote Sensing	477
259	W. M. Sackinger R. D. Nelson Geophys. Inst. U. of Alaska	Experimental Measurements of Sea Ice Failure Stresses Near Ground Structures	687
261	William R. Hunt Claus-M. Naske Geophys. Inst. U. of Alaska	Beaufort Sea, Chukchi Sea, and Bering Strait Baseline Ice Study Proposal	689
265	Lewis H. Shapiro Richard D. Nelson Geophys. Inst. U. of Alaska	Development of Hardware and Procedures for <u>in situ</u> Measurement of Creep in Sea Ice	700
267	Albert E. Belon Geophys. Inst. U. of Alaska	Operation of an Alaskan Facility for Applications of Remote-Sensing Data to OCS Studies	731
289	Thomas C. Royer IMS/U. of Alaska	Mesoscale Currents and Water Masses in the Gulf of Alaska	739
307	Robin S. Muench IMS/U. of Alaska	Historical and Statistical Oceanographic Data Analysis and Ship of Opportunity Program	745
335	R. J. Callaway Chester Koblinsky Coastal Pollution Br./EPA	Transport of Pollutants in the Vicinity of Prudhoe Bay, Alaska	749
347	James L. Wise AEIDC William A. Brower NCC	Marine Climatology of the Gulf of Alaska and the Bering and Beaufort Seas (and Climatic Atlases)	751

TRANSPORT

<u>Research Unit</u>	<u>Proposer</u>	<u>Title</u>	<u>Page</u>
367	R. Michael Reynolds Bernard Walter PMEL	Coastal Meteorology in the Gulf of Alaska	757
407	R. Lewellen Arctic Research	A Study of Beaufort Sea Coastal Erosion, Northern Alaska	759
435	Jan Leendertse Rand Corp.	Modeling of Tides and Circulations of the Bering Sea	763
436	Roger Schlueter et al. Dames and Moore	Oil Spill Trajectory Analysis - Lower Cook Inlet, Alaska	765
519	Frank Carsey U. of Wash.	Coastal Meteorology of the Alaskan Arctic Coast	829



QUARTERLY REPORT

Project No: RW0000 R7120856

Research Unit: No. 48

Reporting Period: July 1 -
September 30, 1976

Development and Operation of HF Ocean Current Mapping Radar Units

Principal Investigator: Donald E. Barrick

Submitted: February 7, 1977

CURRENT-MAPPING RADAR PROGRAM

PROGRESS REPORT

(1 September 1976)

A. Background. Eighteen months ago a team was organized within NOAA's Wave Propagation Laboratory to build, test, and operate an HF radar system for mapping near-surface ocean currents in coastal areas. Two radar units — separated by some 40 km — are required to produce a current-vector map. Each radar unit was to be self-contained, van or helicopter transportable, low-powered, and digital-controlled; the output product, namely the map of surface-current vectors, was to be available at the site within minutes after the radar measurements. Primary funding for the program came from OCSEAP (Outer Continental Shelf Environmental Assessment Program, a joint BLM/NOAA program), with smaller amounts of funding from the U.S. Coast Guard and ERDA.

The principle of operation of the system involves backscatter from moving ocean waves which in turn are being transported by an underlying current field. These motions are detected and measured as "Doppler" shifts (frequency displacements of the received echo signal from the transmitted signal). The origin of the sea echo is obtained in polar coordinates; range from the radar is related to the time delay between signal transmission and reception, whereas azimuth angle is obtained from phase differences at three simple receiving antenna elements. While the concept had been analyzed theoretically, and elements of the system had been tried experimentally over the past decade, this project was essentially unique in that the system was built from "scratch" within a very short period of time. Most projects involving the development of remote-sensing instruments evolve over many years. For example, one might start with a surplus microwave radar system, replace the receiver with a more sensitive version, add a digital signal processing capability, increase the transmitter power, add Doppler processing software, and finally, bring the entire operation of the radar system under computer control. Such an evolution of improvements might typically occur over a period of ten to fifteen years. In our case, however, we had to begin with no existing radar hardware and accomplish all of the above tasks within a period of eighteen months.

At the inception, we envisioned Phase I of our program ending with the first testing and validation of the new hardware and software in the field. Thus the "milestone" point would be obtaining experimental evidence — in map form — that such a system can indeed measure and map ocean current fields. To this end it was decided that the first field tests would be conducted looking eastward from Miami, Florida because of (i) the existence of the known current pattern of the Gulf Stream, and (ii) independent oceanographic observations for comparison, to be provided by scientists from Nova University and The University of Miami.

B. Achievement of Milestone. Design, construction, procurement, and final assembly of the components into the first radar unit pair was completed in June, 1976. Software development and testing for the field units paralleled the hardware construction. A major technical report (enclosed herein) was

prepared describing the concept, supporting analyses, hardware and software as they existed in May. Finally the gear was taken to Fort Lauderdale for the first field tests in early July. It was planned to bring both radar units into operation first at Fort Lauderdale before separating the sites in order to produce a complete current-vector map. Electronic laboratories for this hardware/software checkout were made available by Nova University.

In early August, the team began operating the radar from a van on the beach, using a portable gasoline generator for power. The first evidence that the system was working properly came in the form of sea-echo Doppler spectra from the receiver; one such spectrum is shown as Fig. 1, measured at a range of 27 km from the radar. These records exhibit the expected behavior of sea echo as shaped by the Gulf Stream current. It is with such data that the current-vector maps are constructed using mathematical algorithms.

The final proof of proper operation, however, is the production of a "current map." In order to obtain a feeling for what a "one-site" current map of the Gulf Stream should look like, data published by Dr. Walter Düing of the University of Miami were plotted on the same map grid as the output of our radar. Figure 2 illustrates this current field as it would be viewed from one site at Fort Lauderdale. What is shown is the "mean" flow, averaged over time so that short-term meanderings and eddies are removed. Since one radar site (alone) can "see" only that component of the current vector from a given ocean patch which points toward or away from the radar (the "radial" component), Düing's complete vector field was used to obtain the one-site "radial" vector map shown in Fig. 2. Thus the map shown represents a Gulf Stream flowing from South to North parallel to the shore, with zero velocity near shore but increasing to a maximum, ~ 5 knot velocity about 40 km from shore.

Data measured from the radar were then used to generate a one-site radial current map, which is shown in Fig. 3. The measurements for this map represent one 128-second run, with some smoothing done to remove noisy data points. This map was produced by the actual software to be used in the radar's field minicomputers. The agreement between expected and measured current data leaves no doubt that the radar system works and is capable of doing the job for which it was designed. The maps represent a 3 x 3 km grid scale, and the maximum range actually exceeds somewhat the predicted 70 km. When simultaneous measurements are made at the Miami radar site, total vector field maps will be plotted by the software.

C. Future Efforts. The current-mapping radar — presently being tested in Florida — is an instrument that represents a revolutionary breakthrough in oceanography. It is not, however, to the point where it can be utilized effectively by just anyone. There are at least three tasks which must be accomplished during our "Phase II" over the next several months before this transfer of technology is completed.

1. Hardware/software validation. When we look at the very first, crude current-map output of Fig. 3, several questions arise in our own minds. Are the features seen in the current map all "true," or might some be products of faulty system elements? For example, if spurious phase response were

present in the receiving antenna, the geographic locations of the currents shown could be skewed azimuthally from their actual positions. These hardware/software doubts can be conclusively answered only after several tests supported by independent current measurements. One such test will be conducted in Florida during September in conjunction with Nova University.

Other questions which must be answered by careful future testing have to do with the precision or accuracy of the current measurements. Of even more importance is the very basic question: what does the instrument actually measure and how is this related to other desired oceanographic quantities? We know already that the radar is measuring the change in phase velocity of a surface gravity wave (in this case, a 6-meter-long wave) produced by underlying currents. Such radar observations occur over space-fixed areas (typically 3 x 3 km). How these wave phase-velocity changes are related to mean surface water transport when the current varies with depth and over the observed patch area are as yet uncertain. Since the sea-echo due to the waves is a random variable, and the currents to some extent vary randomly with time, and finally because of additive atmospheric noise and undesired higher-order sea echo, the total signal is a very complex random variable. Thus, some type of data averaging is necessary, and this in turn must be interpreted in terms of the oceanographic variables being observed. Again only carefully planned field tests will provide conclusive answers to these questions.

2. Hardware/software modifications. In order to provide flexibility to handle unforeseen test situations in the field, the hardware for the first radar unit-pair was "overdesigned." Carbon copies of these units would be more expensive, larger and heavier, and more complex to operate than is necessary. For example, it is anticipated that microprocessors will replace the minicomputers in the field radars (at a reduction in size and cost, with an attendant increase in reliability), but this will be possible only after experience in the field has shown the optimal operational mode for the system. We intend to redesign many of the key hardware elements as field experience indicates more effective alternatives.

Likewise, many signal-processing software packages presently exist and are being evaluated against both simulated and real radar data. It is not yet clear which versions produce the most accurate current maps until several careful field tests have been completed. Ultimately it is desirable that a user have a single, complete tape containing all of the proven software; assembling programs in the field is next to impossible.

3. Correlative/predictive analyses. While the thought of producing current-vector maps in the field over 3000 km² areas every half hour sounds indeed impressive, such maps are not an end in themselves. Of more importance to users are the questions: (i) how are the observed current fields related to their causative driving forces such as winds, tides, earth rotation, nonlinear wave-wave interactions, storm surges, coastal and bottom topography, and (ii) how can one use such current-field outputs to predict the transport of particles (e.g., oil, heated effluent, bottom sediment, etc.) in the water?

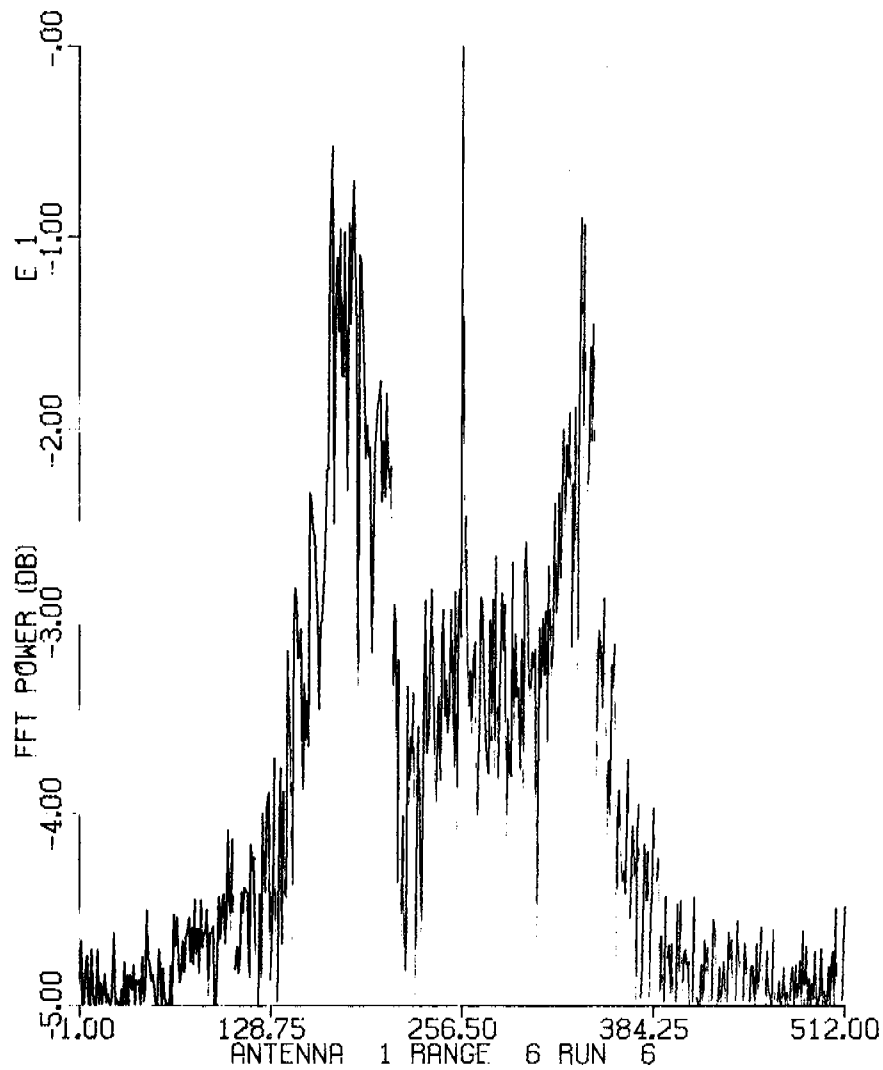
The correlation of current fields with their various driving forces must be established by detailed field experiments combined with careful data analyses. When a user is able to forecast with some degree of accuracy how a given storm, for example, will change the current patterns in a coastal region, then the value of the instrument will very definitely be established.

At present we have developed several software programs which employ the current-field maps to analyze and predict further transport. For example, we have programs which (i) calculate "upwelling" and "downwelling" from the horizontal surface divergence, and (ii) calculate trajectories vs time of floating particles, given an arbitrary starting point in the current field. These programs — and many others — must be validated against actual observations.

D. Required Funding. With the completion of Phase I, our program now branches in two directions. Because OCSEAP has provided 85% of the overall funding for Phase I, we plan to begin a separate effort for them beginning October 1. This will consist of the procurement of two additional radar unit pairs (under our supervision) and preparations to field these units in Alaska in the summer of 1977. Funding for this effort will come entirely from OCSEAP.

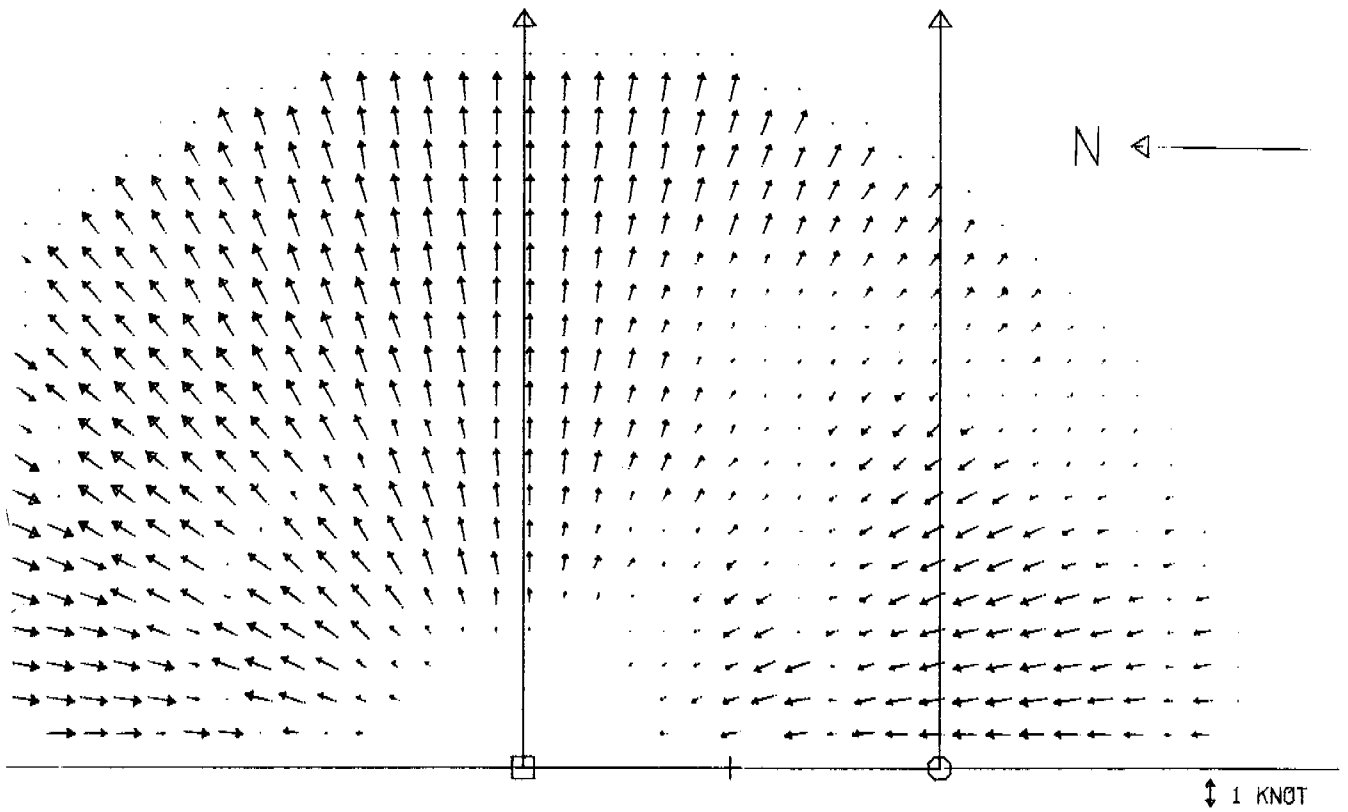
The second portion of the Phase II current-mapping radar development program involves the tasks discussed in Section C above. These include both field experimentation and further design and analysis studies in Boulder. These efforts are necessary before the technology represented by this revolutionary oceanographic instrument can be effectively utilized by others. The two radar units already in existence will be available throughout the next fiscal year for such experiments.

We require other-agency support to accomplish these Phase II efforts. Thus far, ERDA has provided total financial support of \$50,000 in Fiscal Year 1976. We are requesting \$100,000 additional funding in Fiscal Year 1977. With this support, we are planning field experiments (i) in Puget Sound in November and December, 1976; (ii) in the Gulf of Mexico (near Galveston) in January and February, 1977; and (iii) in the Lower Cook Inlet in Alaska in April and May, 1977. Independent ground-truth validation of the currents will be obtained in each case and compared with our radar data. Observations of other relevant oceanographic and meteorological variables will be made also. Each experiment is presently being planned with a different set of goals in mind. Brief reports will be issued on the comparisons and findings resulting from each experiment. We will welcome a close liaison with cognizant ERDA scientists during these experiments, soliciting their suggestions and keeping them informed of our progress and problems.



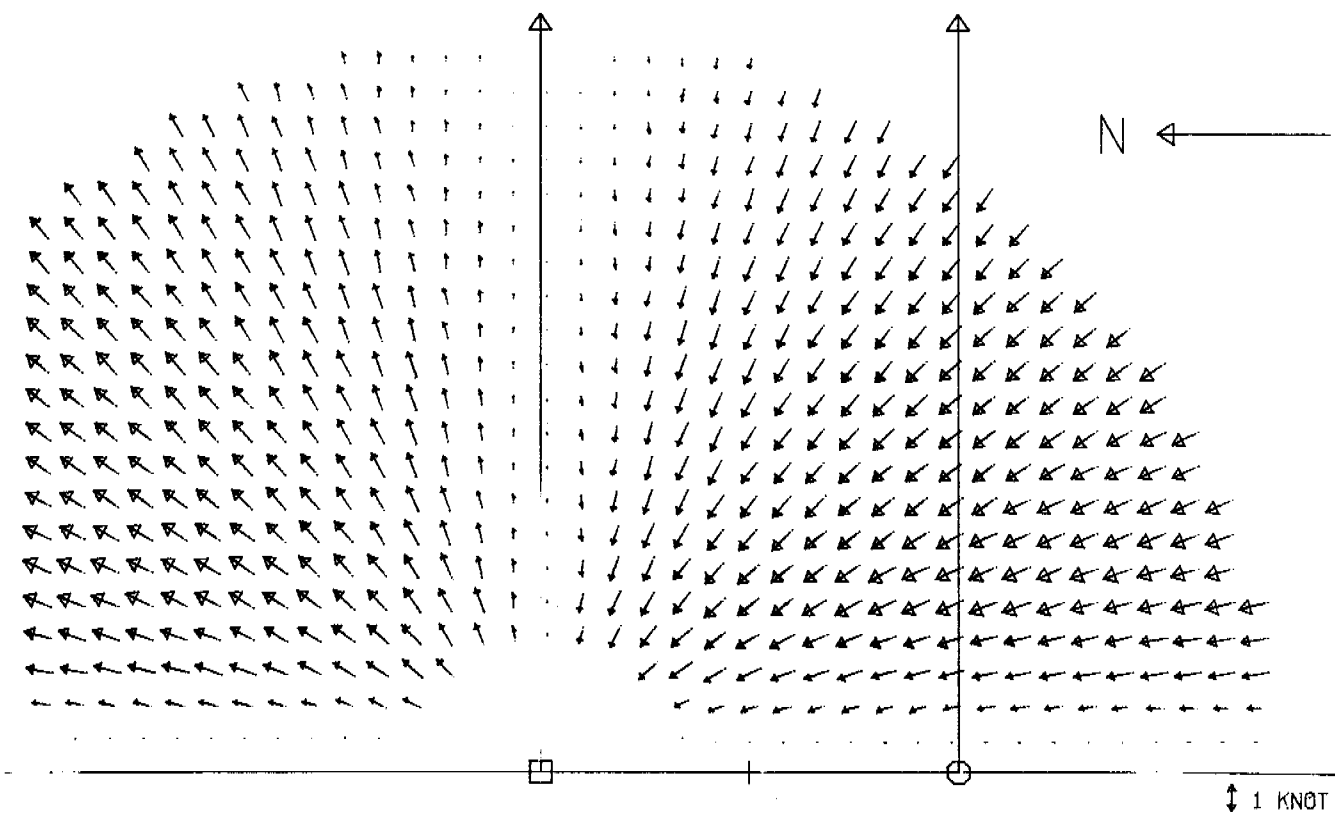
REAL PEAK	5415	REAL RMS	621.55
RMS/AVERAGE	0.00	FF	
IMAG PEAK	10905	IMAG RMS	796.89

Figure 1.
318



MIAMI BEACH AREA			
SITE#1 : FORT LAUDERDALE			
LATITUDE(D.M.S)=	26	0	0
LONGITUDE(D.M.S)=	80	8	46
ALFA(DEG)=	90.0	XSITE(KM)=	-18.5296
SITE#2 : MIAMI BEACH			
LATITUDE(D.M.S)=	25	40	0
LONGITUDE(D.M.S)=	80	8	46
ALFA(DEG)=	-90.0	XSITE(KM)=	18.5296
MAXIMUM RANGE=	66.0	NUMBER CELLS=	18
TRUE NORTH(DEG)=	90.0000		

Figure 3.



MIAMI BEACH AREA			
SITE#1 : FORT LAUDERDALE			
LATITUDE(D,M,S)=	26	0	0
LONGITUDE(D,M,S)=	80	8	46
ALFA(DEG)=	90.0	XSITE(KM)=	-18.5296
SITE#2 : MIAMI BEACH			
LATITUDE(D,M,S)=	25	40	0
LONGITUDE(D,M,S)=	80	8	46
ALFA(DEG)=	-90.0	XSITE(KM)=	18.5296
MAXIMUM RANGE= 66.0 NUMBER CELLS= 18			
TRUE NORTH(DEG)= 90.0000			

Figure 2.

QUARTERLY REPORT

Project No: RW0000 R7120856

Research Unit: No. 48

Reporting Period: October 1 -
December 31, 1976

No. of Pages: 5

Development and Operation of HF Ocean Current Mapping Radar Units

Principal Investigator: Donald E. Barrick

Submitted: February 4, 1977

CURRENT-MAPPING RADAR PROGRAM

Progress Report 1 January 1977

I. Abstract

The first simultaneous two-site data were obtained in mid-October of 1976. Surface current maps were generated by combining the data from the two sites, one at Fort Lauderdale and one at South Mission Beach. This map shows surface currents consistent with previously measured Gulf-Stream flows in the area off the southern coast of Florida. To this date, two-site data have been taken on October 19, 20, 26, 27, 28, 29, 30 and December 14. An example of the map is shown at the back of the report.

At this time, there is no direct supporting surface current measurements made during our radar operations. However, the results are consistent with the general magnitudes, directions, and shear of the Gulf Stream in that area, giving confidence that the radar system and data processing techniques are working properly.

II. Objectives

The objectives of the current mapping radar program for the next calendar year are to: 1) Improve the reliability of existing hardware, 2) Optimize the field software through ground truth testing, 3) Determine the accuracy of the maps via ground truth testing, 4) Obtain and interpret current data from Alaska.

To accomplish the first objective, repairs were made to some of the components corroded by the humid salt air of Florida. Steps are being taken to improve the reliability in the field, and modifications are being made to bring the nearest range gate closer than 12 to 15 km from shore. The receiver was modified in order to obtain better signal-to-noise ratios at the near ranges, and this will possibly improve this ratio at the more distant ranges.

Because of problems with antenna cables, work is being done with the antenna switches to eliminate two of the three receiver antenna cables. Presently they must all be within 1/4 inch in length relative to each other, a difficult task when each cable is 1500 feet long. Special care must be taken not to stretch them when moving them. These switches will now be located at the antennas, and thus the extra two cables can be eliminated; mismatched cable lengths will therefore no longer be a problem.

Additional work being done on the system since returning from Florida includes a new calibration circuit to check-out the entire data flow loop, a new lighter power supply, a modification of the solid state buffer to reduce parity errors, and a new video display that can plot the time series data and FFT in real time. The latter will be useful for ascertaining that the data is good.

Since the October tests much effort has been devoted to Item 2, namely software development for the field system. This involves various kinds of signal processing techniques of the two-site data to remove some of the random-like fluctuations from the derived currents. These techniques include the averaging of several two-minute runs together, statistical thresholding tests, and filtering techniques. New data from other locations are now needed to verify how these techniques work where the flow is not as uniform as the Gulf Stream. Another concept is being tried to increase the area covered by the two radars. The software for these techniques should be completed over the next few months, and some of the experiments in Puget Sound will be devoted to the verification of these techniques.

Plans for accomplishing Item 3, namely establishing the current-map accuracy, involve returning to Florida within a few weeks, and to then take the system to Puget Sound for further comparisons. The present plan is to return to the Fort Lauderdale-Miami area and take surface current observations with the dual-site radar simultaneous with a surface drifter observations. The drifters would be put into the water at various distances from shore and tracked with a ship for about 15 minutes to determine the surface velocity. This would be done on a line halfway between the two radars from 10 km at the nearest point from shore to a maximum of 60 km.

The next set of observations will be in Puget Sound sometime in April or May. In this area, the currents are more complicated and will vary in magnitude from 0 to 2 M/s depending on the location within the Sound and the tidal phase. These tests will give us a chance to check out the current mapping techniques with more complex current patterns. For comparison, we will have assistance from PMEL, who will track several drifters in various range cells with a small boat containing a mini-ranger. These observations will be made over several days. We feel that these observations in a more complicated environment are essential for checking out the radar theory, hardware, and software before proceeding to Alaska where ground truth will be more difficult to obtain. Upon accomplishing Item 1 through 3, we feel we will be able to go to an area in Alaska and obtain interpretable current data. Two potential locations are either Cook Inlet or Kodiak Island. The scheduled operations in Alaska will be sometime this summer.

III. Field Activities

The current-mapping radar program has gone to the Miami-Ft. Lauderdale area in October and December and has resulted in two-site surface-current maps. Direct comparisons of drifter measured surface currents were not possible either because of weather or because the ship was unavailable. However, the results are consistent with the known Gulf-Stream patterns; the fact that the system produced these results in an indication that the agreement between the radar output and other surface current observations in the upper 50 cm of the ocean will be close. To this date, two site data have been collected on October 19, 20, 26, 27, 28, 29, 30 and December 14.

IV. Results

Appended to this report is a surface current map, perhaps the most concise form of our results so far. This shows part of the Gulf Stream between the Miami-Ft. Lauderdale area from about 12 km to 60 km from shore.

V. Preliminary Interpretations of Results

In the map, one can see a definite increase in the current magnitude as a function of the distance from the shore. The maximum current is about 3 m/s. Publications by Duing and others show that these values are reasonable, but are subject to some temporal variations. We did observe a variation of as much as 50% in the current values during the times of our observations.

VI. Problems Encountered/Recommended Changes

Most of the problems we have encountered thus far have been hardware related. Since returning with the radars to Boulder, effort has been made to eliminate these problems in the field. We found the very moist salt air to be the most damaging to the hardware.

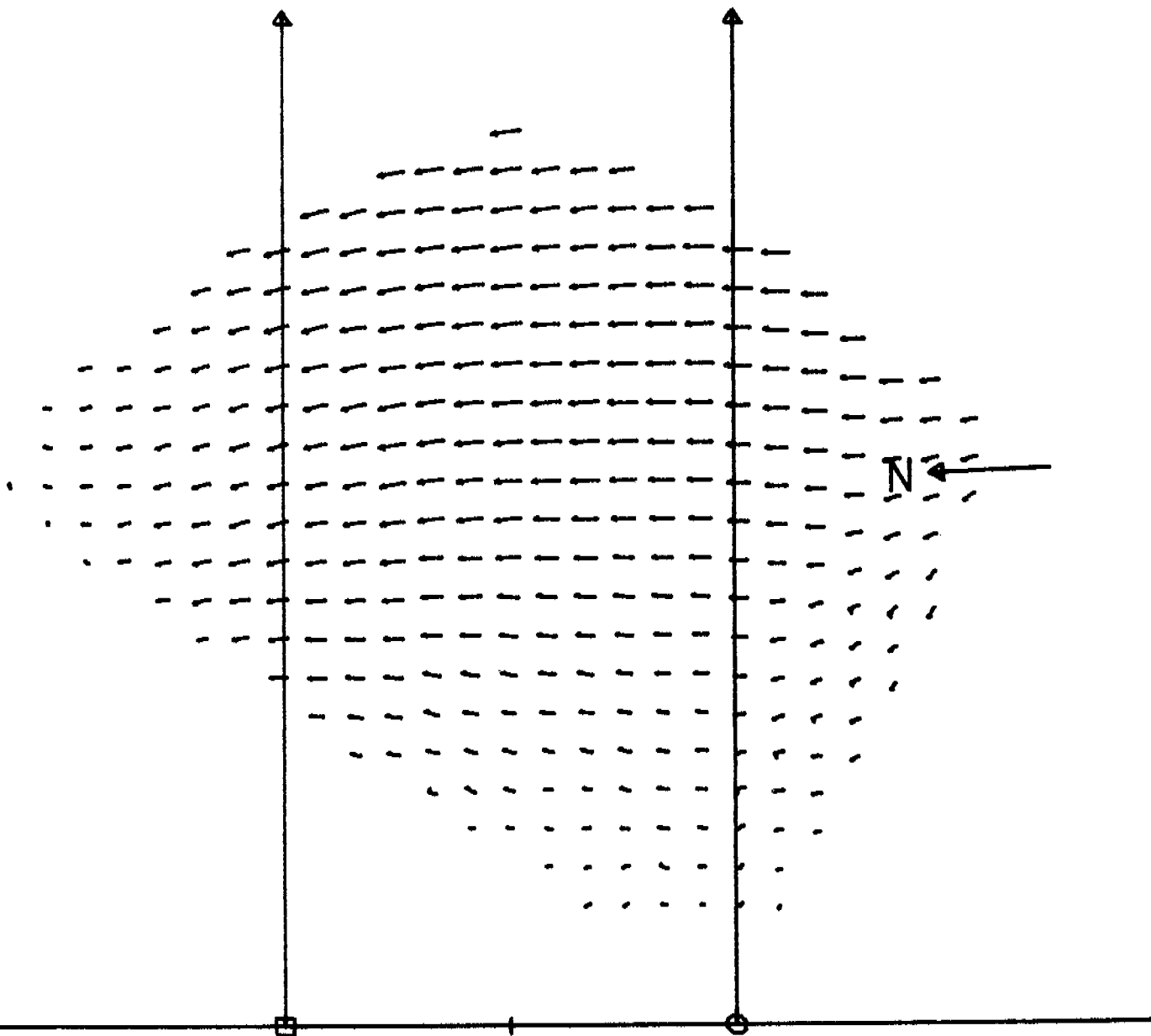
VII. Estimate of Funds Expended

(From July 1975 through September 30, 1976)

Fiscal Year 1975 - - - - -	\$240K
Fiscal Year 1976 and 1976T - -	<u>\$365K</u>
Total	\$605K

VIII. Bibliography

D. E. Barrick and M. Evans, "Implementation of Coastal Current Mapping HF Radar System", Progress Report No. 1, July 1976, NOAA Tech. Report, ERL 373 - WPL 47.



KNBT 1

October 20, 1976

MIAMI BEACH AREA			
SITE#1 = POINT LAUDONDALE			
LATITUDE(D.L.S.°)	28	9	1
LONGITUDE(D.L.S.°)	-80	0	28
ALPITUDE=0.0	XSITE000=		-17.0000
SITE#2 = MIAMI BEACH			
LATITUDE(D.L.S.°)	25	48	0
LONGITUDE(D.L.S.°)	-80	7	28
ALPITUDE=0.0	XSITE000=		17.0000
MAXIMUM RANGE= 75.0 NUMBER CELLS= 25			
TRUE NORTH DEG= 102.715			

USCOMM - S&L

QUARTERLY REPORT

RU 81 - Beaufort Shelf Surface Currents

I. TASK OBJECTIVES

The primary objectives of the proposed program are twofold:
(1) to determine surface current patterns under different wind regimes; and (2) to develop a model capable of predicting wind driven surface water motions. The original area of interest was the Beaufort Sea shelf between Point Barrow and Demarcation Point. However, ice conditions in the Beaufort Sea were severe. The alternate study area, the northeast Chukchi Sea, was chosen to work in.

II. FIELD/LABORATORY ACTIVITIES

- A. Cruises - completed
- B. Station Locations - See Attached Chart
- C. Data Collected

All the data (187 stations) have been processed and put on IBM data cards. A table with current speed and direction is attached.

D. Milestone Chart and Data Submission Schedule

The data is being sent the first week in January 1977. The final report will be completed by 1 April 1977.

III. RESULTS - See Attached Data Table

IV. PROBLEMS ENCOUNTERED - None

V. ESTIMATE OF FUNDS EXPENDED

This quarter only \$800 has been expended on computer and quality control time.

Position

Sta. ID.	Latitude	Longitude	Date	Time	Speed (cm/sec)	Heading (°T)
5A	70°47.7'	159°43.1'	8 Aug	1545	13.0	267°
5B	70°49.7'	159°49.4'	8 Aug	1547	9.3	017°
5C	70°51.1'	159°54.1'	8 Aug		11.8	008°
5D	70°54.2'	160°5.1'	8 Aug		5.8	111°
5E	70°55.2'	160°8.1'	8 Aug			
6B	70°53.2'	160°9.0'	8 Aug	1417	14.6	079°
6A	70°48.4'	159°52.4'	8 Aug		3.8	178°
7A	70°46.1'	159°58.3'	8 Aug		5.6	231°
8A	70°40.3'	160°17.8'	9 Aug	0956	35.7	306°
8C	70°43.7'	160°27.9'	9 Aug	1024		
8E	70°50.4'	160°52.8'	9 Aug	1040	18.0	115°
8F	70°51.6'	160°55.5'	9 Aug	1048	8.3	020°
8G	70°53.7'	161°2.4'	9 Aug	1054		
8H	70°54.9'	161°6.6°	9 Aug	1101		
9B	70°39.4'	160°27.5'	9 Aug	1337	32.6	350°
9D	70°45.4'	160°48.7'	9 Aug	1410	30.3	066°
9G	70°57.2'	161°28.1'	9 Aug	1457	12.6	032°
9H	70°59.6'	161°36.9'	9 Aug	1503	9.5	048°
10A	70°34.6'	160°15.7'	9 Aug	1648	9.0	190°
10B	70°35.7'	160°19.8'	9 Aug	1655	15.6	196°
10C	70°39.0'	160°31.1'	9 Aug	1658	13.3	110°
10F	70°43.5'	160°47.6'	9 Aug	1718	21.1	089°
10G	70°48.6'	161°5.3'	9 Aug	1635	12.8	194°
10J	70°54.7'	161°25.3'	9 Aug	1758	31.3	228°
10K	70°56.8'	161°32.9'	9 Aug	1807	33.9	071°
9K	71°1.1'	161°42.0'	9 Aug	1820	29.6	102°

Position

Sto. ID.	Latitude	Longitude	Date	Time	Speed (cm/sec)	Heading (°T)
11K	70°54.3'	161°42.5'	9 Aug	1830	30.7	111°
11J	70°48.4'	161°34.6'	9 Aug	1838	33.1	060°
11B	70°33.6'	160°45.2'	10 Aug	1928	11.9	122°
11C	70°38.3'	161°0.6'	10 Aug	1945	23.6	064°
19A	70°23.2'	161°49.4'	11 Aug	0925	6.61	259°
19B	70°25.5'	161°49.4'	11 Aug	0935	7.82	253°
19D	70°34.3'	161°49.4'	11 Aug	0956	9.81	103°
19E	70°37.8'	161°49.4'	11 Aug	1017	25.0	099°
19F	70°38.8'	161°49.4'	11 Aug	1025	24.6	016°
19G	70°43.6'	161°49.4'	11 Aug	1030	22.1	143°
19H	70°44.4'	161°49.4'	11 Aug	1040	26.7	128°
18B	70°16.4'	161°26.1'	11 Aug	1403	23.3	228°
18C	70°24.0'	161°26.1'	11 Aug	1408	52.9	238°
18D	70°21.6'	161°26.1'	11 Aug	1416	39.4	233°
18E	70°25.6'	161°26.1'	11 Aug	1422	40.0	245°
18F	70°26.8'	161°26.1'	11 Aug	1427	53.3	248°
18G	70°32.7'	161°26.1'	11 Aug	1443	14.4	217°
18H	70°36.9'	161°26.1'	11 Aug	1448	12.0	213°
18J	70°41.7'	161°26.1'	11 Aug	1458	11.1	210°
18K	70°44.3'	161°26.1'	11 Aug	1505	17.4	150°
15A	70°22.3'	160°50.2'	11 Aug	1645	53.0	217°
15B	70°27.4'	161°6.7'	11 Aug	1655	46.6	243°
15C	70°29.7'	161°14.6'	11 Aug	1706	35.5	238°
15D	70°31.5'	161°20.7'	11 Aug	1718	24.2	243°
15E	70°32.8'	161°25.5'	11 Aug	1731	31.9	251°
15F	70°36.5'	161°37.2'	11 Aug	1742	13.0	217°

Position

<u>Eq</u>	<u>Latitude</u>	<u>Longitude</u>	<u>Date</u>	<u>Time</u>	<u>Speed (cm/sec)</u>	<u>Heading (°T)</u>	
20D	71°9.3'	159°8.0'	14 Aug	1642	19.2	214°	
20C	71°7.3'	159°5.8'	14 Aug	1658			
20B	71°4.7'	159°3.1'	14 Aug	1704	64.7	056°	
20A	70°57.0'	158°54.9'	14 Aug	1711	27.0	082°	
21A	70°55.0'	158°43.1'	14 Aug	1726	7.4	267°	
21A	70°55.0'	158°43.1'	14 Aug	1730	5.0	267°	
21C	71°2.9'	158°49.2'	14 Aug	1743	58.8	061°	
21C	71°2.9'	158°49.2'	14 Aug	1745	60.0	058°	
21D	71°5.7'	158°50.9'	14 Aug	1750			Failure
21E	71°7.6'	158°52.3'	14 Aug	1804	55.9	056°	
21F			14 Aug				
21G	71°13.6'	158°56.9'	14 Aug	1820	14.5	242°	
22G	71°16.2'	158°46.4'	14 Aug	2050	44.5	236°	
22E	71°10.8'	158°42.0'	14 Aug	2108			
22D	71°1.4'	158°35.1'	14 Aug	2120	23.7	204°	
22C	70°53.0'	158°28.2'	14 Aug	2131	17.5	262°	
23G	71°16.6'	158°25.1'	14 Aug		20.0	249°	
23A	70°50.6'	158°5.1'	14 Aug	2201	5.4	242°	
23B	71°2.3'	158°13.7'	15 Aug	1040	24.9	052°	
23C	71°4.1'	158°15.1'		1046	28.1	050°	
23D	71°5.5'	158°16.3'		1056	18.7	081°	
23E	71°11.6'	158°21.1'		1145	48.1	044°	
23F	71°13.7'	158°23.9'		1200	14.0	036°	
23H	71°17.7'	158°26.0'		1206	3.9	284°	
23J	71°21.2'	158°28.9'		1223	36.6	232°	
23K	71°24.6'	158°31.4'	15 Aug	1233	70.4	266°	

Position

Sta. ID.	Latitude	Longitude	Date	Time	Speed (cm/sec)	Heading (°T)
25K	71°26.9'	158°27.4'	15 Aug	1239	60.7	254°
24K	71°29.6'	158°27.1'		1242	28.0	267°
24/25J	71°21.8'	158°21.4'		1301	32.4	264°
24/25H	71°21.1'	158°20.3'		1309	11.2	226°
24G	71°16.3'	158°17.3'		1325	14.1	036°
24F	71°14.5'	158°15.7'		1528	26.1	068°
24E	71°12.8'	158°14.4'		1535	44.4	081°
24D	71°10.1'	158°12.6'		1541	25.1	066°
24C	71°7.7'	158°10.8'		1550	20.5	085°
24B	71°4.8'	158°8.3'		1558	10.6	079°
24A	70°55.3'	158°1.8'		1606	8.2	197°
25A	71°1.4'	157°54.9'		1629	7.1	332°
25B	71°2.3'	157°56.0'		1631	10.1	052°
25C	71°4.2'	157°58.1'		1634	21.8	048°
25D	71°8.3'	158°3.5'		1644	21.4	084°
25F	71°12.9'	158°9.1'			40.7	065°
26A	71°1.6'	157°39.1'			4.8	200°
26B	71°3.7'	157°41.7'			6.3	002°
26C	71°4.8'	157°43.0'			29.9	034°
26D	71°8.2'	157°47.2'			23.0	064°
26E	71°12.8'	157°52.8'			20.8	090°
26F	71°15.3'	157°55.9'			26.2	093°
26G	71°16.2'	157°57.7'			27.4	090°
26H	71°18.9'	158°1.6'			11.8	189°
26J	71°29.3'	158°8.1'				
26K	71°30.7'	158°17.1'	15 Aug			

Position

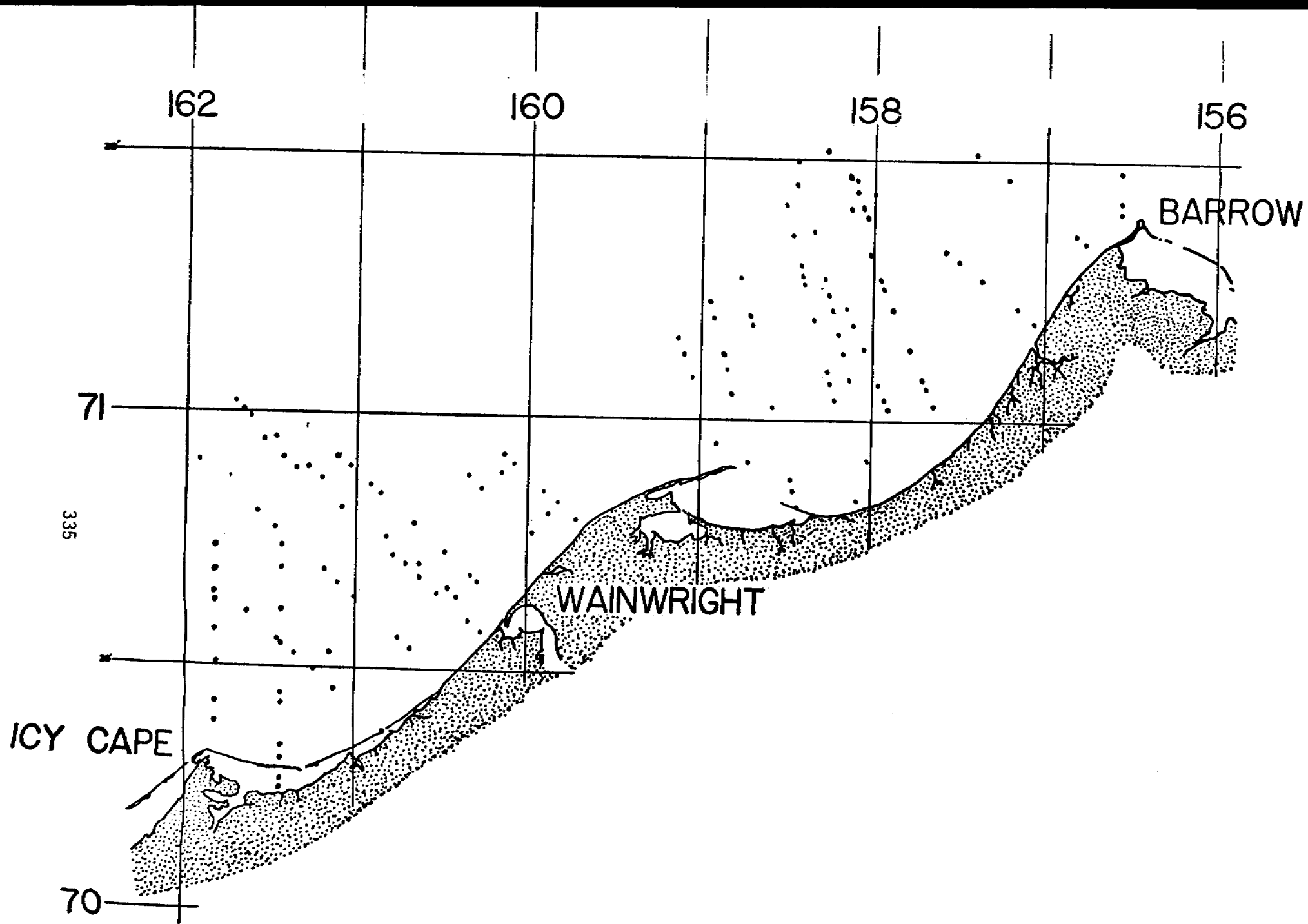
Sto. ID.	Latitude	Longitude	Date	Time	Speed (cm/sec)	Heading (°T)
27K	71°33.5'	158°15.4'	15 Aug			
27H	71°26.3'	158°6.4'	15 Aug		108.1	250°
27G	71°24.4'	158°4.0'	15 Aug		51.9	251°
27F	71°23.4'	158°2.9'	15 Aug		23.8	234°
29A	71°11.5'	157°3.7'	16 Aug	1650	34.2	041°
29B	71°13.1'	157°9.9'		1704	11.7	036°
29C	71°16.3'	157°22.0'		1710	60.4	059°
29D	71°18.4'	157°29.8'		1720	56.1	078°
29E	71°19.5'	157°34.5'		1734	74.5	061°
29F	71°25.9'	158°0.0'		1744	29.1	295°
29G	71°27.5'	158°5.6'		1752	15.8	294°
30D	71°30.5'	157°24.1'		1814	5.8	189°
30D	71°30.5'	157°24.1'		1815	5.5	185°
30C	71°27.8'	157°13.0'		1820	9.8	084°
30B	71°21.6'	156°49.5'		1855	87.0	054°
30A	71°20.8'	156°46.8'		1907	75.6	052°
1B	71°25.1'	156°34.2'		1943	156.7	045°
1C	71°28.1'	156°34.2'		2006	84.1	041°
1D	71°29.1'	156°34.2'		2017	17.3	045°
1E	71°32.1'	156°34.2'	16 Aug	2024	46.7	070°
2A	71°15.7'	156°6.6'	17 Aug	1620	22.7	151°
2B	71°23.7'	156°6.6'	17 Aug	1635	12.2	040°
2C	71°24.7'	156°6.6'	17 Aug	1642	25.3	055°
2D	71°26.7'	156°6.6'	17 Aug	1649	113.8	079°
2E	71°31.7'	156°6.6'	17 Aug	1838	48.2	087°
2F	71°33.7'	165°6.6'	17 Aug	1846	36.3	093°

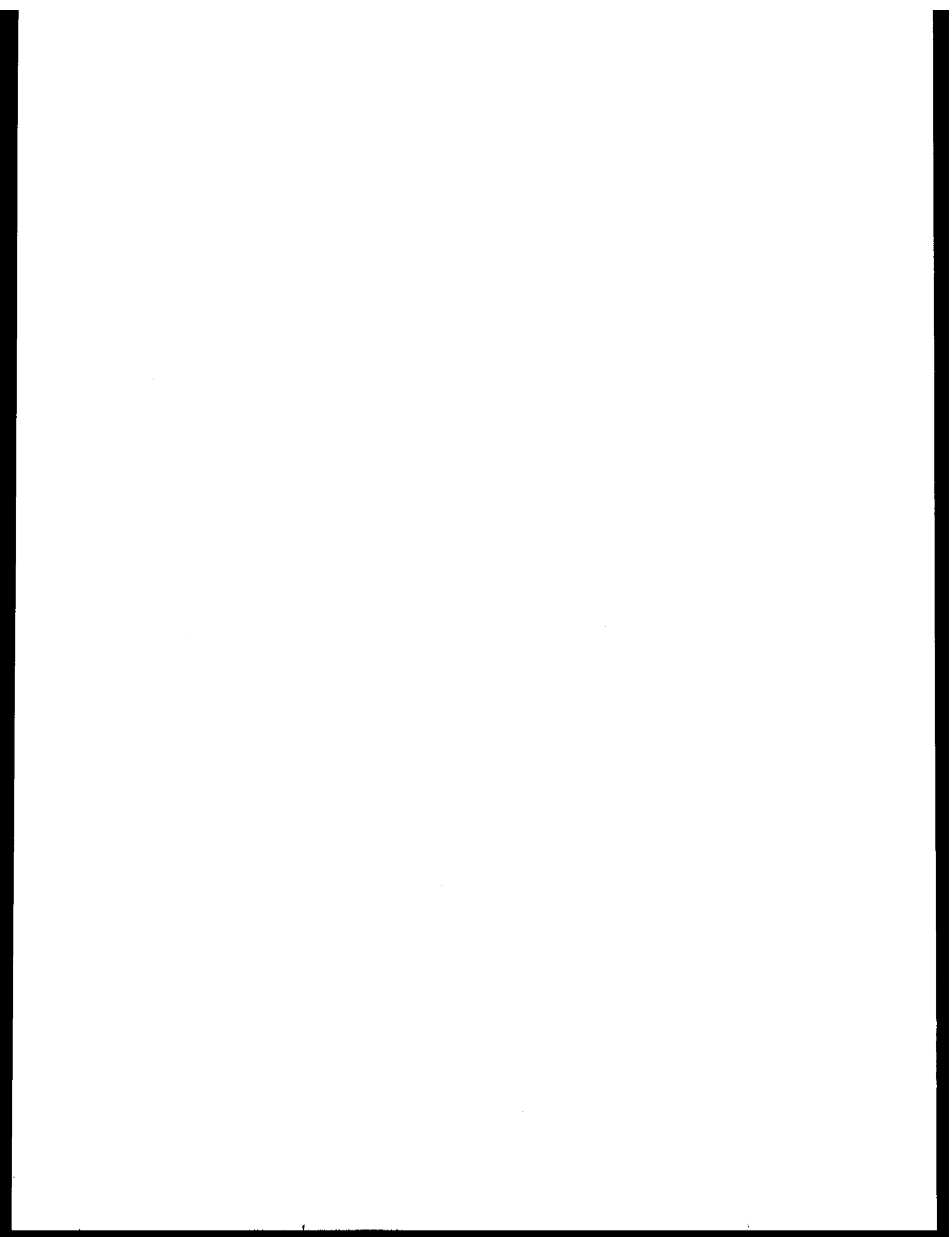
Position

Stn ID	Latitude	Longitude	Date	Time	Speed (cm/sec)	Heading (°T)
2G	71°39.7'	156°6.6'	17Aug	1900	49.7	228°
3H	71°41.7'	155°54.6'		1911	21.9	204°
3G	71°35.7'	155°54.6'		1921	66.9	059°
3F	71°32.7'	155°54.6'		1930	122.8	051°
3E	71°27.7'	155°54.6'		1940	23.7	313°
3D	71°24.7'	155°54.6'		1945	20.9	329°
3C	71°22.7'	155°54.6'		1953	34.7	309°
3B	71°17.7'	155°54.6'		1958	9.8	238°
3A	71°13.7'	155°54.6'	17 Aug	2014	22.1	207°
4G	71°28.0'	155°42.6'	19 Aug	1758	81.7	086°
4F	71°23.0'	155°42.6'		1806	9.3	354°
4E	71°17.0'	155°42.6'		1821	14.7	279°
4D	71°16.0'	155°42.6'		1828	13.7	274°
4D	71°16.0'	155°42.6'		1834	11.8	274°
4C	71°15.0'	155°42.6'		1845	29.1	230°
4B	71°13.0'	155°42.6'	19 Aug	1855	20.4	273°
4A	71°12.0'	155°42.6'	19 Aug	1900	20.5	295°
8E	71°5.0'	152°35.4'	20 Aug	1145	12.1	037°
8D	71°4.0'	152°35.4'		1153	9.5	018°
8C	70°59.0'	152°35.4'		1201	17.5	016°
8B	70°57.0'	152°47.4'		1208	11.7	358°
8A	70°54.0'	152°35.4'		1217	26.9	359°
9A	70°39.4'	152°6.6'		1242	12.6	041°
9B	70°50.4'	152°6.6'		1301	9.2	329°
9C	70°54.4'	152°6.6'		1312	6.0	050°
9D	70°55.4'	152°6.6'	20Aug	1317	14.5	036°

Position

Sta. ID.	Latitude	Longitude	Date	Time	Speed (cm/sec)	Heading ($^{\circ}$ T)
9E	70°59.4'	152°6.6'	20 Aug	1326	6.3	050°
9H	71°0.4'	152°6.6'		1335	13.4	052°
11K	71°6.3'	151°8.4'		1539	16.1	115°
11J	71°5.3'	151°8.4'		1545	8.5	182°
11H	71°4.3'	151°8.4'		1555	7.0	158°
11G	71°0.3'	151°8.4'		1607	2.7	341°
11G	71°0.3'	151°8.4'		1609	4.0	330°
11F	70°53.3'	151°8.4'		1625	14.4	313°
11E	70°51.3'	151°8.4'		1637	4.7	340°
11D	70°47.3'	151°8.4'		1646	9.1	303°
11D	70°47.3'	151°8.4'		1646	9.1	303°
11C	70°41.3'	151°8.4'	20 Aug	1655	14.4	237°



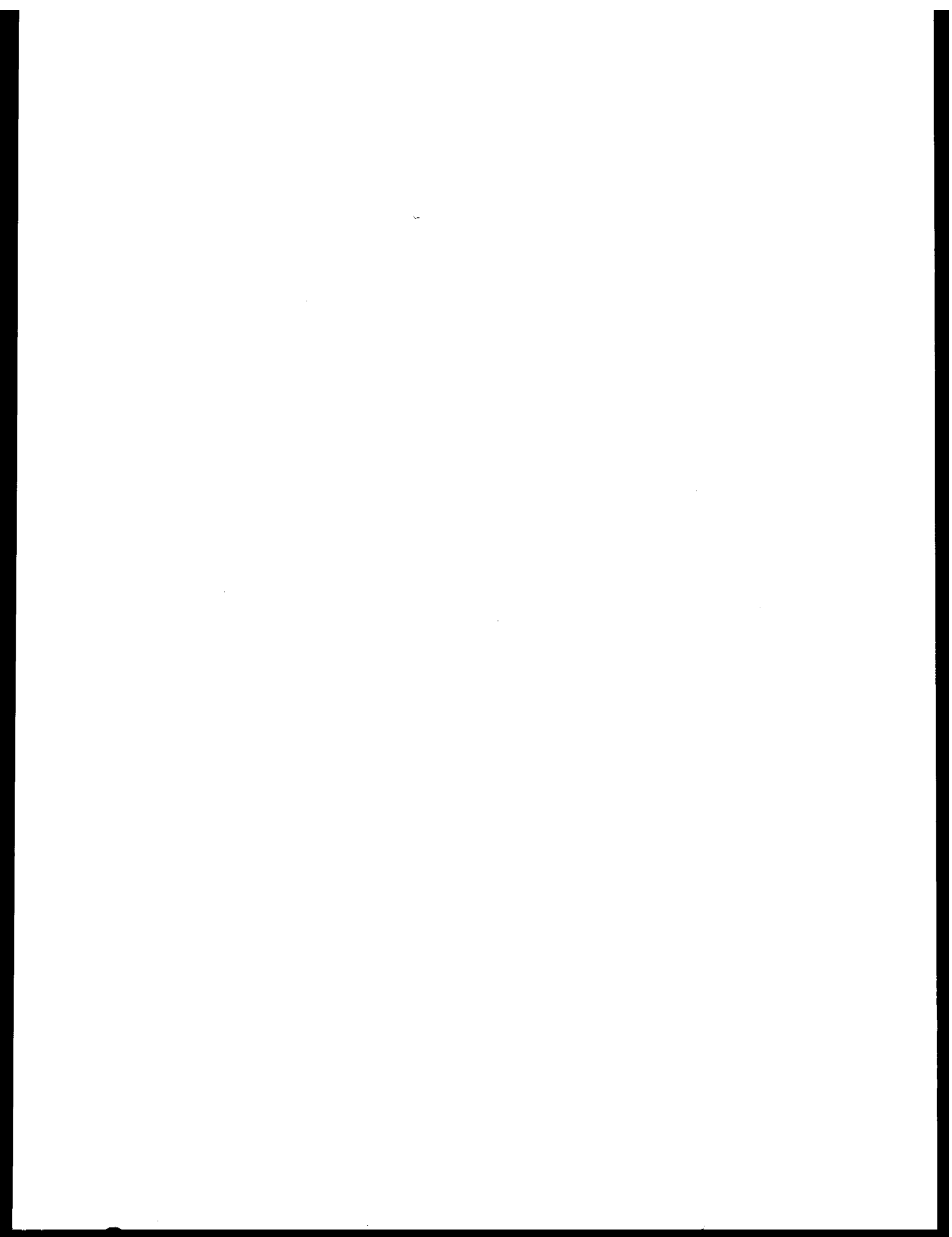


RU# 81

Supplemental reference:

Hufford, G. L., Lissauer, I. M., and Welsh, J. P. 1976. Movement of Spilled Oil Over the Beaufort Sea Shelf - A Forecast. Final report no. CG-D-101-76, 83 pp.

Available through NTIS, Springfield, VA 22161



QUARTERLY REPORT

Contract No.:

03-5-022-67, T.O. #3

Research Unit No.:

91

Reporting Period:

1 October 1976-31 December 1976

Number of Pages:

10

Current Measurements in Possible Dispersal Regions of the Beaufort Sea

Knut Aagaard

Department of Oceanography
University of Washington
Seattle, Washington 98195

31 December 1976

A76-76

I. Objectives

To provide long-term Eulerian time series of currents at selected locations on the shelf and slope of the Beaufort Sea, so as to describe and understand the circulation and dynamics; and in conjunction with the STD program, to examine the possible spreading into the Canadian Basin of waters modified on the Beaufort shelf.

II. Field Activities

The current meter field work was coordinated with that of the STD project (RU #151), with first arrival Barrow on 3 October 1976 and final departure 6 November 1976. The current meter work was completed on 28 October. The field party consisted of Knut Aagaard (5-28 October), Clark Darnall (3-28 October), and Steve Harding (3-23 October), all of the Department of Oceanography, University of Washington; Fred Karig (3-28 October) of the Applied Physics Laboratory, University of Washington; and Mike Cushman (18-27 October) of the Naval Arctic Research Laboratory, Barrow. The aircraft, a Bell 205, I.D. No. N2215W, was on charter from ERA Helicopters. In addition, we spent one day in the Barrow Canyon area aboard the U.S.C.G.C. *Glacier*.

Our immediate objectives were to retrieve the six current meters deployed last April in Barrow Canyon and north of Oliktok, and to install four new ones north of Lonely. All the instruments are designed to record temperature and current speed and direction. The moorings are launched through a hole cut in the ice; a complete deployment normally takes about 5-6 hours. The moorings are designed to release the anchor on command and come up to the underside of the ice. They are then located by acoustic ranging and bearing techniques, a hole is cut through the ice in their general vicinity, and divers used to attach a retrieval line to the mooring.

The moorings are then winched in. A typical mooring is shown in the attached figure. Mooring data for the instruments deployed in April are found in the quarterly report of 30 June, and data for the instruments deployed this fall are given below.

Latitude: 71°28.7'N

Longitude: 152°08.9'W

Sounding: 205 m

Upper current meter: RCM-4 #1309, 30 min. sample interval,
3 channels (°M, spd, temp)

Lower current meter: RCM-4 #1310, 30 min. sample interval,
3 channels (°M, spd, temp)

Acoustic release: AMF 322, channel 5, interrogate 9 KHz,
reply 10 KHz.

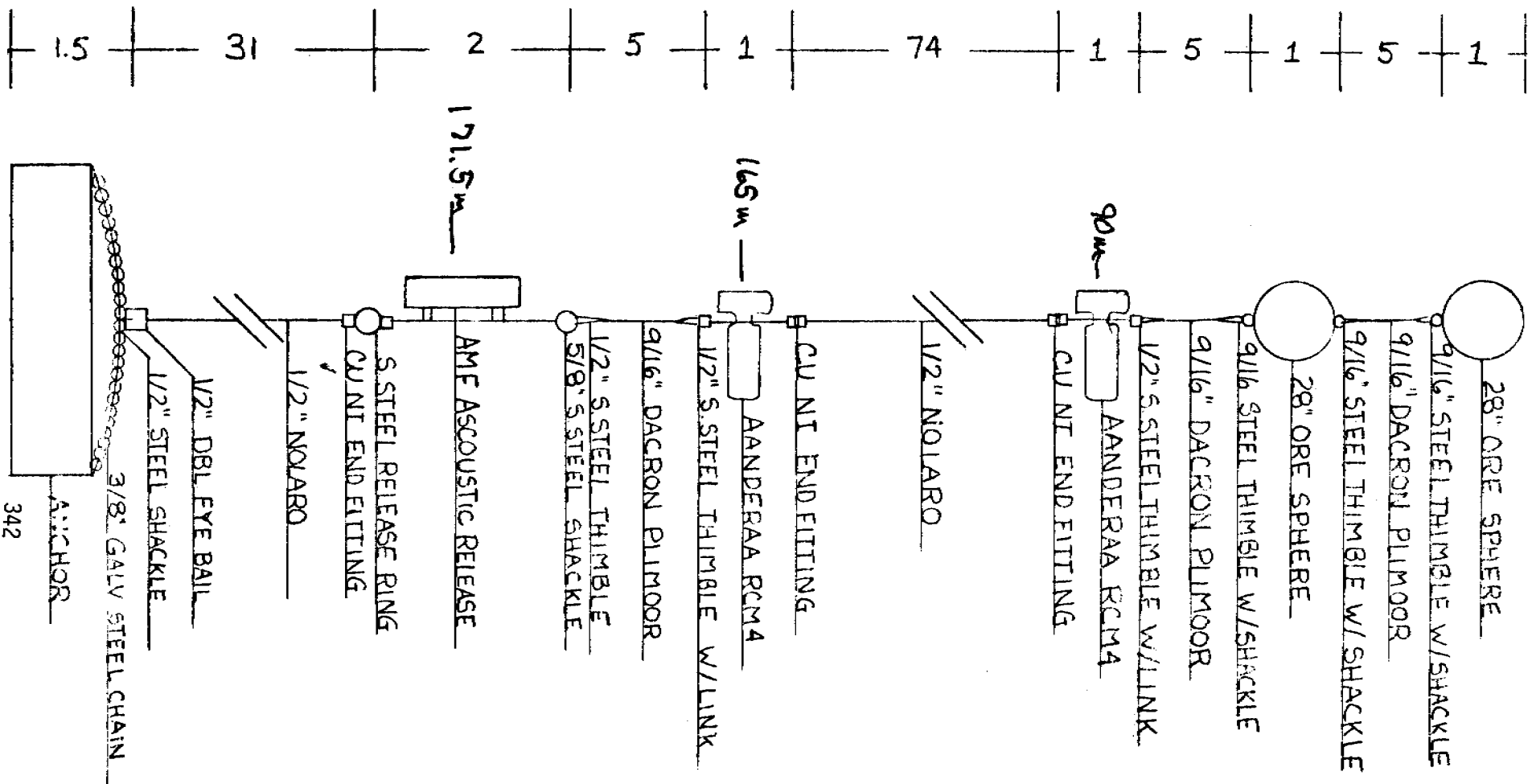
Deployment: 0204 on 16 October 1976, GMT

Nominal instrument depths: upper current meter - 90 m
lower current meter - 165 m
acoustic release - 172 m

III. Results

Despite the considerable and best efforts of all involved, the field work was only partially successful. Some of the reasons for this are indicated in this section and some in Section V of this report.

During the first part of October the entire north coast of Alaska was essentially ice-free to a distance seaward of about 50 miles. In the absence of ice we were able to obtain use of the *Glacier* for one day to recover the Barrow Canyon mooring. Both current meters from this mooring were successfully recovered on 6 October. Unfortunately, however, both tape recorders had stopped after running only a short time; effectively, no data were obtained. We have used these instruments in the Arctic for five and one-half years with no such problems. We have concluded that the fresh magnetic tapes



CURRENT MEASUREMENTS # 2

SCALE: N/A *	APPROVED BY:	DRAWN BY: SDH
DATE: 10 SEPT. 76		REVISED:
LONELY 200M MOORING		
* LENGTHS IN METERS		DRAWING NUMBER:

had in fact been delivered to us with a considerable amount of moisture in the iron oxide, and when the sealed instruments (which incidentally did contain dessicant material, following our normal practice) were exposed to the cold atmosphere prior to deployment, the tape froze to the head. When retrieved, the tapes were in fact stuck firmly to the tape head, preventing tape advance. Indeed, current meter no. 1014 was still running, but only because the tape drive had succeeded in breaking the tape just past the tape head, presumably immediately after freezing to it. We are now looking at the possibilities for force-drying new tapes.

Lack of ice from which to work and a servo failure on the helicopter kept us from further retrieval or deployment attempts until 15 October. The time was spent in diver training, laying fuel and equipment caches, and exploring open-water alternatives. That is, we wanted to turn to our advantage the complete absence of ice, and we concocted a number of interesting schemes to do so, but each was duly frustrated by various circumstances.

On 15 October we were able to fly, and a mooring with two current meters was deployed in water 205 m deep north of Lonely. The ice proved of marginal strength in handling the heavy loading during deployment, but outside of very cold feet all went well. On 17 October we attempted deployment of the second mooring north of Lonely. Such deployments require the use of an echo sounder as the predetermined depth has to be found quite precisely. Unfortunately, the sounder failed, and despite emergency repairs on the ice we were unable to bring the sounder output to an adequate level. The problem proved in part to be an intermittent inside the sealed and welded transducer, requiring factory repairs. We therefore had to terminate this portion of the work without having deployed the last two current meters.

On 18 October we moved from Barrow to Deadhorse to begin recovery of the current meters north of Oliktok. After a day of poor weather we began flying again on the 20th. We landed first at the site of the mooring nearest shore. The release responded immediately to interrogation and was fired at 1924 GMT, but a long series of frustrations, including severe helicopter icing and impossible flying weather, prevented final recovery until five days later when the mooring was pulled safely up at 0130 GMT on 25 October. Again one of the tape recorders had failed to function due to the tape freezing to the head. The other meter (no. 660) appeared to have run satisfactorily.

The next day we interrogated the third mooring, but stormy weather forced us to delay recovery. The release was fired just after 1930 GMT on 27 October and responded perfectly. Through a series of transponder and pinger soundings we located its approximate position under the ice, but a series of problems, the most severe of which was very poor underwater visibility for the divers, prevented recovery. We searched for the mooring all day on the 28th, covering a wide area, but never obtained a release reply. It is almost certain that strong northerly winds the previous night had blown the ice and mooring onshore, causing the release to drag bottom and damaging the exposed boot transducer.

In summary, while all the moorings and releases functioned properly, we recovered only four of the six current meters. Of these four, only one appeared to have functioned satisfactorily, apparently because the magnetic tape, although new, contained moisture. The tapes are presently being processed.

IV. Preliminary Interpretation

None.

V. Problems Encountered

We were plagued by a long series of mishaps and adverse conditions. Of these the apparently faulty tapes of course loom large, changing what should have been a situation of four good current records into one of only one. The bad weather and ice conditions were also important factors. When we tried recovery of the moorings from the *Glacier* in August-September, heavy ice had prevented us from doing so; while ice-free conditions in October, when no ship could be found to take advantage of the situation, caused us to lose a week of flying during the period of longest daylight. On the whole, the weather was poor during the entire trip. The worst conditions occurred during the second half of October. To illustrate, I quote portions of my journal from 19-27 October.

"Tuesday, 19 October. Winds easterly at 25 knots, blowing snow and sand. Poor visibility, unable to fly at any time."

"Wednesday, 20 October. Winds easterly at 25 knots as we got out on the ice after taking off at 0800. Overcast. [Then follows a description of locating and releasing the mooring, and triangulating it with our acoustic bearing equipment.] We took two more bearings by walking around the assumed triangle, ending up at a point 80-90 yards south or southsoutheast, where we could hear the pinger reply through the ice. Tried to rig the ADF [radio direction finding equipment], but darkness caught up with us, and we had to leave before being done. Returned to Deadhorse at 1810, once again with the low fuel warning light on."

"Thursday, 21 October. Winds west at 12 knots, 600 foot overcast. Took off at 0830 for Oliktok to refuel, then headed out. Had to turn back 12 miles short of the site as icing was fairly severe, with the windshield nearly completely obscured. Returned to Oliktok, then Deadhorse."

"Friday, 22 October. Overcast, fog, visibility too poor to fly."

"Saturday, 23 October. Took off at 0900 but had to turn around almost immediately because of low visibility. Snow, northerly winds, temperature dropping during the evening."

"Sunday, 24 October. Westerly winds this morning, minus 10 degrees F, cloudy, patchy fog. After a delay due to a frozen throttle control we took off shortly after 1000. Went to Oliktok, fueled, and began a search [for the mooring released on 20 October. A search utilizes our acoustic equipment which has an effective range of 4-5 miles, so that the procedure is to land at a grid of points, cut a hole in the ice and interrogate at each site]. Returned to Oliktok for refueling and resumed the search. [Late in the afternoon we found the mooring] about 7½ miles south of our position on leaving it four days ago. We sounded the site in a triangle about 80 m on a side, locating the supposed mooring position. We hung an orange poncho on one pole [an ADF antenna support] and at 1655 headed for Deadhorse, encountering considerable fog on the way. Unfortunately the last filter on our fuel pump had clogged at Oliktok in the afternoon, and so we had not topped up. Some distance from shore the low fuel warning light went on, and we had to set down [about five miles short of Deadhorse. We eventually got a drum of fuel out] and arrived back at 1830. [During the day we had had trouble with an erratic and low output from the power amplifier of the interrogation equipment, and this gave us very poor range in our search, probably less than one mile. This is why the search had taken such a long time.]"

"Monday, 25 October. Northeast winds, mostly cloudy, minus 5 degrees F. Took off at 0850 and headed straight for the site [about 65 miles away]. Hunted briefly, landed and sounded the mooring right away. Flew right to the site [using the indicated bearing] and began setting up. Clark made a short preliminary dive; then he and Mike went in. They had trouble maintaining depth, [and some distance out from the diving hole] Mike's regulator froze open and when he went for the other one it was frozen shut. He signaled to Clark [and grabbed Clark's reserve regulator. They were at that point quite deep and with their buoyancy trim upset] were sinking quite rapidly. Clark inflated the unisuit and they came up; we pulled them in [laterally to the diving hole]. It was a dangerous situation. In retrospect both felt they had had some nitrogen narcosis. [The mooring was recovered later that same day, the lower current meter coming out of the water at 1632.]"

"Tuesday, 26 October. Blowing snow, fog, strong northeast winds. Took off at 0915, went to Oliktok for fuel, and proceeded out, having trouble with the GLOBAL (Navigation System) near the end. Picked up the release at about 3½ miles [this mooring had a ranging capability in its release, as had had the Barrow Canyon one] and made three more landings, finally ending up about 700 yards out. The wind was blowing 25 knots and the visibility was very poor. It was clearly impossible to release and recover the mooring, the time being past 1230 and the weather deteriorating. [Then follows a discussion of the navigation problems and positioning.] We refueled at Oliktok and proceeded to Deadhorse in very poor visibility."

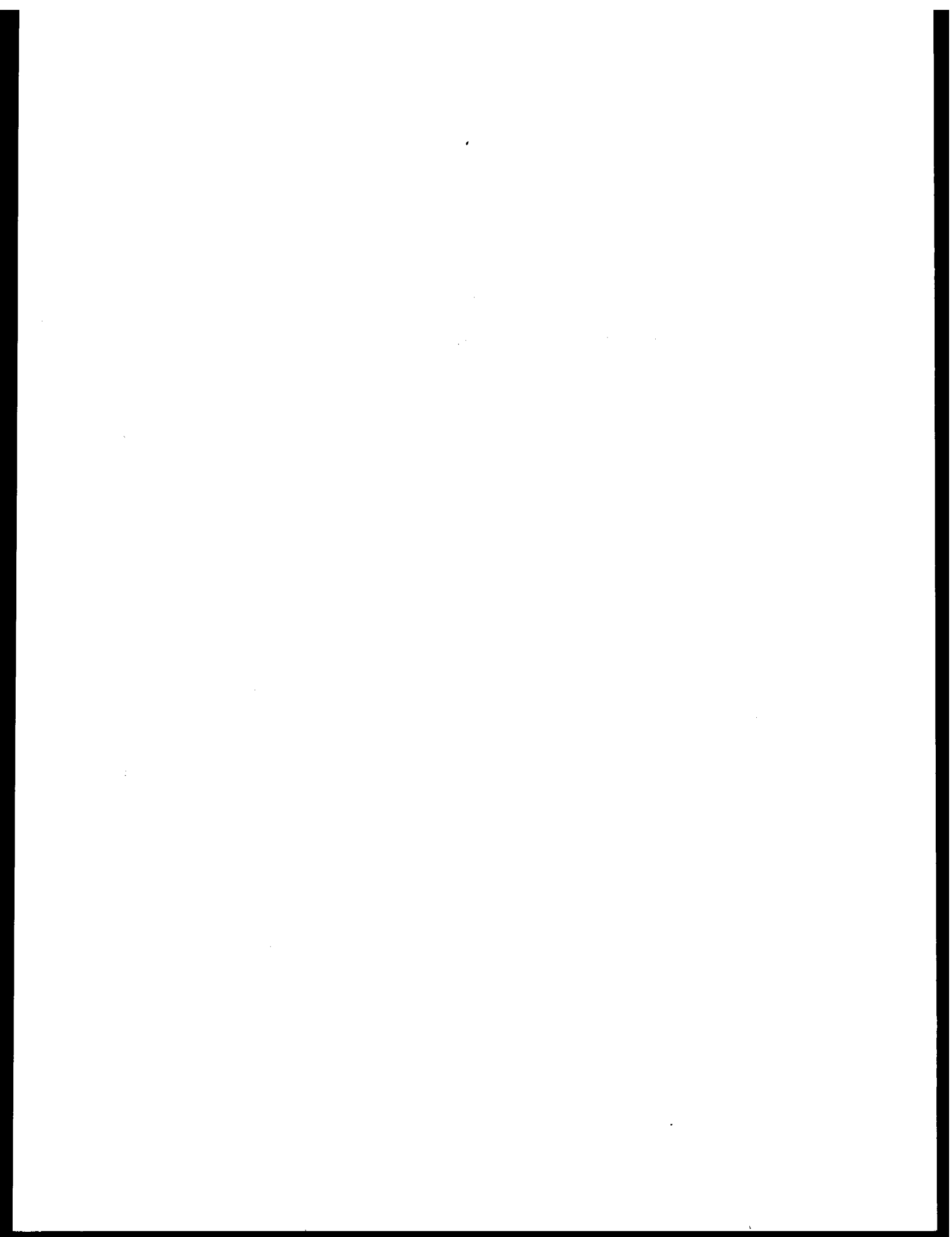
"Wednesday, 27 October. Cloudy, mostly with fog, temperatures about zero, and winds eastnortheast becoming northnortheast at about 12 knots. [Then follows a description of the mooring release and subsequent ranging and triangulation. We had some trouble with a cold wind on the surface, several

people getting lightly frostbitten. More importantly, the visibility was very poor for the divers due to a dark sky and a thick and dense layer of ice crystals in the water. Therefore they could not see the mooring unless it was very close to them. The result of the generally poor light conditions also present on the surface was that we had to call off the day's operation at 1645 without having retrieved the mooring.] We had very poor visibility on the way back, compounded by rapid icing of the wind shield as we came close to land. It was a difficult landing [we had to come in with the doors open in order to see]."

These excerpts illustrate the kinds of problems we had. Let it be recorded, however, that through almost five weeks of continuous field work on this and the STD project, both helicopter crew and scientific personnel performed above all reasonable expectations. For example, Elmer Hutchinson, the ERA mechanic, not only looked after the aircraft, but he also went out on the ice with us each day, assuming our tasks for his own, whether manhandling heavy equipment or assembling machinery with frozen fingers. Each person behaved in such a way that every problem became a challenge rather than an unpleasantness. This was our fifth OCSEAP field trip in the Beaufort Sea. None have been easy, but all have been a pleasure thanks to my colleagues' good will, hard work, and genuine comradeship.

VI. Estimate of Funds Expended (30 November 1976)

TOTAL ALLOCATION (5/16/75-9/30/77):	\$188,542
A. Salaries	11,820
B. Benefits	1,363
C. Travel	4,134
D. Equipment	47,683
E. Supplies	18,200
F. Computer Costs	35
G. Shipping	4,401
H. Other Direct Costs	1,309
I. Indirect Costs	<u>5,177</u>
TOTAL EXPENDITURES:	<u>94,122</u>
REMAINING BALANCE:	\$94,420



RU# 111

NO REPORT WAS RECEIVED

A final report is expected next quarter

the first two cases, the first two terms of the series are the same, and the third term is different.

In the third case, the first two terms are different, and the third term is the same as the second term.

In the fourth case, the first two terms are different, and the third term is different from the second term.

In the fifth case, the first two terms are the same, and the third term is different from the second term.

In the sixth case, the first two terms are different, and the third term is the same as the second term.

In the seventh case, the first two terms are different, and the third term is different from the second term.

In the eighth case, the first two terms are the same, and the third term is different from the second term.

In the ninth case, the first two terms are different, and the third term is the same as the second term.

In the tenth case, the first two terms are different, and the third term is different from the second term.

In the eleventh case, the first two terms are the same, and the third term is different from the second term.

In the twelfth case, the first two terms are different, and the third term is the same as the second term.

In the thirteenth case, the first two terms are different, and the third term is different from the second term.

In the fourteenth case, the first two terms are the same, and the third term is different from the second term.

In the fifteenth case, the first two terms are different, and the third term is the same as the second term.

In the sixteenth case, the first two terms are different, and the third term is different from the second term.

In the seventeenth case, the first two terms are the same, and the third term is different from the second term.

In the eighteenth case, the first two terms are different, and the third term is the same as the second term.

In the nineteenth case, the first two terms are different, and the third term is different from the second term.

In the twentieth case, the first two terms are the same, and the third term is different from the second term.

In the twenty-first case, the first two terms are different, and the third term is the same as the second term.

In the twenty-second case, the first two terms are different, and the third term is different from the second term.

In the twenty-third case, the first two terms are the same, and the third term is different from the second term.

In the twenty-fourth case, the first two terms are different, and the third term is the same as the second term.

Quarterly Report

Contract #03-5-022-56
Research Unit #123
Task Order #18
Reporting Period 10/1 - 12/31/76
Number of Pages 3

ACUTE TOXICITY - PACIFIC HERRING ROE IN
THE GULF OF ALASKA

Dr. Ronald L. Smith
Institute of Marine Science
University of Alaska
Fairbanks, Alaska 99701

I. Task Objectives

Objectives for this quarter included hiring and overseeing a technician for the hydrocarbon analyses. We have also tried to make arrangements for scanning electron microscopy of control and experimental herring larvae.

II. Field and Laboratory Activities

A. Ship or field work:

None.

B. Scientific party involved in project:

R. L. Smith	Principal Investigator
J. Pearson	Associate Investigator
J. A. Cameron	Research Assistant
C. Akert	Research Technician

C. Methods:

Scanning EM work was performed on herring larvae using standard EM procedures employed at Oregon State University. Gas chromatographic analyses of tissues and water samples collected during this project were performed using the techniques of Dr. David Shaw, IMS, University of Alaska. GC-MS techniques were employed in an effort to identify the fractions appearing on the chromatographs.

D. Sample localities:

None.

E. Data analyzed:

Some 60 scanning electron microscope photographs were taken of a variety of control and exposed larvae. Copies of some of these photos will be included in the final report on this project. Those photographs illustrate several malformations which could not be observed under the dissecting microscope. These include the following:

- erosion of pectoral fin
- malformed mouth, incapable of closing completely
- missing branchiostegal membrane
- missing maxillary bone.

Chromatographic analyses show that the exposed larvae and unhatched eggs did accumulate hydrocarbons. We will report on the identity of these hydrocarbons in the final project report, soon upcoming.

IV. Problems Encountered

One very critical problem encountered during this quarter deals with the procedures used in sample preparation for gas chromatography. Either through imprecise instructions or sloth on the part of the technician (or both) no internal marker was added to the tissue and water sample extracts. Since these extracts were not evaporated to a uniform volume, we have no way of expressing hydrocarbon levels quantitatively. In the final report we will only be able to make qualitative statements about what is there and some observations about relative levels in the different exposure groups compared to the controls. This will be the major drawback of the entire study.

OCS COORDINATION OFFICE

University of Alaska

ENVIRONMENTAL DATA SUBMISSION SCHEDULE

DATE: December 31, 1976

CONTRACT NUMBER: 03-5-022-56 T/O NUMBER: 18 R.U. NUMBER: 123

PRINCIPAL INVESTIGATOR: Dr. R. L. Smith

No environmental data are to be taken by this task order as indicated in the Data Management Plan. A schedule of submission is therefore not applicable¹.

The final report is being prepared.

NOTE: ¹ Data Management Plan has been approved and made contractual.

QUARTERLY REPORT

Contract #R7120846
#R7120847

Research Unit #138, 139, 147

Reporting Period: 1 October -
31 December 1976

Number of Pages : 3

GULF OF ALASKA STUDY OF MESOSCALE
OCEANOGRAPHIC PROCESSES (GAS-MOP)

Dr. S. P. Hayes

Dr. J. D. Schumacher

Pacific Marine Environmental Laboratory
National Oceanic and Atmospheric Administration
3711 - 15th Avenue N. E.
Seattle, Washington 98105

January 1, 1977

I. TASK OBJECTIVES

- Eulerian measurements of the velocity field at several positions and levels
- Measurements of the along- and cross-shelf sea surface slope
- Process study to understand the interrelations among the velocity field, the bottom pressure gradient, the density field, and the wind field in order to determine the dynamics of the circulation on the continental shelf.

II. FIELD OR LABORATORY ACTIVITIES

A. Cruises:

1. NOAA ship *DISCOVERER* RP-4-D1-76B LEV VI

Scientific Party:

Carl Pearson	Chief Scientist	PMEL
Rick Miller	Sea Surface Slope, CTD	UW
Roger Osland	Sea Surface Slope	UW
Lf(jg) Dan Dreves	Current Meter Arrays	PMEL
Jerry Hood	Stellite Tracked Buoys	AOML

B. Methods:

Plessey 9040 CTD

Plessey 8400 Digital Data Logger

Aanderaa RCM-4 current meters

PTG pressure temperature gauges

AMF releases

C. Sample Localities:

KISS 1A	57°44.7'N	154°43.7'W
KISS 2A	58°37.2'N	153°05.0'W
KISS 3A	58°45.3'N	152°10.6'W
KISS 4A	58°01.9'N	151°56.4'W
KISS 5A	56°33.2'N	152°39.5'W
WGC-2D	57°34.6'N	150°48.6'W
WGC-3B	55°11.5'N	156°58.0'W
62-I	59°38.1'N	142°05.0'W
SLS-13	59°45.4'N	141°33.0'W
SLS-14	59°39.5'N	141°42.0'W
SLS-15	59°19.2'N	142°06.3'W

D. Data Collected or Analyzed:

1.	KISS 1A	deployed - 2 current meters
	KISS 2A	deployed - 2 current meters
	KISS 3A	deployed - 2 current meters
	KISS 4A	deployed - 2 current meters
	KISS 5A	deployed - 2 current meters
	WGC-2D	recovered- 3 current meters
	WGC-2E	deployed - 2 current meters, 1 PTG
	WGC-2E	deployed - 2 current meters, 1 PTG
	WGC-3B	recovered- 3 current meters
	WGC-3C	deployed - 2 current meters
	62I	recovered- 4 current meters

62J	deployed - 4 current meters
SLS-13	recovered- 1 PTG
SLS-14	recovered- 2 current meters, 1 PTG
SLS-15	lost - 1 PTG
SLS-19	deployed - 2 current meters
SLS-20	deployed - 2 current meters, 1 PTG
SLS-21	deployed - 2 current meters, 1 PTG

2. 38 CTD casts were taken, tapes are being processed.

III. RESULTS

These new data sets are being processed and analyzed.

IV. PROBLEMS ENCOUNTERED/RECOMMENDED CHANGES

Moorings SLS-5 failed to respond to a release command.

Attempts may be made to recover this array by dragging.

V. ESTIMATE OF FUNDS EXPENDED (1 October 1976 - 31 December 1976)

Salaries/Benefits/Overhead	\$ 56,250
Travel and Per Diem	3,500
Equipment	-0-
Other Direct Costs	
Expendable Supplies	\$10,750
Contractual Services	8,750
Calibration	2,500
Shipping	2,750
Publication	1,250
Total	<u>\$ 85,750</u>

QUARTERLY REPORT
DRAFT

Research Unit 140
Reporting Period Ending 9/30/76
P.I. Jerry Galt

Status Report on Numerical Modeling RU #140 as of FY 76T

Present Accomplishments

To describe the present status of the model development, we may once again refer to the enclosed figure. In the diffusion subroutine, the "stochastic current analysis" subroutines have been completed. They have been used on current meter data in the Gulf of Alaska and wind data from the NE Gulf and Kodiak regions. These subroutines have not been documented yet, but the products of the analysis have been accumulated in a data report and relevant sections forwarded to Department of the Interior investigators. The "random walk parameterization" has been tested and compared to the more complex analysis. This simpler subroutine has been combined with rudimentary advective and pollutant reaction component subroutines for initial testing.

In the advective subroutine the "diagnostic circulation model" has been developed, documented and used in the Gulf of Alaska and the Kodiak region where the required observational data have been available. Presently, the FORTRAN code is being updated so that it will run more efficiently on smaller core computers. The computer code has been used in the OCSEAP program and is also being used for additional research at AOML (MESA studies) and the Naval Postgraduate School. The "time dependent barotropic mode simulation" algorithm has been used to key the diagnostic model to current meter observations and the resulting trajectories for the NE Gulf of Alaska have been incorporated in a report and passed on to BLM for consideration. Appropriate but fragmentary input data are being used for numerical experimentation for the Kodiak region. Initial results are being compiled for a briefing to BLM researchers working on the draft EIS for Kodiak. The "ice drift model" and "shallow water current simulation" are in the early theoretical development stage. The "tidal current prediction" algorithm is presently being tested and interfaced with coastline specification routines. The "response analysis modeling" is in the planning stage in close cooperation with tidal analysis studies being carried out by other PMEL investigators (Dr. Mofjeld). A number of "regional meteorology models" have been tested and verified with environmental situations where data is available. The choice of a particular model has been made on the basis of these tests and an efficient FORTRAN code is under development. The "wind drift synthesis" which interfaces the regional meteorology model to the advection subroutine is receiving concomitant consideration.

A few examples of "pollutant reaction subroutine" algorithms have been tested. These are little more than exercises to date, with the primary intention being to test model component interfaces. The major sub-routines in this section are expected from Dr. Mattson (OCSEAP researcher at CEDDA) and close coordination with his research is underway and will continue.

Work has recently begun on standardizing the "software subroutines". This is felt to be a crucial part of making the model an effective tactical tool in the environmental assessments. The model results must be clearly displayed and easily understood if the research is to fulfill its important role of integrating and synthesizing OCSEAP research results into a form useful for decision-makers. Constant interplay with other OCS researchers and briefings to BLM staffs are helping to refine the actual needs for the software development. In addition, studies of other graphics specialists' research and the delivery of appropriate computer hardware are contributing to the continuing maturation of the conceptualized software design. To date, subroutines to handle components of "digitization of geophysical setting", "input-output presentation", "restart-Zoom techniques" and "resource overlay techniques" have been started. The general software development requires additional work, and this facet of the research is receiving significant attention.

The major modeling components of our research for shelf and shelf break regions, are based on the diagnostic model. We have used this in a number of cases and feel that it is dynamically correct and gives us responsible answers. We initially planned to have this model highly automated so that it could be easily run in any area with very little set-up time involved. In doing this, we ran into three specific program problems. The first related to how to handle spurious density data, the second dealt with generating a triangle mesh from the original station data, and the third dealt with how to incorporate the boundary conditions in a consistent manner. Initially, we broached all of these using trial and error techniques (largely out of desperation). More recently, we have been developing automated techniques to handle these problems. The triangle generation is now working in reliable form. The techniques for spurious density data have greatly simplified the problems associated with this form of input data. For boundary conditions, an auxiliary model is under development. This will identify which boundary conditions are strongly coupled and which ones are essentially independent. In addition, it will guarantee overall model continuity in the transport. By the time this is completed, we should be well on the way to a more general model that can be used in a quick response model.

The model has been used, as you know, in the Gulf of Alaska primarily to examine summer data. We have also run it in the northeast Gulf to examine winter data, but those results are in a very preliminary stage and are probably not reliable due to defects in boundary condition specifications. By the time we get the new boundary condition routine running, we should be able to correct this problem easily. Another region where we have run a model is around Kodiak Island. For Kodiak, we took density data that Tom Royer sent us and made a series of model runs which we were able to send to BLM in less than two weeks. The current meter data to check the model was very limited and we essentially got no real input from it. Another modeling area which we were working on is to represent time-dependent variance in the pollution trajectories. To do this, we are looking at the time-dependent currents, both from the model and from the observed current meter records. Combined with both these we are incorporating time-dependent winds, both from direct time series obtained from Flow Numerical Weather Center and from the analysis of those records in stochastic form.

PRESENT DEVELOPMENT MODEL

Activity is concentrating in a number of new areas. First of all, we are looking into how pressure data can be directly input into the diagnostic model to specify boundary conditions. Secondly, we are exploring finite element formulations for near shore circulation models (water depths less than an Ekman depth). Finally, we are working on the oil trajectory model with major emphasis going to I/O development, graphics and modeling interfacing.

If you still feel that working through some tests is an important requirement for verifying the models or keeping BLM happy, we can certainly work towards that. To run the model to any region, we need STD data and some estimate of the appropriate boundary conditions. These boundary conditions come from either current meter information or direct pressure measurements. In a sense the two are independent, so given one, we could compare the results of the other. To date, the only form of boundary condition verification information that we have has available is the current meter records. If we were to try and run an experiment where we plan to do direct comparisons to current meter input and pressure gauge input, it would probably have to be in the Icy Bay region where the data sets are available. Tom Royer, Stan Hayes, and myself intend to do this but we do not feel that it had as high a priority as some of the other things we were doing, in particular, the extension of the model results to Kodiak and the oil trajectory work.

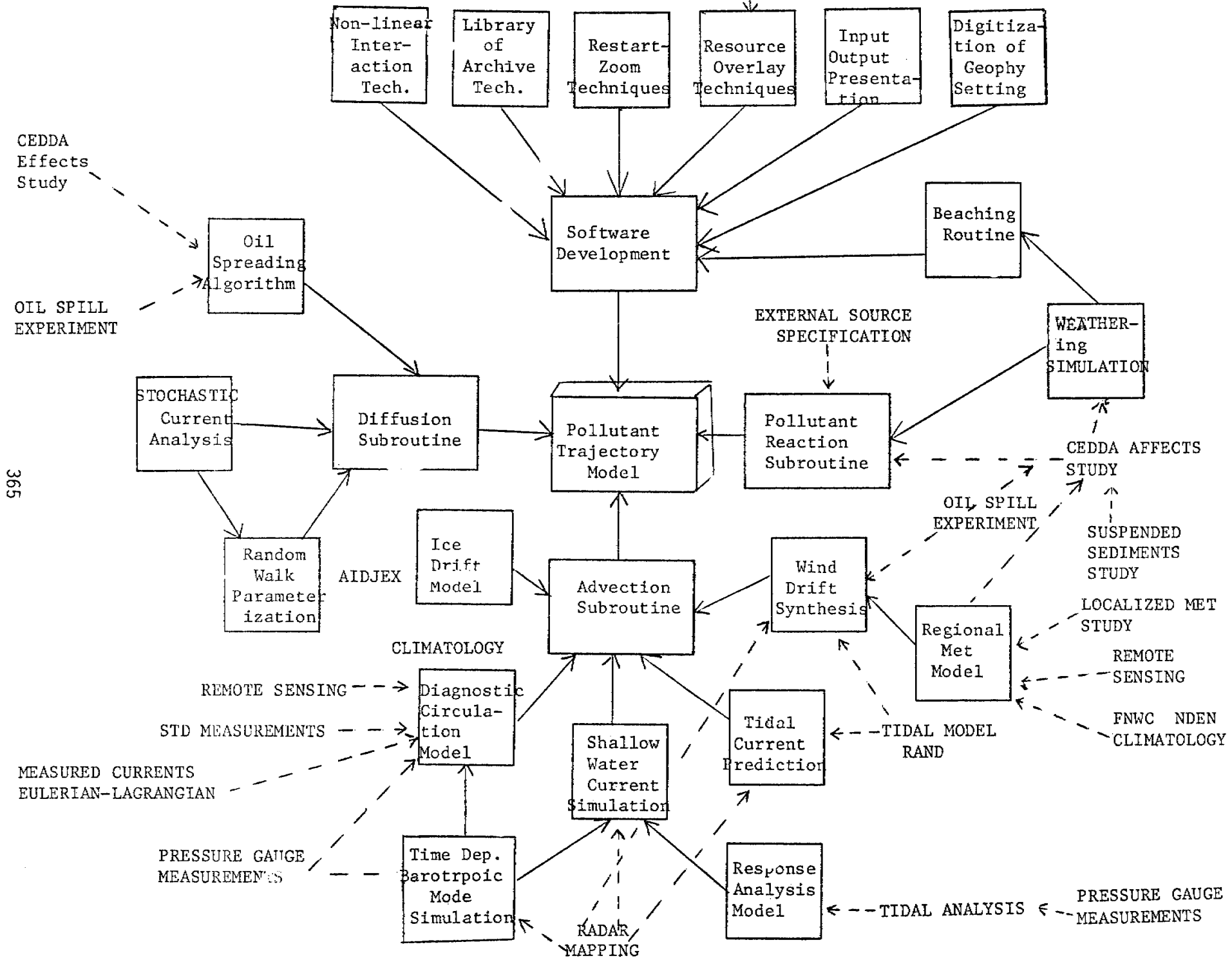
Planned Work

In order to come up with a more detailed description of how and when the basic model will be applied to various Alaska OCS regions, I must first explain the conceptual basis behind its modular design. The model is constructed as a central program which is interactive with: 1) a research scientist, 2) the software routines, and 3) the three major process subroutines (diffusion, advection, pollutant reaction). To this level the model is absolutely general. Whatever region is being studied, there will be a researcher, some software so he or she can communicate with the programs, and three basic processes that can effect the distribution of a given variable. The model domain is at this point unspecified, the number of dimensions and resolution are also not determined (or limited at least in theory).

Beyond this basic core model the process subroutines call on some combination of the particular algorithms that: 1) they can address, 2) that represent an appropriate physical phenomenon for the region of study, and 3) that have the required empirical data to run. This, then, is what makes the model apply to a particular area. The program asks the researcher where the model is to be run, what resolution is needed, what parameters control the spill, which advective processes dominate in the study area, etc., etc.

The research proposed for this work unit can be easily divided into two part. The first part deals with perfecting the computer software, communications interface, graphics presentation and interrogative program elements so that the entire model can be efficiently linked and run with a minimal amount of effort. Clearly, this part of the development is non-site specific. The work has already begun. Key equipment purchases have been made and delivery is expected in November. By April, this part of the model development should be operative and going through extensive testing. By the end of the contract period this should be completed with appropriate documentation.

BIOLOGICAL RECONNAISSANCE



365

QUARTERLY REPORT

RESEARCH UNIT: 140
REPORTING PERIOD ENDING: 12/31/76
P.I.: JERRY GALT

Introduction

The modeling effort as described in the work statement is substantially on target. The project is advancing as five developmental pieces. These pieces and their proponents are as follows:

1. Diagnostic model - Galt, Watabayashi
2. Trajectory model - Galt, Pease
3. Advanced model - Galt, Karpen
4. Meteorological model - Overland, Han, Galt
5. Ice dynamics model - Overland, Galt

The progress and prognosis for each piece is outlined in the following pages.

Diagnostic Model

The diagnostic model has been tried several times and, with careful attention to boundary conditions and a few minor details, we can make it work. We have completed an automatic technique to generate a triangle mesh from original station data. We have also developed methods to handle spurious density data, although the technique still requires some small manual adjustments to be made. We are working to make this method fully automatic.

A large effort is being made to formulate an auxiliary model which will incorporate boundary conditions into the diagnostic model in a consistent manner. To this point, the boundary conditions have been set by trial and error, and a less arbitrary and more automatic system based on pressure data over the region is being developed.

Schedule for Next Quarter:

1. Fully automate methods to handle spurious density data for the diagnostic model.
2. Complete and test auxiliary model to handle boundary conditions.
3. Complete model runs for the winter test case for the Gulf of Alaska.

Pollutant Trajectory Model

The five component processes which can be used to run the preliminary pollutant trajectory model are:

1. Real-time currents using NEGOA current meter data for the region keyed to the results of the diagnostic model.
2. Mean currents based on the same current meter data and also keyed to the results of the diagnostic model.
3. Stochastic currents based on a Markov analysis of the same current meter record.
4. Real-time winds using FNWC data for the region over the same time period.
5. A combined mean and stochastic wind based on an analysis of the same wind record.

The FORTRAN code for this preliminary model is written. The first four sections are debugged and results for Summer 1974 for the real current and the real current plus real wind are included (Fig. 1, 2). Figure 3 shows the diagnostic model results to which the cases in figures 1 and 2 were keyed. The sections on stochastic processes are in the final stages of preparation.

The graphics routine is still under development, although a preliminary version was used to prepare the figures presented here. We are trying to find a format which will maximize the information content of the plots without causing confusion. We also are working on a scaling package to match plots to any particular NOS chart.

Schedule for Next Quarter:

1. The graphics routine will be systematized and efforts will be made to have the plots scaled to a standard chart.
2. All the components should be debugged and run for the summer case and plotted uniformly.
3. If the winter case for the diagnostic model is available soon, then the complete set should be run for the winter case also.
4. Documentation of the program should be brought up to date.

REAL CURRENT ONLY

GULF OF ALASKA TRAJECTORY PLOT

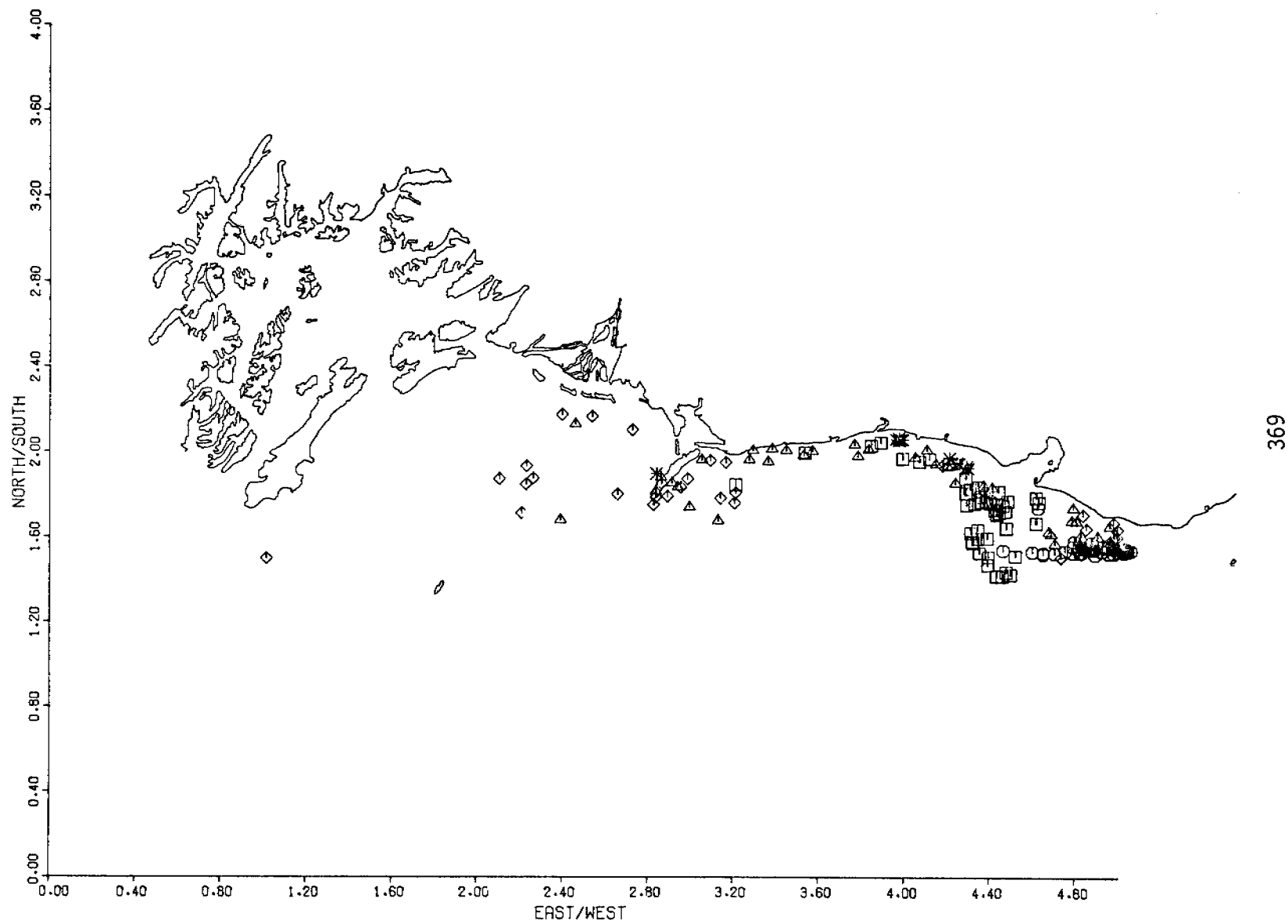


Figure 1

REAL CURRENT AND REAL WIND

GULF OF ALASKA TRAJECTORY PLOT

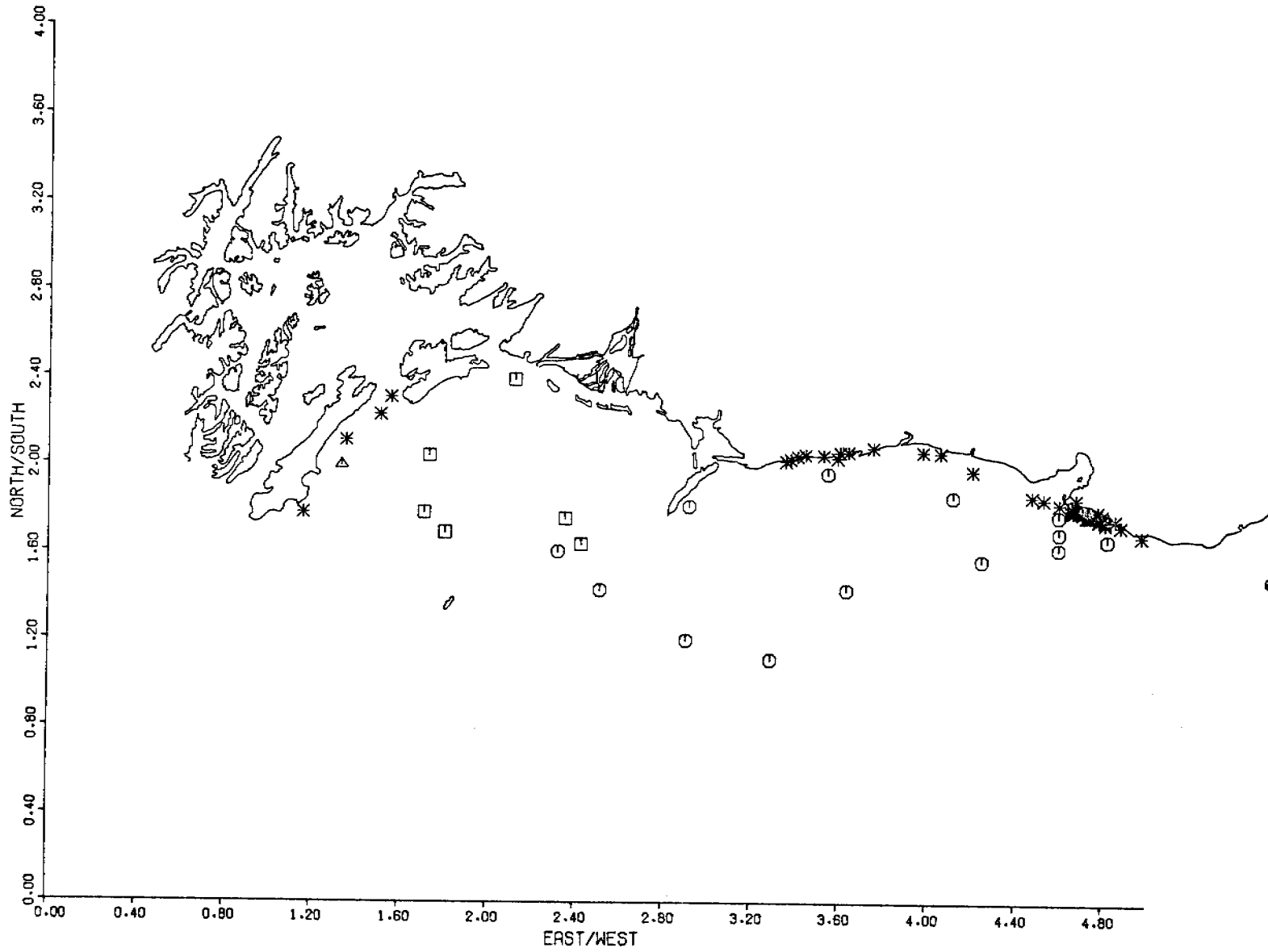


Figure 2

SURF VELOCITY

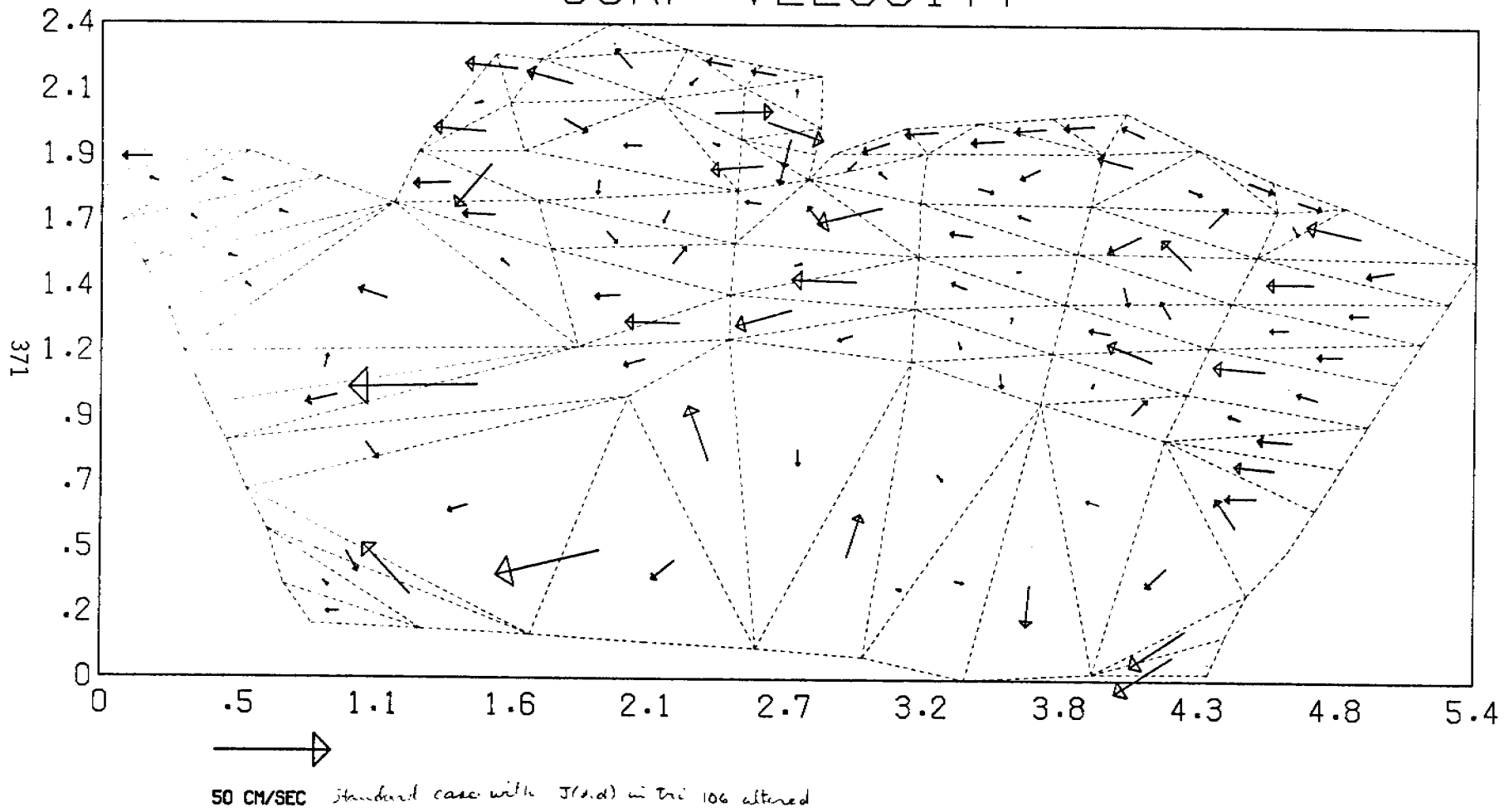


Figure 3

Advanced Model for Oil Slick Motion

The advanced model for oil slick motion is an interactive model run on a dedicated minicomputer. The specification of all model parameters is made by the model operator as the program is being run. The allowable options are given to the model operator by the program.

The model is being documented at two levels. The first level of documentation is for an operator who only wants to run the program. The documentation specifies how to start the model, gives an example of a model run, and explains how to obtain different types of model output. The second level of documentation is for the operator who wants to modify the program or run it on another computer. This documentation includes the location of all computer specific statements, the internal structure of the program, a description of the function of each subroutine and their calling sequences. Also included in this documentation is a detailed description of the structure of the data files needed to run the model and generated by it. The documentation is presently about 50% completed. The basic model structure has been completed. A test spill can be advected across the area being modeled. Work continues on modeling wind forced motion of a slick. Several theoretical approaches are being investigated for modeling differential oil slick motion. A review of literature references obtained through NOAA's OASIS system is approximately one third completed.

Constraints encountered have been specific formulation of differential oil slick motion and the integration of the Lagrangian Elements used to represent a spill to obtain information that can be contoured.

Schedule for next quarter:

1. Bring model documentation up to developmental level of the model.
2. Optimize and refer the computer code for the model.
3. Accelerate review of the literature. An additional request was made to OASIS for monthly updates of new literature. This information should start arriving early in the quarter.
4. Continued developmental work on wind forcing and differential oil slick motion.

Regional Meteorological Model

Initial studies of near shore winds in the Gulf of Alaska OCS regions have indicated significant modification of the large scale synoptic patterns. In order to get a quantitative understanding of these phenomena, we have evaluated the suitability of three regional surface wind models, proposed by Lavoie (1972), Danard (1972), and Fosberg (1976), in terms of estimating coastal influence. All three models treat the boundary layer as a well mixed slab, have modest computer requirements, and are well suited to orographically controlled regions such as the Alaskan Coastline. They all can estimate local winds from synoptic scale pressure charts in terms of topography and land-water contrasts in roughness and heating. Our preference is Lavoie's model; he solves a complete set of primitive equations to steady state subject to fixed boundary conditions, while Danard's lack of the continuity equation and Fosberg's neglect of momentum and temperature advection on the downwind environment make their approaches less general.

Lavoie's original model has been extended and generalized to be easily adaptable to a large variety of coastal configurations to be covered by OCSEAP. This was accomplished by streamlining the computer code and reformulating the problem for a latitude-longitude grid, the normal format of elevation data. Lavoie's arrangement of defining all variables at all grid points has been replaced by the more efficient single Richardson lattice in which the primary variables, two velocity components and inversion height, are staggered in space and time. This arrangement eliminates the problem of over specification of boundary conditions and also removes the numerical artifact of two grid oscillations in the velocity and height fields caused by gravity waves propagating only along a subset of the entire grid.

Schedule for Next Quarter:

1. Implement improvements in the version of the model for Yukatat Peninsula Region.
2. Generalize the input statements to handle climatological storms.

Modeling for Beaufort Sea Ice Dynamics

For most of the year, the Beaufort Sea is covered with a lid of ice. This lid is a complex jumble of flows, holes and ridges with ice of various thicknesses having different strengths and resistances to deformation. This ice cover acts as a filter through which the wind stress must operate to drive the ocean. The dynamics of sea ice are complicated and the mechanical characteristics of aggregate flows are significant controlling parameters. In many instances, stress can be effectively transmitted over hundreds of kilometers. Regional algorithms that incorporate ice dynamics on this scale as well as complex coastal geometries will be essential for acceptable results. Single point schemes will always give limited results.

In conjunction with this project, work has begun at AIDJEX (Arctic Ice Dynamics Joint Experiment) to adapt their developed Ice Model to the forecasting problem in coastal regions. The experimental design for the original AIDJEX experiment consisted of an arbitrary region offshore in the middle of the Beaufort Sea surrounded by ice buoys and with an extensive meteorological array. The three questions to be resolved for forecasting and assessment are the effect of inclusion of a high shear zone caused by the presence of a coastline, the model sensitivity to the lack of data on the open boundaries, and the model sensitivity to smoothed atmospheric input represented by the National Weather Service three day forecasts.

The AIDJEX model will be rerun for the AIDJEX area with a limited set of meteorological and boundary data and compared with the complete AIDJEX calculation and the verification data taken during AIDJEX. The final project results are in the form of two sets of recommendations. The first is what grid size, domain, and minimum input data are necessary to solve for ice motion in the coastal zone, and second, how can the model output such as ice state, strain, and stress state be interpreted to provide necessary forecasting aids for problems such as the summer opening of transportation routes and ice damage to structures.

Schedule for Next Quarter:

1. AIDJEX will present a Seminar on the results of the first six months of this project.
2. The final configuration of the test cases will be determined.

QUARTERLY REPORT

Contract No.: 03-5-022-67, TA 4

Research Unit Numbers: 141, 145, 148

Reporting Period: 1 October-31 December 1976

Number of Pages: 7

Bristol Bay Oceanographic Process (B-BOP)

J. D. Schumacher¹

R. L. Charnell¹

L. K. Coachman²

1. Department of Oceanography
University of Washington, WB-10
Seattle, Washington 98105
2. Pacific Marine Environmental Laboratory
3711 - 15th Avenue N.E.
Seattle, Washington 98105

31 December 1976

A76-77

I. Objectives

This study is a joint program between the University of Washington and the Pacific Marine Environmental Laboratory (ERL/NOAA) to provide water mass and circulation information over the eastern Bering Sea continental shelf for the Outer Continental Shelf Environmental Assessment Program.

II. Field Activities

Cruises: See attached cruise report and summaries of hydrographic and instrument data.

Meetings: Bering Sea Ecological Processes Workshop, Salishan Lodge, Oregon, 3-6 October 1976 (R. Charnell, T. Kinder; no cost to B-BOP budget). OCSEAP Physical Oceanographer and Meteorological Principal Investigator Workshop, Lake Quinalt, Washington, 13-15 October 1976 (R. Charnell, T. Kinder, J. Schumacher).

III. Results

See attached summary for the data being processed now.

IV. Preliminary Interpretation of Results

A. A scientific paper "Fine-Structure Instability in Outer Bristol Bay" by L. K. Coachman and R. L. Charnell, based on March 1976 CTD data, has been submitted to *Deep Sea Research*.

B. Data from the most complete CTD survey (June, 1976) is being analyzed carefully; distribution maps will be available for the annual report (March, 1977).

C. We are focusing on the analysis of the most complete suite of current meter data, that from the summer of 1976. Our intention is to prepare a

preliminary analysis of these data during the next quarter, but a complete analysis will require more time.

D. We are comparing pressure data from the periphery of Bristol Bay with the results from the Fleet Numerical Weather Center model. Early results are promising, and indicate that atmospheric variable time series can be constructed for comparison with the time series data obtained from current meters and pressure gauges.

V. Problems Encountered

The scheduling of ship time continues to be a serious problem. Hydrographic surveys have been hampered by both inadequate ship time and inappropriate timing of cruises. Thus, both areal coverage and temporal resolution have been less than desirable.

Preliminary plans for the 1977 field season indicate that either we must rely upon an exceptionally early break-up of the ice, or accept a data loss by planning to recover instrument moorings in mid-summer. While this problem may yet be resolved satisfactorily, we believe that the ship scheduling has affected B-BOP adversely, both scientifically and logistically, and therefore decreased the efficiency of our efforts.

VI. Estimate of Funds Obligated (FY77)

A. Salaries	7,490
B. Benefits	1,058
C. Indirect Costs	3,745
D. Supplies & Other Direct Costs	11,392
E. Equipment	-0-
F. Travel	<u>2,400</u>
TOTAL	<u>\$26,085</u>

B-BOP INSTRUMENT SUMMARY

DATE	LOCATION	INSTRUMENTS ¹	DAYS ²	REMARKS
7 Sept.- 4 Nov. 1975	BC-4A 58-37.0 168-14.0 55 m	2 RCM-4 1 TG-2	58	
6 Sept.- 21 Sept. 1975	BC-1A 55-24.6 167-57.5 201 m	2 RCM-4 1 TG-2	3, 16	Trawled
8 Sept.- 5 Nov. 1976	BC-2A 57-04.3 163-19.5 65 m	2 RCM-4 1 TG-2	58	
4 Nov. 1975	BC-1B 55-24.0 167-58.0 205 m	2 RCM-4 1 TG-2	0	Trawled
4 Nov. 1975- 14 June 1976	BC-4B 58-37.0 168-14.1 55 m	2 RCM-4 1 TG-2	228 da	Partial recovery
5 Nov. 1975- 30 May 1976	BC-2B 57-03.7 168-21.8 65 m	2 RCM-4 1 TG-2	207 da	
6 Nov. 1975- 16 Mar. 1976	BC-3A 55-01.5 165-10.3 115 m	2 RCM-4	130 da	
16 Mar.- 29 May 1976	BC-3B 55-01.3 165-04.8 116 m	2 RCM-4 1 TG-2	8, 73 da	
19 Mar.- 12 June 1976	BC-12A 55-48.2 163-54.1 97 m	2 RCM-4	15,85	

¹RCM-4: Aanderaa recording current meter, model 4.
TG-2,3: Aanderaa pressure gauges, models 2 and 3.

²Number of days of usable data.

B-BOP INSTRUMENT SUMMARY CONT.

DATE	LOCATION	INSTRUMENTS ¹	DAYS ²	REMARKS
20 Mar.- 30 May 1976	BC-7A 55-42.3 163-01.3 67 m	2 RCM-4 TG-2	71 da (TG-2)	
22 Mar.- 6 June 1976	BC-13A 55-30.2 166-01.7 122 m	2 RCM-4 1 TG-2		
31 May- 26 Sept. 1976	BC-2C 57-03.7 163-21.3 119 m	2 RCM-4 1 TG-2	23, 118 da	
29 May- 28 Sept. 1976	BC-3C 55-01.8 165-09.8 114 m	2 RCM-4	122 da	
30 May- 27 Sept. 1976	BC-6A 56-32.1 162-35.3 76 m	2 RCM-4	125 da	
6 June- 29 Sept. 1976	BC-13B 55-30.1 165-49.4 122 m	2 RCM-4 1 TG-2	35 da	Trawled
30 May- 27 Sept. 1976	BC-14A 56-02.3 161-50.0 51 m	2 RCM-4 1 TG-3	124 da	TG-3 not recovered
31 May- 26 Sept. 1976	BC-15A 57-36.4 162-45.2 51 m	2 RCM-4 TG-2	118 da	one RCM-4 lost
1 June- 23 Sept. 1976	BC-10A 57-16.6 169-32.8 66 m	1 RCM-4 1 TG-3	~ 60 da	
1 June- 24 Sept. 1976	BC-8A 57-58.5 168-49.5 73 m	2 RCM-4	~ 60 da	

¹RCM-4: Aanderaa recording current meter, model 4.
TG-2,3: Aanderaa pressure gauges, models 2 and 3.

²Number of days of usable data.

B-BOP INSTRUMENT SUMMARY

5

DATE	LOCATION	INSTRUMENTS ¹	DAYS ²	REMARKS
30 May- 27 Sept. 1976	BC-5A 56-49.2 163-06.6 70 m	2 RCM-4	119 da	
1 June- 25 Sept. 1976	BC-4C 58-35.8 168-20.7 58 m	2 RCM-4 1 TG-3	~ 60 d Faded	
2 June- 24 Sept. 1976	BC-9A 59-14.0 167-36.1 39 m	2 RCM-4	~ 60 d	
2 June- 24 Sept. 1976	BC-11A 59-40.9 167-13.6 31 m	1 TG-3	~ 90 d	
27 Sept. 1976	BC-2D 57-02.3 163-25.7 66 m	2 RCM-4 1 TG-2		
29 Sept. 1976	BC-13C 55-47.2 165-13.8 108 m	2 RCM-4 1 TG-2		
26 Sept. 1976	BC-15B 57-37.7 162-44.9 46 m	2 RCM-4 1 TG-2		
21 Sept. 1976	BC-17A 56-34.0 167-33.0 108 m	2 RCM-4		
25 Sept. 1976	BC-4D 58-36.6 168-21.7 55 m	2 RCM-4 1 TG-3		
24 Sept. 1976	BC-9B 59-13.0 167-42.0 40 m	2 RCM-4 1 TG-3		

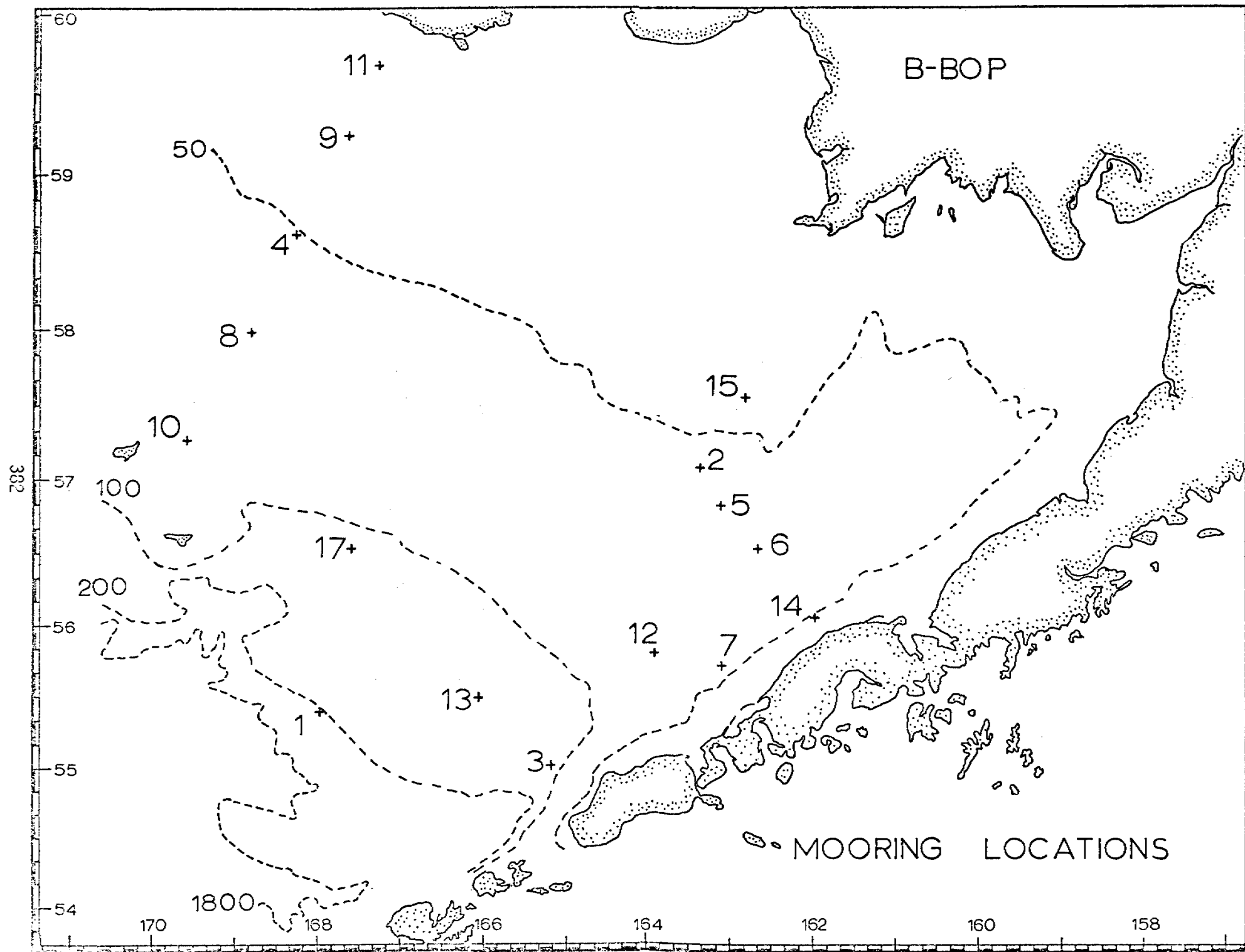
¹RCM-4: Aanderaa recording current meter, model 4.
TG-2,3: Aanderaa pressure gauges, models 2 and 3.

²Number of days of usable data.

B-BOP HYDROGRAPHIC DATA SUMMARY

DATES	STATIONS ¹	CRUISE	REGION	REMARKS
2-11 Sept. 1975	41	Discoverer RP-4-DI-75B Leg II	Outer Bristol Bay	
4-8 Nov. 1975	14	Miller Freeman RP-4-MF-75B Leg I	Outer Bristol Bay	Analog data only
16-23 Mar. 1976	27	Moana Wave RP-4-MW-76A Leg II	Unimak Pass	Stations near ice edge
16-18 June 1976	19	Miller Freeman RP-4-MF-76A Leg IV	Nearly entire B-BOP grid less deep slope	3 lines of closely spaced (~ 5 nm) stations; 2 are across 50 m front
7-18 June 1976	152	Moana Wave RP-4-MW-76A Leg VII		
3-10 Aug. 1976	85	Acona 233	AS/CA inter- action zone	Moana Wave aborted after massive elec- tronic failure
5-9 Aug. 1976	30	Moana Wave RP-4-MW-76C Leg II		
21-30 Sept. 1976	66	Moana Wave RP-4-MW-76C Leg II	AS/CA inter- action zone	Digitizer failure on Moana Wave
29 Sept-2 Oct. 1976	42	Acona		

¹Does not include stations occupied at mooring sites or outside B-BOP grid.



QUARTERLY REPORT

Contract No.: R7120840

Task Order No.: 141E

Quarter Ending 31 December 1976

Number of pages: 11

Norton Sound/Chukchi Sea Oceanographic
Processes (N-COP)

L. K. Coachman¹

R.L. Charneil²

J.D. Schumacher²

K. Aagaard¹

R.D. Muench²

1. Department of Oceanography
University of Washington, WB-10
Seattle, Washington 98105
2. Pacific Marine Environmental Laboratory
3711 - 15th Avenue N. E.
Seattle, Washington 98105

31 December 1976

Task Title: NORTON SOUND/CHUKCHI SEA OCEANOGRAPHIC PROCESSES (N-COP)

Report Period 1 October - 31 December 1976

I. Task Objectives:

The general objectives of the Norton - Chukchi oceanographic program are:

- 1) Verification of fluctuations in the predominantly northward transport through the system.
- 2) Delineation of the bifurcation of northward flow which occurs west of Point Hope.
- 3) Definition of time and space scales of eddies ubiquitous in the system and acquisition of data contributing to a dynamical description.
- 4) Definition of the circulation in Norton and Kotzebue sounds.

II. Field Activities:

A cruise was carried out in the region east of St. Lawrence Island and Norton Sound aboard R/V DISCOVERER during 26 September-9 October 1976. In addition to providing the most detailed current and hydrographic data yet available from Norton Sound, a meteorological program carried out synoptically with the oceanographic work provided detailed meteorological data. While the meteorological program is not included in this OSCEAP research unit (141), the data are complementary to the oceanographic data. All aspects of the cruise are detailed in an appended cruise report.

Atmospheric pressure data are now being received on a routine basis from existing meteorological stations at Cape Romanzof, Nome, Tin City, Kotzebue and Cape Lisburne. Such data are also being received from stations established specifically for this project at Savoonga, on St. Lawrence Island, and at Port Clarence. These data are all in the form of analog traces of pressure in time (barograph charts) and will need to be digitized prior to analysis.

III. Results:

Since the hydrographic data from the cruises carried out on this project are just now going through the final stages of routine processing, they are not yet available for analysis. A preliminary analysis of anchored current measure obtained in the Bering Strait has suggested that water transport was on the order of 10^6 m sec⁻¹ northward, in agreement with past estimates.

IV. Problems Encountered:

None.

V. Expenditures:

FY 77 funds have not been received for this research unit. An estimate of costs incurred is included on the attached sheet.

Estimate, based on projected FY 77 expenditures, of costs incurred during quarter ending 31 December 1976.

	<u>PMEL</u>	<u>UW</u>	<u>Total</u>
A. Salaries, Benefits, Overhead	\$24,000	\$13,814	\$37,814
B. Equipment	-	-	-
C. Supplies	1,000	4,750	5,750
D. Travel	1,750	1,500	3,250
E. Computer	-	2,500	2,500
F. Other direct	<u>2,500</u>	<u>12,823</u>	<u>15,323</u>
Total	\$29,250	\$35,387	\$64,637

Cruise Report
RP4-DI-76B, Leg V
26 September - 9 October, 1976.

To: Clinton D. Upham
Captain, NOAA
Commanding Officer
NOAA Ship DISCOVERER

From: Robin D. Muench (Chief Scientist, Leg V) *RDM*
Research Oceanographer
Pacific Marine Environmental Laboratory
Seattle, Washington

INTRODUCTION

This cruise has contributed to Phase 2 in a physical oceanographic survey of Norton Sound, Bering Straits, Kotzebue Sound and the Chukchi Sea. This is a joint program between NOAA/PMEL and the University of Washington. In addition, this cruise carried out research as part of the joint NOAA/PMEL and University of Washington program for studying Arctic coastal meteorology.

The general objectives of the Norton-Chukchi oceanographic program are: 1) verification of fluctuations in the predominantly northward transport through the system; 2) delineation of the bifurcation of northward flow which occurs west of Point Hope; 3) definition of time and space scales of eddies ubiquitous in the system and acquisition of data contributing to a dynamical description; and 4) definition of the circulation in Norton and Kotzebue Sounds. This cruise concentrated on the last objective, specifically, the circulation in Norton Sound.

The meteorological experiment was aimed at measuring the modification of an arctic air mass by a warmer ocean surface. Synoptic scale systems through the Alaskan area are periods when arctic air blows from the N to NE over Norton Sound and Bristol Bay. The air picks up large amounts of sensible heat and water vapor from the ocean as it moves offshore. This experiment is discussed further in Attachment A.

SCIENTIFIC PARTY:

This scientific party during Leg V was composed of the following personnel:

- 1) Physical Oceanography Program
Robin D. Muench, Research Oceanographer, PMEL (C/S)
Marilyn Pizzello, Physical Science Technician, PMEL
- 2) Arctic Coastal Meteorology Program
Mike Reynolds, Research Oceanographer, PMEL
Al Macklin, Oceanographer, UW

METHODS AND ACCOMPLISHMENTS

1. Physical Oceanography Program

One current meter mooring consisting of: 1) an Aanderaa RCM-4 Current Meter at a depth 10 meters above the bottom; 2) an AMF Model 242 Acoustic Release; and 3) subsurface flotation, sufficiently deep to escape the keel of the winter ice cover, was deployed at NC-16 southeast off St. Lawrence Island (see Attachment B). Since this meter will not be recovered until August, 1977, the timer was set for 30 minute intervals.

Salinity/temperature/depth measurements were made along a traverse southeast of St. Lawrence Island and on a grid throughout Norton Sound. Lowering rate of the underwater unit was 10 m/min. to minimize lowering rate error and preserve evidence of any fine structure. A temperature and salinity calibration were obtained on each cast. Locations of all stations are given in Attachment B.

Four 25-hour time series in salinity/temperature/depth and current speed and direction at 5 meter intervals throughout the water column were obtained at Stations 22, 24, 25 and 26 of the Norton Sound grid. CTD casts were made hourly on the hour during these time series, while current measurements were made hourly on the half hour.

The current measurements were made using a modified Aanderaa RCM-4 Current Meter with a deck read-out unit. The ship was anchored during each 25-hour station. Calibration samples for salinity and temperature were obtained every third cast during the time series stations.

In conjunction with the meteorology program, a close-spaced salinity/temperature/depth section was run offshore from Nome. Due to the high sampling rate, calibration samples were obtained only at the first and final casts of this series. As part of the same program, a 10-hour time series of salinity/temperature/depth and currents was occupied from an anchored position about 4 miles off Nome. Position of these stations are listed in Attachment B.

2. Arctic Coastal Meteorology Program

Attachment A.

CONSTRUCTIVE SUGGESTIONS

In my opinion this cruise has gone extremely smoothly, and I can think of no areas needing improvement.

ACKNOWLEDGEMENTS

Despite the loss of some meteorological gear, this has been a most successful cruise. The physical oceanographic program has been able to accomplish actually more than was proposed. Of particular merit have been the ship's willingness to occupy stations in relatively shallow (less than 10 fathoms) waters and to adjust quickly to changes in plan which resulted from the nature of the meteorology program. All of the ship's personnel gave tremendously of their time and energy, but special thanks to Captain Upham, LT(jg) Simpson, Lieutenant Commander McGee, Chief Survey Technician Murray and the Survey Technicians and Deck personnel who aided in our operations.

ATTACHMENT A

Meteorological Subprogram

Anticipated Goals

The meteorological program is primarily interested in the development of an unstable atmospheric boundary layer such as occurs when an arctic continental air mass blows out over open ocean. On this particular cruise the following experiments were planned:

- a. Field trial, calibration, and use of the new meteorological boom.
- b. Tethersonde profiles of the lower boundary layer. A kite was proposed as an alternate to the helium filled kytoons, especially during windy conditions.
- c. Radiosonde ascents.

The prime conditions for a successful experiment are N.E. winds blowing continental air offshore, but light enough to allow tethersonde studies.

Field Program

The final arrangement of meteorological stations was:

- a. A trackline of stations, lined approximately with the mean wind flow offshore. The spacing of the stations was logarithmic, allowing increased definition of the nearshore region. The trackline (Table A1) was occupied twice.
- b. An anchor station close to shore where the day/night transition could be studied in detail (Table A2).

Operational Comments

The tethersonde experiments suffered badly, mainly due to problems in launching a kite or balloon in the ship induced turbulence. Future plans must concentrate on a reliable and safe launching technique. The test kite was lost overboard due to a fouled tail which made the kite unstable. Later, a kytoon and sonde were lost when the tether line parted. After three successful flights with a second balloon and sonde, the sonde was lost during a launch when turbulence shook the package hard enough to break it's antenna-attachment bar.

The bow boom system proved most reliable and operational. The system is mechanically sound, easy to assemble and easy to swing inboard for maintenance. Data recording with PODAS worked well. The RF interference encountered during GATE was also experience here, but a shielding error was discovered which may alleviate future problems. The main problem with PODAS was insufficient software preparation which made processing of the acquisition tape impossible. Hopefully this will be rectified before the computer is disassembled for maintainance in November.

Radiosondes as usual worked reliably.

TABLE A1

Meteorological Station Summary - Trackline

Station	Time-GMT	Approximate Position	Radio-sonde	Tether-sonde	Surface Weather	Remarks
	09/30=0036	162°10' 64°17.3'	NS1		9.2 957 68.5	Eastern Norton Sound
	10/01-0011	165°31.3' 64°25.7'	NS2		8.1 035 80	Approx. 5 mi. fm Nome
	10/02-0007	165°24.3' 64°11.2'	NS3		6.7 113 74	Approx. 19 mi S. of Nome
	02-1814	" " " "	NS4		7.1 072 73	" " "
N1	03-2354	165°25.0' 64°29.1'	NS5	N-BLP-1	7.9 071 61	One mile off Nome
N2	0210	165°28.0' 64°27.0'	NS6	N-BLP-1	8.8 050 54	BLP line broke
N3	0418	165°30.31' 64°27.18'	NS7		8.8 056 60	Four mi. off Nome
N4	0525	165°37.2' 64°23.8'	NS8		7.0 055 67	Eight mi. off Nome
N5	0643	165°50.5' 64°18.1'	NS9		7 054 68	Sixteen mi. off Nome
N6	0847	166°16.6' 64°06.8'	NS10		6.5 050 72	Thirty Two mi. off Nome
N5B	1042	165°51.1' 64°18.1'	NS11		4 052 68	Sixteen mi. off Nome
N4B	1222	165°35.8' 64°25.0'	NS12		2.8 052 68	Eight mi. off Nome
N3B	1415	165°30.3' 64.27.4	NS13		1.5 050 70	Four mil off Nome
N2B	1505	165°25.92' 64°28.08'	NS14		.5 049 84	Met Boom Orientation Test
N1B	2045	165°25.0' 64°29.0'		N-BLP-2		Test Flight with BLP#2 Sonde
N2C	2145	165°36.2' 64°28.0'	NS15		4 041 50	

TABLE A2

Meteorological Station Summary - Anchor Station N3C

Time-GMT Radiosonde	Radio- sonde	Tether- sonde	Surface Weather	Remarks
10/03-2327	NS16		5.1 036 41%	
10/04-0001	NS17	NS-BLP-3	4.7 030 47	
0425	NS18	NS-BLP-4	3.0 023 64	
0625	NS19		2.9 026 64	BLP Sonde antenna broke, Sonde lost
0713	NS20		2.7 029 68	
0753	NS21		2.9 029 67	
0848	NS22		2.9 031 67	
0950	NS23		2.1 028 68	

ATTACHMENT B

CORSEC. NO.	GRID NO.	DAY/TIME E	LATITUDE N	LONGITUDE W	STD DEPTH m	WATER DEPTH m
----------------	-------------	---------------	---------------	----------------	----------------	------------------

EAST ST. LAWRENCE ISLAND SECTION

1	7	27-0850	63-12.6	168-36.2	22	26
2	8	1008	63-05.8	168-21.6	19	42
3	9	1105	63-01.7	168-07.7	31	35
4	10	1213	62-54.3	167-52.1	18	21
5	11	1312	62-48.9	167-37.6	24	27
6	12	1412	62-43.9	167-22.6	30	34
7	13	1506	62-38.9	167-07.5	31	35
8	14	1615	62-33.9	166-52.3	25	29
9	15	1721	62-29.5	166-39.3	19	23
10	NC-16	1813	62-36.4	166-53.7	26	29

NORTON SOUND GRID

11	16	27-2354	63-21.8	165-43.4	21	24
12	17	28-0217	63-43.0	165-54.0	22	26
13	18	0421	64-04.9	166-08.7	20	24
14	19	0532	64-14.5	166-14.0	20	24
15	20	0631	64-22.8	166-07.5	23	27
16	21	0740	64-27.1	165-59.8	29	33
17	22	0900	64-26.1	165-31.6	22	26
18	23	0958	64-20.1	165-29.3	20	23
19	24	1059	64-11.3	165-21.1	16	19
20	25	1222	63-53.9	165-20.5	16	19
21	26	1357	63-37.6	165-04.1	13	17
22	27	1612	63-17.3	165-24.2	16	20
23	28	2048	63-49.7	164-21.8	12	17
24	29	2227	63-58.1	164-47.3	15	18
25	30	2330	64-07.7	164-50.3	14	17
26	31	29-0112	64-15.0	164-48.5	11	15
27	32	0218	64-21.4	164-56.0	29	32
28	33	0332	64-26.2	164-31.5	23	26
29	34	0446	64-17.9	164-10.0	12	16
30	35	0608	64-06.1	164-03.7	18	22
31	36	0822	63-41.7	163-46.2	11	15
32	37	1016	63-36.7	163-07.1	10	14
33	38	1145	63-49.9	163-14.8	14	18
34	39	1342	64-15.6	163-13.9	16	20
35	40	1449	64-23.2	163-35.0	15	19
36	41	1702	64-16.0	162-44.0	19	25
37	42	1843	63-58.2	162-35.2	14	21
38	43	2001	63-43.5	162-28.7	11	15
39	44	2133	63-51.7	161-49.1	15	18
40	45	2310	64-05.2	161-50.4	15	19
41	46	30-0034	64-18.3	162-10.5	15	19
42	47	0202	64-15.0	161-26.7	12	16
43	48	0341	63-55.2	161-18.5	9	13
44	49	0515	63-39.8	161-21.5	10	14

CONSEC. NO.	GRID NO.	DAY/TIME Z	LATITUDE N	LONGITUDE W	STD DEPTH m	WATER DEPTH m
----------------	-------------	---------------	---------------	----------------	----------------	------------------

25-HOUR TIME SERIES STATION

45-73	22	30-1415 01-1904	64-25.8	165-31.7	23	27
74-97	24	01-2207 02-2105	64-11.2	165-24.3	15	19

CLOSE-SPACED METEOROLOGICAL TRANSECTS

98	N-1	03-0130	64-29.0	165-25.3	10	14
99	N-2	0317	64-28.2	165-26.0	13	17
100	N-3	0433	64-27.1	165-30.4	20	24
101	N-4	0533	64-23.8	165-37.2	24	28
102	N-5	0649	64-18.1	165-50.5	16	20
103	N-6	0833	64-06.7	166-16.2	21	25
105	N-5B	1051	64-18.2	165-51.2	16	21
106	N-4B	1227	64-25.1	165-35.3	27	31
107	N-3B	1334	64-27.1	165-30.4	20	24
108	N-2B	1457	64-28.1	165-26.1	14	18
109	N-1	1948	65-28.5	165-24.3	11	15
110	N-2C	2220	64-27.9	165-26.3	13	17

10-HOUR METEOROLOGICAL TIME SERIES STATIONS

111- 120	N-3C	04-0028- 04-0900	64-26.7	165-30.8	20	24
-------------	------	---------------------	---------	----------	----	----

25 HOUR TIME SERIES STATIONS

121- 146	25	04-1309- 05-1406	63-54.0	165-20.1	15	19
147- 171	26	05-1700- 06-1700	63-37.8	165-02.3	13	17

CURRENT METER MOORING NC-16

Agency - PMEL

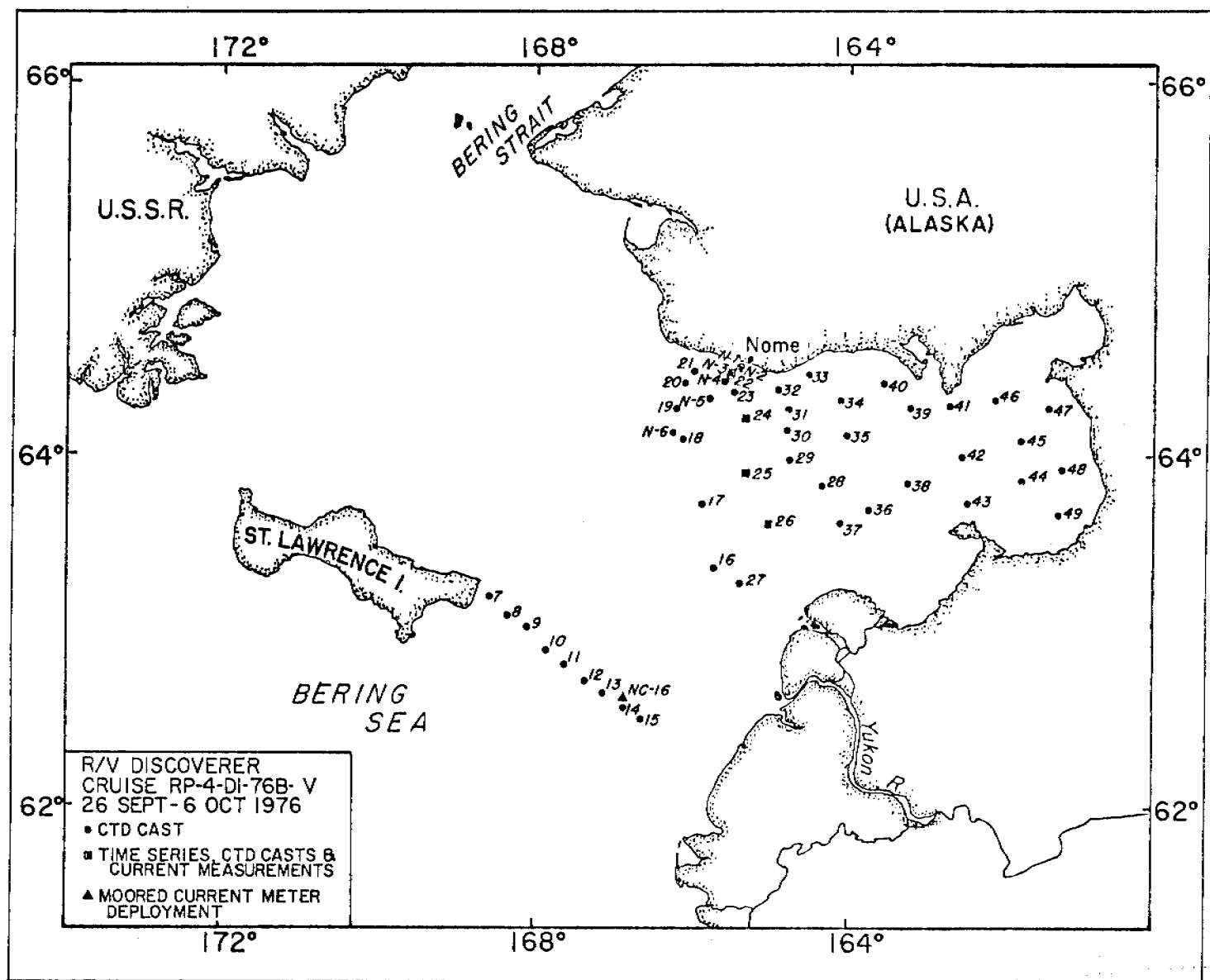
Deployment Date/time Z September 1976: 27-2007

Position: 62°37:0'N 166°53.2'W

Loran C Rates: X - 18090.09 Y - 29921.01

Depth: 19 meters

Receiver channel: 9



QUARTERLY REPORT

Contract No.:

03-5-022-67, T.O. #1

Research Unit No.:

151

Reporting Period:

1 October 1976-31 December 1976

Number of Pages:

4

STD Measurements in Possible Dispersal Regions of the Beaufort Sea

Knut Aagaard

Department of Oceanography
University of Washington
Seattle, Washington 98195

31 December 1976

A76-75

I. Objectives

To examine by means of STD measurements the possible sinking and spreading into the Canadian Basin of waters modified on the Beaufort shelf. Such sinking and spreading constitute an unexplored but possibly very important dispersal mechanism.

II. Field Activities

The STD field work was coordinated with that of the current meter project (RU #91), with first arrival Barrow on 3 October 1976 and departure 6 November 1976. The STD stations were accomplished during 31 October-4 November (GMT), the field party consisting of Knut Aagaard and Clark Darnall, both of the Department of Oceanography, University of Washington. The aircraft, a Bell 205, I.D. no. N2215W, was on charter from ERA Helicopters.

Two sets of CTD stations, each consisting of two parallel lines normal to the coast, were run across the shelf. One set was off Lonely and the other off Oliktok. Typical station spacing was five miles and parallel line spacing 15 miles. The methods were essentially the same as those employed the previous contract year. One important improvement on the earlier technique was a redesigned sensor package sufficiently small to permit its deployment through an eight-inch auger hole. This greatly expedited casts but did reduce the opportunities for the scientific party to further develop their expertise with ice chisels.

The stations are listed on the following page.

CTD Stations

<u>Station No.</u>	<u>Date, GMT</u>	<u>Time, GMT</u>	<u>Latitude, N</u>	<u>Longitude, W</u>	<u>Sounding, m</u>
1	31 October 1976	0049	70°55.2'	150°08.2'	24
2	31 October 1976	0129	70°59.6'	150°07.0'	25
3	31 October 1976	1937	71°04.2'	150°04.3'	32
4	31 October 1976	2030	71°09.4'	150°02.1'	45
5	31 October 1976	2104	71°14.1'	149°59.9'	303
6	31 October 1976	2220	71°19.0'	149°57.4'	--
7	31 October 1976	2319	71°15.0'	149°14.5'	--
8	1 November 1976	0028	71°08.2'	149°18.5'	54
9	1 November 1976	1935	70°52.2'	149°24.0'	26
10	1 November 1976	2008	70°57.3'	149°21.6'	31
11	1 November 1976	2044	71°02.3'	149°19.8'	34
12	1 November 1976	2117	71°07.4'	149°18.6'	44
13	1 November 1976	2154	71°12.9'	149°17.9'	117
14	3 November 1976	2123	71°12.7'	152°18.9'	36
15	3 November 1976	2155	71°17.3'	152°10.4'	50
16	3 November 1976	2225	71°21.9'	152°04.5'	70
17	3 November 1976	2258	71°26.7'	151°58.0'	216
18	3 November 1976	2338	71°31.2'	151°50.7'	>440
19	4 November 1976	2016	71°21.8'	152°58.1'	86
20	4 November 1976	2048	71°25.4'	152°49.7'	71
21	4 November 1976	2118	71°30.3'	152°43.0'	73
22	4 November 1976	2149	71°35.3'	152°36.0'	136
23	4 November 1976	2250	71°39.2'	152°28.7'	250
24	4 November 1976	2336	71°44.0'	152°23.8'	--

III. Results and IV. Preliminary Interpretation

Processing and analysis of data are continuing. All data tapes from the previous contract year have been submitted. Data listings from this past trip are presently being filtered and calibrated. Preliminary examination of these listings indicate a somewhat different hydrographic regime than the previous year, pointing out the need for caution in regarding any one year as typical.

V. Problems Encountered

We now have a very smoothly running CTD program, having sorted out most of the problems on earlier trips; from landing to takeoff we can do a complete station on the inner shelf in 20-25 minutes. However, it's important to realize that the work is done under difficult conditions and that hazards are always present, any one of which can jeopardize the effort. To illustrate, I quote from my journal of 29 October: "Cloudy, light westerly winds, temperatures just below zero. Took off [from Deadhorse] at 0900, fueled at Oliktok and proceeded to farthest station on western leg [about 50 miles out] and began the CTD cast. A generator malfunction forced a temporary halt to the cast with about 60 m of wire out, and we began pulling up to start the cast again. A sheet of ice had moved across the hole on the underside however, and the CTD sensors were suddenly stuck. There was active ice movement in the area but no surface indication of anything near the hole; we drilled and chiseled to no avail, for the underneath piece had moved a considerable distance by this time. Diving was our only chance. We took off at 1130 direct to Deadhorse [73 miles away], fueled and loaded on the diving gear, and headed back. Found the site with no trouble, as we had left the gas cans to mark the spot. [By pulling in wire til the sensor package was tightly against the subsurface ice jam], the meter wheel indicated a lateral distance to the fish

[sensor package] of about 26 m. Stepping off this distance, plus a bit more, and going off to the left, we found single thickness ice [i.e., no subsurface rafting]. Cut the diving hole, and Clark went down. Found the fish quickly in a mess of rafted ice and tied on to it with an extension of his tending line, then dropped his own diving weight and cut the fish loose from the wire. We took the load on the tending line and hauled diver and gear in with nothing lost. [The adjacent ice had been ridging actively since our return and] by the time we had loaded up the ridging was only ten feet from the helicopter. We returned to Deadhorse about 1530. We had been very close to having lost the whole CTD program for the season." We were equipped to re-terminate the sensors and did so that same evening; the next day we ran the first CTD stations.

VI. Estimate of funds expended (30 November 1976)

TOTAL ALLOCATION (5/16/75-9/30/77):		\$142,627
A. Salaries	9,543	
B. Benefits	1,079	
C. Expendable Supplies & Equipment	3,743	
D. Permanent Equipment	23,277	
E. Travel	3,333	
F. Computer	160	
G. Other Direct Costs	18,850	
H. Indirect Costs	<u>4,599</u>	
TOTAL EXPENDITURES:		<u>64,584</u>
REMAINING BALANCE:		\$78,043

Quarterly Report

Research Unit # 208
Reporting Period 10/1/76-12/31/76
Number of Pages: 6

YUKON DELTA COASTAL PROCESSES STUDY

William R. Dupré
Department of Geology
University of Houston
Houston, Texas 77004

12/30/76

QUARTERLY REPORT

I. Task Objectives

The overall objective of this project is to provide data on geologic processes active within the Yukon-Kuskokwim delta in order to aid in the evaluation of the potential impact of scheduled oil and gas exploration and possible production. In particular, attention has been focused on the following:

- 1) Study the processes along the Yukon-Kuskokwim delta shoreline (e.g., tides, waves, sea-ice, river input) in order to develop a coastal classification including morphology, coastal stability, and dominant direction of longshore transport of sediments. (Task D-4, B-2).
- 2) Study the hydrology and sediment input of the Yukon and Kuskokwim Rivers as they largely determine the sediment budget of the northern Bering Sea. (Task B-11, B-2).
- 3) Determine the type and extent of Quaternary faulting and volcanism in the region. (Task D-6).
- 4) Reconstruct the late Quaternary chronology of the delta complex in order to determine:
 - a) frequency of major shifts in the course of the Yukon River.
 - b) effects of river diversion on coastal stability.
 - c) relative age of faulting and volcanism.
 - d) frequency of major coastal storms as recorded in chenier-like sequences along the coast.

II. Field and Laboratory Activities

A) Field Trip Schedule:

none

B) Scientific Party

not applicable

C) Methods

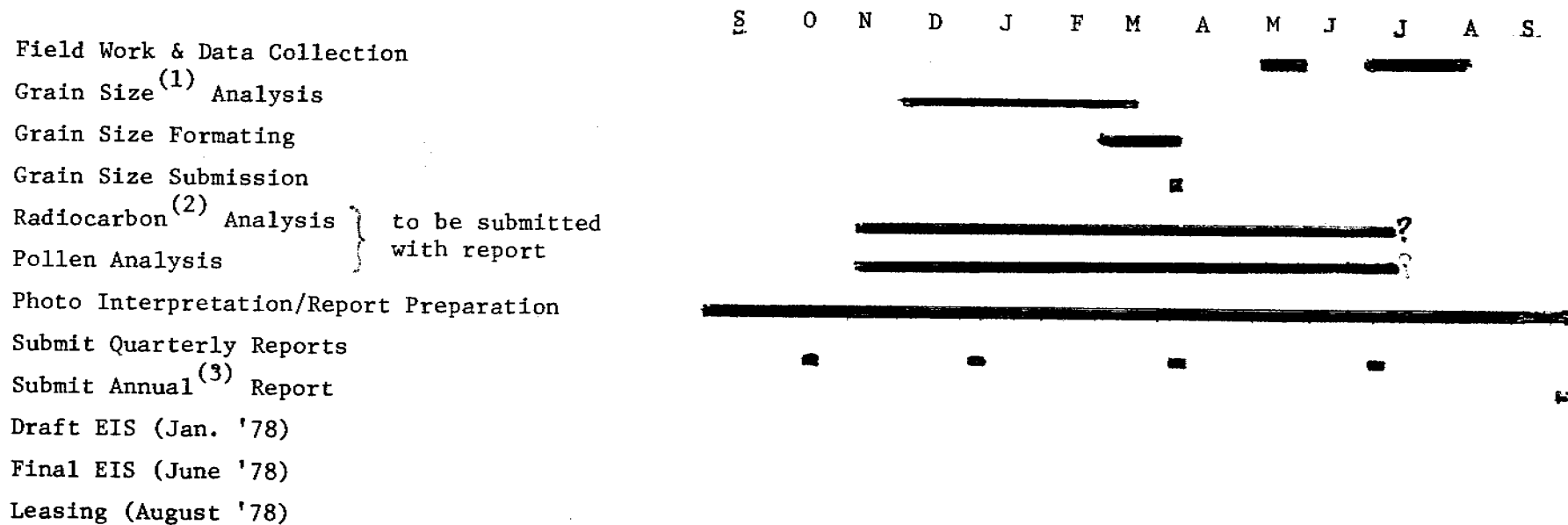
- 1) Textural analysis of beach and river deposits by seiving - in progress
- 2) Radiocarbon dating of wood and peat - in progress
- 3) Interpretation of Landsat imagery for evidence of offshore sediment transport

D) Data analysed

- 1) Number and type of samples collected
not applicable
- 2) Number and type of analyses
 - a) Textural analyses: 10 completed, 90 in progress
 - b) Radiocarbon analyses: 13 in progress

E) Milestone Chart and Data Submission Schedules

- 1) See Figure 1
- 2) The textural analyses have been delayed approximately two months because of delays and uncertainty of funding for FY 77 which prevented contracting the work. Radiocarbon dates are delayed because of backlogs, and final submission may not be until June.



- 1. Approx. 100 samples
- 2. Approx. 25 samples
- 3. Final Report if Funding Not Continued

Figure 1: ACTIVITY/MILESTONE/DATA MANAGEMENT CHART

III. Results:

The geologic map and coastal stability map are in progress, as are most of the textural and radiocarbon analyses. One figure is included, however, to show the utility of using Landsat imagery to determine offshore sediment transport patterns (Figure 2).

IV. Preliminary interpretation of results:

A comparison of sediment plumes off the Yukon delta (as delineated by Landsat imagery) with the distribution of modern shelf sediments, oceanic currents and water masses suggest a strong correlation between the Alaska coastal waters and present-day sedimentation patterns.

Much of the sediment from the Yukon River enters the Bering Sea to the southwest. Once on the shelf, however, it is diverted sharply to the north and northwest where it is transported within the Alaska coastal water with little or no mixing with oceanic water to the west. The modern shelf sediment as mapped by McManus and others is also confined to areas within the coastal water, suggesting that the contact between coastal and oceanic water is an effective barrier to diffusion of sediment to the west and that advective shelf sediment transport is dominant in the area.

It seems likely that the dispersion patterns as defined by Landsat imagery and oceanic measurements is a good indication of how pollutants might behave once introduced to the marine environment. Thus pollutants are likely to be confined to the coastal waters or transported to the north and northwest (i.e. offshore) under most summer, fair weather

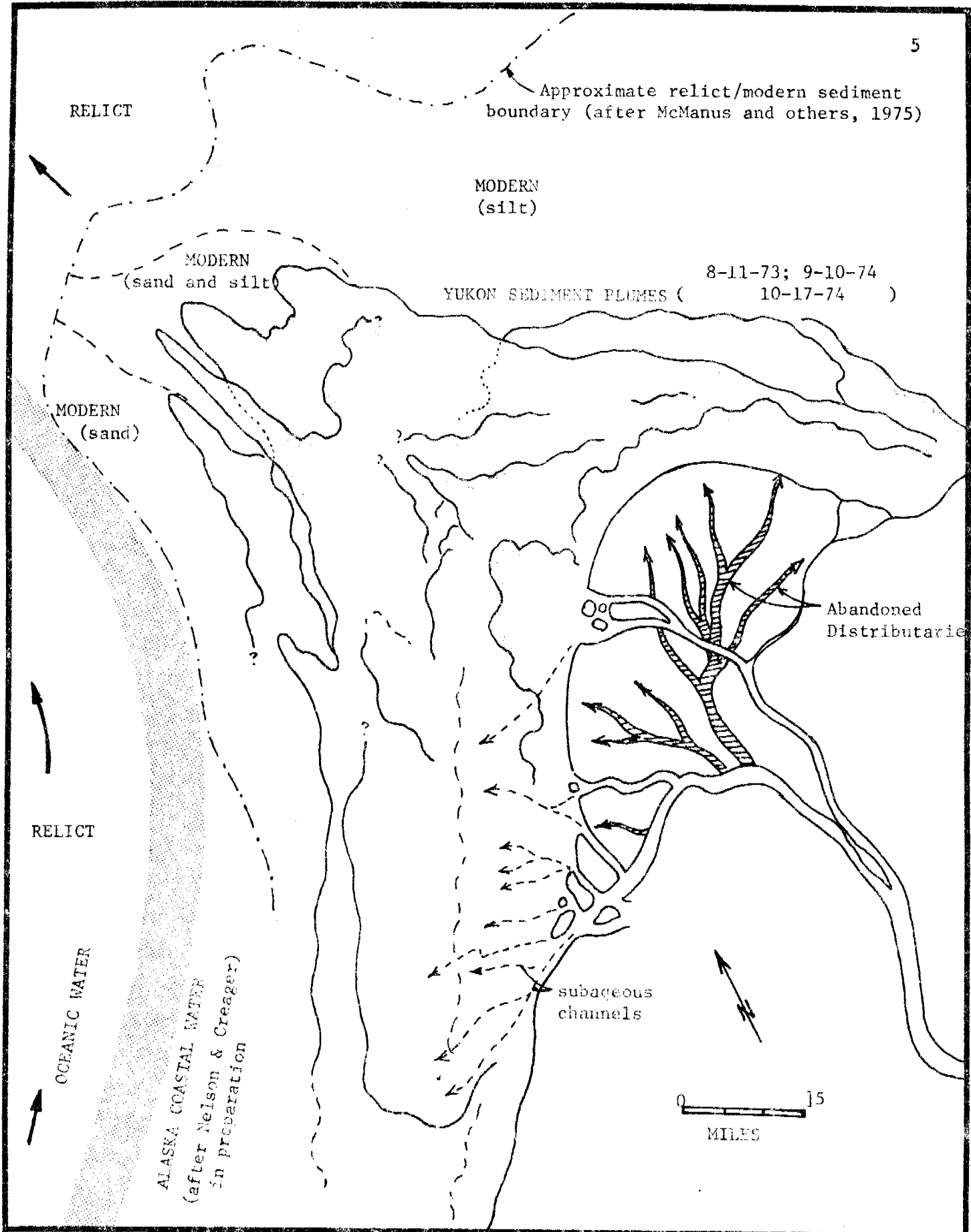


Figure :
 Comparison of offshore sediment plumes, modern and relict shelf sediments,
 and oceanic currents and water masses off the Yukon delta.

conditions. What is urgently lacking, however, is information on winds, waves, and currents under storm and winter ice conditions. In addition, there is limited evidence that bedload transport of sediments is more sensitive to nearshore bathymetry and seems more likely to be transported to the southwest in some areas than is suspended sediment.

V. Problems encountered/recommended changes

The only serious problem was the delay in approval of funding which delayed sample preparation and analysis.

VI. Estimate of funds expended:

A) Salary:

assistant @ \$3,25/hr.	\$195.00
------------------------	----------

B) Sample preparation:

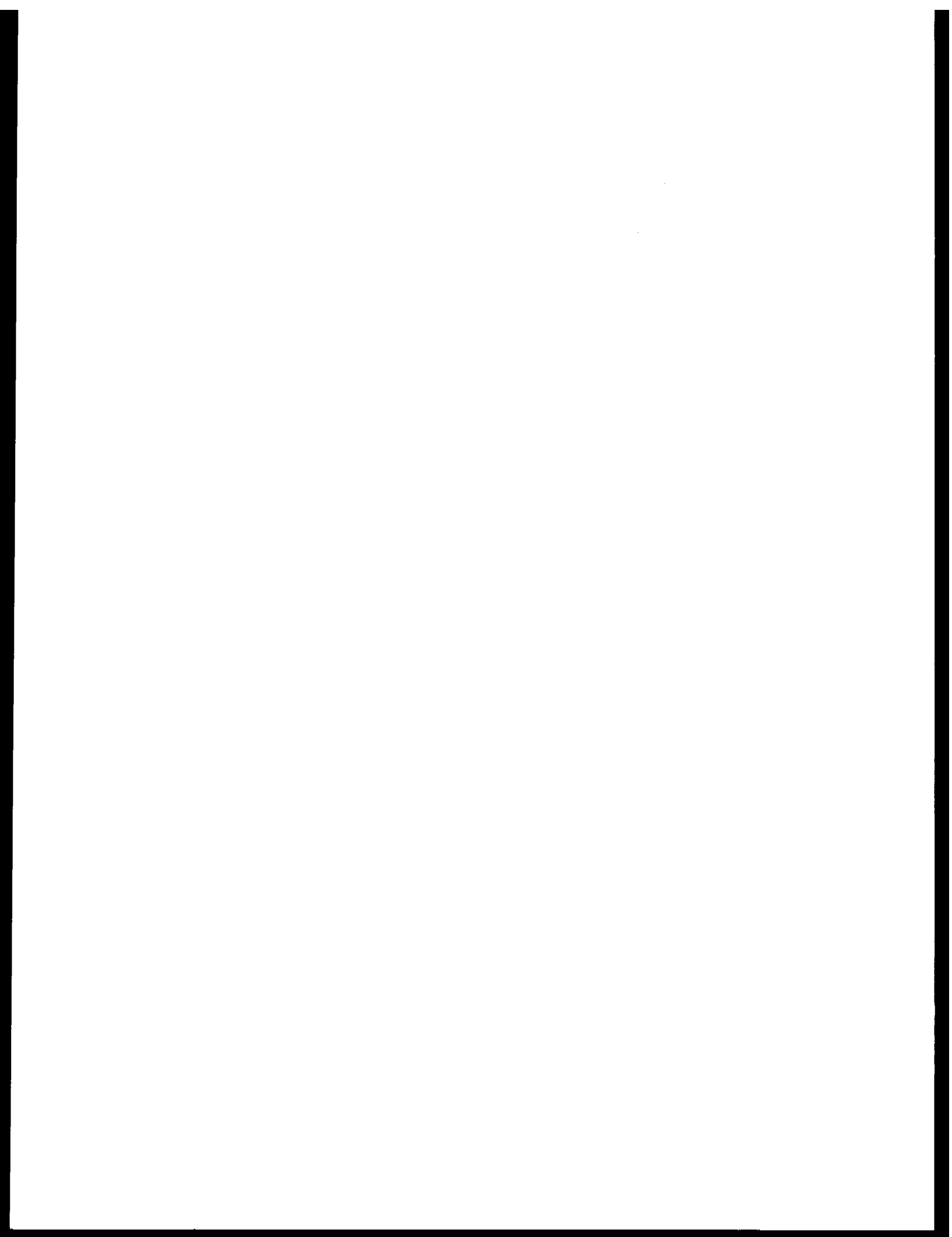
10 textural analyses @ \$25./sample	250.00*
-------------------------------------	---------

C) Equipment:

1) Reference material	75.00
2) Drafting material	25.00
3) Xeroxing	<u>25.00</u>

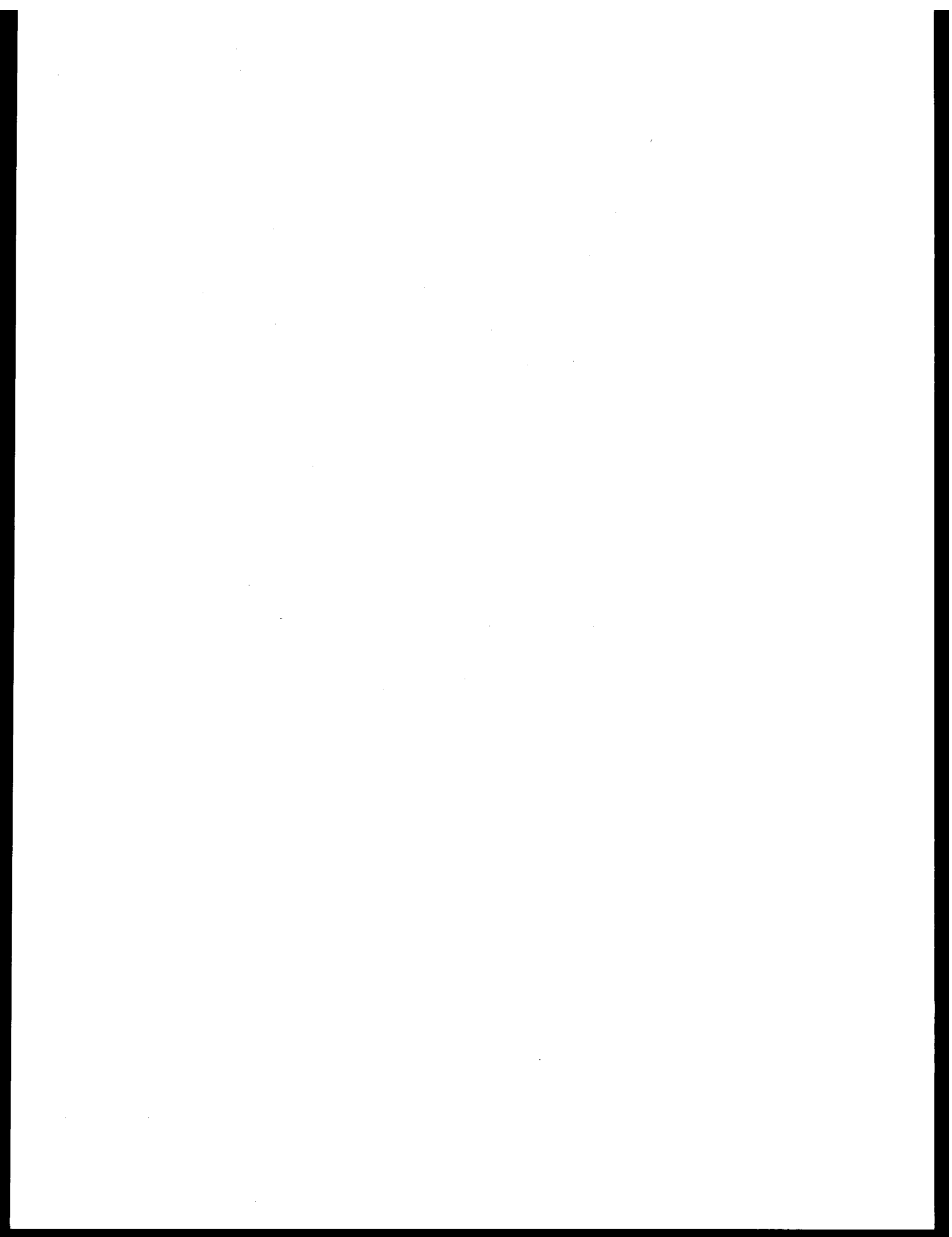
Estimated Total Expenditures	\$570.00
------------------------------	----------

* includes formatting



RU# 217

NO REPORT WAS RECEIVED



QUARTERLY REPORT

Contract #03-5-022-91

Research Unit #244

Reporting Period: Sept. 1 - Dec. 31, 1976

Number of Pages: 59

STUDY OF CLIMATIC EFFECTS ON FAST ICE EXTENT
AND ITS SEASONAL DECAY ALONG THE BEAUFORT AND
CHUKCHI COASTS

Principal Investigator

R. G. Barry

Acting Director, Professor of Geography

Institute of Arctic and Alpine Research

University of Colorado

Boulder, Colorado 80309

31 December, 1976

I. TASK OBJECTIVES

The primary objective of this study is to assess the role of climate factors in determining the extent and seasonal decay of fast ice along the Beaufort and Chukchi coasts. Activities this quarter have concentrated on continuation of ice mapping for the Beaufort and Chukchi sectors and synoptic and analysis for the Chukchi sector.

II. ACTIVITIES

1. Field

None

2. Office

A. Period

1 September - 31 December 1976

B. Personnel

R. G. Barry, Principal Investigator

R. E. Moritz, Research Assistant

J. C. Rogers, Research Assistant

R. Keen, Research Assistant

G. Wohl, Research Assistant

M. Eccles, Programming Consultant

R. Straub, Work Study Student

S. Chapman, Work Study Student

C. Methods

1. Remote Sensing Data

a. Maps of Ice Surface Morphological Characteristics

Mapping and interpretation methods for this task are described in our last Quarterly Report (9/30/76: Section II.2.C.1.b).

b. Ice Truthing 1976 OCS SLAR Imagery

A joint effort between this project and Dr. Stringer's group has been undertaken to determine the type of ice information contained on the May, 1976 SLAR imagery obtained for OCS.

The methods used by INSTAAR workers are described in this section.

Hard-copy SLAR images at three scales (1:1000,000; 1:500,000; 1:250,000) were placed on the zoom transfer scope and areas of different tone were mapped on standard projections. Photograph numbers and flight transects from our 1976 fields (see Quarterly Report 6/30/76: section II.1.A. and Figure 1) were then plotted on the same maps. Our photographs and field notes were then used to compare visually-observed ice types with the tone on the SLAR images.

2. Meteorological data: Chukchi Synoptic types

The daily catalog of synoptic types for the Chukchi sector was described in the last Chukchi Quarterly Report (9/30/76: section II.2.C.2.). Using these data, several synoptic parameters have been determined as follows:

- (i) Percentage frequency of each type for each month for the period 1946-74.
- (ii) A matrix of synoptic type transitions. $A(I,J)$, giving the number of transitions from type I to type J, has been computed for each month and for the annual total.
- (iii) If N_I , N_J and N_{Total} are the frequencies of type I, type J, and all types, respectively, then $B(I,J) = N_I N_J / N_{Total}$ is the frequency of transitions from type I to type J if the types

occur randomly. The ratio of actual to random occurrences $A(I, J) / B(I, J)$ has been computed for the year and for three seasons (defined below).

(iv) The median duration of persistence of duration of each type has also been determined. The persistence is assumed to be a first-order Markov process, where

$$P(I) = A(I, I) / N(I)$$

is the probability that type I will be succeeded the next day with type I.

$$T_{1:2}(I) = \ln(0.5) / \ln P(I)$$

is the half-life of the persistence, i.e. the time at which the probability of continuing occurrence of type I drops to 0.5. The same argument applies to the days preceding a chosen date. Hence, the median length of a spell of type I is given

$$T_m = 2 T_{1:2}(I).$$

Substituting the expected random matrix $B(I, I)$ for $A(I, I)$ yields the expected persistence (Tr) assuming random occurrences of type I. This has also been computed for each type.

(v) The degree of change in type frequency between months has been used as a basis for identifying seasons of predominant circulation regime.

$$\Delta_1 = \sum_I | f_m(I) - f_{m-1}(I) |$$

is the sum of the absolute values of the between-month difference in frequency of each type.

$$\Delta_2 = \left| \sum_{I,J} | A_m(I, J) - A_{m-1}(I, J) | \right|$$

is an analogous sum of differences for the transition matrices. Similar calculations were made for the sum of the squares of the differences in both cases.

3. Interaction Case Studies

Large Grounded Ridges off Oliklok, 1975-1976

It has been reported (Kovacs, 1976) that a very large, elongate shear ridge field was grounded about 60 km N and NE of Oliktok Point at some time during winter-spring, 1975. These ridges constitute the largest such grounded feature we have observed on 4 years of Beaufort Sea Coast LANDSAT imagery. Furthermore, 1976 SLAR imagery and summer, 1975 and 1976 LANDSAT data show that this formation was unusually stable and long-lasting. Our preliminary analyses indicate that the feature originated under somewhat anomalous weather and ice-motion conditions and that subsequent fact ice development in Harrison Bay was greatly influenced by it, hence the importance of a case study approach.

The methods employed here are primarily related to remotely-sensed data analysis techniques. Postions of the ridge field and tonal variations on its surface were mapped from 1:500,000 scale LANDSAT prints using techniques described in our last Quarterly Report (section: II.2.C.1.b.). The breakup and decay of the field are mapped for summers, 1975 and 1976. Winter, 1975 LANDSAT images were inspected in order to bracket the date of establishment of the feature. Additionally, several meteorological data sets, NOAA-4 imagery and SLAR images were analyzed to pin down the formation mechanisms and structure of the feature, and its subsequent influence on Harrison Bay ice.

E. Data Collected/Analyzed

1. Remote Sensing Data

a. Maps of Ice Surface Morphological Characteristics

The following LANDSAT scenes ($1:10^6$ scale transparencies) have been mapped for the decay season 1974 in the Barrow sector:

<u>Date</u>	<u>Scene ID</u>
6/29/74	1706-21322
7/3	1710-21551
7/15	1722-21202
7/16	1723-21260
7/20	1727-21485
7/21	1728-21540
8/22	1760-21302
9/8	1777-21240

Additional data used in the mapping analysis include 1:250,000 scale X-band SLAR images, flown April 29, 1974, and 1:132,000 Color IR photography flown June 21, 1974.

The following LANDSAT scenes ($1:10^6$ scale transparencies) have been mapped for the decay season 1973 in the Kotzebue sector:

<u>Date</u>	<u>Scene ID</u>
5/17/73	1298-22161
6/01	1313-21585
6/18	1330-21525
6/22	1334-22155
7/09	1351-22095

b. Ice Truthing 1976 OCS SLAR Imagery

Photographic contact prints of several SLAR images were obtained from the Geophysical Institute files (courtesy of

Dr. W. Stringer) during our summer, 1976, ice-reconnaissance flights. As listed in OCS Arctic Project Bulletin #10, the tracks include numbers 1,2,3,4, and 5. Other data used in the analysis are hand-held, aerial oblique, color photographs and field notes.

2. Synoptic Catalog

The synoptic catalog of daily MSL pressure pattern types for the Chukchi sector has been analyzed for 1946-74 by the methods described in 2.C.2. above.

3. Interaction Case Studies

Ridge-building off Oliktok Point, 1975

The following LANDSAT scenes have been mapped and analyzed to date:

<u>Date</u>	<u>Scene ID</u>
3/25/75	1975-21163
3/26	1976-21221
4/20	2088-21178
7/21	2180-21281
9/12	2233-21213
11/3	2285-21094

Other remotely-sensed data analyzed for this case study include a 1:1,000,000 scale SLAR image (Designated track #5, OCS Arctic Project Bulletin #10).

Daily wind speeds and wind directions have been extracted from the NOAA NCC publication "Local Climatological Data" for Barrow and Barter Island, March-April, 1975. These data are used to study the wind-effects on ridge-building processes. Also used were the atmospheric pressure, surface wind stress, and

geostrophic wind fields from the AIDJEX data banks, for April, 1975. The stress data are calculated using boundary-layer models, as discussed in Leavitt (1975) and Brown (1975).

III. RESULTS / DATA PRODUCTS

1. Ice Features

A. Working maps have been drawn and interpreted for 1976 for the Barrow sector. Maps for 1976 for the Barter Island sector have also been prepared in draft. The final products will be forwarded to the OCS Arctic Project office upon transfer to the OCS UTM base map.

Maps of surface morphology of fast ice in Kotzebue Sound area for 1973 are included as Figures 1-5 with detailed legends. Work on 1974 is in progress.

B. Ice Truthing OCS SLAR Imagery

Analysis of SLAR for the Beaufort coast is still underway. A full report will follow in our next Quarterly.

C. LARSYS Analysis of LANDSAT Radiance Data

Analysis of the results of our project with LARS is proceeding further (see Quarterly Report, 9/30/76 for initial results). A formal publication should be ready for inclusion in our next report.

2. Synoptic Climatology

A. Magnetic Tape Archive of Pressure-Pattern Catalog for the Beaufort Sector

A daily listing of atmospheric pressure-pattern types and related statistics has been filed with the OCS Project Office, Juneau. The methods and initial results of this classification scheme were

reported in our Annual Report (3/31/76). The data are available to any interested OCS investigator. The significance of each pattern-type for ice-formation and breakup processes is currently under investigation (see Appendix 1).

B. Synoptic data for the Chukchi sector

Maps of the 22 MSL synoptic pressure pattern types are included (Figures 6-27). The isolines are standard deviations (0.5 intervals) from the normalized pressure values. (The objective technique used to develop the classification is described in Beaufort Sea Annual Report, March, 1976.

3. Climate-Fast Ice Interaction

In this section the results of an initial attempt to determine the climatic factors associated with the extent and decay of fast ice along the Beaufort Sea Coast during the summer are presented. Due to the nature of the data, the analysis also applies to the climatic factors which would affect the summertime retreat of pack ice in the Beaufort Sea. This study is an extension of the work done on case studies # 1 and # 2 presented in our last quarterly report (pp. 33-39).

The data consist of:

a.) Climatological data obtained from the "Local Climatological Data" for Barrow, Alaska since 1953. Included are daily temperature data in the form of thawing degree days (TDD's), cloud cover data, wind speed and direction, barometric pressure, and geostrophic wind data which have been described in previous reports.

b.) Barnett's (1976) data regarding the extent of the retreat of fast and pack ice by Sept. 15 of each year since 1953.

A preliminary analysis of the relationship between the individual meteorological parameters and the ice extent and retreat by Sept. 15 of each year was carried out for temperature/ice relationships in the last quarterly report (pp. 33-35). There it was found that a high relationship existed between summertime thawing degree days and the extent of ice retreat northward. The completion of this analysis is shown in Tables 1-4.

(i) Table 1: which shows the relationship between the average number of days with 12 categories of direction during the 12 severe and 11 light summers since 1953 (including 1975). The severe summers are those in which the distance northward from Point Barrow to the 4/8 ice concentration boundary (southernmost) is zero or only a few kilometers by Sept. 15. Light ice summers are those in which a major retreat of the pack ice occurs and include (in order of increasing severity) 1958, 1968, 1962, 1961, 1973, 1963, 1959, 1972, 1954, 1974, 1957 (Barnett, 1976).

(ii) Table 2 shows the relationship between the geostrophic wind direction during the severe and light ice summers. The average number of days geostrophic wind direction during the severe/light ice summers are given after the wind directions were divided into eight categories.

(iii) Table 3 shows the relationship between the average number of summer days with a given synoptic type category (only the major synoptic types are included) during both severe and light ice summers.

(iv) Table 4 shows the number of days with a given geostrophic wind direction category (see Table 2) during each of the individual

years 1953 to 1974 as well as the average summertime U and V component of the wind. The tabulation of the individual light ice summers is given above, all other summers being considered severe.

IV. INTERPRETATION

1. Ice Mapping

Interpretation of the ice maps for the Barrow, Barter Island, and Kotzebue Sound sectors is in progress.

We have reviewed the terminology proposed for fast-ice zonation for spring, fall, and winter by Reimnitz et al. (1976) and Stringer's (1974) earlier definitions, in connection with our mapping. In terms of the focus of Project RU#244, these categories provide a useful starting point but are insufficient by themselves to characterize the fast ice zone during the summer decay season. For example, no distinction is made of older ice incorporated into the fast ice zone although such occurrences significantly alter the local break-up pattern. Our mapping to date has shown noticeable spatial variations in fast ice zonation along the Beaufort Sea coast. These will be characterized in detail as a more complete record is built up for the three sectors under investigation (Barrow, Prudhoe, Barter Island).

2. Synoptic Characteristics

a.) The monthly frequency of the synoptic types and their transition matrices have been used to define synoptic circulation seasons, as described in 2.C.2. (v). All four indices described show that the greatest inter-monthly changes occur between May/June, August/September and October/November. Three synoptic seasons can then be recognized, respectively:

Summer (June-August), Autumn (September-October), and Winter (November-May).

The graph of average type frequencies over the year (Figure 28) shows that the autumn represents a two month transition in the switch from summer to winter regimes.

b.) The transition matrix (Table 5) shows that most types are preceded and followed by the same type more often than by a different type. Most exceptions to this occur when the transition to (or from) type 1 is more frequent. Type 1 occurs 30.7% of the days, and from random transitions one would expect type 1 to be involved a large number of times. This effect is removed in Table 6, showing the ratio of observed to expected random transitions. In virtually every case, the ratio is greater for the persistence transition than for any transition involving another type. The only exception concerns type 20, for which the ratio is greater for transition to types 7, 18, and 19 than for persistence. Type 7 is very similar to type 20 (a central low), while the transitions to types 18 and 19 are so rare (2 and 4 times respectively, out of 10,592 days) that the ratio is meaningless.

Since the ratio is an approximate measure of the relative importance of deterministic physical processes compared to random processes, then it is clear that over time periods of 24 hours (the sampling interval), persistence is the dominant physical process. It is probable than over longer time periods, other physical processes, namely the motion and evolution of synoptic features, will dominate.

c.) The relative importance of persistence among the various types is indicated in Table 7. Type 1 exhibits the longest duration, averaging 4 days, while type 20 is the most likely to change to another type,

enduring 0.4 days on the average.

The ratio of median observed persistence to median expected (random) persistence is generally between 2 and 3, and is greater than 1 in all cases. Types 1 and MD (missing data) have the greatest ratios. For type 1, this is probably because the dominant feature of that type, the Gulf of Alaska low, is outside the grid, and therefore the type classification is less sensitive to changes in location or structure of the dominant feature. The high ratio for days with missing data is due to the tendency for missing data to occur in blocks of several days. Type 20 has the lowest ratio, consistent with its low display of persistence discussed earlier. NT (no type) also has a low ratio, indicating that it represents temporary stages in the transition between types.

3. Interaction Case Studies

Ridge-Building off Oliktok Point, 1975

The results of the analysis are still in the preliminary stage. However, the following tentative results seem to be worth stating:

- a.) It is likely (from LANDSAT sequential images) that the ridges were built at the seaward edge of shore-continuous ice off Oliktok; i.e. they did not form elsewhere and drift aground.
- b.) The ridges formed between March 26, 1975 and April 20, 1975 and thus represent a "late"-season extension of continuous ice.
- c.) A severe wind storm accompanied an intense low pressure center into the Beaufort Sea on April 15, 1975. Calculated wind stress data show a maximum in the vicinity of the large ridge field. The directions indicate southeastward ice motions during the ridging.

It may be that such motions cause more severe deformation than the ("normal") westward motions.

d.) The existence of this large feature during summer and freeze-up, 1975 seems to have influenced greatly the nature of the 1976 fast ice in the vicinity (to shoreward).

4. Climate - Fast Ice Interaction

Some general conclusions can be drawn from the results of section III. 3 (b), Tables 1-4 .

a.) There is a strong tendency for N - NE (350° - 040°) surface winds to occur more frequently during severe ice summers, while light ice summers are characterized by S - SE (140° - 190°) winds (Table 1). The differences across these four categories of direction are significant at the 5% level by t test.

b.) There is a tendency for geostrophic winds between 286° to 150° to occur during severe ice summers, whereas light ice summers are characterized by geostrophic winds between 151° - 285° (Table 2). None of these differences are statistically significant, however, for reasons discussed below.

c.) Synoptic types 2 and 15 are more frequent in light ice summers, implying more frequent southerly flow over the Beaufort Sea coast near Barrow (Table 3). However, type 5 is also associated with southerly flow and Table 3 shows it is slightly more frequent in severe ice summers. None of the differences are statistically significant.

d.) There is little relationship between geostrophic winds and the relative severity of summer ice conditions (Table 4). Wendler (1973)

showed a generally close relationship between geostrophic winds and ice movement on a 5-day basis. It should be noted from Table 4 that in summer 1969 (the year examined by Wendler) there was excellent correspondence between the winds and the type of summer (severe) which occurred. Northerly winds (categories 1 and 2) predominated in 1969 (27 total days) and the U and V components of the geostrophic wind indicate predominantly northwesterly flow. During many other summers, however, there was little relationship between the geostrophic wind directions and the general ice conditions. For example, during the mild summers of 1958, 1959, and 1972 northeasterly and easterly winds prevailed while during the severe ice summers of 1953, 1956, 1965, and 1967 southerly winds predominated.

The results of this analysis, and the thawing degree day analysis in the last quarterly report, suggest that there is a good qualitative relationship between temperature and surface wind direction with ice conditions, when a summer is considered to be either severe or mild. The previously suggested good correspondence between geostrophic winds and ice conditions does not exist.

The apparent relationships between climatic parameters and fast ice conditions have been examined by stepwise regression analysis. The meteorological data are: accumulated degree-days, barometric pressure, surface wind speed, and mean cloud cover. The ice data (dependent variable) were changed to the actual distance northward from Point Barrow (nautical miles) to the 4/8 ice concentration boundary on Sept. 15.

Two regression analysis were performed. In the first the data used consisted of:

Y = Distance from Point Barrow northward to the boundary of 4/8 ice concentration on Sept. 15.

X₁ = Summer maximum accumulated Thawing Degree Days (TDD's).

X₂ = Preceeding winter maximum accumulated freezing degree days (FDD's). This is a relative measure of maximum ice thickness.

X₃ = The U or west-east component of the geostrophic wind from July 1 to Sept. 10.

X₄ = The V or south-north component of the geostrophic wind from July 1 to Sept. 10.

X₅ = Barrow barometric pressure July + Aug. divided by 2.

X₆ = Barrow mean surface wind speed July + Aug. divided by 2.

X₇ = Barrow mean cloud cover July + Aug. divided by 2.

In the second stepwise regression analysis the data consisted of:

Y = Distance from Point Barrow northward to the boundary of 4/8 ice concentration on Sept. 15.

X₁ = Summer maximum accumulated thawing degree days.

X₂ = # of summer days* with geostrophic wind categories 4 and 5.

X₃ = # of summer days* with geostrophic wind categories 8 and 1.

X₄ = # of summer days* with geostrophic wind category 2.

X₅ = # of summer days* with surface winds 140° to 220°.

X₆ = # of summer days* with surface winds 350° to 070°.

X₇ = # of summer days* with surface winds 080° to 130°.

X₈ = # of summer days* with synoptic types 2 and 15.

Where * indicates that July 1 to Sept. 10 are the summer days except for X₈ where only July and Aug. days are used.

Table 8 shows the correlation matrix for both regression analysis. Table 9 shows the statistical results of both regression analysis including the order in which a particular variable emerged in the analysis, its regression coefficient, the percentage of additional variance it accounts for, and its F-ratio.

The results of the correlation tables for analysis # 1 indicate that distance to the ice edge is most highly correlated with the summer TDDs and the V component of the geostrophic wind. However, the latter is not statistically significant (F-ratio) and only adds 0.9% to the total explained variance. The most important parameters accounting for the variance in Y are TDD's wind speed (surface), and barometric pressure which together account for 80.1% of the total variance; all 7 parameters together account for 82.3% of the variance.

Of interest also from Table 8 is the high correlation between TDDs and the V component of geostrophic wind ($r=0.579$), and between the barometric pressure and winter FDDs (0.456) and with the U geostrophic wind component ($r=0.494$). High positive correlation occurs between the two geostrophic components ($r=0.544$) suggesting winds tend to be northeasterly and southwesterly, and negative between barometric pressure and cloud cover ($r=0.703$).

In the second regression analysis where frequency data are used, the only statistically significant factor besides TDDs is X_5 , the number of days with southerly surface winds. Again, the surface winds seem to be of more importance than the geostrophic winds with X_5 , X_6 , and X_1 accounting for 9.8% of the variance while X_2 , X_3 , and X_4 account for only 3.5% of the variance and variable X_3 is not significant enough to be included in the equation. The correlation matrix, nonetheless, shows a fairly good correlation between Y and X_2 although the correlations between Y and the surface winds (X_5 , X_6) are much higher. The most important geostrophic wind direction frequency was the easterly component, and based on correlations in analysis # 1

(X_3 with X_5 , $r=0.494$) the relationship between the easterlies and barometric pressure is worth investigating.

Other high correlations from analysis # 2 exist between the number of days with southerly surface winds (X_5) and the number of days with synoptic types 2 and 15 (X_8) ($r=.785$). This agrees with the findings of case study # 2 in the last quarterly report where types 2, 5, and 15 were found to be associated with southerly winds. A correlation of $r=0.576$ exists between geostrophic wind category 4 (easterly-northeasterly and northerly and northeasterly surface winds (X_4 vs. X_6)). Otherwise the table shows high negative correlations between opposite wind directions.

The results of the regression analysis indicate the importance of air temperature and winds in the decay of the ice cover. The role of barometric pressures in the process is now assumed to be related to winds, but will have to be investigated more closely. Other factors of importance can be obtained from the stepwise regression analysis:

- (i) The statistical insignificance of wintertime freezing degree days suggest that the thickness of the ice from the previous winter is of little importance in the melting and retreat of the ice cover. This is based upon established relationships between freezing degree days and ice thickness found by Zubov and others.
- (ii) The fact that temperature accounts for about 65% of the variance, and that most basic meteorological parameters combined with temperature account for over 80% of the variance, suggests that oceanographic factors and ice dynamics probably do not play a major role in the

removal of the winter ice in summer.

(iii) The relative unimportance of cloud cover suggests that some elements of the radiation budget which are highly and negatively correlated to cloud cover, such as total incoming solar radiation, are also relatively unimportant.

(iv) The unimportance of geostrophic winds, which has already been discussed.

The results from the regression analysis and the more subjective analysis presented via Table 1-4 provide a basis for analyzing the physical relationships between the ice and the atmosphere. Work expanding this statistical model into a physical model showing the ice/climate relationships will continue in the upcoming months. Specifically the answer to several problems will be sought:

(i) Whether or not it is meaningful to assume temperature on the land at Barrow is really important in analysis of ice decay since the winds may determine the temperatures at Barrow. That is, a more careful analysis of the relationship between wind direction and speed and temperature will be carried out.

(ii) Since temperature is of primary importance in the regression, although it may cover up some the variance the wind, it must be determined if the temperatures are influencing how much ice decays, or if the decaying ice (by some unknown agent) determines what the summer temperatures will be.

(iii) The results of the regression model will be expanded, primarily toward analyzing the relationship between climate and the fast ice. Because of the large number of severe summers in the last 23

summers (with little or no northward retreat past the fast ice boundary at about the 20 meter isobath) the fast ice was to some extent represented in the results, although the data relate mainly to pack ice retreat. Attempts will be made to correlate climate/ice relationships based only in the fast ice region using LANDSAT imagery.

(iv) The relationships between barometric pressure, storms, and winds and their influence on ice decay need to be analyzed further.

V. PROBLEMS/RECOMMENDATIONS

None.

VI. ESTIMATE OF FUNDS EXPENDED

\$66,000.

SUMMARY

The results from a regression analysis of climatic parameters and distance to the pack ice margin, and a more subjective interpretation of the meteorological data, are viewed as laying the basis for analyzing the physical relationships between the ice and the atmosphere. Several meteorological factors of importance have been identified: air temperature expressed as thawing degree days, the number of days with southerly surface winds, barometric pressure and wind speed. Other factors which do not seem to be of importance are geostrophic winds, the previous winter's accumulation of freezing degree days and therefore ice thickness, cloud cover, and perhaps also incoming solar radiation, if one make an assumption about its relationship between cloud cover.

The physical model of the atmosphere's influence on ice decay in the summer depends upon the interaction, or non-interaction, of the above factors with ice and the precise nature of those relationships has to be determined.

REFERENCES

- Brown, R.A., 1975. Planetary boundary layer models and parameters for AIDJEX, 1975-76. AIDJEX Bull. No. 29, 113-130.
- Kovacs, A., 1976. Ground ice in the fast ice zone along the Beaufort Sea coast of Alaska. CRREL Rep. U. S. Army, Hanover.
- Leavitt, E., 1975. Determination of air stress from AIDJEX surface layer data. AIDEX Bull. No. 28, 11-20.
- Reimnitz, E., Toimil, L., and Barnes, R., 1976. Development of the stamuklu zone and its relation to arctic shelf processes and morphology, Beaufort Sea, Alaska. U.S.Geol. Surv., Menlo Park, Calif., Final Report of NASA. (Contract 5-7024-AG).
- Wendler, G., 1973. Sea ice observation by means of satellite. J. Geophys. Res. 78, 1427-48.

Table 1

MEAN FREQUENCIES AND STANDARD DEVIATIONS OF OCCURRENCE OF WIND DIRECTIONS
 (0° to 360°) BETWEEN JULY 1 AND SEPT. 8 AT BARROW DURING LIGHT
 AND SEVERE ICE SUMMERS

		WIND DIRECTION (TENS OF DEGREES)												
		35-01	02-04	05-07	08-10	11-13	14-16	17-19	20-22	23-25	26-28	29-31	32-34	
	\bar{X}	5.25	7.75	9.92	12.25	5.25	1.92	1.33	3.42	7.33	6.58	5.17	2.58	
St Dev.		2.99	2.60	4.81	5.34	4.71	1.93	1.56	3.06	4.23	3.18	2.41	1.88	Severe Ice Summers
	\bar{X}	2.91	3.82	7.82	15.91	7.91	4.18	3.45	3.54	7.09	5.27	4.09	2.91	
St Dev.		2.26	1.94	5.27	5.09	4.09	2.48	2.11	2.46	3.70	2.76	2.59	1.81	Light Ice Summers

* For example 35-01 equals 350° to 010° or approximately northerly winds.

Table 2

MEAN FREQUENCIES AND STANDARD DEVIATIONS OF THE EIGHT
 GEOSTROPHIC WIND CATEGORIES NEAR BARROW DURING
 LIGHT AND SEVERE ICE SUMMERS*

	TYPE								
	1	2	3	4	5	6	7	8	
\bar{X}	7.73	20.91	9.73	5.27	8.55	8.09	5.45	4.45	
St. Dev.	3.52	7.23	2.83	3.32	4.97	4.37	4.25	3.14	Severe Ice Summers
\bar{X}	6.82	15.73	9.18	6.09	10.45	9.55	4.73	4.09	
St. Dev.	2.52	7.93	5.91	4.11	4.91	4.80	3.00	2.70	Light Ice Summers

* Data base for each summer was July 1 to Sept. 10.

CATEGORY 1: Direction 016^o to 060^o
 CATEGORY 2: Direction 061^o to 105^o
 CATEGORY 3: Direction 106^o to 150^o
 CATEGORY 4: Direction 151^o to 195^o

CATEGORY 5: Direction 196^o to 240^o
 CATEGORY 6: Direction 241^o to 285^o
 CATEGORY 7: Direction 286^o to 330^o
 CATEGORY 8: Direction 331^o to 015^o

Table 3

MEAN FREQUENCIES AND STANDARD DEVIATIONS OF MAJOR BEAUFORT
SEA SYNOPTIC TYPES DURING LIGHT AND SEVERE ICE SUMMERS

		SYNOPTIC TYPE									
		1	2	3	4	5	6	8	14	15	
	X	8.27	11.64	2.36	3.73	6.18	6.00	3.36	3.09	3.09	
	St Dev.	6.44	7.17	1.57	2.72	4.00	5.39	2.77	2.39	3.53	Severe Ice Summers
	X	8.36	14.91	.91	4.45	5.91	5.64	4.00	2.09	5.36	
	St Dev.	6.90	6.83	1.04	2.42	3.83	3.61	2.05	1.51	2.38	Light Ice Summers

* Data base for each summer was July 1 to Aug. 31.

Table 4

TABULATION BY SUMMERS OF THE NUMBER OF DAYS WITH A GIVEN GEOSTROPHIC WIND
CATEGORY AND THE SUMMER AVERAGE WESTERLY AND SOUTHERLY WIND COMPONENTS.

		GEOSTROPHIC WIND CATEGORY								U	V
SUMMER	DAYS	1	2	3	4	5	6	7	8		
1974	62	12	5	7	4	14	10	5	5	ND	ND
1973	70	4	9	4	8	11	18	9	7	1.50	1.46
1972	72	4	21	21	3	6	5	7	5	-2.28	-0.09
1971	71	14	20	13	6	5	4	4	5	-2.17	-1.37
1970	71	10	28	8	4	5	4	7	5	-2.16	-1.06
1969	72	5	12	7	3	8	10	14	13	0.88	-1.22
1968	72	5	23	13	9	11	9	1	1	-2.13	1.15
1967	70	3	20	4	10	20	10	0	3	-0.89	1.32
1966	72	5	30	10	7	10	5	2	3	-3.63	-0.34
1965	70	7	19	11	10	14	3	2	4	-1.73	1.18
1964	71	6	27	11	9	2	13	2	1	-2.15	-0.12
1963	72	7	15	15	9	10	5	9	2	-1.52	.50
1962	72	5	8	5	13	12	13	6	10	0.48	.93
1961	71	6	15	15	5	12	7	6	5	-1.38	.40
1960	72	9	32	10	2	7	3	4	5	-4.08	-1.30
1959	56	10	22	2	3	5	8	3	3	-2.04	-1.63
1958	57	8	25	7	1	6	6	1	3	-2.42	-0.55
1957	58	3	7	5	5	11	14	9	4	0.87	.44
1956	62	4	15	8	1	9	15	7	3	-.04	.28
1955	72	12	14	14	4	5	11	7	5	-.47	-0.29
1954	72	6	5	5	11	22	18	4	1	1.66	3.11
1953	69	10	13	11	2	9	11	11	2	0.43	.07

CATEGORY 1: Direction 016° to 060°
 CATEGORY 2: Direction 061° to 105°
 CATEGORY 3: Direction 106° to 150°
 CATEGORY 4: Direction 151° to 195°

CATEGORY U: + westerly

CATEGORY 5: Direction 196° to 240°
 CATEGORY 6: Direction 241° to 285°
 CATEGORY 7: Direction 286° to 330°
 CATEGORY 8: Direction 331° to 015°

CATEGORY V: + southerly

Table 5

PER MIL TRANSITION MATRIX FOR CHUKCHI TYPES, ANNUAL

TO FROM	1	2	3	4	5	6	7	8	9	10	11	12	13	14	15	16	17	18	19	20	21	22	NT	MD
1	218	19	0	13	4	5	1	0	1	0	10	0	9	10	0	2	5	0	0	0	1	2	5	1
2	11	45	3	1	2	8	2	1	5	1	2	4	2	2	1	0	5	2	1	0	0	2	4	0
3	0	1	20	1	1	0	1	5	4	4	0	6	0	0	1	0	0	0	1	2	0	0	2	0
4	24	1	0	44	1	1	0	2	0	2	4	0	3	3	1	3	0	0	0	0	1	1	2	0
5	10	1	0	4	10	0	0	1	1	0	1	0	4	0	1	0	1	0	0	0	2	0	1	0
6	1	2	3	1	0	7	1	1	1	2	0	2	0	1	0	2	0	0	0	0	0	0	2	0
7	1	5	0	0	0	0	3	0	0	0	1	1	0	0	0	0	2	0	1	0	0	0	1	0
8	0	0	2	6	2	0	0	6	2	2	0	0	1	0	1	1	0	0	0	1	0	0	2	0
9	0	4	5	0	3	1	0	2	12	1	0	2	1	0	1	0	1	0	1	0	1	1	2	0
10	1	0	4	2	0	0	1	2	1	7	1	2	0	1	3	0	0	0	0	0	0	0	2	0
11	15	1	0	3	2	0	1	0	0	0	9	0	0	0	1	0	2	0	0	0	0	0	1	0
12	0	5	7	0	0	1	2	0	2	1	0	8	0	0	0	0	0	1	1	0	0	0	1	0
13	6	3	0	3	2	2	0	1	3	0	0	0	9	1	0	1	0	0	0	0	0	1	3	0
14	4	3	0	1	0	2	1	0	0	1	2	1	1	3	1	1	0	0	0	0	0	0	2	0
15	2	0	1	4	1	0	1	1	0	1	2	0	0	0	4	0	0	0	0	0	0	1	0	2
16	1	0	1	4	0	1	0	1	0	2	0	0	0	0	0	3	0	0	0	0	0	0	1	0
17	5	7	0	0	2	0	1	0	1	0	1	0	1	0	0	0	5	0	0	0	0	0	0	0
18	0	0	1	0	0	0	1	0	0	0	0	0	0	0	1	0	0	1	0	0	0	0	0	0
19	0	0	1	0	1	0	0	0	1	0	0	0	0	0	1	0	0	0	0	2	0	0	1	0
20	0	1	0	0	0	0	1	0	0	0	0	0	0	0	0	0	0	0	0	0	0	0	0	0
21	1	0	0	3	0	0	0	1	0	1	1	0	0	0	1	0	0	0	0	0	0	2	0	0
22	1	1	0	1	1	0	0	1	1	0	0	0	1	0	0	0	0	0	0	0	0	2	0	0
NT	3	3	3	3	2	1	1	2	2	2	2	2	2	1	2	1	1	0	1	0	0	0	5	0
MD	2	1	0	0	0	0	0	0	0	0	0	0	0	0	0	0	0	0	0	0	0	0	0	2

Table 6

RATIO OF MATRIX TO EXPECTED CHANCE MATRIX, ANNUAL

	TO	1	2	3	4	5	6	7	8	9	10	11	12	13	14	15	16	17	18	19	20	21	22	NT	MD
FROM																									
1	2.3	.6	.0	.5	.4	.5	.1	.0	.1	.1	.1	.8	.0	.8	1.5	.1	.3	.7	.1	.0	.0	.4	.8	.4	.7
2	.4	4.2	.6	.1	.6	2.7	1.0	.2	1.4	.2	.6	1.3	.6	.7	.4	.2	2.0	3.7	.6	.7	.2	1.8	.9	.8	.8
3	.0	.1	7.9	.1	.4	.2	.9	3.5	2.3	2.9	.1	4.1	.1	.1	1.3	.2	.2	1.2	1.9	5.5	.9	.2	1.1	.0	.0
4	.8	.1	.0	5.0	.4	.3	.2	.7	.1	.6	1.1	.1	.9	1.6	.6	2.0	.1	.0	.0	.6	.6	.9	.6	.8	.8
5	1.0	.2	.0	1.1	7.7	.2	.0	.7	.6	.0	.8	.0	3.1	.0	.8	.0	1.6	.6	.8	.5	4.3	.0	.5	.0	.0
6	.1	.8	2.1	.5	.0	8.3	1.3	1.0	.8	2.9	.5	2.3	.1	.9	.6	4.6	.1	3.6	1.0	1.2	1.4	1.5	1.9	.6	.6
7	.2	2.9	.3	.0	.7	.5	9.9	.0	.5	.0	1.5	2.4	.0	.0	1.0	.0	3.7	3.3	5.2	2.9	.0	.0	1.5	1.7	.0
8	.1	.1	1.3	2.4	1.7	.1	.0	8.2	1.5	2.8	.2	.5	1.1	.2	1.4	3.0	.2	.0	.4	4.0	.4	.4	1.7	2.4	.0
9	.0	1.1	2.4	.0	2.2	.5	.0	1.6	8.7	1.0	.1	1.7	.6	.0	.7	.3	1.0	.0	3.0	2.3	2.0	1.6	1.6	1.2	.0
10	.1	.1	3.0	.7	.0	.4	2.0	3.3	.5	8.5	1.1	2.2	.2	.9	5.1	.6	.0	.7	1.3	1.8	1.0	.0	1.5	.0	.0
11	1.3	.3	.0	.7	1.6	.1	1.8	.0	.0	.3	6.8	.0	.0	.3	1.7	.2	1.8	.0	.3	.9	1.3	.0	.5	1.7	.0
12	.0	1.7	4.2	.1	.1	.8	2.7	.5	2.2	1.0	.1	9.1	.2	.0	.4	.0	.0	4.0	4.1	.6	.0	.0	1.2	.0	.0
13	.5	.9	.1	.9	1.4	1.6	.1	.9	1.9	.2	.1	.2	7.8	.7	.3	1.9	.1	.6	.0	.5	.8	2.6	1.9	.4	.0
14	.6	1.2	.3	.5	.2	2.7	3.2	.8	.0	1.2	2.1	1.0	.7	7.1	1.2	2.8	.5	.0	.0	.8	.0	.0	1.8	.0	.0
15	.3	.1	.7	2.2	1.8	.0	3.2	1.2	.4	2.1	2.3	.0	.3	.2	8.8	.0	.4	.0	1.8	.8	4.6	.0	1.8	.0	.0
16	.1	.1	1.0	2.6	.5	2.2	.0	2.3	.7	3.8	.0	.6	.5	1.1	1.5	9.9	.0	.0	.0	.0	.0	3.3	1.2	1.0	.0
17	.7	3.0	.1	.1	1.8	.1	1.7	.5	.9	.0	.8	.3	.7	.2	.0	.0	9.1	.0	.8	.0	.4	.9	.4	2.0	.0
18	.0	1.0	2.8	.2	2.2	.0	7.6	.8	.5	2.8	1.1	.7	.0	.0	6.7	1.3	.9	9.9	2.0	.0	.0	.0	.5	.0	.0
19	.0	.1	1.9	.2	4.0	.0	2.6	1.8	2.3	1.7	.3	.9	.3	.0	5.5	.0	.8	.0	9.9	1.8	3.9	.0	1.4	1.6	.0
20	.3	1.4	.3	.2	2.4	.6	6.7	.0	2.3	.0	.5	.6	2.5	.0	.0	.0	3.7	7.4	7.1	6.5	.0	.0	1.7	.0	.0
21	.3	.0	.0	2.8	.8	.3	.5	2.6	1.0	3.7	2.1	.0	.0	.0	3.2	.6	.0	2.0	1.0	.0	9.9	.0	1.0	.0	.0
22	.2	.7	.0	1.6	1.7	1.1	.0	2.3	1.6	1.1	.6	.0	2.3	.5	.5	2.0	.9	.0	.0	.0	4.2	9.9	2.0	3.4	.0
NT	.3	.7	1.2	.7	1.4	.9	1.9	2.1	1.1	1.6	1.3	1.5	1.3	1.0	2.6	1.7	1.0	.5	1.7	2.2	.7	1.0	3.4	1.6	.0
MD	.8	.9	1.2	.8	.9	.0	.8	1.2	.4	.5	1.3	.0	.4	.0	.8	2.0	.0	.0	1.6	.0	.0	1.7	.4	9.9	.0

Table 7

Median duration of persistence of synoptic types (T_m , days), and ratio to duration expected from random occurrence (T_r).

Type	T_m	T_m/T_r
1	4.1	3.5
2	1.7	2.7
3	1.5	3.3
4	1.8	3.1
5	1.1	2.6
6	1.0	2.5
7	.8	2.3
8	.9	2.4
9	1.2	3.0
10	1.0	2.5
11	1.0	2.4
12	1.1	2.7
13	1.1	2.6
14	.8	2.1
15	.8	2.3
16	.9	2.6
17	.9	2.4
18	.7	2.5
19	.9	3.0
20	.4	1.5
21	.8	2.6
22	.7	2.5
NT	.7	1.6
MD	1.0	3.7

NT = No Type

MD = Missing Data

Table 8

CORRELATION MATRICES FOR STEPWISE REGRESSION

Analysis 1

	Y	X ₁	X ₂	X ₃	X ₄	X ₅	X ₆	X ₇
Y	1.000	.809	.248	.271	.614	.162	.269	.048
X ₁		1.000	.123	.260	.579	.078	.063	.205
X ₂			1.000	.359	.222	.456	.194	.414
X ₃				1.000	.544	.494	.333	.338
X ₄					1.000	.225	.163	.022
X ₅						1.000	.122	.703
X ₆							1.000	.024
X ₇								1.000

Analysis 2

	Y	X ₁	X ₂	X ₃	X ₄	X ₅	X ₆	X ₇	X ₈
Y	1.000	.809	.469	.298	.355	.578	.632	.250	.357
X ₁		1.000	.424	.268	.357	.428	.593	.455	.225
X ₂			1.000	.382	.440	.472	.614	.134	.499
X ₃				1.000	.111	.262	.203	.227	.325
X ₄					1.000	.619	.576	.227	.665
X ₅						1.000	.358	.380	.785
X ₆							1.000	.429	.434
X ₇								1.000	.322
X ₈									1.000

Table 9

RESULTS OF THE TWO STEPWISE REGRESSION ANALYSIS
OF METEOROLOGICAL DATA AND ICE CONDITIONS

	Variable Reg. An. # 1	Regr. Coeff.	% Variance Accounted For	F-ratio	Variable Regression Anal. # 2	Regres- sion Coeff.	% Variance Accounted For	F-ratio
Summer TDD	X ₁	0.262	65.4%	37.80	TDD X ₁	0.219	65.4%	37.80
Windspeed	X ₆	18.152	7.2%	4.97	S Wind X ₅	5.074	6.5%	4.43
Pressure	X ₅	-164.676	7.5%	6.74	NE Wind X ₆	-4.821	2.4%	1.68
V Component	X ₄	13.876	0.9%	0.83	NE* X ₄	2.800	3.4%	2.56
Winter FDD	X ₂	-0.012	0.6%	0.53	E Wind X ₇	-1.826	0.9%	0.71
-U Component	X ₃	1.952	0.4%	0.36	Types X ₈	-0.984	0.4%	0.29
Cloud	X ₇	7.631	0.3%	0.23	2, 15			
			82.3%		SE-SW* X ₂	-0.321	0.1%	0.04
							79.1%	

(* geostrophic)

Fig. 1: 17 May 1973, ID No. 1298-22161

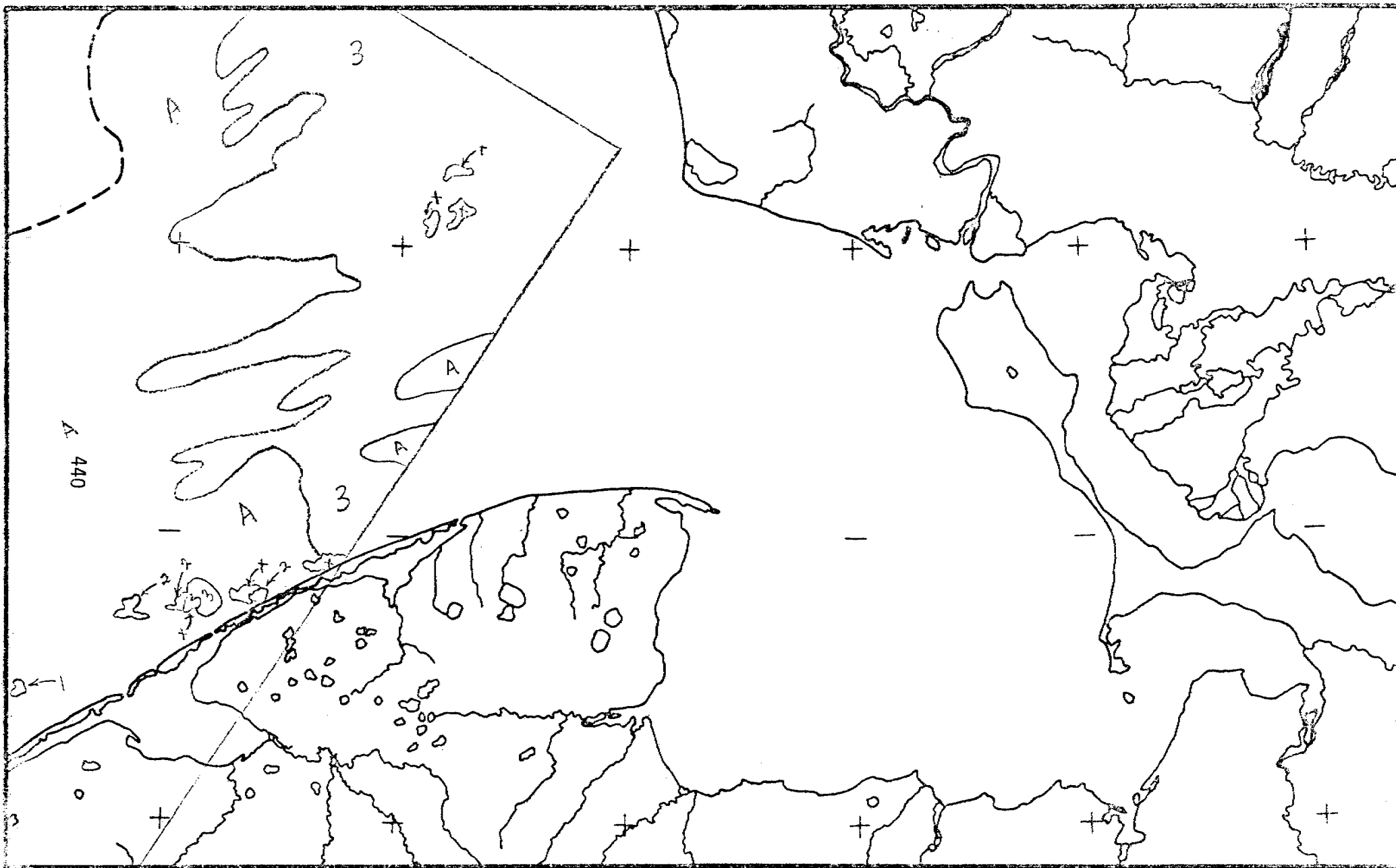
Legend X open water

A pack ice

1 & newly formed ice. Area 1 is older and thicker
2 than that labeled area 2.

3 general area of ice with leads. The leads are
are of various widths and lengths but are
oriented SW-NE.

All ice areas on the frame (except those labeled 1, 2, or 3)
show no difference in tone.



SHOREFAST SEA ICE
SURFACE MORPHOLOGICAL CHARACTERISTICS
CHUKCHI SEA COAST: KOTZEBUE SOUND SECTOR

Fig. 2: 01 June 1973, ID No. 1313-21585

Legend X open water

A pack ice - with melt water on the surface

1 this is flat first year ice making up the largest single ice type in the sound. This ice generally contains small cracks which can drain the water on the ice surface from the very immediate area.

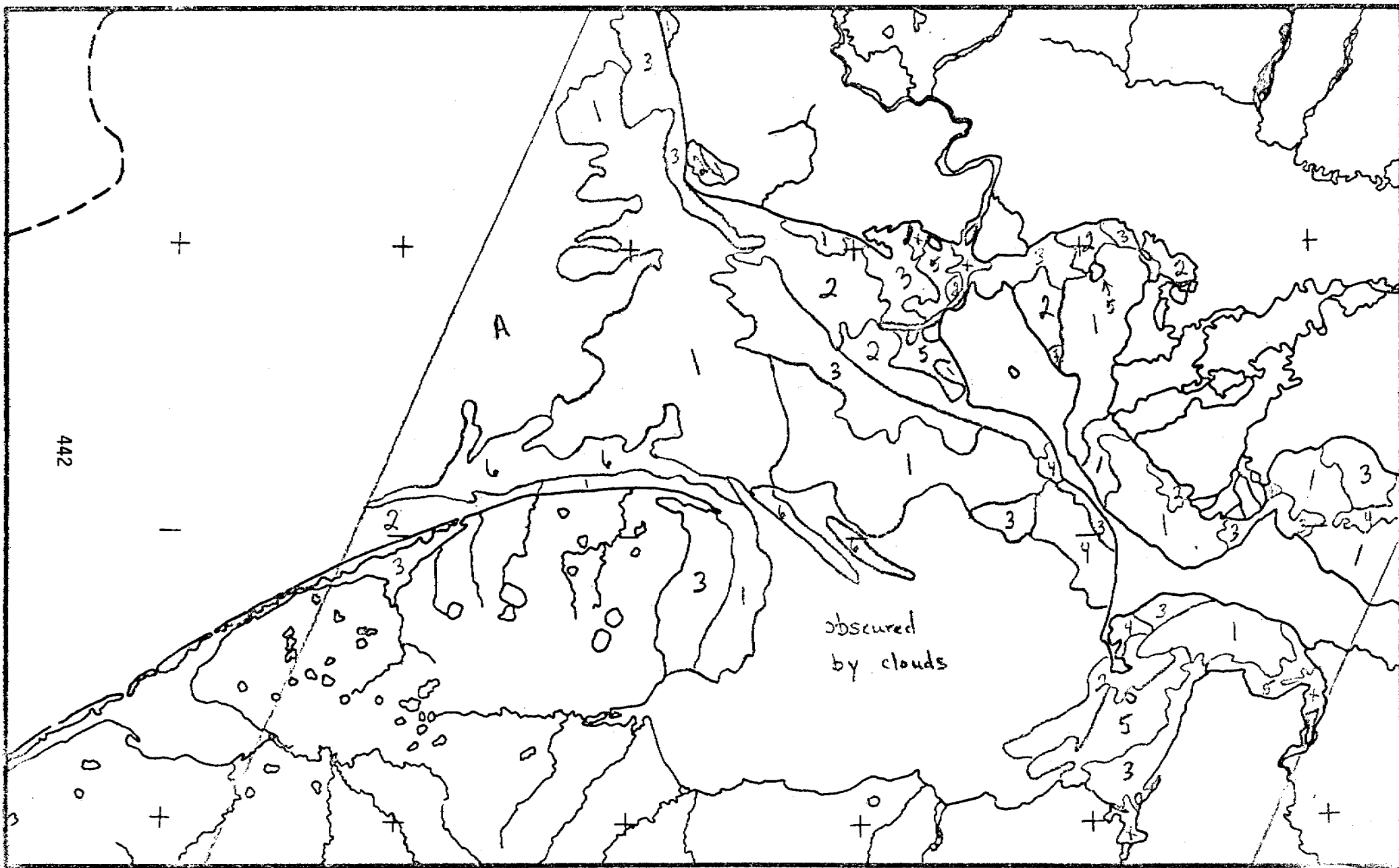
2 represents ice which would seem to be a mixture of first year types producing a mottled appearance due to spatial variation in surface melting.

3 is of the same ice as number 1 but here there is more melt water on the surface probably in the form of deeper water while water extent on the surface is probably not much greater than for type 1.

4 small areas of ice that have more water on the surface than area 3 has the same relation to area 3 as area 3 has to area 1.

5 areas with extensive and deep meltwater on the surface, also transected with small cracks.

6 generally areas of flat ice containing large cracks with open water. The ice is predominately types 1 and 2.

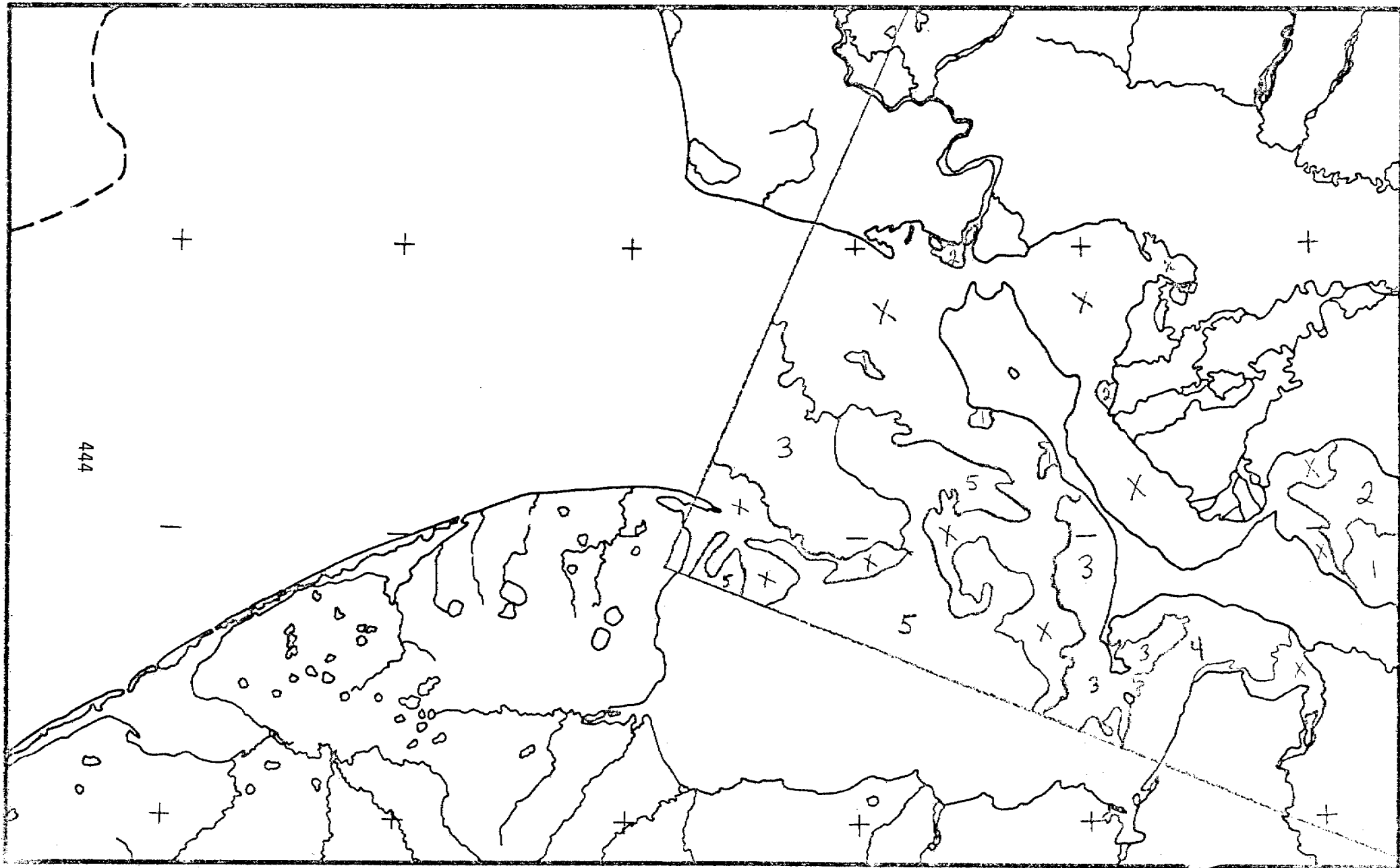


SHOREFAST SEA ICE
SURFACE MORPHOLOGICAL CHARACTERISTICS
CHUKCHI SEA COAST: KOTZEBUE SOUND SECTOR

Fig. 3: 18 June 73, ID No. 1330-21525

Legend X open water

- 1 flat ice with uniform amount of water on its surface also containing leads.
- 2 mostly flat ice with more melt water on its surface than area 1. Not as uniform in amount of water or topography.
- 3 this ice has a mottled appearance due to the incorporation of floes with varying amounts of melt water on their surfaces. No major areas of pressure ridging can be detected.
- 4 much like area 2 but with increased melt water on the surface and containing areas of open water between some floes.
- 5 areas of non-continuous ice composed of floes of varying sizes. Identifiable ice is of type 3 but the degree of break up (as much as 80% water) warrants a separate category.

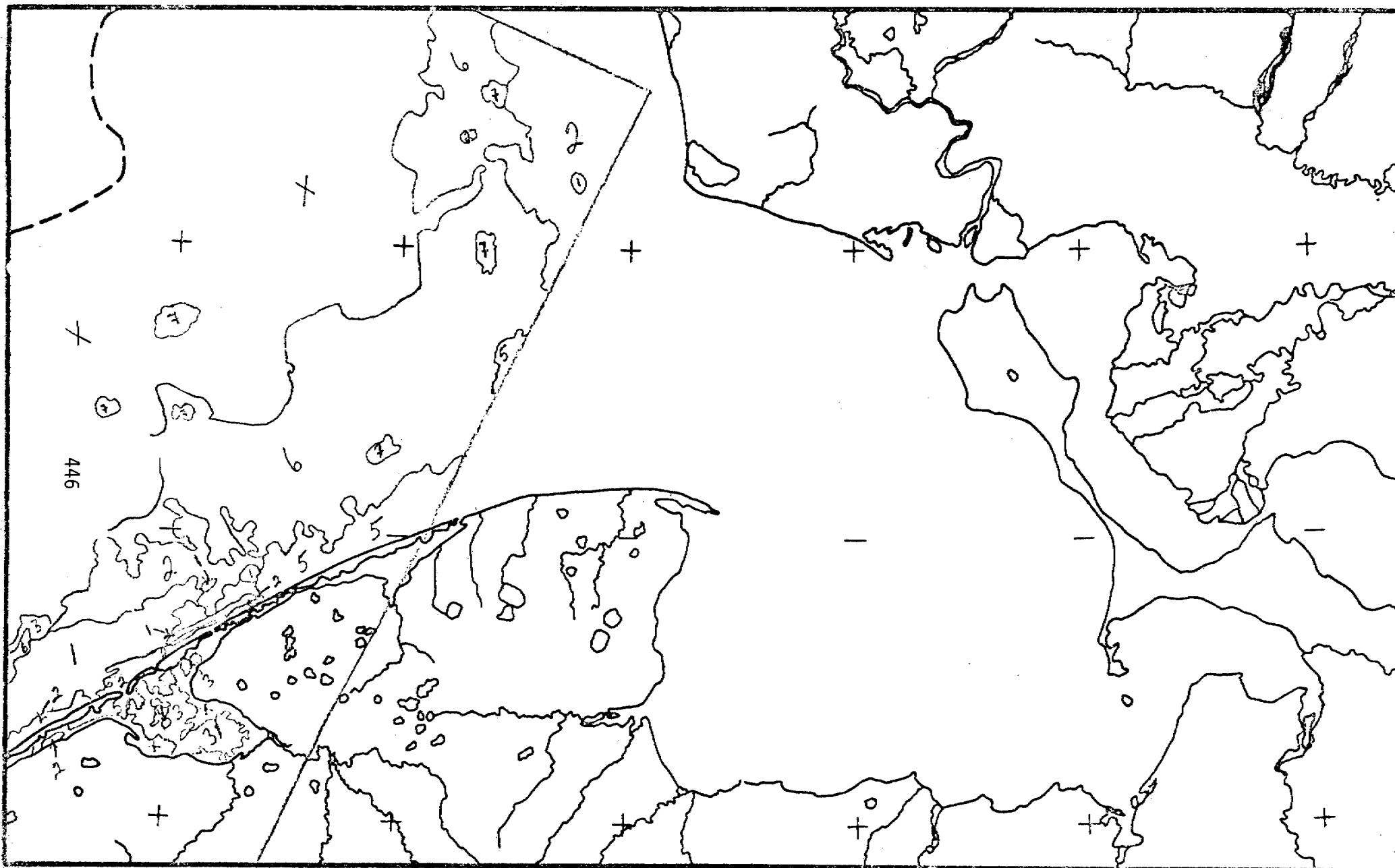


SHOREFAST SEA ICE
SURFACE MORPHOLOGICAL CHARACTERISTICS
CHUKCHI SEA COAST: KOTZEBUE SOUND SECTOR

Fig. 4: 22 June 73, ID No. 1334-22155

Legend X open water

- 1 generally continuous ice that is relatively well drained. There is indication of pressure ridging in these areas as there is in all other areas of continuous ice.
- 2 the same as type 1 but with more melt water on the ice surface.
- 3 is made of ice floes of large areal extent which are flat and have a uniform melt water cover.
- 4 the same as type 3 but with a greater amount of melt water on the surface.
- 5 this type indicates areas of non-continuous ice (ice coverage of 80-30%) composed of ice of type 2.
- 6 the same as type 5 but more rarefied ice (ice coverage 30-5%).
- 7 individual floes of large areal extent exhibiting drainage patterns probably related to ridging. Indications point to them being composed of first year ice.



SHOREFAST SEA ICE
SURFACE MORPHOLOGICAL CHARACTERISTICS
CHUKCHI SEA COAST: KOTZEBUE SOUND SECTOR

Fig. 5: 09 July 1973, ID No. 1351-22095

No map.

Ice is entirely absent except for some areas of non-continuous ice (ice coverage about 25%) near the mouth of Kotzebue Sound. There are also a few floes of large extent in the same area.

Figs. 6 - 27. Maps of the key days of Chukchi MSL pressure-pattern types. (Isolines are at intervals of 0.5 x standard deviation; high and low centers are indicated.)

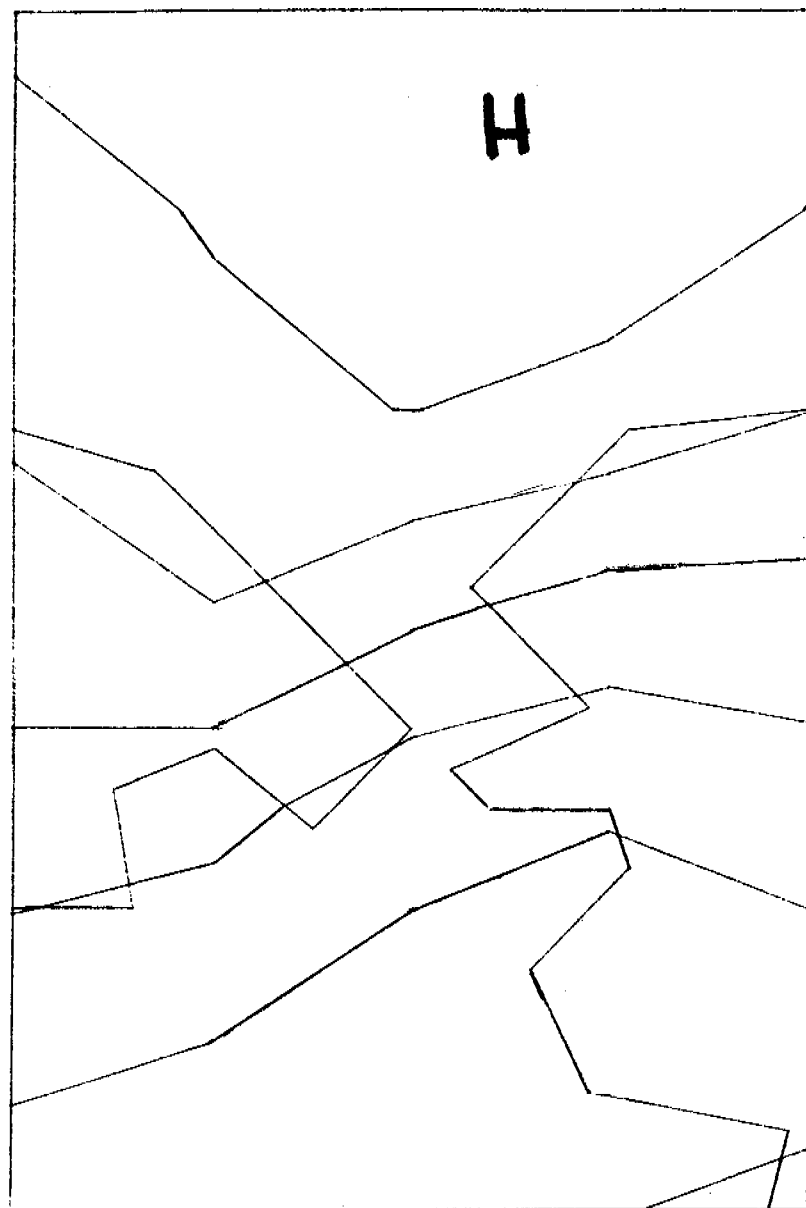


Fig. 6 Chukchi Key Day 1, March 14, 1970

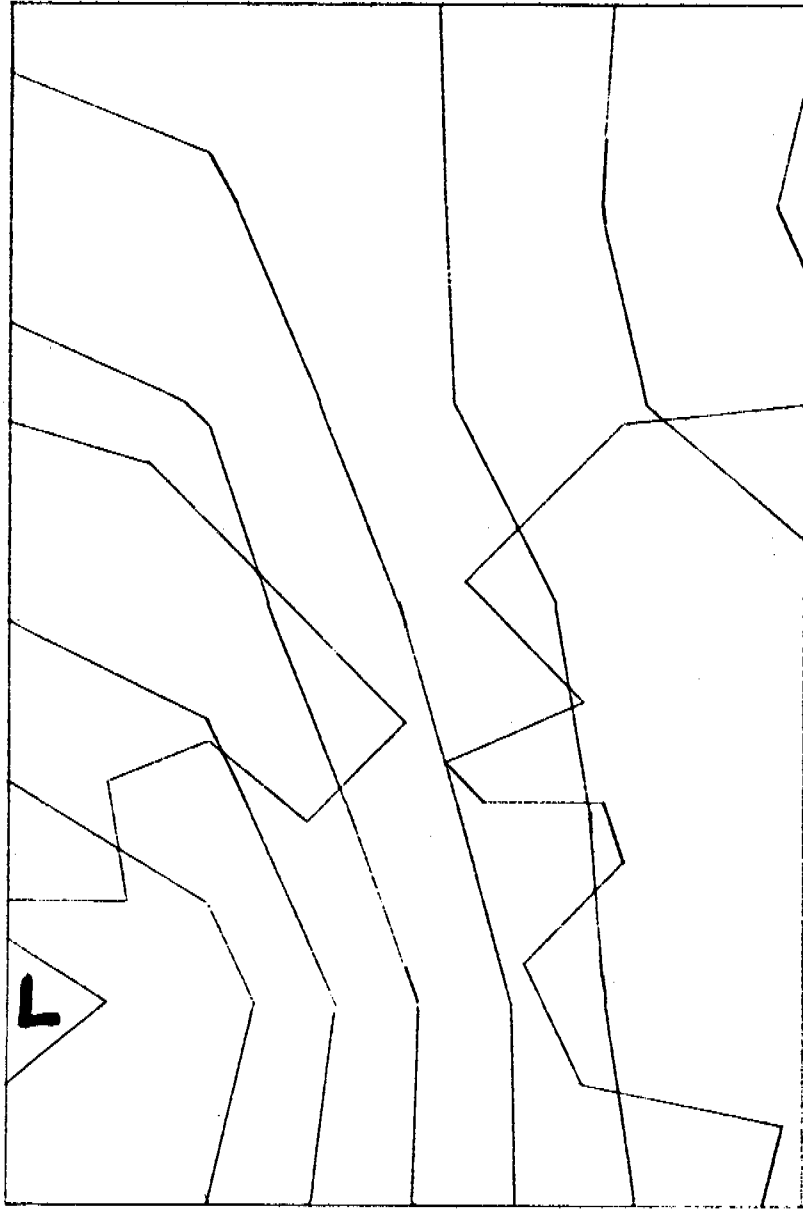


Fig. 7 Chukchi Key Day 2, Aug. 7, 1968

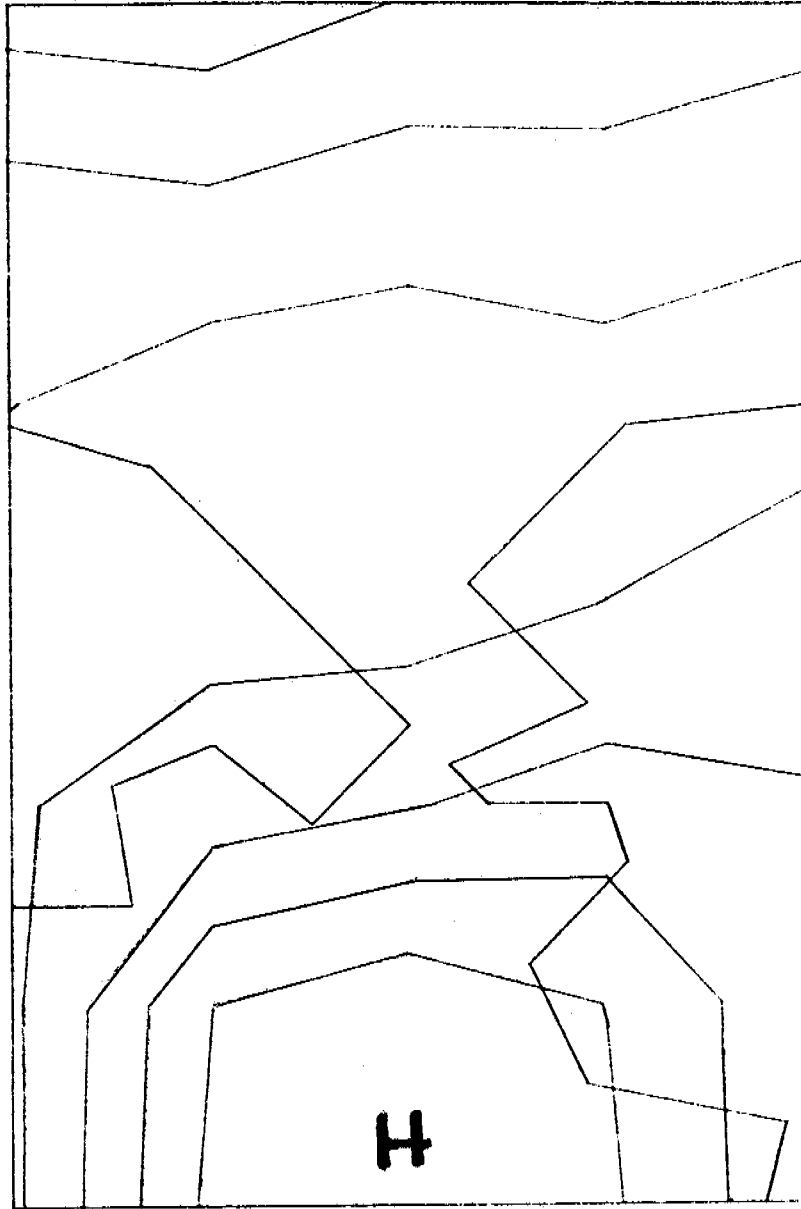


Fig. 8 Chukchi Key Day 3, March 20, 1967

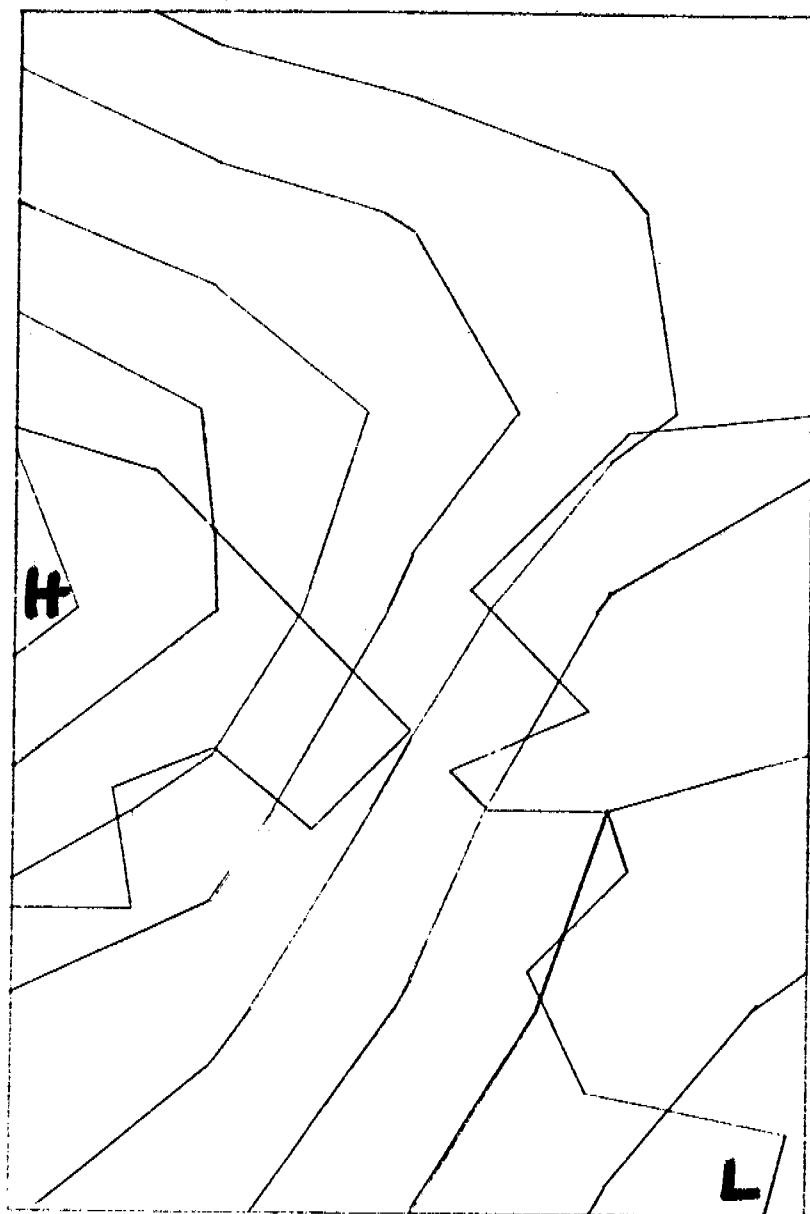


Fig. 9 Chukchi Key Day 4, Feb. 2, 1961

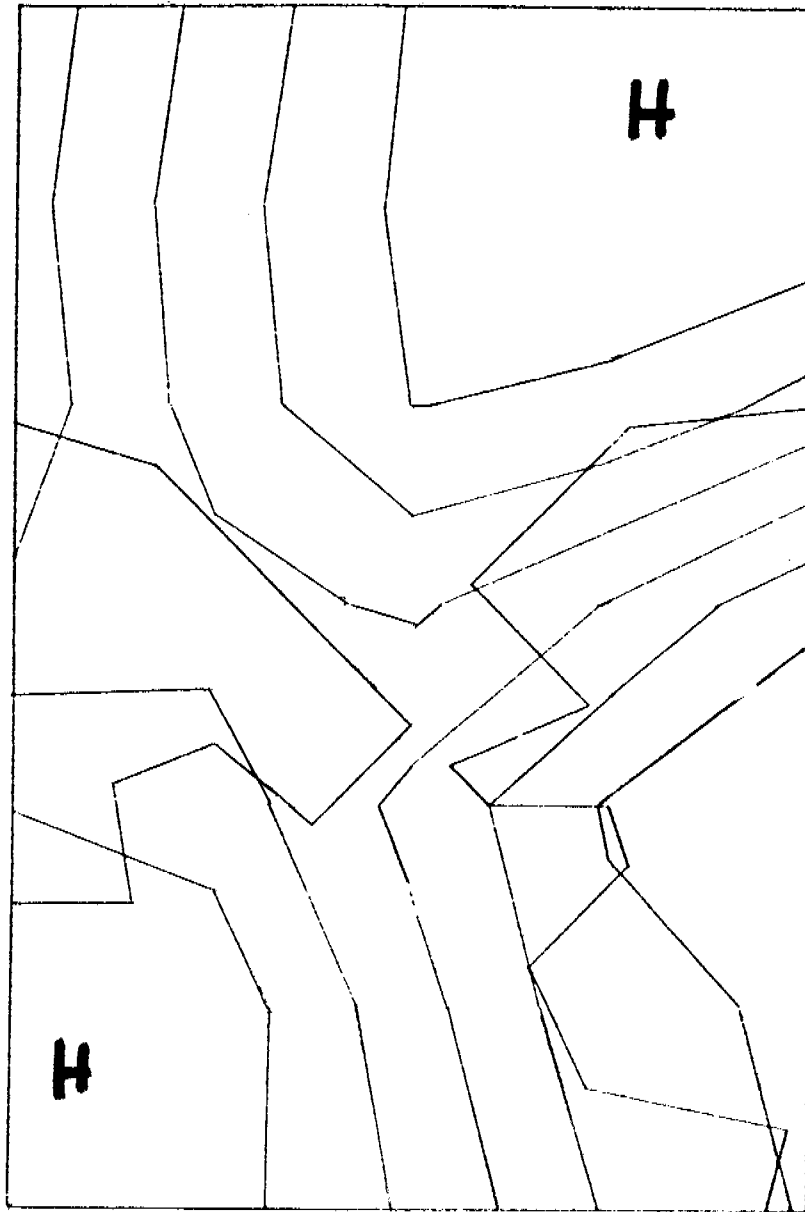


Fig. 10 Chukchi Key Day 5, June 23, 1969

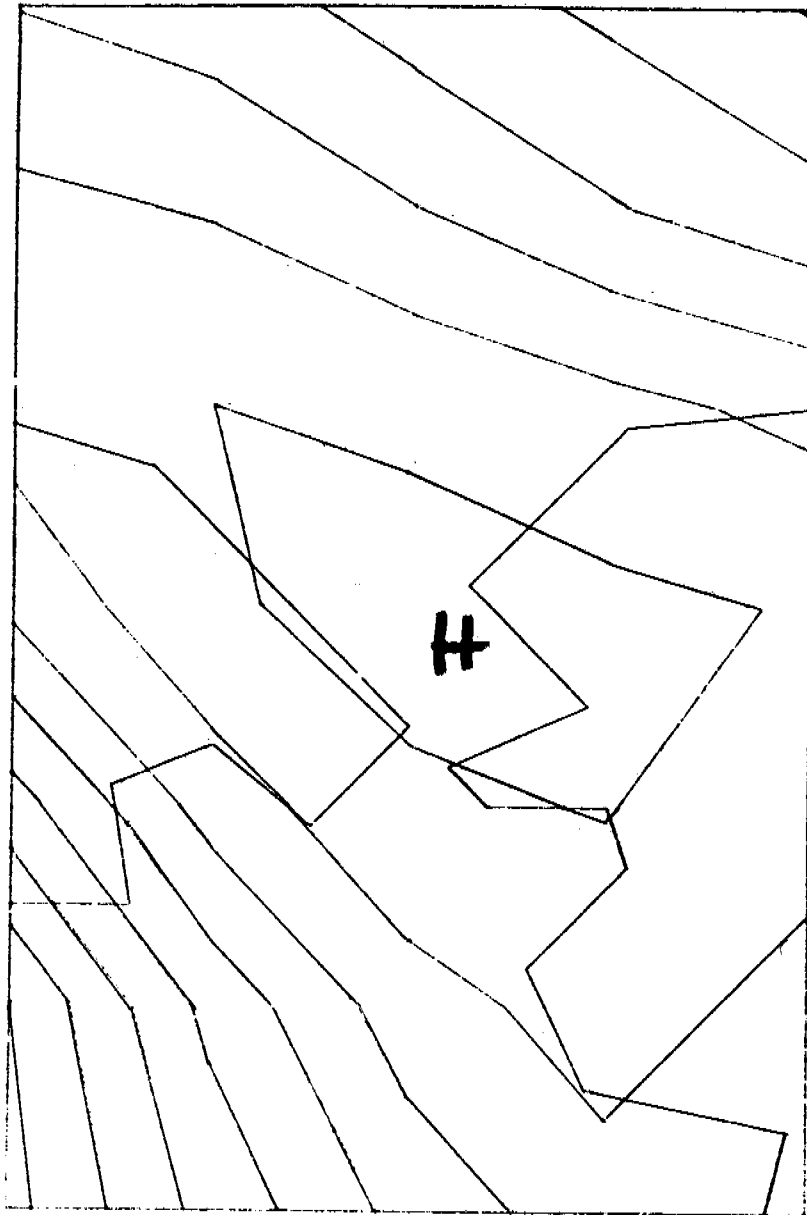


Fig. 11 Chukchi Key Day 6, March 12, 1955

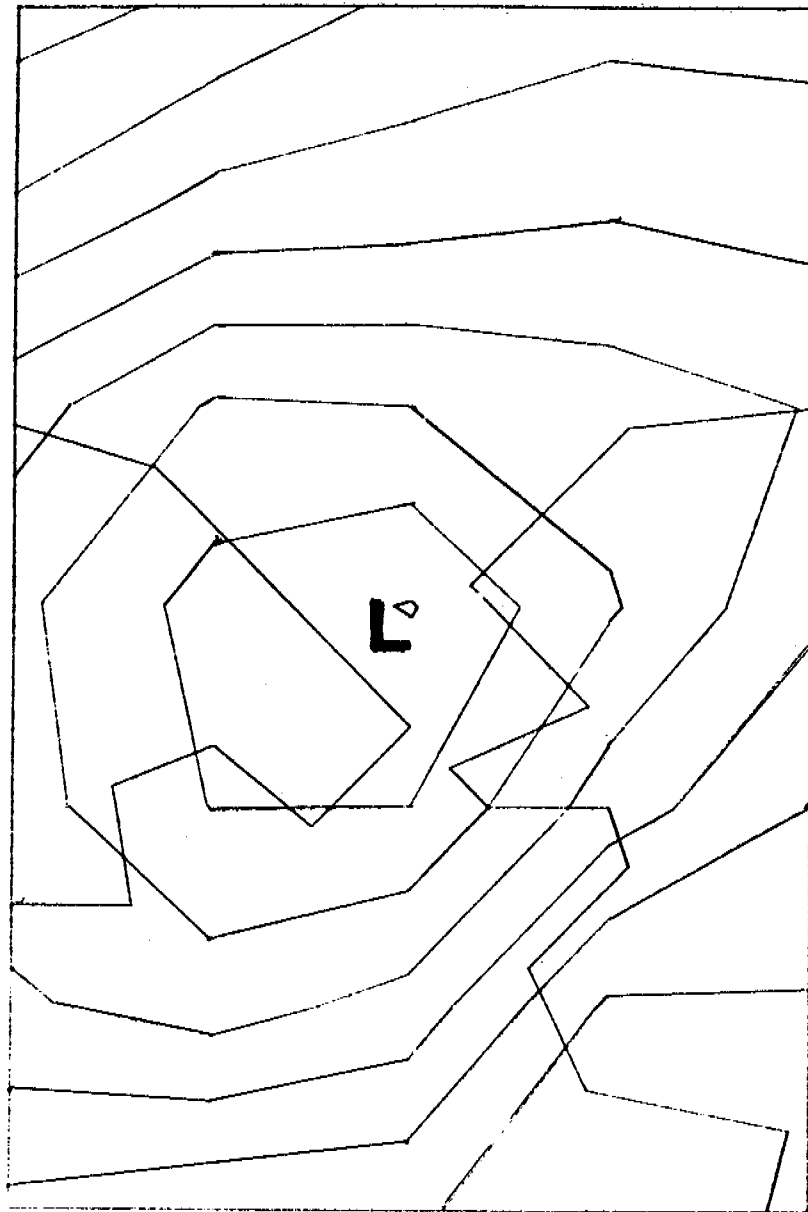


Fig. 12 Chukchi Key Day 7, July 16, 1966

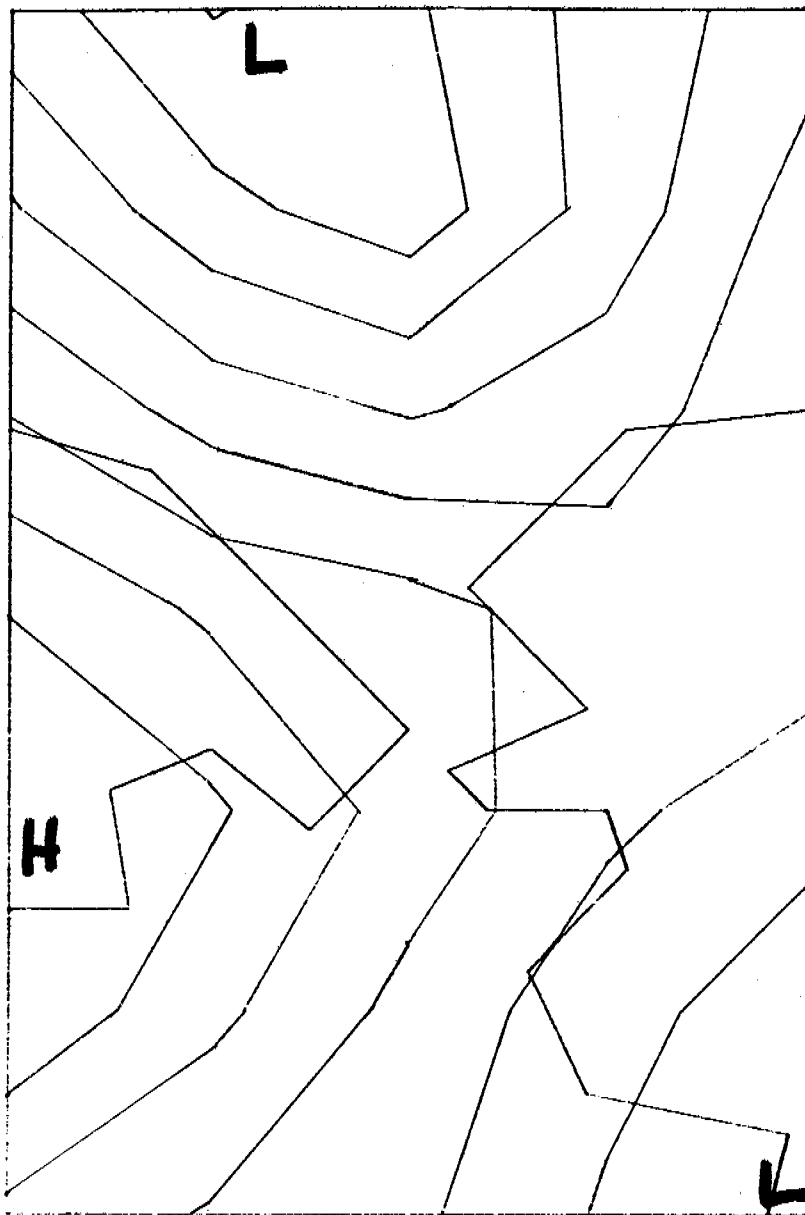


Fig. 13 Chukchi Key Day 8, Sept. 26, 1957

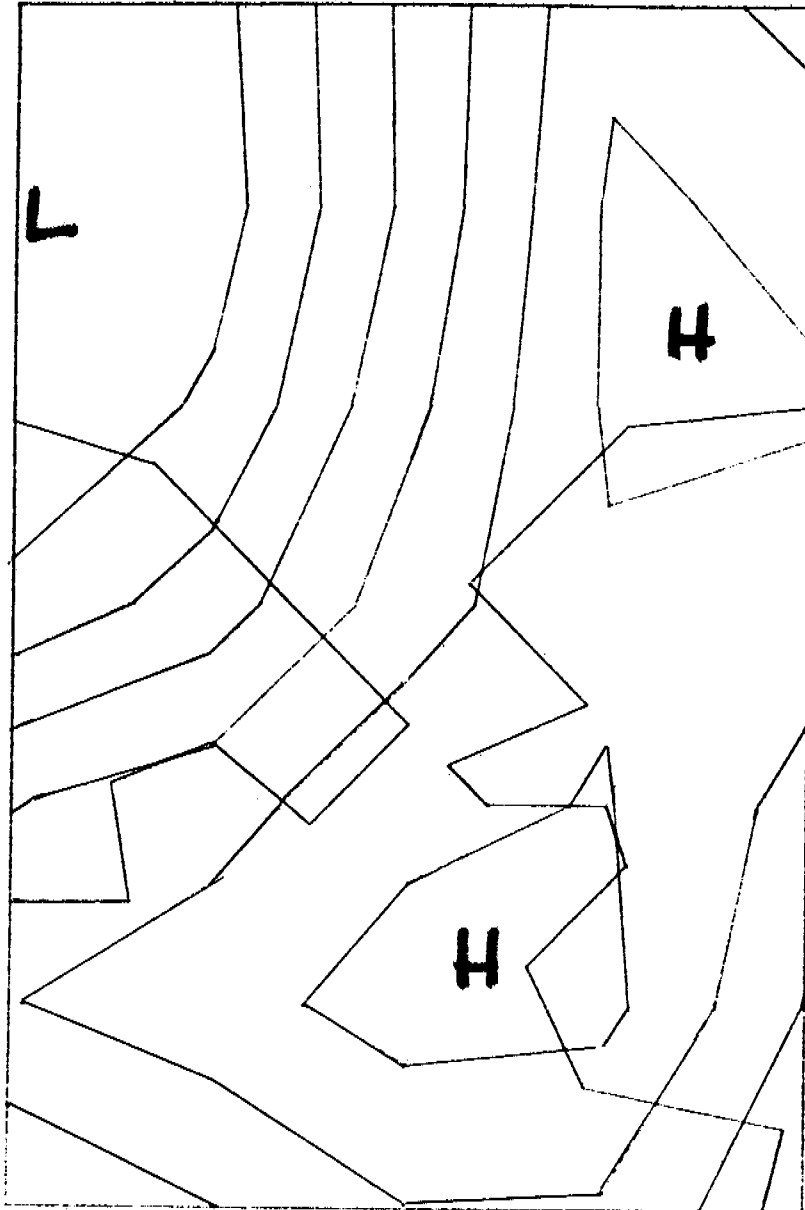


Fig.14 Chukchi Key Day 9, April 17, 1948

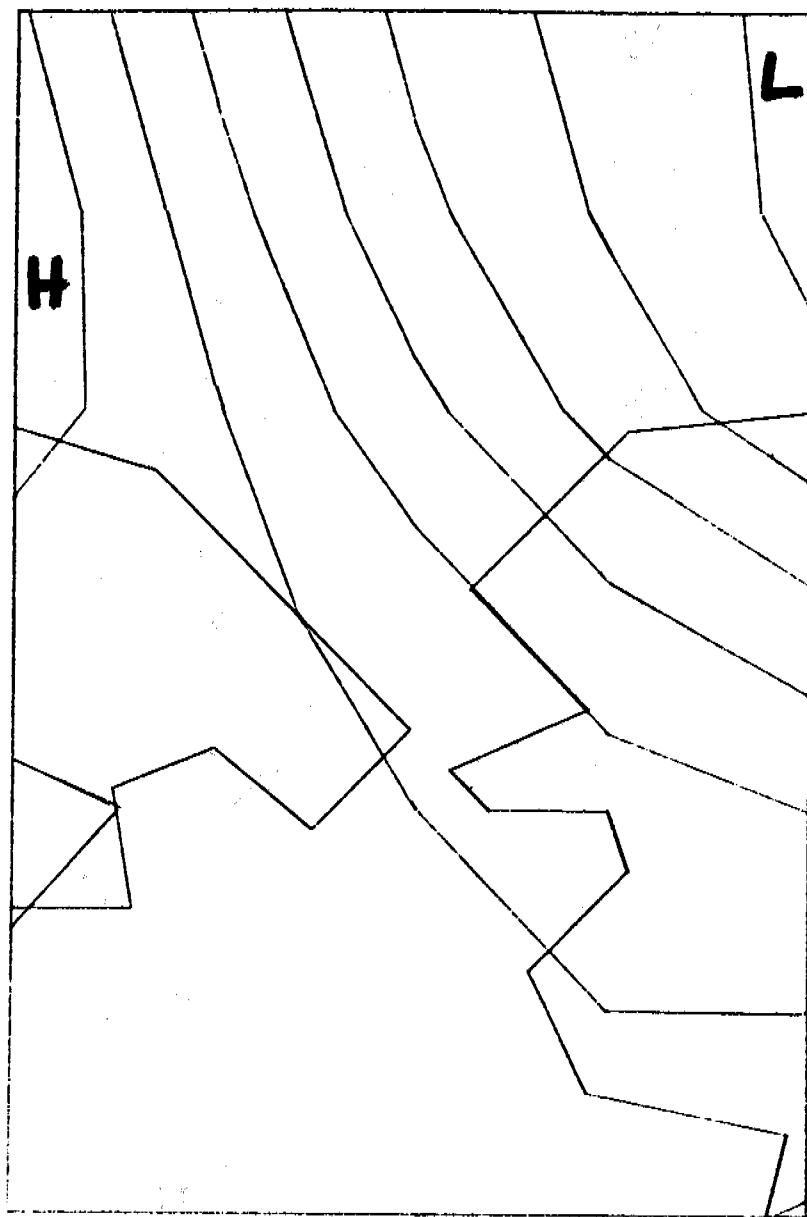


Fig.15 Chukchi Key Day 10, Aug. 28, 1948

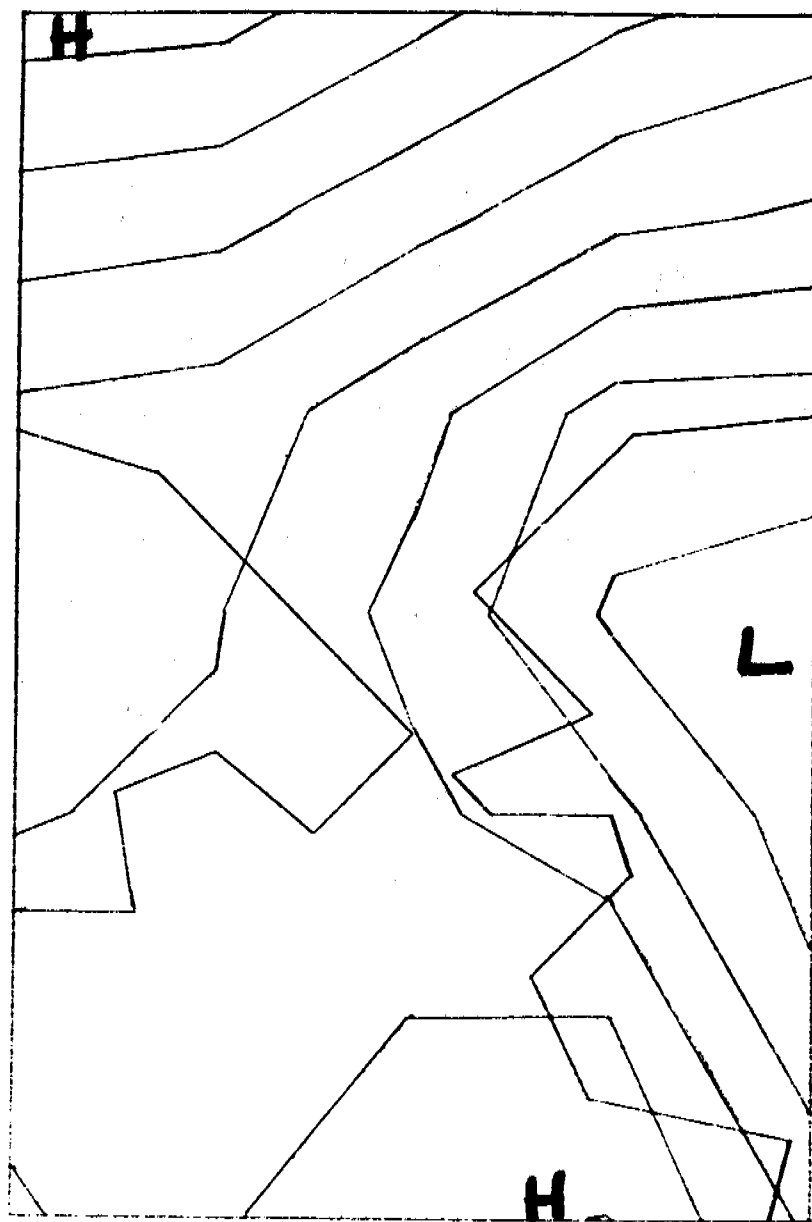


Fig. 16 Chukchi Key Day 11, Feb. 4, 1955

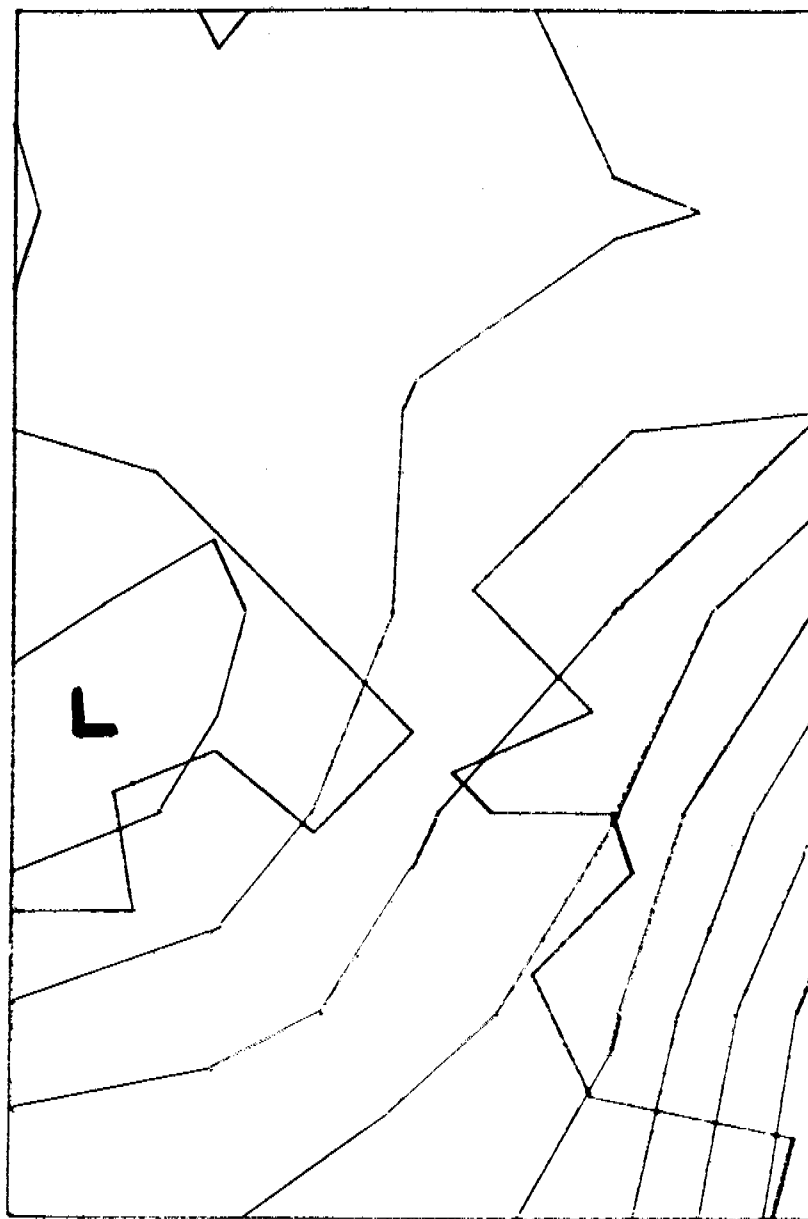


Fig.17 Chukchi Key Day 12, Sept. 8, 1948

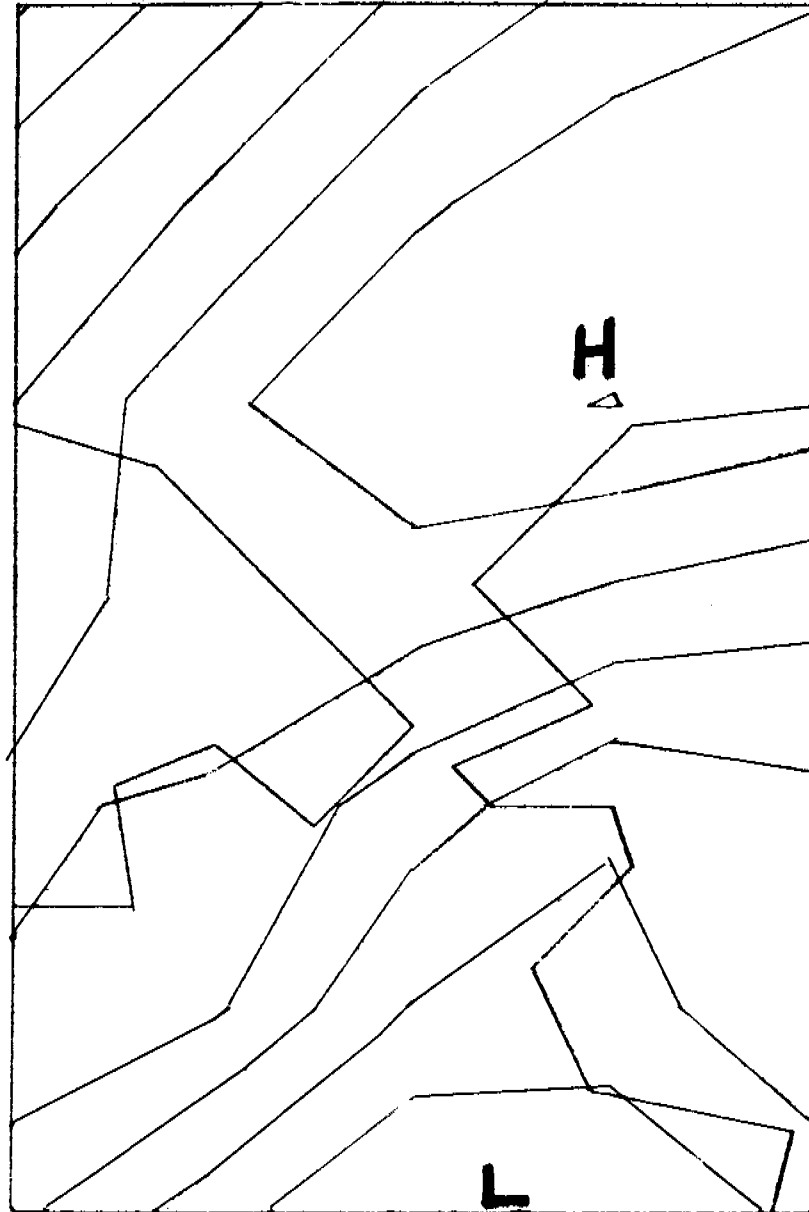


Fig. 18 Chukchi Key Day 13, June 16, 1969

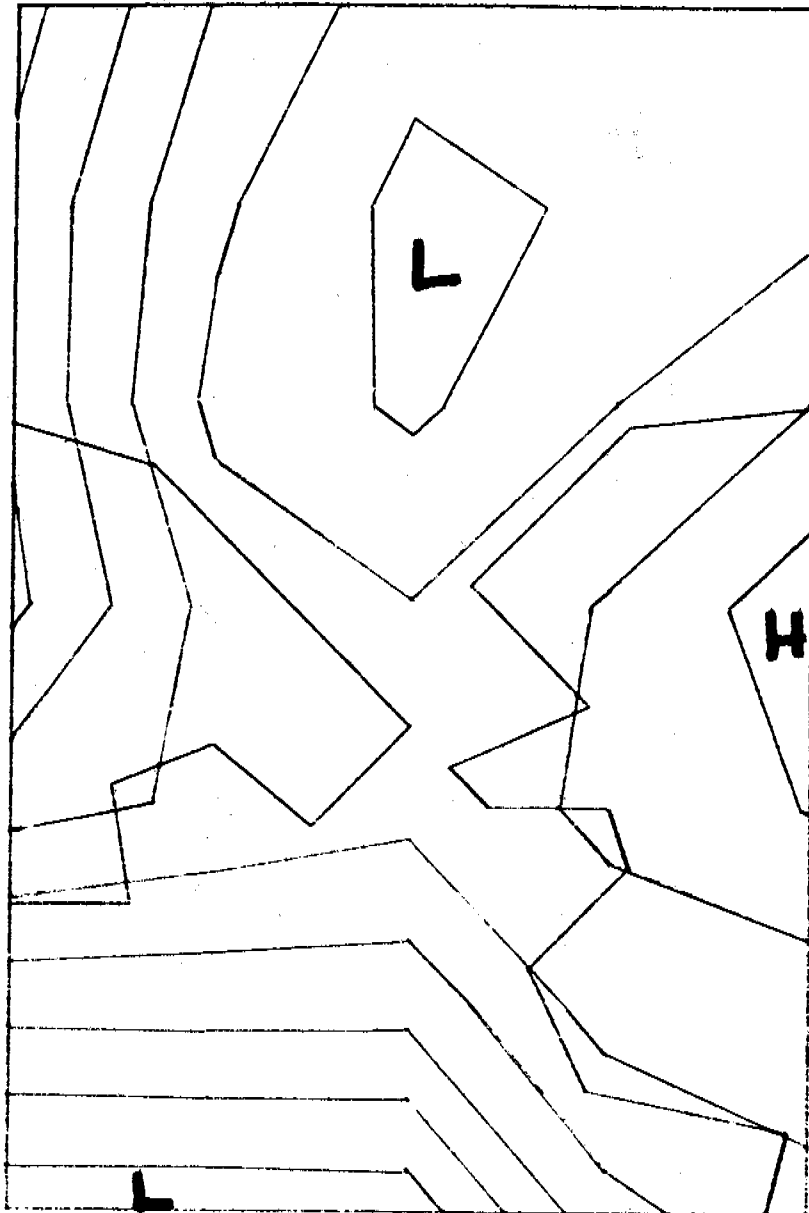


Fig.19 Chukchi Key Day 14, Dec. 19, 1966

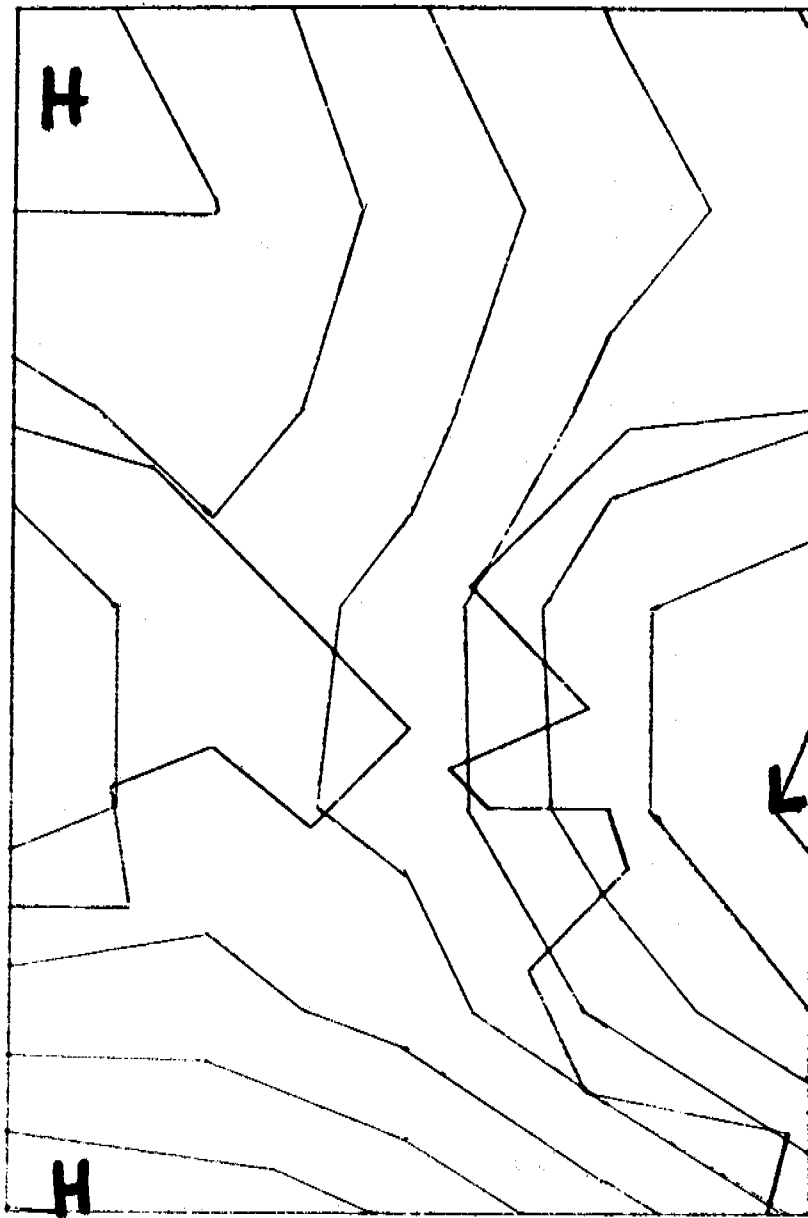


Fig.20 Chukchi Key Day 15, June 16, 1960

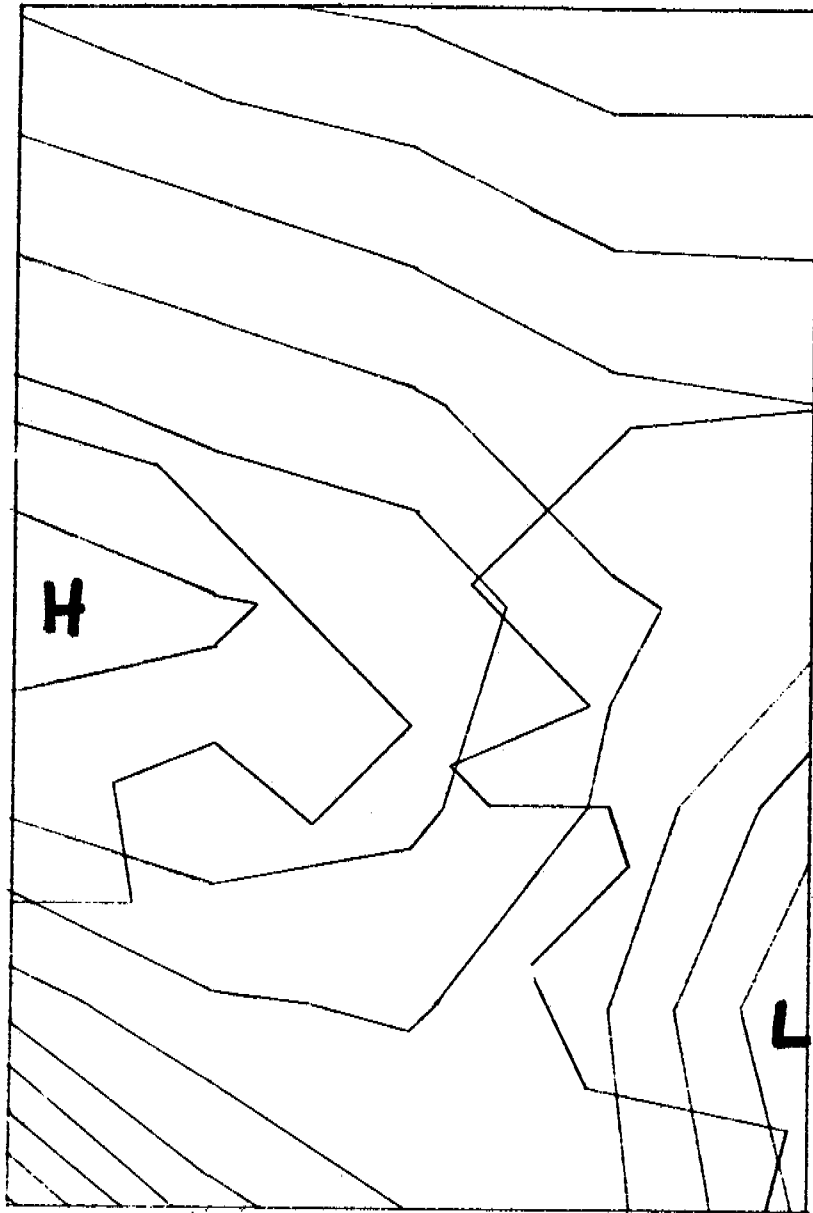


Fig.21 Chukchi Key Day 16, March 4, 1956

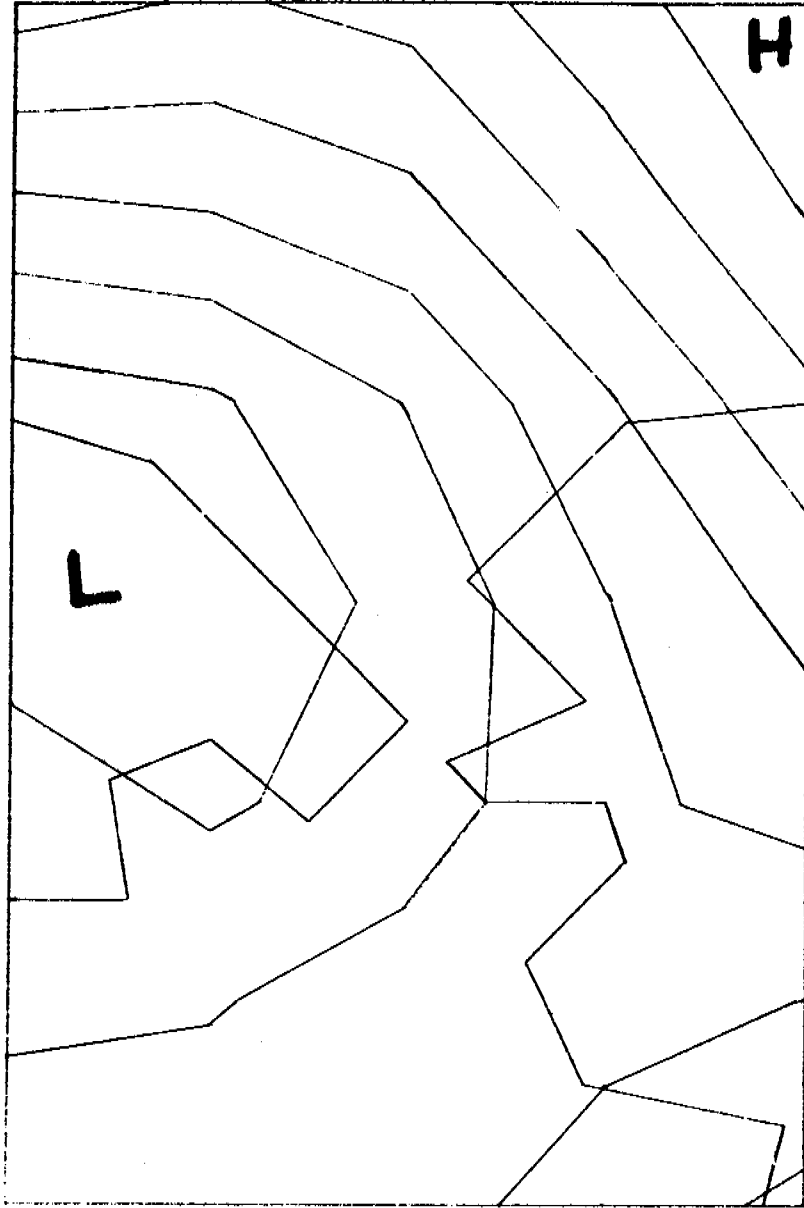


Fig.22 Chukchi Key Day 17, Dec. 26, 1968

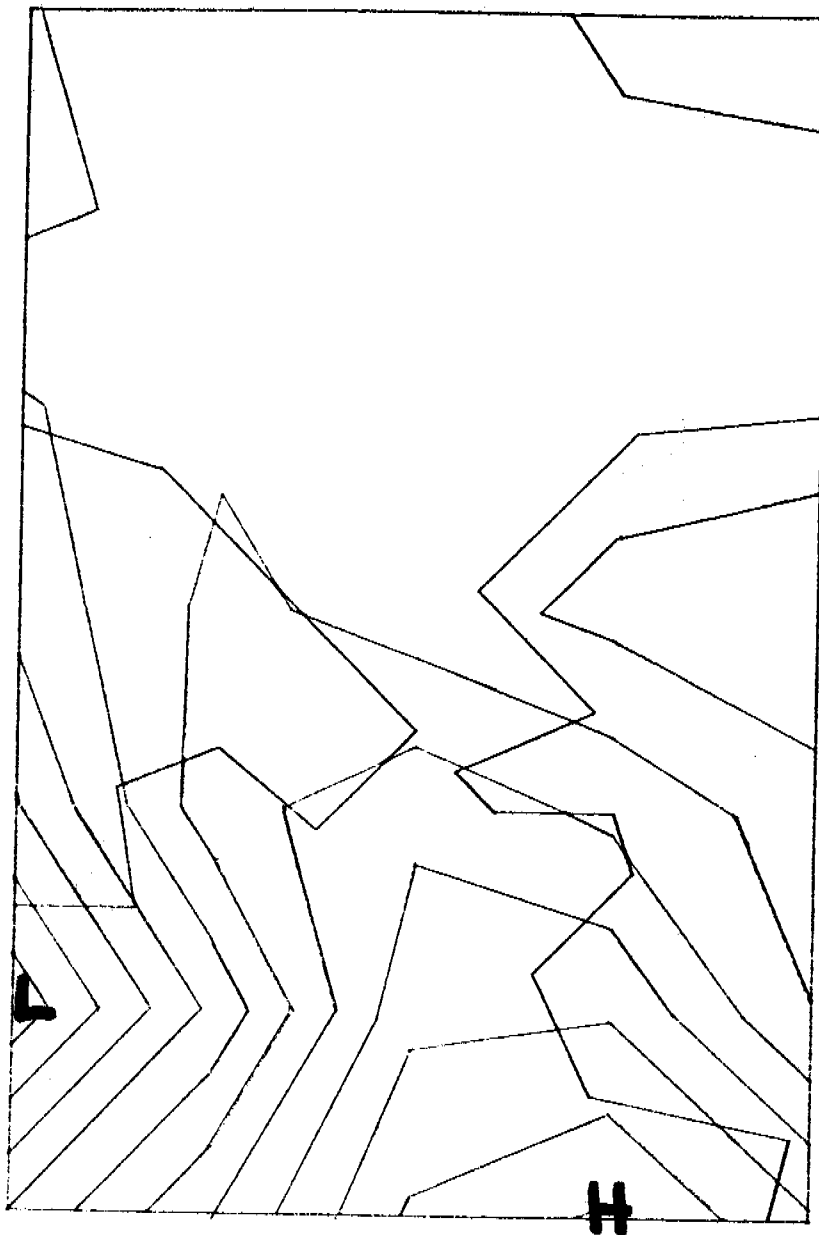


Fig. 23 Chukchi Key Day 18, July 19, 1963

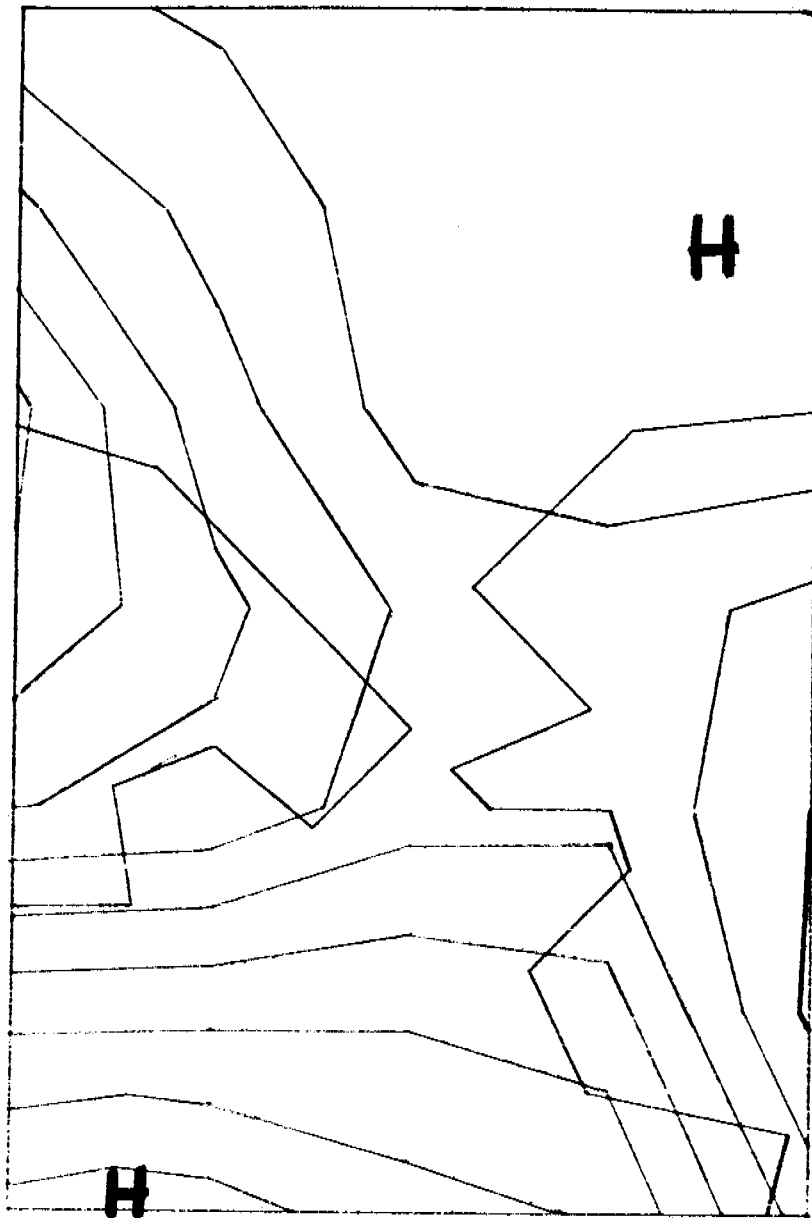


Fig.24 Chukchi Key Day 19, Oct. 17, 1964

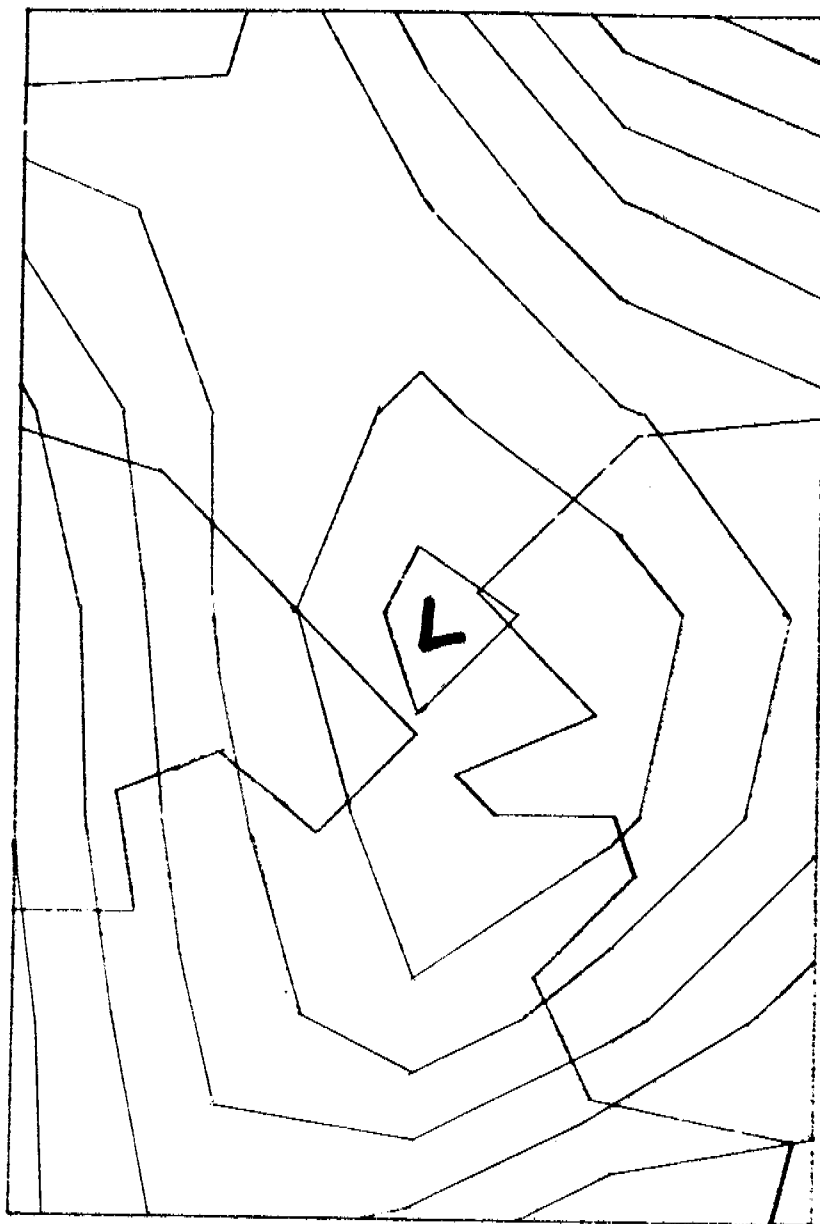


Fig.25 Chukchi Key Day 20, April 24, 1959

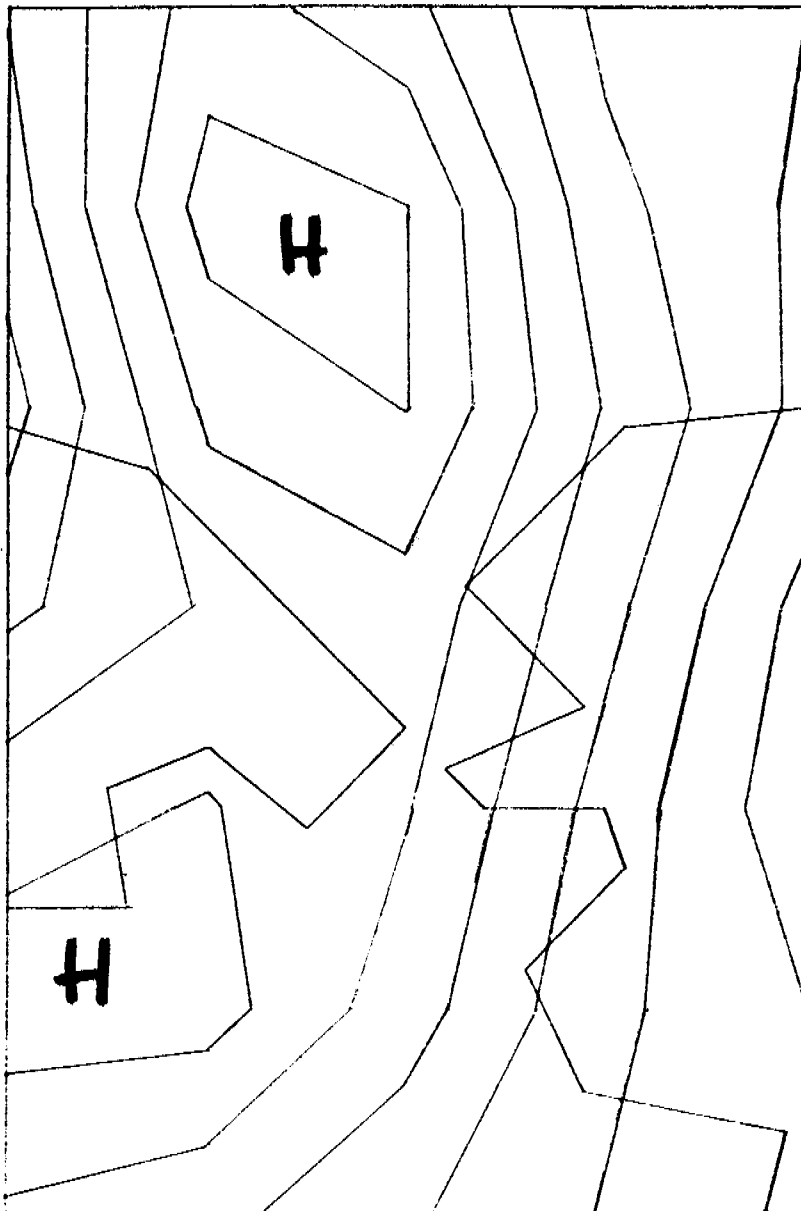


Fig.26 Chukchi Key Day 21, June 7, 1970

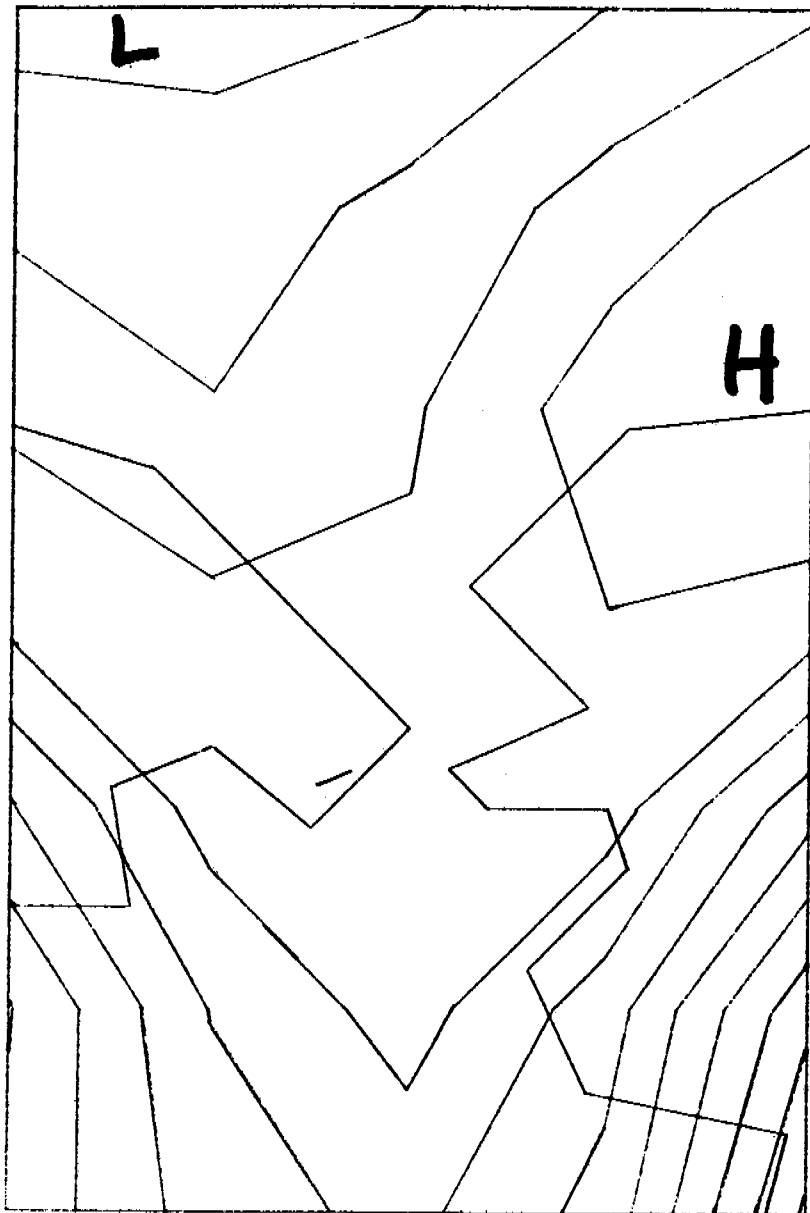


Fig.27 Chukchi Key Day 22, Jan. 1, 1956

% FREQUENCY OF CHUKCHI SYNOPTIC TYPES

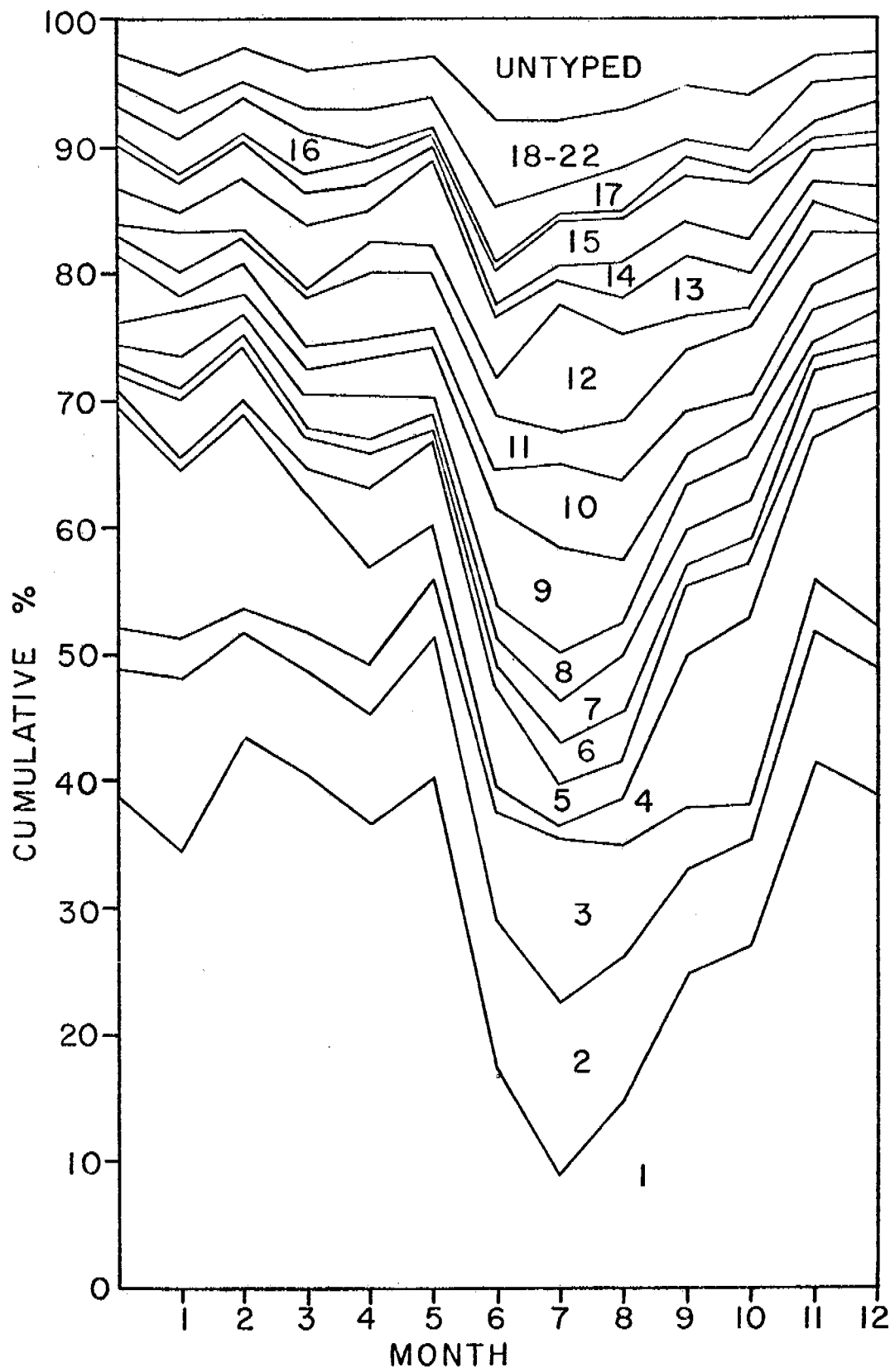


Fig. 28

APPENDIX 1

Documentation for Tape Containing Daily
Catalog of Pressure Pattern Types for
Beaufort Sea, Jan. 1966 - Aug. 1976.
OCS # RU 244, Contract # 03-5-022-91

The tape contains information on the daily, 1200 z MSL pressure pattern in the sector 120°-170° W, 60°-80° N. The daily catalog runs from 1/1/1946 to 8/31/1974. The tape is coded, BCD even-parity., tape density is 800 BPI. The card image format is as follows (one card per day):

1946 Δ12 Δ31 ΔΔΔ4 ΔΔ11.8 ΔΔ1013.6 ΔΔ1014.1 ΔΔΔ13.71 ΔΔ36

Field 1 Year

Field 2 Month

Field 3 Day

Field 4 Pressure Type (see Annual Report, 3/31/76).

Field 5 $\sum \Delta^2$ score against "key day" for type.

Field 6 Central Pressure (mb and tenths).

Field 7 Mean Pressure (mb and tenths)

Field 8 Pressure Standard Deviation (mb and hundredths).

Field 9 Number of points

Δ = space

The output list from the type has been checked, and there are two days with errors in the numeric fields, these are:

9/22/1956 Field 5.

1/11/1973 Fields 7 & 8.

TITLE: Mechanics of Origin of Pressure Ridges, Shear Ridges and Hummock Fields in Landfast Ice

PERIOD: October 1, 1976-December 31, 1976

PRINCIPAL INVESTIGATORS: Lewis H. Shapiro and William D. Harrison
Geophysical Institute, University of Alaska

I. TASK OBJECTIVES: To determine the mechanics of origin of pressure ridges, shear ridges and hummock fields in landfast ice.

II. FIELD AND LABORATORY SCHEDULE: Evaluation of results and continuation of preliminary theoretical work.

III RESULTS AND INTERPRETATION:

As noted in the last quarterly report, a bathymetric survey was conducted within the field of view of the University of Alaska radar system at Barrow. A bathymetric map of the area has been prepared to aid in interpretation of ridging patterns. In addition, E. Riemnitz of the U. S. Geological Survey had the opportunity to examine the records acquired during the survey (which was done with a continuously recording fathometer), and pointed out that numerous gouges in the sea floor were visible on the data. Accordingly, we attempted to determine the distribution of gouges with water depth in the survey area.

The number of gouges which penetrated more than 1 foot into the sea floor were identified and counted by selected intervals of water depth. The length of ship track over each depth interval was identified, and an average number of gouges per nautical mile of track was calculated for each such interval. Samples of the data and a plot of the results are attached.

A total of 32.7 nautical miles of track was covered during the survey, and most legs were run at a high angle to the coast. Thus, the counts are probably biased toward gouges which are oriented parallel to the coast. Note also that the relatively high number of gouges in the 95-99 foot depth interval largely reflects counts in one small area, and may not be representative of the average. However, gouges were found in depths to 120 feet, the limit to which the survey was extended.

The sea floor was sufficiently rough that it was difficult to establish an accurate datum from which to measure the depth of penetration of the gouges. However, it appears that most were in the range of 2-5 feet. The maximum penetration observed was 9 feet.

Based upon the data shown, the change in gouge density across the 30 foot depth contour appears to be real, but the question of the significance of variations in the remainder of the data requires further study.

During the past quarter we began a study of the vibration of ice sheets as an indicator of increasing stress. The work is being done by Dr. Howard Bates of the Geophysical Institute staff.

The study is based on the following observations of vibrations of landfast ice sheets with periods in the range of almost 6-10 cycles per minute.
1) At Barrow during July, 1975 the landfast ice sheet was driven ashore forming a line of ridges on the beach. A tide gauge was operating on the ice sheet, and recorded the passage of waves with amplitudes of up to 2 inches, and with the periods noted above, for several hours prior to the movement. The vibration was confirmed by examination of 8mm time-lapse movies of the movement episode which included the location of the tide gauge in the field of view.

2) In April 1976, similar vibrations were recorded at Barrow by the tide gauge (again fixed to the ice), and an array of stress transducers installed nearby in the ice sheet. Unfortunately, the output from the stress transducers was not being continuously recorded prior to the start of the vibrations, so that the magnitude of the stress build-up (if any) associated with the start of the movements is not known. The amplitude of the stress changes during the vibrations was about 2 psi.

3) R. D. Nelson (pers. comm.) reported that records from a stress transducer array located north of Cross Island in Spring 1976 recorded several examples of cycling of stresses with amplitudes of a few pounds per square inch and periods as above which followed episodes of increases in the stress level of the ice of about 10 psi.

4) Radar observations at Barrow include several examples of vibrational of the ice sheets (of unknown periods) as precursors to movement. These have been noted for drifting pack ice as well as landfast ice.

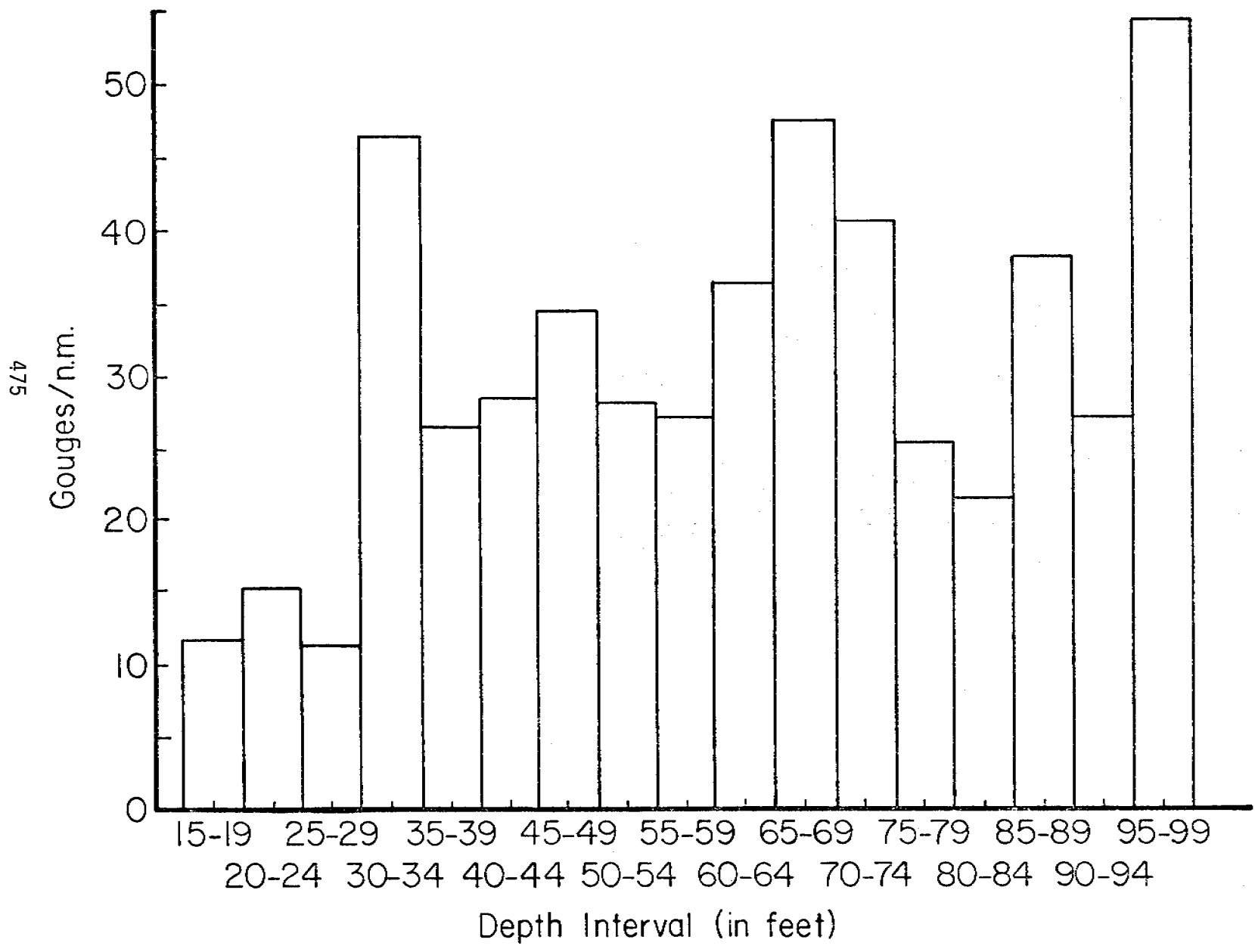
Based upon these observations, there is an apparent relationship between the buildup of stress in the ice, and the initiation of the vibrations in the observed frequency range, and the problem is being examined.

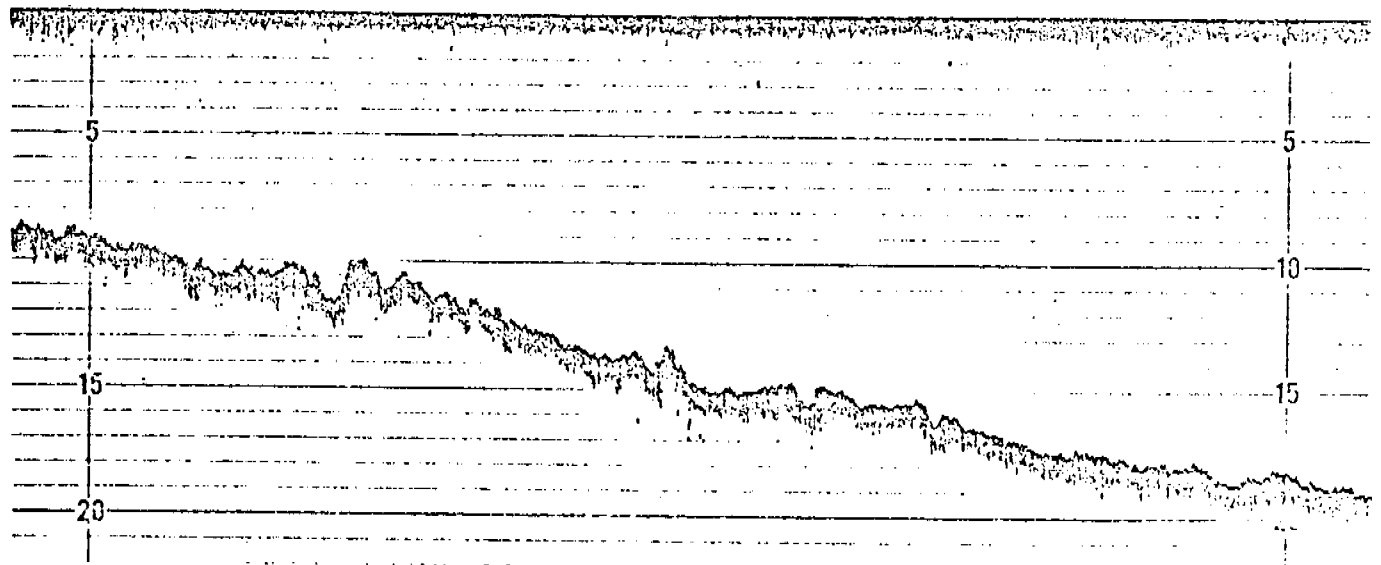
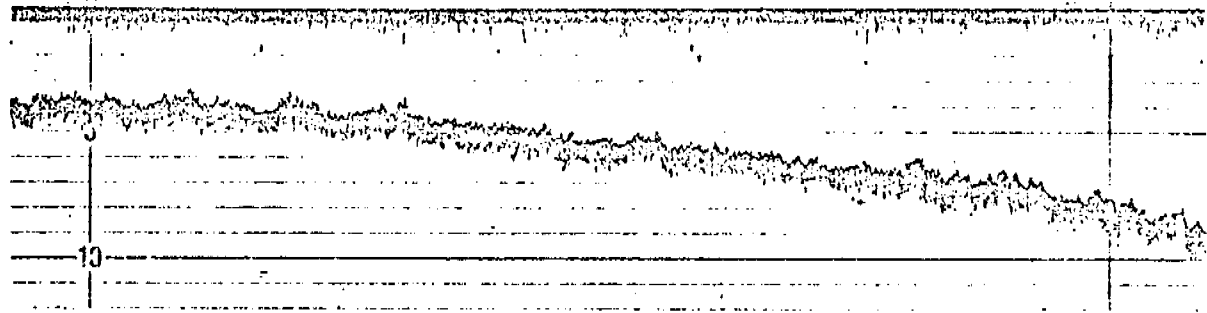
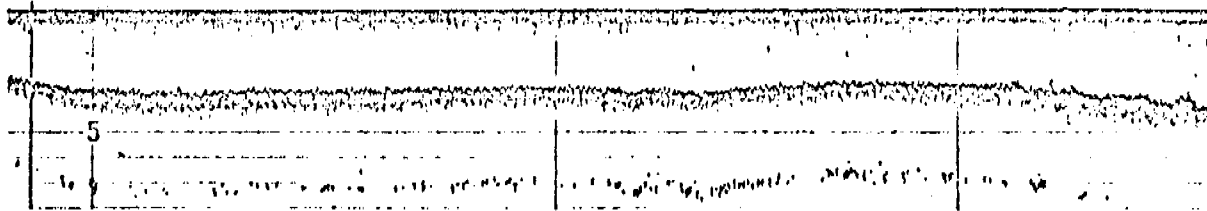
The approach is based upon the assumption that the stress build-up in the ice sheet is due to in-plane wind loading, with the vibration initiated by out-of-plane loading resulting from failure of the ice at some distance from the point where the vibrations are observed. The ice sheet has been analyzed as an elastic plate on an elastic foundation, with the ice-water system coupled by a pressure proportional to the displacement at the interface. This yields an eigenvalue in the proper frequency range, but two major problems still exist concerning this solution: (1) the assumption that the coupling between the ice and water is proportional to pressure needs to be verified, and (2) the solution gives a narrow spectral line while observations by other investigators indicate that the spectrum should be rather wide. Studies of these problems are continuing.

In conjunction with the above, we are examining the role of wave motion of the sea ice-water system as an energy sink in the process of formation of pressure ridges. This work is still in a preliminary stage and results are not yet available.

IV. PROBLEMS ENCOUNTERED: none.

V. ESTIMATED FUNDS EXPENDED: \$10,000.





┌────────── 1/4 n.m. ─────────┐
Depths in Fathoms

Quarterly Report

Contract #03-5-022-55
Research Unit # 257/258
Task Order # 5/8
Reporting Period 10/1 - 12/31/76
Number of Pages 210

MORPHOLOGY OF BEAUFORT, CHUKCHI AND BERING SEAS
NEAR SHORE ICE CONDITIONS BY MEANS OF SATELLITE AND
AERIAL REMOTE SENSING

Dr. W. J. Stringer
Research Associate
Geophysical Institute
University of Alaska
Fairbanks, Alaska 99701

January 1, 1977

OCS COORDINATION OFFICE

University of Alaska

Quarterly Report for Quarter Ending December 31, 1976

Project Title: Morphology of Beaufort, Chukchi and Bering Seas Near Shore Ice Conditions by Means of Satellite and Aerial Remote Sensing.

Contract Number: 03-5-022-55

Task Order Number: 8

Principal Investigator: W. J. Stringer

I. Task Objectives:

The objective of this study is to develop a comprehensive morphology of near shore ice conditions along the ice-frequented portions of the Beaufort, Chukchi and Bering Sea coasts of Alaska. This comprehensive morphology will include a synoptic picture of the development and decay of fast ice and related features, and in the absence of fast ice, the nature of other ice (pack ice, ice islands, hummock fields, etc.) which may occasion the near shore areas in other seasons. Special emphasis will be given to consideration of potential hazards to offshore facilities and operations created by dynamic ice events. Based on satellite observations available since 1972, a historical perspective of near shore ice dynamics will be developed to aid in determining the statistical rate of occurrence of ice hazards.

II. Field and Laboratory Schedule:

This project has no field schedule. All remote sensing aircraft data is to be provided by project management. Occasional field reconnaissance flights will be carried out on an unscheduled basis. The work does not involve laboratory activities.

III. Results:

Using LANDSAT band 7 hard copy produced at 1:500,000 scale, preliminary Beaufort Sea near shore ice maps have been compiled for the early summer (July) ice season of 1975, and preliminary Chukchi Sea near shore ice maps have been compiled for the 1973, 1974, and 1975 winter, spring and summer ice seasons as well as the late winter 1976 ice season. Particular care, described in earlier reports, has been taken to locate ice features as well as the bathymetric 10-fathom contour. Half-size (1:1 million scale) reproductions of these maps have been reproduced here as Appendix A.

IV. Preliminary Interpretations:

Preliminary Interpretations based on this quarter's work can be found in Appendix A.

V. Plans for Next Reporting Period:

During this quarter we will participate in the Beaufort Sea Synthesis meeting to be held in Barrow, Alaska the week of February 7, 1977.

Synthesis maps representing compilation of preliminary results to date will be prepared for that meeting. Following the meeting, the synthesis maps will be revised based on discussions with other investigators and representatives of project management and presented in our annual report due at the end of the reporting period.

VI. Problems Encountered/Recommended Changes:

None.

VII. Appendices:

(Appendix A, attached.)

APPENDIX A

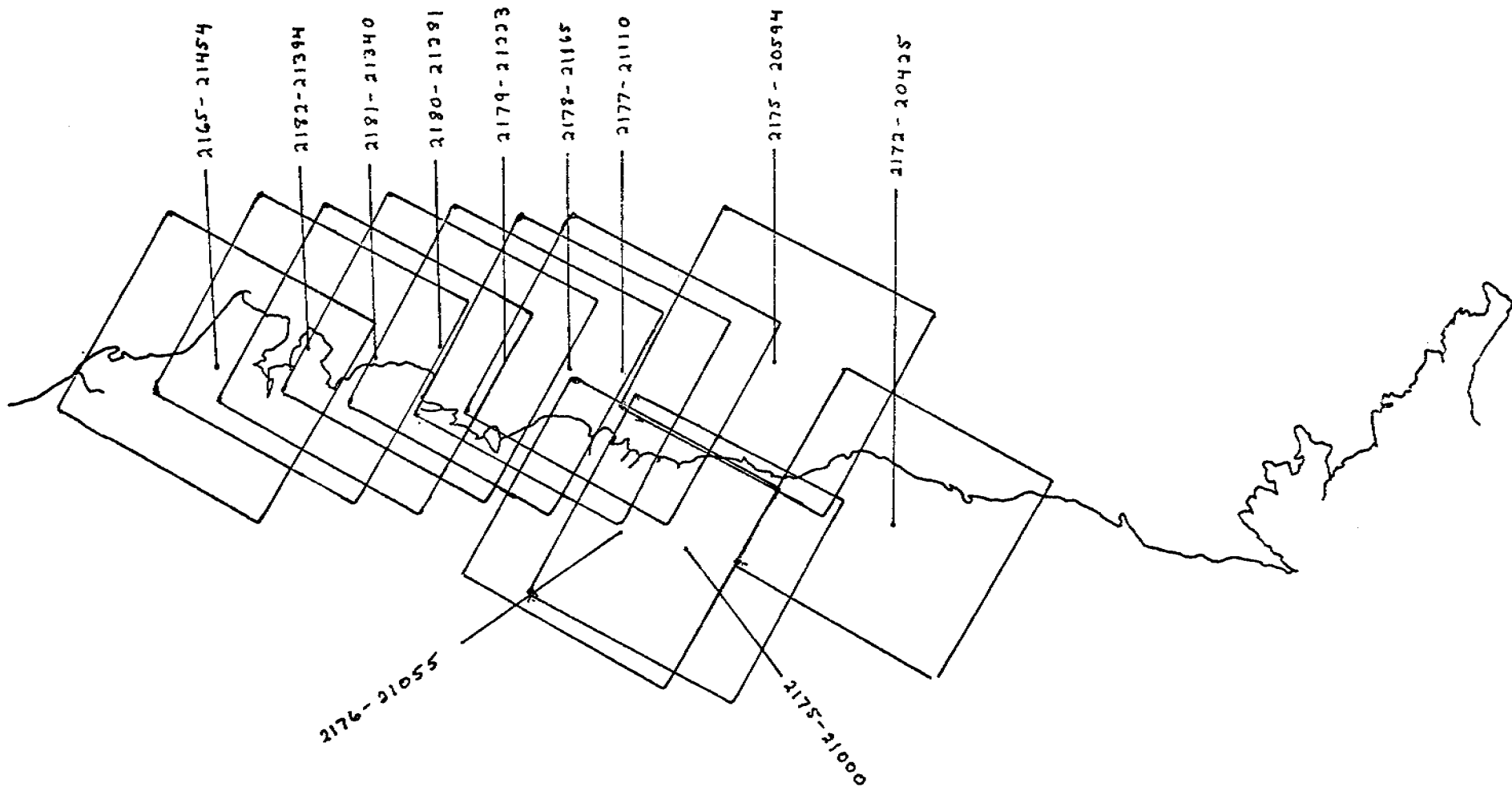
SYMBOLS USED AND THEIR MEANING

Listed below are the symbols used to map near shore ice conditions from LANDSAT imagery. This list of symbols has evolved during the mapping project and reflects ice conditions which can be detected on LANDSAT imagery as well as those ice conditions considered important in the understanding of near shore ice dynamics.

A	River Overflow	Used to denote areas where river water has overflowed onto sea ice.
B	Boundary	Denotes boundary between what appear to be two different ice types even though the two ice types may not be differentiated.
Bn	Broken New Ice	Sheet of new ice which has been broken - usually into an irregular pattern
Bpn	Broken Pans and New Ice	A sheet of young or first year ice is broken into pans followed by the freezing of the voids to the new ice stage, followed by the breaking of this entire matrix. Several cycles of this process may be evident, but the most recently-formed ice has developed to the new ice stage.
Bpy	Broken Pans and Young Ice	A sheet of young or first year ice is broken into pans followed by the freezing of the voids to the young ice stage followed by the breaking of this entire matrix. Several cycles of this process may be evident, but the most recently-formed ice has developed to the young ice stage.
By	Broken Young Ice	Sheet of young ice which has been broken - usually into an irregular pattern
C	Contiguous Ice	Ice stationary and continuous from shore without apparent fractures. This ice is at the time of observation fast with respect to the shore. The symbol is placed within large expanses of such ice and along the landward side of the seaward edge of such ice. Contiguous ice is not necessarily bounded on the seaward edge by grounded ice and can therefore extend seaward considerable distances.
Cf	Fractured Contiguous Ice	Contiguous ice which although not separated from shore by an open lead, is fractured by leads - often perpendicular to the shore.
D	Decayed Ice	Rotting or decaying ice, characterized by a dark mottled effect indicating holes and puddling.

F	Floe	Separately identifiable ice floe. Symbol used to denote floes distinctly visible against background even when completely frozen into surrounding ice.
Fw	Floes in Water	Open water with numerous floes of various sizes (see "Up".)
Fy	First Year Ice	Ice cover of age and thickness beyond "young" stage. Used principally to denote large expanses of ice in either contiguous or offshore category. May be composed of single sheet, many pans frozen together, or many pans compressed, and frozen together. Thickness on the order of 30-70 cm.
Fyb	First Year Broken	A broken or fragmented expanse of first year ice.
G	Grounded	Ice which clearly appears to be grounded.
H	Hummock Field	Large expanses of piled ice.
I	Young Ice	Ice appearing light grey on LANDSAT imagery. Can be single sheet or exhibit a variety of conditions (broken, compressed, rafted etc.). Thickness on the order of 10-30 cm.
L	Lead	A lead, usually open, but may be so narrow that this can not be determined. Large leads denoted by two lines showing boundaries, narrow leads denoted by single line.
M	New Ice	Characterized by dark shade of grey, smooth texture, may exhibit a number of conditions (see I). Thickness on the order of 0-10 cm.
N	Newly Frozen Lead or Polynya	Either new or young ice. Symbol usually written within distinct boundary.
O	Old Frozen Lead	A lead with ice sufficiently old to have either turned light grey or be covered with snow.
P	Partly Frozen Lead	Partly frozen lead. Ice conditions not uniform (as distinct from M) and may vary from new ice to late stages of young ice.
Pn	Pans in Matrix of New Ice	A sheet of young or first year ice had broken into pans and the surrounding water has frozen to the young ice stage.

R	Ridge	Denotes shear or pressure ridge or system of ridges.
S	Smooth Ice	Usually used to denote ice of uncertain age in protected areas.
T	Tidal or Tension Cracks	Cracks in near shore ice opened by either tidal action or thermal tension. Identification may be indirect (snow drifts, drainage pattern etc.)
Up	Unconsolidated Pack	A broken sheet of ice of any age beyond young ice which has been compressed to the point that open water voids are quite small but are not frozen over (see FW).
W	Water	Open water - symbol often used to denote specific area enclosed by line.
Y	Polynya	More specific than W. Most often used to denote area of open water on lee side of obstruction.
Z	Zone of Shear	Symbol used to denote location of apparent shearing motion on image. The symbol may be specifically located on a lead where shearing motion is taking place, a closed lead where shear piling of ice is apparently occurring or in an ice field where characteristic pattern of leads caused by shearing forces can be seen.

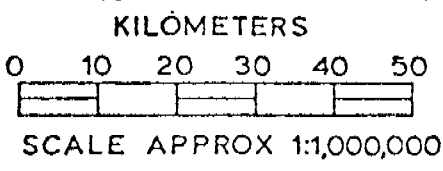
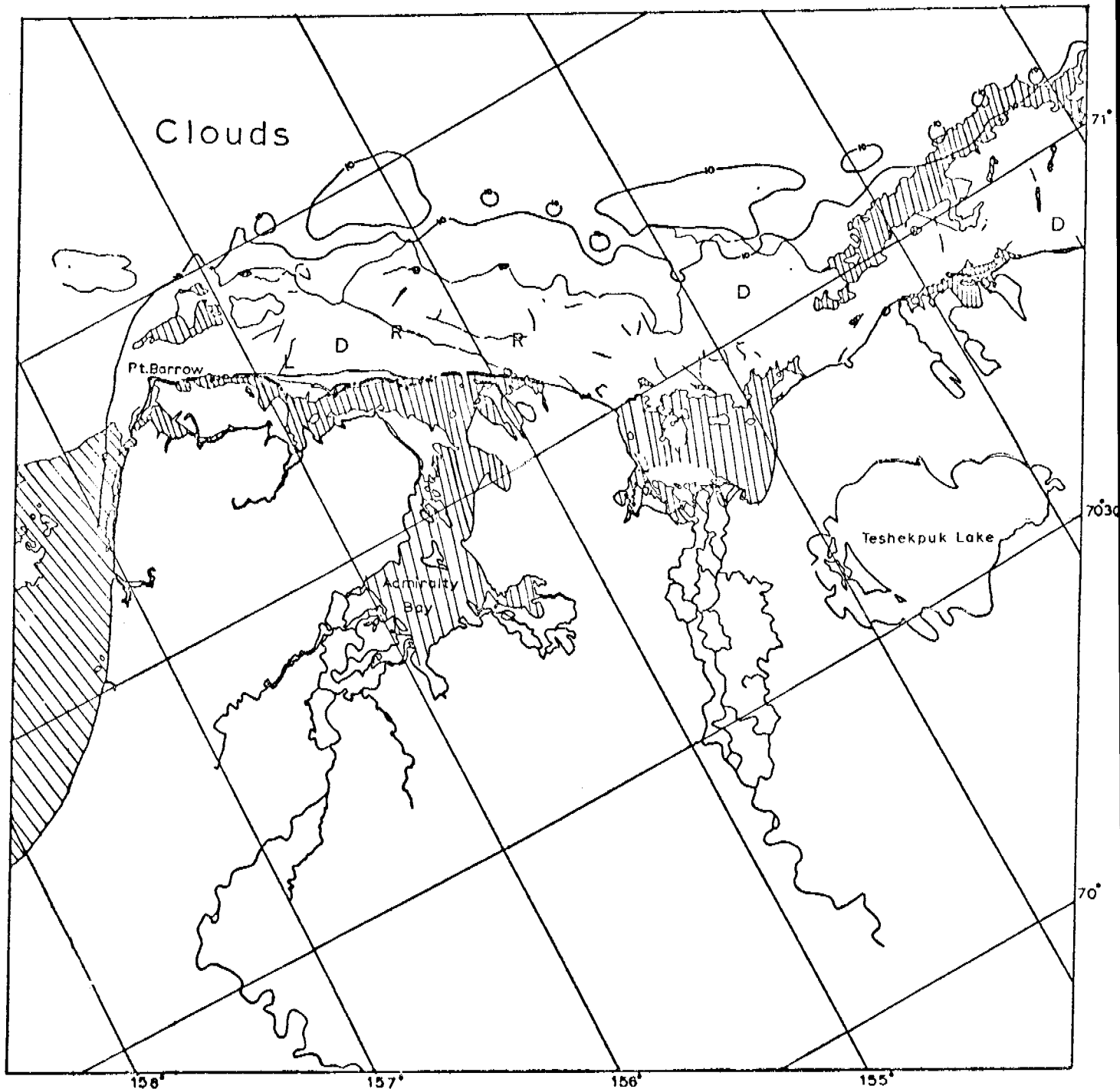


BEAUFORT SEA
6 JULY - 23 JULY 1975
Images 2165 - 2182

Scenes 2172-20425 through 2182-21394

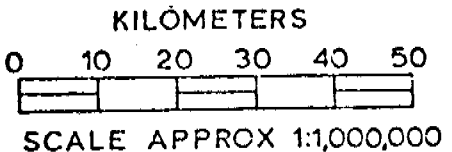
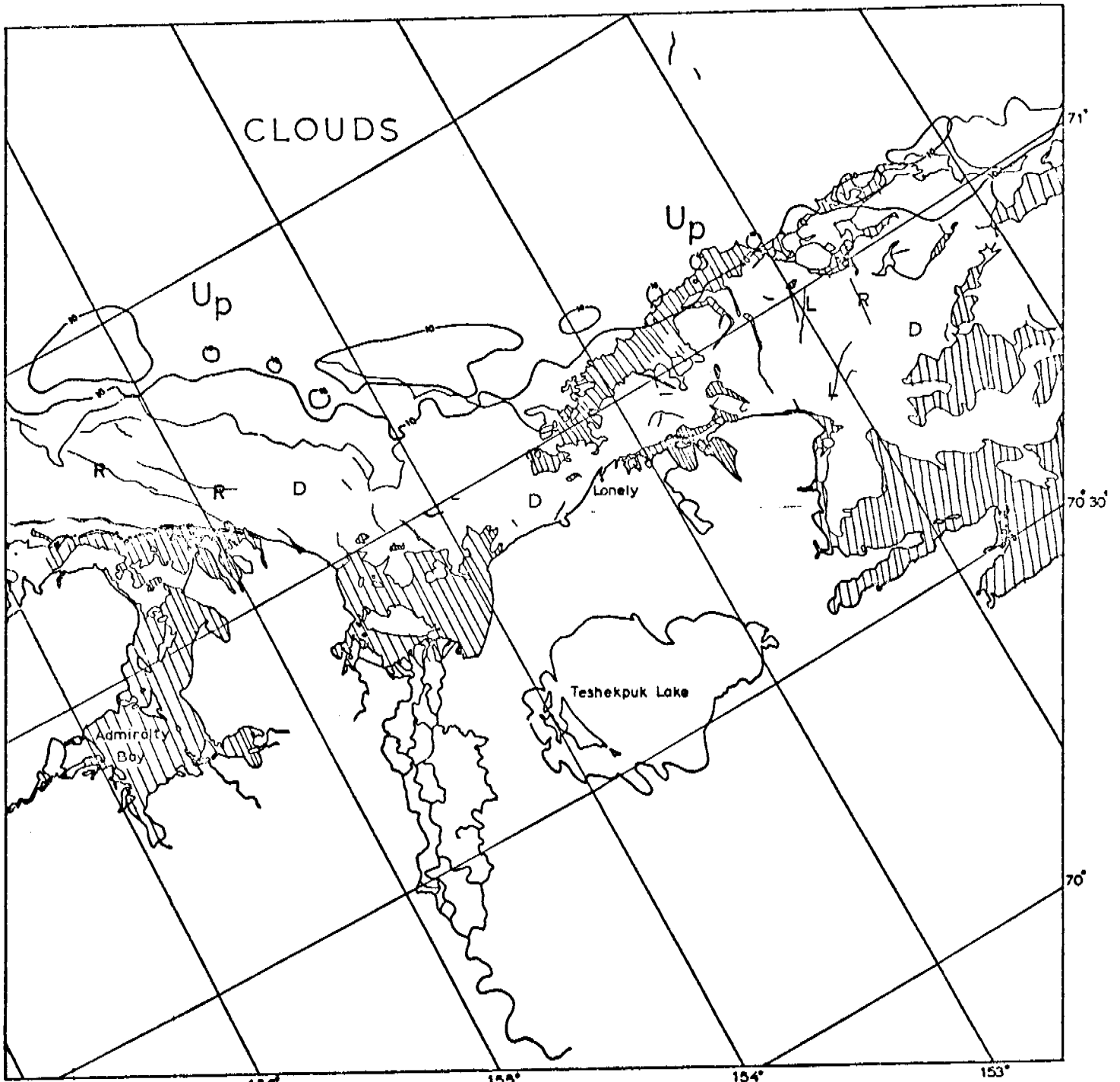
These scenes show the Beaufort Sea Coast between July 13-23, 1975. The chief value of this summer imagery is the identification of ice features remaining in place in mid summer and therefore very likely grounded. Ice yet grounded at this date was probably well grounded much of the past ice season.

Although thin clouds obscure much of the coast, it is still possible to trace ice boundaries along much of the coast. Of particular interest in the Harrison Bay area is the large complex of apparently grounded ridges mapped far off shore.



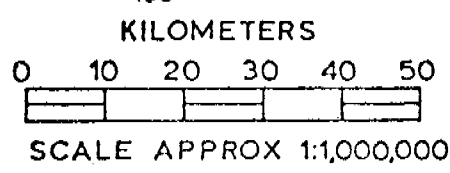
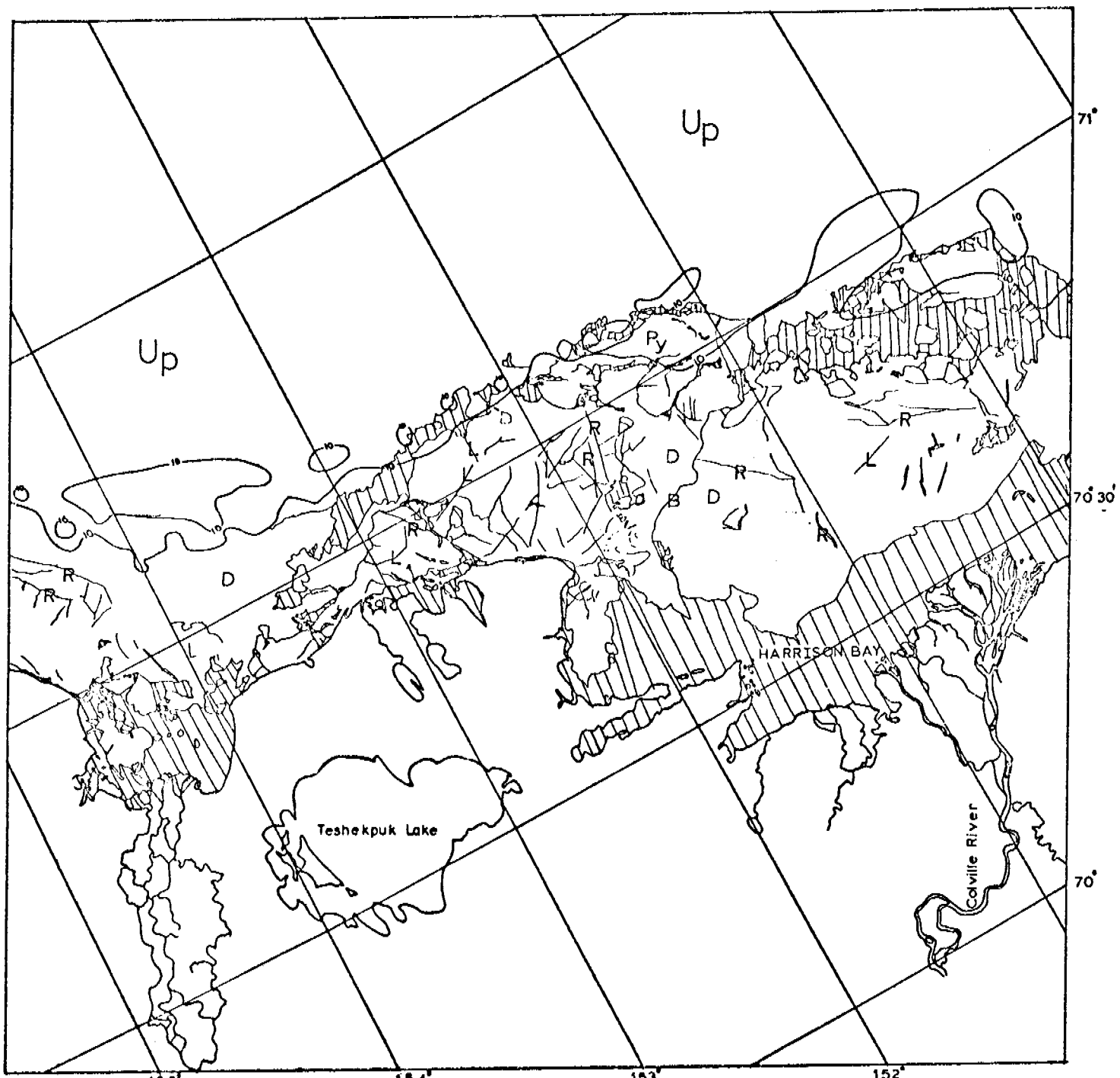
BEAUFORT SEA

E-2182-21394-7
23 JULY 1975



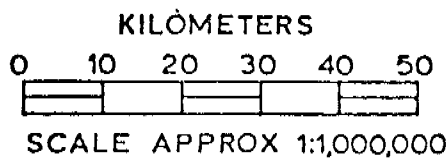
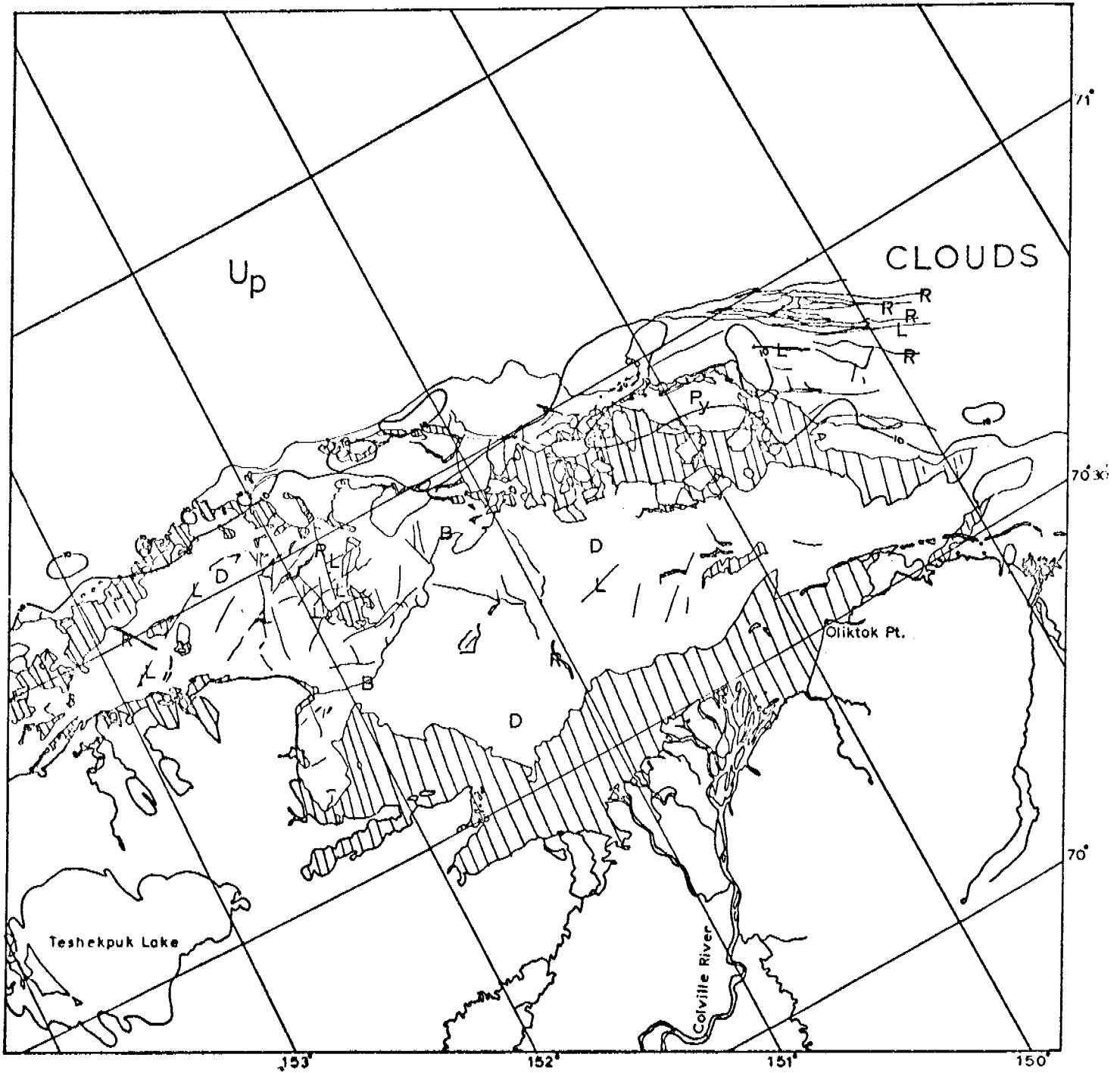
BEAUFORT SEA

E-2181-21340-7
22 JULY 1975



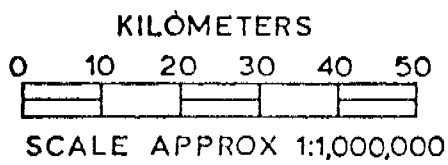
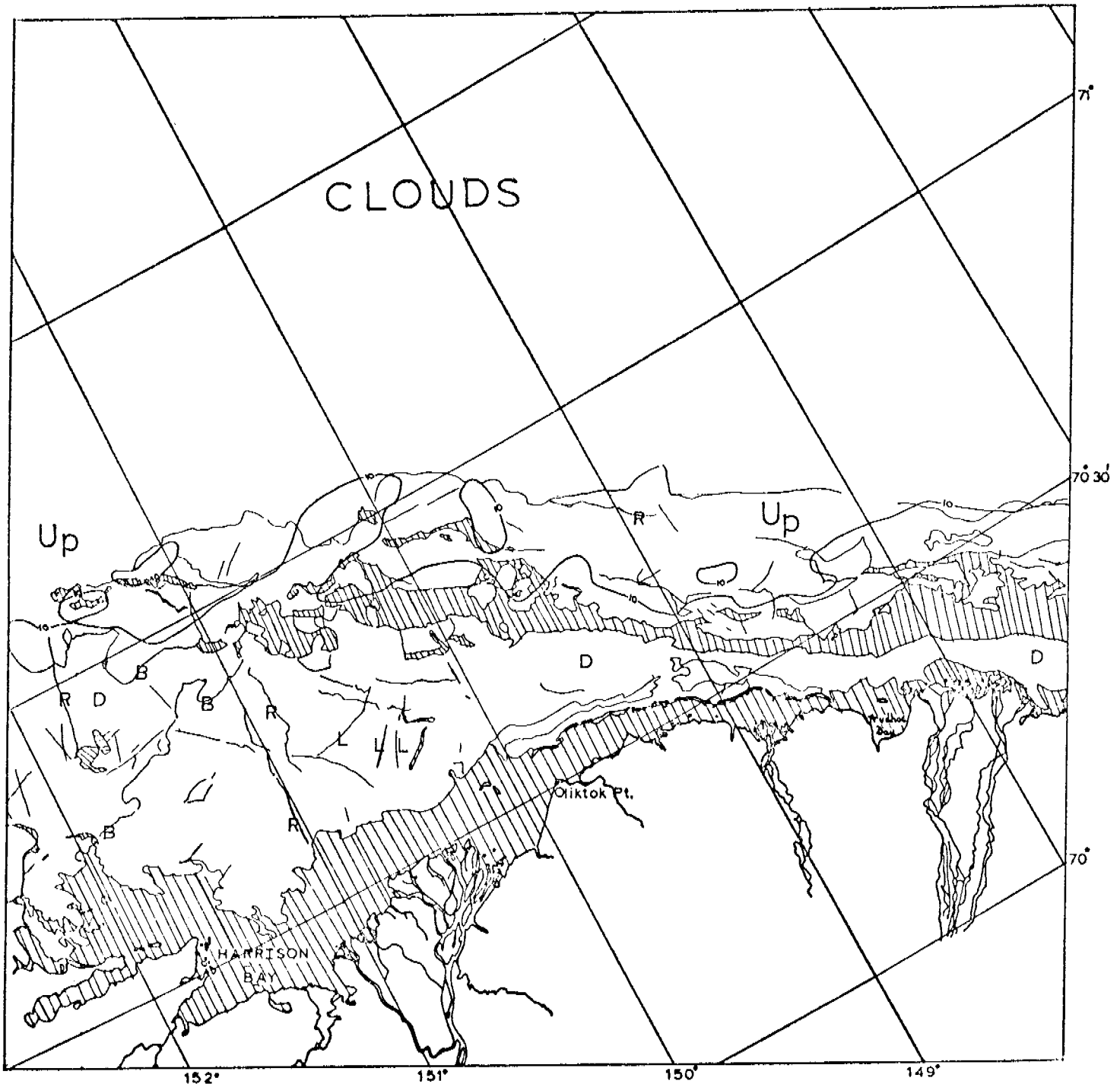
BEAUFORT SEA

E-2180-21281-7
21 JULY 1975



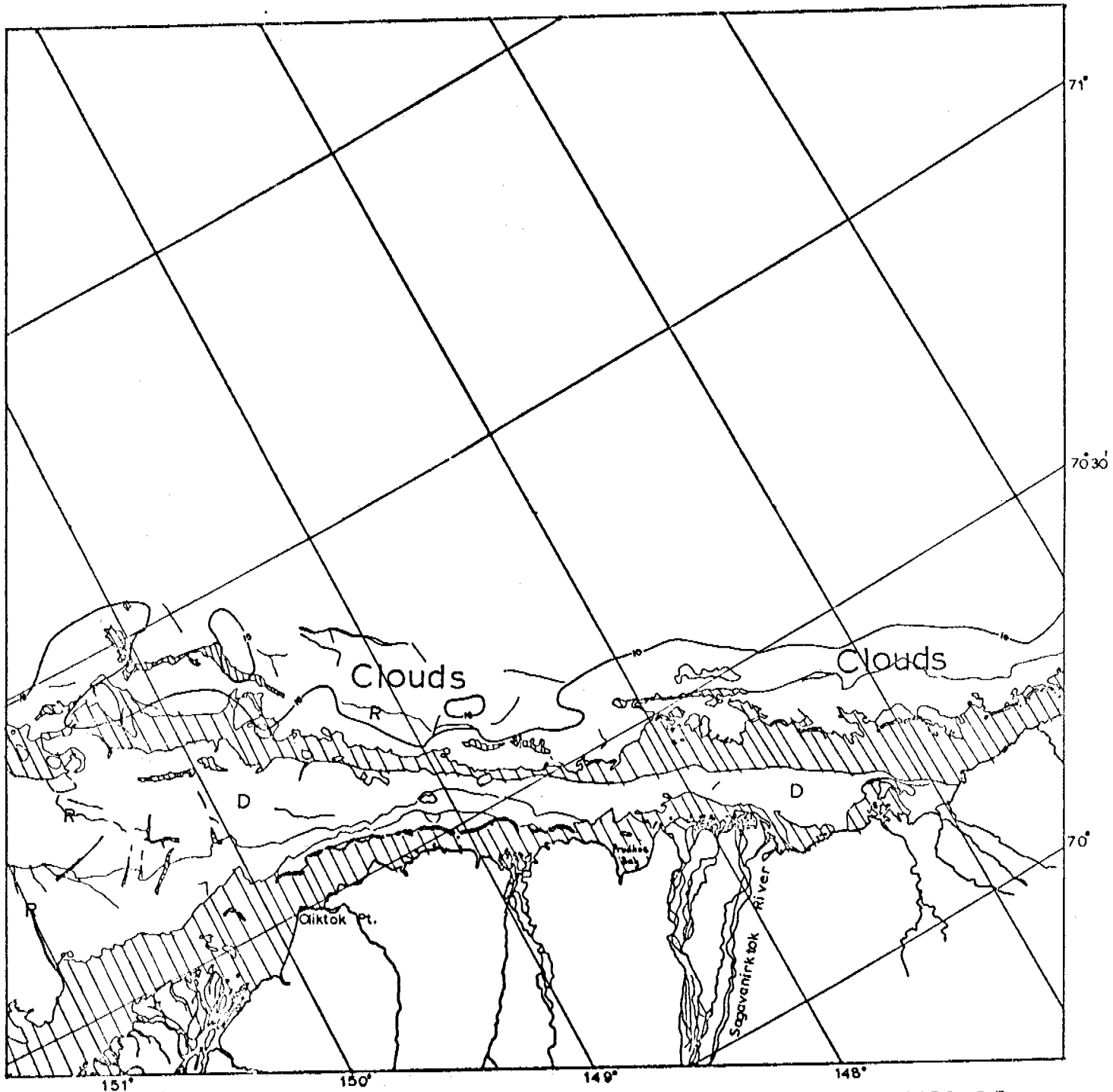
E-2179-21223-7
20 JULY 1975

BEAUFORT SEA



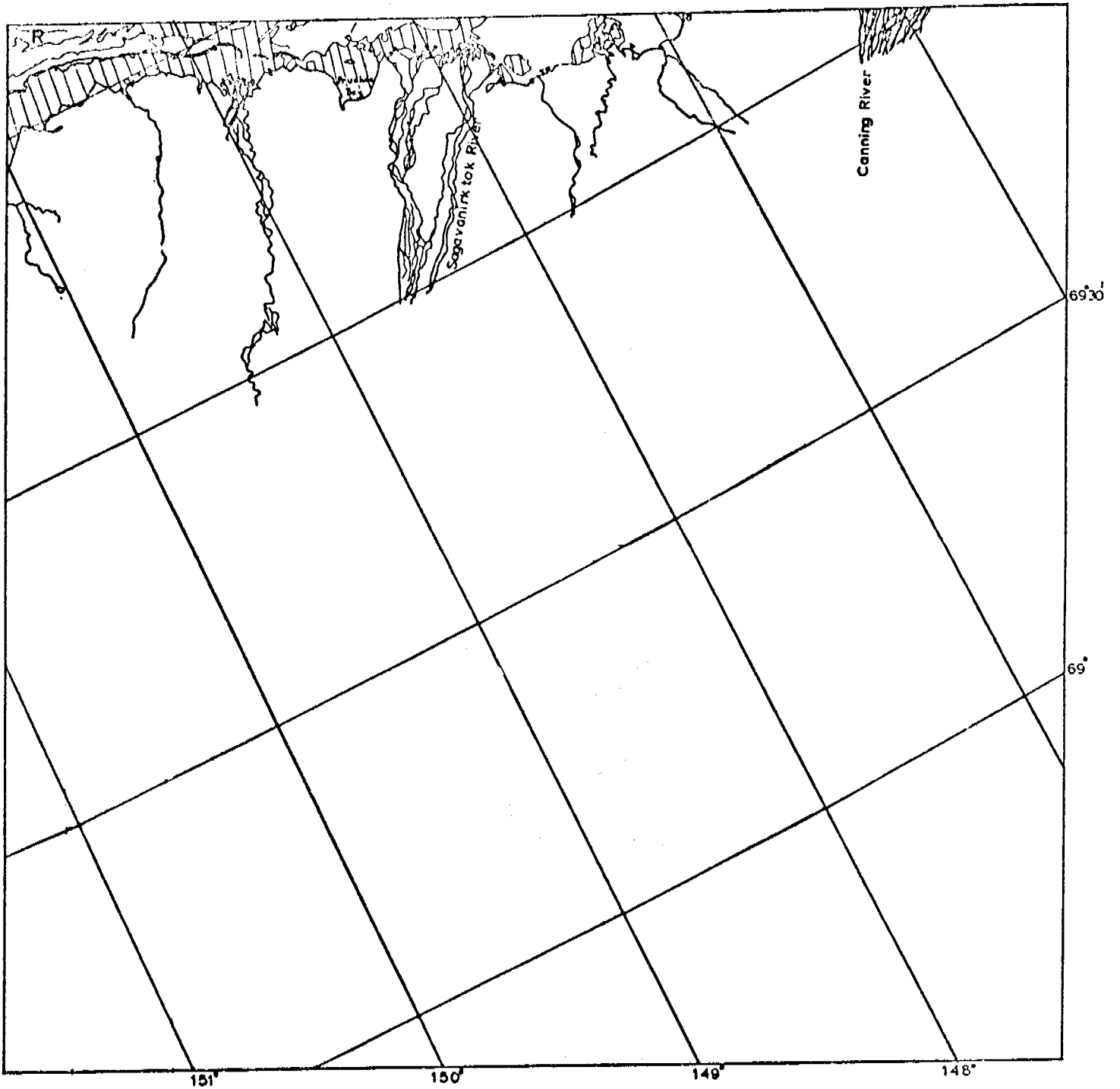
E-2178-21165-7
19 JULY 1975

BEAUFORT SEA



E-2177-21110-7
18 JULY 1975

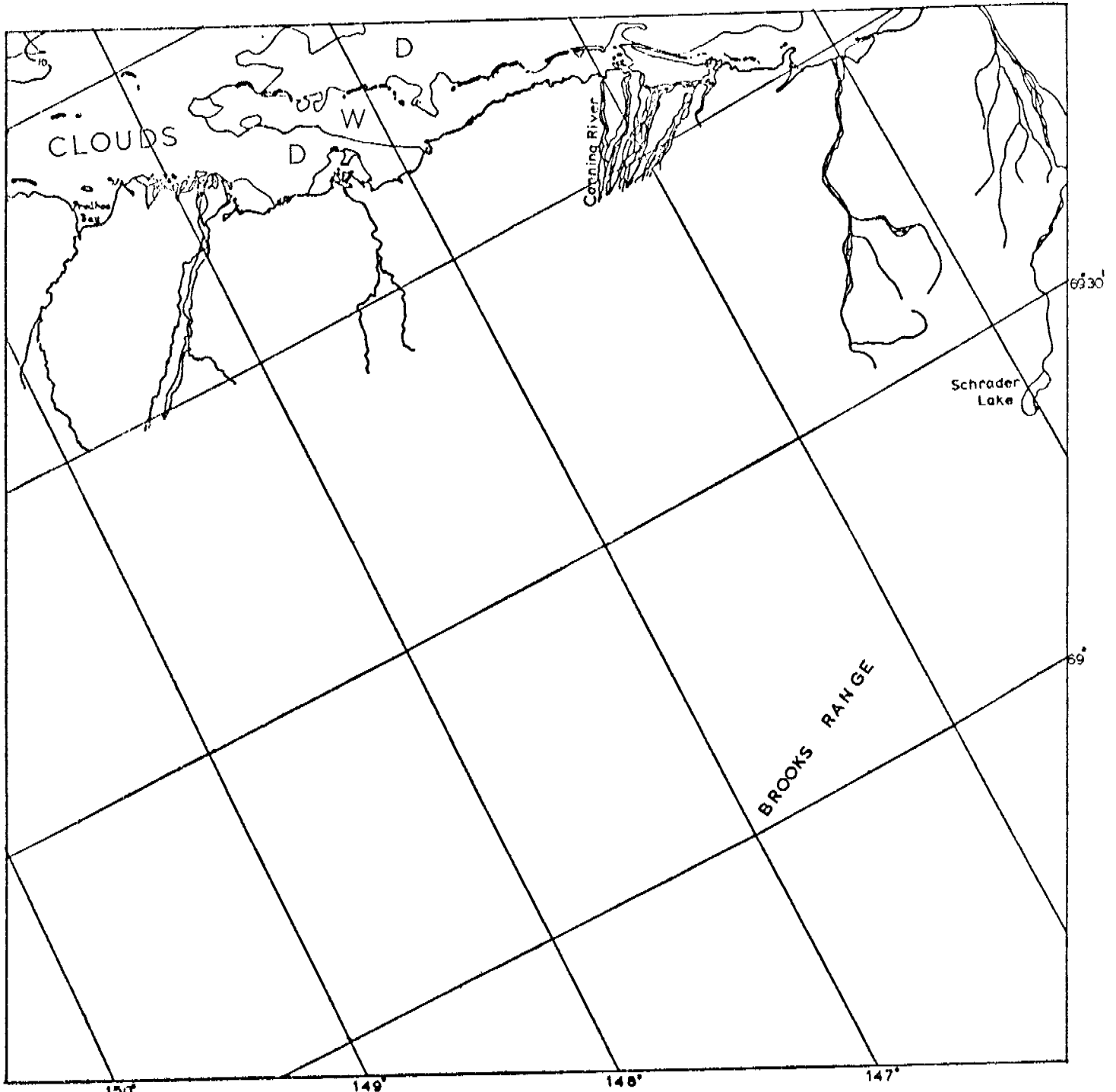
BEAUFORT SEA



KILÓMETERS
0 10 20 30 40 50
SCALE APPROX 1:1,000,000

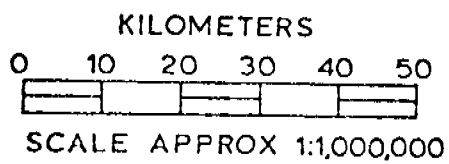
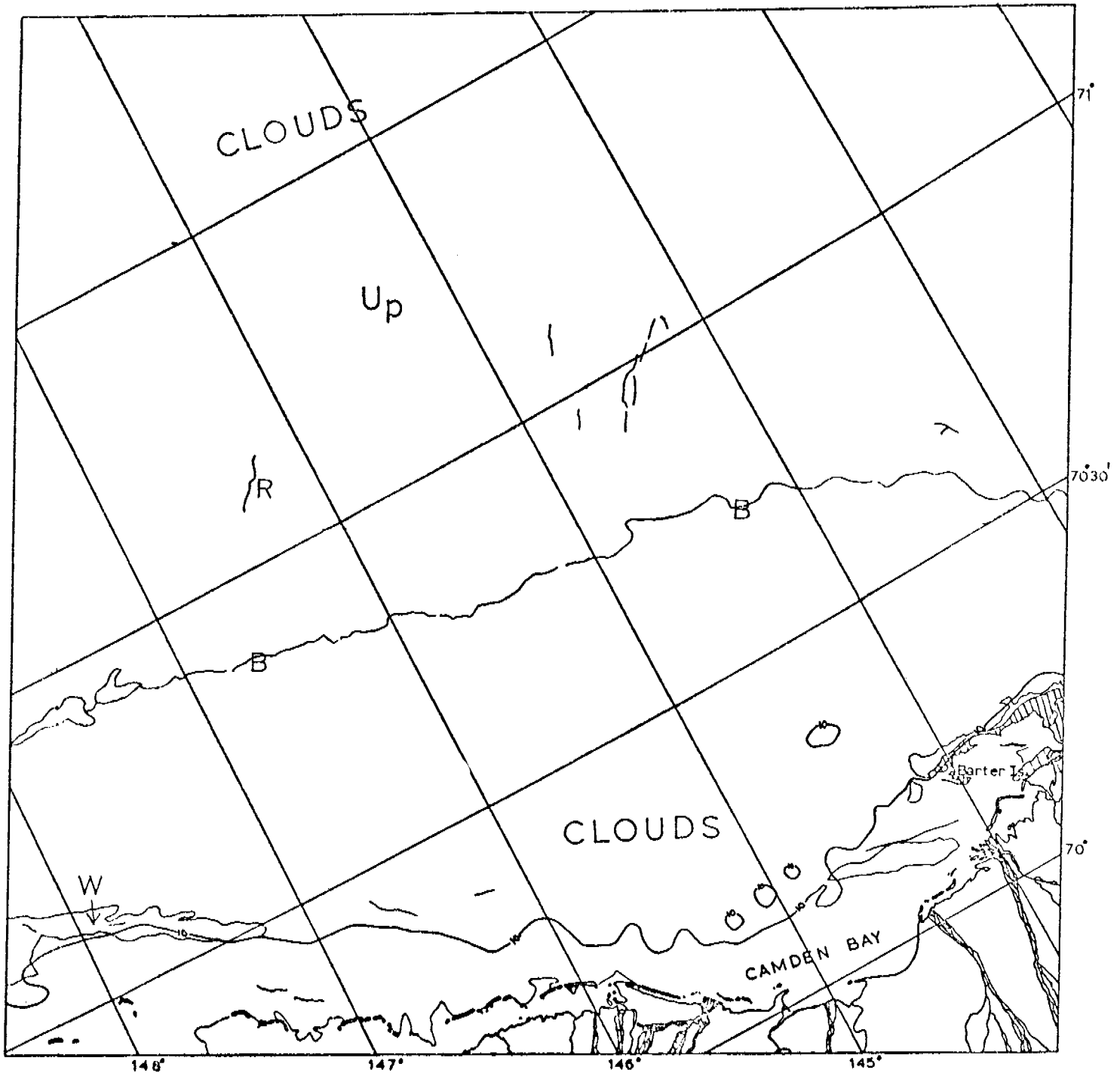
E-2176-21055-7
17 JULY 1975

BEAUFORT SEA



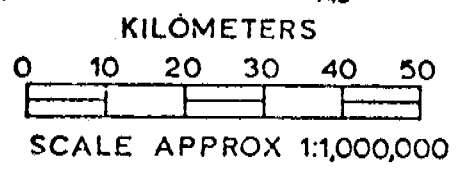
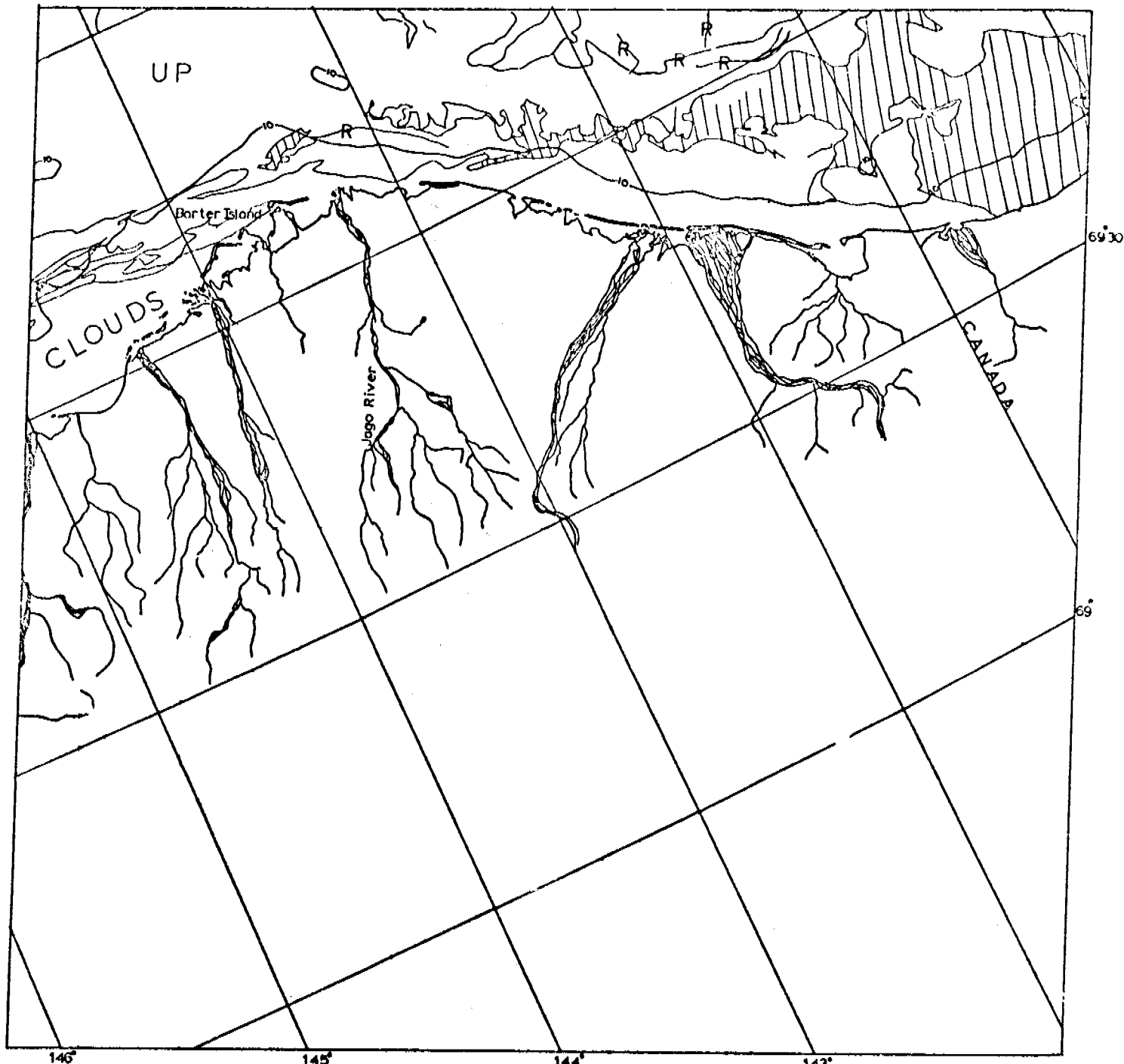
E-2175-21000-7
16 JULY 1975

BEAUFORT SEA



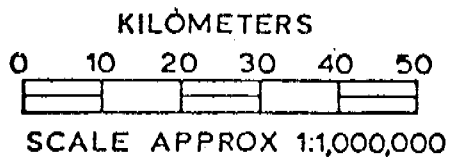
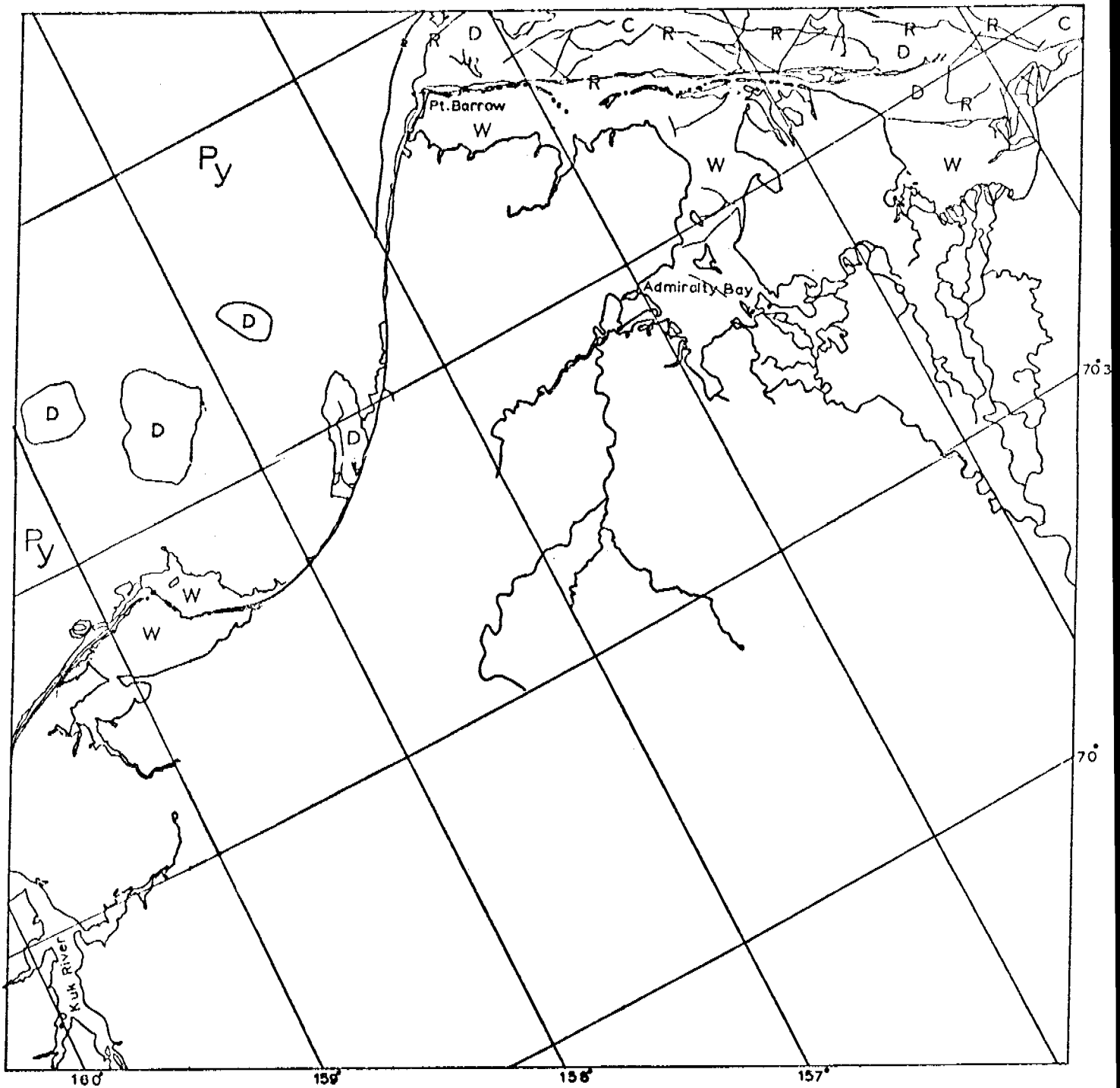
E-2175-20594-7
16 JULY 1975

BEAUFORT SEA



BEAUFORT SEA

E-2172-20425-7
 13 JULY 1975



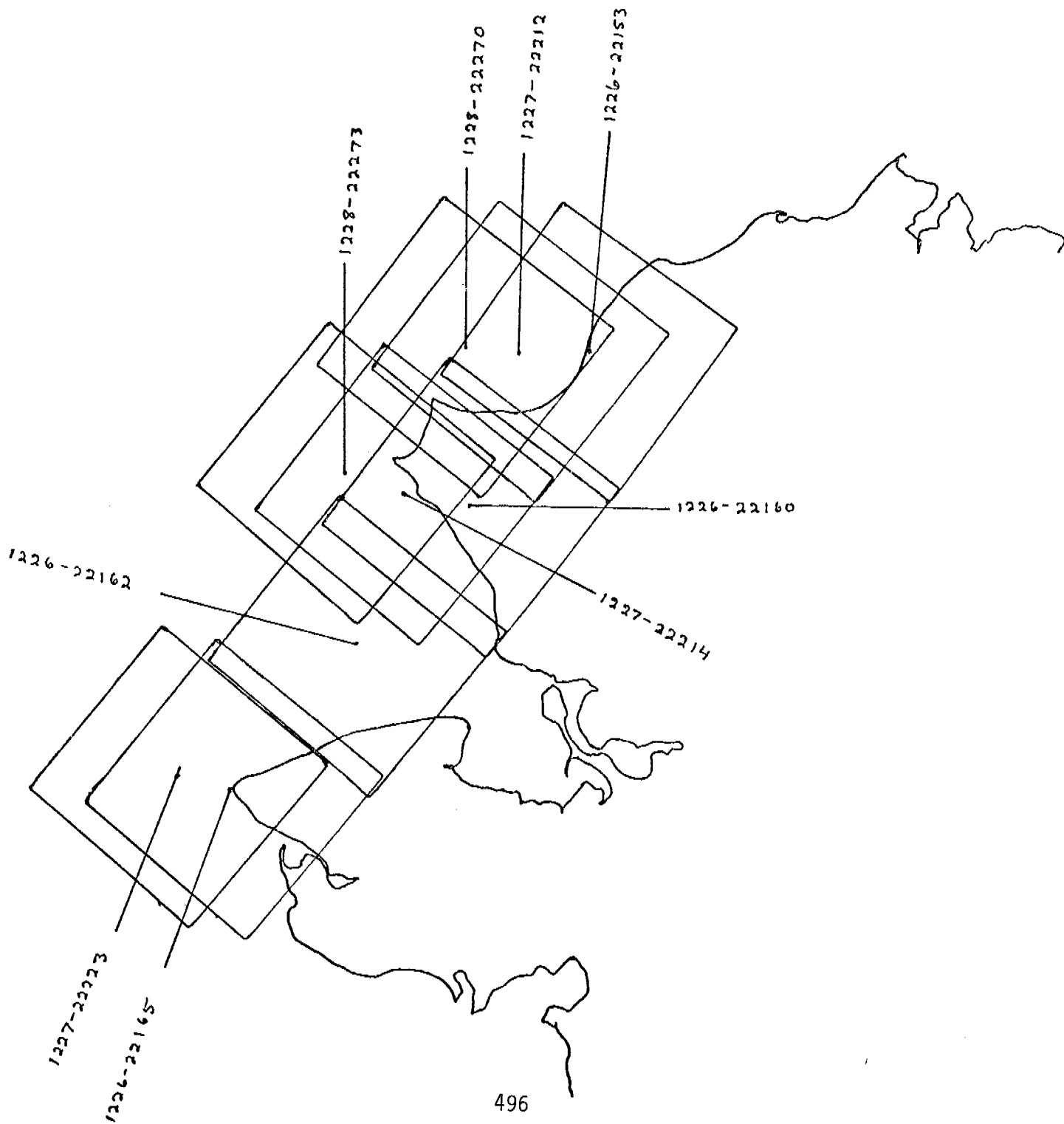
E-2165-21454-7
6 JULY 1975

BEAUFORT SEA

CHUKCHI SEA

2 - 19 MARCH 1973

Images 1222 - 1239

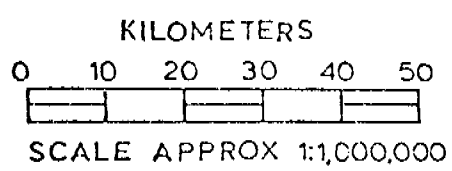
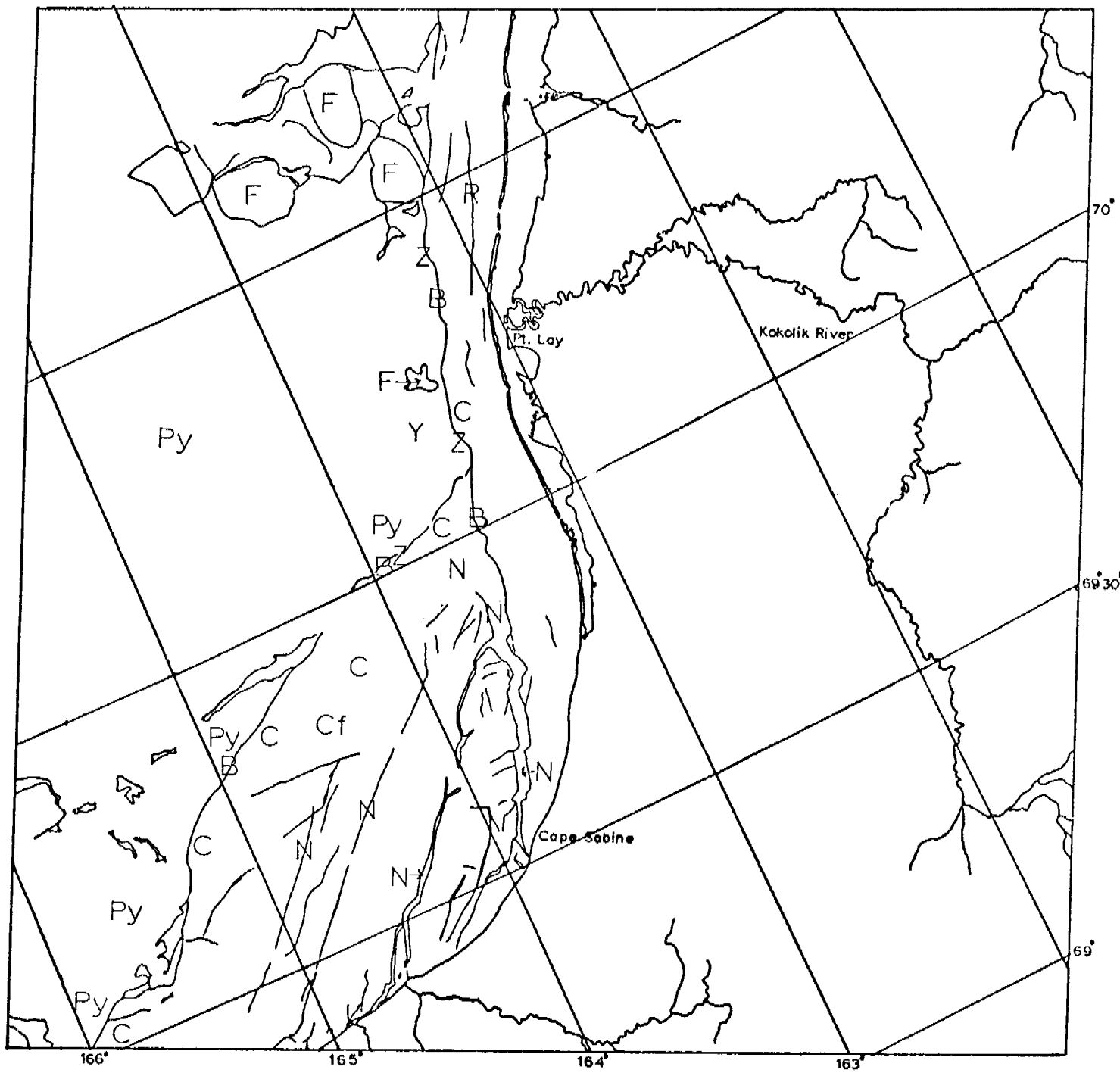


Scenes 1226-22153 }
 1226-22160 } adjacent scenes
 1226-22162 }
 1226-22165 }
 1227-22214
 1227-22223
 1228-22270 } adjacent scenes
 1228-22273 }

These scenes show the Point Lay to Cape Prince of Wales portion of the Chukchi coast between March 6-8, 1973. The configuration of oceanic ice indicates that several cycles of ice formation and subsequent breakage have taken place, with ice being driven out Bering Strait with a velocity of 0.6 km/hour or 17cm/sec.

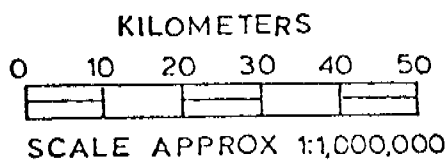
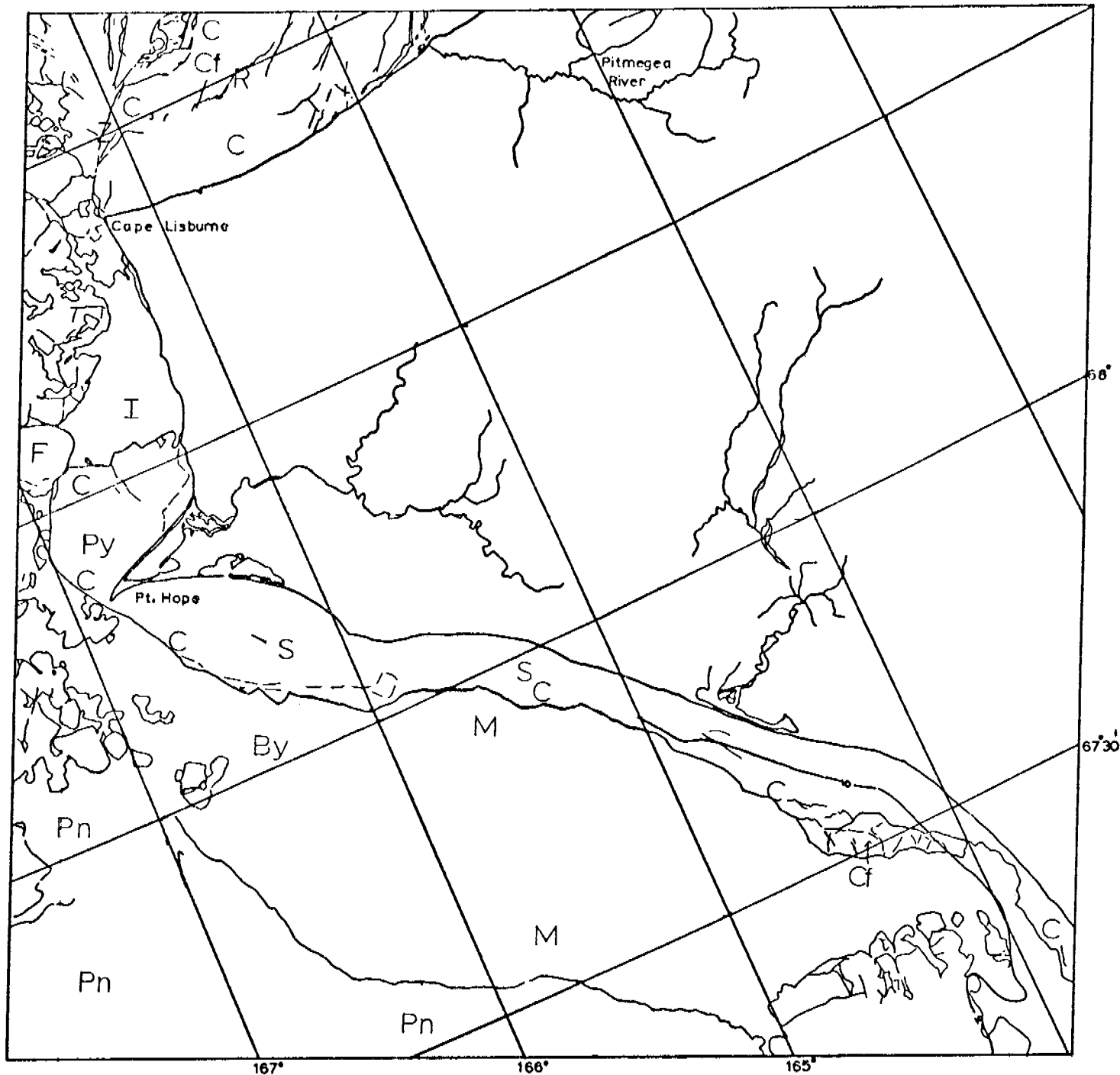
There is a large expanse of contiguous ice extending northward from Cape Prince of Wales which may be grounded on shoals in that area. To the north, contiguous ice extends seaward both north and south of Point Hope. There is some evidence of large ridge systems on the seaward side of the contiguous ice to the north. However, from the north of that apron to Cape Lisburne there is no contiguous ice although the 10 fathom contour is considerably seaward of the coast.

To the north of Cape Lisburne the seaward edge of the contiguous ice roughly follows the 10-fathom contour. In the Point Lay area several ridges can be found parallel to the coast.



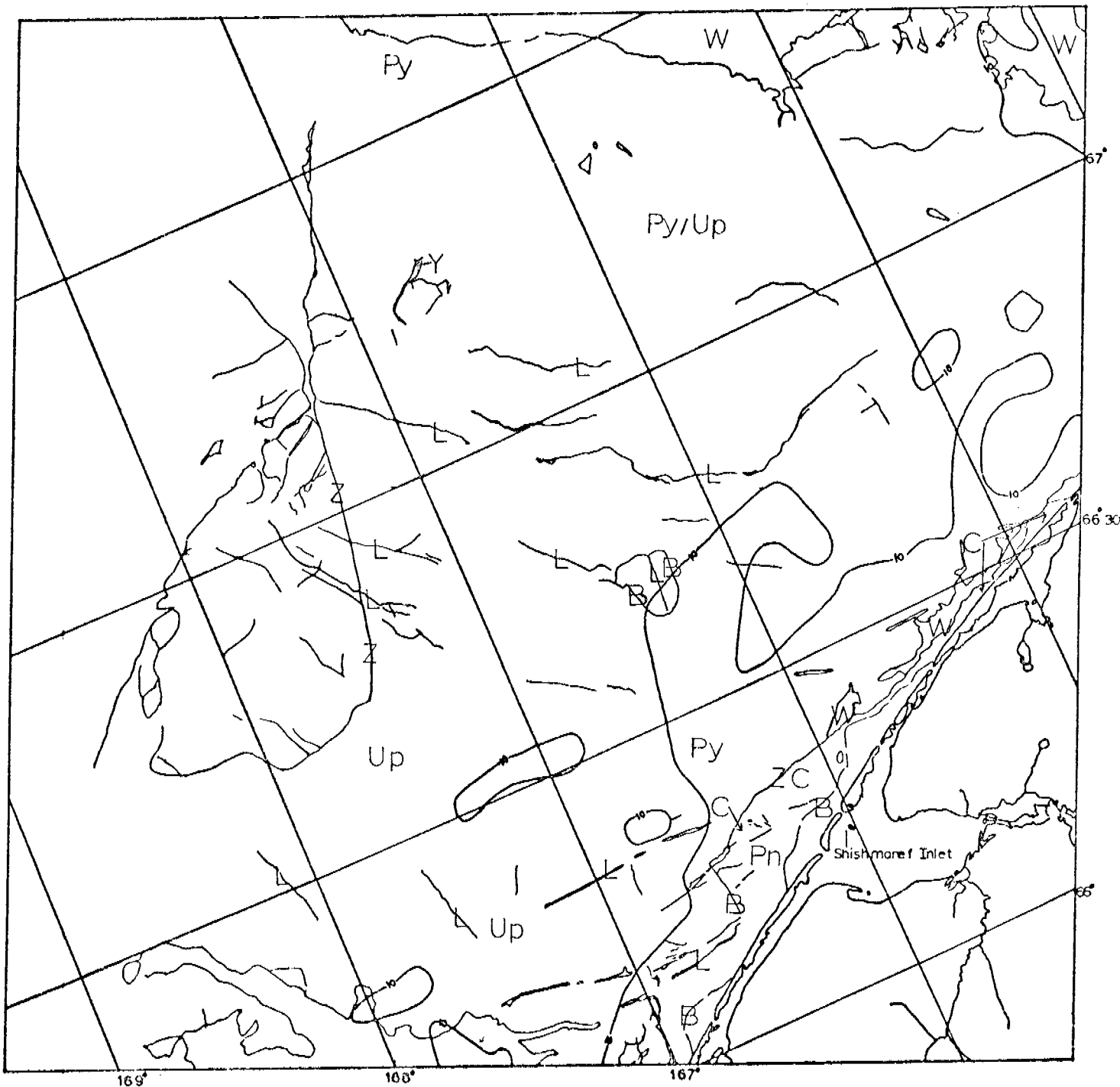
E-1226-22153-7
6 MARCH 1973

CHUKCHI SEA



E-1226-22160-7
6 MARCH 1973

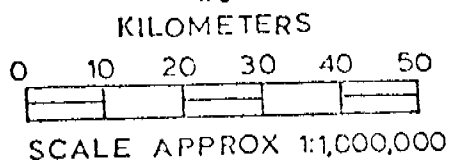
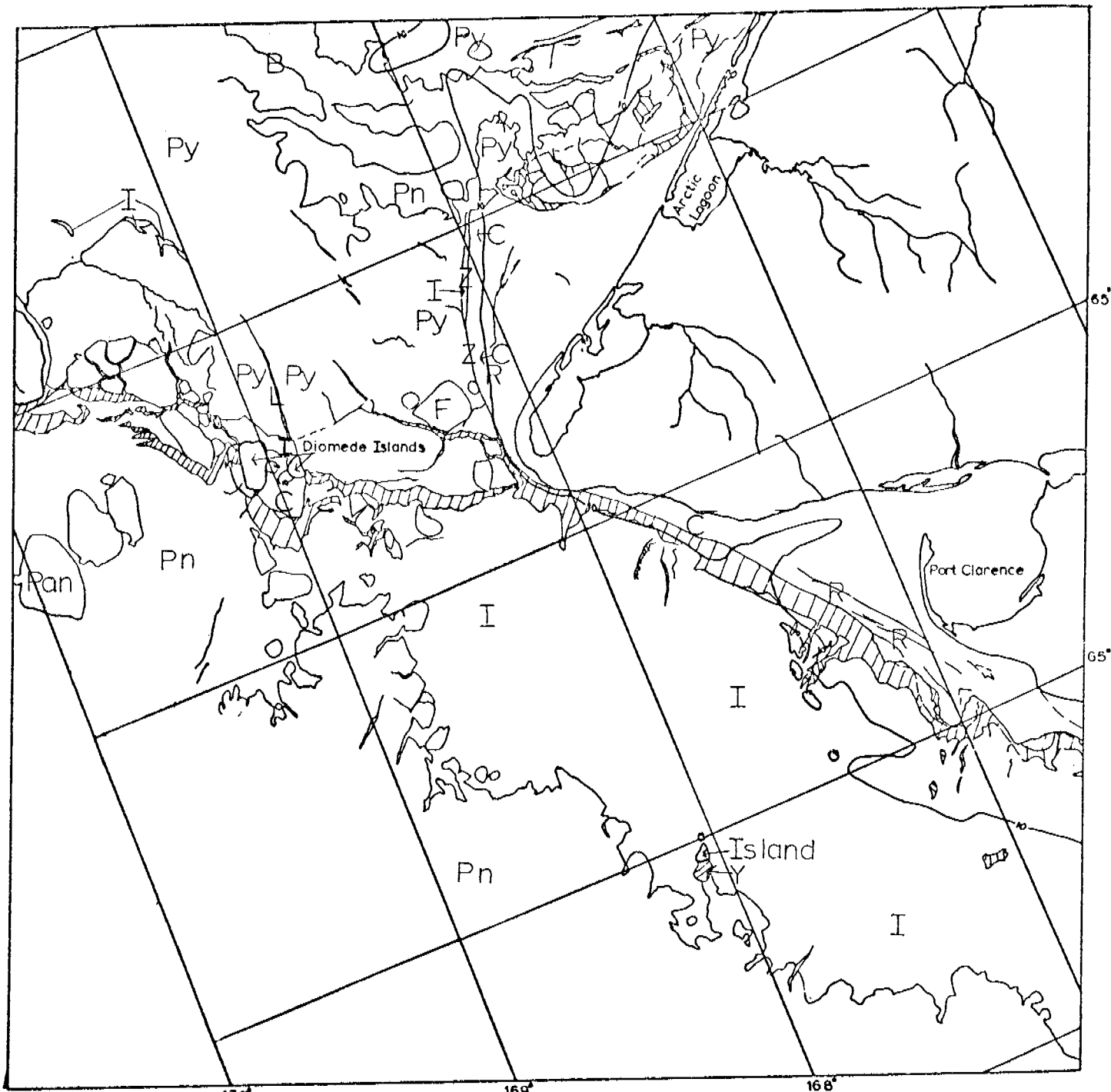
CHUKCHI SEA



KILOMETERS
 0 10 20 30 40 50
 SCALE APPROX 1:1,000,000

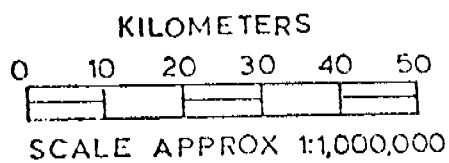
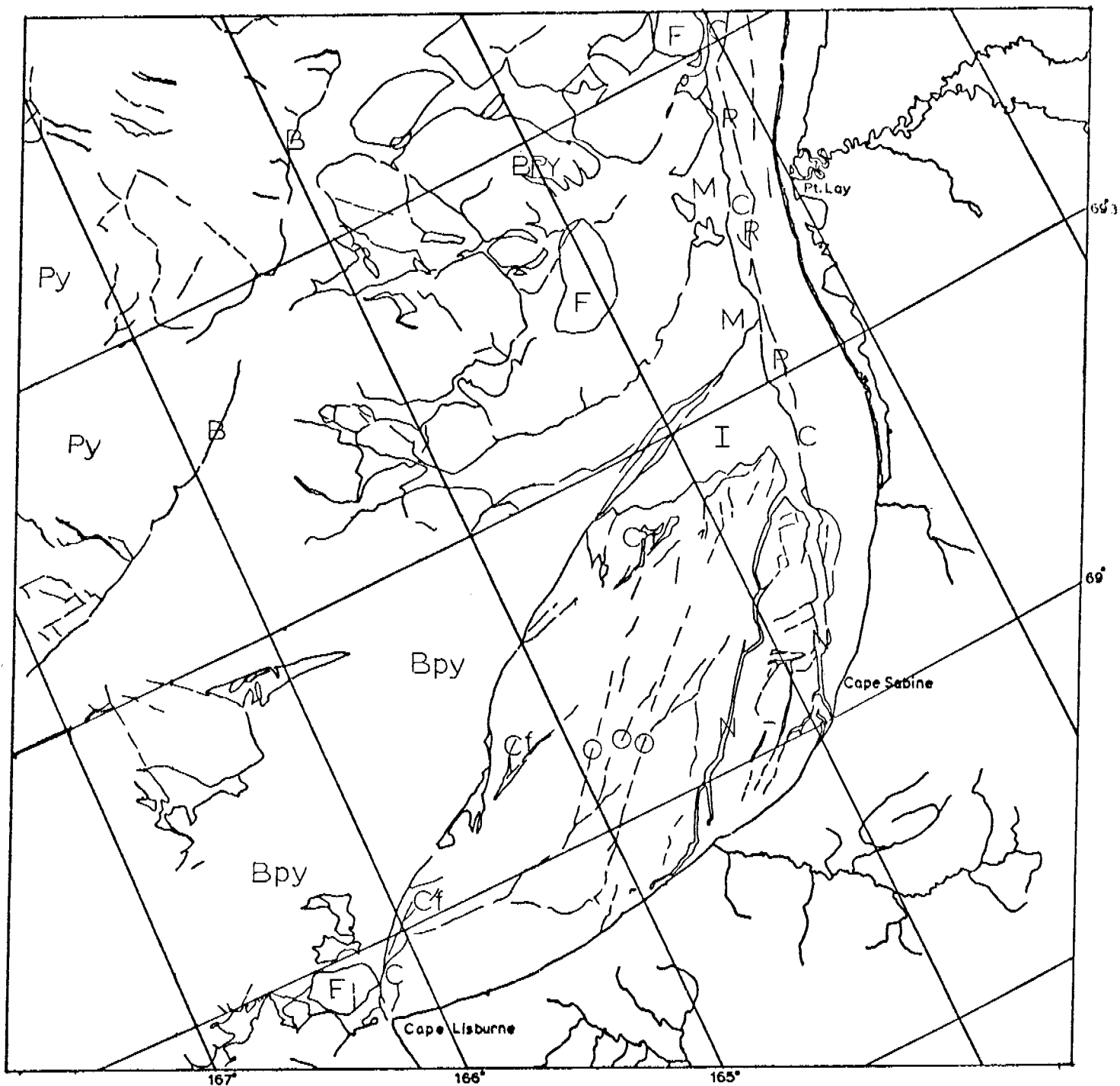
CHUKCHI SEA

E-1226-22162-7
 6 MARCH 1973



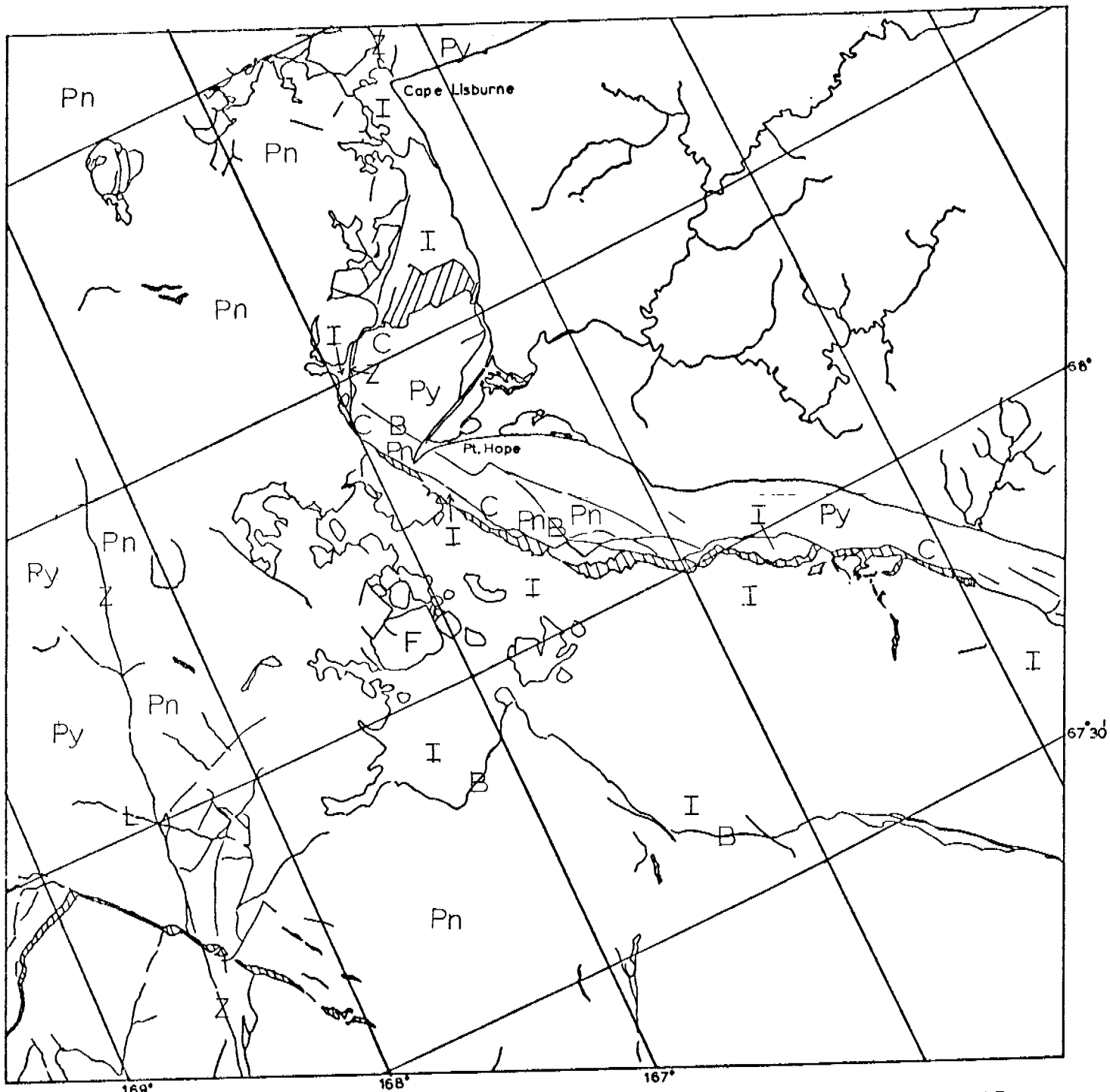
E-1226-22165-7
6 MARCH 1973

CHUKCHI SEA



CHUKCHI SEA

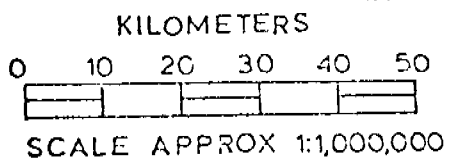
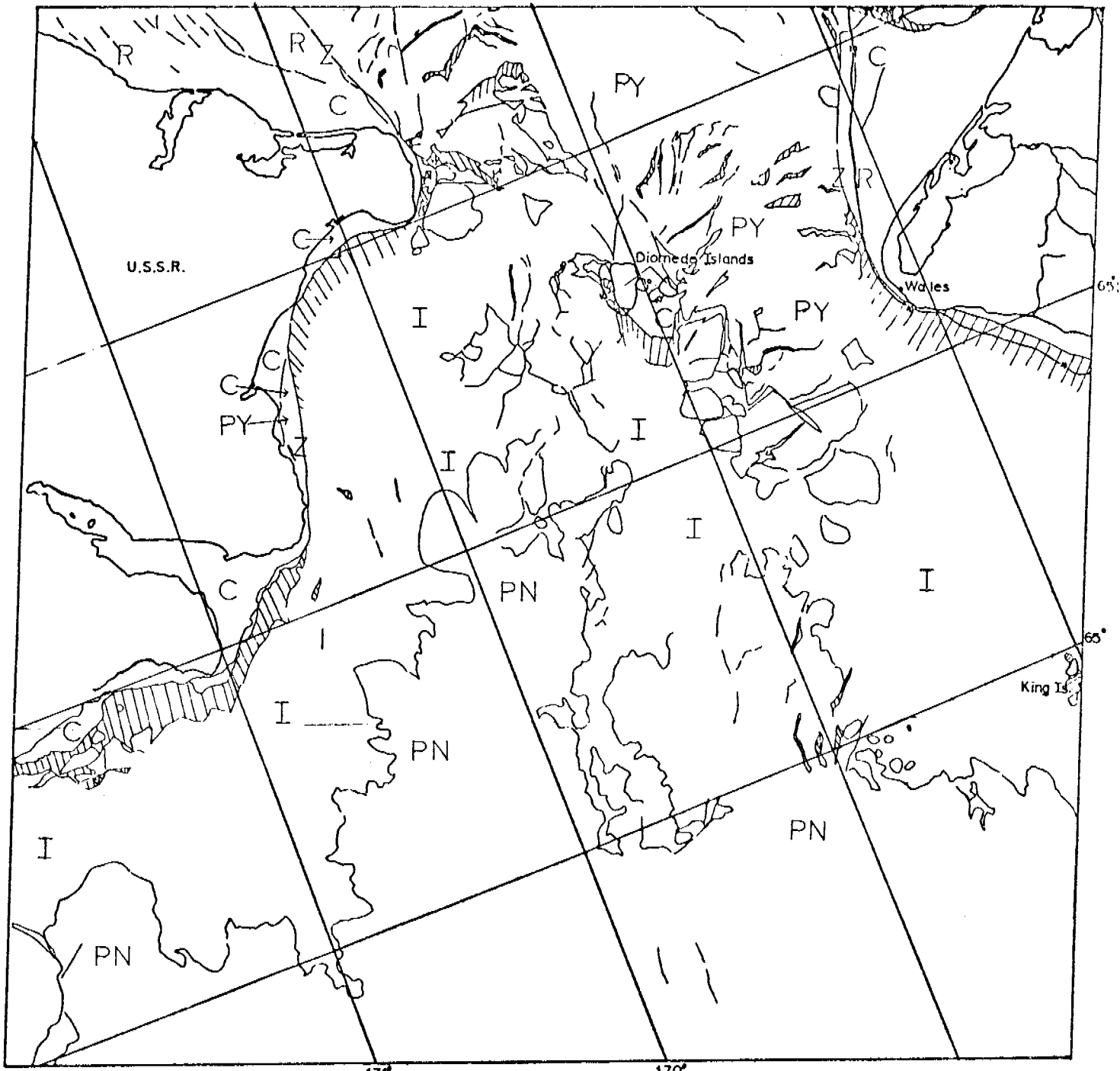
E-1227-22212-7
7 MARCH 1973



KILOMETERS
 0 10 20 30 40 50
 SCALE APPROX 1:1,000,000

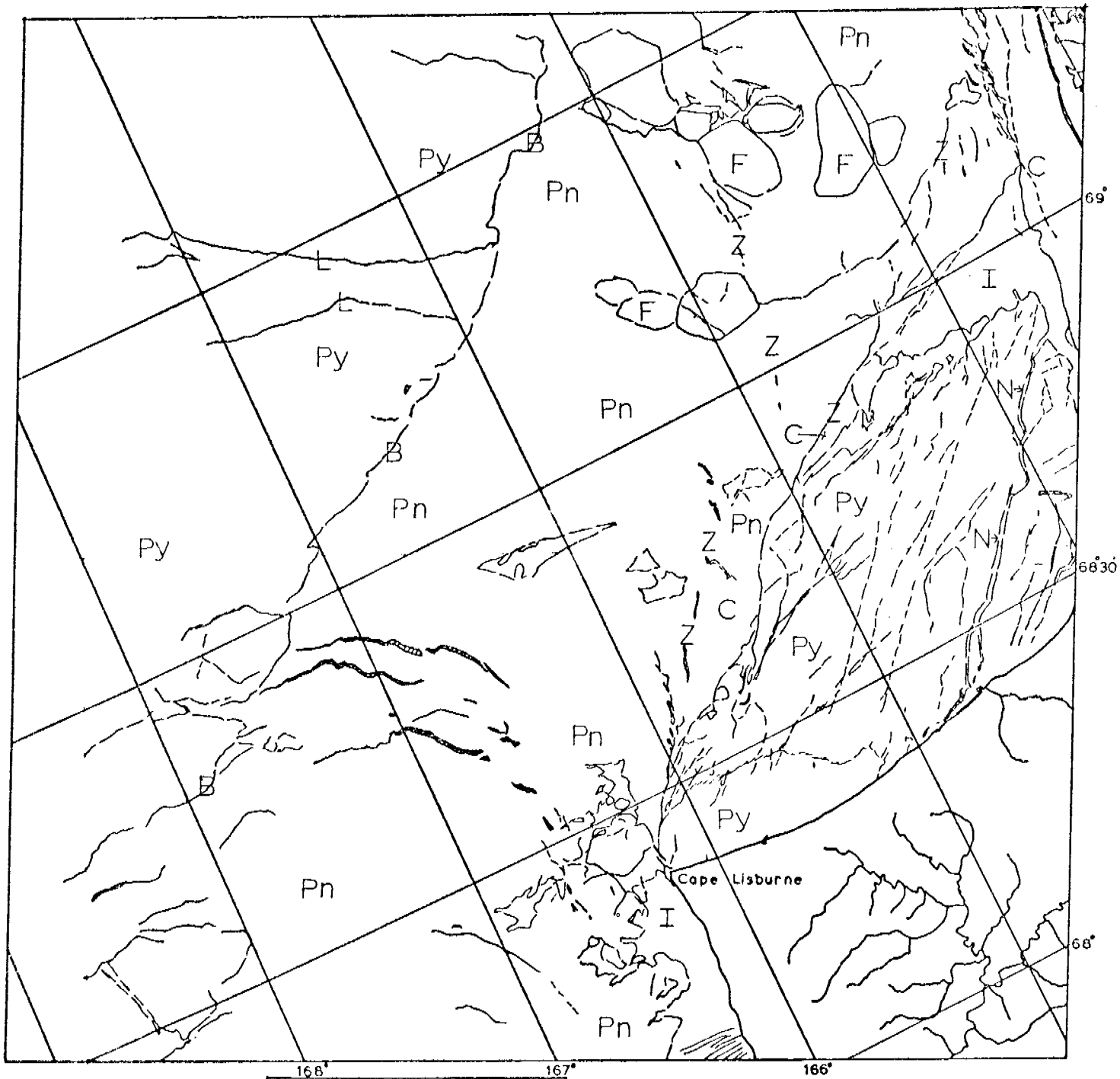
CHUKCHI SEA

E-1227-22214-7
 7 MARCH 1973



CHUKCHI SEA

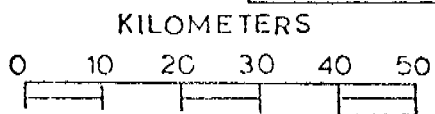
E-1227-22223-7
7 MARCH 1973



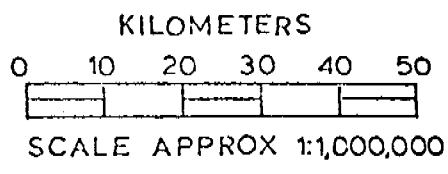
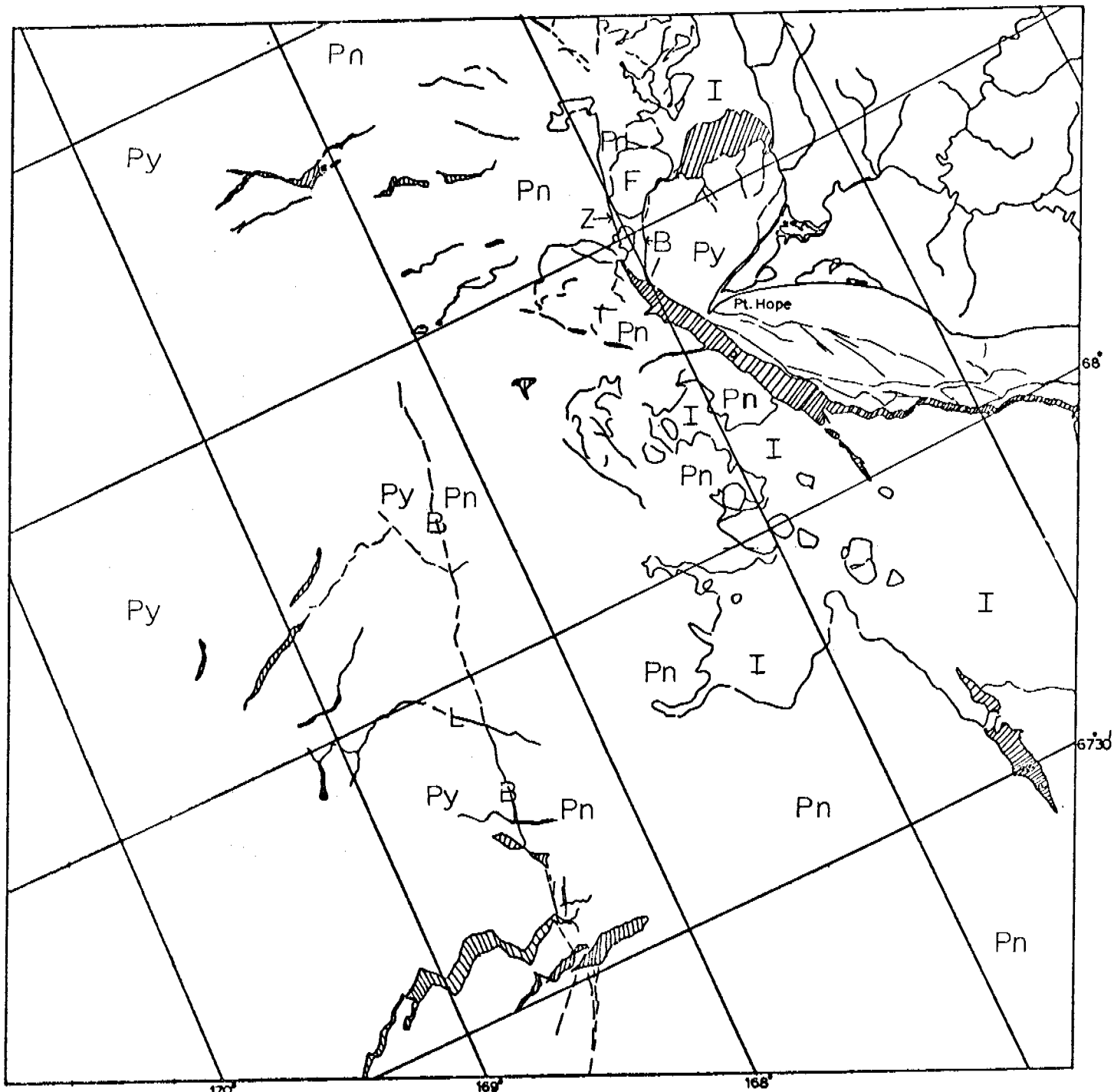
SYMBOLS	
	open water
	water crack
	refrozen crack
	shorefast ice or lead edge or: (delineates thinner ice)
	pressure ridge
	ice flow
	grounded, if known
	hummock

E-4228-22270-7

8 MARCH 1973



CHUKCHI SEA

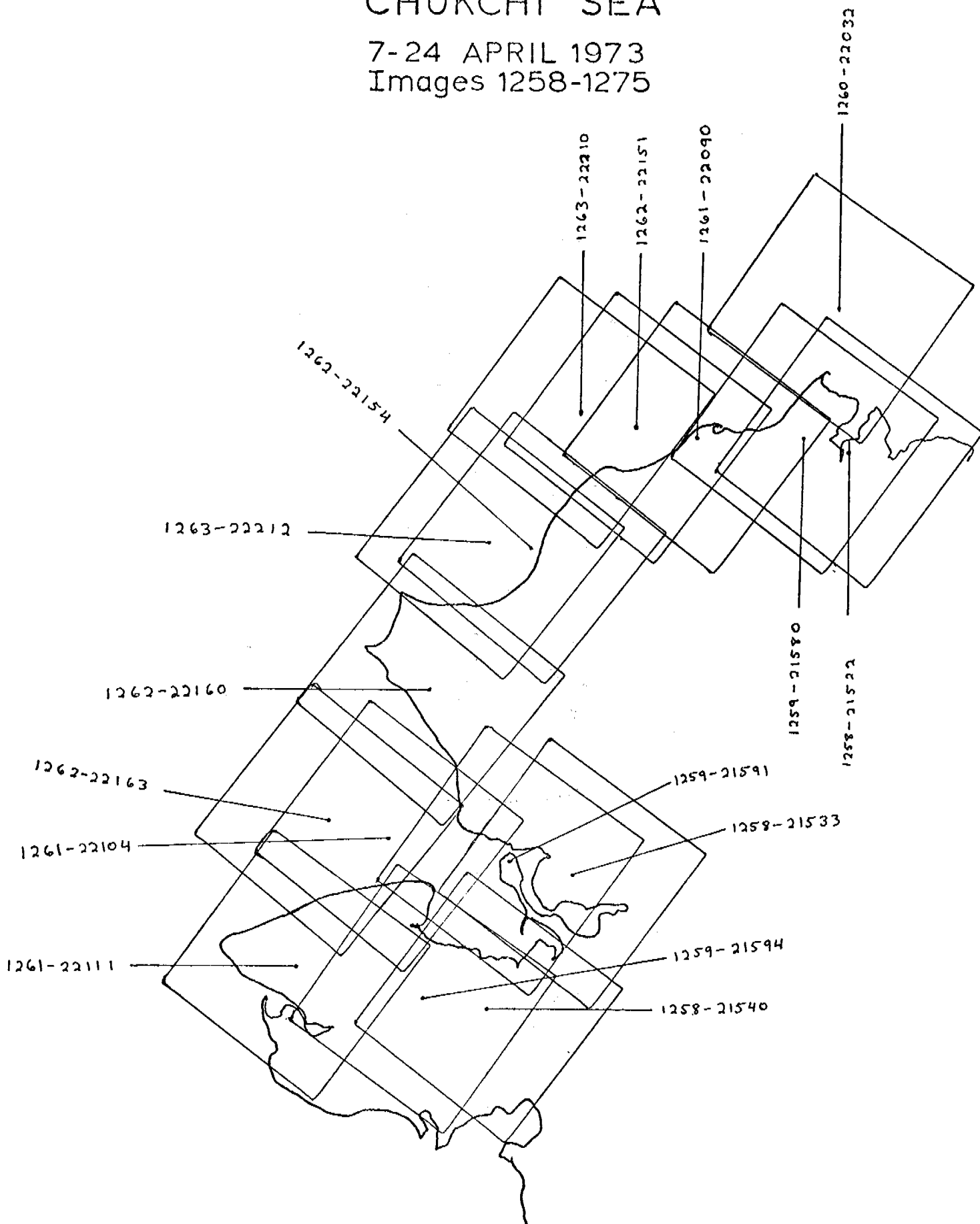


E-1228-22273-7
8 MARCH 1973

CHUKCHI SEA

CHUKCHI SEA

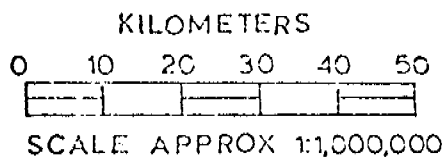
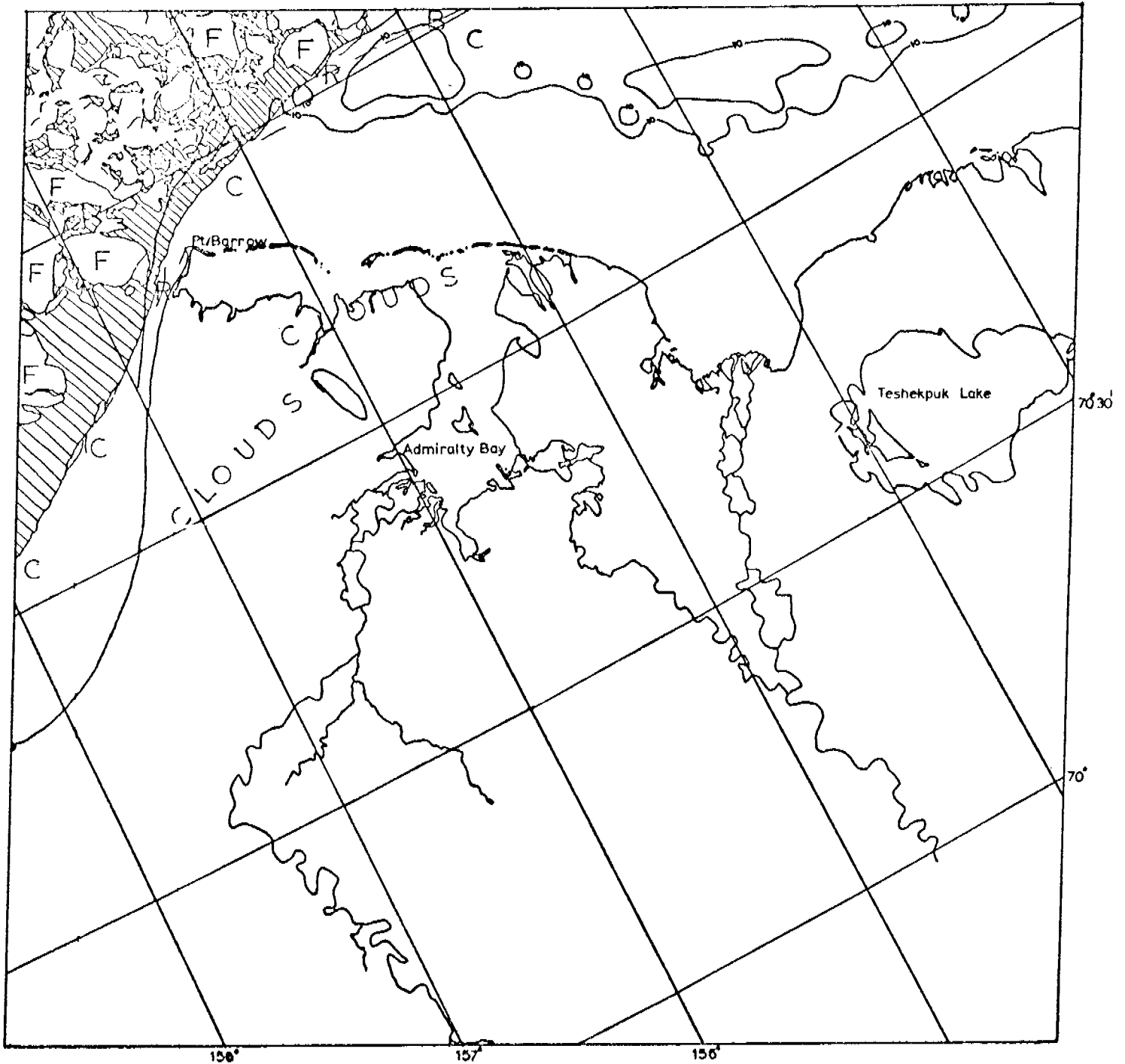
7-24 APRIL 1973
Images 1258-1275



Scenes	1258-21522}	adjacent pair
	1258-21533}	
	1258-21540	
	1259-21580	
	1259-21591	
	1260-22032	
	1261-22090	
	1261-22104}	adjacent pair
	1261-22111}	
	1262-22151}	adjacent triplet
	1262-22154}	
	1262-22160}	
	1263-22210}	adjacent pair
	1263-22212}	

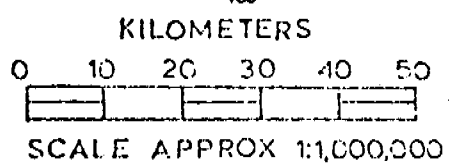
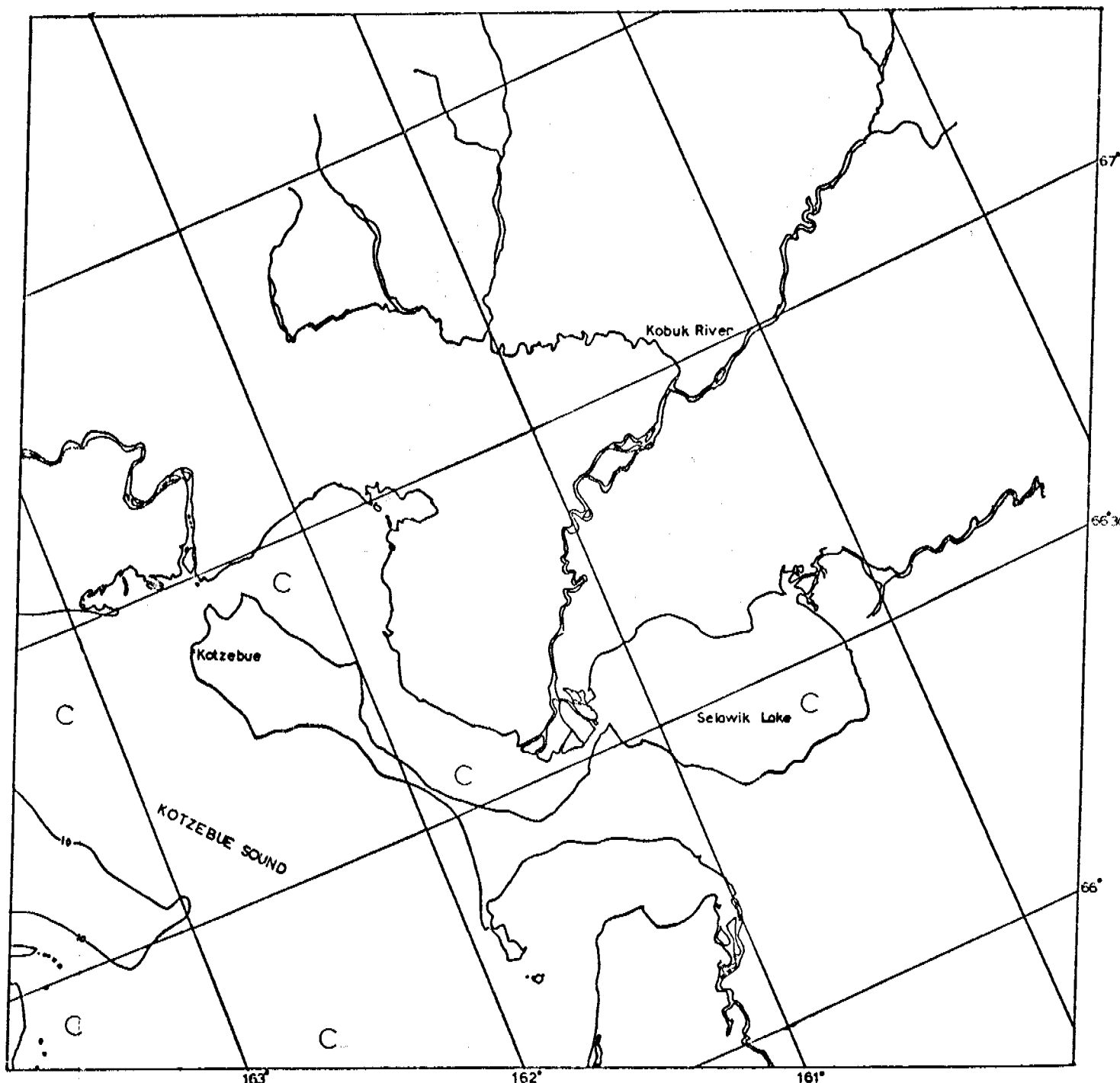
These scenes show the Chukchi coast between April 7-12, 1973. Kotzebue Sound is filled with contiguous ice out to a line between Cape Krusenstern and Cape Espenberg. A large lead has opened up along that line and down along the Espenberg Peninsula to the south.

At this time a relatively narrow band of fractured and mobile ice extending southward from Barrow along the coast. There is evidence along the coast in the form of polynyas on the south side of prominent features that this entire column of ice is moving southward. Although considerable amounts of contiguous ice have been mapped for this series few ridge systems were evident-partly because of thin clouds obscuring these details.



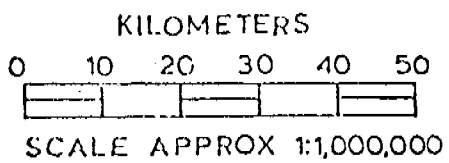
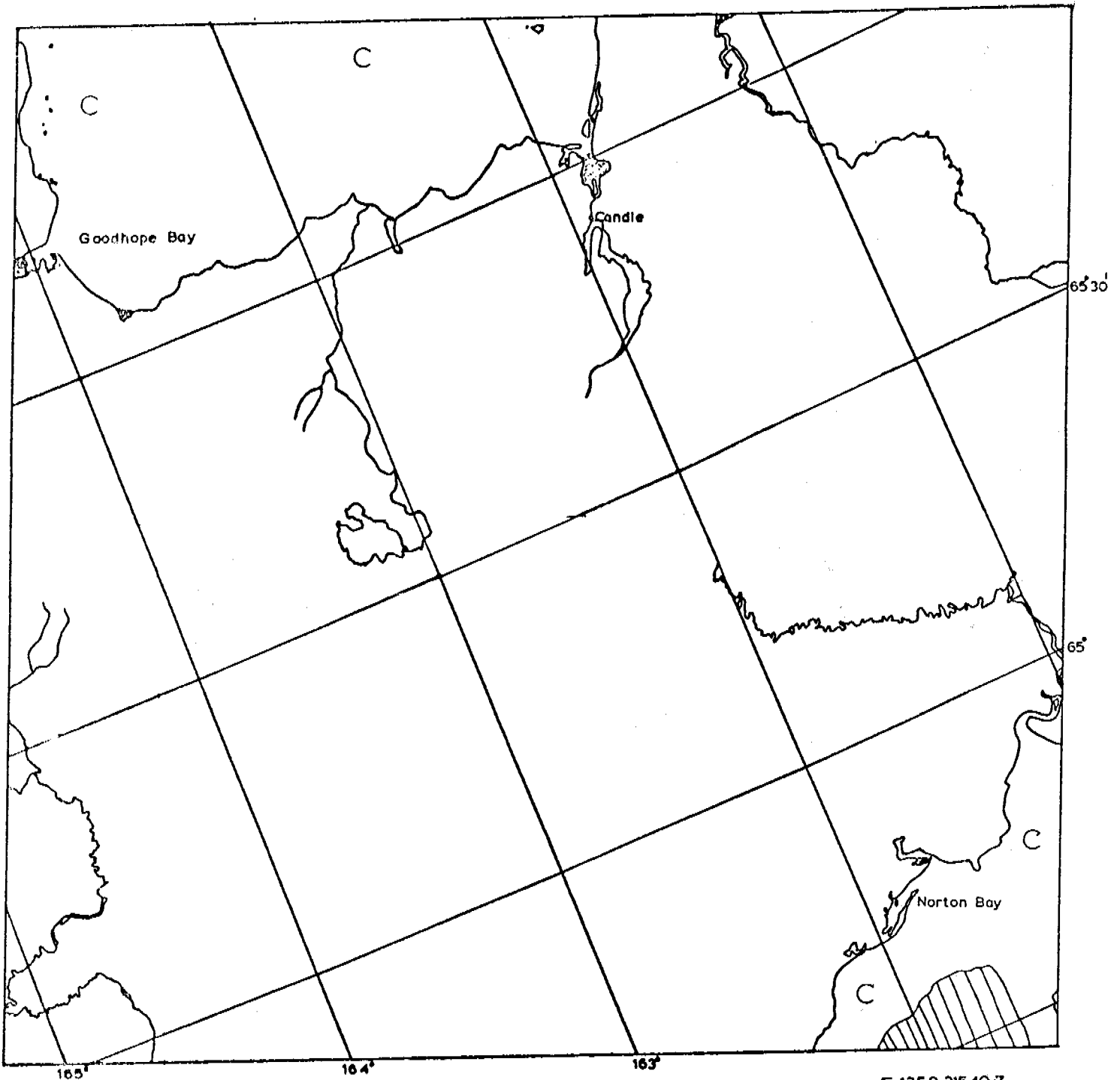
E-1258-21522-7
7 APRIL 1973

CHUKCHI SEA



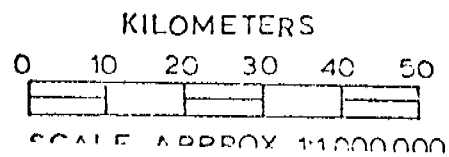
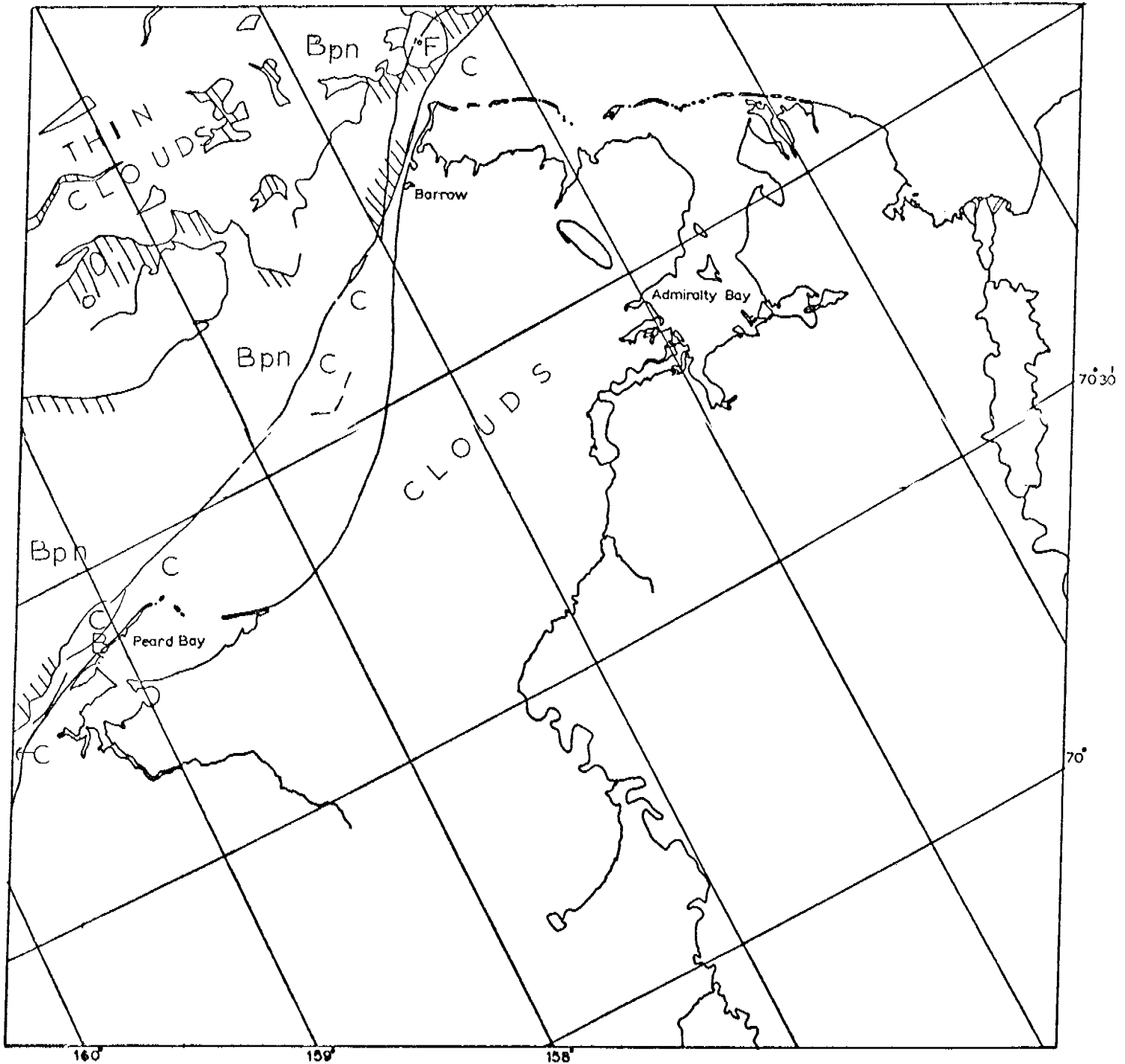
E-1258-21533-7
7 APRIL 1973

CHUKCHI SEA



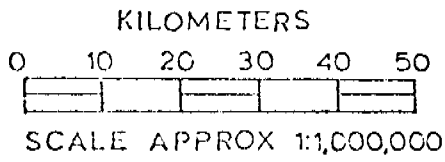
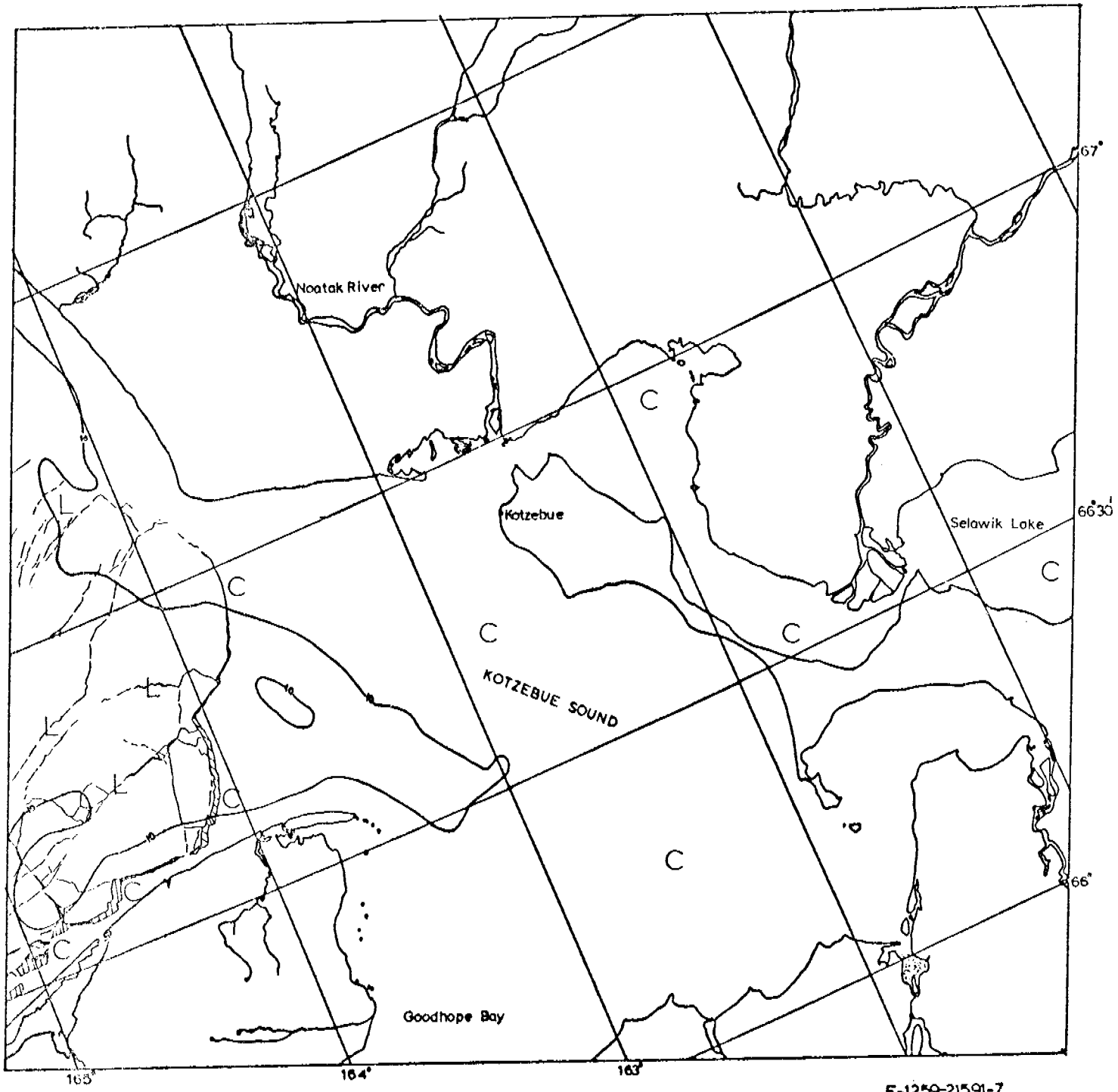
E-1258-21540-7
7 APRIL 1973

CHUKCHI SEA



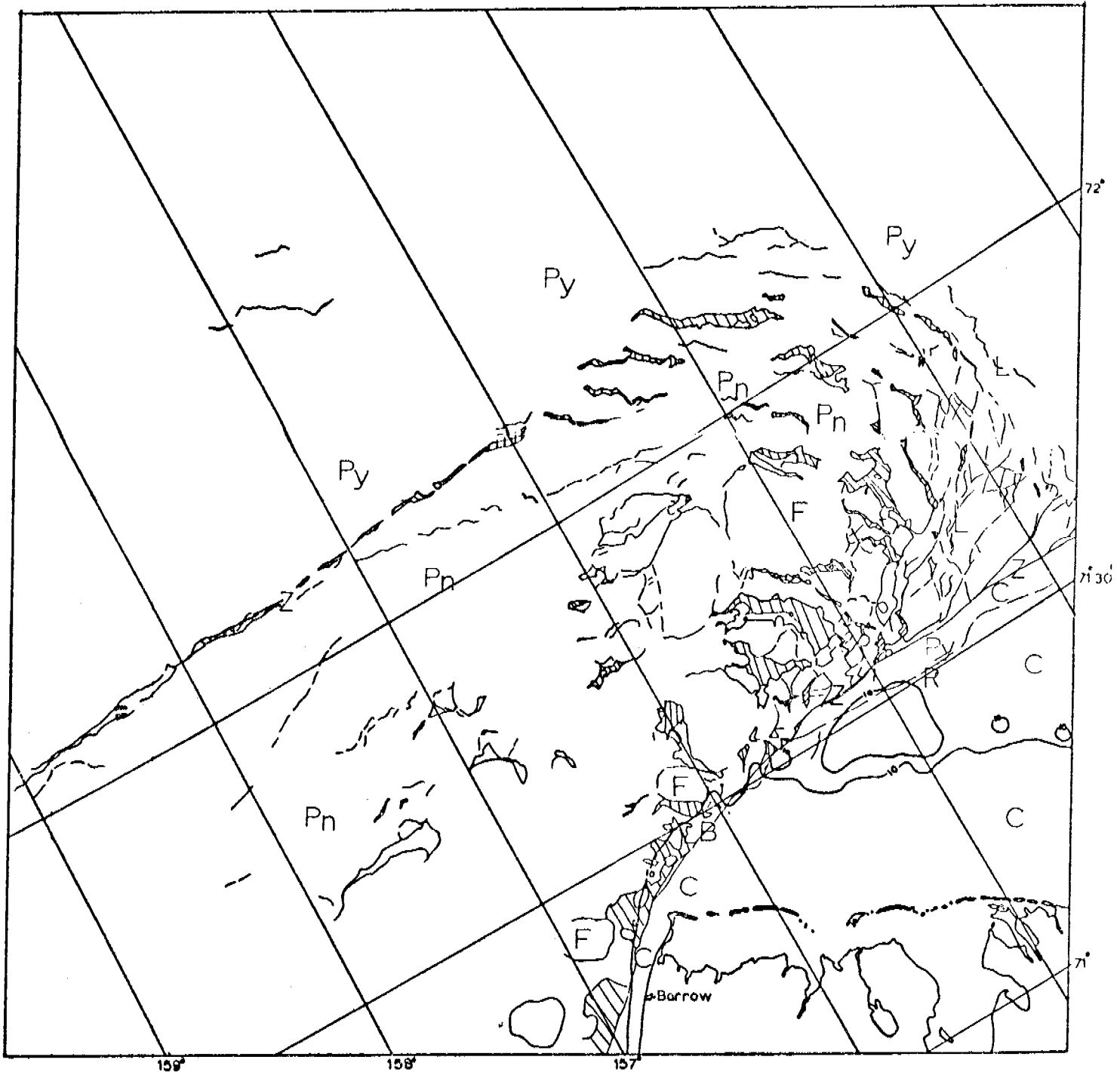
E-1259-21580-7
8 APRIL 1973

CHUKCHI SEA



E-1259-21591-7
8 APRIL 1973

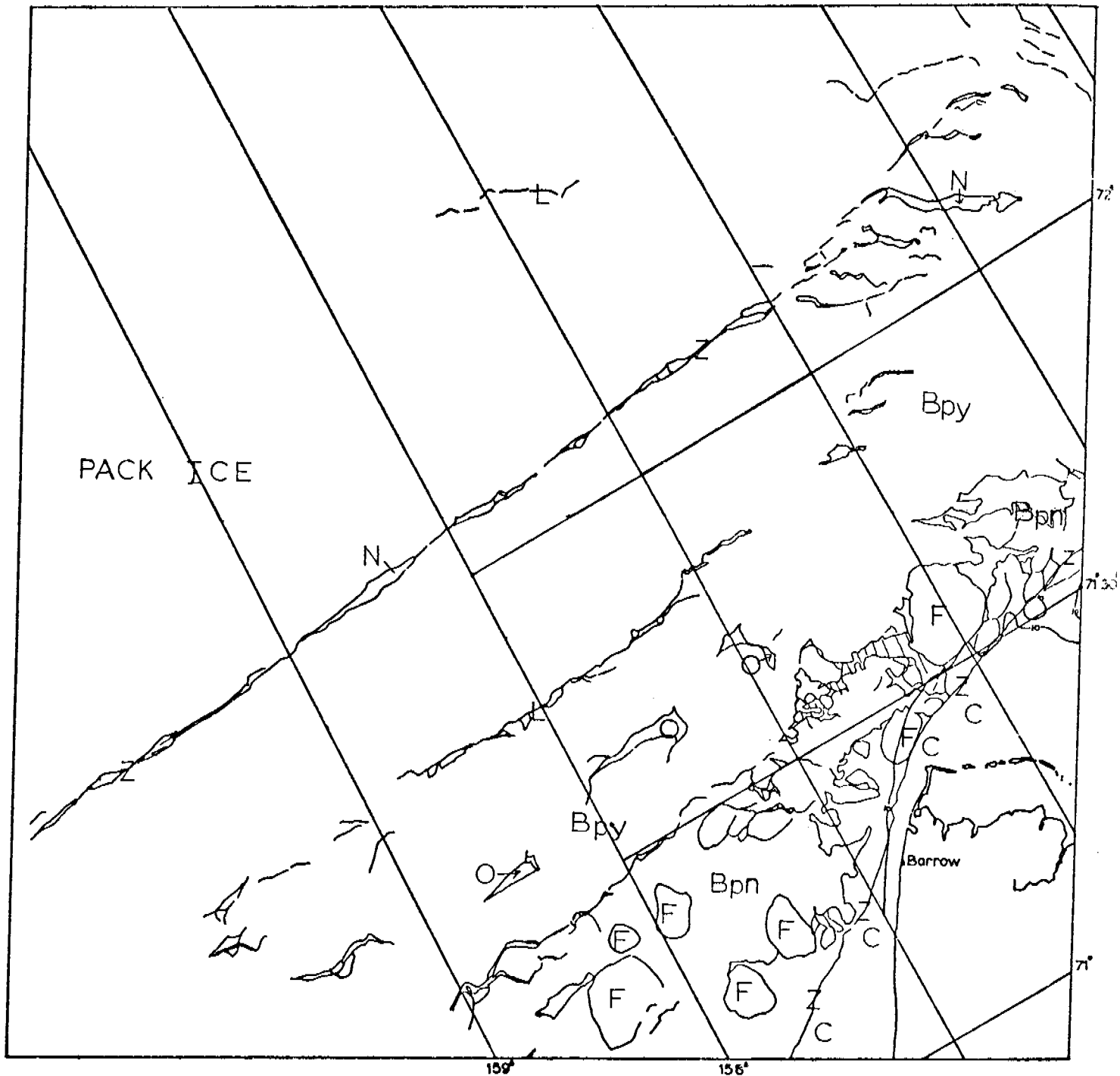
CHUKCHI SEA



KILOMETERS
 0 10 20 30 40 50
 SCALE APPROX 1:1,000,000

E-1260-22032-7
 9 APRIL 1973

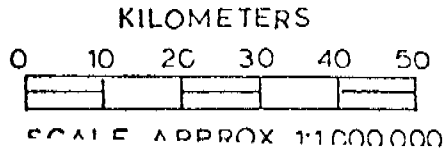
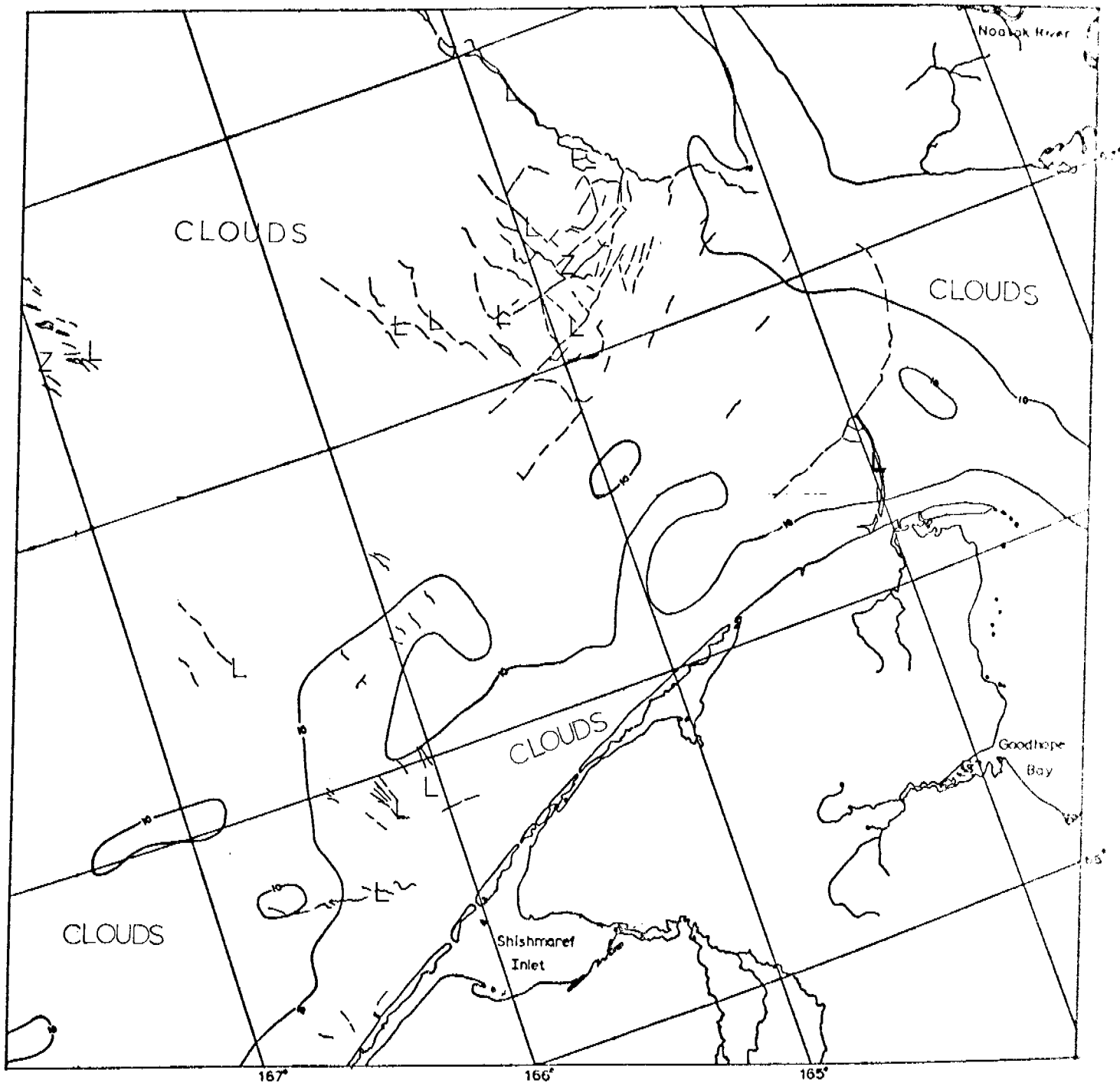
CHUKCHI SEA



KILOMETERS
 0 10 20 30 40 50
 SCALE APPROX 1:1,000,000

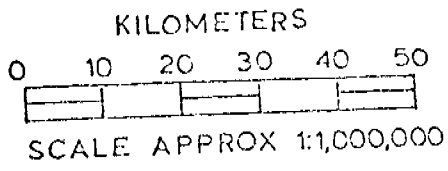
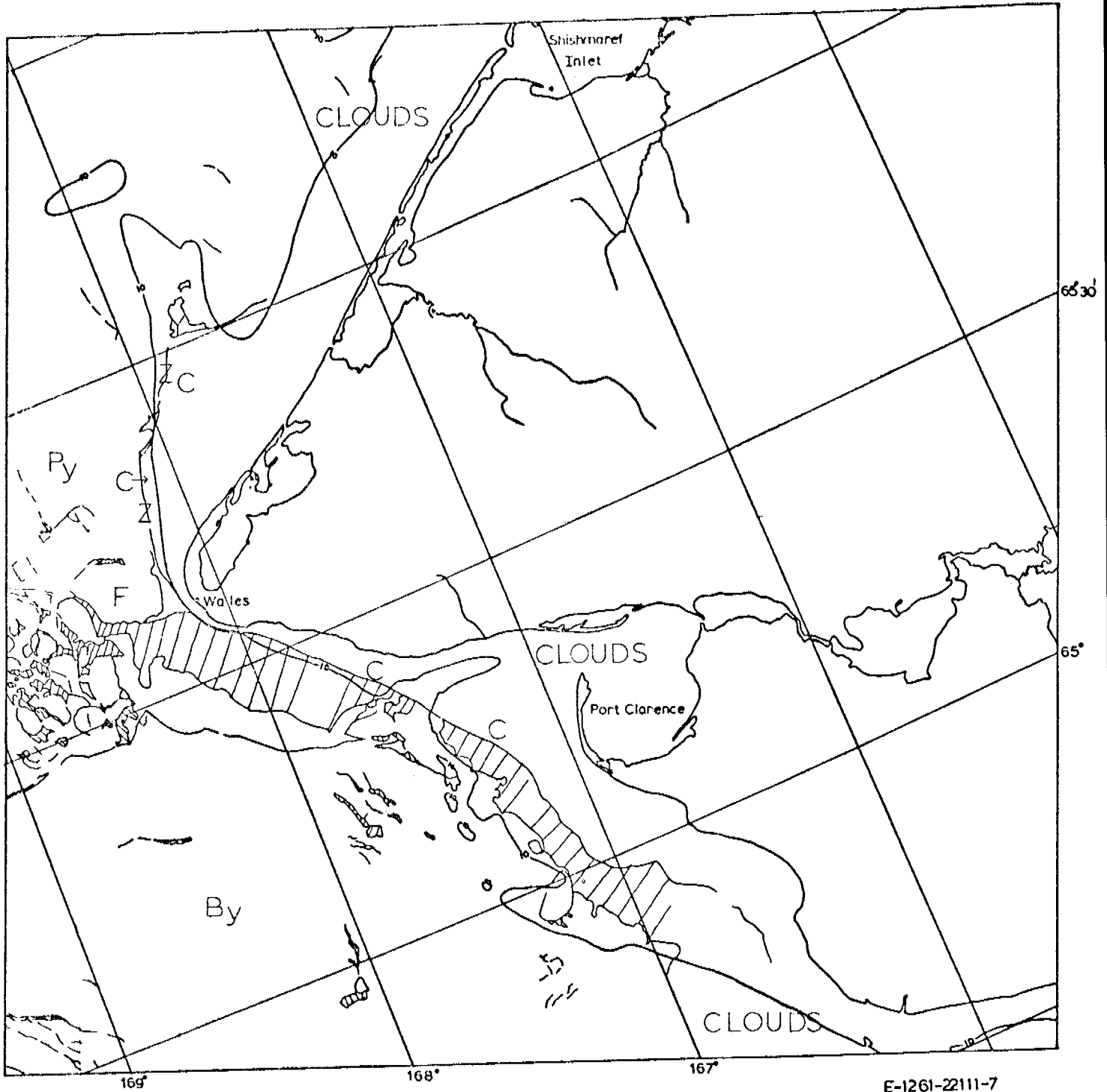
CHUKCHI SEA

E-1261-22090-7
 10 APRIL 1973



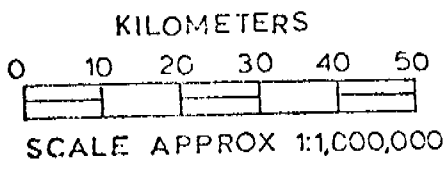
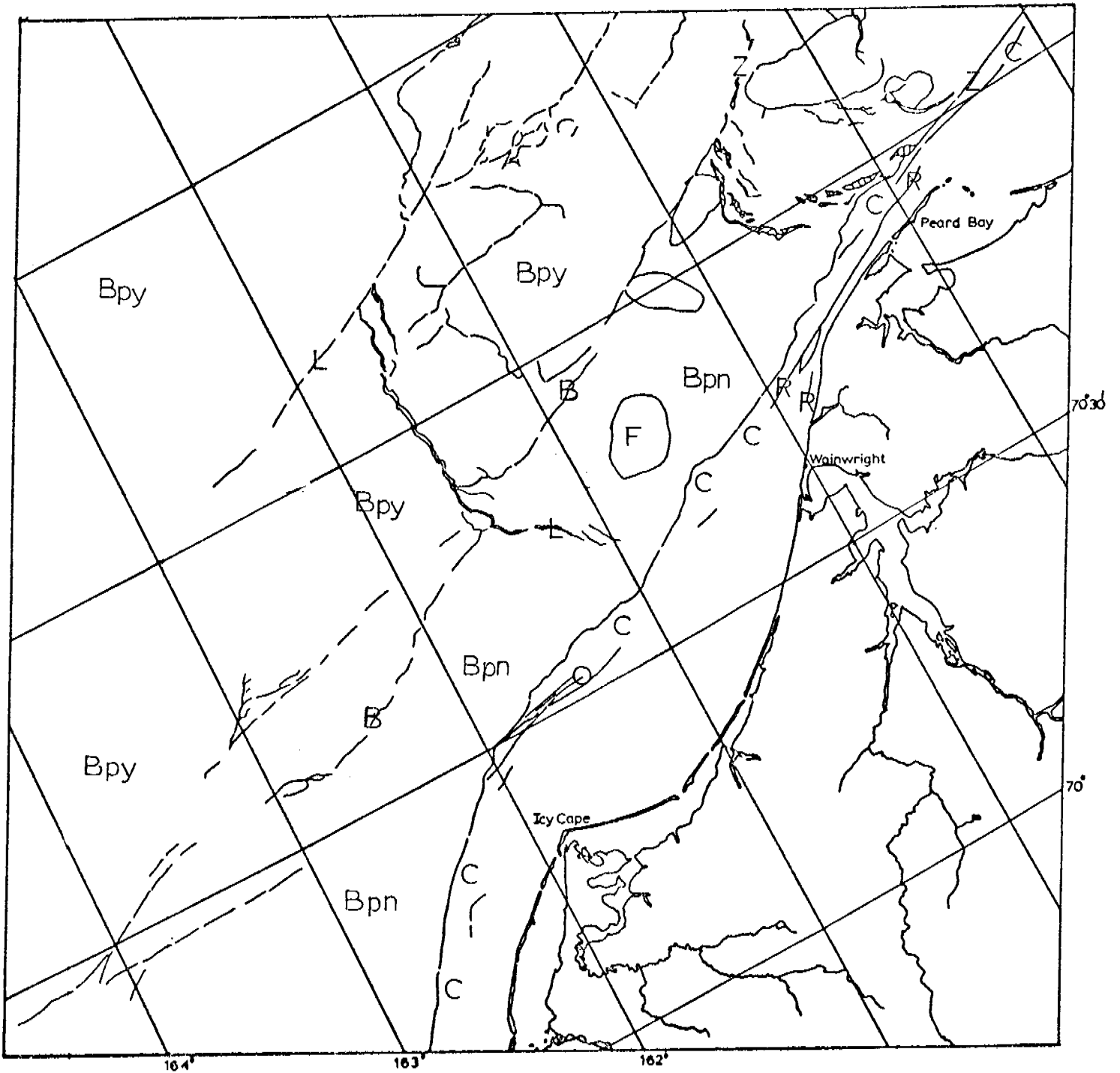
E-1261-22104-7
10 APRIL 1973

CHUKCHI SEA



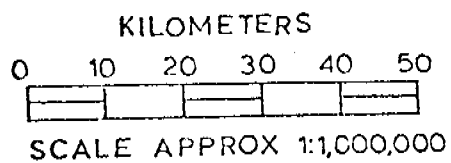
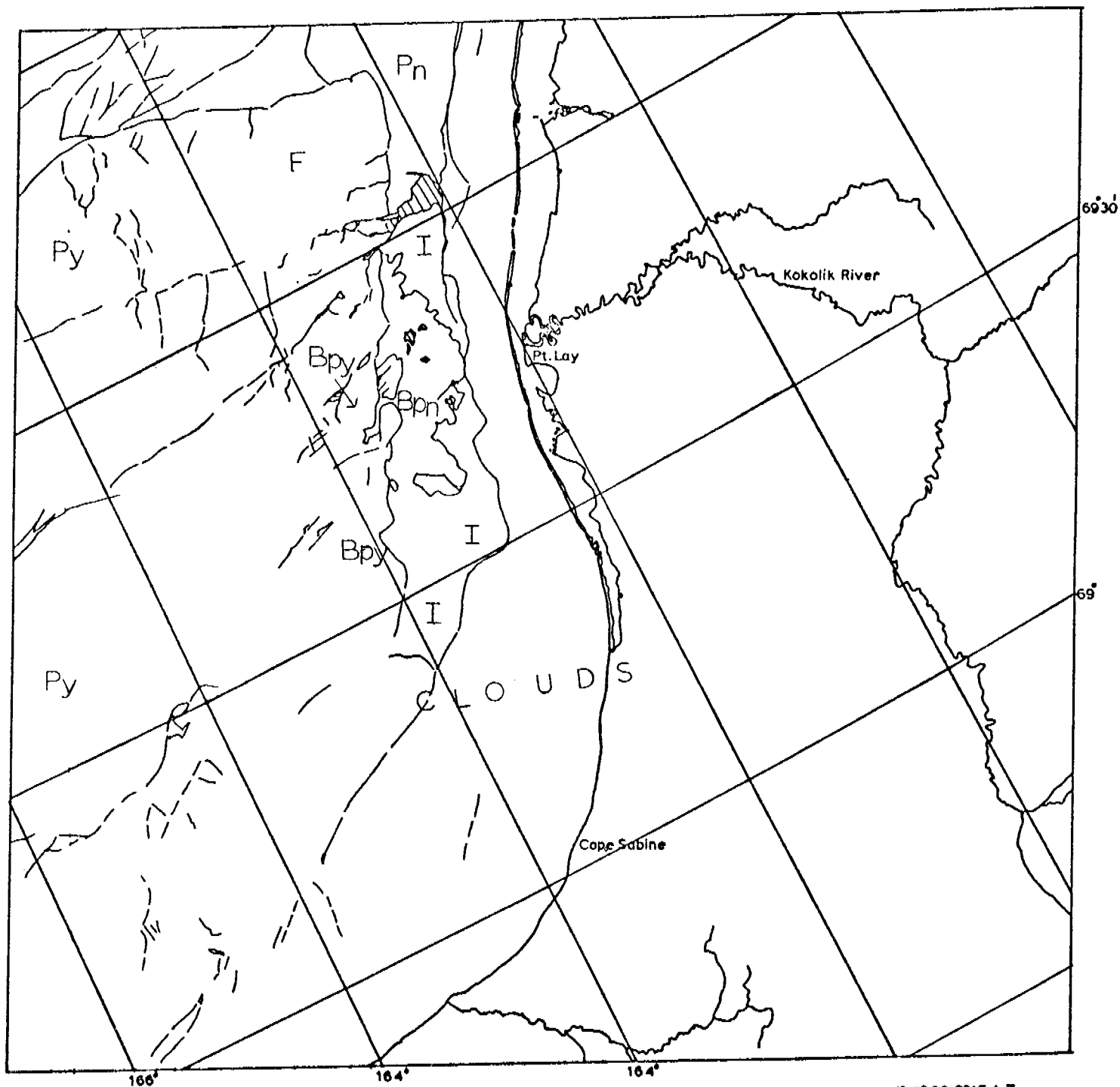
E-1261-22111-7
10 APRIL 1973

CHUKCHI SEA



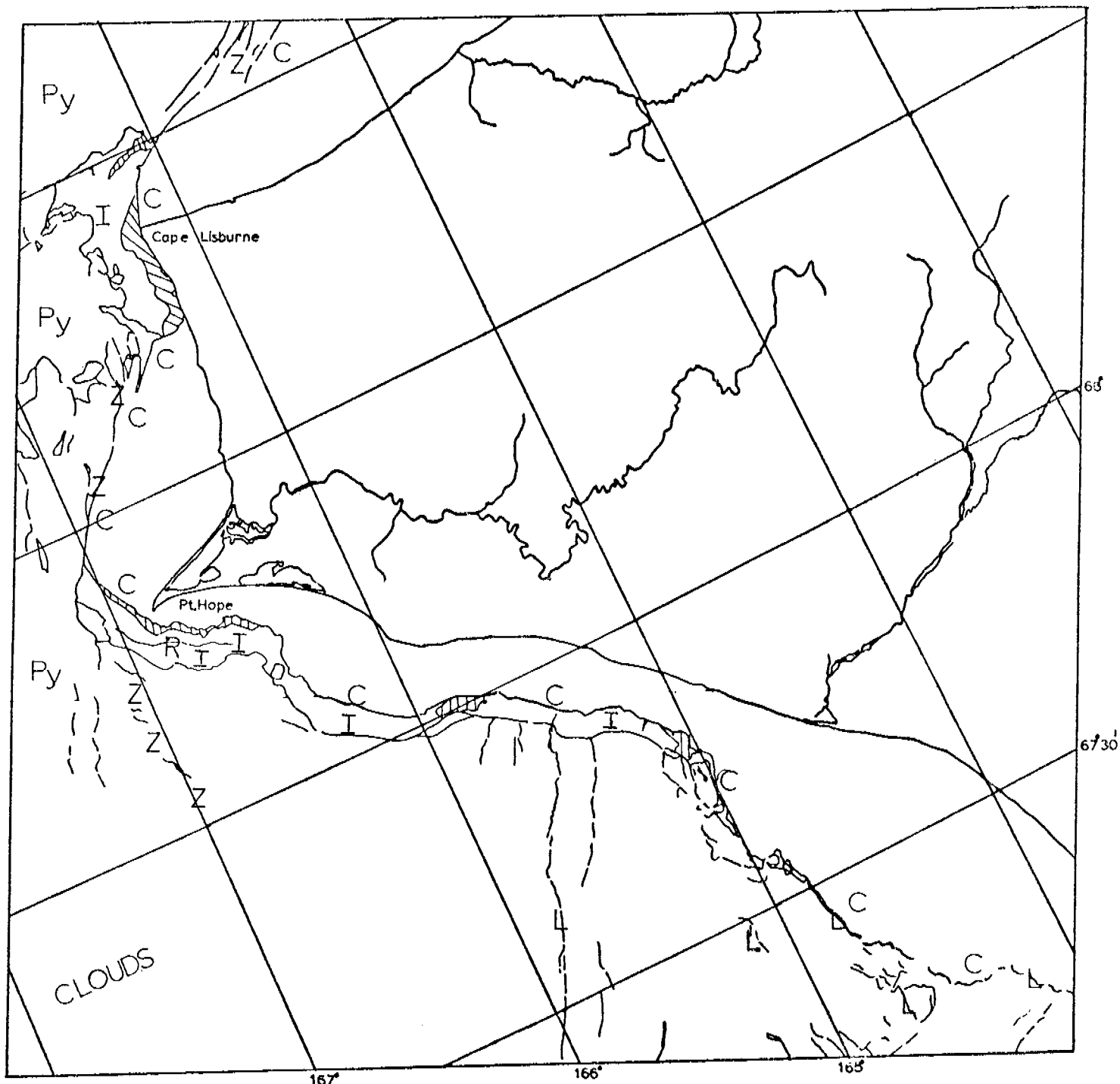
CHUKCHI SEA

E-1262-22151-7
11 APRIL 1973



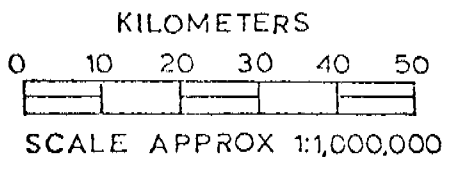
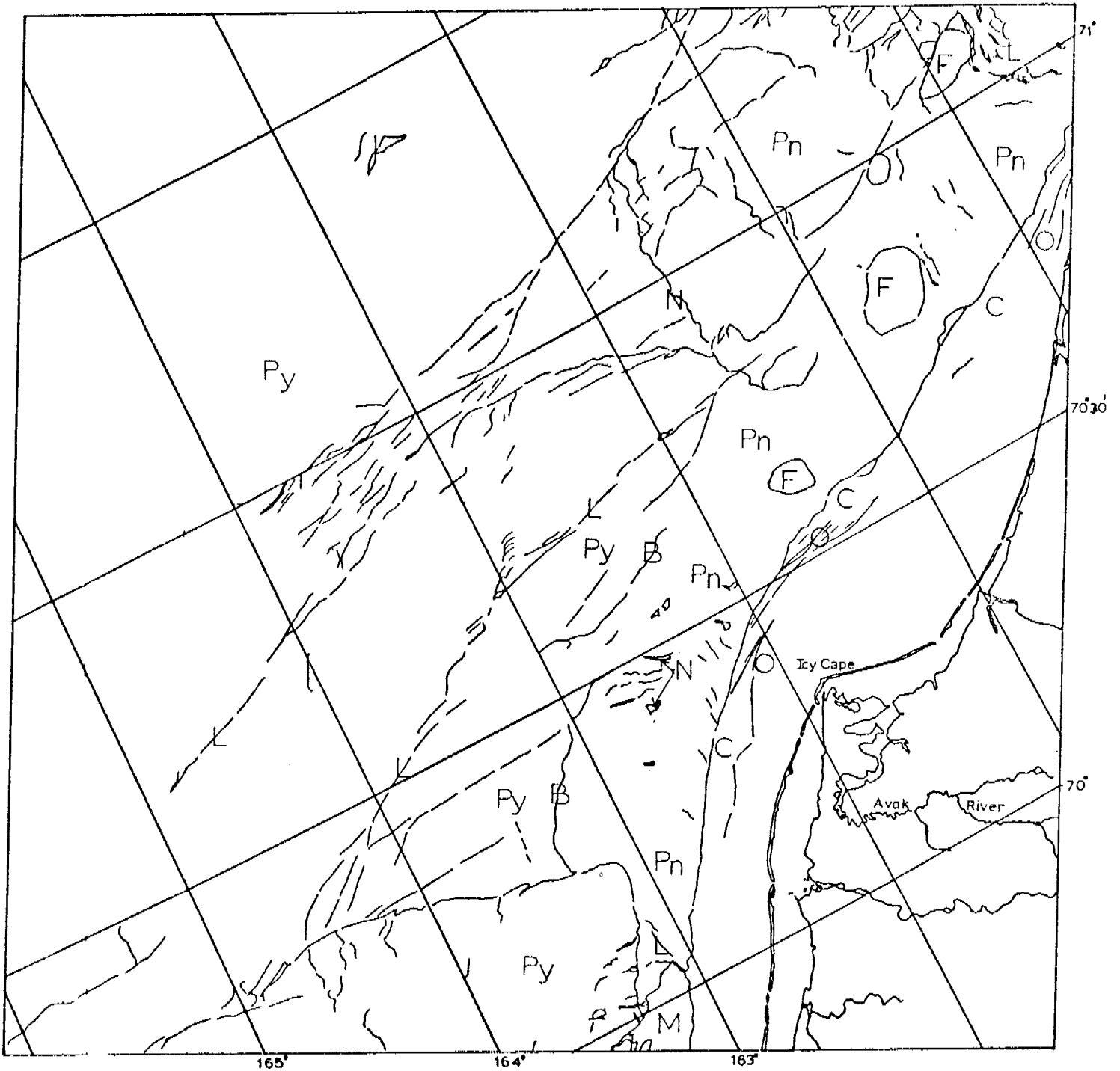
E-1262-22154-7
11 APRIL 1973

CHUKCHI SEA



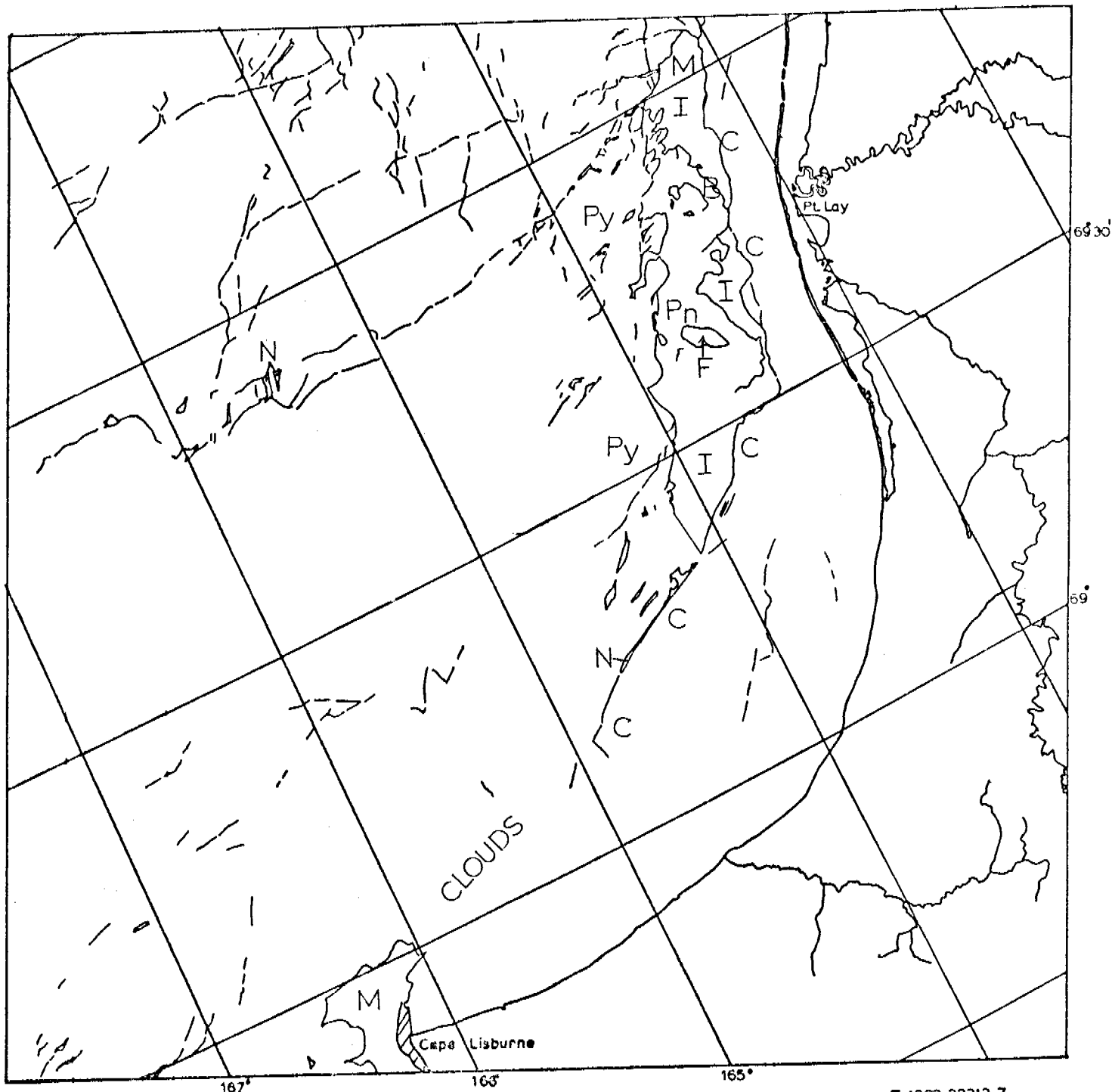
E-1262-22160-7
11 APRIL 1973

CHUKCHI SEA



E-1263-22210-7
12 APRIL 1973

CHUKCHI SEA



KILOMETERS
 0 10 20 30 40 50
 SCALE APPROX 1:1,000,000

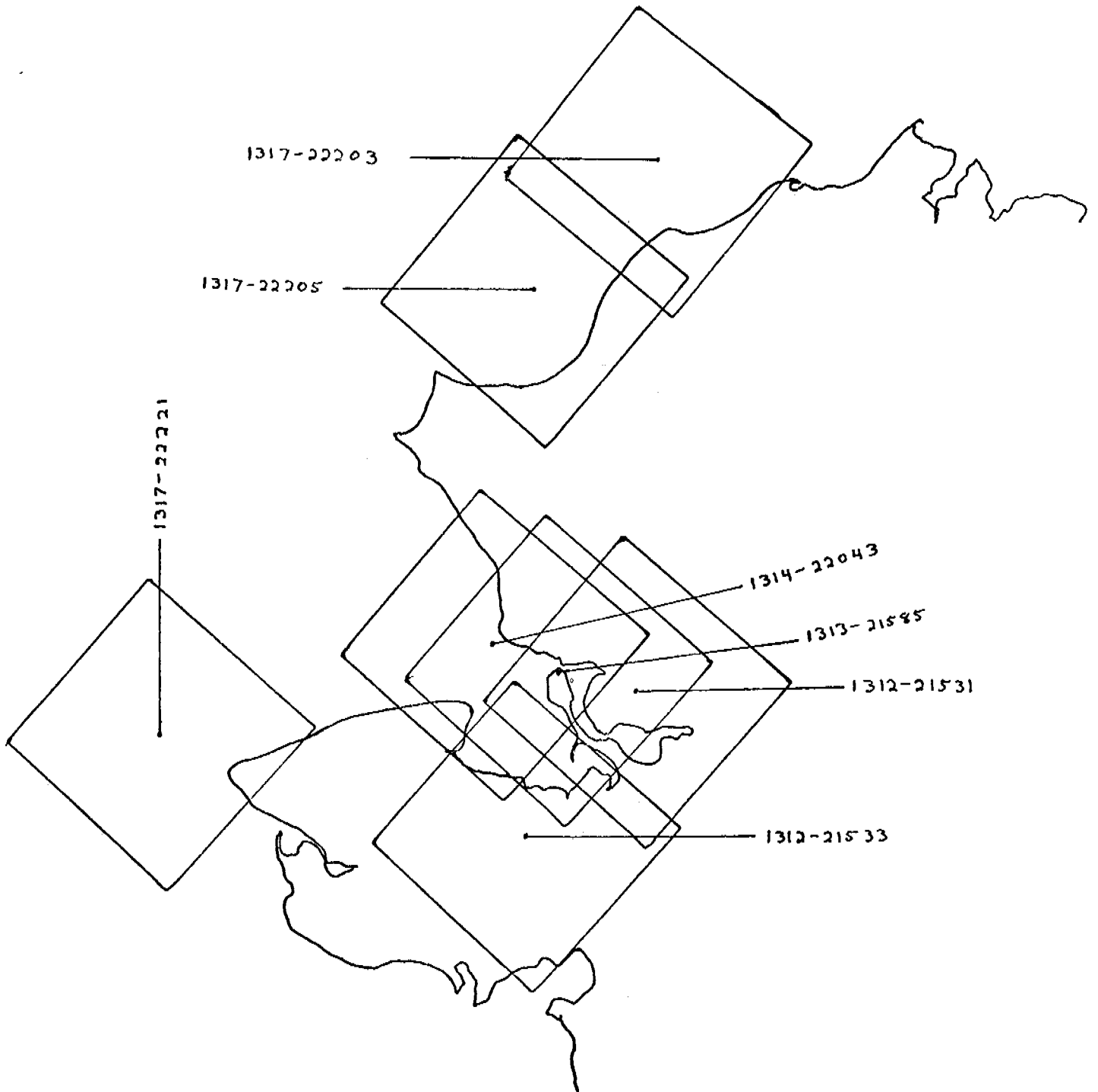
E-1263-22212-7
 12 APRIL 1973

CHUKCHI SEA

CHUKCHI SEA

31 MAY-17 JUNE 1973

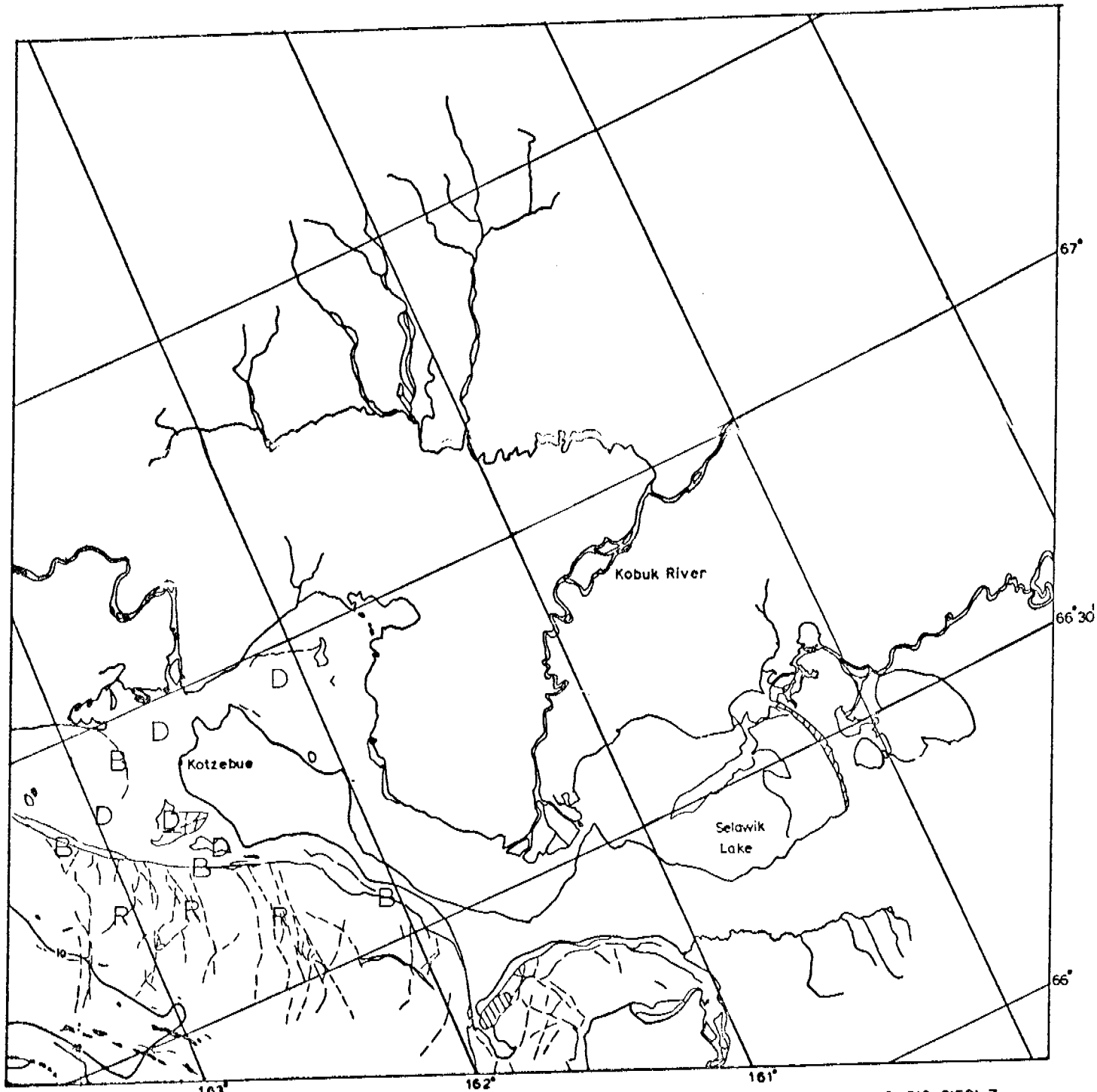
Images 1312-1329



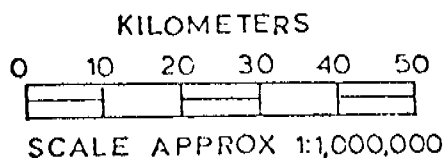
Scenes 1312-21531 } adjacent pair
1312-21533 }
1313-21585
1314-22043
1316-22153
1317-22203 } adjacent pair
1317-22205 }
1317-2221

These scenes show the Kotzebue Sound, Point Lay and Bering Strait portions of the Chukchi coast between May 31 and June 5, 1973. This series of scenes shows near shore ice features formed during the previous winter. Many small ridges have been mapped in the Kotzebue sound region. These include an extensive ridge system which extends along the Baldwin Peninsula NW to Cape Krusenstern. To the south, the last remaining contiguous ice along the Espenberg indicates the probable extent of grounded ice.

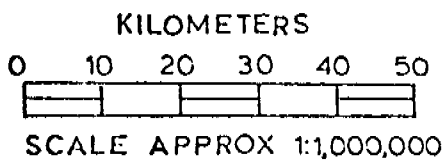
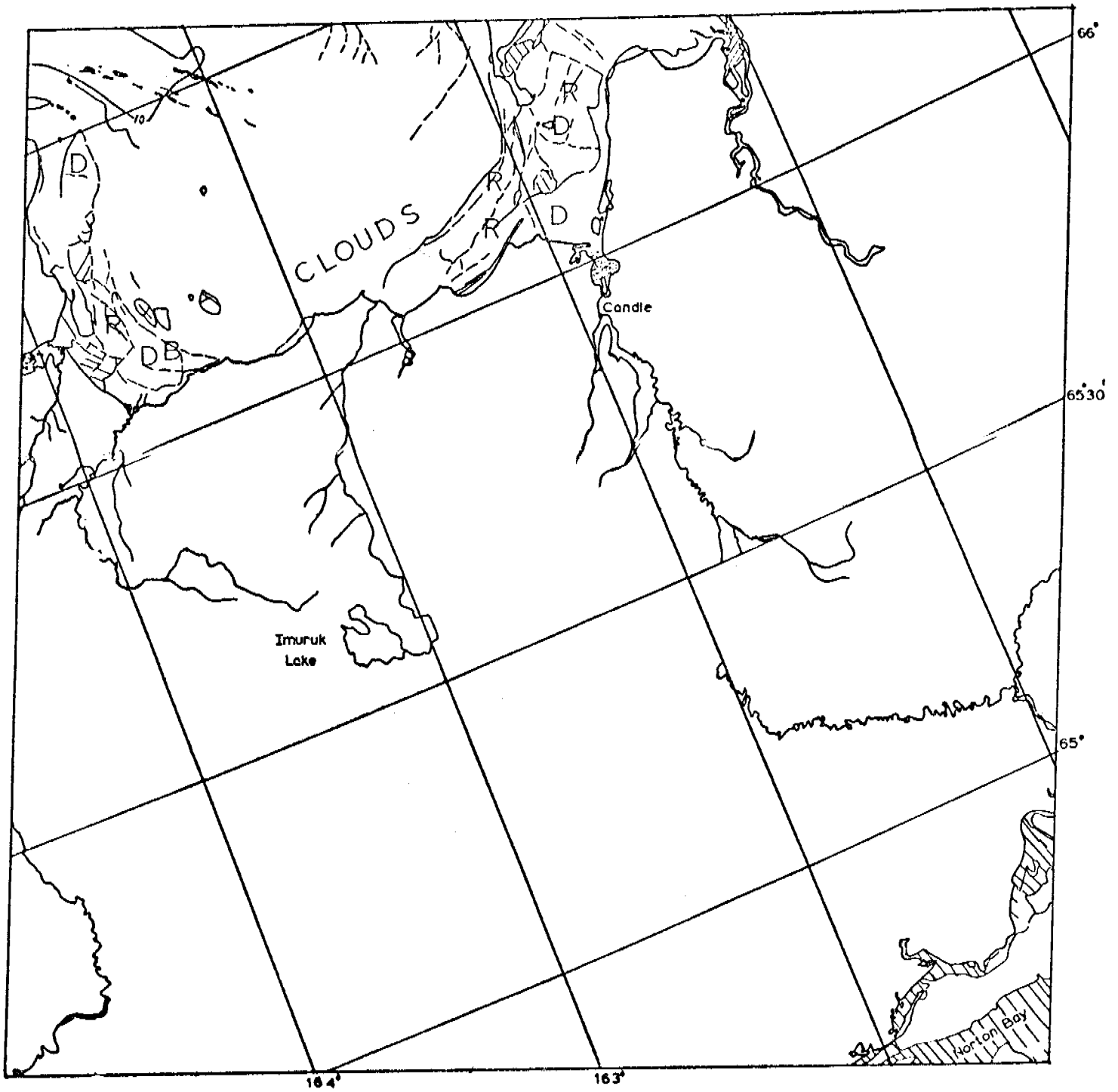
To the north, in the Point Lay-Icy Cape area there are also extensive regions of remaining contiguous ice. Considerable grounded ice remains on Blossom Shoals. Farther to the south, where massive ridging did not occur, it appears that in the absence of these protective features, the near shore apron has been considerably eroded.



E-1312-21531-7
31 MAY 1973

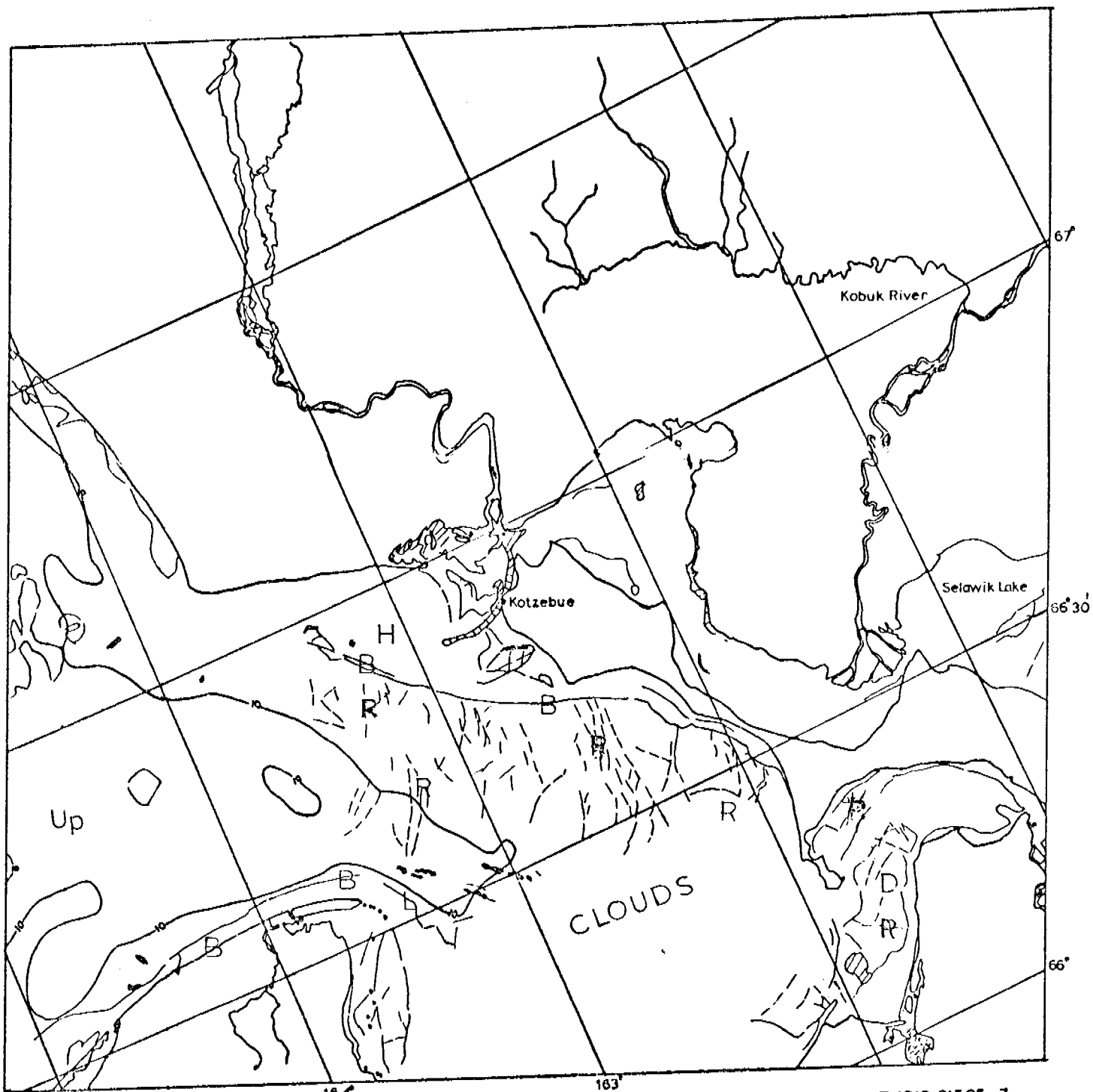


CHUKCHI SEA

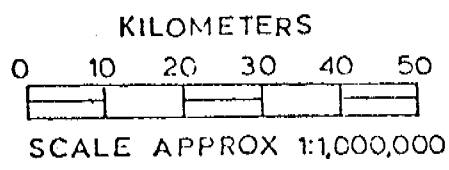


E-1312-21533-7
31 MAY 1973

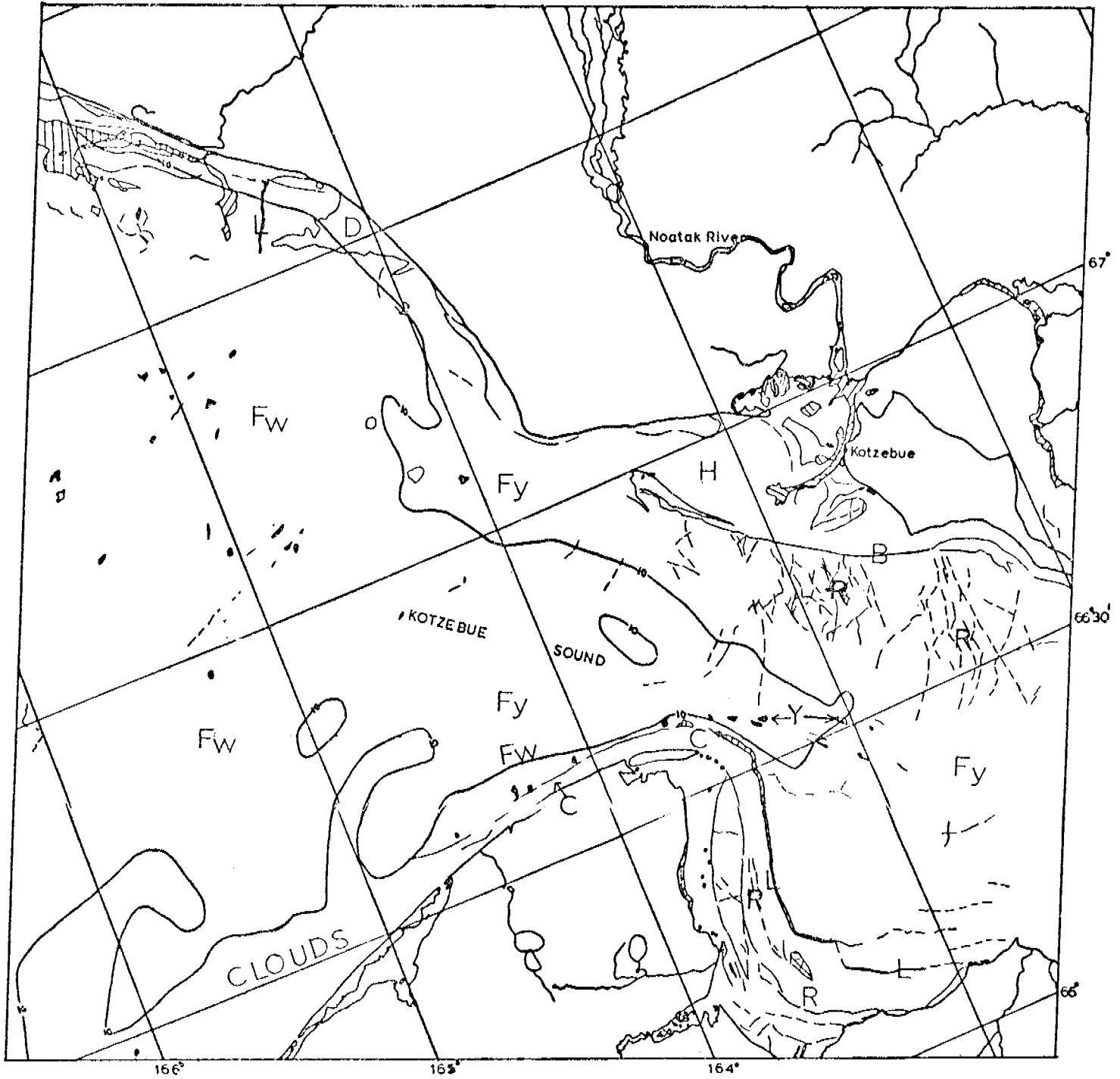
CHUKCHI SEA



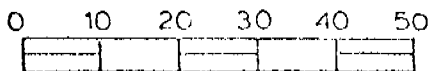
E-1313-21585-7
1 JUNE 1973



CHUKCHI SEA



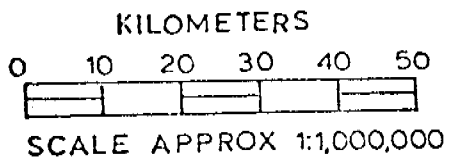
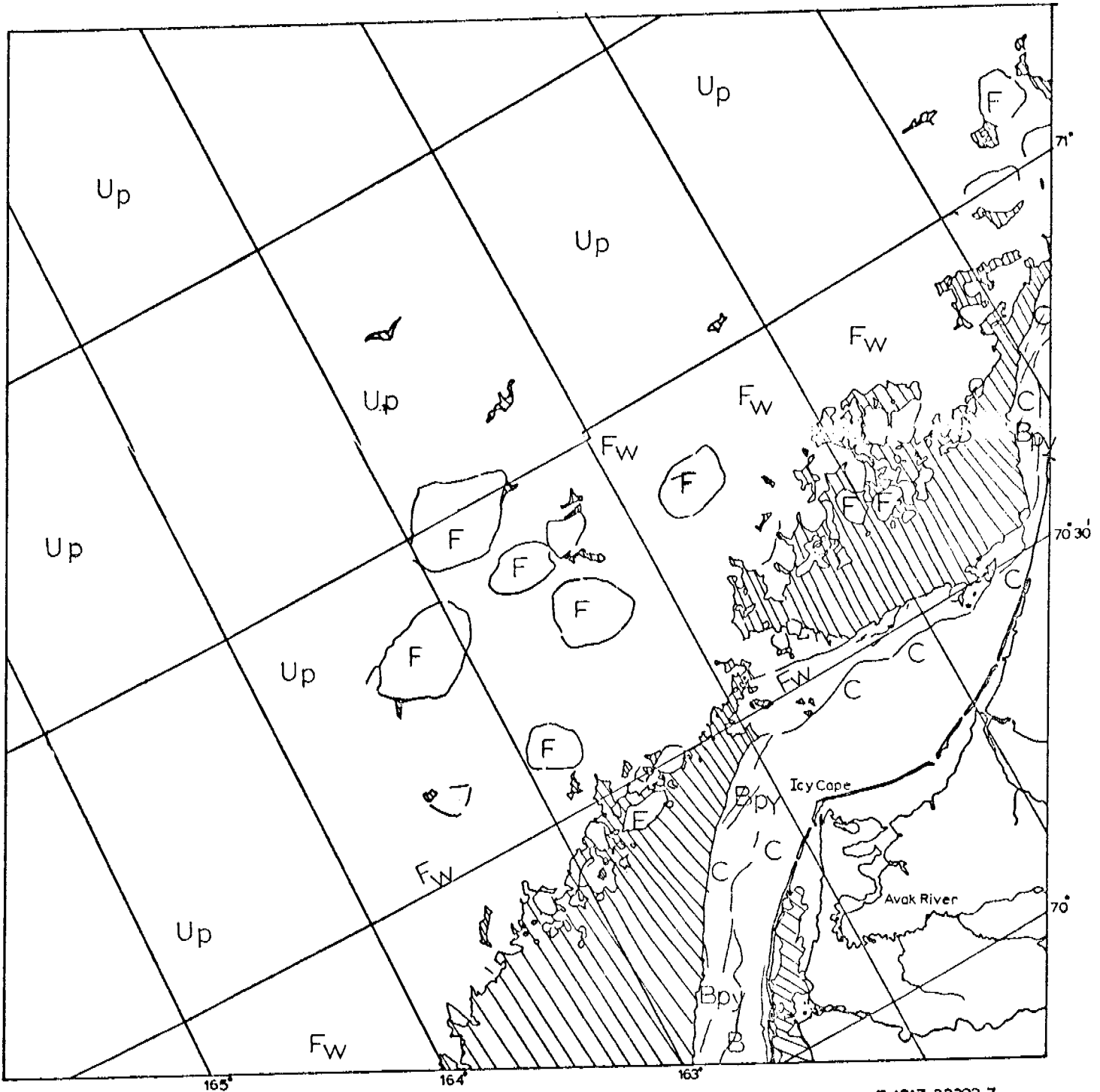
KILOMETERS



SCALE APPROX 1:1,000,000

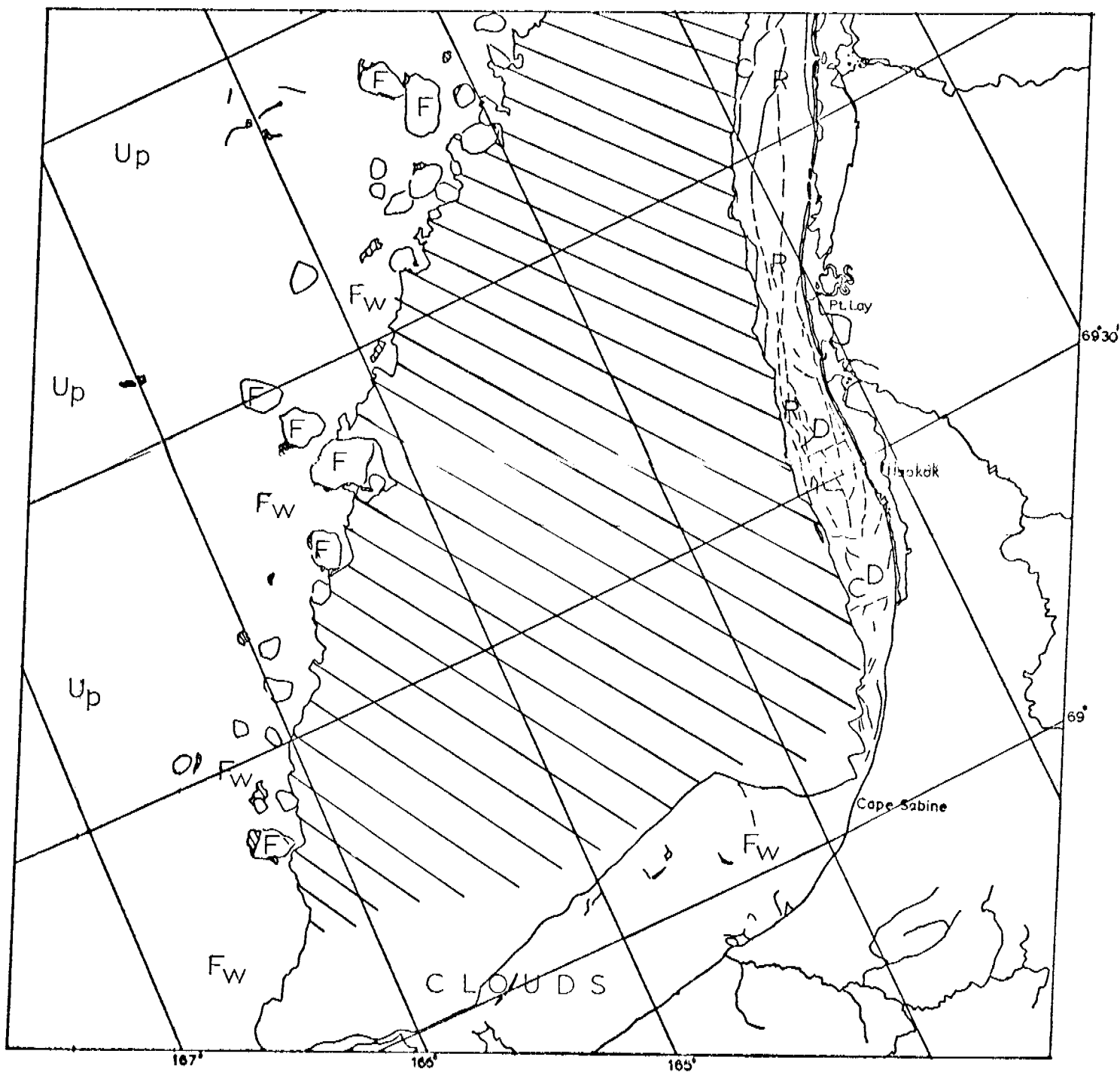
E-1314-22043-7
2 JUNE 1973

CHUKCHI SEA



CHUKCHI SEA

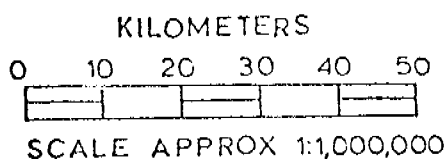
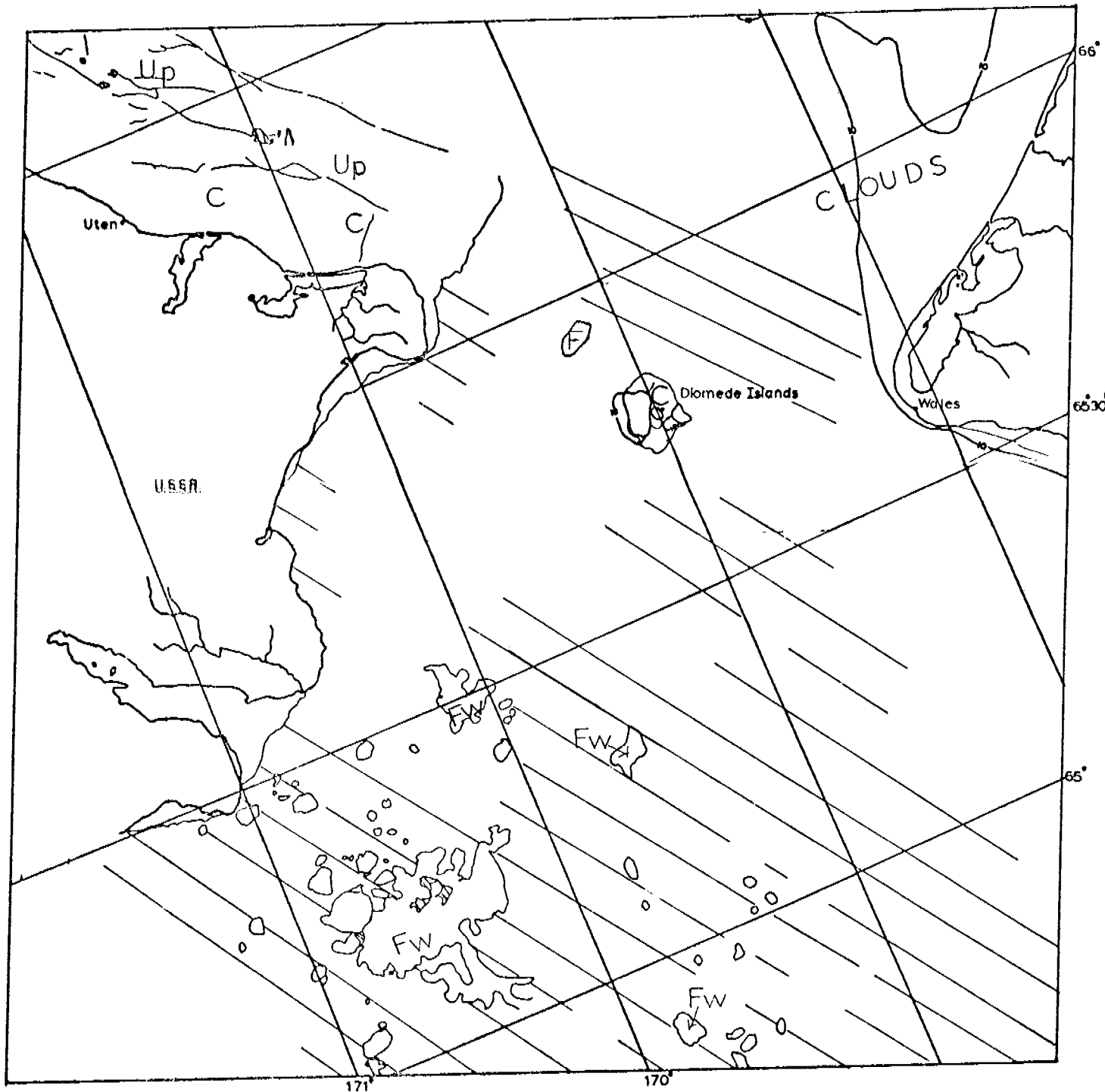
E-1317-22203-7
 5 JUNE 1973



KILOMETERS
 0 10 20 30 40 50
 SCALE APPROX 1:1,000,000

E-1317-22205-7
 5 JUNE 1973

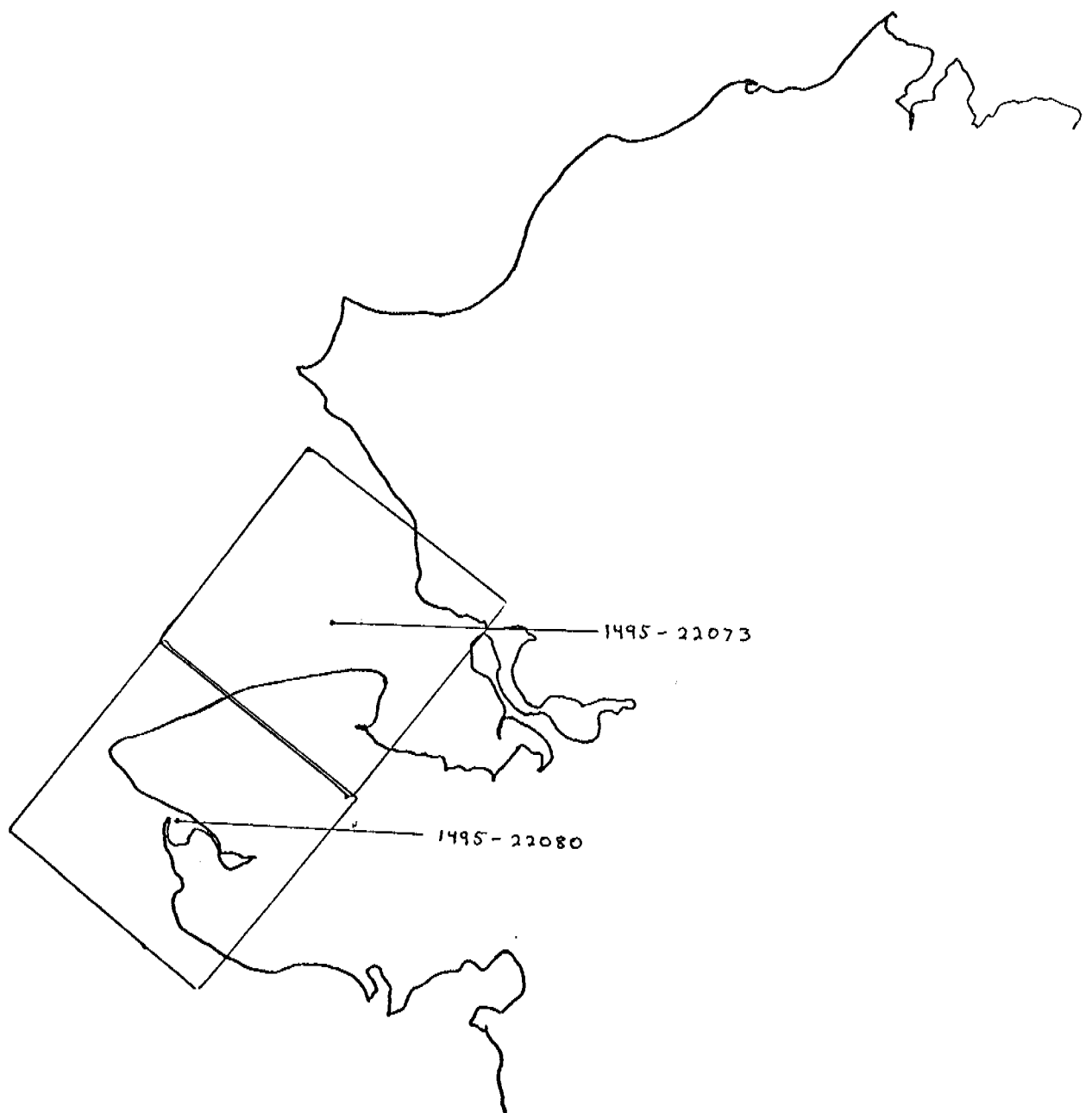
CHUKCHI SEA



E-1317-22221-7
5 JUNE 1973

CHUKCHI SEA

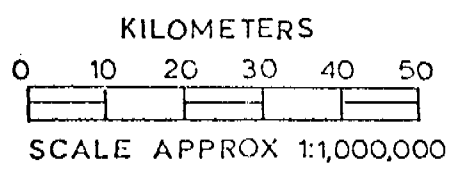
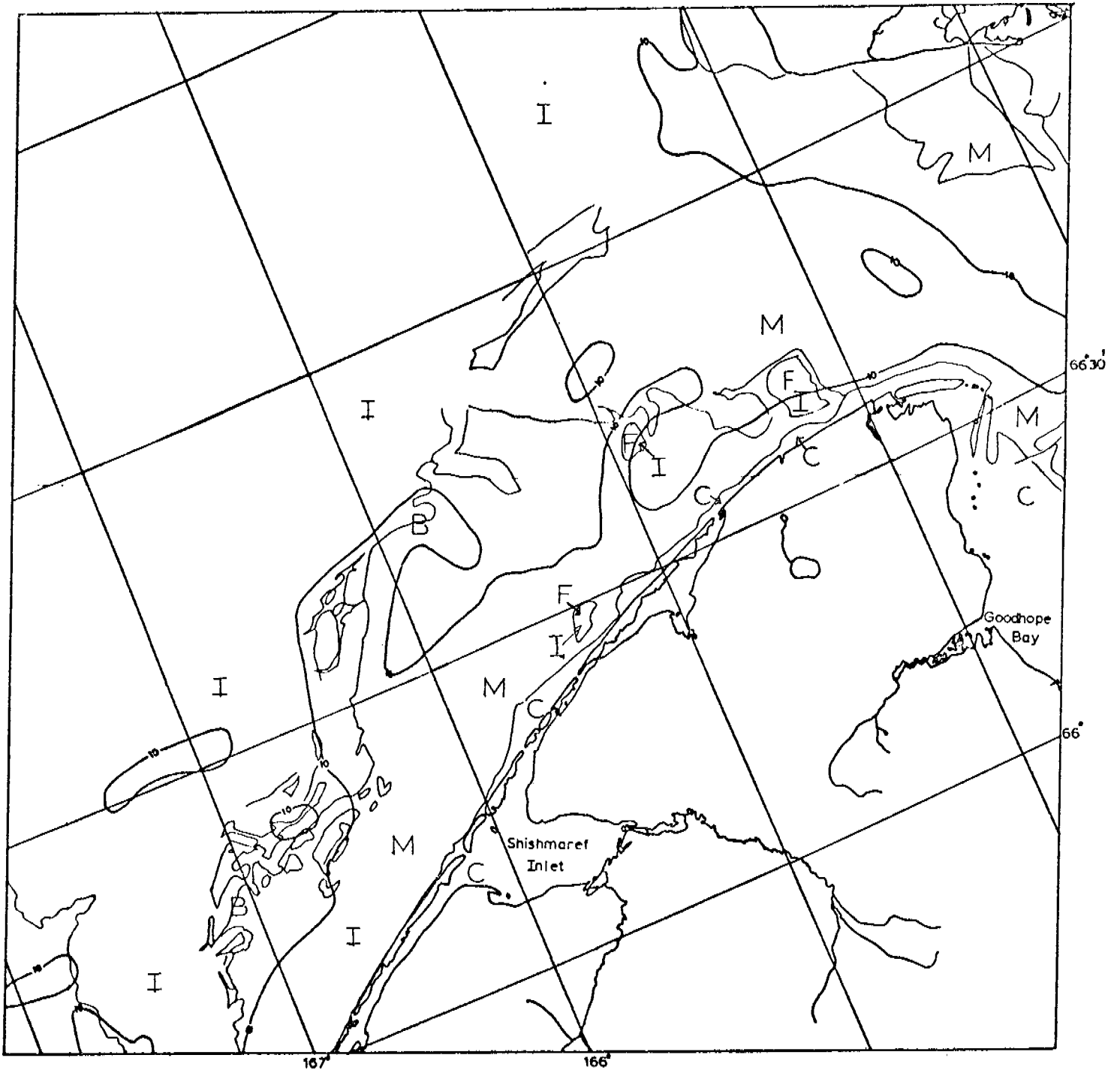
CHUKCHI SEA
27 NOVEMBER-14 DECEMBER
1973
Images 1492-1509



Scenes 1495-22080

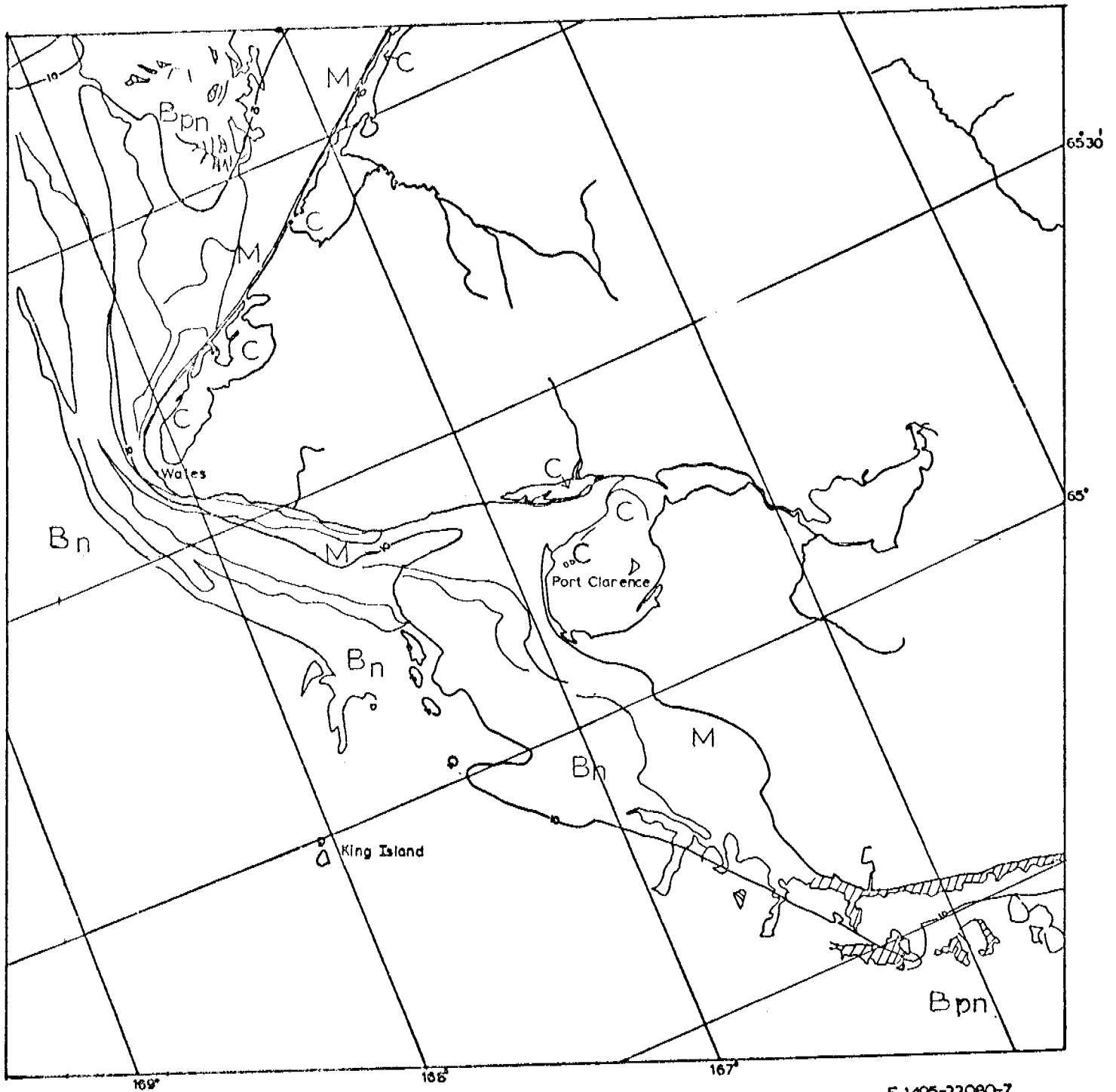
1495-22073

These two scenes show the Cape Prince of Wales area on November 30, 1973. The solar elevation angle at the time of acquisition was one degree. At this time the oceanic ice consists of new to young ice. Along the coast a thin irregular ribbon of contiguous ice can be found adjacent to the shore.

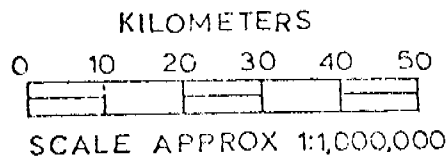


E-1495-22073-7
30 NOV. 1973

CHUKCHI SEA



E-1495-22080-7
30 NOV. 1973

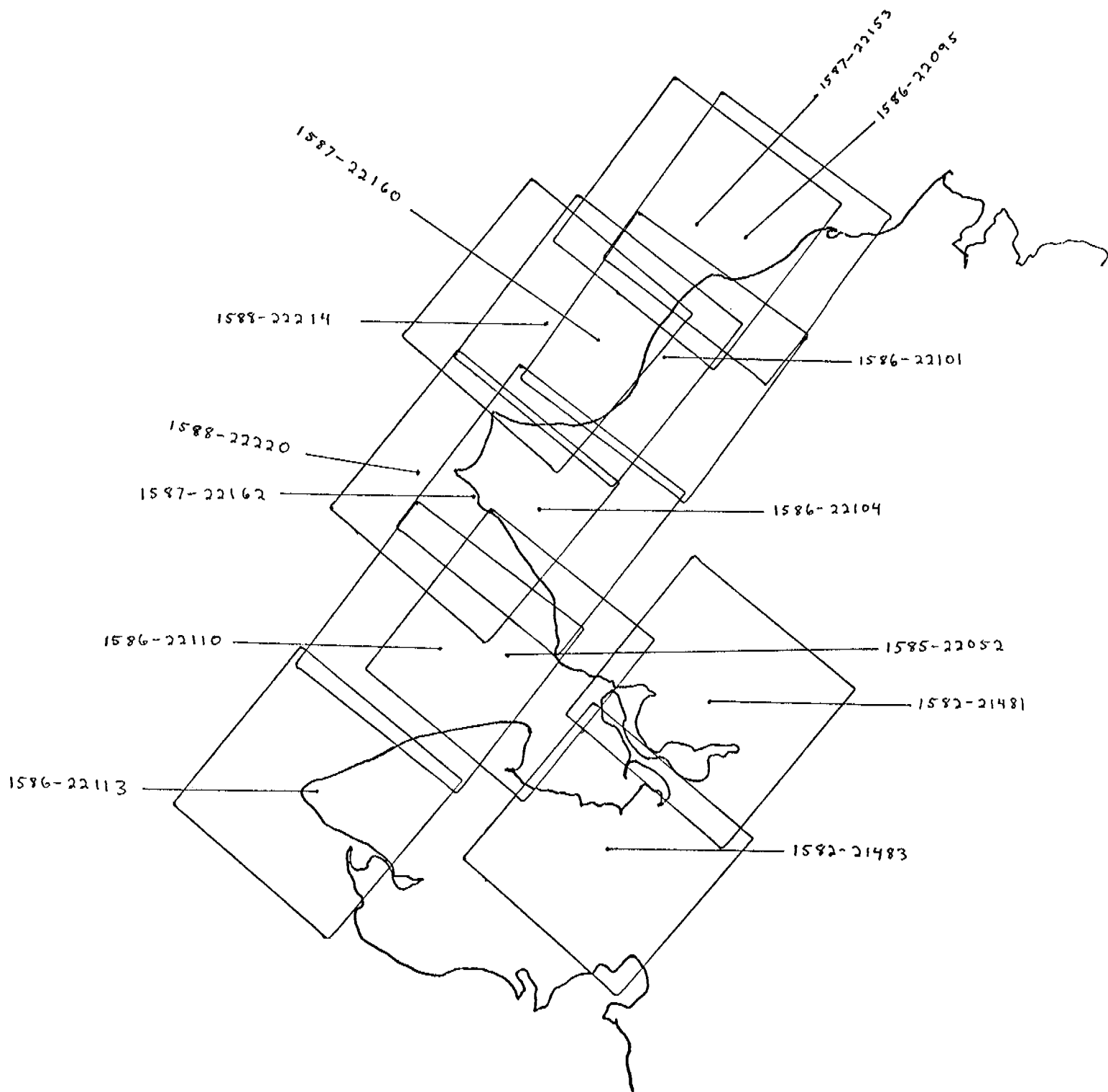


CHUKCHI SEA

CHUKCHI SEA

25 FEBRUARY-14 MARCH
1974

Cycle 1582-1599



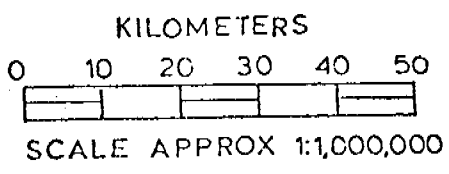
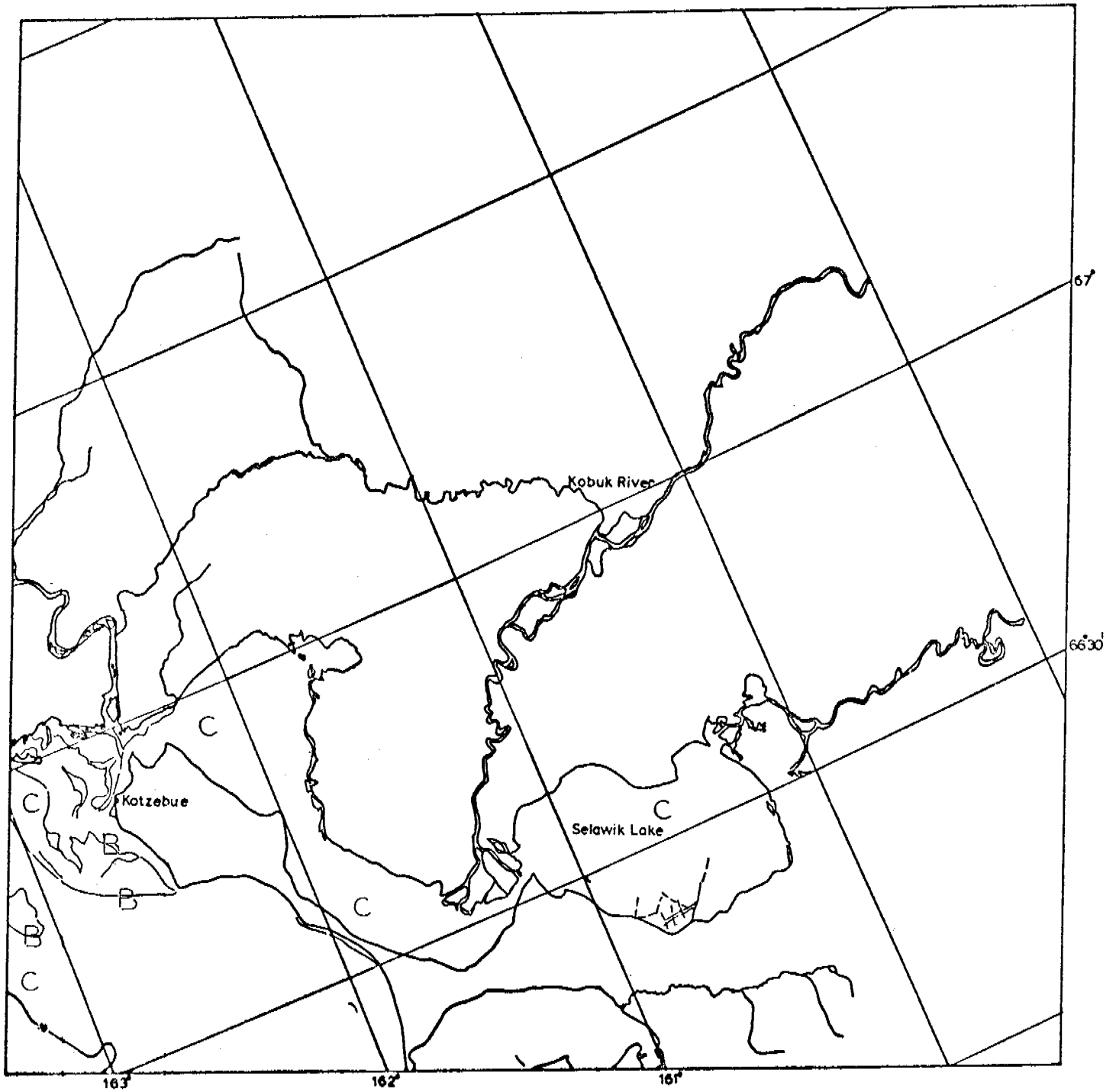
Scenes	1582-21481 } 1582-21483 }	adjacent pair
	1582-22052	
	1586-22095 } 1586-22101 }	adjacent pair
	1586-22110 } 1586-22113 }	adjacent pair
	1587-22160 } 1587-22162 } 1587-22153 }	adjacent triplet
	1588-22214 } 1588-22220 }	adjacent pair

These scenes show the portion of the Chukchi coast from Bering Strait to Point Franklin between February 25 and March 3, 1974. At this time Kotzebue Sound is covered with continuous first year ice out to a line well beyond the entrance to the sound. At that location a large lead has opened up in a large sweeping curve from south to north. This lead has frozen over to the late new ice stage at this time. However, to the west many new leads are opening up as part of a general system of ice motion to the northwest.

At Bering Strait there is evidence of ice motion northward through the strait. Long trails of new ice to the north of King Island and the Diomedes indicate that this motion has been taking place for some time.

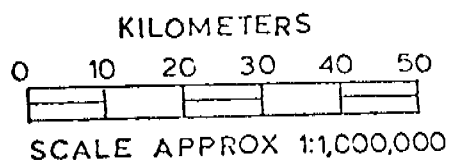
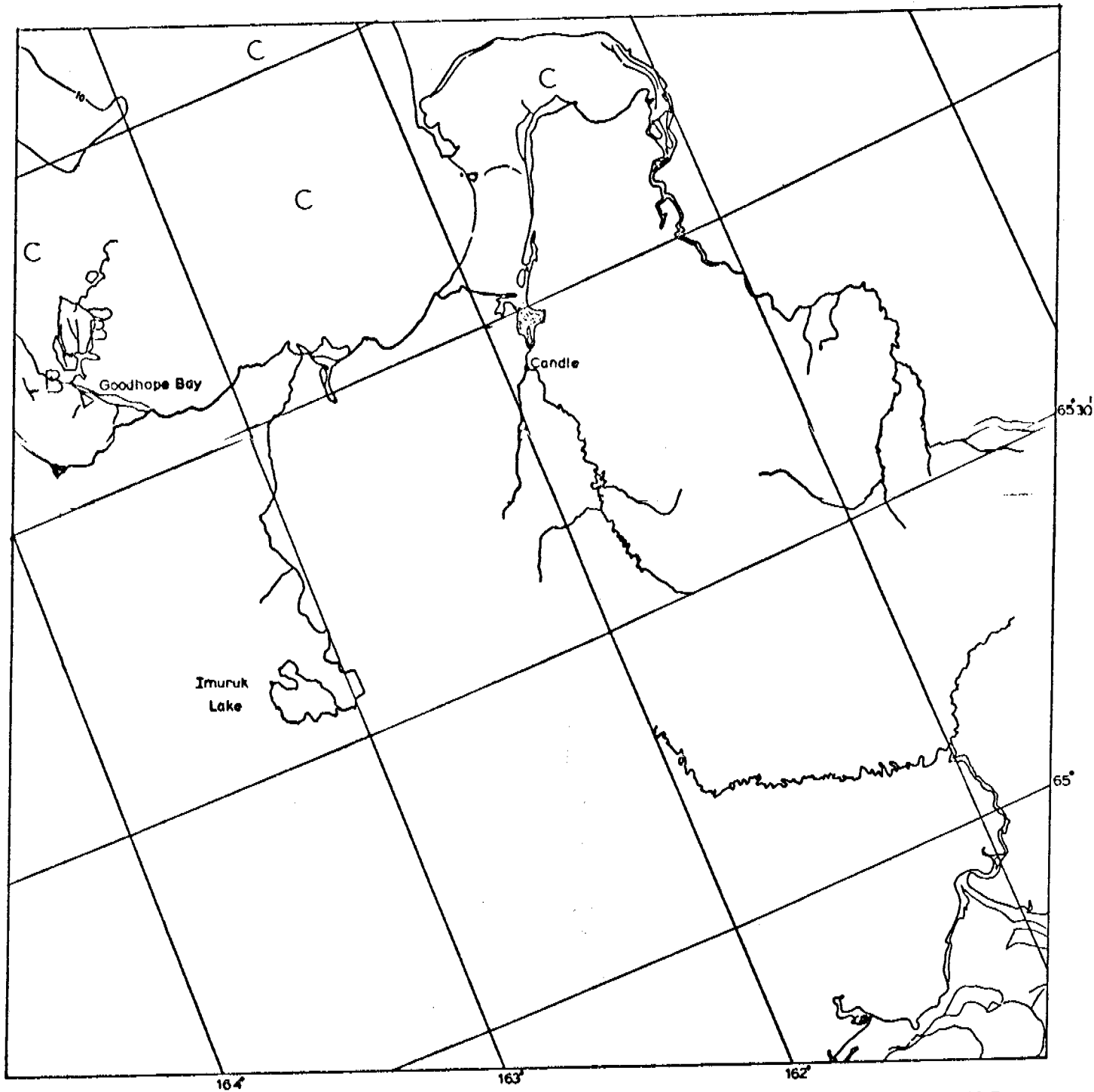
To the north of Cape Prince of Wales there are two groups of extension shear ridge systems forming a narrow "V" pointed to the south. These ridge systems are very likely at least partly grounded on shoals in this area and form the western side of an extensive area of contiguous ice. At this time however, a lead has formed which is cutting off the western side of the "V"--indicating that its anchoring (if any) was not very great.

Farther to the north extensive ridging appears across Blossom Shoal and from Point Franklin southward along the coast to a point just south of Wainwright.



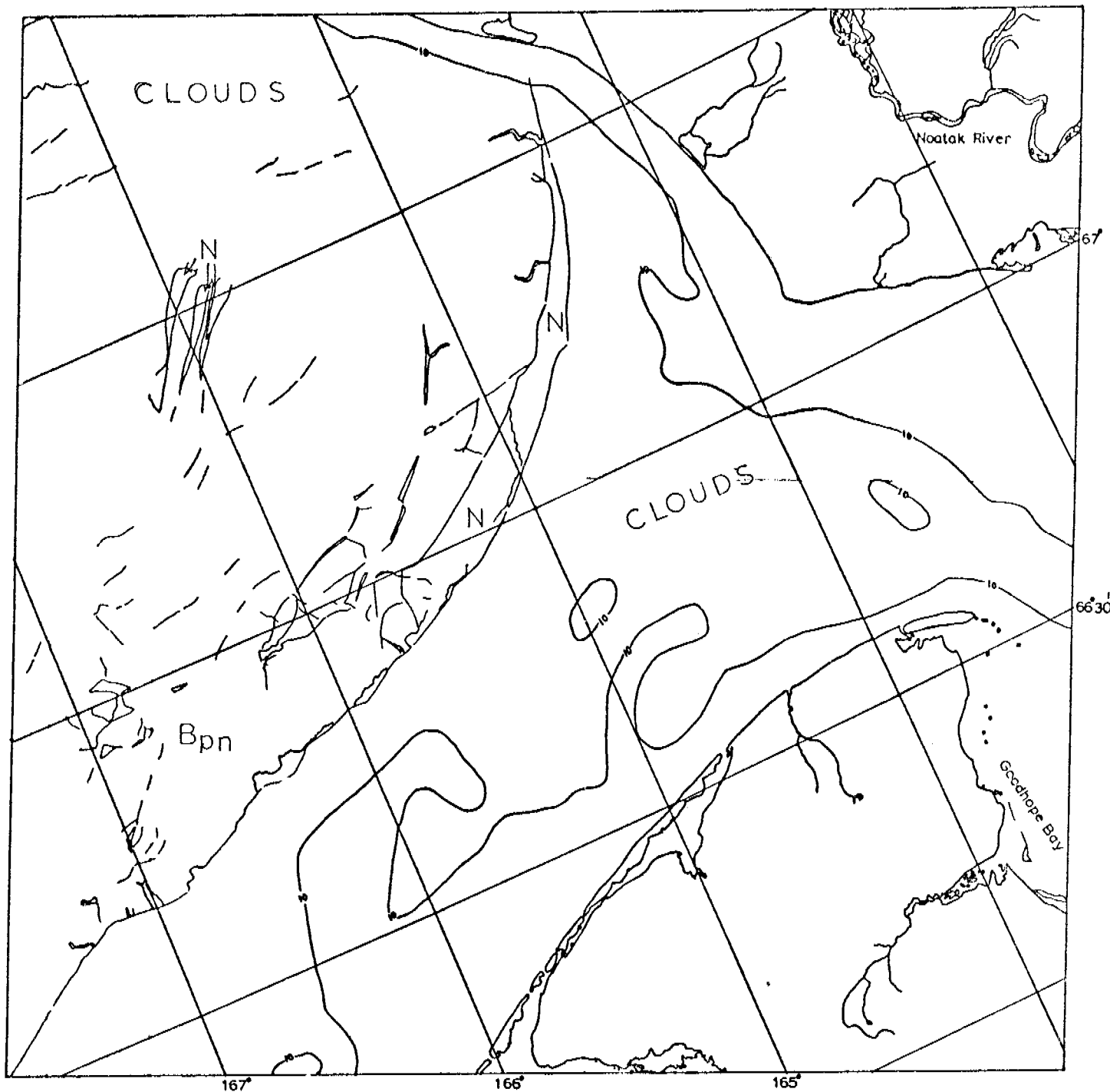
E-1582-21481-7
25 FEB. 1974

CHUKCHI SEA



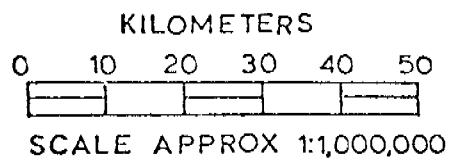
E-1582-21483-7
25 FEB. 1974

CHUKCHI SEA

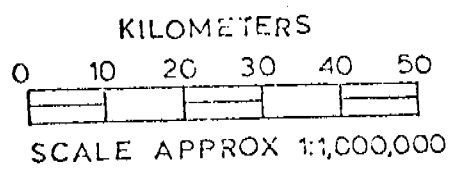
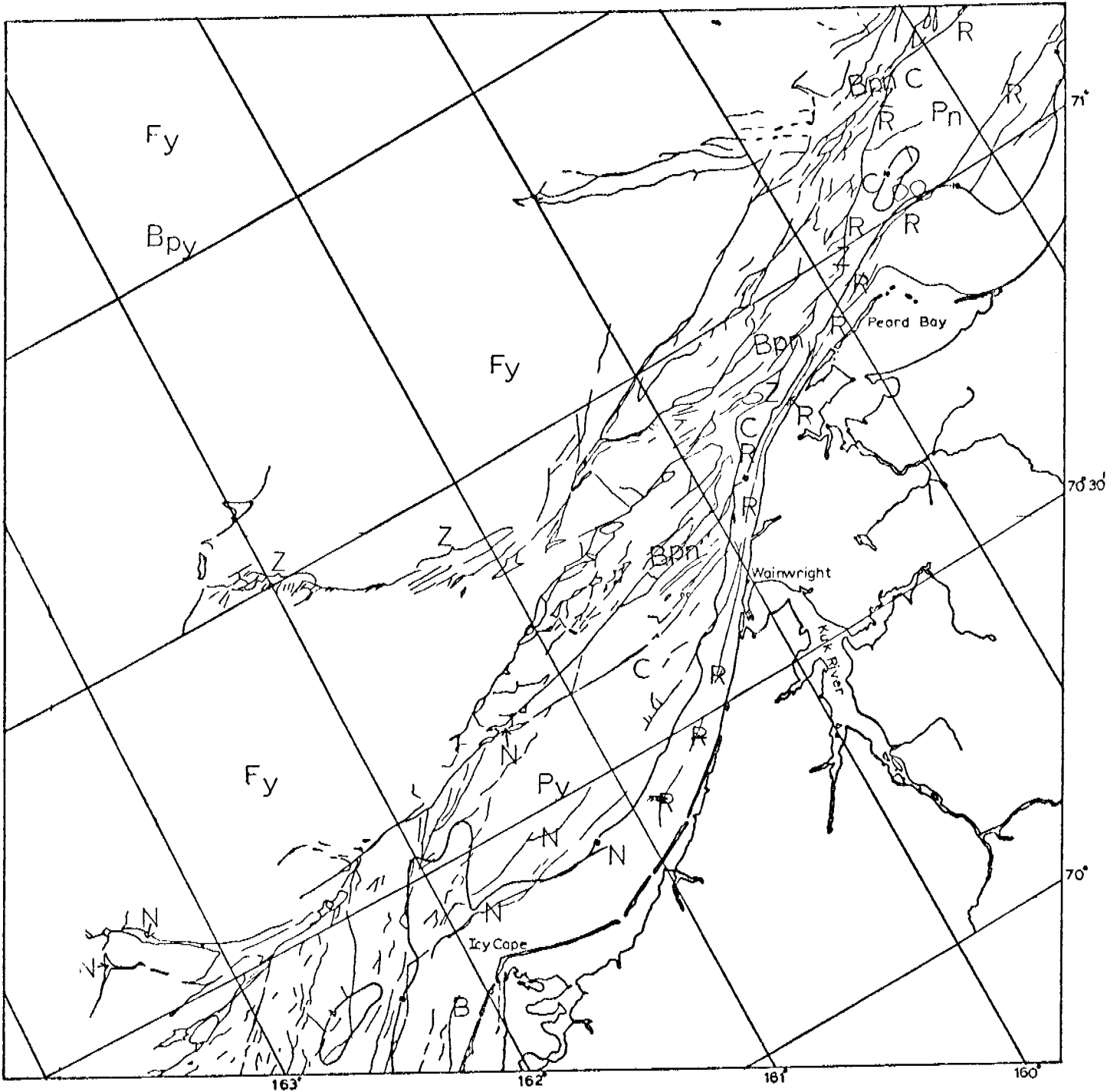


Entire scene covered with thin clouds.

E-1585-22052-7
28 FEB. 1974

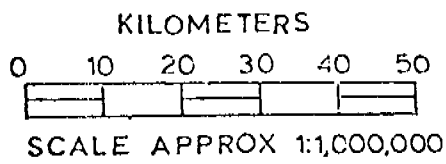
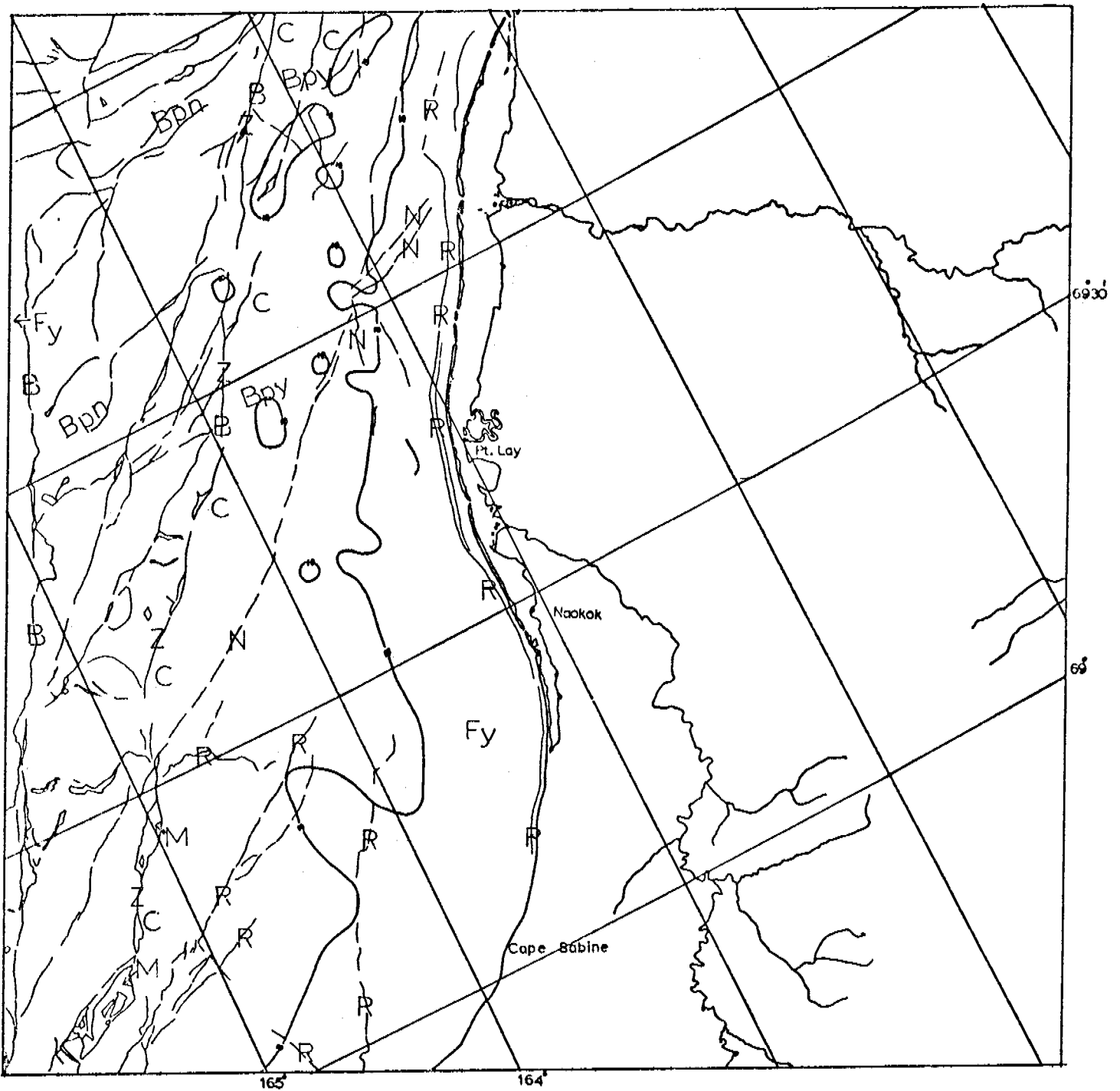


CHUKCHI SEA



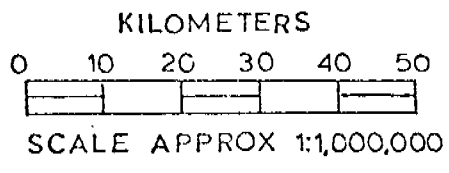
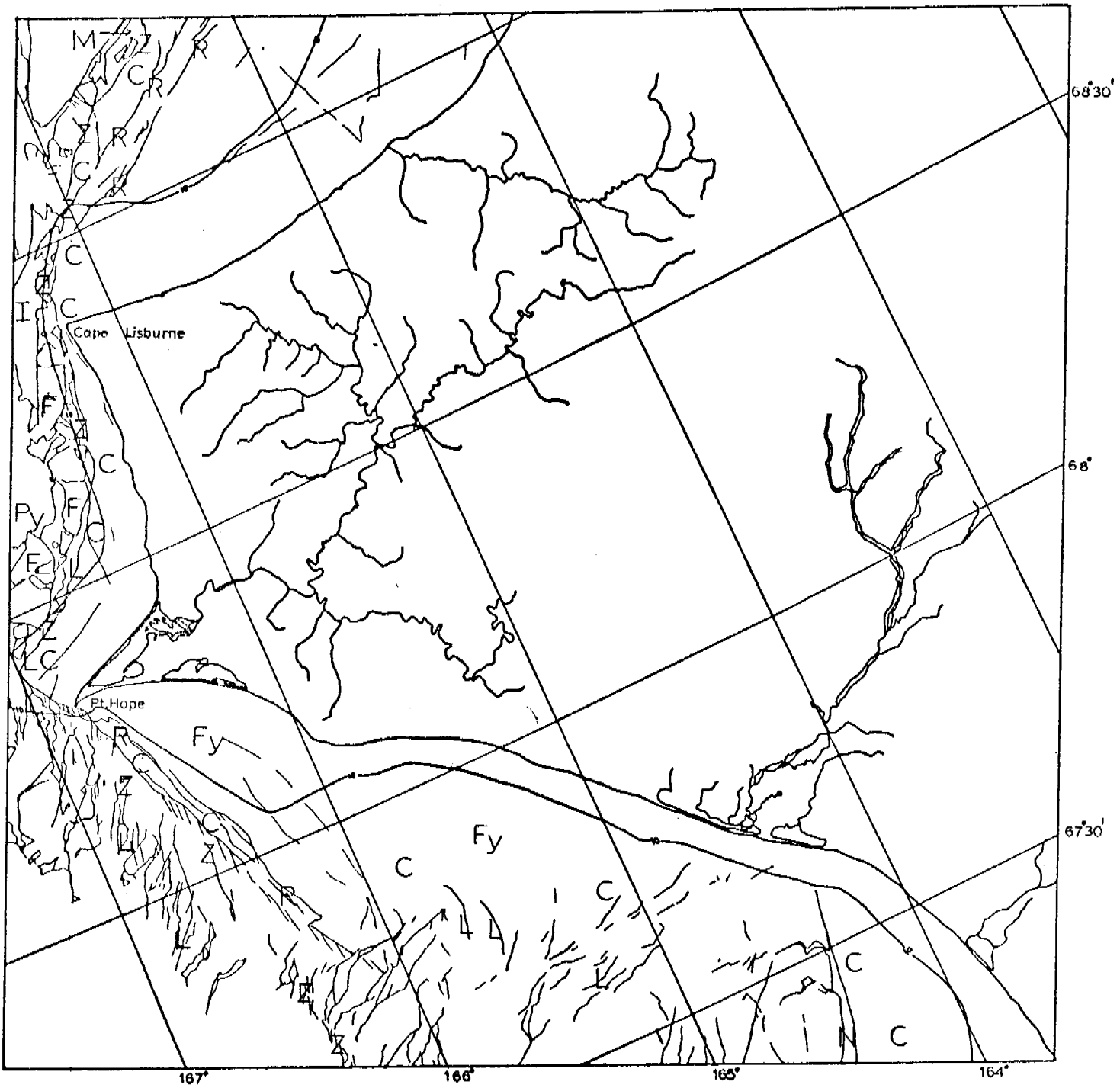
CHUKCHI SEA

E-1586-22095-7
1 MARCH 1974



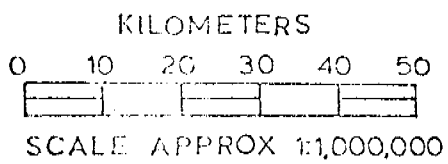
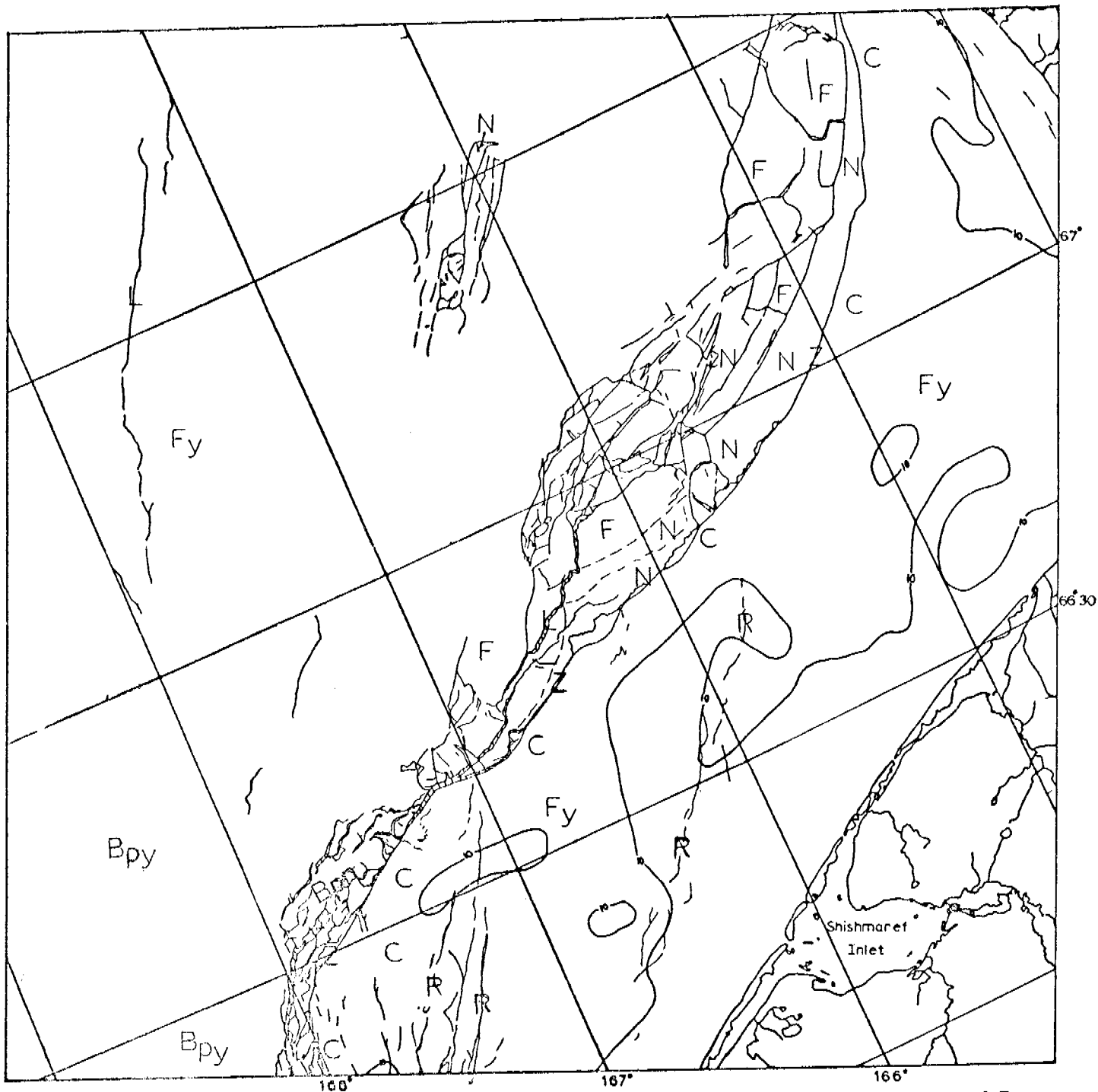
E-1586-22101-7
1 MARCH 1974

CHUKCHI SEA



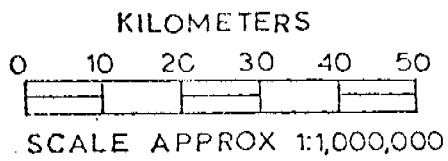
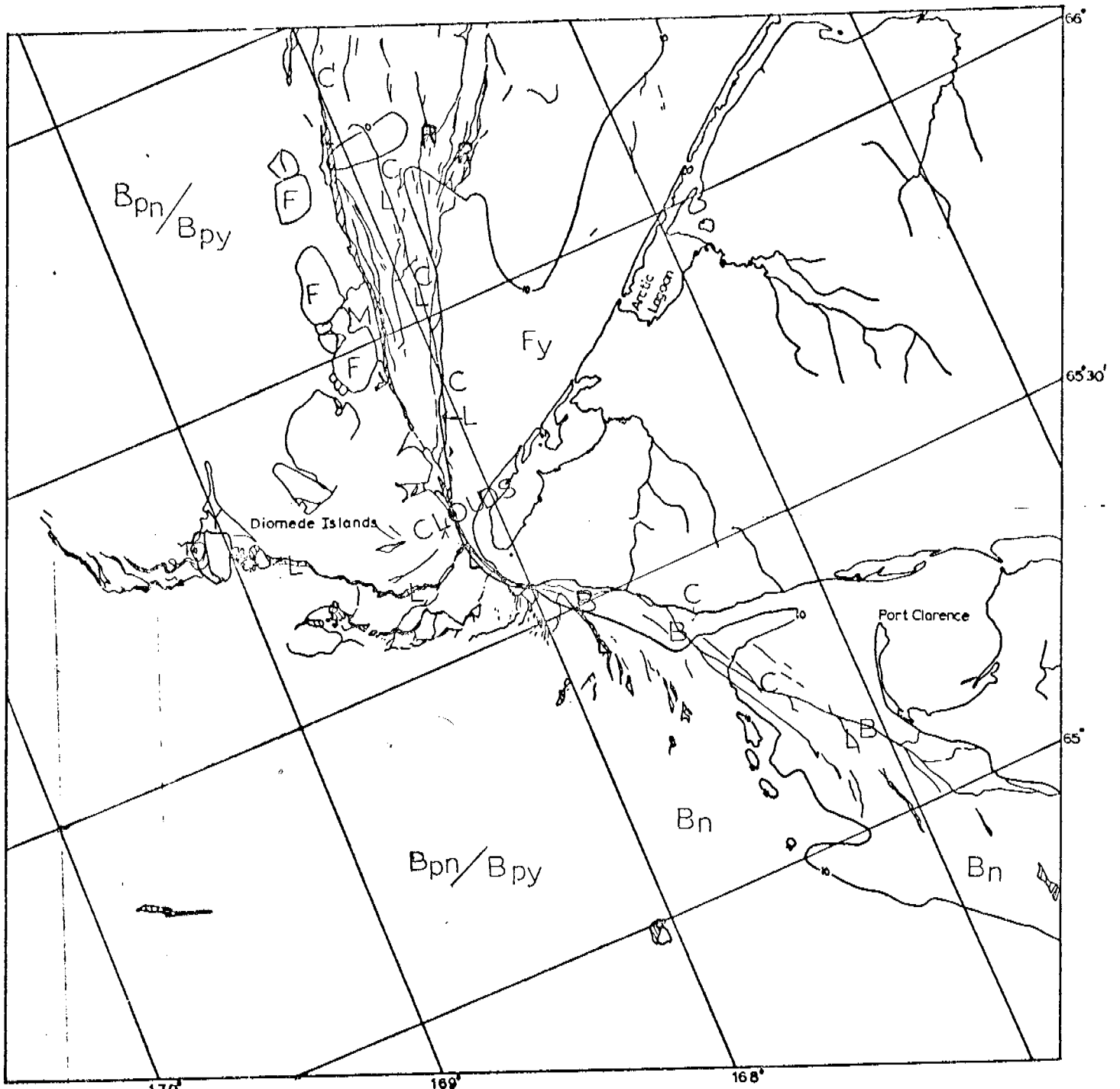
E-1586-22104-7
1 MARCH 1974

CHUKCHI SEA



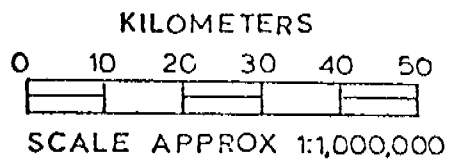
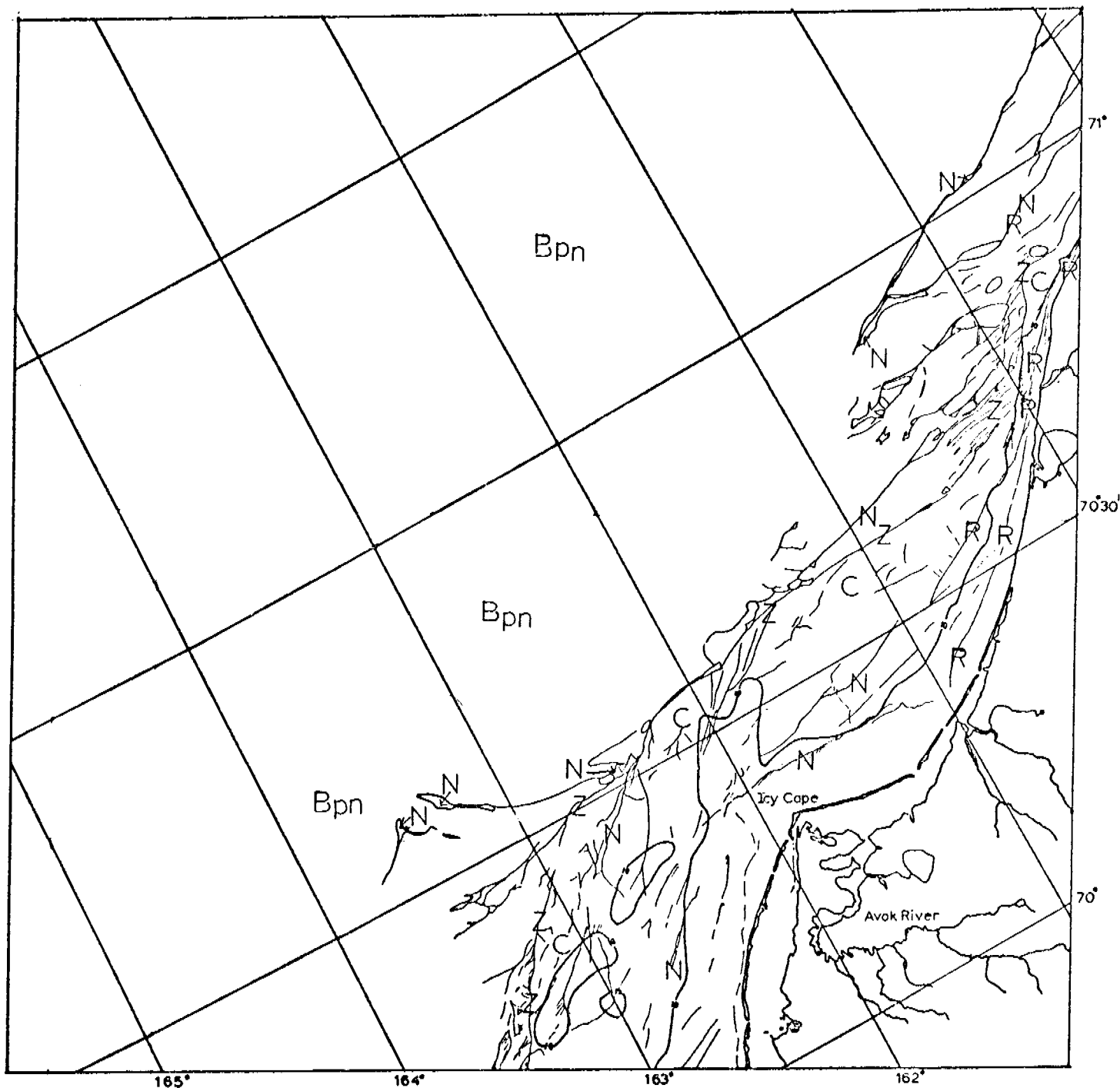
CHUKCHI SEA

E-1586-22110-7
1 MARCH 1974



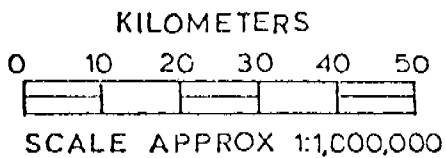
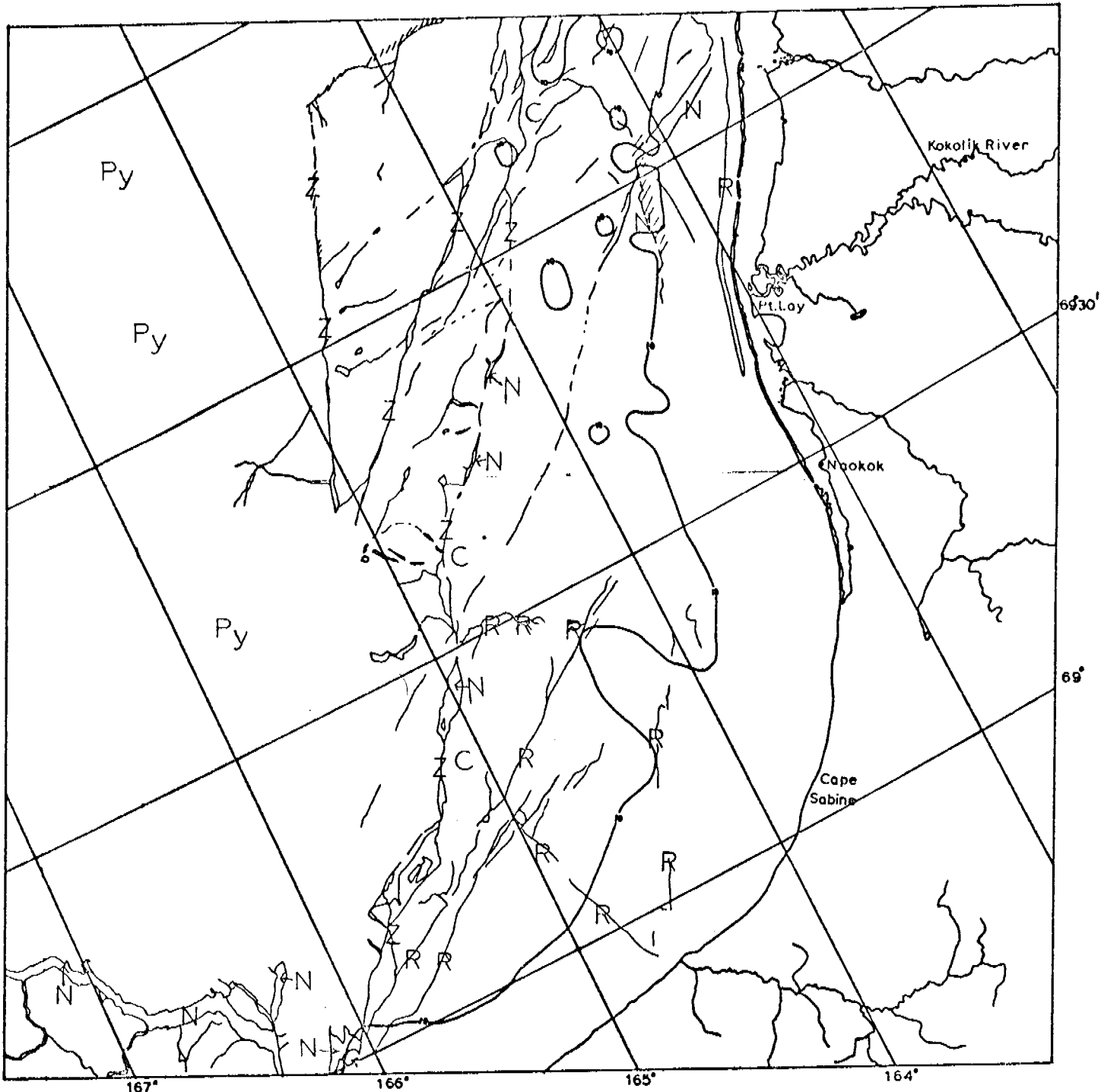
CHUKCHI SEA

E-1586-2213-7
1 MARCH 1974



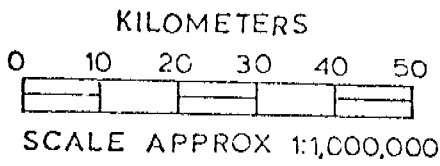
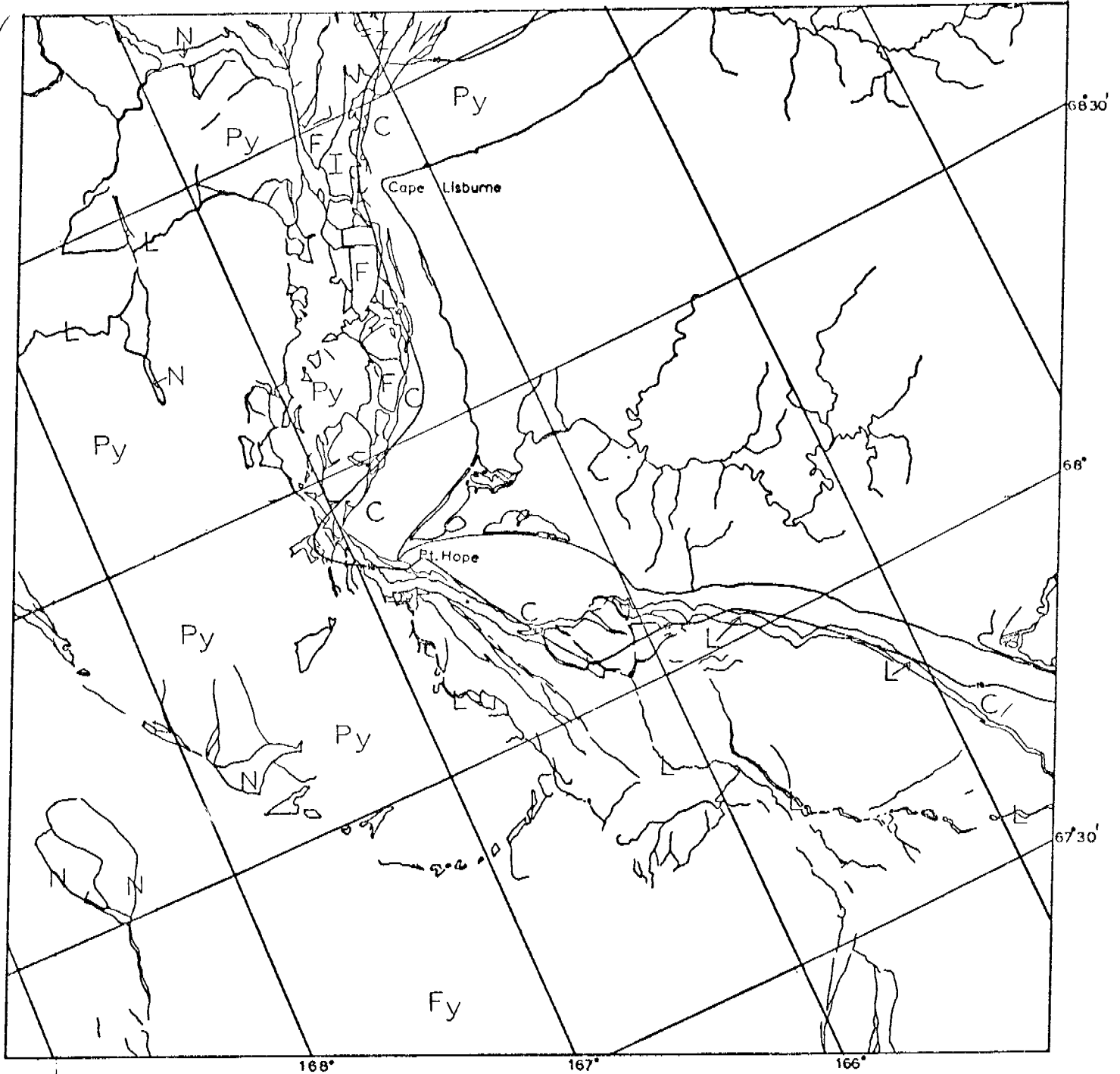
E-1587-22153-7
2 MARCH 1974

CHUKCHI SEA



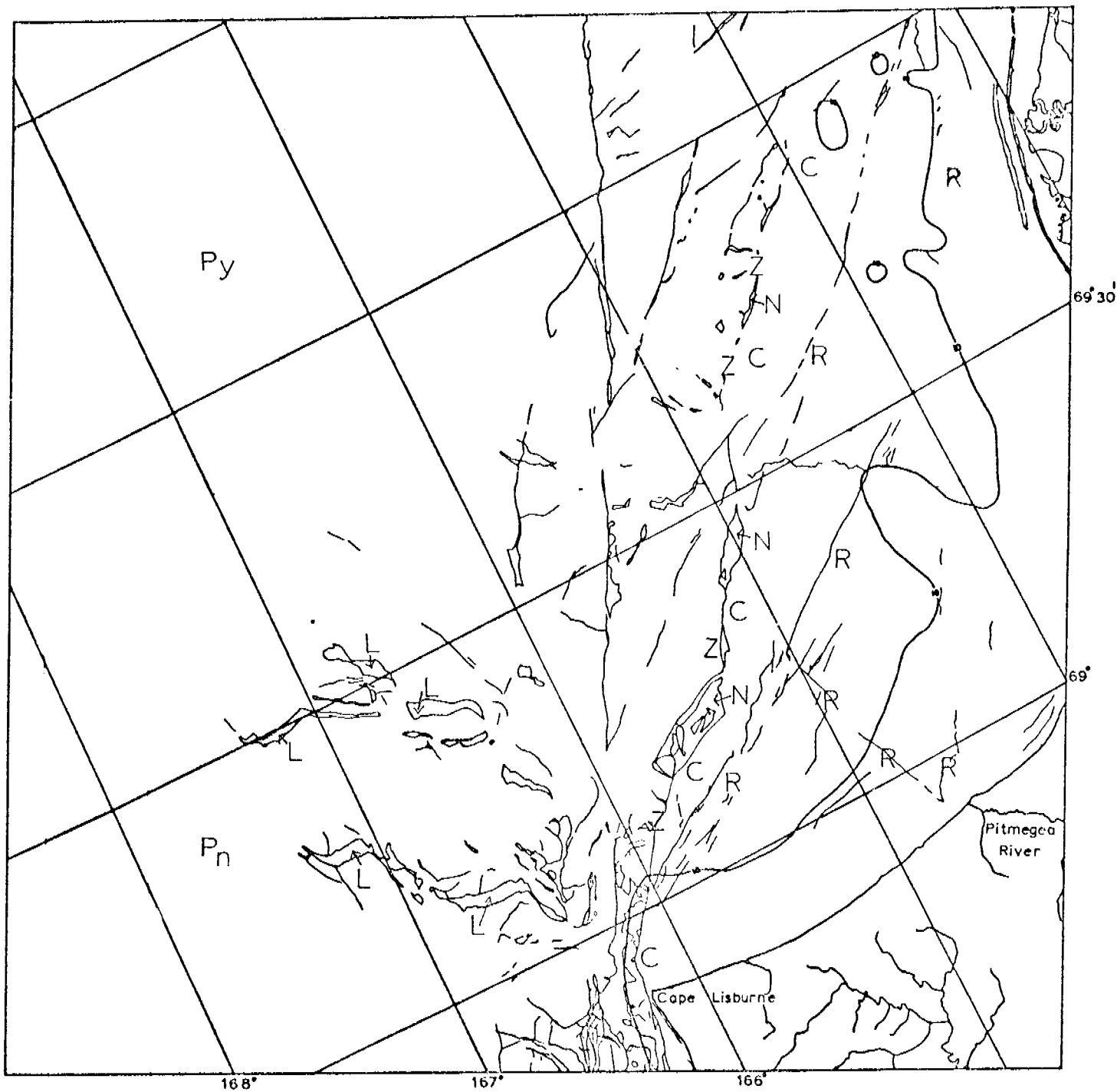
E-1587-22160-7
2 MARCH 1974

CHUKCHI SEA



E-1587-22162-7
2 MARCH 1974

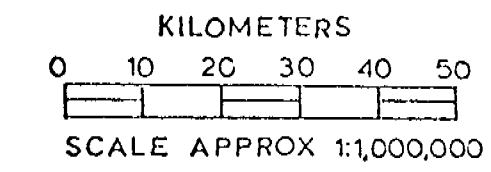
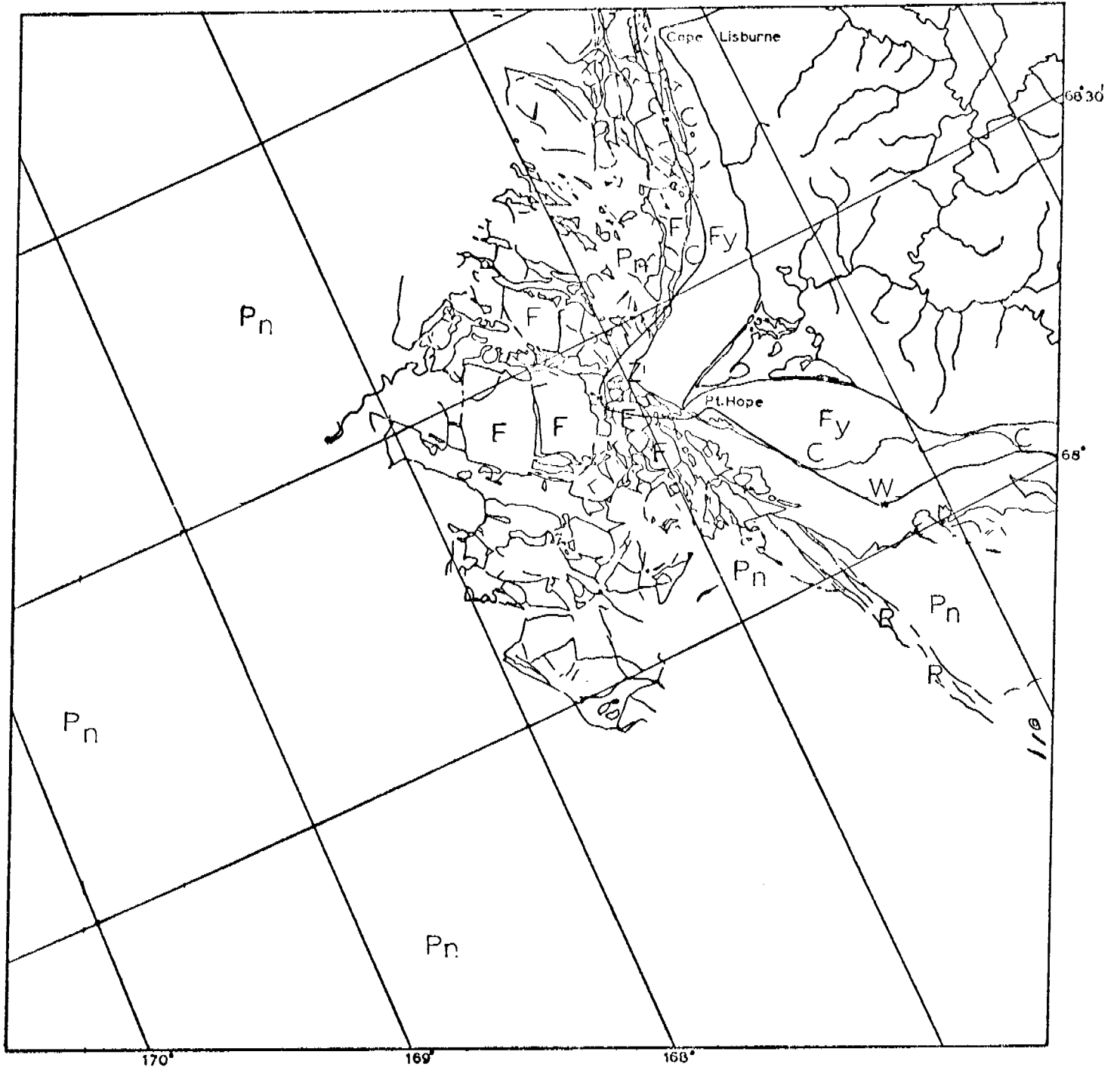
CHUKCHI SEA



KILOMETERS
 0 10 20 30 40 50
 SCALE APPROX 1:1,000,000

CHUKCHI SEA

E-1588-22214-7
 3 MARCH 1974



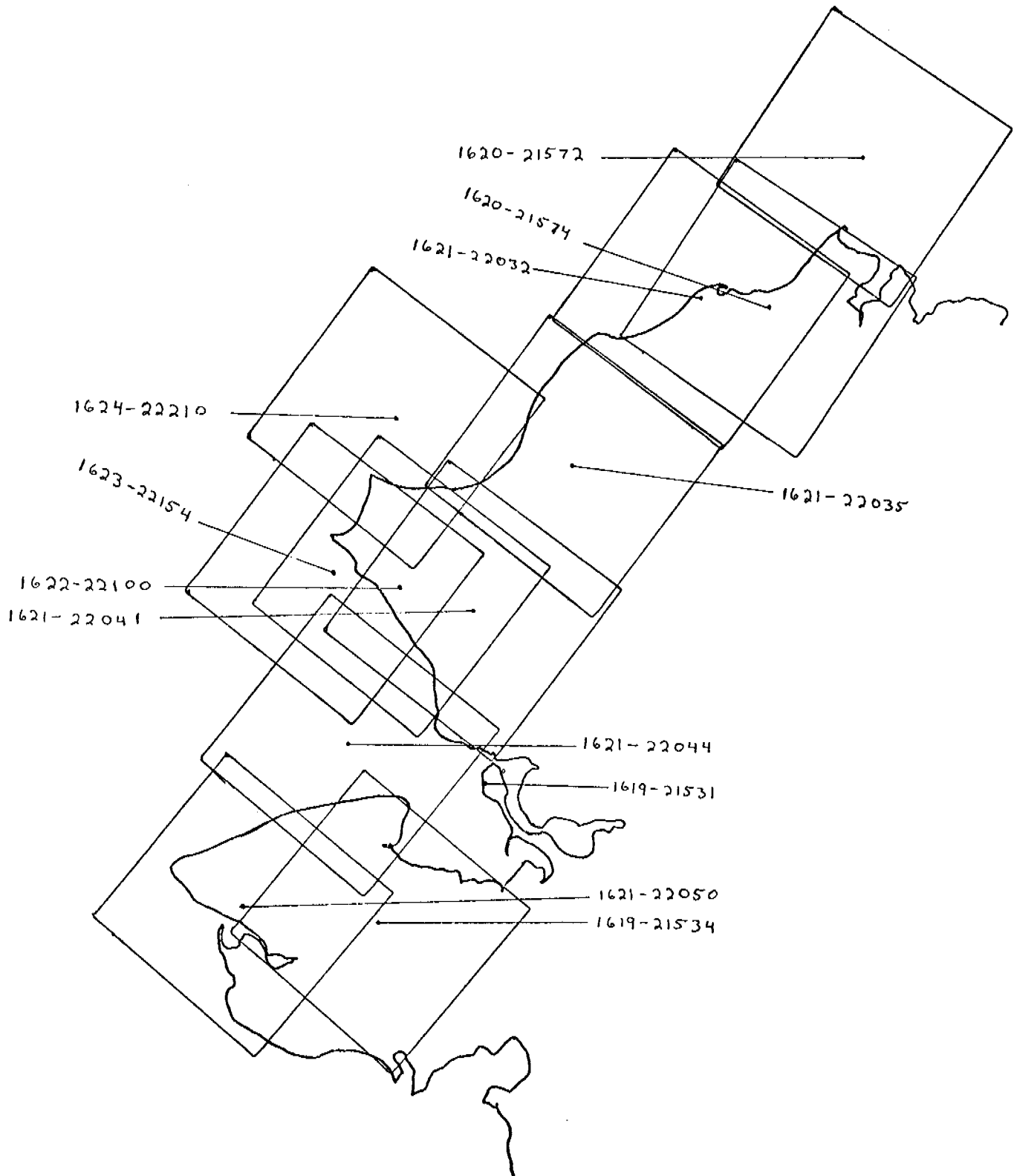
E-1588-22220-7
3 MARCH 1974

CHUKCHI SEA

CHUKCHI SEA

2-19 APRIL 1974

Cycle 1618-1635



Scenes 1619-21531
1619-21534
1620-21572
1620-21574
1621-22032
1621-22035
1621-22041
1621-22044
1621-22050

1622-22100
1623-22154
1624-22210

These scenes show the Chukchi coast between Barrow and Cape Rodney for April 3-8, 1974. It is apparent that considerable ice motion had been taking place recently but has ceased long enough for the formation of new ice. Very recently a new lead has opened up running down the coast at places somewhat off shore from the contiguous ice from Barrow to Cape Lisburne ending there in a system of polynyas. Starting from a polynya south of Point Hope a recently formed lead forms the edge of contiguous ice across the outer portion of Kotzebue Sound, and then after approaching the coast south of Cape Espenberg, strikes seaward meeting fractured ice and open water approximately 50 km north of Bering Strait.

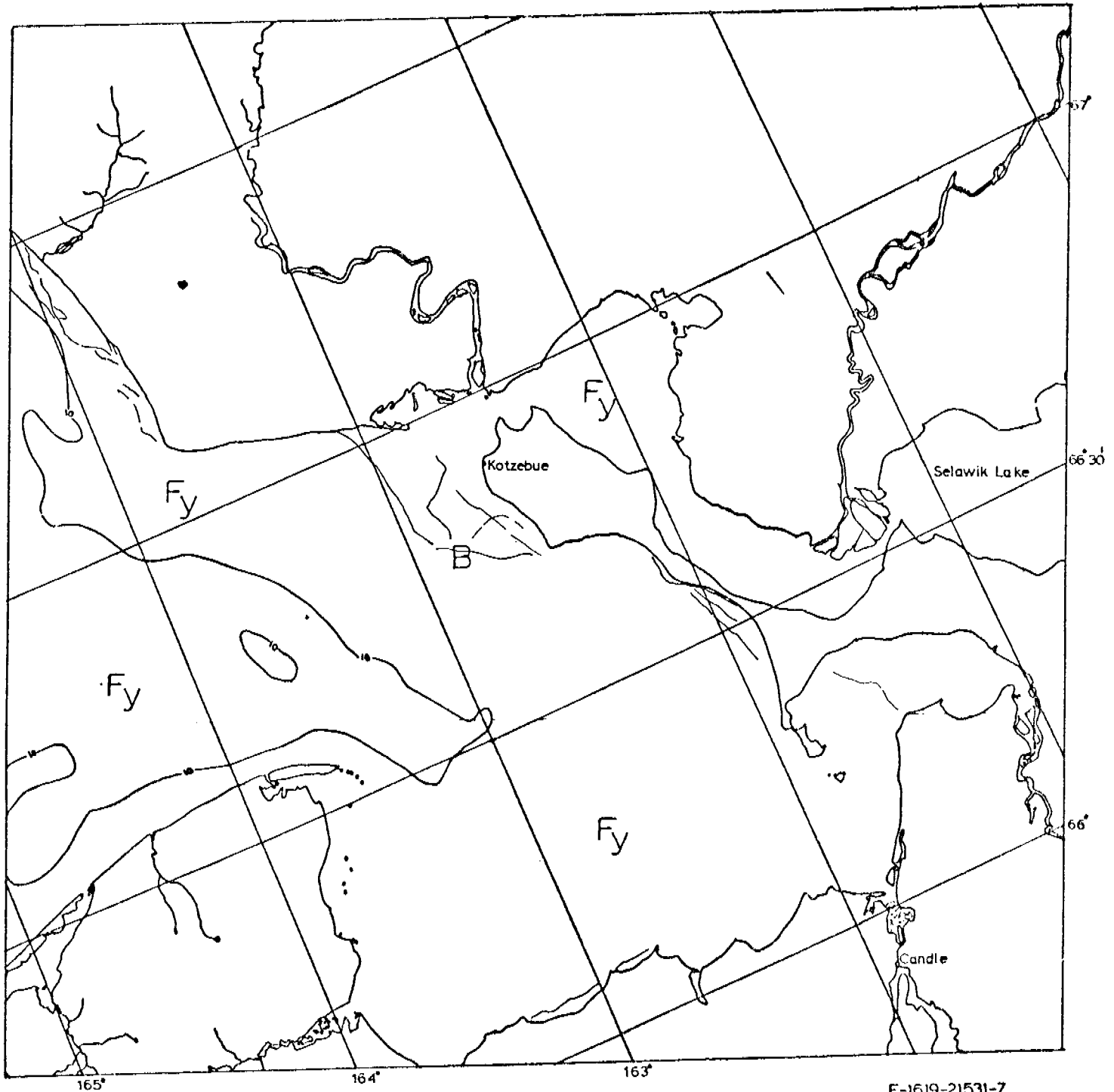
At Bering Strait the edge of contiguous ice strikes west of north from Cape Prince of Wales while the coast runs east of north. Hence a large triangularly shaped area of contiguous ice is formed with the closed lead striking seaward from the Espenberg Peninsula as the northern boundary. This piece of contiguous ice is situated over shoals and may be grounded. The entire Kotzebue Sound is contiguous ice at this time. Southeast of Point Hope a large polynya forms the seaward boundary of contiguous ice.

Northwest of Point Hope a large apron of contiguous ice can be found situated above shoals in the same location. This apron ends midway between Point Hope and Cape Lisburne where the edge of contiguous ice abruptly moves almost to the shore line---well inshore of the 10-fathom contour.

North of Cape Lisburne is another large apron of contiguous ice with many indications of current and past stress relief. Just as with the apron of contiguous ice north of Point Hope, the edge of contiguous ice then runs shoreward coming quite close to shore well within the 10-fathom contour.

The edge of contiguous ice then moves seaward passing Blossom Shoals well seaward of the 10-fathom contour (but perhaps controlled by shoals more seaward than the Blossom group) and then coastward to pass Point Franklin in close coincidence with the 10-fathom contour, and again passing Barrow close to the 10-fathom contour.

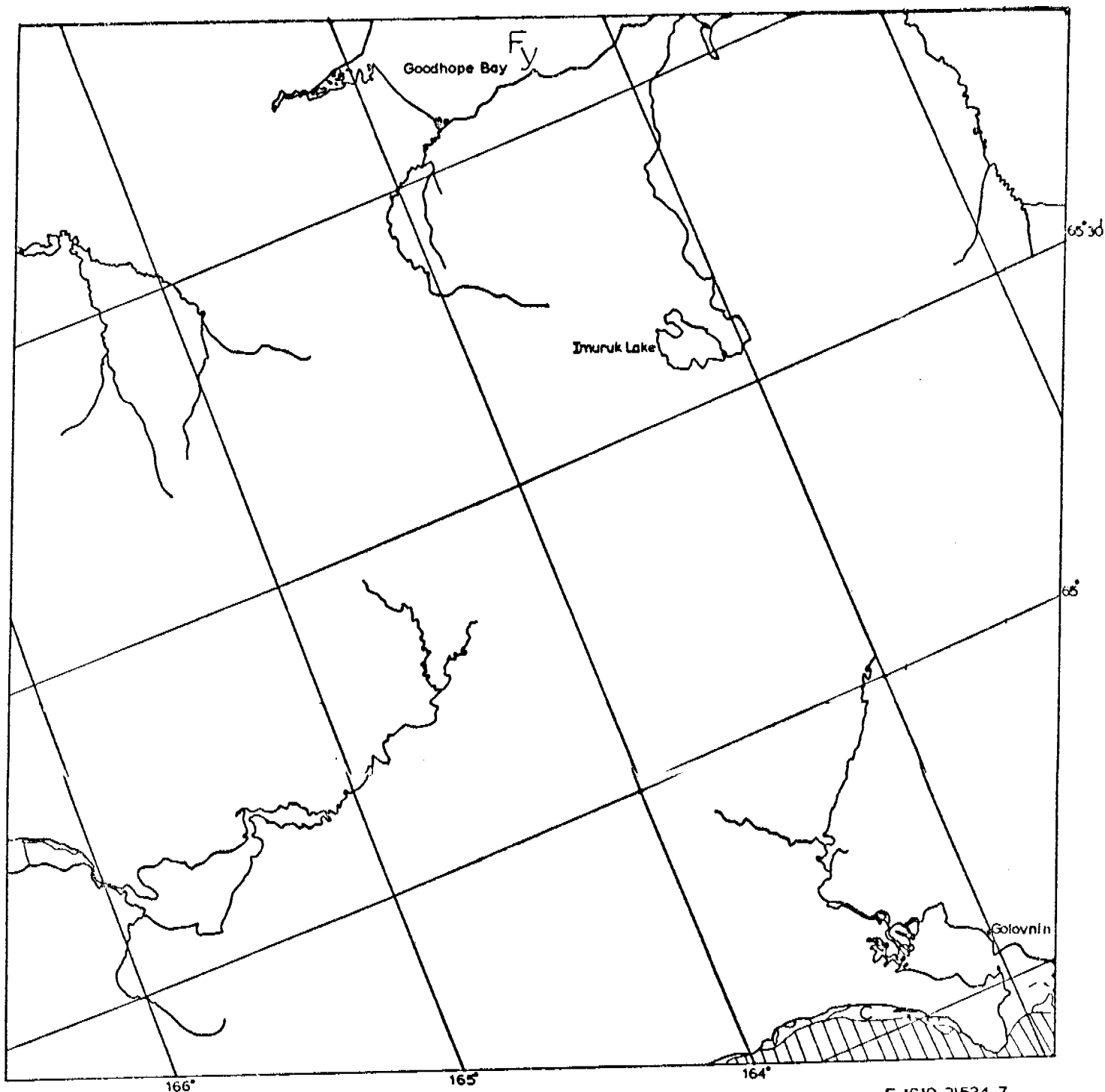
Evidence of ridging can be found in the contiguous ice off Barrow, parallel to the coast past Point Franklin, on Blossom Shoals and north of Cape Prince of Wales.



KILOMETERS
 0 10 20 30 40 50
 SCALE APPROX 1:1,000,000

CHUKCHI SEA

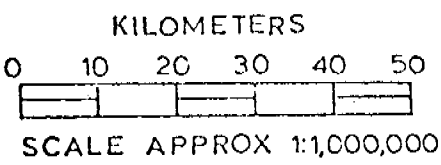
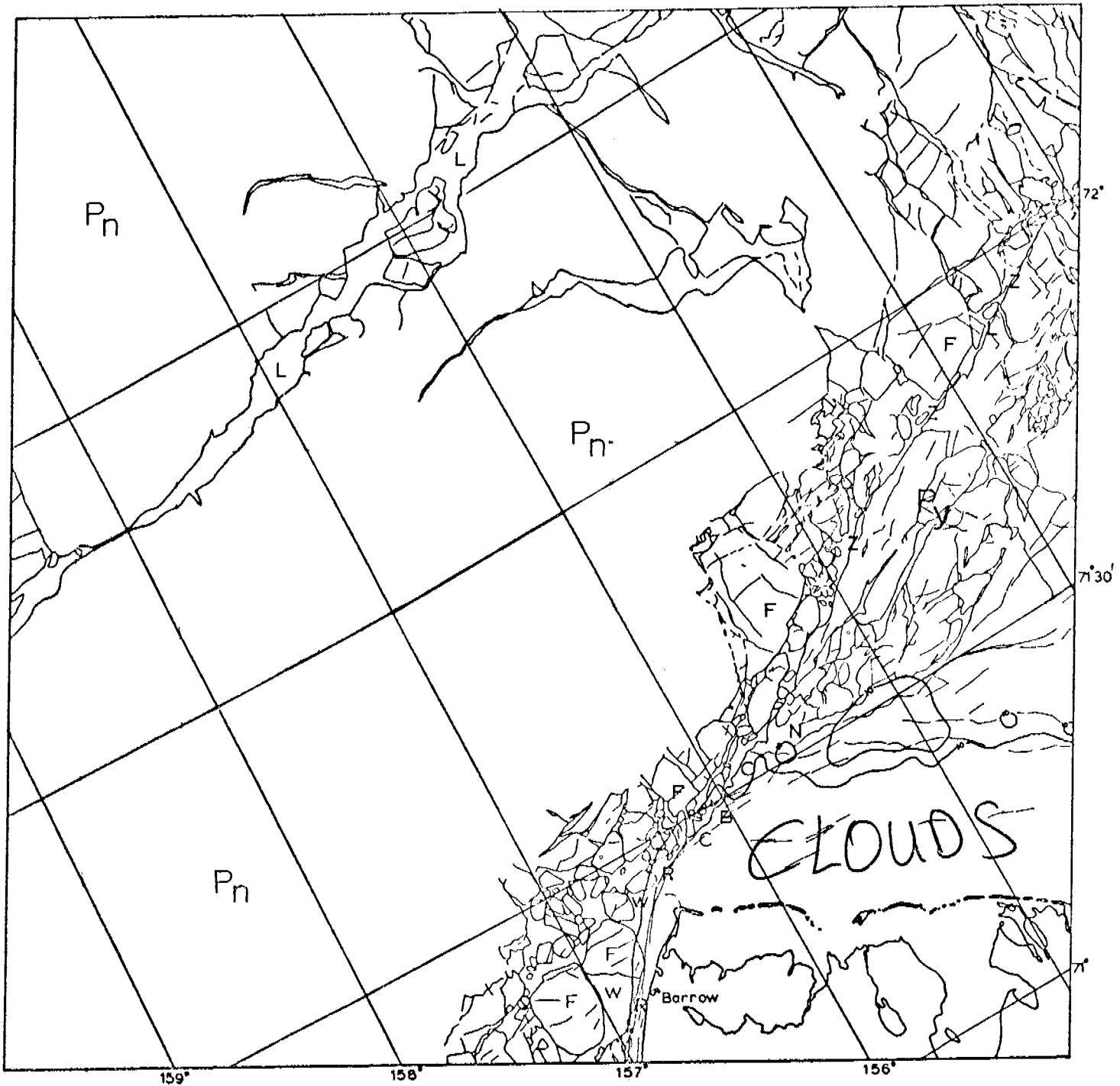
E-1619-21531-7
 3 APRIL 1974



KILOMETERS
0 10 20 30 40 50
SCALE APPROX 1:1,000,000

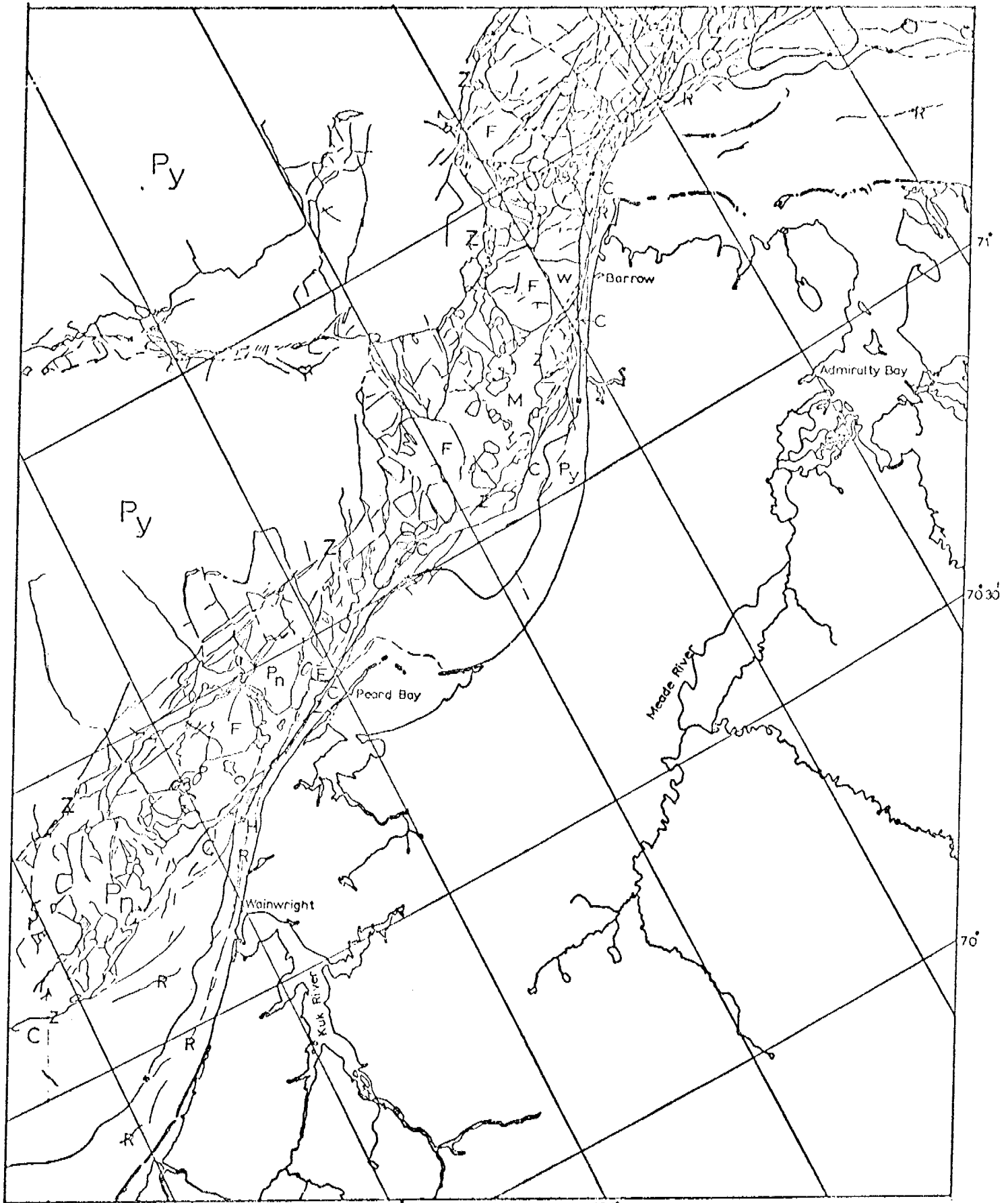
CHUKCHI SEA

E-1619-21534-7
3 APRIL 1974



CHUKCHI SEA

E-1620-21572-7
 4 APRIL 1974



KILOMETERS

0 10 20 30 40 50

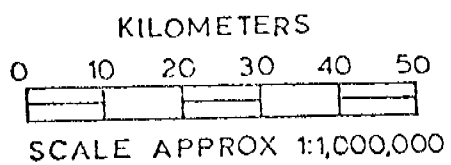
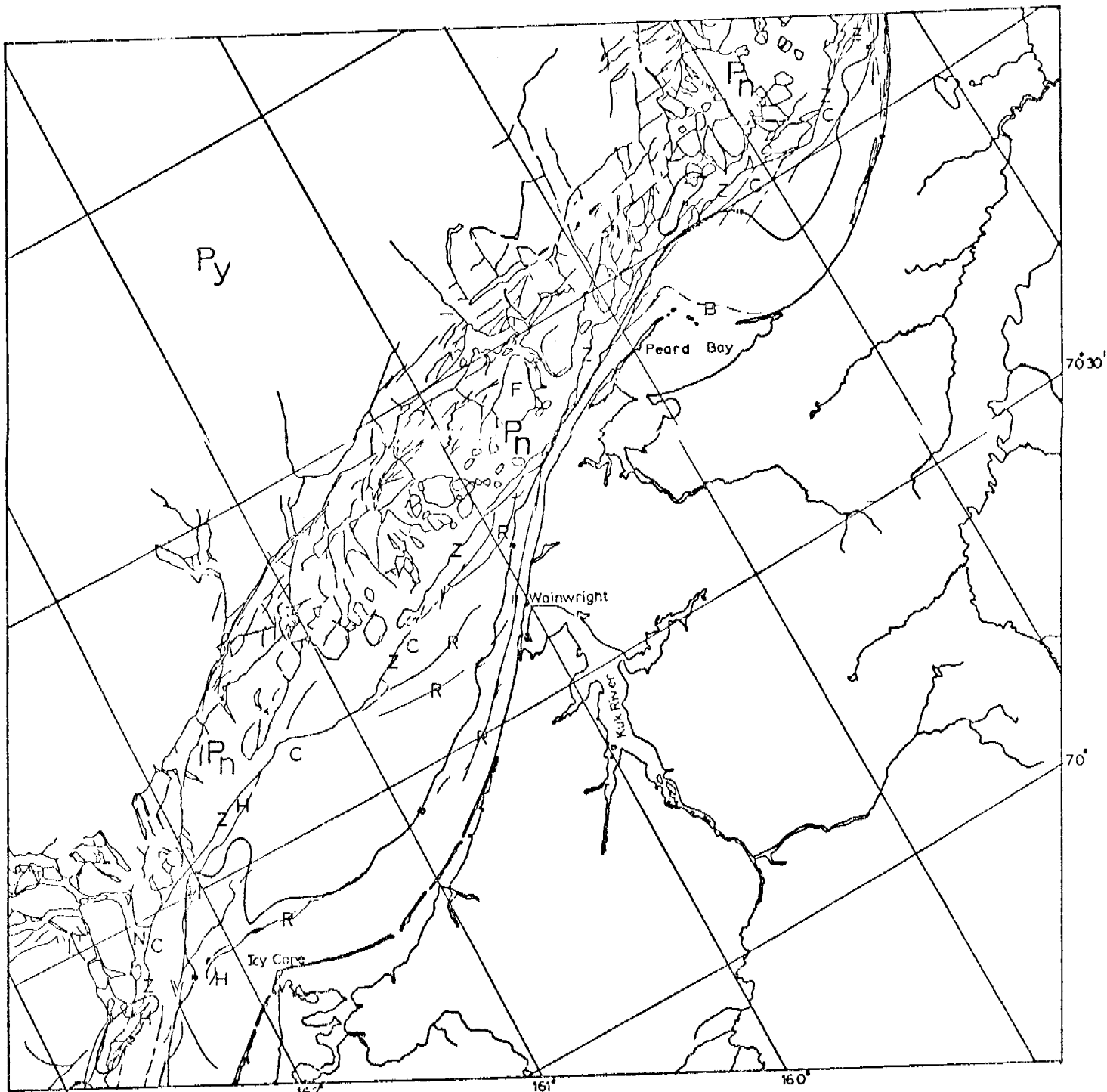


SCALE APPROX 1:1,000,000

CHUKCHI SEA

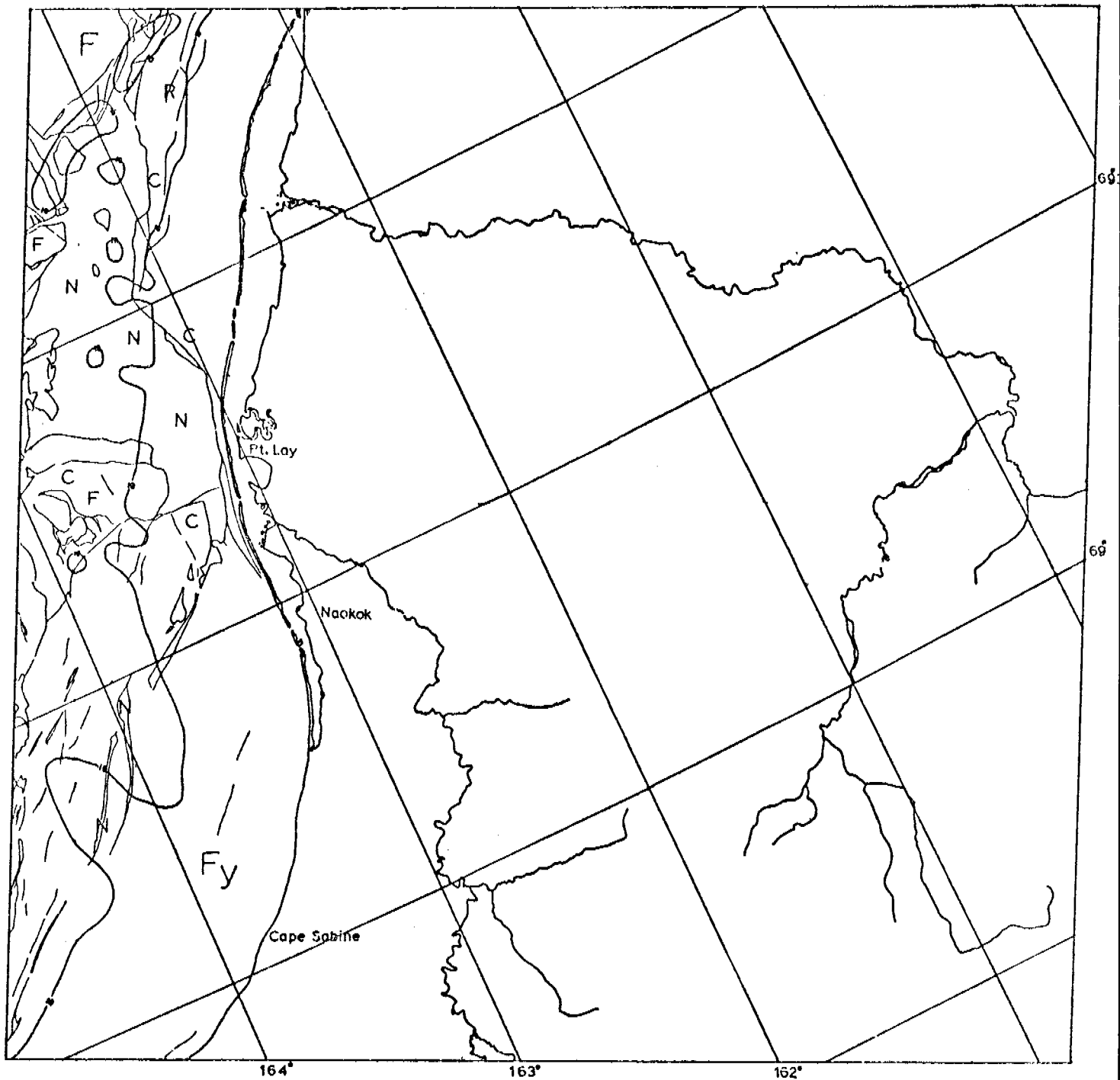
E-1620-21572-7
E-1620-21574-7

4 APRIL 1974

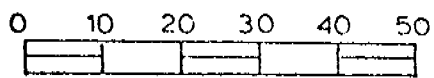


CHUKCHI SEA

E-1621-22032-7
5 APRIL 1974



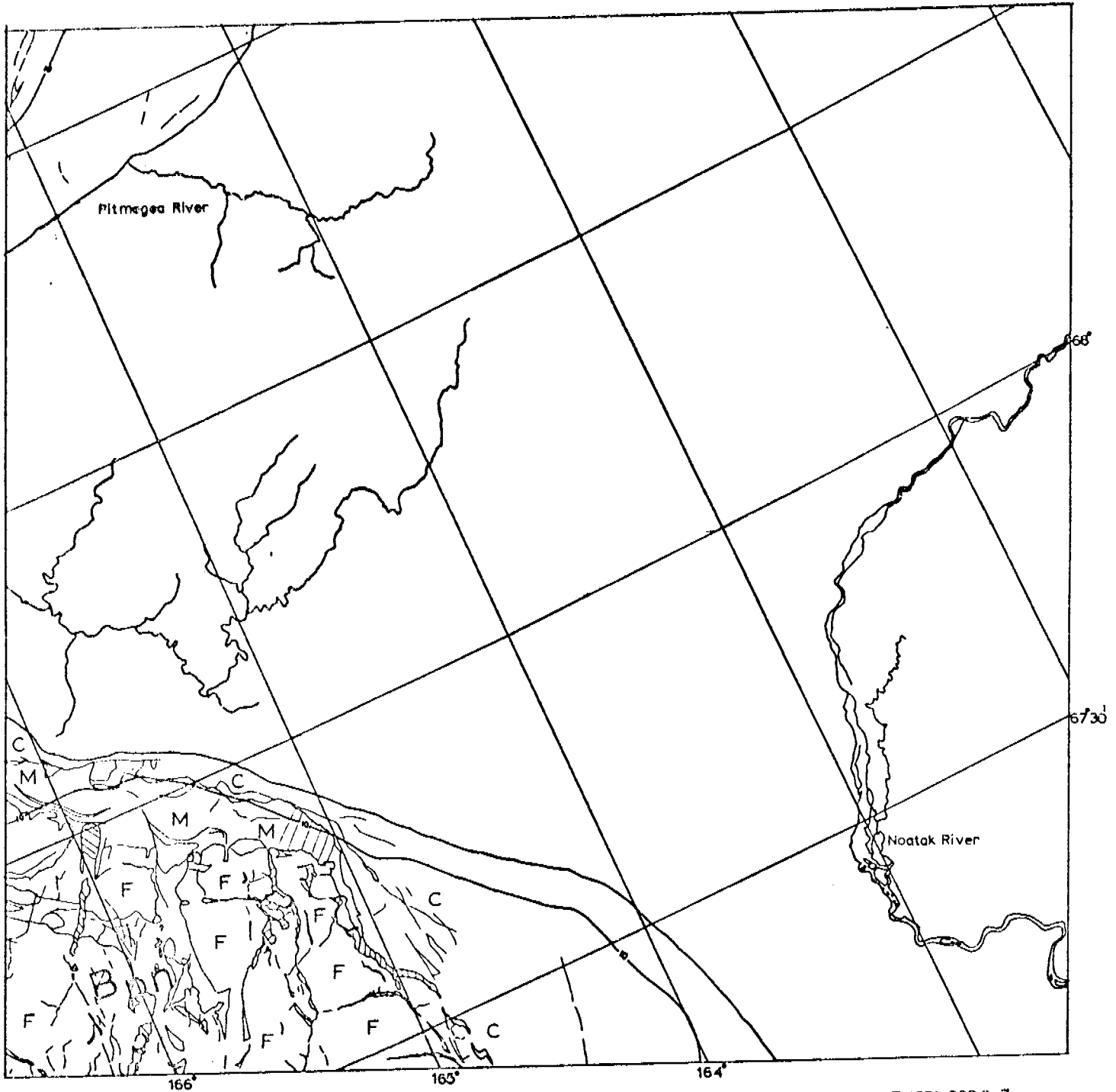
KILOMETERS



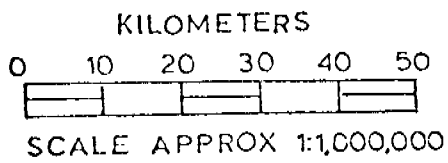
SCALE APPROX 1:1,000,000

E-1621-22035-7
5 APRIL 1974

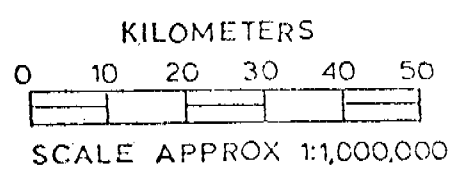
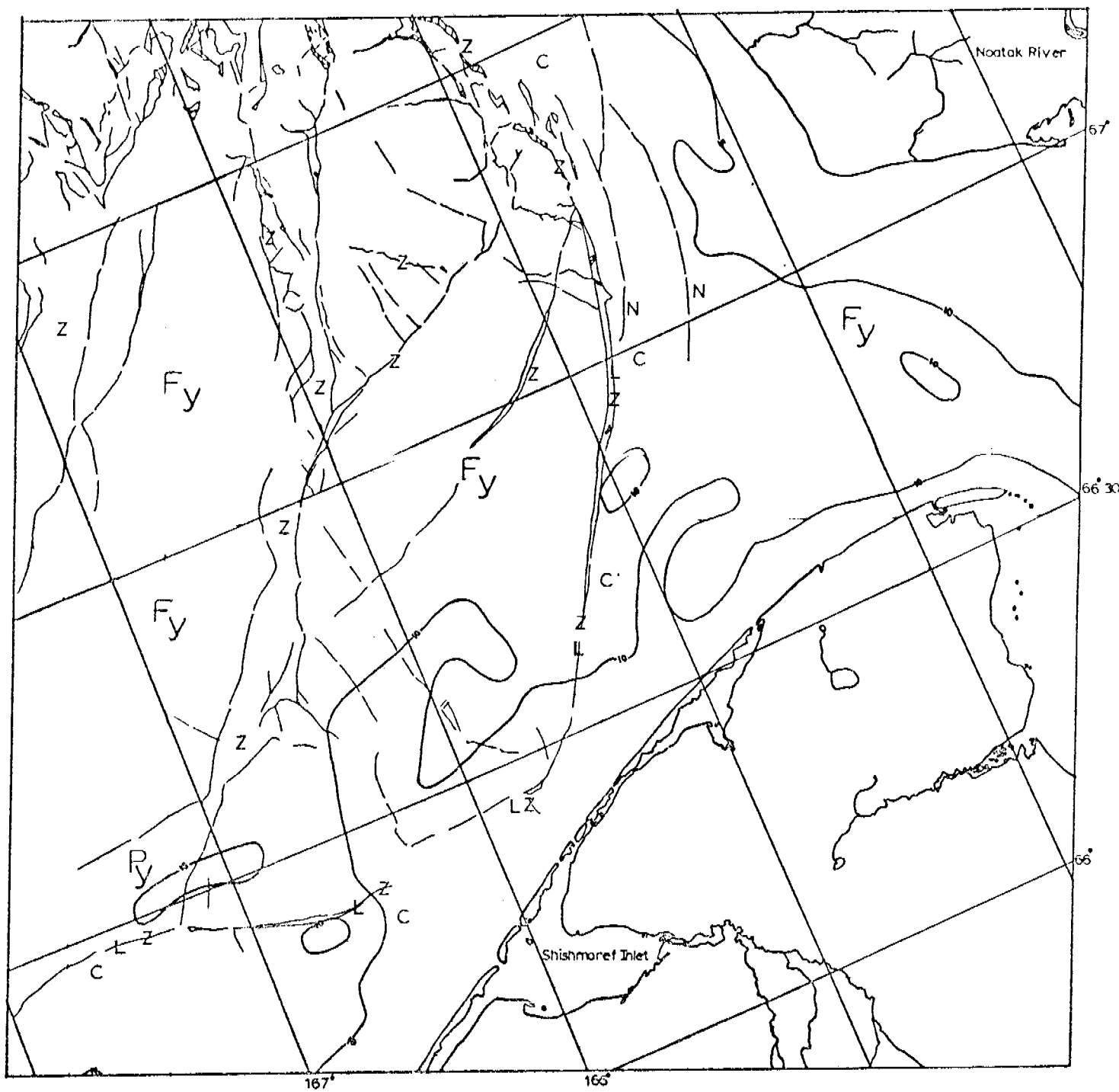
CHUKCHI SEA



E-1621-22041-7
5 APRIL 1974

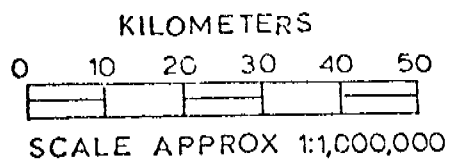
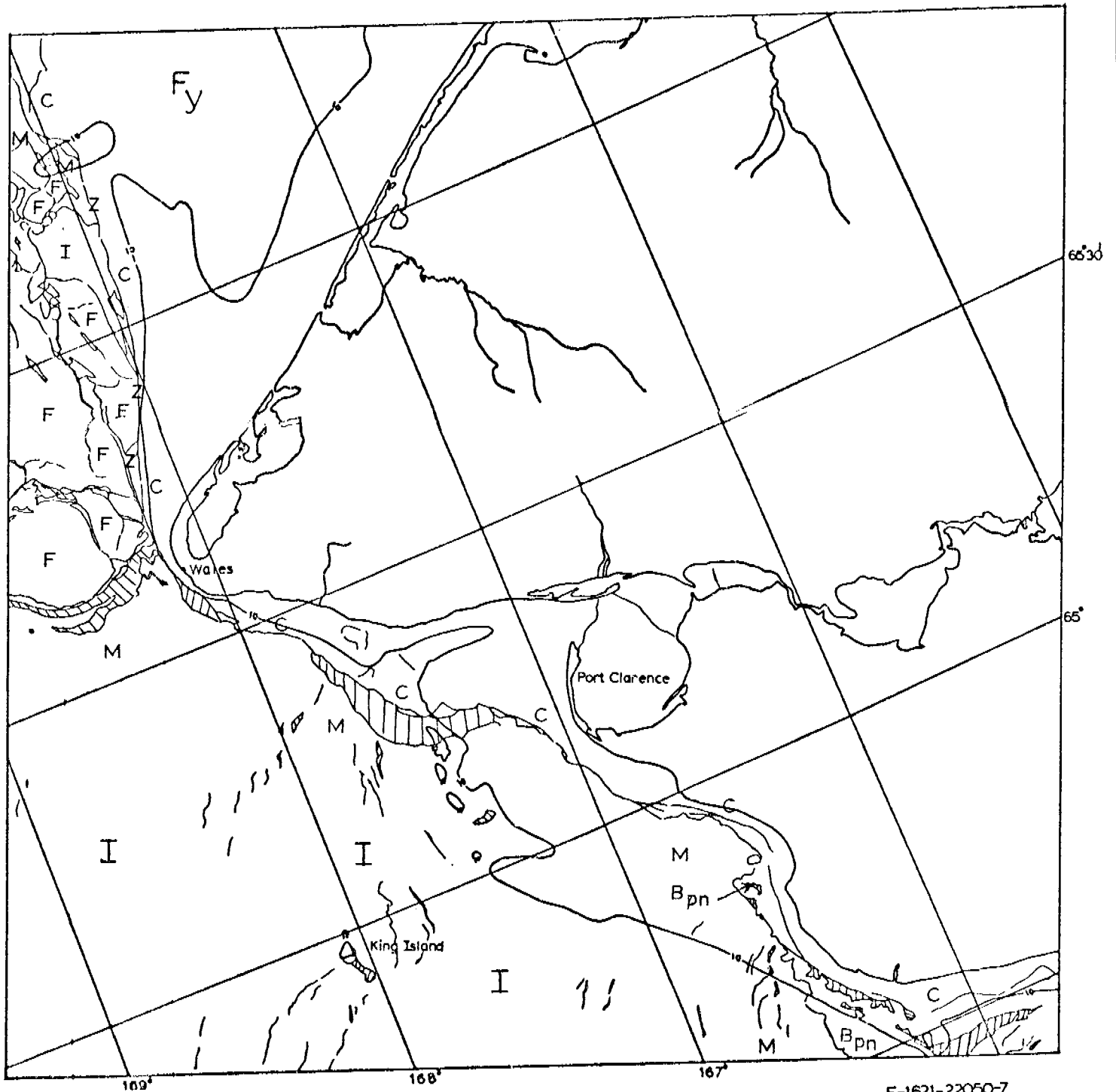


CHUKCHI SEA



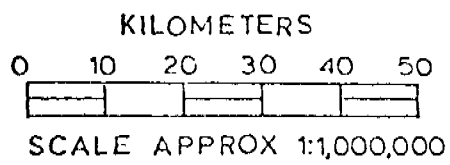
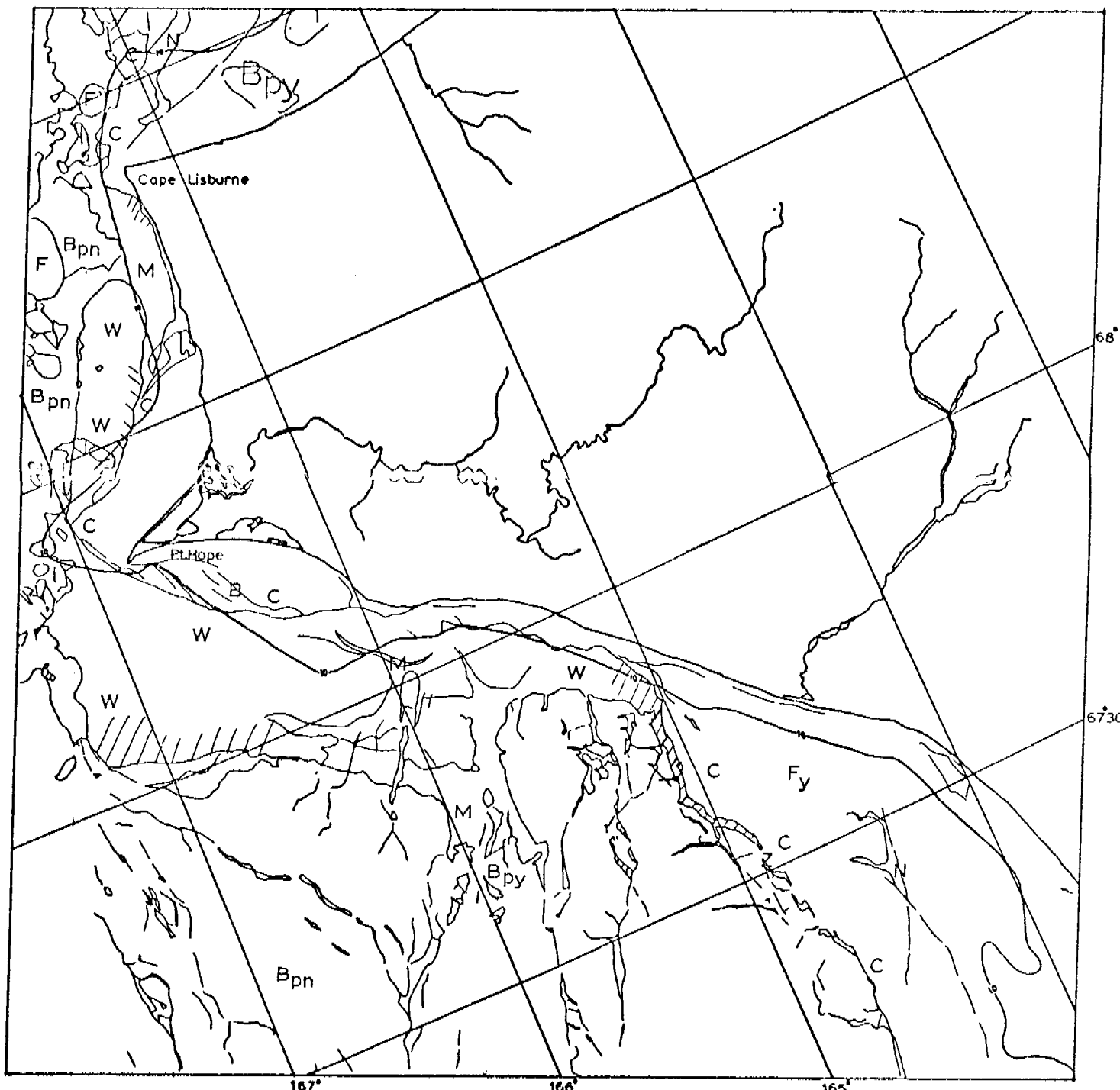
E-1621-22044-7
5 APRIL 1974

CHUKCHI SEA



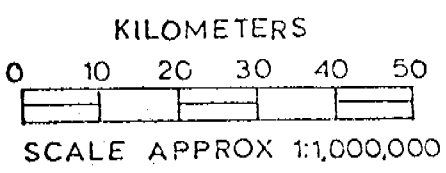
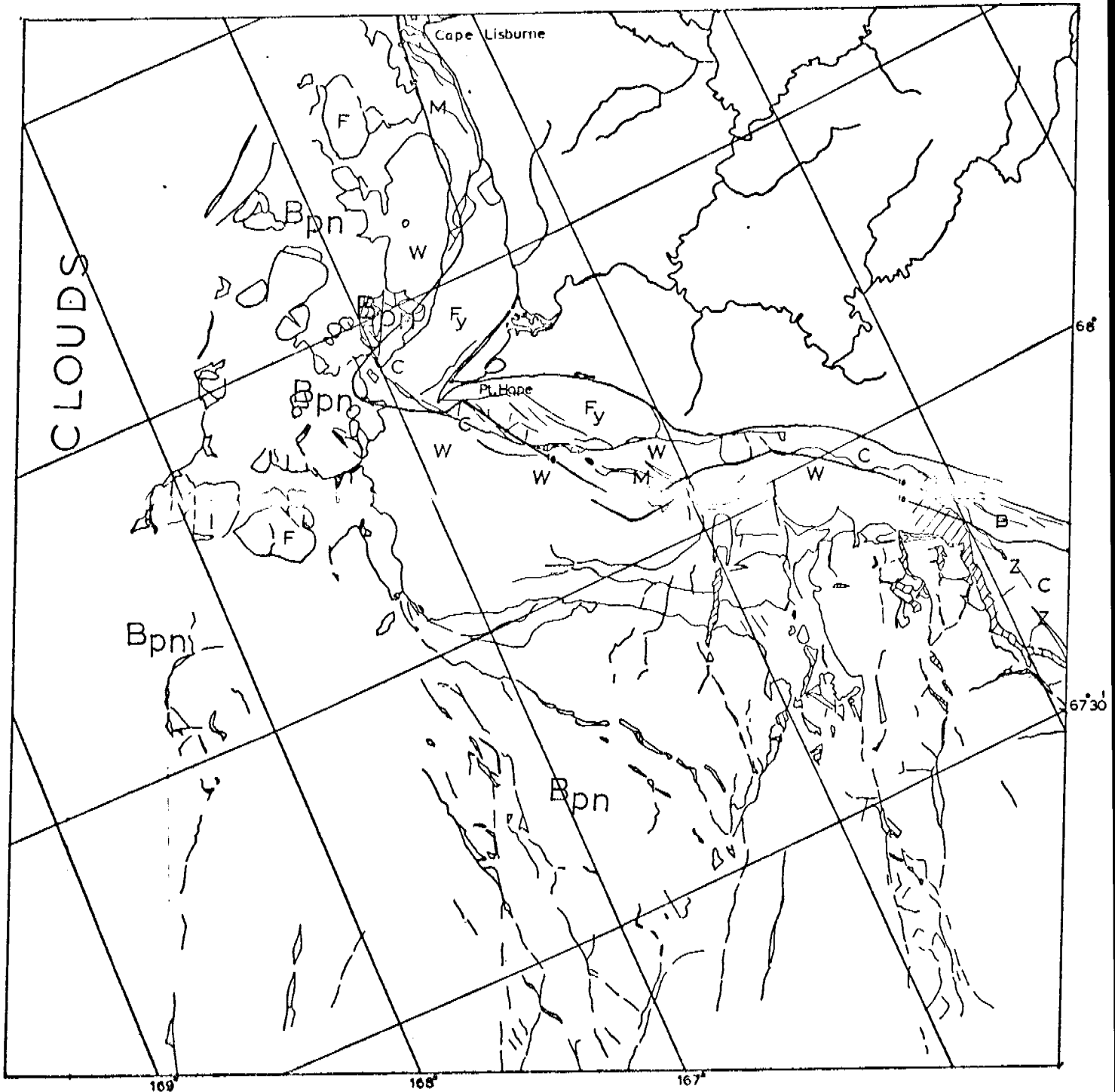
E-1621-22050-7
5 APRIL 1974

CHUKCHI SEA



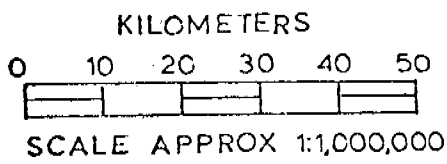
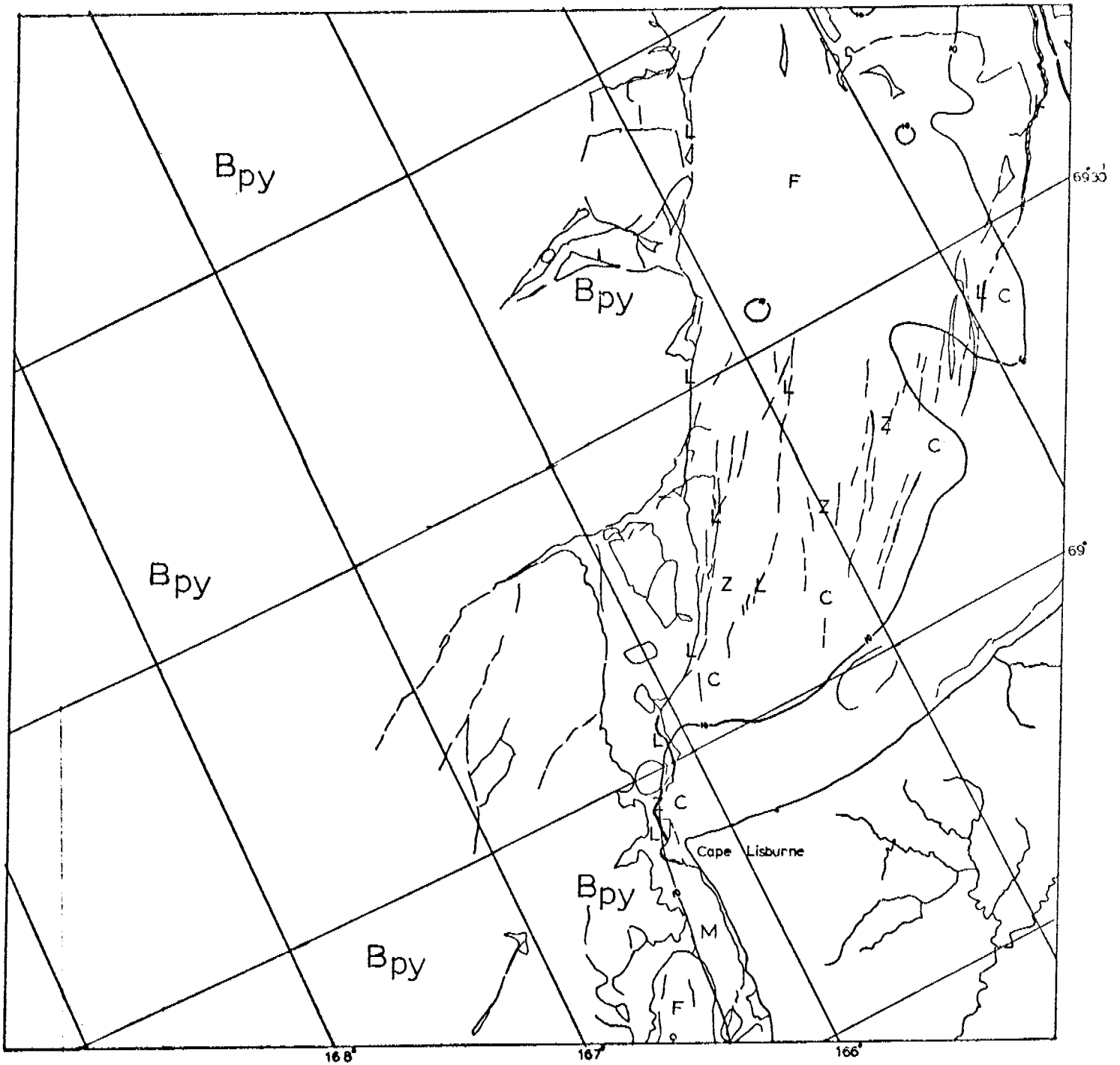
E-1622-22100-7
6 APRIL 1974

CHUKCHI SEA



E-1623-22154-7
7 APRIL 1974

CHUKCHI SEA



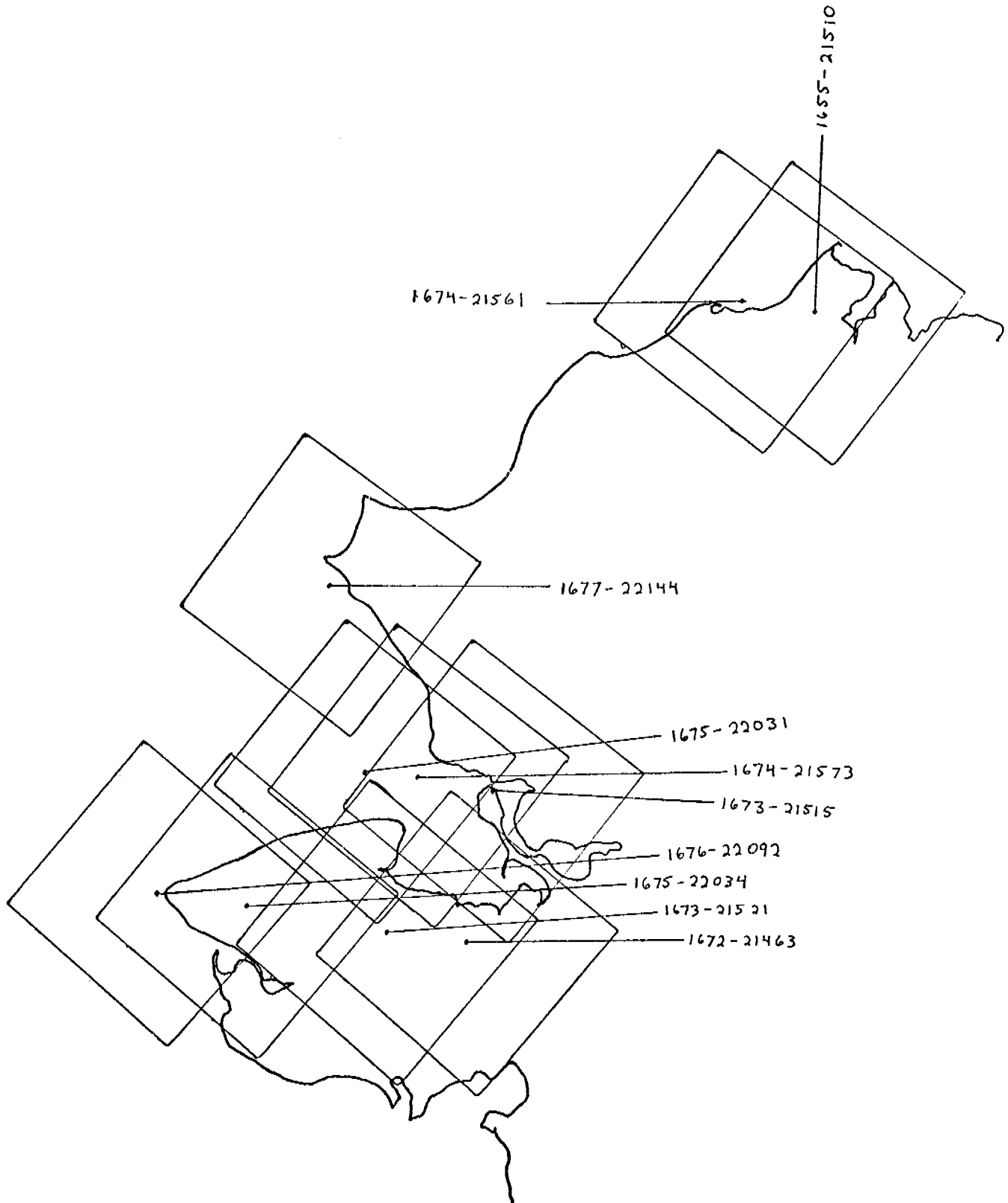
CHUKCHI SEA

E-1624-22210-7
8 APRIL 1974

CHUKCHI SEA

26 MAY - 12 JUNE 1974

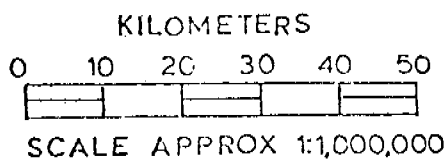
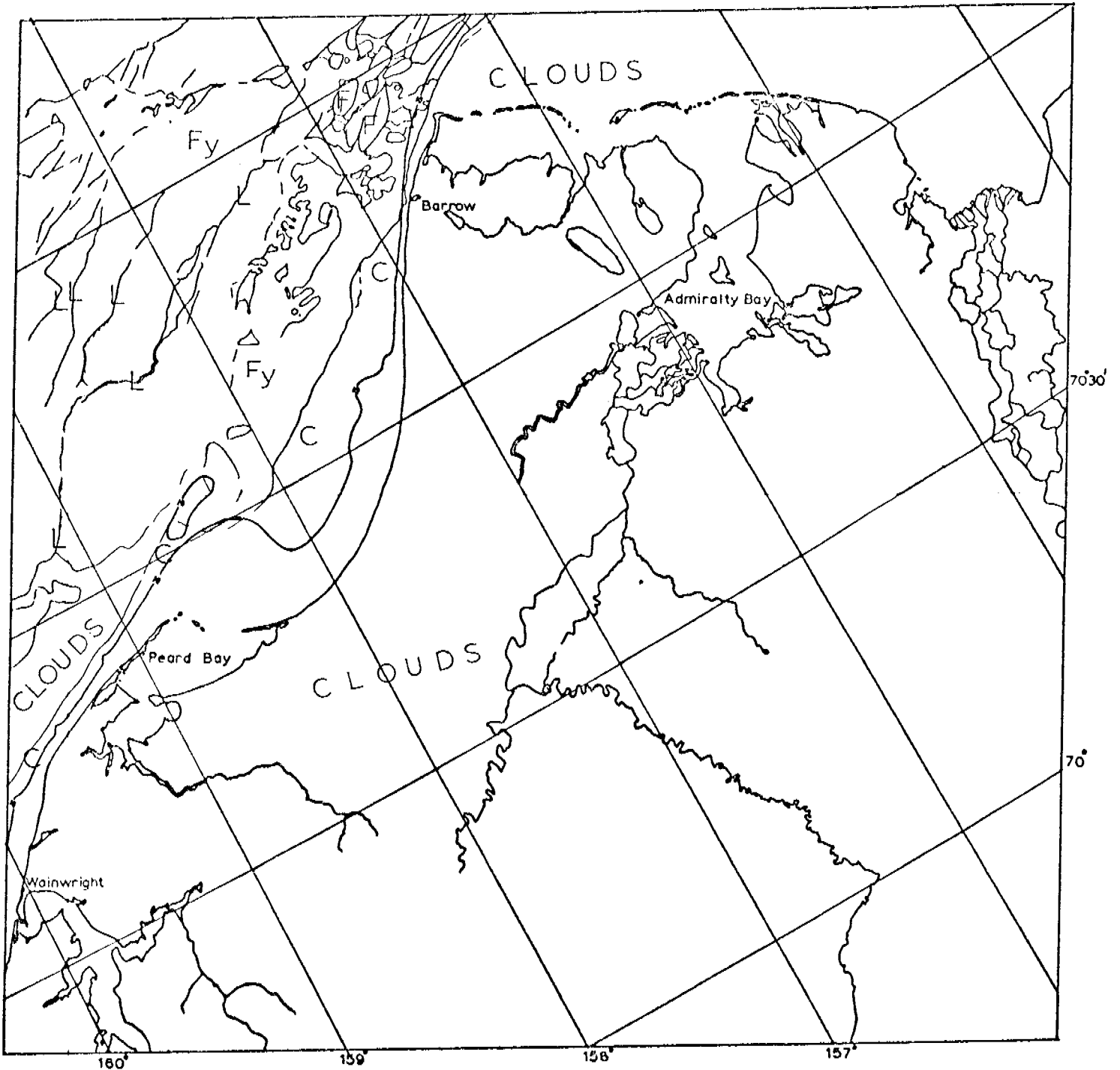
Cycle 1672 - 1689



Scenes 1672-21463
1673-21515
1673-21521
1674-21561
1674-21573
1675-22031
1675-22034
1676-22092
1676-22141

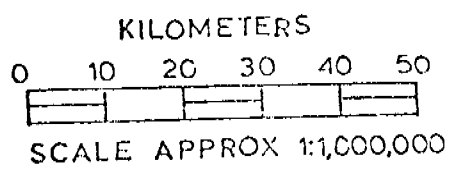
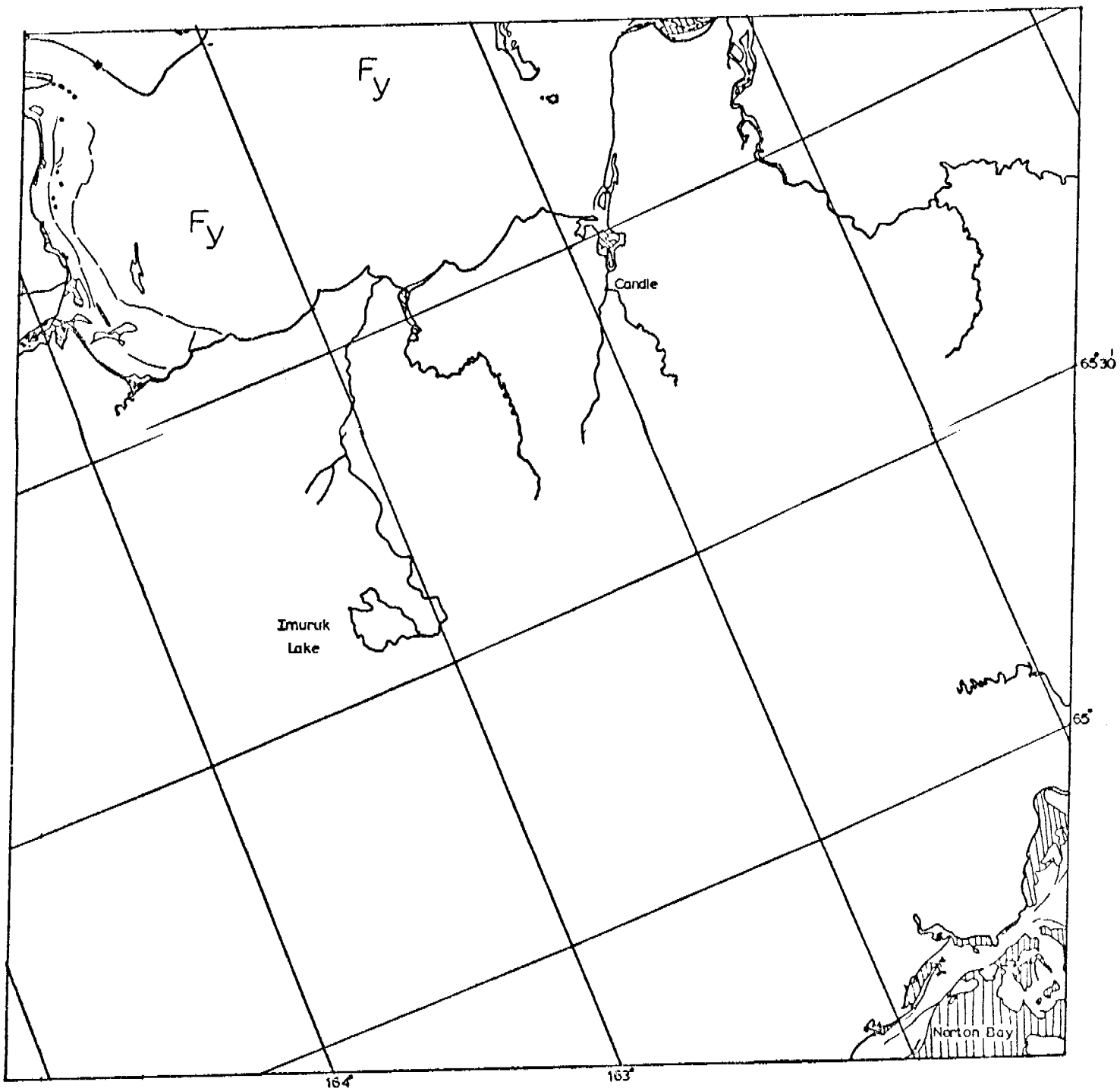
These scenes show the Chukchi coast for the period May 26-31, 1975 between Bering Strait and Barrow with the exception of a few areas in between. At this time the oceanic ice has been broken into pans and no freezing is taking place. The chief value of this imagery is the identification of ice remaining contiguous with shore and hence the ice which has been protected by grounded ice features.

Starting northward from Cape Prince of Wales we note a large expanse of ice remaining over the shoals just to the north. There is evidence of ridges on the seaward boundary of this ice. The ice within Kotzebue sound remains in place and unbroken. It does not appear to be bounded by grounded ice. To the north, a small apron of ice remains next to the shore to Point Hope where again a large area of ice remains coinciding with shoals. This situation repeats at Cape Lisburne. Far to the north, an apron of ice remains off Wainwright and Point Franklin apparently held in place by grounded ridges.



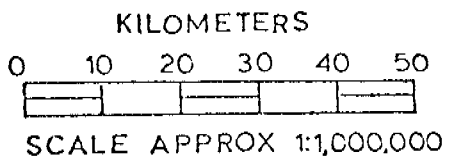
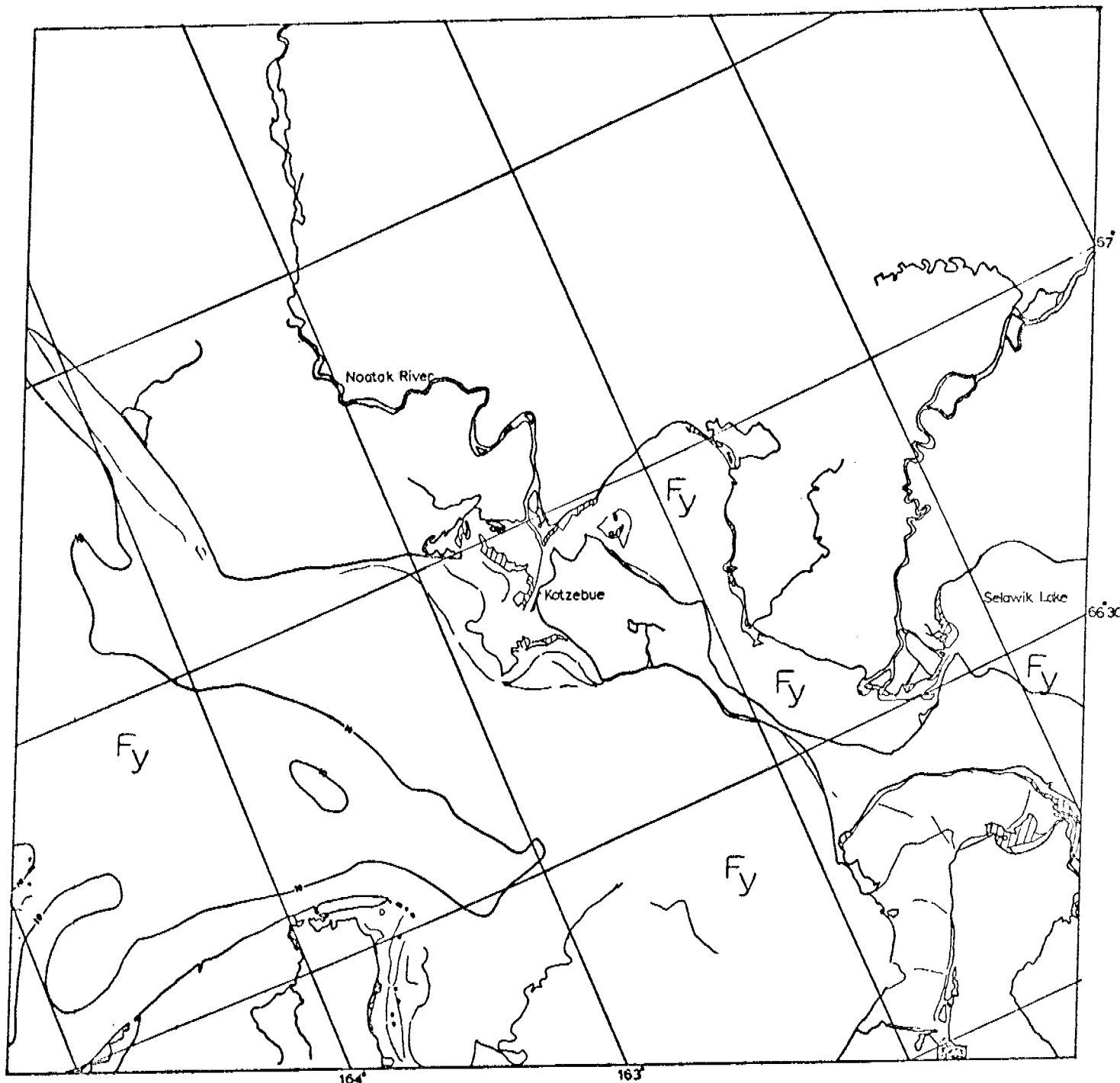
E-1655-21510-7
9 MAY 1974

CHUKCHI SEA



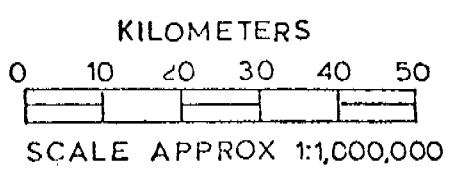
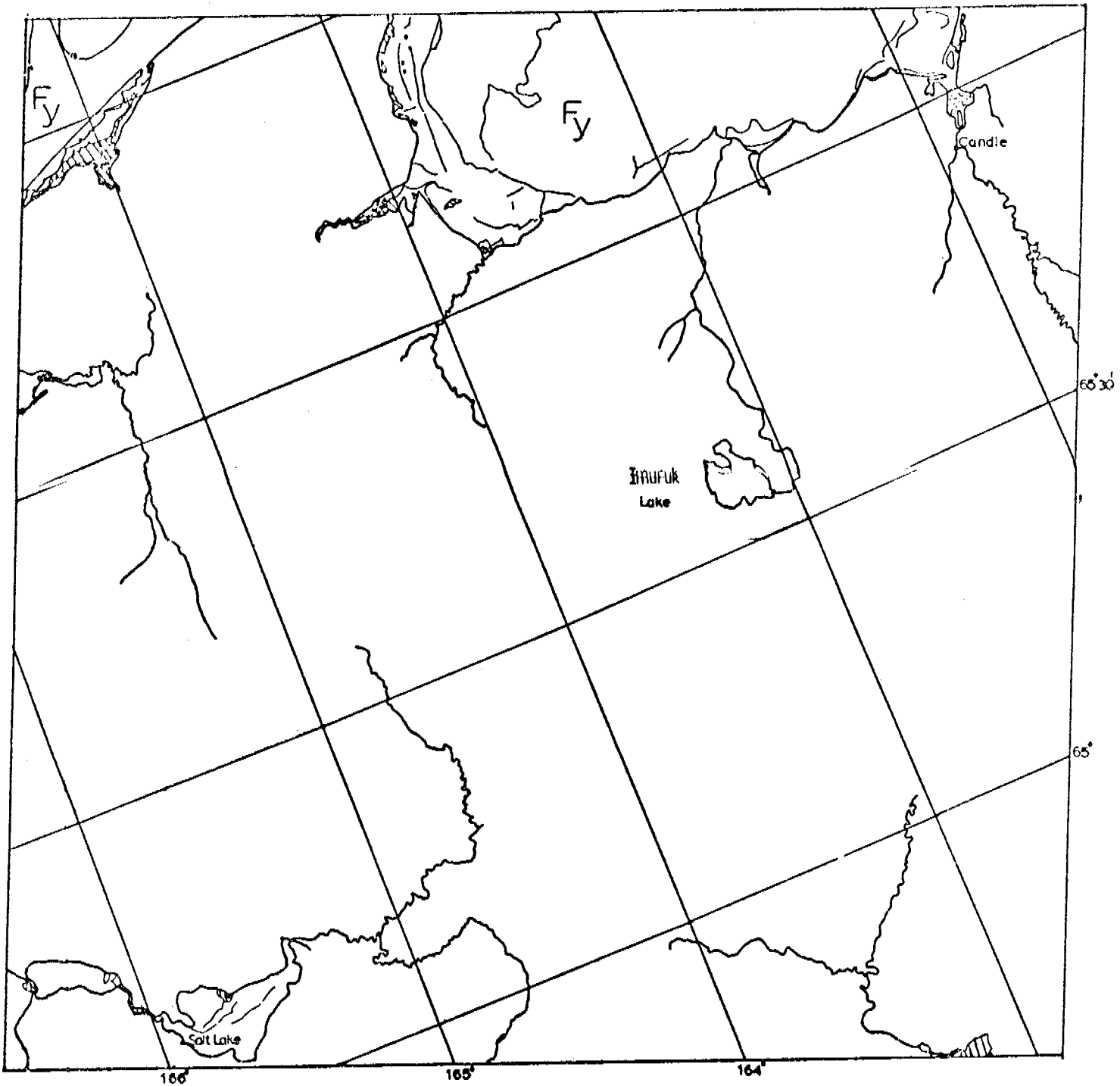
CHUKCHI SEA

E-1672 21463-7
26 MAY 1974



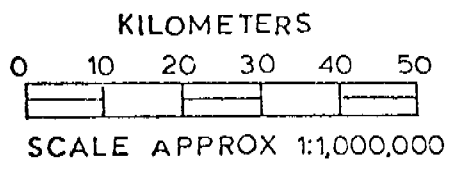
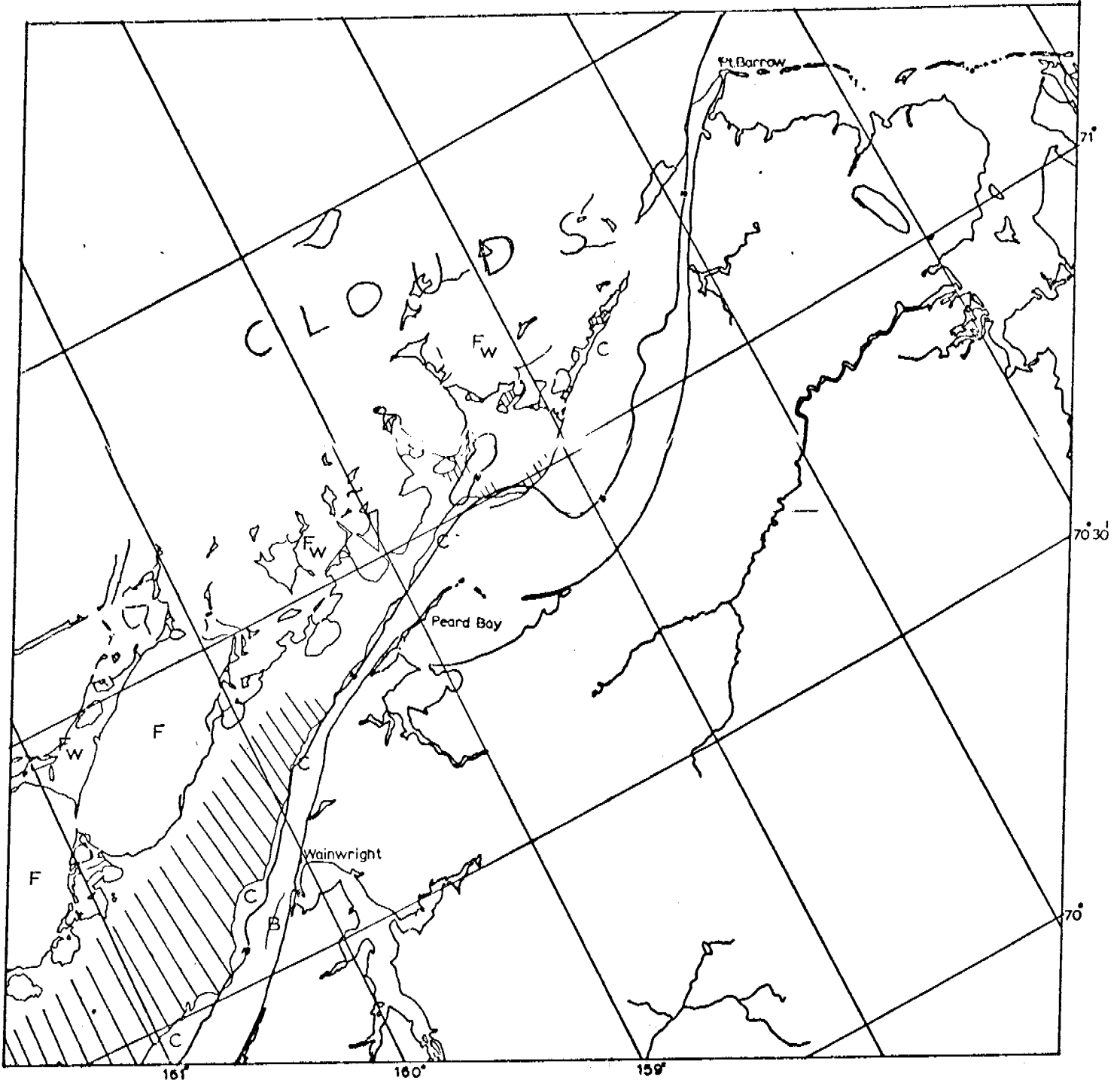
CHUKCHI SEA

E-1673-21515-7
27 MAY 1974



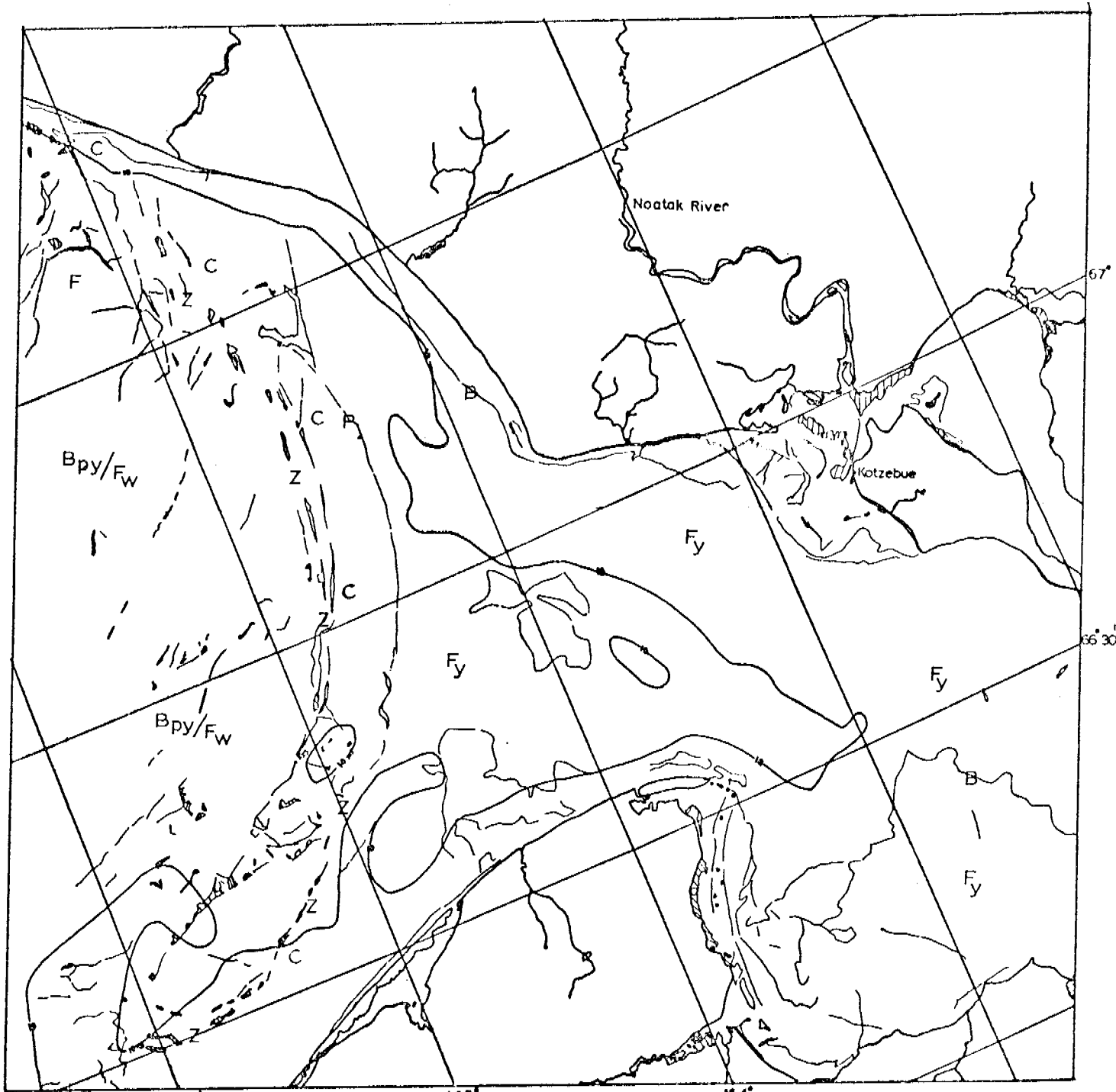
E-1673-21521-7
27 MAY 1974

CHUKCHI SEA



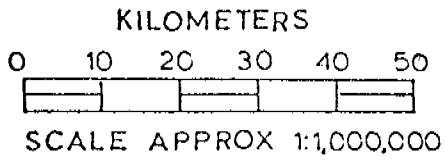
E-1674-21561-7
28 MAY 1974

CHUKCHI SEA

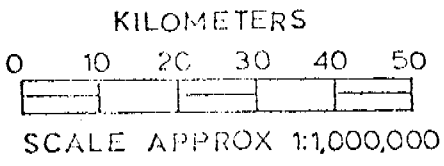
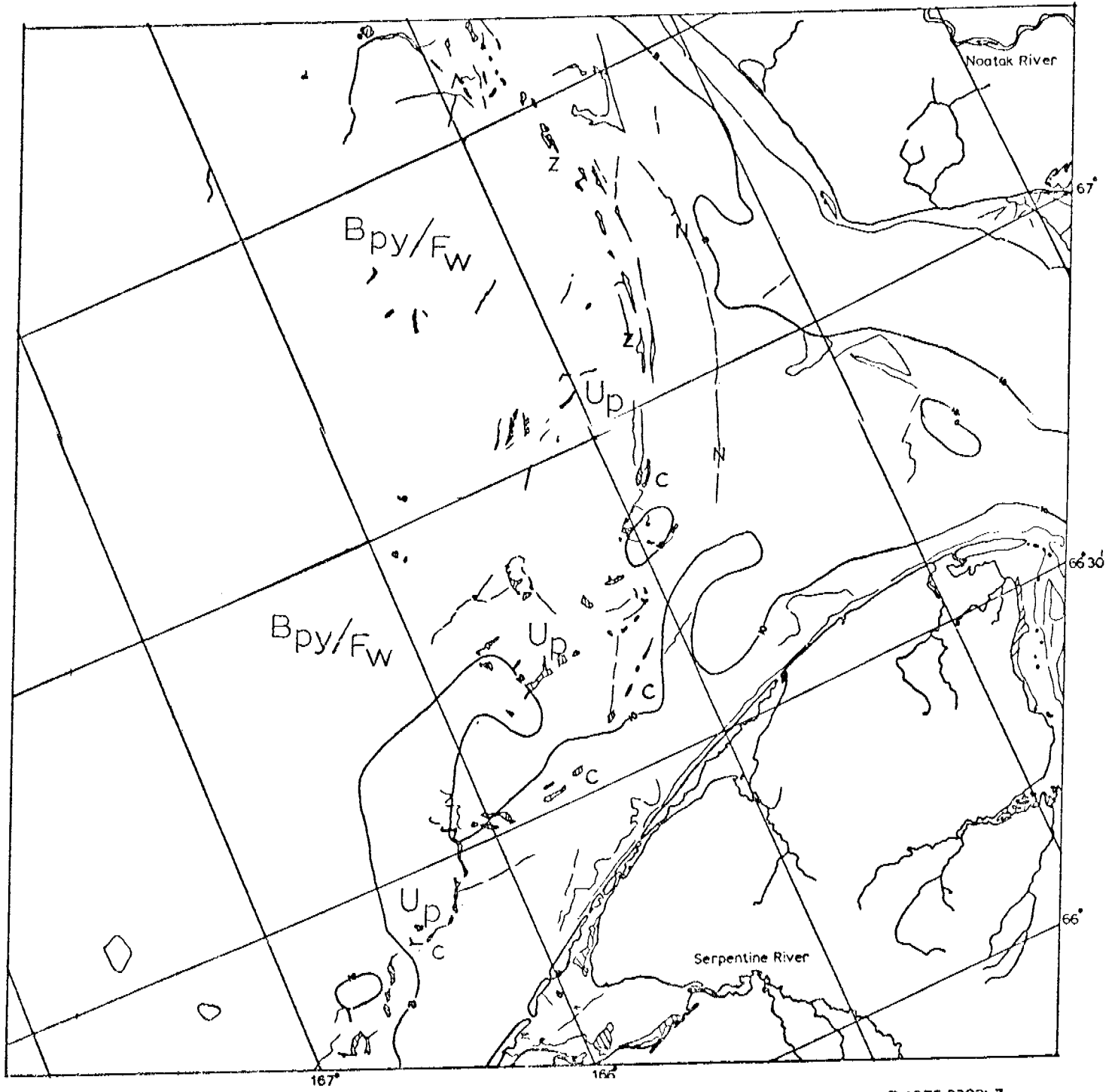


E-1674-21573-7

28 MAY 1974

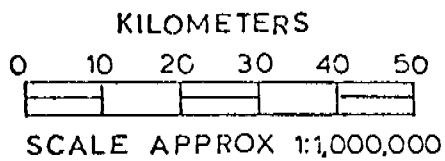
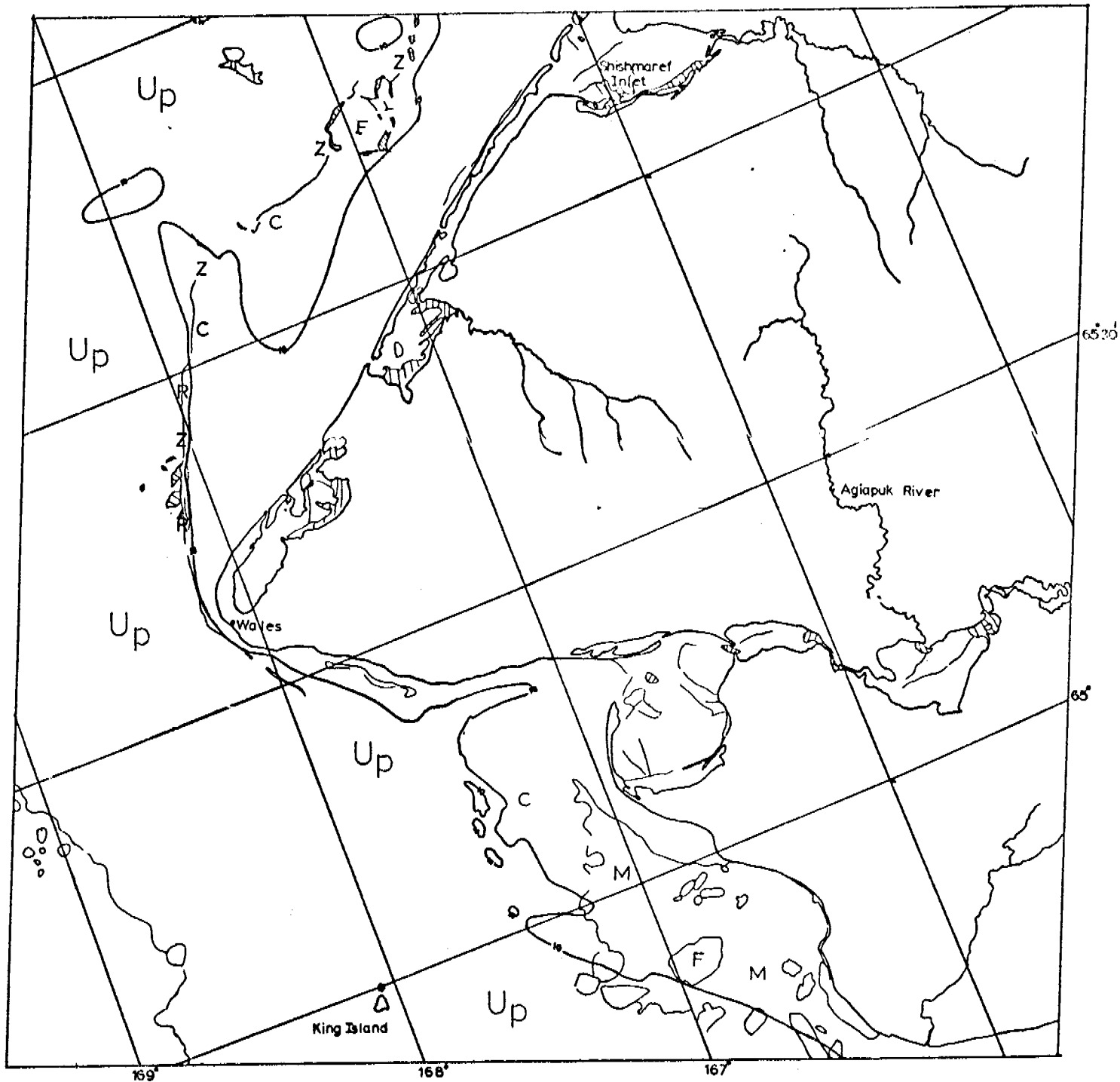


CHUKCHI SEA



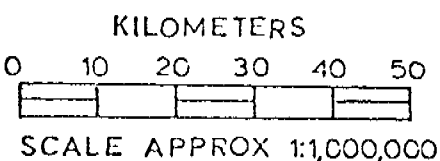
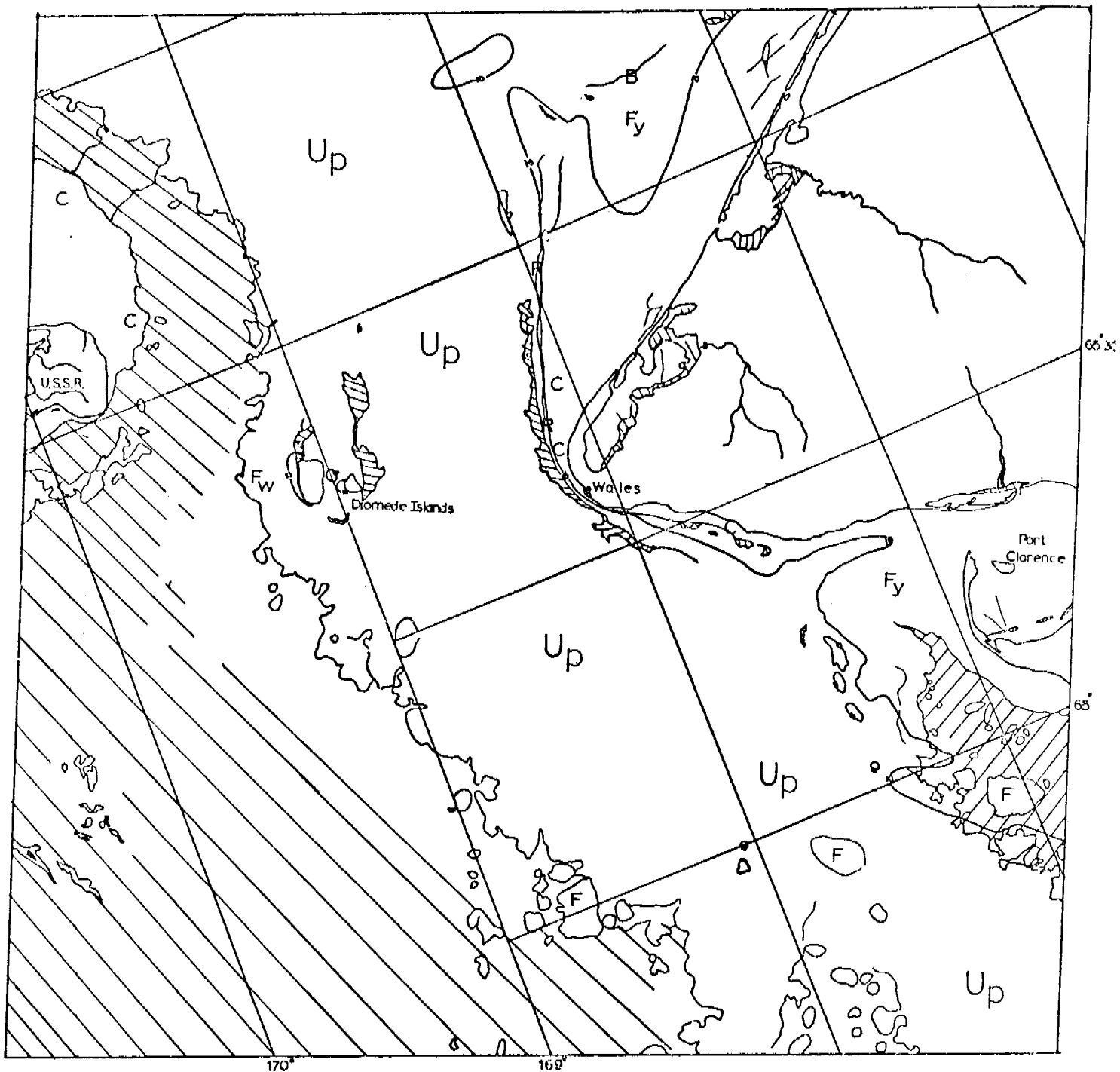
E-1675-22031-7
29 MAY 1974

CHUKCHI SEA



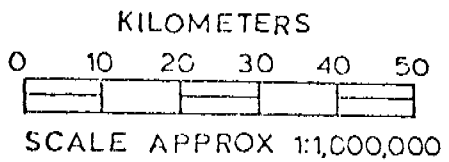
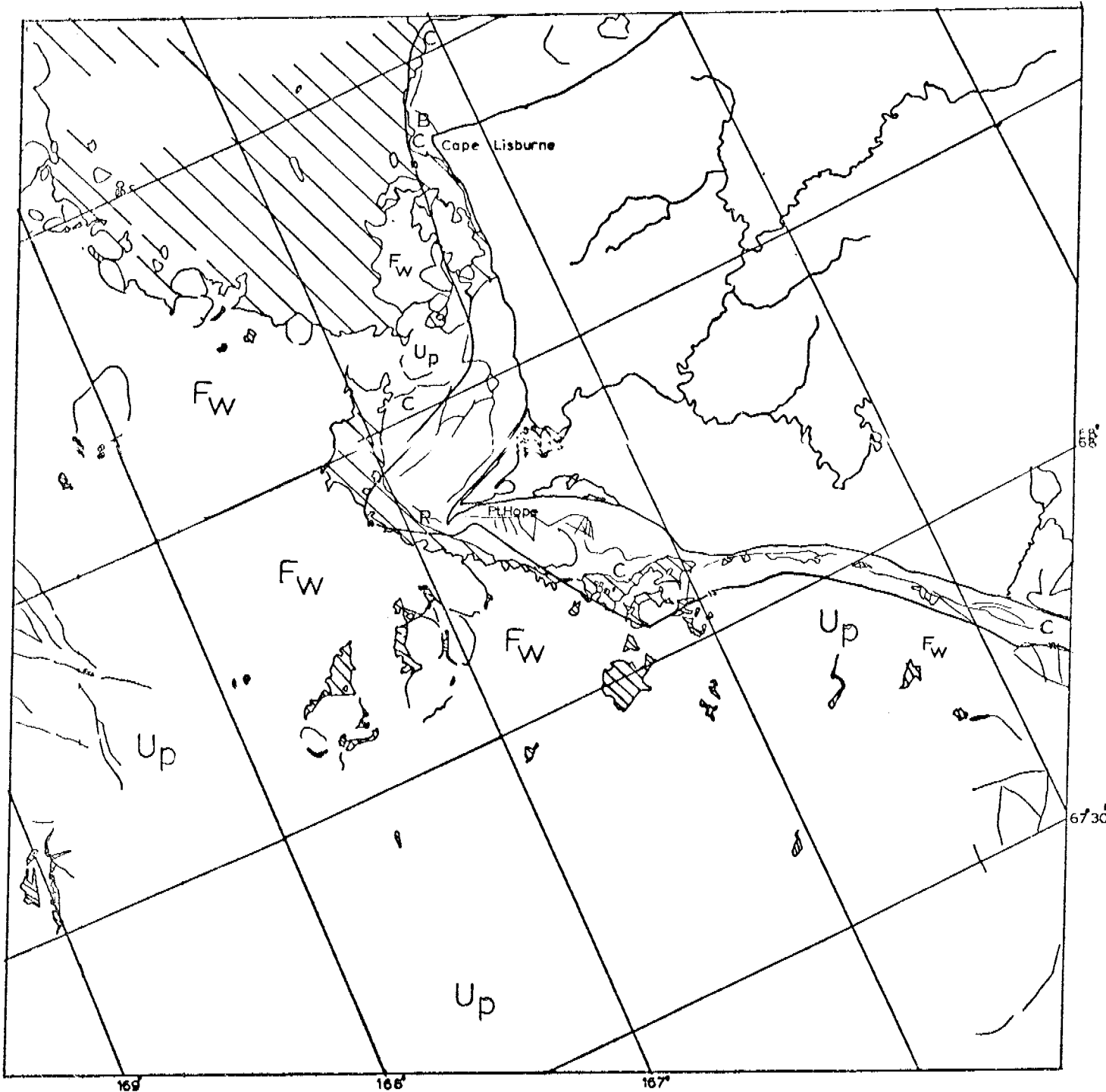
E-1675-22034-7
29 MAY 1974

CHUKCHI SEA



CHUKCHI SEA

E-1676-22092-7
30 MAY 1974



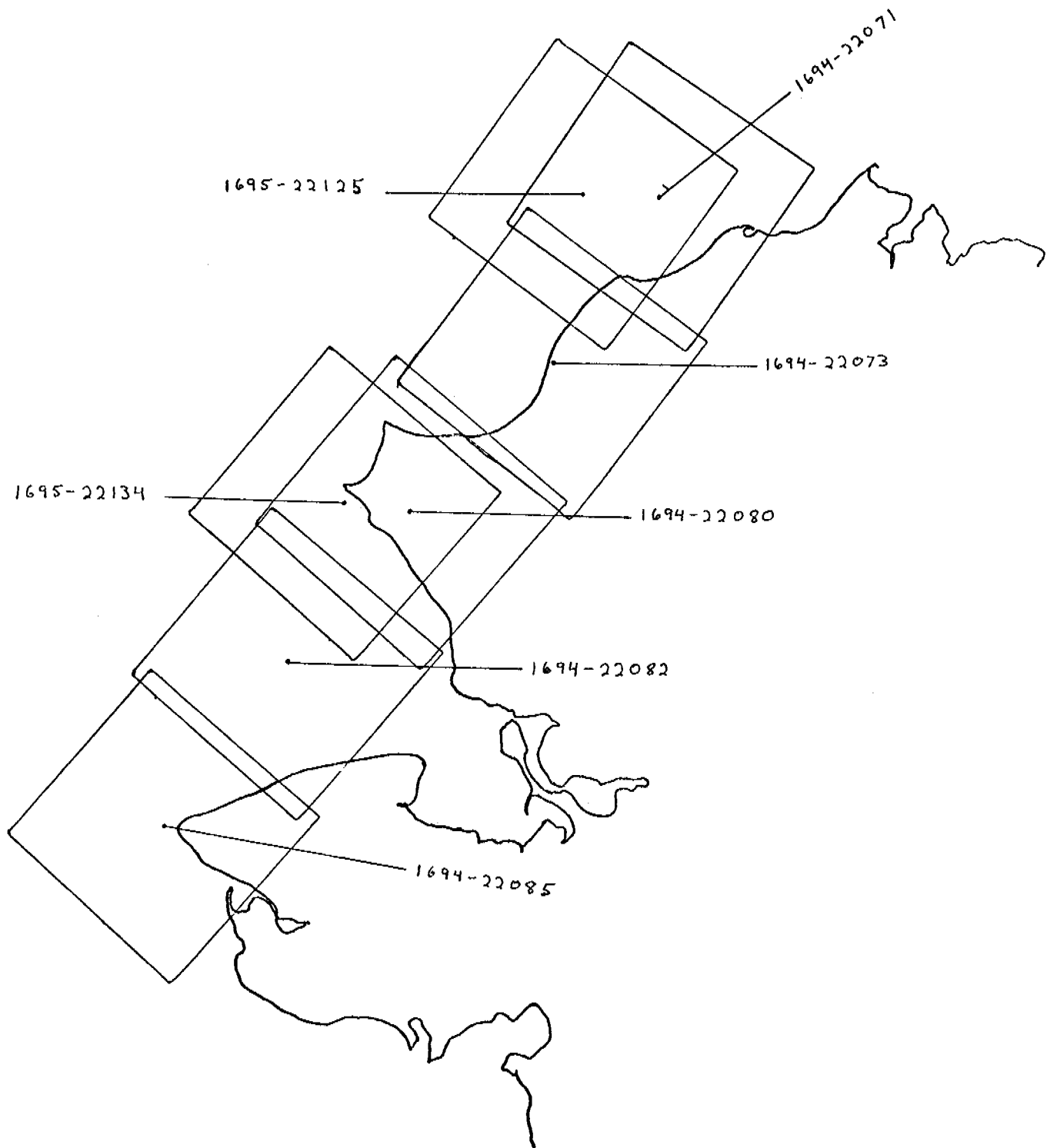
E-1677-22141-7
31 MAY 1974

CHUKCHI SEA

CHUKCHI SEA

13-30 JUNE 1974

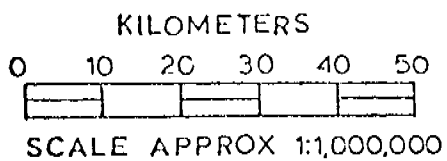
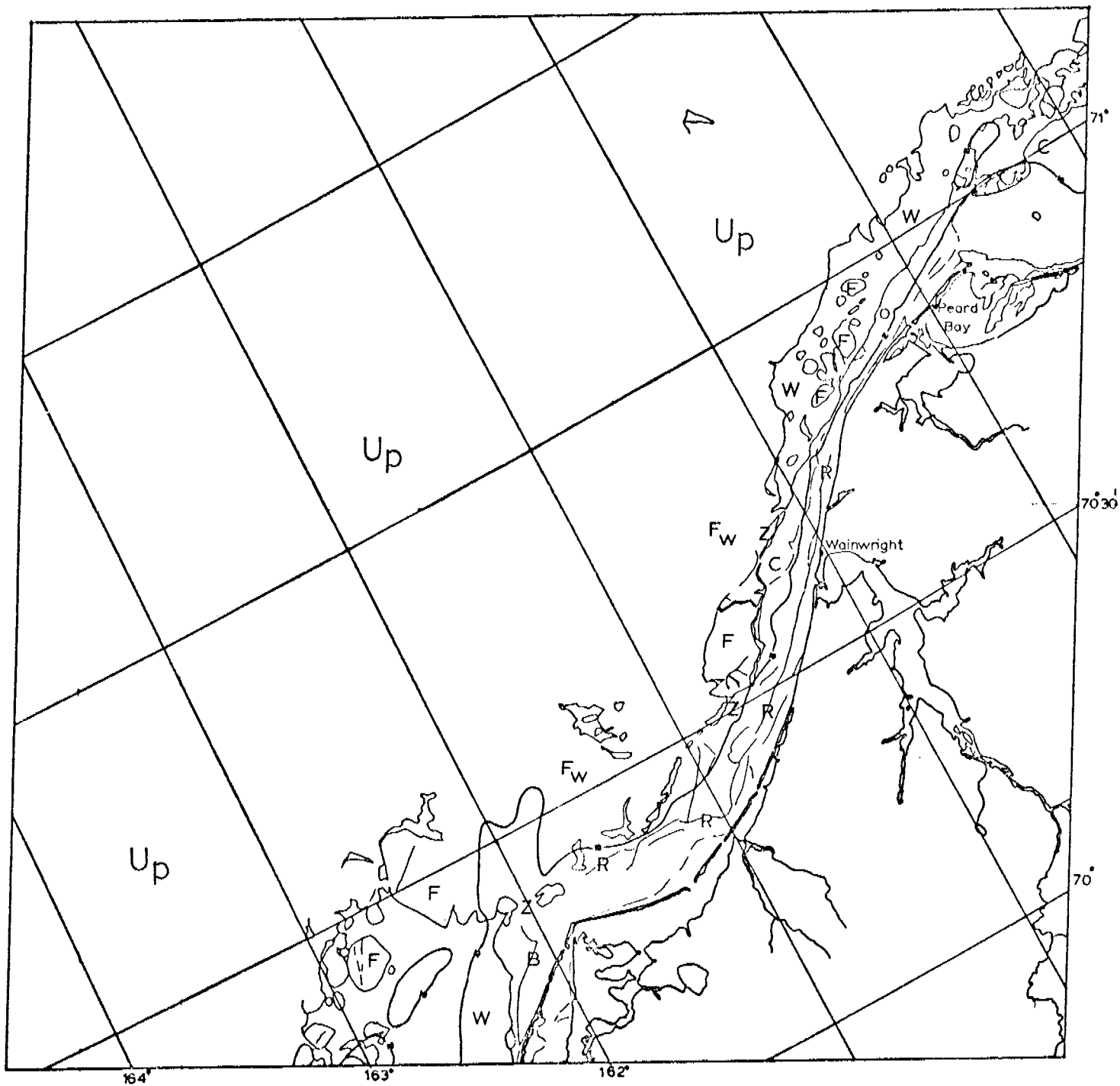
Cycle 1690-1707



LANDSAT scenes 1694-22073 through 1695-22134

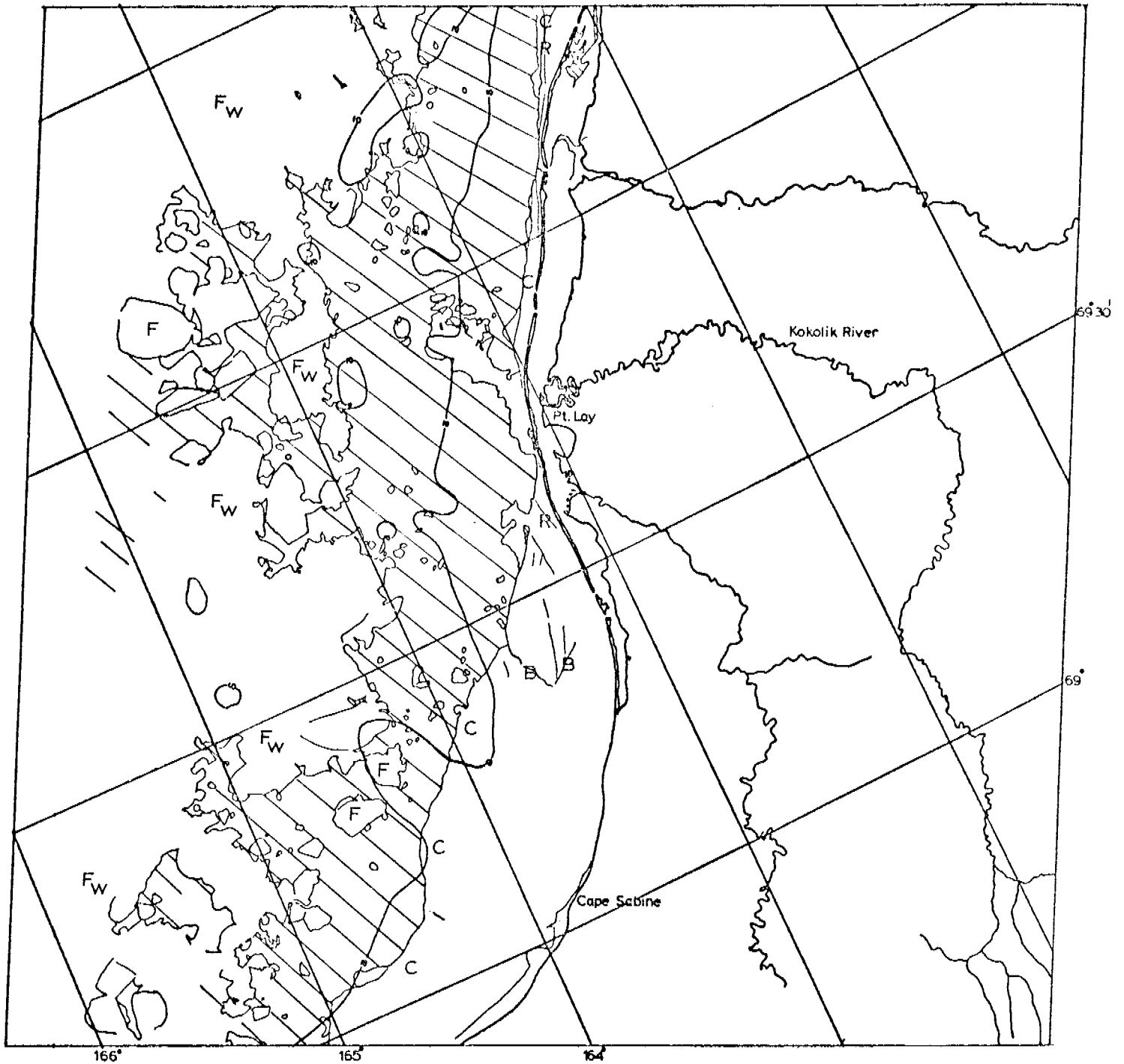
These scenes show the Chukchi coast on June 17-18, 1974, between Bering Strait and Point Franklin. The chief value of these images is to locate ice remaining in place and very likely to be well grounded, protected or both. Starting north from Bering Strait we find that ice formerly appearing to be grounded on shoals to the north has broken up and largely moved away. At Point Hope, some ice appears to remain along the shore to the southeast and on shoals to the immediate northwest. Only one small remnant of ice appears to remain stranded on shoals northwest of Cape Lisburne.

South of Icy Cape a small ribbon of ice remains along the coast widening at Blossom Shoals and narrowing again at Point Franklin.

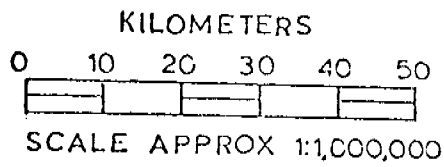


E-1694-22071-7
17 JUNE 1974

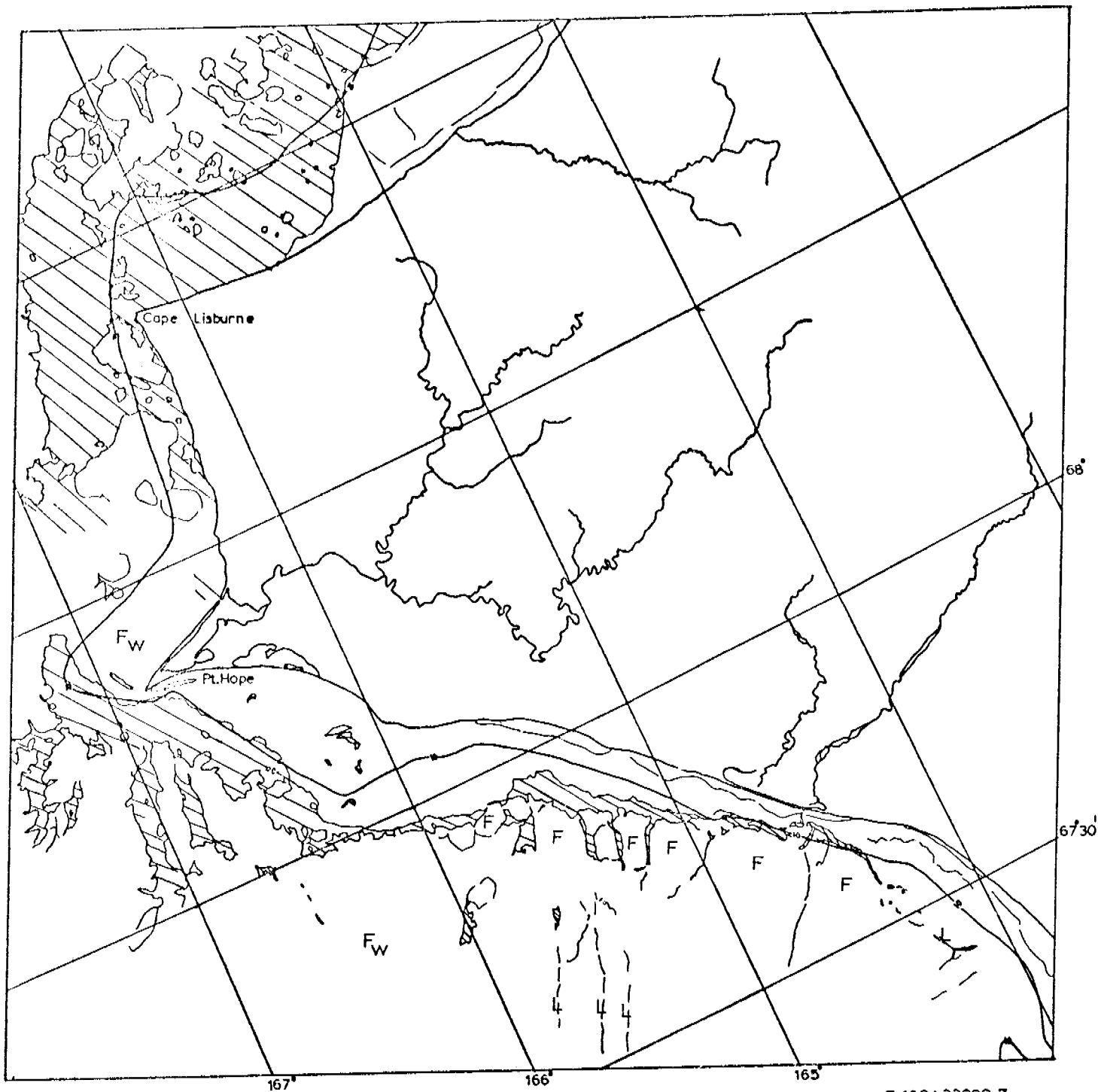
CHUKCHI SEA



E-1694-22073-7
17 JUNE 1974



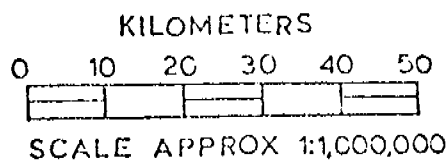
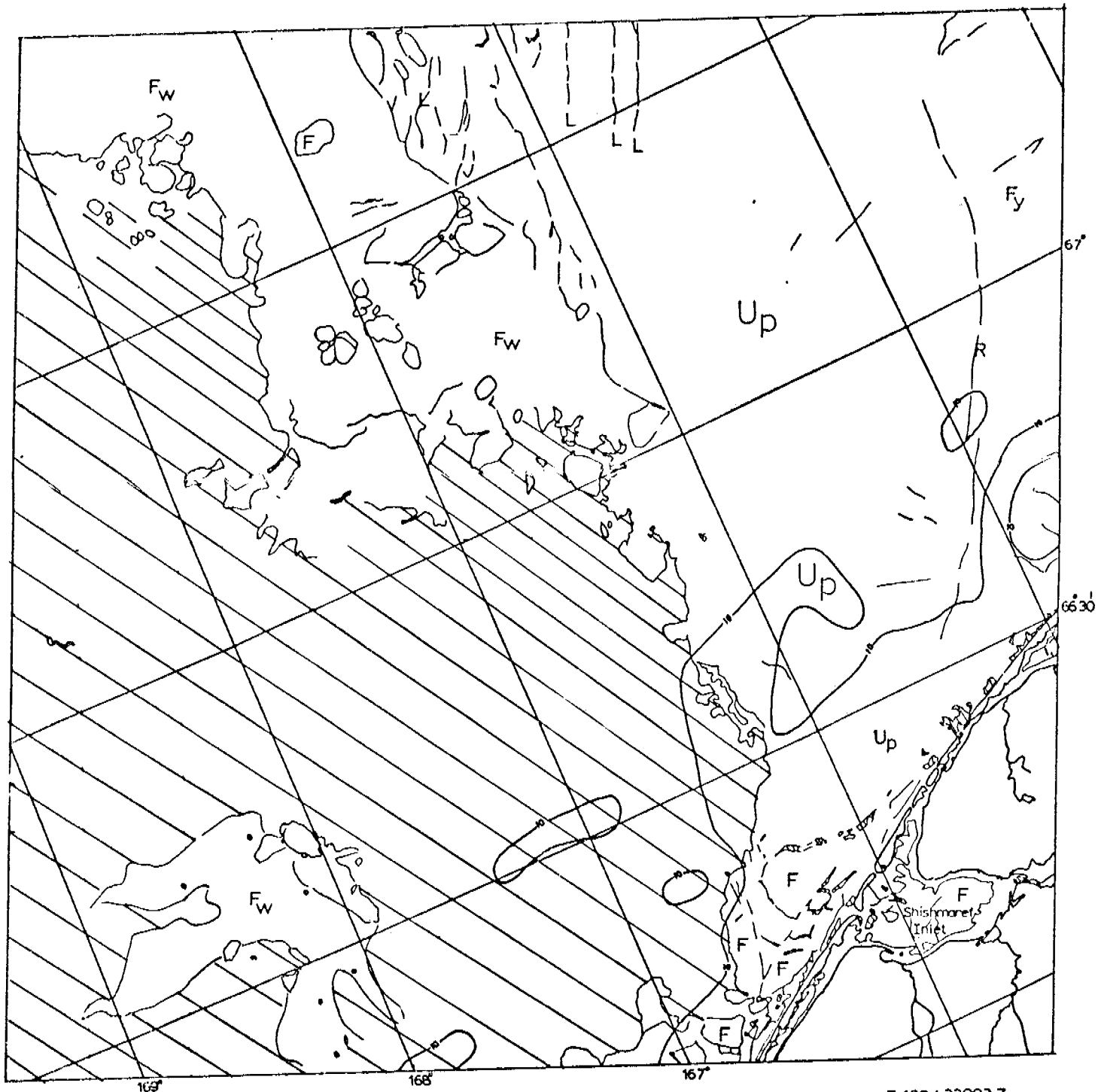
CHUKCHI SEA



KILOMETERS
 0 10 20 30 40 50
 SCALE APPROX 1:1,000,000

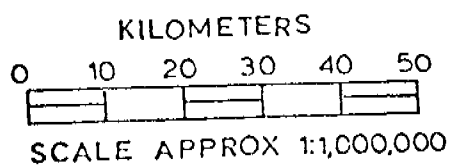
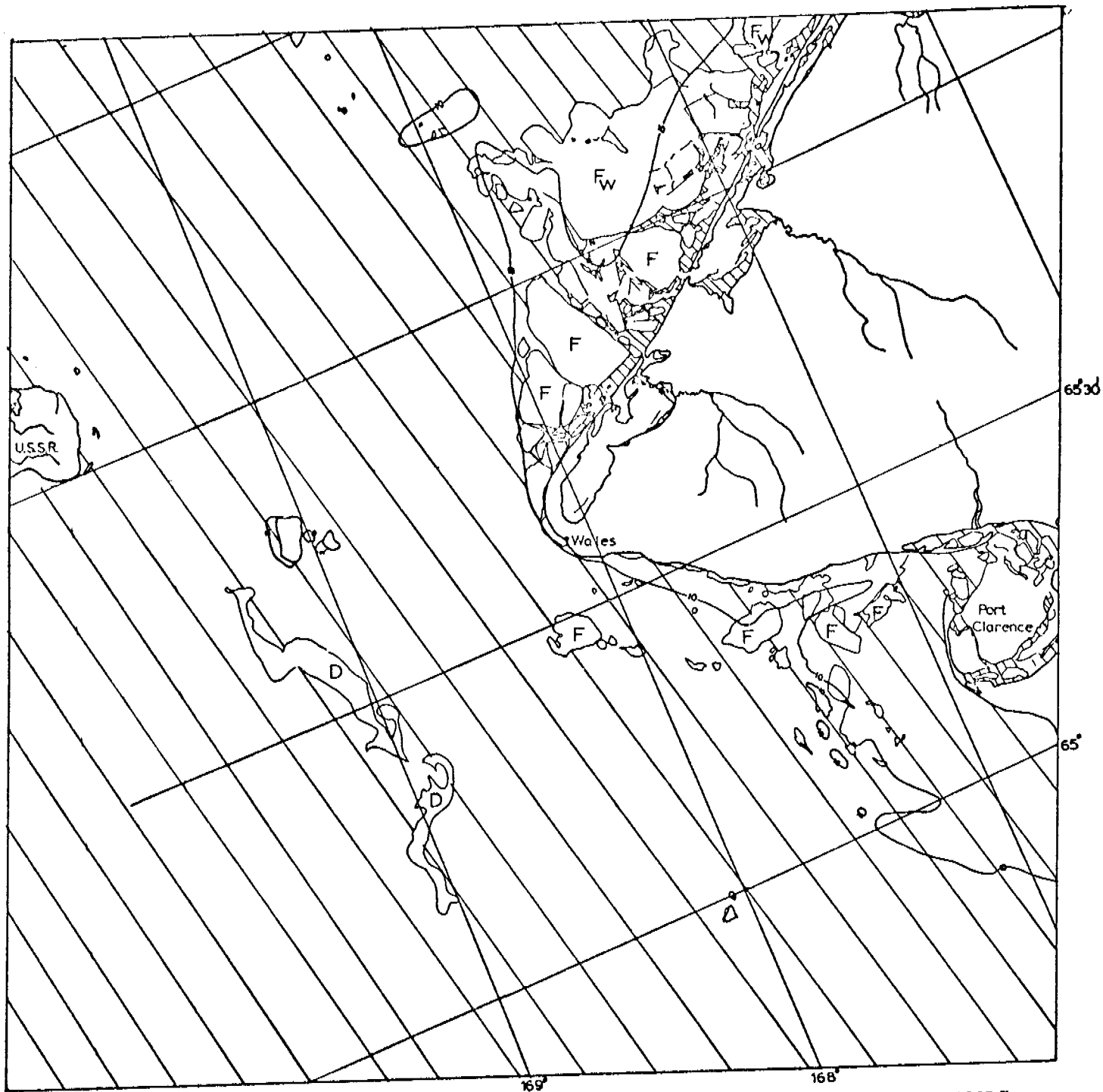
CHUKCHI SEA

E-169422080-7
 17 JUNE 1974



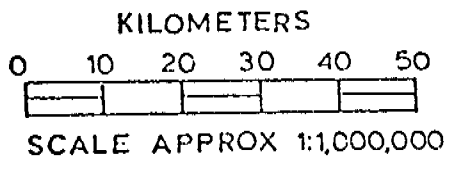
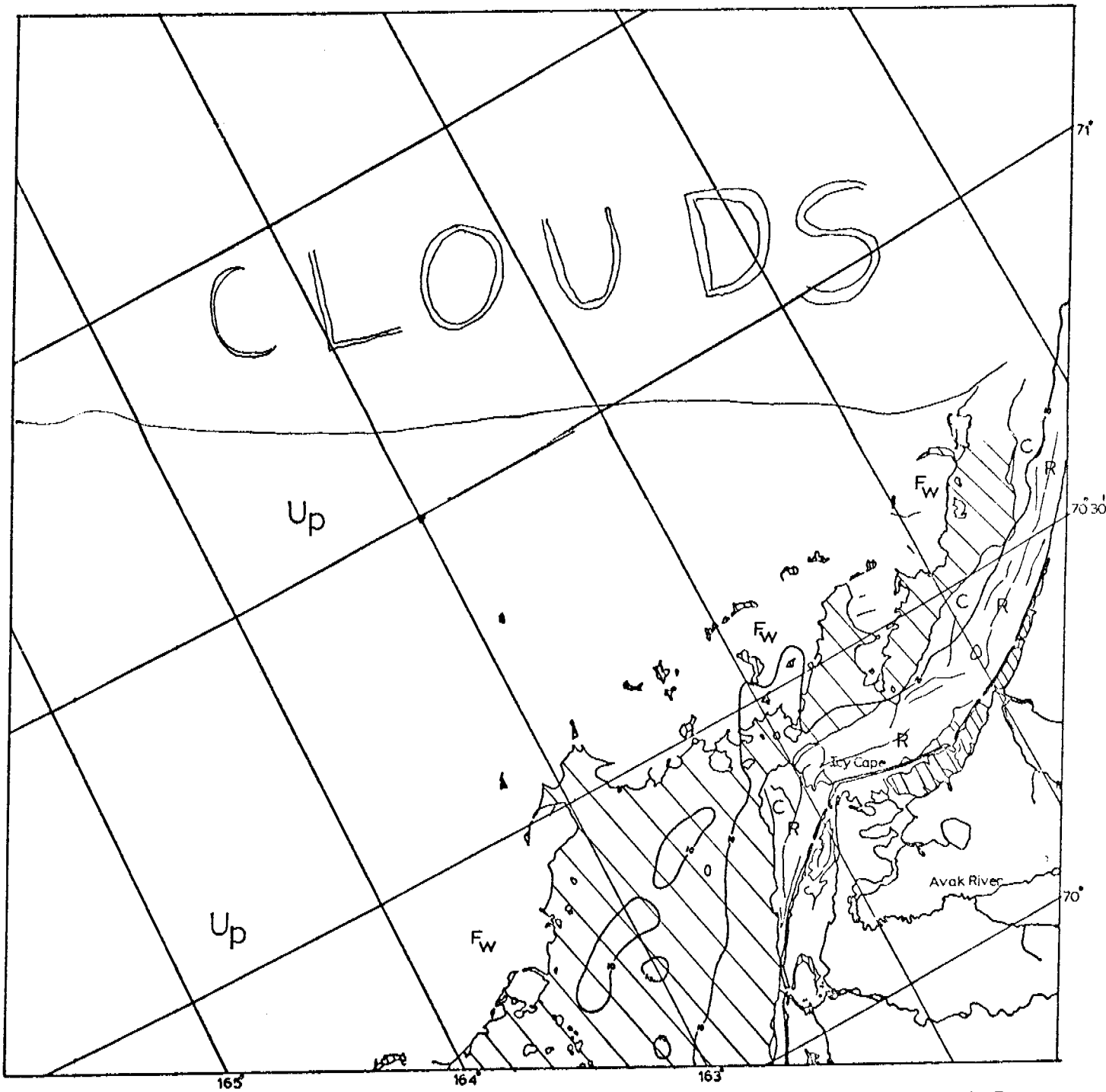
E-1694-22082-7
17 JUNE 1974

CHUKCHI SEA



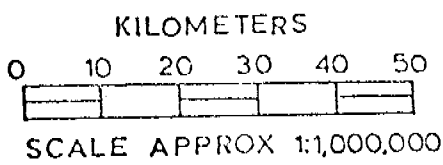
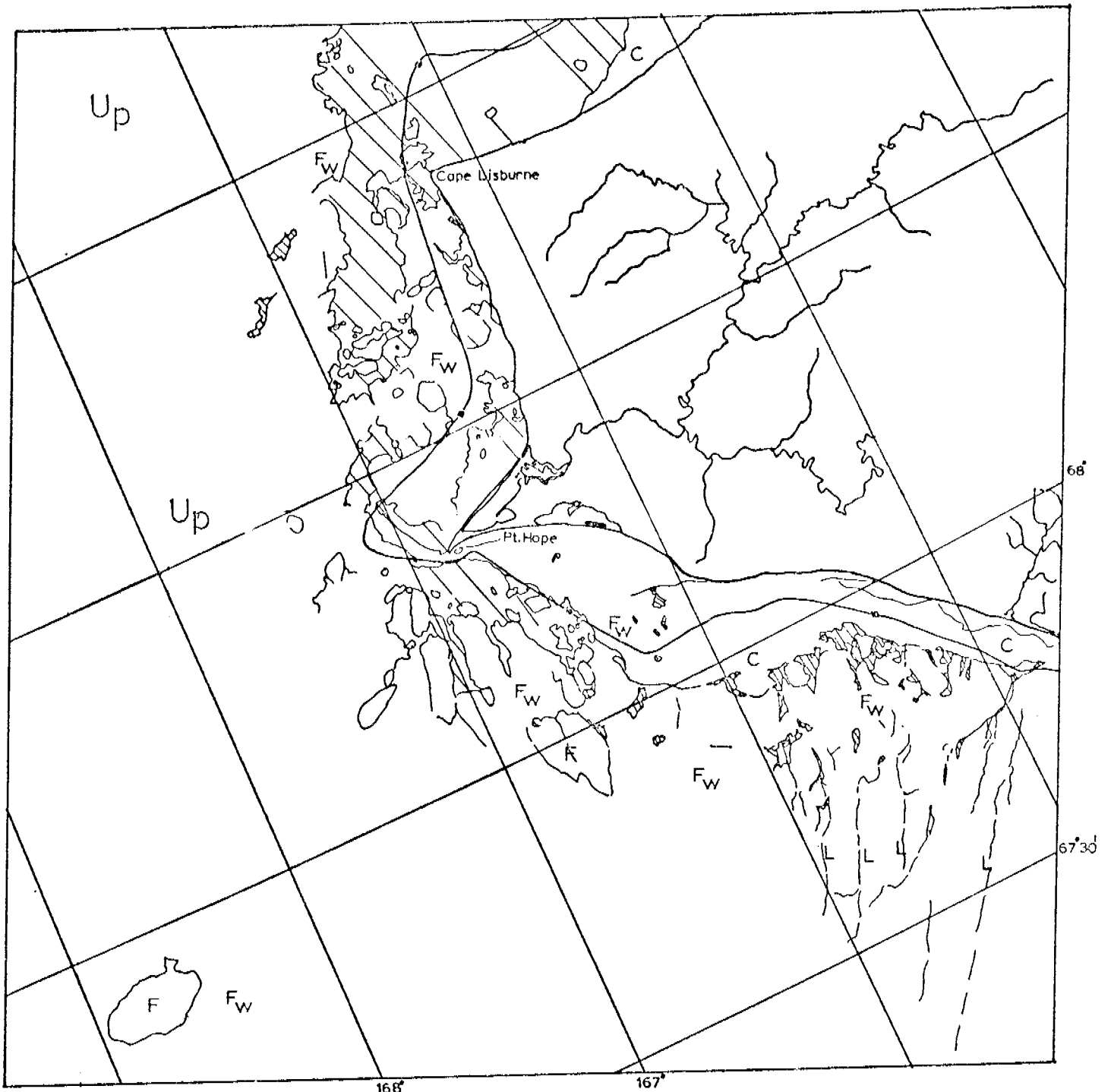
CHUKCHI SEA

E-1694-22085-7
17 JUNE 1974



E-1695-22125-7
18 JUNE 1974

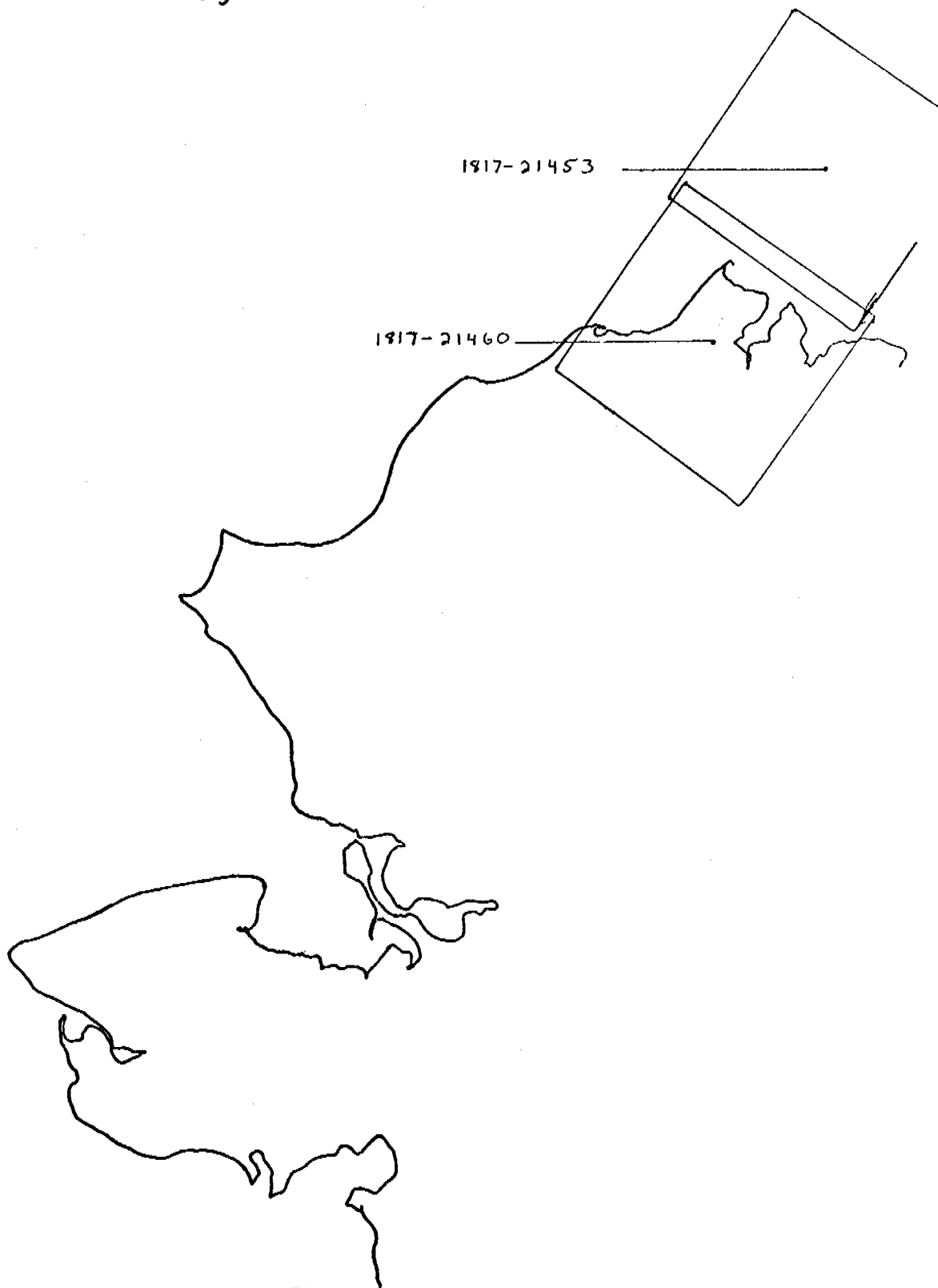
CHUKCHI SEA

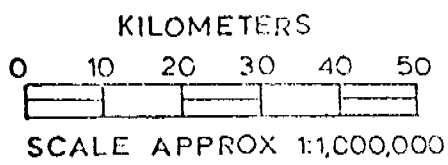
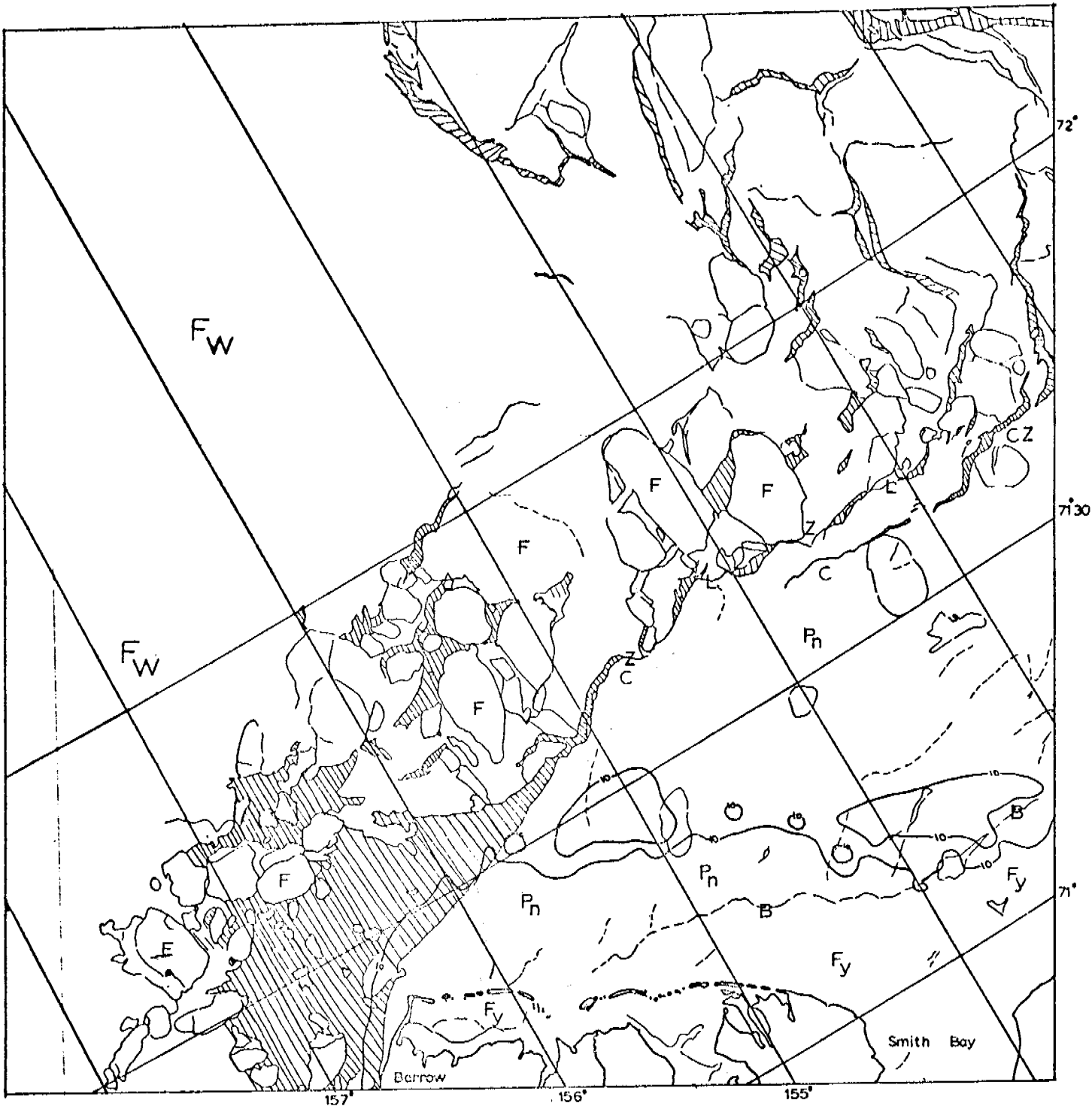


CHUKCHI SEA

E-1605-22134-7
 18 JUNE 1974

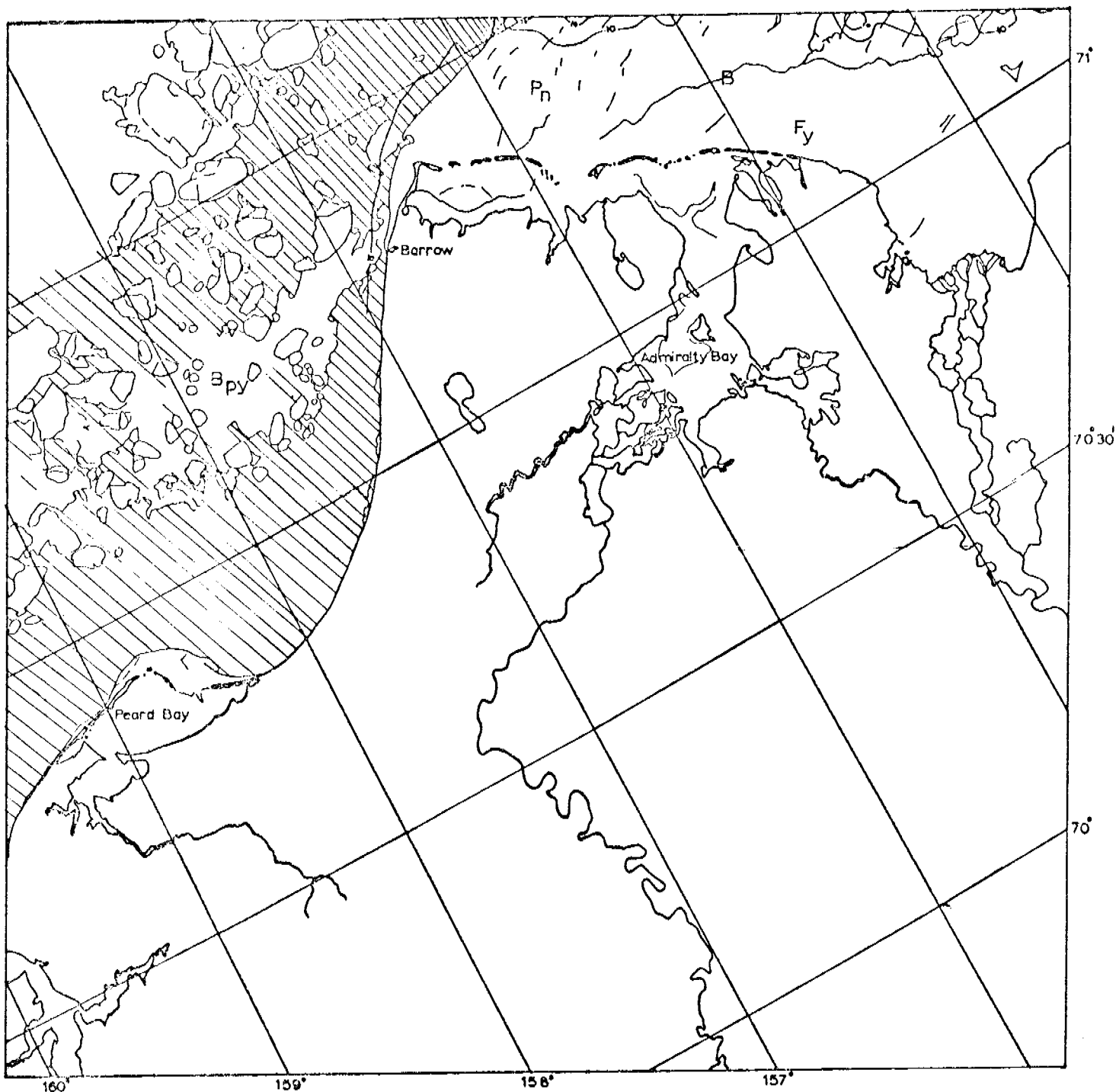
CHUKCHI SEA
17 OCTOBER-3 NOVEMBER
1974
Cycle 1816-1833





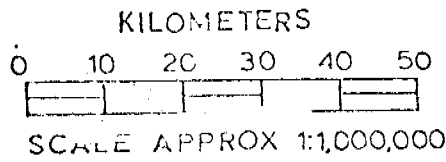
CHUKCHI SEA

E-1817-21453-7
18 October 1974



160° 159° 158° 157°

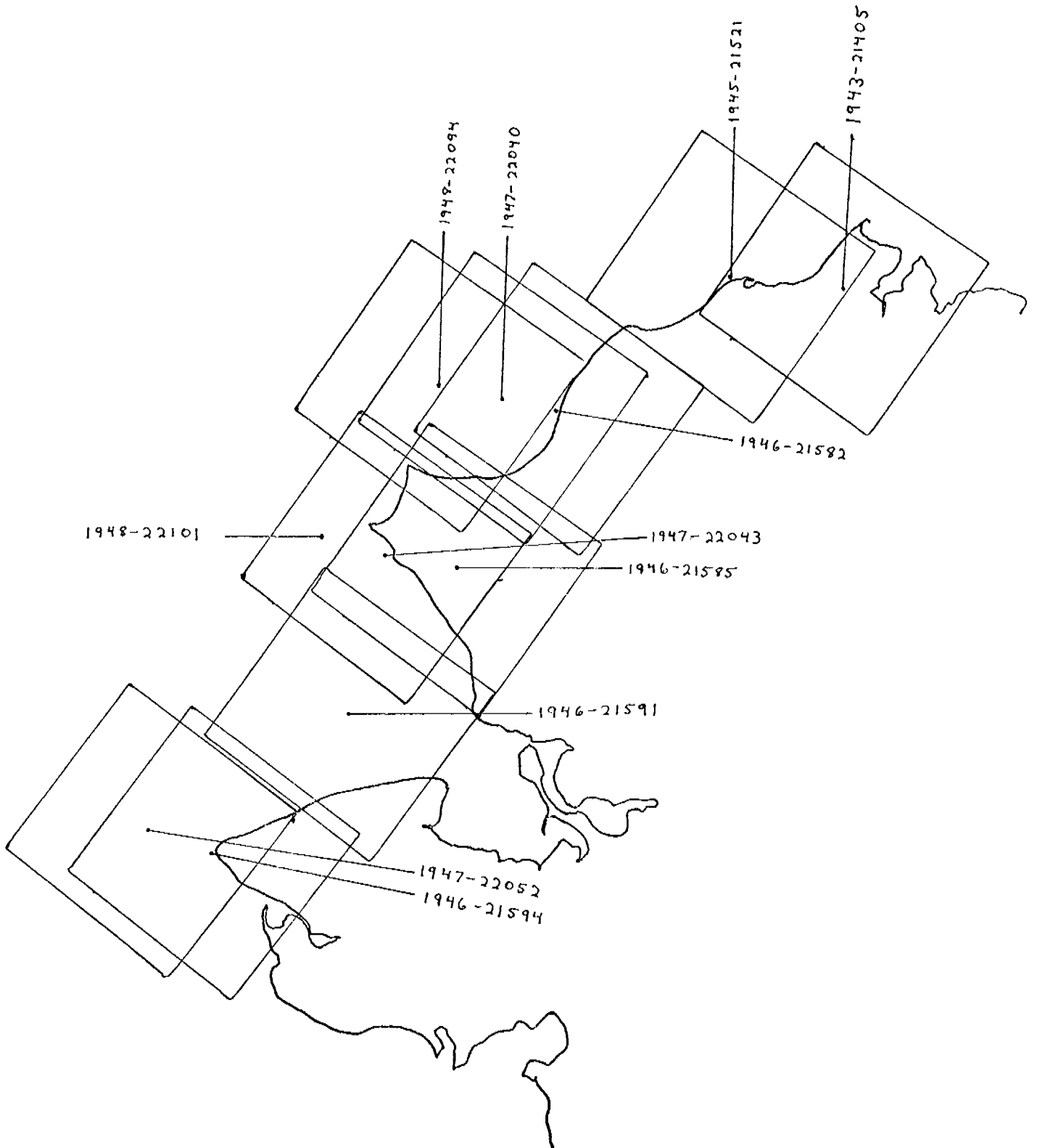
71°
70°30'
70°



E-1817-21460-7
18 October 1974

CHUKCHI SEA

CHUKCHI SEA
20 FEBRUARY - 9 MARCH 1975
Cycle 1942-1959



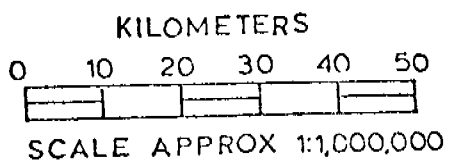
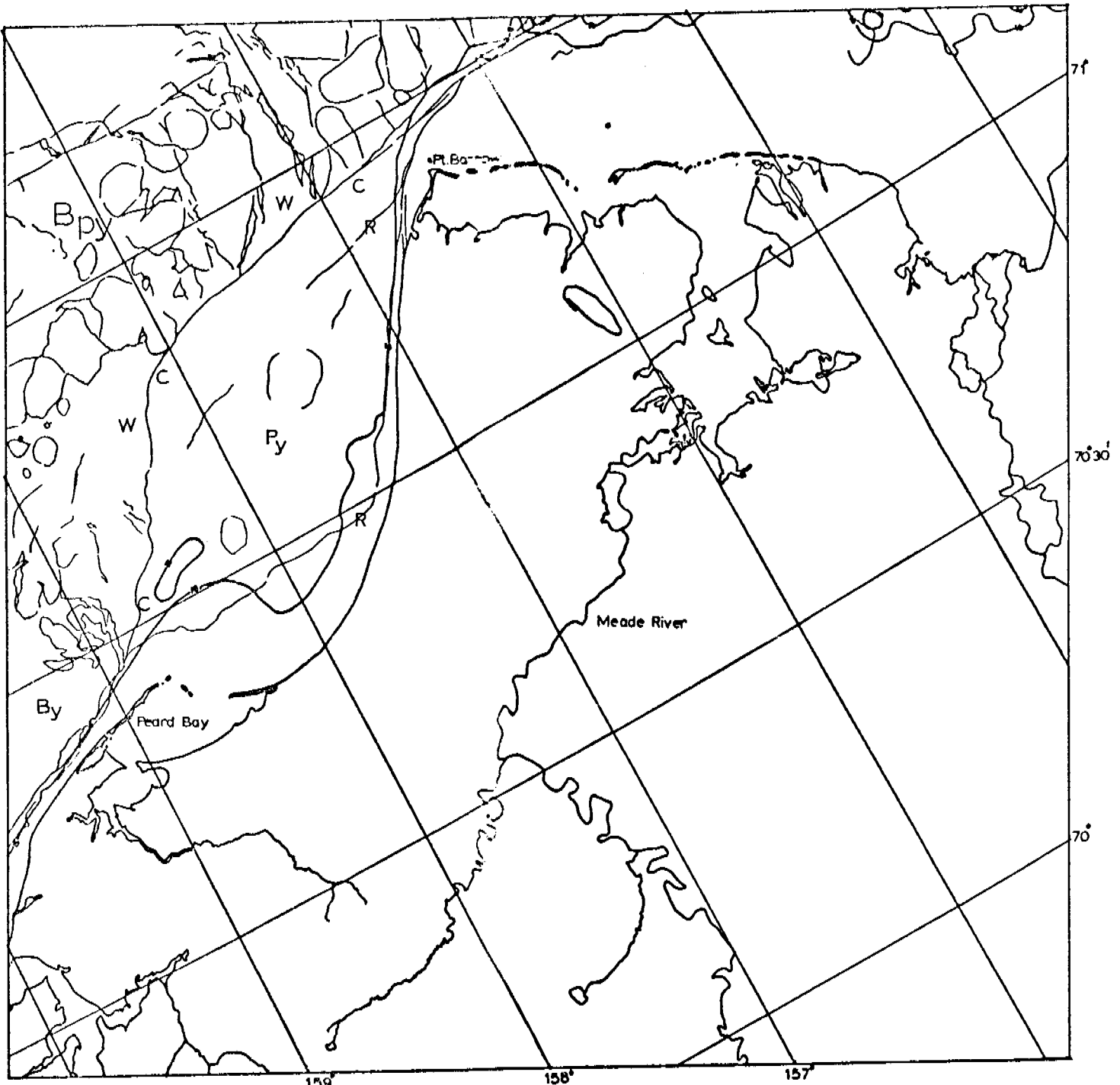
Scenes 1943-21405 through 1948-22101

These scenes yield coverage of ice conditions along the Chukchi coast from Cape Prince of Wales to Barrow between February 20-28, 1975. It is apparent that the ice has been in motion with the formation of much new ice for some time. A broad zone of moving ice presents a shearing surface from Barrow to Bering Strait clearly illustrating in many places which ice is firmly fixed with respect to the shore.

Starting northward from Bering Strait, a large expanse of contiguous ice with some apparently grounded ridges is found to the north. Farther north, opposite Kotzebue Sound (and over deep water) this ice is considerably fractured, ending in a newly frozen polynya southeast of Point Hope. On the north side of the polynya, a narrow ribbon of contiguous ice is found next to the shore.

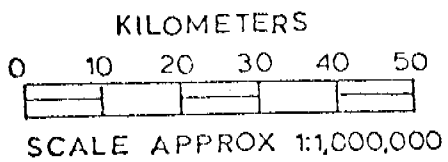
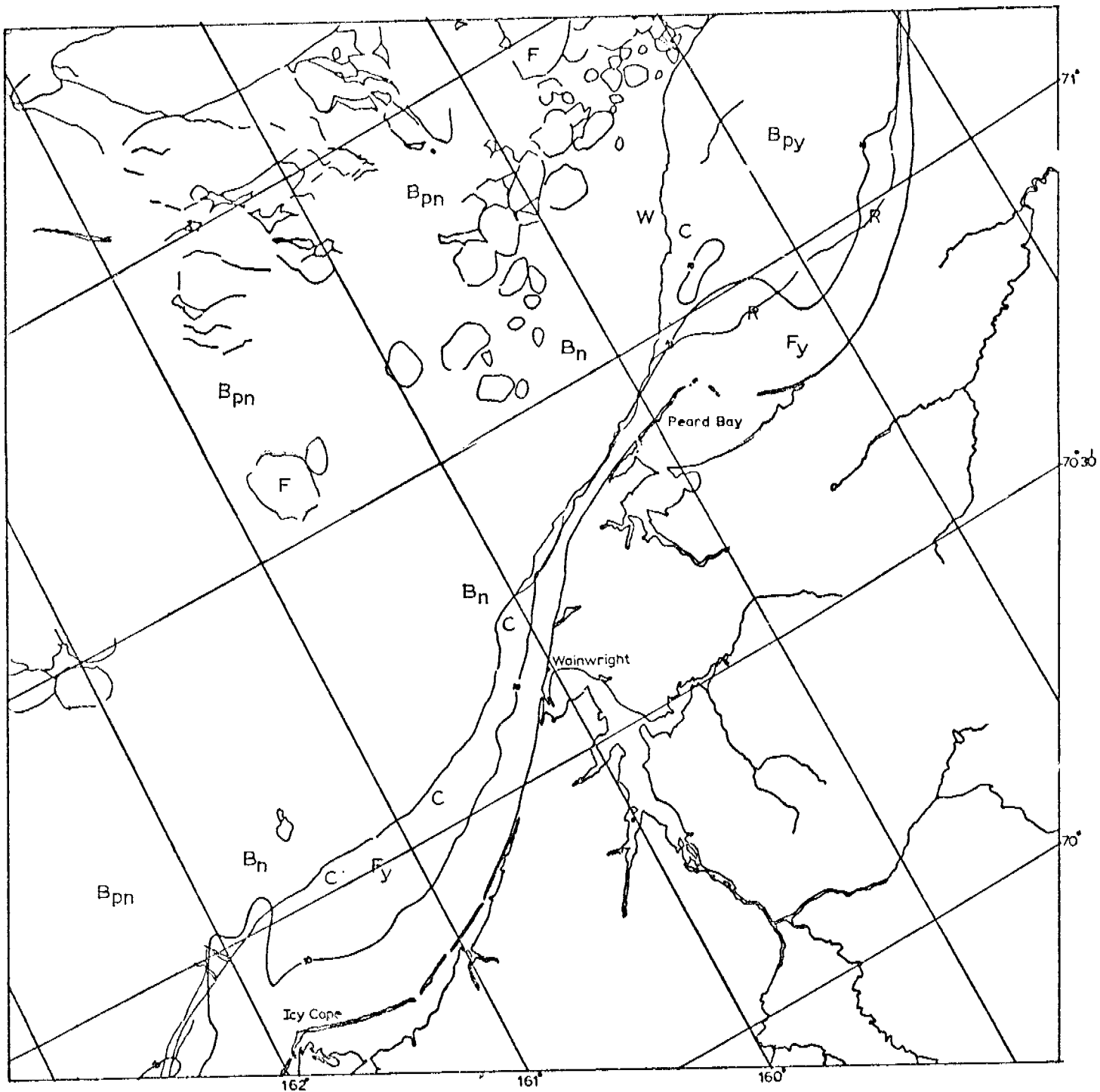
Northwest of Point Hope and Cape Lisburne large expanses of contiguous ice coincide with shoals some distance from shore. Some evidence of ridges can be found on the seaward side of these areas of ice.

Farther north, the edge of contiguous ice appears to have been formed by the breaking away of ice moving seaward. However, large ridges can be seen on Blossom Shoal, from Point Franklin to the south, and off Barrow within the apron of contiguous ice.



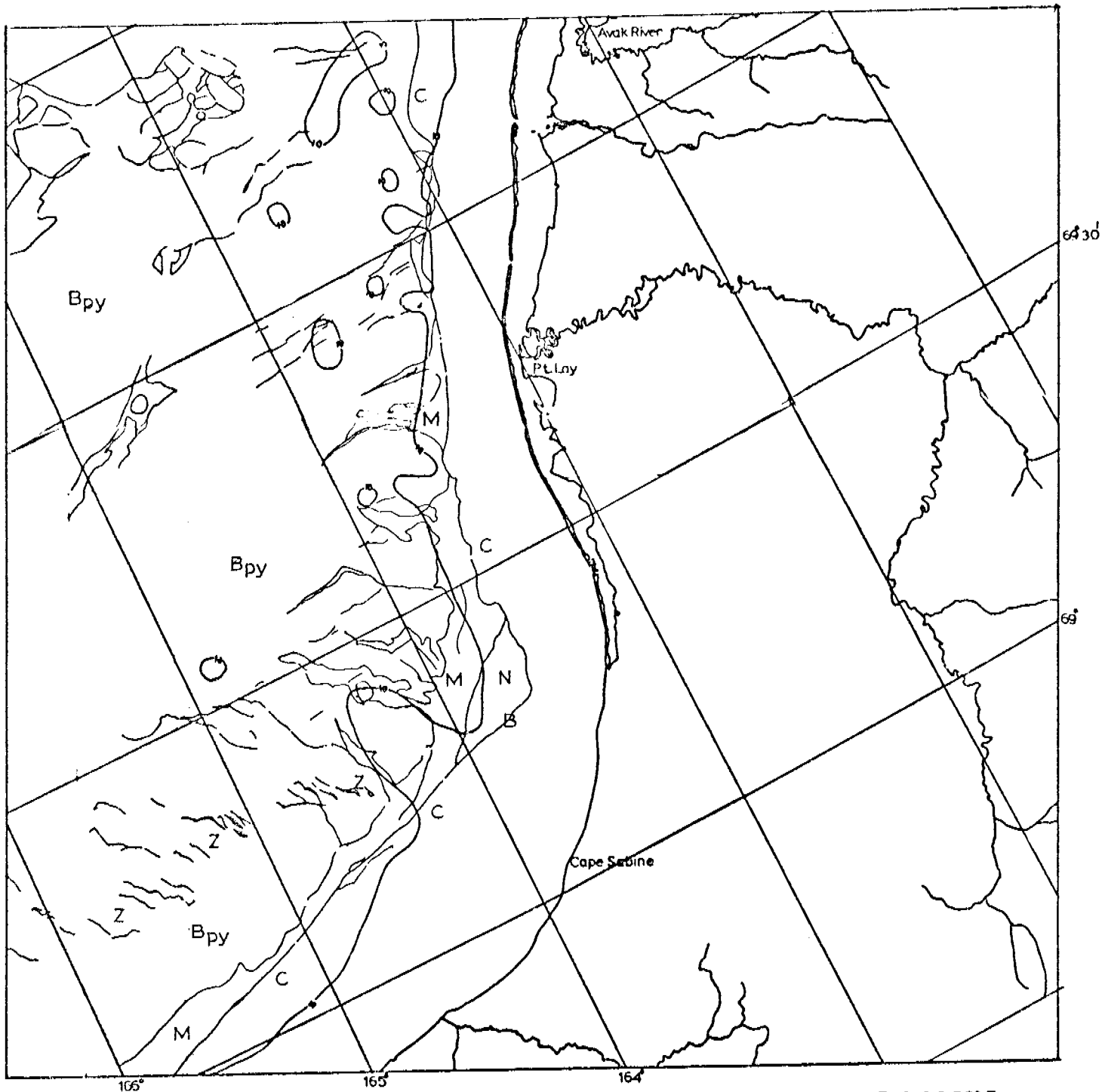
E-1943-21405-7
21 FEB. 1975

CHUKCHI SEA

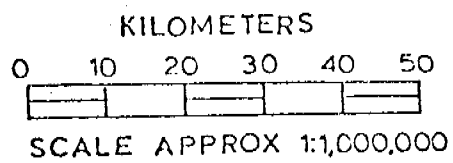


E-1945-2152-7
23 FEB. 1975

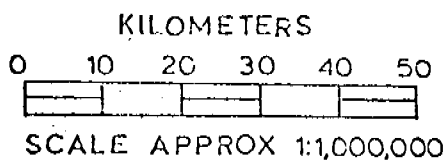
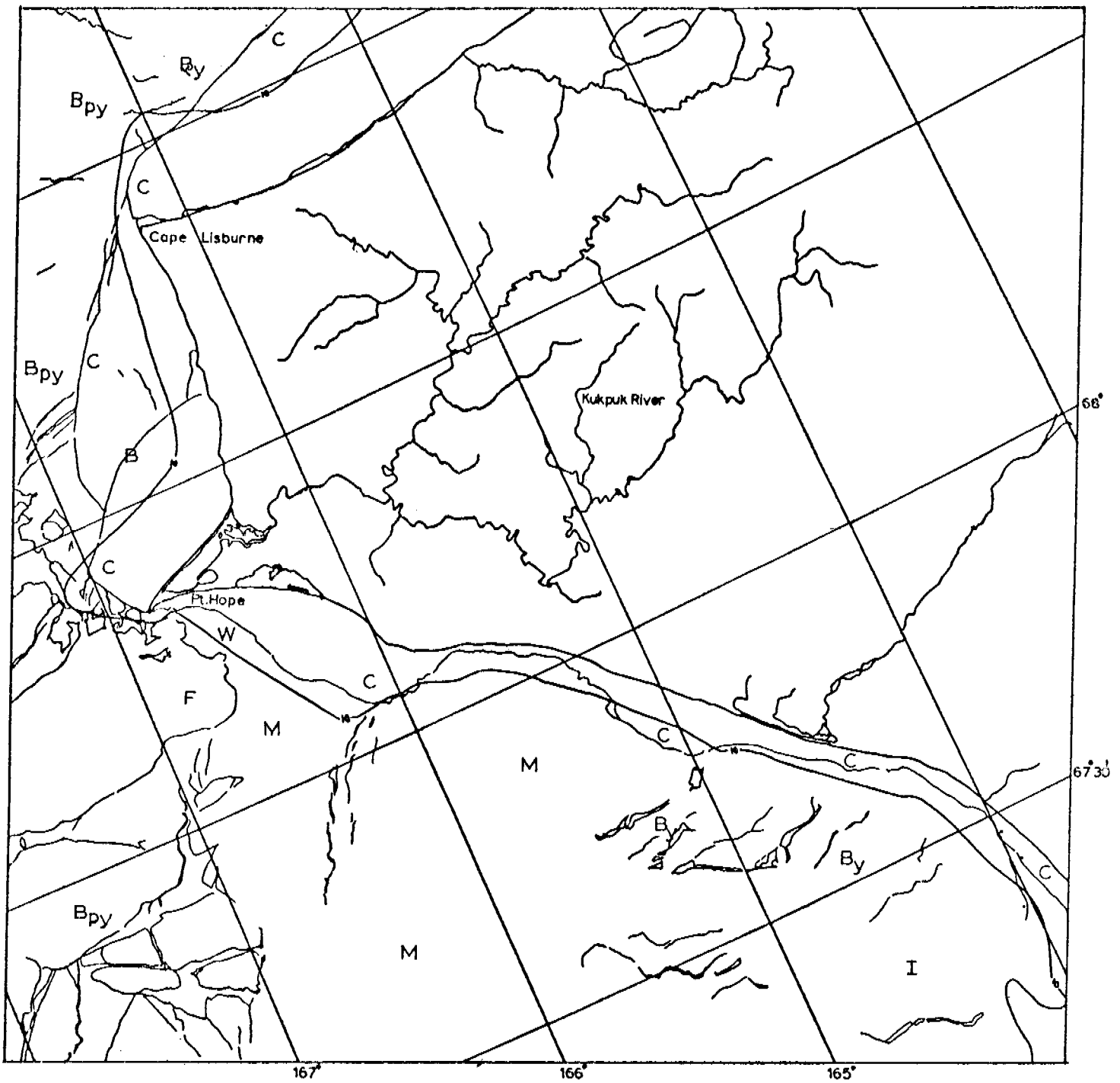
CHUKCHI SEA



E-1946-21582-7
24 FEB. 1975

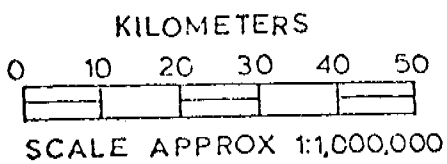
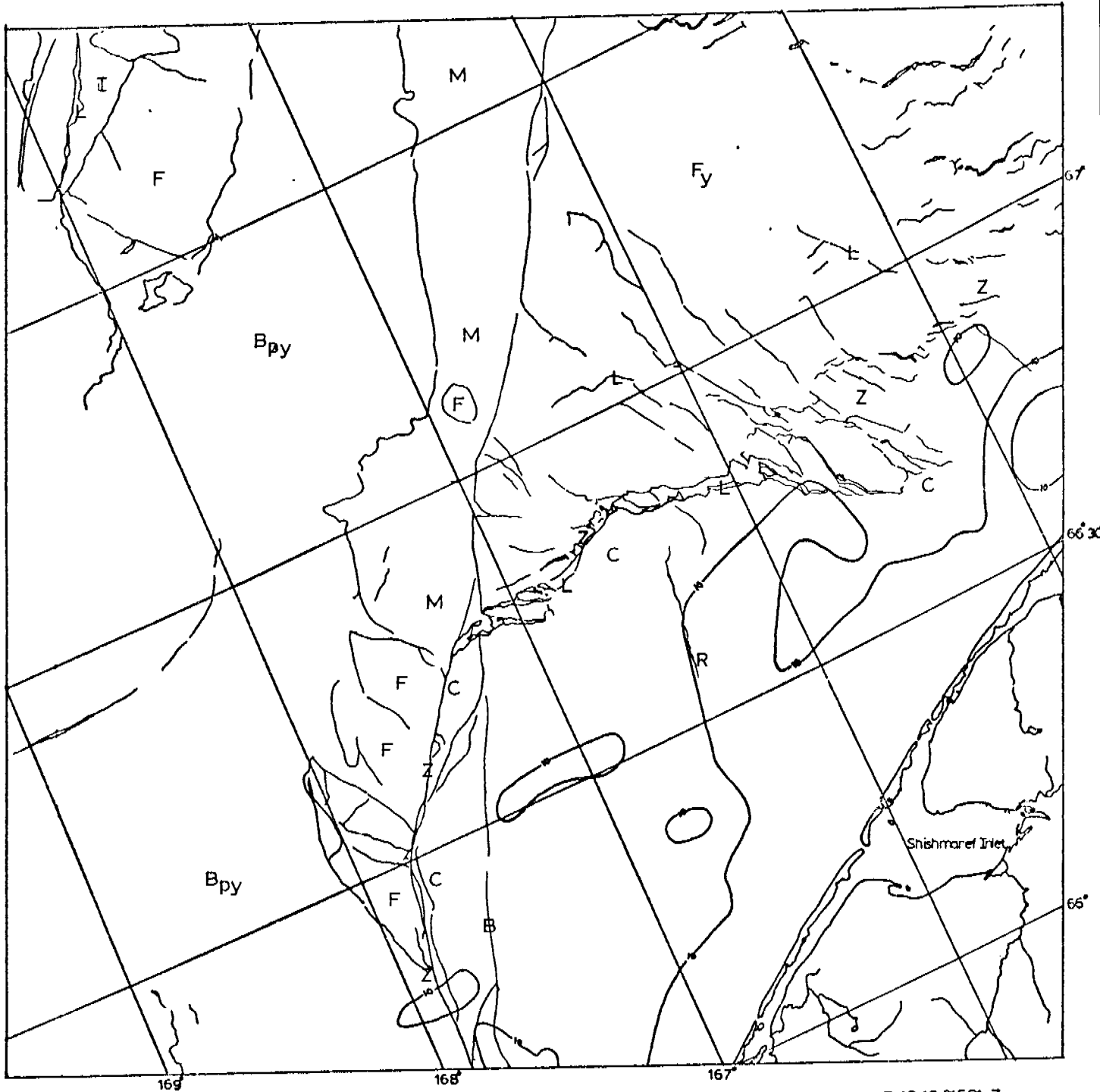


CHUKCHI SEA



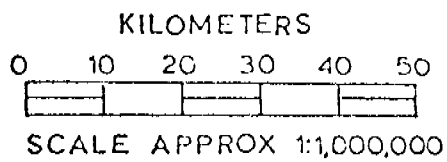
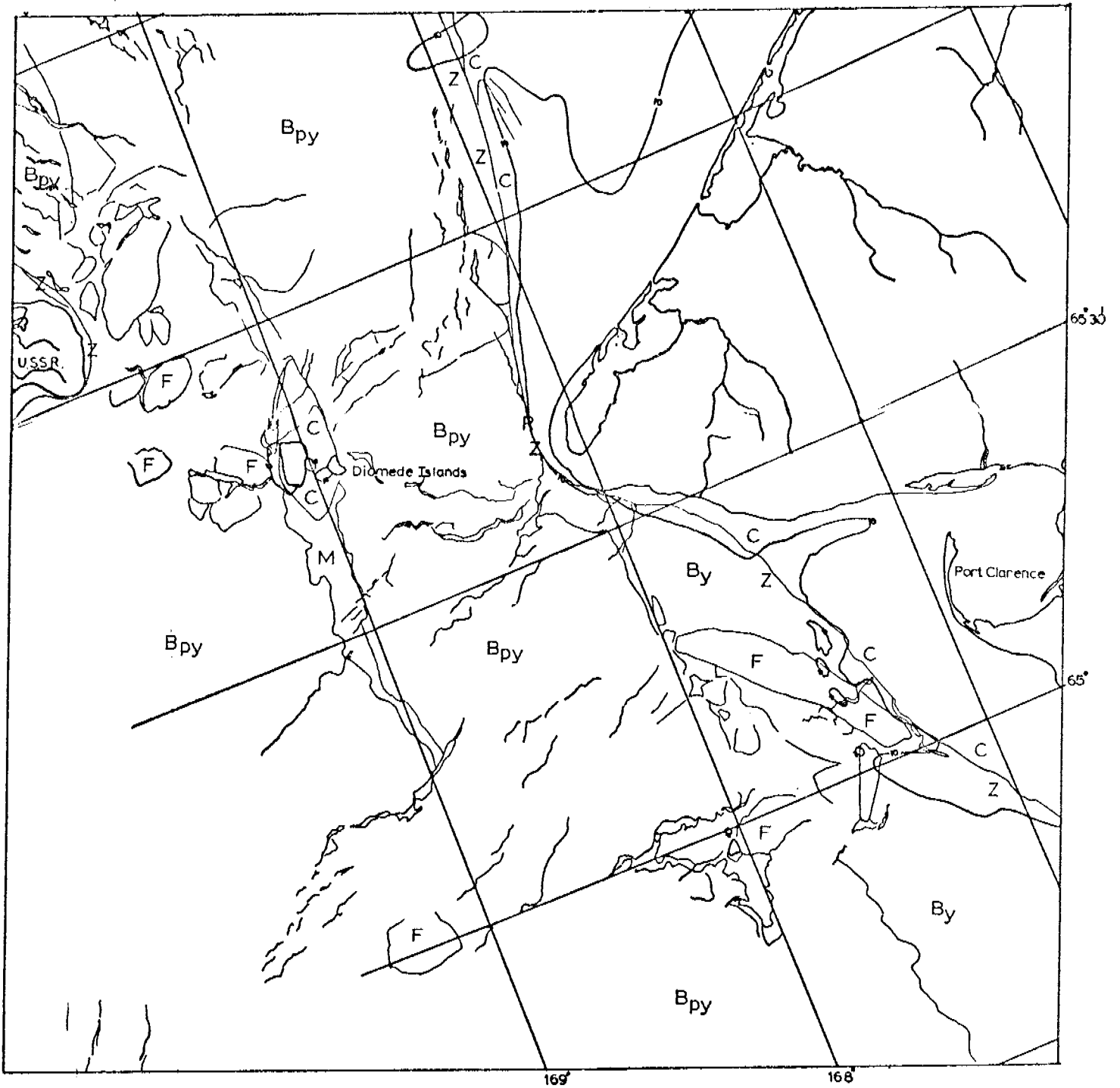
E-1946-21585-7
24 FEB. 1975

CHUKCHI SEA



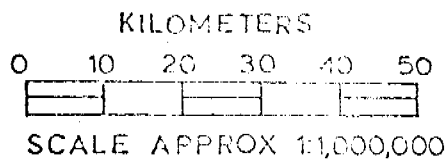
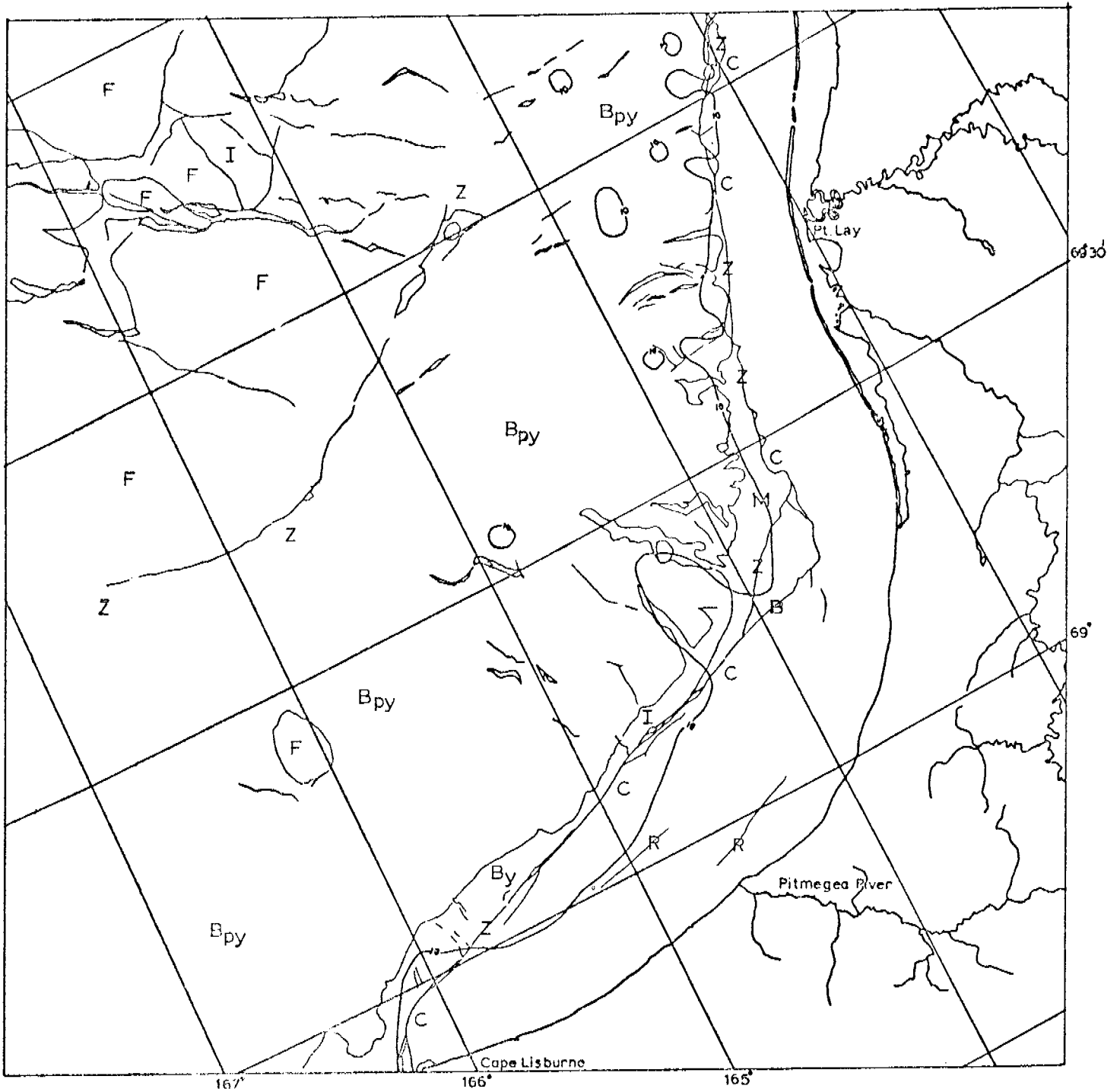
E-1946-21591-7
24 FEB. 1975

CHUKCHI SEA



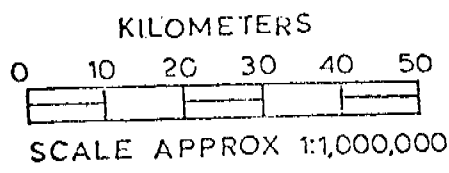
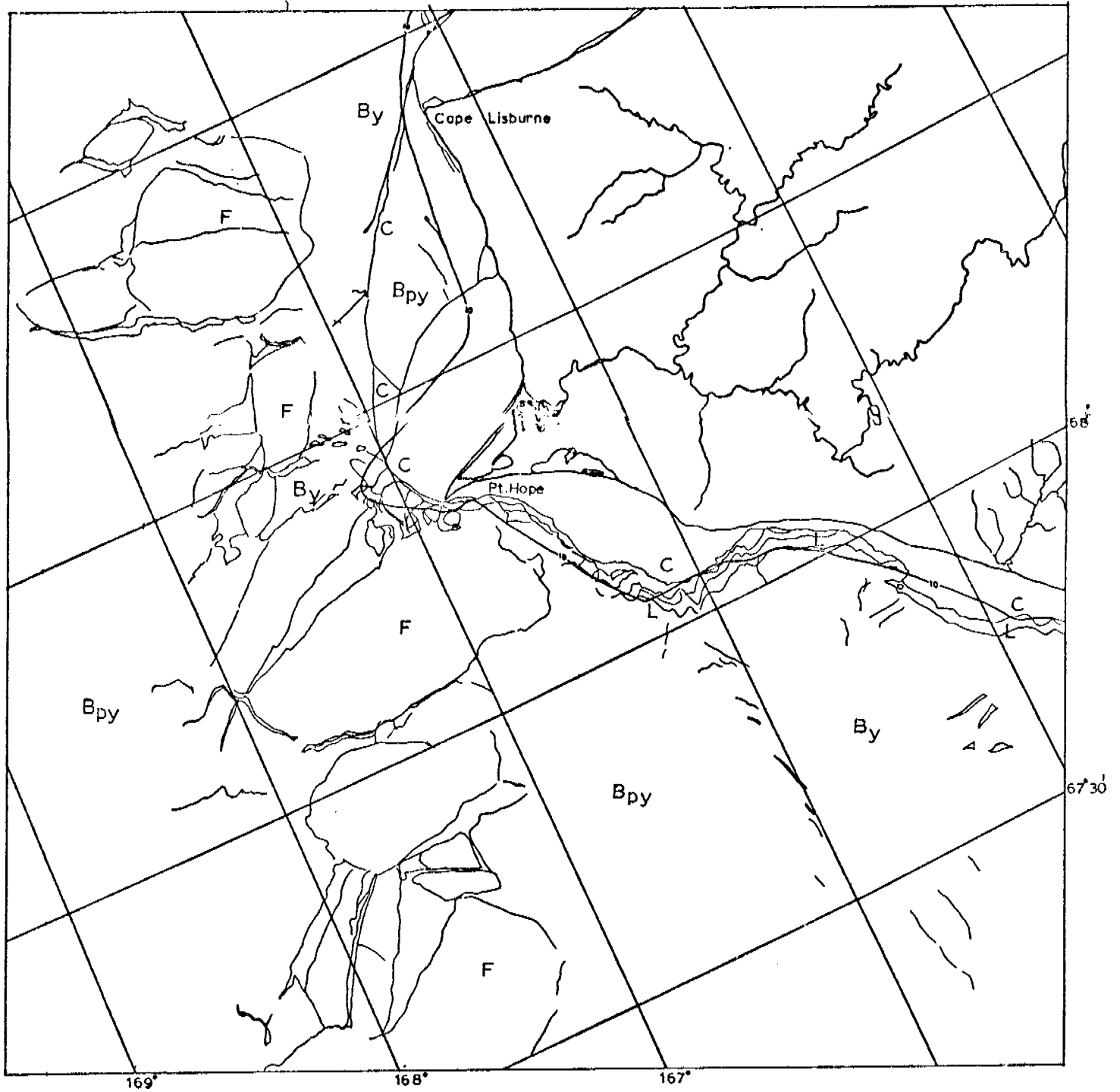
E-1946-21594-7
24 FEB. 1975

CHUKCHI SEA



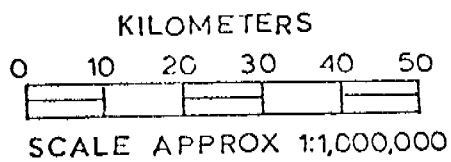
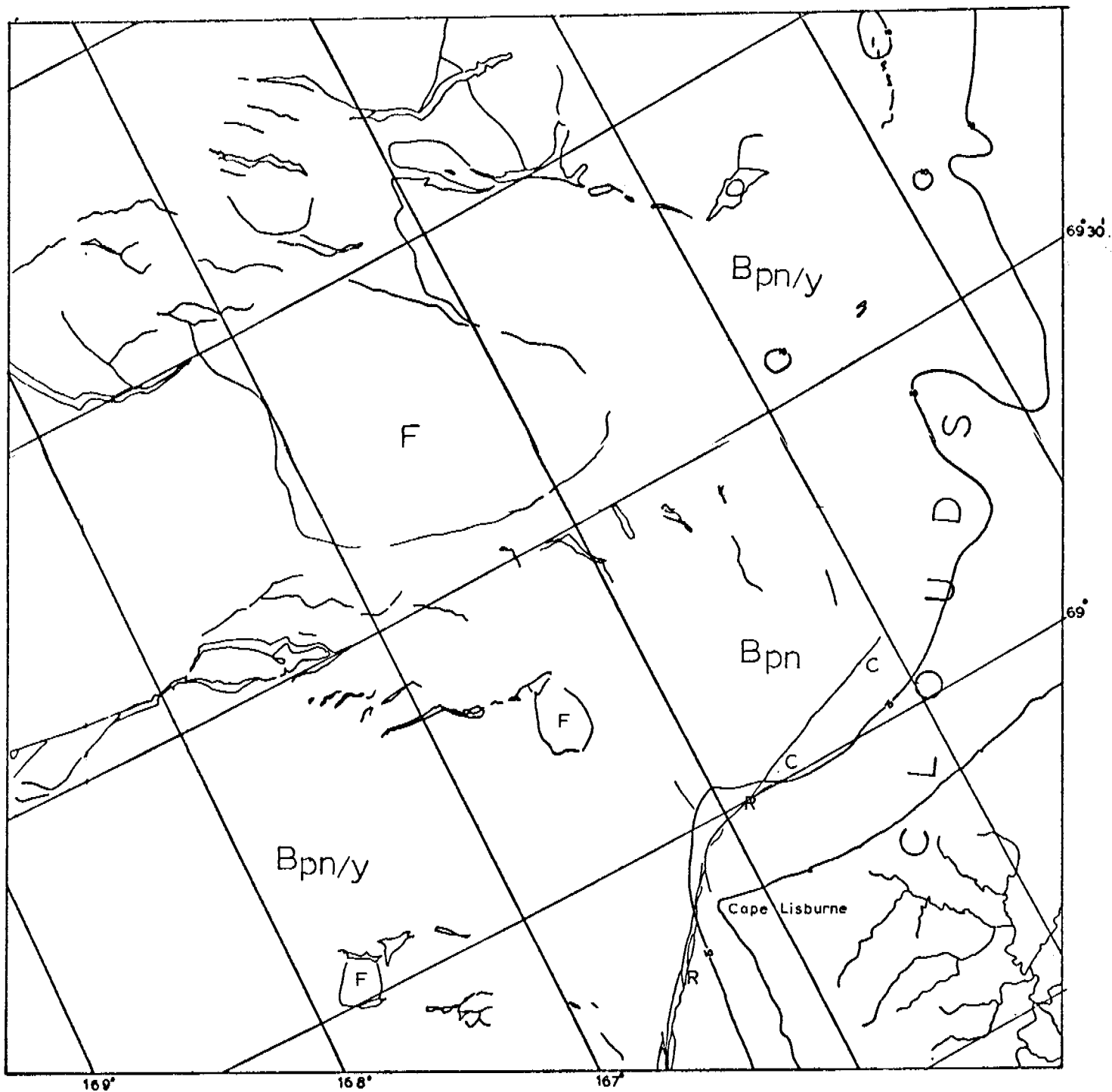
E 1947-22040-7
25 FEB. 1975

CHUKCHI SEA



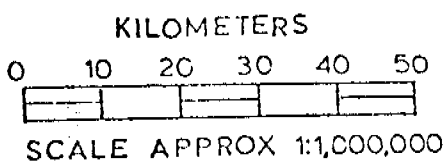
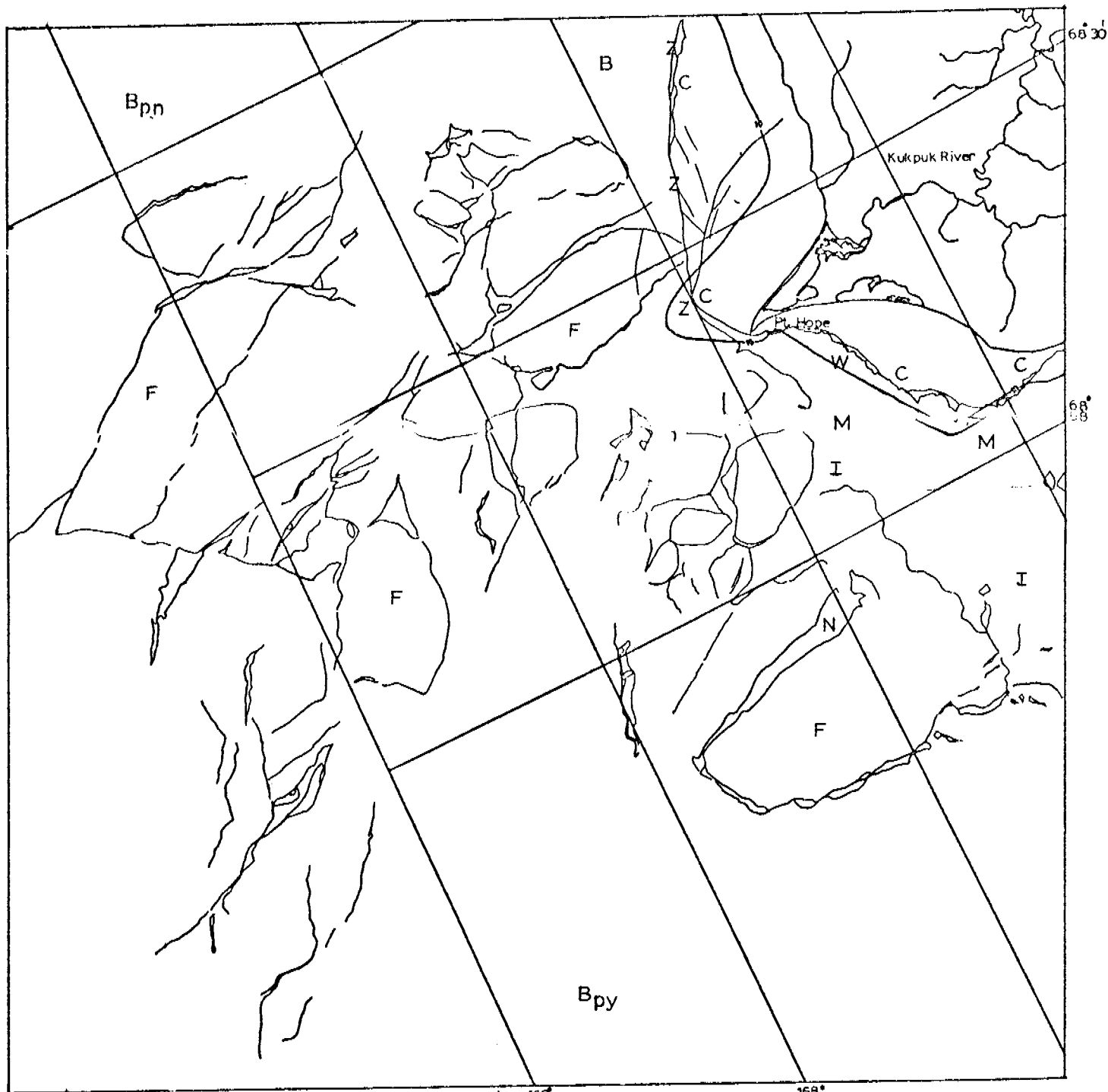
E-1947-22043-7
25 FEB. 1975

CHUKCHI SEA



E-1948-22094-7
26 FEB. 1975

CHUKCHI SEA



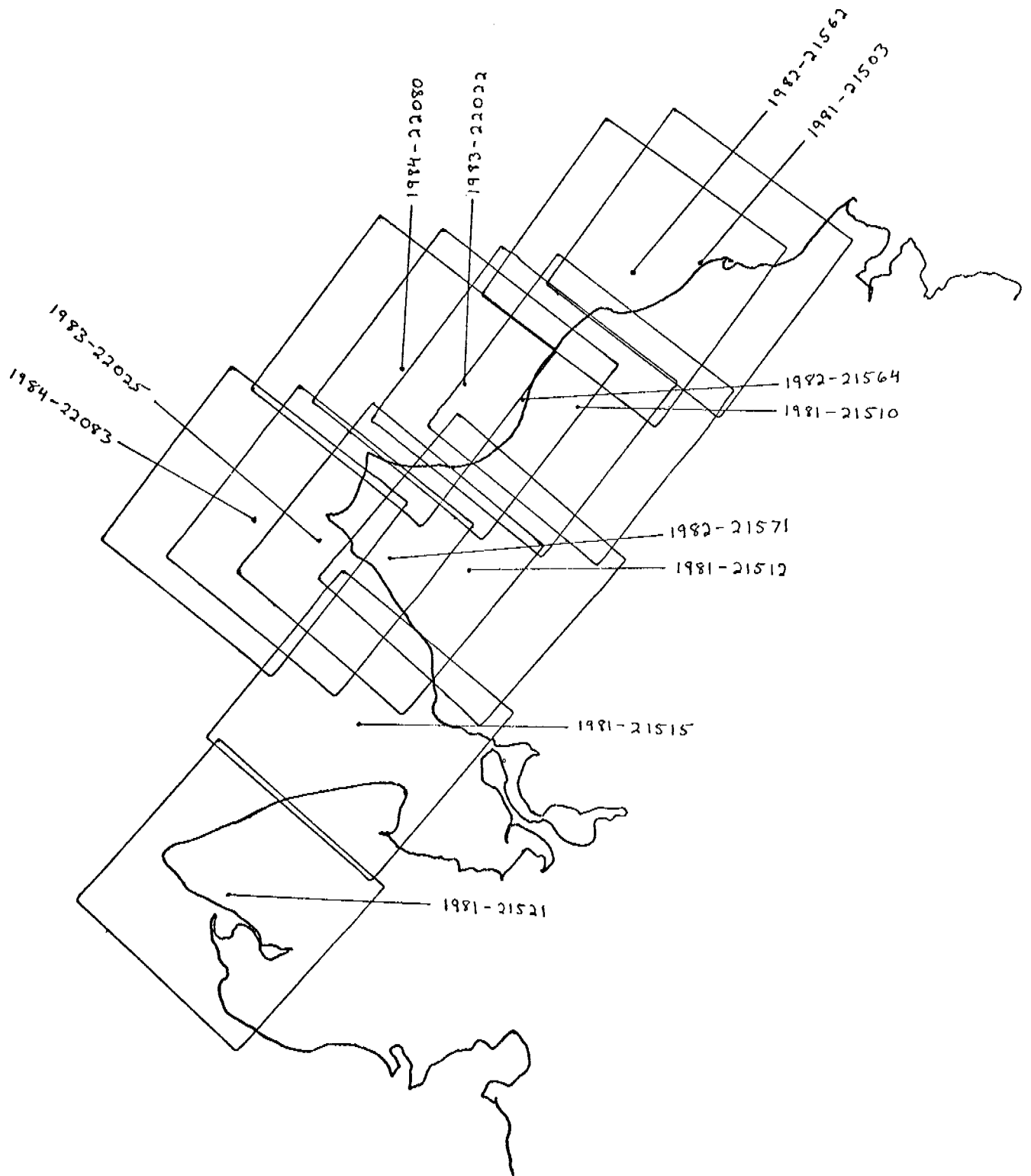
E-1948-22101-7
26 FEB. 1975

CHUKCHI SEA

CHUKCHI SEA

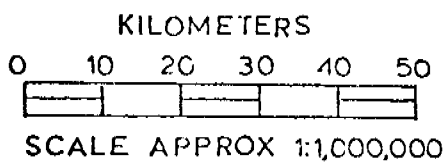
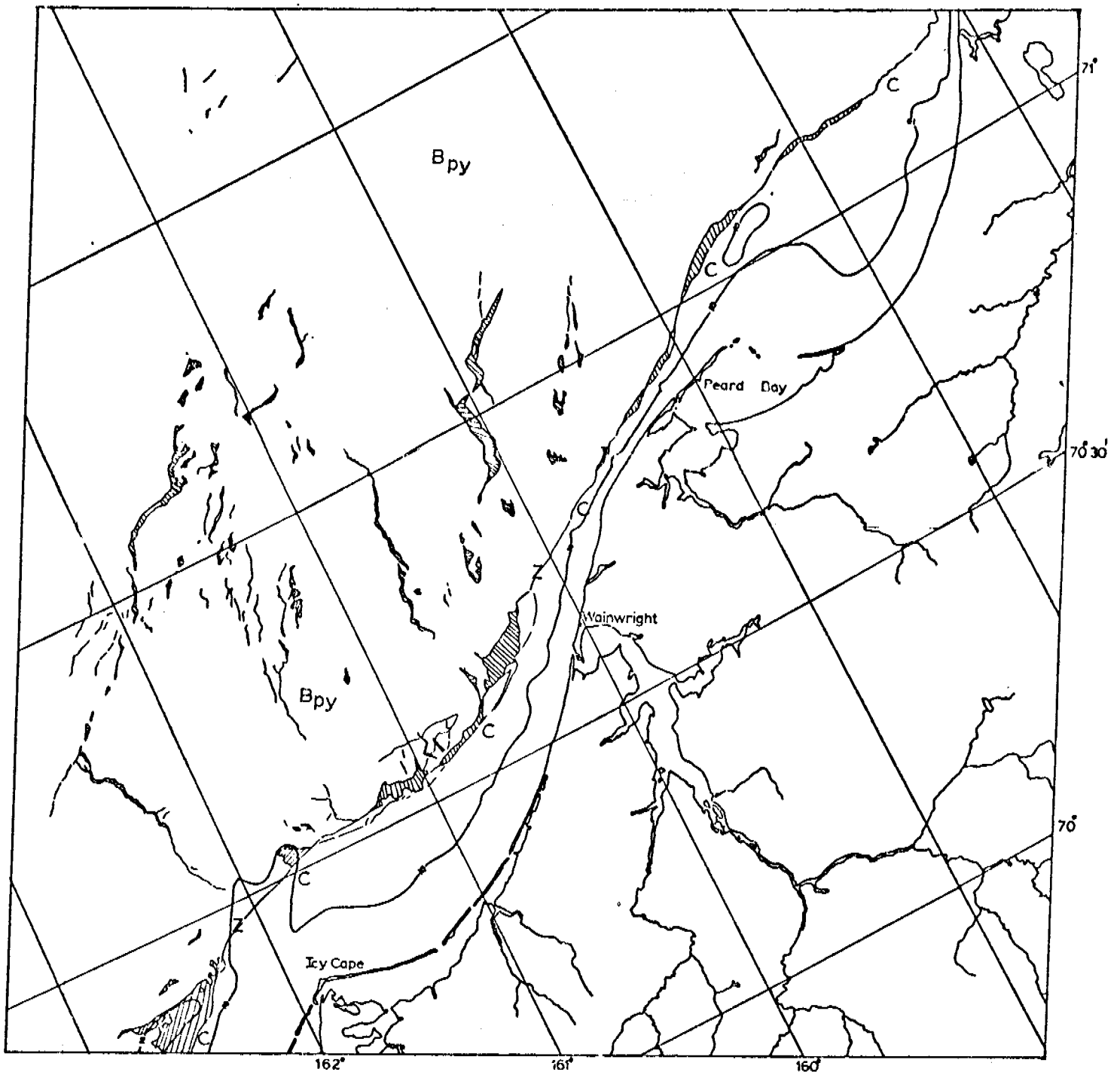
28 MARCH-14 APRIL 1975

Cycle 1978 - 1995



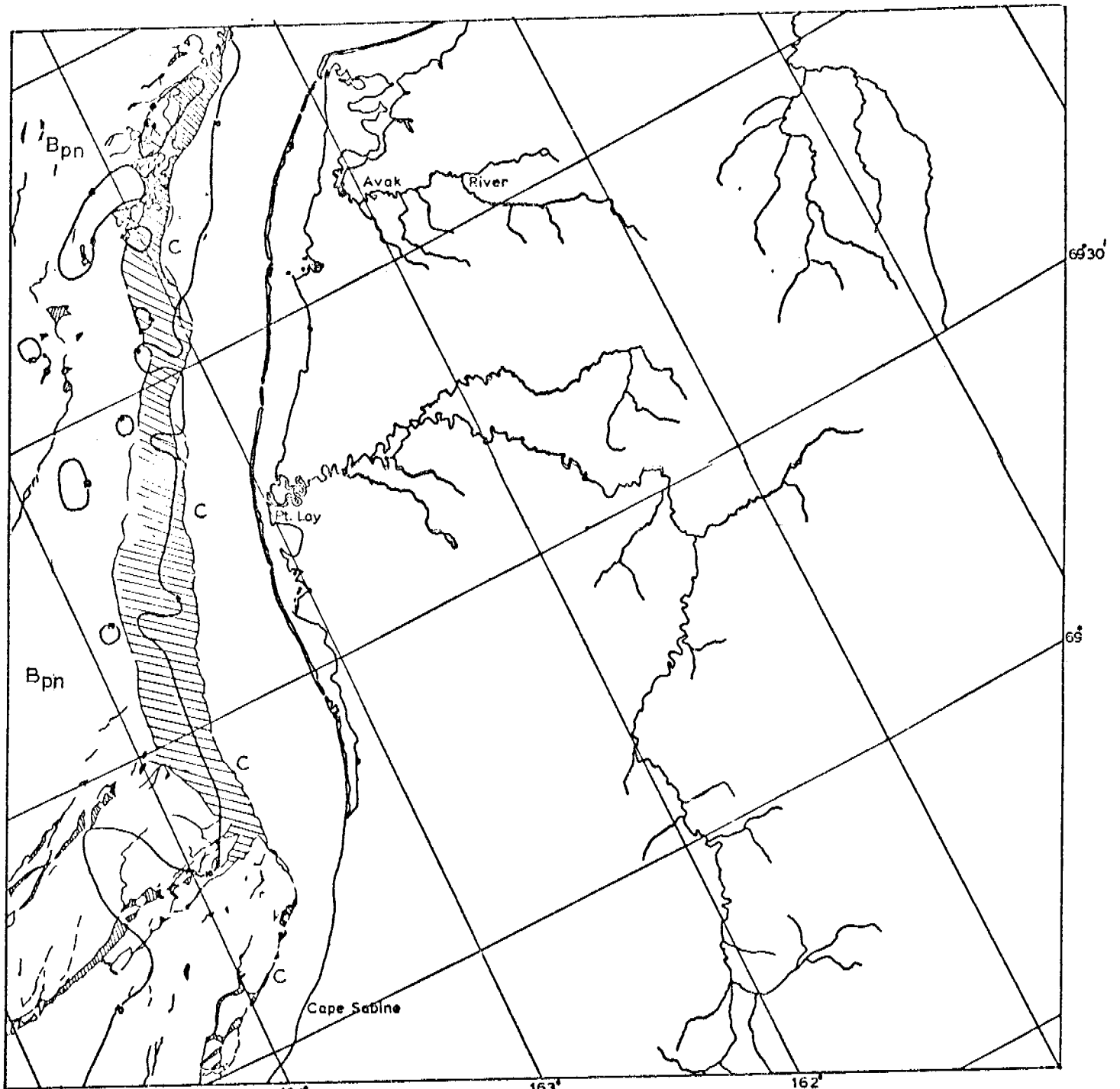
Scenes 1981-21503 through 2080-22151

These scenes show the Chukchi coast for the period March 31 through April 12, 1975. As in the previous cycle of imagery mapped the ice appears to have been in motion for some time. The active edge of ice appears to have changed little since the previous cycle of images with the exception of outer Kotzebue sound where additional ice has become mobilized. Large expanses of apparently grounded ice can be found on shoals north of Cape Prince of Wales, Point Hope, and on Blossom Shoals. Indentations in contiguous ice shoreward of the 10-fathom contour can be found southeast of Point Hope, south of Cape Lisburne and south of Icy Cape, following the pattern established earlier.

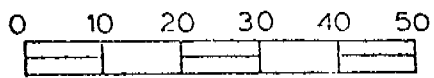


E-1981-21503-7
31 MARCH 1975

CHUKCHI SEA



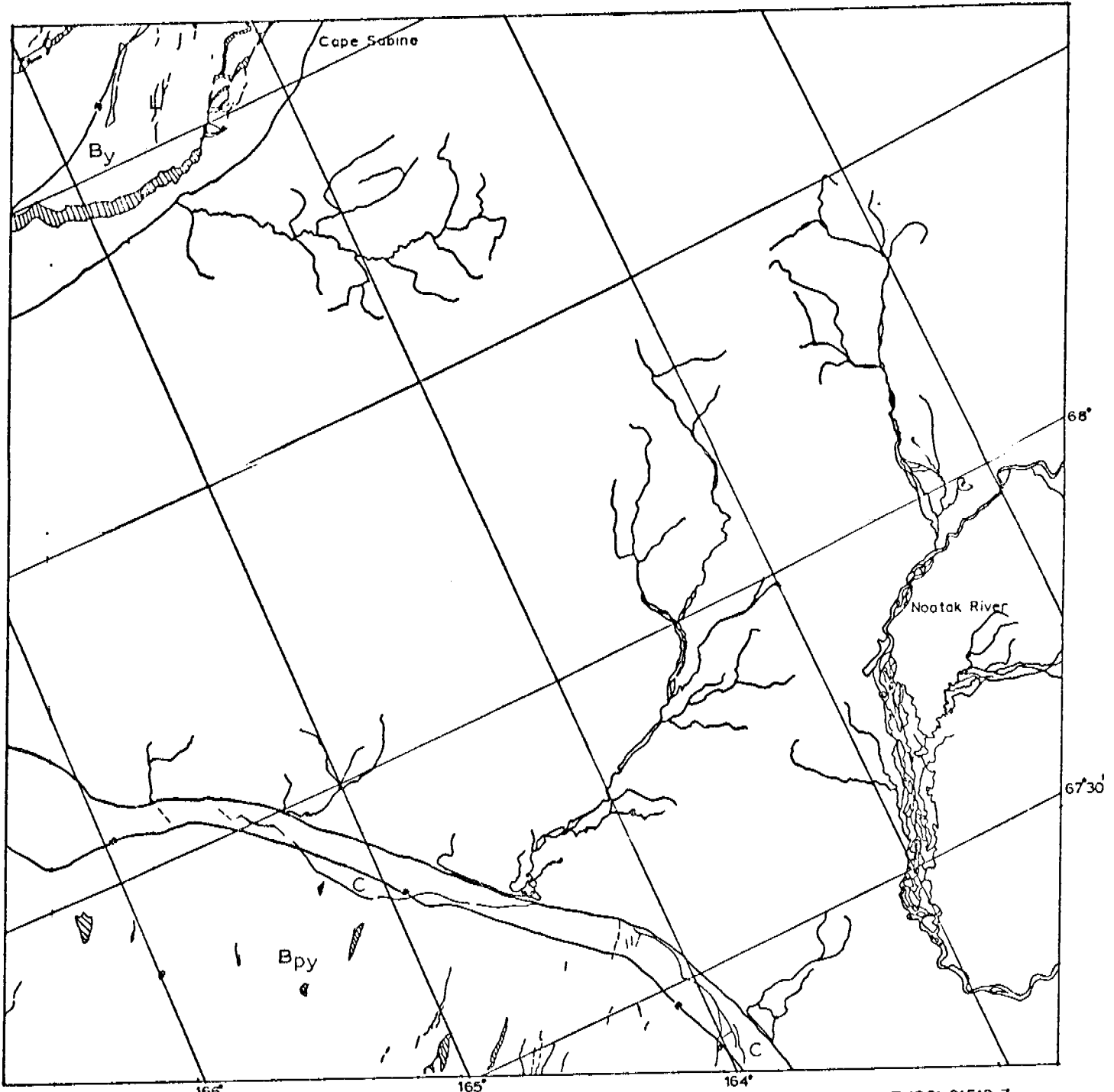
KILOMETERS



SCALE APPROX 1:1,000,000

E-1931-21510-7
31 MARCH 1975

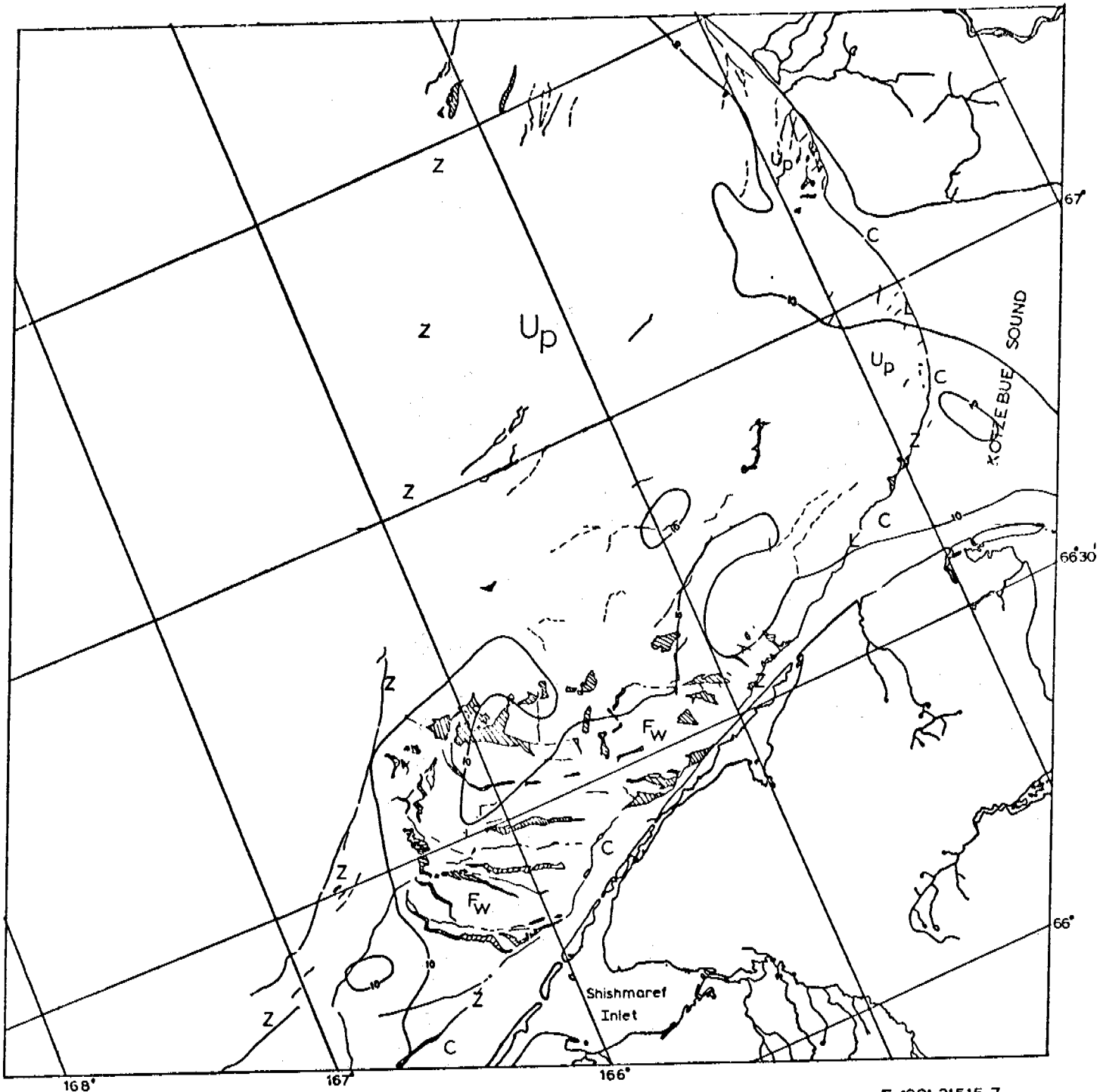
CHUKCHI SEA



E-1981-21512-7
31 MARCH 1975

KILOMETERS
0 10 20 30 40 50
SCALE APPROX 1:1,000,000

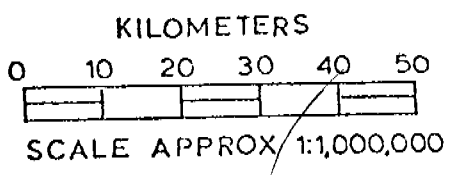
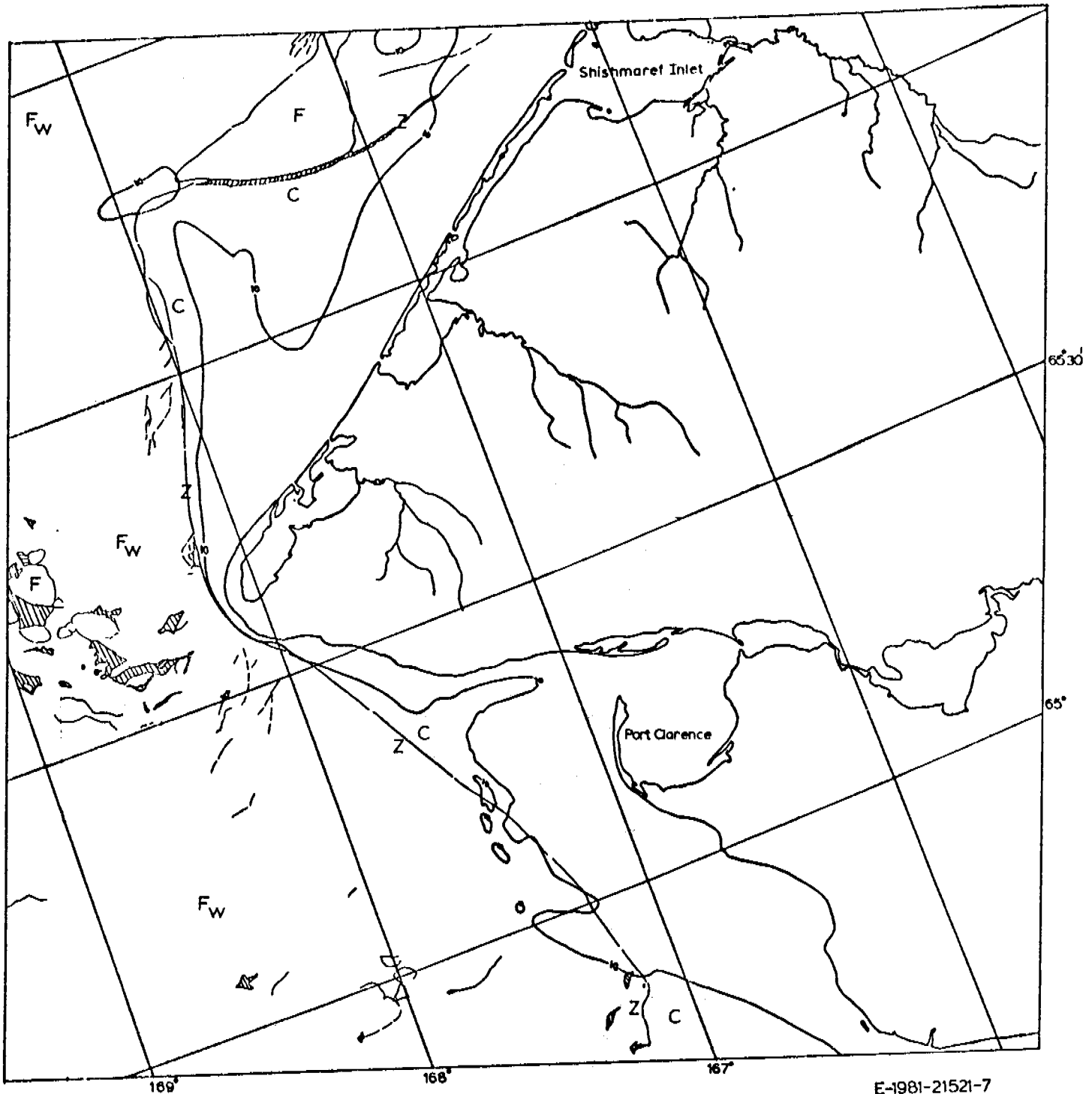
CHUKCHI SEA



KILOMETERS
 0 10 20 30 40 50
 SCALE APPROX 1:1,000,000

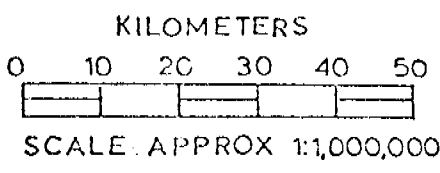
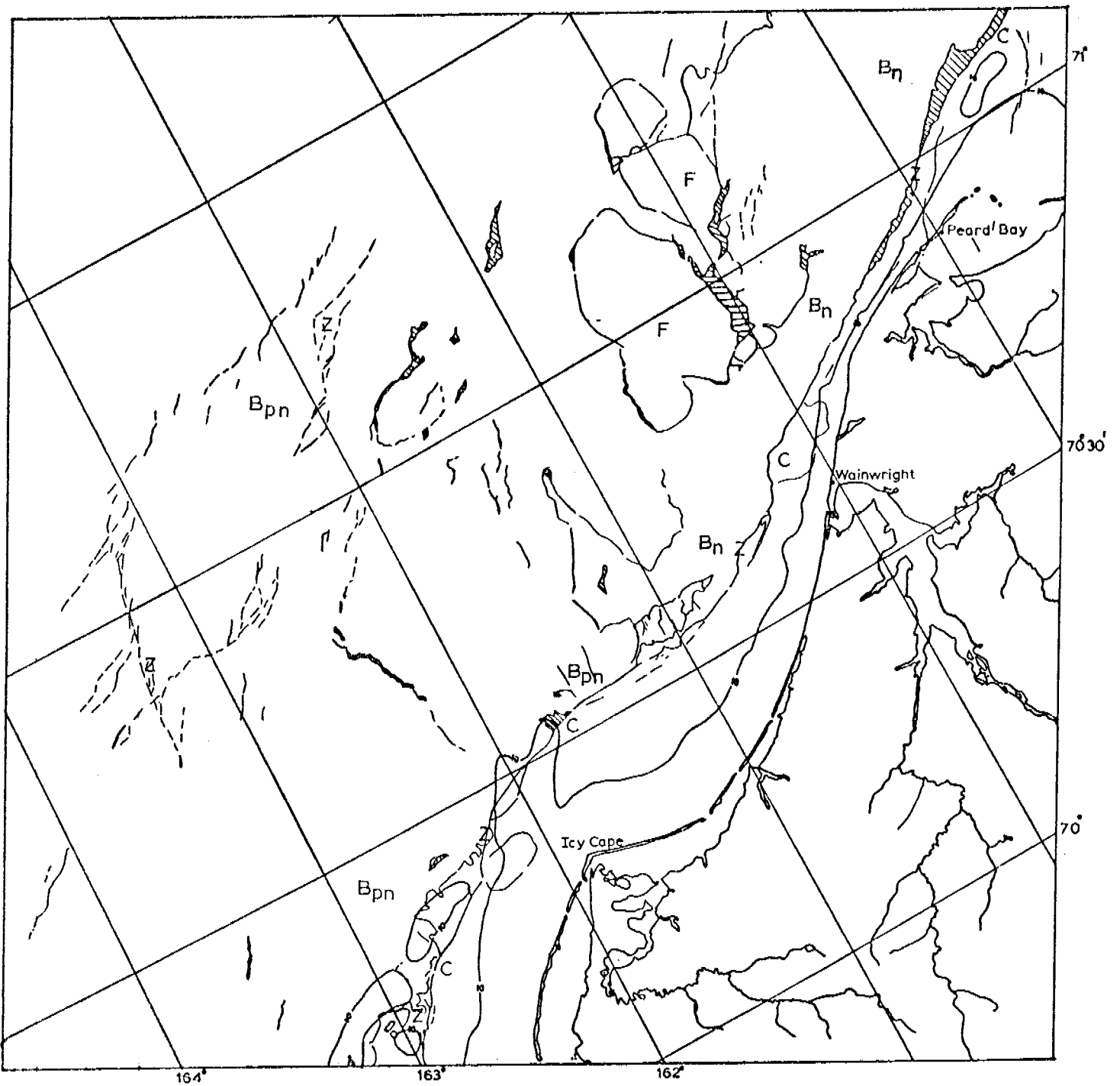
E 1981-21515-7
 31 MARCH 1975

CHUKCHI SEA



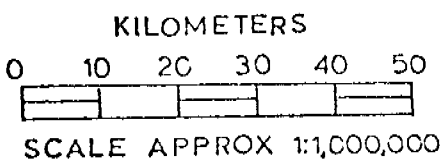
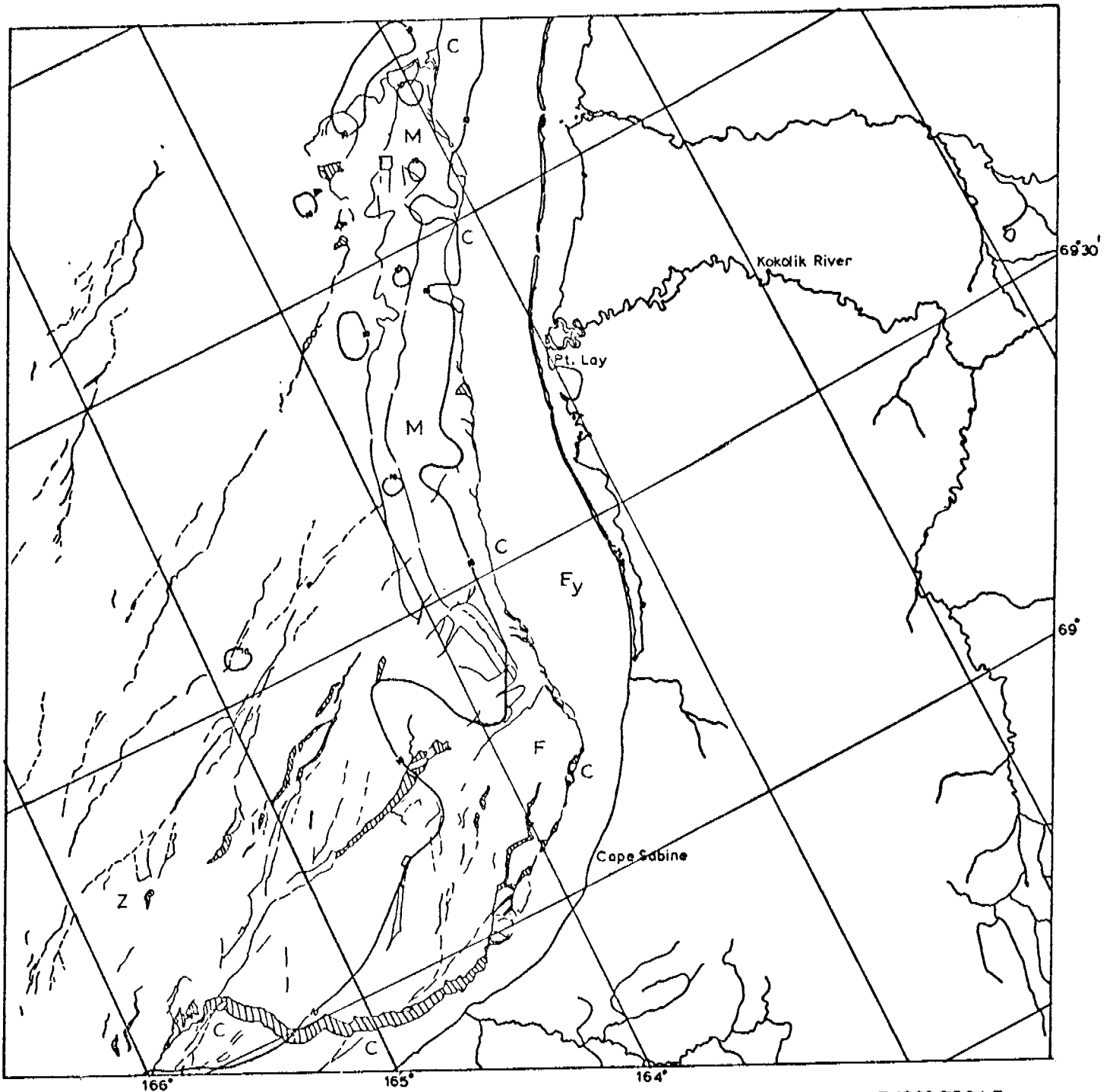
E-1981-21521-7
31 MARCH 1975

CHUKCHI SEA



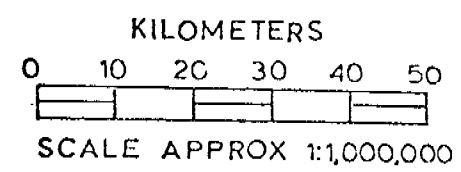
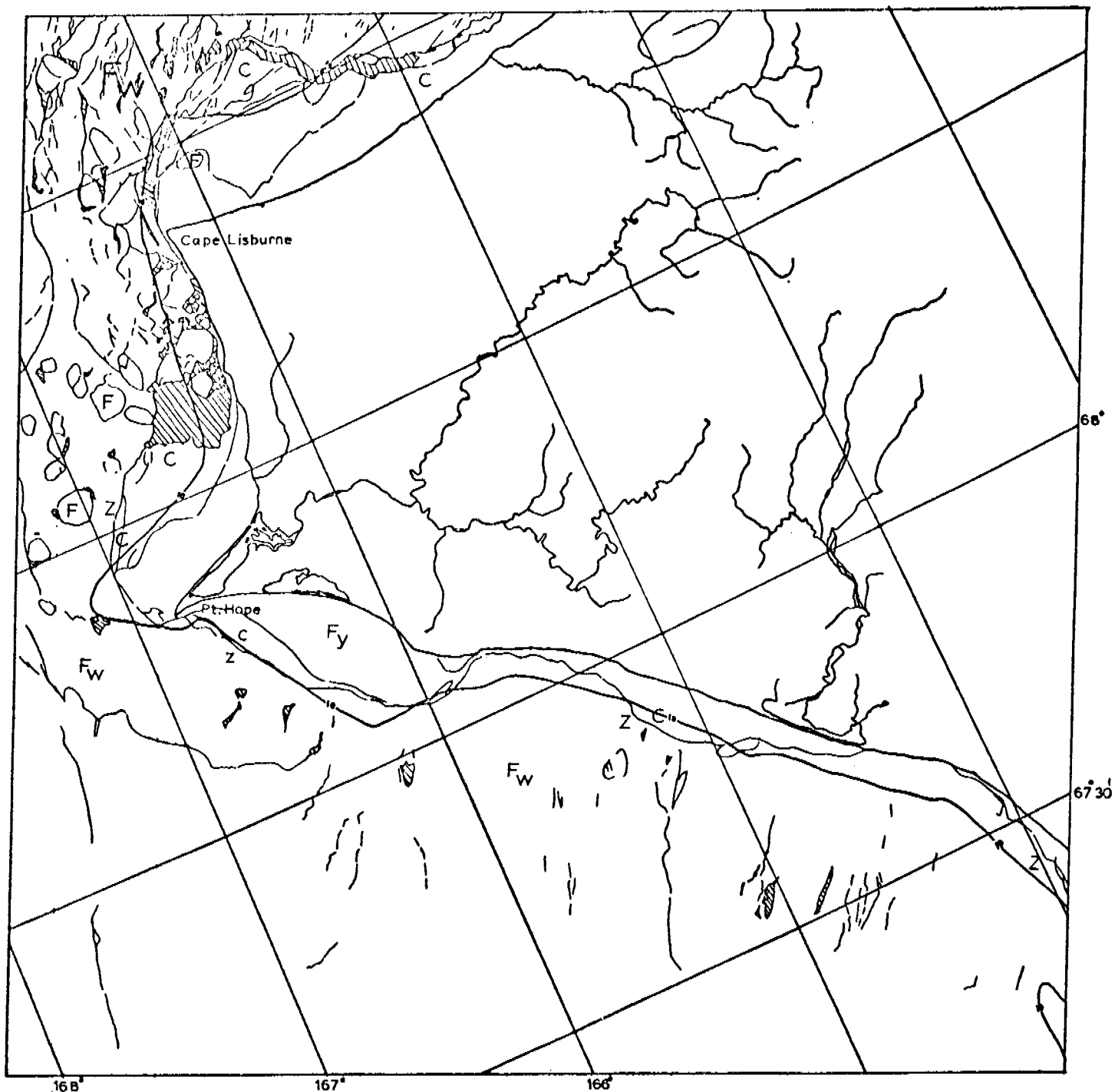
E-1982-21562-7
1 APRIL 1975

CHUKCHI SEA



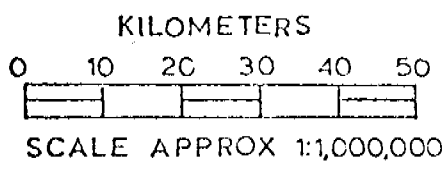
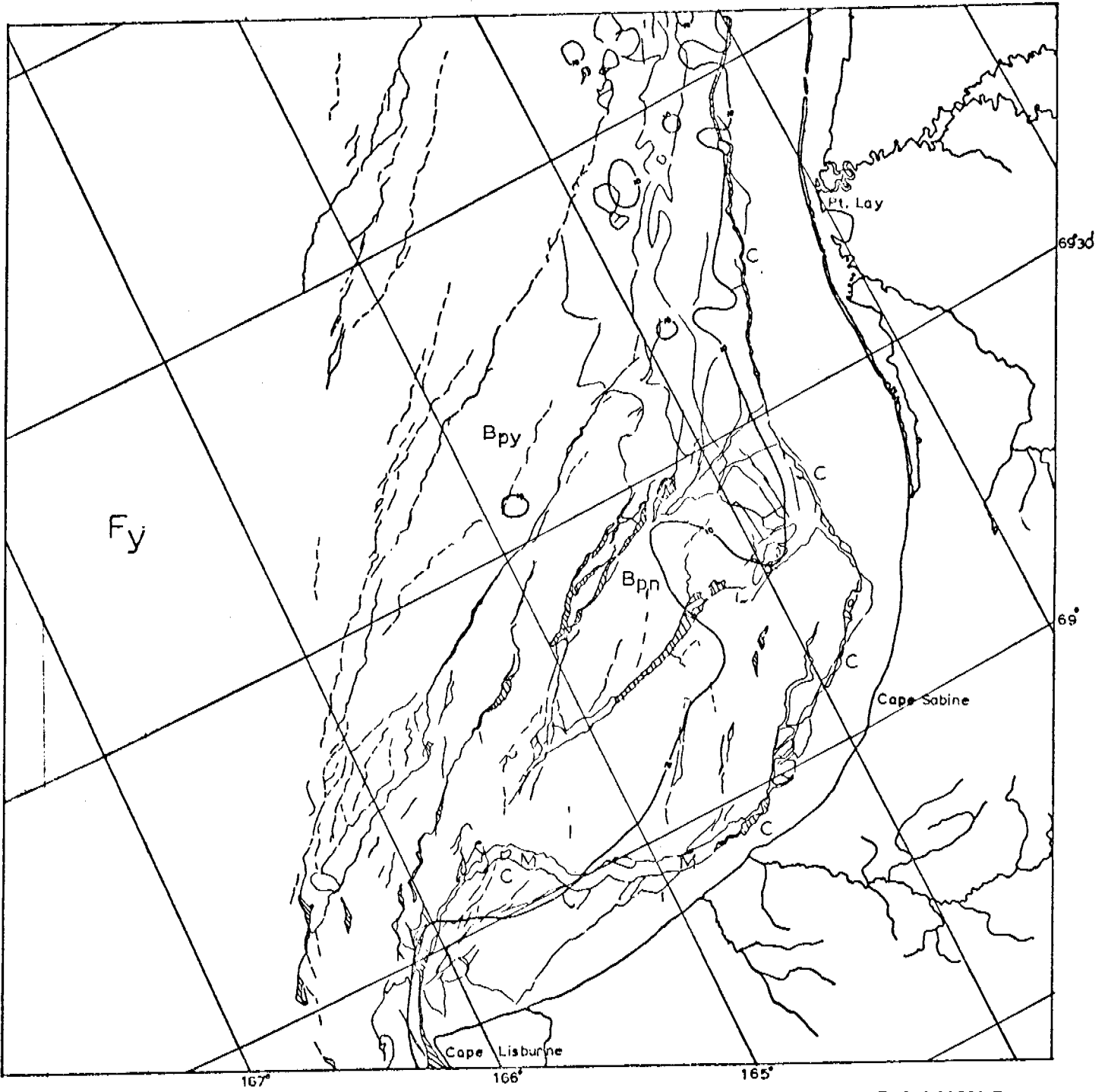
E-1982-2564-7
1 APRIL 1975

CHUKCHI SEA



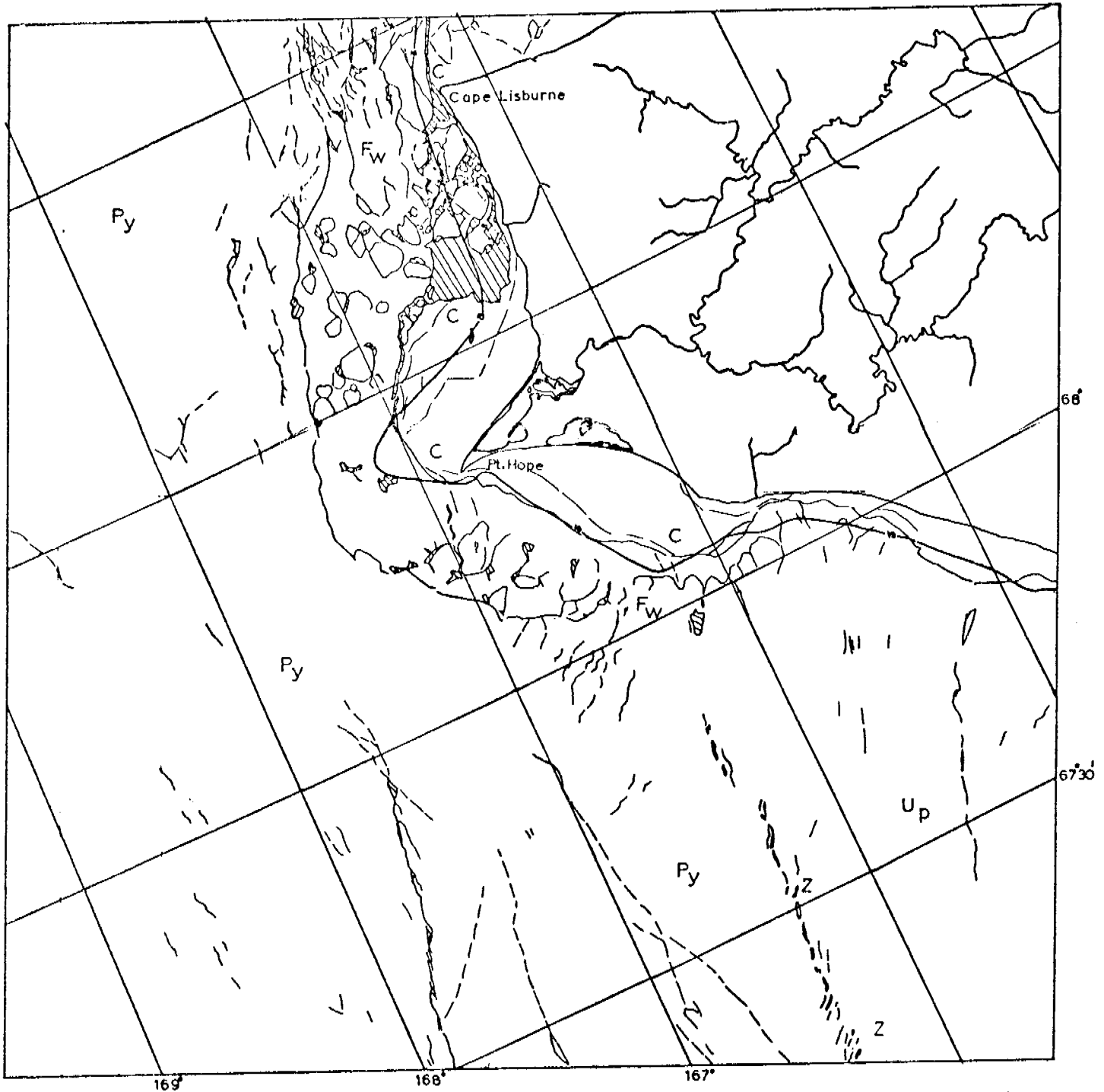
E-1982-21571-7
1 APRIL 1975

CHUKCHI SEA



E-1983-22022-7
2 APRIL 1975

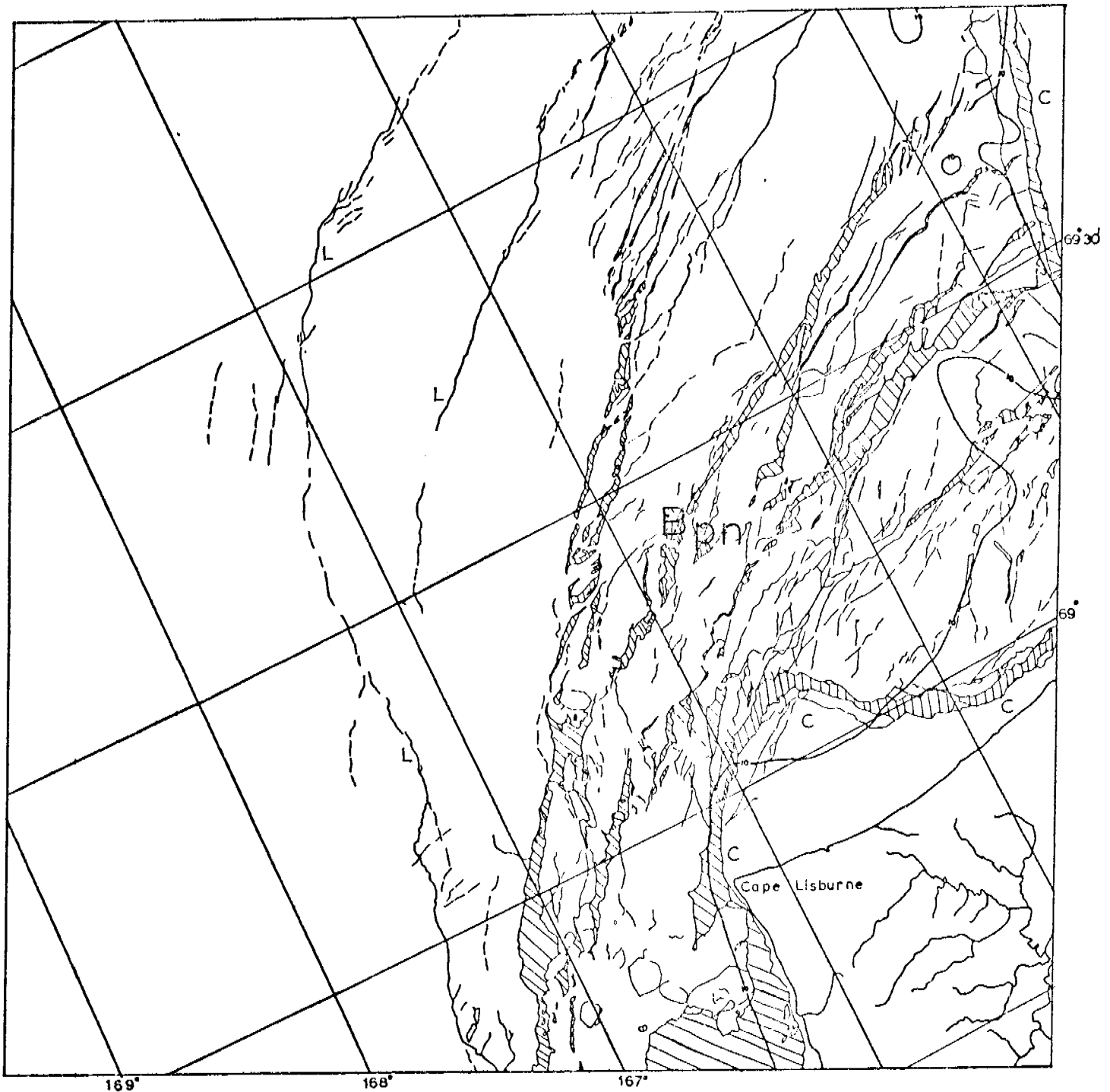
CHUKCHI SEA



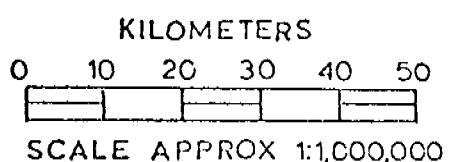
KILOMETERS
 0 10 20 30 40 50
 SCALE APPROX 1:1,000,000

E-1983-22025-7
 2 APRIL 1975

CHUKCHI SEA

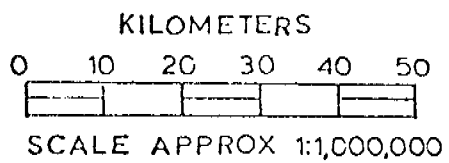
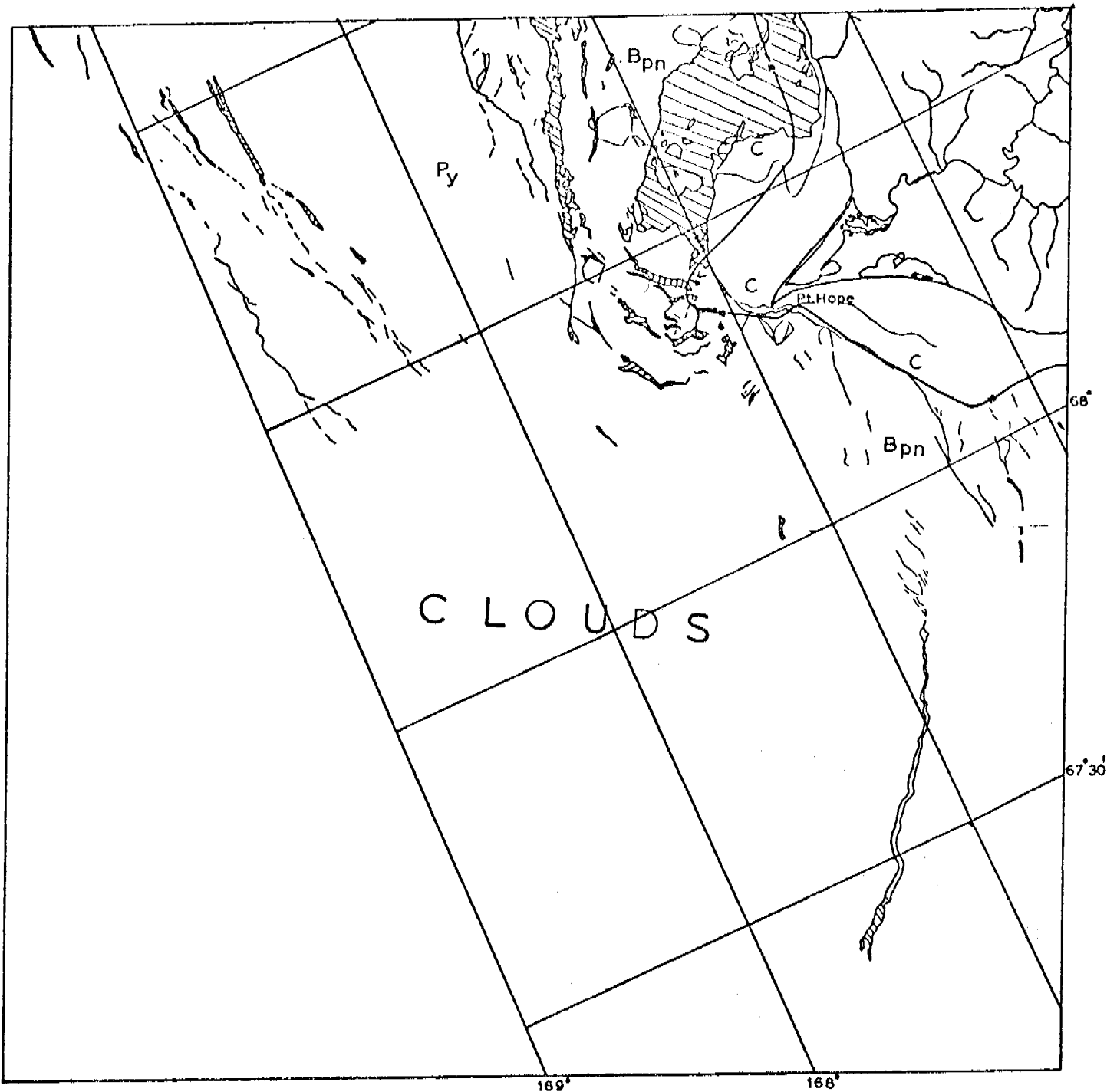


169° 168° 167°



E-1984-22080-7
3 APRIL 1975

CHUKCHI SEA



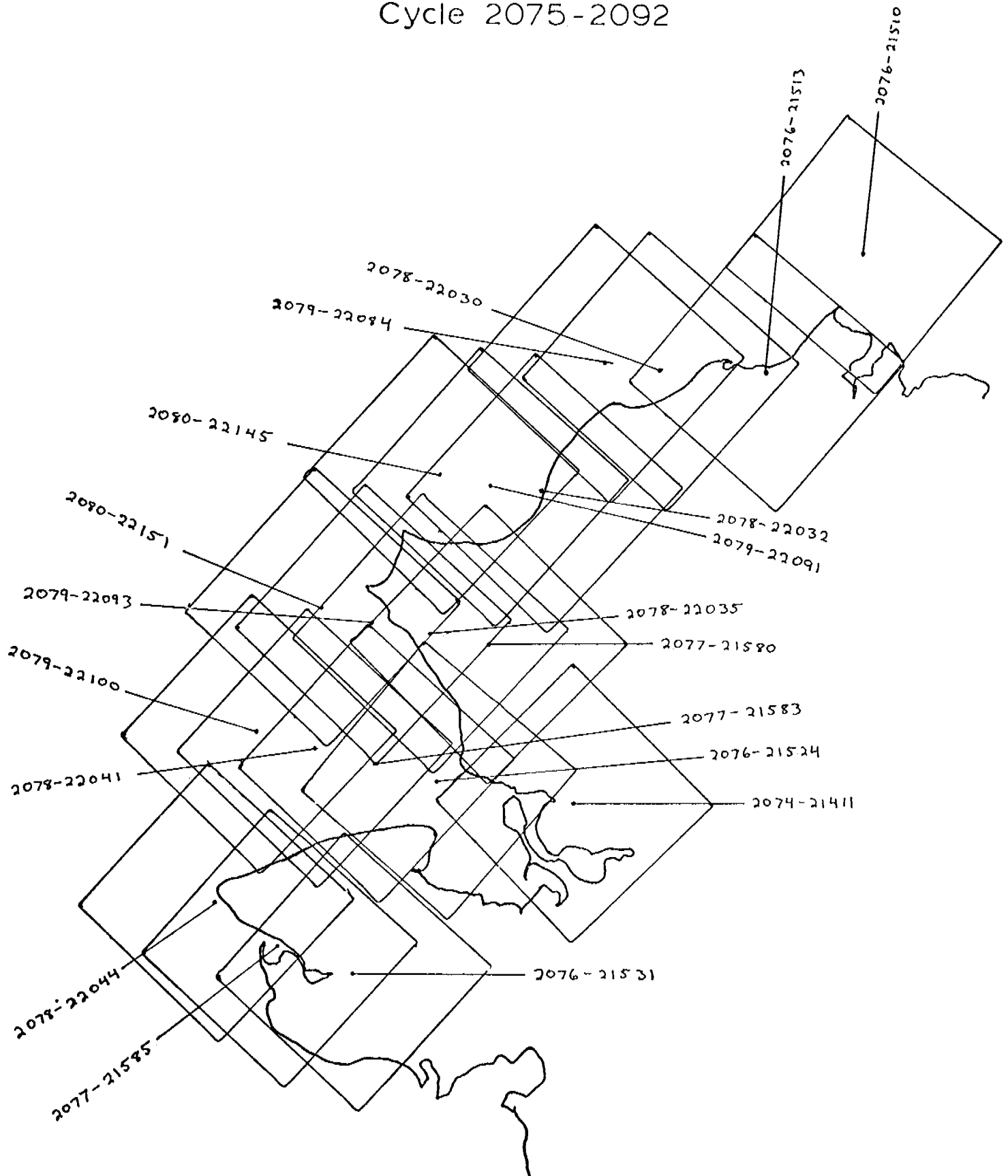
E-1984-22083-7
3 APRIL 1975

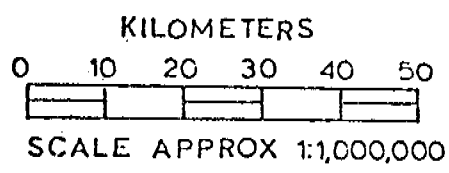
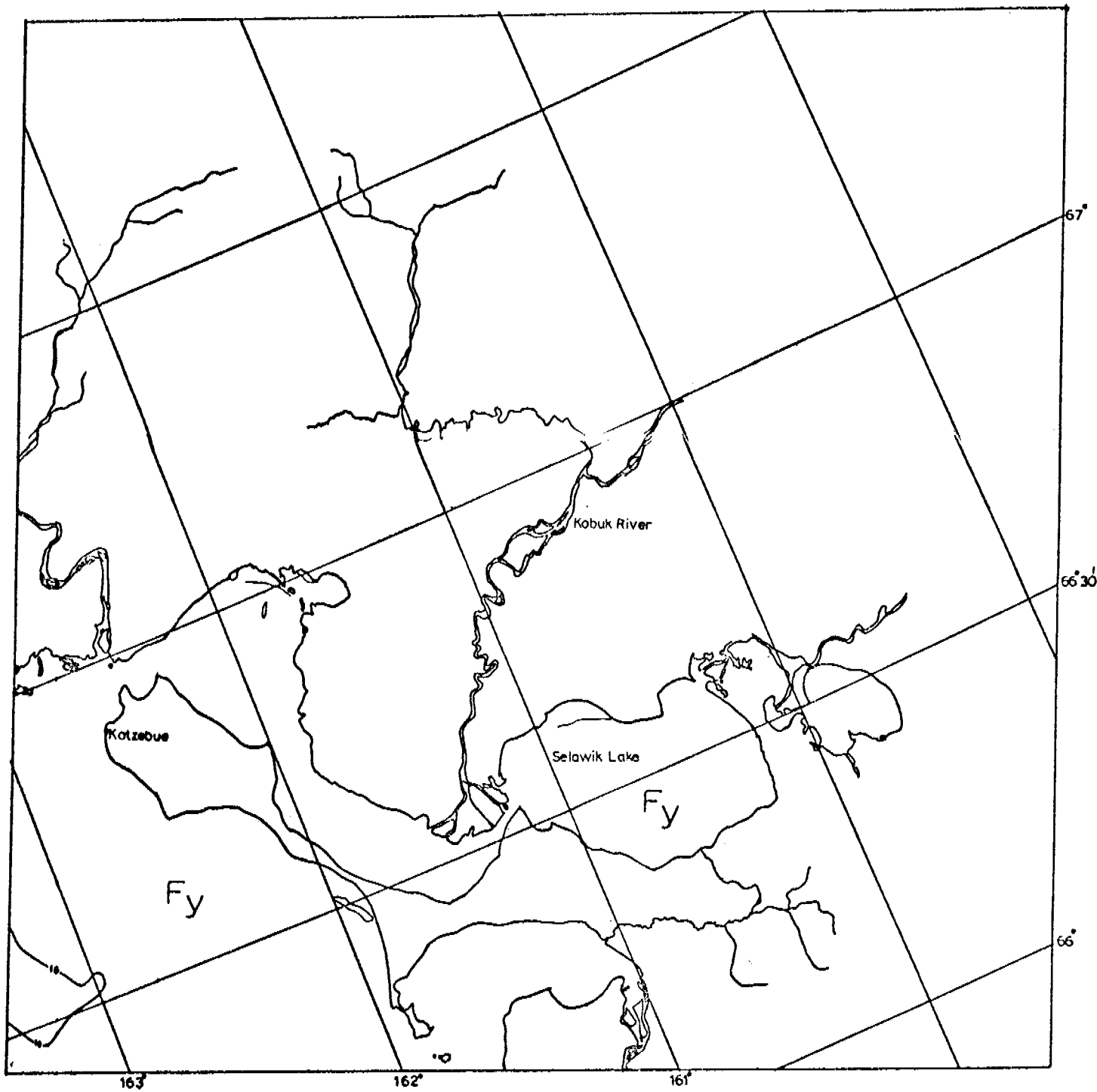
CHUKCHI SEA

CHUKCHI SEA

6-23 APRIL 1975

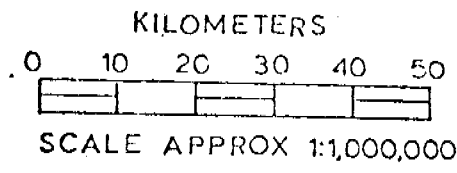
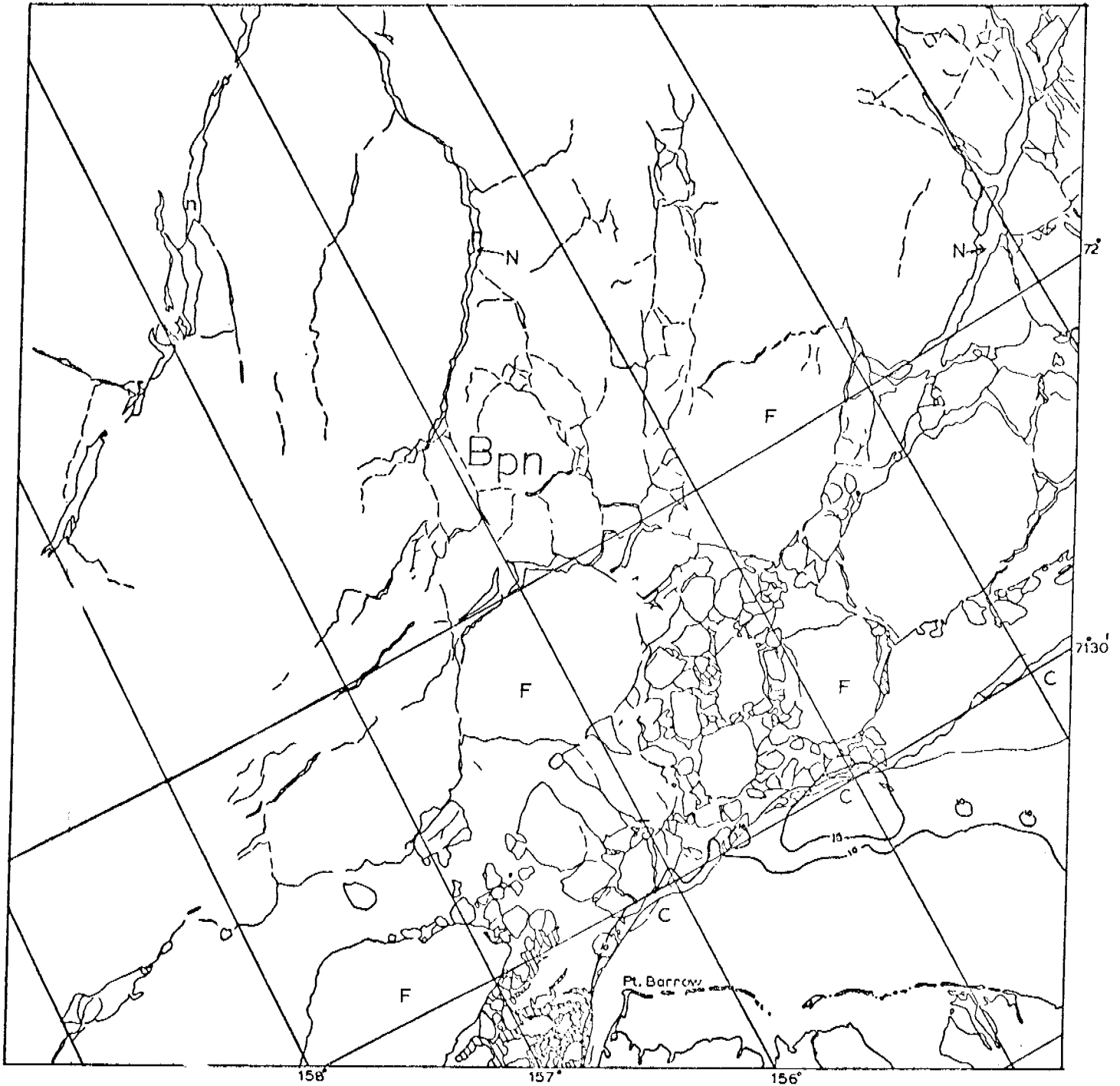
Cycle 2075-2092





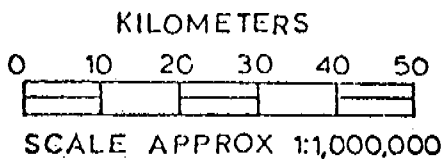
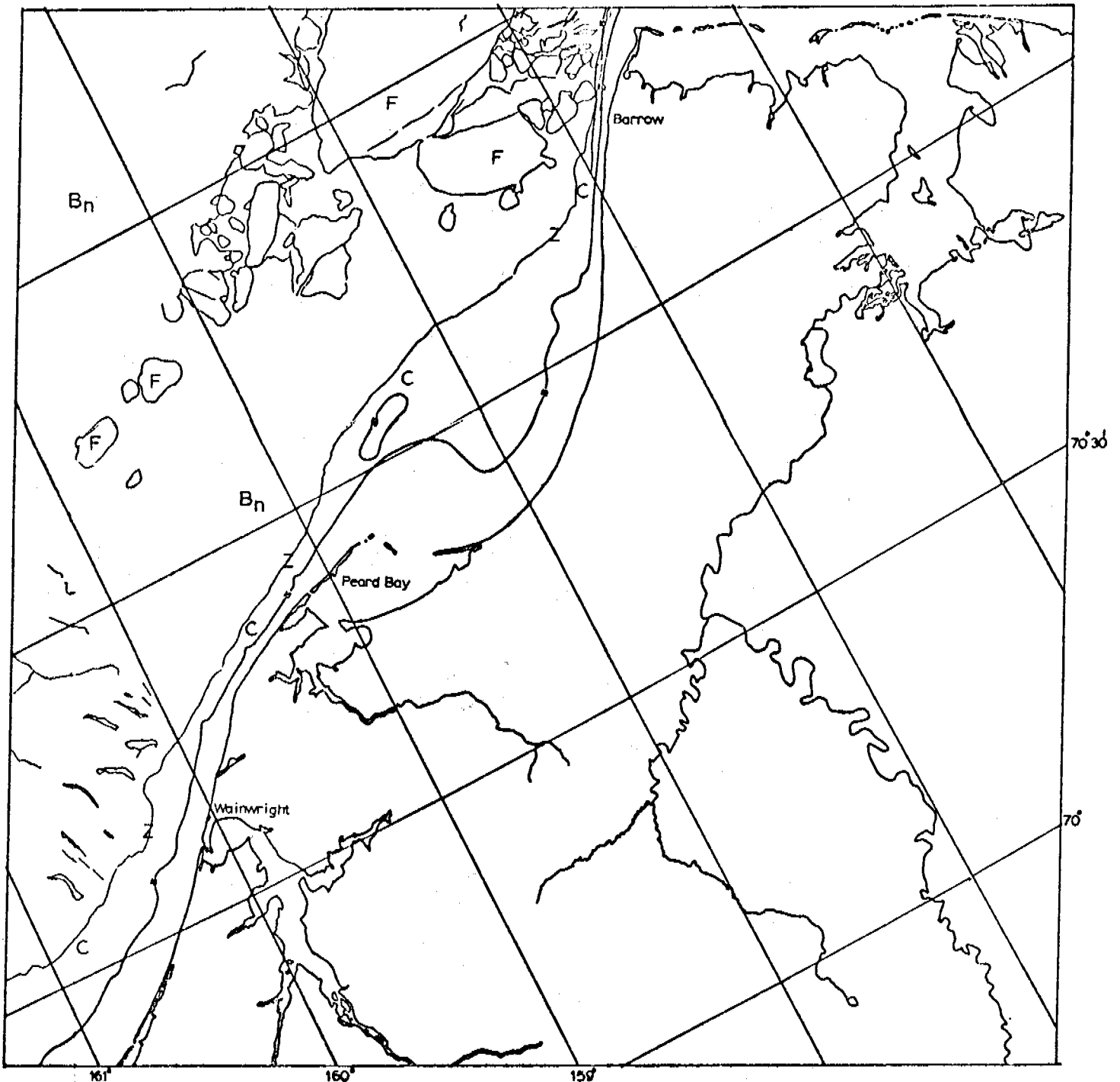
E-2074-21411-7
6 APRIL 1975

CHUKCHI SEA



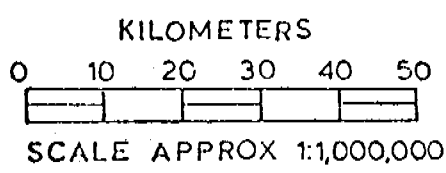
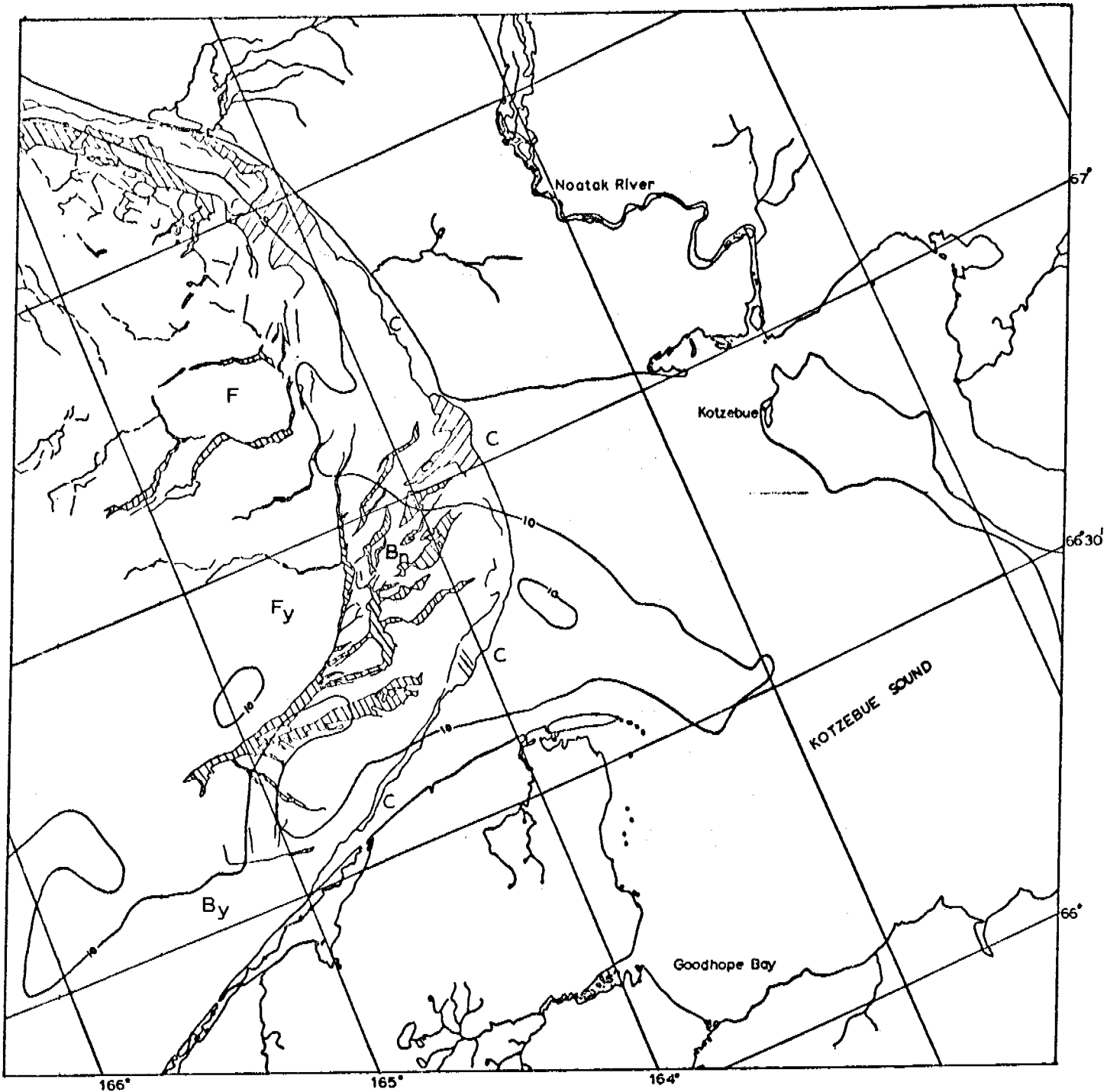
6-2076-21510-7
8 APRIL 1975

CHUKCHI SEA



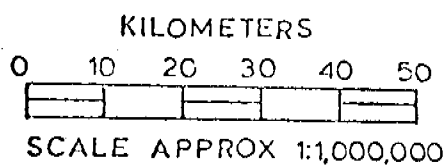
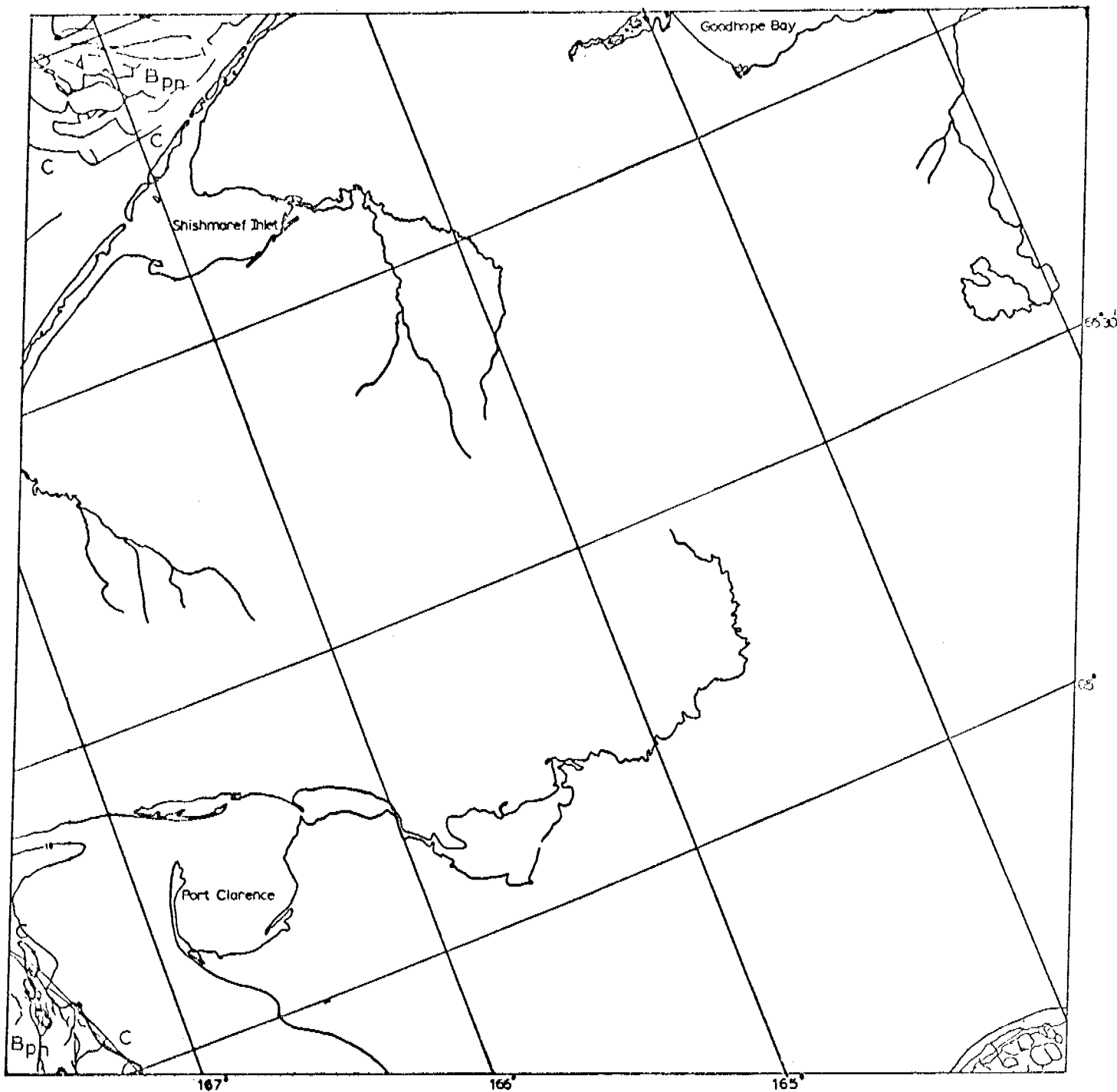
E-2076-21513-7
8 APRIL 1975

CHUKCHI SEA



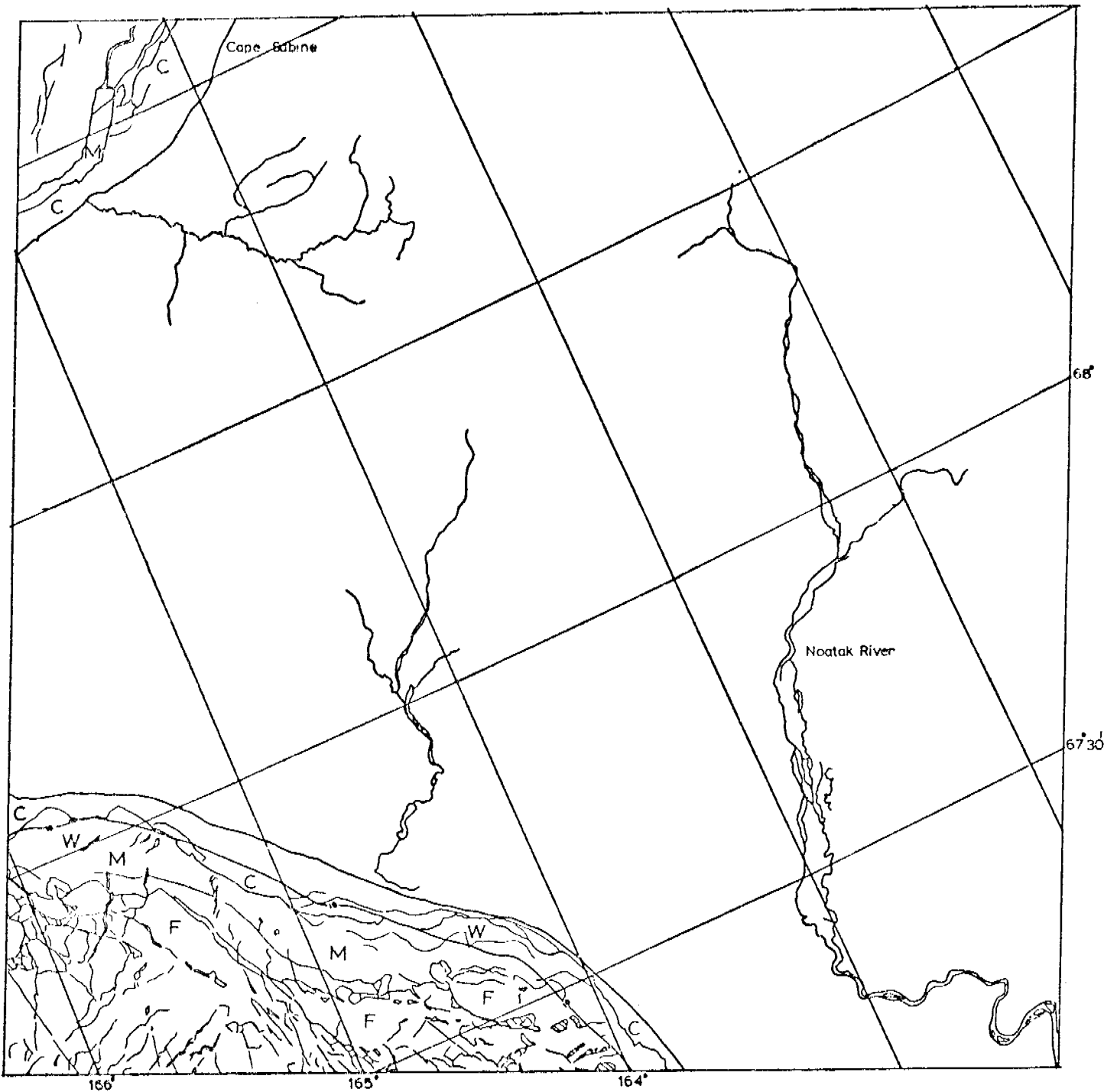
E-2076-21524-7
8 APRIL 1975

CHUKCHI SEA



E-2076-21531-7
B APRIL 1975

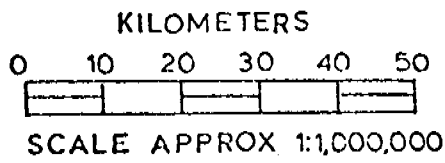
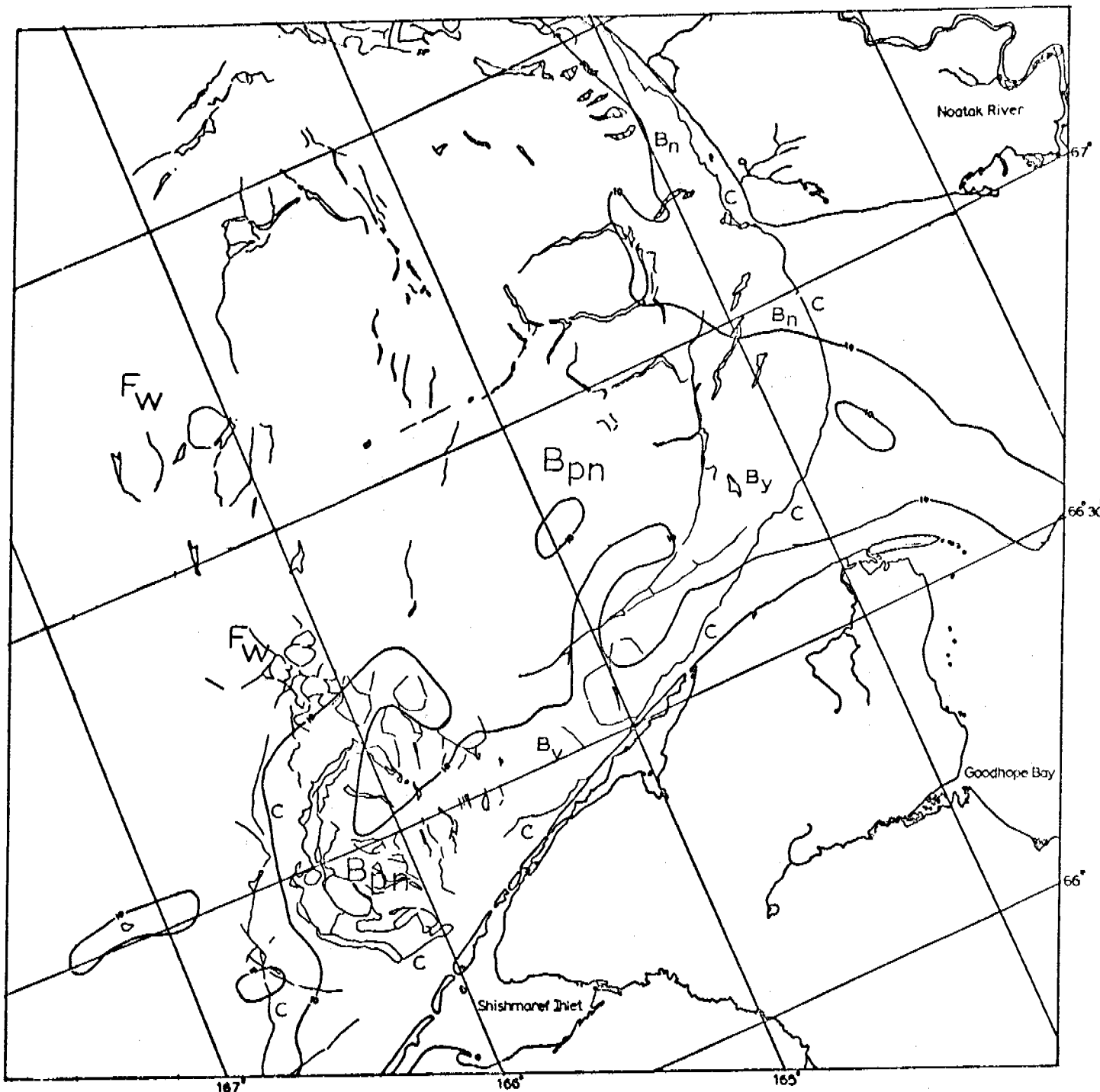
CHUKCHI SEA



KILOMETERS
 0 10 20 30 40 50
 SCALE APPROX 1:1,000,000

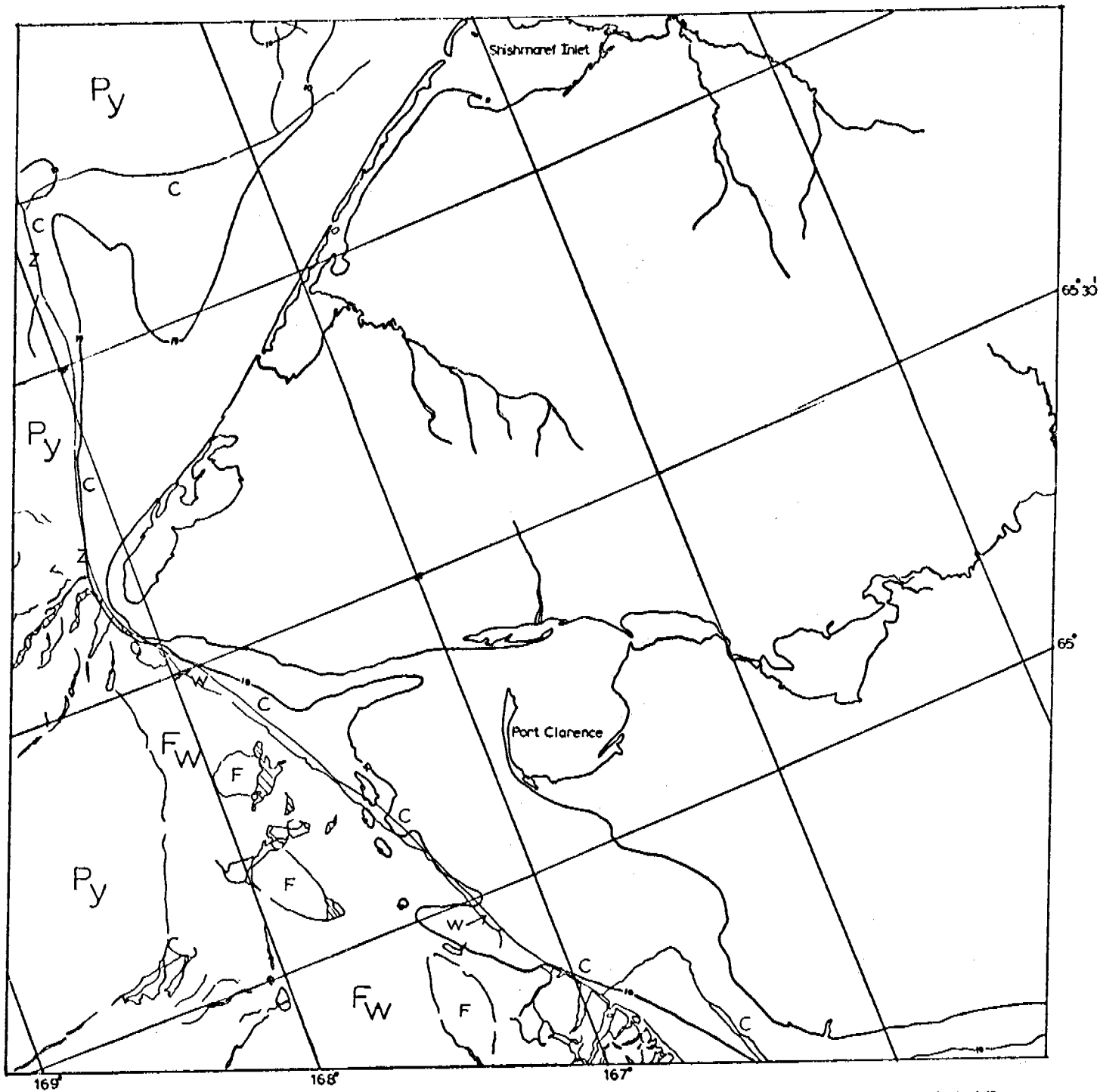
CHUKCHI SEA

E-2077-21580-7
 9 APRIL 1975



E-2077-21583-7
9 APRIL 1975

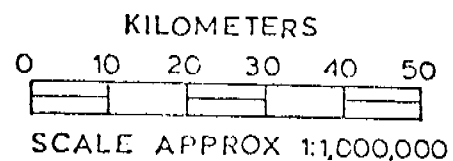
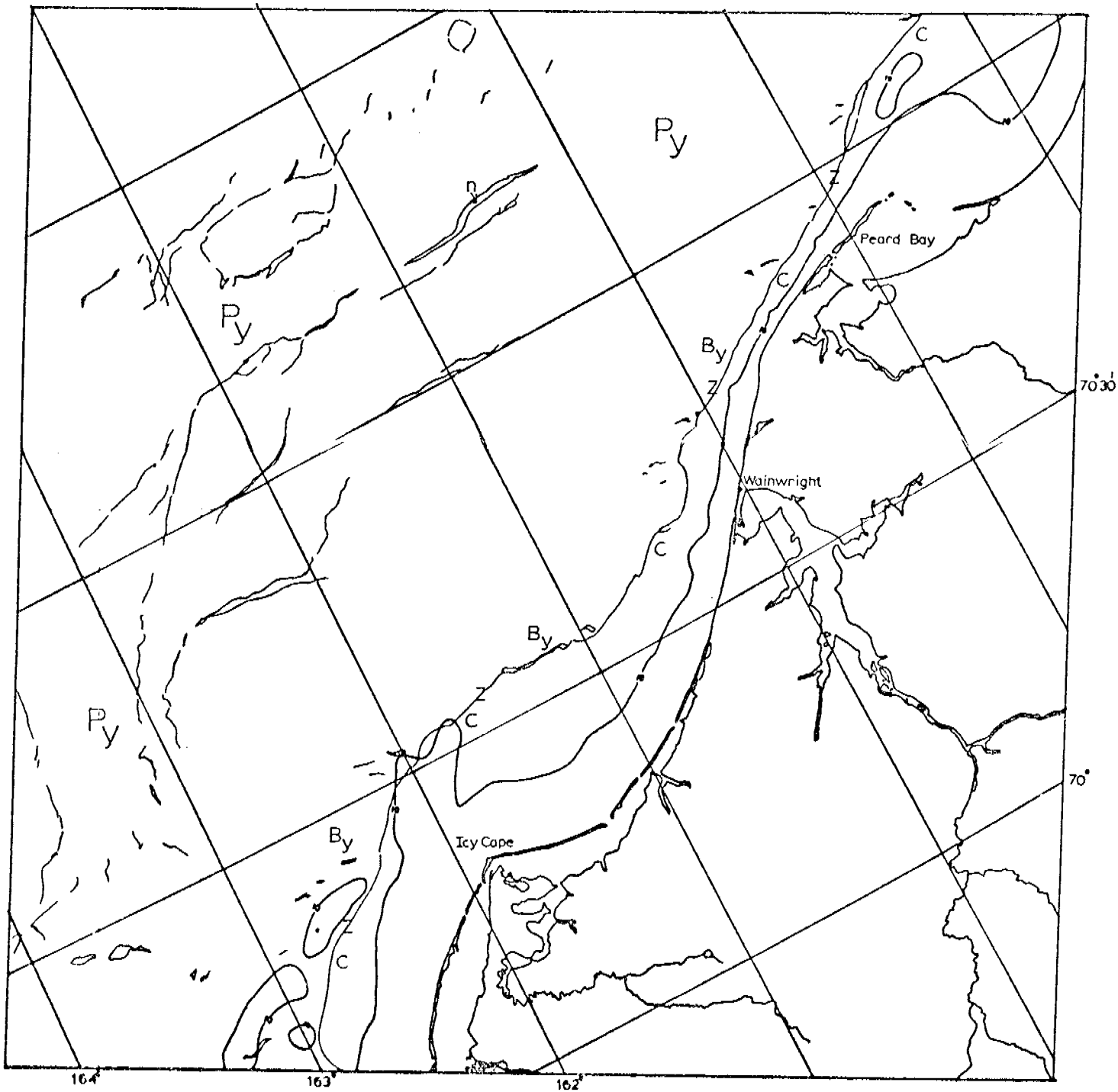
CHUKCHI SEA



E-2077-21503-7
9 APRIL 1975

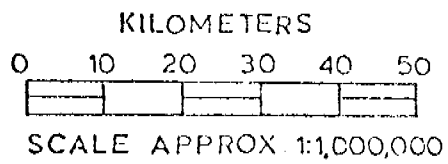
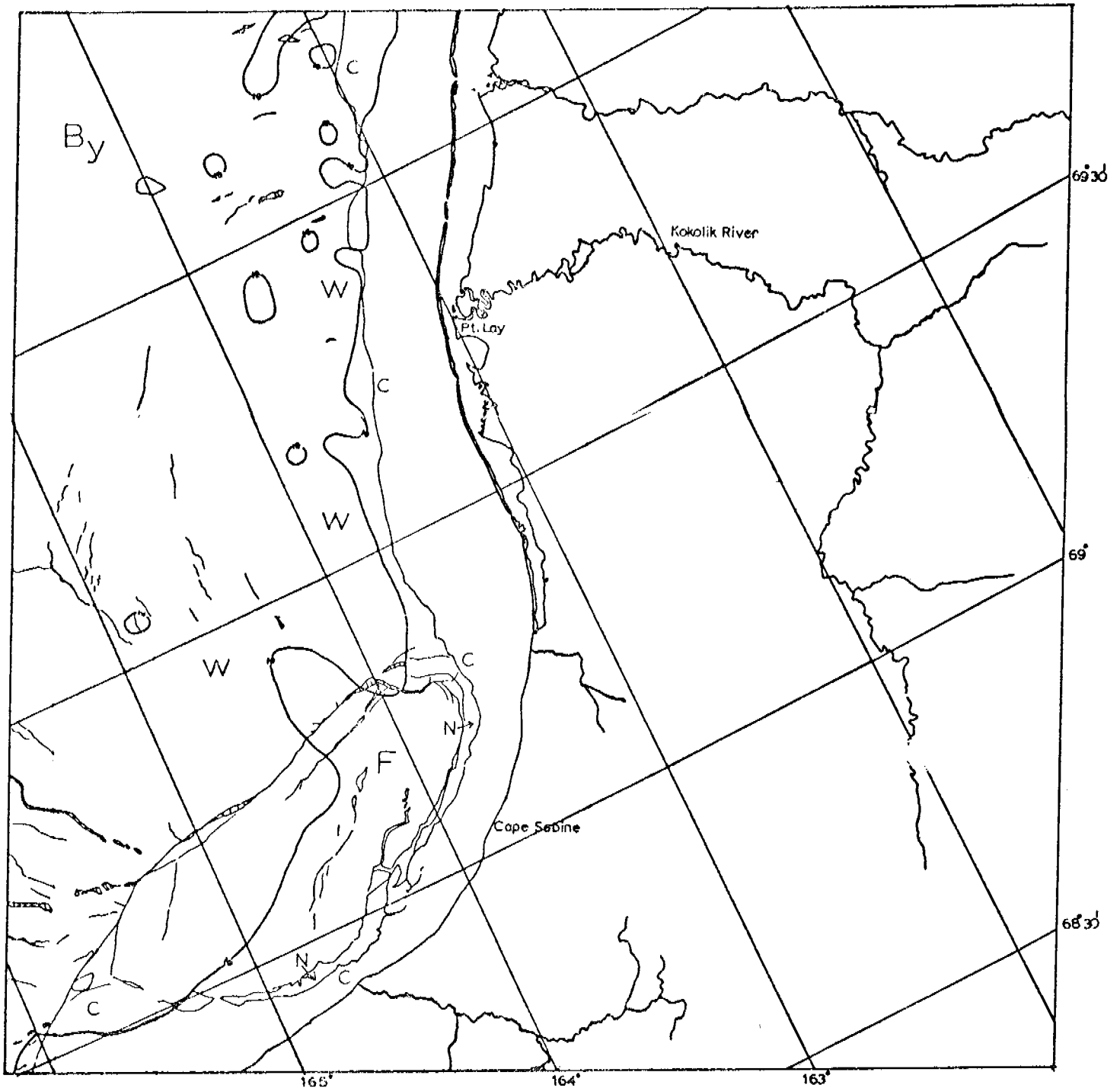
KILOMETERS
0 10 20 30 40 50
SCALE APPROX 1:1,000,000

CHUKCHI SEA



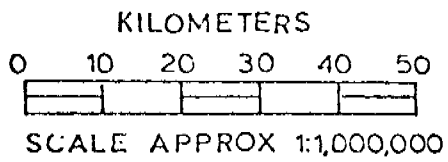
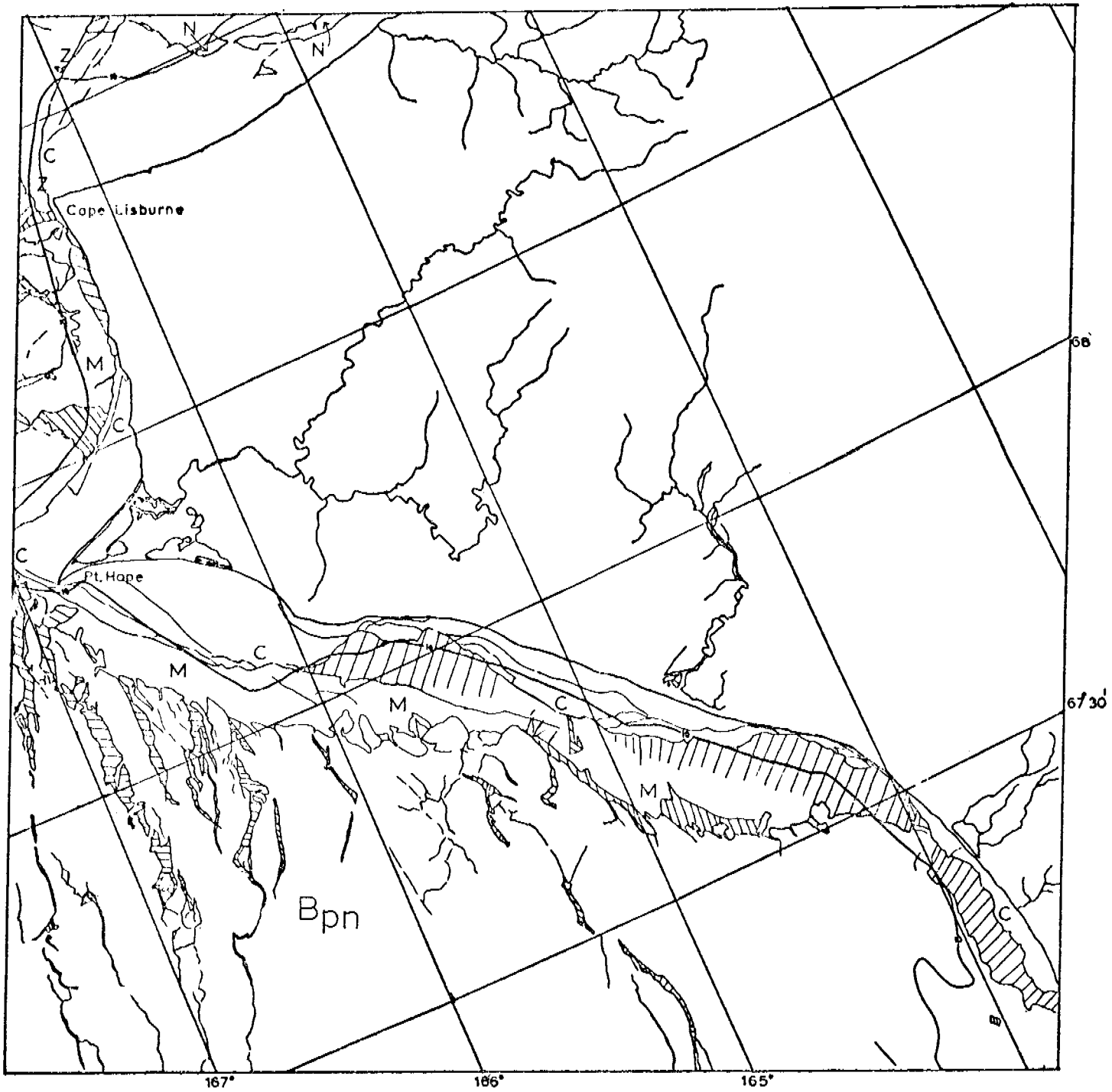
E-2078-22030-7
10 APRIL 1975

CHUKCHI SEA.



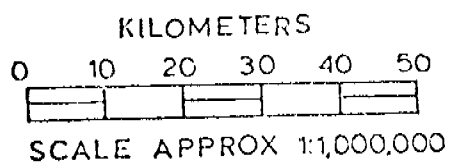
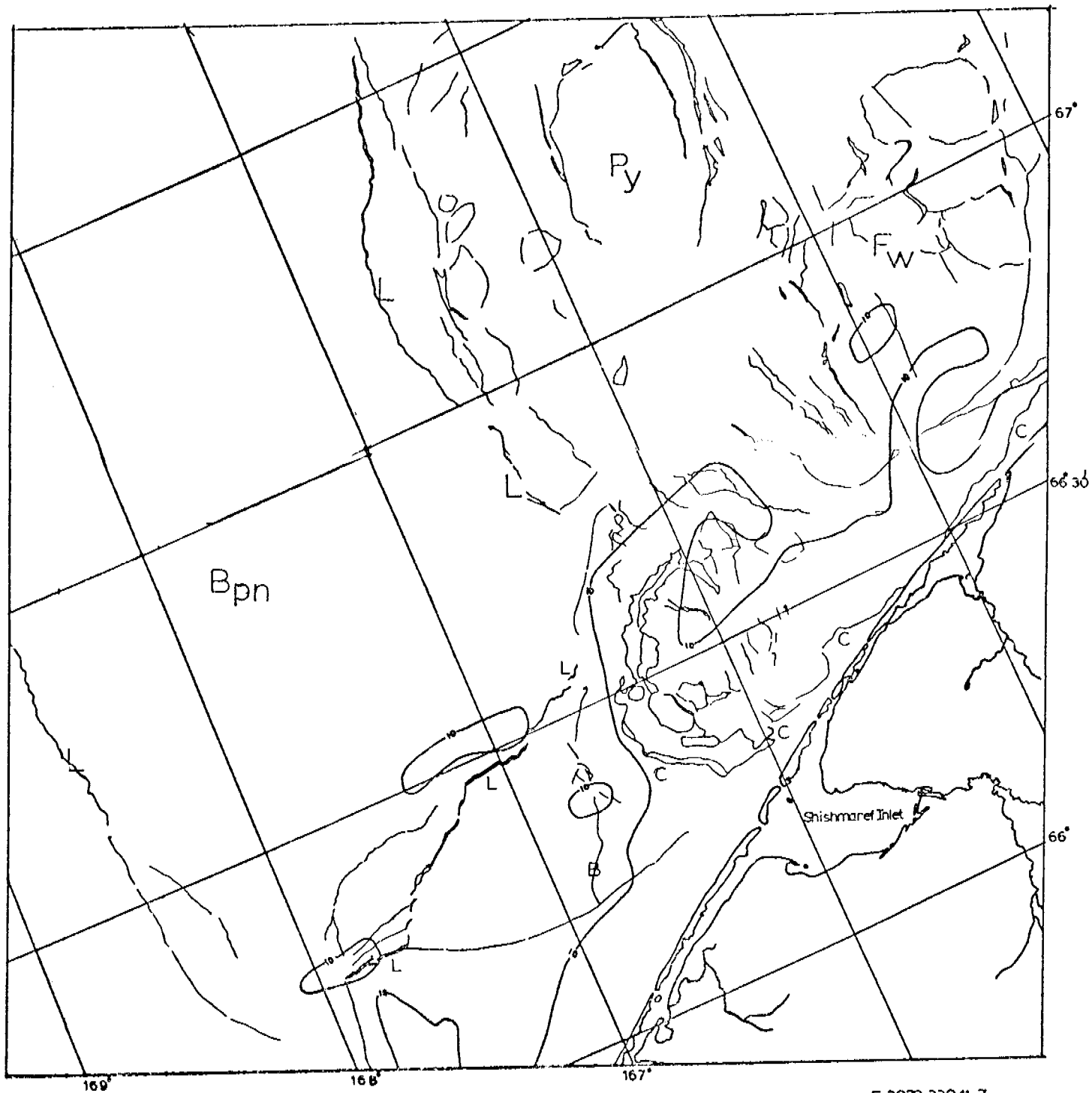
CHUKCHI SEA

E-2078-22032-7
10 APRIL 1975



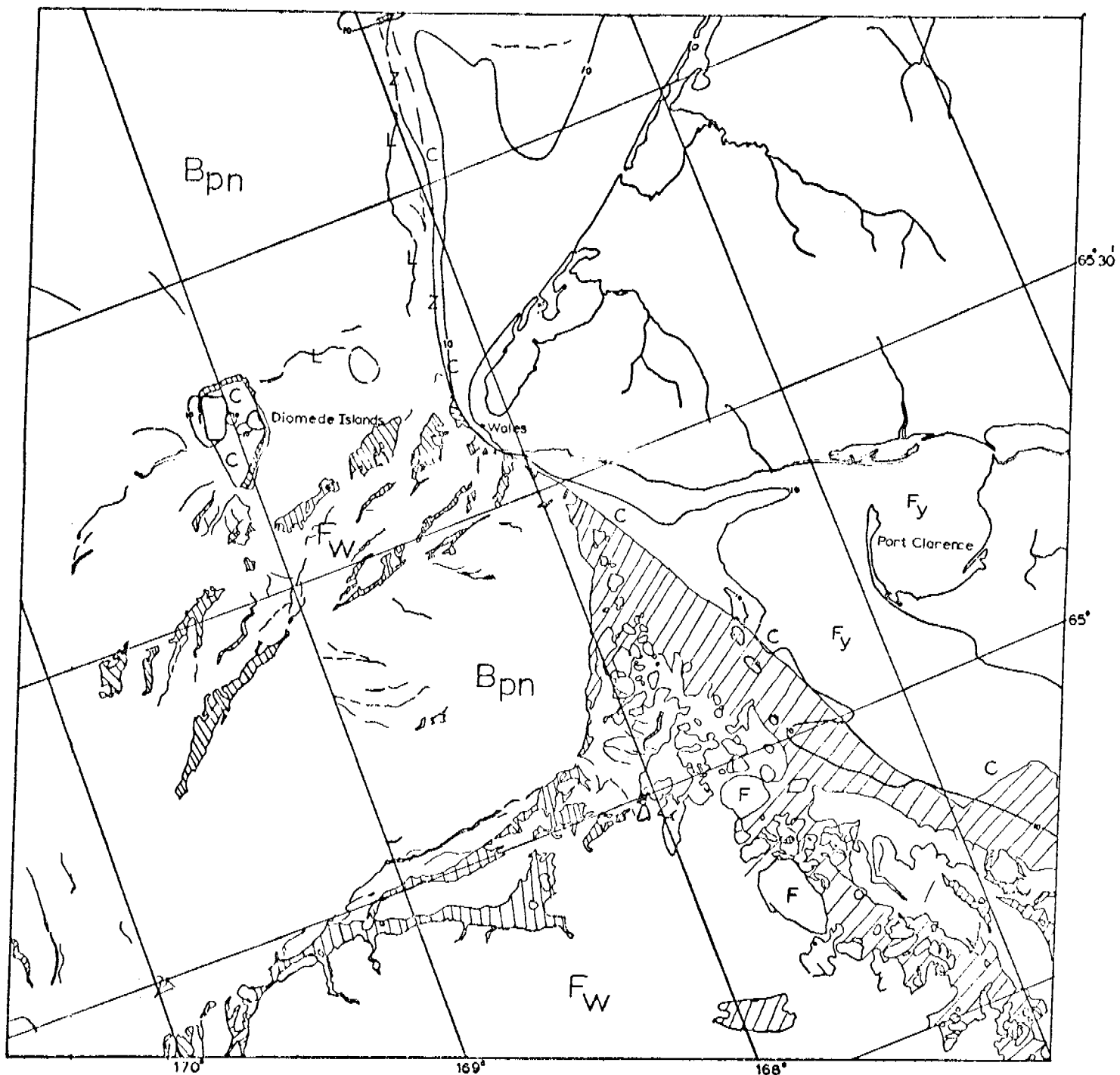
E-2078-22035-7
10 APRIL 1975

CHUKCHI SEA

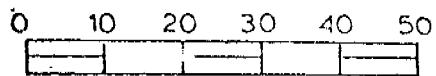


CHUKCHI SEA

E-2078-22041-7
10 APRIL 1975



KILOMETERS

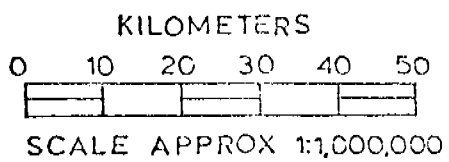
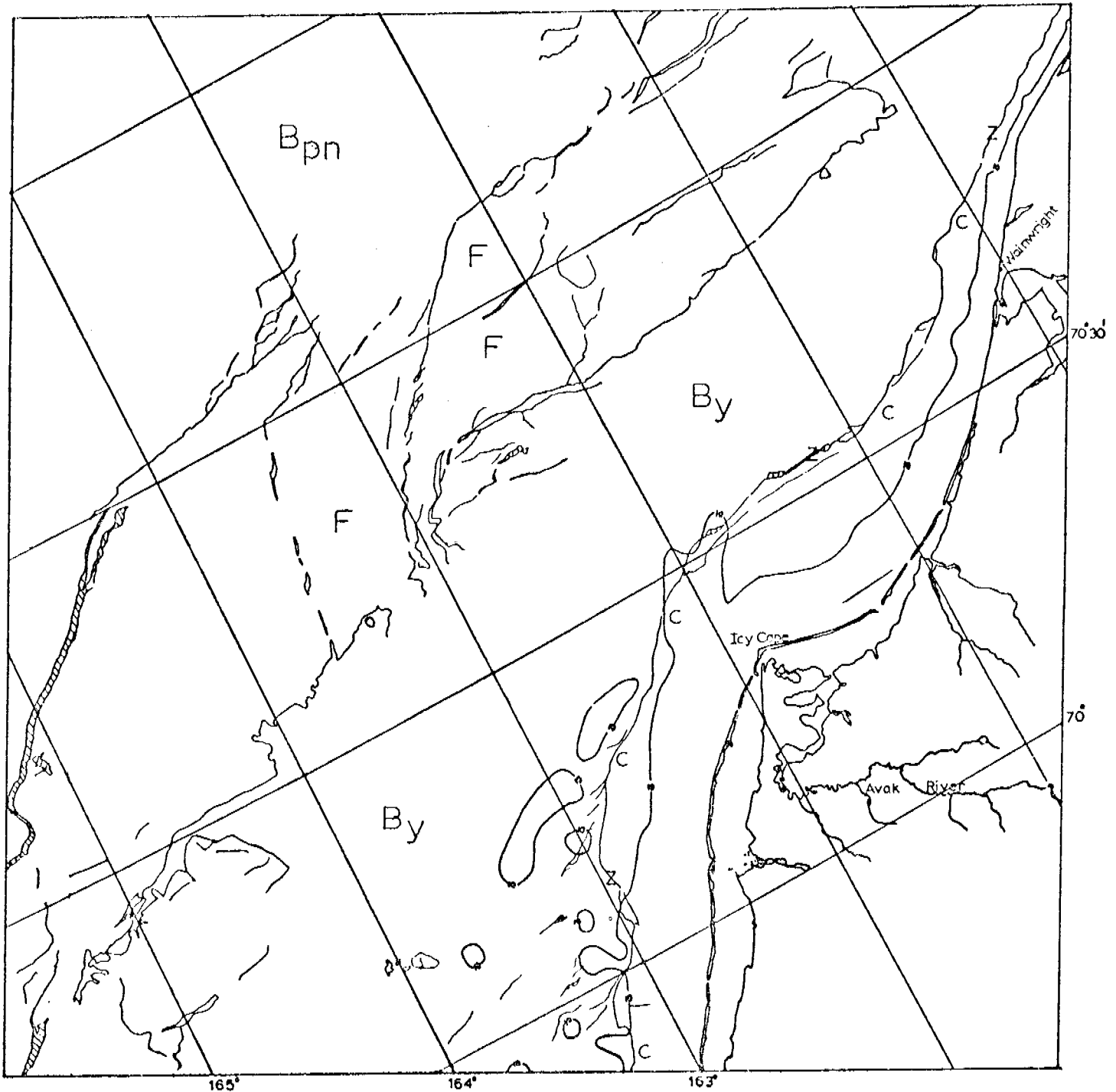


SCALE APPROX 1:1,000,000

E-2078-22044-7

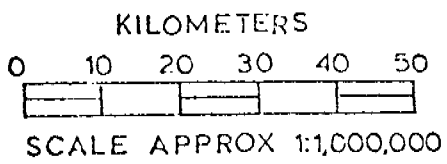
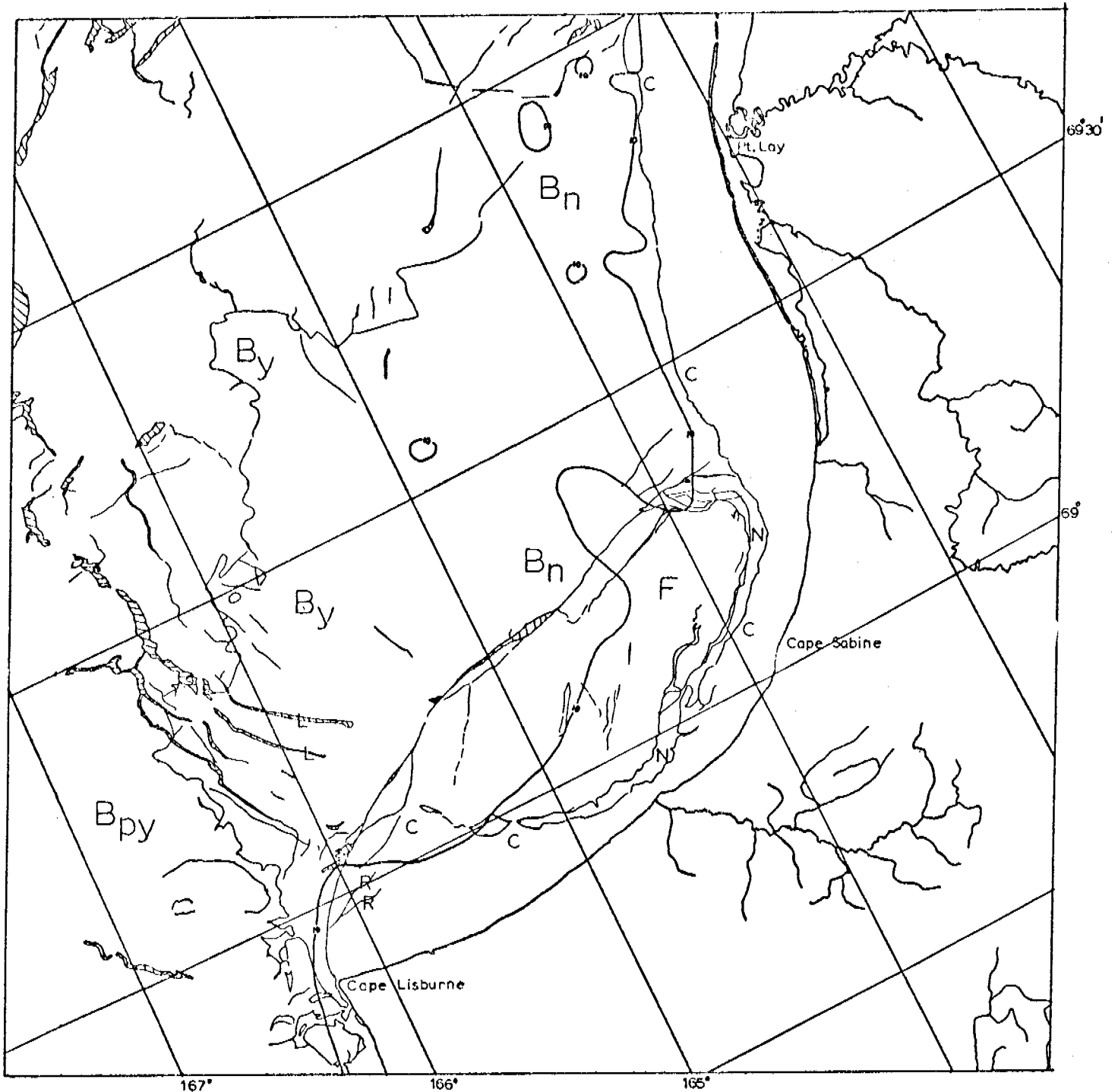
10 APRIL 1975

CHUKCHI SEA



E-2079-22084-7
11 APRIL 1975

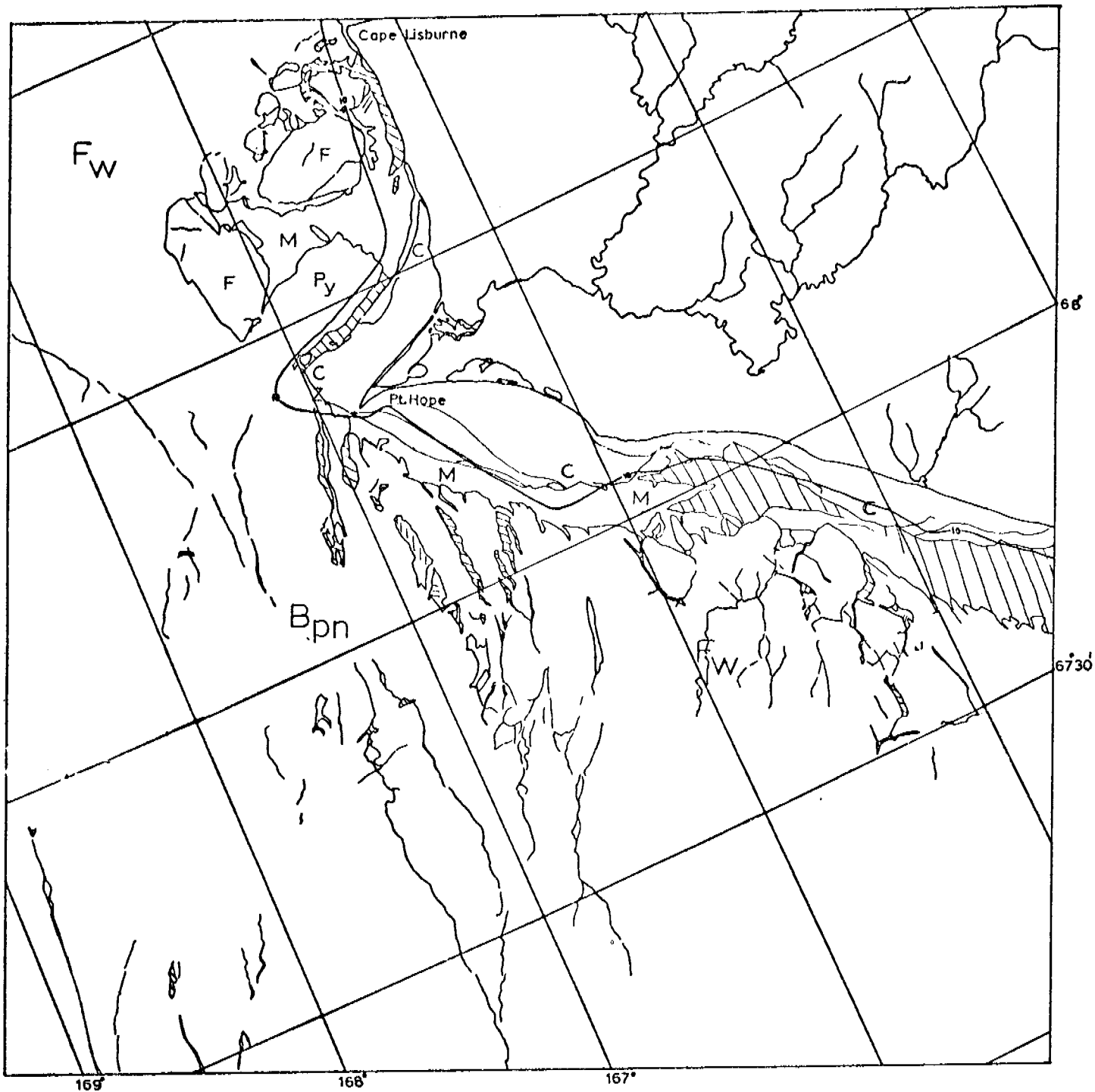
CHUKCHI SEA



E-2079-22091-7

11 APRIL 1975

CHUKCHI SEA

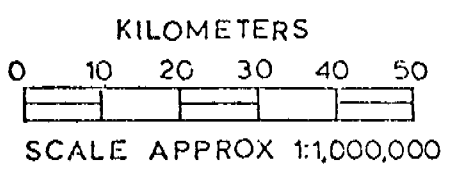
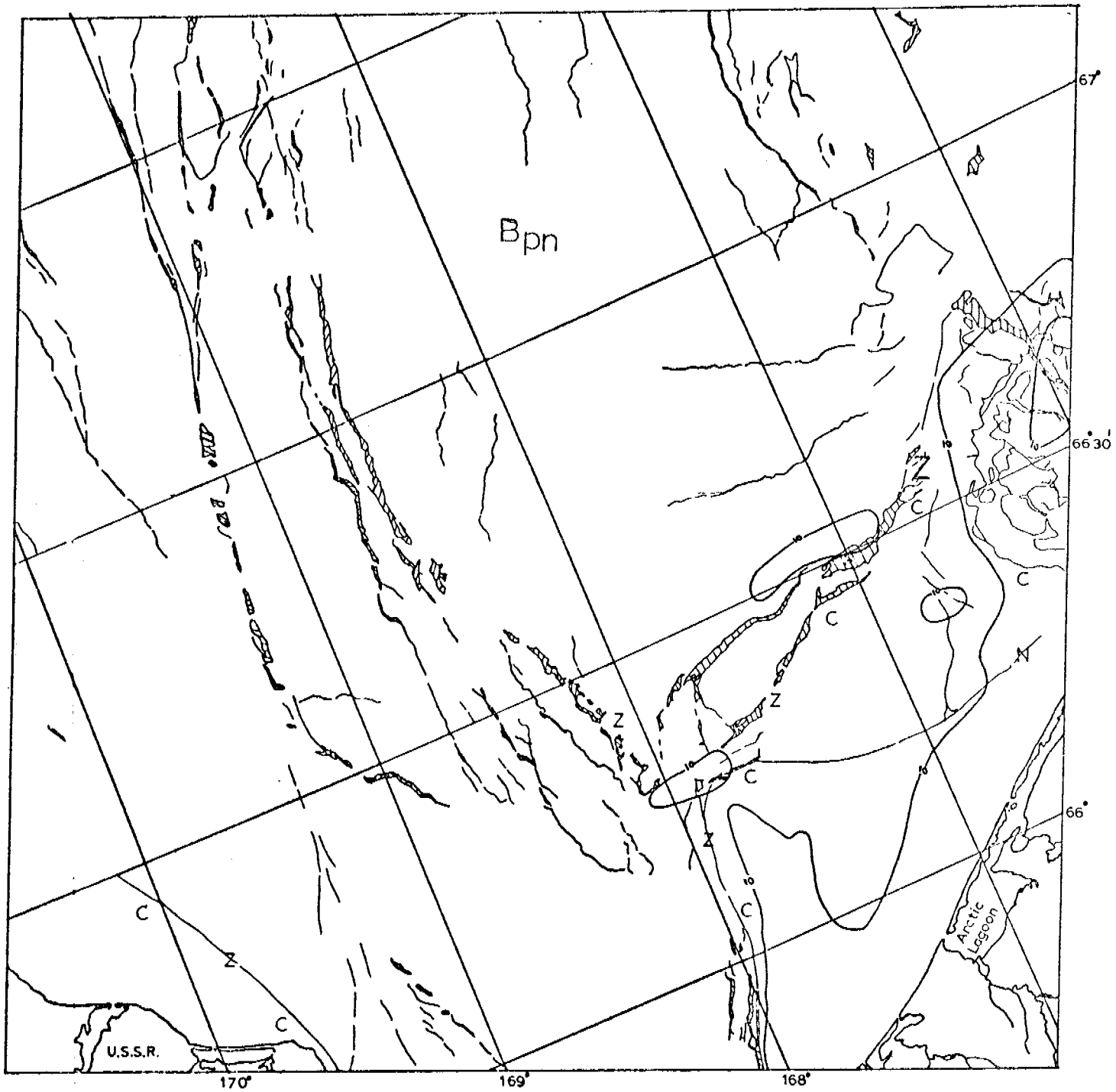


E-2079-22093-7

11 APRIL 1975

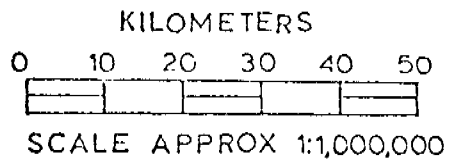
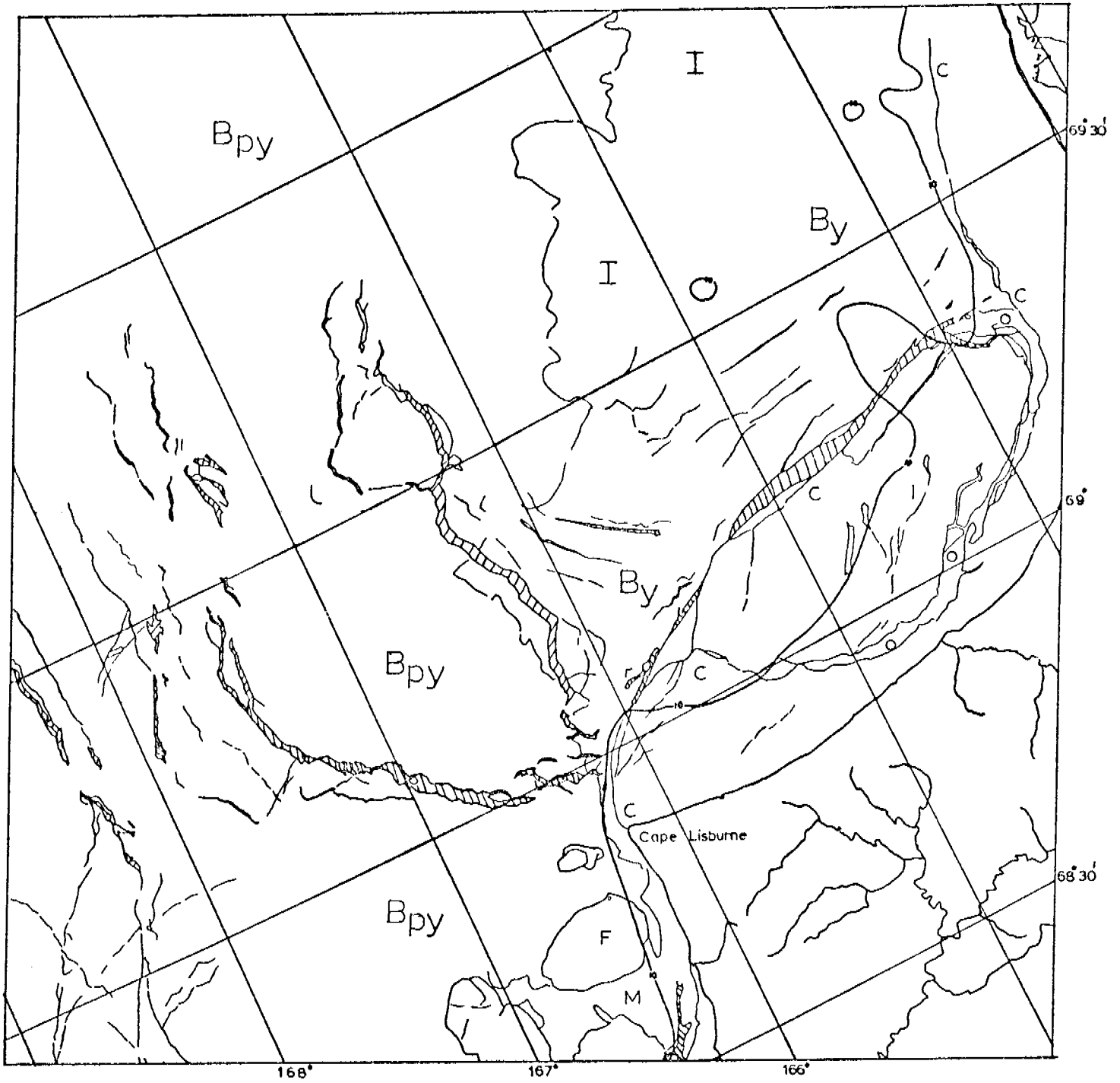
CHUKCHI SEA

KILOMETERS
 0 10 20 30 40 50
 SCALE APPROX 1:1,000,000



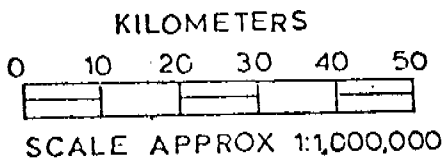
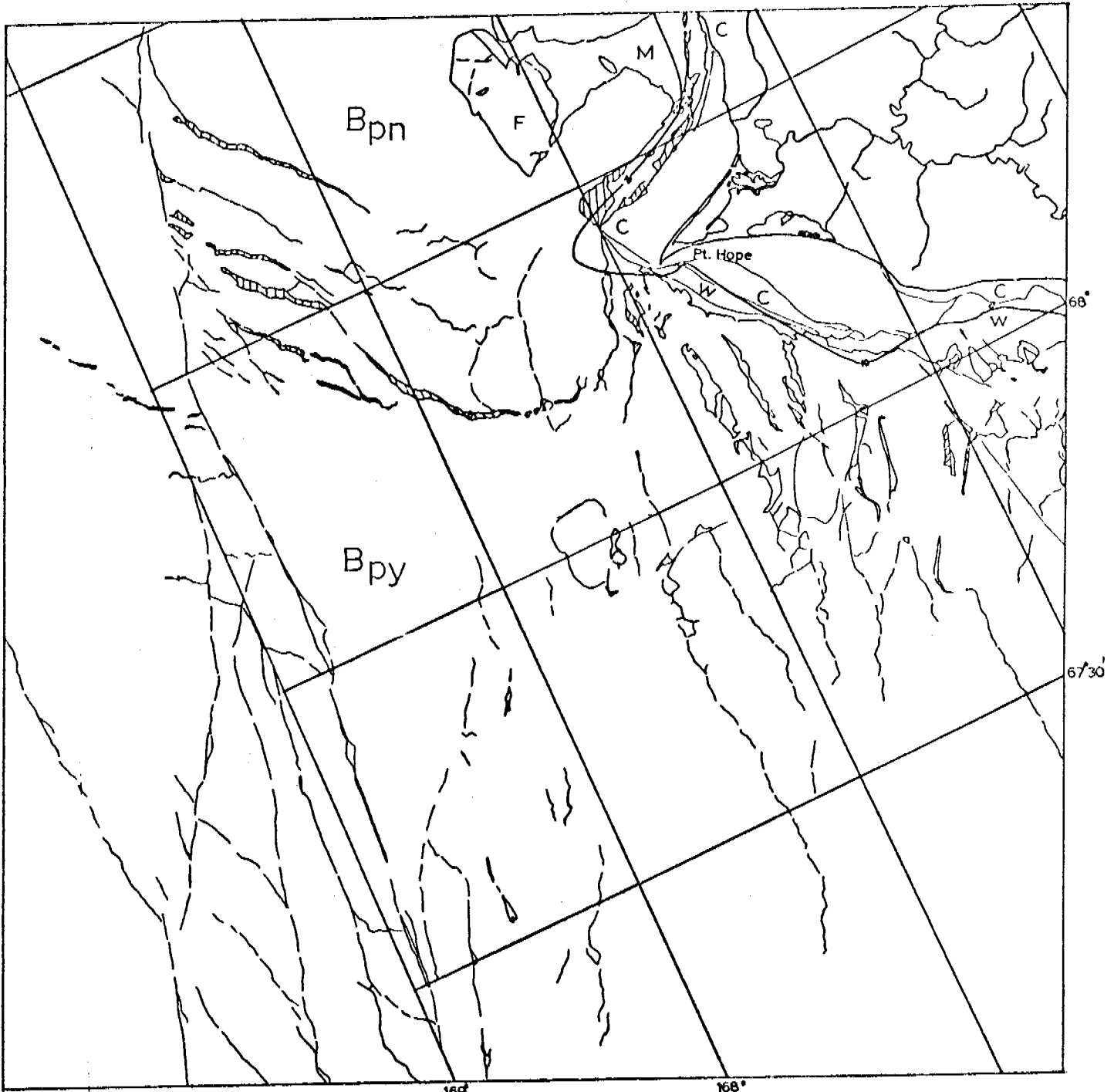
E-2079-22100-7
11 APRIL 1975

CHUKCHI SEA



E-2080-22145-7
12 APRIL 1975

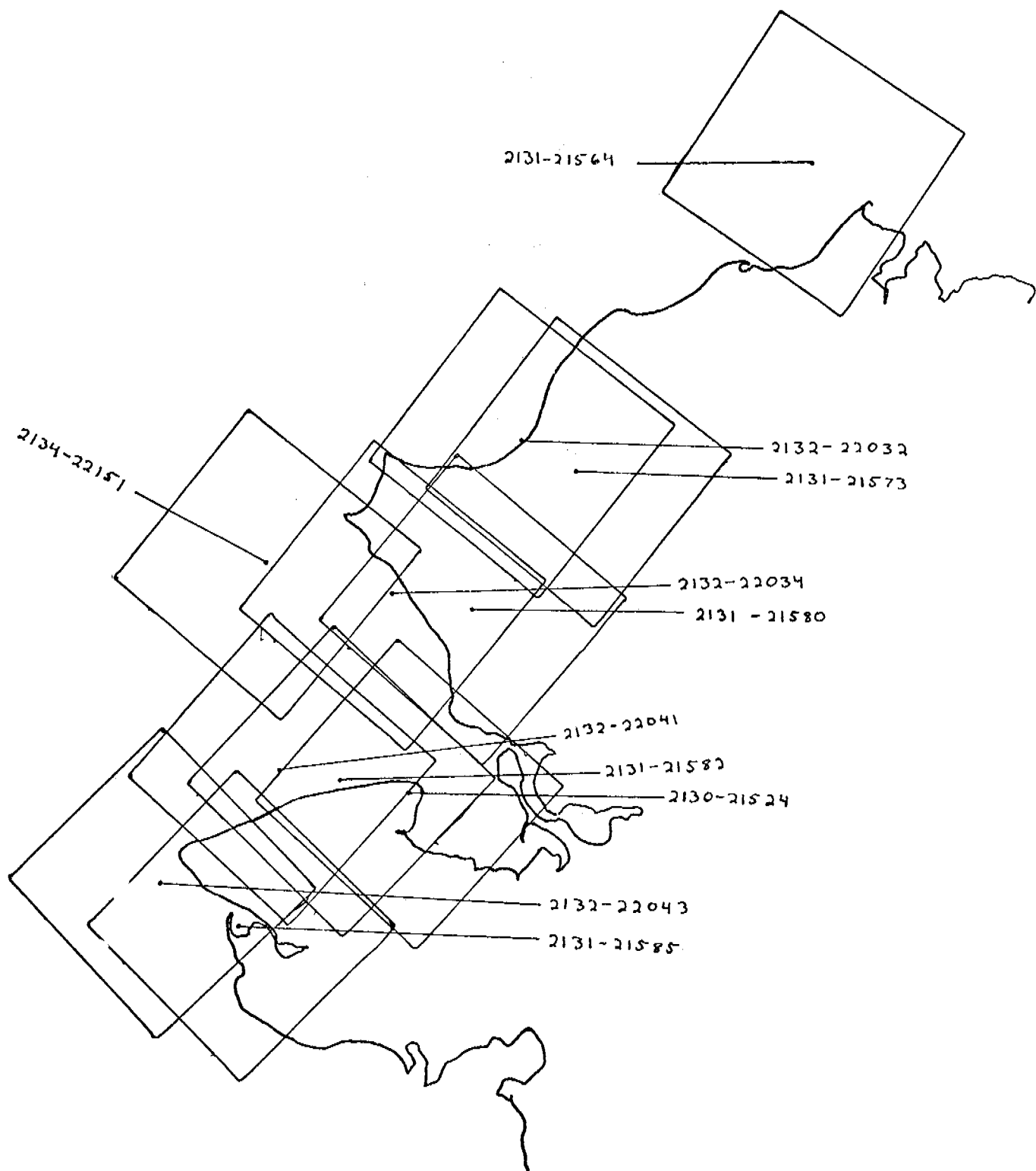
CHUKCHI SEA



CHUKCHI SEA

E-2080-22151-7
12 APRIL 1975

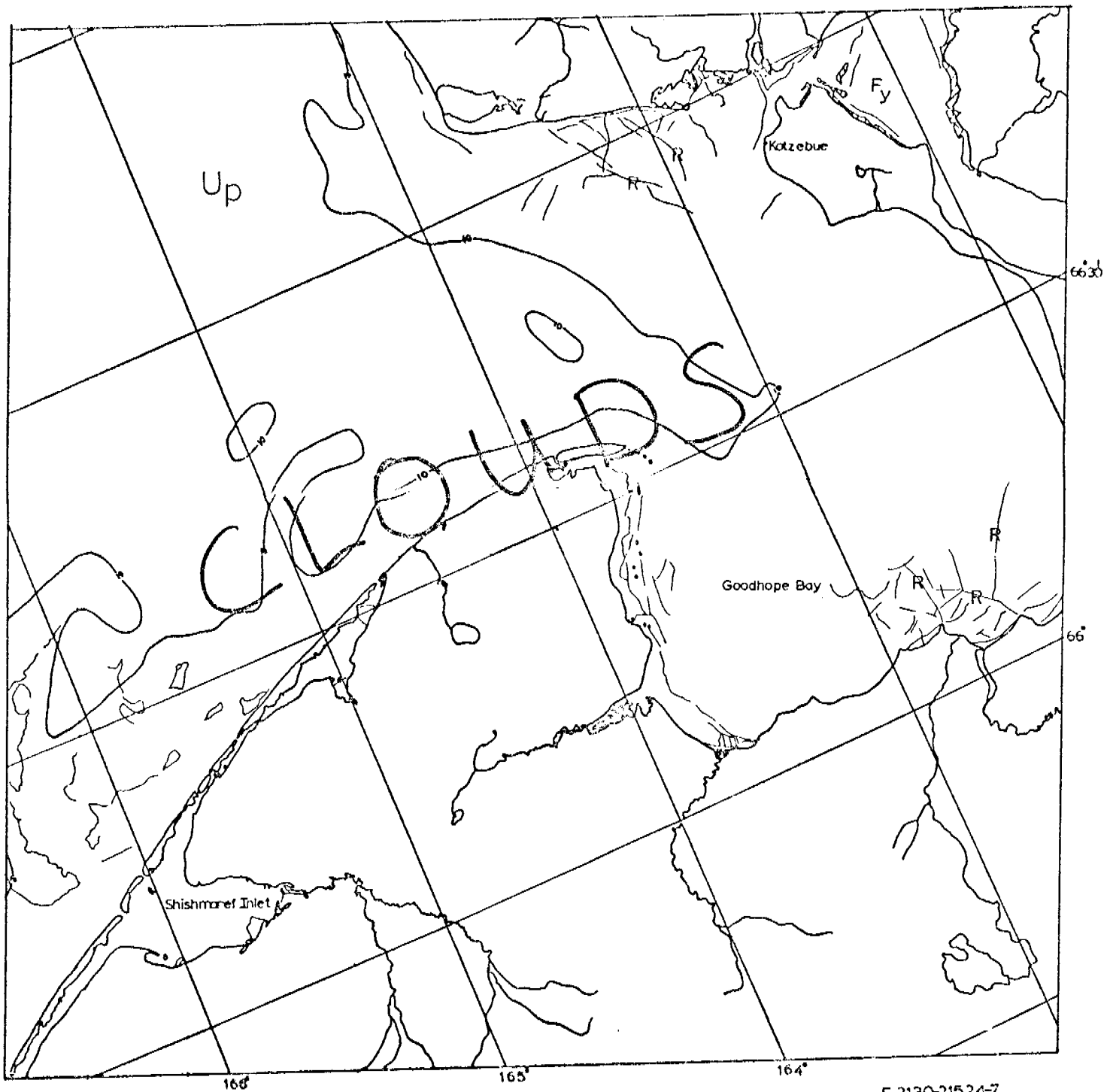
CHUKCHI SEA
30 MAY-16 JUNE 1975
Cycle 2128-2145



Scenes 2130-21524 through 2165-21454

These scenes show major portions of the Chukchi coast between June 1-6 and on July 6, 1975. The major value in this imagery is documentation of ice apparently stranded, protected by stranded ice or protected by geographic features and remaining in place at this late time.

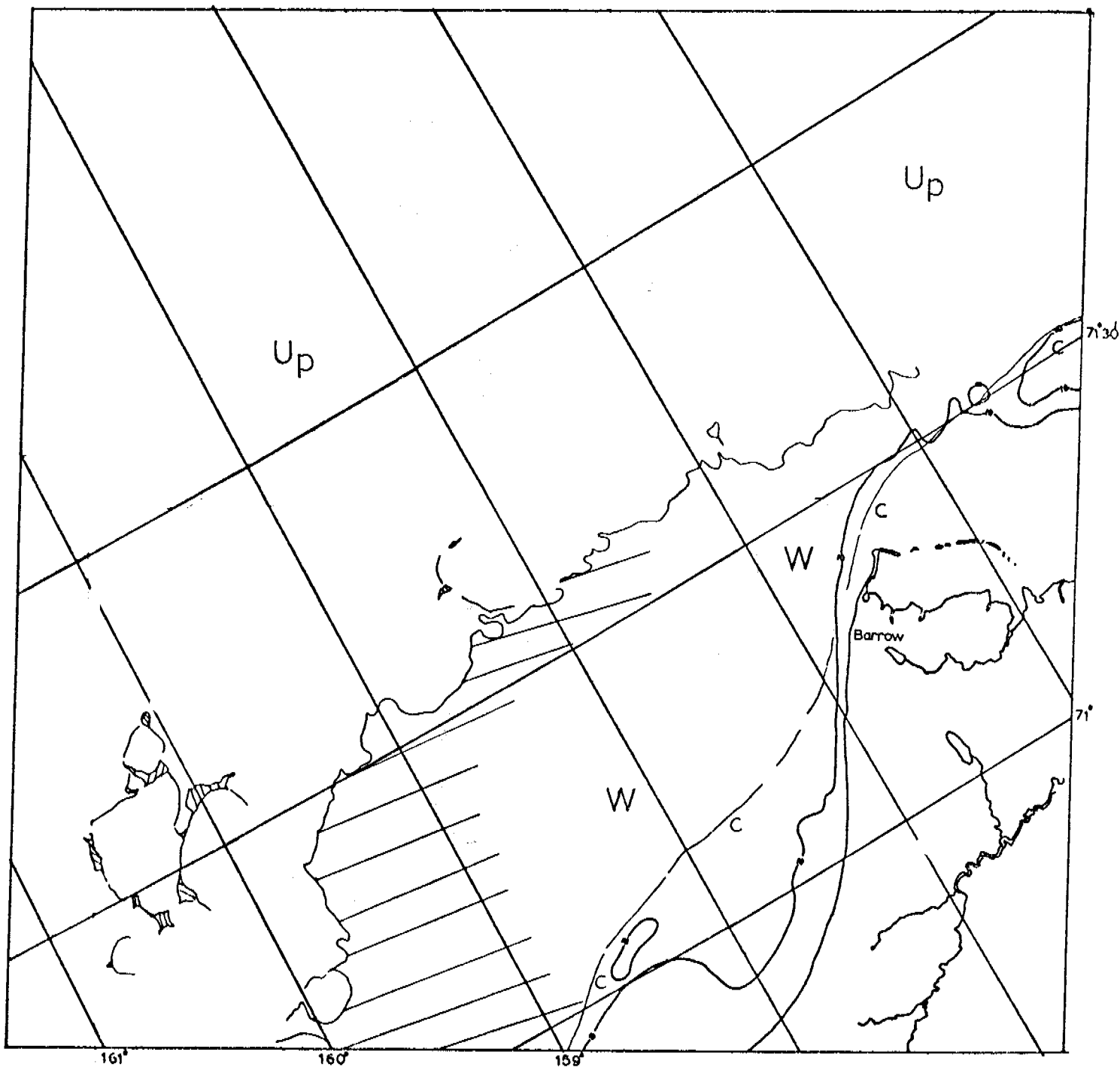
North of Cape Prince of Wales, ice remains over the large expanse of shoals in that area. Near shore ridges remain off Cape Krusenstern. Along the coast between there and Point Hope areas of ice remains in various protected locations. At Point Hope and Cape Lisburne ice remains-apparently stranded on shoals to the north. Just north of Cape Lisburne the contiguous apron indents toward the shore well inside the 10-fathom contour, and then broadens again.



KILOMETERS
 0 10 20 30 40 50
 SCALE APPROX 1:1,000,000

CHUKCHI SEA

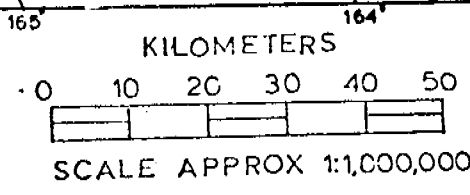
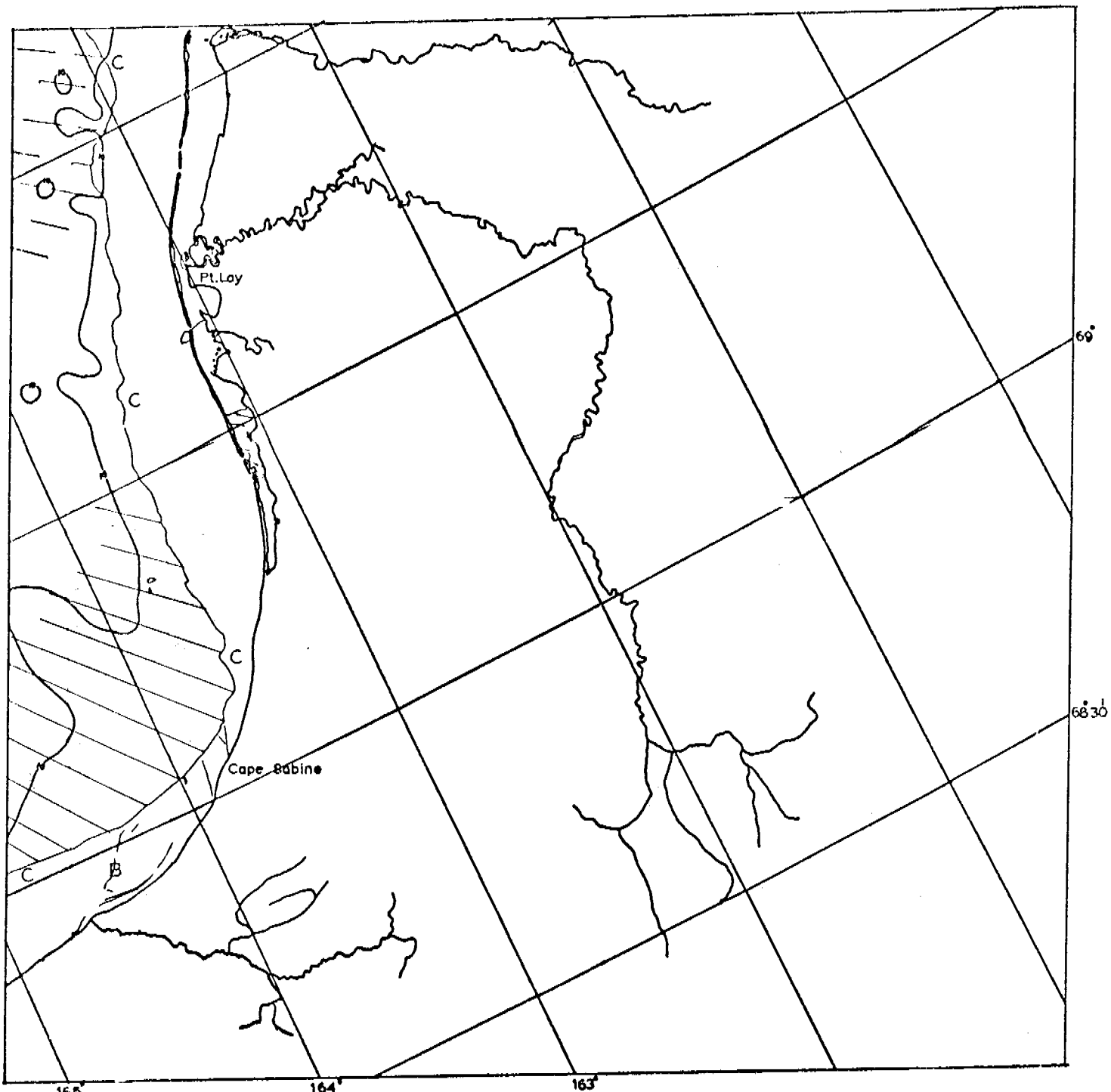
E-2130-21524-7
 1 JUNE 1975



KILOMETERS
 0 10 20 30 40 50
 SCALE APPROX 1:1,000,000

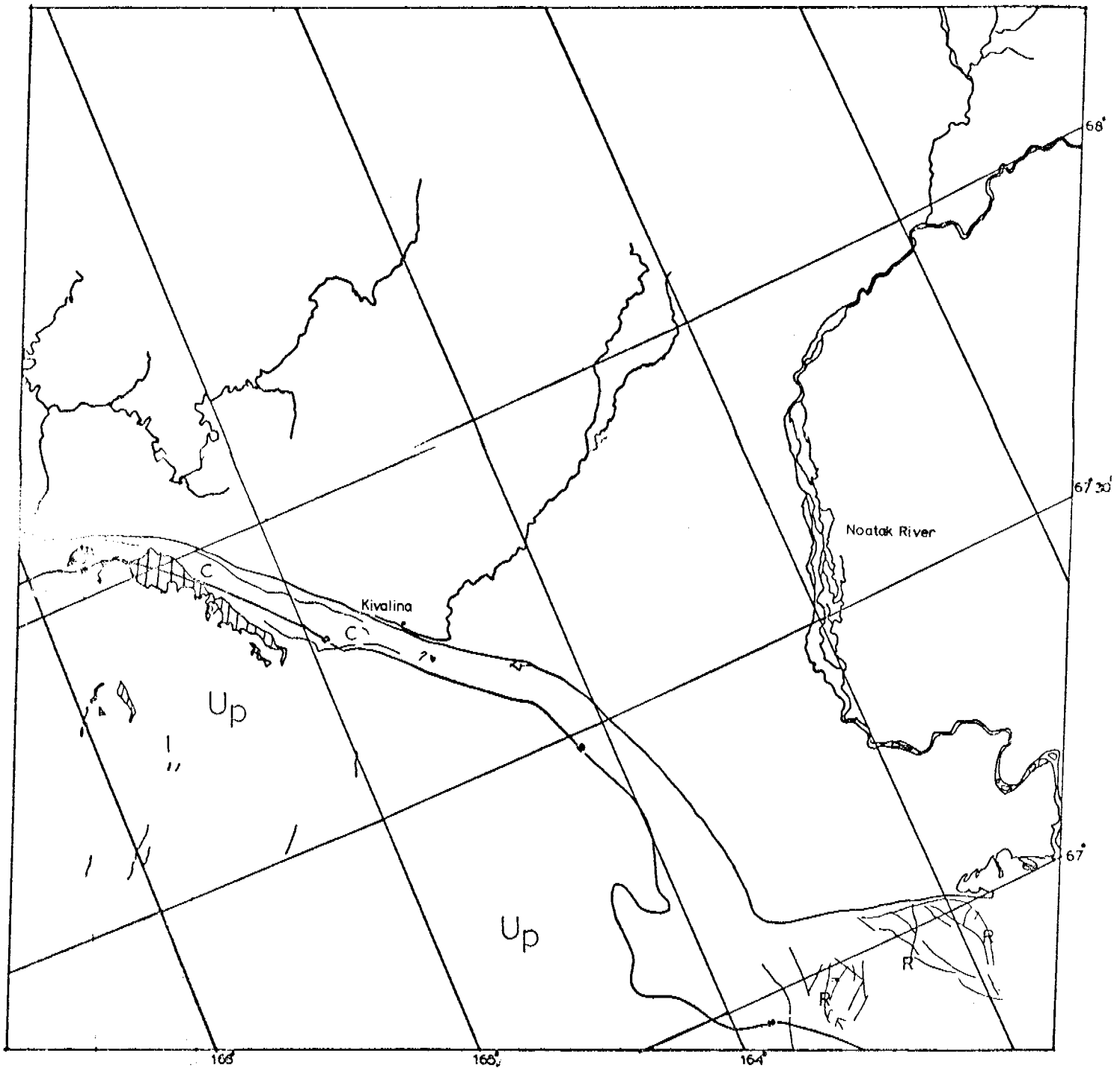
CHUKCHI SEA

E-2131-21564-7
 2 JUNE 1975



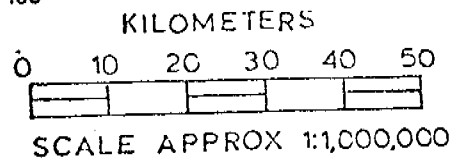
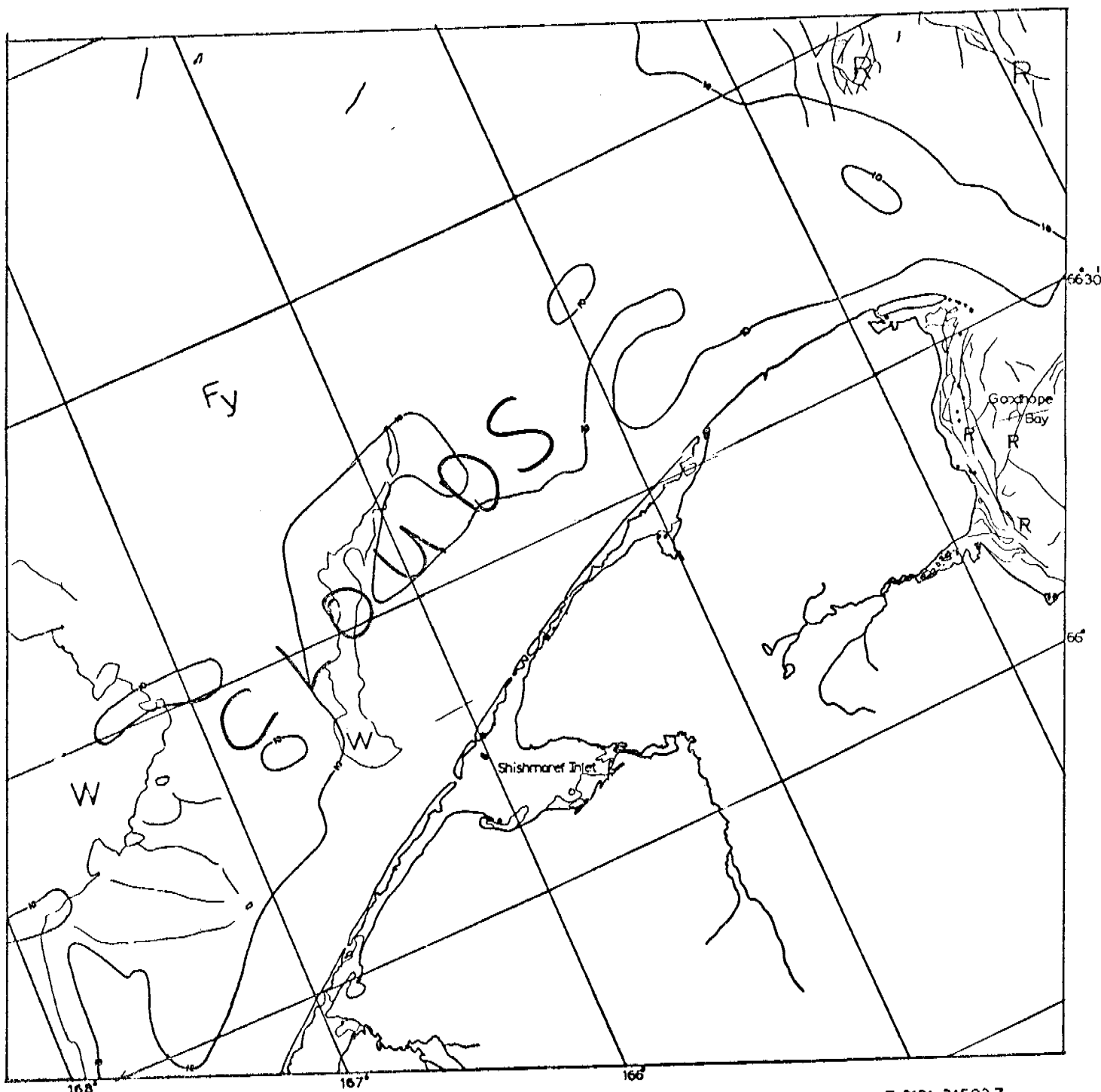
E-2131-21573-7
2 JUNE 1975

CHUKCHI SEA



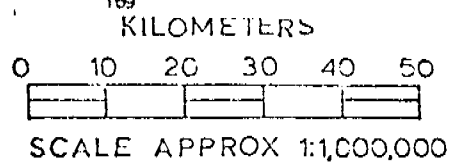
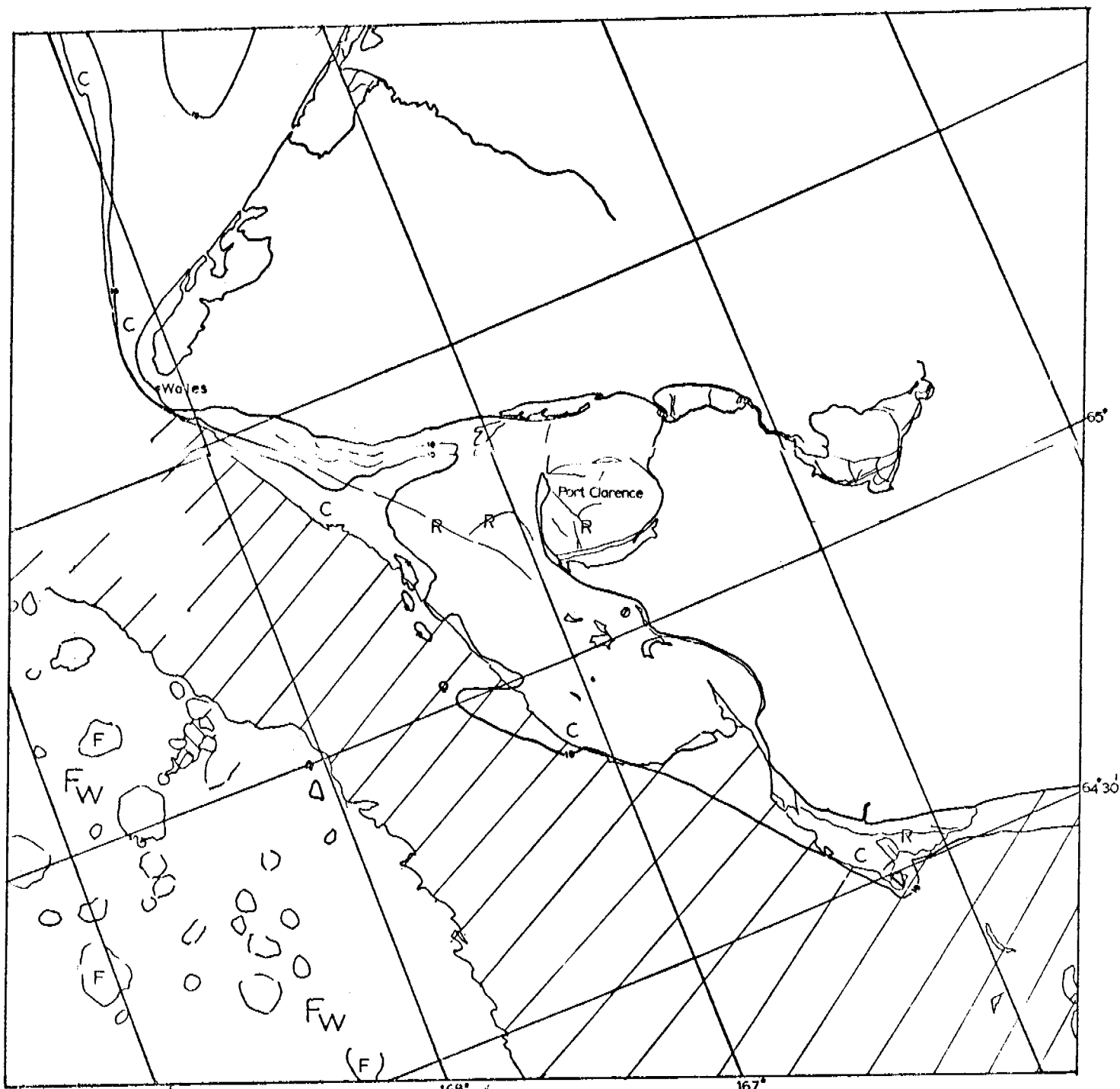
E-2131-21580-7
2 JUNE 1975

CHUKCHI SEA



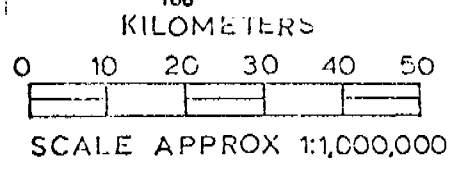
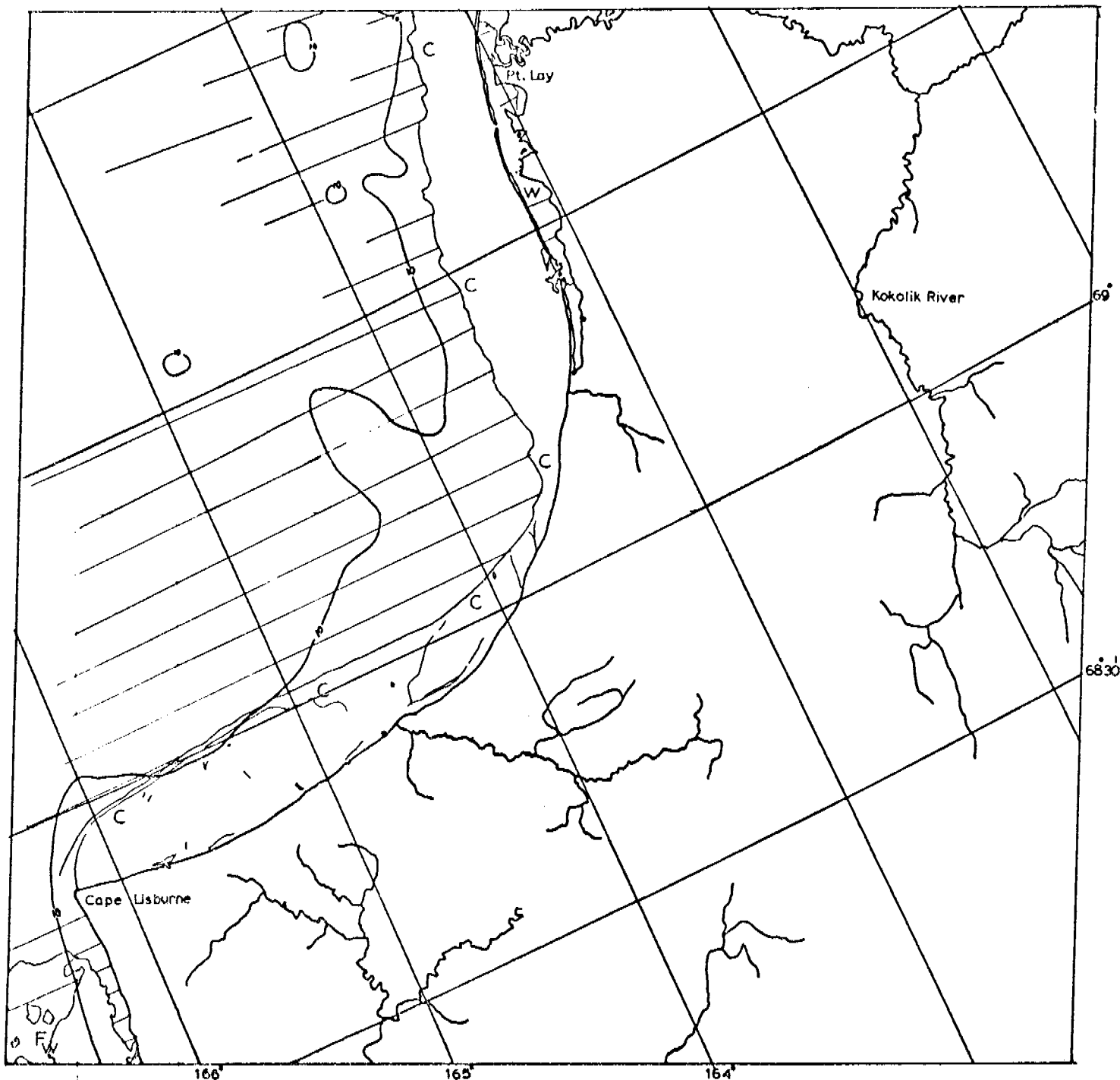
CHUKCHI SEA

E-2131-21582-7
2 JUNE 1975



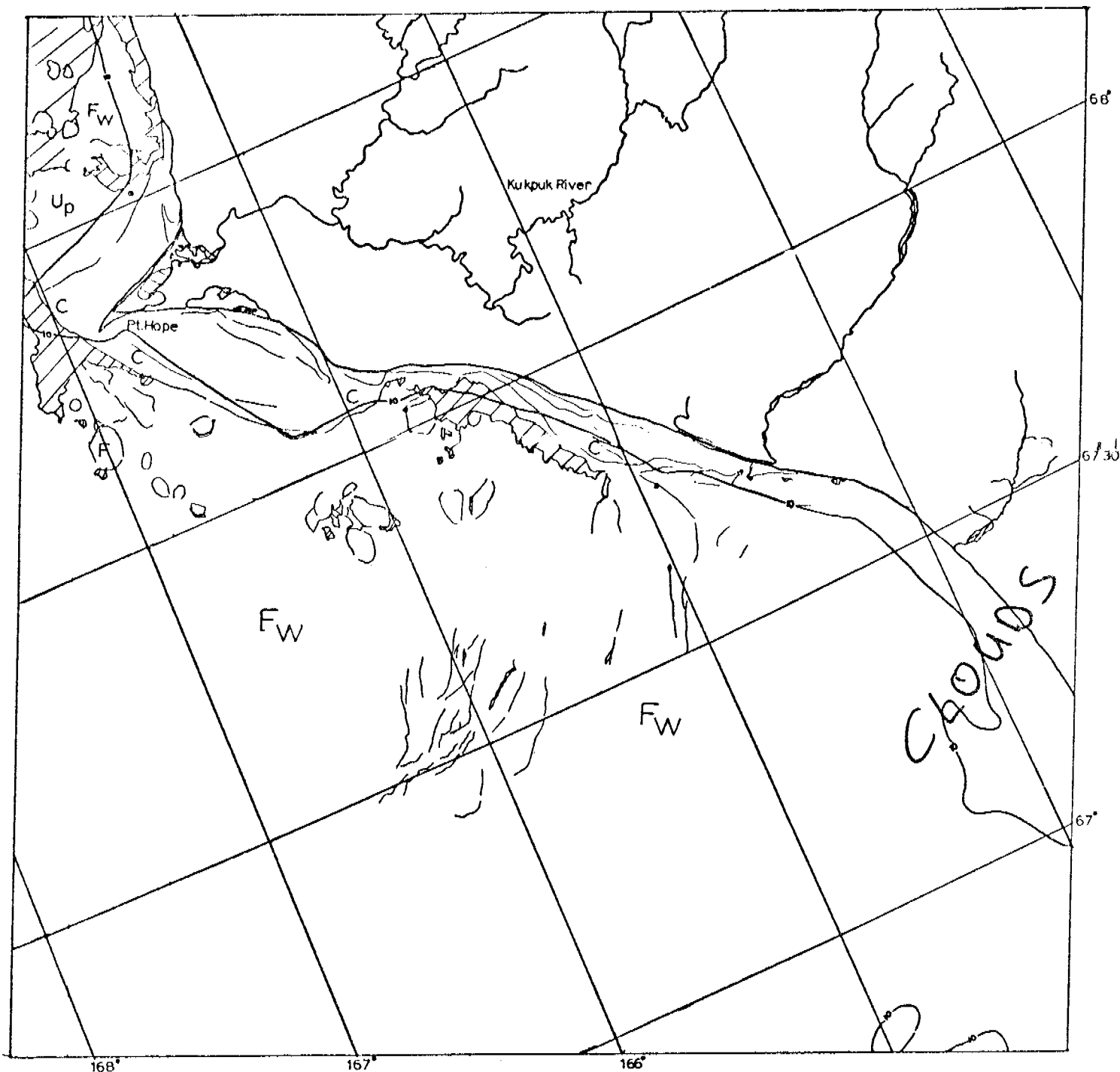
E-2131-21585-7
2 JUNE 1975

CHUKCHI SEA



E-2132-22032-7
3 JUNE 1975

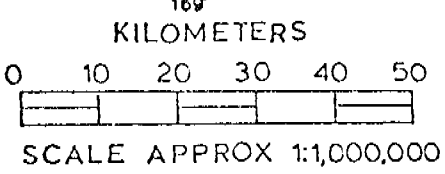
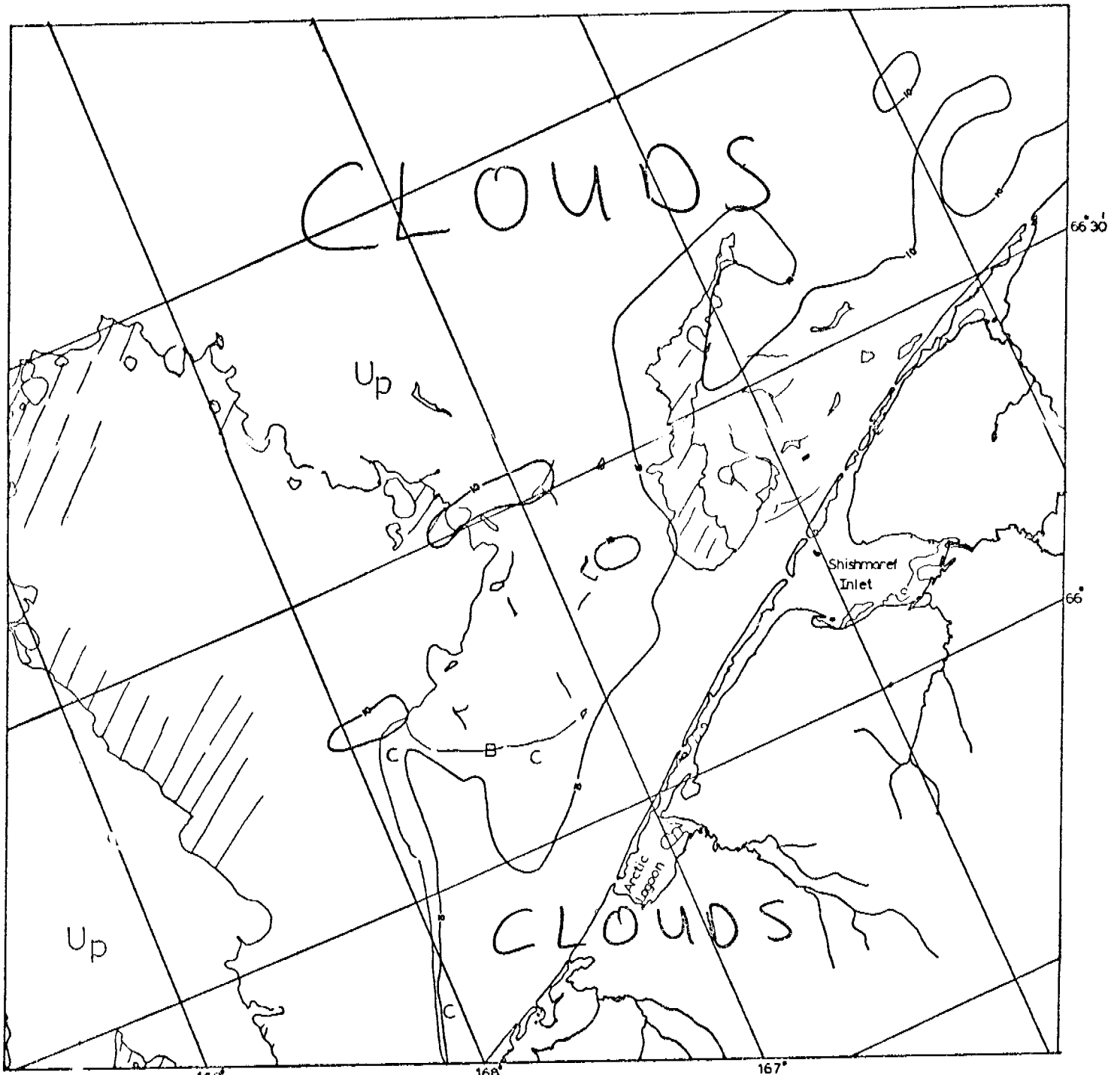
CHUKCHI SEA



KILOMETERS
 0 10 20 30 40 50
 SCALE APPROX 1:1,000,000

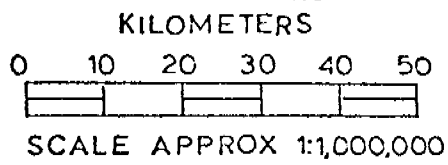
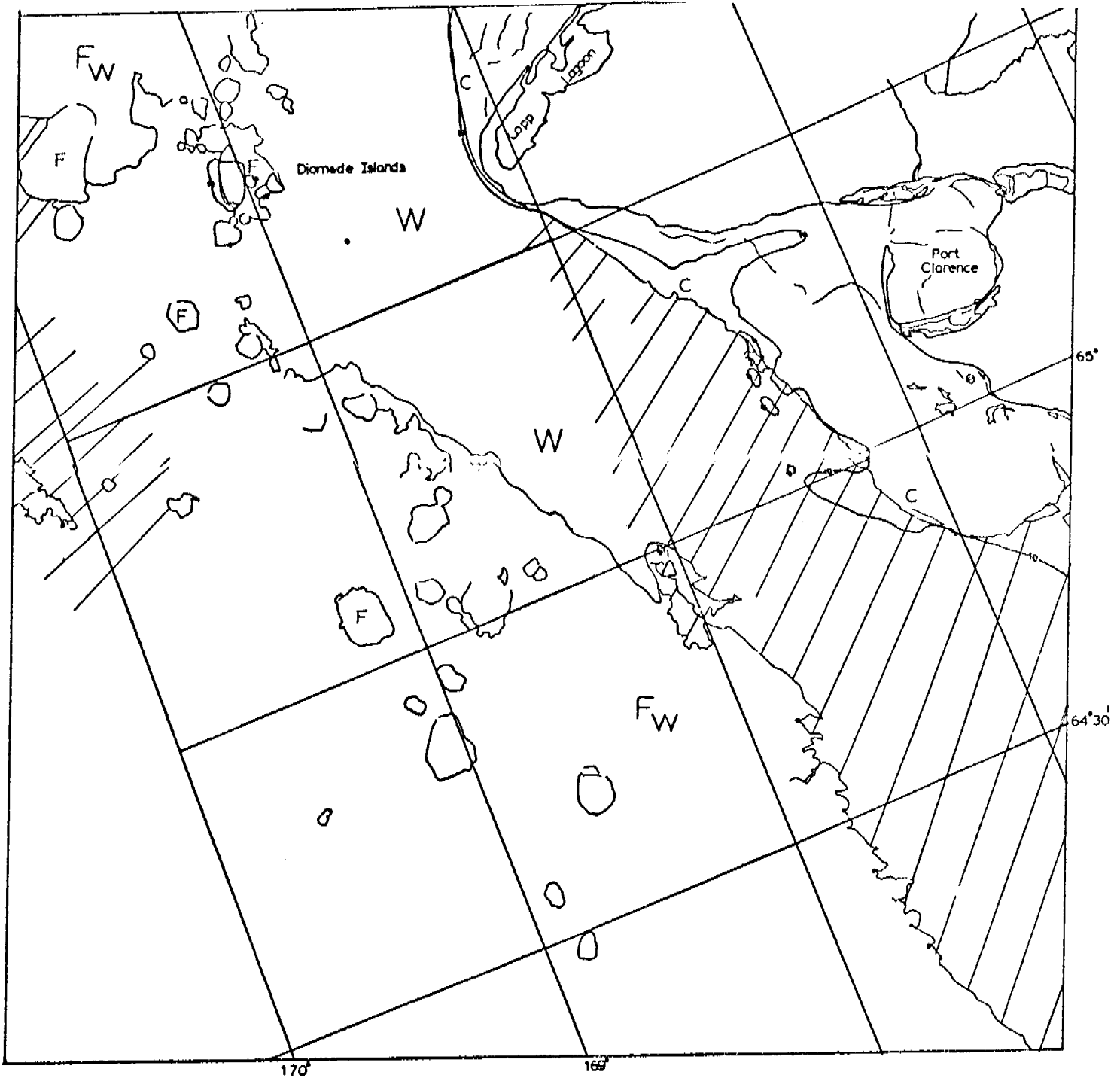
CHUKCHI SEA

E-2132-22034-7
 3 JUNE 1975



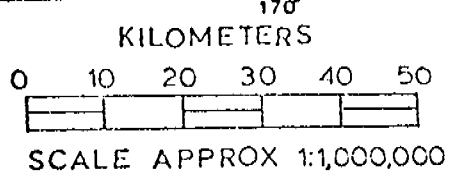
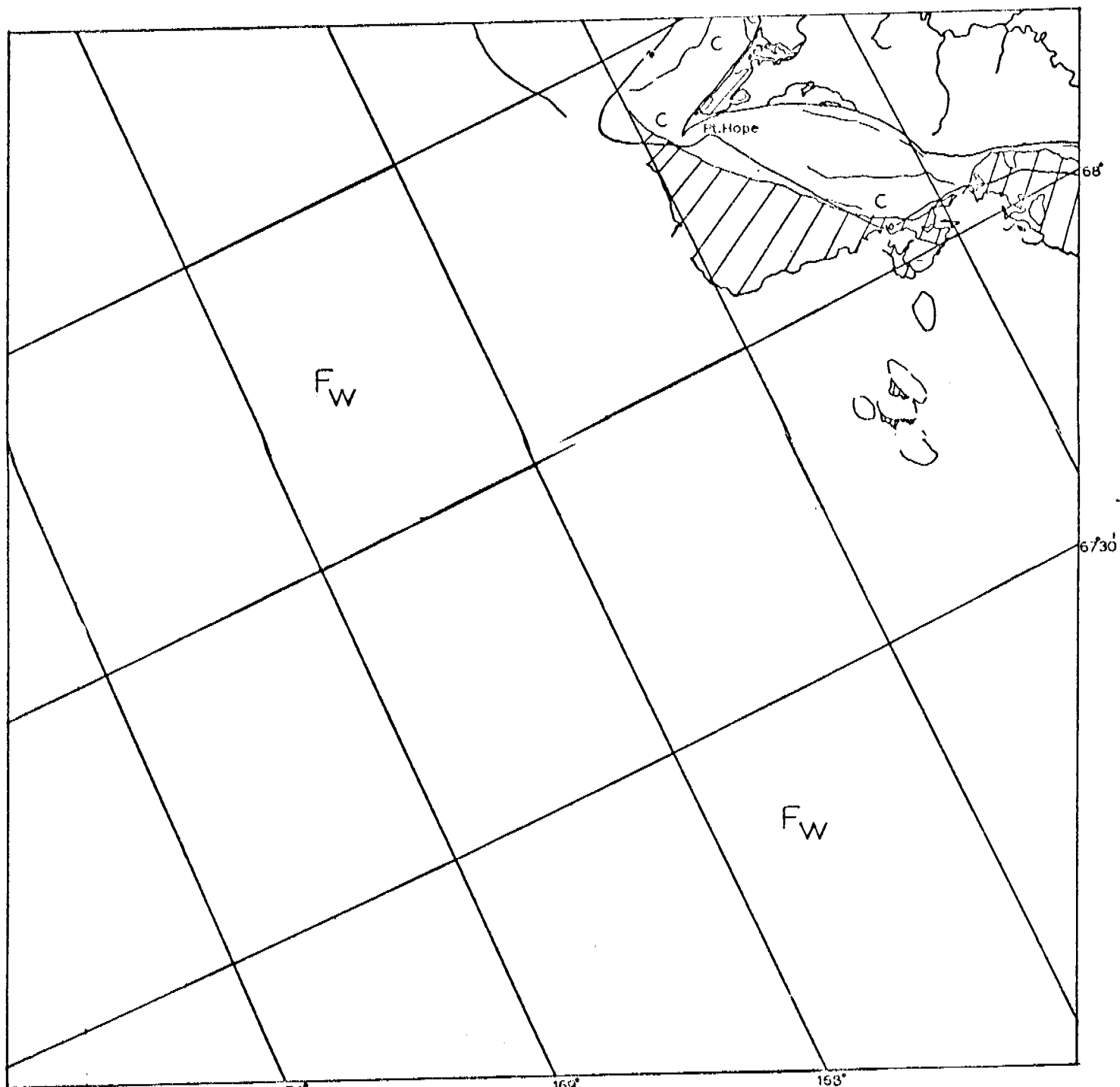
E-2132-22041-7
3 JUNE 1975

CHUKCHI SEA



CHUKCHI SEA

E-2132-22043-7
3 JUNE 1975

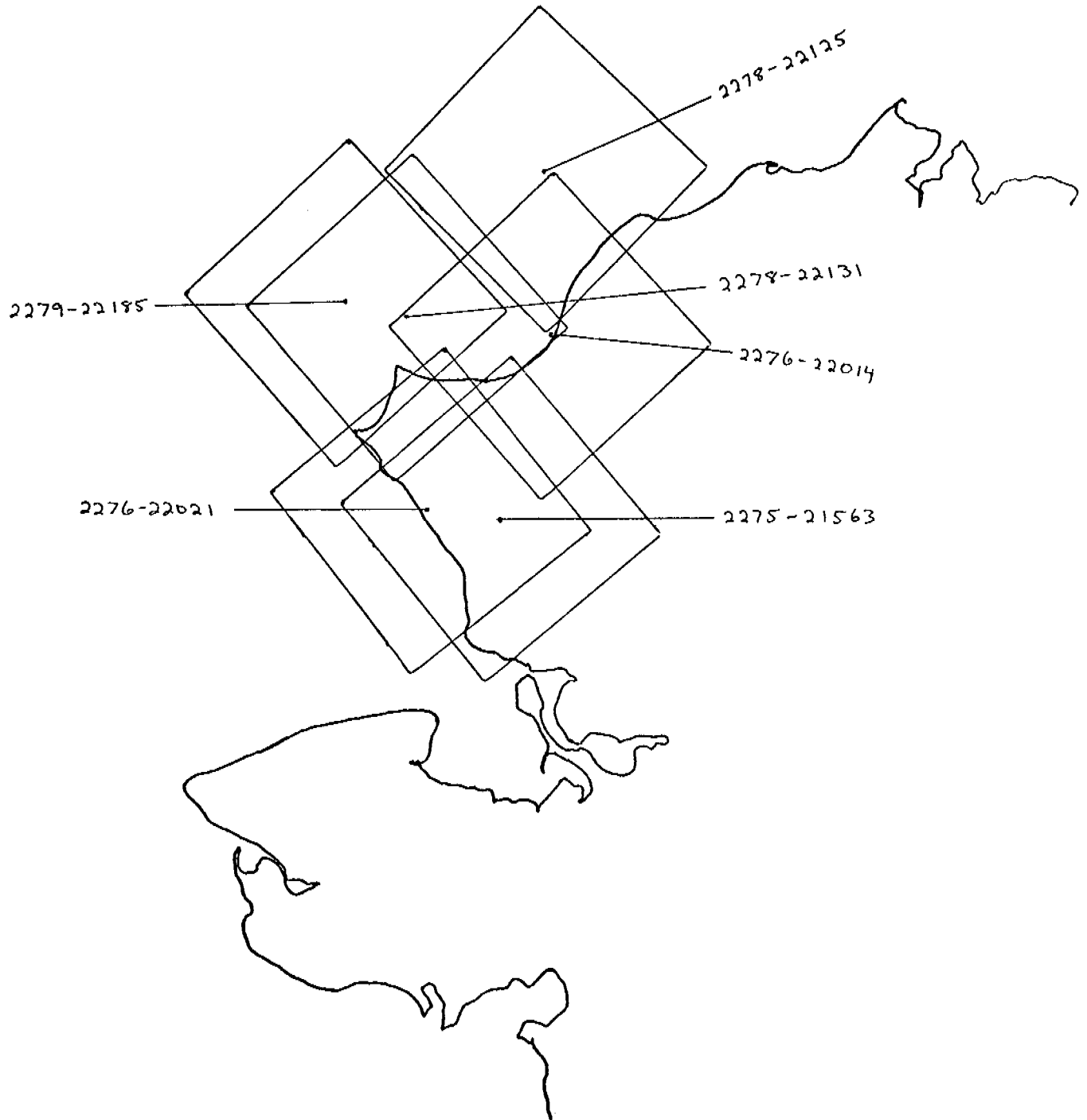


E-2134-22151-7
5 JUNE 1975

CHUKCHI SEA

CHUKCHI SEA

21 OCTOBER - 8 NOVEMBER 1975
Cycle 2272-2290



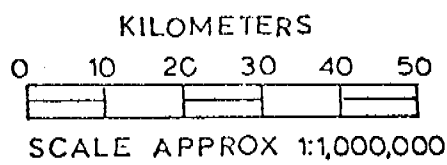
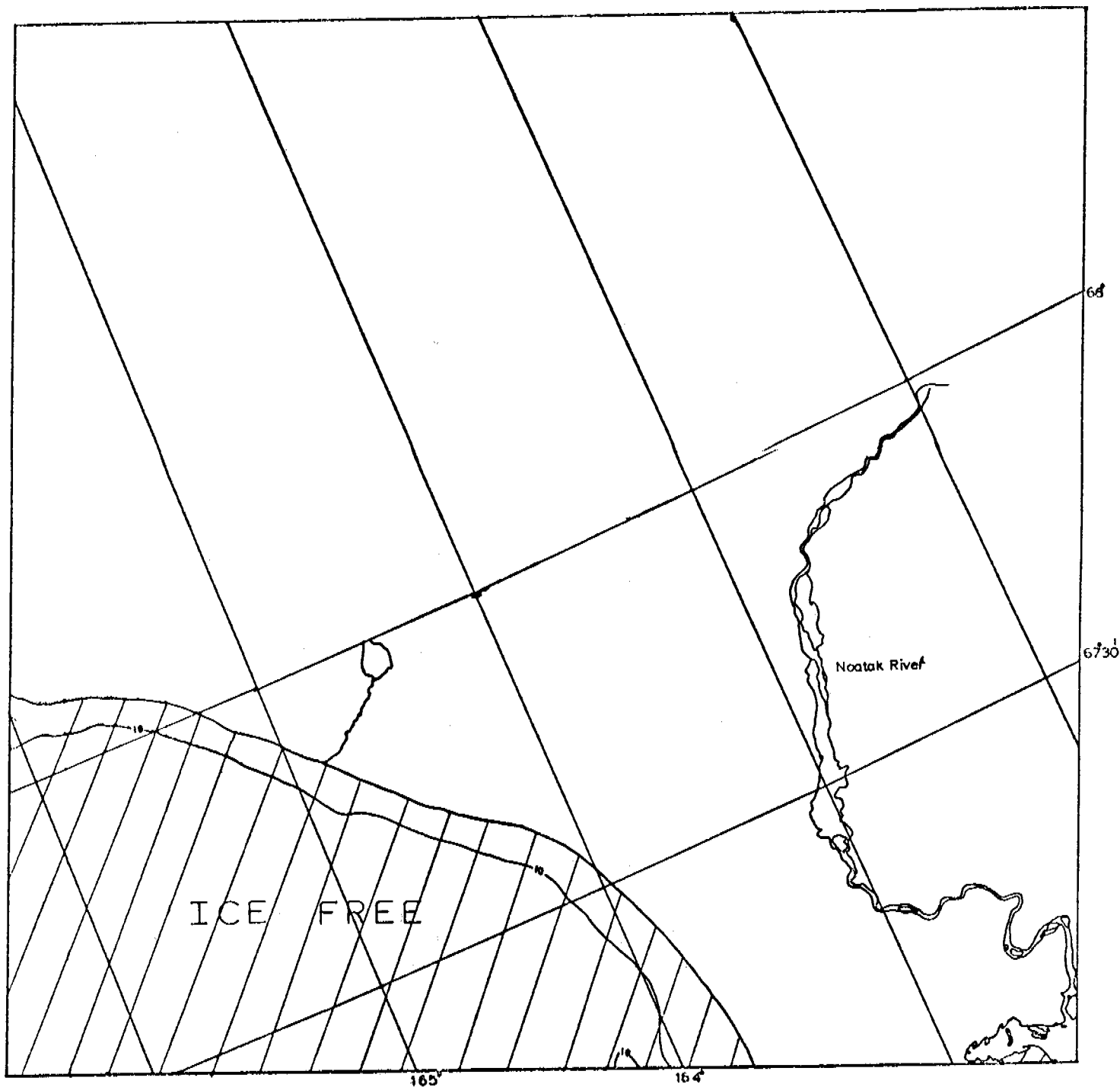
Scenes 2275-21563

2276-22014 } adjacent pair
2276-22021 }

2278-22125 } adjacent pair
2278-22131 }

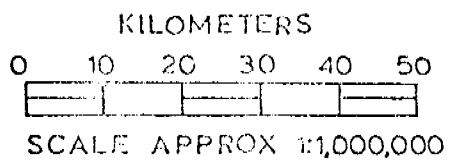
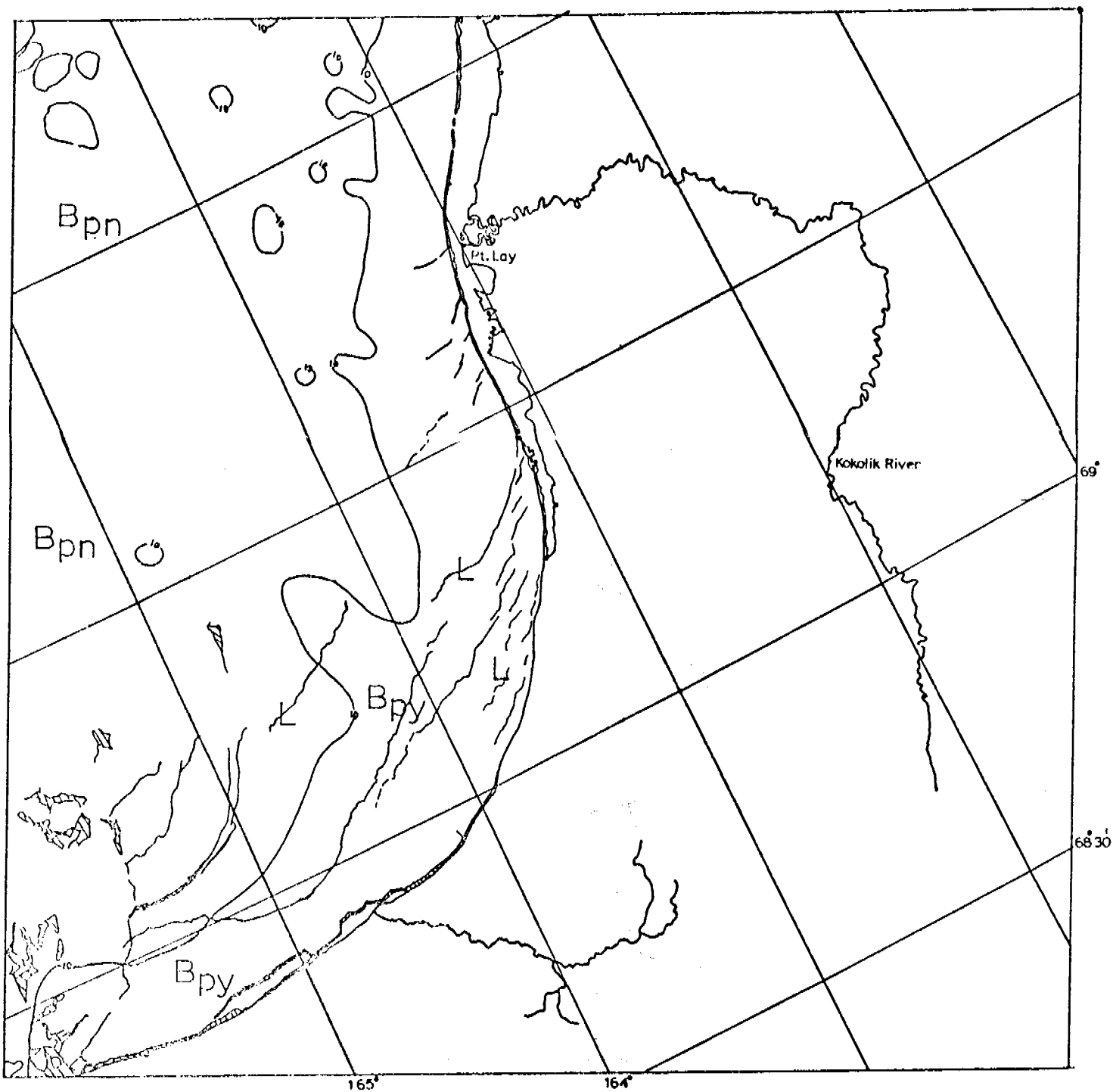
2279-22185

These scenes show the Cape Lisburne area for October 24-28, 1975. The ice in these scenes is from young to new and is repeatedly being broken up with new ice forming in the newly-created voids. Cloud patterns indicate shifting wind systems responsible for fragmentation of the ice. Ice piling in the near shore areas has been limited to locations very close to the break. No large shear or pressure ridges have been formed.



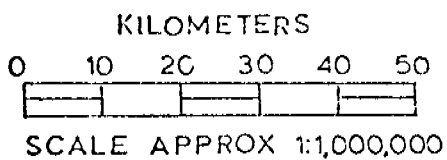
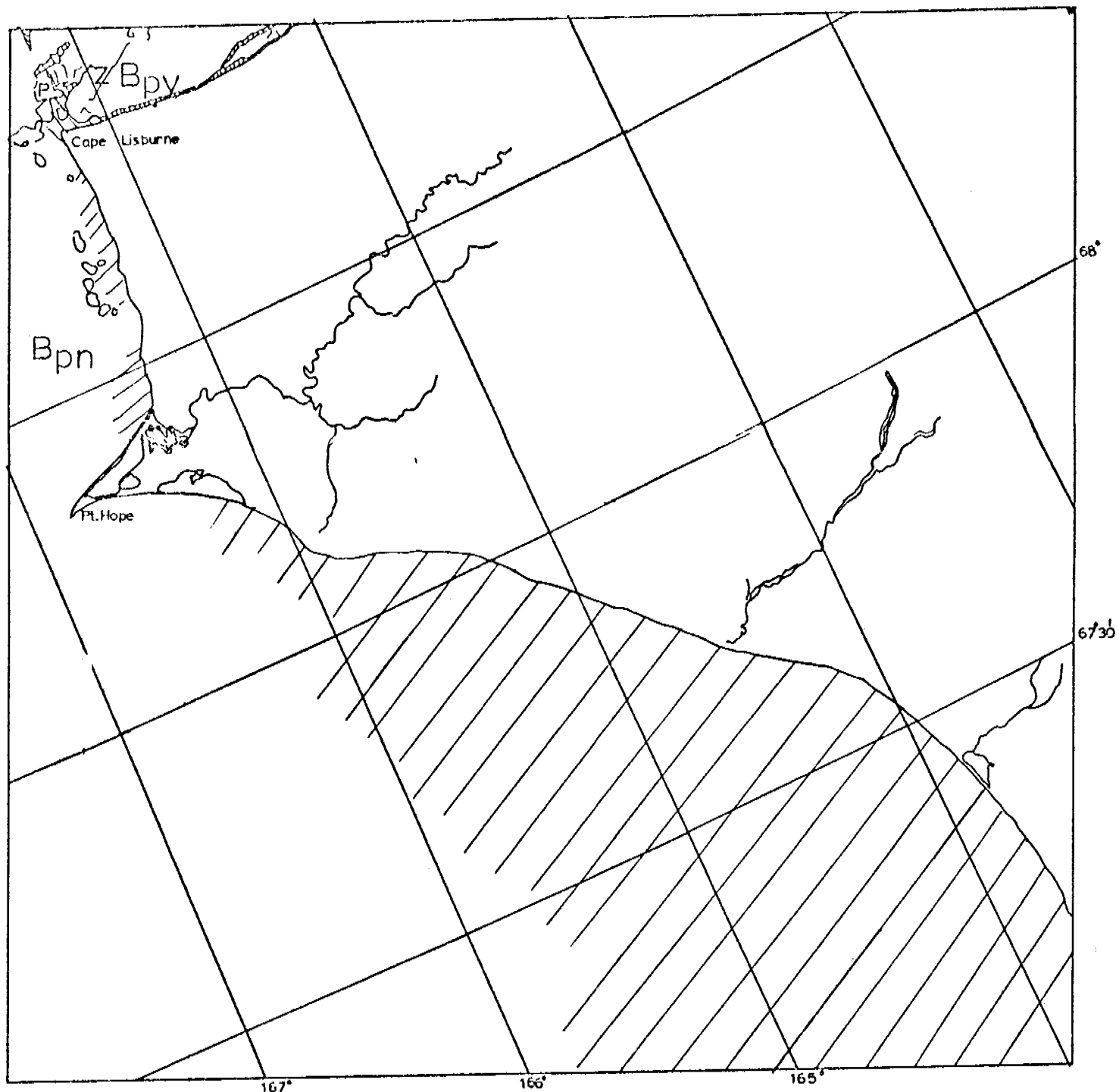
E-2275-21563-7
24 OCT. 1975

CHUKCHI SEA



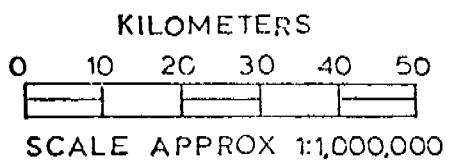
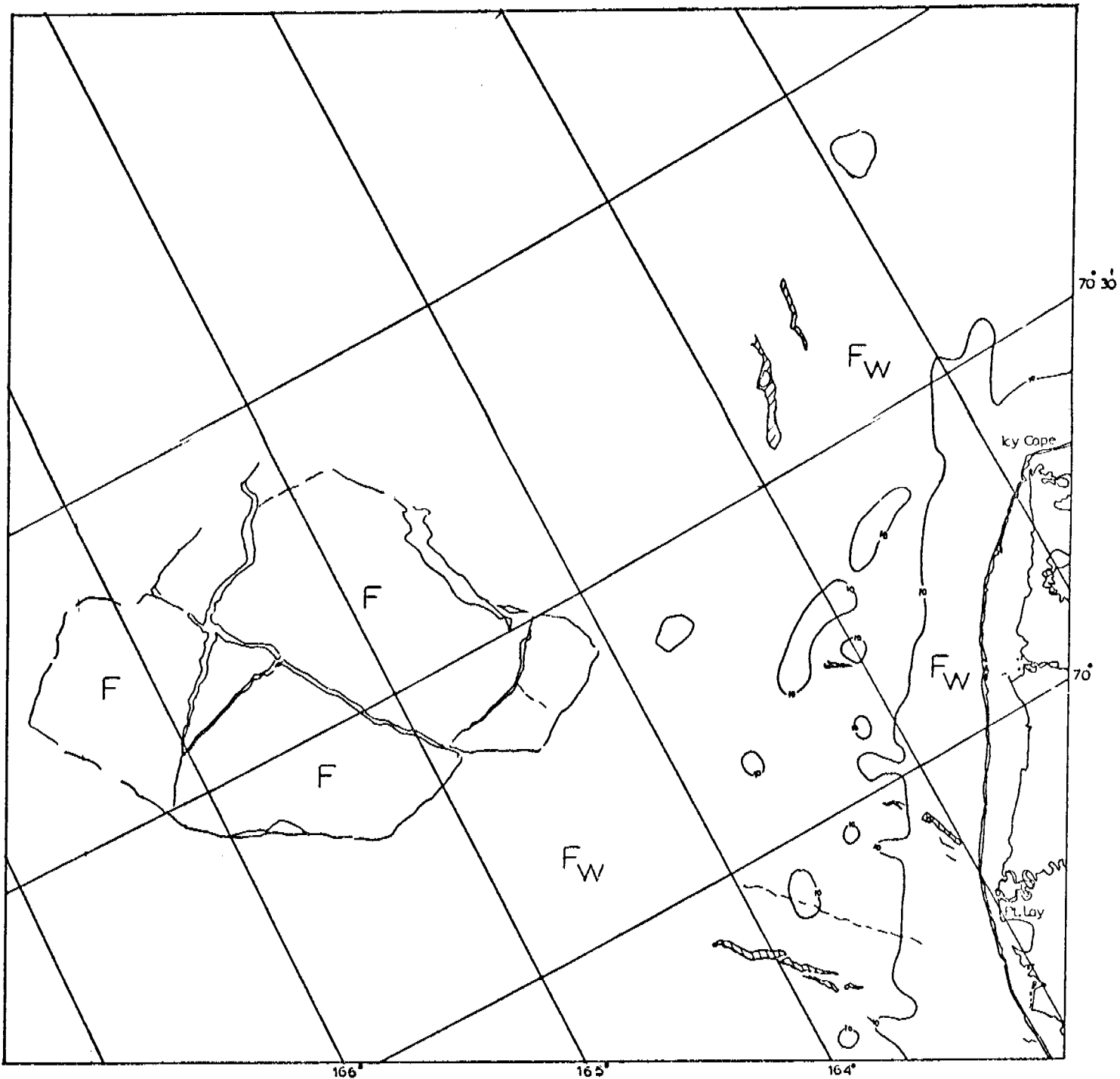
E-2276-22014-7
25 OCT. 1975

CHUKCHI SEA



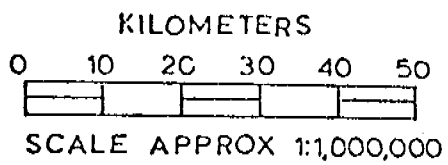
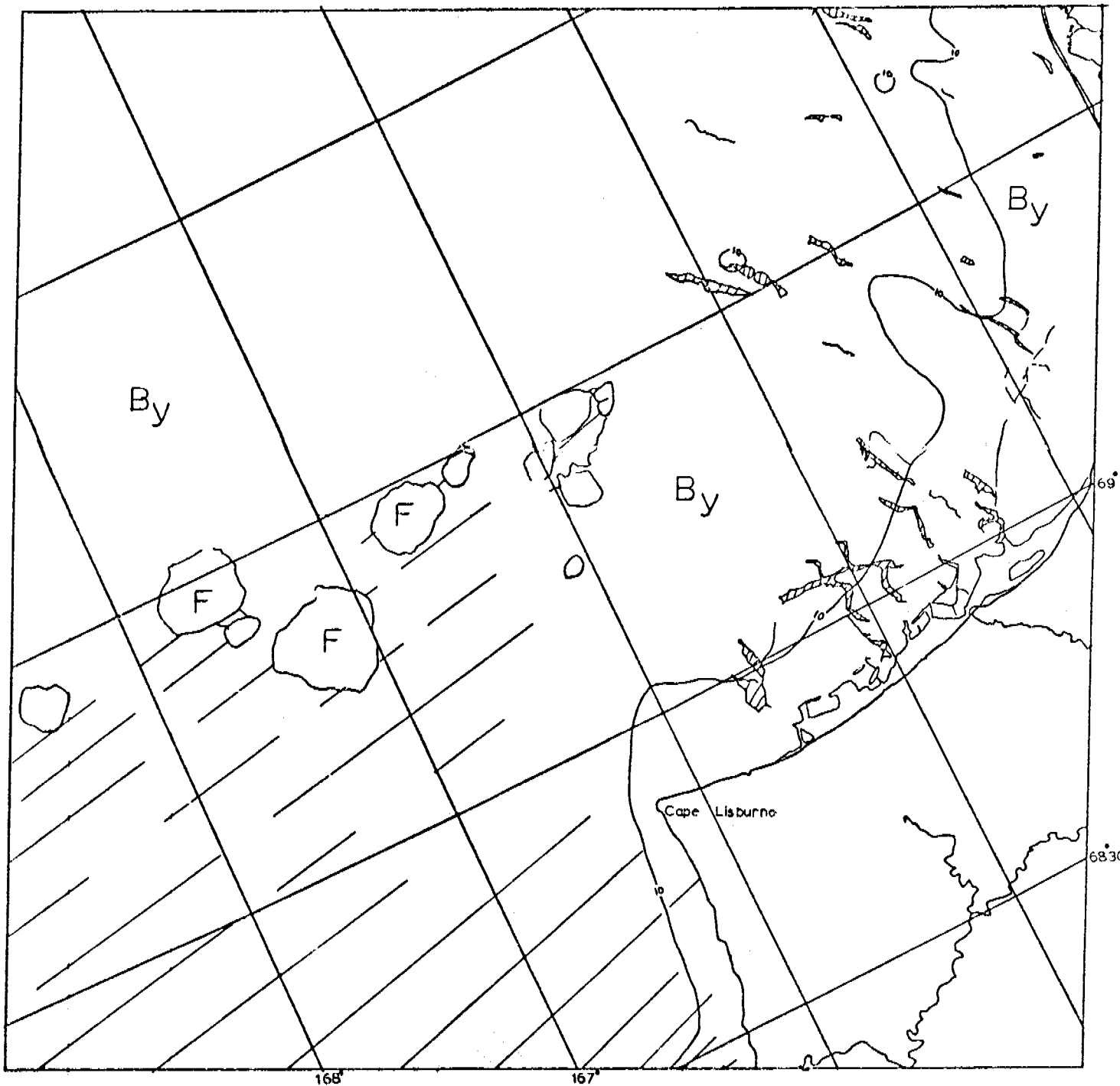
E-2276-22021-7
25 OCT. 1975

CHUKCHI SEA



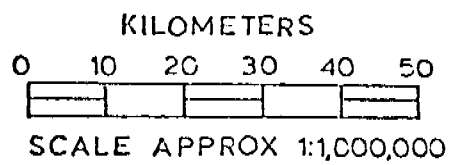
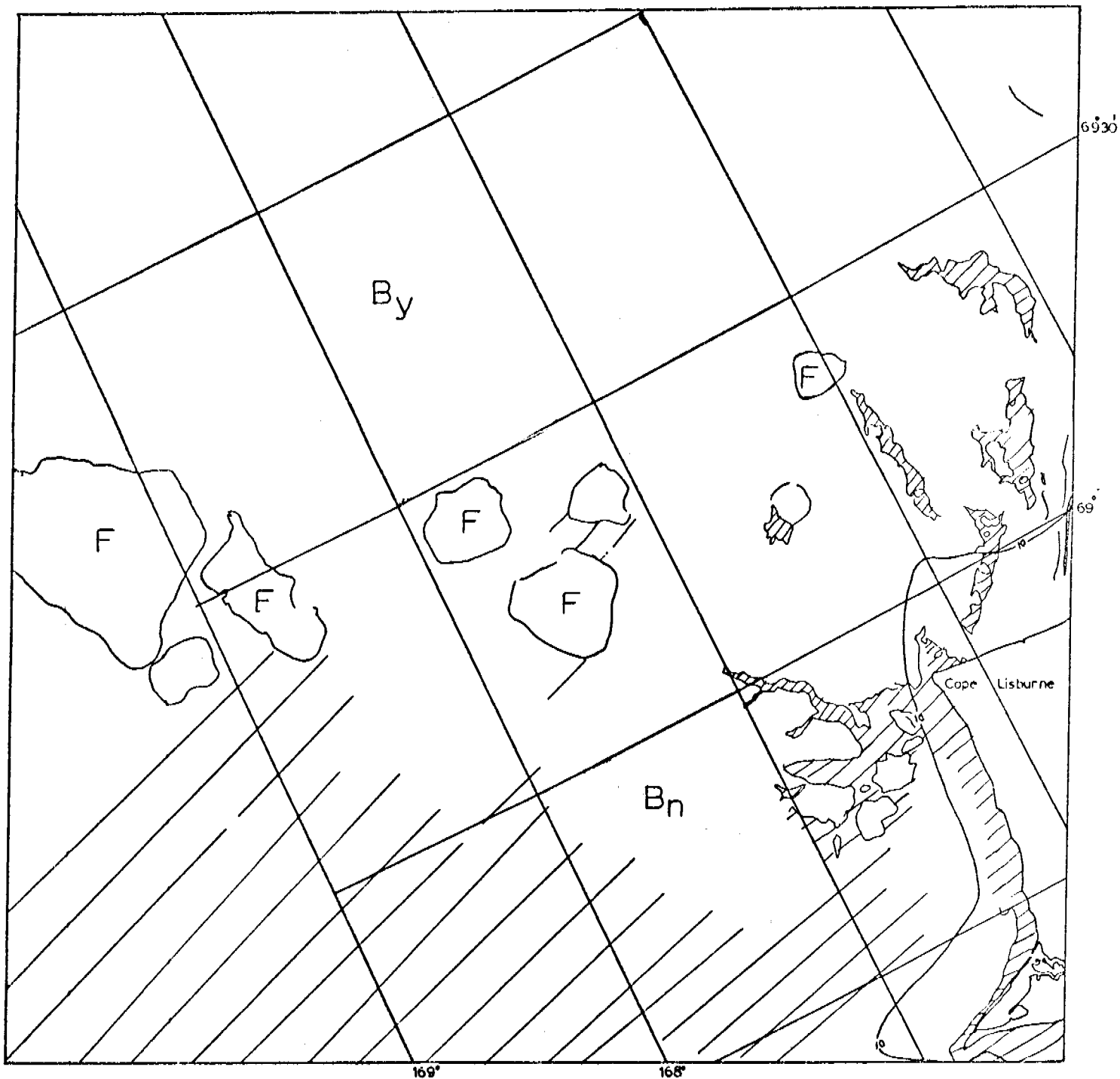
E-2278-22125-7
27 OCT. 1975

CHUKCHI SEA



E-2278-22131-7
27 OCT. 1975

CHUKCHI SEA



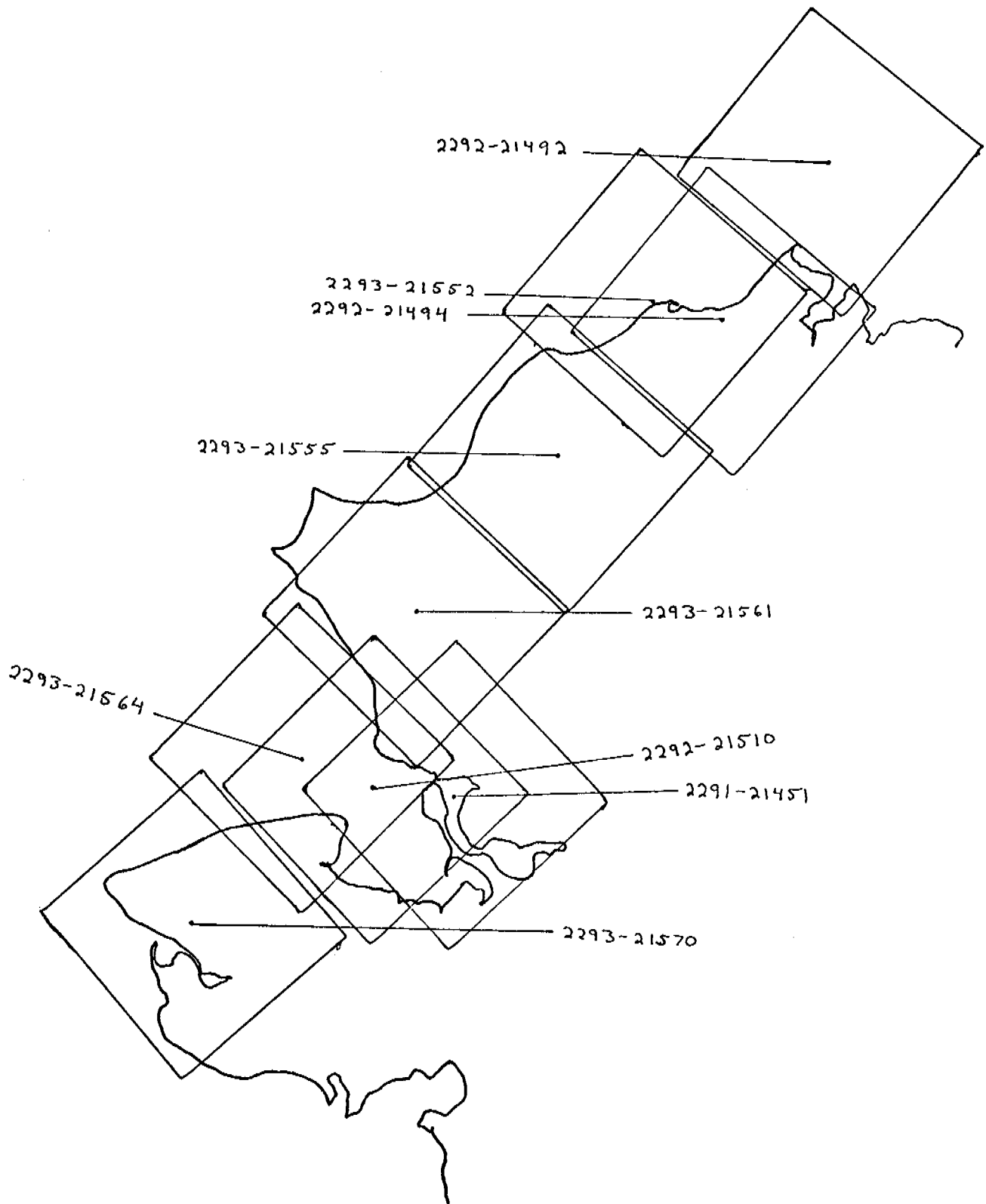
E-2279-22185-7
28 OCT. 1975

CHUKCHI SEA

CHUKCHI SEA

9-26 NOVEMBER 1975

Cycle 2291-2308



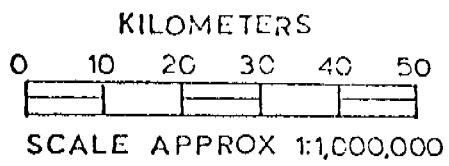
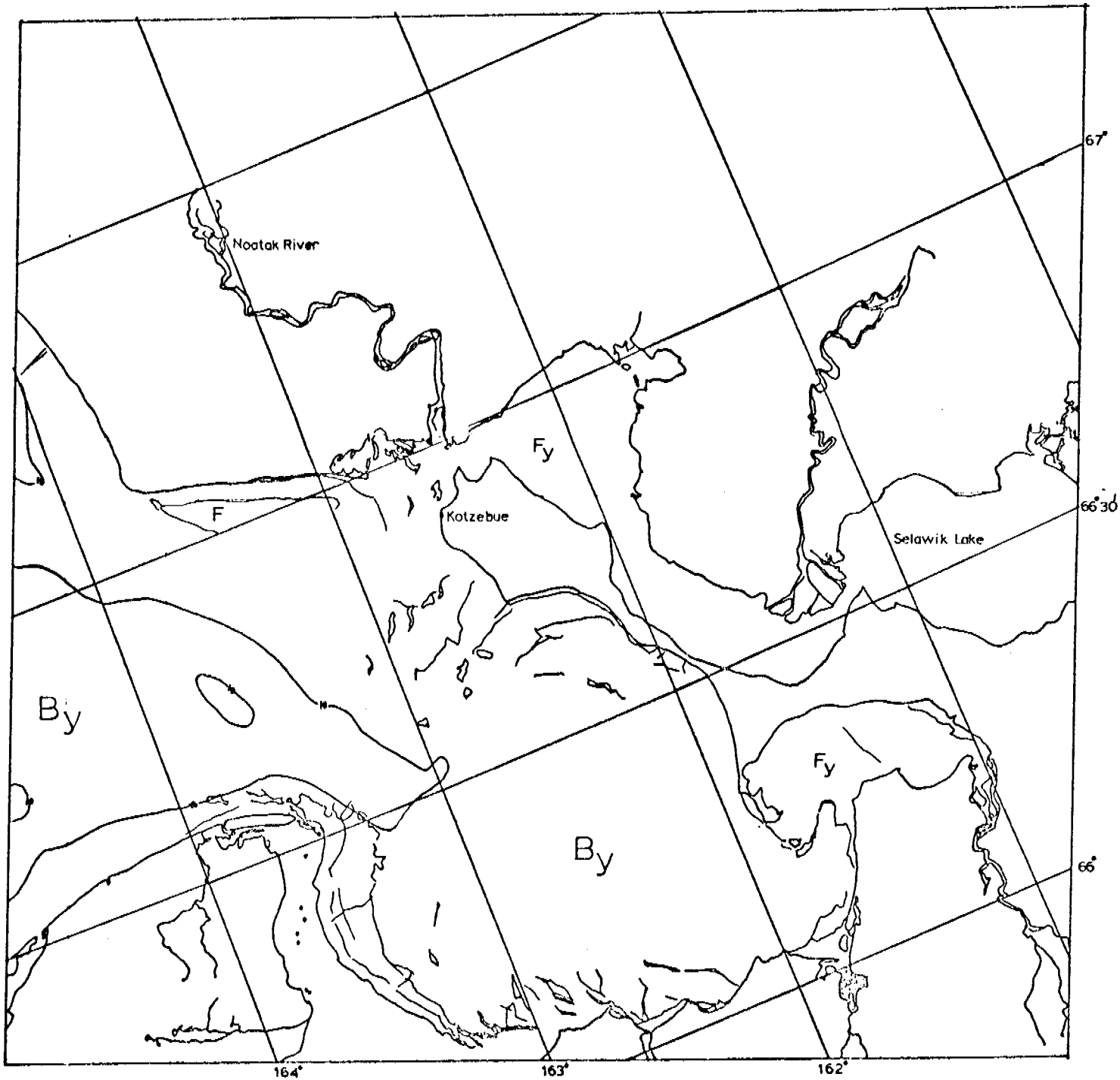
Scenes 2291-21451

2292-21492 } adjacent pair
2292-21494 }

2292-21510

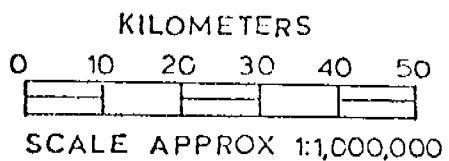
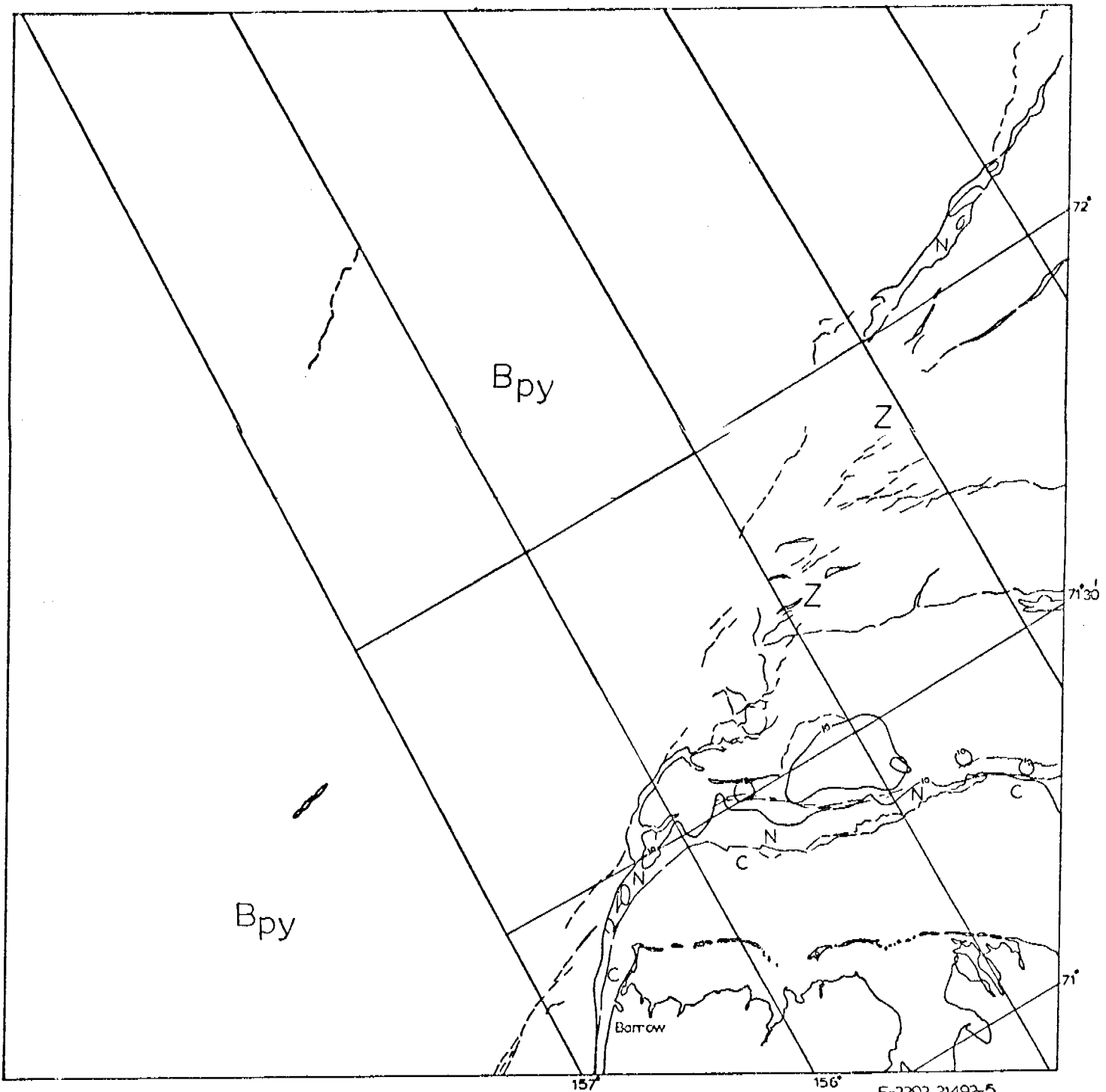
2293-21552 }
2293-21555 } group of 5 adjacent scenes
2293-21561 }
2293-21564 }
2293-21570 }

These scenes show the Chukchi Coast of Alaska for the period of November 9-11, 1975 between Barrow and Nome. At this time large expanses of contiguous ice can be found along the coast. However, there is no evidence of large grounded ridge systems that would be required to produce ice which would remain shore fast for the remainder of the winter season.



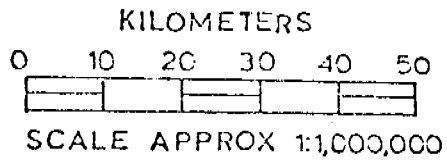
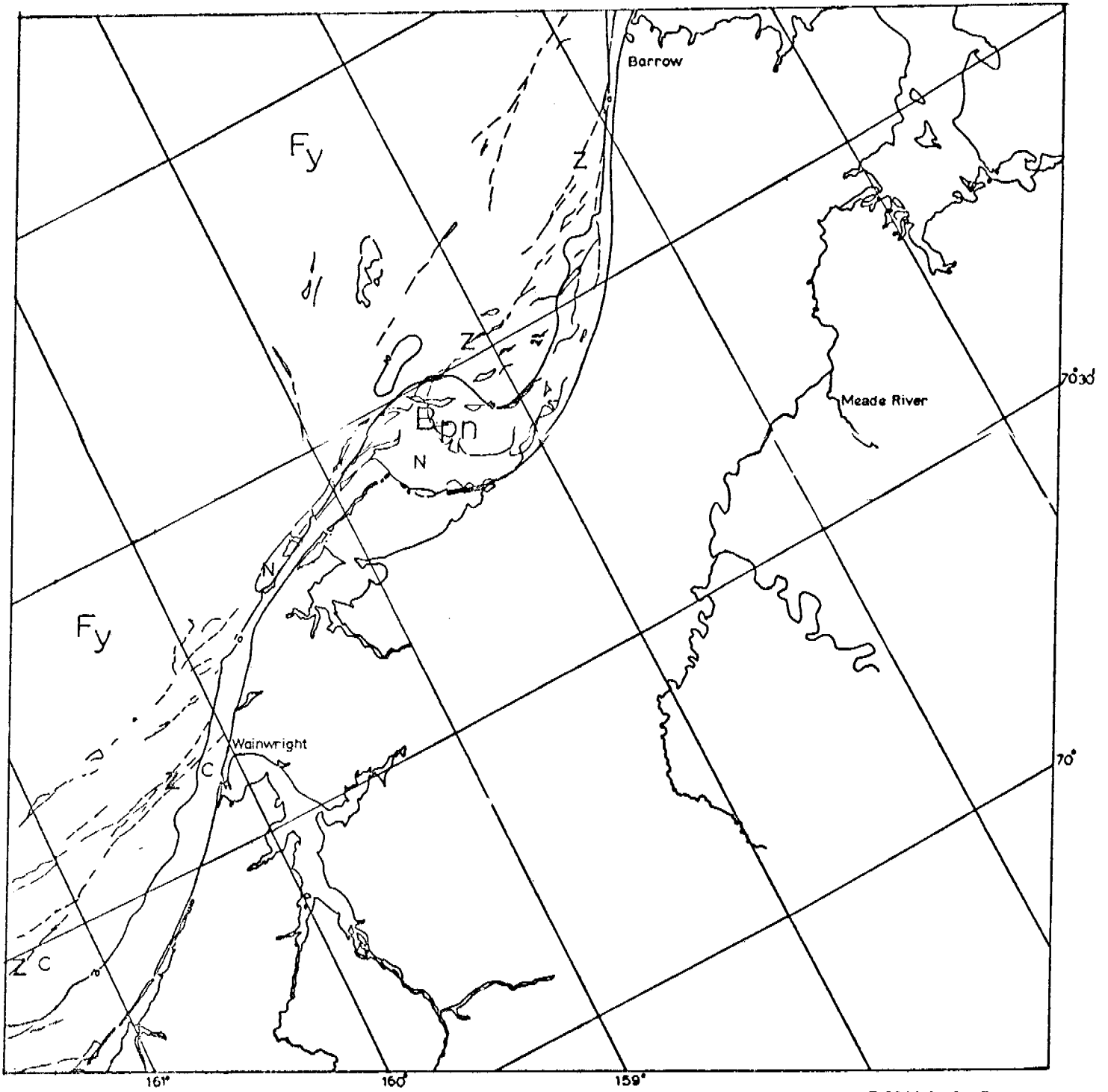
CHUKCHI SEA

E-2291-21451-7
9 Nov. 1975



CHUKCHI SEA

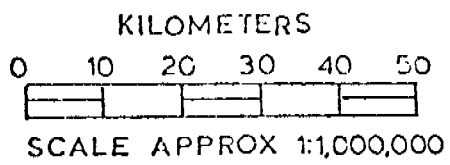
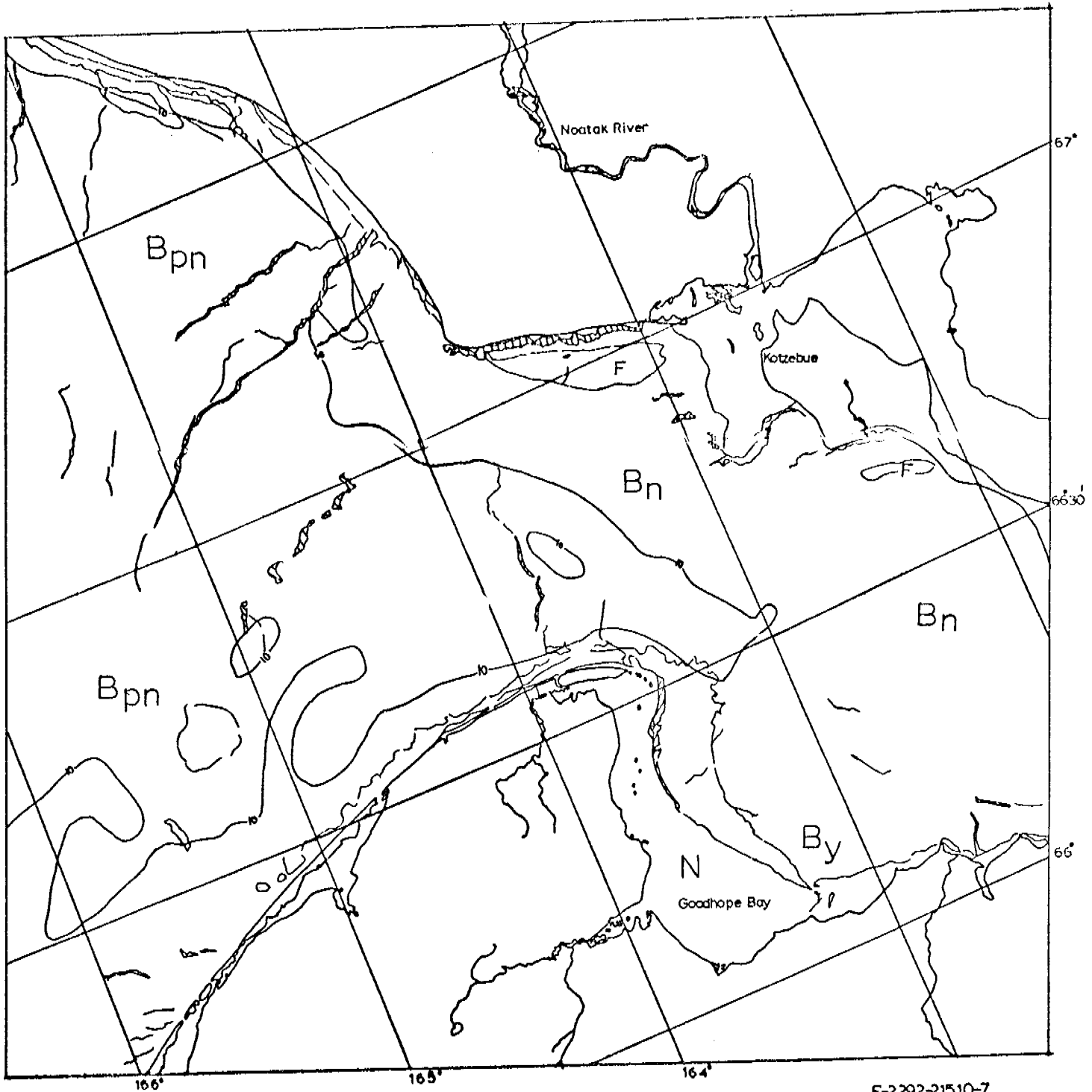
E-2292-21492-5
10 NOV. 1975



CHUKCHI SEA

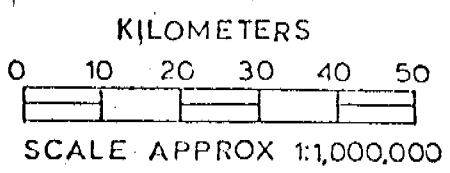
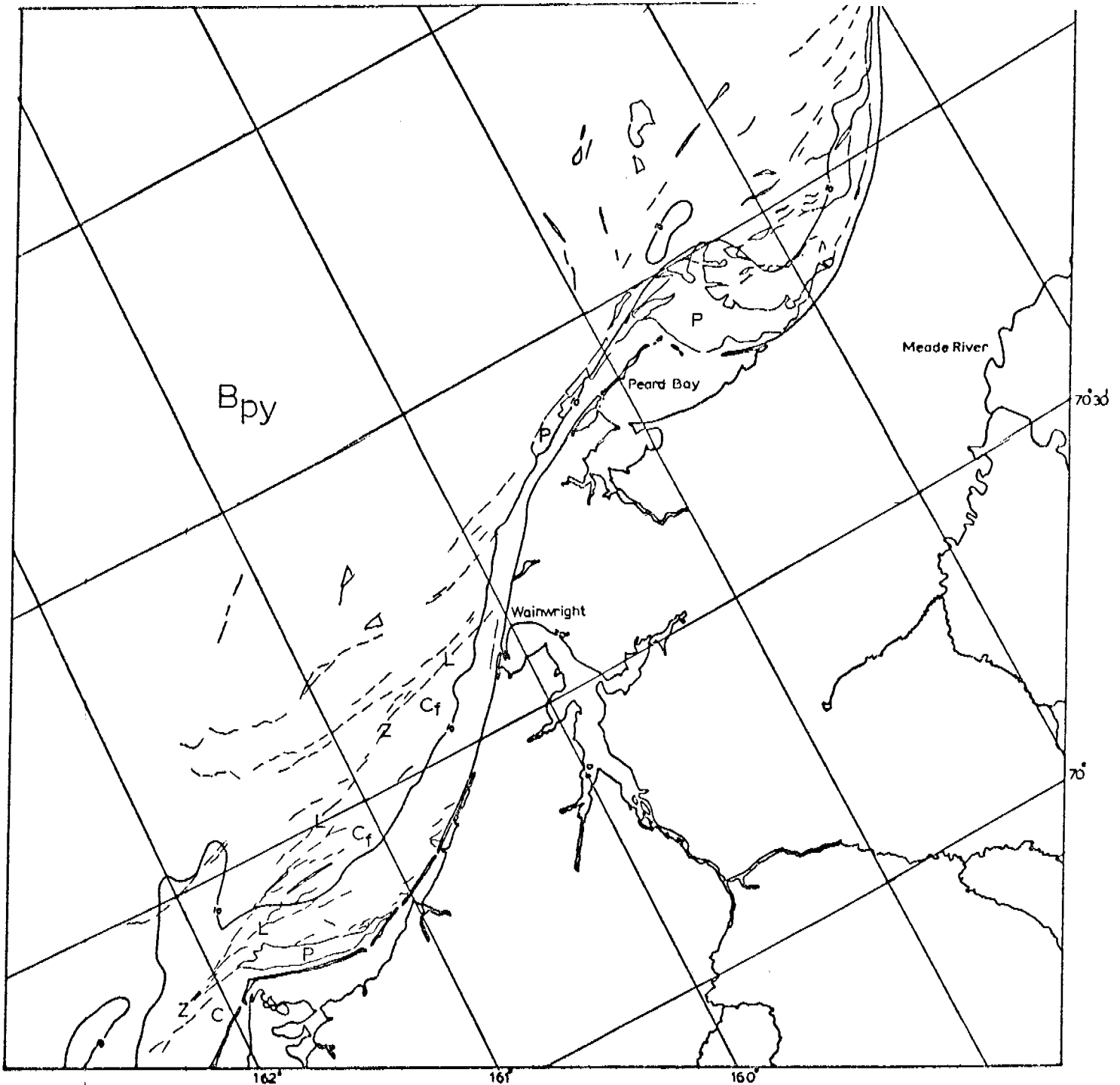
E-2292-21494-5

10 NOV, 1975



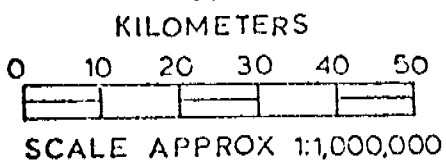
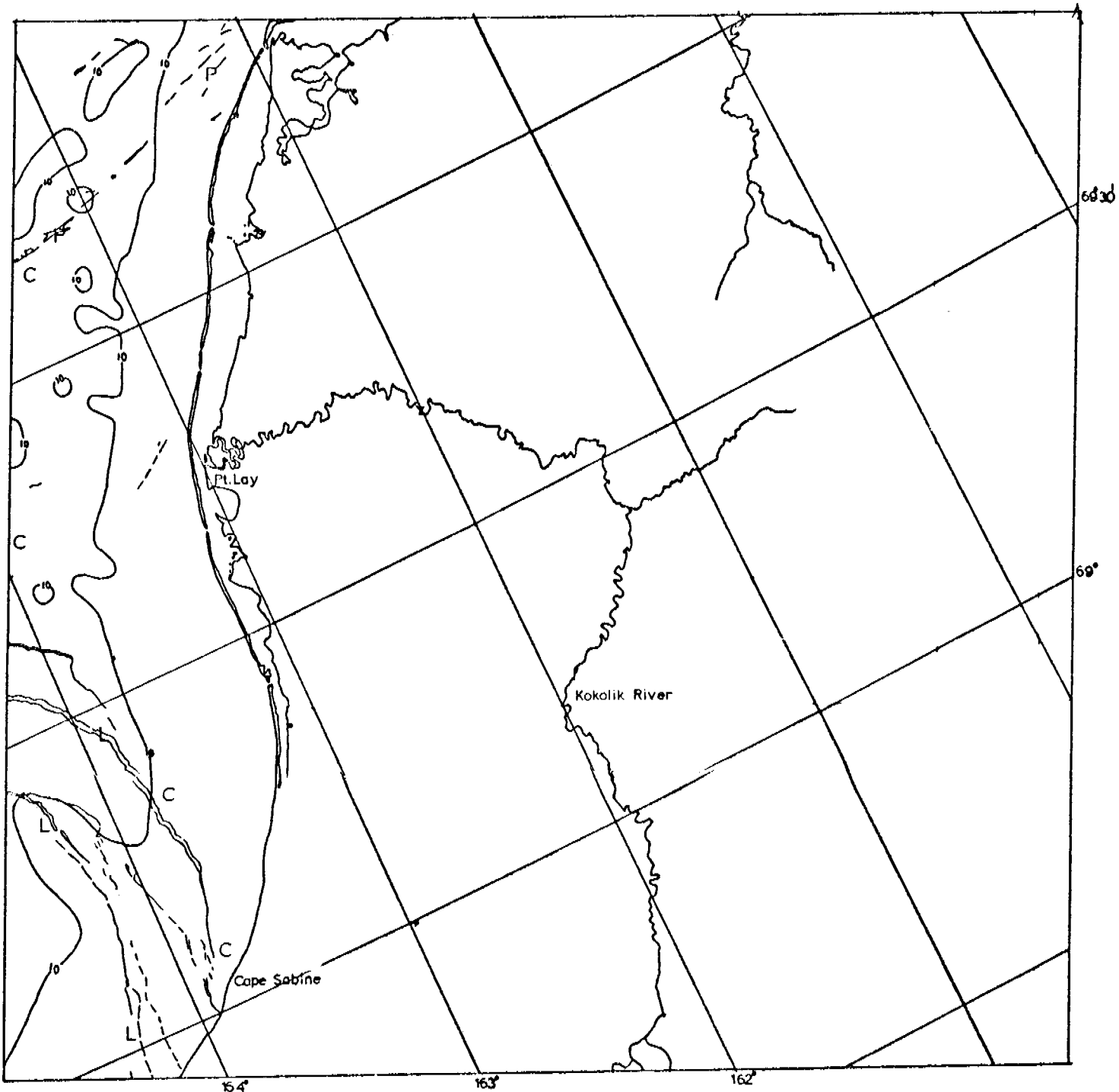
E-2292-21510-7
10 NOV. 1975

CHUKCHI SEA



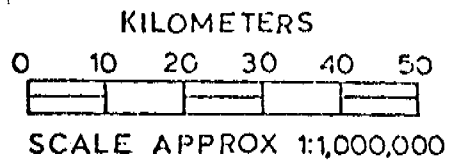
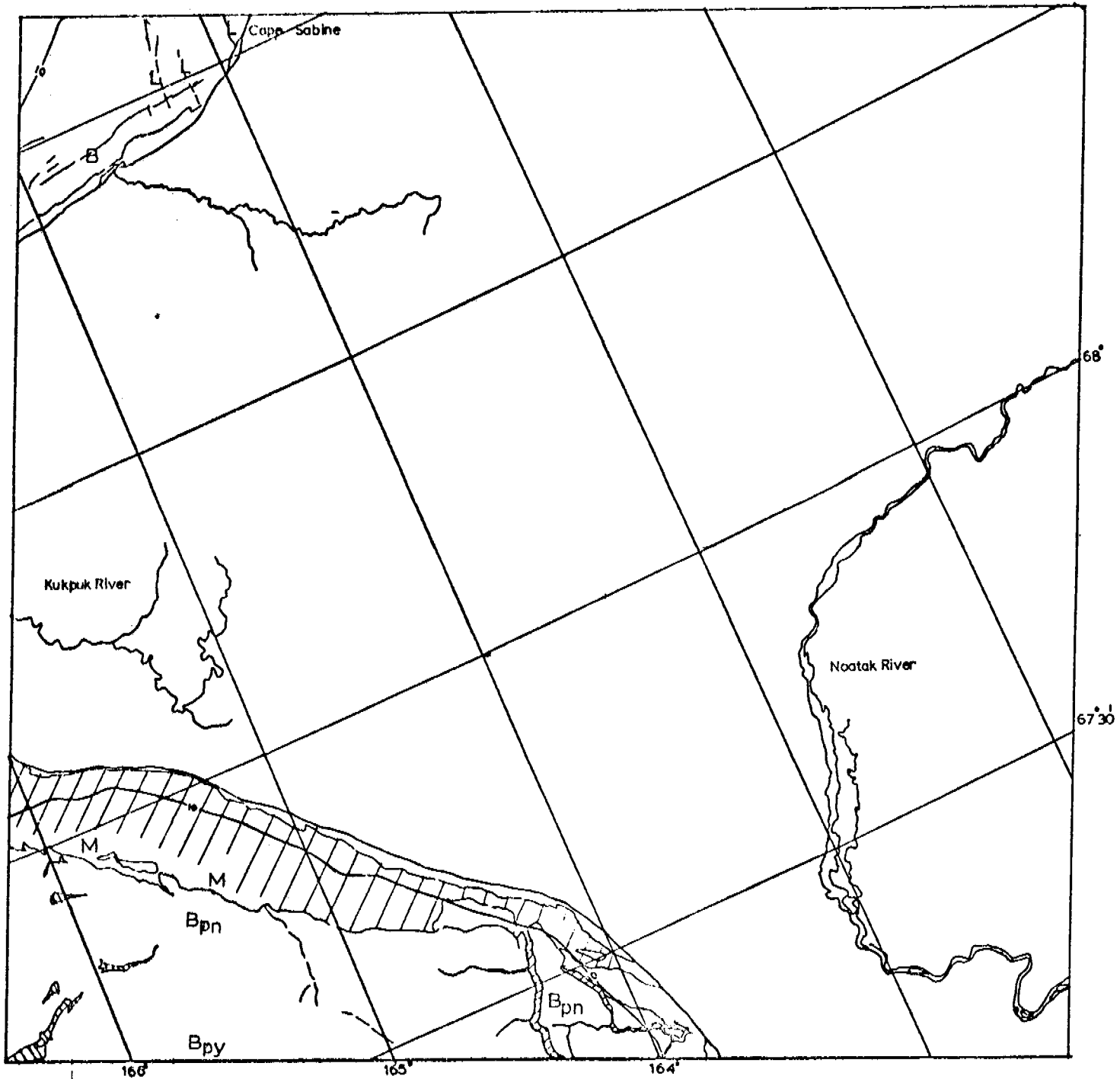
E-2293-21552-5
11 NOV. 1975

CHUKCHI SEA



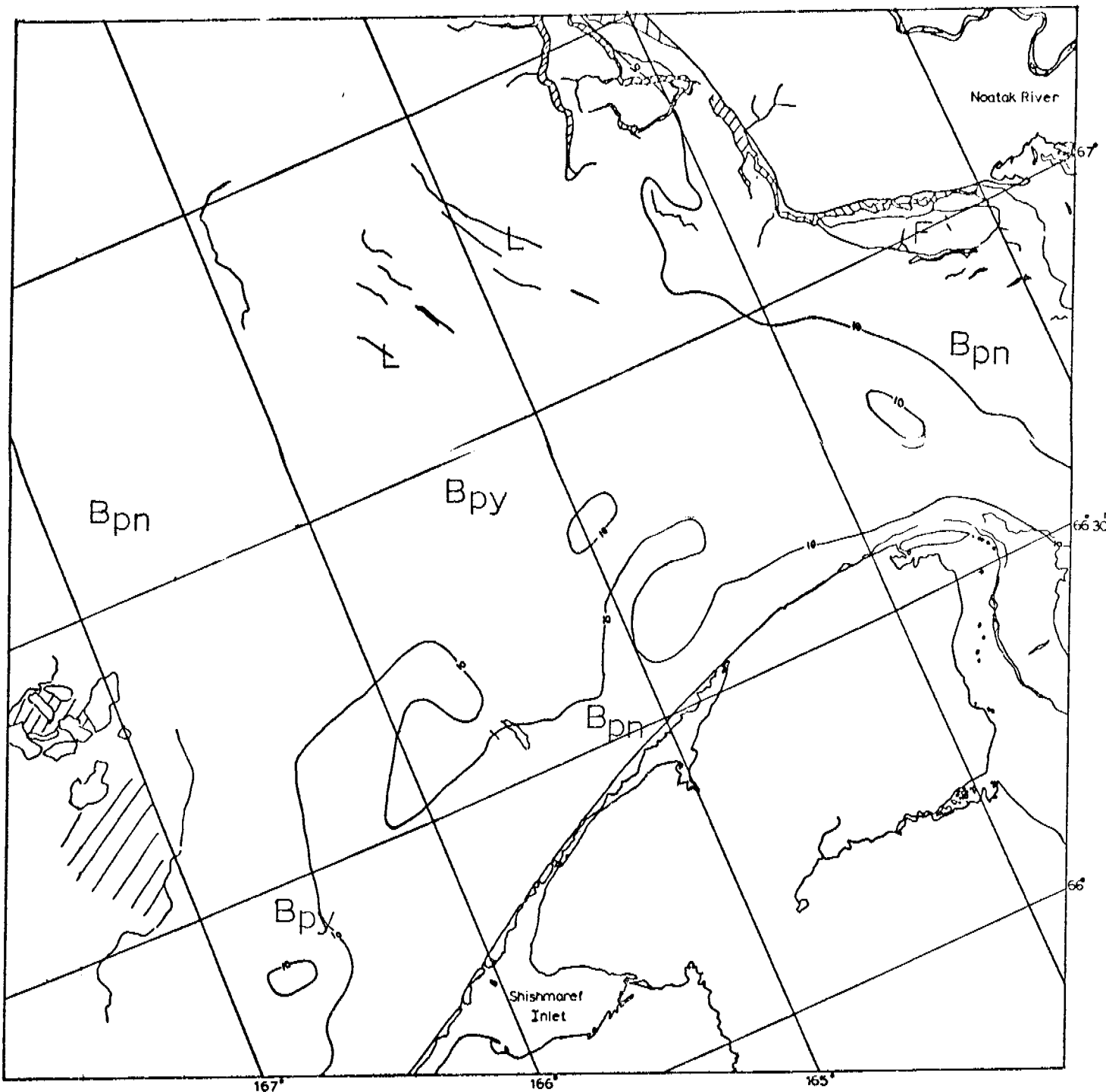
E-2293-21555-5
11 NOV. 1975

CHUKCHI SEA

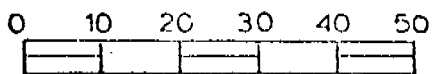


E-2293-2561-7
11 NOV. 1975

CHUKCHI SEA



KILOMETERS

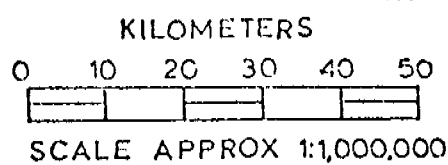
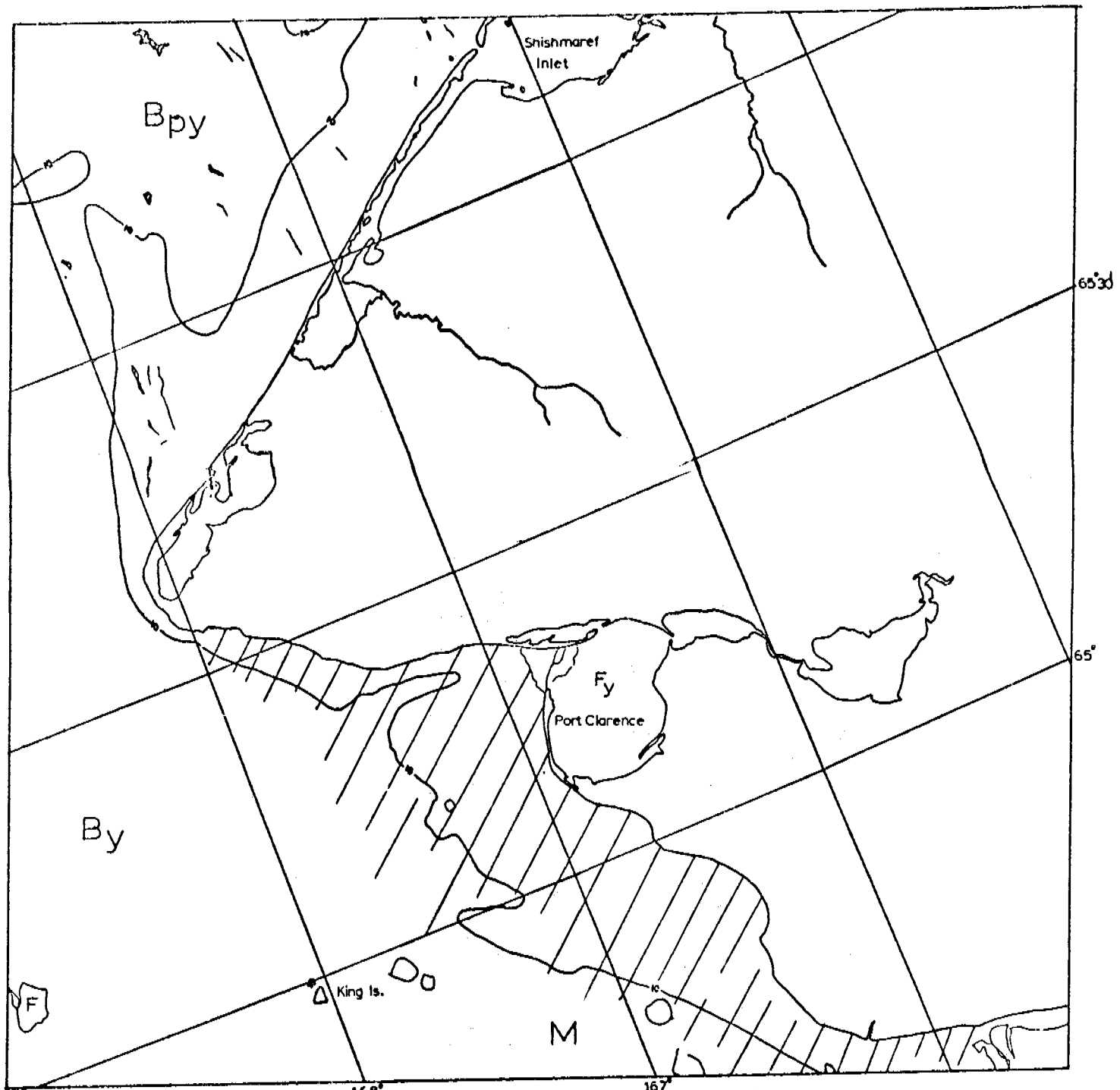


SCALE APPROX 1:1,000,000

E-2293-21564-7

11 NOV. 1975

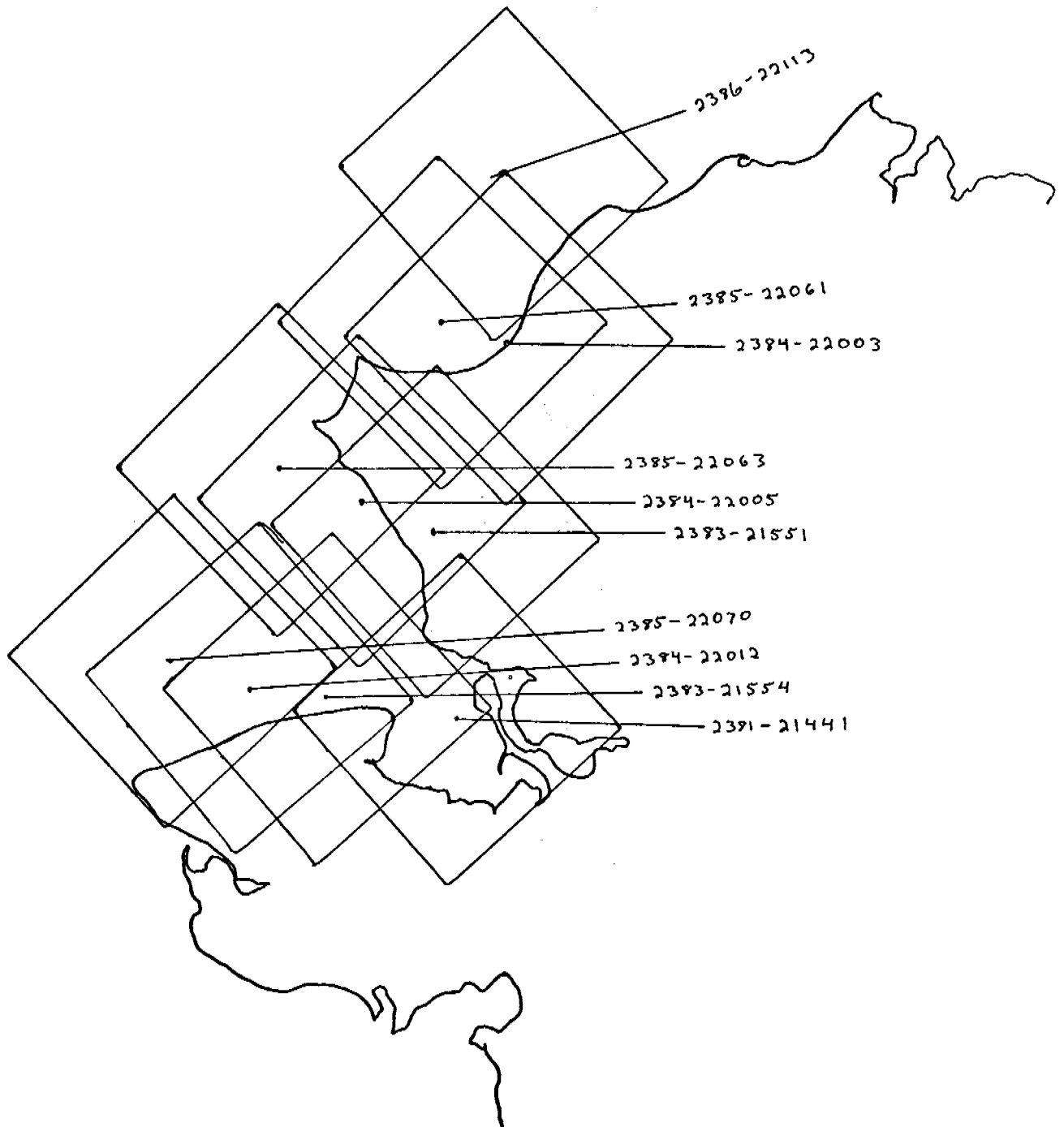
CHUKCHI SEA



E-2293-21570-7
11 NOV. 1975

CHUKCHI SEA

CHUKCHI SEA
6-23 FEBRUARY 1976
Cycle 2381-2398



Scenes 2381-21441

2383-21551 } adjacent pair
 2383-21554 }

2384-22003 } adjacent triplet
 2384-22005 }
 2384-22012 }

2385-22061 } adjacent triplet
 2385-22063 }
 2385-22070 }

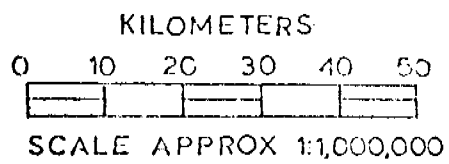
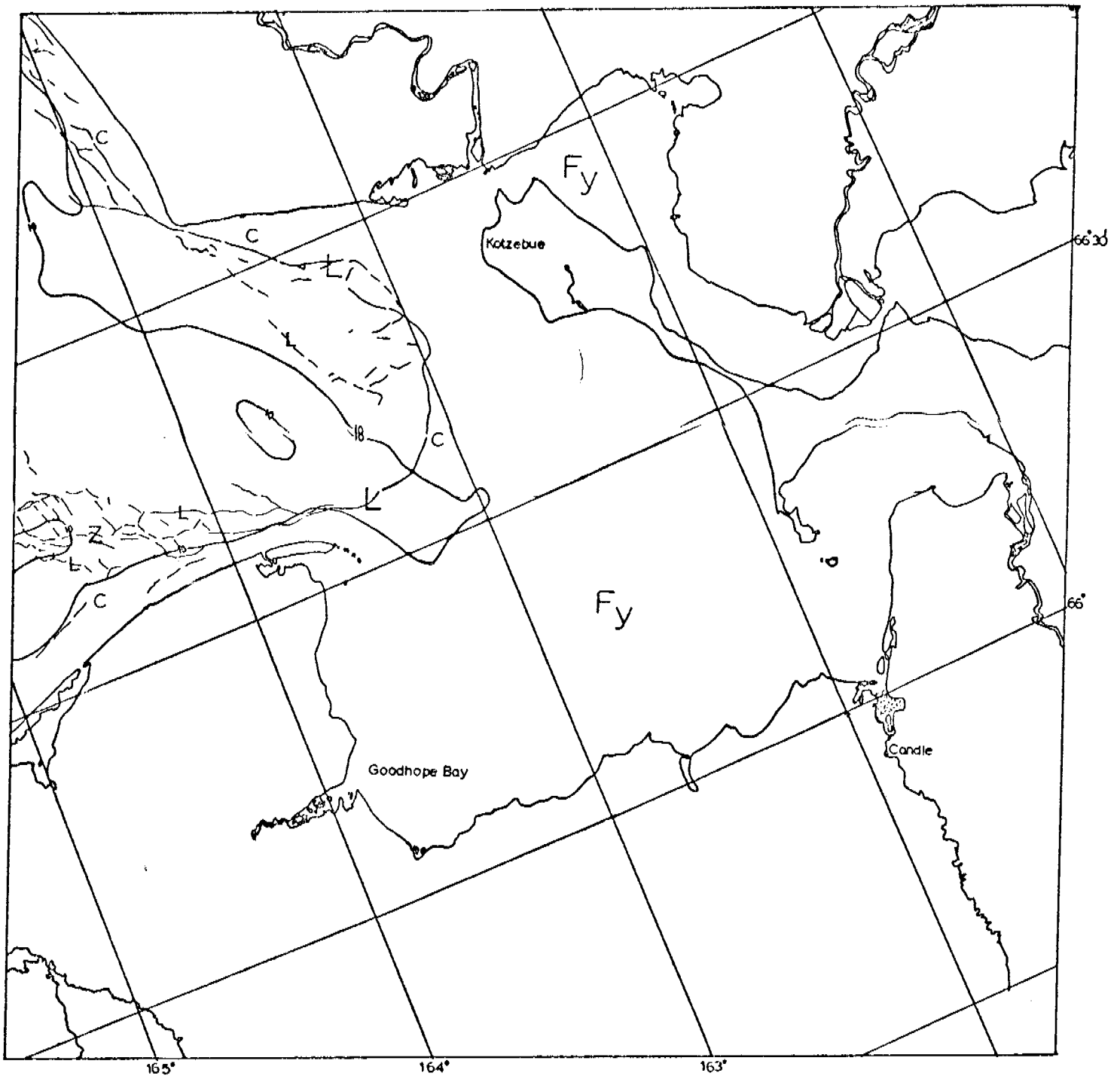
2386-22113

These scenes show the Kotzebue sound region between Point Lay and Bering Strait for the period February 7-12, 1976.

At this time the inner part of Kotzebue sound is covered with smooth first-year ice. There is a sideways "U"-shaped indentation of pressured ice protruding into the sound with associated shearing effects along its arms. The three sets of adjacent images show dynamic processes at work in the lower Chukchi sea: Winds appear to be forcing the ice southward through Bering Strait. Associated with this is a large polynya south of Point Hope. However, the open water in the polynya is freezing to the young ice almost as fast as it is formed. Immediately south of this polynya is a funnel-shaped area of highly pressured ice which shows considerable compaction even within the one day observation period between the second and third adjacent scene triplets.

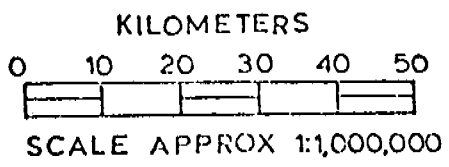
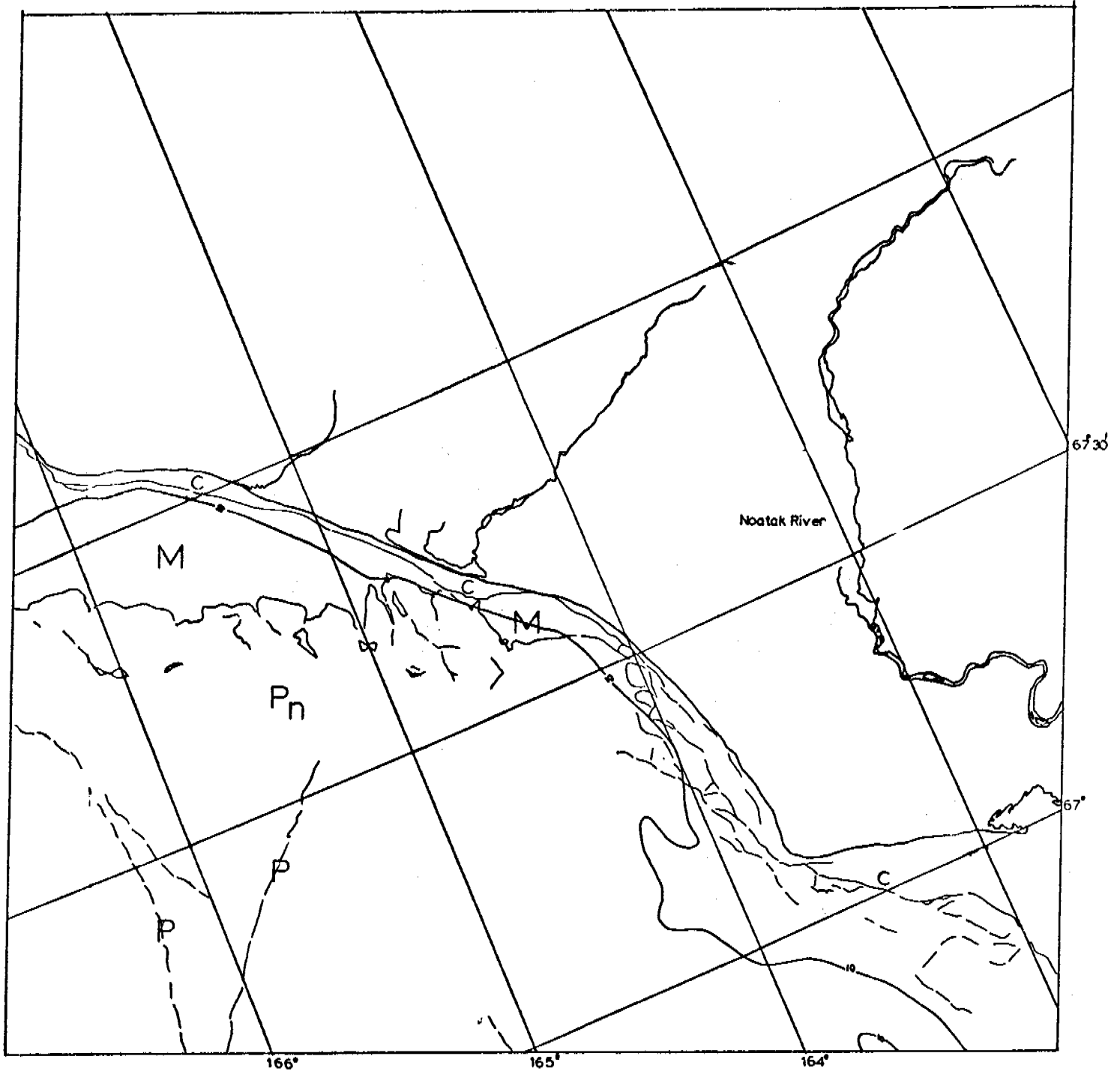
Immediately south (50 km) of the "spout" of the funnel is a large north-south shear ridge hummock field extending northward from Cape Prince of Wales. It would appear that this large feature has been created by the construction of large massive shear ridges over shoals in this area with the result that the ridges easily become grounded and stabilized. At this time, a line of shear can be traced northward from Cape Prince of Wales, past the ridge system, and up the westward side of the funnel.

To the north, ice appears to be shearing past Point Hope, leaving an accumulation of ice on the shoals just to the north of Point Hope. North of Cape Lisburne a smooth apron of first year ice extends to approximately the 10-fathom contour. Approaching Blossom Shoals, there are increasing indications of large ridges along the seaward edge of the apron ending in a large hummock field at Blossom Shoals.



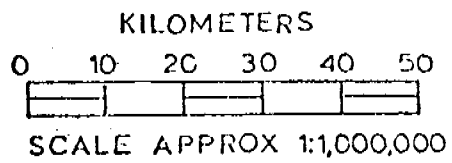
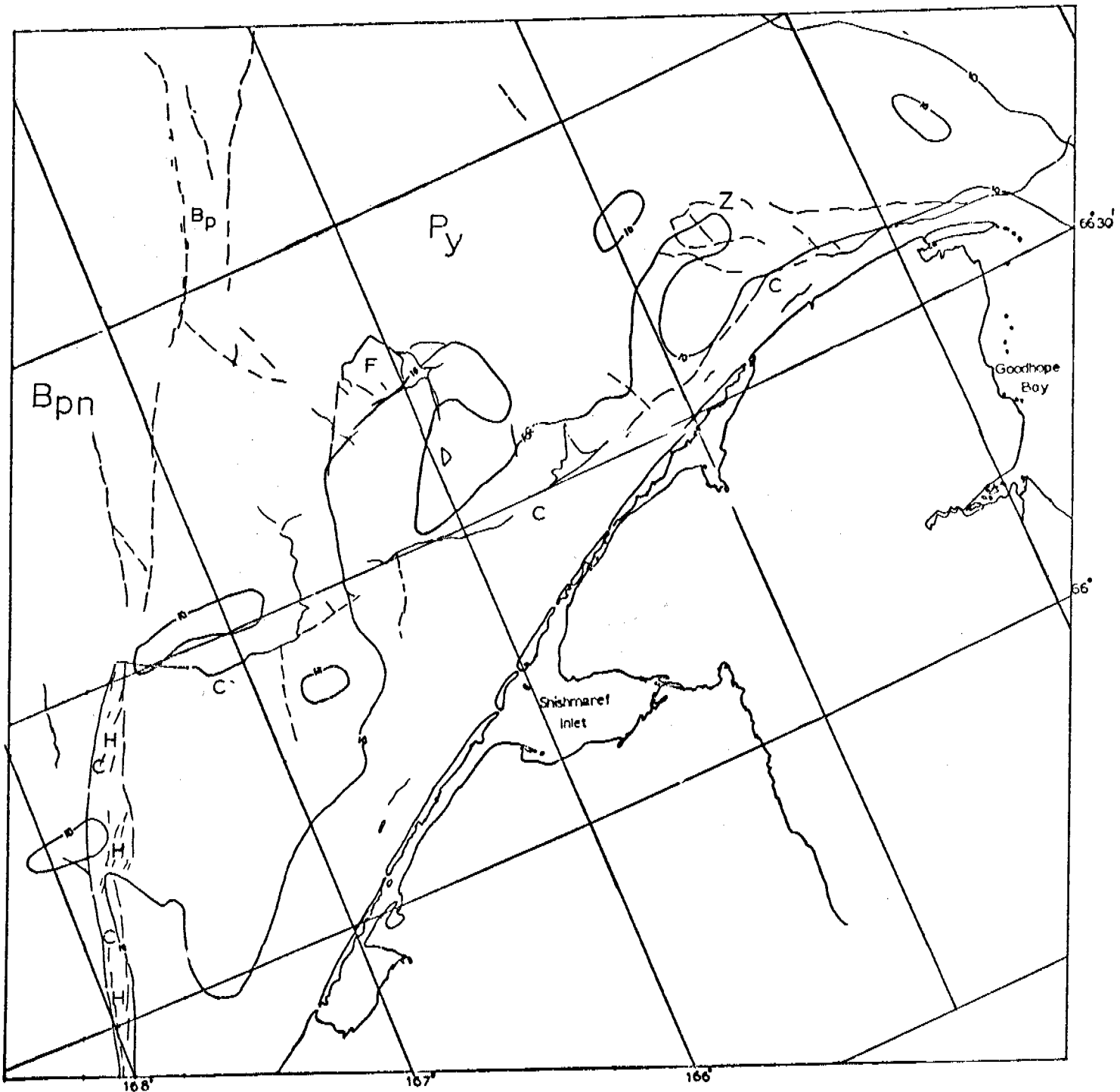
E-2381-21441-7
7 FEB. 1976

CHUKCHI SEA



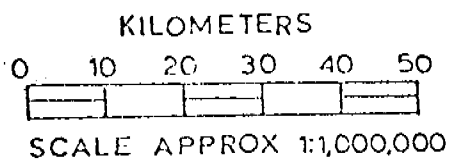
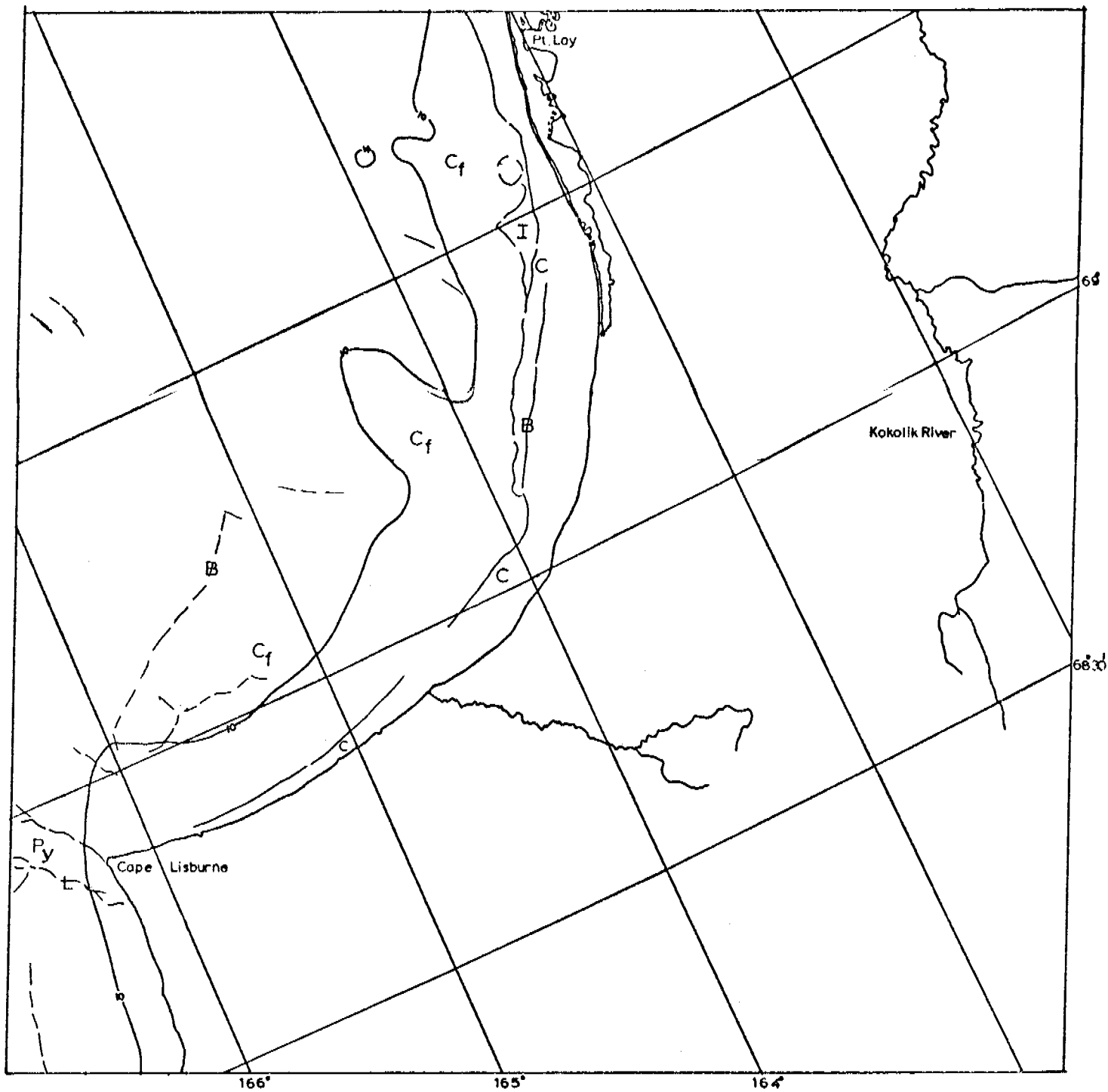
CHUKCHI SEA

E-2383-21551-7
9 FEB. 1976



E-2383-21554-7
9 FEB. 1976

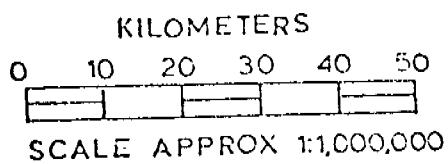
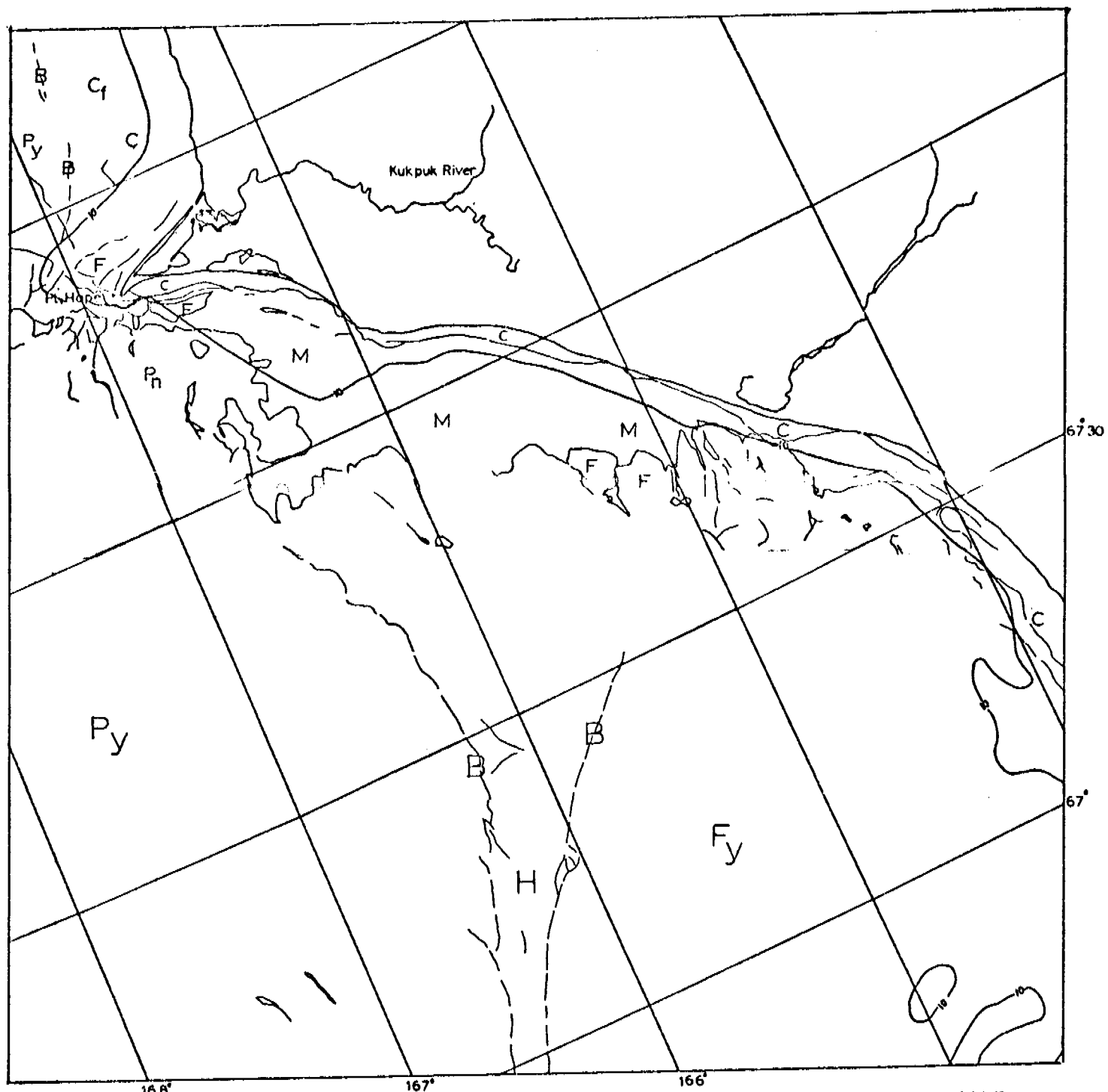
CHUKCHI SEA



CHUKCHI SEA

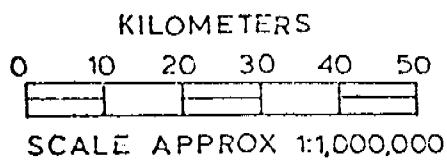
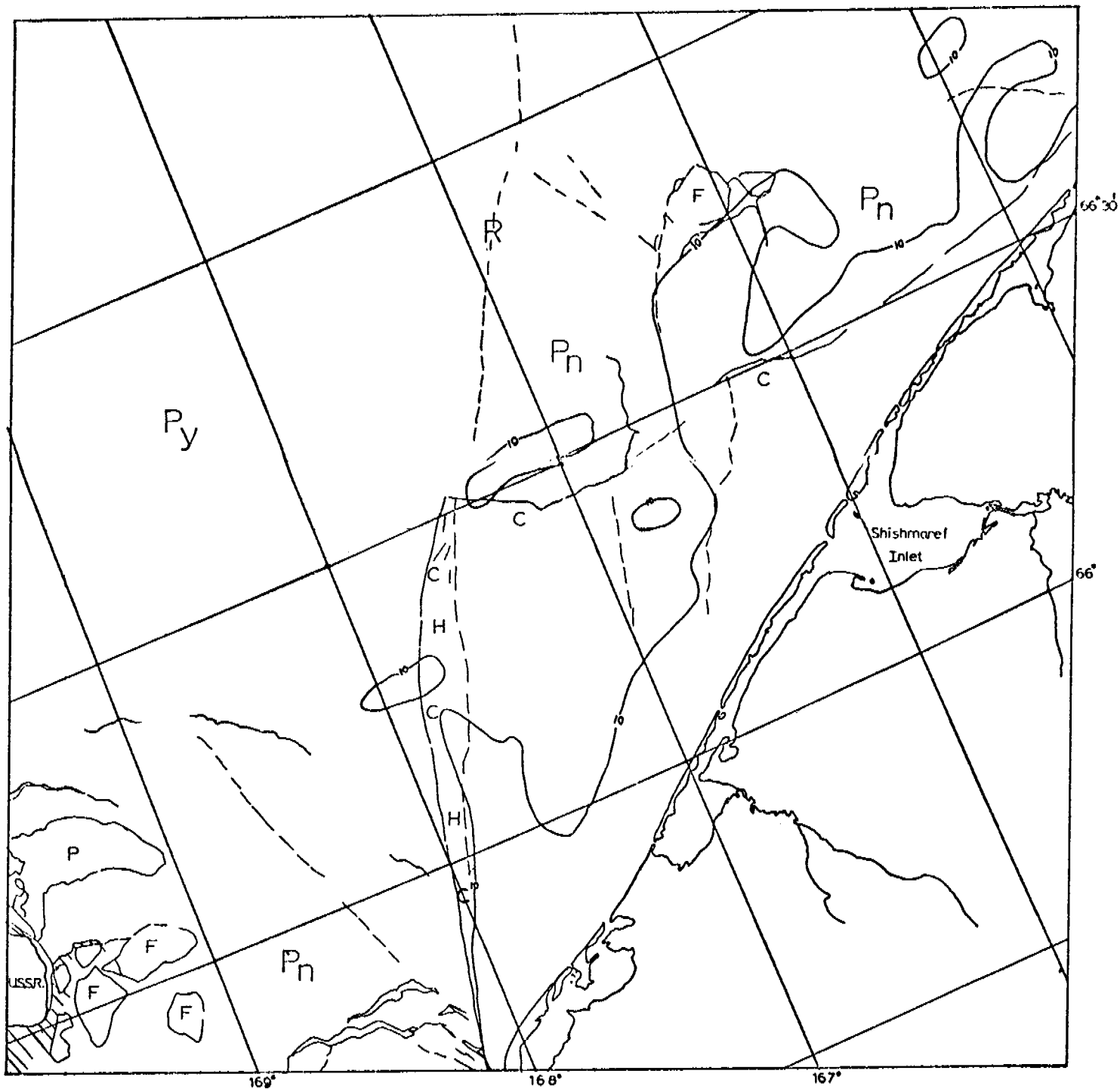
E-2384-22003-7

10 FEB. 1976



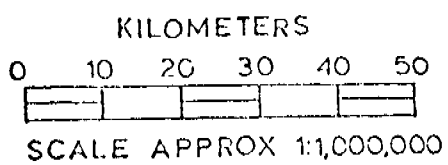
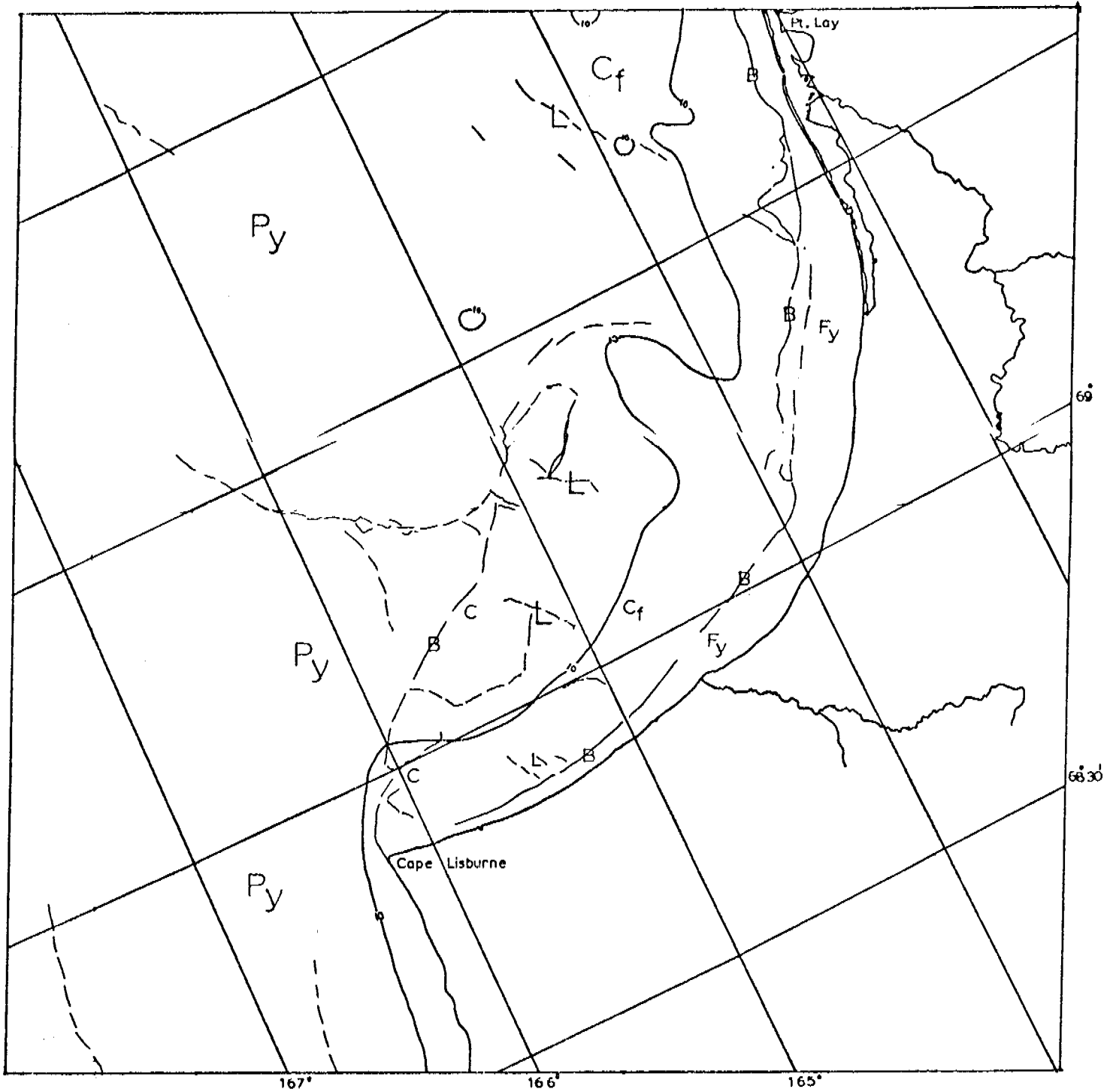
E-2384-22005-7
10 FEB. 1976

CHUKCHI SEA



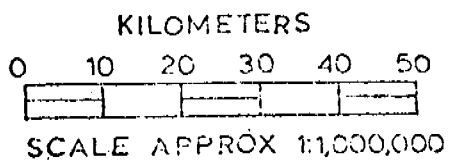
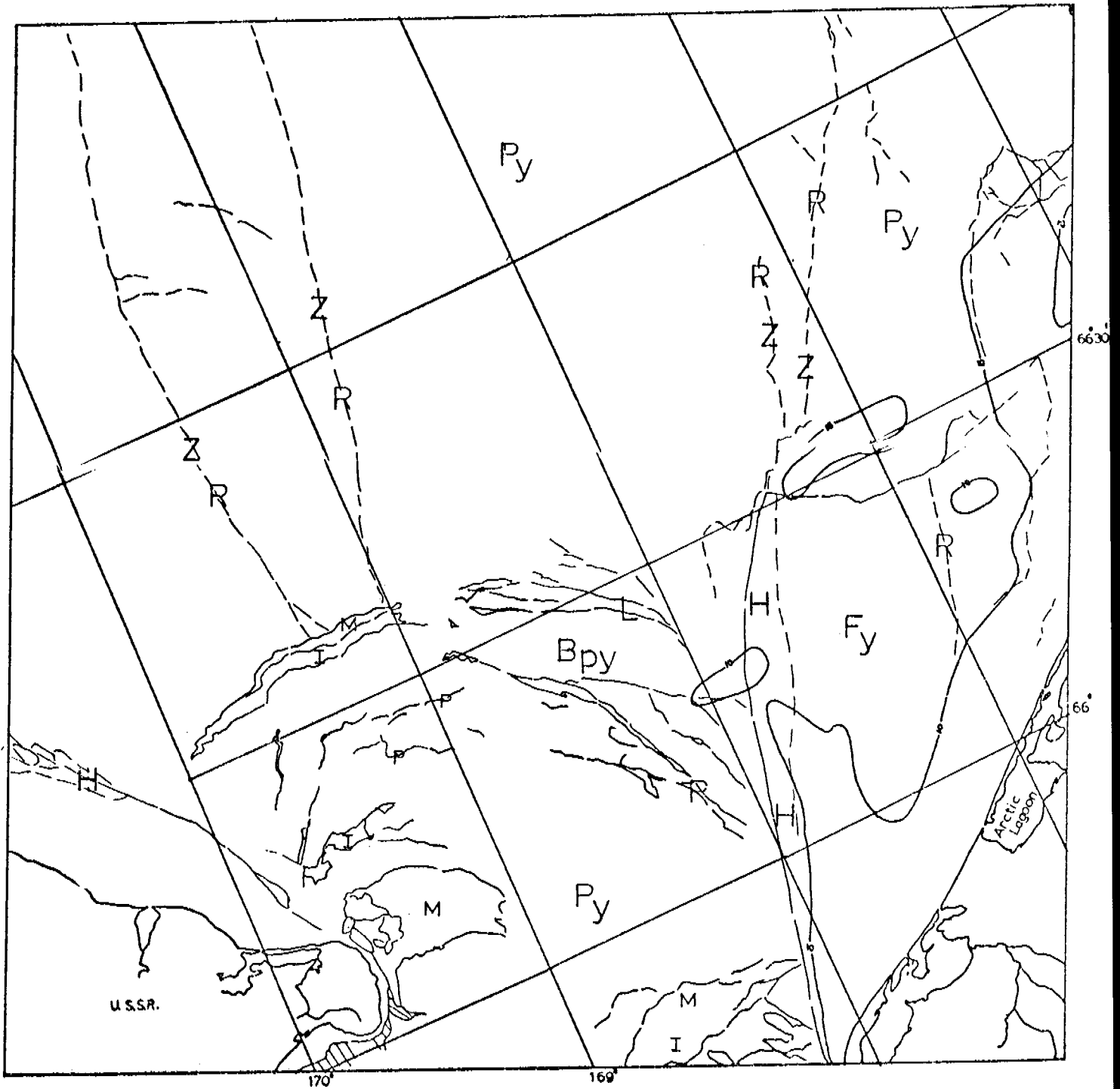
E-2384-22012-7
10 FEB. 1976

CHUKCHI SEA



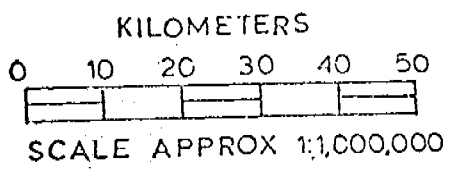
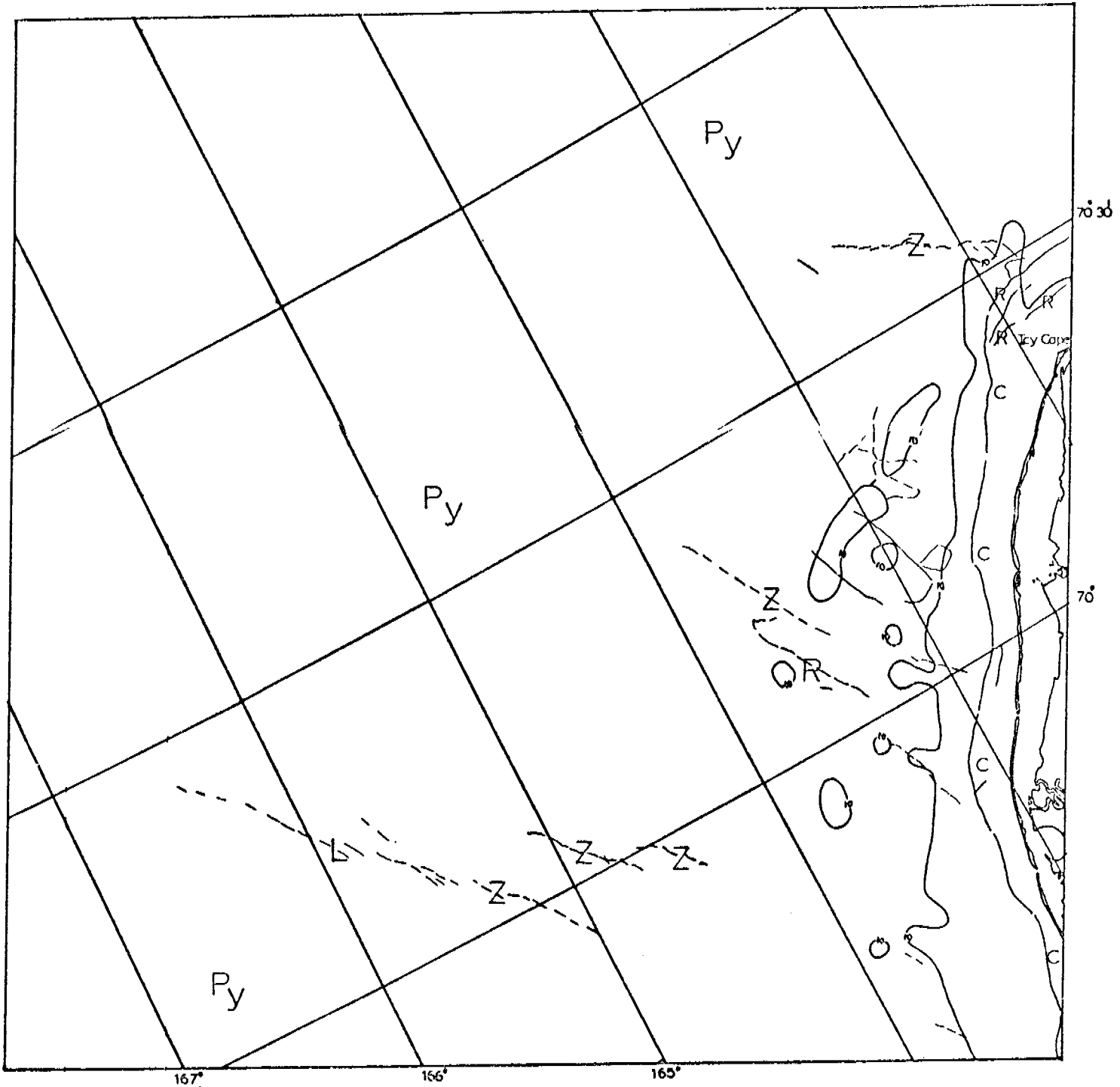
CHUKCHI SEA

E-2385-2206-7
11 FEB. 1976



E-2385-22070-7
11 FEB. 1976

CHUKCHI SEA



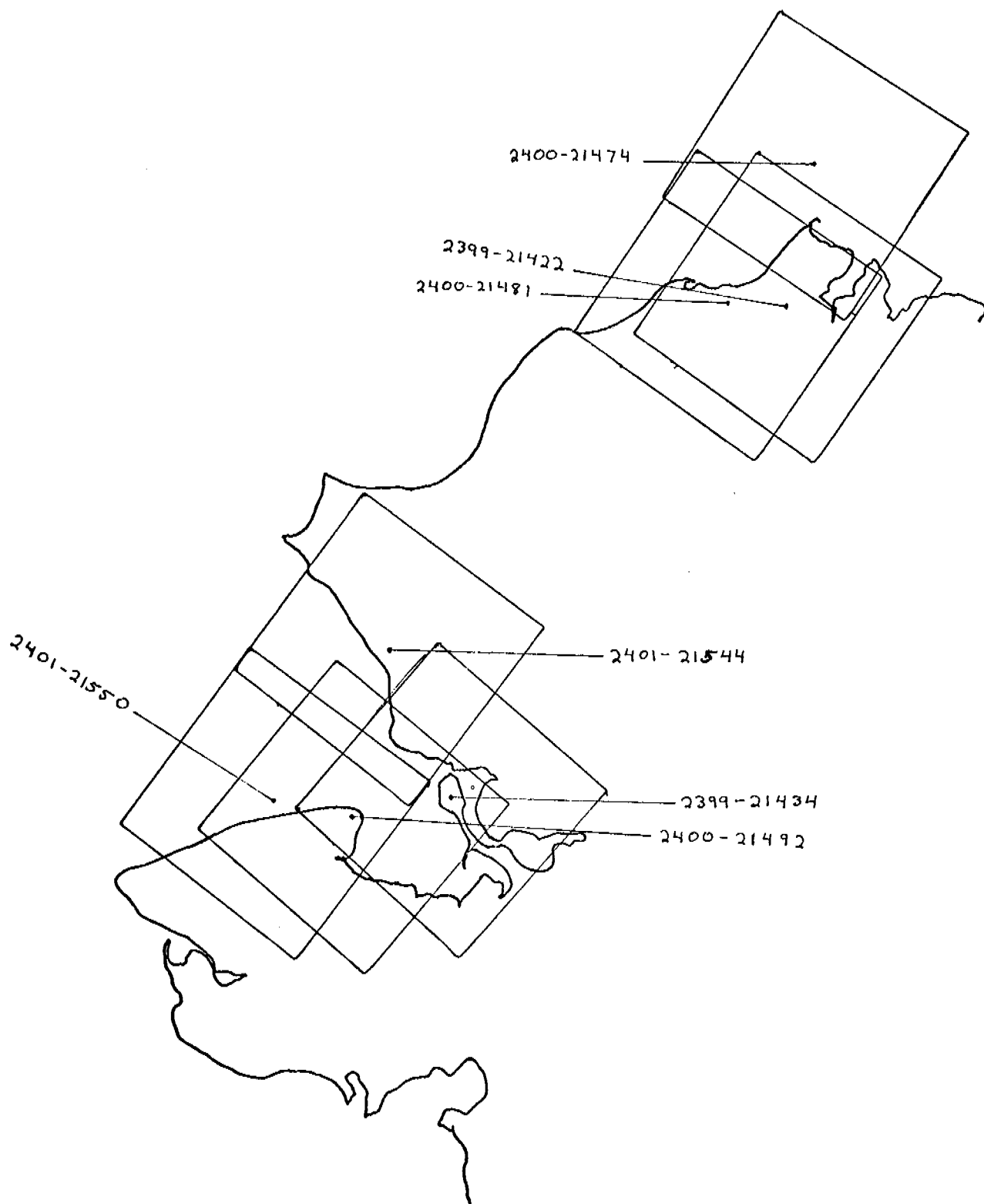
CHUKCHI SEA

E-2386-22113-7
12 FEB. 1976

CHUKCHI SEA

24 FEBRUARY -12 MARCH 1976

Cycle 2399 -2416

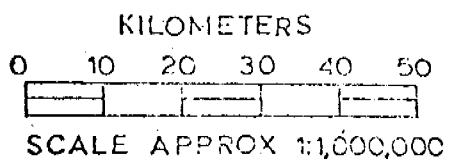
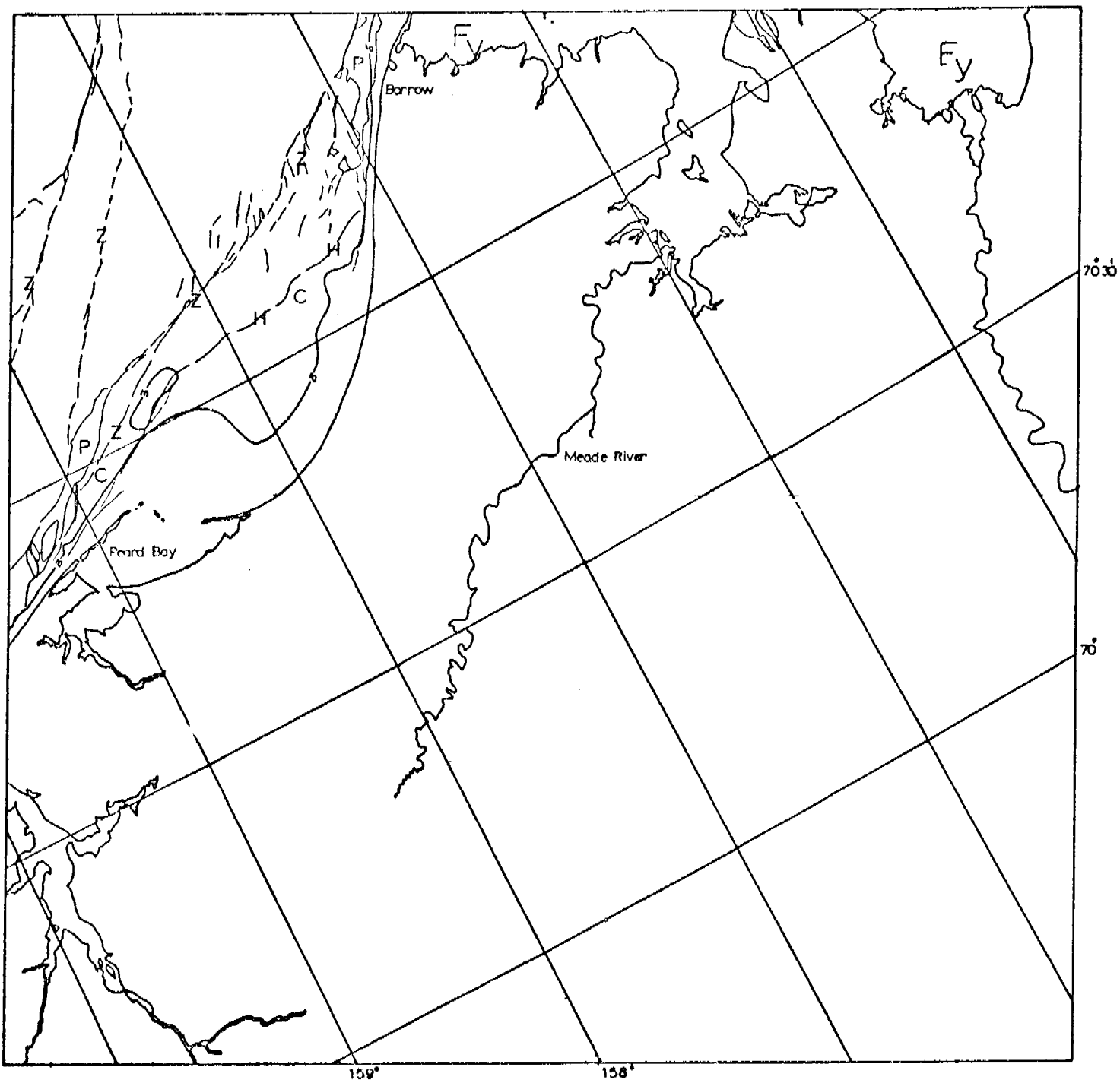


Scenes 2399-21422 } adjacent pair
 2399-21434 }
 2400-21474 } adjacent pair
 2400-21481 }
 2400-21492
 2401-21544
 2401-21550

These scenes show portions of the Chukchi coast between Barrow and Cape Prince of Wales for the period February 25-27, 1976. At this time all ice in Kotzebue Sound including that between Cape Krusenstern and Cape Espenberg is contiguous and well frozen-in. There appears to be a very massive hummock field west of Cape Krusenstern.

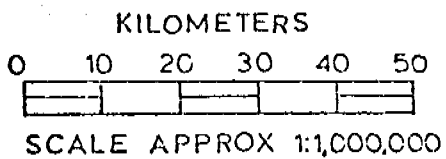
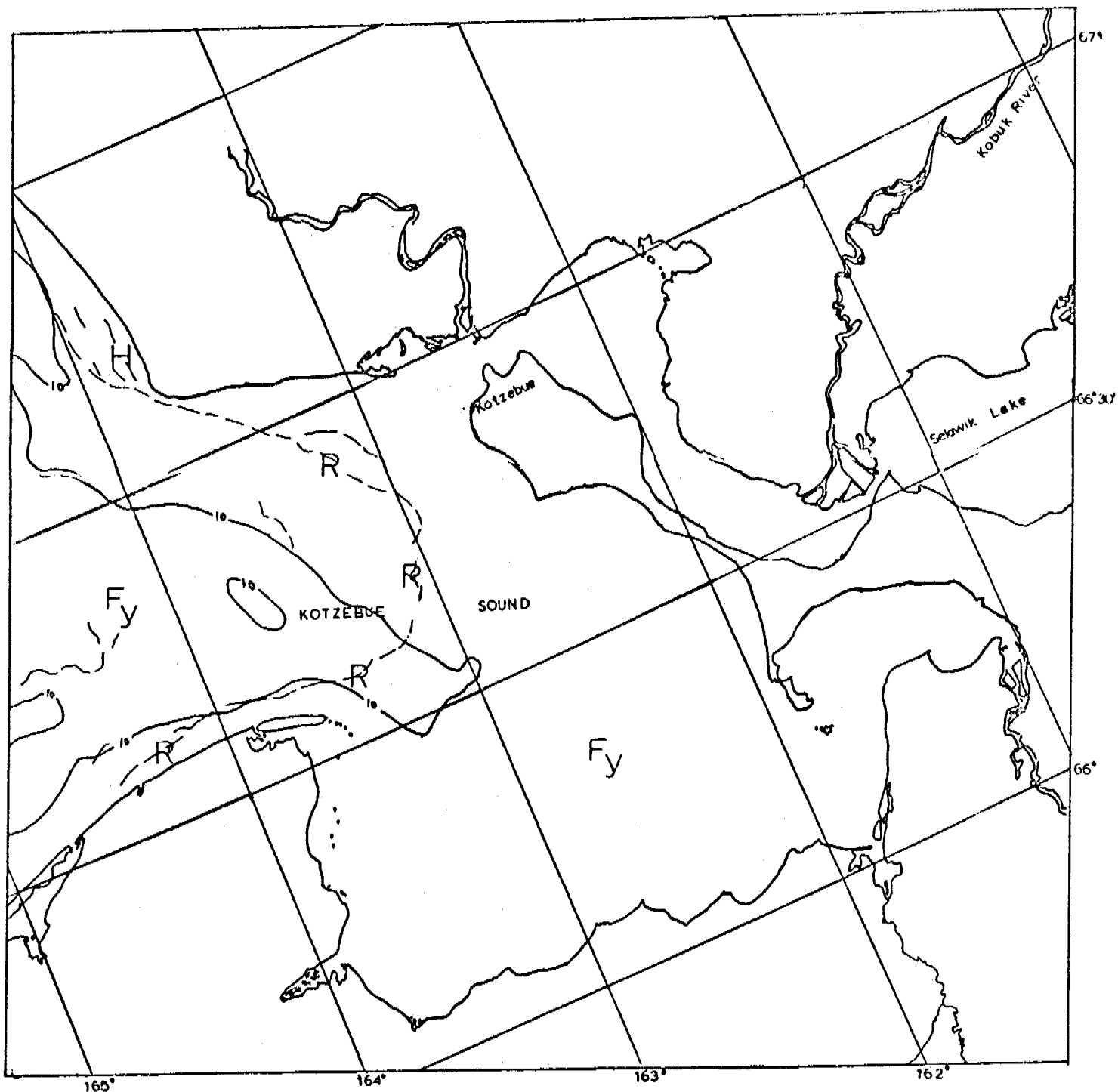
Further west, all along the Chukchi Coast, north-south leads are opening up reflecting a WSW motion of oceanic ice. This dynamic event is illustrated in the Point Franklin area where during the one day between scenes 2399-21422 and 2400-21481, a large lead has opened up considerably inshore of the previous zone of shear. The new lead coincides closely with a large ridge system running roughly parallel to the coast.

The new lead system is freezing rapidly and at Barrow has reached the young ice stage. Far to the south the large shear ridge hummock field mapped north of Cape Prince of Wales remains fixed during this event.



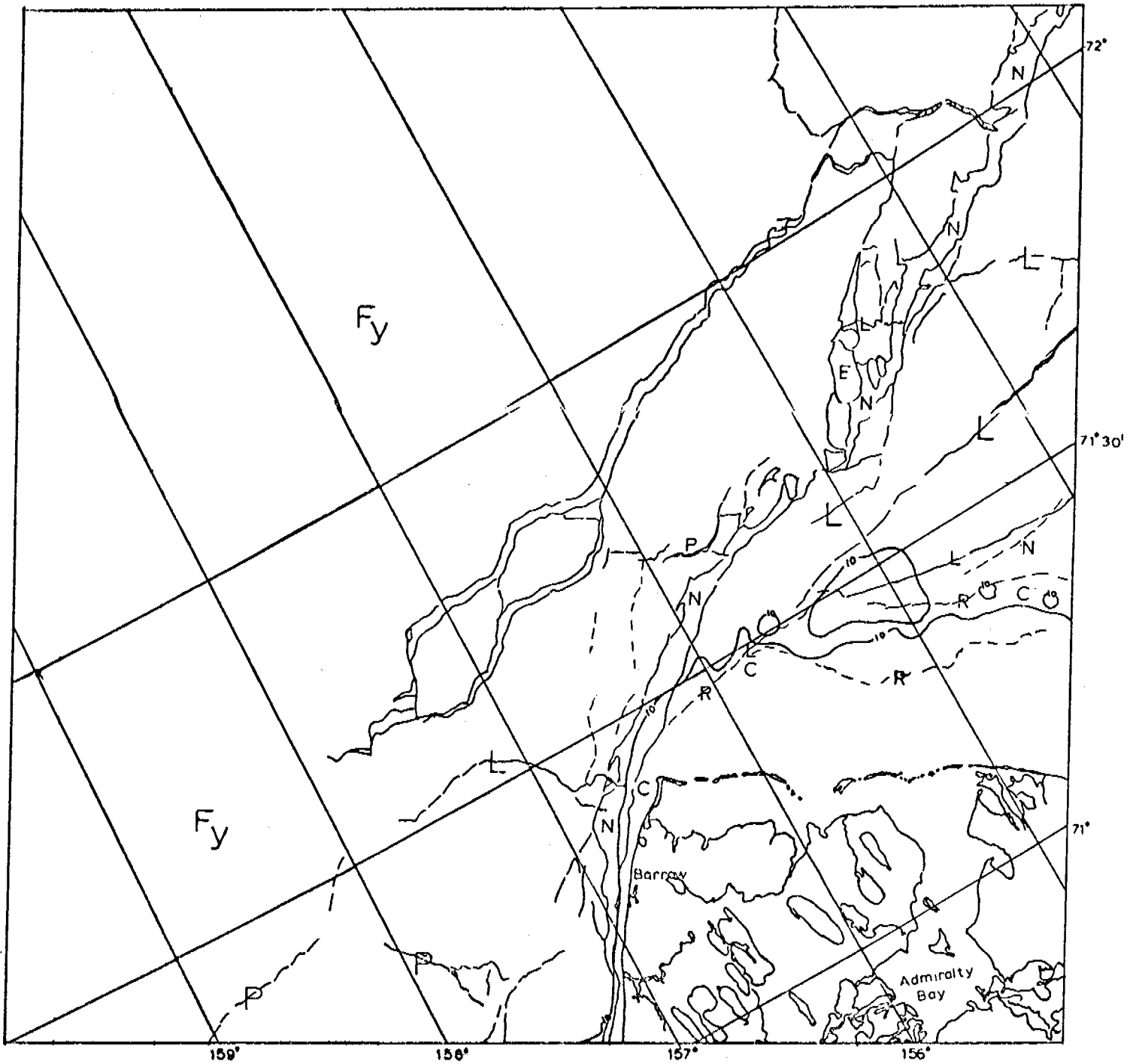
CHUKCHI SEA

E-2399-21422-7
25 FEB. 1976



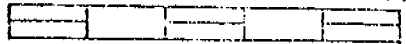
E-2399-21434-7
25 FEBRUARY 1976

CHUKCHI SEA



KILOMETERS

0 10 20 30 40 50

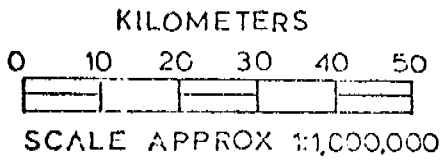
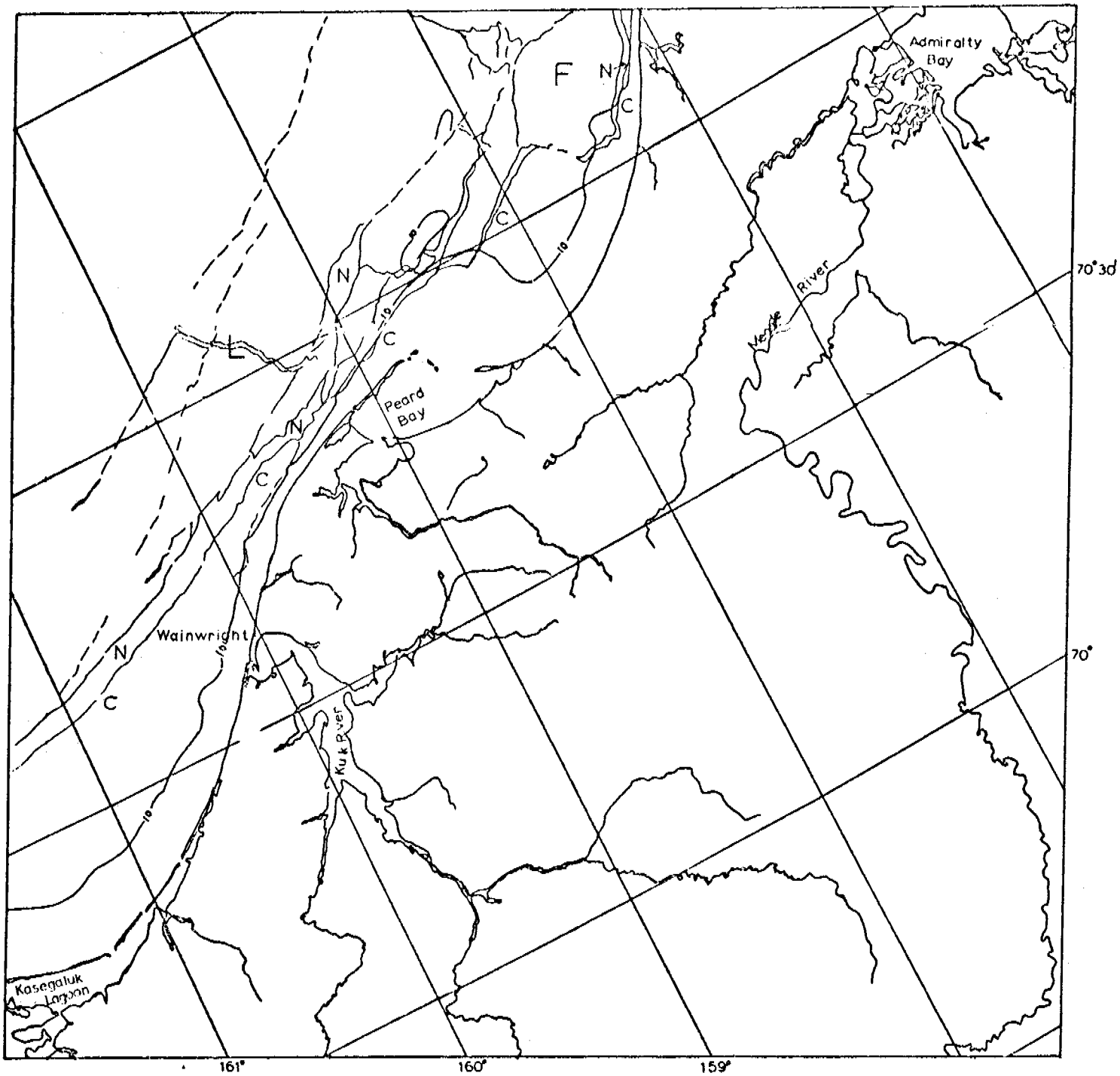


SCALE APPROX 1:1,000,000

E-2400-21474-7

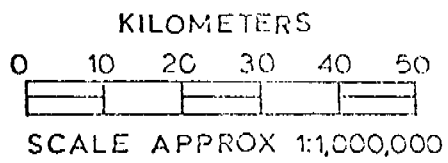
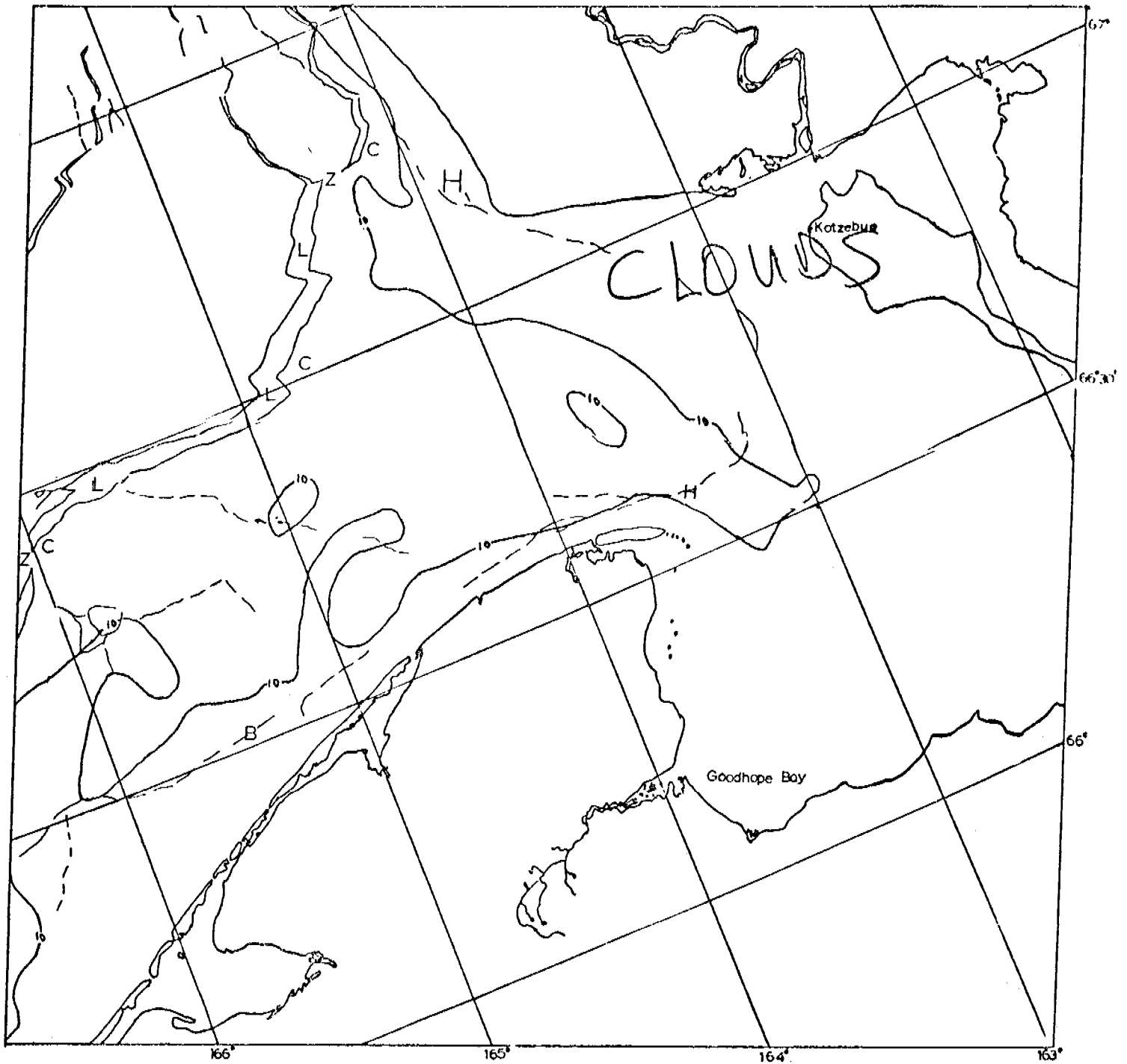
26 FEBRUARY 1976

CHUKCHI SEA



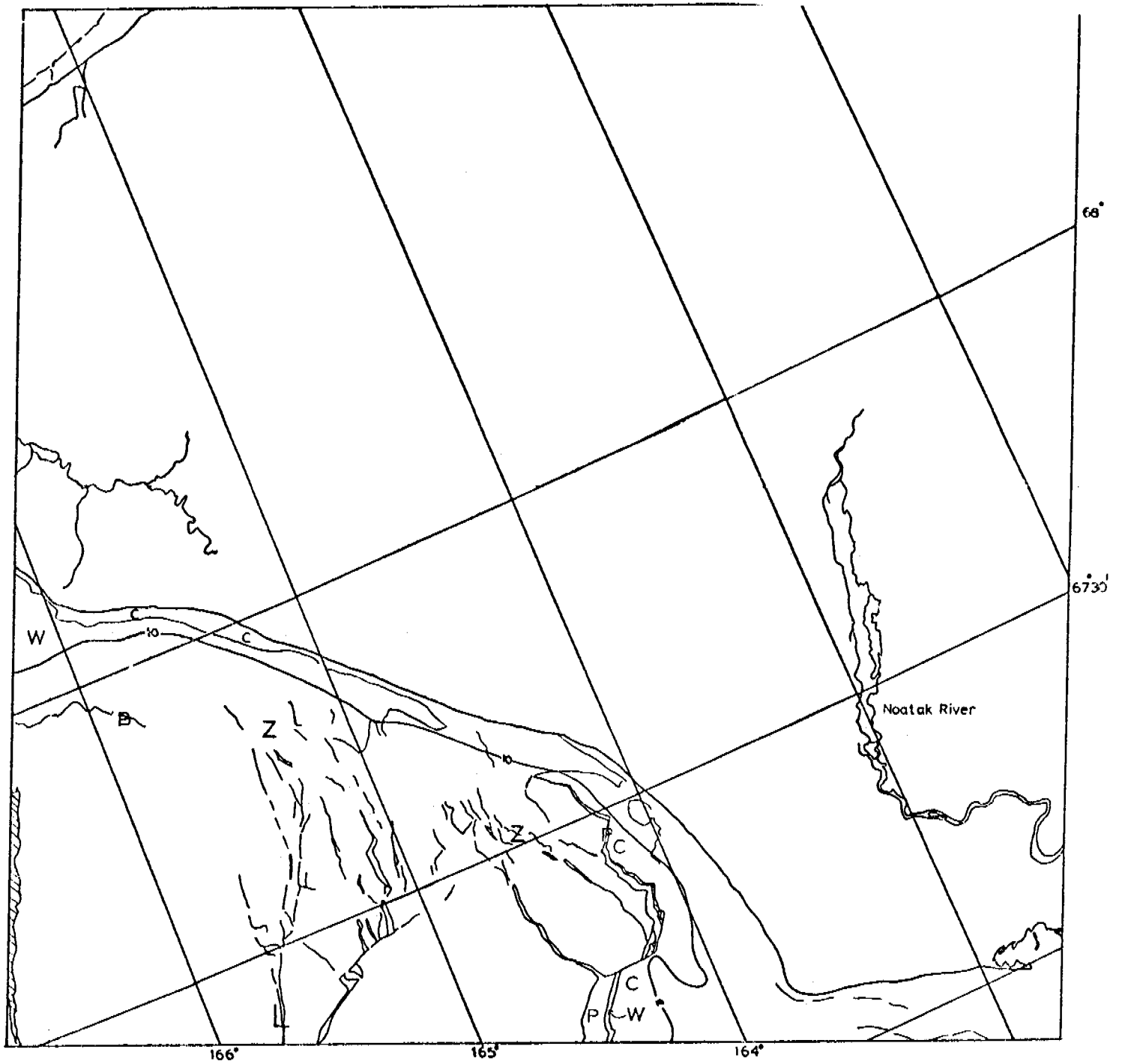
E-2400-21481-7
26 FEB 1976

CHUKCHI SEA



E-2400-21492-7
26 FEBRUARY 1976

CHUKCHI SEA



KILOMETERS
 0 10 20 30 40 50
 SCALE APPROX 1:1,000,000

E-2401-21544-7
 27 FEB. 1976

CHUKCHI SEA

OCS Coordination Office

University of Alaska

Quarterly Report for Period Ending Dec. 31, 1976

Project Title: Experimental Measurements of Sea Ice Failure Stresses
Near Ground Structures

Contract No.: 03-5-022-55 RU #: 259

Task Order No.: 7

Principal Investigators: W.M. Sackinger, R.D. Nelson

I. Task Objectives.

The objectives of this study are to measure, in-situ, the stresses generated in a sea ice sheet as it fails in the vicinity of a static obstacle, and the rate of approach of the ice sheet during this process.

II. Field or Laboratory Activities.

No field activities took place during the past quarter. Interpretation of data from previous experiments was continued. Additional testing, calibration, and checkout of equipment built last year was begun, in preparation for ice stress measurements in the spring of 1977.

III. Results.

Comparison of digitally-recorded data with simultaneously-recorded paper charts was continued.

IV. Preliminary interpretation of results.

The abruptly-increasing event which occurred near the end of the recorded telemetry experiment was determined to be caused by abnormal instrument operation during final stages of battery depletion and battery failure. Both digital and analog records showed this equipment-related behavior.

Prior to the battery failure, many apparently-random compressive events took place, which were recorded on all three sensor channels. These events, which were in the range 20-60 psi, could be associated with general movements and floe-floe interactions which would normally occur on the compressive side of a grounded obstacle prior to the onset

of actual ridgebuilding and fracture. The time sequence of these minor events is being examined to determine, if possible, the duration of such stresses, the correlation of stresses observed in the three directions, and an approximate measure of the average stresses thus created.

However, it appears that conditions of ice fracture near the transducers were not recorded during the experimental period.

V. Problems encountered/recommended changes.

Measurements for the coming year will include provision for longer-lasting telemetry batteries, continuous recording at a shoreline site, and instrument package recovery in case of abnormal ice movements away from the shoreline.

VI. Estimate of funds expended.

\$73,324.

QUARTERLY REPORT

Contract No. 03-5-022-55

Research Unit No. 261

Reporting Period:

Oct. 1 - Dec. 31, 1976

BEAUFORT SEA, CHUKCHI SEA, AND BERING STRAIT

BASELINE ICE STUDY PROPOSAL

William R. Hunt

and

Claus-M. Naske

Dec. 31, 1976

QUARTERLY REPORT
BEAUFORT SEA, CHUKCHI SEA, AND BERING STRAIT
BASELINE ICE STUDY PROPOSAL

I. Task Objectives:

The investigators are working on a data supplement to the charts which show seasonal navigational conditions from 1870 to 1970. This supplement presents all pertinent ice information and navigational information which is available in ship logs of whaling vessels, U. S. Coast Guard ships, and trading ships.

II. Field Activities:

The researchers gathered data from source centers. Two more trips to Washington, D. C. to the National Archives and other resource centers were made in this quarter.

III. Results:

A sample of ice data gathered that lends itself to chronological narrative rather than cartographic representation is included with this report.

An effort is being made to gather and report on all unusual ice conditions and all available navigational information which is not included on maps.

ICE DATA FROM LOG BOOKS OF MOTOR VESSEL "PATTERSON" 1926 to 1936

SEASON 1926

- July 14, 1926, Caught up with main ice pack few miles north of Wainwright.
- July 16, Arrived at Barrow 7:30 A.M., after working ice in shallow water inside of ground ice all the way from Point Belcher.
- July 27, ARRIVED AT HERSCHEL ISLAND. Worked through ice all the way from Point Barrow. (Herschel 9.10 A.M.)
- Aug. 29, LEFT HERSCHEL FOR POINT BARROW.at 6.45 A.M.
- Sept. 7, ARRIVED AT BARROW at 10.30 A.M.
Had to work ice from Herschel to Flaxman Island, but very little ice between Flaxman Isl. and Point Barrow. Spent time looking for Whales off Harrison Bay, and westward. Worked through scattered ice from Barrow to Wainwright, then no more ice.

SEASON 1927

- July 23, 1927, Up to southern edge of ice pack at 2.30 A.M. about 20 miles south of Cape Smyth. Had to work ice along the beach.
ARRIVED AT BARROW at 9.25 A.M.
- July 29, ARRIVED AT HERSCHEL ISLAND. Worked ice all the way from Point Barrow to Herschel. Quite heavy in places.
- Sept. 2, LEFT HERSCHEL ISLAND westbound at 8.30 A.M.
- Sept. 8, ARRIVED AT POINT BARROW, found clear water from Herschel to Demarcation Point, and then scattered ice all the way to Barrow. No ice south of Barrow.

SEASON 1928

- July 7, ARRIVED AT POINT HOPE. Ice all along Coast.
- July 13, ARRIVED AT ICE CAPE. Tough going along the beach that far. Ice pack hard on Blossom Shoals, so felt our way through channel between the shoals.
- July 18, ARRIVED AT BARROW AT NOON.
- July 29, ARRIVED HERSCHEL ISLAND. Had worked ice all the way from Point Barrow to Demarcation Point, then clear water to the eastward.
- Aug. 30, WESTBOUND FROM HERSCHEL ISLAND at 9 A.M.
- Sept. 4, ARRIVED AT POINT BARROW at 9.55 P.M. More or less scattered ice all the way from Herschel to Barrow. No ice south of Barrow.

SEASON 1929

- July 4th ARRIVED POINT HOPE. Considerable ice south of Point Hope from K but clear water to Northward, except in vicinity of Icy Cape.
- July 13, ARRIVED AT BARROW. Ice pack hard against ground ice from Barrow Village (Cape Smyth) to Barrow, so started to break through winter ice between the beach and the ground ice. (Ridge). Took 31 1/2 hours steady bucking and some blasting to break through the 8 miles from Tom Gordon's place, to Point Barrow. C.T. Pedersen never left the Crow's Nest in that time. Had to rub over the bottom at times. Ice Pack impassable East of Point until July 28th.
- Aug. 6, ARRIVED AT HERSCHEL ISLAND. Worked ice all the way from Point Barrow.
- Aug. 28, WESTBOUND FROM HERSCHEL ISLAND at 3.20 A.M.
- Sept. 2, ARRIVED AT POINT BARROW at 1.35 A.M. Encountered some ice here and there between Barter Island and Point Barrow. No ice south of Barrow.

SEASON 1930

- July 21st, First ice near Wainwright.
- July 23, ARRIVED POINT BARROW, at 10.45 P.M.
- Aug. 1, ARRIVED HERSCHEL ISLAND at 6 P.M. Found open water all the way from Point Barrow to Demarcation, then heavy packed ice on July 29th all the way to Herschel.
- Aug. 30, LEFT HERSCHEL ISLAND for San Francisco, at 2.30 A.M.
- Sept. 3, ROUNDED POINT BARROW AT 10.40 A.M. Found more or less ice all the way from Herschel to Barrow, and then to the southward as far as Icy Cape.

SEASON 1931 - Bad ice year

- July 9, FOUND ICE PACK AT POINT HOPE and to the north. Prevailing westerly winds kept the ice pack hard against the land.
- July 14, ARRIVED AT ICY CAPE.
- July 26, Still dodging ice around Icy Cape. Sighted the "BAYCHIMO" steaming northward at 12.10 P.M.
- July 28, Southwest Gale. Had to come south few miles for shelter on north side of Ice Cape. "Baychimo" also at anchor near by.
- July 31, ARRIVED AT WAINWRIGHT at 11.45 PM.

- Aug. 4, BAYCHIMO AND "PATTERSON" still at Wainwright, waiting for ice pack to slack up. Got under way and working north at 11.50 P.M.
- Aug. 10, Reached shelter under Seahorse Islands in Peard Bay, at 3.10 A.M. Off along the beach to the north is slack ice at 4.30 A.M. Baychimo following a couple miles behind. Could see ice pack closing fast, and low fog building up from ice pack, so headed south full speed for shelter at the Sea Horses. We passed the "Baychimo" but she went right on to the northward. The fog was raising up fast, and in a few minutes after we had passed the "Baychimo", I could tell by her masts above the low fog that she was trying to turn around and come out of the pack, but was helpless, and was shoved close into the ground ice along the beach, where we could see her when the fog lifted.
- Aug. 11, Ice pack slacked a little in the evening, letting the "Baychimo" out of the trap she was in, and she anchored close by us at 9 P.M.
- Aug. 13, Sent Mr. Ford and 7 natives in skin canoe with outboard motor, to try to reach Barrow with first class mail.
- Aug. 14, Canoe returned to ship. They had found ice shoved up on beach and not water enough to float the canoe up along the beach, as seen from high cliff.
- Aug. 20th Light N.E. breeze at 2.40 A.M. slacked ice pack. Both ships working north along the beach.
- Aug. 21, ARRIVED AT BARROW at 9 A.M.
- Aug. 22, Found more or less ice along Coast from Barrow to Beechey Point, where we arrived at 5.25 P.M. and started landing supplies for trading post.
- Aug. 23, Left Beechey Point at 6.30 A.M. Ice Pack hard on Cross Island, so took to the lagoon inside of all these islands. N.N.E. wind with light snow and freezing hard.
- Aug. 24, Out of lagoon at Newport Island at 3.45 A.M., having saved about 40 miles of hard going outside of the Islands.
- Aug. 26, ARRIVED AT HERSCHEL ISLAND, AFTER landing outfit at Barter Island Trading Post. Worked ice all the way from outlet to lagoon at Newport Island. The "Baychimo" arrived few hours ahead of us.
- Aug. 28, "Baychimo" left for Coronation Gulf at 3 P.M. but returned to Herschel at 8 P.M. on account of ice pack tight.
- Aug. 29, "Baychimo" sailed again at 8 A.M. but returned at 3 P.M.
- Aug. 30. "Baychimo" sailed at 4 A.M. and kept going East for Coppermine.
- Sept. 5, "Patterson" left Herschel Island for home.

Sept. 9, ARRIVED AT BARROW, 2.55 P.M. Found ice pack in all the way to Icy Cape. Mostly slack ice inside of ground ice, but tough going in places. Trader at Wainwright reported later that ice pack shoved up on beach 9 hours after we left there, and did not slack up all winter. S. S. "Baychimo" was 3 days behind us and failed to get out. She froze in about 10 miles south of Seahorse Islands, was carried away by ice pack early 1932.

SEASON 1932

July 26, ARRIVED HERSCHEL ISLAND at 10.30 A.M. Found more or less ice from Barrow to Barter Island, then clear water to Herschel Island.

Aug. 23, LEFT HERSCHEL ISLAND at 9. P.M.

Aug. 26, ARRIVED AT BARROW at 10.50 P.M. Ran into scattered ice a few miles east of Cross Island, and the same all the way to Barrow. Also had to work through heavy scattered ice all the way from Barrow to Icy Cape along beach.

SEASON 1933

July 15, 1933, Ice pack tight north of Point Hope, and had to return to Point Hope.

July 16, Found ice pack had slacked enough to allow us to work around Cape Lisburne and worked along the beach. Spent many days bucking and blasting ice inside of the ground ice, as the ice pack was slowly moving north in a tight mass against the outside of the ground ice. Used 30 blasts in 8 hours one day, and many blasts in other days.

July 28, Arrived at Icy Cape. Sighted ship far out in Ice Pack, (later found to be the abandoned S. S. "Baychimo"). Ice pack very tight against land, but moving north about a mile per hour.

Aug. 6th ARRIVED AT WAINWRIGHT at 10.12 A.M. Got under way at 1.40 P.M. At 4.30 P.M. we were abreast of the old "Baychimo" camp on the beach. The "Baychimo" was then approximately 7 miles directly offshore from the place where she had been lifted up and carried away by the ice pack in a southwest gale about 18 months or more before. She had been drifting all over the Arctic Ocean in the meantime.

Aug. 10, ARRIVED AT POINT BARROW.

Aug. 17, ARRIVED AT HERSCHEL ISLAND at 8.35 P.M. Worked ice all the way from Point Barrow, and had to do some blasting to get around Cross Island.

Sept. 5, LEFT HERSCHEL ISLAND FOR BARROW at 4.10 A.M.

Sept. 8, ARRIVED AT POINT BARROW. Worked through scattered ice from Herschel to Barter Island, but no ice west of Barter Island.

SEASON 1934

- July 20th ARRIVED AT POINT BARROW at 1.40 P.M. Worked first ice getting around Cape Lisburne on July 15th, and found fairly slack ice long the beach to Icy Cape, then clear water in places to the north.
- July 26, ARRIVED AT HERSCHEL ISLAND at 3 A.M. More or less close ice from Barrow to Demarcation Point, then clear water to Herschel Island.
- Sept. 9, LEFT HERSCHEL ISLAND at 2 A.M.
- Sept. 11, ARRIVED AT BARROW at 6.07 A.M. Found clear water all the way, except some small scattered ice near Herschel.

SEASON 1935

- July 14, ARRIVED AT WAINWRIGHT. More or less ice in sight.
- July 16, ARRIVED AT POINT BARROW at 5.30 P.M., after working ice close inshore all the way from Wainwright.
- July 30, ARRIVED HERSCHEL ISLAND at 6.50 A.M. We left Barrow in fairly slack ice on July 18th, with the "St. Roch" following close behind us. We turned back at 10 A.M. and steamed back a few miles where the "St. Roch" appeared to be stuck in some partly rotten ice between two large floes of ice. We went into this rotten ice at full speed and broke her clear. Then both vessels proceeded Eastward.
- Aug. 10, THE "ST. ROCH" ARRIVED AT HERSCHEL ISLAND from Westward at noon.
- Aug. 27, LEFT HERSCHEL ISLAND FOR BARROW at 9.15 P.M.
- Aug. 30, ARRIVED AT POINT BARROW at 8.17 P.M. Found only scattered ice in places, then clear water from Smith Bay to Barrow. No ice encountered to southward, except ice pack in sight of the Sea Horse Islands, and south to Pt. Belcher.

SEASON 1936

- July 13th Went into slack ice north of Cape Lisburne
- July 26, ARRIVED AT POINT BARROW at 5.20 P.M. Had tough going along beach all the way.
- Aug. 2, ARRIVED HERSCHEL ISLAND. Fairly good going in places from Barrow.
- Sept. 4, Left Herschel Island and spent 12 hours blasting and bucking to get around N.W. point of Island as ice pack against mud bank.
- Sept. 8, ARRIVED AT POINT BARROW at 2 A.M. Ice all the way. Clear south.

(1) The Arctic ice pack is usually never far off the east between Barrow and Herschel, or Baillie Island, and a spell of strong westerly wind brings it back to shore as a rule. The summer of 1912 was about the real safe year for navigation between Point Barrow and Cambridge Bay that I can recollect, since 1894. However, I did not enter the Arctic from 1904 to 1907, inclusive, but several whaling steamers were forced to spend the winter in the vicinity of Herschel Island in 1904 or 1905, as the pack was against the shore, and winter set in very early. I was master of the little whaling schooner "Elvira in 1912 and we did encounter some ice on the way to Herschel but we had several prolonged North East gales in August and all the ice was driven out of the Beaufort Sea, and I estimated that the ice pack must have been about 200 miles off shore along the Coast between Herschel and Barrow. We cruised for whales about 100 miles off the coast from Herschel Island to Harrison Bay without seeing any sign of ice, and no ice blink, and it was the same all the way to Barrow, as we cruised along far off shore, after killing three Bowhead whales in near Harrison Bay. The year 1902 was also an open season along in August and September. I was mate in a little sailing schooner in that year and N.E. gales again drove the pack far off shore. Such N.E. gales will clear the whole Arctic Coast, but there are years when westerly winds prevail, and they make it a cold and icy season, with an early freeze-up. However, a vessel reaching Point Barrow on or about August 1st has a reasonable good chance of making it in to Cambridge Bay, and out around Barrow again, especially in a vessel built for ice work. I have never had a vessel that was built for use in the Arctic, but managed to get through the ice and out again, except 1913.

(2) As mentioned above, August 1st is about an average date on which a vessel should figure on reaching Barrow. There can be whole month variation in the seasons. In 1931 it was physically impossible for a vessel to reach Herschel Island before August 26th, as against July 26th in 1932. The "Baychimo" (H.B. Co.) was three days behind us coming out from Herschel in 1931 and was frozen in just south of the Sea Horse Islands, and was carried off by the ice pack during a S.W. gale early in 1932, as you no doubt know. She was a very good vessel for the Arctic as she was built for the Baltic ice work. The 10,000 ton Russia Ice Breaker "Krassin" could not do anything against the Western Arctic ice pack in the vicinity of Point Barrow when she went up there in Aug. 1937 in search of the Russian plane which was lost, after crossing over the North Pole.

(3) There are no harbours for a large vessel between Herschel Island and Point Barrow, but there are a few points of land which afford some shelter from certain winds. Pauline Cove at Herschel Island is a small harbour, and 3 1/2 fathoms of water is about all there is in the opening of the harbour, shaling to about two fathoms in about a quarter mile towards the head of the bay. There is no shelter between Herschel Island and Baillie Island, but some shelter behind the S.W. sandspit of the main island, for a vessel drawing up to 18 feet. I found that this shelter had shoaled up some after we wintered there in 1899 - 1900. A vessel drawing less than 18 feet can get inside of the sandspit of Cape Bathurst, at the eastern end of Baillie Island, but there is not much swinging room inside of the sandspit, and there is a shoal extending well out from the island across the entrance to the harbour, with a narrow channel along the Cape Bathurst sandspit. The next Harbour

east is Langton Bay, some miles east from Horton River, and if I remember correctly it could accommodate a large vessel, as I think there is from five to eight fathoms of water inside. I have not been in there since 1895, so am not sure about the depth, but Captain Larsen of the "St. Roch" will know. He will also know all about the harbour at Booth Island, Pierce Point and eastward to Cambridge Bay.

(4) Some years there are mostly westerly winds, making an icy season. There is also much calm weather (in which we pray for a northeaster). Such winds are very scarce in many years.

(5) It is quite shallow along the Coast from Point Barrow to Baillie Island, and a few shoals close in, but the largest shoal is between Herschel Island and Kay Point, but nearer Kay Point. There is a depth of six feet of water or less on this shoal. If the Coast is fairly clear of ice east of Barrow, or only scattered ice, we always kept outside of seven fathoms of water, and always kept the hand lead going.

(6) Yes, we always had considerable fog in the Arctic, but not so much during the latter part of the open season.

(7) The main pack usually moves along with the current in a solid pack, but at times it is slack on the edge. In the early part of the season, there is much heavy ground ice along the coast in from 7 to 12 fathoms of water, and the pack moves back and forth on the outside of this ground ice, depending on the direction of the winds. A N.E. wind of near gale force will create a three to four knot current setting west along the Coast and lowering the water several feet if

the wind lasts a few days. This current appears to be swifter along the shore between the beach and the ground ice, but it will open up many small leads, or leave the ice slack enough to work through, and the main pack will move out of sight of land in a few hours, even though the wind is blowing on to the shore a couple of points or more. A strong S.W. wind will create a strong current setting eastward, and bring the pack into the beach, if there is no heavy ground ice to keep it off. This wind blows off the land a couple points, but the ice comes in just the same, and the water rises a few feet in a prolonged gale. It has often been said that there must be some land to the northward, causing the pack to set inshore in a S.W. gale.

SEVENTH QUARTERLY REPORT

TITLE: Development of Hardware and Procedures for *In-Situ* Measurement of Creep in Sea Ice

PERIOD: October 1, 1976 - December 31, 1976

PRINCIPAL INVESTIGATORS: Lewis H. Shapiro and Richard D. Nelson
Geophysical Institute, University of
Alaska

I. TASK OBJECTIVE: To develop hardware and procedures for *in-situ* measurement of creep sea ice.

II. SCHEDULE: Evaluation of Results

III-IV. RESULTS AND INTERPRETATION

During the past year we have been reviewing the results of Peyton's (1966) creep tests on sea ice samples. Within the past quarter enough results became available to permit a preliminary report to be prepared. The preliminary nature of the following discussion is emphasized - much more data remains to be evaluated. The same is true of the derivations of the equations of the viscoelastic models presented below. As an example, the viscous components of the strain were assumed to follow a hyperbolic sine relationship between the stress and the strain rate. This appears to agree well with the data, but other functional relationships, which might fit better, remain to be investigated. In addition, in the interest of brevity, the derivations have not, in general, been presented with the degree of thoroughness or rigor which would be expected in a formal publication. Finally, the reader is referred to Peyton (1966) for description of sampling methods, preparation and description of test specimens and experimental techniques.

The total data set consists of approximately 190 creep tests in uniaxial compression. The curves for all of these have been plotted,

and the tests were sorted by sample orientation, test temperature and load. The groupings by temperature and orientation include from 1 to 9 tests, with most having less than 5. Thus, there is neither the range of loads nor the repetition of tests for averaging which would be needed in order for the mechanical properties of the ice to be determined for any given set of conditions. However, useful information and suggestions for additional work can be obtained as discussed below.

The following discussion is based upon the results of 70 of Dr. Peyton's experiments which represent most of the samples from groups of 4 or more tests. Samples from depths of 8, 17, 48 and 60 inches at temperatures from -6°C to -21°C are included. Those referred to below as "vertical" were loaded along a direction normal to the ice sheet and, therefore, normal to the c-axis orientation. "Horizontal" samples were loaded in the plane of the ice sheet at a specified orientation to the dominant c-axis direction. Orientation and temperatures are indicated in the figures where the data appears.

The quality of the data is generally good in the sense that the creep curves are smooth. In some cases, apparently irregular data points were found to be the result of errors in calculation or transcription of the data and these were corrected by reference to the original notes.

To the present, we have referred to the tests as "creep tests". However, examination of the curves shows that this description needs to be modified. Some of the tests were true creep tests, with steady-state creep approached closely. However, many of the tests were actually stress-rupture tests in which tertiary creep leading to failure was

initiated at some time during primary creep. Interpretation of this type of test is described in Grant and Mullendore (1965). The results of a series of stress-rupture tests on sea ice, by bending of simply supported beams, are given in Kingery and French (1963).

Finally, a peculiar feature of some of the data is the presence of one or more discontinuities in the creep curves. These are points at which the strain rate instantaneously increases, as if an incremental load was applied at that time as in a two-step creep test, then gradually decreases toward a steady-state creep rate which is higher than that just prior to the discontinuity. A typical example is shown in Figure 1. These features, termed here "jump points" were previously found in Peyton's data by Karlsson (1972) who considered them to be strain-rate dependent plastic yield points in the viscoelastic flow field, and modeled them as such following the theory suggested by Naghdi and Murch (1963). An alternative explanation is considered below.

ORGANIZATION OF THE DATA

A minimum value of the strain-rate was determined, by inspection, for each strain-time curve. For creep tests, this value is simply the slope of the "best fit" straight line to the linear portion of the curve; that is, the steady-state strain rate. For stress-rupture tests, it is the slope of the curve at the inflection point at the onset of tertiary creep. If the curve included a "jump" point, then the minimum strain rate was taken as the slope of the curve at the jump. The time to the minimum strain rate of stress-rupture tests was also measured, as were the time to the first jump point in any test and the total duration

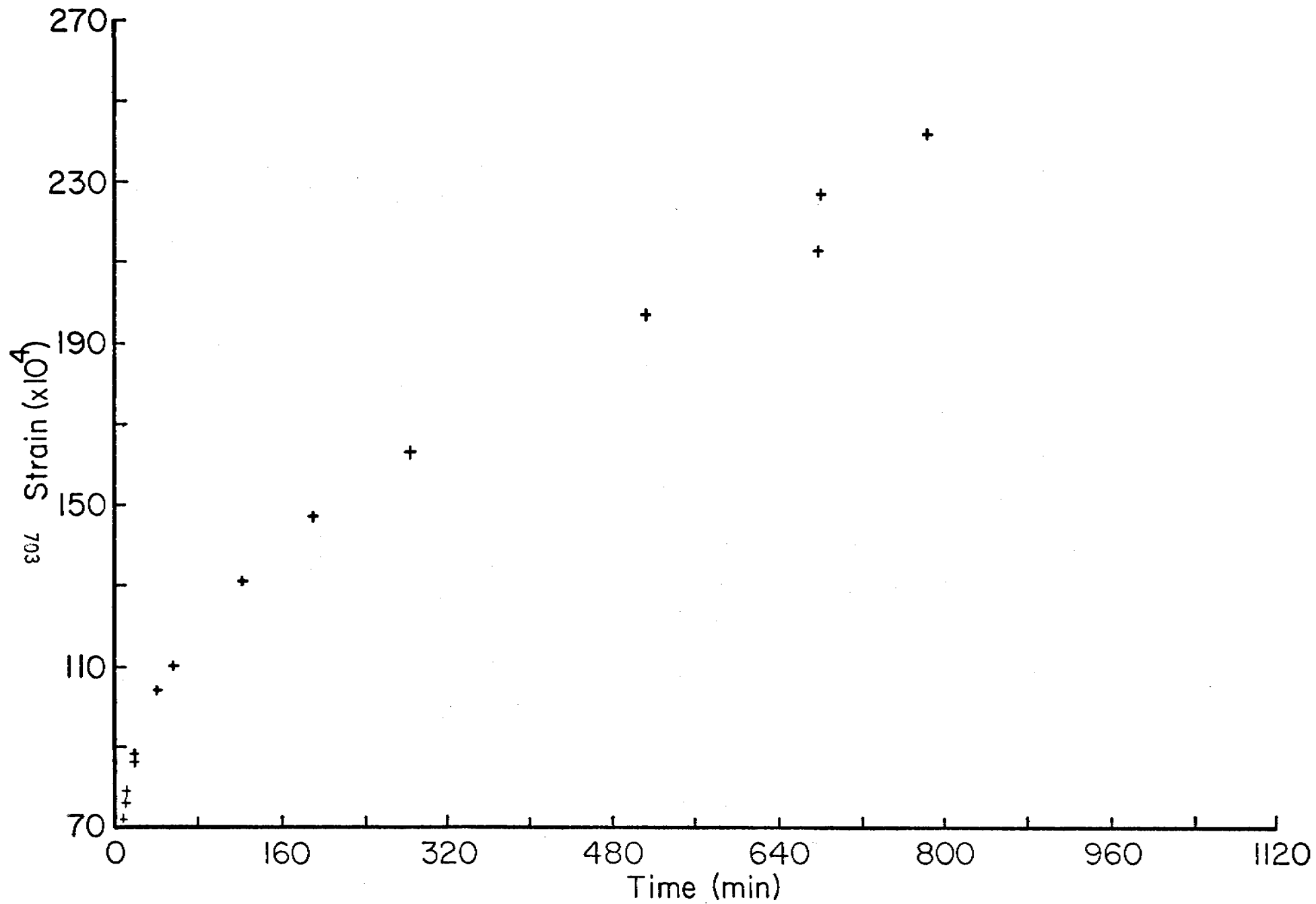


Figure 1. Typical jump point in a strain-time curve, from Peyton's (1966) experiment 37; 8" vertical sample at -18.7°C , and loaded at 16.9 kg/cm^2 .

of the test for creep tests in which neither rupture nor jumps occurred. The total strain of the sample at the minimum strain rate or at the end of a creep test was also recorded. Finally, the time to rupture of the stress rupture tests was taken as the time asymptote of the strain-time curve. Note that this was estimated in most cases because the samples were unloaded prior to total collapse. However, errors in these estimates probably do not exceed a few percent but, of course, cannot be accurately measured.

A plot of time to rupture vs. stress is given in Figure 2 for all of the vertical samples. Tests in which jump points occur are also indicated, as are the durations of the creep tests. Stress vs. time to minimum strain rate for the same tests is plotted in Figure 3. In both cases, the points fall into reasonably well-defined linear zones (compare with Kingery and French, 1963). Note that there is no clear separation with respect to temperature, but this may reflect the relatively small number of samples. Of particular interest, however, are the positions of the jump points. Clearly, these are not random occurrences, but instead, fall within the main trends of the plots. From the available data, the association with the minimum creep rate seems to be preferred, but in either case, it is clear that the jump points are associated with the failure process. This is discussed further below.

Finally, the value of the minimum strain rate for all the vertical specimens is plotted against stress in Figure 4. Note again that the minimum strain rates for those tests which include jump points fall within the trend. The scatter in this plot is somewhat greater than that of Figures 2 and 3, but this may be partially due to the fact that

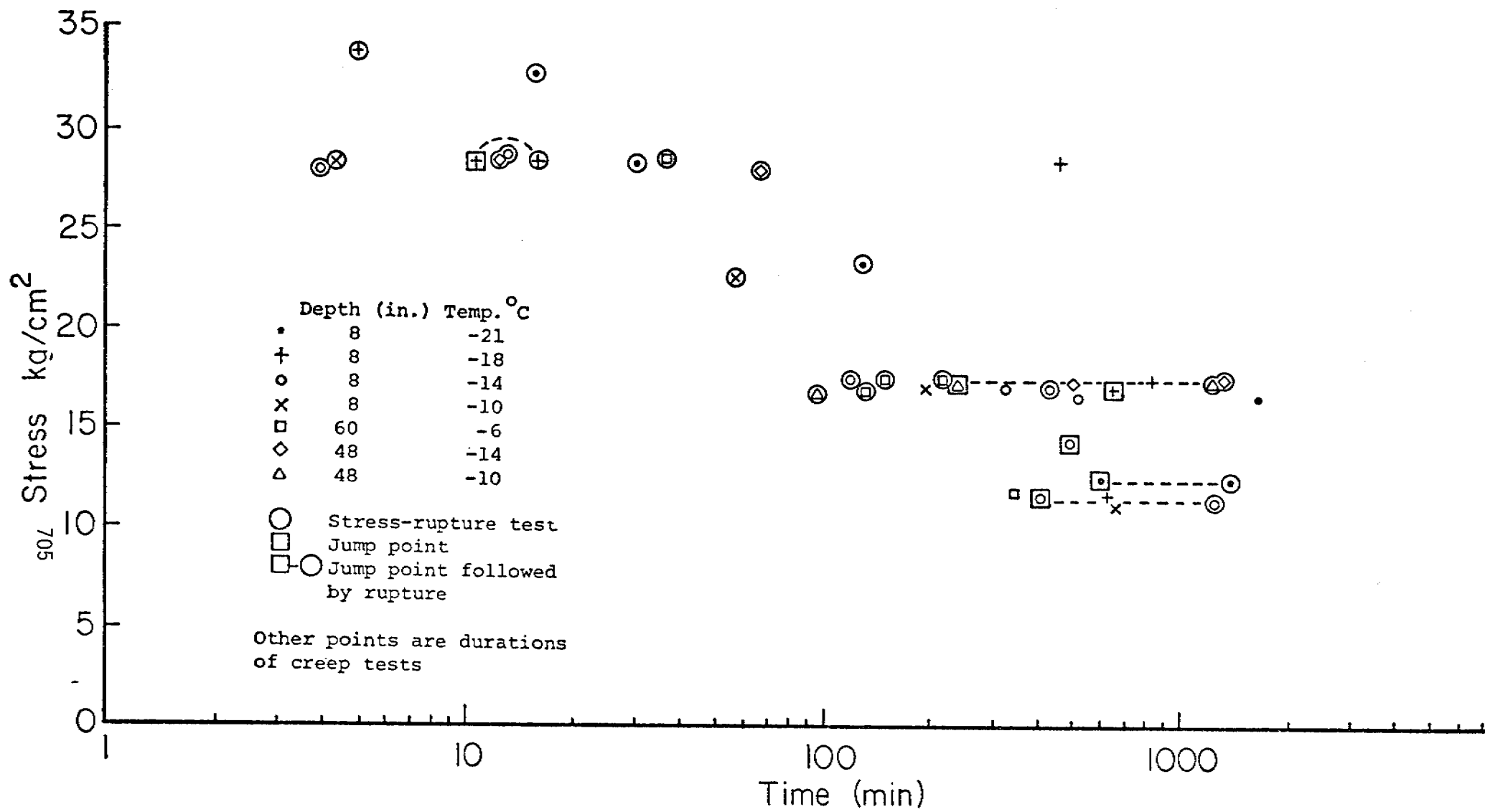


Figure 2. Stress vs. time to rupture for vertical samples.

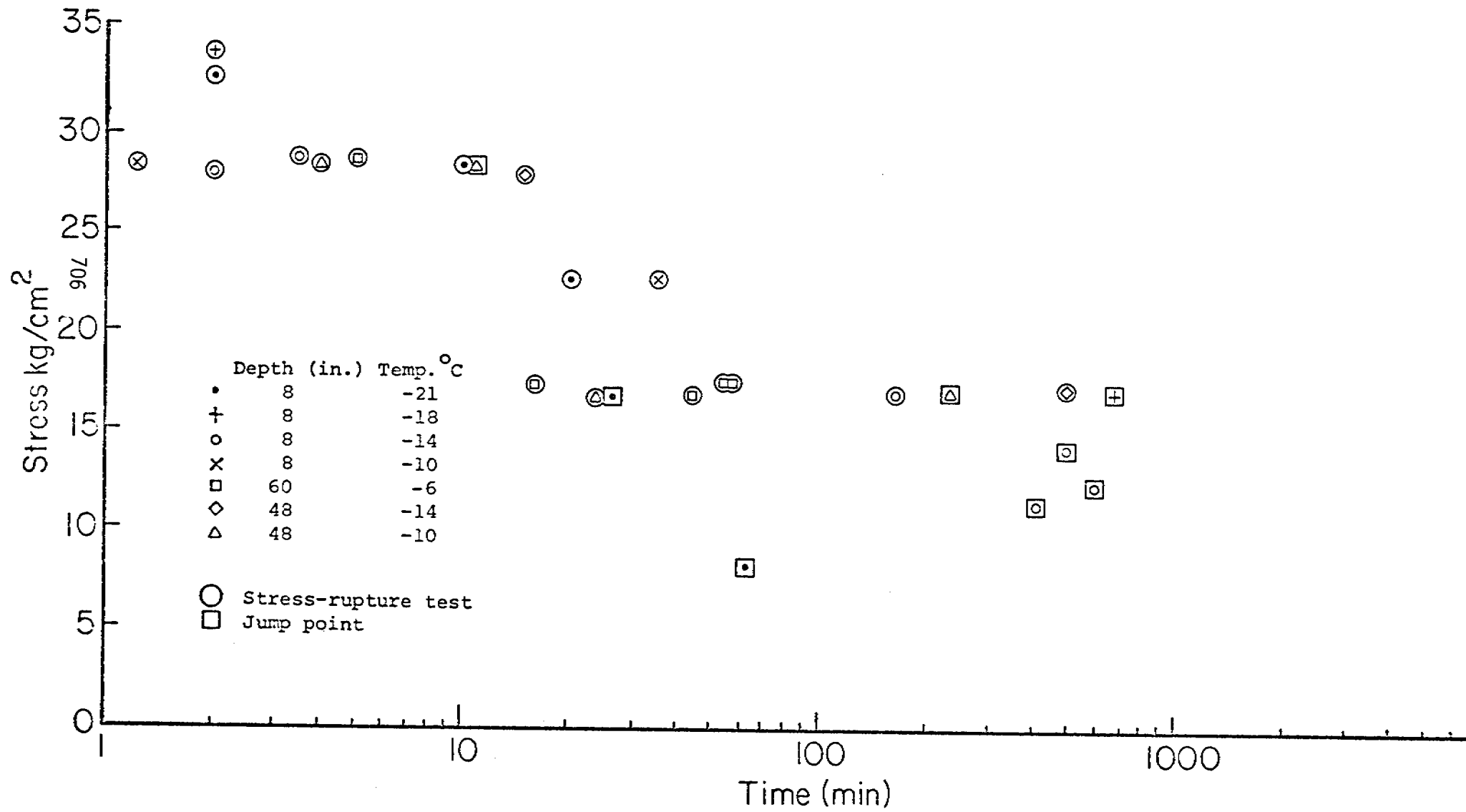


Figure 3. Stress vs. time to minimum strain rate for vertical samples.

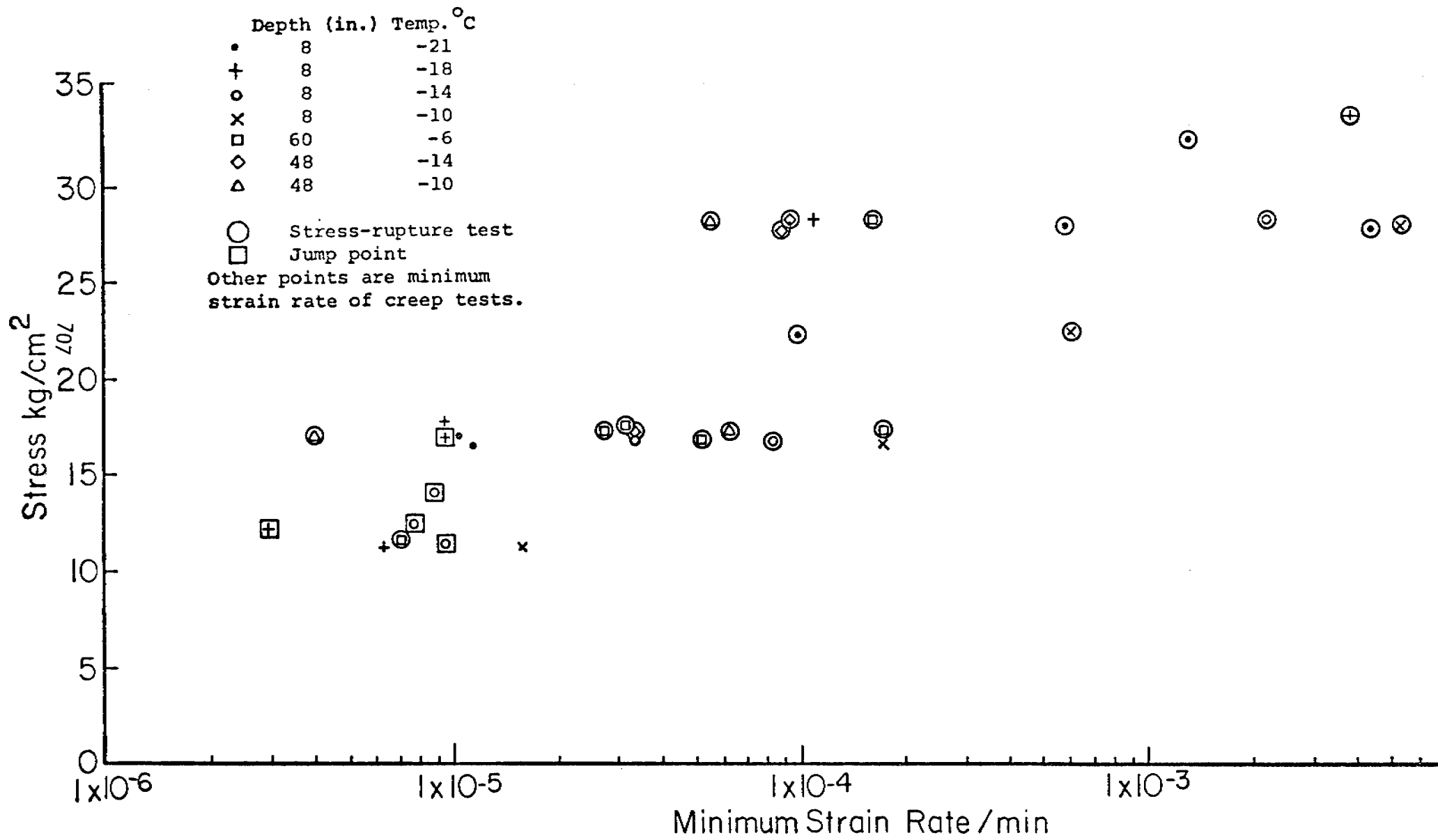


Figure 4. Stress vs. minimum strain rate for vertical samples.

the spacing between data points of the creep curves was often too great for the minimum strain rate to be measured with accuracy. Thus, errors must be present in some of the plotted values.

Figures 5 and 6 show the same plots for horizontal samples (loading in the plane of the ice sheet). These show a wider scatter with poorer definition of the trends. However, two sets of samples within this group are of particular interest: those from 60" depth at various orientations to the c-axis, and a set from 17" depth with randomly oriented c-axes.

The data from the 60" depth samples clearly shows the effect of orientation on the time to rupture. The samples loaded at 45° to the c-axes are obviously weakest, while the results from those loaded at 0° and 90° tend to overlap. Note that one of the tests at 0° orientation was run to rupture at about 2800 minutes at a load of 2 kg/cm², although a jump point appeared at about 160 minutes.

The results from the 17" horizontal samples represent the largest single group of tests under the same conditions of temperature and orientation, and clearly show the association between stress and time to rupture and minimum strain-rate.

DISCUSSION OF THE DATA

It is of interest to compare the plots of stress vs. time to rupture and time to minimum strain rate for the vertical samples (Figures 2 and 3). In the semi-log plots used, the zones defined by these appear to be sub-parallel, so that the time span between the occurrence of the minimum creep rate and of rupture may be some regular multiple of the time to minimum creep rate. It is obvious that there is insufficient

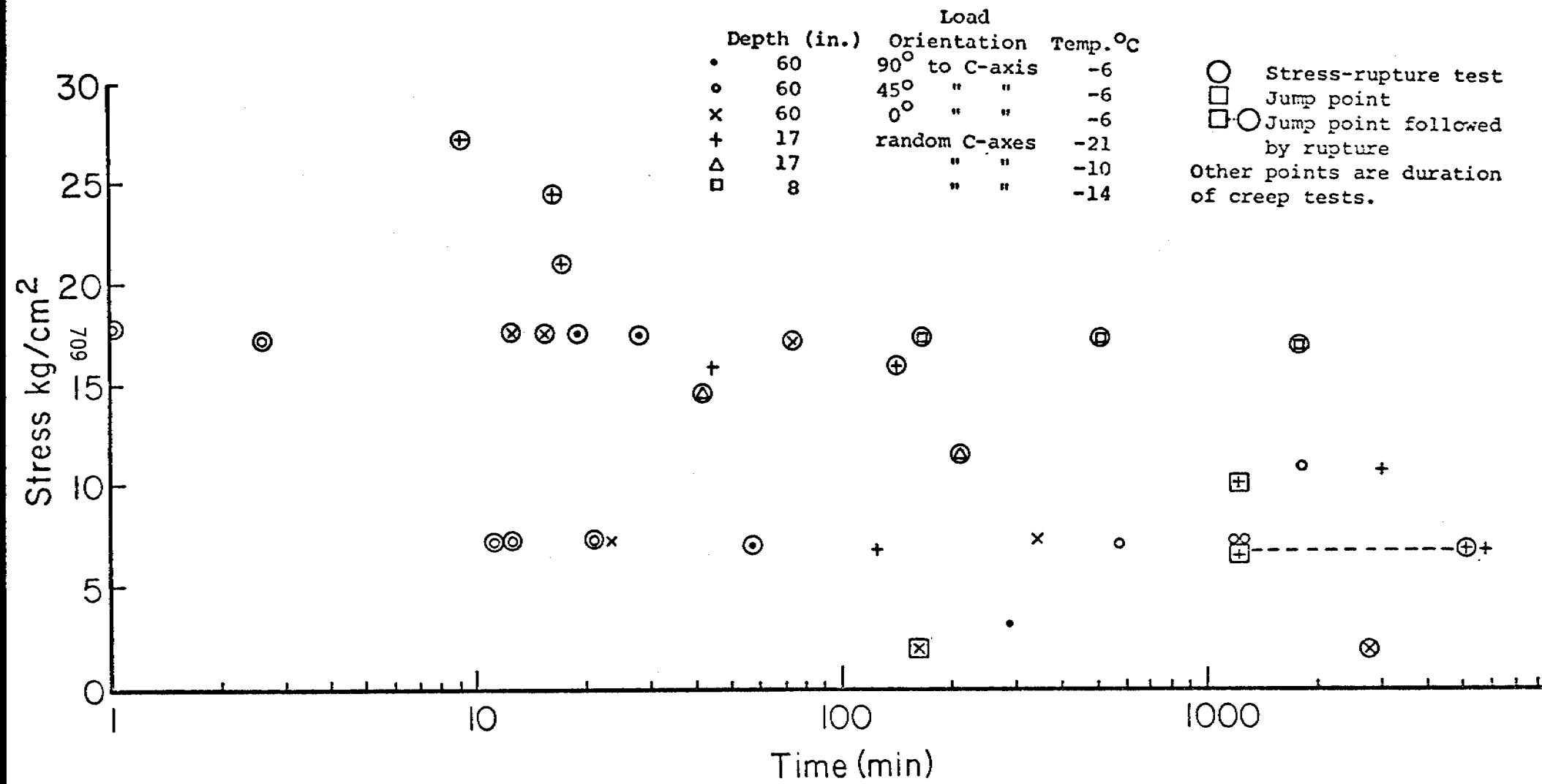


Figure 5. Stress vs. time to rupture-horizontal samples.

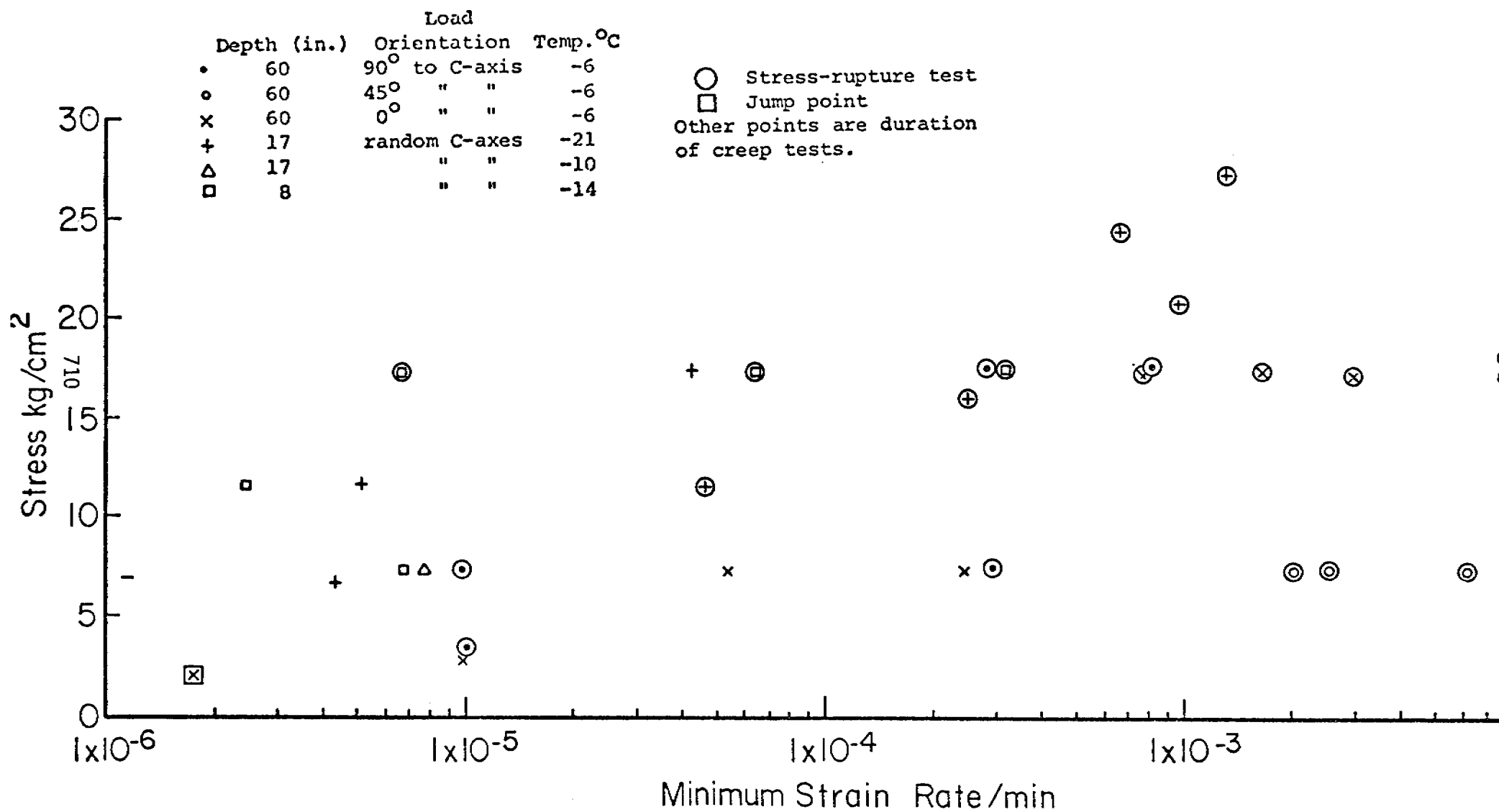


Figure 6. Stress vs. minimum strain rate for horizontal samples.

data to do more than suggest this as a possibility but, if verified (particularly for tension tests), this may have application in considering safety factors for offshore installations or for loads on floating ice sheets.

The relative lack of scatter in the vertical samples of Figures 2, 3 and 4 is somewhat surprising in view of the range of temperatures and ice types represented. It is possible that the number of tests is simply not large enough to represent the full range of typical values so that the lack of scatter is fortuitous. However, it should be noted that in all the tests shown, the loading direction was parallel to the basal planes and normal to the c-axis orientation. Thus, the relationship between the load direction and the directional properties of the sample were similar for all tests.

The apparent relationship between the stress and the minimum strain-rate and the stress and time to minimum strain-rate in the vertical samples suggests the possibility of some correspondence between the stress and the strain at minimum strain-rate. A plot of these is shown in Figure 7a, and a similar plot for the horizontal samples is shown in Figure 7b. In both data sets there is an apparent tendency to cluster, with a trend to increasing strain with increasing load. The data from Figures 7a and 7b are replotted in Figure 8 for purposes of comparison. These show a distinct overlap between the points for both data sets which is unexpected in view of the range of ice types, temperatures, loads and sample orientations represented. This is a potentially important result if it is accepted that the inflection point or first jump point in a strain-time curve represents the initiation of processes

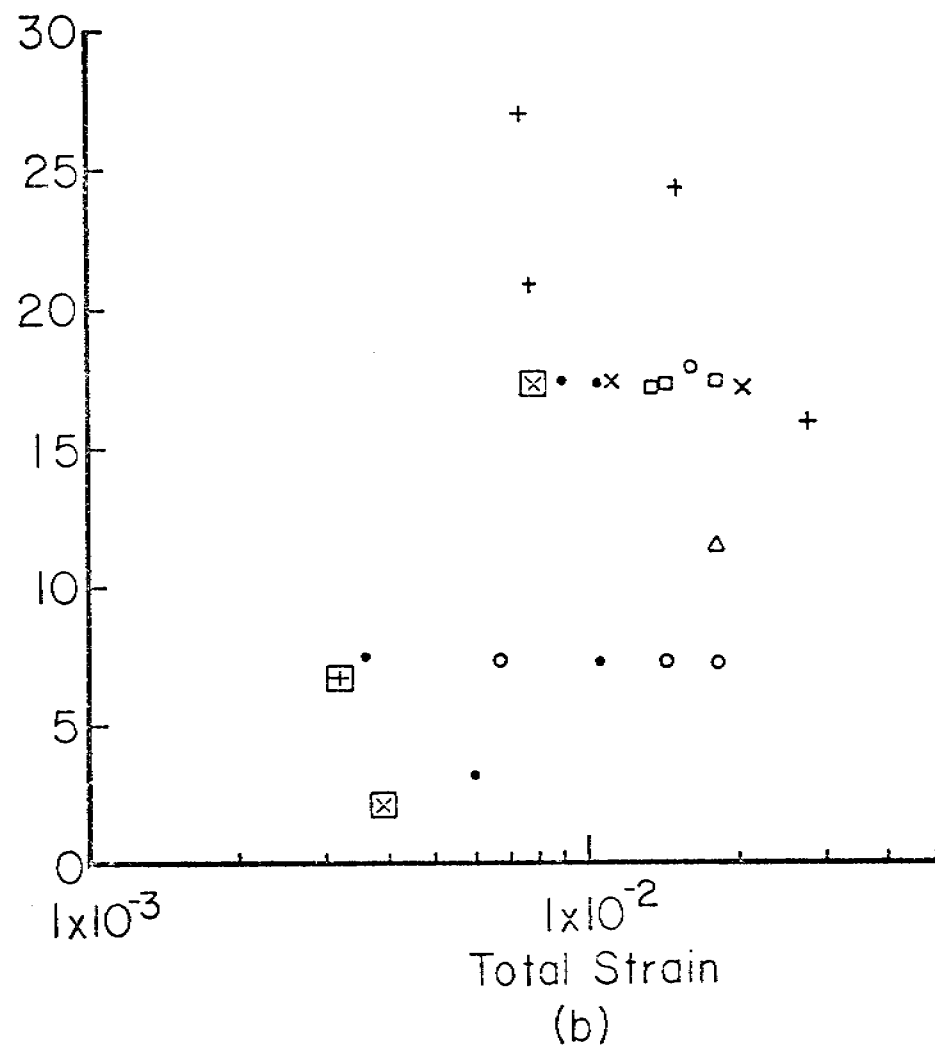
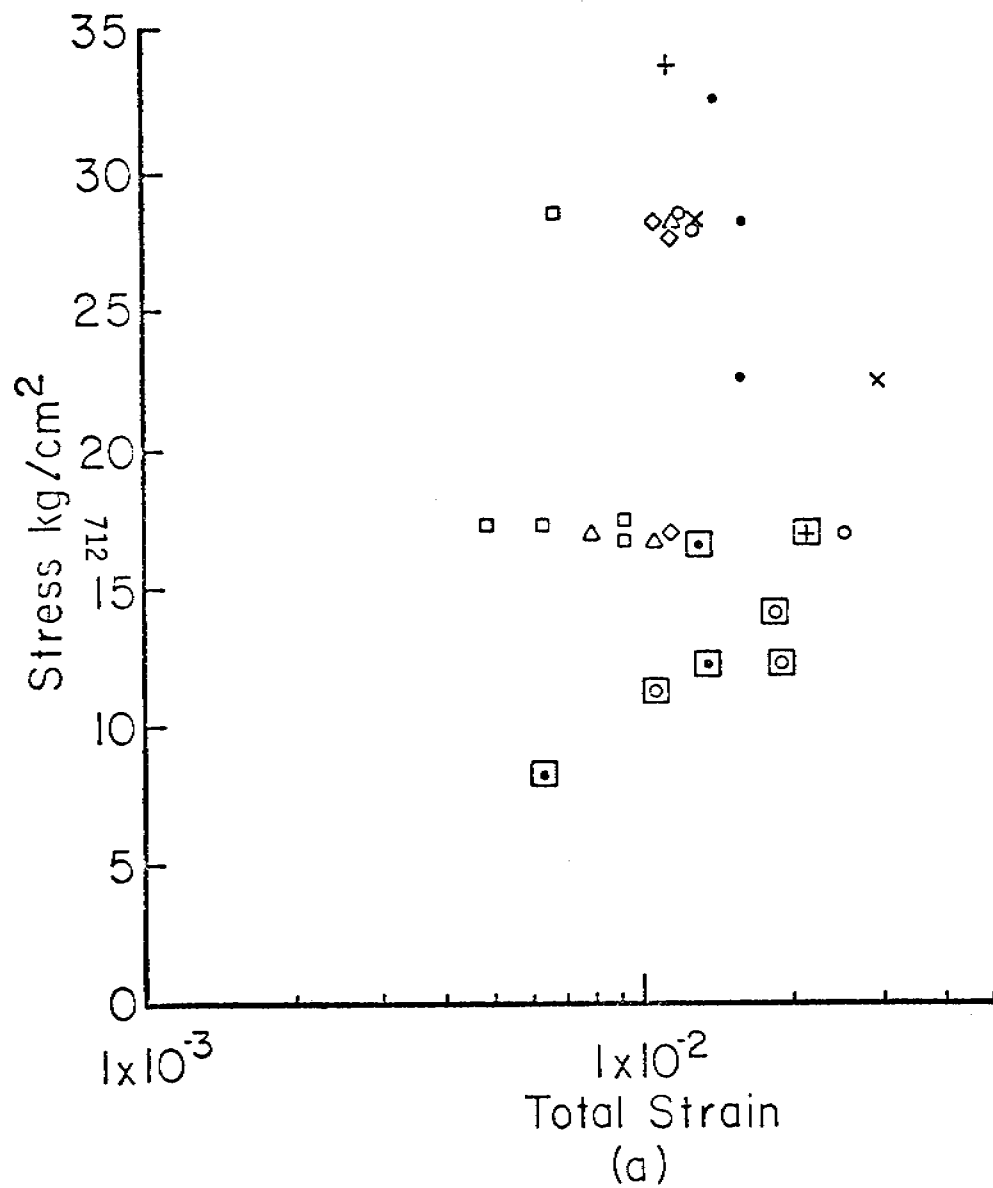


Figure 7a,b. Stress vs. total strain at minimum strain rate. (a) vertical samples; (b) horizontal samples. Points outlined by squares are jump points; the remainder are from stress-rupture tests. Symbols are the same as in previous figures.

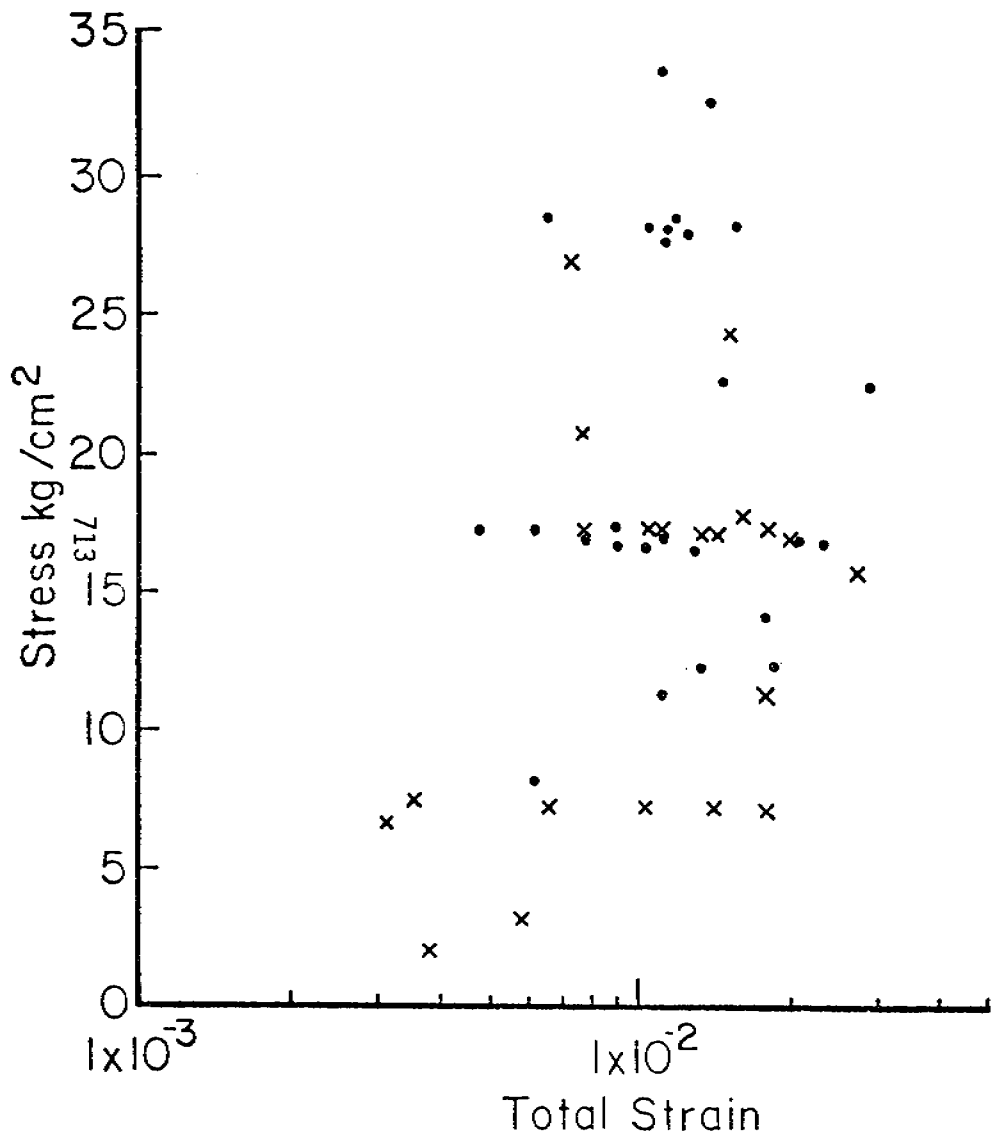


Figure 8. Stress vs. total strain at minimum strain rate for both horizontal (x) and vertical (-) samples.

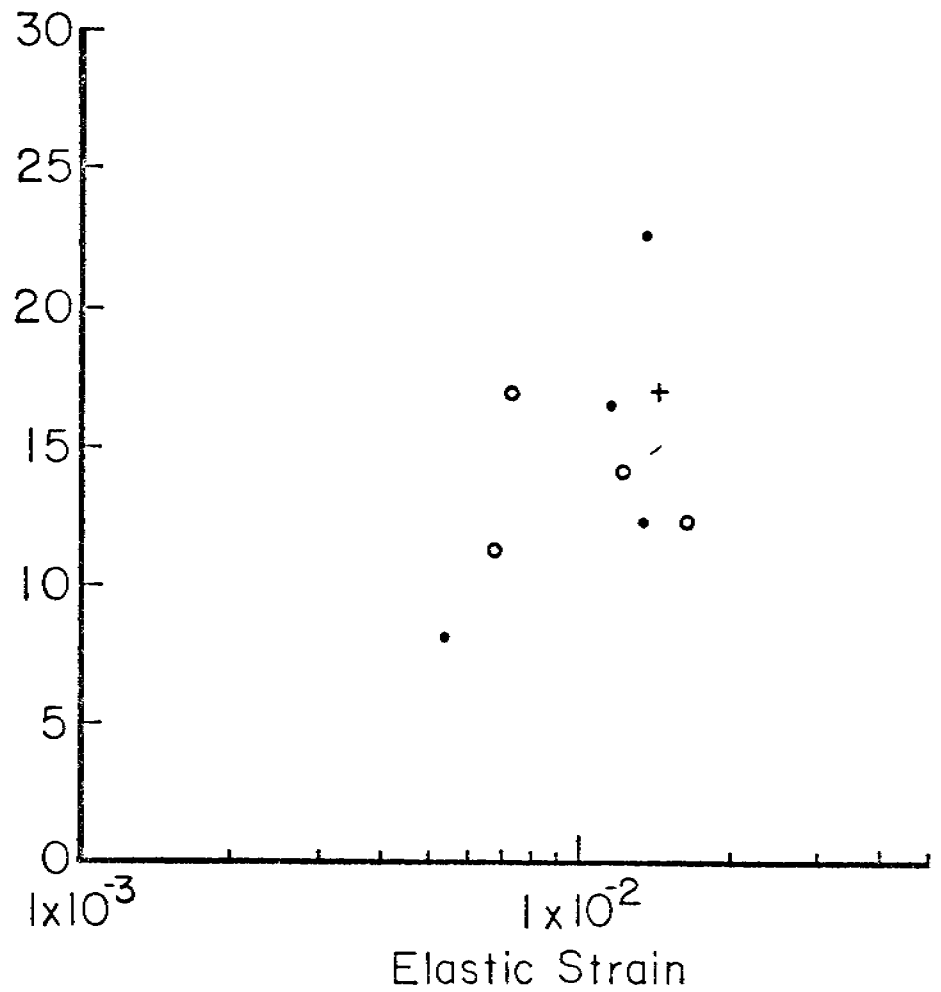


Figure 9. Stress vs. elastic strain at minimum strain rate for 8" vertical samples. Symbols as in previous figure.

leading to failure. The data in Figure 8 implies that the position of these points in the curve is primarily strain dependent and relatively independent of temperature and orientation with respect to load.

In fact, this cannot be strictly true, because sea ice is a visco-elastic material, so that some of the strain represents a dissipation of energy by flow. Thus, failure cannot depend upon the total strain, but instead, must depend upon the elastic component of the strain through which energy can be stored. Accordingly, using methods indicated in the next section, it has been possible to separate the viscous from the elastic strain for a few of the vertical samples. A plot of the results is shown in Figure 9, although there are too few points to indicate any decrease in scatter of the data. In addition, errors in the positions of these points could be as great as $3-4 \times 10^{-3}$ in the strain. These result from inaccuracies in the value of the initial elastic strain, which would tend to increase the calculated elastic strain, and from errors in measurement of the viscous strain which must, of necessity, be too great. This is discussed more fully below.

It should also be emphasized that elastic strain in a single direction in itself cannot provide a failure criteria. Instead, a full 3-dimensional description of the elastic strain is required, through which the strain energy density can be calculated. An approach to the problem is given in Reiner (1960).

Finally, further discussion of the significance of the jump points to the failure process is indicated. Figure 10 shows the stress-rupture curve of a horizontal sample from 60" depth, loaded parallel to the c-axis at -6°C . The dashed lines between the data points have been added

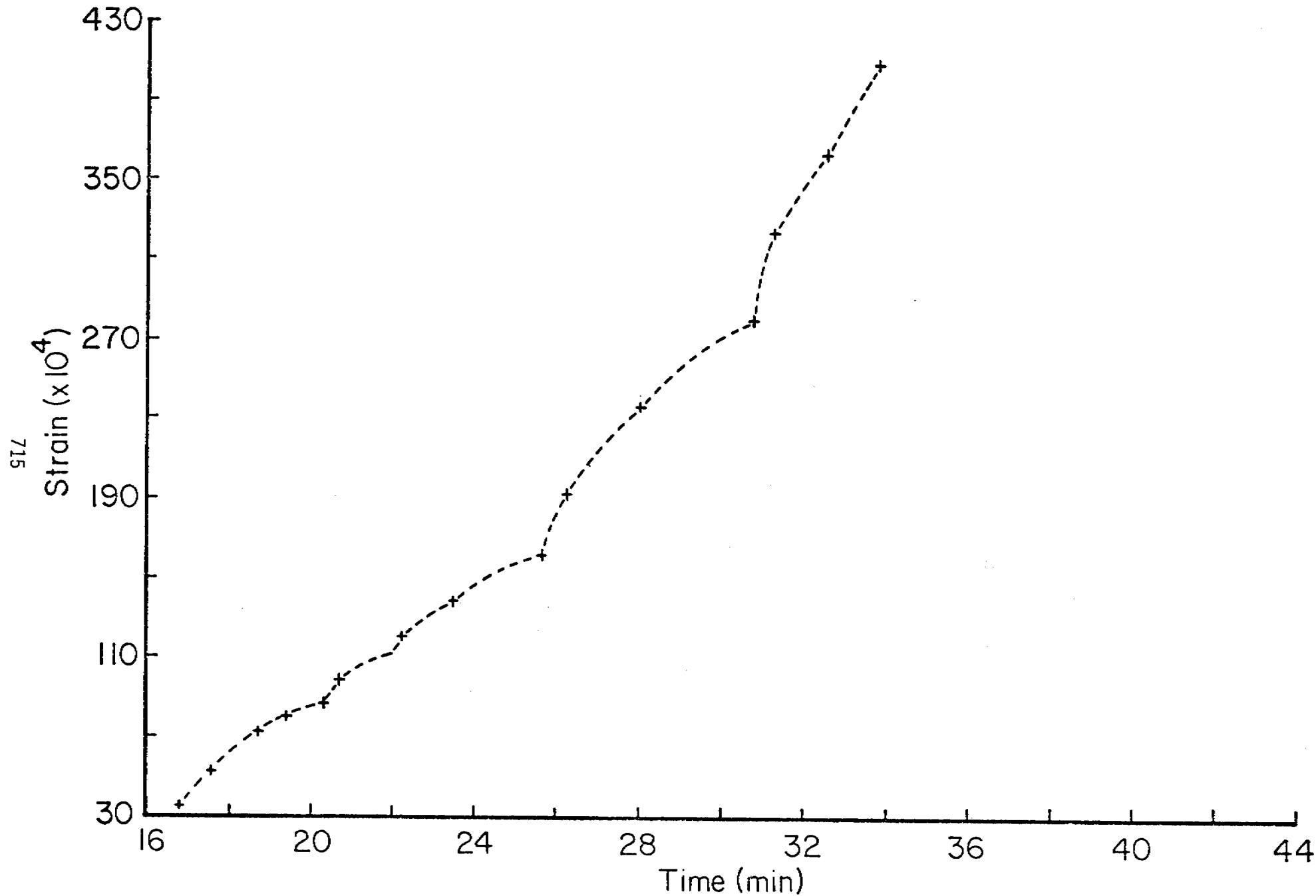


Figure 10. Stress-rupture curve points from Peyton's (1966) experiment 91; 60" horizontal sample at -6°C , loaded parallel to c-axes at 17.4 kg/cm^2 . Dashed line indicates possible interpretation of tertiary creep as a series of jump points.

to show a possible interpretation of the tertiary segment of the curve as a series of jumps. This suggests that tertiary creep may in some instances be considered to be a series of closely spaced jump points which, even if not true, may provide a means of modelling this part of the curve.

Considering Figure 1 to represent a typical jump point, it is apparent that it shows an initial elastic reaction followed by flow. As noted above, this part of the creep curve appears to be similar to those which result from two-stage creep tests so that, in effect, the stress on the sample appears to have been suddenly increased at that point. This is what would be expected if failure had occurred within some volume of the sample at the indicated time, so that the load carrying capacity of some fraction of the cross-sectional area of the sample was effectively reduced. The stress across the remainder of the cross-section of the sample then increases, thus leading to failure. This is essentially the process described in Maser (1972).

VISCOELASTIC STRESS-STRAIN LAWS FOR SEA ICE

The initial approach to analysis of the data from Peyton was based upon the work of Tabata (1958) who fitted the results of a series of creep tests on sea ice to a 4-parameter, one-dimensional model of a linear viscoelastic solid (Figure 11), and obtained values of the relevant constants. This is the simplest viscoelastic model which includes all the elements of a creep-recovery curve (except for tertiary creep leading to failure) and is thus a useful starting point.

The differential equation which describes the behavior of the model is

$$(1) \quad \dot{\epsilon} + \tau_2 \ddot{\epsilon} = \frac{1}{\eta_1} \dot{\sigma} + \left(\frac{1}{k_1} + \frac{\tau_2}{\eta_1} + \frac{1}{k_2} \right) \dot{\sigma} + \frac{\tau_2}{k_1} \ddot{\sigma}$$

where σ and ϵ are stress and strain, the dot indicates differentiation with respect to time, $\tau_2 = \eta_2/k_2$, and η_1 , η_2 , k_1 , k_2 refer to the constants of the model in Figure 11. The derivation of equation (1) can be found in standard textbooks of linear viscoelasticity (i.e., Bland, 1960). For creep tests, the load is given by

$$(2) \quad \sigma(t) = \sigma^* u(t)$$

where σ^* is a constant, and $u(t)$ is the unit step function. Substituting (2) into (1) and integrating gives the equation for strain as a function of time as

$$(3) \quad \epsilon(t) = \left(\frac{1}{k_1} + \frac{1}{k_2} + \frac{t}{\eta_1} - \frac{1}{k_2} e^{-t/\tau_2} \right) \sigma^*$$

The elements of the creep curve can readily be deduced from equation (3) and the model. Note that equation (1) can also be integrated for constant load rate or constant strain rate.

Attempts to fit equation (3) to Peyton's creep curves gave unsatisfactory results.

In order to obtain a better fit to the creep curves the dashpots in the model were assumed to obey a non-linear stress-strain law which was taken in the form of a hyperbolic sine relationship between the stress and strain rate. (Note that Krausz and Eyring (1975) describe the application of models of this type in studies of the deformation of textiles and polymers.) Then, letting $\epsilon_V(t)$ represent the strain in the Voigt model, the strain-rate is given by

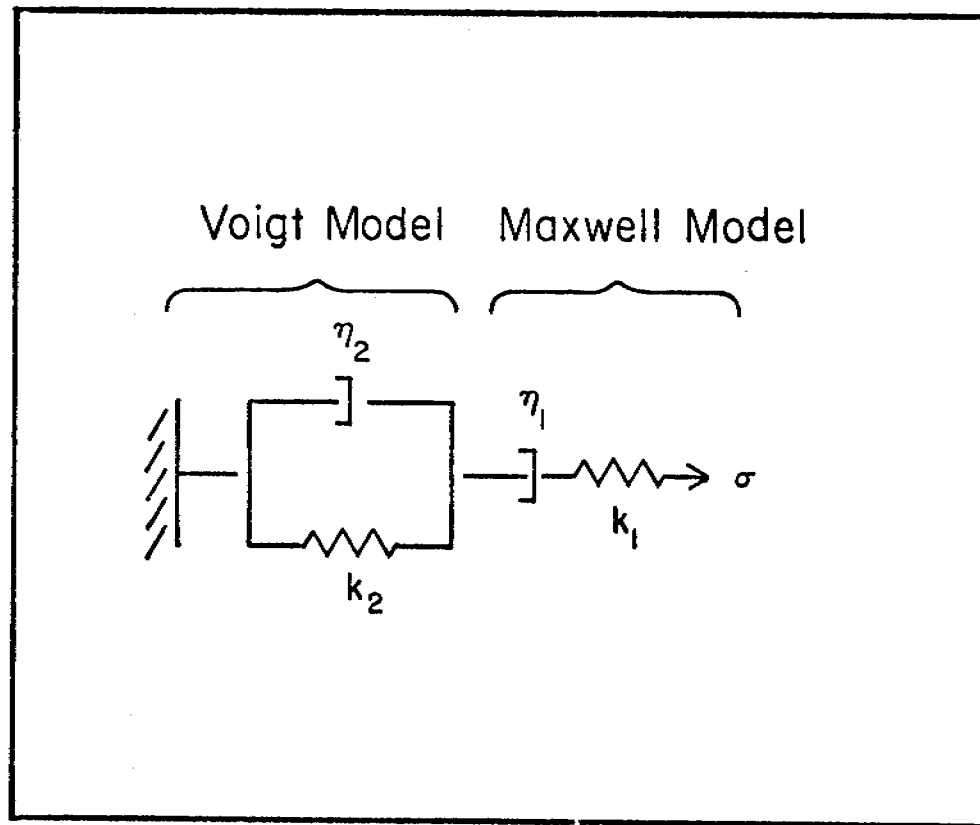


Figure 11. Spring-dashpot model of a 4-parameter linear-viscoelastic solid.

$$(4) \quad \dot{\epsilon}_V(t) = A \sinh \phi \sigma_1(t)$$

in which $\sigma_1(t)$ is the stress on the dashpot of the Voigt model and A and ϕ are constants. The strain on the element is simply

$$(5) \quad \epsilon_V(t) = \frac{\sigma_2(t)}{k_2}$$

where $\sigma_2(t)$ is the stress on the spring of the Voigt model. Then, equilibrium requires that, for a load $\sigma(t)$ applied to the total 4-parameter model,

$$(6) \quad \sigma(t) = \sigma_1(t) + \sigma_2(t)$$

Introducing (6) and (5) into (4) then gives

$$(7) \quad \dot{\epsilon}_V(t) = A \sinh \phi [\sigma(t) - k_2 \epsilon_V]$$

For a constant load ($\sigma(t) = \sigma^*$) equation (7) can be integrated and rearranged to give

$$(8) \quad \epsilon_V(t) = \frac{\sigma^*}{k_2} - \frac{2}{\phi k_2} \tanh^{-1} \left(e^{-A\phi k_2 t} \tanh \frac{\phi \sigma^*}{2} \right)$$

the creep curve of the Voigt model alone.

To extend the law to the total 4-parameter model, note that the strain in the spring of the Maxwell model is

$$(9) \quad \epsilon_1(t) = \frac{\sigma(t)}{k_1}$$

while the strain rate of the dashpot of the Maxwell model is assumed to be

$$(10) \quad \dot{\epsilon}_2(t) = B \sinh \theta \sigma(t)$$

where B and θ are constants.

The strain of the total 4-parameter model is simply the sum of the strains in the elements of the model arranged in series, which is

$$(11) \quad \epsilon_T(t) = \epsilon_V(t) + \epsilon_1(t) + \epsilon_2(t)$$

Then for $\sigma(t) = \sigma^*$, substituting (8), (9) and (10) into equation (11), and noting that $\dot{\epsilon}_2(t) = \dot{\epsilon}_2^* = \text{constant}$ when $\sigma(t) = \sigma^*$, gives

$$(12) \quad \epsilon_T(t) = \frac{\sigma^*}{k_1} + \dot{\epsilon}_2^* t + \frac{\sigma^*}{k_2} - \frac{2}{\phi k_2} \tanh^{-1} \left(e^{-A\phi k_2 t} \tanh \frac{\phi \sigma^*}{2} \right)$$

the creep curve of the total model.

In principal, the constants in equation (12) can be determined by fitting the equation to an experimentally determined creep curve. This is presently being done using Marquardt's (1963) maximum neighborhood method. To date, satisfactory fits to the data have been obtained for about 25 creep curves, but more are required before any results can be discussed. It is noteworthy, however, that creep curves calculated using the parameters determined by the fit seldom show errors of greater than 2% when compared with the original data points.

In fitting the curve, the modulus k_1 is not treated as a free parameter, but instead is calculated from the strain at the first data point of the creep curve if that point was measured within one minute of the application of the load. This is clearly in error, because the strain from the Voigt model and the dashpot of the Maxwell model are included in this value, although their combined contribution should be no greater than two orders of magnitude less than the strain in the spring of the Maxwell element. Note that a more significant error is indicated by comparison of the initial strain with the strain recovered

within the first minute after the specimen is unloaded. Unfortunately, there are few recovery curves in the data for non-rupture tests with no jump points, upon which to base a comparison. Those which are available, however, indicate that the initial strain is greater than the recovered strain by as much as 50% (i.e., magnitude of 1 to 4×10^{-3}). This affects the computation of the elastic strain in the total model as a function of time, so that the data points of Figure 9 would be translated to lower values. However, the error does not enter into the curve fitting process, and therefore does not affect the computed values of the remaining parameters.

In some of Peyton's tests, stress-strain data were taken during loading and, when available, these were plotted to determine k_1 . However, the errors in total strain are still present in the creep curves for these tests.

The source of this error is probably at least partially experimental, resulting from taking up "slack" in the loading system and the specimen. However, the possibility that some of the difference is due to strain dependent changes in the mechanical properties of the sample cannot be ignored based upon the available data.

From equation (12) and the model (Figure 11), it is apparent that the only viscous component of the strain at any time is that associated with the dashpot of the Maxwell model, represented by the second term on the right side of the equation. This quantity can be estimated for those experimental creep curves which appear to have nearly reached the steady-state creep phase by measuring the minimum strain-rate and multiplying by the time. Subtraction of this value at any time from the curve gives

the value of the elastic strain (including the errors above) at that time. The values of the elastic strain shown in Figure 9 were determined in this way. Note that the value of the strain-rate measured must be too large, so that the error introduced tends to compensate that in the estimate of the initial strain.

CONSTANT LOAD-RATE TESTS

The stress-strain law for the 4-parameter model with non-linear dashpots can also be derived for the case in which the specimen is loaded at a constant load rate. Fitting this model to experimental data would then, in principal, permit all of the parameters of equations (10) to be evaluated.

The derivation follows that for the constant load problem. Equation (4) is integrated and substituted into (5) to obtain an expression for $\sigma_2(t)$ in terms of $\sigma_1(t)$. Then, substituting into (6), gives

$$(13) \quad \sigma(t) = \sigma_1(t) + Ak_2 \int \sinh \phi \sigma_1(t) dt$$

For constant load rate tests, the load as a function of time is given by

$$\sigma(t) = \dot{\sigma}^* t$$

where $\dot{\sigma}^*$ is the constant rate of loading. Substituting into (13) and differentiating with respect to time then gives

$$\dot{\sigma}^* = \dot{\sigma}_1(t) + Ak_2 \sinh \phi \sigma_1(t)$$

or

$$(14) \quad \int_0^{\sigma_1} \frac{d\sigma_1'}{C - \sinh \phi \sigma_1'} = Ak_2 \int_0^t dt'$$

where the primes indicate dummy variables and the substitution $C = \dot{\sigma}^*/Ak_2$ has been used. Using the substitution

$$z = C - \sinh \phi \sigma_1'$$

and noting the limits on z as σ_1' gives from zero to σ_1 , (14) becomes

$$(15) \quad -\frac{1}{\phi} \int_{\beta}^{\beta - \sinh \phi \sigma_1} \frac{dz}{z(z^2 - 2Cz + C^2 + 1)^{1/2}} = Ak_2 t$$

In the quadratic term of the denominator $b^2 - 4ac = -4$, ($4ac > b^2$), so that (15) integrates to (Dwight, 1947, #380.111)

$$\frac{1}{\phi C^{1/2}} \sinh^{-1} \frac{bz+2c}{z(4ac-b^2)^{1/2}} \Big|_{\beta}^{\beta - \sinh \phi \sigma_1} = Ak_2 t$$

and

$$\frac{1}{\phi(1+C^2)^{1/2}} \left[\sinh^{-1} \left(\frac{1 + C \sinh \phi \sigma_1}{C - \sinh \phi \sigma_1} \right) - \sinh^{-1} \frac{1}{C} \right] = Ak_2 t$$

Then, introducing the substitutions

$$D = \phi(1 + C^2)^{1/2} k_2 A$$

$$E = \sinh^{-1} \frac{1}{C}$$

and solving for $\sigma_1(t)$ gives

$$(16) \quad \sigma_1(t) = \frac{1}{\phi} \sinh^{-1} \left[\frac{C \sinh (Dt + E) - 1}{C + \sinh (Dt + E)} \right]$$

The stress-strain law for the Voigt model can then be found from equations (5), (6) and (16), since

$$\epsilon_V(t) = \frac{\sigma_2(t)}{k_2} = \frac{\sigma(t) - \sigma_1(t)}{k_2}$$

so that [recalling that $\sigma(t) = \dot{\sigma}^* t$]

$$(17) \quad \epsilon_V = \frac{\sigma}{k_2} - \frac{1}{\phi k_2} \sinh^{-1} \left[\frac{C \sinh(D \frac{\sigma}{\dot{\sigma}^*} + E) - 1}{C + \sinh(D \frac{\sigma}{\dot{\sigma}^*} + E)} \right]$$

To extend the results to the 4-parameter model, note that from (9), the spring of the Maxwell model strains as

$$(18) \quad \epsilon_1(t) = \frac{\sigma^* t}{k_1}$$

while the strain-rate of the dashpot is (from 10)

$$\dot{\epsilon}_2(t) = B \sinh \theta \sigma^* t$$

The dashpot strain is therefore

$$(19) \quad \epsilon_2(t) = \frac{C}{\theta \dot{\sigma}^*} \cosh \theta \dot{\sigma}^* t$$

Then, substituting (17), (18) and (19) into (11) gives the stress-strain curve for the total model,

$$(20) \quad \epsilon_T(t) = \frac{\sigma(t)}{k_1} + \frac{C}{\theta \dot{\sigma}^*} \cosh \theta \sigma(t) + \frac{\sigma(t)}{k_2} - \frac{1}{k_2 \phi} \sinh^{-1} \left[\frac{C \sinh(D \frac{\sigma}{\dot{\sigma}^*} + E) - 1}{C + \sinh(D \frac{\sigma}{\dot{\sigma}^*} + E)} \right]$$

where, as above, the strain in the spring of the Maxwell model is given by the first term, while the second term is the strain in the dashpot of the same model.

One additional point should be noted here which provides a further test of the suggestion above that failure is dependent on the elastic strain. The only viscous strain represented in equation (20) is that given by the second term on the right, which describes the strain in the

dashpot of the Maxwell element. The elastic strain of the model is therefore given by the remaining three terms. It is thus possible to calculate the value of $\sigma(t)$, for any value of constant load rate $\dot{\sigma}^*$, at which the elastic strain reaches some specified value corresponding to failure. This has been done with the elastic strain fixed at a value of 6×10^{-3} and load rates ranging up to $500 \text{ kg/cm}^2/\text{min}$. The results are plotted to give the curve of "compressive strength" vs. load rate shown in in Figure 12. The values of the parameters are arbitrary. For purposes of comparison, Figure 13 shows plots of experiment curves of strength vs. load rate taken from Peyton (1966). The similarity is apparent, and thus tends to reinforce the hypothesis of the elastic strain dependency of failure, at least over the range of values indicated.

It should be noted that because the model does not include any elements which would lead to a decrease in strength with increasing load rate, that hypothesis is not excluded by the result presented here.

CONSTANT STRAIN RATE TESTS

Finally, for the sake of completeness, the derivation of the stress-strain law for constant-strain rate tests of the non-linear 4-parameter model will be outlined.

Let $\dot{\epsilon}^*$ be the applied constant strain rate. Then, this must equal the sum of the strain rates in the individual elements, so that

$$\dot{\epsilon}^* = \dot{\epsilon}_V(t) + \dot{\epsilon}_1(t) + \dot{\epsilon}_2(t)$$

where $\epsilon_V(t)$, $\epsilon_1(t)$ and $\epsilon_2(t)$ are defined above. Then from (4), the derivative of (9), and (12)

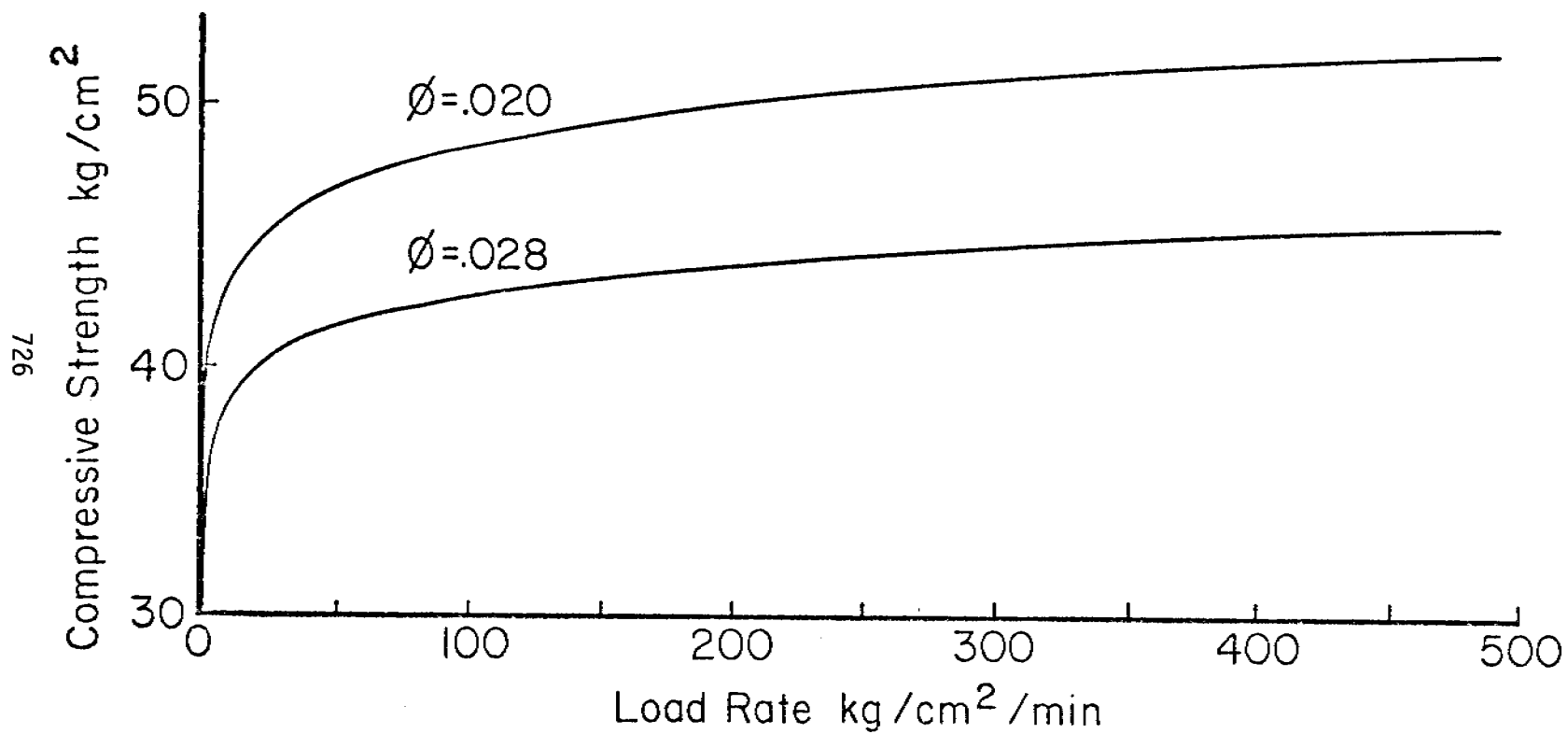


Figure 12. "Compressive strength" as calculated assuming failure occurs when the elastic strain in equation (20) reaches 6×10^{-3} . Values of the constants were $k_1 = 1.4 \times 10^4$ kg/cm², $k_2 = 7.02 \times 10^3$ kg/cm², $A = 5 \times 10^{-6}$ /min. Values of ϕ as indicated.

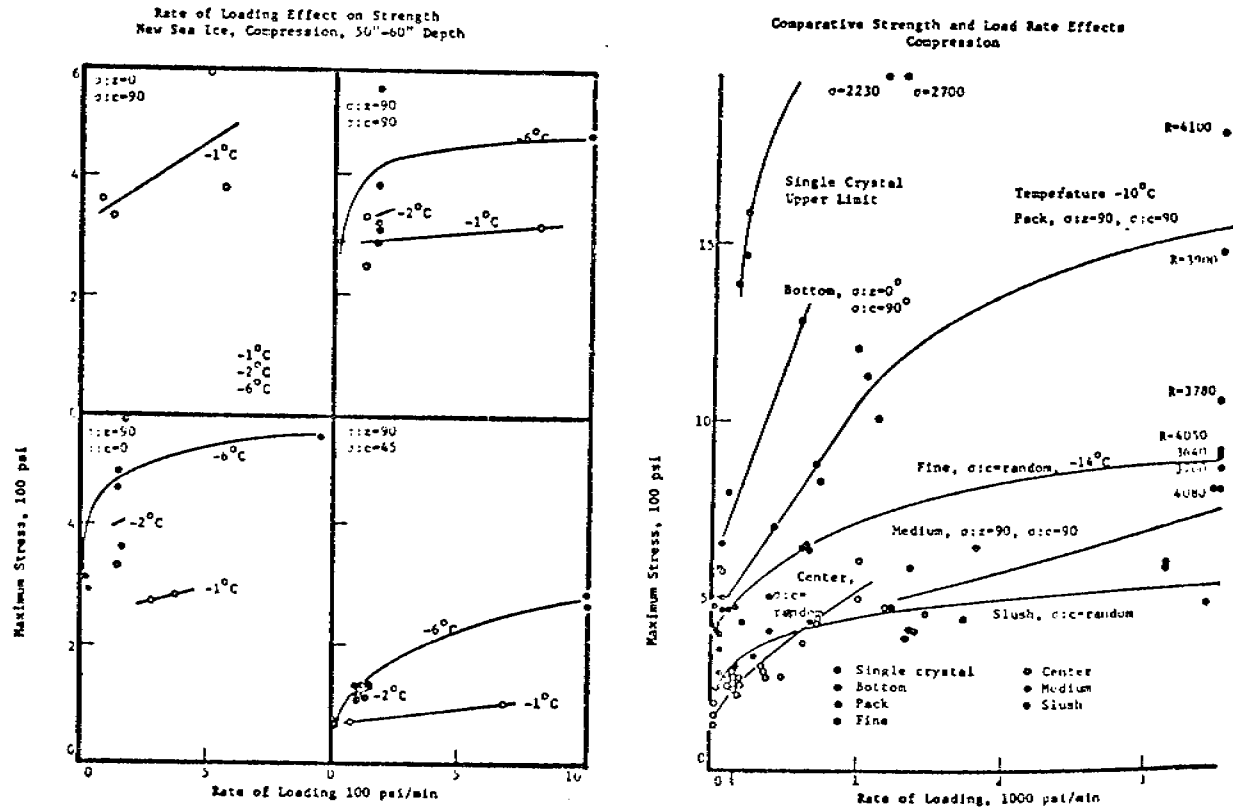


Figure 13. Experimental curves of compressive strength vs. loading rate from Peyton (1966).

$$(21) \quad \dot{\epsilon}^* = A \sinh \phi \sigma_1(t) + \frac{\dot{\sigma}(t)}{k_1} + B \sinh \theta \sigma(t)$$

Similarly, the strain at time t is

$$\dot{\epsilon}^* t = \epsilon_v(t) + \epsilon_1(t) + \epsilon_2(t)$$

or, from (5), (9) and the integral of (10)

$$(22) \quad \dot{\epsilon}^* t = \frac{\sigma_2(t)}{k_2} + \frac{\sigma(t)}{k_1} + B \int \sinh \theta \sigma(t) dt$$

Solving (21) for σ_1 and (22) for σ_2 , and substituting into equation (6) then gives

$$(23) \quad \sigma(t) = \frac{1}{\phi} \sinh^{-1} \frac{\dot{f}}{A} + k_2 f$$

where

$$f = \dot{\epsilon}^* t - \frac{\sigma(t)}{k_1} - B \int \sinh \theta \sigma(t) dt$$

Equation (23) can be differentiated to remove the inverse hyperbolic sine, and then rearranged to

$$\dot{f}^4 - \frac{2}{k_2} \dot{\sigma} \dot{f}^3 + \frac{\dot{\sigma}^2 + k_2^2}{k_2^2} \dot{f}^2 - \frac{2}{k_2} \dot{\sigma} \dot{f} + \frac{\dot{\sigma}^2}{k_2^2} = \frac{1}{\sigma^2 A^2 k_2^2} \ddot{f}^2$$

which is a complicated (algebraically) non-linear ordinary differential equation which should be solvable by numerical methods. However, the possibility of obtaining a closed form solution still has not been excluded.

DISCUSSION

It is important to note that introducing non-linear dashpots into the 4-parameter model removes the results from the firm foundation of

the theory of linear viscoelasticity. It is intuitively reasonable that such models may eventually be associated with the integrals of the stress-strain laws of non-linear viscoelasticity but we know of no examples of this in the literature. A possible approach to this problem is presently being examined. Further, the equations given are one-dimensional, and the form of the analogous 3-dimensional law is not established. This must be done before the anisotropy of the material can be considered. Thus, for the present, the models should be taken only as a means of examining the energy balance in the sample and for what information can be obtained regarding the changes in these quantities during deformation.

REFERENCES CITED

- Bland, D. R., 1960, The Theory of Linear Viscoelasticity, Pergamon Press, New York, 125 p.
- Dwight, H. B., 1957, Tables of Integrals and Other Mathematical Data, Macmillan Co., New York, 288 p.
- Grant, N. J. and Mullendore, A. W., 1965, Deformation and Fracture at Elevated Temperatures, M.I.T. Press, Cambridge, Mass., 211 p.
- Karlsson, T., 1972, A viscoelastic-plastic material model for drifting sea ice, in Sea Ice, Proc. Conf. Reykjavik, Iceland, May 10-13, 1971, p. 188-195.
- Kingery, W. D. and French, D. N., 1963, Stress-rupture Behavior of Sea Ice, in Ice and Snow - Processes, Properties and Applications, (W. D. Kingery, ed.), M.I.T., Cambridge Mass., p. 124-129.
- Krausz, A. S. and Eyring, H., 1975, Deformation Kinetics, John Wiley and Sons, New York, 398 p.
- Marquardt, D. W., 1963, An algorithm for least-squares estimation of non-linear parameters, J. Soc. Indust. Appl. Math., 11, p. 431.
- Maser, K. R., 1972, An analysis of the small-scale strength testing of ice, M.I.T. Sea Grant Office, Rept. No. MITSG 72-6, 137 p.
- Naghdi, P. M. and Murch, S. A., 1963, On the mechanical behavior of viscoelastic-plastic solids, J. Appl. Mech., 30, p. 321-328.
- Peyton, H. R., 1966, Sea Ice Strength, Geophysical Institute, University of Alaska, Report UAG R-182, 273 p.
- Reiner, M., 1960, Plastic Yielding in Anelasticity, J. Mech. Phys. Solids, 8, p. 255-261.
- Tabata, T., 1958, Studies on viscoelastic properties of sea ice, in Arctic Sea Ice, U.S. National Academy of Sciences, National Research Council, Pub. 598, p. 139-147.

Q U A R T E R L Y R E P O R T

Contract # 03-5-022-55, task 10
Research Unit # 267
Reporting Period, October 1 to
December 31, 1976
Number of Pages - 7

OPERATION OF AN ALASKAN FACILITY
FOR APPLICATIONS OF REMOTE-SENSING DATA TO OCS STUDIES

Albert E. Belon
Geophysical Institute
University of Alaska

December 31, 1976

OPERATION OF AN ALASKAN FACILITY
FOR APPLICATIONS OF REMOTE-SENSING DATA TO OCS STUDIES

Principal Investigator: Albert E. Belon
Affiliation: Geophysical Institute, University of Alaska
Contract: NOAA # 03-5-022-55
Research Unit: #267
Reporting Period: October 1 to December 31, 1976

I. TASK OBJECTIVES

The primary objective of the project is to assemble available remote-sensing data of the Alaskan outer continental shelf and to assist other OCS investigators in the analysis and interpretation of these data to provide a comprehensive assessment of the development and decay of fast ice, sediment plumes and offshore suspended sediment patterns along the Alaskan coast from Yakutat to Demarcation Bay.

II. LABORATORY ACTIVITIES

A. Operation of the Remote-Sensing Data Library

We continued to search periodically for new Landsat imagery of the Alaskan coastal zone entered into the EROS Data Center (EDC) data base. As a result 164 cloud-free Landsat scenes were selected and ordered from EDC at a cost of \$5215. These data products, which are gradually received from EDC, complete our files of Landsat data from the launch of the first satellite, July 26, 1972, with at least the following data products.

- 70mm positive transparencies of multispectral scanner (MSS) spectral bands 4, 5 and 7
- 70mm negative transparency of MSS, spectral band 5
- 9½ inch print of MSS, spectral band 6

This unusually large order for Landsat data products resulted from a notification, received from EDC in mid-December, that the purchase cost of Landsat transparencies and prints would increase from \$3.00 to \$8.00 each on January 1, 1977. Normally we order one print from each new scene, as it is revealed by periodic computer searches, and we delay ordering the transparencies until the prints have been received and the data quality has been assessed. The notification of the price increase prompted frantic activity in December to bring the acquisition of all selected transparencies up-to-date before the price increase took effect.

In addition custom prints were ordered to construct mosaics of the Beaufort Sea and the Chukchi Sea for summer (August) and winter (March-April) of 1975 and 1976 in preparation for the Arctic Project Office's synthesis meeting to be held at Barrow on February 7-11, 1977.

We continued to receive and catalog daily copies of NOAA satellite imagery of Alaska in both the visible and infrared spectral bands under a standing order with the NOAA/NESS Fairbanks Satellite Data Acquisition Station. 368 NOAA scenes at a total cost of \$1656 were acquired in 10" positive transparency format during the reporting period.

We received and catalogued 1316 frames of color aerial photography acquired for OCSEAP by the National Ocean Survey's Buffalo aircraft in June and July 1976. These data provide complete coverage of the Bering Sea and Chukchi coast from the Yukon Delta to Cape Lisburne for which little aerial photography was previously available. The data also include several short film strips of strategic areas in the northern Gulf of Alaska and Cook Inlet.

We also received and catalogued 167 frames of high altitude aerial photography acquired for OCSEAP by the NASA Ames Research Center U-2 aircraft in October 1976. These data provide color-infrared and high resolution black and white coverage of the coasts of the northeast gulf of Alaska from Yakutat to Valdez and northern Prince Williams Sound from Whittier to Valdez.

A catalog of all remote-sensing data acquired for OCSEAP during 1976 was prepared and distributed to all OCS investigators in December 1976 through the NOAA/OCSEAP Arctic Project Bulletin No. 12. It is included as an appendix to this quarterly report.

B. Operation and Maintenance of Data Processing Facilities

Most of the remote-sensing data processing equipment was kept operational during the reporting period and was utilized by numerous OCS investigators. This equipment includes a variety of small and large light tables which are used almost continuously, a multi-format stereo-light table for viewing aerial roll films, a zoom transfer scope for transferring thematic data onto maps, a color-additive viewer for color-combining multispectral or multirate images (Landsat and sea-ice radar), a VP-8 image analyser for density-slicing satellite and aircraft photographs, a digital image recorder for transferring digital imagery data to black and white or color photographic film, and a variety of other viewing and standard photographic instruments.

The CDU-200 Digital Color Display System continued to be plagued with troubles and repeated break-downs, all related to its digital disc memory which requires extraordinarily stable and accurate timing and synchronization pulses in order to correctly transfer data from tape to disc and from disc, through a minicomputer, to the color television display screen. We have finally decided to replace the disc memory with a solid-state random access memory which will cure all the current problems and provide additional capabilities for interactive data manipulations. The substantial costs of this modification (~\$15,000) will be shared by several user projects of the Geophysical Institute. It is expected that the modified system will be operational by late spring 1977. In the meantime the operational VP-8 image analyser and the digital image recorder should meet most of the present needs of OCS users.

C. Development of Data Analysis and Interpretation Techniques

Most of the current needs of OCS investigators are met by data processing techniques which have been developed or adapted to OCS needs by our project. These include techniques of visual photo-interpretation, custom printing of black and white or color images for specific purposes (details of shoreline morphology, sea-ice sediments suspended in offshore waters etc.), color-coding of multirate images, false-color reconstitution of multispectral images, density-slicing and various types of digital data manipulations (high resolution density-slicing, multispectral histogram construction, reflectivity profiles etc.).

In cooperation with other projects of the Geophysical Institute we are now in the process of converting a series of NASA computer programs for automatic classification of Landsat data on our computing facilities. These include an "Isoclass" spectral clustering program (converted during the last period) for spectral separation of various types of sea ice as well as land features, a "Maximum Likelihood Classifier" program for mapping the sea-ice types identified by the "Isoclass" program, and a "Geometric Correction" program for rectifying the map-like images produced either from the raw data tapes or from the classified data tapes generated by the "Maximum Likelihood Classifier" program. The latter two programs will be converted during the next quarterly period.

Although we have utilized such techniques in the past using commercial computing facilities in California, and are therefore convinced of their applicability to the OCSEAP program, few OCSEAP investigators have used them so far. One outstanding exception is Dr. Roger Barry (RU #244). We believe that the local availability of these powerful programs and interpretation techniques will generate increased use by OCSEAP investigators.

D. Assistance to OCS Investigators

During the last quarterly period twenty-eight OCS investigators requested our project to provide them with substantial and often repeated assistance ranging from data searches and orders to operation of data processing equipment and digital analysis of Landsat data.

Data purchases by OCS investigators totalled \$586.00 for orders placed to the EROS Data Center, \$89.00 for orders placed to the National Ocean Survey, and several hundred dollars in work orders for urgent or custom reproduction of selected data, principally SLAR data. In addition many OCS investigators performed analyses of library copies of data in our facility.

Dr. William Stringer (RU #257), Dr. Jan Cannon (RU #99) and Dr. John J. Burns (RU #230,232,248 and 249) continued to be frequent and heavy users of our data and facilities. Bruce Krogman of the National Marine Fisheries Service and connected with four projects (RU #67,68,69 and 70) dealing with marine mammals in different areas of the Alaskan coastal zone also utilized our facilities extensively to order Landsat imagery.

At the request of the Arctic Project Office the principal investigator of our project attended the OCSEAP Bird Investigator's Workshop in Anchorage on October 20-22, 1976 and presented a lecture on remote-sensing applications and capabilities, as part of a panel

of physical scientists convened for the purpose of discussing data and services available from meteorology, climatology, and remote-sensing that can be of use to OCS bird investigators. An attempt was also made to identify major environmental events or conditions that could have had a bearing on bird phenology and reproductive success in summer 1976. (see Arctic Project Bulletin No. 12 for a summary of the meeting). As a result of general and individual discussions held at this meeting several OCSEAP bird biologists are now using remote-sensing data through the facilities provided by our project. Three of the major users in this group are George Divoky and his assistants (RU #196 and RU #330) who spent numerous hours analyzing remote-sensing data in our facility, Leonard Peyton (RU #458) who is using NOS color aerial photography to map bird habitat in the Norton Bay region, and George Hunt (RU #83) who requested our project to perform analyses of sea-surface temperatures from NOAA satellite data, and ice-edge locations from Landsat data in the vicinity of the Pribilof Islands. Arrangements have also been made with George Hunt to perform similar analyses on suitable future NOAA and Landsat data during the 1977 season. Discussions were also initiated with Peter Myers (RU #172) concerning bird habitat mapping from Landsat digital data.

In preparation for the OCSEAP Arctic Project Office workshop to be held in Barrow on February 7-11, 1977 we have been selecting satellite and aircraft data to illustrate sea-ice conditions during winters and summers 1975 and 1976 and sediment transport in the Beaufort and Chukchi Seas during summers 1975 and 1976. The selected images will be custom printed to emphasize sea-ice or sediments. The Landsat images will be used to construct black and white mosaics on 1:1,000,000 scale base maps. The NOAA satellite and aircraft images will be enlarged to appropriate scales. It is believed that these remote-sensing data products will be quite useful to compare with and help in synthesizing the results of other OCSEAP arctic projects.

The project coordinated the acquisition of high-altitude aerial photography of the Alaskan coastal zone by the NASA/Ames U-2 aircraft during early October 1976. This data acquisition program, which was performed at no-cost to OCSEAP, had been previously negotiated with NASA as secondary to the primary mission which was high-altitude stratospheric sampling. Problems with the sampling instruments caused postponement of the mission from June to October, and similar problems in October caused the mission to be reduced from two to one week. As a result, and because of unfavorable cloud-cover elsewhere, the only aerial photography obtained in October 1976 covered the north-central Gulf of Alaska and Prince Williams Sound. These data were recorded on color-infrared and high-resolution black and white film. It is hoped that our informal arrangements with NASA/Ames can be continued and that further attempts to acquire aerial photography of other areas of the coastal zone can occur during the next scheduled U-2 mission in June 1977.

SLAR data obtained over the Beaufort and northern Chukchi Seas by the NASA Lewis Research Center and the Coast Guard in August and September 1976 has not yet been received by our project for the use of OCS investigators. Apparently the low density and contrast of the films has caused serious problems in reproducing it for us.

An experimental test of the capabilities of the University of Kansas prototype side-looking radar (SLAR) was performed at Barrow in December 1976 using the C-117 NARL aircraft as a platform. Our project processed and evaluated the film obtained during these tests. The results were disappointing. When compared with conventional SLAR data previously obtained by the Motorola SLAR of the Army's Mohawk remote-sensing aircraft, the U. of Kansas SLAR exhibits three serious deficiencies:

- a) the film format is small (70mm vs. 5") and is not continuous, i.e. there are coverage gaps between frames. In principle this problem can be resolved by a change in the design of the recording system, i.e. recording on magnetic tape with subsequent transfer from tape to film in our facilities; but this would substantially increase the costs of data acquisition
- b) there is often a density gradation across the SLAR frame. This may be simply due to maladjustment of ramp voltages during the test flights; if so it is correctable and would not be a serious problem
- c) the SLAR images of sea-ice appear "fuzzy" and exhibit pronounced lack of contrast and detail. Since the scan lines themselves are sharp, the problem is likely to be inherent to the SLAR rather than its recording system. Comparison of sea-ice data with data of Kansas agricultural fields obtained with the same system shows the latter to be of better, though still insufficient, quality. Therefore it may be that the characteristics of sea-ice as a radar reflector enhances basic deficiencies of the system. In view of the results of this test, the Arctic Project Office and our project are reconsidering other SLAR systems (Westinghouse and Motorola) which may be available on loan from other agencies.

The disappointing results obtained with the U. of Kansas prototype SLAR system are clearly a set-back in the Arctic Project Office's plans to establish an airborne remote-sensing data acquisition facility at Barrow because the prevalent cloud cover on the arctic coast makes an all-weather system (SLAR) an essential component of this facility. Other components of the system are a laser profilometer and an aerial camera presently available at NARL, and a multiband aerial camera which our project is acquiring on loan from the U.S. Fish and Wildlife Service. Thus it is possible to at least start a remote-sensing data acquisition program in time for monitoring the 1977 sea-ice break-up, and we are hopeful that a SLAR system may also be available and operational by that time. With this in mind, the Arctic Project Office has requested a proposal from NARL for the airborne remote-sensing data acquisition program and a companion amended proposal from our project for the photographic processing of the data acquired by NARL.

III. RESULTS

A catalog of all remote-sensing data acquired for OCSEAP during 1976 was prepared and distributed to all OCS investigators in December 1976 through the NOAA/OCSEAP Arctic Project Bulletin No. 12. It is included as an appendix to this quarterly report.

The operation of data processing facilities, the assistance provided to OCSEAP investigators, and the results of these two activities are described in the previous section of this report.

IV. PRELIMINARY INTERPRETATION OF RESULTS

This project provides technical support to the other OCS projects. Therefore disciplinary data interpretations are reported by the individual user projects.

V. PROBLEMS ENCOUNTERED/RECOMMENDED CHANGES

None of substance or unusual character during the reporting period.

The 166% increase, effective January 1, 1977, in the price of Landsat data products commonly ordered from the EROS Data Center will severely restrict our financial ability to order the available cloud-free Landsat scenes of the Alaskan coastal zones in the five data products which we previously purchased. As a result, starting January 1, 1977 we will order only the 9½" prints of MSS spectral band 6 as soon as they become available, and we will order the other data products subsequently and selectively based on data quality and need by frequent OCSEAP users.

VI. ESTIMATES OF FUNDS EXPENDED

The estimated expenses of the project during the reporting period were approximately \$20,000. In addition, outstanding obligations related to standing orders for Landsat and NOAA satellite data products totalled \$14,022.13.

A P P E N D I X

See Arctic Project Bulletin No. 12, Remote Sensing Data for OCS Studies

Quarterly Report

Contract #03-5-022-56
Research Unit #289
Task Order #19
Reporting Period 10/1 - 12/31/76
Number of Pages 5

MESOSCALE CURRENTS AND WATER MASSES IN THE
GULF OF ALASKA

Dr. Thomas C. Royer
Institute of Marine Science
University of Alaska
Fairbanks, Alaska 99701

January 1, 1977

I. Task Objectives

To continue gathering hydrographic data over the continental shelf region of the Gulf of Alaska in the eastern portion (GASSE), western portion (GASSO) and Kodiak Island region (KISS). To continue to monitor currents and sea level at a permanent station location ($58^{\circ} 41.1' N$, $148^{\circ} 21.6' W$) in the Gulf of Alaska.

II. Field Activities

The NOAA ship Surveyor was used to gather 65 CTD stations in the N. E. Gulf of Alaska grid (GASSE) from 7 - 18 September. The same ship was used from 19 September - 20 October to occupy 78 stations on the Kodiak Island grid (KISS). The Moana Wave was used from 7 - 24 September to occupy 35 stations in the northwestern grid (GASSO). This data gathering effort had several interruptions in it. The NOAA ship Miller Freeman occupied GASSE (modified FY '77), KISS and a portion of the GASSO grid from 1 - 23 November. Total CTD stations for this cruise was 155 with one current meter recovery and deployment at station 9.

III. Results

Computer procedures for determining the baroclinic transport from the hydrographic data have been converted to the University's new Honeywell computer system. Examination of eleven transects of the Seward station line indicate a mean transport of about 1.5 sverdrups ($1.5 \times 10^6 \text{ m}^3/\text{s}$) westward relative to 120 db. Over a two week period, this transport increased to 2.4 sverdrups, however. (See table below)

Typically, there is a minimum westward flow in the region between GASSE stations 6 and 8. This flow pattern is believed due to the fresh, low density surface water which has passed to the south of Kayak Island. Often there exists an eastward flow between stations 6 and 8. The most significant event of this type was in November 1975 when there was a 0.4 sverdrup eastward flow between stations 6 and 8 with a surface velocity of 16 cm/sec eastward. The current meter data from station 9 should allow us to determine the barotropic current component in order to determine the direction and magnitude of the net transport.

Transports Relative to 120 db (Seward Line)

Date	Transport, s.v.
July 1974	1.65
June 1975	1.69
Nov. 1975	1.44 (.22 eastward)
Feb. 1976	1.43
Feb. 1976	1.94
Feb. 1976	2.36
April 1976	1.52

The flow reversal is supported by the surface IR satellite data east of the Seward line. A diagram of dynamic height gradients for all transects of the Seward line is enclosed. The autumn increase in near-shore baroclinic flow is clear from this diagram. However, few other seasonal changes are apparent.

A brief inspection of the current meter data at station 9 for July - November 1976 reveals maximum current speeds at 20 m of greater than 90 cm/sec. The flow appears to be along topographic lines, that is, southward. Further analysis of these data continue.

IV. Problems Encountered

As stated in the last quarterly report, the problem of collecting CTD or STD using the PMC CTD manual is being addressed by Institute personnel. A critique is being prepared. However, it is extremely important that while data are being gathered, for which this research unit is responsible, a project representative be aboard the vessel.

The cruise aboard the Moana Wave was hampered due to a malfunction in the digitizer which should have been corrected prior to the ship's departure since the problem was known to exist by cruise personnel on the prior cruise. Several ship days were lost on this problem though nearly all data are recoverable. The Moana Wave itself caused some delays and extra travel expenses since the cruise was cancelled at one time after one day of sailing. The problem involved the malfunction of the variable pitch propellers.

The operations aboard the Miller Freeman suffered from rough equipment handling by the ship's deck crew. The array placed at station 9 was damaged in deployment. Its recovery is now questionable.

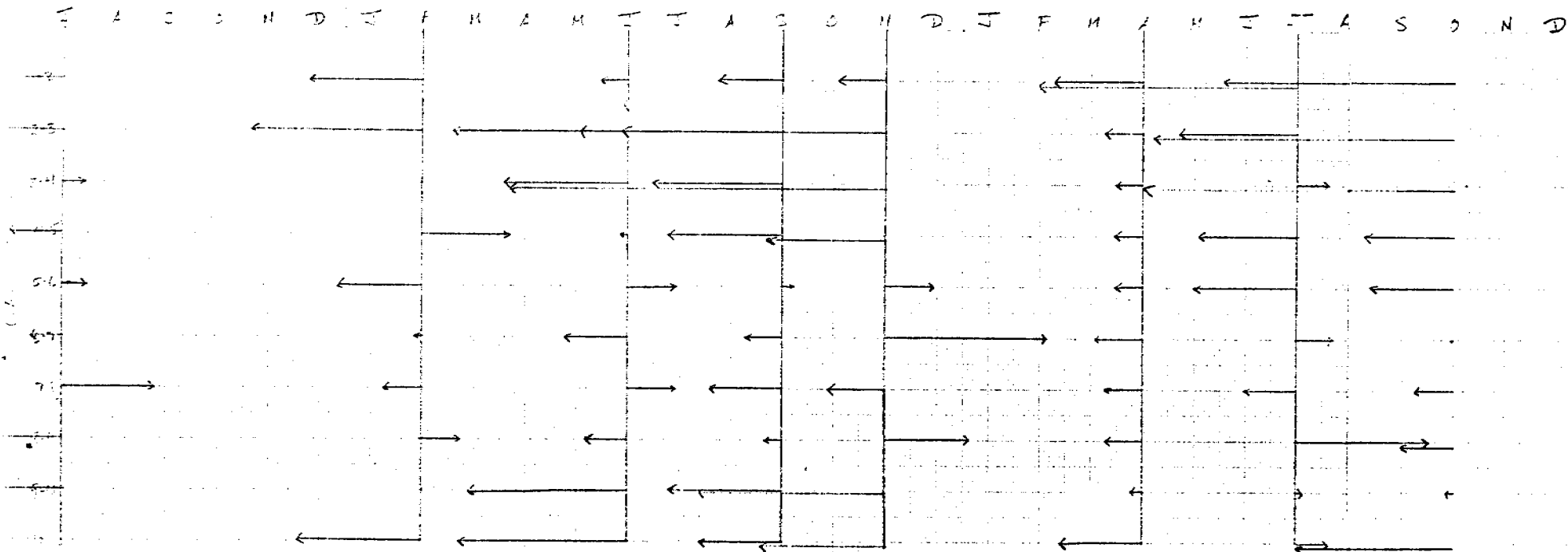
Delays and changes in the project funding have caused some serious problems. The modification of the budget after 1/3rd of the cruises was completed was especially crippling. Since it was requested that the cuts be made in the field work, this requires a virtual elimination of all field work after April 1977. A more timely adjustment would have allowed a reduction in the number of stations without elimination of all sampling. The funding delay has also not allowed us to purchase the graphics unit which is essential to a comprehensive display of the hydrographic data. We expect that the earliest date to have this unit on line is now late spring or early summer.

Finally, the termination of the CTD field work in the Gulf of Alaska is questionable due to the findings presented in this report. The ramifications are not known at this point in time due to the incomplete analysis of the current meter data at station 9. However, future plans for detailed process studies will be forthcoming in the next few months based on additional analysis of these data.

1974

1975

1976



742

Sound Line
 Dynamic Height Difference (0-1200)

0.10 dy unit

OCS COORDINATION OFFICE

University of Alaska

ENVIRONMENTAL DATA SUBMISSION SCHEDULE

DATE: December 31, 1976

CONTRACT NUMBER: 03-5-022-56

T/O NUMBER: 19

R.U. NUMBER: 289

PRINCIPAL INVESTIGATOR: Dr. T. C. Royer

Submission dates are estimated only and will be updated, if necessary, each quarter. Data batches refer to data as identified in the data management plan.

<u>Cruise/Field Operation</u>	<u>Collection Dates</u>		<u>Estimated Submission Dates</u> ¹		
	<u>From</u>	<u>To</u>	<u>Batch 1</u>	<u>2</u>	<u>3</u>
Acona #193	7/1/74	7/9/74	submitted	None	None
Acona #200	10/8/74	10/14/74	submitted	None	None
Acona #202	11/18/74	11/20/74	submitted	None	None
Acona #205	2/12/75	2/14/75	submitted	None	None
Acona #207	3/21/75	3/27/75	submitted	None	None
Acona #212	6/3/75	6/13/75	submitted		
Oceangrapher #805	2/1/75	2/13/75	submitted	None	None
Silas Bent #811	8/31/75	9/28/75	Submitted		
Discoverer #812	10/3/75	10/16/75	(a)		
Surveyor #814	10/28/75	11/17/75	submitted		
Discoverer #816	11/23/75	12/2/75	(b)	None	None
Station 60	6/2/74	9/10/74	None	Unknown	None
Station 64	4/28/75	5/20/75	None	Unknown	None
Station 9	Current meter, not available in field.				
Station 9	Pressure gauge, not available in field.				
Moana Wave MW 001	2/21/76	3/5/76	submitted		
Moana Wave MW 003/004	4/20/76	5/21/76	submitted		
Moana Wave MW005	9/22/76	8/1/76	(c)		
Surveyor SU 003	9/7/76	9/17/76	(c)		

<u>Cruise/Field Operation</u>	<u>Collection Dates</u>		<u>Estimated Submission Dates</u> ¹		
	<u>From</u>	<u>To</u>	<u>Batch 1</u>	<u>2</u>	<u>3</u>
Surveyor	9/20/76	10/2/76	(c)		
Miller Freeman	11/1/76	11/19/76	(c)		
Moana Wave	10/7/76	10/16/76	(c)		

- Note: ¹ Data Management Plan and Data Formats have been approved and are considered contractual.
- (a) Parent tapes were coded in PODAS format, tapes were submitted to F. Cava as requested.
 - (b) Data useless due to malfunction of shipboard data logger.
 - (c) Data will be processed in FY '77 contingent upon approval of and funding for extension of this project for FY '77.

Quarterly Report

Contract #03-5-022-56
Research Unit #307
Task Order #14
Reporting Period 10/1 - 12/31/76
Number of Pages 2

HISTORICAL AND STATISTICAL OCEANOGRAPHIC DATA
ANALYSIS AND SHIP OF OPPORTUNITY PROGRAM

Dr. Robin S. Muench
Institute of Marine Science
University of Alaska
Fairbanks, Alaska 99701

January 1, 1977

I. Task Objectives

To obtain temperature, salinity, dissolved oxygen, nutrient and meteorological data on an opportunity (not-to-interfere) basis from oceanographic vessels operating in the southeastern Bering Sea region, to analyze this data and to incorporate it into the ongoing analysis of historical data.

II. Field Activities

None.

III. Results

Cruise data for the Surveyor cruises was submitted to OCSEAP. Final details of archiving the ship of opportunity data for the Bering Sea were completed.

OCS COORDINATION OFFICE

University of Alaska

ENVIRONMENTAL DATA SUBMISSION SCHEDULE

DATE: December 31, 1976

CONTRACT NUMBER: 03-5-022-56

T/O NUMBER: 14

R.U. NUMBER: 307

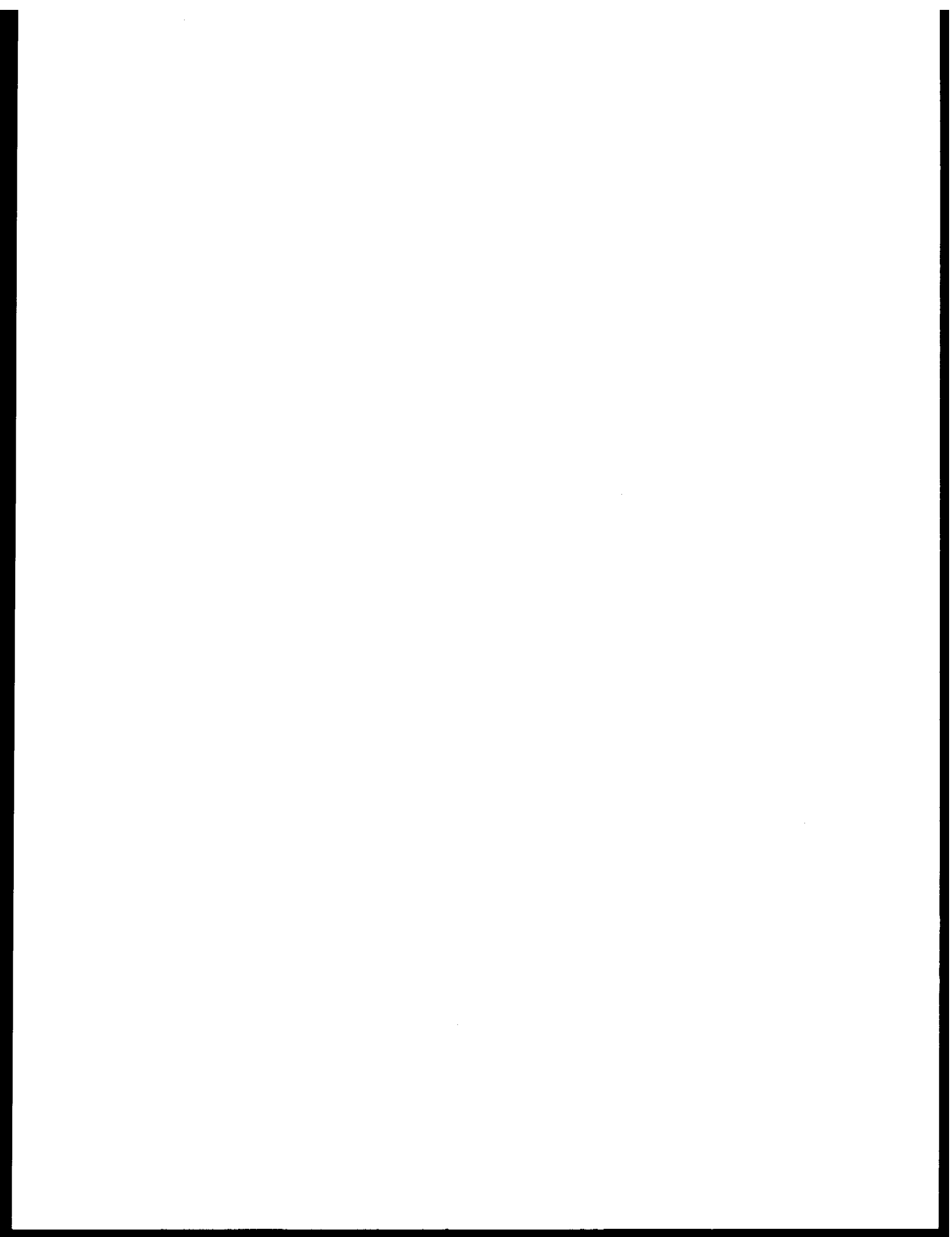
PRINCIPAL INVESTIGATOR: Dr. R. D. Muench

Submission dates are estimated only and will be updated, if necessary, each quarter. Data batches refer to data as identified in the data management plan.

<u>Cruise/Field Operation</u>	<u>Collection Dates</u>		<u>Estimated Submission Dates</u> ¹
	<u>From</u>	<u>To</u>	<u>Batch 1</u>
Acona #197	7/20/75	7/30/75	submitted
Discoverer Leg I & II #808	5/15/75	6/19/75	submitted
Discoverer Leg I #810	8/9/75	8/28/75	(a)
Miller Freeman #815	11/19/75	11/26/75	submitted
Surveyor 001/002	3/76	4/76	submitted

All data to be submitted under this task order, for this contract have now been submitted.

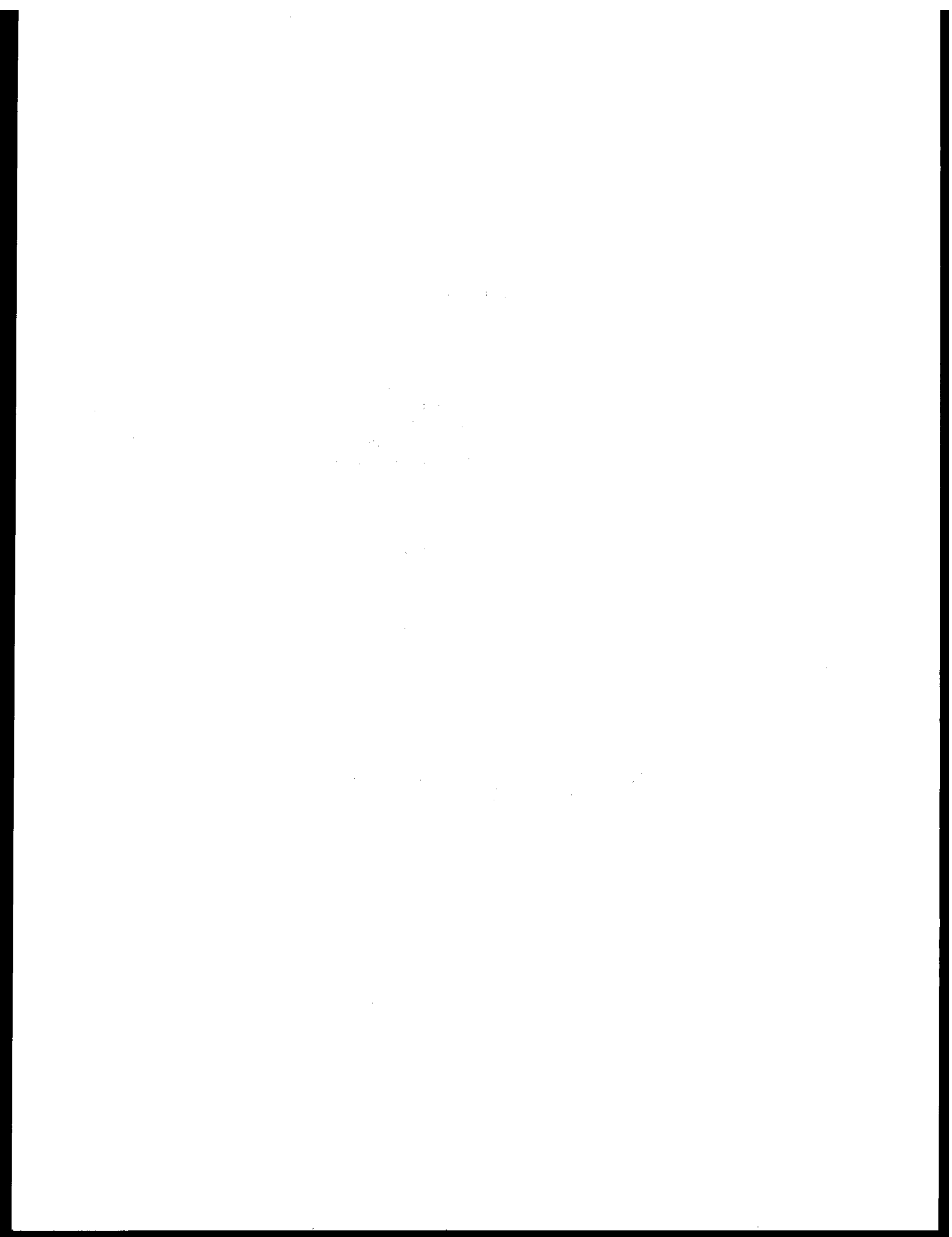
- NOTE:
- ¹ Data Management Plan and Data Format have been approved and are considered contractual.
 - (a) Parent tapes were coded in PODAS format, tapes were submitted to F. Cava as requested.



RU# 335

NO REPORT WAS RECEIVED

A final report is expected next quarter



QUARTERLY REPORT

Contract No. 03-5-022-56
Research Unit No. 347
Reporting Period: October 1, 1976,
through December 31, 1976
Number of Pages: 1

MARINE CLIMATOLOGY OF THE GULF OF ALASKA
AND THE BERING AND BEAUFORT SEAS

James L. Wise

Arctic Environmental Information and Data Center
University of Alaska

December 17, 1976

December 17, 1976

QUARTERLY REPORT

For the Period Ending December 31, 1976

I. Task Objectives:

To determine and publish the knowledge of the climatological conditions of that portion of Alaska that is important to OCS development.

II. Field and Laboratory Activities:

This portion of the project has no field or laboratory activities. It is a joint project with the National Climatic Center (NCC) in Asheville, North Carolina. AEIDC responsibilities are to provide extremes of all weather elements, information on coastal damage resulting from wind generated storm flooding, check analysis work done at NCC, and through our graphics department, prepare materials for publication, including contracting for and supervising the publication of the three marine atlases.

III. All data to be used in the atlas have been compiled either here at AEIDC or at the NCC. The NCC has developed additional data relationships on persistence of winds and visibilities and recurrence intervals for winds and waves since the last report. The persistence graphs and legends for graphs and isopleth analyses are expected here from the NCC by the end of this reporting period. Recurrence interval data on winds and waves, monthly storm tracks and cyclogenesis areas, and the NCC's portion of the texts are expected here sometime in the next quarter.

In the preparation of the data for printing by AEIDC Graphics, paste up of graphs is 90 percent complete, preparation of isopleth maps is 15 percent complete and typesetting of data and text is approximately 15 percent complete. It is expected that the AEIDC Graphics work on preparing the data for printing will proceed at a faster pace after the first of the year when several projects with deadlines of December 31, 1976 have been completed.

IV. N/A

V. N/A

OCS COORDINATION OFFICE

University of Alaska

ESTIMATE OF FUNDS EXPENDED

DATE: December 31, 1976

CONTRACT NUMBER: 03-5-022-56

TASK ORDER NUMBER: 25

PRINCIPAL INVESTIGATOR: Mr. James L. Wise

(Period July 1, 1975 - December 31, 1976* (18 mos.))

	<u>Total Budget</u>	<u>Expended</u>	<u>Remaining</u>
Salaries & Wages	57,286	26,576	30,710
Staff Benefits	10,284	4,853	5,431
Equipment	-	-	-
Travel	2,045	1,345	700
Other	<u>6,126</u>	<u>5,405</u>	<u>721</u>
Total Direct	75,741	38,179	37,562
Indirect	<u>30,147</u>	<u>14,452</u>	<u>15,695</u>
Task Order Total	105,888	52,631	53,257

*Preliminary cost data, not yet fully processed.

Quarterly Report

Contract No. N/A
Research Unit No: 347
Reporting Period: October 1, 1976,
 through December 31
Number of Pages: 2

"Marine Climatology of the Gulf of Alaska
and the Bering and Beaufort Seas"
Climatic Atlases (3)

Principal Investigators

James L. Wise
Associate in Climatology
Arctic Environmental Information
and Data Center
University of Alaska
707 'A' Street
Anchorage, AK 99501
Comm: (907) 279-4523

William A. Brower, Jr. (D5312)
Applied Climatology Branch
National Climatic Center
Federal Building, Room 401
Asheville, NC 28801
Comm: (704) 258-2850, x266
FTS: 672-0266

December 23, 1976

Quarterly Report

I. Task Objectives

To compile and publish a descriptive climatology of that portion of the Alaskan waters and coastal areas that are important to resource development of the outer continental shelf (OCS).

II. Field and Laboratory Activities

This project has no field or laboratory activities. It is a joint effort by the AEIDC and the NCC to produce a climatic atlas for each of three Alaskan marine and coastal areas: the Gulf of Alaska (50° - 65° N, 130° - 165° W); the Bering Sea (50° - 65° N, 155° - 180° W); and the Beaufort Sea (65° - 75° N, 140° - 180° W).

NCC is to provide monthly climatological analyses in the form of 360 isopleth charts and some 10K statistical graphs. The analyses are to be based on 600,000 surface marine observations and two million (3-hourly) observations for 49 (selected) coastal stations contained in NCC's digital data base. AEIDC is to provide extremes of all weather elements and information on coastal damage resulting from wind generated weather elements, check analysis work done by NCC, and prepare all materials for publication. (AEIDC will provide an independent quarterly report).

III. Results

Computer processing of the digital data is complete. This includes the computer-to-microfilm production of the 10K statistical graphs and the computer plotting of 360 charts. The graphs have been processed and the 360 isopleth charts have been analyzed and edited by staff meteorologists and all have been mailed to AEIDC to prepare for printing. (Microfilm copies of the charts and graphs and glossy prints of the charts are being held by NCC for reference during preparation of the materials for print by AEIDC and can be made available to OCSEAP PI's and others at cost for reproduction).

NCC is currently preparing the graph/map legends for all the parameter sets, and these should be ready for mailing to AEIDC by 15 January. All remaining items NCC is to provide to AEIDC (by the end of January) are: storm track trajectory/cyclogenesis information; marine wind and wave return period tables; atlas text describing NCC's products. (Refer to PI's April-June 1976 Report, Vol. 2, pp. 461-488 for the description of atlas contents.)

2.

IV. Preliminary Interpretation of Results

The U. S. Navy Marine Climatic Atlas of the World, Vol. II, North Pacific Ocean (1959), one of eight volumes in a series of atlases of the world which is currently being updated by the Navy, has had wide acceptance as an authoritative reference for large-scale operational planning and research.

The present study will provide three atlases to represent the total of the Alaskan waters in greater detail and each will be based on more than 20 years of additional data. Also, as marine data are typically sparse in the near coastal zone, a zone of sharp gradients and complex climate, data for the 49 coastal stations were included. Such a combination should provide the best possible climatological picture for the coastal waters of Alaska.

V. Problems Encountered

A computer-visual inventory of the digital surface marine data file disclosed a sparcity of data north of 60° latitude. To permit a better climatic description of the Bering and Beaufort Seas, marine observations were digitized from manuscript forms archived at NCC for the period 7/73-12/74 and digital data for 22 additional coastal stations held in NCC's file were combined with data of the 27 stations originally selected. However, as there were little data available in NCC's digital file for the land and marine area east of Barter Island, the Beaufort Sea Atlas will contain only a limited climatic description of the Mackenzie Bay area.

VI. Estimate of Funds Expended

The \$84.5K allotted for FY-76, 76T periods were expended as of 6/15/76; \$15K of the \$25K approved for FY-77 have been provided during 76T to permit continuation of the Project and was expended by 9/30/76. Of the remaining \$10K for FY-77, \$5.2K remains as of 12/15/76. Preparation of the three atlases is well underway and all are scheduled for completion in FY-77.

QUARTERLY REPORT

Contract: #R7120848

Research Unit: 357

Reporting Period: 1 July -
30 September 1976

Number of Pages: 1

COASTAL METEOROLOGY IN THE GULF OF ALASKA

R. Michael Reynolds
Bernard Walter

Pacific Marine Environmental Laboratory
National Oceanic and Atmospheric Administration
3711 - 15th Avenue, N.E.
Seattle, Washington 98105

October 1, 1976

I. TASK OBJECTIVES

- A. Description of wind conditions near coast in northeast Gulf of Alaska, especially, it pertains to modification of katabatic flow offshore.
- B. Comparison and selection of a mesoscale model which suitably describes the offshore wind field.

II. Field or Laboratory Activities

- A. Cruises: DISCOVERER cruise to Norton Sound, 26 September - 8 October. Offshore air modification was studied on a line from Nome. Data from this cruise will be compared to measurements in the Gulf of Alaska. Also, a bow boom was evaluated. The boom was adapted from the GATE system for PMEL studies. Radiosondes and BLP profiles were taken in addition to the surface measurements.
- B. Laboratory Development: A microcomputer controlled datalogger has been developed for operation of the meteorological boom system. The boom can now be used on any ships (i.e., not restricted to PODAS) in Alaskan operations, and software allows specialized computations before tape storage.
- C. Other Activities
 - 1. Michael Reynolds attended the AMS Conference on Coastal Meteorology in Virginia Beach, Va. on 20 - 23 September.
 - 2. Bernard Walter attended the ERL sponsored conference on Mesoscale meteorology.

QUARTERLY REPORT

Contract no. 03-6-022-35126
Research unit no. 407
Reporting period: 1 April -
30 June 1976.
Number of pages: 3

A STUDY OF BEAUFORT SEA COASTAL EROSION
NORTHERN ALASKA

Robert Lewellen
P.O. Box 2435
Littleton, Colorado 80161
759

1 July 1976

I. TASK OBJECTIVES.

Search, evaluate, and synthesize existing literature and data on erosional and depositional rates and patterns of sediments along the Alaskan sea coasts. Compile maps of erosional and depositional rates and patterns.

Evaluate present rates of change in coastal morphology, with particular emphasis on rates and patterns of man-induced changes. Locate areas where coastal morphology is likely to be changed by man's activities and evaluate the effect of these changes, if any. The relative susceptibility of different coastal areas will be evaluated.

II. FIELD OR LABORATORY ACTIVITIES.

A. Ship or Field Trip Schedule.

1. Dates, name of vessel, aircraft, NOAA or chartered, (none required for this project).

B. Scientific Party.

1. Names, affiliation, role, (not applicable).

C. Methods.

1. Field sampling or laboratory analysis. Methods include the use of published and unpublished materials documents, and data, sequential aerial photography and standard air photo mensurational techniques.

D. Sample localities/ship or aircraft tracklines. The temporal sampling scheme is a function of when sequential aerial photography or ground measurements exist. This coverage is adequate.

E. Data collected or analyzed.

1. Number and types of samples/observations. Numerous observations are currently being processed, but will not be available until the next quarterly report.
2. Number and types of analyses. (all are aerial photography measurements except for a few ground measurements).
3. Miles of trackline. (not applicable to this project).

III. RESULTS.

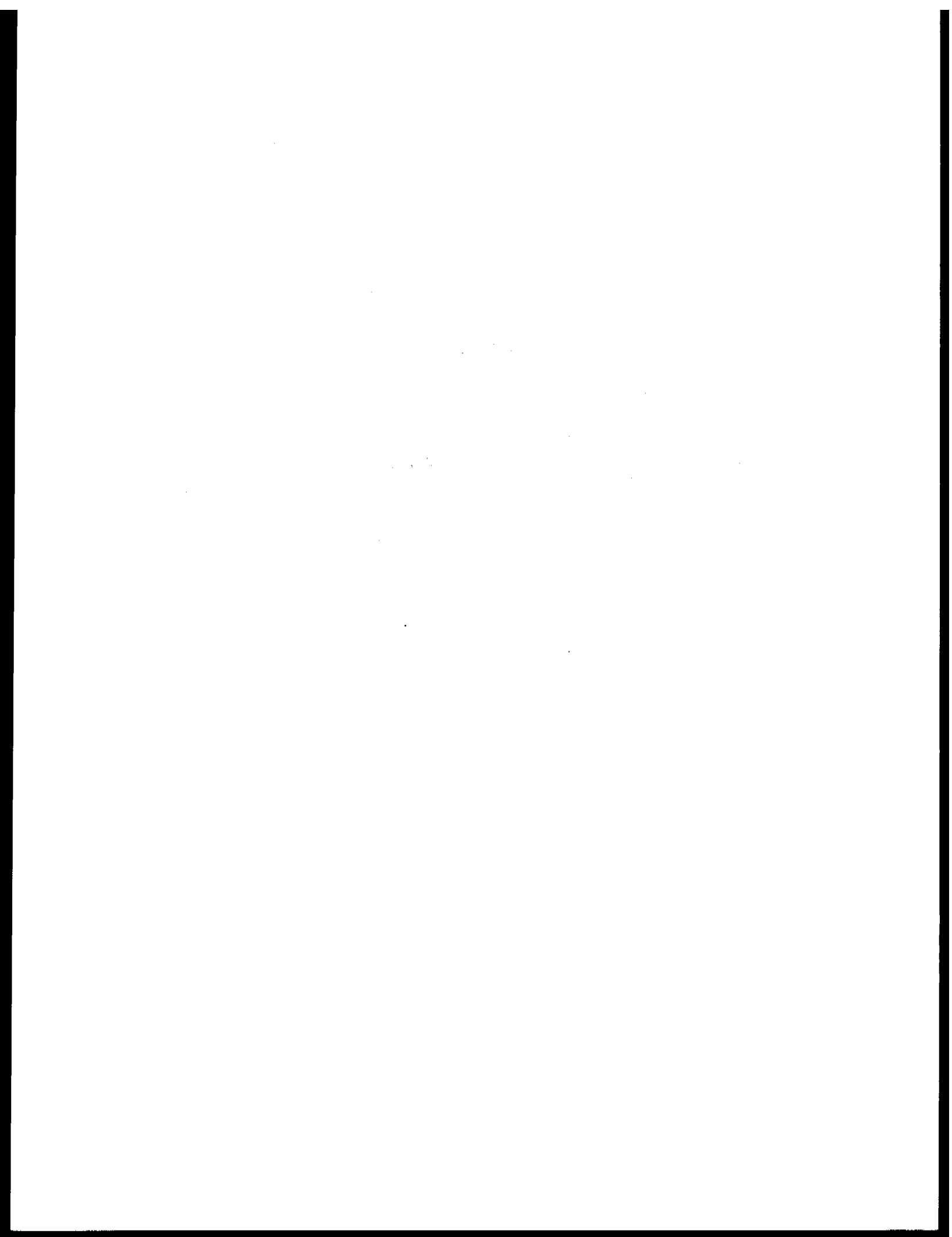
No results are available for this report.

- IV. PRELIMINARY INTERPRETATION OF RESULTS. The coastline is definitely eroding in permafrost terrain; and in other cases permafrost is rapidly aggrading in areas of recent deposition.

- V. PROBLEMS ENCOUNTERED/RECOMMENDED CHANGES. (none).

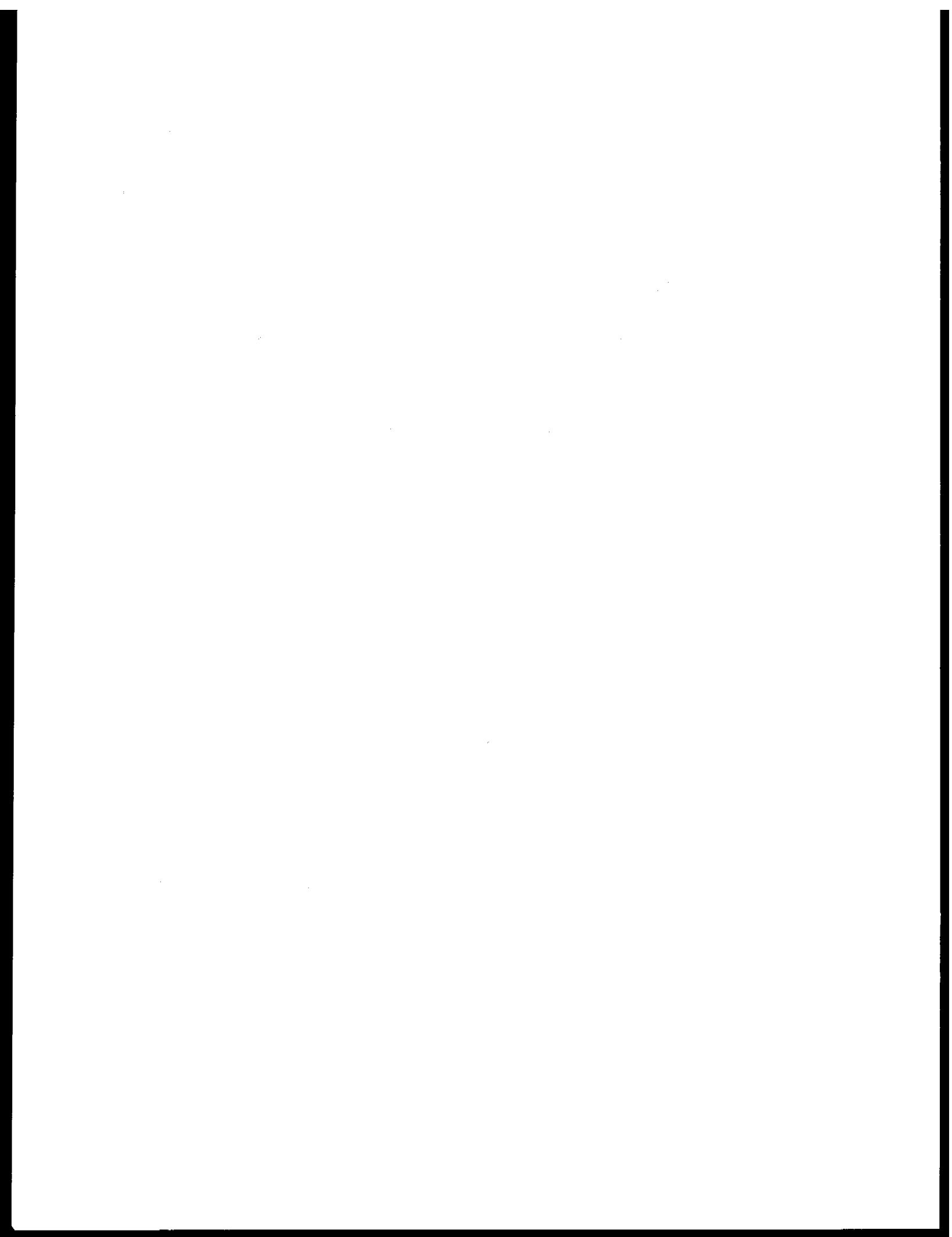
- VI. ESTIMATE OF FUNDS EXPENDED. (approximately \$ 10,500).

Remarks: Very little time was spent on the project since there was a prior commitment to do field work until the end of May 1976.



RU# 435

NO REPORT WAS RECEIVED



RU# 436

OIL SPILL TRAJECTORY ANALYSIS
LOWER COOK INLET, ALASKA
FOR
NATIONAL OCEANIC AND ATMOSPHERIC ADMINISTRATION

DAMES & MOORE
JOB NUMBER 6797-003-20

MARCH 8, 1976

March 8, 1976

Bureau of Land Management
Alaska Outer Continental Shelf Office
800 "A" Street
Anchorage, Alaska 99501

Attention: Mr. Dan Patton
Oceanographer Geologist

Gentlemen:

Final Report
Oil Spill Trajectory Analysis
Lower Cook Inlet, Alaska
For National Oceanic and
Atmospheric Administration

This Final Report and the attached computer graphics contain the results of Dames & Moore's "quick-response" study as discussed in our Confirmation Letter of February 14, 1976. The scope and depth of treatment for this project have been approved and monitored by the Bureau of Land Management, Alaska OCS Office in Anchorage. All contractual and financial matters have been coordinated with the National Oceanic and Atmospheric Administration, Boulder, Colorado.

We trust that the enclosed reports (2 copies) and the original computer graphics satisfy your immediate needs. Should you require any additional information or clarification of the attached material, please do not hesitate to contact us.

It has been a pleasure working with you on this quick-response effort.

Yours very truly,

DAMES & MOORE



Richard C. Miller
Associate



Alan A. Allen
Associate

RCM:AAA:sed
Attachment

TABLE OF CONTENTS

	<u>Page</u>
Transmittal Letter	
I. DAMES & MOORE OIL SPILL MODEL	1
II. INPUT DESCRIPTIONS	7
A. Hypothetical Spill Scenarios	7
B. Oceanography	8
C. Meteorology	13
III. RESULTS	22
References	32
Computer Output	(Bound Separately)

LIST OF PLATES

		<u>Following Page</u>
Plate 1	Tidal Currents (Average Maximums, Speed in Knots)	1
Plate 2	Spill Sites and Computer Grid System	9
Plate 3	Net Surface Circulation (Speed in Knots)	11
Plate 4	Wind Patterns 1 & 2	13
Plate 5	Wind Patterns 3 & 4	13
Plate 6	Wind Patterns 5 & 6	13
Plate 7	Wind Pattern 7	13
Plate 8	Wind Pattern 8	13
Plate 9	Potential Boundary Contact Zones for Spill Site 1	32
Plate 10	Potential Boundary Contact Zones for Spill Site 2	32
Plate 11	Potential Boundary Contact Zones for Spill Site 3	32
Plate 12	Potential Boundary Contact Zones for Spill Site 4	32
Plate 13	Potential Boundary Contact Zones for Spill Site 5	32
Plate 14	Potential Boundary Contact Zones for Spill Site 6	32
Plate 15	Potential Boundary Contact Zones for Spill Site 7	32
Plate 16	Potential Boundary Contact Zones for Spill Site 8	32
Plate 17	Potential Boundary Contact Zones for Spill Site 9	32
Plate 18	Potential Boundary Contact Zones for Spill Site 10	32

LIST OF PLATES, (Cont.)

		<u>Following Page</u>
Plate 19	Potential Boundary Contact Zones for Spill Site 11	32
Plate 20	Potential Boundary Contact Zones for Spill Site 12	32
Plate 21	Potential Boundary Contact Zones Composite for Sites 1-12	32
Plate 22	Annual Percent Probability of Exposure for Winds Evaluated - Spill Site 1	32
Plate 23	Annual Percent Probability of Exposure for Winds Evaluated - Spill Site 2	32
Plate 24	Annual Percent Probability of Exposure for Winds Evaluated - Spill Site 3	32
Plate 25	Annual Percent Probability of Exposure for Winds Evaluated - Spill Site 4	32
Plate 26	Annual Percent Probability of Exposure for Winds Evaluated - Spill Site 5	32
Plate 27	Annual Percent Probability of Exposure for Winds Evaluated - Spill Site 6	32
Plate 28	Annual Percent Probability of Exposure for Winds Evaluated - Spill Site 7	32
Plate 29	Annual Percent Probability of Exposure for Winds Evaluated - Spill Site 8	32
Plate 30	Annual Percent Probability of Exposure for Winds Evaluated - Spill Site 9	32
Plate 31	Annual Percent Probability of Exposure for Winds Evaluated - Spill Site 10	32
Plate 32	Annual Percent Probability of Exposure for Winds Evaluated - Spill Site 11	32
Plate 33	Annual Percent Probability of Exposure for Winds Evaluated - Spill Site 12	32
Plate 34	Annual Percent Probability of Exposure for Winds Evaluated - Cumulative for Sites 1-12	32

LIST OF TABLES

		<u>Page</u>
Table 1	Frequencies and Number of Circulation Patterns (Putnins) for Eight Directions	19
Table 2	Direction, Speed, and Frequency of Eight Wind Patterns	21
Table 3	Boundary Contact Cells	23

I. DAMES & MOORE OIL SPILL MODEL

Oil spilled on the water's surface may be transported far from the original spill location under the influence of winds, waves, and currents. These and other forces also cause an oil film to spread, distort, and change in physicochemical characteristics throughout its existence. Based on presently available knowledge of the processes involved, Dames & Moore has constructed a simulation model of surface oil spill behavior that accounts for the most important aspects of surface transport and spreading.

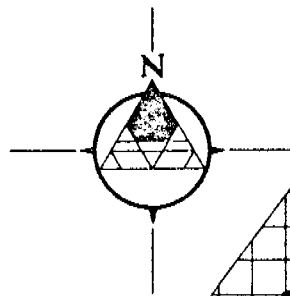
The primary factors affecting oil transport are winds, currents, and to a lesser extent waves. In this study, we neglected both wave effects and wind/wave interaction. Under these conditions, it is generally, although not universally, accepted that oil movement can be reasonably represented as the vectorial sum of the surface current velocity and approximately 3 percent of the local surface wind velocity. In this study, the current was treated as the sum of the tidal driven component and the net circulation component (see Section IIB for a more detailed discussion of these current components). Thus, the total velocity vector of the centroid of an oil slick may be written as

$$\bar{u}_{oil} = .03 \bar{u}_{wind} + \bar{u}_{tidal} + \bar{u}_{net} \quad (1)$$

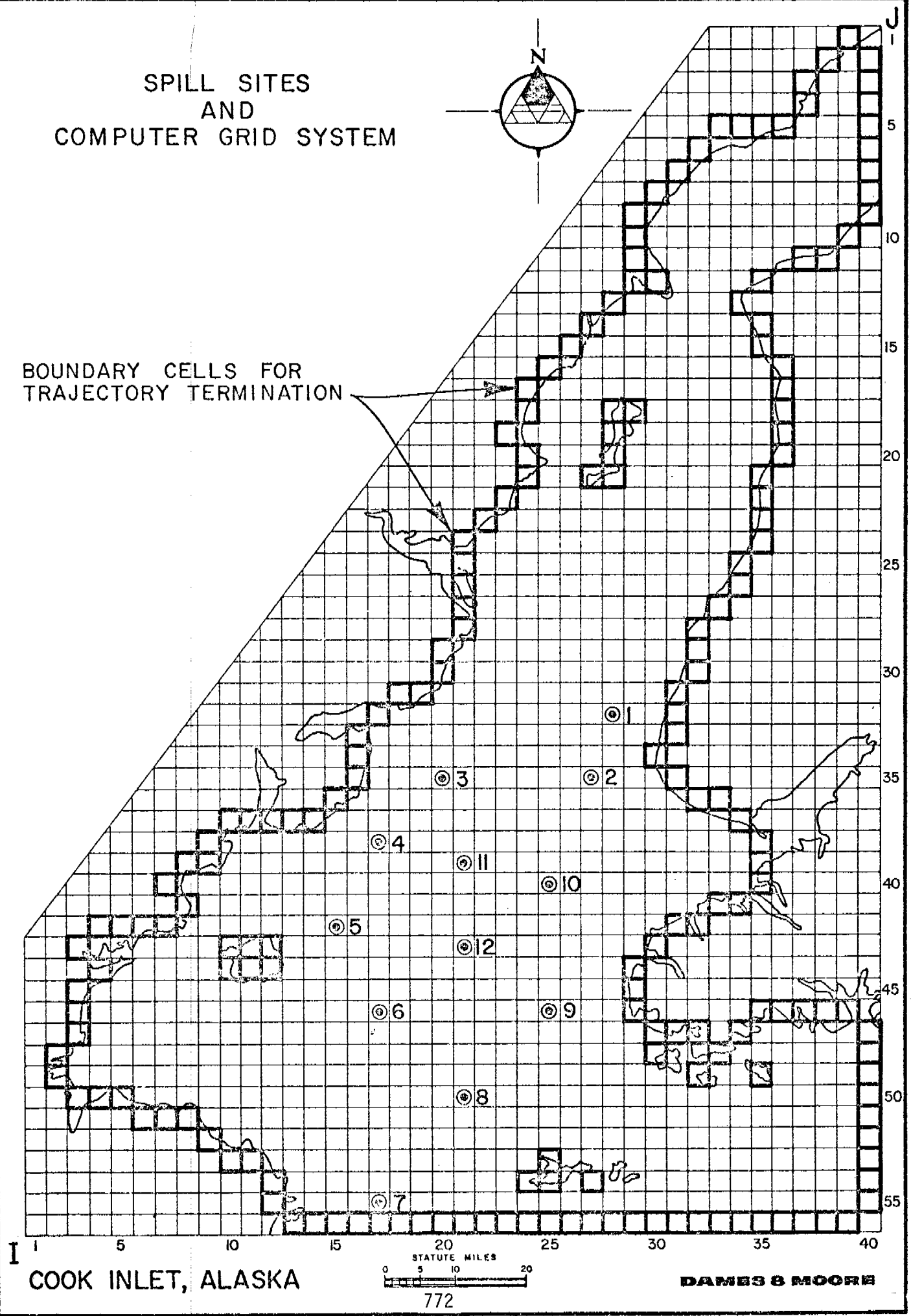
A grid system as illustrated in Plate 1 was used as a framework to input both wind and current data as well as to define the geometry of Cook Inlet itself. This grid system was selected so that the cells defined by the grid lines correspond to the lease tracts as defined on chart "Outer Continental Shelf Official Protraction Diagram, No. 5-3 and 5-4" (U.S. Department of Interior, BLM). Each cell is 4,800 meters on a side.

(3 miles)

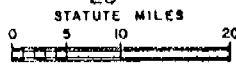
SPILL SITES AND COMPUTER GRID SYSTEM



BOUNDARY CELLS FOR
TRAJECTORY TERMINATION



COOK INLET, ALASKA



DAMES & MOORE

772

PLATE I

Characteristic features of the Inlet required by the model such as land and water areas and open water boundaries are prescribed by assigning to each cell an index that defines the predominate feature of that cell. Land boundaries were chosen to represent the "best" approximation of the geographic extent of the Inlet.

Data defining the spatial and temporal variation of the wind and current fields are prescribed at the intersection of the grid lines. Since the number of intersection points can become large (there are over 2,300 for the grid shown in Plate 1), the model has been designed to accept values only at every n^{th} intersection point where "n" is any integer up to the maximum dimension of the grid. Selection of this quantity is based on the variability of each field and the level of detail of the input data; for this study, the current field data were input at every 2nd point and the wind field data at every 4th point.

The temporal variation of each of these fields is defined by specifying the entire spatial distribution at one or more times. If only one distribution is given for a field, that field is taken to be constant throughout the period of simulation. This was, in fact, the case for both the net drift and wind data for this study.

The tidal cycle was defined by specifying the tidally driven current at four points in the tidal cycle: at maximum ebb and flood, and at the two slack points midway between maximum tides. This results in a "sawtooth" representation of the tidal variation with time.

Using a three-way linear interpolation scheme on the two spatial dimensions and on time, the fields specified in this manner suffice to define

the total drift vector given by Equation 1 for the entire area of interest for all time. The movement of an oil slick centroid is uniquely determined by this drift vector field.

For example, suppose that the centroid is at a location (x_0, y_0) at time t . The drift vector (u_0, v_0) computed at that point then determines the new location (x_n, y_n) at time $t+\Delta t$ by

$$x_n(t+\Delta t) = x_0(t) + u_0\Delta t, \text{ and} \quad (2a)$$

$$y_n(t+\Delta t) = y_0(t) + v_0\Delta t. \quad (2b)$$

For display purposes, the track of the centroid is defined by a sequence of cells through which the centroid passes rather than by the coordinate values themselves.

The capability to handle spreading of an oil slick due to gravity, surface tension, wind and current shear forces, and shoreline/slick interaction is presently within the numerical capabilities of the model. However, since the terminally coherent spill size of even a 10,000 bbl spill is on the order of 10 square miles or approximately equal to the grid size chosen in the model, spreading would not significantly influence the results of this study.

Since the centroid location is defined for display purposes as being within some cell, the effects of spreading would, at most, result in the display of an additional cell under normal conditions. This extent of spreading is not significant compared to other uncertainties in the wind and current data, thereby leading to the conclusion that spreading would not be included in the present study.

In addition to the input wind and current conditions and the basic grid system, the other important parameters required by the model are summarized below with values given for the spill scenarios considered in this study.

Time step (Δt) = 0.4 hours

This is the time step used in Equations (2a and 2b) to compute slick centroid movement. It was chosen so that the maximum centroid displacement in any one time step would always be less than one cell width.

Stop time = 149.04 hours = 6.21 days

The stop time defines the period over which centroid movement is simulated. It was chosen to cover 12 complete tidal cycles or just over 6 days. The period of the predominate tidal cycle in Cook Inlet is 12.42 hours.

Initial tidal phase

The ultimate disposition of the oil slick depends on the point in time within the tidal cycle at which the spill occurs. Four points along the tidal cycle were selected for simulation: maximum flood and ebb and the two slack tides midway between the extreme. Note that it is only coincidental that these times match those where data was input. This is not required by the model.

Output from the model takes the form of a "printer-plotter" map showing a gridded map of the Inlet with one trajectory per map superimposed. Land areas are denoted by the symbol "@," water boundaries by an asterisk,

the spill site by a completely darkened cell and, finally, open water areas are denoted by unmarked (plain white) zones.

Note that several bays are delimited from the main body of water within Cook Inlet by one or more water boundary cells. Within these bays, the detailed nature of the wind and water current fields is not sufficiently well known to permit an accurate simulation of spill movement. For those cases where the trajectory intersects one of these boundary cells, we have terminated that simulation and conclude that oil would, in fact, enter the bay but that its subsequent behavior is not determined.

The trajectories of the slick centroid are traced by a series of unique symbols and numbers; a different symbol is used to mark trajectories that started at the four different times in the tidal cycle as defined in the table below:

Tidal Phase	Symbol	Starting Tidal Phase
1	0	maximum ebb
2	X	slack, entering flood tide
3	+	maximum flood
4	=	slack, entering ebb tide

The numerals 1-8 along the trajectory serve as time markers, each integer being a submultiple of 14 hours. For example, the digit 5 denotes that the slick centroid was within the marked cell 70 hours ($5 \times 14 = 70$) after the spill occurred.

The trajectory is terminated when either time exceeds 149.04 hours or the trajectory intersects a land or water boundary cell.

II. INPUT DESCRIPTIONS

A. Hypothetical Spill Scenarios

The 12 spill sites shown in Plate 1 were selected by the Anchorage OCS Project Office of the Bureau of Land Management as representative areas for possible exploratory drilling. Scenarios for potential oil spills at these locations were evaluated without consideration for volume or rate of release of oil. Further, all sites were treated independently, and the probability of a spill occurring at any location was considered equal.

Using existing oceanographic and meteorological information, the objective of this study was to estimate the time to impact and the probability of exposure for the coastal regions of Cook Inlet. The effects of evaporation, dispersion and wind/wave interaction were not considered in this study.

B. Oceanography

The oceanographic inputs to the model were limited to surface currents. Wind drift currents induced by local surface winds in lower Cook Inlet were computed from the eight surface wind patterns discussed in Section C. Wind wave effects on oil were not considered.

Current information was provided as input to the oil spill model in two components: (1) tidal current speed and direction and (2) net circulation drift speed and direction. The vector summation of these two components represent the surface water motion in the absence of a local surface wind.

Tidal Current Component

Tidal currents were developed from data obtained during the 1973 and 1974 NOAA oceanographic cruises in Cook Inlet. Computer analysis of this data was available for 23 stations in lower Cook Inlet. Since most of the measurements in the upper portions of lower Cook Inlet were not available in analyzed form, peak values were obtained via personal communication.

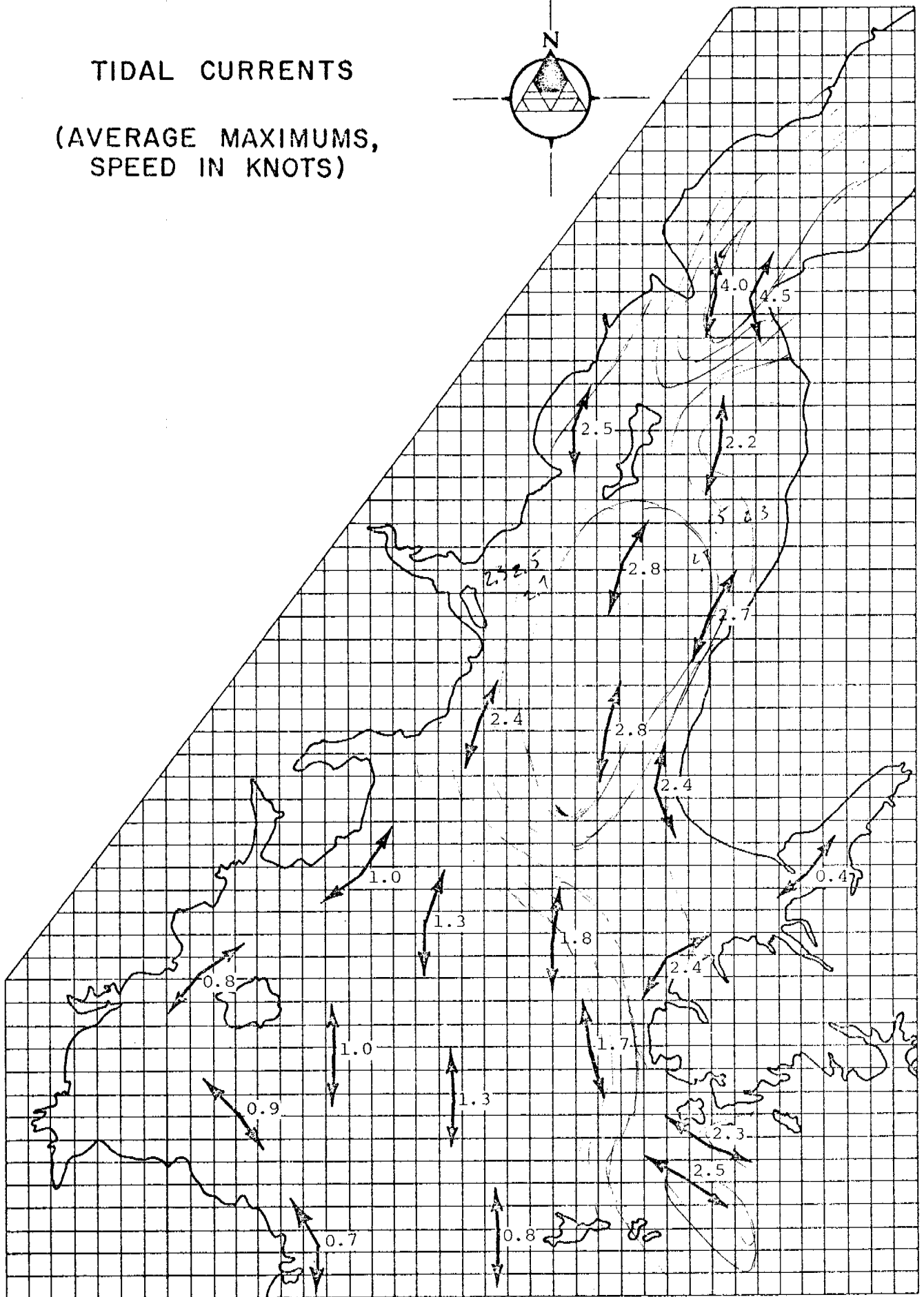
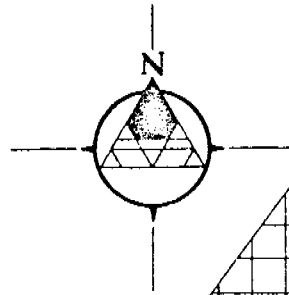
For the 23 stations for which computer analysis was available, estimates of the average maximum current were prepared by tabulating peak current velocities for all ebb and flood tide conditions. Average maximum values for both the ebb and flood tide were calculated as the mathematical average of all peak values. Data input to the spill model is representative of the average maximum current for both ebb and flood tide.

For most of the stations for which analyzed data was available the data was relatively uniform; for example, tidal cycles and peak speeds were easily discernible. Exceptions included Stations 21, 25, and 26. At Station 21, north of Augustine Island, currents were observed to rotate steadily in a clockwise direction. At low slack tide currents were westerly; however, by peak flood tide, currents were northerly. At high slack tide currents were easterly and at peak ebb tide currents were southerly. At Station 25, off Cape Douglas, currents flowed continually in a southerly direction, probably as a result of an overriding southerly net drift component. Records for Station 26, east of Augustine Island, were quite variable and may possibly be attributed to the complex flow patterns around Augustine Island, especially on a flood tide.

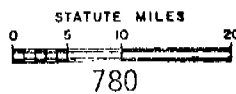
In general, it was also noted that directions of tidal currents became quite variable when the velocity dropped below 0.5 knots. This condition is most frequent in areas of the inlet south of Kachemak Bay and west of the Barren Islands.

Since most of the 1974 NOAA tidal current data was not readily available as computer printouts for areas north of Anchor Point, current speeds and directions were approximated from peak flood and ebb currents. This peak flow data was provided for six 1974 stations by Mr. Muirhead of the Oceanographic Division of the National Ocean Survey in Rockville, Maryland. Values obtained were reduced by a factor of 1.4 as determined from correlation of available records to obtain the average maximum tidal current. Plate 2 displays the currents which were determined from both the 1973 and 1974 NOAA data and which were used as input.

TIDAL CURRENTS
 (AVERAGE MAXIMUMS,
 SPEED IN KNOTS)



COOK INLET, ALASKA



DAMES & MOORE

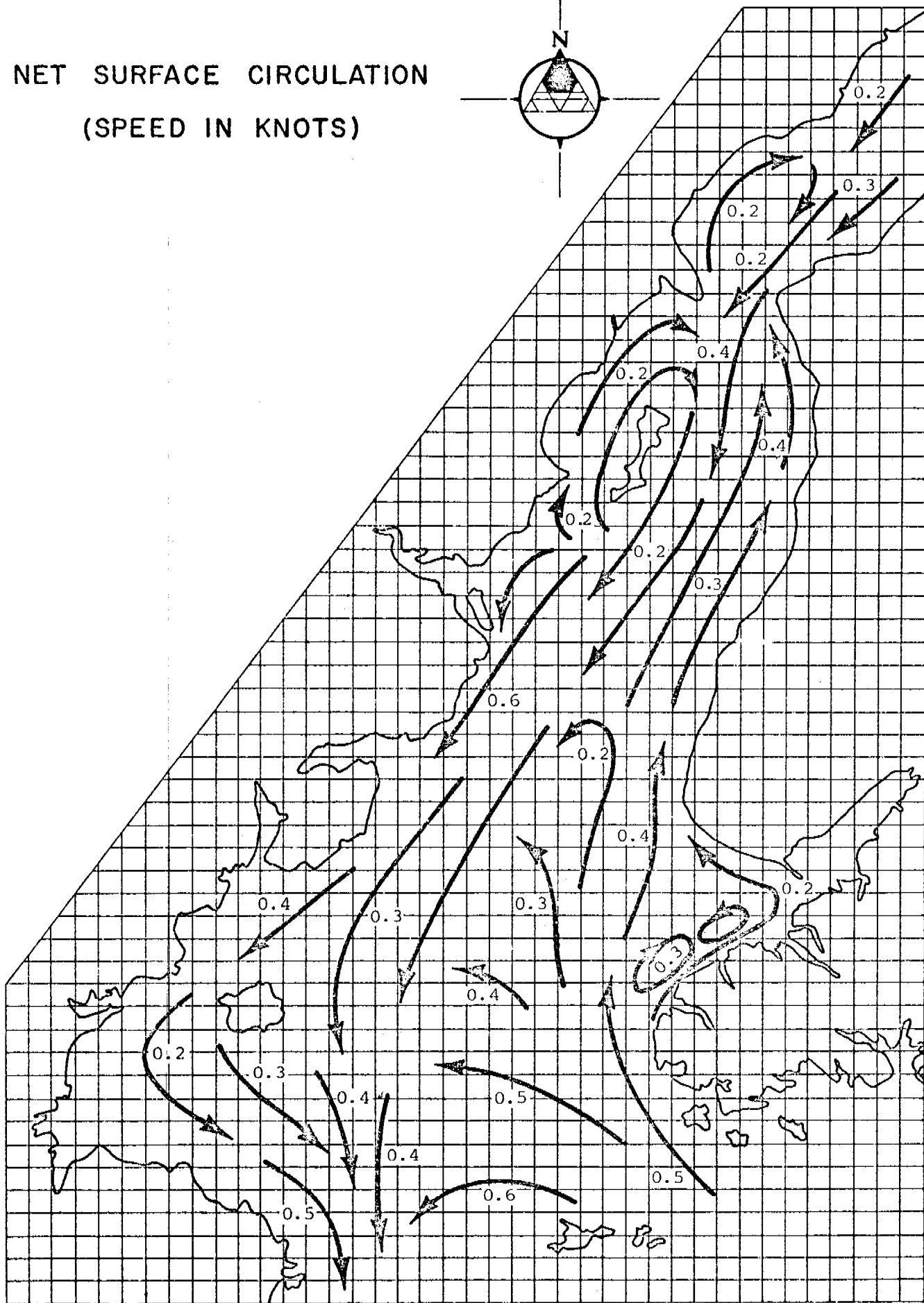
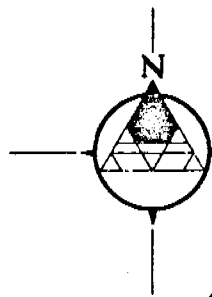
Results of previous computer models of Cook Inlet, most notably Mungal (1973), were also utilized to extrapolate remaining data gaps for input to the oil spill model.

Net Drift Component

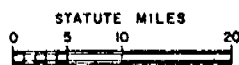
The net drift component of current represents the net movement of water due to the overall circulation patterns in Cook Inlet. In recent years numerous investigators including Wright (1975), Burbank (1974) and Alaska Department of Fish and Game (1975) have attempted to describe the circulation patterns in lower Cook Inlet. Wright (1975) utilized drift cards to determine the overall movement of waters in the inlet. His results provide information only on the location of deployment and point of stranding on the beach of drift cards and, hence, do not describe the path taken by the surface water. Alaska Department of Fish and Game (1975) conducted an extensive radar drogue study within Kachemak Bay and these results have been incorporated into this analysis. Burbank (1974) utilized ERTS photography to assess the gross circulation patterns in the inlet above Augustine Island. Burbank's results provided much of the information used to determine the directions of the net drift component.

Estimates of the magnitude of the net drift component were derived in part from the results of ADF&G work in Kachemak Bay and in part from variations between the average maximum flood and ebb tides as observed in the NOAA data. Plate 3 illustrates the inferred circulation of lower Cook Inlet.

NET SURFACE CIRCULATION
(SPEED IN KNOTS)



COOK INLET, ALASKA



782

DAMES & MOORE

PLATE 3

C. Meteorology

Meteorological inputs were limited to the development of representative surface wind patterns from historical data.

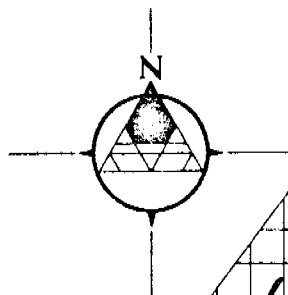
Plates 4-8 show the eight wind patterns that were used in this study. These eight patterns were selected from 22 broad scale circulation patterns for Alaska first identified and defined by Putnins (1966). For each of Putnins' 22 types we investigated the wind flow in lower Cook Inlet, combining those types that resulted in the same basic direction of wind flow. Table 1 gives the number of types and the total frequency for each of the eight directions for the months of January, April, July, and October, plus the annual frequency.

For each direction, the mean speeds for different areas in Cook Inlet can be estimated based on observed speeds at nearby land stations over a period of approximately 17 years (Putnins, 1969). However, for each direction there will be times when extreme winds will occur and times when very light winds will occur. Based on cursory analysis of wind speed and direction tabulations for Alaskan coastal stations, we estimate the distribution of winds by frequency and speed range to be as follows:

<u>Speed Range</u>	<u>Frequency</u>	<u>Description</u>
<0.5x	15%	low
0.5x - 1.5x	60%	normal
1.5x - 2.5x	20%	high
>2.5x	5%	very high

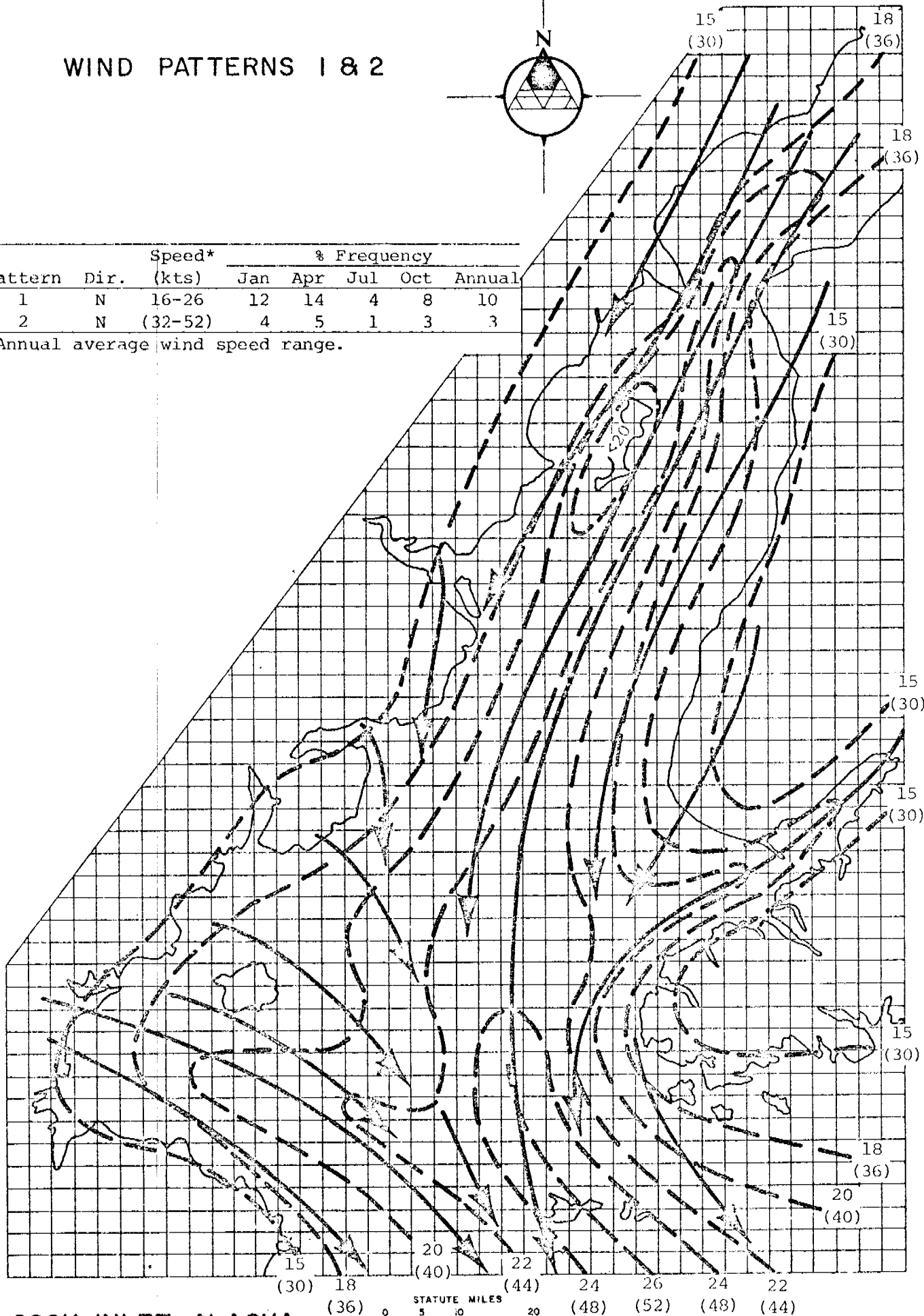
Where x is the mean speed.

WIND PATTERNS 1 & 2



Pattern	Dir.	Speed* (kts)	% Frequency				
			Jan	Apr	Jul	Oct	Annual
1	N	16-26	12	14	4	8	10
2	N	(32-52)	4	5	1	3	3

*Annual average wind speed range.

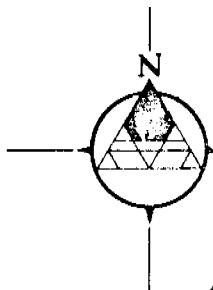


COOK INLET, ALASKA

STATUTE MILES
0 5 10 20

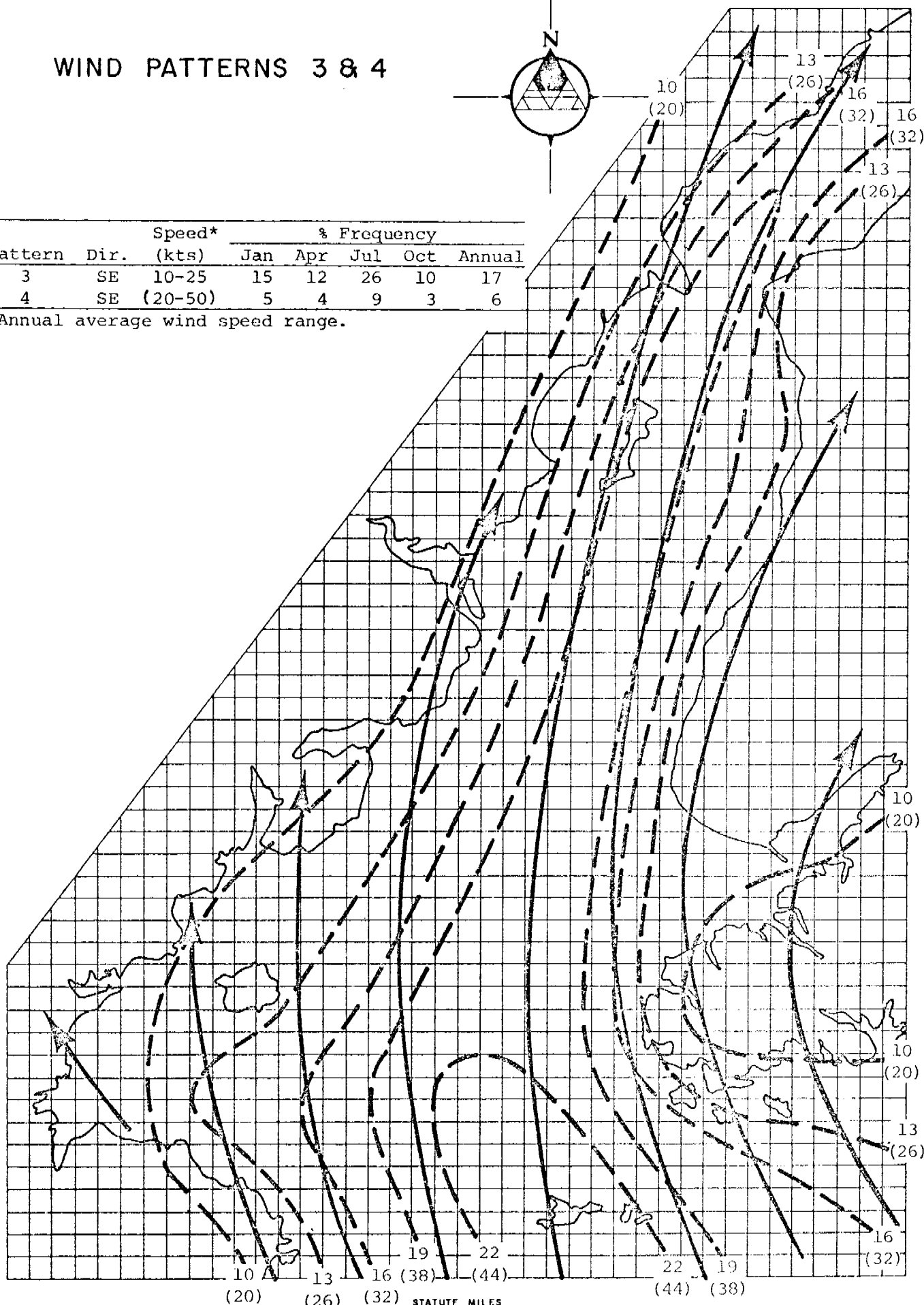
DARRIS & MOORE

WIND PATTERNS 3 & 4

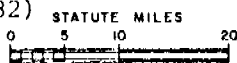


Pattern	Dir.	Speed* (kts)	% Frequency				
			Jan	Apr	Jul	Oct	Annual
3	SE	10-25	15	12	26	10	17
4	SE	(20-50)	5	4	9	3	6

*Annual average wind speed range.



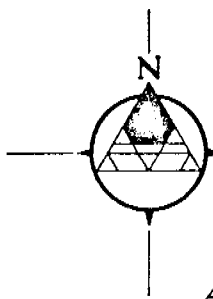
COOK INLET, ALASKA



785

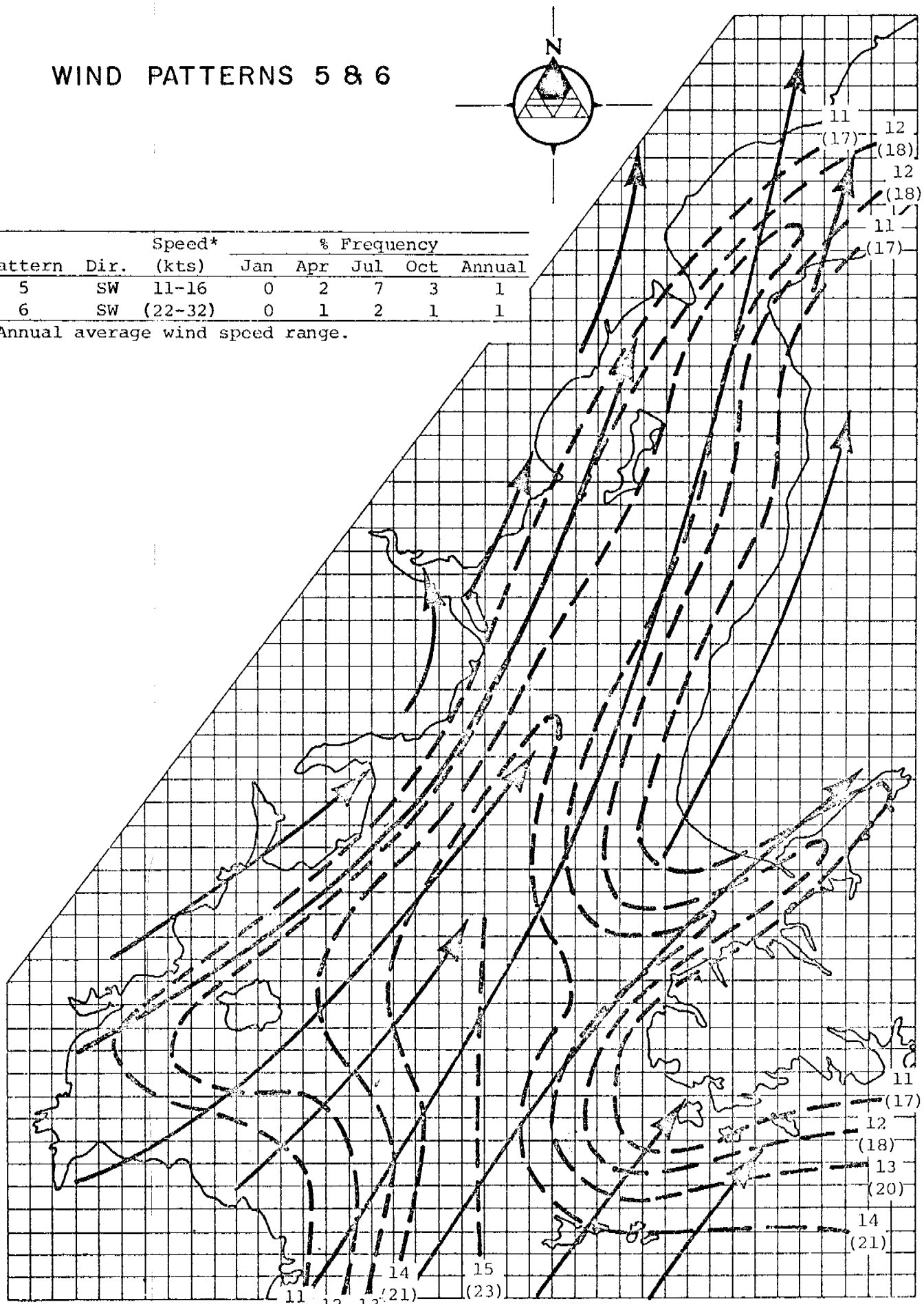
DAMES & MOORE

WIND PATTERNS 5 & 6

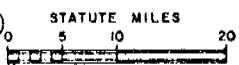


Pattern	Dir.	Speed* (kts)	% Frequency				
			Jan	Apr	Jul	Oct	Annual
5	SW	11-16	0	2	7	3	1
6	SW	(22-32)	0	1	2	1	1

*Annual average wind speed range.

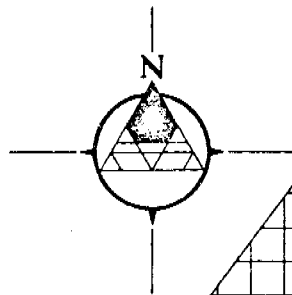


COOK INLET, ALASKA



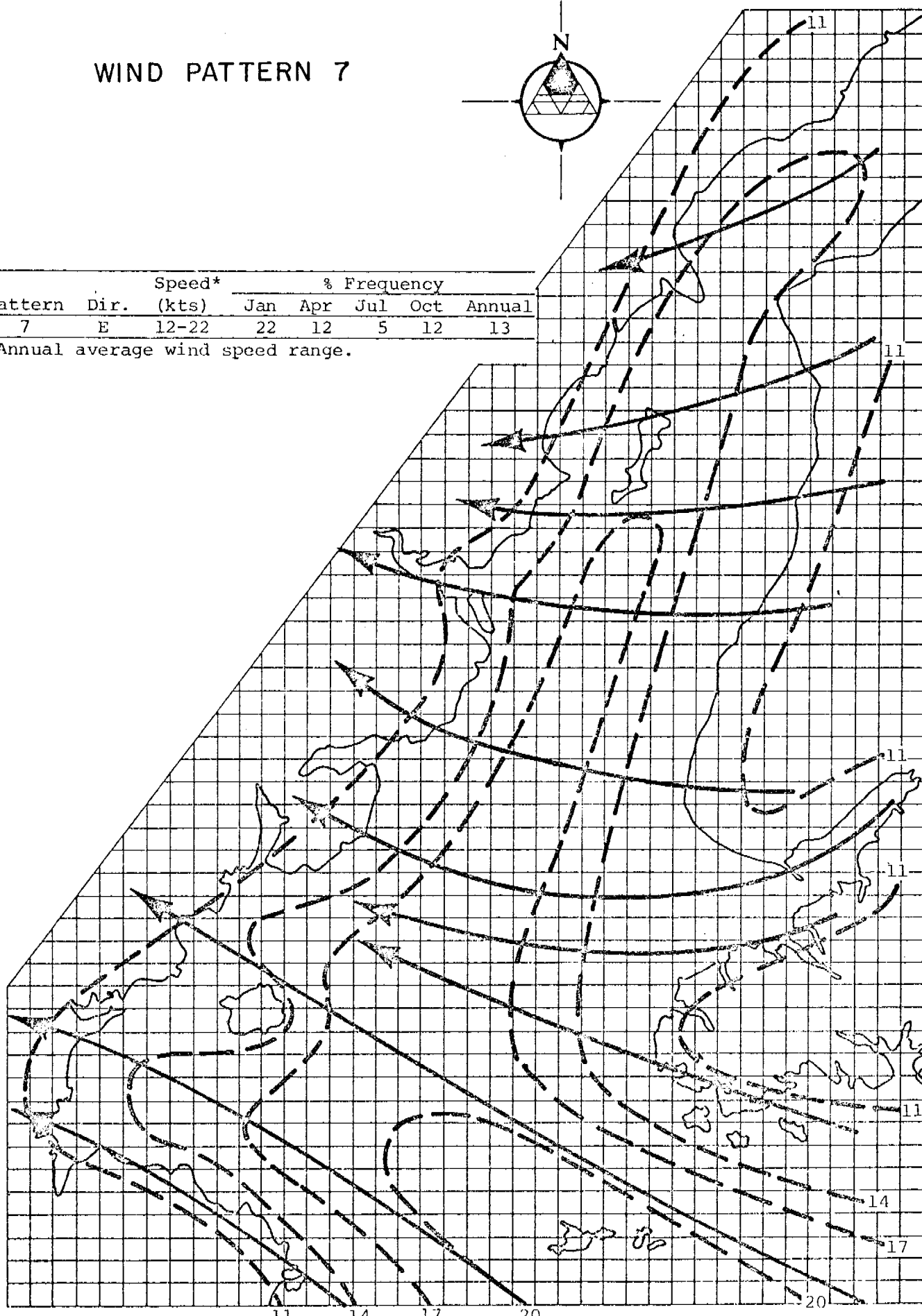
DAWES & MOORE

WIND PATTERN 7

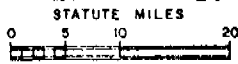


Pattern	Dir.	Speed* (kts)	% Frequency				Annual
			Jan	Apr	Jul	Oct	
7	E	12-22	22	12	5	12	13

*Annual average wind speed range.



COOK INLET, ALASKA

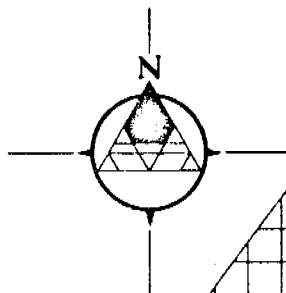


787

DAMES & MOORE

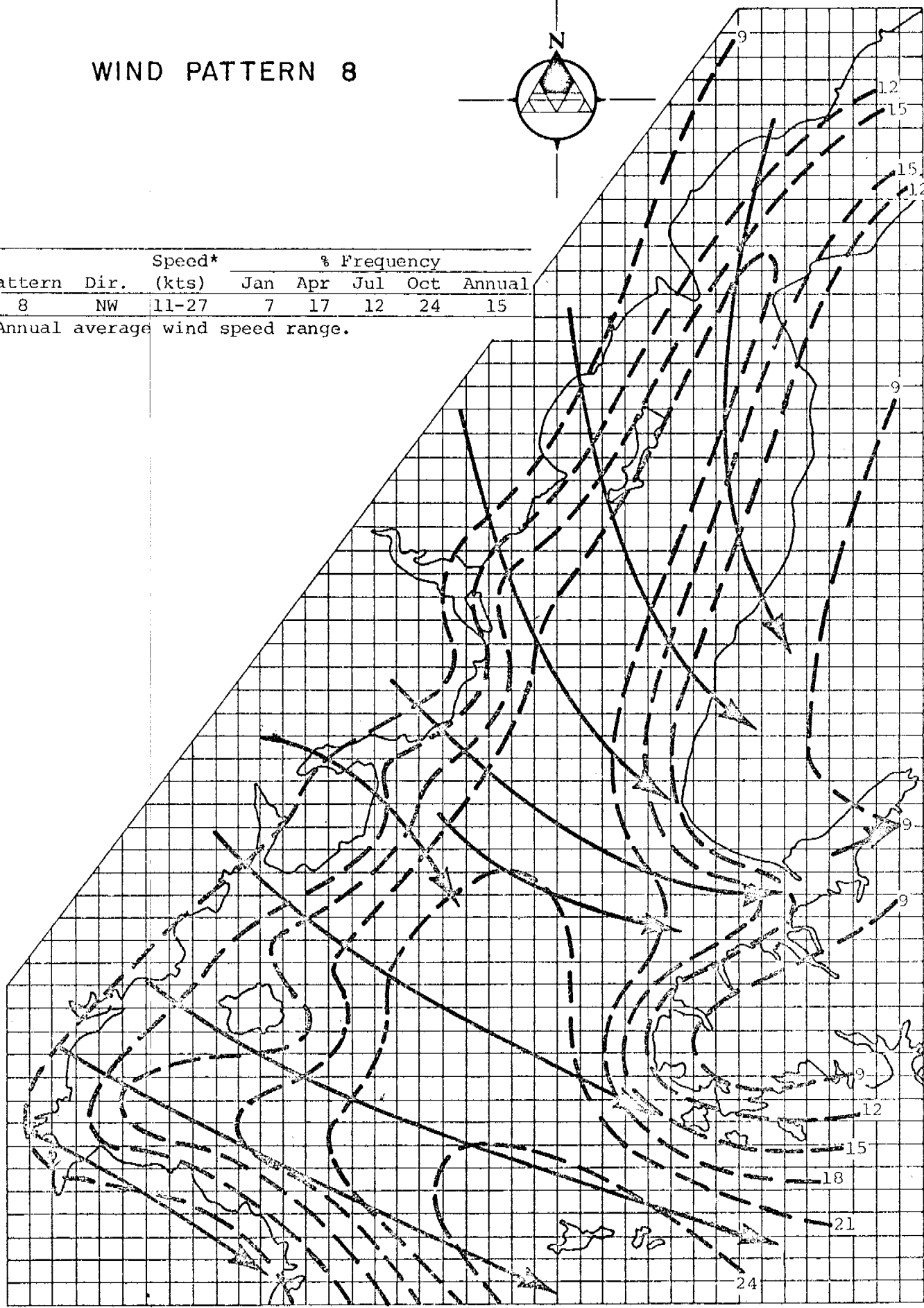
PLATE 7

WIND PATTERN 8

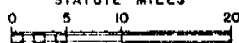


Pattern	Dir.	Speed* (kts)	% Frequency				
			Jan	Apr	Jul	Oct	Annual
8	NW	11-27	7	17	12	24	15

*Annual average wind speed range.



COOK INLET, ALASKA



788

DAMES & MOORE

TABLE 1
FREQUENCIES AND NUMBER OF CIRCULATION PATTERNS (PUTNINS)
FOR EIGHT DIRECTIONS

<u>Direction*</u>	<u>Number of 'Types'</u>	<u>Jan</u>	<u>Apr</u>	<u>July</u>	<u>Oct</u>	<u>Annual</u>
N	4	20.5	22.5	6.8	13.7	16.0
NE	2	2.6	2.7	0.7	1.8	2.0
E	4	37.0	19.3	8.7	20.7	21.1
SE	6	25.5	19.7	43.2	17.3	27.5
S	1	0.3	2.2	5.0	0.4	1.6
SW	1	0.8	3.3	12.4	5.0	5.2
W	2	1.0	2.0	3.2	1.4	2.2
NW	2	12.1	28.2	20.1	39.6	24.2

*Lower Cook Inlet - vicinity Barren Islands

Five of the eight wind patterns selected for this study were "normal" wind speed patterns and therefore the frequency that they represent is 60% of the total frequency for those particular directions. Three of the wind patterns were "high" wind patterns and their frequencies were 20% of the total frequency for the particular directions that they represent. Table 2 gives a breakdown of the direction, speed range, and frequency for each of the eight wind patterns selected for this study. Three directions were not represented in the analysis, NE, S, and W; their total annual frequency is only 5.8% (see Table 1). For each of the five directions that were analyzed neither the low speed range nor the very high speed range were evaluated. The total frequency of the eight patterns selected is approximately 66% (Table 2).

There are some limitations and weaknesses in the above scheme. First of all, Putnins' typology may be off somewhat, i.e., secular changes in weather type frequency may have occurred since the 1946-1963 period which Putnins used. Also Putnins' typology is too subjective -- better, more objective approaches are available. In particular, it would be better to restrict the coverage to just Cook Inlet and vicinity and type the basic pressure patterns that occur there. Computerized schemes for doing this have been developed elsewhere and could be adopted. Finally, real data in such spots such as Kalgin Island, the Barren Island, Cape Douglas, Saint Augustine Island, etc. would aid immeasurably in determining the actual speeds that prevail in Cook Inlet. While such information was unavailable for this study the values used herein are based in part on actual observations made in Cook Inlet, such as those reported by low flying planes and those reported by ships.

TABLE 2

DIRECTION, SPEED, AND FREQUENCY OF EIGHT WIND PATTERNS

<u>Pattern</u>	<u>Direction (a)</u>	<u>Speed (b)</u>	<u>Jan</u>	<u>Apr</u>	<u>Frequency (%)</u>		<u>Annual</u>
					<u>July</u>	<u>Oct</u>	
1	N	16-26	12	14	4	8	10
2	N	32-52	4	5	1	3	3
3	SE	10-25	15	12	26	10	17
4	SE	20-50	5	4	9	3	6
5	SW	11-16	0	2	7	3	3
6	SW	22-32	0	1	2	1	1
7	E	12-22	22	12	5	12	13
8	NW	11-27	7	17	12	24	15
Total Frequency			67	65	67	65	66

(a) Lower Cook Inlet - vicinity Barron Islands.

(b) Annual mean speed range, Cook Inlet in knots.

III. RESULTS

The hypothetical spill scenarios and the oceanographic and meteorological data described in the previous sections, were used with Dames & Moore's Oil Spill Model. The computer output was graphically displayed using printer-plotter graphics, while a separate listing was compiled of such information as boundary contact cell locations and times to impact.

The computer graphics have been bound separately and provided to the Bureau of Land Management, Alaska OCS Office in Anchorage. A tabular listing of the boundary contact cells for each simulated spill trajectory and the associated times to impact (assuming a maximum 6-day trajectory) is provided in Table 3.

Plates 9-20 (also at the end of this section) are graphic illustrations of the tabularized data, giving information on the likely shoreline termination cell for each of the 384 trajectories simulated. The actual cells contacted by each trajectory have been identified for each spill site by one or more numbers adjacent to the cell. The number represents the wind pattern(s) used to produce a trajectory termination at that cell. The dots over each number indicate the number of times that cell was contacted for each set of four trajectories for each wind pattern. Recall that the four trajectories were for spills occurring at four different phases of the tide.

As indicated on each plate, the times to impact for each cell are given as: possible within 1 day, 3 days, or 6 days. Trajectories that

TABLE 3

BOUNDARY CONTACT CELLS *

	SITE 1			SITE 2		
	Cell Location		Time to Impact (hrs)	Cell Location		Time to Impact (hrs)
	I	J		I	J	
Wind 1						
Tidal Phase 1	18	56	98	18	56	73
Tidal Phase 2	18	56	79	18	56	70
Tidal Phase 3	18	56	77	18	56	69
Tidal Phase 4	18	56	90	18	56	73
Wind 2						
Tidal Phase 1	21	56	61	21	56	50
Tidal Phase 2	21	56	56	21	56	45
Tidal Phase 3	21	56	55	20	56	45
Tidal Phase 4	21	56	61	21	56	52
Wind 3						
Tidal Phase 1	24	21	34	23	22	48
Tidal Phase 2	23	22	39	21	28	28
Tidal Phase 3	24	21	36	23	22	54
Tidal Phase 4	27	14	50	23	22	44
Wind 4						
Tidal Phase 1	27	21	19	27	14	45
Tidal Phase 2	27	14	41	24	21	34
Tidal Phase 3	27	14	39	24	21	32
Tidal Phase 4	27	21	20	27	21	23
Wind 5						
Tidal Phase 1	24	21	37	22	23	56
Tidal Phase 2	27	21	38	20	30	32
Tidal Phase 3	27	21	37	21	28	33
Tidal Phase 4	27	21	35	27	21	45
Wind 6						
Tidal Phase 1	28	18	38	27	21	37
Tidal Phase 2	27	21	34	24	21	46
Tidal Phase 3	28	18	37	24	21	42
Tidal Phase 4	28	18	34	28	21	32
Wind 7						
Tidal Phase 1	20	29	20	16	33	30
Tidal Phase 2	18	31	27	16	35	30
Tidal Phase 3	19	31	24	16	35	30
Tidal Phase 4	20	30	18	16	33	31
Wind 8						
Tidal Phase 1	32	30	14	30	34	15
Tidal Phase 2	31	33	17	30	34	16
Tidal Phase 3	31	31	9	30	34	13
Tidal Phase 4	31	31	11	30	34	17

*6-day truncation employed on time to contact.

TABLE 3 (Cont.)

BOUNDARY CONTACT CELLS

	SITE 3			SITE 4			
	Cell Location		Time to Impact (hrs)	Cell Location		Time to Impact (hrs)	
	I	J		I	J		
Wind 1							
Tidal Phase 1	18	56	57	Tidal Phase 1	18	56	52
Tidal Phase 2	18	56	55	Tidal Phase 2	18	56	51
Tidal Phase 3	18	56	57	Tidal Phase 3	18	56	50
Tidal Phase 4	18	56	60	Tidal Phase 4	18	56	50
Wind 2							
Tidal Phase 1	20	56	35	Tidal Phase 1	20	56	31
Tidal Phase 2	20	56	34	Tidal Phase 2	20	56	30
Tidal Phase 3	20	56	35	Tidal Phase 3	20	56	29
Tidal Phase 4	20	56	36	Tidal Phase 4	20	56	31
Wind 3							
Tidal Phase 1	17	32	29	Tidal Phase 1	15	36	20
Tidal Phase 2	16	34	21	Tidal Phase 2	13	37	25
Tidal Phase 3	16	35	20	Tidal Phase 3	14	37	23
Tidal Phase 4	17	32	22	Tidal Phase 4	14	37	18
Wind 4							
Tidal Phase 1	19	31	13	Tidal Phase 1	16	35	11
Tidal Phase 2	18	31	18	Tidal Phase 2	15	36	12
Tidal Phase 3	19	31	16	Tidal Phase 3	15	36	10
Tidal Phase 4	19	31	12	Tidal Phase 4	16	35	12
Wind 5							
Tidal Phase 1	No Contact			Tidal Phase 1	No Contact		
Tidal Phase 2	No Contact			Tidal Phase 2	No Contact		
Tidal Phase 3	No Contact			Tidal Phase 3	No Contact		
Tidal Phase 4	No Contact			Tidal Phase 4	No Contact		
Wind 6							
Tidal Phase 1	19	31	18	Tidal Phase 1	No Contact		
Tidal Phase 2	20	30	28	Tidal Phase 2	No Contact		
Tidal Phase 3	19	31	23	Tidal Phase 3	No Contact		
Tidal Phase 4	20	30	23	Tidal Phase 4	No Contact		
Wind 7							
Tidal Phase 1	16	35	13	Tidal Phase 1	12	37	20
Tidal Phase 2	15	36	13	Tidal Phase 2	9	38	34
Tidal Phase 3	15	36	13	Tidal Phase 3	9	38	38
Tidal Phase 4	16	35	13	Tidal Phase 4	14	37	14
Wind 8							
Tidal Phase 1	No Contact			Tidal Phase 1	25	53	81
Tidal Phase 2	No Contact			Tidal Phase 2	24	54	80
Tidal Phase 3	27	54	140	Tidal Phase 3	24	54	84
Tidal Phase 4	No Contact			Tidal Phase 4	25	53	82

TABLE 3 (Cont.)

BOUNDARY CONTACT CELLS

	SITE 5			SITE 6		
	Cell Location		Time to Impact (hrs)	Cell Location		Time to Impact (hrs)
	I	J		I	J	
Wind 1						
Tidal Phase 1	18	56	40	18	56	26
Tidal Phase 2	18	56	40	18	56	24
Tidal Phase 3	18	56	40	18	56	25
Tidal Phase 4	18	56	42	18	56	29
Wind 2						
Tidal Phase 1	19	56	24	19	56	16
Tidal Phase 2	19	56	23	19	56	15
Tidal Phase 3	19	56	24	19	56	16
Tidal Phase 4	19	56	25	19	56	17
Wind 3						
Tidal Phase 1	10	37	56	10	37	97
Tidal Phase 2	10	37	58	10	37	104
Tidal Phase 3	10	37	59	10	37	102
Tidal Phase 4	11	37	52	10	37	96
Wind 4						
Tidal Phase 1	13	37	21	13	37	39
Tidal Phase 2	12	37	24	13	37	44
Tidal Phase 3	12	37	23	13	37	42
Tidal Phase 4	13	37	21	13	37	40
Wind 5						
Tidal Phase 1	No Contact			18	56	118
Tidal Phase 2	No Contact			18	56	106
Tidal Phase 3	No Contact			18	56	105
Tidal Phase 4	No Contact			18	56	112
Wind 6						
Tidal Phase 1	20	30	86	20	30	95
Tidal Phase 2	20	30	92	20	30	102
Tidal Phase 3	20	30	90	20	30	99
Tidal Phase 4	20	30	88	20	30	97
Wind 7						
Tidal Phase 1	7	42	34	3	47	95
Tidal Phase 2	12	43	12	2	48	102
Tidal Phase 3	12	43	11	2	48	102
Tidal Phase 4	8	41	32	3	47	96
Wind 8						
Tidal Phase 1	22	56	64	22	56	50
Tidal Phase 2	21	56	61	21	56	41
Tidal Phase 3	22	56	65	21	56	46
Tidal Phase 4	22	56	66	22	56	52

TABLE 3 (Cont.)

BOUNDARY CONTACT CELLS

	SITE 7			SITE 8		
	Cell Location		Time to Impact (hrs)	Cell Location		Time to Impact (hrs)
	I	J		I	J	
Wind 1						
Tidal Phase 1	17	56	2	19	56	17
Tidal Phase 2	17	56	1	20	56	15
Tidal Phase 3	17	56	1	19	56	18
Tidal Phase 4	17	56	1	19	56	18
Wind 2						
Tidal Phase 1	17	56	2	21	56	12
Tidal Phase 2	17	56	1	21	56	10
Tidal Phase 3	17	56	1	21	56	10
Tidal Phase 4	17	56	1	21	56	11
Wind 3						
Tidal Phase 1	15	56	25	10	37	133
Tidal Phase 2	17	56	4	10	37	142
Tidal Phase 3	16	56	10	10	37	141
Tidal Phase 4	12	54	57	10	37	127
Wind 4						
Tidal Phase 1	11	37	84	14	37	48
Tidal Phase 2	11	37	87	13	37	54
Tidal Phase 3	11	37	87	13	37	52
Tidal Phase 4	12	43	57	13	37	48
Wind 5						
Tidal Phase 1	17	56	6	18	56	99
Tidal Phase 2	17	56	3	18	56	88
Tidal Phase 3	17	56	2	18	56	95
Tidal Phase 4	17	56	8	18	56	103
Wind 6						
Tidal Phase 1	17	56	7	20	30	114
Tidal Phase 2	17	56	3	20	30	121
Tidal Phase 3	17	56	9	20	30	118
Tidal Phase 4	17	56	9	20	30	107
Wind 7						
Tidal Phase 1	16	56	6	5	50	93
Tidal Phase 2	16	56	3	8	51	70
Tidal Phase 3	17	56	1	8	51	70
Tidal Phase 4	16	56	8	5	50	93
Wind 8						
Tidal Phase 1	18	56	4	24	54	32
Tidal Phase 2	17	56	2	24	56	40
Tidal Phase 3	17	56	1	24	56	38
Tidal Phase 4	18	56	3	24	54	34

TABLE 3 (Cont.)

BOUNDARY CONTACT CELLS

	SITE 9			SITE 10		
	Cell Location		Time to Impact (hrs)	Cell Location		Time to Impact (hrs)
	I	J		I	J	
Wind 1						
Tidal Phase 1	19	56	36	18	56	54
Tidal Phase 2	20	56	32	18	56	52
Tidal Phase 3	20	56	34	19	56	54
Tidal Phase 4	19	56	37	18	56	56
Wind 2						
Tidal Phase 1	22	56	22	21	56	34
Tidal Phase 2	22	56	19	21	56	32
Tidal Phase 3	22	56	19	21	56	33
Tidal Phase 4	22	56	23	21	56	35
Wind 3						
Tidal Phase 1	15	36	57	17	32	48
Tidal Phase 2	12	37	74	16	34	52
Tidal Phase 3	13	37	70	17	32	61
Tidal Phase 4	15	36	54	17	32	45
Wind 4						
Tidal Phase 1	19	31	37	21	28	28
Tidal Phase 2	18	31	45	20	29	31
Tidal Phase 3	18	31	42	20	29	30
Tidal Phase 4	19	31	35	21	28	27
Wind 5						
Tidal Phase 1	22	23	86			No Contact
Tidal Phase 2		No Contact				No Contact
Tidal Phase 3		No Contact				No Contact
Tidal Phase 4		No Contact				No Contact
Wind 6						
Tidal Phase 1	30	34	33	20	30	37
Tidal Phase 2	30	34	36	20	30	44
Tidal Phase 3	32	29	52	20	30	39
Tidal Phase 4	28	21	61	21	28	39
Wind 7						
Tidal Phase 1	12	43	49	9	39	54
Tidal Phase 2	3	47	111	7	40	67
Tidal Phase 3	3	47	112	9	39	55
Tidal Phase 4	7	40	85	9	39	56
Wind 8						
Tidal Phase 1	30	43	27	32	36	78
Tidal Phase 2	29	44	20			No Contact
Tidal Phase 3	29	44	19	32	36	84
Tidal Phase 4	30	43	22	32	36	107

TABLE 3 (Cont.)

BOUNDARY CONTACT CELLS

	SITE 11			SITE 12		
	Cell Location		Time to Impact (hrs)	Cell Location		Time to Impact (hrs)
	I	J		I	J	
Wind 1						
Tidal Phase 1	18	56	52	18	56	39
Tidal Phase 2	18	56	49	18	56	34
Tidal Phase 3	19	56	49	19	56	38
Tidal Phase 4	18	56	54	18	56	39
Wind 2						
Tidal Phase 1	20	56	31	20	56	24
Tidal Phase 2	20	56	29	20	56	22
Tidal Phase 3	20	56	28	20	56	22
Tidal Phase 4	20	56	33	20	56	25
Wind 3						
Tidal Phase 1	15	36	33	11	37	66
Tidal Phase 2	14	37	41	11	37	76
Tidal Phase 3	14	37	40	11	37	72
Tidal Phase 4	16	35	34	12	37	62
Wind 4						
Tidal Phase 1	18	31	29	16	35	27
Tidal Phase 2	17	32	27	15	36	33
Tidal Phase 3	18	31	33	16	35	32
Tidal Phase 4	19	31	25	17	32	40
Wind 5						
Tidal Phase 1	No Contact			No Contact		
Tidal Phase 2	No Contact			No Contact		
Tidal Phase 3	No Contact			No Contact		
Tidal Phase 4	No Contact			No Contact		
Wind 6						
Tidal Phase 1	20	30	39	19	31	63
Tidal Phase 2	20	30	46	20	30	74
Tidal Phase 3	20	30	43	19	31	70
Tidal Phase 4	20	30	41	20	30	60
Wind 7						
Tidal Phase 1	9	39	44	12	43	32
Tidal Phase 2	7	40	55	12	44	35
Tidal Phase 3	7	40	56	12	44	34
Tidal Phase 4	9	39	46	12	43	35
Wind 8						
Tidal Phase 1	No Contact			27	54	117
Tidal Phase 2	29	44	120	27	54	105
Tidal Phase 3	No Contact			27	54	95
Tidal Phase 4	No Contact			27	54	110

do not contact a boundary cell within six days are ignored -- it is interesting to note that only 38 trajectories out of the 384 run did not terminate at a boundary cell in less than six days.

Plates 9-20 also contain contact cells that do not have specific trajectory information (wind pattern numbers and dots) associated with them. These cells have been selected, and given estimated time-to-impact values, based upon a careful examination of the entire trajectory for each spill simulation. The use of only four tidal phases for initiation of a spill, and the representation of the coastline with 3 x 3 mile squares, clearly require the need for some judgement in expanding the specific computer-generated contact cells to a more realistic potential contact zone.

Plate 21 illustrates a summation of the boundary contact zones for each of the 12 sites. For the eight wind patterns and oceanographic conditions selected for use in this study, Plate 21 shows those portions of the coastline that could conceivably be reached by oil spilled from any one of the 12 potential spill sites. It should be recognized that the lower boundary cells in Plates 9-21 represent open water at the mouth of Cook Inlet. A total of 131 trajectories out of 384 evaluated passed through these open water cells.

An assessment of possible shoreline contamination for the sites and conditions selected in this study is possible based upon the results in Plates 9-21. However, due consideration should be given to the percent frequency of occurrence for each wind pattern and its associated contamination zones onshore. To facilitate such an evaluation the percent frequency of occurrence for each wind pattern is provided in the upper left hand corner of each plate.

To further assist in the development of frequency - dependent exposure levels, the annual percent probability of exposure for each spill site is shown in Plates 22 through 33. The information given in these plates has been derived from the model output data for the eight wind patterns evaluated. The annual percent probability of occurrence of the wind patterns shown in Plates 9 through 20 were used to construct these exposures.

As an example of the technique used in constructing Plate 22, consider the most southwestern cell in Kalgin Island (Coordinates 27, 21). Turning to Plate 9, it is seen that wind Patterns 4, 5, and 6 have a potential to propagate a surface slick to this cell. The cumulative probability of wind Patterns 4, 5, and 6 occurring in a year is 10 percent. Hence, the southwestern cell of Kalgin Island in Plate 22 is coded in the 10-15 percent range. Following this technique all cells in Plates 22 through 33 were constructed.

In using Plates 22 through 33 it is important to emphasize that the potential exposure zones do not reflect the time to impact, the dosage of any impact, nor the biological effects that might be anticipated. Only the annual percent probability has been addressed involving the likelihood that if oil is spilled at the indicated site, it will reach the cell in question. Further, the results are limited by the eight wind fields selected for this study.

Plate 34 gives the cumulative results for all 12 sites. It was constructed by summing the probabilities for each cell for each spill site and then dividing by the number of sites. It gives the percent probability of exposure at each cell, assuming that a single annual spill is equally probable from any one of the 12 potential spill sites. The relative

exposure levels along the coastline thus provide an indication, within the limitations of the model and available input data, of those portions of the inlet which are most likely to be impacted by an oil spill from the 12 sites under consideration.

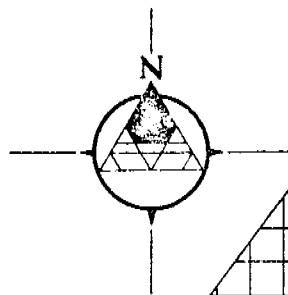
It should be recognized that an assessment of shoreline exposure to oil must include both the likelihood of contamination, as well as the time elapsed prior to contamination. The potential shoreline contact zones for each spill site, as well as the composite contact zones for all 12 sites, should be interpreted with due consideration for the fact that relatively infrequent wind conditions can result in the contamination of normally low exposure areas (based on frequency of occurrence) in a very short period.

For example, a spill from Site 1 is shown in Plate 22 to have a greater probability of coastal contact in the Kalgin Island area, approximately 40 miles to the north, than on the adjacent coastline, less than 10 miles to the east (assuming a spill of adequate volume to propagate this distance). While this information is of use in the assessment of impact frequency in one area versus another, Plate 9 illustrates that under certain wind conditions (Wind Pattern 8) the adjacent coastline could be contaminated in less than 24 hours. The less likely, though possible, events involving shorter times to impact could be more significant in some areas because of the greater volume of oil likely to exist at the surface upon impact, dosage and toxicity considerations, and the shorter response time available for spill containment, diversion, and cleanup operations.

REFERENCES

- Alaska Department of Fish & Game, 1975. Miscellaneous data obtained from radar drogue study.
- Burbank, D. C., 1974. Suspended Sediment Transport and Deposition in Alaskan Coastal Waters. Univ. of Alaska, Master Thesis. 222 p.
- Mungal, J. C. H., 1973. Cook Inlet Tidal Stream Atlas. Univ. of Alaska, Inst. of Marine Science, Report R73-6, 24 p.
- Putnins, Pauls, 1966. Studies on the meteorology of Alaska: First Interim Report (The sequences of basic weather patterns over Alaska), U.S. Department of Commerce, ESSA, EDS, Silver Spring, MD 20910, 107 p.
- Putnins, Pauls, 1969. Studies on the meteorology of Alaska: Final Report (Weather situations in Alaska during the occurrences of specific basic weather patterns), U.S. Department of Commerce, ESSA, Research Laboratories, Boulder CO 80302, 267 p.
- Wright, F. F., 1975. Surface Circulation of Lower Cook Inlet - A Drift Card Study. Prepared for the Alaska Dept. of Fish and Game.

POTENTIAL BOUNDARY CONTACT ZONES FOR SPILL SITE I

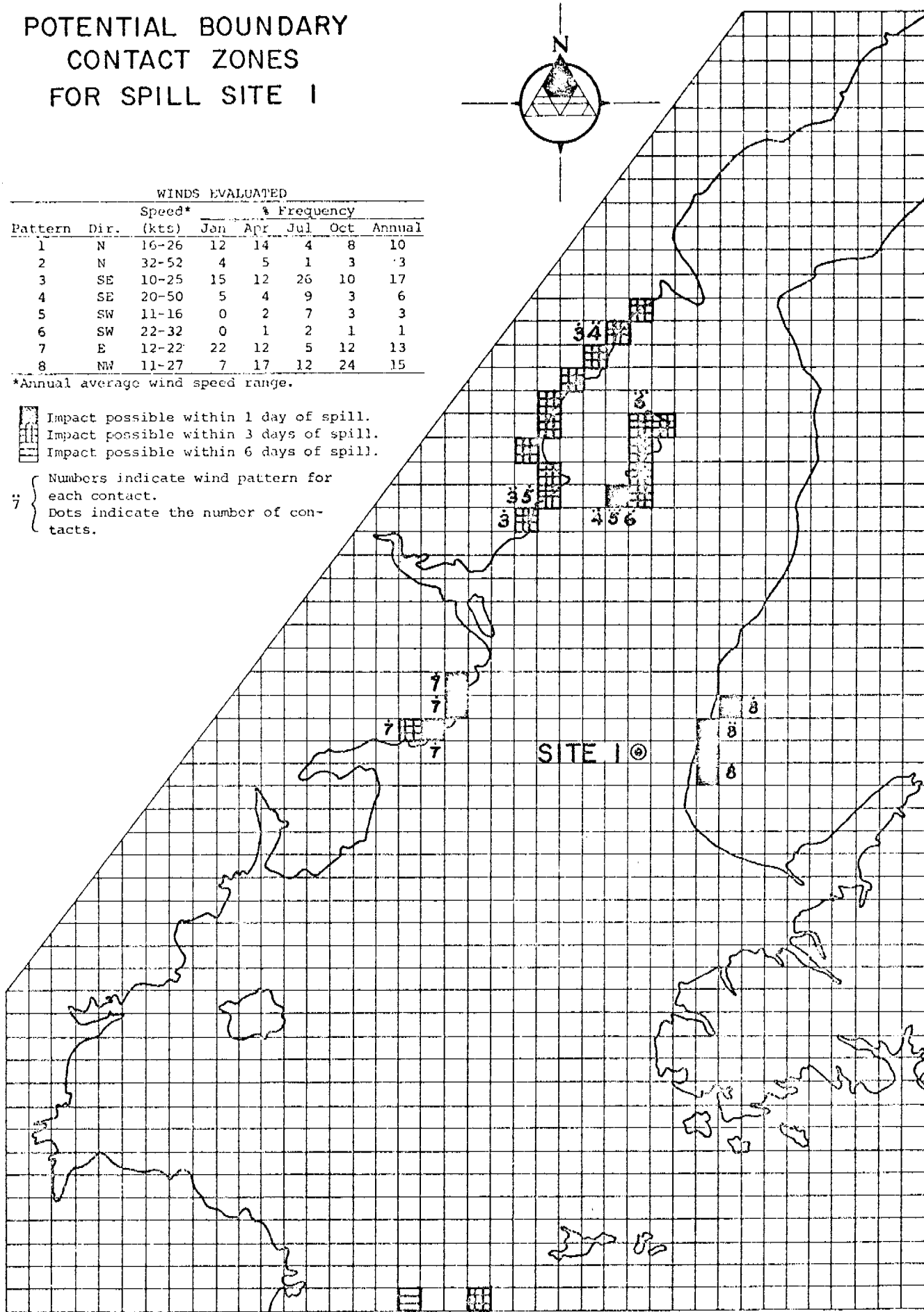


Pattern	Dir.	WINDS EVALUATED					
		Speed*	% Frequency				
		(kts)	Jan	Apr	Jul	Oct	Annual
1	N	16-26	12	14	4	8	10
2	N	32-52	4	5	1	3	3
3	SE	10-25	15	12	26	10	17
4	SE	20-50	5	4	9	3	6
5	SW	11-16	0	2	7	3	3
6	SW	22-32	0	1	2	1	1
7	E	12-22	22	12	5	12	13
8	NW	11-27	7	17	12	24	15

*Annual average wind speed range.

- Impact possible within 1 day of spill.
- Impact possible within 3 days of spill.
- Impact possible within 6 days of spill.

- Numbers indicate wind pattern for each contact.
- Dots indicate the number of contacts.



COOK INLET, ALASKA

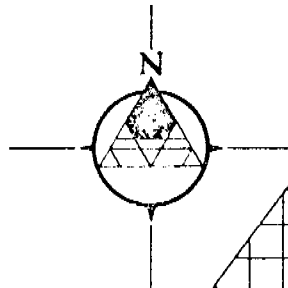


803

DANHS & MOORE

PLATE 9

POTENTIAL BOUNDARY CONTACT ZONES FOR SPILL SITE 2

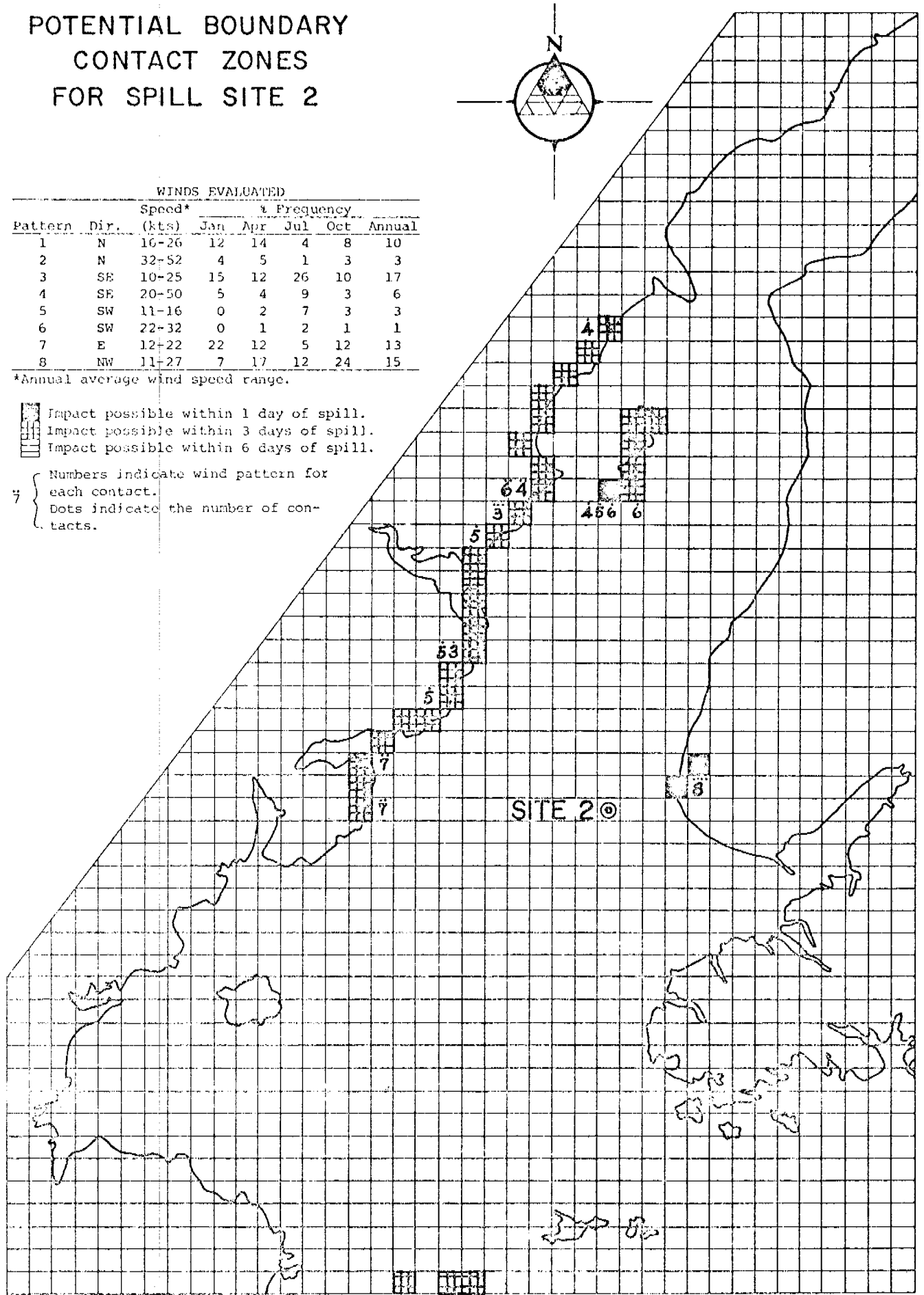


Pattern	Dir.	WINDS EVALUATED					
		Speed* (Kts)	Frequency				Annual
			Jan	Apr	Jul	Oct	
1	N	16-26	12	14	4	8	10
2	N	32-52	4	5	1	3	3
3	SE	10-25	15	12	26	10	17
4	SE	20-50	5	4	9	3	6
5	SW	11-16	0	2	7	3	3
6	SW	22-32	0	1	2	1	1
7	E	12-22	22	12	5	12	13
8	NW	11-27	7	17	12	24	15

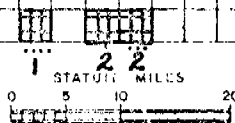
*Annual average wind speed range.

- Impact possible within 1 day of spill.
- Impact possible within 3 days of spill.
- Impact possible within 6 days of spill.

7 { Numbers indicate wind pattern for each contact.
Dots indicate the number of contacts.

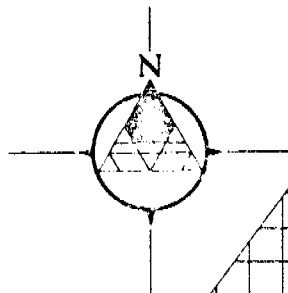


COOK INLET, ALASKA



DAMES & MOORE

POTENTIAL BOUNDARY CONTACT ZONES FOR SPILL SITE 3

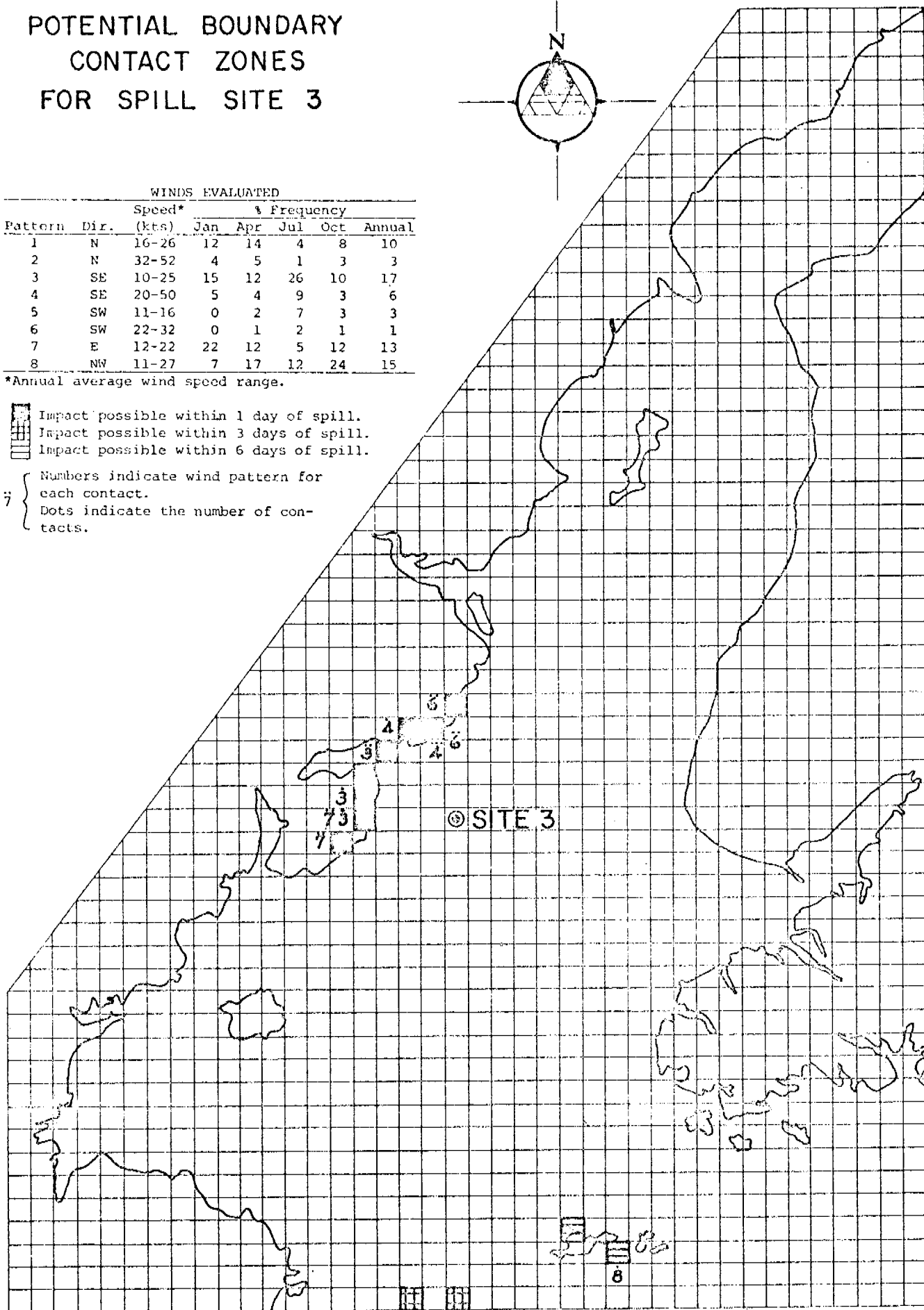


WINDS EVALUATED							
Pattern	Dir.	Speed* (kts)	% Frequency				Annual
			Jan	Apr	Jul	Oct	
1	N	16-26	12	14	4	8	10
2	N	32-52	4	5	1	3	3
3	SE	10-25	15	12	26	10	17
4	SE	20-50	5	4	9	3	6
5	SW	11-16	0	2	7	3	3
6	SW	22-32	0	1	2	1	1
7	E	12-22	22	12	5	12	13
8	NW	11-27	7	17	12	24	15

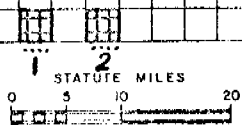
*Annual average wind speed range.

- Impact possible within 1 day of spill.
- Impact possible within 3 days of spill.
- Impact possible within 6 days of spill.

- Numbers indicate wind pattern for each contact.
- Dots indicate the number of contacts.

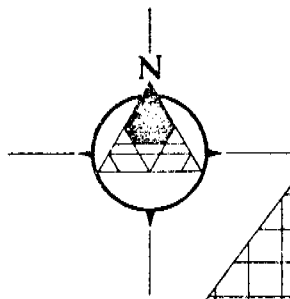


COOK INLET, ALASKA



DAVIS & BROWN

POTENTIAL BOUNDARY CONTACT ZONES FOR SPILL SITE 4

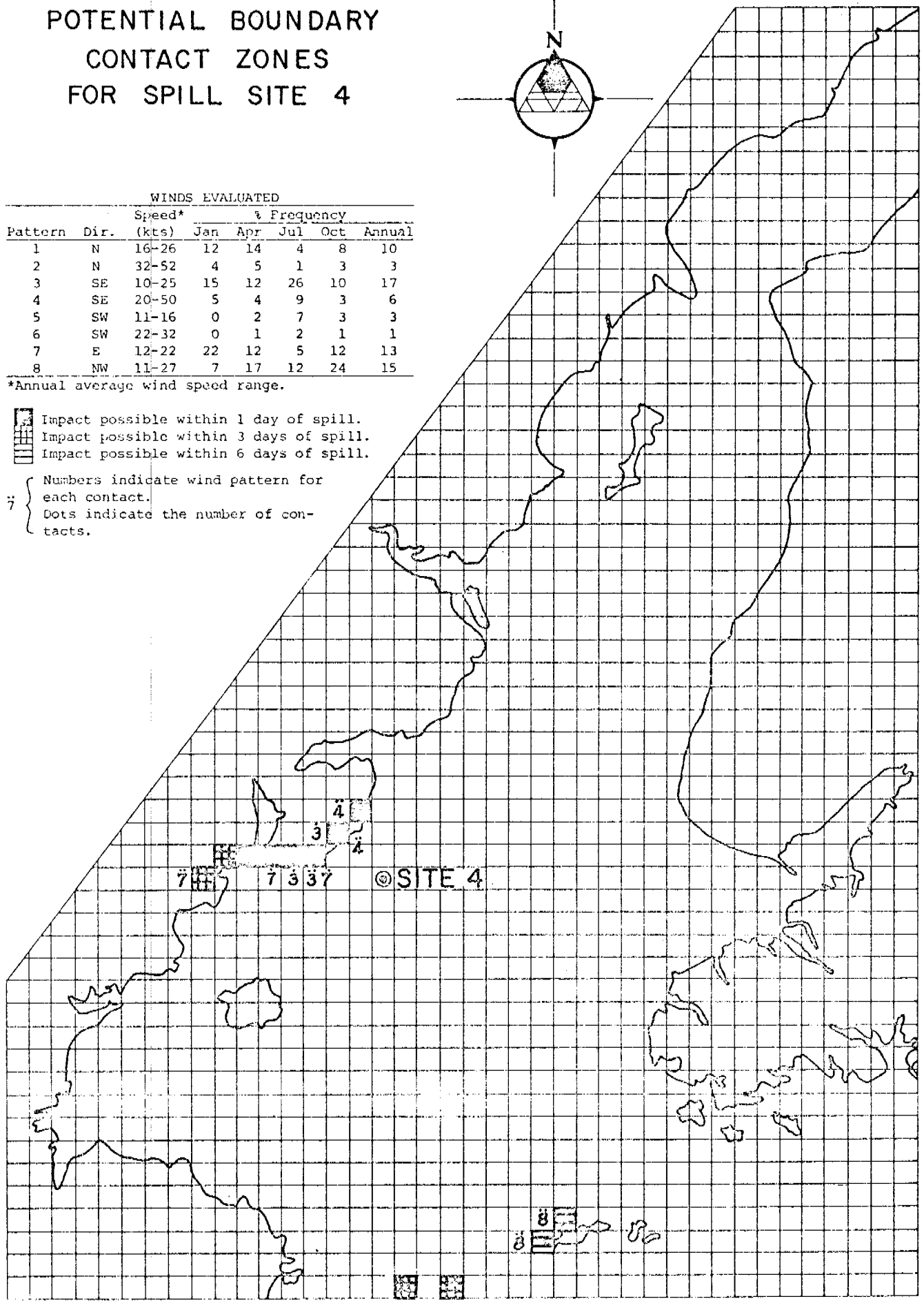


Pattern	Dir.	WINDS EVALUATED					
		Speed* (kts)	Jan	Apr	Jul	Oct	Annual
1	N	16-26	12	14	4	8	10
2	N	32-52	4	5	1	3	3
3	SE	10-25	15	12	26	10	17
4	SE	20-50	5	4	9	3	6
5	SW	11-16	0	2	7	3	3
6	SW	22-32	0	1	2	1	1
7	E	12-22	22	12	5	12	13
8	NW	11-27	7	17	12	24	15

*Annual average wind speed range.

- Impact possible within 1 day of spill.
- Impact possible within 3 days of spill.
- Impact possible within 6 days of spill.

Numbers indicate wind pattern for each contact.
 Dots indicate the number of contacts.

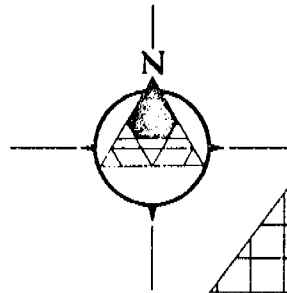


COOK INLET, ALASKA



DAMES & MOORE

POTENTIAL BOUNDARY CONTACT ZONES FOR SPILL SITE 5

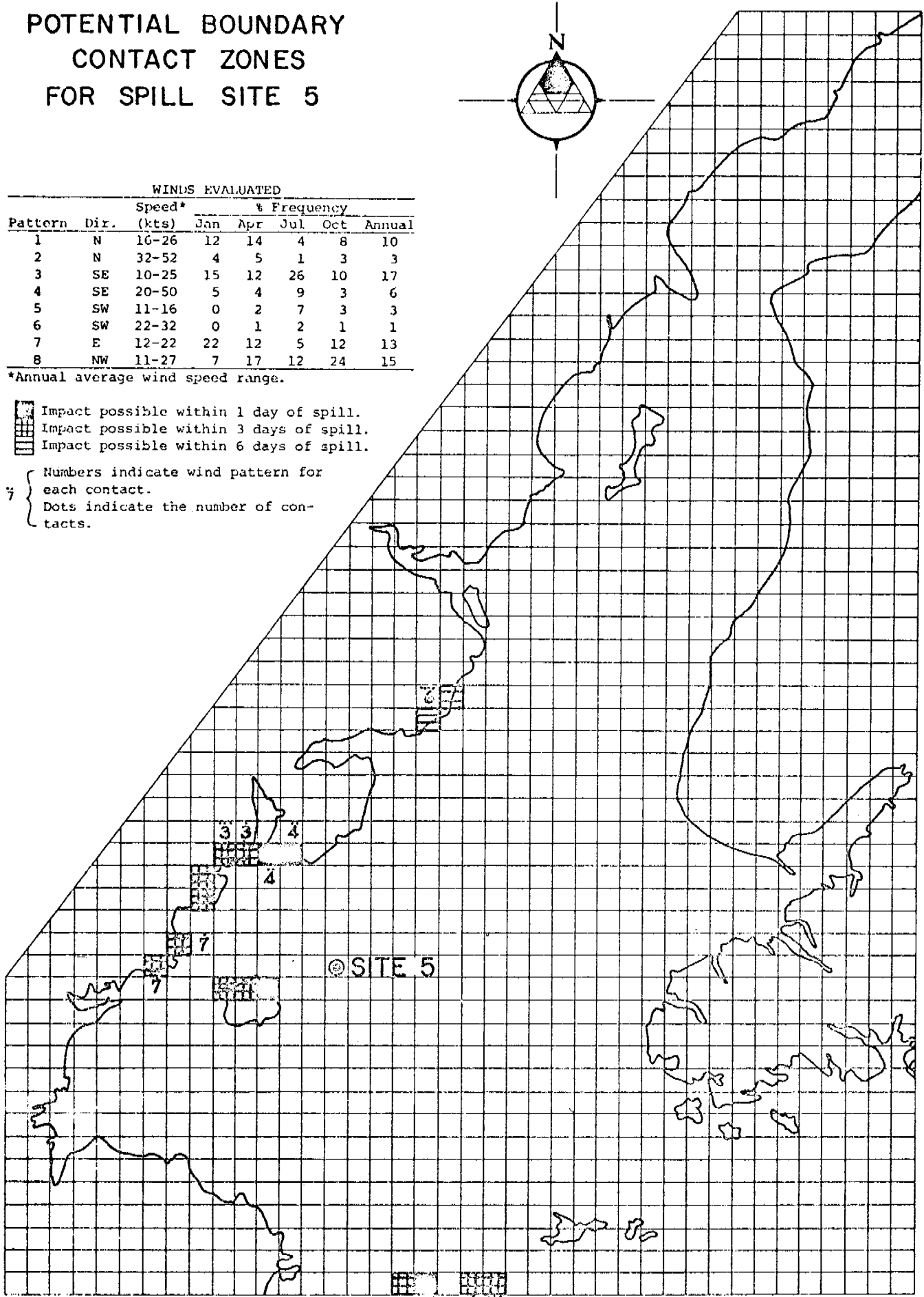


WINDS EVALUATED							
Pattern	Dir.	Speed* (kts)	% Frequency				Annual
			Jan	Apr	Jul	Oct	
1	N	16-26	12	14	4	8	10
2	N	32-52	4	5	1	3	3
3	SE	10-25	15	12	26	10	17
4	SE	20-50	5	4	9	3	6
5	SW	11-16	0	2	7	3	3
6	SW	22-32	0	1	2	1	1
7	E	12-22	22	12	5	12	13
8	NW	11-27	7	17	12	24	15

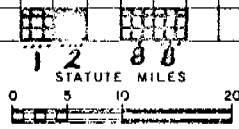
*Annual average wind speed range.

- Impact possible within 1 day of spill.
- Impact possible within 3 days of spill.
- Impact possible within 6 days of spill.

Numbers indicate wind pattern for each contact.
Dots indicate the number of contacts.

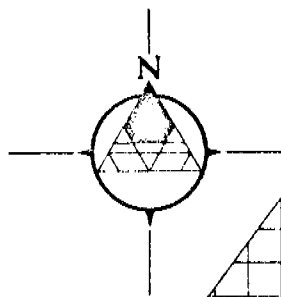


COOK INLET, ALASKA



DAMES & MOORE

POTENTIAL BOUNDARY CONTACT ZONES FOR SPILL SITE 6

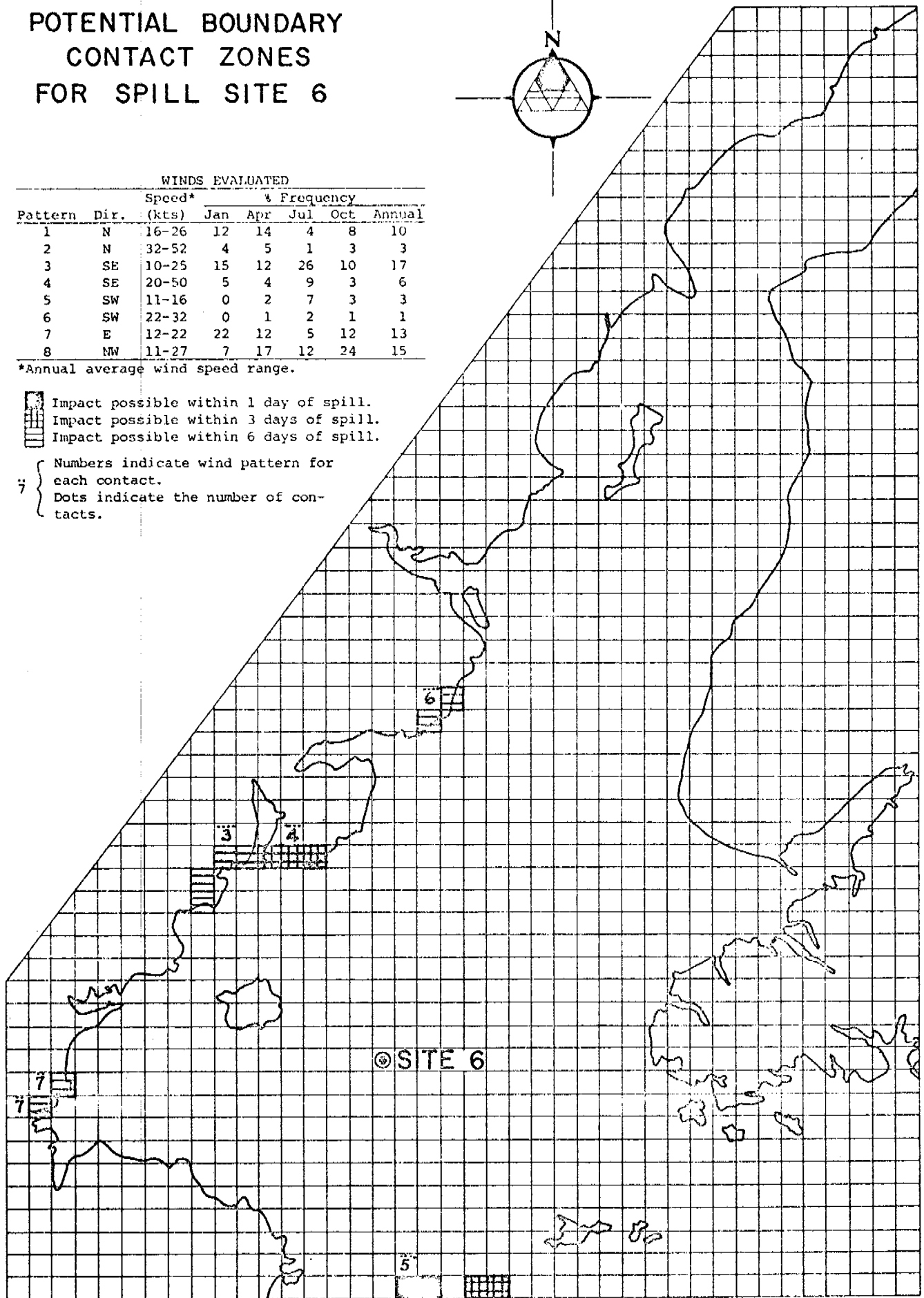


Pattern	Dir.	WINDS EVALUATED					
		Speed* (kts)	% Frequency				
			Jan	Apr	Jul	Oct	Annual
1	N	16-26	12	14	4	8	10
2	N	32-52	4	5	1	3	3
3	SE	10-25	15	12	26	10	17
4	SE	20-50	5	4	9	3	6
5	SW	11-16	0	2	7	3	3
6	SW	22-32	0	1	2	1	1
7	E	12-22	22	12	5	12	13
8	NW	11-27	7	17	12	24	15

*Annual average wind speed range.

- Impact possible within 1 day of spill.
- Impact possible within 3 days of spill.
- Impact possible within 6 days of spill.

Numbers indicate wind pattern for each contact.
Dots indicate the number of contacts.

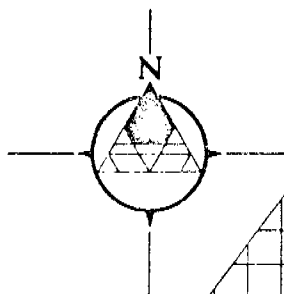


COOK INLET, ALASKA



DAMES & MOORE

POTENTIAL BOUNDARY CONTACT ZONES FOR SPILL SITE 7

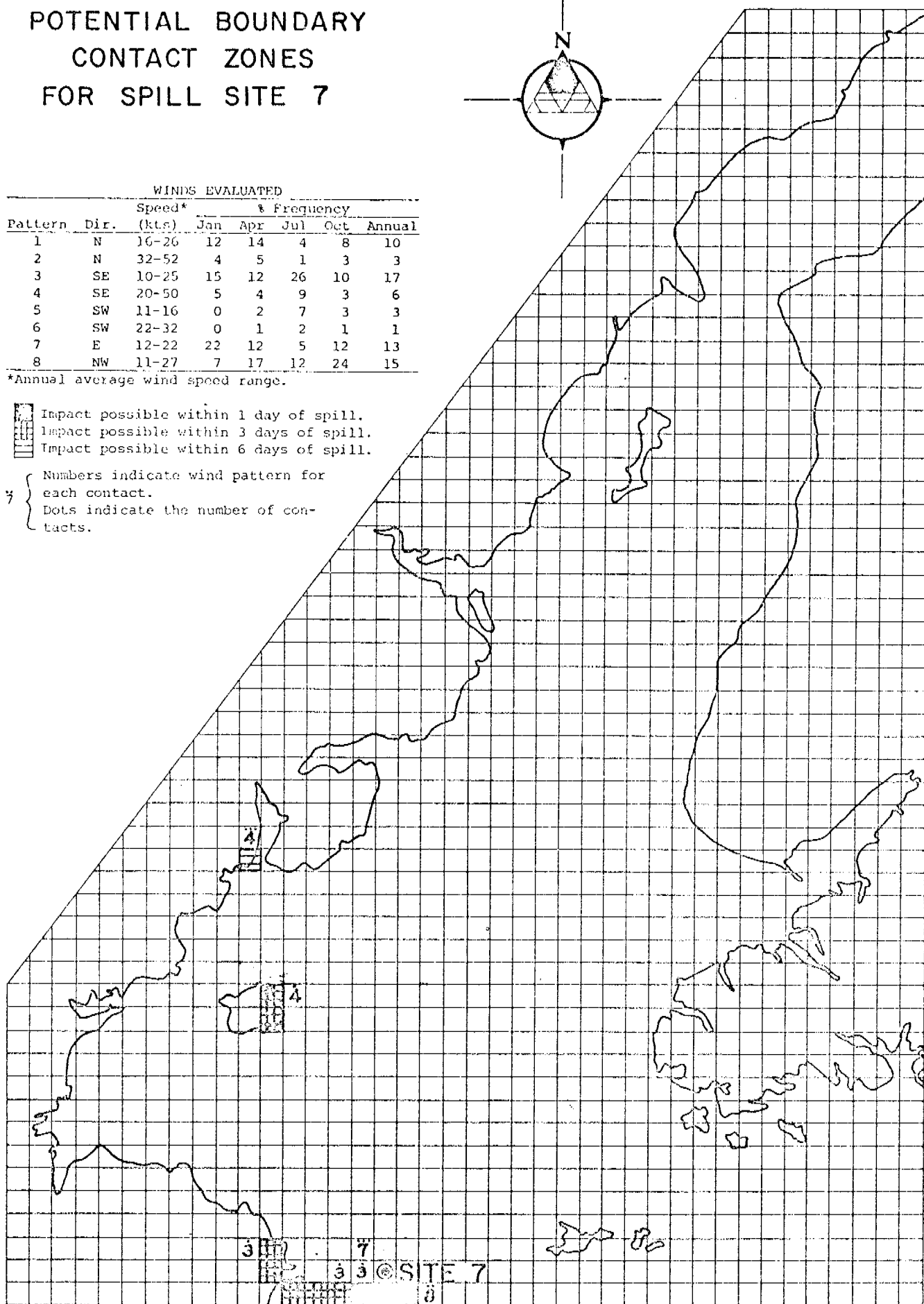


Pattern	Dir.	WINDS EVALUATED					
		Speed* (kts)	% Frequency				Annual
1	N	16-26	12	14	4	8	10
2	N	32-52	4	5	1	3	3
3	SE	10-25	15	12	26	10	17
4	SE	20-50	5	4	9	3	6
5	SW	11-16	0	2	7	3	3
6	SW	22-32	0	1	2	1	1
7	E	12-22	22	12	5	12	13
8	NW	11-27	7	17	12	24	15

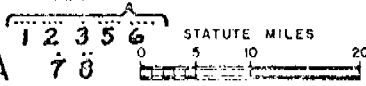
*Annual average wind speed range.

- Impact possible within 1 day of spill.
- Impact possible within 3 days of spill.
- Impact possible within 6 days of spill.

Numbers indicate wind pattern for each contact.
 Dots indicate the number of contacts.

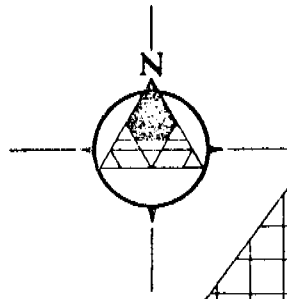


COOK INLET, ALASKA



DANIEL S. MOORE

POTENTIAL BOUNDARY CONTACT ZONES FOR SPILL SITE 8

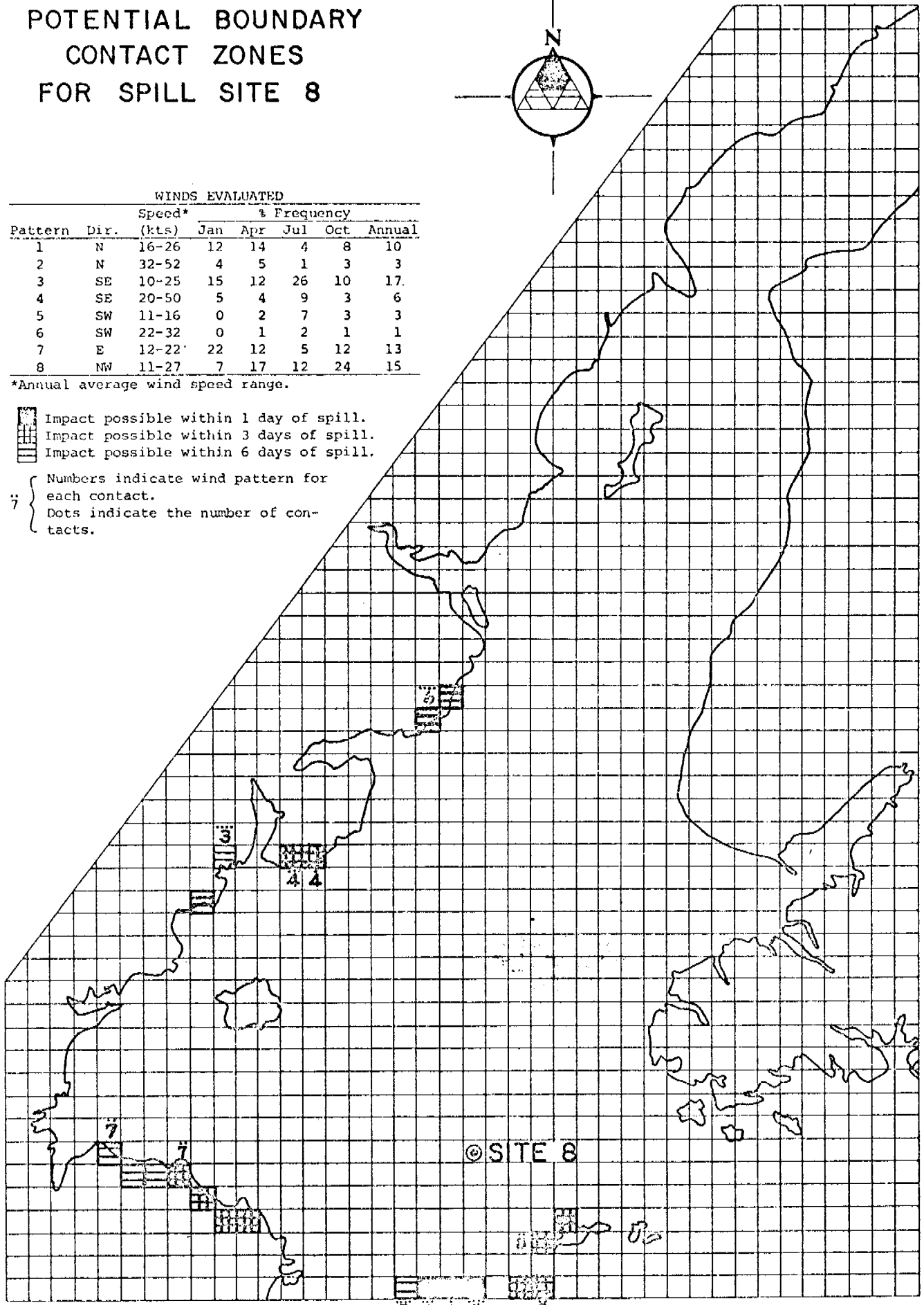


		WINDS EVALUATED					
Pattern	Dir.	Speed* (kts)	% Frequency				
			Jan	Apr	Jul	Oct	Annual
1	N	16-26	12	14	4	8	10
2	N	32-52	4	5	1	3	3
3	SE	10-25	15	12	26	10	17
4	SE	20-50	5	4	9	3	6
5	SW	11-16	0	2	7	3	3
6	SW	22-32	0	1	2	1	1
7	E	12-22	22	12	5	12	13
8	NW	11-27	7	17	12	24	15

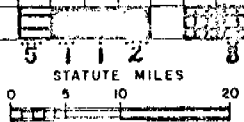
*Annual average wind speed range.

- Impact possible within 1 day of spill.
- Impact possible within 3 days of spill.
- Impact possible within 6 days of spill.

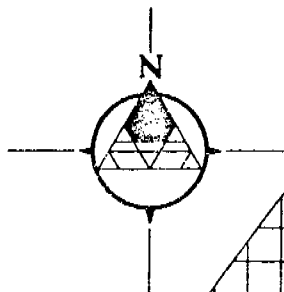
- { Numbers indicate wind pattern for each contact.
- { Dots indicate the number of contacts.



COOK INLET, ALASKA



POTENTIAL BOUNDARY CONTACT ZONES FOR SPILL SITE 9

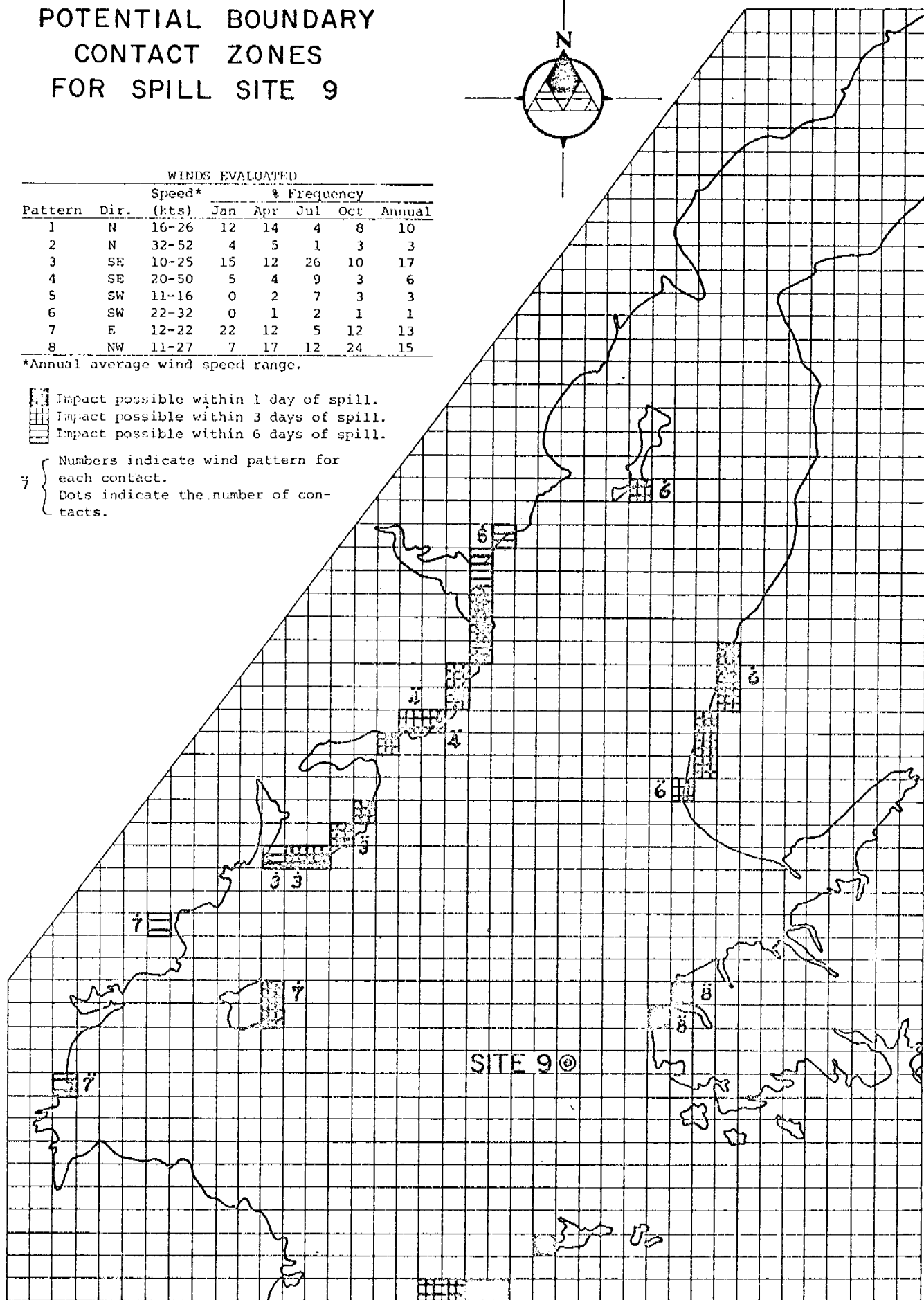


WINDS EVALUATED							
Pattern	Dir.	Speed*	% Frequency				
		(kts)	Jan	Apr	Jul	Oct	Annual
1	N	16-26	12	14	4	8	10
2	N	32-52	4	5	1	3	3
3	SE	10-25	15	12	26	10	17
4	SE	20-50	5	4	9	3	6
5	SW	11-16	0	2	7	3	3
6	SW	22-32	0	1	2	1	1
7	E	12-22	22	12	5	12	13
8	NW	11-27	7	17	12	24	15

*Annual average wind speed range.

- Impact possible within 1 day of spill.
- Impact possible within 3 days of spill.
- Impact possible within 6 days of spill.

Numbers indicate wind pattern for each contact.
Dots indicate the number of contacts.

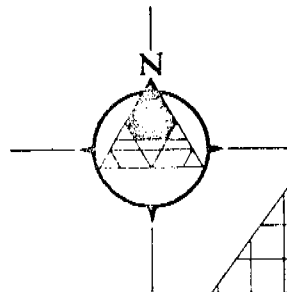


COOK INLET, ALASKA



DAMES & MOORE

POTENTIAL BOUNDARY CONTACT ZONES FOR SPILL SITE 10

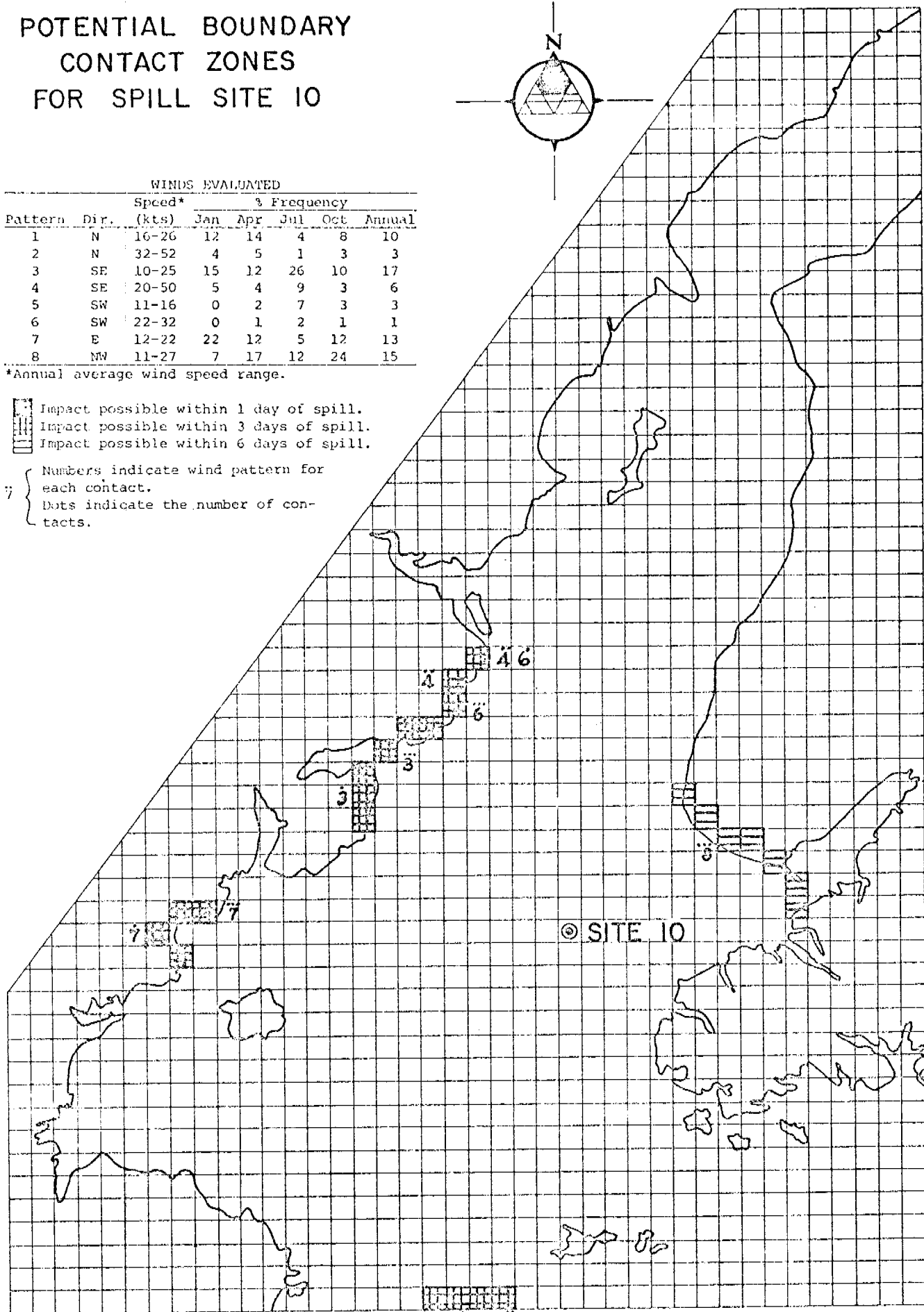


WINDS EVALUATED							
Pattern	Dir.	Speed* (kts)	% Frequency				
			Jan	Apr	Jul	Oct	Annual
1	N	16-26	12	14	4	8	10
2	N	32-52	4	5	1	3	3
3	SE	10-25	15	12	26	10	17
4	SE	20-50	5	4	9	3	6
5	SW	11-16	0	2	7	3	3
6	SW	22-32	0	1	2	1	1
7	E	12-22	22	12	5	12	13
8	NW	11-27	7	17	12	24	15

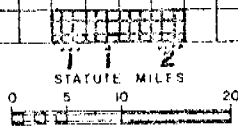
*Annual average wind speed range.

- Impact possible within 1 day of spill.
- Impact possible within 3 days of spill.
- Impact possible within 6 days of spill.

- Numbers indicate wind pattern for each contact.
- Dots indicate the number of contacts.

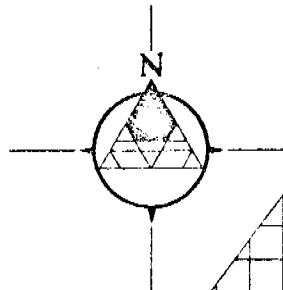


COOK INLET, ALASKA



DAWES & MOORE

POTENTIAL BOUNDARY CONTACT ZONES FOR SPILL SITE II

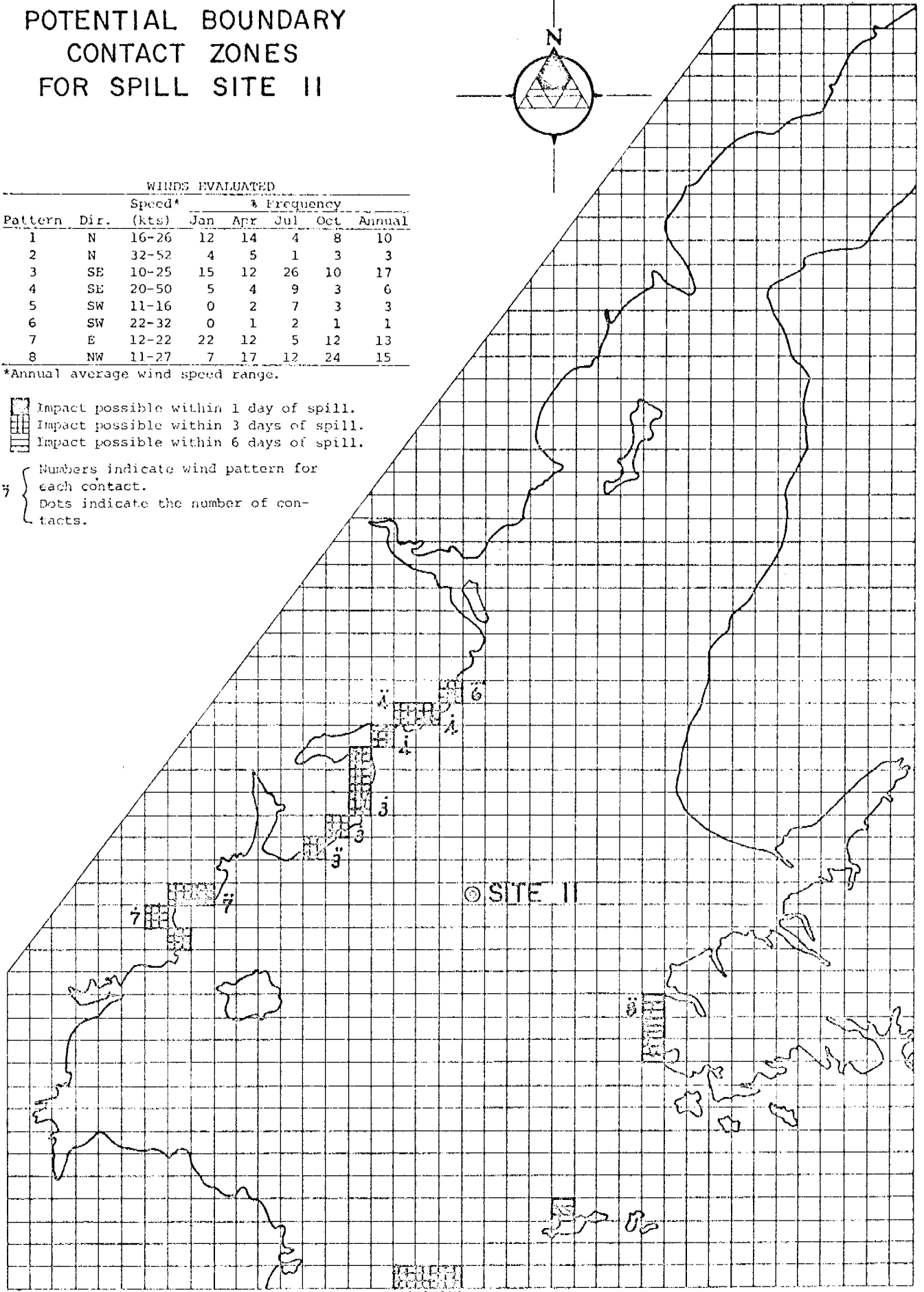


Pattern	Dir.	WINDS EVALUATED					
		Speed*	% Frequency				
		(kts)	Jan	Apr	Jul	Oct	Annual
1	N	16-26	12	14	4	8	10
2	N	32-52	4	5	1	3	3
3	SE	10-25	15	12	26	10	17
4	SE	20-50	5	4	9	3	6
5	SW	11-16	0	2	7	3	3
6	SW	22-32	0	1	2	1	1
7	E	12-22	22	12	5	12	13
8	NW	11-27	7	17	12	24	15

*Annual average wind speed range.

- Impact possible within 1 day of spill.
- Impact possible within 3 days of spill.
- Impact possible within 6 days of spill.

Numbers indicate wind pattern for each contact.
 Dots indicate the number of contacts.

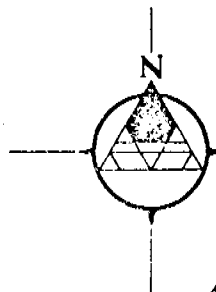


COOK INLET, ALASKA



DANIELS & ANDRE

POTENTIAL BOUNDARY CONTACT ZONES FOR SPILL SITE 12

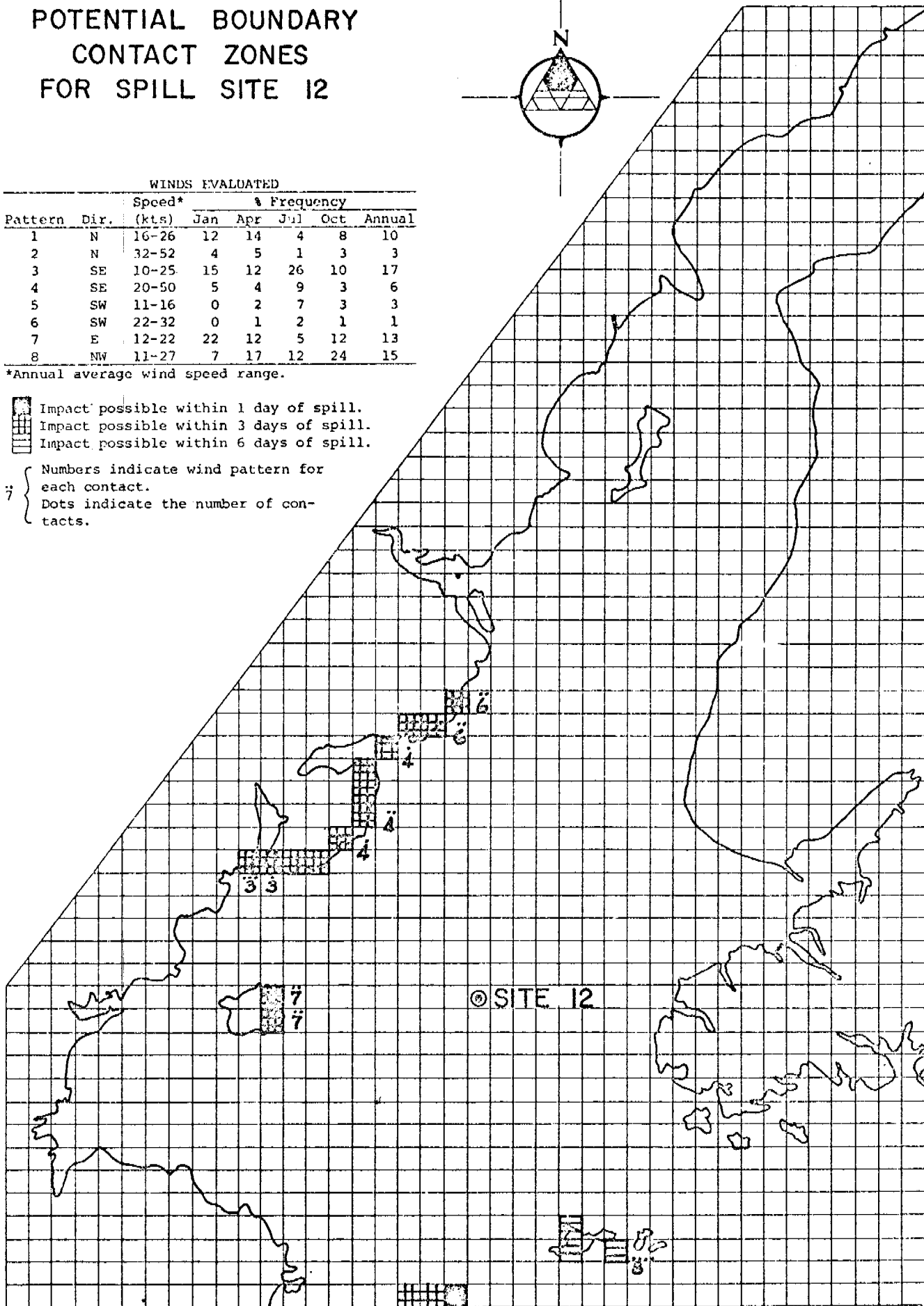


WINDS EVALUATED							
Pattern	Dir.	Speed* (kts)	% Frequency				Annual
			Jan	Apr	Jul	Oct	
1	N	16-26	12	14	4	8	10
2	N	32-52	4	5	1	3	3
3	SE	10-25	15	12	26	10	17
4	SE	20-50	5	4	9	3	6
5	SW	11-16	0	2	7	3	3
6	SW	22-32	0	1	2	1	1
7	E	12-22	22	12	5	12	13
8	NW	11-27	7	17	12	24	15

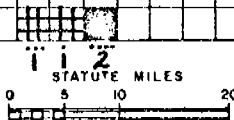
*Annual average wind speed range.

- Impact possible within 1 day of spill.
- Impact possible within 3 days of spill.
- Impact possible within 6 days of spill.

Numbers indicate wind pattern for each contact.
Dots indicate the number of contacts.

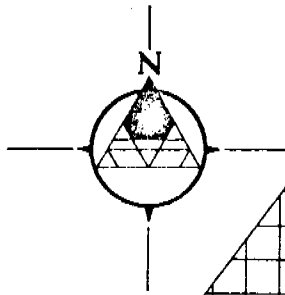


COOK INLET, ALASKA



DAMES & MOORE

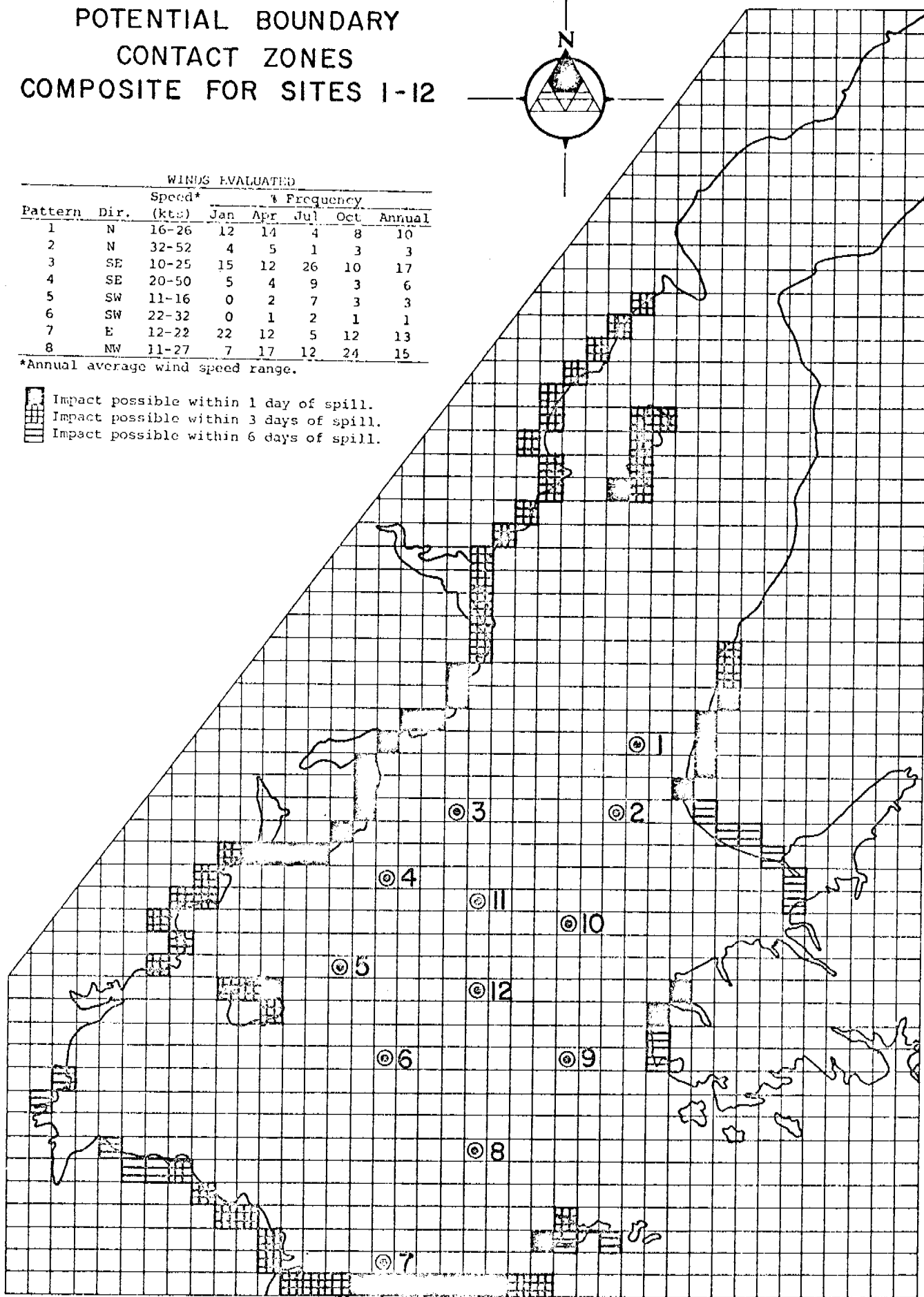
POTENTIAL BOUNDARY CONTACT ZONES COMPOSITE FOR SITES 1-12



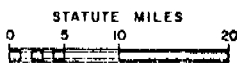
Pattern	Dir.	WINDS EVALUATED					
		Speed* (kts)	Jan	Apr	Jul	Oct	Annual
1	N	16-26	12	14	4	8	10
2	N	32-52	4	5	1	3	3
3	SE	10-25	15	12	26	10	17
4	SE	20-50	5	4	9	3	6
5	SW	11-16	0	2	7	3	3
6	SW	22-32	0	1	2	1	1
7	E	12-22	22	12	5	12	13
8	NW	11-27	7	17	12	24	15

*Annual average wind speed range.

- Impact possible within 1 day of spill.
- Impact possible within 3 days of spill.
- Impact possible within 6 days of spill.



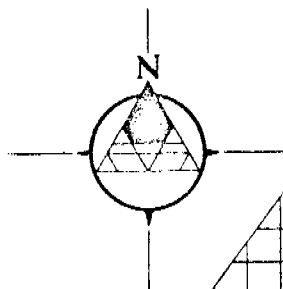
COOK INLET, ALASKA



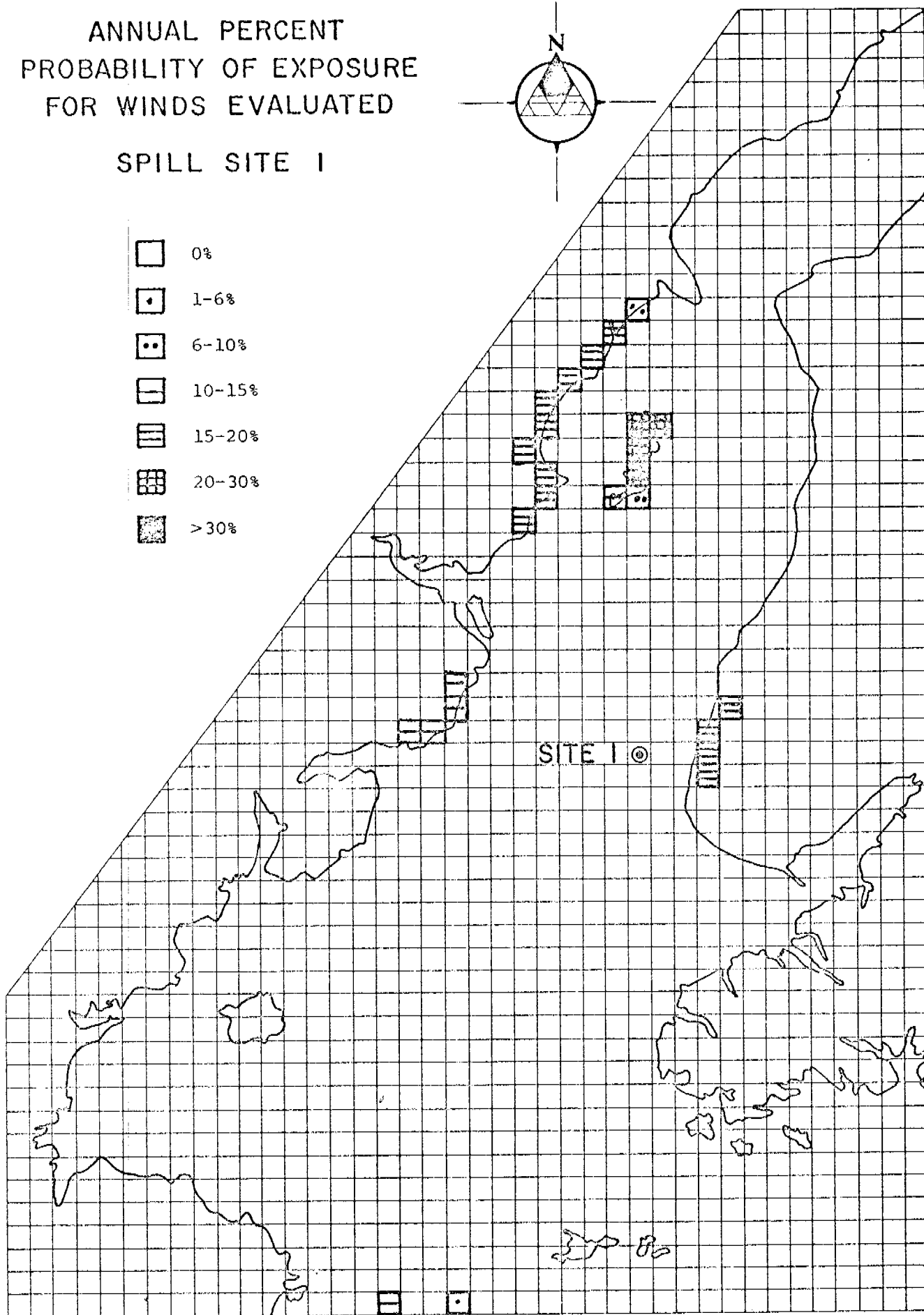
DANES & MOORE

ANNUAL PERCENT
PROBABILITY OF EXPOSURE
FOR WINDS EVALUATED

SPILL SITE I

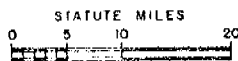


- 0%
- ◼ 1-6%
- ◼ 6-10%
- ◼ 10-15%
- ◼ 15-20%
- ◼ 20-30%
- ◼ >30%



SITE I ⊙

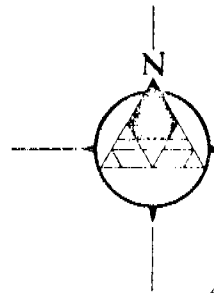
COOK INLET, ALASKA



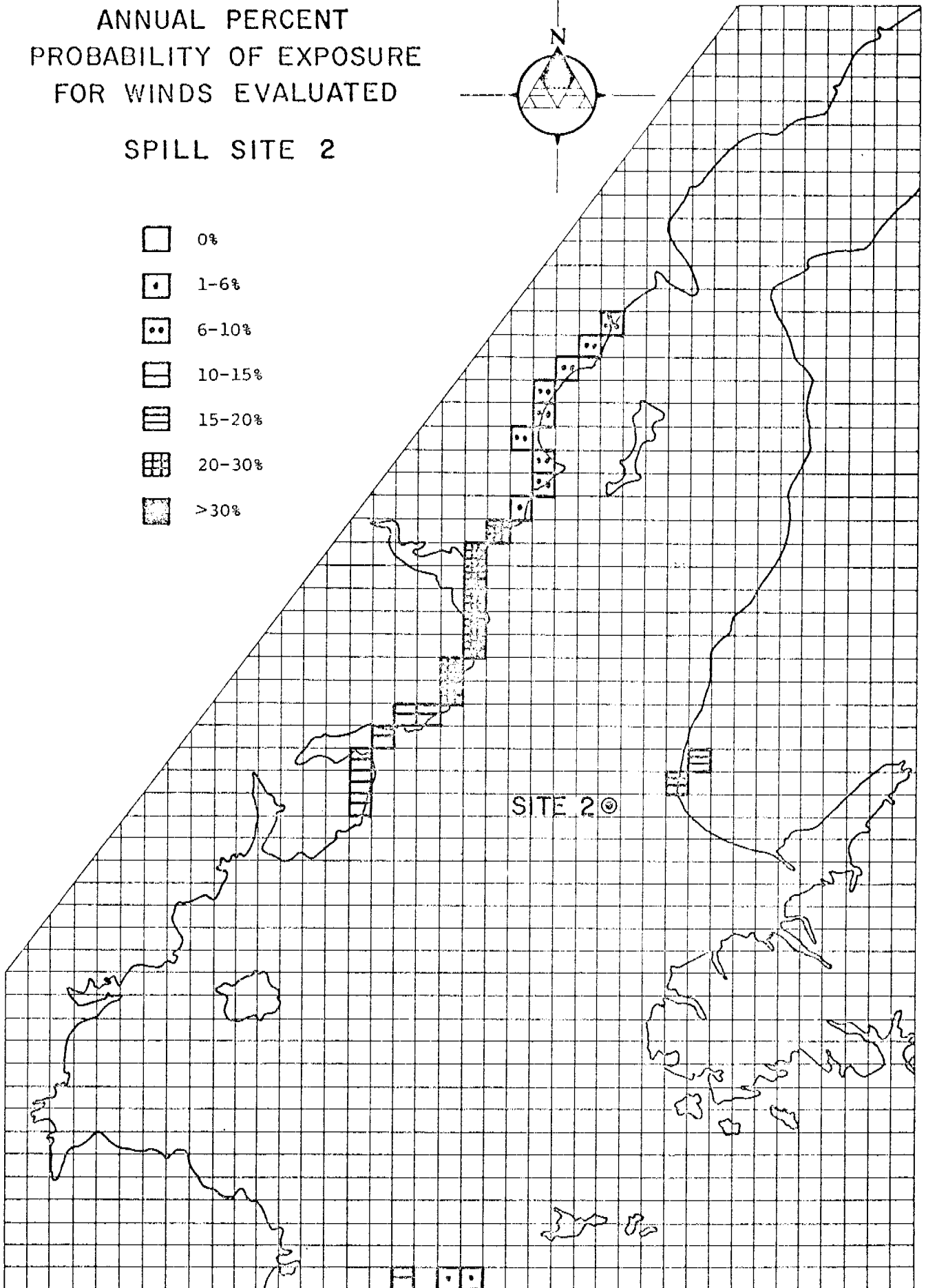
DAVIS & MOORE

ANNUAL PERCENT
PROBABILITY OF EXPOSURE
FOR WINDS EVALUATED

SPILL SITE 2

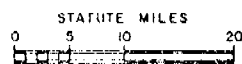


- 0%
- ◻• 1-6%
- ◻•• 6-10%
- ◻▬ 10-15%
- ◻▬▬ 15-20%
- ◻▬▬▬ 20-30%
- ◻▬▬▬▬ >30%



SITE 2 ©

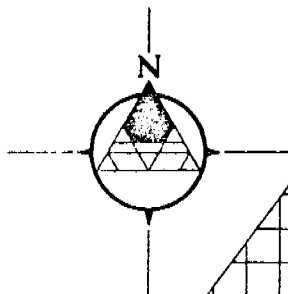
COOK INLET, ALASKA










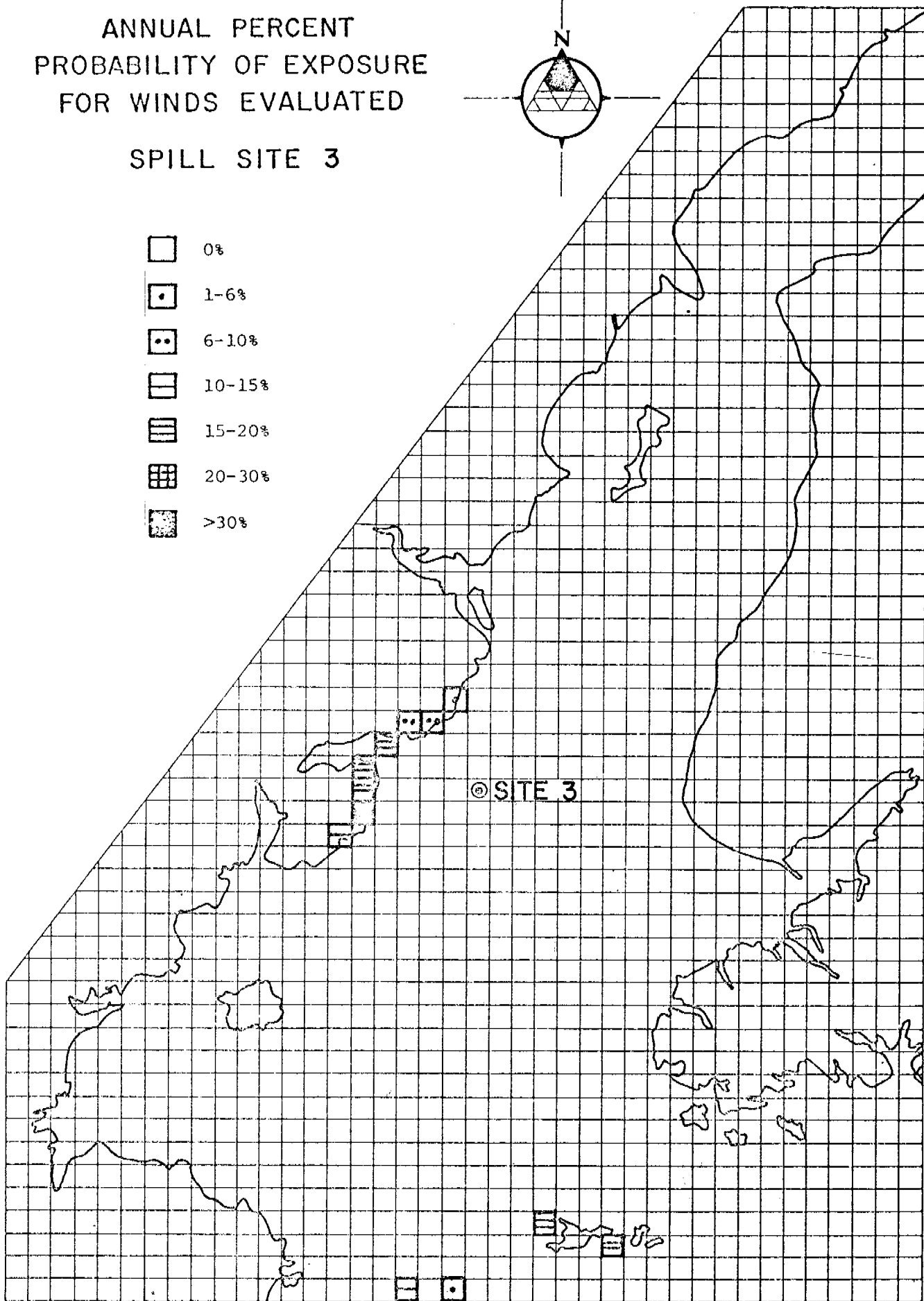
DAMES & MOORE

ANNUAL PERCENT
PROBABILITY OF EXPOSURE
FOR WINDS EVALUATED

SPILL SITE 3



-  0%
-  1-6%
-  6-10%
-  10-15%
-  15-20%
-  20-30%
-  >30%



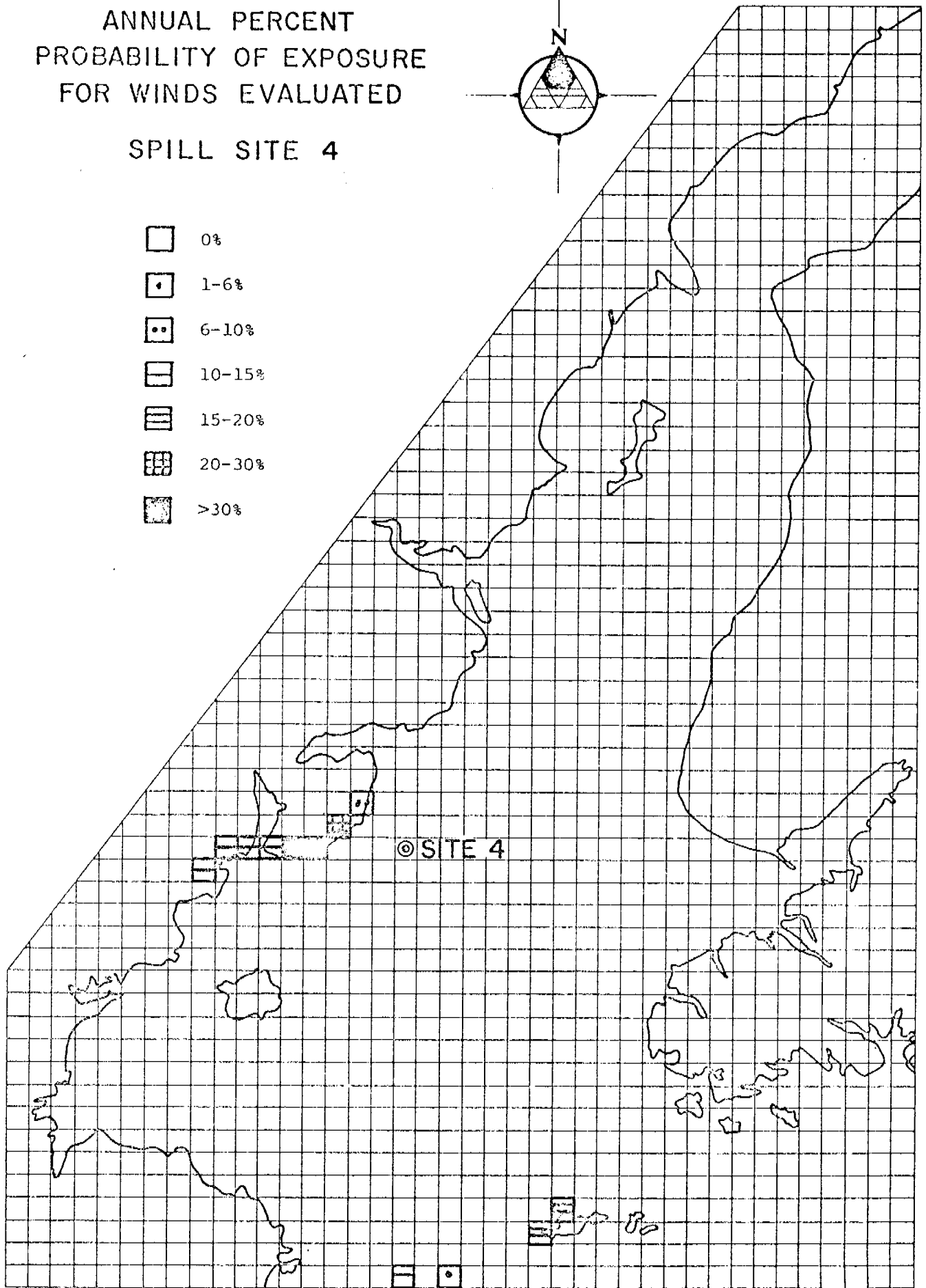
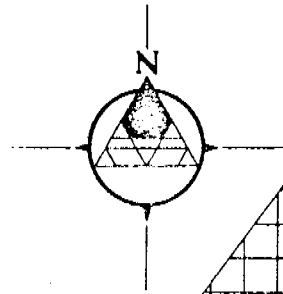
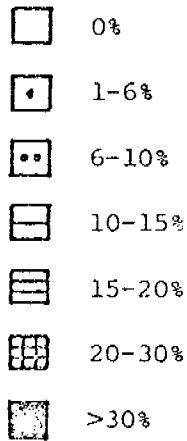
COOK INLET, ALASKA



DAMES & MOORE

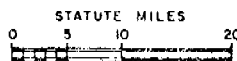
ANNUAL PERCENT
PROBABILITY OF EXPOSURE
FOR WINDS EVALUATED

SPILL SITE 4



© SITE 4

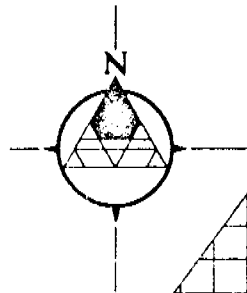
COOK INLET, ALASKA






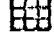



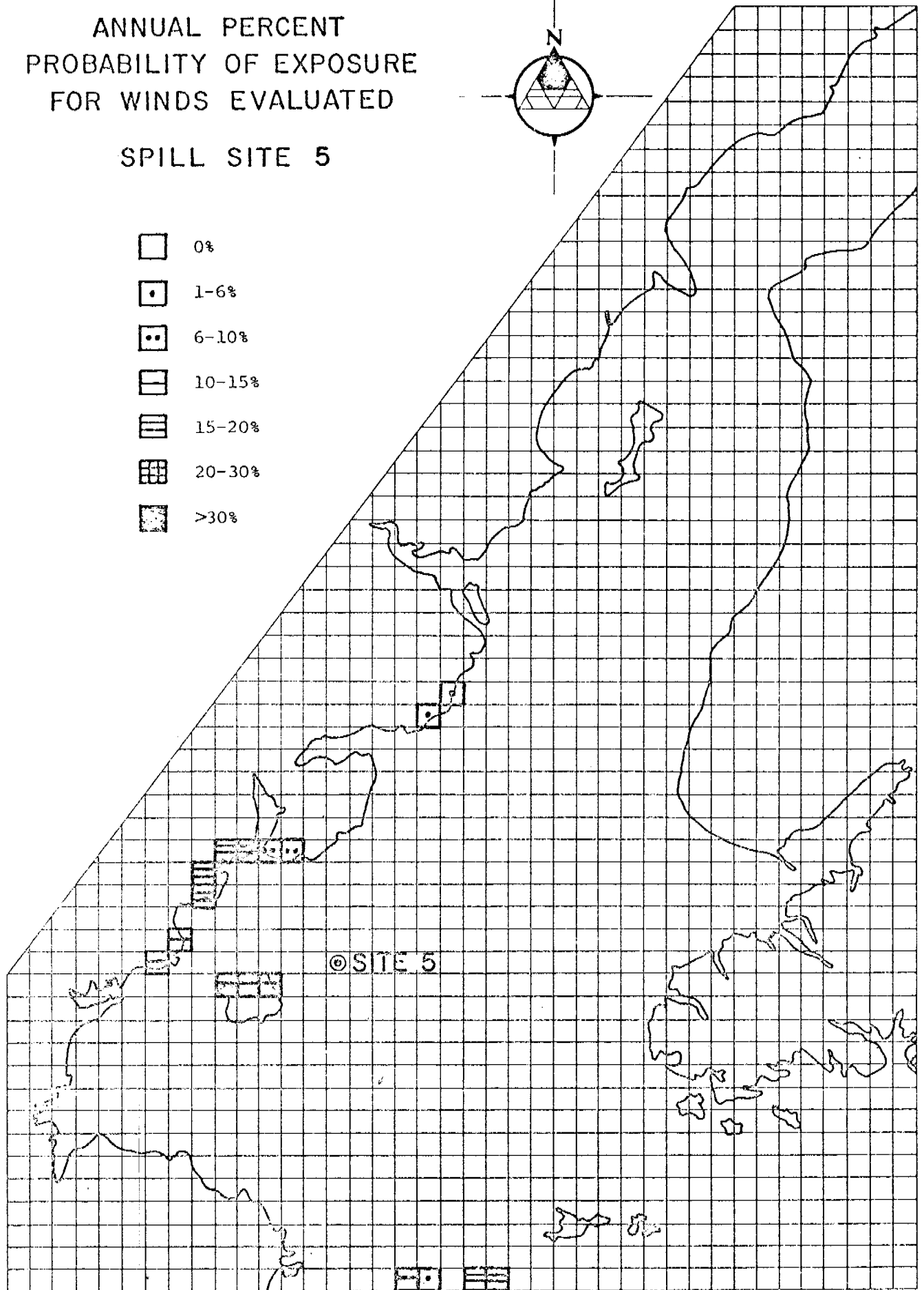
DAMES & MOORE

ANNUAL PERCENT
PROBABILITY OF EXPOSURE
FOR WINDS EVALUATED

SPILL SITE 5



-  0%
-  1-6%
-  6-10%
-  10-15%
-  15-20%
-  20-30%
-  >30%



⊙ SITE 5

COOK INLET, ALASKA



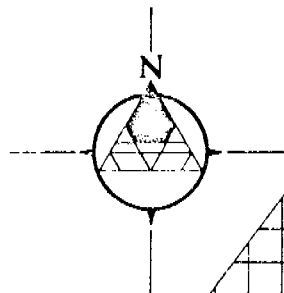
820

DAMES & MOORE

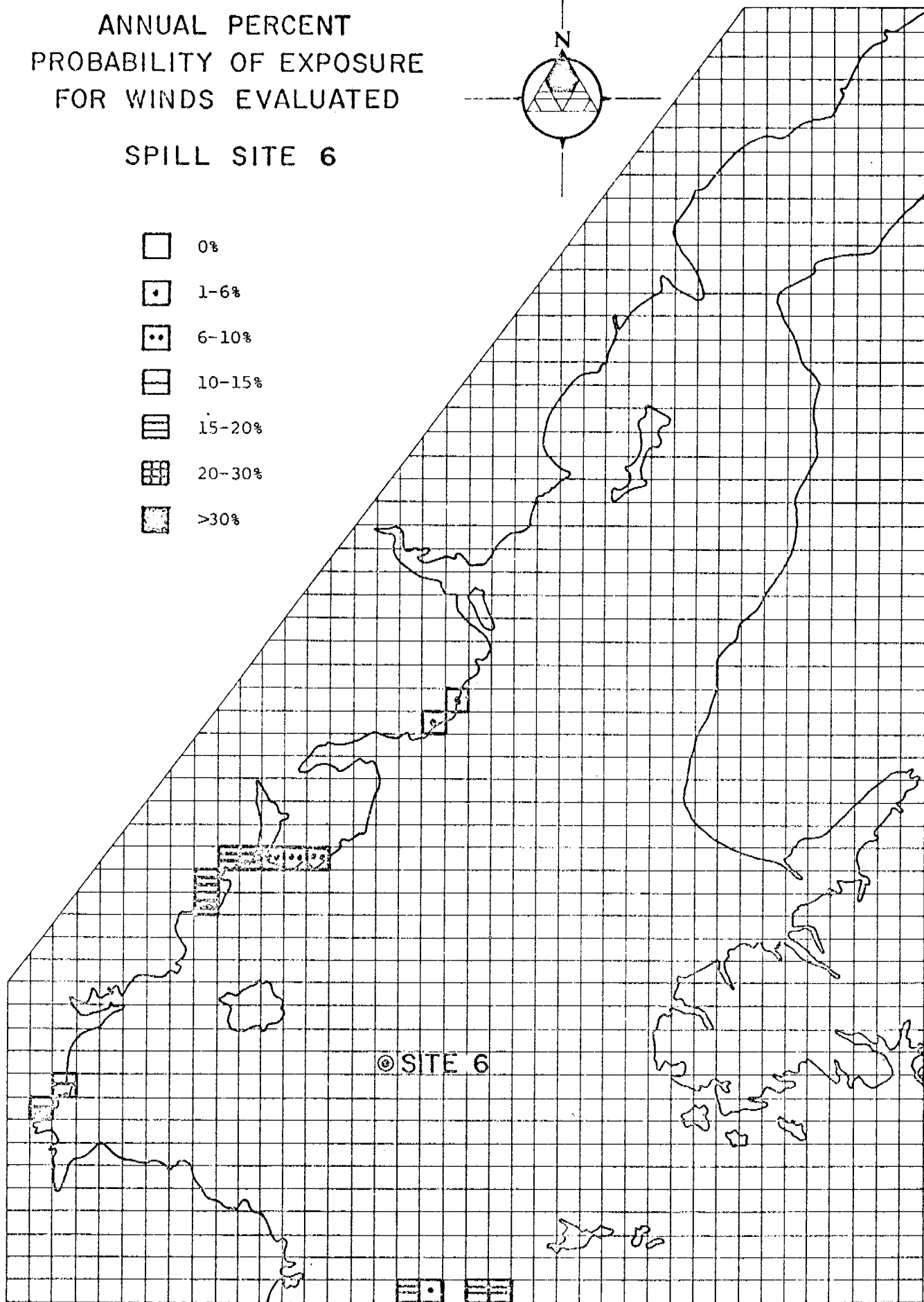
PLATE 26

ANNUAL PERCENT
PROBABILITY OF EXPOSURE
FOR WINDS EVALUATED

SPILL SITE 6

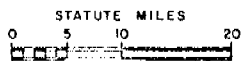


- 0%
- ◻• 1-6%
- ◻◻ 6-10%
- ◻◻◻ 10-15%
- ◻◻◻◻ 15-20%
- ◻◻◻◻◻ 20-30%
- ◻◻◻◻◻◻◻ >30%



© SITE 6

COOK INLET, ALASKA



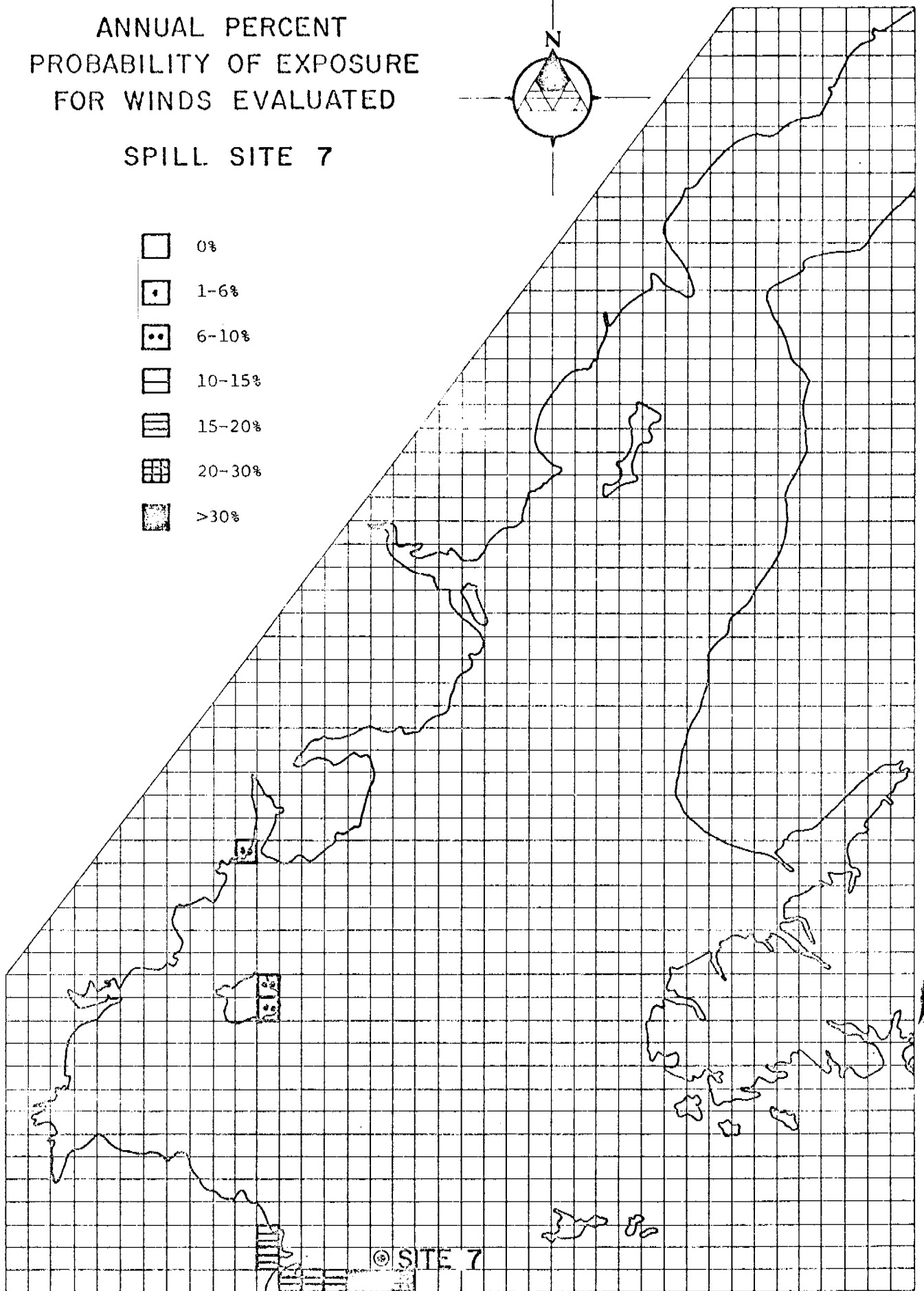
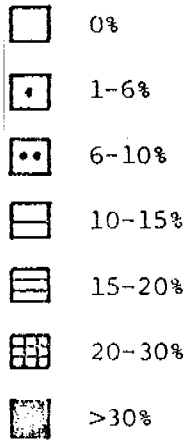
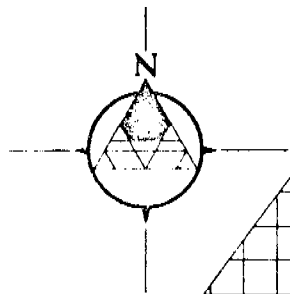
821

DAMES & MOORE

PLATE 27

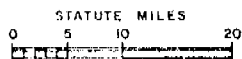
ANNUAL PERCENT
PROBABILITY OF EXPOSURE
FOR WINDS EVALUATED

SPILL SITE 7



⊙ SITE 7

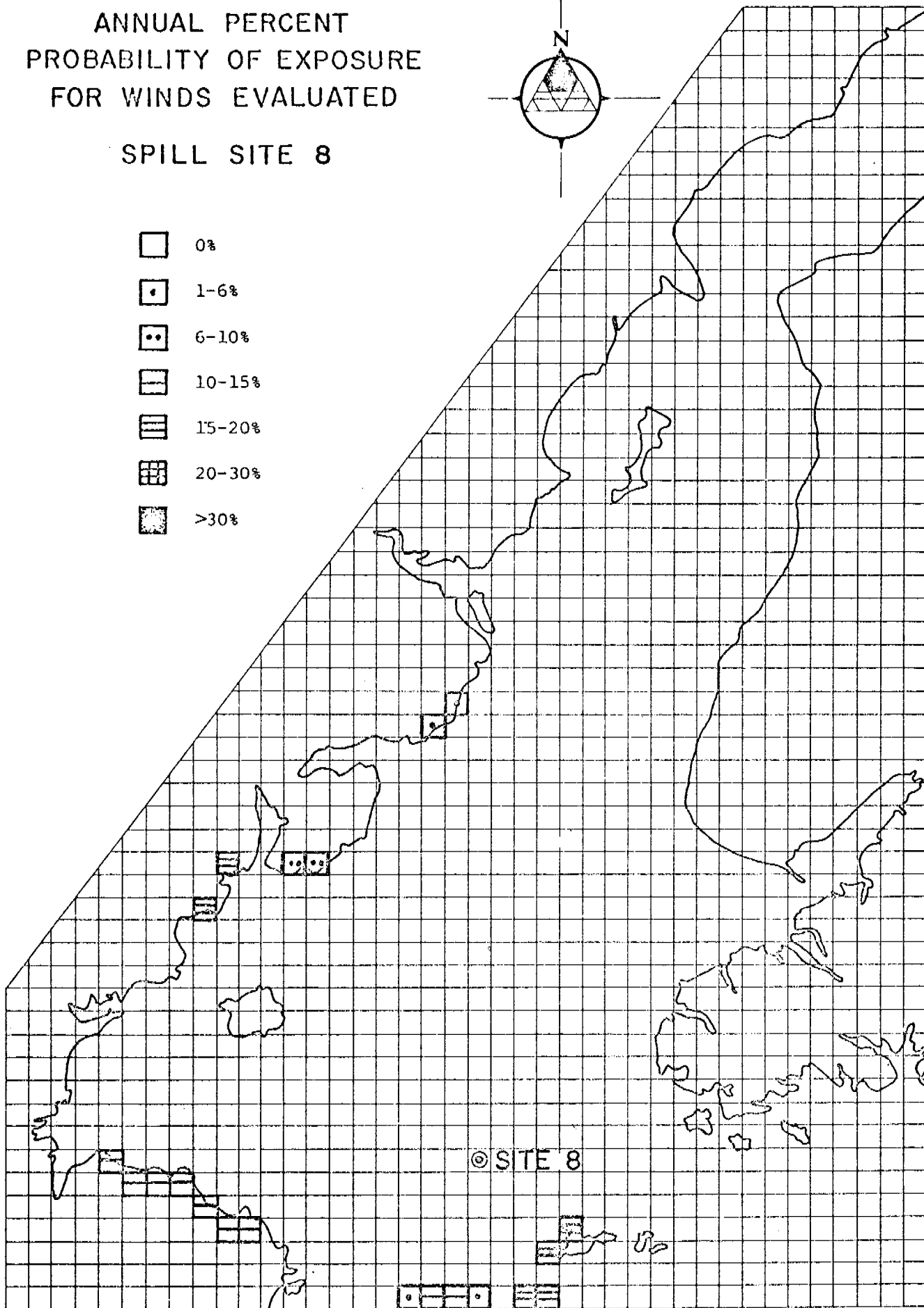
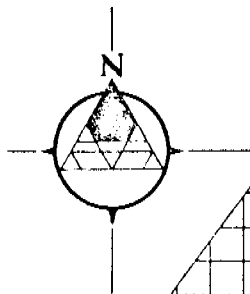
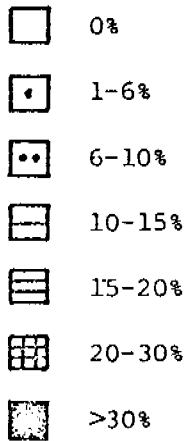
COOK INLET, ALASKA



DAMES & MOORE

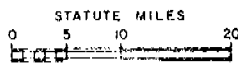
ANNUAL PERCENT
PROBABILITY OF EXPOSURE
FOR WINDS EVALUATED

SPILL SITE 8



© SITE 8

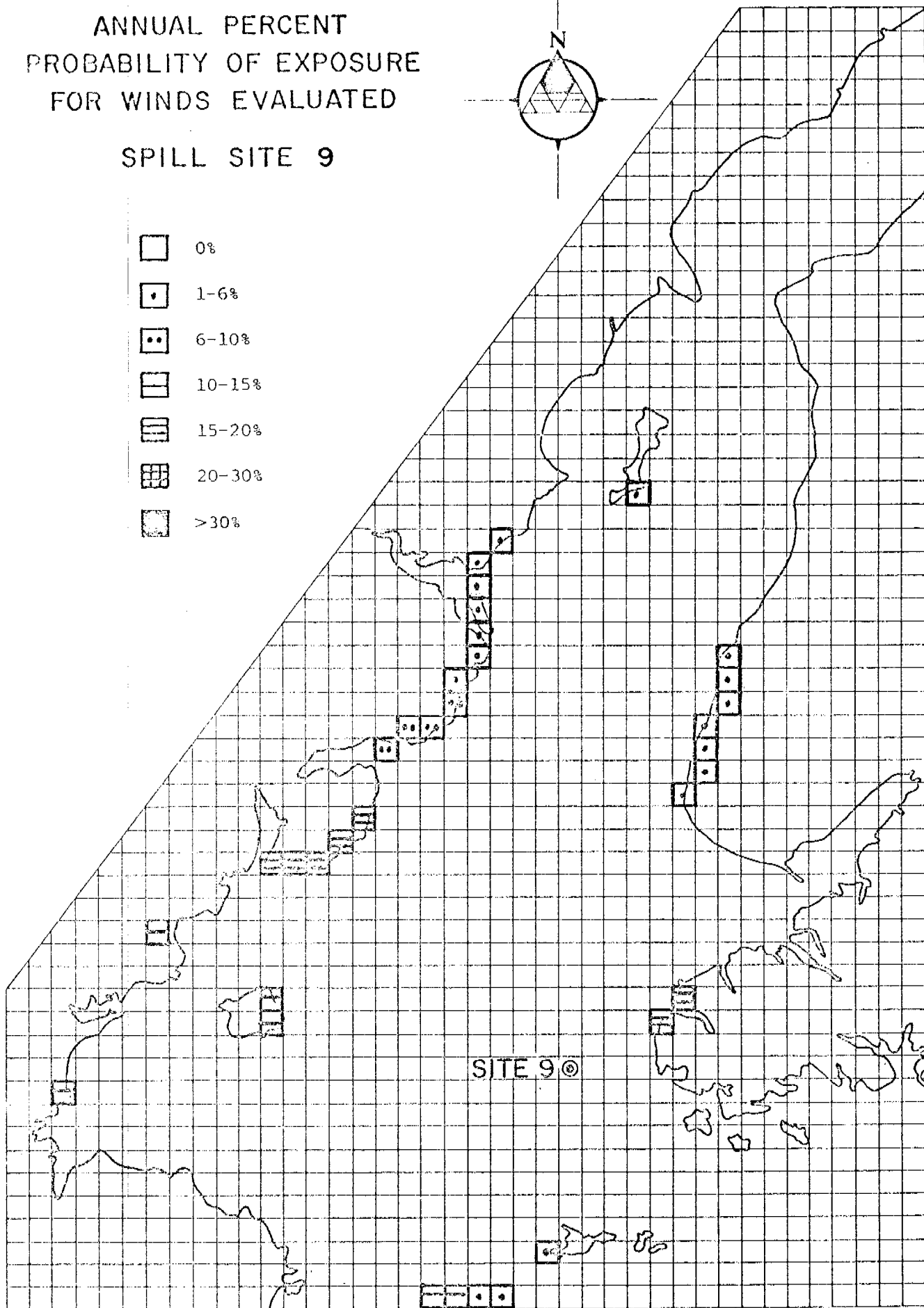
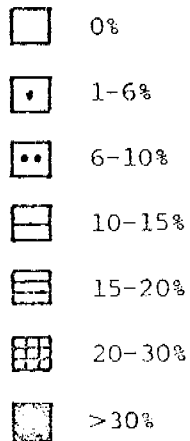
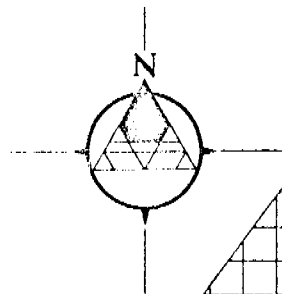
COOK INLET, ALASKA



DAMES & MOORE

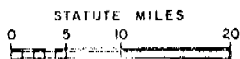
ANNUAL PERCENT
PROBABILITY OF EXPOSURE
FOR WINDS EVALUATED

SPILL SITE 9



SITE 9

COOK INLET, ALASKA



DAMES & MOORE

